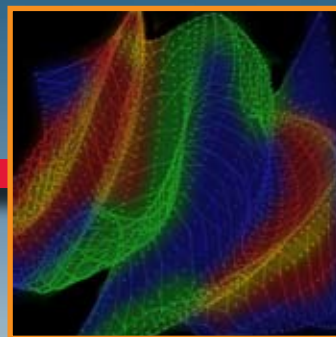


Linking Science and Technology for Global Solutions

TMS2008

137th Annual Meeting & Exhibition

**March 9-13, 2008
Ernest Morial Convention Center
New Orleans, Louisiana, USA**



Register before February 11 at www.tms.org/annualmeeting.html

TMS2008

137th Annual Meeting & Exhibition

**March 9-13, 2008
Ernest Morial Convention Center
New Orleans, Louisiana, USA**

TMS 2008 is bringing top materials scientists and engineers from around the world together to address some of today's global challenges:

- ▶ Resolving technology and techno-management issues for the production of aluminum, metal castings, steel, automotive and electronic materials
- ▶ Optimizing energy utilization and addressing environmental impacts
- ▶ Developing materials for high-performance applications
- ▶ Achieving process improvement for a variety of materials under a variety of conditions
- ▶ Preparing future materials scientists and engineers

These issues and more are presented in 56 symposia covering four major themes:

Light Metals

Extraction, Processing, Structure and Properties

Emerging Materials

Materials and Society

TMS 2008 addresses these global challenges with traditional programming presenting new developments, such as . . .

9th Global Innovations Symposium

Aluminum Reduction Technology

Bulk Metallic Glasses

Magnesium Technology 2008

Materials in Clean Power Systems III

Ultrafine Grained Materials

. . . with new partnerships represented . . .

American Physical Society and TMS present Integrated Computational Materials Engineering symposia.

The Chinese Society for Metals delegation, led by Professor Liu Yongcai, deputy secretary general, and the Indian Institute of Metals delegation, led by Dr. Sanak Mishra, vice president and chairman of the ferrous division, provide perspective in the Materials and Society symposia.

Linking Science and Technology for Global Solutions

... and **new perspectives** for discussion ...

Climate Change and Greenhouse Gas Emissions

Features leaders from the world's largest aluminum companies: Alcan, Alcoa, BHP Billiton, Chalco and Hydro Aluminum

Energy Conservation in Metals Extraction and Materials Processing

Presents current and potential technology and methodologies for energy saving techniques

IOMMMS Global Materials Forum 2008: Creating the Future MS&E Professionals

Highlights approaches from China, India, Japan and the United States

Materials for Infrastructure: Building Bridges in the Global Community

Includes special guided tour for symposium attendees covering the geology of the Katrina disaster. See page 27 to learn how you can leave a lasting impression on New Orleans!

Role of Engineers in Meeting 21st Century Societal Challenges

Addresses energy, transportation, housing, health and recycling issues

Sloan Industry Centers Forum: Techno-Management Issues Related to Materials-Centric Industries

Considers aluminum, metal processing, steel, automotive, paper and wood

With 56 symposia, three short courses, six lectures, eight networking receptions, 130+ exhibitors, one free collected proceedings CD-ROM, and thousands of your colleagues from 70 countries, **TMS 2008 offers you the opportunity to learn, network and advance global solutions for today's materials challenges.**

Register online at www.tms.org/annualmeeting.html or see page 22.

Table of Contents

Symposia by Theme	4
Symposia Alphabetically	6
Lectures	11
Continuing Education	13
Networking Events	14
Exhibition	16
Especially for Students	18
Proceedings	20
Registration	21
Housing	23
Tours	25
Hands-On New Orleans	27

Register online at www.tms.org/annualmeeting.html

Light Metals

Alumina and Bauxite
 Aluminum Alloys: Fabrication, Characterization and Applications
 Aluminum Reduction Technology
 Carbon Dioxide Reduction Metallurgy
 Cast Shop Technology
 Characterization of Minerals, Metals and Materials
 Computational Thermodynamics and Kinetics
 Electrode Technology
 Frontiers in Process Modeling
 Magnesium Technology 2008
 Materials Informatics: Enabling Integration of Modeling and Experiments in Materials Science
 Recycling

Related Lecture and Short Courses:

- *"Innovations in Steel Production – Animations for Aluminium Technologies?"*
- *Furnace Systems and Technology*
- *Grain Refinement of Aluminium Alloys: Theory and Practice*
- *Greenhouse Gas Emissions*

See page 12 for details.

Extraction, Processing, Structure and Properties

3-Dimensional Materials Science
 9th Global Innovations Symposium: Trends in Integrated Computational Materials Engineering for Materials Processing and Manufacture
 Acta Materialia Gold Medal Symposium: Recent Developments in Rare Earth Science and Technology
 Advances in Roasting, Sintering, Calcining, Preheating and Drying
 APS Frontiers of Computational Materials Science
 Aqueous Processing
 Biological Materials Science
 Bulk Metallic Glasses V
 Carbon Dioxide Reduction Metallurgy
 Characterization of Minerals, Metals and Materials
 Complex Oxide Materials: Synthesis, Properties and Applications
 Computational Thermodynamics and Kinetics

Creating the ICME Cyberinfrastructure: an Interdisciplinary Technology Forum
 Deformation Twinning: Formation Mechanisms and Effects on Material Plasticity – Experiments and Modeling
 Emerging Interconnect and Packaging Technologies
 Emerging Methods to Understand Mechanical Behavior
 Energy Conservation in Metals Extraction and Materials Processing
 Enhancing Materials Durability via Surface Engineering
 Frontiers in Process Modeling
 Hael Mughrabi Honorary Symposium: Plasticity, Failure and Fatigue in Structural Materials – from Macro to Nano
 Hot and Cold Rolling Technology
 Hume-Rothery Symposium: Nanoscale Phases
 Materials Informatics: Enabling Integration of Modeling and Experiments in Materials Science
 Materials Processing Fundamentals
 Mechanical Behavior, Microstructure and Modeling of Ti and Its Alloys
 Mechanics and Kinetics of Interfaces in Multicomponent Materials Systems
 Minerals, Metals and Materials under Pressure
 Neutron and X-Ray Studies for Probing Materials Behavior
 Particle Beam-Induced Radiation Effects in Materials
 Phase Stability, Phase Transformations and Reactive Phase Formation in Electronic Materials VII
 Pyrometallurgy
 Recent Industrial Applications of Solid-State Phase Transformations
 Recycling
 Refractory Metals 2008
 Structural Aluminides for Elevated Temperature Applications
 Ultrafine-Grained Materials: Fifth International Symposium

Related Lectures:

- *"Computational Modeling of Metals Processing: Past, Present and Future"*
- *"Smelting and Refining – Faster, Smoother, Cheaper, Safer"*
- *"High Performance Structural Metals: an Undervalued but Critical Enabling Technology"*
- *Nanoscale Metal Silicides*

See page 11 for details.

Symposia Listed by Theme

Emerging Materials

2008 Nanomaterials: Fabrication, Properties and Applications
3-Dimensional Materials Science
4th Lead-Free Solders Technology Workshop
9th Global Innovations Symposium: Trends in Integrated
Computational Materials Engineering for Materials Processing
and Manufacture
Acta Materialia Gold Medal Symposium: Recent Developments in
Rare Earth Science and Technology
Advances in Semiconductor, Electro Optic and Radio
Frequency Materials
Biological Materials Science
Bulk Metallic Glasses V
Carbon Dioxide Reduction Metallurgy
Characterization of Minerals, Metals and Materials
Complex Oxide Materials: Synthesis, Properties and Applications
Computational Thermodynamics and Kinetics
Creating the ICME Cyberinfrastructure: An Interdisciplinary
Technology Forum
Emerging Interconnect and Packaging Technologies
Energy Conservation in Metals Extraction and
Materials Processing
Enhancing Materials Durability via Surface Engineering
Frontiers in Process Modeling
Hael Mughrabi Honorary Symposium: Plasticity, Failure and Fatigue
in Structural Materials – from Macro to Nano
Hume-Rothery Symposium: Nanoscale Phases
Materials in Clean Power Systems III: Fuel Cells, Hydrogen, and
Clean Coal-Based Technologies
Materials Informatics: Enabling Integration of Modeling and
Experiments in Materials Science
Mechanics and Kinetics of Interfaces in Multicomponent
Materials Systems
Micro-Engineered Particulate-Based Materials
Neutron and X-Ray Studies for Probing Materials Behavior
Particle Beam-Induced Radiation Effects in Materials
Phase Stability, Phase Transformations and Reactive Phase
Formation in Electronic Materials VII
Recycling
Structural Aluminides for Elevated Temperature Applications
Ultrafine-Grained Materials: Fifth International Symposium

Related Short Course:

- *Nanomechanical Characterization*

See page 13 for details.

Materials and Society

Climate Change and Greenhouse Gas Emissions
IOMMMS Global Materials Forum 2008: Creating the Future
MS&E Professionals
Materials for Infrastructure: Building Bridges in the
Global Community
National Materials Advisory Board Town Hall Meeting on Assessing
Corrosion Education
Role of Engineers in Meeting 21st Century Societal Challenges
Sloan Industry Centers Forum: Techno-Management Issues
Related to Materials-Centric Industries

About Materials and Society

Many of the programs and activities fit broadly under the umbrella of Materials and Society—from many symposia and presentations in the technical program to the community outreach that will be performed on-site. Many invited speakers will examine opportunities for the materials science and engineering community to proactively address the complex technological, professional, educational, societal, environmental, infrastructural and economic issues that challenge the sustainability of today's world. We are all challenged to improve the world as we know it for those in developing countries and to secure it for future generations.

Related Lecture and Short Course:

- *"Design for the Other 90%"*
- *Greenhouse Gas Emissions*

See page 11 for details.

Turn to the alphabetical listing of the symposia on the following pages for descriptions.

2008 Nanomaterials: Fabrication, Properties and Applications

...development, manufacture and application of functional nanomaterials

- Functional applications of nanomaterials
- Nanostructure fabrication
- Carbon nanostructures
- Quantum-dots

3-Dimensional Materials Science

...advanced characterization, modeling and microanalysis

- 3-D visualization and modeling
- 3-D microstructural evolution
- Microscopy techniques
- Microanalysis methods

4th Lead-Free Solders Technology Workshop

...TMS-Surface Mount Technology Association forum addressing critical needs

- Solder systems
- Packaging technologies
- Reliability
- Legislation

9th Global Innovations Symposium: Trends in Integrated Computational Materials Engineering for Materials Processing and Manufacture

...TMS-American Physical Society plenary discussions of advancements in materials modeling across length scales, and manufacturing impact

- Nuclear materials
- Ceramics
- Aluminum
- Nanomaterials

Acta Materialia Gold Medal Symposium: Recent Developments in Rare Earth Science and Technology

...in honor of Karl Gschneidner Jr.

- Single crystals
- Characterization and properties
- Novel applications
- Recent advancements

Advances in Roasting, Sintering, Calcining, Preheating and Drying

...state-of-the-art in processing technologies

- Iron ore
- Alumina
- Rotary kiln systems

Advances in Semiconductor, Electro Optic and Radio Frequency Materials

...development, fabrication and application of emerging technologies

- Medical device semiconductors
- Nanomaterials
- Photovoltaics

Alumina and Bauxite

...mining and refining of raw materials for aluminum production

- Alumina refinery design and development
- Alumina refinery safety and integrity
- Bauxite and digestion
- Precipitation

Aluminum Alloys: Fabrication, Characterization and Applications

...advancements in aluminum for today's marketplace

- Alloy characterization
- Alloy development
- Aluminum products and applications

Aluminum Reduction Technology

...conversion of alumina to aluminum

- Alternative processes
- Anode design and operation
- Cell fundamentals and phenomena
- Environmental and plant improvements
- Process control developments

Aluminum Reduction Symposium Organizer Martin Iffert:

"(This symposium) has a strong focus on sustainability and environmental aspects in the aluminum smelting process. This includes firsthand information about the European emission trading scheme and the influence on energy prices, smelter economy and environment."

APS Frontiers of Computational Materials Science

...American Physical Society forum on progress in computational materials methods

Aqueous Processing

...recent progress

- Alternative leaching processes
- Precious metals
- Process-stability relationships
- New strategies and techniques

Biological Materials Science

...development of biological materials and biomaterial devices

- Biocompatibility
- Mimicking biological systems
- Bioinspired design
- Mechanical and environmental response

Bulk Metallic Glasses V

...state-of-the-art development

- Mechanical behavior
- Characterization
- Modeling
- Processing

Carbon Dioxide Reduction Metallurgy

(sponsored by TMS, American Iron and Steel Institute, and Canadian Institute of Mining, Metallurgy and Petroleum)

...state-of-the-art carbon dioxide metallurgical reduction and decreased use of carbon

- Green production of light metals
- Green production of steel
- Carbon sequestration
- Electrochemical reduction of carbon dioxide

Cast Shop Technology

...melting and metal treatment of aluminum

- Sustainability and environmental issues
- Cast house operations and melting
- Cast shop safety
- Casting, solidification and microstructures

Characterization of Minerals, Metals and Materials

...techniques for characterizing materials across a spectrum of systems and processes

- Characterization of mechanical and physical properties of materials
- Characterization of processing of materials
- Characterization of structure across length scales

Climate Change and Greenhouse Gas Emissions

...industry leaders discuss progress and challenges for the materials industries

- Alcan
- Alcoa
- BHP Billiton
- Chalco
- Hydro Aluminum

Complex Oxide Materials: Synthesis, Properties and Applications

...interdisciplinary forum bridging materials research and application

- Novel functional oxide thin films
- Nanostructures
- Oxides for energy technologies
- Ferroelectrics, multiferroics, piezoelectrics and dielectrics

Computational Thermodynamics and Kinetics

...TMS-American Physical Society symposia on fundamental modeling methods and application for materials structures

- Integrated Computational Materials Engineering (ICME)
- Microstructure properties and evolution
- Phase transformations
- Nanoscale systems

Creating the ICME Cyberinfrastructure: an Interdisciplinary Technology Forum

...TMS-American Physical Society roundtable

- State-of-the-art capabilities
- CyberDesign
- Roadmapping development needs

Deformation Twinning: Formation Mechanisms and Effects on Material Plasticity—Experiments and Modeling

...progress in fundamentals of deformation twinning

- Texture, twinning and hardening
- Constitutive modeling
- Electron microscopy
- Flow and fracture

Electrode Technology

(formerly Carbon Technology)

...anodes and cathodes used in aluminum reduction

- Sustainability and environmental issues
- Anode technology and production
- Carbon anodes
- Inert anode materials

Emerging Interconnect and Packaging Technologies

...advanced lead-free solder and packaging technologies

- Electromigration
- Microstructures and characterization
- Processing and reliability issues
- Whisker growth, design and modeling

Emerging Methods to Understand Mechanical Behavior

...advanced characterization and analytical methods

- Orientation imaging microscopy
- Texture evolution
- Nanomechanical testing
- Static, dynamic and cyclic testing

Energy Conservation in Metals Extraction and Materials Processing

...technologies to reduce energy consumption for material production

- Energy and environmental conservation
- Enhanced energy efficiency
- Alternate technologies
- Modeling, simulation and application experiences

Enhancing Materials Durability via Surface Engineering

...recent advancements in surface engineering and modification for life enhancement

- Coatings for environmental, thermal and wear resistance
- Residual stresses
- Graded and novel structures
- Modeling

Frontiers in Process Modeling

...advancing materials development

- Hot-rolling technologies
- Deformation of materials
- Primary metal production

Hael Mughrabi Honorary Symposium: Plasticity, Failure and Fatigue in Structural Materials—from Macro to Nano

...deformation and fracture mechanisms

- Single crystals
- Mathematical modeling
- Cyclic, static and dynamic loading
- Damage evolution

Help to celebrate Professor Hael Mughrabi's lifelong accomplishments at a dinner held in his honor on Monday, March 10.

See the registration form on page 22.

Hot and Cold Rolling Technology

...advanced hot- and cold-rolled products

- Texture development
- Process modeling
- Surface quality

Hume-Rothery Symposium: Nanoscale Phases

...fundamentals of structure and stability of nanoscale phase materials

- Microstructural evolution and stability
- Nano/tera scale integration
- Microscopy
- Nanowires, nanovolumes and nanocrystallization

IONMMS Global Materials Forum 2008: Creating the Future MS&E Professionals

...global forum with speakers representing TMS, Association for Iron & Steel Technology, Chinese Society for Metals, Indian Institute of Metals, Japan Institute of Metals, and Mining and Materials Processing Institute of Japan

- Pre-college/K-12
- Innovative university education programs
- Lifelong learning
- International cooperation
- Innovative use of technology

Magnesium Technology 2008

...all aspects of magnesium production, properties and application

- Primary production
- Alloy development
- Performance
- Global market

Materials for Infrastructure: Building Bridges in the Global Community

(sponsored by TMS, Chinese Society for Metals, and Indian Institute of Metals)

...forum devoted to infrastructure needs for the global community

- Buildings
- Public utilities
- Bridges

Materials in Clean Power Systems III: Fuel Cells, Hydrogen, and Clean Coal-Based Technologies

...in-depth coverage of advances in clean power

- Fuel cells
- Hydrogen
- Clean coal

Materials Informatics: Enabling Integration of Modeling and Experiments in Materials Science

...TMS-American Physical Society symposium advancing techniques and application of materials informatics

- Titanium alloys
- Superalloys
- Neural networks
- CyberDesign

Materials Processing Fundamentals

...design, synthesis and control of materials processes and processing

- Solidification processing
- Optimization of thermomechanical processing
- Numerical simulations
- Microstructural evolution

Mechanical Behavior, Microstructure and Modeling of Ti and Its Alloys

...progress towards predictive constitutive and damage models for titanium

- Refinement and processing
- Microstructural evolution
- Microstructure-property relationships
- Modeling and property prediction

Mechanics and Kinetics of Interfaces in Multicomponent Materials Systems

...performance-enabling interfaces across materials systems and applications

- Metal-ceramics, metal-semiconductors and metal-polymer interfaces
- Creep
- Electromigration
- Dynamic and static performance

Micro-Engineered Particulate-Based Materials

...production, characterization and utilization

- In situ nanocomposites
- Corrosion and passivation
- Aluminum
- Stainless steel

Minerals, Metals and Materials under Pressure

...interdisciplinary forum connecting theory and experiment

- Pressure-induced phase transformations
- Simulations and modeling
- High rate plasticity
- Damage and failure mechanisms

National Materials Advisory Board Town Hall Meeting on Assessing Corrosion Education

...review current status and address future needs

- Effectiveness of existing engineering curricula
- Actions to enhance corrosion-based skill and knowledge base of graduating and practicing engineers

Neutron and X-Ray Studies for Probing Materials Behavior

...progress in advanced materials characterization

- Mechanical response
- Thermal treatment
- Texture development
- Microstructural evolution

Neutron Symposium Organizer Rozaliya Barabash:

"The idea to put together two diffraction methods will demonstrate the uniqueness of both of them and mutual complementary possibilities."

Particle Beam-Induced Radiation Effects in Materials

...experimental and theoretical radiation materials science

- Damage evolution
- In situ analysis
- Radiation-induced diffusion
- Nanoscale testing

Phase Stability, Phase Transformations and Reactive Phase Formation in Electronic Materials VII

...thermodynamics and kinetics for phase stability electronic materials

- Phase evolution and stability
- Electro- and thermo-migration
- Solder interfacial reactions

Pyrometallurgy

...advanced pyrometallurgical methods

- Nonferrous pyrometallurgy
- Lead refining
- Titanium production
- Smelter improvements

Recent Industrial Applications of Solid-State Phase Transformations

...utilizing phase transformations for new products

- TRIP steels
- Friction stir welding
- Nickel-based alloys
- Magnesium

Recycling

...recycling of engineered materials today

- Light metals
- Electronic materials
- Precious metals
- Reducing environmental impact

Refractory Metals 2008

...processing and performance

- Oxidation and thin films
- Processing and mechanical deformation

Role of Engineers in Meeting 21st Century Societal Challenges

...AIME keynote session on energy, transportation, housing, health and recycling

Sloan Industry Centers Forum: Techno-Management Issues Related to Materials-Centric Industries

...in-depth coverage of business issues facing aluminum, steel, automotive, wood, paper and metal processing industries

Structural Aluminides for Elevated Temperature Applications

...fundamentals and application

- Alloy design
- Processing and fabrication
- Microstructure-property relationships
- Applications

Ultrafine-Grained Materials: Fifth International Symposium

...technological advancements in design, manufacture and application

- Severe plastic deformation
- Nanocrystalline materials
- Thermal stability
- Deformation and fracture

Women in Science Breakfast Lecture*

“Design for the Other 90%”

Monday, March 10 • 7 to 8 a.m.

Speaker: Cynthia E. Smith, Curator, “Design for the Other 90%” Exhibit, Smithsonian’s Cooper-Hewitt, *National Design Museum*

“Design for the Other 90%” explores a growing movement among designers to develop solutions for the 5.8 billion people across the globe (90 percent of the world’s total population) not traditionally served by the professional design community. Through local and global partnerships, individual designers and organizations are finding unique ways to address the lack of basic necessities faced by the poor and marginalized around the world.

**Advance registration required*

Young Leaders Tutorial Luncheon Lecture

“Computational Materials Science & Engineering: What is it and how do we Take Advantage?”

Monday, March 10 • noon to 1:30 p.m.

Speaker: Katsuyo Thornton, Assistant Professor, Materials Science and Engineering, *University of Michigan*
Recipient of the TMS Early Career Faculty Fellow Award

This lecture will address why experimentalists and theorists should become familiar with and utilize many of the standard materials science and engineering computational tools. An overview of the available methodologies, their applications and case studies will be presented.

Note: An optional box lunch may be purchased on the registration form.

Institute of Metals/Robert Franklin Mehl Lecture

“High Performance Structural Metals: an Undervalued but Critical Enabling Technology”

Monday, March 10 • 12:30 to 1:30 p.m.

Speaker: James C. Williams, Department of Materials Science and Engineering, *The Ohio State University*

This talk will describe some of the past advances in structural materials and outline some important opportunities going forward. The reality (or lack thereof) of some of the trendy topics also will be assessed and some relative value comparisons will be offered.

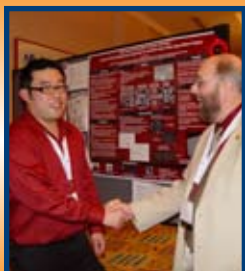
William Hume-Rothery Award Lecture

Nanoscale Metal Silicides

Monday, March 10 • 2 p.m.

Speaker: L.J. Chen, Department of Materials Science and Engineering, *National Tsing Hua University*

In this talk, an historical account of evolving roles of metal silicides in the context of integrated circuits device applications will be presented. Epitaxial growth of metal silicides on silicon and formation of amorphous interlayers in the metal/Si systems will be reviewed. In addition, synthesis and applications of metal silicide nanowires will be described, and the future outlook will be addressed.



Show your support for the upcoming leaders of our profession!

Attend the TMS Technical Division Student Poster Contest.
Monday, March 10
5 to 6:30 p.m.

Leave a Lasting Impression on New Orleans

Turn to page 27 to learn how you can help the city that has welcomed the TMS Annual Meeting & Exhibition many times.



Extraction & Processing Division Luncheon Lecture*

“Computational Modeling of Metals Processing: Past, Present and Future”

Tuesday, March 11 • 12:30 to 2 p.m.

Speaker: Brian G. Thomas, Wilkins Professor, Mechanical Engineering, *University of Illinois*; Director, *Continuous Casting Consortium*

This talk will recall the early days of process modeling as well as cover recent examples, including fluid flow, heat transfer and stress analysis of processes such as continuous casting of steel. The future of computational modeling will also be contemplated.

**Advance registration required*

Extraction & Processing Division Distinguished Lecture

“Smelting and Refining—Faster, Smoother, Cheaper, Safer”

Tuesday, March 11 • 2 to 2:45 p.m.

Speaker: David G.C. Robertson, Professor, Metallurgical Engineering, *University of Missouri-Rolla*

The purpose of research and development in pyrometallurgy is to achieve at least one of the goals mentioned above (faster, smoother, cheaper, safer). This lecture will review how basic research at the university can contribute to meeting these important goals, using examples mainly from work carried out by the author and his colleagues.

Light Metals Division Luncheon Lecture*

“Innovations in Steel Production—Animations for Aluminium Technologies?”

Wednesday, March 12 • 12:30 to 2:30 p.m.

Speaker: Reiner Kopp, Professor Emeritus, *Institute of Metal Forming, RWTH Aachen University*

This lecture outlines some highlights of manufacturing new steel products and asks the question as to whether or not these innovations in steel could be animations for the development of aluminium products.

**Advance registration required*

For greater detail on any of the annual
meeting lectures and speakers, visit
www.tms.org/annualmeeting.html.



Grain Refinement of Aluminium Alloys: Theory and Practice

Short Course • Sunday, March 9 • 8 a.m. to 6 p.m.

Instructors

Paul Cooper, *London and Scandinavian Metallurgical Co.*
Douglas Granger, *GRAS*
Wolfgang Schneider, *Hydro Aluminium GmbH*
Peter Schumacher, *University of Leoben*
David StJohn, *Cast Metals Manufacturing*

Who Should Attend

- Professional or technical representatives in the aluminium casting industry
- University researchers

Learn About

- Fundamentals of nucleation and grain growth
- Fundamentals of grain refinement with TiB₂ and TiC
- Grain refiner alloys, grain refiner tests and grain size measurement
- Influence of grain refinement on product quality
- Practice of grain refinement in DC casting and shape casting
- Influence of casting conditions on grain refinement

Greenhouse Gas Emissions

Short Course • Sunday, March 9 • 9 a.m. to 3:30 p.m.

Instructors

Halvor Kvande, *Hydro Aluminum*
Jerry Marks, *J. Marks & Associates*
Alton Tabereaux, *Consultant*

Who Should Attend

- HSE professionals
- Aluminum industry operational employees
- Others wanting to learn more about greenhouse gas emissions and their reduction

Learn About

- Environmental challenges facing the global aluminum business
- Reducing greenhouse gas emissions from aluminum smelters
- Anode effects in industrial electrolysis cells
- Action plans and activities to minimize future negative environmental impact and achieve a greener future

Nanomechanical Characterization Tutorial • Sunday, March 9 • 1 to 5 p.m.

Instructors

Erica T. Lilleodden, *GKSS Research Center*
Brad L. Boyce, *Sandia National Laboratories*

Who Should Attend

- Scientists and engineers interested in mechanical behavior of materials at small scales, particularly nanoscale and nanostructured materials and micro and nanoscale devices
- Students, post-doctoral researchers, early career as well as senior scientists and engineers involved in academic research and industrial applications of thin films and nanomaterials subject to mechanical loads

Learn About

- Current state-of-the-art test methods
- Emerging methods
- Nanoindentation-based techniques
- MEMS-based techniques

Furnace Systems and Technology

3rd Annual Workshop • Monday Afternoon,
March 10-Wednesday, March 12

Presentations from 15 companies covering:

- Basic combustion, energy savings and furnace productivity improvement
- Melting furnaces
- Burners designs
- Emissions and abatement
- Recirculating process furnaces
- Metal circulation, cleaning and dross processing
- Casting
- Refractory issues and practices
- Contract engineering
- Rotary delay/decorating systems

Get additional details about these courses and
register online at www.tms.org/annualmeeting.html
or see page 22.

President's Welcoming Reception

Sunday, March 9 • 6 to 8 p.m.

Seven Networking Receptions for Select Symposia

Visit www.tms.org/annualmeeting.html for details.

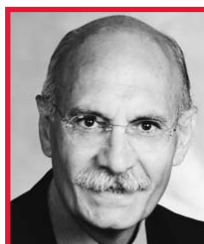
137th TMS and AIME Honors and Awards Presentation

With Installation of 2008 TMS President

Tuesday, March 11 • 6 p.m. Reception (Cash Bar) • 7 p.m. Dinner



Robert D. Shull
2007 TMS President



Diran Apelian
2008 TMS President



Dan Thoma
2007 AIME President

Join us as we honor those outstanding individuals who have contributed greatly to materials science and engineering through TMS and AIME. Following the awards presentation, the TMS 2007 and 2008 presidents will address the society. Order your tickets on the registration form.

About the 2008 TMS President

Diran Apelian is Howmet professor of engineering and director of the Metal Processing Institute at Worcester Polytechnic Institute, where he has worked for more than 15 years. Professor Apelian's research interests and expertise are in materials processing, and specifically, solidification and net-shape manufacturing. He is credited for pioneering work in various areas of solidification processing: molten metal processing and filtration of metals; aluminum foundry engineering; plasma deposition; and spray casting/forming. Professor Apelian has more than 400 publications to his credit and four books, which he has co-edited. He has served on, and chaired, several national materials advisory boards for the National Research Council. Professor Apelian has been an active member of TMS for more than 30 years and is the chair of the steering committee for this year's materials and society symposia.

Society Awards

TMS Fellow Class of 2008

- Tsu-Wei Chou, *University of Delaware*
- Campbell Laird, *University of Pennsylvania*
- David E. Laughlin, *Carnegie Mellon University*
- S. Lee Semiatin, *U.S. Air Force Research Laboratory*

Alexander R. Scott Distinguished Service Award

J. Wayne Jones, *University of Michigan*

Application to Practice Award

Gregory Yurek, *American Superconductor*

Bruce Chalmers Award

Alain Karma, *Northeastern University*

Champion H. Mathewson Award

Adam Badri, *Royal Dutch Shell*

Early Career Faculty Fellow

Katsuyo Thornton, *University of Michigan*

Educator Award

Robert L. Snyder, *Georgia Institute of Technology*

Institute of Metals/Robert Franklin Mehl Award

James C. Williams, *The Ohio State University*

John Bardeen Award

Pallab Bhattacharya, *University of Michigan*

Leadership Award

Bruce A. MacDonald, *National Science Foundation*

Robert Lansing Hardy Award

Ken Gall, *Georgia Institute of Technology*

TMS Foundation Shri Ram Arora Award

Sasanka Deka, *National Chemical Laboratory*

William Hume-Rothery Award

L.J. Chen, *National Tsing Hua University*

Division Awards

Electronic, Magnetic & Photonic Materials Division

Distinguished Scientist/Engineer Award

Iver Anderson, *Iowa State University*

Distinguished Service Award

Sung Kang, *IBM*

Extraction & Processing Division

Distinguished Lecturer

David G.C. Robertson, *University of Missouri-Rolla*

Distinguished Service Award

V. Ramachandran, *RAM Consultants*

Science Award

- Ortavio Fortini, *Carnegie Mellon University*
- Richard Fruehan, *Carnegie Mellon University*

Technology Award

- Alex Moyano, *Codelco-Chile*
- Carlos Caballero, *Codelco-Chile*
- Roberto Mackay, *Codelco-Chile*
- Pedro Morales, *Codelco-Chile*
- Domingo Cordero, *Codelco-IM2*
- Jonkion Font, *Codelco-IM2*

Light Metals Division

Distinguished Service Award

Barry Welch, *Welbank Consulting*

Light Metals Award

- Sebastien Leboeuf, *Alcan Inc.*
- Claude Dupuis, *Alcan Inc.*
- Bruno Maltais, *STAS*
- Marc-Andre Thibault, *STAS*
- Einar Smarason, *Alcan Iceland Ltd.*

Technology Award

Alton Tabereaux, *Technical Consultant*

Materials Processing & Manufacturing Division

Distinguished Scientist/Engineer Award

Brian Thomas, *University of Illinois*

Structural Materials Division

Distinguished Scientist/Engineer Award

S. Lee Semiatin, *U.S. Air Force Research Laboratory*

Distinguished Service Award

Marc Meyers, *University of California, San Diego*

Other Awards

2008 Acta Materialia Inc. Gold Medal Award

Karl A. Gschneidner Jr., *Iowa State University and Ames Laboratory, U.S. Department of Energy*

AIME Distinguished Service Award

Alexander R. Scott, retired, *The Minerals, Metals & Materials Society*

AIME Honorary Member

Robert H. Wagoner, *The Ohio State University*

Visit **Science Avenue**, **Technology Avenue** or **Innovation Boulevard** in the exhibition hall where 130+ exhibitors have the newest products and services you need to advance your work.

Exhibition Hours:

Monday, March 10 • noon to 6 p.m.
Tuesday, March 11 • 9:30 a.m. to 5:30 p.m.
Wednesday, March 12 • 9:30 a.m. to 3 p.m.

Enjoy a hosted grand opening reception on Monday, March 10, 5 to 6 p.m., and a snack break on Wednesday, March 12, 12:15 to 2 p.m., while you visit with representatives from these industries:

Light Metals Production and Processing

- Cast shop technology: combustion and furnace technology, grain refiners/hardeners, molten metal filtration and pumps, refractory and insulation products
- Industrial process control and automation, sensors
- Primary production equipment and services: carbon technology and supplies, combustion and furnace technology, HF measurement systems, industrial gases

Materials Research and Development

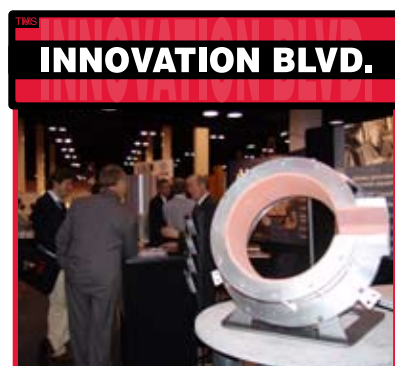
- Characterization equipment: analysis, instrumentation, measurement, microscopy, x-ray fluorescence
- Emerging materials: biomaterials, fuel cells, nanomaterials
- Materials for R&D: alloys, rare earths, precious metals, minerals, chemicals
- Surface processes: coatings, thin films, surface modification

Products and Services for the Materials Science and Engineering Profession

- Professional services: consulting, contracting, engineering, R&D
- Publishers: journals, reference publications
- Software Vendors: design, modeling, process simulation, thermodynamics, phase diagrams
- Technology resources: collaborative programs and centers, national laboratories, nongovernmental organizations

To become an exhibitor or sponsor an event, contact:

Joe Rostan • (724) 776-9000, ext. 231, or (800) 759-4TMS • jrostan@tms.org



Our Sponsors

BP Coke	Registration Counter	Life Cycle Engineering	Registration Bag Insert
Burner Dynamics Inc.	Registration Bag Insert	Mitsubishi International Company	General Meeting
Carbone Savoie	Coffee Break	Oxbow Carbon & Minerals LLC	General Meeting
ConocoPhillips	General Meeting	SEC Carbon (Sumitomo)	Registration Bag Insert
Elsevier Ltd.	Exhibit Hall Snack	Sentech Precimeter Inc.	Registration Bag Insert
GE Water & Process Technologies	Lanyards	SGL Carbon LLC	Coffee Break
Harbison-Walker Refractories	Event Signs, Banner and Information Booth	Solios Environnement	Registration Bags
Hatch	Coffee Break (Monday Morning)	TCP Petcoke Corporation	General Meeting
Jacobs Consultancy Inc.	TMS Today Newsletter (Tuesday)	Thermo-Calc Software Inc.	Registration Bag Insert
		Vabco	Coffee Break (Monday Afternoon)

Exhibiting Companies	Booth No.	Exhibiting Companies	Booth No.	Exhibiting Companies	Booth No.
ABB Analytical	606	Gouda Vuurvast	329	Opsis AB	220
Acuity VCT		Graphite Engineering & Sales	209	Outotec Ltd.	321
(formerly Benchmark Automation)	232	Graphite Machining Inc.	332	Parker Hannifin	539
Alcan Group	309	Hamilton Research & Technology		Pipeline Systems	127
Aleasur	704	PVT Ltd.	832	Pyrotek Inc.	301
Almeq Norway AS	428	Hauck Manufacturing Company	227	Resco Products	103
ALTECH SMV Ltd.	721	Heggset Engineering	238	Rex Materials Group	533
Aluminium International Today	TBD	Hencon BV	545	Riedhammer GmbH	121
Aluminium Times	TBD	Hertwich Engineering	708	Rigaku	815
Aluminum Corporation of China	222	HMR Group AS	339	SELEE Corporation	501
AUMUND Foerdertechnik GmbH	722	HRV Engineering Group	723	Sente Software	231
B&P Process Equipment Systems LLC	331	Hysitron	643	SenTech Precimeter Inc.	805
BHS Marketing/Western Briquette	345	iCrane Systems	632	Shenzhen Aida Aluminum	
Bloom Engineering	304	IMPEC AS	139	Alloys Co. Ltd.	809
Boreal Laser	136	Industries 3R Inc.	206	Shimadzu Scientific Instruments Inc.	344
Brochot	639	Innovatherm GmbH + Co. KG	631	SMV AS	720
Bruker AXS	114	International Magnesium Association	TBD	Solios Environment	513
Buehler Ltd.	806	Jayne Industries	101	Starcyl Cylinders/MAC	203
Burner Dynamics Inc.	110	JEOL USA Inc.	837	STAS	609
Buss ChemTech AG	631	Jervis B. Webb Company	725	Stellar Materials Inc.	700
C.A. Picard International	233	Kabert Industries	605	SUAL Group	131
Carl Zeiss Microlmaging	214	KB Alloys Inc.	621	Taylor & Francis Group/CRC Press	819
Carl Zeiss SMT	212	KBM Affilips BV	715	Thermal Ceramics	507
Ceradyne Inc.	100	KEMPE International	620	Thermcon Ovens BV	804
Chongqing Runji Alloy Co Ltd.	814	L.P. Royer Inc.	221	ThermoCalc Software	444
CMI Novacast Inc.	113	Laeis GmbH	631	Thermo Scientific Niton Analyzers	107
Colt International	644	Life Cycle Engineering	115	Thermo Scientific-Scientific Instruments	106
CompuTherm LLC	820	Light Metal Age	205	Thorpe Technologies Inc.	308
CSM Instruments	712	Maerz-Gautschi	600	Urja Products PVT. Limited	713
Cytec Industries Inc.	731	Maruzen International Co. Ltd.	245	Wagstaff Inc.	521
Dantherm Filtration Inc.	239	McAllister Mills Inc.	625	Zircar Ceramics Inc.	711
Darco Southern	104	MECFOR Inc.	339		
DMC Clad Metal Division	738	Mechatherm International Ltd.	626		
EBSD Analytical Inc.	710	Metallurg Aluminium	320		
ECL	312	Metallurgical Society of CIM	745		
EDAX Inc.	707	Mid-Mountain Materials Inc.	213		
Eirich Machines Inc.	211	MINTEQ International Inc.	118		
Erico	705	Morgan AM&T/National			
FEI Company	730	Electrical Carbon	810		
FFE Minerals	223	Murlin Chemical Inc.	201		
GE Energy	322	N.A. Water Systems	821		
GE Water & Process Technologies	324	Nalco Company	601		
Giesel Verlag GmbH-Verlag für		National Filter Media	739		
Fachmedien	TBD	NKM Noell Special Cranes GmbH	527		
Gillespie & Powers Inc.	831	North American Manufacturing Co. Ltd.	432		
GLAMA Maschinenbau GmbH	613	Novelis	300		
GNA Alutech Inc.	724	Olympus Micro Imaging Division	109		



Students - Don't miss this opportunity!

TMS 2008 is a perfect opportunity for materials science and engineering students to learn how to prepare for a career in the materials field, make important professional contacts, and share enjoyable times outside the classroom with fellow students and professionals.

Students who are Material Advantage members may attend the technical sessions, lectures, exhibition and all student activities listed on this page for an advance registration fee of only \$25. The advance registration fee for students who are not members is \$50, which includes a free year of membership in the Material Advantage Student Program.

Sunday, March 9

2nd Annual Materials Bowl

Preliminary Elimination Rounds • noon

Championship Match • 8:30 to 9 p.m.

Team Registration Deadline: December 15, 2007

A total of \$3,500 in prize money is awarded in this “Jeopardy”-style knowledge and trivia competition as well as the Materials Bowl Trophy! Currently, the trophy resides with the 2007 champions, Florida International University. Student chapters are invited to select a team of four chapter members to represent its school for the 2008 Materials Bowl. Eighteen teams will compete in preliminary elimination rounds, with the winners moving on to semifinal matches. The championship match will culminate at the Student Networking Mixer. View the official rules online and register your team early to be part of this exciting competition!

Orientation • 2 to 3 pm.

Find out all you need to know about student activities at TMS 2008 and meet other students with similar interests.

Career Forum • 3:30 to 5 p.m.

Representatives from key materials industries will provide personal insights on career preparation strategies, offer tips on how to develop and foster rewarding careers, and answer your questions.

Career Tips Session • 5 to 6 p.m.

Discover what human resource representatives are looking for when reviewing resumes and interviewing candidates.

Student Networking Mixer • 9 to 11 p.m.

This networking mixer provides a relaxed, casual and fun atmosphere for students, faculty members, and government and industry representatives to make connections and share experiences of professional growth.

Monday, March 10

TMS Technical Division Student Poster Contest • 5 to 6:30 p.m.

Deadline to Apply: January 10, 2008

Both undergraduate and graduate students are encouraged to participate in this dynamic and interactive event. Each of the TMS technical divisions is awarding \$500 to the best undergraduate poster and \$500 to the best graduate poster. A top prize of \$2,500 is awarded by TMS for the “Best of Show” poster.

Ambassador Awards

Judges will select two student authors from among the poster award winners to receive the TMS Student Ambassador awards. The “ambassadors” will receive sponsorship from TMS to represent the society at a 2008 international conference. Two alternate ambassadors will also be chosen in the event the initial award winners are unable to attend the conference.

Visit www.tms.org/annualmeeting.html and click on the student page from the menu for full details about any of these student events.

Subsidize the Cost of Attending TMS 2008

Become a Student Monitor!

Deadline to Apply: December 29, 2007

Student monitors are assigned to attend technical sessions to assist as follows:

- Record the number of attendees for each paper presented in a given session.
- Report any malfunctions of audio/visual equipment to appropriate staff.
- Aid presenters with operation of room lights.

Monitors receive \$40 for each one-half day session monitored. Monitor positions are filled as applications are received.

For more information about submitting an application:

- Visit www.tms.org/annualmeeting.html and click on the student page from the menu.
- Contact Cheryl Moore, technical programming assistant, at (724) 776-9000, ext. 252; (800) 759-4TMS; or cmoore@tms.org.

Apply for Travel Reimbursement!

Each Material Advantage chapter is eligible to receive \$500 per calendar year in travel reimbursement for members to attend the TMS annual meeting. The travel reimbursement form must be submitted with original receipts by March 28, 2008.

Visit www.tms.org/annualmeeting.html and click on the student page from the menu for the form.

Donate a Door Prize

Student chapter members are asked to donate school logo items to the cache of items TMS will be donating for door prizes at the Student Networking Mixer. The more prizes donated, the better your chances to win! Let TMS know what you plan to bring to donate by e-mailing Bryn Stone at bstone@tms.org.



Collected Proceedings CD-ROM

To provide added value for attendees, those registering in the following categories receive a free CD-ROM containing select proceedings:

- Members
- Nonmember Authors
- Nonmembers
- TMS Senior Members
- Exhibitors Full Conference

The CD-ROM will include:

- Multiple symposia proceedings
- Keynote presentations
- Links to additional resource information
- Table of contents

Each symposium will be presented as an individual publication on the CD-ROM, with its own table of contents, standard publication reference numbers, and copyright information. Please visit www.tms.org/annualmeeting.html for a complete listing of the symposia to be included on the CD-ROM.

The CD-ROM is also available for purchase in advance on the registration form or on-site during the annual meeting. The cost per CD-ROM is \$150; student price is \$75.

Printed Proceedings

For those interested in purchasing printed copies of individual symposia, arrangements can be made before, during and after the annual meeting. To order in advance or after the meeting, contact:

TMS Customer Service • (724) 776-9000, ext. 256, or (800) 759-4TMS • E-mail jsmith@tms.org

Arrangements may also be made at the meeting by visiting the TMS Publications Sales area.



**MATERIALS
TECHNOLOGY** TMS



6 Online Communities of Learning

Education
Integrated Computational Materials Engineering
Lead-Free Solders
Magnesium
Materials for Nuclear Power
Superalloys

Share your knowledge with colleagues and benefit from theirs, and utilize resources specific to your technical interest.

Site Features:

Articles
News
Discussion Boards
Digital Resources*
Publications
Conferences

Visit www.materialstechnology.org today!

*Exclusive to TMS members

Register before February 11, 2008, to qualify for the advance registration rate. You save \$100!

Two Ways to Register

1. Online at www.tms.org/annualmeeting.html with our secure form
2. Complete the form on the next page and mail or fax with your payment.

Your registration includes these valuable learning and networking events:

- | | |
|---|---|
| 1. Technical Sessions (Monday through Thursday) | 10. President's Welcoming Reception (Sunday) |
| 2. ICME Technology Forum* (Sunday) | 11. Networking Receptions |
| 3. Lead-Free Solders Technology Workshop* (Sunday) | 12. Exhibition (Monday through Wednesday) |
| 4. Women in Science Breakfast Lecture* (Monday) | 13. Hosted Grand Opening Reception in Exhibit Hall (Monday) |
| 5. Young Leaders Tutorial Lecture+ (Monday) | 14. Snack Break in Exhibit Hall (Wednesday) |
| 6. Institute of Metals/Robert Franklin Mehl Lecture (Monday) | 15. Collected Proceedings CD-ROM |
| 7. William Hume-Rothery Award Lecture (Monday) | |
| 8. Student Poster Contest (Monday) | |
| 9. Extraction & Processing Division Distinguished Lecture (Tuesday) | |

*Please sign up to attend on the meeting registration form as space is limited.

+Young Leaders lecture is free. You may order lunch on the meeting registration form.

Location

All conference events, including registration, technical sessions and the exhibition, will take place at the Ernest N. Morial Convention Center; all committee meetings will be held at the Hilton New Orleans Riverside Hotel.

Advance Registrant Check-In and On-Site Registration, Hall J:

Sunday, March 9	11 a.m. to 8 p.m.
Monday, March 10	7 a.m. to 6 p.m.
Tuesday, March 11	7 a.m. to 5:30 p.m.
Wednesday, March 12	7 a.m. to 5 p.m.
Thursday, March 13	7 to 10 a.m.

Policies

Registration Policy

All attendees and meeting participants (authors, exhibitors, etc.) must register for the conference. Badges must be worn for admission to technical sessions, the exhibition and social functions.



Americans With Disabilities Act

TMS strongly supports the federal Americans with Disabilities Act (ADA) which prohibits discrimination against, and promotes public accessibility for, those with disabilities. In support of, and in compliance with, ADA, we ask those requiring specific equipment or services to contact TMS Meeting Services in advance.

Audio/Video Recording Policy

TMS reserves the right to all audio and video reproductions of presentations at TMS sponsored meetings. Recording of sessions (audio, video, still photography, etc.) intended for personal use, distribution, publication or copyright without the express written consent of TMS and the individual authors is strictly prohibited. Contact TMS Technical Programming at (724) 776-9000, ext. 212, to obtain a waiver release.

Photography Notice

By registering for the conference, all attendees acknowledge that they may be photographed by TMS personnel while at events, and that those photos may be used for promotional purposes.

Questions? Contact:

TMS Meeting Services • (724) 776-9000, ext 243, or (800) 759-4TMS

ADVANCE REGISTRATION FORM
Advance Registration Deadline: February 11, 2008**Payment must accompany form.**

Forms received past this date will be processed at the on-site fee.

WEBwww.tms.org/AnnualMeeting.htmlWeb registration requires
credit card payment.**FAX****USA: (724) 776-3770**Fax registration requires
credit card payment.**MAIL****Return with TMS Meeting Services**
payment to: 184 Thorn Hill Road
Warrendale, PA 15086**1. Member of:** ☐ TMS ☐ AIST ☐ SME ☐ SPE Member Number: _____☐ Dr. ☐ Prof.☐ Mr. ☐ Mrs. ☐ Ms. _____

Last Name

First Name

Middle Initial

Informal First Name to Appear on Badge: _____ Date of Birth: _____

mm / dd / yyyy

Employer/Affiliation: _____ Title: _____

Address: ☐ Business ☐ Home _____

City: _____ State/Province: _____ Zip/Postal Code: _____ Country: _____

Telephone: _____ Fax: _____

E-mail: _____

2. Registration Fees:**Advance Fees
Through 2/11/08****On-Site Fees
After 2/11/08**

<input type="checkbox"/> Member.....	\$555	M.....	\$655	ML
<input type="checkbox"/> Nonmember Author *	\$645	NMA.....	\$745	NMAL
<input type="checkbox"/> Nonmember *	\$705	NM.....	\$805	NML
<input type="checkbox"/> Recent Graduate Member	\$395	RG.....	\$495	RGL
<input type="checkbox"/> Student Member ##	\$25	STU.....	\$50	STUL
<input type="checkbox"/> Student Nonmember ## *	\$50	STUN.....	\$100	STUNL
<input type="checkbox"/> TMS Senior Member.....	\$395	RM.....	\$495	RML
<input type="checkbox"/> TMS Retired Senior Member	\$100	RS.....	\$495	RSL
<input type="checkbox"/> Exhibitor Full Conference.....	\$555	E.....	\$555	EL
<input type="checkbox"/> Exhibit Only.....	\$50	EO.....	\$50	EOL

Registration TOTAL \$ _____

* Includes TMS membership for 2008

Students must attach a copy of school student identification card.

6. Social Function Tickets:

Fee

Quantity

Total

Mon. 3/10/08	Hael Mughrabi Honorary Dinner	\$70	_____	\$_____ MD
	"Women in Science" Breakfast	\$0	_____	\$_____ SB
	TMS-AIME Banquet	\$70	_____	\$_____ AD
	Tables of 8	\$560	_____	\$_____ AD8
Tues. 3/11/08	Table Sign to Read			
	Extraction & Processing Division Luncheon.....	\$45	_____	\$_____ EP
	Tables of 8	\$360	_____	\$_____ EP8
	Table Sign to Read			
Wed. 3/12/08	Light Metals Division Luncheon	\$45	_____	\$_____ LM
	Tables of 8	\$360	_____	\$_____ LM8
	Table Sign to Read			

Social Function TOTAL \$ _____

For any special dietary needs, please contact
Meeting Services at (724) 776-9000, ext. 243.**3. Publications/Collected Proceedings:**

Those registering at the member, nonmember author, nonmember, TMS senior member and exhibitor full conference levels will receive a free TMS 2008 collected proceedings CD-ROM.

The CD-ROM may also be purchased below. Note: CD-ROMS will not be available after the meeting. They must be picked up at the meeting; none will be shipped.

	Attendee	Student	Quantity
<input type="checkbox"/> CD-ROM	\$150	\$75	_____
Publications TOTAL \$ _____			

Visit the Publications Sales area at the meeting to purchase CD-ROMs or print volumes of selected symposia proceedings. After the meeting, individual symposia proceedings volumes may be purchased online at the TMS Knowledge Resource Center, <http://doc.tms.org>.**4. Continuing Education:****Advance Fees Through 2/11/08**

	Member	Nonmember
<input type="checkbox"/> Grain Refinement Short Course* (Sunday)	\$475	\$560
<input type="checkbox"/> Greenhouse Gas Emissions Short Course* (Sunday)	\$475	\$560
<input type="checkbox"/> Nanomechanical Characterization Tutorial (Sunday)	\$100	\$125

	Conference Registrants	Nonregistrants
<input type="checkbox"/> ICME Technology Forum (Sunday)	\$0	\$50
<input type="checkbox"/> Lead-Free Solders Technology Workshop (Sunday)	\$0	\$50

Continuing Education TOTAL \$ _____

* Includes meal

5. Furnace Systems and Technology Workshop:

	Member	Nonmember	Total
Monday 3/10/08-Wednesday 3/12/08	\$200	\$250	\$_____

7. Tutorial Luncheon Tickets:

Monday 3/10/08

Fee

Quantity

Total

The Young Leaders Tutorial Lecture is free.

You may purchase the optional box lunch for\$35 _____ \$_____ EM

8. 2008 Membership Renewal: For current TMS members only

<input type="checkbox"/> Professional Member.....	\$105	FM
<input type="checkbox"/> Recent Graduate (2006 or 2005).....	\$52.50	JM
<input type="checkbox"/> (ACerS/AIST/ASM/TMS) Material Advantage Student Member	\$25	ST

9. Hands-On New Orleans Service Project:**Amount**

- ☐ I wish to participate in the service project on Saturday, March 8.....\$0 HOP
- ☐ I wish to contribute financially to the TMS Foundation for project costs..... \$25 TFP

10. Payment Enclosed:☐ Check, Bank Draft, Money Order

Make checks payable to TMS. Payment must be made in U.S. dollars drawn on a U.S. bank.

☐ Credit Card Expiration Date _____

Card No. _____

☐ Visa ☐ MasterCard ☐ Diners Club ☐ American Express

Cardholder Name _____

Signature _____

11. TOTAL FEES PAID.....\$ _____**Refund Policy:** Written requests must be mailed to TMS, post-marked no later than February 11, 2008. A \$75 processing fee is charged for all cancellations. **No refunds will be processed after February 11, 2008.**

Receive a special reduced rate by reserving your hotel before January 28, 2008.

Two ways to reserve your hotel:

1. Visit www.tms.org/annualmeeting.html and click on "Housing" from the menu.
2. Use the form on the next page.

About the Hilton New Orleans Riverside Hotel

The Hilton New Orleans Riverside Hotel is the headquarters hotel for this year's conference. It has a prime location with restaurants, shopping and entertainment close by. Located on the banks of the Mississippi River, the Hilton gives you the best New Orleans has to offer – all within easy walking distance.

Connected to the Hilton is the Riverwalk Marketplace, with more than 140 stores and a great food court. The historic French Quarter is a mere three blocks away, and the famous Aquarium of the Americas and the IMAX Theater is only one block away.

For Your Convenience

TMS has contracted a block of rooms at the Hilton New Orleans Riverside Hotel, and at an additional 15 hotels available through Travel Planners, to ensure attendees are able to obtain housing at reduced rates. Therefore, TMS has assumed a financial liability for any and all rooms in the block that are not reserved. TMS asks that you reserve your room at these hotels in order to limit financial liability for the overall success of the meeting. Thank you.

Guest Hospitality

A special guest hospitality area will be hosted each day from 7 a.m. to 9:30 a.m. in the Hilton New Orleans Riverside Hotel. TMS will sponsor a continental breakfast for the convenience of guests of meeting attendees.

Airport Shuttle

For discounted airport transportation, visit Airport Shuttle online at www.tms.org/annualmeeting.html and click on "Housing" from the menu.



TMS2008

137th Annual Meeting & Exhibition

March 9-13, 2008

Ernest Morial Convention Center, New Orleans, LA

HOUSING RESERVATION FORM

Mail or fax this housing form to:

Travel Planners Inc., 381 Park Ave. South, New York, NY 10016

FAX: (212) 779-6128 • PHONE: (800) 221-3531

In local New York City area or international, call (212) 532-1660.

(CHOOSE ONLY ONE OPTION.)

Making a reservation is easier than ever through Travel Planners' real-time Internet reservation system! Just log on to www.tms.org/AnnualMeeting.html, and click on "Housing Reservations." View actual availability, learn about hotel features and services, and obtain local city and sightseeing information. Most importantly, receive instant confirmation of your reservation!

Reservations must be received at Travel Planners by: Monday, January 28, 2008

Arrival Date _____ Departure Date _____

Last Name _____ First Name _____ MI _____

Company _____

Street _____ Address _____

City _____ State/County _____ Zip/Postal Code _____ Country _____

Daytime Phone _____ Fax _____

Additional Room Occupants _____

E-mail _____ (Confirmation will be sent via e-mail if address is provided.)

Nonsmoking Room Requested _____ Special Needs _____

Indicate 1st, 2nd, and 3rd hotel choice:

1. _____
2. _____
3. _____

Type of Accommodations: (check one)

- ☐ Single 1 person/1bed ☐ Double 2 people/1bed ☐ Twin 2 people/2 beds
☐ Triple 3 people/2 beds ☐ Quad 4 people/2 beds

If all three requested hotels are unavailable, please process this reservation according to: (check one) ☐ ROOM RATE ☐ LOCATION

In order to ensure that rooms are available for attendees, TMS has contracted a block of rooms at the headquarters hotel, Hilton New Orleans Riverside Hotel, along with each of the hotels listed. TMS assumes financial liability for any and all rooms that are not reserved in the blocks. Therefore, attendees are strongly encouraged to reserve rooms at the hotels listed. This will help to limit undue expenses and secure the success of TMS 2008. Thank you.

Confirmations: A confirmation is e-mailed, faxed or mailed from Travel Planners Inc. once the reservation has been secured with a deposit or credit card. The hotels do not send confirmations. If you do not receive a confirmation within seven days, please call Travel Planners Inc.

Changes/Cancellations: All changes and cancellations in hotel reservations must be made with Travel Planners Inc. until five business days prior to arrival and are subject to the individual hotel's cancellation policies. Cancellations and changes within five days of arrival MUST be made with the hotel directly. Many hotels impose fees for early departure. This rate is set by each hotel and may vary accordingly. Please reconfirm your departure date at the time of check-in.

Reservations/Deposits: All reservations are being coordinated by Travel Planners Inc. Arrangements for housing must be made through Travel Planners Inc. and NOT with the hotel directly. Reservations via Internet, phone or fax are accepted with a major credit card only. Housing forms and written requests are accepted with a major credit card or deposit of one night's room and tax payable to Travel Planners Inc. Check must be drawn in U.S. funds on a U.S. bank. No wire transfers are accepted. Deposit policies are set by each hotel and are outlined on the hotel confirmation.

Please read all hotel information prior to completing and submitting this form to Travel Planners Inc. Keep a copy of this form. Use one form per room required. Make additional copies if needed.

HEADQUARTERS

Hilton New Orleans Riverside Hotel

\$237 single/double

\$287 Executive Towers single/double

Best Western St. Christopher Hotel

\$139 single/double

Country Inn & Suites

\$139 single/double

Courtyard by Marriott Convention Center

\$179 single/double

Embassy Suites New Orleans Convention Center Hotel

\$189 single/\$209 double

Hampton Inn & Suites Convention Center

\$169 single/double

Hilton Garden Inn New Orleans

\$175 single/double

Hotel New Orleans (formerly Holiday Inn Select)

\$159 single/double

Loews New Orleans Hotel

\$209 single/double

Marriott New Orleans at the Convention Center

\$249 single/double

Residence Inn by Marriott Downtown Convention Center

\$189 single/double

SpringHill Suites by Marriott Convention Center

\$179 single/double

St. James Hotel

\$149 single/double

The Pelham Hotel

\$139 single/double

W New Orleans

\$199 single/double

Wyndham Riverfront

\$199 single/double

Deposit Payment: ☐ Check ☐ American Express ☐ MasterCard ☐ VISA ☐ Discover ☐ Diners

Account Number _____ Expiration Date _____

Cardholder Name _____ Authorized Signature _____



City and Katrina

Sunday, March 9 or Monday, March 10 • 1 to 4 p.m. • \$35 per person

Explore all that makes New Orleans America's most European city. As you ride by beautiful Jackson Square, your tour guide will reconstruct the first days of the old French City. The sights and sounds of the mighty Mississippi River, St. Louis Cathedral, Cabildo and Pontalba buildings are some of the highlights of this area. You will continue past the French Market and the U.S. Mint.

Then, to New Orleans greatest challenge, the tour will proceed by the three levees that "breached" as the tour guide provides a chronology of events leading up to Hurricane Katrina and the days immediately following the disaster. You will travel through parts of the Ninth Ward and Lakeview, some of the hardest hit areas of New Orleans as well as witness the revival of the city by citizens who refuse to give up.

Next is Esplanade Avenue, the outermost boundary of the French Quarter, where you will see a stunning display of the many fine Creole homes with delicate wrought iron fences and balconies. Passing by one of the city's oldest cemeteries, you will learn about the unique above ground burial system. Across Bayou St. John is the spacious city park with its lush greenery and scenic lagoons. Located on the park's grounds is the New Orleans Museum of Art set among the overhanging oak trees and Spanish moss.

Continuing toward the lakefront, which was also affected by the hurricane, you will see Lake Pontchartrain with its lovely setting for exclusive residences, water sports, outdoor activities and many fine seafood restaurants. Following the crescent of the river to the old town of Carrollton and the route of the St. Charles streetcar, you will pass Tulane and Loyola Universities as the ancient oaks of Audubon Park come into view. The heart of uptown showcases some of the city's loveliest neighborhoods, while the Garden District is distinguished by its Greek revival architecture and splendid gardens.



Houmas House

Tuesday, March 11 • 9 a.m. to 1 p.m. • \$40 per person

One of the most visited antebellum plantation homes near New Orleans is the Houmas House Plantation. With spectacular gardens, Houmas was used as the filming location for "Hush, Hush, Sweet Charlotte," starring Bette Davis.

Located in the small river community of Darrow, Houmas sits on a few acres on the Mississippi River, much smaller than the 20,000 acres that it once had. The house was built in 1840 by Col. John Smith Preston on land originally owned by the Houmas Indians.

The preservation of this home is superior, and the furnishings are period appropriate. It is lived in and entertained in, even today. Your guides, dressed in period costumes, make the history of this plantation home come alive for you!



Jean Lafitte Swamp Adventure

Wednesday, March 12 • 9:30 a.m. to 12:30 p.m. • \$50 per person

Enjoy a journey by boat, Cajun style, into the heart of Louisiana's beautiful and natural swamplands. Your boat will travel deep into the swamps and meandering bayous of this exciting region. Be sure to bring your camera as you may encounter exciting and beautiful animals at any time—alligators, snakes, nesting eagles, egrets, white-tailed deer, mink and nutria. Your guide will be a native of the area who will bring history alive by recounting the exploits of pirate Jean Lafitte and his band as they plied these waters. Louisiana's mysterious waters, moss-draped bayous and the adventure of Jean Lafitte await you!

TMS2008

137th Annual Meeting & Exhibition

March 9-13, 2008

Ernest Morial Convention Center, New Orleans, LA

TOUR REGISTRATION FORM

Type or print clearly. Copy the completed form for your records.

Return this form with appropriate fee to:

MAIL: DMI-Conventions, Laura Swann, 4220 Howard Avenue, New Orleans, LA 70125

FAX: (504) 592-0529 / E-MAIL: lswann@visitnola.com / TELEPHONE: (504) 587-1604

Registration Deadline: February 27, 2008

All tour prices are in U.S. dollars and include all taxes, gratuities, entrance fees, etc. You will receive notification from DMI confirming availability of the tours you have selected. See below for refund cancellation policy.

Tour Attendee Information:

Last Name _____ First Name _____

Street _____ City _____

State/Province _____ Country _____ Postal Code _____

Home Telephone _____ Work Telephone _____

Fax _____ E-mail _____

Name of Hotel in New Orleans _____

Tours:	Hours	No. of People	Cost	Total
March 9, 2008				
City and Katrina Tour	1 to 4 p.m.	_____ x	\$35	= \$ _____
March 10, 2008				
City and Katrina Tour	1 to 4 p.m.	_____ x	\$35	= \$ _____
March 11, 2008				
Houmas House	9 a.m. to 1 p.m.	_____ x	\$40	= \$ _____
March 12, 2008				
Jean Lafitte Swamp Tour	9:30 a.m. to 12:30 p.m.	_____ x	\$50	= \$ _____
Total (in U.S. dollars):\$				_____

Payment Information:

Credit card orders will be charged to your account upon receipt of your tour registration form.

☐ VISA Credit Card Number _____

☐ MasterCard Expiration Date _____

Name on Card _____

Signature (required) _____

REFUND/CANCELLATION POLICY

Cancellations received by February 27, 2008, will receive a refund less a \$5 per tour administrative fee. Cancellations received after February 27, 2008, will not receive a refund. Should a catastrophic event occur that adversely affects the overall conference, written notice must be received by DMI Conventions for a refund subject to a \$5 administration fee.

Cancellation requests must be made in writing and addressed to: DMI-Conventions, MMM308, 4220 Howard Avenue, New Orleans, LA 70125, or faxed to (504) 592-0529. Refunds will be made via check following the conference.

SOCIAL PROGRAM INFORMATION

Tickets will be distributed at the social program registration desk at the ENMCC, Hall I, for all preregistered guests. Early registration is recommended in order to guarantee your space. DMI has the right to cancel any tours if the minimum number of attendees is not met. If a tour is cancelled due to lack of minimum attendance, registrant will be notified by DMI after the registration deadline, and the registration fee refunded in full, unless an alternate choice is selected by registrant.

Hands On

Be The Change. Volunteer. | NEW ORLEANS

You Can Make a Difference in New Orleans

Volunteer with **TMS** and "Hands On New Orleans" on Saturday, March 8, to make a direct impact on a community affected by Hurricane Katrina.

The city of New Orleans and the surrounding Gulf Coast region continue to recover from the effects of Hurricane Katrina in 2005. TMS is partnering with Hands On New Orleans to take a team of volunteers into a community still rebuilding from the hurricane. You can help in one or more school renovation projects, such as enhancing science and math classrooms, painting science labs and classrooms, or landscaping.

Hands On New Orleans is affiliated with the national Hands On Network and specializes in developing and implementing high impact service projects. Since the hurricane, the local organization has leveraged the power of more than 4,000 visiting volunteers who gave more than 500,000 hours of service to the recovery and rebuilding of the Gulf Coast.

Saturday's Schedule

- Continental breakfast and project orientation
- Volunteers transported to project site with equipment and supplies provided
- Lunch on-site
- Evening reception

To be part of this special event, sign up on the conference registration form. Space is limited. You can also show your support by contributing \$25 to the TMS Foundation to help offset the project costs.

Corporate sponsorship opportunities are also available by contacting:

Joe Rostan • (724) 776-9000, ext. 231, or (800) 759-4TMS • jrostan@tms.org

Leave a lasting impression on the city that has welcomed the TMS Annual Meeting & Exhibition many times.

All contributions to the TMS Foundation are tax deductible in the United States. Pennsylvania residents may obtain the official registration and financial information of the TMS Foundation from the Pennsylvania Department of State by calling, toll-free within Pennsylvania, 1-800-732-0999. Registration does not imply endorsement.



Room	Sunday	Monday		Tuesday		Wednesday		Thursday
	PM	AM	PM	AM	PM	AM	PM	AM
271		Micro-Engineered Particulate-Based Materials: Session I	Micro-Engineered Particulate-Based Materials: Session II	Materials Informatics: Enabling Integration of Modeling and Experiments in Materials Science: Informatics and Materials Property Design	Materials Informatics: Enabling Integration of Modeling and Experiments in Materials Science: Informatics and Combinatorial Experiments and Materials Characterization	Materials Informatics: Enabling Integration of Modeling and Experiments in Materials Science: Informatics and Materials Theory and Modeling	Materials Informatics: Enabling Integration of Modeling and Experiments in Materials Science: Informatics and Cyberinfrastructure	
		General Abstracts: Extraction and Processing: Session I	General Abstracts: Extraction and Processing: Session II	IOMMS Global Materials Forum 2008: Creating the Future MS&E Professional	Materials for Infrastructure: Building Bridges in the Global Community: Session I	Materials for Infrastructure: Building Bridges in the Global Community: Session II	The Role of Engineers in Meeting 21st Century Societal Challenges -- AIME Keynote Session	
273		Ultrafine-Grained Materials: Fifth International Symposium: Modeling, Theory, and Property	Ultrafine-Grained Materials: Fifth International Symposium: Processing and Materials	Ultrafine-Grained Materials: Fifth International Symposium: Stability, Technology, and Property	Ultrafine-Grained Materials: Fifth International Symposium: Properties	Ultrafine-Grained Materials: Fifth International Symposium: Deformation Mechanisms	Ultrafine-Grained Materials: Fifth International Symposium: Structure and Evolution	
274		2008 Nanomaterials: Fabrication, Properties, and Applications: CNT	2008 Nanomaterials: Fabrication, Properties, and Applications: Nanomaterials Synthesis	2008 Nanomaterials: Fabrication, Properties, and Applications: Device	2008 Nanomaterials: Fabrication, Properties, and Applications: Application	2008 Nanomaterials: Fabrication, Properties, and Applications: Random Topics	2008 Nanomaterials: Fabrication, Properties, and Applications: Theory	
275		Emerging Interconnect and Packaging Technologies: Pb-Free Solders: Fundamental Properties, Interfacial Reactions and Phase Transformations	Emerging Interconnect and Packaging Technologies: Pb-Free and Sn-Pb Solders: Electromigration	Emerging Interconnect and Packaging Technologies: Advanced Interconnects	Emerging Interconnect and Packaging Technologies: Pb-Free Solder: Tin Whisker Formation and Mechanical Behavior	Emerging Interconnect and Packaging Technologies: Pb-Free Solders: Reliability and Microstructure Development	Emerging Interconnect and Packaging Technologies: Pb-Free Solders and Other Interconnects: Microstructure, Modeling, and Test Methods	
276		Hume-Rothery Symposium - Nanoscale Phases: Session I	Hume-Rothery Symposium - Nanoscale Phases: Session II	Hume-Rothery Symposium - Nanoscale Phases: Session III	Hume-Rothery Symposium - Nanoscale Phases: Session IV	General Abstracts: Electronic, Magnetic, and Photonic Materials Division: Session I	General Abstracts: Electronic, Magnetic, and Photonic Materials Division: Session II	
277		Complex Oxide Materials - Synthesis, Properties and Applications: ZnO Nanostructures and Thin Films	Complex Oxide Materials - Synthesis, Properties and Applications: Novel Functionality from Complex Oxide Heterointerfaces	Complex Oxide Materials - Synthesis, Properties and Applications: Functionally Cross-Coupled Heterostructures	Complex Oxide Materials - Synthesis, Properties and Applications: Epitaxial Oxides: Ferroelectric, Dielectric, and (Electro-)Magnetic Thin Films	Complex Oxide Materials - Synthesis, Properties and Applications: Scaling, Dynamics, and Switching	Complex Oxide Materials - Synthesis, Properties and Applications: Ferroelectric/ Dielectric Oxides	

Sunday	Monday		Tuesday		Wednesday		Thursday	Room
PM	AM	PM	AM	PM	AM	PM	AM	
	Advances in Semiconductor, Electro Optic and Radio Frequency Materials: Silicon-Based Optoelectronics and Microelectronics	Advances in Semiconductor, Electro Optic and Radio Frequency Materials: Compound Semiconductors and Beyond	Phase Stability, Phase Transformations, and Reactive Phase Formation in Electronic Materials VII: Session I	Phase Stability, Phase Transformations, and Reactive Phase Formation in Electronic Materials VII: Session II	Phase Stability, Phase Transformations, and Reactive Phase Formation in Electronic Materials VII: Session III	Phase Stability, Phase Transformations, and Reactive Phase Formation in Electronic Materials VII: Session IV		278
	Mechanics and Kinetics of Interfaces in Multi-Component Materials Systems: Mechanics of Adhesion, Friction and Fracture	Mechanics and Kinetics of Interfaces in Multi-Component Materials Systems: Nanoscale Structures and Simulations	Mechanics and Kinetics of Interfaces in Multi-Component Materials Systems: Mechanical Properties of Interfaces	Mechanics and Kinetics of Interfaces in Multi-Component Materials Systems: Interfacial Microstructures and Effects on Mechanical and Physical Properties	Mechanics and Kinetics of Interfaces in Multi-Component Materials Systems: Joint Session with Advances in Semiconductors, Electro Optic and Radio Frequency Materials			279
	Recent Developments in Rare Earth Science and Technology - Acta Materialia Gold Medal Symposium: Session I	Recent Developments in Rare Earth Science and Technology - Acta Materialia Gold Medal Symposium: Session II	Recycling: Electronics Recycling	Recycling: Micro-Organisms for Metal Recovery	Recycling: Light Metals	Recycling: General Sessions		280
	Advances in Roasting, Sintering, Calcining, Preheating, and Drying: Advances in Thermal Processing	9th Global Innovations Symposium: Trends in Integrated Computational Materials Engineering for Materials Processing and Manufacturing: Session I	9th Global Innovations Symposium: Trends in Integrated Computational Materials Engineering for Materials Processing and Manufacturing: Session II	Aqueous Processing - General Session: Aqueous Processing General Abstracts				281
	General Abstracts: Materials Processing and Manufacturing Division: Solidification and Casting	General Abstracts: Materials Processing and Manufacturing Division: Composition Structure Property Relationships I	General Abstracts: Materials Processing and Manufacturing Division: Composition Structure Property Relationships II	General Abstracts: Materials Processing and Manufacturing Division: Films, Coatings, and Surface Treatments	General Abstracts: Materials Processing and Manufacturing Division: Forging, Forming, and Powder Processing			282
	Materials Processing Fundamentals: Solidification and Deformation	Materials Processing Fundamentals: Process Modeling	Materials Processing Fundamentals: Powders, Composites, Coatings and Measurements	Materials Processing Fundamentals: Smelting and Refining	Pyrometallurgy - General Sessions: Pyrometallurgy			283
	Characterization of Minerals, Metals, and Materials: Emerging Characterization Techniques	Characterization of Minerals, Metals, and Materials: Characterization of Extraction and Processing	Characterization of Minerals, Metals, and Materials: Characterization of Microstructure and Properties of Materials I	Characterization of Minerals, Metals, and Materials: Characterization of Microstructure and Properties of Materials II	Characterization of Minerals, Metals, and Materials: Characterization of Microstructure and Properties of Materials III	Characterization of Minerals, Metals, and Materials: Characterization of Microstructure and Properties of Materials IV	Characterization of Minerals, Metals, and Materials: Characterization of Microstructure and Properties of Materials V	284

Room	Sunday	Monday		Tuesday		Wednesday		Thursday
	PM	AM	PM	AM	PM	AM	PM	AM
285		Emerging Methods to Understand Mechanical Behavior: Imaging Methods	Emerging Methods to Understand Mechanical Behavior: Digital Image Correlation	Emerging Methods to Understand Mechanical Behavior: Indentation and Dynamic Methods	Emerging Methods to Understand Mechanical Behavior: Subscale Methods	Emerging Methods to Understand Mechanical Behavior: Electron and Neutron Diffraction	Emerging Methods to Understand Mechanical Behavior: X-Ray Diffraction	
		3-Dimensional Materials Science: ONR/DARPA Dynamic 3-D Digital Structure Program	3-Dimensional Materials Science: Large Datasets and Microstructure Representation I	3-Dimensional Materials Science: Large Datasets and Microstructure Representation II	3-Dimensional Materials Science: Modeling and Characterization across Length Scales I	3-Dimensional Materials Science: Modeling and Characterization across Length Scales II	3-Dimensional Materials Science: Modeling and Characterization across Length Scales III	3-Dimensional Materials Science: Modeling and Characterization across Length Scales IV
286		Recent Industrial Applications of Solid-State Phase Transformations: Superalloys and TRIP Steels/ Automotive Steels	Recent Industrial Applications of Solid-State Phase Transformations: Alloy Design, Microstructure Prediction and Control	Frontiers in Process Modeling: Metallurgical Reactors	Frontiers in Process Modeling: Casting and General Modeling	Energy Conservation in Metals Extraction and Materials Processing: Session I	Energy Conservation in Metals Extraction and Materials Processing: Session II	
	Computational Thermodynamics and Kinetics: Poster Session	Computational Thermodynamics and Kinetics: Defect Structure I	Computational Thermodynamics and Kinetics: Defect Structure II	Computational Thermodynamics and Kinetics: Phase Field Crystal	Computational Thermodynamics and Kinetics: Functional Materials	Computational Thermodynamics and Kinetics: Phase Transformations	Computational Thermodynamics and Kinetics: Integrated Computational Materials Engineering	Computational Thermodynamics and Kinetics: Diffusion and Phase Stability
287		Magnesium Technology 2008: Magnesium Plenary Session	Magnesium Technology 2008: Wrought Alloys I	Magnesium Technology 2008: Wrought Alloys II	Magnesium Technology 2008: Wrought Alloys III	Magnesium Technology 2008: Advanced Magnesium Materials	Magnesium Technology 2008: Corrosion, Surface Finishing and Joining	
			Magnesium Technology 2008: Primary Production	Magnesium Technology 2008: Thermodynamics and Phase Transformations	Magnesium Technology 2008: Casting	Magnesium Technology 2008: Alloy Microstructure and Properties	Magnesium Technology 2008: Creep Resistant Magnesium Alloys	
288		Aluminum Alloys: Fabrication, Characterization and Applications: Development and Applications	Aluminum Alloys: Fabrication, Characterization and Applications: Processing and Properties	Aluminum Alloys: Fabrication, Characterization and Applications: Modeling	Aluminum Alloys: Fabrication, Characterization and Applications: Alloy Characterization	Aluminum Alloys: Fabrication, Characterization and Applications: Corrosion and Protection	Aluminum Alloys: Fabrication, Characterization and Applications: Composites and Foams	
				Carbon Dioxide Reduction Metallurgy: Mechanisms	Carbon Dioxide Reduction Metallurgy: Ferrous Industry	Carbon Dioxide Reduction Metallurgy: Electrolytic Methods		
289		Sustainability, Climate Change and Greenhouse Gas Emissions Reduction:	Cast Shop Technology: Sustainability in the Casthouse	Cast Shop Technology: Casthouse Operation	Cast Shop Technology: Melt Handling and Treatment	Cast Shop Technology: Foundry Ingots and Alloys	Cast Shop Technology: Casting Processes and Quality Analysis	Cast Shop Technology: Modelling
		Responsibility, Key Challenges and Opportunities for the Aluminum Industry	Alumina and Bauxite: HSEC	Alumina and Bauxite: Equipment	Alumina and Bauxite: Bauxite	Alumina and Bauxite: Additives	Alumina and Bauxite: Operations	Alumina and Bauxite: Precipitation/ Conclusion

Sunday	Monday		Tuesday		Wednesday		Thursday	Room
PM	AM	PM	AM	PM	AM	PM	AM	
		General Abstracts: Light Metals Division: Session I	General Abstracts: Light Metals Division: Session II	Electrode Technology Symposium (formerly Carbon Technology): Anode Manufacturing and Developments	Hot and Cold Rolling Technology: Session I	Aluminum Reduction Technology: Reduction Cell Modelling		297
		Aluminum Reduction Technology: Sustainability and Environment	Aluminum Reduction Technology: Cell Development Part I and Operations	Aluminum Reduction Technology: Process Control	Aluminum Reduction Technology: Aluminum Industry in Mid-East	Aluminum Reduction Technology: Fundamentals, Low Melting Electrolytes, New Technologies	Aluminum Reduction Technology: Cell Development Part II	298
		Electrode Technology Symposium (formerly Carbon Technology): Carbon Sustainability and Environment Aspects	Electrode Technology Symposium (formerly Carbon Technology): Anode Raw Materials and Properties	Electrode Technology Symposium (formerly Carbon Technology): Cathodes Raw Materials and Properties		Electrode Technology Symposium (formerly Carbon Technology): Cathodes Manufacturing and Developments	Electrode Technology Symposium (formerly Carbon Technology): Inert Anode	299
	Deformation Twinning: Formation Mechanisms and Effects on Material Plasticity: Experiments and Modeling: Twin Formation and Growth Mechanisms	Deformation Twinning: Formation Mechanisms and Effects on Material Plasticity: Experiments and Modeling: Twin Effects on Material Deformation I	Deformation Twinning: Formation Mechanisms and Effects on Material Plasticity: Experiments and Modeling: Twinning and Associated Defect Structures	Deformation Twinning: Formation Mechanisms and Effects on Material Plasticity: Experiments and Modeling: Twin Effects on Material Deformation II				383
	Mechanical Behavior, Microstructure, and Modeling of Ti and Its Alloys: Processing: Design, Control and Optimization	Mechanical Behavior, Microstructure, and Modeling of Ti and Its Alloys: Phase Transformation and Microstructure Development I	Mechanical Behavior, Microstructure, and Modeling of Ti and Its Alloys: Phase Transformation and Microstructure Development II	Mechanical Behavior, Microstructure, and Modeling of Ti and Its Alloys: Microstructure/ Property Correlation I	Mechanical Behavior, Microstructure, and Modeling of Ti and Its Alloys: Microstructure/ Property Correlation II	Mechanical Behavior, Microstructure, and Modeling of Ti and Its Alloys: Physical/ Mechanical Property Prediction		384
	Minerals, Metals and Materials under Pressure: New Experimental and Theoretical Techniques in High-Pressure Materials Science	Minerals, Metals and Materials under Pressure: Shock-Induced Phase Trans- formations and Microstructure	Minerals, Metals and Materials under Pressure: Electronic, Magnetic and Optical Properties of Materials under High Pressure	Minerals, Metals and Materials under Pressure: High Pressure Phase Transitions and Mechanical Properties				385

Room	Sunday	Monday		Tuesday		Wednesday		Thursday
	PM	AM	PM	AM	PM	AM	PM	AM
386		Hael Mughrabi Honorary Symposium: Plasticity, Failure and Fatigue in Structural Materials - from Macro to Nano: Dislocations: Work Hardening, Patterning, Size Effects I	Hael Mughrabi Honorary Symposium: Plasticity, Failure and Fatigue in Structural Materials - from Macro to Nano: High-temperature Mechanical Properties: Creep, Fatigue and Thermomechanical Fatigue	Hael Mughrabi Honorary Symposium: Plasticity, Failure and Fatigue in Structural Materials - from Macro to Nano: Dislocations: Work Hardening, Patterning, Size Effects II	Hael Mughrabi Honorary Symposium: Plasticity, Failure and Fatigue in Structural Materials - from Macro to Nano: Cyclic Deformation and Fatigue of Metals I	Hael Mughrabi Honorary Symposium: Plasticity, Failure and Fatigue in Structural Materials - from Macro to Nano: Mechanical Properties of Ultrafine-Grained (UFG) Metals I	Hael Mughrabi Honorary Symposium: Plasticity, Failure and Fatigue in Structural Materials - from Macro to Nano: Mechanical Properties of Ultrafine-Grained (UFG) Metals II	Hael Mughrabi Honorary Symposium: Plasticity, Failure and Fatigue in Structural Materials - from Macro to Nano: Cyclic Deformation and Fatigue of Metals II
		General Abstracts: Structural Materials Division: Mechanical Behavior of Metals and Alloys	General Abstracts: Structural Materials Division: Mechanical Behavior of Materials	General Abstracts: Structural Materials Division: Structure/Property Relations	General Abstracts: Structural Materials Division: Novel Issues in Materials Processing	General Abstracts: Structural Materials Division: Microstructure/Property Relations in Steel I	General Abstracts: Structural Materials Division: Microstructure/Property Relations in Steel II	
387		Enhancing Materials Durability via Surface Engineering: Residual Stress Effects on Durability	Enhancing Materials Durability via Surface Engineering: Steel and Other Alloys Surface Durability	Enhancing Materials Durability via Surface Engineering: Superalloy Surface Durability	Enhancing Materials Durability via Surface Engineering: Novel Surface Durability Approaches National Academies Corrosion Education Study Community Town Hall Meeting	Refractory Metals 2008: Processing	Refractory Metals 2008: Characterization	Refractory Metals 2008: Properties of Refractory Metals
		Particle Beam-Induced Radiation Effects in Materials: Metals I	Particle Beam-Induced Radiation Effects in Materials: Metals II	Particle Beam-Induced Radiation Effects in Materials: RIS and Multilayers	Particle Beam-Induced Radiation Effects in Materials: Ceramics and Nuclear Fuel Materials	Particle Beam-Induced Radiation Effects in Materials: Carbides, Semiconductors and Other Non-Metals	Particle Beam-Induced Radiation Effects in Materials: Nanostructures	
388		Biological Materials Science: Mechanical Behavior of Biological Materials I	Biological Materials Science: Implant Biomaterials I	Biological Materials Science: Bioinspired Design and Processing	Biological Materials Science: Scaffold Biomaterials	Biological Materials Science: Functional Biomaterials	Biological Materials Science: Mechanical Behavior of Biological Materials II	Biological Materials Science: Implant Biomaterials II
		Neutron and X-Ray Studies for Probing Materials Behavior: Resolving Local Structure	Neutron and X-Ray Studies for Probing Materials Behavior: Diffraction at Small Dimensions	Neutron and X-Ray Studies for Probing Materials Behavior: Phase Transitions and Beyond	Neutron and X-Ray Studies for Probing Materials Behavior: Recrystallization	Neutron and X-Ray Studies for Probing Materials Behavior: Stresses/Strains and Structure	Neutron and X-Ray Studies for Probing Materials Behavior: Scattering and Understanding of Materials Properties	
389		Materials in Clean Power Systems III: Fuel Cells, Hydrogen-, and Clean Coal-Based Technologies: Plenary Session	Materials in Clean Power Systems III: Fuel Cells, Hydrogen-, and Clean Coal-Based Technologies: Gas Separation and CO ₂ Capture	Materials in Clean Power Systems III: Fuel Cells, Hydrogen-, and Clean Coal-Based Technologies: Solid Oxide Fuel Cells: Metallic Interconnects	Materials in Clean Power Systems III: Fuel Cells, Hydrogen-, and Clean Coal-Based Technologies: Metallic Interconnects in SOFCs: Oxidation, Protection Coatings	Materials in Clean Power Systems III: Fuel Cells, Hydrogen-, and Clean Coal-Based Technologies: Metallic Interconnects and Sealing in SOFCs	Materials in Clean Power Systems III: Fuel Cells, Hydrogen-, and Clean Coal-Based Technologies: PEM Fuel Cells and Solar Technologies	Materials in Clean Power Systems III: Fuel Cells, Hydrogen-, and Clean Coal-Based Technologies: Hydrogen Technologies

Sunday	Monday		Tuesday		Wednesday		Thursday	Room
PM	AM	PM	AM	PM	AM	PM	AM	
	Bulk Metallic Glasses V: Structures and Mechanical Properties I	Bulk Metallic Glasses V: Structures and Mechanical Properties II	Bulk Metallic Glasses V: Structures and Modeling I	Bulk Metallic Glasses V: Structures and Mechanical Properties III	Bulk Metallic Glasses V: Glass Forming Ability and Alloy Development	Bulk Metallic Glasses V: Structures and Modeling II	Bulk Metallic Glasses V: Processing and Properties	393
	Structural Aluminides for Elevated Temperature Applications: Applications	Structural Aluminides for Elevated Temperature Applications: Mechanical Behavior	Structural Aluminides for Elevated Temperature Applications: FE and Other Aluminides	Structural Aluminides for Elevated Temperature Applications: Processing and Microstructure Control	Structural Aluminides for Elevated Temperature Applications: Phase and Microstructure Evolution	Structural Aluminides for Elevated Temperature Applications: New Class of Gamma Alloys - & - Poster Session	Structural Aluminides for Elevated Temperature Applications: Environmental Effects and Protection	394
		Sloan Industry Centers Forum: Techno-Management Issues Related to Materials-Centric Industries: Session I	Sloan Industry Centers Forum: Techno-Management Issues Related to Materials-Centric Industries: Session II					397
	Frontiers of Computational Materials Science: Session I							APS, Hall A
Poster Sessions: 2008 Nanomaterials: Fabrication, Properties, and Applications Computational Thermodynamics and Kinetics General Poster Session Hael Mughrabi Honorary Symposium: Plasticity, Failure and Fatigue in Structural Materials - from Macro to Nano Ultrafine-Grained Materials: Fifth International Symposium								Hall 12

2008 Nanomaterials: Fabrication, Properties, and Applications: Application.....	274	Tues PM	207
2008 Nanomaterials: Fabrication, Properties, and Applications: CNT.....	274	Mon AM	59
2008 Nanomaterials: Fabrication, Properties, and Applications: Device.....	274	Tues AM	152
2008 Nanomaterials: Fabrication, Properties, and Applications: Nanomaterials Synthesis.....	274	Mon PM	101
2008 Nanomaterials: Fabrication, Properties, and Applications: Poster Session.....	Hall 1 2	Sun PM	39
2008 Nanomaterials: Fabrication, Properties, and Applications: Random Topics.....	274	Wed AM	260
2008 Nanomaterials: Fabrication, Properties, and Applications: Theory.....	274	Wed PM	308
3-Dimensional Materials Science: Large Datasets and Microstructure Representation I.....	286	Mon PM	102
3-Dimensional Materials Science: Large Datasets and Microstructure Representation II.....	286	Tues AM	153
3-Dimensional Materials Science: Modeling and Characterization across Length Scales I.....	286	Tues PM	209
3-Dimensional Materials Science: Modeling and Characterization across Length Scales II.....	286	Wed AM	262
3-Dimensional Materials Science: Modeling and Characterization across Length Scales III.....	286	Wed PM	309
3-Dimensional Materials Science: Modeling and Characterization across Length Scales IV.....	286	Thurs AM	355
3-Dimensional Materials Science: ONR/DARPA Dynamic 3-D Digital Structure Program.....	286	Mon AM	60
9th Global Innovations Symposium: Trends in Integrated Computational Materials Engineering for Materials Processing and Manufacturing: Session I.....	281	Mon PM	104
9th Global Innovations Symposium: Trends in Integrated Computational Materials Engineering for Materials Processing and Manufacturing: Session II.....	281	Tues AM	155
Advances in Roasting, Sintering, Calcining, Preheating, and Drying: Advances in Thermal Processing.....	281	Mon AM	62
Advances in Semiconductor, Electro Optic and Radio Frequency Materials: Compound Semiconductors and Beyond.....	278	Mon PM	104
Advances in Semiconductor, Electro Optic and Radio Frequency Materials: Joint Session with Mechanics and Kinetics of Interfaces in Multi-Component Materials Systems.....	279	Wed AM	296
Advances in Semiconductor, Electro Optic and Radio Frequency Materials: Silicon-Based Optoelectronics and Microelectronics.....	278	Mon AM	63
Alumina and Bauxite: Additives.....	296	Wed AM	263
Alumina and Bauxite: Bauxite.....	296	Tues PM	210
Alumina and Bauxite: Equipment.....	296	Tues AM	156
Alumina and Bauxite: HSEC.....	296	Mon PM	106
Alumina and Bauxite: Operations.....	296	Wed PM	311
Alumina and Bauxite: Precipitation/Conclusion.....	296	Thurs AM	356
Aluminum Alloys: Fabrication, Characterization and Applications: Alloy Characterization.....	293	Tues PM	211
Aluminum Alloys: Fabrication, Characterization and Applications: Composites and Foams.....	293	Wed PM	312
Aluminum Alloys: Fabrication, Characterization and Applications: Corrosion and Protection.....	293	Wed AM	264
Aluminum Alloys: Fabrication, Characterization and Applications: Development and Applications.....	293	Mon AM	64
Aluminum Alloys: Fabrication, Characterization and Applications: Modeling.....	293	Tues AM	157
Aluminum Alloys: Fabrication, Characterization and Applications: Processing and Properties.....	293	Mon PM	107
Aluminum Reduction Technology: Aluminum Industry in Mid-East.....	298/299	Wed AM	266
Aluminum Reduction Technology: Cell Development Part I and Operations.....	298	Tues AM	159
Aluminum Reduction Technology: Cell Development Part II.....	298	Thurs AM	357
Aluminum Reduction Technology: Fundamentals, Low Melting Electrolytes, New Technologies.....	298	Wed PM	313
Aluminum Reduction Technology: Process Control.....	298	Tues PM	213
Aluminum Reduction Technology: Reduction Cell Modelling.....	297	Wed PM	315
Aluminum Reduction Technology: Sustainability and Environment.....	298	Mon PM	108
Aqueous Processing - General Session: Aqueous Processing General Abstracts.....	281	Tues PM	214
Biological Materials Science: Bioinspired Design and Processing.....	390	Tues AM	160
Biological Materials Science: Functional Biomaterials.....	390	Wed AM	267
Biological Materials Science: Implant Biomaterials I.....	390	Mon PM	110
Biological Materials Science: Implant Biomaterials II.....	390	Thurs AM	358
Biological Materials Science: Mechanical Behavior of Biological Materials I.....	390	Mon AM	66
Biological Materials Science: Mechanical Behavior of Biological Materials II.....	390	Wed PM	316
Biological Materials Science: Scaffold Biomaterials.....	390	Tues PM	215
Bulk Metallic Glasses V: Glass Forming Ability and Alloy Development.....	393	Wed AM	268
Bulk Metallic Glasses V: Processing and Properties.....	393	Thurs AM	359
Bulk Metallic Glasses V: Structures and Mechanical Properties I.....	393	Mon AM	67
Bulk Metallic Glasses V: Structures and Mechanical Properties II.....	393	Mon PM	110
Bulk Metallic Glasses V: Structures and Mechanical Properties III.....	393	Tues PM	216
Bulk Metallic Glasses V: Structures and Modeling I.....	393	Tues AM	161
Bulk Metallic Glasses V: Structures and Modeling II.....	393	Wed PM	317
Carbon Dioxide Reduction Metallurgy: Electrolytic Methods.....	294	Wed AM	270
Carbon Dioxide Reduction Metallurgy: Ferrous Industry.....	294	Tues PM	219
Carbon Dioxide Reduction Metallurgy: Mechanisms.....	294	Tues AM	163
Cast Shop Technology: Casthouse Operation.....	295	Tues AM	164
Cast Shop Technology: Casting Processes and Quality Analysis.....	295	Wed PM	319
Cast Shop Technology: Foundry Ingots and Alloys.....	295	Wed AM	271
Cast Shop Technology: Melt Handling and Treatment.....	295	Tues PM	220
Cast Shop Technology: Modelling.....	295	Thurs AM	361
Cast Shop Technology: Sustainability in the Casthouse.....	295	Mon PM	112
Characterization of Minerals, Metals, and Materials: Characterization of Extraction and Processing.....	284	Mon PM	113

Characterization of Minerals, Metals, and Materials: Characterization of Microstructure and Properties of Materials I.....	284	Tues AM.....	166
Characterization of Minerals, Metals, and Materials: Characterization of Microstructure and Properties of Materials II.....	284	Tues PM.....	221
Characterization of Minerals, Metals, and Materials: Characterization of Microstructure and Properties of Materials III.....	284	Wed AM.....	272
Characterization of Minerals, Metals, and Materials: Characterization of Microstructure and Properties of Materials IV.....	284	Wed PM.....	321
Characterization of Minerals, Metals, and Materials: Characterization of Microstructure and Properties of Materials V.....	284	Thurs AM.....	362
Characterization of Minerals, Metals, and Materials: Emerging Characterization Techniques.....	284	Mon AM.....	69
Complex Oxide Materials - Synthesis, Properties and Applications: Epitaxial Oxides: Ferroelectric, Dielectric, and (Electro-)Magnetic Thin Films.....	277	Tues PM.....	222
Complex Oxide Materials - Synthesis, Properties and Applications: Ferroelectric/Dielectric Oxides.....	277	Wed PM.....	322
Complex Oxide Materials - Synthesis, Properties and Applications: Functionally Cross-Coupled Heterostructures.....	277	Tues AM.....	167
Complex Oxide Materials - Synthesis, Properties and Applications: Novel Functionality from Complex Oxide Heterointerfaces.....	277	Mon PM.....	114
Complex Oxide Materials - Synthesis, Properties and Applications: Scaling, Dynamics, and Switching.....	277	Wed AM.....	274
Complex Oxide Materials - Synthesis, Properties and Applications: ZnO Nanostructures and Thin Films.....	277	Mon AM.....	70
Computational Thermodynamics and Kinetics: Defect Structure I.....	288	Mon AM.....	71
Computational Thermodynamics and Kinetics: Defect Structure II.....	288	Mon PM.....	116
Computational Thermodynamics and Kinetics: Diffusion and Phase Stability.....	288	Thurs AM.....	364
Computational Thermodynamics and Kinetics: Functional Materials.....	288	Tues PM.....	223
Computational Thermodynamics and Kinetics: Integrated Computational Materials Engineering.....	288	Wed PM.....	323
Computational Thermodynamics and Kinetics: Phase Field Crystal.....	288	Tues AM.....	168
Computational Thermodynamics and Kinetics: Phase Transformations.....	288	Wed AM.....	275
Computational Thermodynamics and Kinetics: Poster Session.....	Hall I 2	Sun PM.....	42
Deformation Twinning: Formation Mechanisms and Effects on Material Plasticity: Experiments and Modeling: Twin Effects on Material Deformation I.....	383	Mon PM.....	117
Deformation Twinning: Formation Mechanisms and Effects on Material Plasticity: Experiments and Modeling: Twin Effects on Material Deformation II.....	383	Tues PM.....	225
Deformation Twinning: Formation Mechanisms and Effects on Material Plasticity: Experiments and Modeling: Twin Formation and Growth Mechanisms.....	383	Mon AM.....	73
Deformation Twinning: Formation Mechanisms and Effects on Material Plasticity: Experiments and Modeling: Twinning and Associated Defect Structures.....	383	Tues AM.....	169
Electrode Technology Symposium (formerly Carbon Technology): Anode Manufacturing and Developments.....	297	Tues PM.....	225
Electrode Technology Symposium (formerly Carbon Technology): Anode Raw Materials and Properties.....	299	Tues AM.....	171
Electrode Technology Symposium (formerly Carbon Technology): Carbon Sustainability and Environment Aspects.....	299	Mon PM.....	119
Electrode Technology Symposium (formerly Carbon Technology): Cathodes Manufacturing and Developments.....	299	Wed PM.....	325
Electrode Technology Symposium (formerly Carbon Technology): Cathodes Raw Materials and Properties.....	299	Tues PM.....	226
Electrode Technology Symposium (formerly Carbon Technology): Inert Anode.....	299	Thurs AM.....	365
Emerging Interconnect and Packaging Technologies: Advanced Interconnects.....	275	Tues AM.....	172
Emerging Interconnect and Packaging Technologies: Pb-Free and Sn-Pb Solders: Electromigration.....	275	Mon PM.....	119
Emerging Interconnect and Packaging Technologies: Pb-Free Solder: Tin Whisker Formation and Mechanical Behavior.....	275	Tues PM.....	228
Emerging Interconnect and Packaging Technologies: Pb-Free Solders and Other Interconnects: Microstructure, Modeling, and Test Methods.....	275	Wed PM.....	326
Emerging Interconnect and Packaging Technologies: Pb-Free Solders: Fundamental Properties, Interfacial Reactions and Phase Transformations.....	275	Mon AM.....	74
Emerging Interconnect and Packaging Technologies: Pb-Free Solders: Reliability and Microstructure Development.....	275	Wed AM.....	277
Emerging Methods to Understand Mechanical Behavior: Digital Image Correlation.....	285	Mon PM.....	121
Emerging Methods to Understand Mechanical Behavior: Electron and Neutron Diffraction.....	285	Wed AM.....	278
Emerging Methods to Understand Mechanical Behavior: Imaging Methods.....	285	Mon AM.....	75
Emerging Methods to Understand Mechanical Behavior: Indentation and Dynamic Methods.....	285	Tues AM.....	173
Emerging Methods to Understand Mechanical Behavior: Subscale Methods.....	285	Tues PM.....	229
Emerging Methods to Understand Mechanical Behavior: X-Ray Diffraction.....	285	Wed PM.....	328
Energy Conservation in Metals Extraction and Materials Processing: Session I.....	287	Wed AM.....	279
Energy Conservation in Metals Extraction and Materials Processing: Session II.....	287	Wed PM.....	329
Enhancing Materials Durability via Surface Engineering: Novel Surface Durability Approaches.....	388	Tues PM.....	231
Enhancing Materials Durability via Surface Engineering: Residual Stress Effects on Durability.....	388	Mon AM.....	77
Enhancing Materials Durability via Surface Engineering: Steel and Other Alloys Surface Durability.....	388	Mon PM.....	122
Enhancing Materials Durability via Surface Engineering: Superalloy Surface Durability.....	388	Tues AM.....	175
Frontiers in Process Modeling: Casting and General Modeling.....	287	Tues PM.....	232
Frontiers in Process Modeling: Metallurgical Reactors.....	287	Tues AM.....	177

Frontiers of Computational Materials Science	APS, Hall A.....	Mon AM.....	78
General Abstracts: Electronic, Magnetic, and Photonic Materials Division: Session I.....	276.....	Wed AM.....	280
General Abstracts: Electronic, Magnetic, and Photonic Materials Division: Session II	276.....	Wed PM.....	331
General Abstracts: Extraction and Processing: Session I	272.....	Mon AM.....	78
General Abstracts: Extraction and Processing: Session II	272.....	Mon PM.....	124
General Abstracts: Light Metals Division: Session I.....	297.....	Mon PM.....	125
General Abstracts: Light Metals Division: Session II.....	297.....	Tues AM.....	178
General Abstracts: Materials Processing and Manufacturing Division: Composition Structure Property Relationships I.....	282.....	Mon PM.....	126
General Abstracts: Materials Processing and Manufacturing Division: Composition Structure Property Relationships II	282.....	Tues AM.....	179
General Abstracts: Materials Processing and Manufacturing Division: Films, Coatings, and Surface Treatments.....	282.....	Tues PM.....	233
General Abstracts: Materials Processing and Manufacturing Division: Forging, Forming, and Powder Processing	282.....	Wed AM.....	282
General Abstracts: Materials Processing and Manufacturing Division: Solidification and Casting	282.....	Mon AM.....	79
General Abstracts: Structural Materials Division: Mechanical Behavior of Materials	387.....	Mon PM.....	128
General Abstracts: Structural Materials Division: Mechanical Behavior of Metals and Alloys	387.....	Mon AM.....	81
General Abstracts: Structural Materials Division: Microstructure/Property Relations in Steel I.....	387.....	Wed AM.....	283
General Abstracts: Structural Materials Division: Microstructure/Property Relations of Steels II.....	387.....	Wed PM.....	332
General Abstracts: Structural Materials Division: Novel Issues in Materials Processing	387.....	Tues PM.....	234
General Abstracts: Structural Materials Division: Structure/Property Relations	387.....	Tues AM.....	180
General Poster Session.....	Hall 12.....	Sun PM.....	44
Hael Mughrabi Honorary Symposium: Plasticity, Failure and Fatigue in Structural Materials - from Macro to Nano: Cyclic Deformation and Fatigue of Metals I.....	386.....	Tues PM.....	236
Hael Mughrabi Honorary Symposium: Plasticity, Failure and Fatigue in Structural Materials - from Macro to Nano: Cyclic Deformation and Fatigue of Metals II.....	386.....	Thurs AM.....	333
Hael Mughrabi Honorary Symposium: Plasticity, Failure and Fatigue in Structural Materials - from Macro to Nano: Dislocations: Work Hardening, Patterning, Size Effects I.....	386.....	Mon AM.....	82
Hael Mughrabi Honorary Symposium: Plasticity, Failure and Fatigue in Structural Materials - from Macro to Nano: Dislocations: Work Hardening, Patterning, Size Effects II	386.....	Tues AM.....	182
Hael Mughrabi Honorary Symposium: Plasticity, Failure and Fatigue in Structural Materials - from Macro to Nano: High-Temperature Mechanical Properties: Creep, Fatigue and Thermomechanical Fatigue.....	386.....	Mon PM.....	129
Hael Mughrabi Honorary Symposium: Plasticity, Failure and Fatigue in Structural Materials - from Macro to Nano: Mechanical Properties of Ultrafine-Grained (UFG) Metals I.....	386.....	Wed AM.....	285
Hael Mughrabi Honorary Symposium: Plasticity, Failure and Fatigue in Structural Materials - from Macro to Nano: Mechanical Properties of Ultrafine-Grained (UFG) Metals II	386.....	Wed PM.....	367
Hael Mughrabi Honorary Symposium: Plasticity, Failure and Fatigue in Structural Materials - from Macro to Nano: Poster Session.....	Hall 12.....	Sun PM.....	49
Hot and Cold Rolling Technology: Session I.....	297.....	Wed AM.....	287
Hume-Rothery Symposium - Nanoscale Phases: Session I.....	276.....	Mon AM.....	84
Hume-Rothery Symposium - Nanoscale Phases: Session II.....	276.....	Mon PM.....	131
Hume-Rothery Symposium - Nanoscale Phases: Session III	276.....	Tues AM.....	184
Hume-Rothery Symposium - Nanoscale Phases: Session IV	276.....	Tues PM.....	237
IOMMMS Global Materials Forum 2008: Creating the Future MS&E Professional	272.....	Tues AM.....	185
Magnesium Technology 2008: Advanced Magnesium Materials.....	291.....	Wed AM.....	288
Magnesium Technology 2008: Alloy Microstructure and Properties	292.....	Wed AM.....	289
Magnesium Technology 2008: Casting	292.....	Tues PM.....	238
Magnesium Technology 2008: Corrosion, Surface Finishing and Joining	291.....	Wed PM.....	335
Magnesium Technology 2008: Creep Resistant Magnesium Alloys	292.....	Wed PM.....	336
Magnesium Technology 2008: Magnesium Plenary Session	291/292.....	Mon AM.....	85
Magnesium Technology 2008: Primary Production	292.....	Mon PM.....	132
Magnesium Technology 2008: Thermodynamics and Phase Transformations	292.....	Tues AM.....	186
Magnesium Technology 2008: Wrought Alloys I.....	291.....	Mon PM.....	133
Magnesium Technology 2008: Wrought Alloys II.....	291.....	Tues AM.....	188
Magnesium Technology 2008: Wrought Alloys III	291.....	Tues PM.....	240
Materials for Infrastructure: Building Bridges in the Global Community: Session I.....	272.....	Tues PM.....	242
Materials for Infrastructure: Building Bridges in the Global Community: Session II	272.....	Wed AM.....	291
Materials in Clean Power Systems III: Fuel Cells, Hydrogen-, and Clean Coal-Based Technologies: Gas Separation and CO ₂ Capture	392.....	Mon PM.....	135
Materials in Clean Power Systems III: Fuel Cells, Hydrogen-, and Clean Coal-Based Technologies: Hydrogen Technologies	392.....	Thurs AM.....	368
Materials in Clean Power Systems III: Fuel Cells, Hydrogen-, and Clean Coal-Based Technologies: Metallic Interconnects and Sealing in SOFCs	392.....	Wed AM.....	292
Materials in Clean Power Systems III: Fuel Cells, Hydrogen-, and Clean Coal-Based Technologies: Metallic Interconnects in SOFCs: Oxidation, Protection Coatings	392.....	Tues PM.....	243
Materials in Clean Power Systems III: Fuel Cells, Hydrogen-, and Clean Coal-Based Technologies: PEM Fuel Cells and Solar Technologies.....	392.....	Wed PM.....	338

Materials in Clean Power Systems III: Fuel Cells, Hydrogen-, and Clean Coal-Based Technologies: Plenary Session	392.....	Mon AM.....	86
Materials in Clean Power Systems III: Fuel Cells, Hydrogen-, and Clean Coal-Based Technologies: Solid Oxide Fuel Cells: Metallic Interconnects	392.....	Tues AM.....	189
Materials Informatics: Enabling Integration of Modeling and Experiments in Materials Science: Informatics and Cyberinfrastructure	271.....	Wed PM.....	339
Materials Informatics: Enabling Integration of Modeling and Experiments in Materials Science: Informatics and Combinatorial Experiments and Materials Characterization	271.....	Tues PM.....	244
Materials Informatics: Enabling Integration of Modeling and Experiments in Materials Science: Informatics and Materials Property Design	271.....	Tues AM.....	191
Materials Informatics: Enabling Integration of Modeling and Experiments in Materials Science: Informatics and Materials Theory and Modeling	271.....	Wed AM.....	293
Materials Processing Fundamentals: Powders, Composites, Coatings and Measurements.....	283.....	Tues AM.....	192
Materials Processing Fundamentals: Process Modeling.....	283.....	Mon PM.....	136
Materials Processing Fundamentals: Smelting and Refining.....	283.....	Tues PM.....	245
Materials Processing Fundamentals: Solidification and Deformation.....	283.....	Mon AM.....	86
Mechanical Behavior, Microstructure, and Modeling of Ti and Its Alloys: Microstructure/Property Correlation I.....	384.....	Tues PM.....	246
Mechanical Behavior, Microstructure, and Modeling of Ti and Its Alloys: Microstructure/Property Correlation II.....	384.....	Wed AM.....	294
Mechanical Behavior, Microstructure, and Modeling of Ti and Its Alloys: Phase Transformation and Microstructure Development I.....	384.....	Mon PM.....	138
Mechanical Behavior, Microstructure, and Modeling of Ti and Its Alloys: Phase Transformation and Microstructure Development II.....	384.....	Tues AM.....	193
Mechanical Behavior, Microstructure, and Modeling of Ti and Its Alloys: Physical/Mechanical Property Prediction	384.....	Wed PM.....	340
Mechanical Behavior, Microstructure, and Modeling of Ti and Its Alloys: Processing: Design, Control and Optimization.....	384.....	Mon AM.....	88
Mechanics and Kinetics of Interfaces in Multi-Component Materials Systems: Interfacial Microstructures and Effects on Mechanical and Physical Properties	279.....	Tues PM.....	247
Mechanics and Kinetics of Interfaces in Multi-Component Materials Systems: Joint Session with Advances in Semiconductors, Electro Optic and Radio Frequency Materials	279.....	Wed AM.....	296
Mechanics and Kinetics of Interfaces in Multi-Component Materials Systems: Mechanical Properties of Interfaces.....	279.....	Tues AM.....	194
Mechanics and Kinetics of Interfaces in Multi-Component Materials Systems: Mechanics of Adhesion, Friction and Fracture.....	279.....	Mon AM.....	89
Mechanics and Kinetics of Interfaces in Multi-Component Materials Systems: Nanoscale Structures and Simulations	279.....	Mon PM.....	139
Micro-Engineered Particulate-Based Materials: Session I	271.....	Mon AM.....	90
Micro-Engineered Particulate-Based Materials: Session II.....	271.....	Mon PM.....	140
Minerals, Metals and Materials under Pressure: Electronic, Magnetic and Optical Properties of Materials under High Pressure.....	385.....	Tues AM.....	196
Minerals, Metals and Materials under Pressure: High Pressure Phase Transitions and Mechanical Properties	385.....	Tues PM.....	249
Minerals, Metals and Materials under Pressure: New Experimental and Theoretical Techniques in High-Pressure Materials Science	385.....	Mon AM.....	91
Minerals, Metals and Materials under Pressure: Shock-Induced Phase Transformations and Microstructure	385.....	Mon PM.....	140
National Academies Corrosion Education Study Community Town Hall Meeting	388.....	Tues PM.....	232
Neutron and X-Ray Studies for Probing Materials Behavior: Diffraction at Small Dimensions.....	391.....	Mon PM.....	141
Neutron and X-Ray Studies for Probing Materials Behavior: Phase Transitions and Beyond.....	391.....	Tues AM.....	197
Neutron and X-Ray Studies for Probing Materials Behavior: Recrystallization	391.....	Tues PM.....	250
Neutron and X-Ray Studies for Probing Materials Behavior: Resolving Local Structure	391.....	Mon AM.....	92
Neutron and X-Ray Studies for Probing Materials Behavior: Scattering and Understanding of Materials Properties	391.....	Wed PM.....	341
Neutron and X-Ray Studies for Probing Materials Behavior: Stresses/Strains and Structure	391.....	Wed AM.....	297
Particle Beam-Induced Radiation Effects in Materials: Carbides, Semiconductors and Other Non-Metals.....	389.....	Wed AM.....	299
Particle Beam-Induced Radiation Effects in Materials: Ceramics and Nuclear Fuel Materials	389.....	Tues PM.....	251
Particle Beam-Induced Radiation Effects in Materials: Metals I	389.....	Mon AM.....	94
Particle Beam-Induced Radiation Effects in Materials: Metals II	389.....	Mon PM.....	143
Particle Beam-Induced Radiation Effects in Materials: Nanostructures	389.....	Wed PM.....	342
Particle Beam-Induced Radiation Effects in Materials: RIS and Multilayers	389.....	Tues AM.....	198
Phase Stability, Phase Transformations, and Reactive Phase Formation in Electronic Materials VII: Session I.....	278.....	Tues AM.....	199
Phase Stability, Phase Transformations, and Reactive Phase Formation in Electronic Materials VII: Session II.....	278.....	Tues PM.....	253
Phase Stability, Phase Transformations, and Reactive Phase Formation in Electronic Materials VII: Session III	278.....	Wed AM.....	300
Phase Stability, Phase Transformations, and Reactive Phase Formation in Electronic Materials VII: Session IV	278.....	Wed PM.....	343
Pyrometallurgy - General Sessions: Pyrometallurgy	283.....	Wed AM.....	301

Recent Developments in Rare Earth Science and Technology - Acta Materialia Gold Medal Symposium: Session I.....	280.....	Mon AM.....	95
Recent Developments in Rare Earth Science and Technology - Acta Materialia Gold Medal Symposium: Session II.....	280.....	Mon PM.....	144
Recent Industrial Applications of Solid-State Phase Transformations: Alloy Design, Microstructure Prediction and Control.....	287.....	Mon PM.....	145
Recent Industrial Applications of Solid-State Phase Transformations: Superalloys and TRIP Steels/Automotive Steels.....	287.....	Mon AM.....	96
Recycling: Electronics Recycling.....	280.....	Tues AM.....	201
Recycling: General Sessions.....	280.....	Wed PM.....	345
Recycling: Light Metals.....	280.....	Wed AM.....	302
Recycling: Micro-Organisms for Metal Recovery.....	280.....	Tues PM.....	255
Refractory Metals 2008: Characterization.....	388.....	Wed PM.....	346
Refractory Metals 2008: Processing.....	388.....	Wed AM.....	303
Refractory Metals 2008: Properties of Refractory Metals.....	388.....	Thurs AM.....	369
Sloan Industry Centers Forum: Techno-Management Issues Related to Materials-Centric Industries: Session I.....	397.....	Mon PM.....	147
Sloan Industry Centers Forum: Techno-Management Issues Related to Materials-Centric Industries: Session II.....	397.....	Tues AM.....	202
Structural Aluminides for Elevated Temperature Applications: Applications.....	394.....	Mon AM.....	97
Structural Aluminides for Elevated Temperature Applications: Environmental Effects and Protection.....	394.....	Thurs AM.....	370
Structural Aluminides for Elevated Temperature Applications: FE and Other Aluminides.....	394.....	Tues AM.....	203
Structural Aluminides for Elevated Temperature Applications: Mechanical Behavior.....	394.....	Mon PM.....	148
Structural Aluminides for Elevated Temperature Applications: New Class of Gamma Alloys.....	394.....	Wed PM.....	347
Structural Aluminides for Elevated Temperature Applications: Phase and Microstructure Evolution.....	394.....	Wed AM.....	304
Structural Aluminides for Elevated Temperature Applications: Poster Session.....	394.....	Wed PM.....	349
Structural Aluminides for Elevated Temperature Applications: Processing and Microstructure Control.....	394.....	Tues PM.....	255
Sustainability, Climate Change and Greenhouse Gas Emissions Reduction: Responsibility, Key Challenges and Opportunities for the Aluminum Industry.....	295/296.....	Mon AM.....	99
The Role of Engineers in Meeting 21st Century Societal Challenges -- AIME Keynote Session.....	272.....	Wed PM.....	351
Ultrafine-Grained Materials: Fifth International Symposium: Deformation Mechanisms.....	273.....	Wed AM.....	306
Ultrafine-Grained Materials: Fifth International Symposium: Modeling, Theory, and Property.....	273.....	Mon AM.....	99
Ultrafine-Grained Materials: Fifth International Symposium: Poster Session.....	Hall 12.....	Sun PM.....	50
Ultrafine-Grained Materials: Fifth International Symposium: Processing and Materials.....	273.....	Mon PM.....	149
Ultrafine-Grained Materials: Fifth International Symposium: Properties.....	273.....	Tues PM.....	257
Ultrafine-Grained Materials: Fifth International Symposium: Stability, Technology, and Property.....	273.....	Tues AM.....	205
Ultrafine-Grained Materials: Fifth International Symposium: Structure and Evolution.....	273.....	Wed PM.....	352

2008 Nanomaterials: Fabrication, Properties, and Applications: Poster Session

Sponsored by: The Minerals, Metals and Materials Society, TMS Electronic, Magnetic, and Photonic Materials Division, TMS: Nanomaterials Committee
Program Organizers: Seong Jin Koh, University of Texas; Wonbong Choi, Florida International University; Donna Senft, US Air Force; Ganapathiraman Ramanath, Rensselaer Polytechnic Institute; Seung Kang, Qualcomm Inc

Sunday PM
 March 9, 2008

Room: Hall I 2
 Location: Ernest Morial Convention Center

Aluminum Alloy Based Nanocomposites Reinforced with Carbon Nanotubes: *Hyun-joo Choi*¹; Donghyun Bae¹; ¹Yonsei University

Aluminum alloy based nanocomposites reinforced with carbon nanotubes exhibiting high specific strength and toughness are produced by hot rolling of the ball-milled mixture of aluminum alloy powders and MWNTs (Multi-walled carbon nanotubes). Each of MWNTs is well dispersed during the milling and uniaxially aligned along the rolling direction. Especially, the tubes are found to be gradually filled with aluminum atoms as the milling time increases, providing the perfectly sticking interface between the MWNTs and the matrix. The strength of the composites increase with an increase of volume fraction of MWNTs up to 0.03, and the tendency is well matched with the conventional rule of mixture. Finally, the composite sheets containing 3 vol.% MWNTs with an area above 10 inch² exhibit remarkably enhanced strength around 750MPa in tension tests. The details of reinforcing effects of nano-scale tubes including strengthening and toughening mechanism of the MWNTs will be presented.

Cladding of Different Metals and Composites by Laser Process and Their Effects on Mechanical Properties: *Ali Emamian*¹; ¹University of Waterloo-Canada

Cladding is deposition of different material on base metal for different aims like corrosion and erosion resistance or wear resistance or all of them. Depending on type of service, clad material can be made from metal or composites. In this process, we are able to have different aspects of properties related to base metal and cladding material simultaneously. Cladding material will be selected according their abilities and compatibility with base metals and properties. The most important item which must be considered is that clad material has to be able to wet completely by metal surface and be compatible according their surface energies. Otherwise, we cannot have a strong bond between clad and base metal because clad material will be in global shape. In this case oxidation risk also will be increased because of increasing of particles' surface in global state.

Composition Evolution during FePt Nanoparticle Synthesis: *Chandan Srivastava*¹; Jayendra Balasubramanian¹; Gregory Thompson¹; Christoffer Turner¹; John Wiest¹; ¹University of Alabama

FePt nanoparticles are candidate materials for future magnetic storage devices. Variation in composition and size from particle-to-particle is one of the factors limiting their application. In the present study, FePt nanoparticles were synthesized by two different synthetic routes: the iron pentacarbonyl route (involving the co-reduction of Fe and Pt precursors) and the superhydride route (involving a two step reduction of precursors). The mechanism of formation of particles was investigated by structural and compositional characterization of the reaction mixture, extracted at different stages of the synthesis. It was observed that the superhydride route produced particles with a narrower composition and size distribution than iron pentacarbonyl route. These differences will be discussed as a function of the evolution of composition during the synthesis. A Monte Carlo simulation has been performed supporting the mechanism theory and suggesting a thermodynamic limit for the incorporation of Fe into the core of FePt nanoparticles.

Dislocation Interactions with $\Sigma 11$ Tilt Boundaries: *Joshua Askin*¹; Richard Hoagland²; Peter Anderson¹; ¹Ohio State University; ²Los Alamos National Laboratory

Grain boundaries play a critical role in plasticity in nanocrystalline metals, where they act as both sources and sinks of dislocation content. A single set of grain misorientations can create a multitude of grain boundary structures,

depending on the orientation of the grain boundary and rigid body translation of the two grains parallel to the grain boundary. Here we compare the interaction of several grain boundaries in the $\Sigma 11$ tilt orientation with dislocations of differing Burgers vectors. Absorption is a common result, with the perfect dislocation dissociating into grain boundary dislocations or otherwise spreading its core on the grain boundary, lowering total system energy. The details of absorption vary both between boundaries and within a single boundary, as the local atomic configuration changes. Results from atomistic studies are viewed in the context of the gamma surface for the boundary and compared with Peierls-type continuum models of core spreading.

Effect of Nb and Sn on the Transformation of Alpha to Beta Titanium in Ti-35 Nb-2.5 Sn Alloy Using Mechanical Alloying: *Abdel-Nasser Omran*¹; K. Woo¹; D. Kim¹; Sug Won Kim¹; ¹Chonbuk National University, Divisions of Advanced Materials Engineering, Research Center of Industrial Technology

Titanium and its alloys have many uses in different medical fields. In titanium alloys, the principal effect of an alloying element is its effect on the alpha-to-beta transformation temperature. In this work, the niobium has been chosen as β stabilizer, and tin as reducer of elastic modulus. The starting materials were blended and milled using mixing machine (24hr) and high energy ball mill machine (1, 4, and 12 hr respectively). The particles size and phases of the produced powders were analyzed using XRD, SEM, TEM, and PSA. It was found that, the titanium was completely transformed from α to β Ti at milling time 12hr.

Electrical and Optical Properties of ZnO and Gallium Doped ZnO Thin Films Prepared by rf Magnetron Sputtering: Effect of Annealing and UV Radiation: *Ved Verma*¹; Hoonha Jeon²; Minhyon Jeon²; Wonbong Choi¹; ¹Florida International University; ²Inje University

Zinc oxide (ZnO) and Ga doped (1wt%) zinc oxide (GZO) thin films are grown on SiO₂/Si and glass substrates at room temperature by rf magnetron sputtering. The structural properties of both ZnO and GZO thin films are investigated by high resolution x-ray diffraction and atomic force microscopy. Both the ZnO and GZO films grow in preferred orientation of $\langle 001 \rangle$ direction. However, GZO thin film shows higher surface roughness (rms~1.65 nm) than ZnO thin film (rms~1.0 nm). Electrical and optical properties of thin films are investigated by Hall Effect and UV-VIS-NIR spectrometer. Both the thin films show a transmittance, above 80%. The GZO thin films exhibit higher conductivity compared to that of ZnO thin films. With time, ZnO thin films show decrease in conductivity where as GZO thin films demonstrate a stable value, which can be attributed to the passivation of oxygen dangling bond by Ga atoms in GZO thin film.

Forming Surface Nanofilms on Particles of Dispersion Aluminium: *Sergey Lipko*¹; Vladimir Tauson²; Boris Zelberg¹; ¹Siberian Research and Design Institute for Aluminium and Electrode Industry JSC; ²Institute of Geochemistry, SD, RAS

It is considered the influence of various chemical components on powder aluminium composition, produced using the method of gas dispersion of aluminium melt in nitrogen atmosphere and then annealed in different conditions. Powders with particles of different size 5-7 and about 20 mkm were examined. The presence of W makes better the structure of a film and promotes the formation of less strained nitride coating that was seen during comparative analysis of RFES width, pick no. 1s at half of maximum height after aluminium powder annealing in the presence of W in a sealed test-tube with air. It is anticipated that W has catalytic effect promoting the formation of nitric radicals that interact with particles' surface. W belongs to the group of elements with effect of integral accumulation in fine fractions of spray like Zn, Zr and some others (V.V. Skitina and others – DAN, 2003, v.390, no. 4, p.495-498).

Microstructures and Mechanical Properties of Carbon Nanotube/Metal Nanocomposites Processed by Molecular Level Mixing: *Kyung Tae Kim*¹; Thomas Gemming¹; Seung Il Cha²; Soon Hyung Hong³; Juergen Eckert¹; ¹IFW Dresden; ²NIMS; ³KAIST

The carbon nanotube/Cu matrix (CNT/Cu) nanocomposite is fabricated by a novel fabrication process named molecular level process. The novel process for fabricating CNT/Cu composite powders involves suspending CNTs in a solvent by surface functionalization, mixing Cu ions with CNT suspension, drying, calcinating and reducing. The molecular level process produces CNT/Cu composite powders whereby the CNTs are implanted within Cu powders.

The CNT/Cu nanocomposites, consolidated by spark plasma sintering of CNT/Cu composite powders, show the characteristic microstructures which are homogeneous dispersion of CNTs in Cu matrix and interfacial bonding between CNT and Cu. Due to these microstructures, the mechanical properties of CNT/Cu nanocomposite shows about 3 times higher strength and 2 times higher Young's modulus than those of Cu matrix. This strengthening effect of carbon nanotubes is found to be the highest compared to other types of reinforcements for metal matrix composites.

Nanowires of AlN and Si₃N₄ Prepared from Amorphous Powders: Zhao Han¹; Mei Yang¹; Mingli Lv¹; Hongmin Zhu¹; ¹Beijing University of Science and Technology

Aluminum nitride and silicon nitride nano-powders were synthesized through a chemical reduction, of AlCl₃ and SiCl₄ by sodium in liquid ammonia. The product powders were amorphous and spherical agglutinating particles ranging from 1 to 10 nanometers in diameter. Single-crystalline aluminum nitride (AlN) and silicon nitride (Si₃N₄) nanowires with hexagonal structure were prepared by heating the amorphous nano-powders at 1300°C through 1450°C. The products obtained were characterized by X-ray diffraction (XRD), scanning electron microscopy (SEM), transmission electron microscopy (TEM), and selected area electron diffraction (SAED). The results revealed that the products were single-crystalline AlN and Si₃N₄ nanowires. The diameters of the nanowires ranged from 30 to 200 nm, and the lengths were from several micrometers to several decades of micrometers.

Novel Preparation and Characterization of Rare-Earth Nanoparticles and Nanocrystalline Bulks: Xiaoyan Song¹; Jiuxing Zhang¹; Nianduan Lu¹; Markus Rettenmayr²; ¹Beijing University of Technology; ²Friedrich-Schiller-Universität Jena

With a home-developed "oxygen-free" in-situ synthesis system, we produced a series of rare-earth nanoparticles with controllable size. In particular, we proposed an innovative route of preparing ultrafine nanocrystalline bulks with the sequentially performed processes: the amorphization of nanoparticles, nucleation and growth of the short-range ordered "clusters", and the complete nanocrystallization. By these procedures, the grain sizes in the resultant nanocrystalline bulks are much smaller than the initial nanoparticle sizes, representing the advantage of the present technique over the conventional power metallurgy methods. The microstructures and properties of the prepared nano rare-earths have been characterized systematically. The physical, thermal and mechanical properties of the prepared nanostructured bulks are found to be improved remarkably as compared with the conventional polycrystalline bulks. The present preparation technique has potentially wide applications to a big variety of metal nanomaterials that are active in the air.

Photoactive C60 Bridged Tetrameric Osmium and Ruthenium γ -Cyclodextrin Assemblies: Assembly and Spectroscopy: Muath Atmeh¹; ¹Dublin Institute of Technology

Cyclodextrins display a rich host-guest chemistry. A particularly attractive proposition is to combine the properties of CD with luminophores, which may act as reporters of binding or other interactions at the cyclodextrin cavity. Ruthenium and osmium polypyridyl complexes are particularly attractive reporters in this regard because of their visible emission, their useful redox properties. In this contribution, we exploit this ability to design a tetrameric metallocyclodextrins containing photoactive Ru(II) polypyridyl units covalently bonded to γ -CD. The supramolecular assembly consists of cyclodextrin to which two ruthenium (II) or osmium (II) polypyridyl have been covalently linked these CDs then self-assemble with a fullerene moiety in 2:1 ratio to produce the tetramer, Figure 1. Here we describe the synthesis and characterization of the complexes and in particular their spectroscopic electrochemical and photophysical properties. We describe evidence for photoinduced processes and discuss the possibility of electron and energy transfers in these novel supramolecular assemblies.

Physical and Microstructural Properties of Ultra Dispersed Nano-Diamond Reinforced Copper Matrix Composites: Hülya Kaftelen¹; Mustafa Öveçoglu¹; ¹Istanbul Technical University

Ultra dispersed nanodiamond powders were used as a reinforcement material in copper matrix to improve thermal and physical properties of composites. High energy ball milling were performed under Ar atmosphere for four different milling times. The mechanical alloyed composite powders later consolidated

and sintering under protective atmosphere at 1100-1200K. The microstructures of both sintered and mechanical alloyed powders were investigated using XRD, scanning electron microscope (SEM) and EDS analysis. Titanium was also incorporated to enhance interfacial bonding between the nano-diamond and the copper matrix phase.

Preparation of ZnO Nanoparticles, Nanorods and Nanoplatelets by Micro-Emulsion Template Method: Teng Honghui¹; ¹Jilin Normal University

Nano-ZnO particles, nanorods and nanoplatelets were prepared by a micro-emulsion template method. The micro-emulsion consists of surfactant A/ butanol/cyclohexane/water systems=5:1.2:1:X, X are certain specific values (1.0, 1.5, 2.0, 2.5, 3.0ml). The structures of microemulsions were studied from electric conductivities of the water in oil (W/O) microemulsions at different W/O rate, with the electric conductivities of that increasing, the structures of microemulsions change from spherical to double-continued-linear and layered structure. Then, each of zinc chloride and ammonia aqueous solutions instead of water systems, two micro-emulsion systems were established, as original reaction systems, mixed up, nano-ZnO particles, nanorods and nanoplatelets were prepared by the controlling of W/O rate. The particles were spherical or spherical-like with diameter about was 30 to 80nm. The nanorods were uniform in diameter and in length, their mean diameter was 70nm and mean length was 350nm. The mean thickness of nanoplatelets was 60nm.

Processing and Characterization of Ti₂AlC/Nanocrystalline Mg Matrix Composites: Shahram Amini¹; Michel Barsoum¹; ¹Drexel University

The MAX phases - of which Ti₂AlC is a member - are layered machinable, hexagonal ternary carbides and nitrides. Due to their high c/a ratios, the MAX phases deform primarily by the formation of kink bands and consequently are members - together with Mg - of a much larger class of solids labeled kinking nonlinear elastic, KNE. Herein we report on the fabrication and characterization of Ti₂AlC/nanocrystalline Mg matrix composites fabricated by hot pressing and pressureless melt infiltration. Hot-pressing of 50 vol. % Mg and Ti₂AlC powders at 750°C for 1 h at ~45 MPa resulted in fully dense composites. More importantly, fully dense samples were also made by pressureless infiltration of molten Mg into porous preforms of Ti₂AlC under vacuum. The Mg matrix existed in the form of ~35 and 50 nm diameter nanoparticles in hot pressed and infiltrated composites.

Size Dependent Elasticity of Nanowires: Moneesh Upmanyu¹; ¹Colorado School of Mines

We employ a molecular statics approach based on embedded-atom-method (EAM) inter-atomic potentials to study the elasticity of metallic nanowires. Self-consistent comparison with the bulk response in copper clearly shows that the overall nanowire elasticity is primarily due to non-linear response of the nanowire core. While the surface stress induced surface elasticity modifies the behavior for ultra-thin nanowires, their contribution is always considerably smaller than that due to non-linear elasticity of the nanowire core. More importantly, for all three orientations, the surface is softer than an equivalently strained bulk, and the overall nanowire softening or stiffening is determined by orientation dependent core elasticity. Implications for heterostructured nanowires and nanotube bundles will be also discussed.

Structural Identification of Nanocrystals from High Resolution Transmission Electron Microscopy Images: Peter Moeck¹; ¹Portland State University

A novel method for the structurally identification of nanocrystals from high resolution transmission electron microscopy images is described. Components of this method are demonstrated on both experimental and simulated images. There are several levels to this structural fingerprinting method that allow for increasingly discriminatory identifications of crystal structures out of a range of candidate structures from a database. With increasing identification power, these levels are extracting the projected reciprocal lattice geometry, plane symmetry group, structure factor amplitudes, and structure factor phases. If necessary for even higher levels of structural discrimination, the extracted structural information can be extended by direct methods and the errors that have been made by assuming kinematical scattering can be estimated and corrected for. The mainly inorganic subset of the Crystallography Open Database (<http://nanocrystallography.research.pdx.edu/CIF-searchable/cod.php>), with approximately 10,000 structure entries) and the Nano-Crystallography Database (<http://nanocrystallography.research.pdx.edu/CIF-searchable/ncd.php>) can be

employed to facilitate the structural identification by calculating lattice-fringe fingerprint plots.

Study on Nano-Alumina Prepared by Low-Temperature Combustion Synthesis: *Guo Rui¹*; ¹Northeastern University

Al₂O₃ has fine physical and chemical properties. Nanometer α -Al₂O₃ powder was prepared by the method of Low-temperature Combustion Synthesis with aluminum nitrate nonahydrate and urea as raw materials in the muffle furnace and microwave oven. By the means of XRD, TEM, TG-DTA, IR and Malvern Mastersizer measurements, the as-prepared powder was analyzed. The optimum technology process with muffle furnace was: the molar ratio of Al(NO₃)₃·9H₂O/CO(NH₂)₂ was 1 to 2.5, the igniting temperature was 750°C. It was found that the α -Al₂O₃ powders having an average grain size about 40-90nm were sheet structure in a great measure, others were the shape of approximate sphere. The optimum technology process with the microwave oven was: the molar ratio of Al(NO₃)₃·9H₂O/CO(NH₂)₂ was 1 to 2.5; heat power was 900W. The product having an average grain size about 60-90nm was sheet in a great measure.

Surface Modification of PPy Conducting Polymer Nanowires by Sputtered Noble Metals for Gas Sensing: *Jiajun Chen¹*; Lianbin Xu²; Xiaojun Tang¹; Yushan Yan²; Weilie Zhou¹; ¹University of New Orleans; ²University of California at Riverside

Polypyrrole (PPy) conducting polymer can work as the active materials for gas sensor, which has several advantages compared to commercial available metal oxide based sensors: high sensitivity and short response time at room temperature, low cost fabrication and compatible to flexible electronics. PPy nanowires are ideal materials for highly sensitive gas sensors due to their high surface-volume aspect ratio. PPy nanowires were fabricated by electrochemistry methods and multi-nanowire-based field effect transistors (FETs) were prepared by e-beam lithography. Sputtered noble metals were used to modify the PPy nanowire surfaces. The electrical and gas sensing properties of PPy nanowire based FETs were investigated. The role of noble metal modification was discussed.

Synthesis and Characterization of Nano-Spinel Lithium Manganate: *Xinghua Xie¹*; Shilong Yan¹; Hongbo Wu¹; Weiguo Wang¹; Meng Wang¹; Xiaojie Li²; ¹Anhui University of Science and Technology; ²Dalian University of Technology

The formation of metallic nanooxides via detonation reaction was investigated with respect to the presence of an energetic precursor, such as the metallic nitrate and the degree of confinement of the explosive charge. The detonation products were characterized by scanning electron microscopy. The thermal stability of the nanostructures has been examined by heating-treatment at different temperatures. Powder X-ray diffraction, transmission electron microscopy, scanning electron microscopy, thermogravimetric analysis and BET were used to characterize the products. Nano-metallic oxides with diameters from 10 to 50 nm and a variety of morphologies were found. The oxides produced by this cheap method affirmed the validity of detonation synthesis of nano-size powders.

Synthesis and Electrical Properties of Exotic Boron Carbide Nanowires: *Varun Gupta¹*; Steve Miller¹; Giovanni Fanchini¹; Jafar Al-Sharab¹; Manish Chhowalla¹; ¹Rutgers University

Recently, synthesis of one dimensional nano-materials and quasi-one dimensional nanostructures such as nanotubes, nanowires and nanowires (NWs) has gained a large impetus. Boron carbide NWs are particularly significant because of their use in thermoelectric devices and other electronic applications. In this study we explore the role of boron/carbon ratio, temperature, inert gas pressure and dopants (Si and Al) on the morphology, length and diameter of nanowires. Nanowire dimensions show a bimodal distribution with wire length varying from 100nm to 50µm and up to a few millimeters. The elemental composition, morphology and single crystalline nature of the nanowires were analyzed by SEM, EDS, TGA and HRTEM. The effect of Si and Al doping on the conductivity is further evaluated and compared to pure B₄C. This approach can be readily extended to the synthesis of other doped nanostructures, which can offer great opportunities for both fundamental research and technological applications.

Temperature, Thickness and High Energy Si Ions Bombardment Effects on the Thermoelectric Properties of GdFe₄Sb_{6-y}Ge_y Thin Films: *Sadik Guner¹*; Satilmis Budak¹; Claudiu Muntele²; Daryush Ila²; ¹Alabama A&M University, Department of Physics, Center for Irradiation of Materials

We have grown three monolayer GdFe₄Sb_{6-y}Ge_y (y = 2, 4) thin films on silica substrates with varying thickness between 100-1000 nm using electron beam deposition. The high-energy (MeV) Si ion bombardments were performed on samples with varying fluencies (1x10¹⁴-5x10¹⁵). The thermopower, electrical and thermal conductivity measurements were carried out before and after the bombardment on samples to determine the dimensionless figure of merit, ZT. The Si ions bombardment caused changes on the thermoelectric properties of films. The fluence and temperature dependence of cross plane thermoelectric parameters were also reported. Rutherford Backscattering Spectrometry (RBS) was used to analyze the elemental composition of deposited materials and to determine the layer thickness of each film. Research sponsored by the Center for Irradiation of Materials, Alabama A&M University and by the AAMURI Center for Advanced Propulsion Materials under the contract number NNM06AA12A from NASA, and by National Science Foundation under Grant No. EPS-0447675.

The Fabrication Technique for Indium Tin Oxide Nanosized Composite Powder: *Huimin Lu¹*; Xi Zhang¹; ¹Beijing University of Aeronautics and Astronautics

Indium tin oxide (ITO) nanosized composite powder not only can improve sintering properties of target and afford material for big size and super density ITO target, but also can be made into electronic pastes which can be sputtered on cathode ray tube as an effective seclusion screen of electromagnetic interference. In this paper, conductive indium tin oxide (ITO) powder size of nanometer were prepared by the hydrolysis of corresponding metal salts following co-precipitation technique using indium metal ingots and SnCl₄·5H₂O as raw materials. On the purpose of manufacturing functional powders in a large amount and energy-conserving, the factors in whole course were considered, especially the influences of co-precipitation terminal pH value and heat treatment temperature under hydrogen gas on the particle size and power resistance were discussed. The characteristics of powders were investigated by DTA-TG, XRD, TEM.

The Influence of Nano Boehmite on Spinel Formation: *Hamid Zargar¹*; Farhad Golestani Fard¹; Hamidreza Rezaei¹; ¹Iran University of Science and Technology

The effect of nano boehmite as an additive on the formation of spinel at low temperatures (T<1000°C) via solid-state procedure is investigated. In this regard, the homogeneity of prepared mixtures previously studied by performing XRD, FTIR, SEM and MAP. Furthermore, in order to evaluate the morphology of synthesized spinel, SEM has applied. Results are implied that nano boehmite facilitate solid-state spinel formation on magnesia grain at temperatures as low as 700°C. In addition, prepared spinel is in nano scale (<80nm) and homogeneously distributed on, magnesia grains.

Thermoelectric Generator from Sequentially Deposited SiO₂/GdFe₄Sb_{6-y}Ge_y Nanolayers Modified by MeV Si Ions Bombardment: *Sadik Guner¹*; Satilmis Budak²; Claudiu Muntele²; Daryush Ila²; ¹Alabama A&M University, Department of Physics, Center for Irradiation of Materials; Fatih University, Department of Physics; ²Alabama A&M University, Department of Physics, Center for Irradiation of Materials

We have grown 50-100 periodic nano-layers of SiO₂/GdFe₄Sb_{6-y}Ge_y super-lattice electro-cooling system. The deposited multi-layer films have a periodic structure consisting of alternating layers, between 5-20 nm thick each. The super-lattices were then bombarded by 5 MeV Si ions at different fluences ranging from 1x10¹⁴ to 5x10¹⁵ ions/cm² to form nano-cluster structure. Rutherford Backscattering Spectrometry (RBS) specified the total deposit thickness and stoichiometry. We measured the thermoelectric efficiency of the fabricated device before and after MeV bombardments. To accomplish this we measured the cross plane thermal conductivity by 3rd harmonic method, cross plane Seebeck coefficient and cross plane electric conductivity. As predicted the electronic energy deposited due to ionization by MeV Si beam in its track produces nano-scale structures that disrupt and confine phonon transmission therefore reducing thermal conductivity, increasing electron density of state so as to increase Seebeck coefficient and

electric conductivity, thus increasing the figure of merit. Research sponsored by the Center for Irradiation of Materials, Alabama A&M University and by the AAMURI Center for Advanced Propulsion Materials under the contract number NNM06AA12A from NASA, and by National Science Foundation under Grant No. EPS-0447675.

Preparation of Nanosized Zinc Ferrite Particles: *Qing-hua Tian*¹; Xueyi Guo¹; Huang Kai¹; ¹Central South University

Based on the review of technical literatures, the co-precipitation-drying-thermal decomposition was determined for the preparation of nanosized zinc-ferrite. The ammonium bicarbonate was chosen as the co-precipitation agent, and the thermodynamic analyses were done for the solution system of Fe(III)-Zn(II)-NH₃-CO₃—H₂O. The double-jet precipitation process was proposed based on the thermodynamic analyses results. Considering the heavy aggregation among nano-sized particles, the measures were adopted by addition of dispersant in the process of co-precipitation and washing by organic solvent or azeotropic distillation. By TG-DTA analysis, the suitable thermol-decomposition temperature of the zinc ferrite precursor was determined at about 450°C. Kept at this temperature for 2 hours, the pure and well crystalized ZnFe₂O₄ was obtained. SEM Photos of the obtained powder shows that the particles are uniform in size distribution (20nm-50nm) with good dispersivity.

Quantum Size Effect of Electron Density and Its Influence on Interlayer Relaxation of Ultra-Thin Metal Films: *Fei Ma*¹; Shengli Ma²; Kewei Xu²; Paul Chu¹; ¹City University of HongKong; ²Xi'an Jiaotong University

Further minimization of electronic devices and microelectromechanical systems (MEMS) requires the feature sizes of relevant materials to be shrunk significantly. In such a case, boundary effects, such as interfaces and surfaces, become remarkable, especially in nanometer scale, which must affect their microstructures and properties. In this work, we have analyzed the distribution of electron charge density in Cu and Al ultra-thin films using free electron model. The results show that an electrostatic field may come into being due to quantum size effect, and the interlayer separations must relax to decrease the Coulomb energy, the thinner the films, the larger the relaxation. More interestingly, the different electron shell configurations result in two opposite deviating directions of the center of negative charges: inwards for Cu and outwards for Al, and thus two absolutely distinct interlayer relaxations.

Nano-Diamond Coatings for Machining Applications: *Jianwen Hu*¹; *Kevin Chou*¹; Raymond Thompson²; ¹University of Alabama; ²Vista Engineering

Different from microcrystalline diamond (MCD) coatings, nanostructured diamond (nano-diamond) coatings, produced by microwave plasma-assisted chemical vapor deposition with nitrogen gas added, own several unique properties that enhance their machining performance in cutting tool applications. Characterized by nanoindentation, nano-diamond coatings have very high hardness (over 80 GPa vs. ~60 GPa of MCD) and lower elasticity (below 800 GPa vs. ~1100 GPa of MCD) which generates less residual stresses in the coating-substrate system. Moreover, nano-diamond coatings have much smoother topography than MCD coatings. Nano-diamond coatings consist of nanocrystalline diamond grains (average sizes from 5 to 30 nm) imbedded into an amorphous tetrahedral carbon matrix which offers cracking resistance. These distinct attributes jointly result in strong adhesion of nano-diamond coatings. Machining of high-strength Al alloys and composites using diamond tooling shows that nano-diamond coated tools significantly outperform conventional MCD tools, though both of them exhibiting delamination as the major tool failure mode.

The Anodic and Cathodic Processes in Direct Electrochemical Conversion of Solid Metal Chlorides to Metal Nanoparticles in Ionic Liquids: *Linpo Yu*¹; *Huijiao Sun*¹; *Dihua Wang*¹; *Xianbo Jin*¹; *George Chen*²; ¹Wuhan University; ²University of Nottingham and Wuhan University

Solid metal chlorides have been attached to a metallic substrate in the form of either a thin coating or powder and successfully electrochemically reduced to metal nanoparticles in an ionic liquid, 1-butyl-3-methylimidazolium hexafluorophosphate. Particularly, the presentation compares the cyclic voltammograms of cuprous copper in aqueous and ionic liquid electrolyte, and the physicochemical characterisations of the potentiostatic electrolysis products on both cathode and anode. Preliminary findings are also presented for a few other metal chlorides. It is proposed that the formation of the metal nanoparticles

is the result of a combined effect of the slow kinetics of the dissolution-deposition process in the ionic liquids, and also likely the ionic liquid being effective in preventing the metal particles to grow larger as compared with water.

Robust and High Current Cold Electron Source Based on Carbon Nanotube Field Emitters and Electron Multiplier Microchannel Plate: *Raghuandan Seelaboyina*¹; Srinivas Rao Bodepalli¹; Wonbong Choi¹; ¹Florida International University

Vacuum microelectronics has been studied for decades to develop unique devices such as rf-generators, high efficiency flat panel displays, x-ray sources and so on. In recent years field emitters based on carbon nanotubes (CNTs) and other nano materials have demonstrated high emission current densities making them prime candidates for next generation vacuum microelectronic applications. However the emission efficiency and stability of these materials is hindered by non uniform emission and emitter destruction in high electric field conditions. To achieve higher and stable current we have designed and fabricated a unique ceramic microchannel plate (MCP) consisting of high secondary emission yield (SEY) materials. The MCP was fabricated utilizing the optimum design parameters, which include channel dimensions and material properties obtained from charged particle optics (CPO) simulation. In this presentation we will discuss the results on our new microchannel plate design (simulation), fabrication, and field emission current amplification from vertically aligned carbon nanotube tower structures and microchannel plate assembly.

Computational Thermodynamics and Kinetics: Poster Session

Sponsored by: The Minerals, Metals and Materials Society, TMS Electronic, Magnetic, and Photonic Materials Division, TMS Materials Processing and Manufacturing Division, ASM Materials Science Critical Technology Sector, TMS: Chemistry and Physics of Materials Committee, TMS/ASM: Computational Materials Science and Engineering Committee, TMS/ASM: Phase Transformations Committee
Program Organizers: Yunzhi Wang, Ohio State University; Long-Qing Chen, Pennsylvania State University; Jeffrey Hoyt, McMaster University; Yu Wang, Virginia Tech

Sunday PM
March 9, 2008

Room: Hall 12
Location: Ernest Morial Convention Center

Session Chairs: Yunzhi Wang, Ohio State University; Long Qing Chen, Pennsylvania State University; Jeffrey Hoyt, McMaster University; Yu Wang, Virginia Tech

Investigation of Atom Size Effects on Binary Alloys Phase Diagrams Using a Relaxed Monte Carlo Approach: *Mathieu Fevre*¹; *Alphonse Finel*¹; *Yann Le Bouar*²; ¹ONERA; ²CNRS-ONERA

The precise determination of phase diagrams is essential to understand the microstructural evolution in metallic alloys. Theoretical predictions are difficult and usually rely on simplifying assumptions, such as interatomic potentials on a rigid lattice. In this study, we investigate a more realistic situation where atoms can move freely and interact through a position dependent potential. Using relaxed Monte Carlo simulations, we calculate the phase diagram of binary alloys exhibiting a phase separation (Cu-Ag type) or an order-disorder transformation (Cu-Au type). The whole composition range, from low temperature up to the liquid state is considered. By changing the parameters values of the potential, we have systematically studied the evolution of the phase diagram when the difference between the atomic radii of the two components is increased. The understanding of the phase stability in thin films and nanoparticles, where elastic relaxations play a major role is a natural extension of this work.

Prediction of the Thermodynamic Properties of Liquid Alloys by Molecular Interaction Volume Model: *Hongwei Yang*¹; *Dongping Tao*¹; ¹Kunming University of Science and Technology

The thermodynamic properties (for example: activities and mixing enthalpies) of ternary and quaternary liquid alloys are calculated by molecular interaction volume model (MIVM) which is a two-parameter model with the partial molar infinite dilute mixing enthalpies. The predicted values are in agreement with the

experimental data and then indicate that the model is reliable, convenient and economic.

First Principle Calculation of the Structural and Electronic Property of Zr Doped $B_{13}C_2$: *Yu Liang*¹; Ru Hongqiang¹; Jiang Yanli¹; Zuo Liang¹; Xue Xiangxin¹; ¹Northeastern University

The first principle calculations based on density functional theory were carried out to study the stability and electronic properties of three structural unit models of Zr atom doped boron carbides ($B_{13}C_2$) crystal using CASTEP code which employed a plane wave-pseudo potential expansion technology. The calculations results show that Zr atom doped boron carbide is in preference to substituting C atom on the end of boron carbide chain, a representative structural unit containing Zr atom is [C-B-Zr] ϵ^- -[B11C] ϵ^- , while the structural unit without Zr is [C-B-C] ϵ^- -[B11C] ϵ^+ . The band and density of states(DOS) indicates that the coexistence of these two different structural units makes the electrical conductivity increased. As the covalent bond of Zr-B is weaker than those of B-B and B-C, and the thermal conductivity decreases when Zr doped $B_{13}C_2$, the thermoelectric property of Zr doped boron carbides will be improved.

Anharmonic Phonons in A15 V3X Compounds: *Oliver Delaire*¹; Jorge Munoz¹; Matthew Lucas¹; Max Kresch¹; Rebecca Stevens¹; Brent Fultz¹; ¹California Institute of Technology

Using inelastic neutron scattering, we investigated the temperature-dependence of the phonon density of states (DOS) in the A15 compounds V3Si, V3Ge and V3Co. Phonons in V3Si exhibit an anomalous stiffening up to temperatures $T > 500$ K, while V3Co and V3Ge exhibit the more common softening, expected from thermal expansion. We also measured the heat capacity of the compounds, which could be correlated to the trend observed in the phonons. To help interpret experimental results, we performed Density functional theory (DFT) calculations of these materials. The calculated phonon DOS was in good agreement with the low-T measurements. The electronic part of the heat capacity was also obtained from the DFT computations. V3Si and V3Ge are known to exhibit a fairly strong electron-phonon coupling, as evidenced by their rather high superconducting T_c ($T_c = 16$ K for V3Si). Anharmonic couplings arising from phonon-phonon or electron-phonon interactions are used to explain the departure from the quasiharmonic behavior.

Modeling of Dynamic Strain Aging in Solid Solutions: Part II: Multiple Strengthening Mechanisms: *Monica Soare*¹; William Curtin¹; ¹Brown University

Having previously shown that a full rate theory for thermally-activated dislocation motion involving a single rate-dependent dislocation strengthening mechanism is unable to predict a regime of negative strain rate sensitivity, here the analysis is extended to incorporate two concurrent mechanisms, solute strengthening and forest hardening, each of which is influenced by the same time-dependent solute diffusion. Explicitly, solute diffusion toward both (i) temporarily arrested but otherwise mobile dislocations and (ii) forest dislocations formed during the plastic deformation are considered simultaneously. Solute strengthening controls the overall rate dependence so that forest hardening enters the theory as a time, strain, and strain-rate dependent "backstress" acting on the mobile dislocations. The model includes the influence of plastic strain, strain rate, temperature, and solute concentration. Comparisons to experimental data on Al-Mg alloys show broad quantitative agreement, including non-intuitive features such as the non-additivity of solute strengthening and forest hardening at low strain rates.

Solute Drag Simulations in Grain Growth with Realistic Interaction Potential Input from Atomistic Simulations: *Michael Gao*¹; Anthony Rollett¹; Branden Kappes¹; Moneesh Upmanyu²; ¹Carnegie Mellon University; ²Colorado School of Mines

With the solute-grain boundary interaction potentials calculated from atomistic simulations, solute segregation and solute drag phenomena are reexamined using gradient weighted finite element package GRAIN3D coupled with solute diffusion field in 3-dimension grain growth. Specifically, the potential versus distance away from a grain boundary plane are computed using embedded atom method (EAM) for fcc Al with impurity of Mg for a flat tilt grain boundary with tilting angle of 0, 32, 35, 37, 38 and 40 degrees. These measured potentials are then directly input into GRAIN3D to simulate Mg segregation and the

corresponding drag effect during grain growth. Our simulation results are compared with analytical models reported in the literature.

Grain Growth Simulations with Langevin Noise: *Nele Moelans*¹; Frans Spaepen²; ¹Katholieke Universiteit Leuven; ²Harvard University

We have added, in a thermodynamically consistent way, Langevin noise to a diffuse interface (phase field) model for grain growth. With this model we simulated how thermal noise affects grain growth. The total energy content of the simulated system was measured as a function of time. Energy jumps were linked to special events in the grain growth process, for example the disappearance of a grain. Depending on the magnitude of the noise, certain events and processes are induced or accelerated. Furthermore, we studied the stability and occurrence of (local) metastable grain configurations as a function of the magnitude of the noise. Langevin noise is also successful in preventing artificial pinning and drag in simulations, for example as a result of low resolution of the numerical technique.

Phase Field Study of Precipitate Growth Kinetics: Effect of a Misfit Strain: *Rajdip Mukherjee*¹; Thennathur Abinandanan¹; *Mogadalai Gururajan*²; ¹Indian Institute of Science; ²Northwest University

Laraia and Johnson presented a model for the kinetics of growth of an isolated, dilatationally misfitting precipitate. Our study - using a phase field model based on the Cahn-Hilliard equation - is aimed at validating their results through 'computer experiments', since those results are not amenable for direct experimental verification. We first establish the validity of phase field experiments by showing that the parabolic growth coefficient obtained from our phase field simulations is in very good agreement with that obtained through a numerical solution of the classical Zener problem with a variable diffusivity. We then show that the parabolic growth coefficient for a dilatationally misfitting precipitate is in agreement with that obtained from the sharp interface model (modified to account for composition-dependent diffusivity) of Laraia and Johnson. In more supersaturated alloys, since curvature effects are smaller, the agreement between phase field results and those from the sharp-interface model is better.

Microscopic Phase-Field Simulation of the Ni_3Al Phase Separation Process: *Yanli Lu*¹; ¹Northwestern Polytechnical University, School of Materials Science and Engineering

The separation process of Ni_3Al phase in Ni-Al alloy containing 12.5at.% Al was simulated at the atomic scale using the microscopic phase-field model and microelasticity theory. The simulation results show that Ni_3Al phases firstly are formed from the disordered solid solution by the mechanism of non-classical nucleation growth, resulting in the appearance of single ordered domain separated by the antiphase domain boundaries (APBs). With the ordered domains isostructural decomposing and the Al-lean regions disordering spontaneously, the equilibrium state is formed finally. In the whole stage of precipitation, the shape of Ni_3Al phase becomes more regular and their orientation becomes more obvious, at the later stage, Ni_3Al phases present quadrate shape with round corner and align along the [10] and [01] directions.

Development and Calibration of Pseudo-Binary Phase Field Modeling for Microstructural Evolution in Multi-Component Alloys: *Billie Wang*¹; James Lill²; Youhai Wen³; Jeff Simmons⁴; Yunzhi Wang¹; ¹Ohio State University; ²High Performance Technologies Inc.; ³UES Inc.; ⁴Air Force Research Laboratory

Alloy development time is under constant pressure to be reduced. Physics-based modeling promises to make the most efficient use of experimentalist time by identifying processing windows for the formation of desirable microstructures. In order to be incorporated into the development cycle, a model must be calibrated rapidly and accurately, and be computationally efficient. To this end, a pseudo-binary phase field methodology that captures the kinetics of microstructural evolution of a multi-component system was developed. The parameters for the pseudo-binary model were optimized using the simplex method to match experimental measurement on average particle size as function of time. A penalty function was defined to quantify deviation from target parameters and accounts for uncertainty in literature, database and experimental data. Preliminary results will be presented.

Model Study and Forecast on the Behavior of Rare Earth during Solidification Process of Heavy Rail Steel: Liu Chengjun¹; ¹Northeastern University

A thermodynamic model was developed to describe quantitatively elements segregation and inclusions precipitation during solidification process of heavy rail steel. According to the SEM and energy spectrum analysis, the model could completely consist with experimental results. The state of RE and constituents of inclusions in heavy rail steel with different cleanliness were studied. The results as follows: (1) The increment of RE dissolved in heavy rail steel mainly has two stages: the first stage is before the RE second phases were not precipitated, the second stage is after the separation react of the RE second phases reached equilibrium. And the increment of the second stage is more obvious. (2) Under the conditions of the same RE addition, the content of solid lanthanum dissolved in heavy rail steel is more than that of cerium. Alloying function of lanthanum is better than that of cerium.

Numerical Simulation of Twin-Roll Strip Casting Process: Jieyu Zhang¹; Bo Wang²; ¹Shanghai University; ²Inner Mongolia University of Science and Technology

A three-dimensional mathematical model has been developed to simulate fluid flow, heat transfer, and solidification in twin-roll strip casting of steel. The two equation model is used to incorporate the turbulence in fluid flow. The effect of the casting speed, superheat, and roll gap on the flow and temperature field was predicted. The simulation results showed that it was desirable for the wedge metal delivery system to not only gain the uniform of flow and temperature in the pool, but also improve strip quality and ensure casting process.

Thermodynamics of Liquid Phase Sintering of SiC Using Al₂O₃ and Y₂O₃ as Sintering Additives: Hans Seifert¹; Damian Cupid²; Olga Fabricichnaya¹; ¹Technische University Bergakademie; ²University of Florida

A thermodynamic dataset for the Al-C-O-Si-Y system was used for calculations of multicomponent, multiphase reactions. Some aspects of the liquid phase sintering of silicon carbide using alumina and yttria sintering additives were analyzed. The phase relations in the SiC-Al₂O₃, SiC-Al₂O₃-SiO₂ and SiC-Y₂O₃-SiO₂ systems were calculated. Phase fraction diagrams, isopleths, isothermal sections, and potential phase diagrams are presented to illustrate the reactions between silicon carbide and sintering additives. The effect of Ar inert gas as an additional component and the related volume change of the gas phase were considered. In addition, the influence of surface silica on silicon carbide powder is taken into account.

Modeling of Oxygen Kinetics in a Ag/MgO Composite: Nilindu Muthubandara¹; Irina Belova¹; Andreas Oechsner²; Graeme Murch¹; ¹University of Newcastle; ²Technical University of Malaysia

The presence of atomic oxygen at metal/oxide interfaces can significantly affect the physical properties of interfaces and hence the properties of the bulk material. We modeled oxygen diffusion in Ag-MgO composites with a Lattice Monte Carlo method and the finite element method. First, we considered oxygen in-diffusion from a constant surface source solely into a Ag metal matrix: oxygen depth profiles were in excellent agreement with exact results. Next, we simulated oxygen in-diffusion/segregation in the composite permitting and restricting the mobility of oxygen in different scenarios involving the Ag-MgO interface. The (higher temperature) out-diffusion of oxygen from the composite was also simulated and corresponding results obtained for the oxygen depth profiles. In both cases, very good agreement was found between the Lattice Monte Carlo method and the finite element method.

Kinetic Study on Chromium Ore Dissolution in CaO-SiO₂-MgO-Al₂O₃ Melts: Jiang Maofa¹; ¹Northeastern University

To reveal the smelting reduction mechanism of chromium ore for producing stainless steel in converter, the dissolution behavior of chromium ore in CaO-SiO₂-MgO-Al₂O₃ slag system was studied by laboratory experiments, and the effect of different temperature and slag composition on the dissolution rate of chromium ore in slag was investigated. The dissolution mechanism of chromium ore in slag was discussed. A kinetic model for dissolution process of chromium ore was developed on macrokinetics theory for the first time. According to the data of dissolution experiments, the regression expression between the dissolution rate constant and the temperature and slag composition was obtained. It was found that the dissolution process of chromium ore is controlled

by the surface dissolution reaction on conditions of the present experiments, where the temperature has significant effect on the reaction rate constant of chromium ore dissolution. The calculated value of dissolution activation energy is 524.50 kJ·mol⁻¹.

Study on Dynamic Mathematical Model of Ion Exchange Process: Changren Tong¹; Fengli Yang¹; Xiaoxue Zhou¹; ¹Jiangxi University of Science and Technology

Based on the mechanism analysis of fixed-bed ion exchange process, the relationship among solution flow in column, external diffusion, inner diffusion and ion exchange reaction was given an overall consideration, with the aid of thermodynamics, Fick's law of diffusion and flow solution micro-layers idea, dynamic mathematical model on fixed-bed ion exchange process was developed. In the paper, simulation verification based on an example of tungsten ion exchange process was carried out. The results show the dynamic mathematical model was in agreement with ion exchange practical process, and it would provide guidance and reference for ion exchange process.

General Poster Session

Sponsored by: The Minerals, Metals and Materials Society

Sunday PM
March 9, 2008

Room: Hall 12
Location: Ernest Morial Convention Center

On the Phase Diagram and Thermodynamics of the Al-Ca-Cu System: A Combined Approach of Experiments, CALPHAD and First-Principles Calculations: Michael Gao¹; Gary Shiflet¹; Marek Mihalkovic²; Michael Widom²; ¹University of Virginia; ²Carnegie Mellon University

This study combines critical experiments, CALPHAD modeling and first principles calculations to determine the Al-Ca-Cu ternary phase diagram and the quantitative thermodynamics. Using electron microprobe analysis, nine ternary compounds are experimentally identified. Four ternary compounds and three binary compounds are found to have extended Al/Cu solubility. The compound crystal structures are proposed according to first principles calculations. The observed Al/Cu homogeneity ranges are in good agreement with theoretical predictions. Based on current first principles calculations and experimental results, the complete phase diagram of Al-Ca-Cu is updated and the thermodynamic descriptions are determined via CALPHAD modeling.

Microstructure Evolution and Mechanical Properties of In-Situ Fe-Zr-Nb Ultrafine Eutectic Composites: Tae Eung Kim¹; Jin Man Park¹; Ka Ram Lim¹; Won Tae Kim²; Do Hyang Kim¹; ¹Yonsei University; ²Chongju University

Recently, there have been considerable interests in the development of nano/ultrafine grained materials for structural applications. However, applications of these materials are restricted by various reasons such as complex processing route, limited size and low ductility at room temperature. To overcome the limited ductility of these materials, a new concept for the design of composite microstructure with different length scale has been proposed.¹ In this study, we investigated the development of in-situ nano/ultrafine eutectic composites in Fe-Zr-Nb alloy system by tailoring the microstructure during solidification processing. The morphology and distribution of primary phases (α -Fe or Fe₂Zr) and the scale of α -Fe/Fe₂Zr eutectic have been significantly changed depending on the alloy composition. To improve strength and ductility, Cr and C have been added as strengthening elements in ternary Fe-Zr-Nb alloy system. ¹E. Ma *et al.*, "High tensile ductility in a nanostructured metal" NATURE VOL 419, p912-915.

Nano Eutectic Al-Ag₂Al Composites with High Strength and Ductility: Sung Woo Sohn¹; Jin Man Park¹; Tae Eung Kim¹; Ka Ram Lim¹; Won Tae Kim²; Do Hyang Kim¹; ¹Yonsei University; ²Chongju University

Recently, extensive investigations have been carried out on nano/ultrafine structured materials due to outstanding mechanical properties. Nano/ultrafine grained alloys exhibit high strength but lack of ductility, which restricts their application. The Al-Ag system, which contains a eutectic between the Al solid solution and the Ag₂Al compound, has been selected since the slopes of liquidus, solidus and solvus are very different for the two sides. The alloy compositions studied in the present study are Al-xAg (x= 65, 67 and 69 at%). In-situ eutectic

structure has been obtained under the conditions of various cooling rate such as melt spinning, injection casting, and conventional mold casting. Each sample has been carefully observed using secondary electron microscopy (SEM) and transmission electron microscopy (TEM). The cylindrical samples with 1 mm diameter have been tested in compression mode at room temperature, showing the strength of over 800MPa with a notable strain of 25%.

Microstructural Characterization in Cast AlMg Alloy-SiCp Composites: S. Valdez¹; B. Campillo¹; R. Perez¹; L. Martínez¹; A. García H.²; ¹Instituto de Ciencias Físicas-Universidad Nacional Autónoma de México; ²Facultad de Química-Universidad Nacional Autónoma de México

On the present investigation, microstructural behavior of 10 vol% SiCp reinforced composites was investigated. The composites used were produced by vortex technique. In the vortex process, an Al-8.7 wt% Mg as-cast alloy added with SiC particulates were mixed into the steel tubes at 1500 rpm. The metal-matrix composites was characterized with the purpose of knowing and quantifying the present phases, distribution of stiffener and the interaction of SiC particulates with the metal-matrix. Material characterization was made by means of X-ray diffraction (DRX) and scanning electron microscopy (MEB). Composite microstructure is influenced by solidification parameters and processing conditions. Hence, mechanical properties are highly sensible to the microstructure and these are indirectly related to the preparation route, so processing parameters involved have a great importance. Vortex technique generates a composite with non secondary chemical reactions, minimum porosity approx. 5%, and uniform particles distribution in the Aluminum matrix.

Mean Width Evaluation on Regular Grids: Seth Wilson¹; A.D. Rollett¹; ¹Carnegie Mellon University

We develop and compare several methods to compute the mean width (first-order Minkowski functional) of grains represented on regular grids. Error analysis is presented for a variety of shapes with cusps, creases, facets, and curved surfaces whose mean widths are known exactly. We use our mean width measurements to test the 3D generalization of the vonNeumann-Mullins relation conjectured by MacPherson and Srolovitz (Nature 2007), in the context of multiphase field and Monte Carlo models of isotropic normal grain growth. Results are presented for single grains as well as large networks of grains.

Microstructural Studies of Heteroepitaxial Silicon-on-Sapphire by TEM: Titus Dutta¹; Gopinath Trichy¹; Jagdish Narayan¹; ¹North Carolina State University

Silicon on sapphire (SOS) based devices have extremely small parasitic junction capacitance and hence are suitable for high speed-low power applications. The performance of SOS devices depend on the film-substrate interface and defects that arise due to the high misfit (14%) strain. We report on the detailed investigation of misfit defects in the heteroepitaxial Si(100)/r-plane of sapphire system by cross sectional transmission electron microscopy (TEM). The SAED pattern with the zone axis, $\langle 100 \rangle_{\text{Si}} \parallel \langle 01-11 \rangle_{\text{Sap}}$, revealed the following epitaxial relationship: $(040)_{\text{Si}} \parallel (-4-220)_{\text{Sap}}$. Epitaxial growth in this high misfit system is interpreted and explained by domain matching epitaxy, where integral multiples of lattice planes match across the film-substrate interface. HRTEM revealed a sharp interface with no interfacial reaction. The Si film showed extensive twinning, the linear twin density was estimated to be $2 \times 10^5/\text{cm}$. Evidence of ion-channeling within the twinned region has also been demonstrated.

The Change of Microstructure and Hydrogen Permeation of Nb-TiNi Alloys with Various Ti/Ni Ratios: Tetsuya Kato¹; Kazuhiro Ishikawa¹; Kiyoshi Aoki¹; ¹Kitami Institute of Technology

High purity hydrogen is mainly produced by purification of steam reformed gas by using the Pd-based hydrogen permeation alloy membrane. However, Pd is too expensive and rare in resources, so that non-Pd alloys are strongly desired. We have demonstrated that the Nb-TiNi alloys having the Ti/Ni ratio = 1.0 show high hydrogen permeability and large resistance against the hydrogen embrittlement. However, their performance is insufficient for industrial applications. The value of permeability increases with increasing Nb content in the Nb-TiNi alloys with Ti/Ni ratio=1.0, but the higher Nb content alloys suffer from the hydrogen embrittlement. In the present work, the effect of Ti/Ni ratio on the microstructures, crystal structures and permeability of Nb-TiNi alloys is investigated and discussed on the basis of the experimental data.

Synthesis and Hydrogen Absorption of Li-Doped Titanate Nanotube by Hydrothermal Ion Exchange Processing: Yi-Hun Jung¹; Dong Hyun Kim¹; Sun-Jae Kim²; Kyung Sub Lee¹; ¹Hanyang University; ²Sejong University

Titanate nanotubes have been studied for hydrogen storage due to its unique shape of interlayers. However, absorbing reaction occurred only at a high temperature and/or low temperature (at -196°C and over 250°C). In order to improve the hydrogen capacity of titanate nanotubes at RT, Li-doped titanate nanotubes were synthesized by hydrothermal lithium ion exchange processing from titanate nanotube precursor. To prepare the Li-doped TNT, titanate nanotubes powder was mixed with LiOH aqueous solution and the resulting suspension placed in a Ni-lined stainless-steel autoclave at 120°C for 24 hrs. And Li-doped TNT were fired at 100-500°C in vacuum to remove the hydrate in the nanotube. The sorption of hydrogen of the titanate nanotubes was studied by the conventional volumetric pressure-composition isothermal method at RT, 10 to 40atm. Systematic studies of effect of Li dopant in the nanotube and the relationship between interlayer spacing and hydrogen capacity with firing temperature were presented.

The Effect of Addition of Sn, Zr and B on the Microstructure Evolution in Zn-Al Alloy: Ka Ram Lim¹; Jin Man Park¹; Tae Eung Kim¹; Sung Woo Sohn¹; Hee Tae Jeong²; Won Tae Kim¹; Do Hyang Kim¹; ¹Center for Noncrystalline Materials; ²BK21

Zn-Al alloys are well-known to have excellent damping properties when they are quenched from above the eutectoid temperature of 550K. The reduction of the lamella spacing in Zn-22 wt.% Al eutectoid alloy can lead to the increase of damping capacity. In the present study, Zn-22 wt.% Al alloy has been prepared by casting into a copper mold followed by rolling with reduction of ~ 50 %. Almost fully lamella structure has been obtained in Zn-22 wt.% Al alloy by heat treatment under the eutectoid temperature. The lamella spacing is about 200~300 nm. The orientation relationship between lamellae is $[11-20]_{\beta} \parallel [110]_{\alpha}$, $(0001)_{\beta} \parallel (-111)_{\alpha}$, which corresponds to the previous result. The effects of replacement of Zn by Sn, Zr and B on the spacing of lamella have been investigated. In addition, the effect of processing methods such as rolling and reciprocating extrusion on the microstructure and mechanical property has also been investigated.

Plasticity Size Effects: A Mechanism-Based Discrete Dislocation Analysis of Micro-Crystals: P. Guruprasad¹; Amine Benzerga¹; ¹Texas A&M University

Mechanism-based discrete dislocation plasticity (M-DDP) is used to study the effect of dimensional constraint on micro-crystals. The M-DDP framework involves key dislocation mechanisms including junction formation, dynamic source and dynamic obstacle formation, in addition to dislocation nucleation, annihilation and dislocation escape near the surface. Initially high dislocation source density specimens oriented for double-slip are subjected to macroscopically homogeneous deformation with applied strain rate varied between $10^4 - 10^5/\text{s}$. In general all the specimens showed stress strain response typical of bulk crystals highlighted by strong size affected stage II hardening rate (Θ_H). A slight decrease in the flowstress values were observed with decrease in strain rate, nevertheless Θ_H remained significant. The observed strengthening was attributed to the emergence of a net GND density locally. As a consequence of the net GND build-up we observe: (a) Taylor hardening law breaks down (b) strong Bauschinger effect in the specimens below micron scale.

Synthesis and Mechanical Properties of Al₂O₃/Ti₅₀Cu₂₈Ni₁₅Sn₇ Bulk Metallic Glass Composite: Pee-Yew Lee¹; Chih-Feng Hsu¹; ¹National Taiwan Ocean University

In the present study, the preparation of Ti₅₀Cu₂₈Ni₁₅Sn₇ metallic glass composite powders was successfully synthesized by the mechanical alloying of powder mixtures of pure Ti, Cu, Ni, Sn and Al₂O₃ after a 6h milling. In the ball-milled composites, the initial Al₂O₃ particles were homogeneously dispersed in the Ti-based alloy glassy matrix. The metallic glass composite powders were found to exhibit a large supercooled liquid region before crystallization. Bulk metallic glass (BMG) composite compact discs were obtained by consolidating the 6h as-milled composite powders by vacuum hot pressing process. The microstructure of the Ti₅₀Cu₂₈Ni₁₅Sn₇ BMG with 8 vol. % Al₂O₃ additions exhibited an amorphous matrix embedded with Al₂O₃ nanoparticles ranging from 20 to 300 nm. A significant hardness increase with the Al₂O₃ additions can be achieved for the Ti₅₀Cu₂₈Ni₁₅Sn₇ BMG composites. These BMG composites exhibit good mechanical properties of 1880~2190 MPa for compressive strength and 2.0~2.27 for compressive elastic strain.

The Role of Carbide Morphology in High Temperature Deformation of a Modified Single Crystal Nickel-Base Superalloy: *Andrew Wasson*¹; Gerhard Fuchs¹; Elyssa Cutler¹; ¹University of Florida

Carbon additions to single crystal Ni-base superalloys are known to reduce casting defects, surface scale, and oxide inclusions in large blade castings such as those in industrial gas turbines. In this study, the effect of carbon, carbon and boron, and carbon and nitrogen additions on the microstructure, high temperature tensile, creep, and high cycle fatigue behavior of CMSX-4 was examined. All tests were conducted at 850°C. The analysis focused on how the different additions altered the carbide morphology and how this carbide morphology affected the different modes of deformation and failure. The carbon and nitrogen additions produced carbides that were primarily blocky while the other alloys exhibited more script morphology carbides. Fracture surfaces and post-test microstructures were used to show how the carbides affected the various deformation mechanisms.

Thermal Stability of Cu-Sn Metal-Metal Interconnects: *Jemima Fernandez*¹; Megan Frary¹; Amy Moll¹; ¹Boise State University

Cu-Sn is currently being investigated as an alternative to Pb-Sn solders. It is especially interesting for small scale solder bumps and fine pitches. With the appropriate bonding conditions, the preferred phase of Cu-Sn (Cu₃Sn) can be formed at the interface of two bond pads. This phase should be thermodynamically stable (for up to 350°C) and withstand multiple reflow cycles encountered during the assembly process of a multilayer interconnect stack. This paper investigates the thermal stability and reliability of Cu-Sn bonded die with different Sn thicknesses and bonding pressures. The samples are isothermally aged at 125°C ± 10°C and also subjected to thermal cycling from 125°C to -55°C. The samples are analyzed before and after experiments to track any changes in inter-metallic growth, grain-structure, die cracking, package cracking, and bond lifting with analytical tools including Transmission Electron Microscopy (TEM), Scanning Electron Microscopy (SEM) and Electron Back Scattered Diffraction (EBSD).

Phase Transformation into α Phase Enhanced by Substrate Surface Defects in an Alumina Thin Film Grown on Si(001): *Sung Bo Lee*¹; *Eun Kyu Her*¹; *Kyu Hwan Oh*¹; ¹School of Materials Science and Engineering, Seoul National University

A 250-nm-thick Al₂O₃ film was deposited on a Si(100) 4-inch wafer by a radio-frequency (rf) magnetron sputtering and annealed at 1050°C for various times in air. In the matrix composed of fine grains of about 50 nm in diameter, large α -Al₂O₃ grains of about 2-5 μ m in diameter were formed, arranging themselves in rows. The thermal expansion coefficient of alumina is higher than that of silicon, which develops compressive stresses in the film. The observed, enhanced phase-transformation into α -Al₂O₃ is suggested to start at surface steps in the Si wafer which may bring the highest strain energy to the interface between Al₂O₃ film and Si substrate. This phenomenon was analyzed using Electron Backscattered Diffraction (EBSD), Focused Ion Beam (FIB) and Transmission Electron Microscope (TEM).

Slag Detection Technology: *Prasad Goundla*¹; Rizwan Abdul Rahman Rashid¹; Gouni Rajkiran¹; Siva Jyoth Reddy¹; ¹Mahatma Gandhi Institute of Technology

The occurrence of slag during the production of steel is inevitable with the result that the steel loses its quality thereby imposing severe financial losses on producers. Hence Slag Kills Profits. Now thanks to FLIR's advanced Infrared imaging technology, slag can be detected during casting of crude steel. The highly user-friendly, hand-held A20M state-of-the-art tool detects & records the presence of slag and emits a control signal enabling the operator to interrupt the process. The system also comes integrated with software for remote shutdown possibilities. In this paper, we discuss the properties of this technology, its proper usage techniques and its advantages to the steel industry fraternity.

The Study of the Destabilized Effect in NaAlH₄ Using TiN and BN: *Tabbatha Dobbins*¹; *Whitney Fisher*¹; ¹Louisiana Technical University

Destabilized metal hydride systems are gaining increased attention due to their ability to undergo a lowered hydrogen desorption reaction temperature (moving toward targeted temperatures set by the Dept. of Energy). LiBH₄ has been destabilized using MgH₂ (Vajo, Skeith, and Mertens) with a demonstrated lowering of the hydrogen desorption reaction temperature by 90 C (compared to LiBH₄ alone). This research reports on the potential for destabilization of NaAlH₄ using TiN and BN as destabilizer phases. The samples prepared were

NaAlH₄ with varying concentrations of TiN or BN (specifically, 25 mol%, 50 mol%, and 75 mol% concentrations were used). The destabilizer was introduced to the hydride powder system using high energy ball milling (SPEX 8000M mill in WC mill media). After high energy milling, the formation of TiAl (using the TiN destabilizer) was determined by x-ray diffraction. Alternatively, there was no formation of Al-B phases.

Synthesis and Characterization of Bulk Amorphous/Amorphous Composite Alloys through Powder Metallurgy Route: *Pee-Yew Lee*¹; ¹National Taiwan Ocean University

Recently dual-amorphous phases bulk metallic glasses (DAPBMG) consisting of two metallic glassy phases has attracted increasing R&D interests. Similar to the concept of composite material, DAPBMG can be expected to exhibit dual properties of its original ones. In this study, we attempt to prepare the DAPBMG through powder metallurgy route. The amorphous Ni₆₀Nb₂₀Zr₂₀ and Ti₅₀Cu₂₈Ni₁₅Sn₇ alloy powders were synthesized separately by mechanical alloying technique. The dual-phase powders were prepared by mixing corresponding amorphous powders. The amorphous dual-phase powders were then consolidated into DAPBMG discs. The microstructure of DAPBMG discs showed that the Ni₆₀Nb₂₀Zr₂₀ phase is distributed homogeneously within the Ti₅₀Cu₂₈Ni₁₅Sn₇ matrix. The mechanical behavior of the DAPBMG was investigated by hardness test. The measured hardness values follow the rule-of-mixture equation for describing the hardness of the composite materials. The relative density and Vickers microhardness of DAPBMG increase as the amount of Ni₆₀Nb₂₀Zr₂₀ of the bulk samples increases.

Morphological Changes after H₂ Desorption from Ti³⁺-Catalyzed NaAlH₄: *Nicholas Dailey*¹; *Tabbatha Dobbins*²; ¹Grambling State University; ²Louisiana Technical University

With the continuing problem with global warming, a way to properly store hydrogen in cars needs to be established in order to institute environmentally "clean" energy technologies. Our research addresses issues in hydrogen storage materials by studying powder morphology changes. Specifically, Ti³⁺-catalyzed NaAlH₄ is demonstrated to experience morphological changes upon hydrogen desorption at 150C and 200C. After desorption at 150C for 5 minutes, the NaAlH₄ powder appeared to have melted (as indicated by both the powder morphology and the loss in intensity in the x-ray diffraction peaks). Melting occurred prior to any transformation to the product phases. Alternatively, experiments performed at 200C for 5 minutes showed that the powders partially transformed to Na₃AlH₆ and Al product phases. Those powders appear to have also melted and show an increased quantity of spherical porosity (relative to powders which did not undergo desorption).

Metals Industry Air Metals Emissions and Hazard Rankings: *John Heinze*¹; *Karen Hagelstein*²; ¹Environmental Health Research Foundation; ²TIMES Limited

Total releases of metal air emissions (18 metals) from the metals manufacturing industry (SIC33XX) were over 3400 tons in 2005, according to the latest US EPA Toxic Release Inventory data. These emissions represent the largest source of metal air emissions of any industry sector in the US. Because metals have well recognized human health and the environmental hazard properties, metal air emissions can be prioritized not only by the amount of metal compounds released, but also by their hazard properties, also called "toxicity weighting." For example, the five most toxic metals according to EPA's Toxicity Characteristic Leaching Procedure (TCLP) for hazardous waste metal compounds are: mercury, followed by cadmium and selenium, and then arsenic and lead. The Indiana Relative Chemical Hazard Score (IRCHS) and other methods of hazard ranking will be evaluated and compared as methods for prioritizing hazard impacts and environmental management practices in metals manufacturing.

The Influence of Heterogeneity in Grain Boundary Sliding Resistance on the Constitutive Behavior of AA5083: *David Cipoletti*¹; *Allan Bower*¹; *Yue Qi*²; *Paul Krajewski*²; ¹Brown University; ²General Motors R&D Center

Continuum finite element simulations are used to investigate the influence of heterogeneity in grain boundary sliding resistance on the creep response of the aluminum alloy AA5083 when deformed at 450°C. Previous simulations and experiments have demonstrated that under these conditions, grain boundary sliding (GBS) is the dominant deformation mechanism at strain rates below 0.001, and dislocation creep (DC) is the dominant mechanism for higher strain

rates. However, these simulations assumed a uniform resistance to sliding on all grain boundaries. Molecular dynamic simulations indicate that sliding resistance is strongly sensitive to the character of the boundary: high angle boundaries have resistance up to an order of magnitude lower than low angle boundaries. Finite element simulations are used to investigate the influence of the fraction of high angle boundaries f in a polycrystal on its creep response and operative deformation mechanisms. Computation results showed that GBS heterogeneity greatly influenced the constitutive response.

Nanoscale Electrical Properties of NiO Thin Films: *Cheol-Hwan Kim*¹; Hak-Beom Moon¹; Seong-Sik Min¹; Yun-Hyung Jang¹; Jin-Hyung Cho¹; ¹Pusan National University

The electrical properties of NiO thin films have been studied extensively to exploit their resistance change effect to nonvolatile memory devices. To understand the mechanism of the resistance change, we have studied nanoscale electrical properties of NiO thin films grown by RF magnetron sputtering method. The nanoscale electrical properties were measured using the conducting atomic force microscopy (CAFM) and the electric force microscopy (EFM) and the data indicate that the transition of resistance states results from filamentary conducting paths in the NiO thin films. We will discuss the experimental results of the resistance change of NiO thin films in terms of mechanism of filamentary conducting path.

Microstructural Evolution and Mechanical Properties with Addition of Sn in Mg-MM(Misch-Metal) Alloy: *JoonSeok Kyeong*¹; Hyun Kyu Lim¹; Won Tae Kim²; Do Hyang Kim¹; ¹Yonsei University, Department of Metallurgy/NSM Laboratory; ²Cheongju University

Considering the beneficial effect of MM (misch metal) and Sn addition in Mg-based alloys, it is strongly required to investigate Mg-MM-Sn system for casting products as well as wrought products. Therefore, the present study aims to identify the phases in Mg-RE-Sn system, and to evaluate the mechanical properties of Mg-MM-Sn rolled sheets. The Sn addition into the Mg-MM alloy results in the formation of the feather-shaped phase mainly in the interdendritic region when the ratio of Sn to MM is close to 1 in wt%. Although the strength of alloy is decreased with addition of Sn in Mg-MM alloys, the rollability and ductility are improved when the feather-shaped phase is formed in Mg-rich Mg-MM-Sn alloy due to the sound interface without forming any void at the boundary of the feather-shaped phase during tensile loading.

Laser Synthesis of Porous and Textured Ca-P Bio-Ceramic Coating on Ti-6Al-4V: *Sameer Patil*¹; Narendra Dahotre¹; ¹University of Tennessee

In the present work the feasibility of depositing a porous and geometrically textured Calcium Phosphate (CaP) bio-ceramic coating using a continuous wave Nd:YAG laser on a Ti-6Al-4V substrate has been demonstrated. Advantages offered by such porous bio-ceramic coating is its inertness combined with the mechanical stability of the highly convoluted interface that develops when bone grows into the pores of ceramic. Non-destructive phase analysis of the laser processed samples were carried out using XRD. Quantitative estimation of the crystallite size and relative amounts of Ti, TiO₂ and α -tricalcium phosphate (α -TCP) was obtained. Surface porosity measurements indicated a decreasing trend with increasing laser fluence. In the preliminary studies, the bioactivity of the coatings were further proved by the formation of an apatite like layer on the surface of the sample after being immersed in a simulated bio fluid.

Hydrogen Permeability of Pure Nb and NbTi Solid Solution Alloys: *Naoyoshi Ota*¹; Kazuhiro Ishikawa¹; Kiyoshi Aoki¹; ¹Kitami Institute of Technology

In recent years, non-palladium based hydrogen permeation alloys have actively been investigated by several research groups. Group 5 metals such as V, Nb and Ta showing large hydrogen solubility and high hydrogen diffusivity are promising for hydrogen permeation membranes, because hydrogen permeability is the product of hydrogen solubility and hydrogen diffusivity. However, it is recognized that these metals suffer severe hydrogen brittleness and are pulverized spontaneously during hydrogenation. Then, they are unusable as a hydrogen permeation alloy. However, it is still uncertain why they are easily broken in a hydrogen atmosphere. In the present work, hydrogen permeability of as-cast pure Nb and the NbTi alloys prepared by arc melting were successfully measured using a conventional gas permeation method. We discuss why hydrogen permeability of the as-cast pure Nb and the NbTi alloys is measurable on the basis of the microstructural observation.

Layer by Layer Nanoarchitectures Assembled Using Al₂O₃ and ZrO₂ Systems: *Kristan Moore*¹; Tabbetha Dobbins²; ¹Grambling State University; ²Louisiana Technical University

For controlling the content and spatial distribution of interphase boundaries in materials, we have used a technique known as layer-by-layer (LbL) nanoassembly. The principle behind electrostatic self-assembly is the use of polyelectrolytes (for example, polyallylamine hydrochloride as polycation and polystyrene sulfonate as polyanion) to provide a coulombic 'glue' between ceramic particulate layers. The inherent surface charge (zeta-potential) on the particulate systems leads to their attraction to the polyelectrolytes. The self-assembly technique has been used to deposit multilayered ceramic films and also been used to provide nm-particle coverage over μ m-scale colloidal particles. Using LbL nanoassembly, we have prepared various Al₂O₃ and ZrO₂. The concentration of the nanoparticles in suspension and deposition time was studied to affect the degree of microstructure control during self-assembly.

Inoculation of Aluminum Alloys with Nanosized Borides and Microstructure Analysis: *Hermes Calderón*¹; Cicily Smith²; Olga Menéndez¹; O. Marcelo Suárez¹; ¹University of Puerto Rico; ²Austing College

The effect of MgB₂, AlB₂, HfB₂, and NbB₂ nanosized particles on the grain structure and microhardness of AA6061 and AA7075 aluminum alloys was studied. The metal boride powders were processed with a vario-planetary ball milling unit to be afterwards mixed with pure aluminum pellets. The resulting mechanical mixture was added as inoculant to the aforementioned alloys. For comparison the alloys were separately treated with a commercial grain refiner. Changes in grain size were observed: while boride-treated AA7075 presented a dendritic structure, the boride-inoculated AA6061 alloy exhibited equiaxed grain structure. Vickers microhardness tests showed that MgB₂ and HfB₂ were most effective in improving mechanical strength of these aluminum alloys. Additionally, Charpy impact test were performed to identify the effect of inoculation on the treated alloys toughness.

Deformation Behavior of Magnesium Alloys with the Low c/a Ratio: *Beomsoo Shin*¹; Donghyun Bae¹; ¹Yonsei University

Deformation behavior of Mg-Re-Zn-Sn alloy sheets has been investigated. The sheets are produced by the conventional thermomechanical processes. Tensile tests were performed at a strain rate of 1x10⁻³s⁻¹ at room and elevated temperatures. The alloys exhibit superior tensile elongation higher than 25% at room temperature. The deformed microstructure shows that the contribution of deformation twinning to total elongation is not so significant, and non-basal dislocations are frequently observed. The non-basal slips can be activated not by the presence of refined grains, but by the low c/a ratio of alpha magnesium phase. The c/a ratio of the phase is measured to be below 1.6. The details of deformation behavior of the alloys will be presented.

Deformation Behavior of Zr-Based Bulk Metallic Glasses Showing No Catastrophic Failure at Room Temperature: *Jaehyuck Shin*¹; Donghyun Bae¹; ¹Yonsei University

Plastic deformation of bulk metallic glasses (BMGs) at room temperature occurs within the highly localized shear bands in which generated excess free volume is spontaneously coalesced, leading to a catastrophic failure of the BMGs even under compression. Therefore, to prevent the catastrophic failure, atomic clustering kinetics should be retarded. Zr-Al-Cu-Ni BMGs with high thermal activation energy have shown a highly deformable behavior without global failure under compression. In addition, further plastic homogeneity in the macroscopic appearance can be achieved with the addition of minor elements in the Zr-based BMGs due to the formation of abundant nano-scale ordered sites which initiate multiple shear bands. With the consideration of structural thermal stability, together with free volume, deformation behavior of Zr-based bulk metallic glasses which show no catastrophic failure at room temperature will be discussed.

Effect of Cr on the Oxidation Behavior of Ti-46Al-2V Alloy: *Daniela Pilone*¹; Ferdinando Felli¹; ¹Sapienza Università di Roma

Titanium aluminide alloys are already used because of excellent mechanical properties, but are limited to low temperature applications due to insufficient oxidation resistance. When these alloys are subjected to oxidation in air the scale is not a protective Al₂O₃ layer, but a mixture of Al₂O₃ and TiO₂. The oxidation resistance of TiAl intermetallics is known to be significantly affected

by the addition of alloying elements. The oxidation behavior of Ti-46Al-2V was studied and compared with the ones of the same alloy alloyed respectively with 7, 10 and 14 at.% Cr. Isothermal tests were conducted in air at 850 and 950°C. The scale's morphology and composition were studied by means of SEM/EDS and X-ray diffraction. From weight gain curves and cross-sectional microscopy after oxidation exposure it was found that more than 7 at.% of Cr improves the oxidation resistance of the alloy, although it simultaneously reduces its toughness.

Effects of Initial Texture on the Deformation Behaviors of Strip Cast AZ31 Mg Alloy: *Byoung Ho Lee¹; Sung Hyuk Park¹; Chong Lee¹; Wonkyu Bang²; Sangho Ahn²;* ¹Pohang University of Science and Technology; ²Research Institute of Industrial Science and Technology

The effect of initial texture on the deformation behavior of AZ31 Mg alloy was (manufactured by strip casting method) investigated in this work. XRD experiments showed that a strong basal texture (implying that the basal planes of HCP lattice in grains were located parallel to the rolling direction) was formed in the rolled plate, while a weak and random basal texture was formed in a strip cast sheet and cast ingots, respectively. Compressive specimens were obtained in two different directions, ND (normal direction) and RD (rolling direction). Microstructure observations and stress-strain curves showed that twin formation in strip-cast AZ31 Mg alloy was strongly affected by initial textures. Constitutive modeling of materials having different initial textures was also conducted in this work through physically-based modeling.

Effect of Prior Deformation on the Sliding Wear Characteristics of the Ultra-Fine Grained (UFG) Dual Phase Steel: *Yong-suk Kim¹; H. Yu¹; D. Shin²;* ¹Kookmin University; ²Hanyang University

Effect of prior deformation on the sliding wear of the ultra-fine grained (UFG) ferrite-martensite dual phase (DP) steel was investigated. The UFG DP steel was fabricated by the ECAP and subsequent intercritical annealing. The steel was cold rolled before the wear test, and the effect of the prior deformation on the wear was examined. The wear tests were carried out at various loads against a bearing steel ball. The wear rate of the UFG DP steel that did not experience the prior deformation was higher than that of the coarse-grained (CG) DP steel, because of more severe surface shear deformation. The wear rate of the specimens with prior deformation was much higher than that of the specimen without prior deformation. The deformed CG DP specimen showed higher rate than the deformed UFG DP specimen, and the rate-variation of the CG DP steel was much bigger under the same test condition.

Chemical Composition Effects on the Microstructure of Functionally-Graded Aluminum Matrix Composites: *Lilia Olaya-Luengas¹; Marcelo Suarez²;* ¹University of Puerto Rico, Mayagüez

Aluminum matrix composites reinforced with boride dispersoids redefine the limits of aluminum-based materials due to their unique mechanical properties, low density and low-cost processing methods. In addition, by centrifugal casting a functionally-graded composite can be fabricated. The redistribution of the denser dispersoids in the aluminum matrix is further affected by changes in the levels of boron, magnesium, copper and calcium. The present research has been focused on studying the functionalized composite microstructure and the resulting graded mechanical properties. The final goal has been to determine the optimal reinforcement distribution as a function of the chemical composition of the material.

Co-Doping (Ti3+, Fe3+, and Zr4+) in NaAlH4 Powders Studied by Ultra-Small-Angle X-Ray Scattering (USAXS): *Ejiohene Oteri¹; Tabbetha Dobbins¹;* ¹Louisiana Tech University

This study uses ultrasmall angle x-ray scattering (USAXS) to elucidate differences in NaAlH4 particle morphology as dopant type and mill time is varied after co-doping using FeCl3-TiCl3, FeCl3-ZrCl4, and TiCl3-ZrCl4. In these co-doped systems, USAXS was used to track changes in powder surface area using measured particle sizes and volume fractions. The variation in desorption rates in those co-doped systems correlated well with changes in powder surface area—indicating surface reaction rates are the limiting factor in hydrogen desorption kinetics for these systems.

Application of Amide-Impregnated Fiber to Separation of Precious Metals: *Hirokazu Narita¹; Mikiya Tanaka¹; Kazuko Morisaku¹; Ken Tamura²; Daisuke Sakamoto³; Masashi Suzuki³; Tomomi Nadano³;* ¹National Institute of Advanced Industrial Science and Technology; ²Chiba Institute of Technology; ³Saitama Industrial Technology Center

The separation of precious metals in a hydrochloric acid solution using a solvent impregnated fiber (SIF) was investigated. N-disubstituted amide compounds and kapok fibers were used as the separation reagents and the impregnation support, respectively. We synthesized N,N-di-n-octyl-lauramide (DOLA), N,N'-dimethyl-N,N'-di-n-octyl-thiodiglycolamide (MOTDGA) and N,N'-dimethyl-N,N'-di-n-octyl-diglycolamide (MODGA) and prepared the amide-impregnated fibers (amide-IF). The adsorption of some precious and base metals (Au(III), Pd(II), Pt(IV), Rh(III), Fe(III), Cu(II), Ni(II) and Zn(II)) in HCl solutions was carried out batchwise using the DOLA-IF, MODGA-IF and MODGA-IF. The results of the metal adsorption showed that the selective separation of Au(III), Pd(II) and Pt(IV) can be performed using successively the DOLA-IF, MOTDGA-IF and MODGA-IF.

Changes in Hydrogen Permeability and Microstructure of Melt-Spun Nb₄₀Ti₃₀Ni₃₀ Alloy Ribbons by Annealed: *Yuta Seki¹; Koichi Kita²; Kazuhiro Ishikawa¹; Kiyoshi Aoki¹;* ¹Kitami Institute of Technology; ²Mitsubishi Materials Corporation

Pd-Ag based hydrogen permeation alloys are mainly used for separation and purification of hydrogen gas. However, since Pd is too expensive and a rare metal, it is strongly desired to develop non-Pd based alloys. The Nb-TiNi alloys consisting of the bcc-(Nb, Ti) and the B2-TiNi phase show high hydrogen permeability equivalent to that of pure Pd. However, its membrane is prepared by means of complex processes such as cold rolling and intermediate annealing. On the other hand, it is well known that alloy ribbons can at a stroke be obtained by a melt-spinning technique. In the present work, hydrogen permeability, crystal structures and microstructures of melt spun Nb-TiNi alloy ribbons before and after annealing treatments are investigated in order to develop the preparation method of alloy membrane, and it was concluded that melt-spinning technique is effective for the preparation of the Nb-TiNi hydrogen permeation alloy membrane.

Characterization and Research of Nano-Meter ZnO by X-Ray Diffraction: *Cheng Guofeng¹;* ¹Shanghai Institute of Ceramics

The microstructures (average crystallite size and stacking faults probability) and the doped effects of the nano-meter ZnO have been characterized and researched using separating multip-broadening effects method improved by author. The results are following: (1) The crystallite size of studied two group samples are a few hundreds and several nano-meter respectively. The crystallite shape of the two groups ZnO samples nearly are the same polohedron, but the difference among them can be characterized by. (2) The method for separating two-fold and three-fold broadening effects of closed packing hexagonal is not used to the nano-meter ZnO samples, because the selective broadening effects is also not obviously. (3) The selective broadening effects of stacking faults may be ignored, because the stacking faults probability of the two groups ZnO samples is very small.

Measuring Enhanced Elevated Temperature Deformation Using Spark Plasma Sintering Equipment: *Dustin Hulbert¹; Dongtao Jiang¹; Amiya Mukherjee¹;* ¹University of California

A fully dense nanocrystalline ceramic consisting of ZrO2, Al2O3 and MgAl2O4 was deformed at 1150°C at a strain rate on the order of 10⁻² s⁻¹. Spark plasma sintering was used in this study as a means of consolidation as well as for measuring elevated temperature deformation. By using the constitutive equation for elevated temperature plasticity in conjunction with previously measured strain rate sensitivities and activation energies a strain rate on the order of 10⁻⁶ s⁻¹ is predicted at 1150°C. This strain rate is four orders of magnitude slower than that measured using the spark plasma sintering equipment. This suggests some significant enhancement of the kinetics of deformation garnered by the pulsing electric field found inside the SPS chamber.

Elastic-Plastic Stress and Deformation Analysis of Annular Plates under Prescribed Radial Loading: Ahmed Elkholy¹; Abdulazim Falah¹; ¹Kuwait University

A modified form of constitutive equation for an isotropic elastic-plastic deformation of circular plates subjected to radial tensile loading on the inner surface is introduced. The form takes into consideration the effect of rotation of various principal axes and material hardening during the process of continued deformation. Plastic instability analysis of plates is carried out to determine stresses at the onset of cavity formation. Both symmetric and antisymmetric modes of deformation are determined. It was found out that the modified form which is derived in this study leads to deformation stresses which are lower than those obtained when classical plasticity relations are used, and therefore, are comparable with the results obtained experimentally. It is found also that deformation is asymmetric with respect to the plate axis and depends not only on the stress in the current state but also on the prescribed incremental traction ratio and material properties.

Hael Mughrabi Honorary Symposium: Plasticity, Failure and Fatigue in Structural Materials - from Macro to Nano: Poster Session

Sponsored by: The Minerals, Metals and Materials Society, TMS Structural Materials Division, TMS Materials Processing and Manufacturing Division, TMS: High Temperature Alloys Committee, TMS/ASM: Mechanical Behavior of Materials Committee, TMS: Nanomechanical Materials Behavior Committee
Program Organizers: K. Jimmy Hsia, University of Illinois, Urbana-Champaign; Mathias Göken, Universität Erlangen-Nürnberg; Tresa Pollock, University of Michigan - Ann Arbor; Pedro Dolabella Portella, Federal Institute for Materials Research and Testing; Neville Moody, Sandia National Laboratories

Sunday PM Room: Hall 12
March 9, 2008 Location: Ernest Morial Convention Center

Modeling the Influence of Microstructure on Multi-Site Fatigue Damage Evolution in AA7075: Stephen Sintay¹; Joe Fridy²; John Brockenbrough²; Anthony Rollett¹; Hasso Weiland²; ¹Carnegie Mellon University; ²Alcoa, Inc.

Fatigue crack nucleation and growth in AA7075 is observed to be directly correlated with constituent particles. Given the relatively high volume fraction of such particles, and the spectrum fatigue loading experienced by in service aerospace components, it becomes increasingly difficult to answer questions such as; Where and when will fatigue cracks initiate? What is the distribution of cycles required to grow a crack of a certain size? What is the distribution of cracks at a certain number of cycles? and What role does microstructure play in the incubation, nucleation, and growth of fatigue cracks? The goal of this presentation is to outline the progress and strategy of a set of modeling tools designed to explore the influence of microstructure on fatigue damage evolution.

Crack Initiation in AA7050 Due to Cyclic Fatigue: Jonathan LeDonne¹; ¹Carnegie Mellon University

The fatigue life of aerospace aluminum alloys is governed primarily by crack initiation, which is accelerated by the presence particles in the microstructure. Although much is known qualitatively about the relationships between fatigue life and the size of microstructural features, quantitative models suffer because of the lack of detailed microstructural data. Characteristics of coarse constituent particles are investigated for AA7050. Size distributions of second phase particles are characterized. The sizes and positions of particles are analyzed for 2-dimensional orthogonal sections, which are then used for reconstruction of a 3-dimensional microstructure of particles. The conversion assumes that the particles can be approximated as ellipsoids. Fracture surfaces are also investigated to establish a defined fatigue crack-initiating feature. The results are compared to previous results on AA7075.

Multiscale Characterization of Subsurfaces Produced by Dry Sliding Wear: Wenjun Cai¹; Jung Singh¹; Pascal Bellon¹; ¹University of Illinois

Frictional wear resulting from the dry sliding of two metallic bodies under applied load leads to the formation of complex microstructures. Using

a high performance Cu-Ni-Sn bronze as a test material, we combine pin-on-disc wear measurements with SEM and TEM characterization of subsurface microstructures. The sustained plastic deformation produces layers ranging from severely plastically deformed to nanocrystalline layer in the top few microns. SEM and SEM-EBSD are employed to identify these layers, to quantify the strain and strain-rate, and to analyze the crystallographic texture of these layers. Twinning is found to be a significant deformation mode near the surface. Comprehensive TEM analysis combining imaging, nanodiffraction, EDS, EELS, HAADF provides further information at the nanoscale on the structure and chemistry of these layers. A Taylor model is applied to simulate the evolution of the subsurface textures under sliding. Consequences on the design of materials with optimized wear resistance are discussed.

Fatigue Crack Propagation in E319 Cast Aluminum Alloy at Ultrasonic and Conventional Frequencies: Xiaoxia Zhu¹; J. Wayne Jones¹; John Allison²; ¹University of Michigan; ²Ford Motor Company

The fatigue crack propagation behavior of E319 cast aluminum alloy was studied by using both ultrasonic and conventional fatigue techniques in order to understand the potential effect of frequency on fatigue behavior of cast aluminum alloys. Fatigue cracks grew faster at 30 Hz than at 20 kHz in air at both 20 and 250°C. The effect of frequency on the fatigue crack growth rates at all temperatures can be attributed to an environmental effect, particularly the effect of water vapor. For E319, fatigue crack growth rates at a given ΔK increased with increasing water exposure, P/f , until saturation the environment effect occurred. This behavior was characterized by an environmental superposition model for fatigue crack growth. Based on this model, fatigue crack growth rates over the entire range of ΔK in various environments with different water exposure can be predicted and the predictions generally agreed well with the experimental observations.

Using Marked and Unmarked Correlations to Investigate Interactions of Microstructure Attributes in Fatigue of Titanium Alloys and Nickel Superalloys: Craig Przybyla¹; David McDowell¹; ¹Georgia Institute of Technology

Much work has gone into identifying various mechanisms of fatigue crack initiation, but it is still not well known how interactions of microstructure attributes (e.g., grain/phase morphology, orientation/misorientation, etc.) either inhibit or promote fatigue damage. We explore how correlations of various microstructure attributes differ between larger microstructure "representative" volumes and "marked" volumes from fatigue initiation sites identified in physical fatigue specimens of Ti6246 and Rene 88. In addition, new variants of previously described marked correlation functions are employed to explore probabilities of correlations between certain microstructure attributes marked by the magnitudes of the Fatemi-Socie fatigue indicator parameter (which can indicate localized susceptibility to fatigue crack initiation due to microplasticity) calculated using finite element simulations in a microstructure-sensitive constitutive formulation. Linking correlations of microstructure attributes and a fatigue response parameter in this way provides a potentially effective framework to identify the interactions between attributes that either promote or inhibit fatigue damage.

Atomistic Simulations of Dislocation Nucleation in Copper Grain Boundaries under Uniaxial Tension and Compression: Garritt Tucker¹; Mark Tschopp²; David McDowell¹; ¹Georgia Institute of Technology; ²Air Force Research Laboratories/Universal Technology Corporation

Atomistic simulations are used to investigate how grain boundary structure influences dislocation nucleation under uniaxial tension and compression for a specific class of symmetric tilt grain boundaries that contain the E structural unit. After obtaining the minimum energy grain boundary structure, molecular dynamics was employed based on an embedded-atom method potential for Cu at 10 K. Simulation results show that higher nucleation stresses are required in uniaxial compression than in tension. Additionally, analysis of the dislocation nucleation mechanisms show several differences between tension and compression. For instance, partial dislocations are nucleated in tension and full dislocations are nucleated in compression. The tension-compression asymmetry in mechanisms and responses can be partially explained by the resolved stress components on the slip plane on which the dislocation nucleates.

Effect of Interfacial Dislocation Structure on Yield Strength of Nanostructured Metallic Multilayer Thin Films: Qizhen Li¹; ¹University of Nevada, Reno

Metallic multilayer thin films with the nanoscale layer thickness attract great research interest due to their high hardness and strength. The multilayer system studied here is composed of alternating A and B phases with FCC structure and cube-on-cube orientation relationship. A and B have the same layer thickness. A three dimensional cellular automaton dislocation model is used to study the yield strength of this multilayer system. Different interfacial dislocation structures are investigated in the model for the metallic multilayer thin films with different layer thicknesses ranging from several nanometers to hundreds of nanometers. The result will illustrate the influence of interfacial dislocation structure on yield strength of multilayer systems with different layer thickness.

Damage Mechanisms of High Chromium Iron Used in Work Rolls of Hot Rolling Mills: Christian Krempaszky¹; Wenge Zhang¹; Ewald Werner¹; ¹Technical University-Munich

Hot-rolled steel sheets used in automotive applications have to meet high surface quality demands and therefore rolled-in scale often cannot be tolerated. Rolled-in scale is correlated to the deterioration of the work-roll's surface in the first stands of the finishing train. It is established that this deterioration is a result of discontinuous wear, a phenomenon called banding, caused by the thermomechanical loads and the tribochemical environment. By characterization of the complex thermomechanical loads acting on hot rolling mill work-rolls, a special cyclic loading path with mixed load/displacement control modes is employed to simulate the thermomechanical behavior of the work-roll material via a series of laboratory low cycle fatigue (LCF) tests. With increasing load level the cyclic maximum residual tensile stress increases during cyclic deformation, while the fatigue lifetime decreases. These laboratory tests are useful to explain the mechanisms and conditions responsible for surface deterioration and to optimize the process.

Fatigue Life Prediction under Ranking of Heterogeneity Scales in Ni-Base Superalloys: Sushant Jha¹; Michael Caton²; James Larsen²; ¹Universal Technology Corporation; ²US Air Force Research Laboratory

A probabilistic life-prediction approach for powder-processed Ni-Base superalloys is presented. Integral to this approach is the premise that several levels of heterogeneous deformation can develop for any given microstructure and fatigue loading. In the present Ni-Base superalloys, these levels are related to randomly occurring microstructural features such as the non-metallic particle, the void, and certain local configurations of the γ grains. The probability of failure from a heterogeneity scale and the associated lifetime decrease in the order of the increasing scale. The lower-tail response is limited by crack growth due to the probability of instant crack initiation from a suitably higher heterogeneity level. This appears to produce a separation, with a decrease in the stress level, of the mean-lifetime behavior which tends to be controlled by the smaller (and more prevalent) heterogeneity scale and the crack-growth-controlled lower-tail which is governed by a larger (and less frequent) scale.

Microscopic Material Units Governing the Macroscopic Fatigue Behaviour of Cold Drawn Eutectoid Steel: Jesús Toribio¹; Beatriz González¹; Juan Carlos Matos¹; ¹University of Salamanca

This paper analyzes how the cold drawing process influences the fatigue behaviour of eutectoid steel. Macroscopically, the analysis is focussed on the region II (Paris) of the fatigue behaviour in which $da/dN=C(\Delta K)^m$, measuring the constants (C and m) for the different degrees of drawing. From the engineering point of view, the manufacturing process by cold drawing improves the fatigue behaviour of the steels, since the fatigue crack growth rate decreases as the strain hardening level in the material increases. From the microscopical viewpoint, fatigue cracks are transcollonial and exhibit a preference for fracturing pearlitic lamellae, with non-uniform crack opening displacement values, micro-discontinuities, branchings, bifurcations and frequent local deflections that create microstructural roughness. The net fatigue surface increases with cold drawing due to the higher angle of crack deflections.

Damage of APS-TBCs in Thermomechanical Fatigue Tests: Tilmann Beck¹; Olena Trunova¹; Rolf Willi Steinbrech¹; Roland Herzog²; Lorenz Singheiser¹; ¹Research Center Juelich; ²MAN Turbo AG

Thermal barrier coatings (TBCs) are applied to gas turbine blades to increase maximum service temperature. The performance of TBCs under thermomechanical fatigue (TMF) is governed by the TMF cycle, the thermal mismatch between TBC and substrate, and microstructural changes (e.g. sintering of the TBC, oxide scale growth, interdiffusion processes). In the present work a TBC system comprising air plasma sprayed $ZrO_2/8wt.-% Y_2O_3$ with NiCoCrAlY bond coat on CMSX-4 substrate was subjected to out-of-phase TMF with different high temperature dwell times and mechanical load amplitudes. Some specimens were pre-oxidised before TMF testing. TMF without dwell time resulted in fatigue failure of the base material. Pre-oxidation before TMF testing with the same cycle did not significantly change the failure behaviour. However, sufficient long dwell times lead to TBC spallation before fatigue cracking of the base material. The oxidation and fatigue related processes of crack formation and propagation under TMF loading are discussed.

Effect of Plastic Strain on NiTi-Based Shape Memory Alloys: Qizhen Li¹; ¹University of Nevada, Reno

NiTi-based shape memory alloys (SMAs) attract great research interest and have broad applications including actuators, electric switches, pipe couplings, mobile phone antennas, eyeglass frames, dental braces, etc, due to their good mechanical properties. Like human muscles, the SMAs will endure overloading and be deformed plastically in service. It is important to understand how the plastically deformed SMAs will behave subsequently. Mechanical and shape memory properties will be studied for the SMAs with different plastic strains. The results will provide the knowledge about the amount of plastic strain the SMAs can bear.

Surface Stress-Induced Phase Transformations and Shape Memory Effect in Pd Nanowires: Jijun Lao¹; Dorel Moldovan¹; ¹Louisiana State University

Recent experimental and atomistic simulation studies have demonstrated the existence of structural reorientations and shape memory effect (SME) in various metallic face-centered-cubic (fcc) nanowires. Here we use molecular dynamics simulations to investigate the surface-stress-induced phase transformations in Pd crystalline nanowires. For a $\langle 100 \rangle$ initial crystal orientation and wire cross section areas below 4 nm² we show that the surface stress can cause Pd nanowires to undergo a structural reorientation from an initial fcc structure to a body-centered-tetragonal (bct) structure. The simulations also indicate the existence of SME in Pd nanowires which is associated with the existence of a reversible fcc to bct phase transformation. Under tensile loading and unloading the Pd nanowires exhibit recoverable strains of up to 50%; value that is well beyond the typical recoverable strain for most bulk shape memory alloys.

Ultrafine-Grained Materials: Fifth International Symposium: Poster Session

Sponsored by: The Minerals, Metals and Materials Society, TMS Structural Materials Division, TMS Materials Processing and Manufacturing Division, TMS: Shaping and Forming Committee, TMS: Nanomechanical Materials Behavior Committee
Program Organizers: Yuri Estrin, Monash University and CSIRO Melbourne; Terence Langdon, University of Southern California; Terry Lowe, Los Alamos National Laboratory; Xiaozhou Liao, University of Sydney; Zhiwei Shan, Hysitron Inc; Ruslan Valiev, UFA State Aviation Technical University; Yuntian Zhu, North Carolina State University

Sunday PM
March 9, 2008

Room: Hall 12
Location: Ernest Morial Convention Center

Contribution of Texture and Grain Size to Hall-Petch Relation of a Wrought Magnesium Alloy AZ31: Jun Tao¹; Jingtao Wang¹; Deliang Yin¹; Jinqiang Liu¹; ¹Nanjing University of Science and Technology, Department of Materials Science and Engineering

Because of the mixed contribution from both texture and grain size to mechanical properties of wrought Mg alloys, there was a confusion on the slope of Hall-Petch relation of wrought magnesium alloys, especially in

those processed by equal channel angular pressing (ECAP). The experiment is designed in this investigation so that the effect of texture and grain size on yield strength of an AZ31 alloy could be clearly separated. It is concluded that Hall-Petch relation holds valid for the effect of grain size on yield strength in the experimental alloy, as long as no significant difference in the texture of the samples with different grain size. The effect of crystallographic texture on yield strength manifests itself by the different interception on stress axis of Hall-Petch lines with significant difference in texture intensity.

Corrosion and Fretting Wear Behaviour on UFG Ti-13Nb-13Zr Alloy in Ringer's Solution: Anbarasan Viswanathan¹; Geetha Manivasagam¹; C. Richard²; Sathyam Suwas³; R. Asokamani¹; C. Kowandy²; J. Landoulsi²; ¹Vellore Institute of Technology-University; ²Université de Technologie de Compiègne; ³Indian Institute of Science

Corrosion and wear are the prime consideration for a biomaterial that is to be used in the human body, because metal ion released mainly associated with toxicity of surgical implants and can adversely affect the biocompatibility and mechanical integrity. Earlier works clearly indicate that refinement of grain size may enhance the corrosion and mechanical properties in comparison with coarse grain (CG) counterparts. Hence in this work we have attempted to study the corrosion and fretting wear behavior of ultra fine grain (UFG) Ti-13Nb-13Zr developed by Equal channel angular pressing (ECAP) process in simulated body fluid (Ringer's solution). Potentiodynamic anodic polarization and open circuit potential were used to evaluate the corrosion behavior of UFG Ti-13Nb-13Zr in simulated body fluid at 37°C. In addition, fretting wear behavior of UFG Ti-13Nb-13Zr alloys against bearing steel is also evaluated. The results of the corrosion and fretting wear studies will be presented in this paper.

Deformation and Fracture of AZ31 Magnesium Alloy during Equal Channel Angular Pressing: Feng Kang¹; Jing Tao Wang¹; Yong Peng¹; ¹Nanjing University of Science and Technology

The deformation and fracture characteristics of AZ31 magnesium alloy during equal channel angular pressing (ECAP) were established. The isothermal behavior of AZ31 magnesium alloy was determined at temperatures between 150 and 250°C and ram speeds producing average effective strain rates between 0.001 and 0.25s⁻¹. AZ31 magnesium alloy was particularly susceptible to shear localization during ECAP, uniform flow occurred only at high temperatures and low strain rates. Observations of shear banding and shear fracture were interpreted in terms of the tendency for strain concentration as quantified by the flow localization parameter, or the ratio of the normalized flow softening rate to the strain-rate sensitivity. These understandings of the effect of material properties on flow localization tendency are helpful for the selection of processing parameters with uniform flow during ECAP.

Deformation Behavior of Nanocrystalline Metals and Alloys Investigated by Mini-Tensile Test: Lilia Kurmanaeva¹; Yulia Ivanisenko¹; Jörg Weismüller¹; Jürgen Markmann²; Ruslan Valiev³; Hans-Jörg Fecht⁴; ¹Forschungszentrum Karlsruhe GmbH; ²Universität des Saarlandes; ³Ufa State Aviation Technical University; ⁴University of Ulm

The recent past has seen an increasing interest in studies of mechanical properties of nanocrystalline materials (nc). NC materials offer wide application as structural materials thanks to their outstanding mechanical properties. A novel method for the preparation of bulk nanocrystalline materials with a grain size <30 nm using the combination of inert gas condensation and subsequent high pressure torsion was developed. Here, we present results on a comprehensive investigation of the microstructure and mechanical properties of nanocrystalline metals and alloys, namely Pd and Pd-Au, with a mean grain size of 15 nm. Microstructure was investigated by Transmission Electron Microscope (TEM). Mechanical properties of the obtained specimens were studied in tensile test using a dedicated tensile machine for miniature specimens. It was shown that nanocrystalline Pd and Pd-Au alloy exhibits a very high yield stress and a microhardness with sufficient ductility. The obtained results of mechanical properties and microstructure are discussed.

Microstructure and Mechanical Properties of Nanostructured Metal Matrix Composites: Timothy Lin¹; Fei Zhou¹; Quan Yan¹; Chunfu Tan¹; Bob Liu¹; Adolphus McDonald²; ¹Aegis Technology Inc.; ²U.S. Army Aviation and Missile Command

Over last few years Al-based nanostructured metal matrix composites (NMMCs) has attracted increasing interests because of their great potentials in strength enhancement. Presently Aegis Technology is developing a novel class of NMMCs funded by U.S. Army Small Business Innovative Research (SBIR) project, "Light-weight Material for Ballistic Armor". This class of NMMCs, which is based on submicron SiC particulates reinforced nanostructured Al alloy matrix, can be used for not only lightweight armors but also lightweight structures (e.g. anti-wear engine components). Aegis has successfully developed a cost-effective, scalable processing route for the fabrication of NMMCs plates, billets and near-net-shape components. In this poster, Aegis will report its detailed investigations on the characterization of the NMMCS, including (1) Microstructures using TEM, SEM and X-Ray, and (2) Mechanical properties (Tensile, compression, fatigue, fracture toughness, creep and ballistic penetration). These investigations will provide a solid foundation for the further development of this class of NMMCs for a variety of potential applications.

Flow Properties of an Aluminum Alloy Processed by Equal Channel Angular Pressing: Sivaraman Arjunan¹; Uday Chakkingal¹; ¹Indian Institute of Technology Madras

Equal Channel Angular Pressing (ECAP) process is an important process for producing ultra fine grained microstructures in bulk metals and alloys. The microstructures developed after ECAP represent high energy configurations; hence they are inherently unstable and susceptible to flow softening depending upon strain paths employed in subsequent deformation. In the present work aluminum alloy AA 6063 samples were subjected to ECA pressing for up to three passes with a die angle of 105 degree. Compression testing was used to determine the subsequent flow behaviour. Two types of compression test specimen orientations; one parallel to the axis of pressed sample and the other at 45 degree to the axis of the pressed sample were used for the study. The flow curves were plotted and comparative flow properties, flow softening and anisotropic behavior have been studied with respect to number of passes and processing routes. These are correlated to the observed microstructures.

Forging Parameter Effects on the Mechanical Behavior of Cryomilled Al 5083: Troy Topping¹; Byungmin Ahn²; A. Newbery³; Enrique Lavernia¹; ¹University of California, Davis; ²University of Southern California; ³MillStrong Ultra, LLC

Aluminum alloys with nanocrystalline (NC) and ultra-fine grain (UFG) size are of immense interest because of their high strength – typically 30% stronger than conventionally processed alloys of the same composition. For this study, the microstructure and mechanical behavior of UFG Al 5083 plate, produced by the quasi-isostatic forging of cryomilled powder, has been investigated and compared to coarse-grained Al 5083 - in particular, the ability to strengthen the UFG material further by tuning the forging parameters. Experimental forging parameters were used on six plates with approximate dimensions of 10" in diameter and 0.75" in thickness. The effort focuses on increasing strength through reduced grain growth during processing, while maintaining ductility by breaking up prior particle boundaries (PPBs) with high forging pressures. Mechanical tests reveal increased strength in proportion to decreased grain growth, while ductility is maintained at the level of conventional alloys.

Improvement in Both Strength and Ductility in Nanostructured Carbon Steel Produced by High Pressure Torsion and Annealing: Shaohua Xia¹; Lilia Vichiganina²; Jingtao Wang¹; Igor Alexandrov²; Ruslan Valiev²; ¹Nanjing University of Science and Technology; ²Ufa State Aviation Technology University

Nanostructured carbon steels of Fe-0.45%C and Fe-0.65%C were obtained by high pressure torsion and annealing. Combination of high strength and improved uniform elongation was achieved in Fe-0.45%C resulted from formation of bimodal distribution in grain size. By comparing the microstructures and mechanical properties between nanostructured Fe-0.45%C and Fe-0.65%C, we can conclude that in-situ formed micro-meter sized grains in ferrite phase during annealing provide extra strain hardening ability to sustain the uniform elongation as their coarse-grained counterpart. Estimation of the relationship

between volume fraction of micro-meter sized grains and mechanical properties in bimodal steel was also made by associated analysis of results from previous investigations in low carbon steel processed by equal channel angular pressing and annealing.

Improving the Superplastic Properties of an AZ31 Magnesium Alloy by Equal-Channel Angular Pressing: Roberto Figueiredo¹; Terence Langdon¹;

¹University of Southern California

The interest in improving the properties of magnesium alloys has led to the development of technology to refine the grain structure especially through the use of severe plastic deformation. In the present paper, extruded billets of a commercial alloy, AZ31, were processed by Equal-Channel Angular Pressing (ECAP). Optical microscopy and tensile tests were used to evaluate the grain structure and high temperature mechanical properties in order to determine the effect of processing by ECAP. An analysis of grain structure shows that ECAP effectively reduces the average grain size to the range of a few micrometers. High temperature tensile tests demonstrate that ECAP reduces the flow stress of the AZ31 alloy and improves the strain rate sensitivity and the elongation to failure. Superplastic elongations up to more than 1000% were achieved after ECAP with low flow stresses and high strain rate sensitivity.

In-Situ Observation of Deformation of Nanocrystalline Al-Mg Alloy with Bimodal Grain Structure: Byungmin Ahn¹; Enrique Lavarnia²; Steven Nutt¹;

¹University of Southern California; ²University of California, Davis

The tensile properties and deformation response of nanocrystalline Al-Mg alloy (Al 5083) were investigated using a micro-straining unit. Atomized Al 5083 powder was ball-milled in liquid N₂ to obtain a nanocrystalline structure, and blended with 15% unmilled coarse-grained powder to achieve bimodal structure. The blended powder was hot vacuum degassed to remove residual contaminants, consolidated by either cold (CIP) or hot isostatic pressing (HIP), and then forged. The microstructure was observed using an optical microscope. The investigation of tensile and fracture of bimodal structure suggests unusual deformation mechanisms and interactions between ductile coarse-grain bands and nanocrystalline regions.

Mechanical Properties of Ultra Fine Grained Aluminum and Iron Produced by Accumulative Roll Bonding Method: Saeed Tamimi¹; Mostafa Ketabchi¹;

Nader Parvin¹; ¹Tehran Polytechnic University

This work aims to investigate whether accumulative roll bonding (ARB) is an effective grain refinement technique for ultra-low-carbon steel strips containing 0.002% C and pure aluminum. For this purpose, a number of ARB processes were performed at 500°C for IF and 200°C for pure aluminum, with 50% reduction of each rolling pass. The mechanical properties after rolling were obtained. Aluminum and iron's yield and tensile strengths increased by 200–300%. Variations of hardness along the thickness of the samples were obtained using micro hardness tests. It was found that both the grain size achieved, as well as the degree of bonding, depend on number of rolling pass and reduction of area as a whole. In IF steel, mean grain size was obtained about 300nm. The rolling process was stopped in 7th cycle for pure aluminum and 10th cycle for IF steel, when cracking of the edges became pronounced.

Microstructure and Mechanical Properties of ECAP Processed Two-Phase Zinc-Aluminum (Zn-8%Al) Alloy: Majid Al-Maharbi¹;

Mohammed Haouaoui¹; Ibrahim Karaman¹; Gencaga Purcek²; ¹Texas A&M University; ²Karadeniz Technical University

A two-phase zinc-aluminum alloy (Zn-8%Al) has been subjected to severe plastic deformation by equal channel angular extrusion (ECAE). The alloy was successfully extruded at homologous temperatures of 0.52 to 0.55 through different strain paths. The as-cast dendritic structure was eliminated and the α -phase particles were fragmented and dispersed more uniformly into the η -matrix leading to a more homogeneous microstructure. TEM micrographs show that grain sizes were significantly reduced to the ultrafine grain (UFG) sizes. An average increase in strength and elongation of about 53% and 1420% of as-cast values was achieved. Noticeable softening was observed after the first pass, and was attributed to chemical composition homogenization occurring with increasing strain level. The homogenization is assisted by the simultaneous long range diffusion and the refinement of the two phases as revealed by EDS and microhardness measurements which show considerable changes in composition and properties of the individual phases after ECAE.

OIM Study of Microstructure and Texture Heterogeneity during ECAP of Copper: Alexander Zhilyaev¹; Azat Gimazov²; Shrinivasan Swaminathan³; Terry McNelley³; ¹Centro Nacional de Investigaciones Metallurgicas (CENIM), CSIC; ²Russian Academy of Sciences, Institute for Metals Superplasticity Problems; ³Naval Postgraduate School

The heterogeneous deformation of annealed copper subjected to equal channel angular pressing (ECAP) was studied by Orientation Imaging Microscopy. The microstructure and microtexture of a partially pressed Cu billet has been analyzed at the inner and outer corners in the region of the die channel intersection as well as in the middle of the shear zone. Distinctly inhomogeneous deformation of prior annealing twins by interpenetrating slip bands was observed, and some twin-matrix interfaces displayed stair-like offsets. The intense local deformation within the annealing twins is characteristic of dislocation slip and not deformation twinning.

On the Texture Analysis of High Pressure Torsion - Deformed Mg and Cu:

Bartłomiej Bonarski¹; Erhard Schafler¹; Michael Zehetbauer¹; Borys Mikulowski¹; ¹University of Vienna; ²AGH-University of Science and Technology

Polycrystalline pure magnesium (99.8%) and copper (99.99%) have been subjected to High-Pressure Torsion (HPT) at room temperature. A special technique was developed in order to enable the HPT of Mg up to very high shear strains $\gamma \leq 120$ and different hydrostatic pressures (1–8 GPa). The texture development has been analyzed as a function of strain and hydrostatic pressure by systematic X-ray macrotexture investigations and compared with corresponding microhardness measurements. The texture evolution could be described in terms of volume fractions of the following components: (i) {0001}-, {10-11}- and {10-12}- fibres for the case of Mg; (ii) the typical components of shear textures for the case of Cu. From the textures observed, there is evidence for the occurrence of dynamic and static recovery, which turns out to depend not only on the strain but also on the hydrostatic pressure of HPT.

Stored Energy and Recrystallization Temperature of High Purity Copper after Equal Channel Angular Pressing: Yue Zhang¹; Jingtao Wang¹; ¹Nanjing University of Science and Technology

Equal channel angular pressing (ECAP) was conducted at room temperature to impose high strain into high purity copper. Differential Scanning Calorimeter (DSC) was used to estimate the stored energy from ECAP and recrystallization temperature. It was found that the stored energy increases upon ECAP processing until a peak reached at 12 passes, and a slight decrease in stored energy was observed at higher ECAP passes. The recrystallization temperature decreases upon the increase of stored energy up to ~50 J/mol, and reaches a stable value of ~210°C. Partial annealing of an ECAP processed (8 passes) sample by heating to ~185°C at a heating rate of 20°C/min released the stored energy from ~55 J/mol to ~18 J/mol, without substantial change on the recrystallization temperature of the sample. A model was proposed to help understanding the recrystallization mechanism of ultrafine-grained copper and the observations above.

Tailoring the Microstructures of Ultrafine Grained Aluminum through a Two-Step Annealing Process: Naoya Kamikawa¹; Xiaoxu Huang¹; Niels Hansen¹; ¹Riso National Laboratory

Due to microstructural and textural heterogeneities, annealing of nanostructured metals is difficult to control in order to avoid non-uniform coarsening and recrystallization. The present research demonstrates a method to delay such process by annealing at low temperature before annealing at high temperatures. By this two-step process the structure is homogenized and the stored energy is reduced significantly during the first annealing step. As an example high purity aluminum has been deformed to a total reduction of 98.4% by accumulative roll-bonding at room temperature. Isochronal annealing for 0.5 h of the deformed sample shows initiation of recrystallization at about 200°C. However, when introducing an annealing step for 6 h at 175°C the initiation of non-uniform coarsening and recrystallization is significantly delayed. To underpin these observations the structural evolution has been characterized by TEM, showing that extensive annihilation of low-angle dislocation boundaries characterizes the low-temperature annealing step.

TEM Studies on the Effect of Nature of Precipitates in Al-Li Alloy on Microstructural Evolution during Severe Plastic Deformation: *S. Giribaskar¹; Gouthama¹; ¹Indian Institute of Technology, Kanpur, Department of Materials and Metallurgical Engineering*

Fundamental research in the area of severe plastic deformation (SPD) focuses on the mechanisms that reduce grain size effectively down to nanometer range in metallic materials. Evolution of microstructure of Al-Li alloy processed by equal channel angular extrusion (ECAE), using redundant strain route B_C is analyzed using transmission electron microscopy (TEM). At initial stages of deformation, layers of elongated subgrains with alternating arrays of equiaxed subgrains are formed. Observations on the effect of precipitates/second phase particles in the sample on the deformation characteristics and their role on the increased degree of grain fragmentation process is highlighted. The nature of the precipitates on the evolution of the microstructure is elucidated. For this purpose, the Al-Li is solutionized, quenched and aged at different temperatures before subjecting to ECAE. It was observed that optimal thermal treatment leads to most effective grain refinement and consequent ultrafine grained material.

The Effect of Deformation History on the Microstructure and Texture of Annealed ECAE Processed Copper: *Ana Erbi¹; Daudi Waryoba¹; Peter Kalu¹; ¹Florida A&M University-Florida State University College of Engineering*

Grain refinement by equal channel angular extrusion (ECAE) has recently attracted attention due to its effectiveness of producing ultrafine-grained structures in bulk materials. In the present investigation, OFHC Copper ECAE processed at room temperature via route B_C (where the billet is rotated 90° in the same direction between consecutive passes) has shown refinement of the grain size to about 1 μm at 4 passes. On the other hand, a billet swaged first to a 30% reduction and ECAE processed to 4 passes shows a lower grain size refinement to about 3 μm. Both deformation history, however, show a similar grain boundary structure, consisting of about 25% high angle grain boundaries (HAGBs) and 75% low angle grain boundaries (LAGBs). The effect of deformation history on the microstructure and texture of these materials is discussed.

Transmission Electron Microscopy (TEM) Study of the Effect of Machining Parameters on Grain Refinement in Aluminum Alloy Machine Chips: *Lei Dong¹; Judy Schneider¹; ¹Mississippi State University*

The resulting microstructure of machined chips of AA 2195 and AA 2219 were characterized by Transmission Electron Microscopy (TEM). By varying the specimen diameter and rotation and feed speed, different strains and strain rates were imposed on the metal during the cutting process. Dependant on the metal cutting conditions, the resulting microstructure was found to contain either elongated or ultra-fine grains. These observations suggest that the grain refinement mechanisms were influenced by the metal cutting or hot working conditions. The use of metal cutting theory is being explored as a basis of quantifying the optimal conditions for grain refinement during the friction stir welding process.

Effect of Strain Rate, and Deformation Temperature on the Microstructure of an Equal Channel Angular Extrusion (ECAE) Processed Ti-6Al-4V Alloy: *Rabindra Mahapatra¹; Shankar Sastry²; ¹Naval Air Systems Command; ²Washington University*

The Ti-6Al-4V alloy was ECAE processed to produce ultra-fine grains of 1-2 μm. The uni-axial compression experiments to simulate forging parameters subsequent to ECAE processing were carried out to elucidate whether, the ultra-fine grained microstructure of the alloy can be sustained after the deformation. The ECAE processed Ti-6Al-4V alloy showed no significant grain growth when deformed at 750°C, at a strain rate of 0.1"/sec., where as when deformed at same temperature, a strain rate of 0.001"/sec., both the recovery and grain growth were observed.

Microstructural Characteristics of Leadframe Cu Alloys after Accumulative Roll Bonding Process: *Chayong Lim¹; Seungzeon Han¹; Seonghee Lee²; ¹Korea Institute of Materials Science; ²Mokpo National University*

Mechanical properties and formation of nano-sized grains in Cu and Cu-Fe-P alloys by accumulative roll bonding (ARB) process were investigated. Nano-sized grains were successfully obtained in OFC and PMC-90 alloys by ARB process after third cycle. Once the 200 nm grains formed, further reduction in the grain size was not observed up to the 8 ARB process cycles. For both alloys, the tensile strength values increased drastically in the initial stage of ARB process.

The tensile strength values of both alloys tended to saturate after the third ARB process cycle. The tensile elongation value greatly decreased by 1 cycle of ARB process due to the strain hardening. After the third cycle of ARB process, each alloy showed a gradual increase in tensile elongation due to the dynamic recovery. For PMC-90 alloy, the strength value is higher than that of OFC due to addition of the alloying elements.

Synthesis of Al-Al₈₅Ni₁₀La₅ Nanocomposites by Mechanical Milling: *Zhihui Zhang¹; Yizhang Zhou¹; Enrique Lavernia¹; ¹University of California, Davis*

Mechanical milling has been widely used to fabricate metal matrix composites and dispersion-strengthened alloys with the advantage of improved dispersion, enhanced interfacial bonding and refined microstructure. This study reports on the synthesis of an Al-Al₈₅Ni₁₀La₅ nanocomposite by milling a mixture of Al (mean particle size ~60 μm) and amorphous Al₈₅Ni₁₀La₅ powder (particle size 10-25 μm) at a cryogenic temperature. The microstructural evolution during the milling process was investigated using XRD, DSC, SEM and TEM. The results show that nanocrystalline Al matrix with a grain size about 26 nm was obtained and the amorphous powder was fractured and homogeneously distributed in the Al matrix with a whisker shape (1-2 μm thick with an aspect ratio of 1-5). The mechanical behavior of the powder and consolidated bulk composite was also discussed.

Texture Analysis of Materials Subjected to Equal Channel Angular Pressing: *Katrina Houston¹; Srinivasan Swaminathan¹; Jianqing Su¹; Terry McNelley¹; ¹Naval Postgraduate School*

The correlation between the microstructure and texture for aluminum alloys processed by equal channel angular pressing (ECAP) has been studied. The microstructure was characterized using optical microscopy, scanning electron microscopy (SEM) and transmission electron microscopy (TEM). The local textures were discerned using orientation imaging microscopy (OIM) and compared to macro-texture measurements made by X-ray diffraction. Specific emphasis has been given to understanding the long-range arrangement of texture variants in the microstructure. The interfaces between texture variants are pre-cursors to high angle boundaries in repetitive ECAP. The microstructure-mechanical property relations were also examined.

The Relationship between Work Hardening and Grain Size Distribution in Ultrafine Grained Materials: *Babak Raeisinaia¹; Warren Poole¹; Chad Sinclair¹; ¹University of British Columbia*

One anticipates the mechanical response of ultrafine grained materials to be sensitive to heterogeneity arising from a grain size distribution. In the limit of bimodal distributions, experiments appear to support this assertion. For a given strength level, experiments have shown that improvements in uniform elongation can be obtained via manipulating the size distribution. The conclusion is that the grain size distribution can affect both the yielding and the work hardening behaviour. In this work, the role of grain size distribution on the macroscopic properties of ultrafine grained materials has been examined. This is interpreted based on the partitioning of stress and strain between grains within the framework of a self-consistent approach. This approach extends recent efforts focused on yielding to look at the fully plastic work hardening response of polycrystals. The results of this approach are compared with the experimental tensile response of example materials exhibiting heterogeneous microstructures.

Three Pass Twist Extrusion of Pure Aluminum 1100: Experimental Approach: *Amir Reza Shahabi¹; S. Akbari Mousavi¹; ¹University of Tehran, University College of Engineering, School of Metallurgy and Materials Engineering*

Equal channel angular press (ECAP) and Twist extrusion (TE) are two promising types of Severe Plastic Deformation (SPD) methods in order to produce bulk nano-structured materials. TE process has its own profits in comparison to ECAP such as achieving to nanostructure in less number of passes. In this study, three simultaneous counterclockwise twists were performed on the annealed pure Al of type 1100 samples at room temperature and without any inter pass annealing. In order to evaluate the effects of TE, mechanical and metallurgical properties of the nano-Al produced by the twist extrusion process were examined. The results show that the ultimate tensile strength of the nano Al is almost three times greater than that of the original one. In addition, the ductility of the nano Al reduced 58% and the hardness increased 85% approximately. Moreover, the metallographic inspection of the sample is carried out. The study shows the grain

size non uniformity across the cross section of the sample in longitudinal and transversal directions. This matter may be attributed to the difference of mode of deformation from pure shear to simple shear in cross section.

Three Pass Twist Extrusion of Pure Aluminum 1100: Numerical Simulation Approach: *S. Akbari Mousavi*¹; Amir Reza Shahab¹; ¹University of Tehran, University College of Engineering, School of Metallurgy and Materials Engineering

Reviewing lots of articles, it has been approved that Finite Element Method (FEM) is a powerful mean in order to predict and optimize metal forming techniques include more modern ones such as Severe Plastic Deformation (SPD) methods. Equal channel angular press (ECAP) and Twist extrusion (TE) are two promising types in order to produce bulk nano-structured materials. FEM has addressed well for ECAP but its ability for TE process is not so definite yet. In TE process the cubic bulk of material goes through a 90 degree clock or anticlockwise twisted channel die for a couple of turns. In this study, the simulation of three consecutive anticlockwise passes is presented using an explicit finite element method with ABAQUS software. Suitable constitutive relations are used to describe the behavior of Al 1100 during deformation at room temperature. The flow of three simultaneous clockwise twists is presented using von Mises stress and effective plastic strain contours. The positions of the maximum and minimum values of effective strain and von Mises stress are determined and their profile histories are obtained. The average values of equivalent plastic strains at the end of first, second and third simultaneous passes are found to be 1.5, 2.5 and 3, approximately. The mode of deformation also changes from center to corner of the cross section from pure shear to simple shear.

Continuous Equal-Channel Angular Pressing for Producing Long Nanostructured Ti Semi-Products: *Georgy Raab*¹; Yuntian Zhu²; Terry Lowe²; Ruslan Valiev¹; ¹Ufa State Aviation Technical University; ²Los Alamos National Laboratory

We have analyzed major factors that influence the formation of ultrafine-grained structure and evaluated the effectiveness of a continuous equal-channel angular pressing (ECAP) method, ECAP-Conform, for producing nanostructured CP-Ti long rods. In this work we have built a pilot ECAP-Conform machine to process rods with length up to 3 m and diameter up to 7.5 mm. The nanostructured Ti rods produced here have superior strength and fatigue properties, which is of great interest to advanced medical applications in stomatology and traumatology.

Mechanisms of Deformation and Refinement of Grains in Metals by Severe Plastic Deformation: *Georgy Raab*¹; Farid Utyashev²; ¹Ufa State Aviation Technical University; ²Russian Academy of Sciences, Institute for Metals Superplasticity Problems

Grains refinement is considered as an effect of mechanisms of fragments boundaries and bands formation as a result of crystallographic and non-crystallographic shears at bending and/or torsion of a sample. During ECAP and HPT the sample's bending-torsion in a localized deformation center grows and that leads to a non-monotonic deformation and an increase in the angular misorientations of boundaries of the formed bands and fragments. It was shown that the depth of structure refinement depends on the contributions of the required mechanisms in total strain that depend, in their turn, on a scale factor – the dimensions of the deformation center and sample.

Microstructure Refinement of Ti-6Al-4V Titanium Alloy during Warm Deformation: *Sergey Zharebtsov*¹; Maria Murzinova¹; Sergey Mironov¹; Alexander Pshenichnuk¹; Gennady Salishchev¹; Lee Semiatin²; ¹Institute for Metals Superplasticity Problems; ²Air Force Research Laboratory, Materials and Manufacturing Directorate, Wright-Patterson Air Force Base

Microstructure evolution and mechanical behaviour of Ti-6Al-4V titanium alloy during uniaxial compression at 600°C to a height strain of 70% has been investigated. Initially the alloy has a lamellar microstructure. During deformation lamellar microstructure transforms into globular one with a grain size of around 0.4 micrometers. Mechanical behavior of the material is described by the deformation curve with strengthening, softening and steady state flow stage. The microstructure evolution with emphasis on grain boundaries misorientation and mutual turn of alpha and beta phases has been studied. The orientation of phases was determined by means of the EBSD-technique and so-called "single-

reflex" method which based on computation of microdiffraction patterns. It have been revealed that transformation of lamellar microstructure into globular one is associated with loss of coherence of interphase boundaries. As soon as the coherence is lost the deformation localizes within each phase intensifying division of the lamellae into equiaxial fragments.

Room Temperature Relaxation in Copper under High Pressure Torsion Detected by In-Situ Synchrotron Diffraction: *Askar Kilmametov*¹; Gavin Vaughan²; Alain Yavari³; Ruslan Valiev¹; ¹Ufa State Aviation Technical University; ²European Synchrotron Radiation Facilities; ³Institut National Polytechnique de Grenoble

Structural relaxation in severely deformed Cu has been investigated in real time diffraction experiments at room temperature during in situ high pressure torsion (HPT) in high energy synchrotron light. Simultaneous relative changes in Bragg peak's broadening and crystal lattice expansion were under study in loading-unloading regime of torsion straining. Experimental results are consistent with the attribution of the annihilation of crystalline defects generated during HPT. Relaxation kinetics assumed to be controlled by diffusion; therefore the enhanced diffusivity has been estimated due to extremely high excess vacancy concentration, which is typical for those at thermal equilibrium near the melting point.

Superplastic Ultrafine-Grained Sheet Produced out of the Al-Li-Mg-Sc Alloy with Enhanced Mechanical Properties Introduced by ECAP and Rolling: *Nina Yunusova*¹; Rinat Islamgaliev¹; Nikolay Krasilnikov²; Gulnaz Nurislamova; Ruslan Valiev¹; ¹Ufa State Aviation Technical University; ²Ulyanovsk State University

ECAP at elevated temperatures was applied to produce bulk textureless billets with equiaxed grains with a size less than 1 µm in size out of Al-Li-Mg-Sc alloy. The billets demonstrated the effect of high-strain-rate (10⁻¹ s⁻¹) superplasticity (780%) at a relatively low (400°C) temperature. The sheet fabricated out of the billet by warm rolling retained its equiaxed structure with minor grain refinement and exhibited superplasticity with elongation 530% at the same temperature and the strain rate equal to 10⁻² s⁻¹, when compared to the ductility (80%) of a sheet fabricated out of a coarse-grained billet. Short-time annealing of the superplastic sheet at a temperature of solid solution treatment with subsequent aging allowed to use potential of UFG structure and dispersion hardening to achieve very high UTS (690 MPa) retaining the initial ductility.

The Influence of Impurities on Structure and Mechanical Properties of Nanostructured Titanium: *Rinat Islamgaliev*¹; Vil Kazyhanov¹; Askar Kilmametov¹; Alfred Sharafutdinov¹; Ruslan Valiev¹; ¹Ufa State Aviation Technical University

High pressure torsion (HPT) is a well established severe plastic deformation technique for producing nanostructured metallic materials. Using new HPT installation we have investigated the microstructure (grain size, content of omega-phase) and mechanical properties of commercially pure titanium with different content of impurities (VT1-00, VT1-0, Grade 4) processed at various HPT regimes. It was found that content of high pressure omega-phase depends strongly on purity of initial material influencing on strength, ductility and thermal stability of grain structure. Special attention has been paid to investigation of the influence of thermomechanical treatments on nanostructure and mechanical properties.

Influence of Phase Separation on the Mechanical Properties of Pre-Oxidized PM 2000 Alloy: *Carlos Capdevila-Montes*¹; Michael Miller²; Jesus Chao¹; Jose Gonzalez-Carrasco¹; ¹Centro Nacional de Investigaciones Metalúrgicas (CENIM-CSIC); ²Oak Ridge National Laboratory

In the last few years, the ultrafine-grained Fe-based oxide dispersion strengthened (ODS) PM 2000 alloy has been shown to be a viable biomaterial as result of its outstanding combination of mechanical properties and corrosion resistance. After pre-oxidation at 1100°C and phase separation upon aging at 475°C, the room temperature tensile and fatigue properties are suitable for achieving the required biofunctionality for load-bearing implants. Atom probe tomography has revealed that phase separation into Fe-rich alpha and Cr-enriched alpha-prime phases is responsible for the increases in the yield and ultimate tensile strength. However, despite the loss of some ductility, PM 2000 shows ductile behaviour in the necked zone of tensile specimens. This ductility contrasts with the brittle failure observed during the so-called "475°C embrittlement" of other

ferritic alloys. Moreover, PM 2000 aged at 475°C exhibits a higher fatigue limit than that of unaged pre-oxidised material.

Microstructure and Mechanical Properties of Nanocrystalline Fe-C Alloys Processed by Mechanical Milling and Spark Plasma Sintering: *Keiichiro Ohishi¹; Bonta Rao²; Kazuhiro Hono¹; ¹National Institute for Materials Science; ²University of Tsukuba*

Bulk nanocrystalline Fe-C alloys containing different carbon contents were fabricated by mechanical milling and spark plasma sintering (SPS). The samples consolidated by SPS at temperatures in the range of 650-675°C exhibited a good combination of strength and plastic strain in compression. The values of yield and maximum compressive strengths increased with carbon content, while the plastic strains decreased. The microstructure has been characterized using transmission electron microscopy (TEM) and a three-dimensional atom probe (3DAP) to understand the origin of the unusually high yield strength and plastic strain. A bimodal grain structure consisting of fine and coarse grains was observed for all the samples showing high strength and plastic strain. The fine grained region was found to be a duplex phase structure comprised of ferrite and cementite grains. From TEM and 3DAP analyses, the presence of fine oxide particles containing chromium was confirmed.

Microstructure and Mechanical Properties of Ultra Fine Grained Cu-Al and Cu-Zn Alloys: *Martin Heilmair¹; V. Subramanya Sarma²; ¹Otto Von Guericke University; ²Indian Institute of Technology Madras*

Recent studies on ultrafine grained (ufg) electro-deposited Cu containing controlled densities of nanoscale twins revealed a unique combination of very high yield strength (≈ 850 MPa) and good tensile ductility ($\approx 14\%$). Here we aim at producing bulk Cu-5wt.%Zn and Cu-5wt.%Al alloys with ufg matrix and controlled densities of nano/sub-micron twins through varying (i) alloying additions (reducing the stacking fault energy SFE compared to pure Cu), (ii) deformation (rolling) temperatures and (iii) annealing treatments. Grain sizes were found in the range of 0.6 to 1.2 μm (including twin boundaries in the evaluation). The Cu-Al alloy shows significantly improved strength in comparison to the Cu-Zn alloy at tensile comparable ductilities $>30\%$. This is attributed to the much stronger contribution of Al to solid solution strengthening. Contrary, the yield stress dependence on grain size is much stronger for Cu-Zn. Possible reasons will be discussed incorporating strain rate sensitivity tests to understand the deformation mechanisms.

Microstructure of a FeCoV Alloy after Equal Channel Angular Pressing and Tempering: *Zhongze Du¹; Jingtao Wang²; Qingjuan Wang¹; ¹Xi'an University of Architecture and Technology; ²Nanjing University of Science and Technology*

Equal channel angular pressing (ECAP) of a FeCoV alloy was carried out at room temperature via route A up to 4 passes. The microstructure of the FeCoV alloy after ECAP and subsequent tempering were characterized by transmission electron microscopy (TEM). The FeCoV alloy transformed into a fine lath structure with the width of lath decreasing obviously with ECAP passes. The average width of lathes was 90nm after four passes of ECAP, with dislocation tangles inside the lath. These lath structure would breaks and transforms into a fine lath, when increasing ECAP passes. Although tempering after four passes ECAP had little effect on its lath shape of the microstructure, carbide particles and nanometer precipitates appeared inside the lathes after tempering, indicating the decomposition of the microstructure.

Direct Metal Particulate Production Using Modulation-Assisted Machining: *James Mann¹; Chris Saldana¹; Srinivasan Chandrasekar¹; W. Compton¹; Kevin Trumble¹; ¹Purdue University*

Continuous production of Al 6061-T6 particulate using modulation-assisted machining (MAM) is demonstrated. Superimposition of a controlled, low-frequency modulation in conventional machining causes chips to form as discrete particles. By adjusting the conditions, equiaxed, platelet, and fiber shaped particles having narrow size distributions can be produced. Large-strain deformation leads to microstructure refinement and enhanced hardness. The process is applicable to a wide range of alloys and appears to be intrinsically scalable for large-volume production.

Effect of Initial Microstructure on Strain Hardening Behavior of Ultrafine Grain Dual-Phase Steel Produced by Severe Plastic Deformation: *Young Gun Ko¹; Dong Hyuk Shin²; ¹Massachusetts Institute of Technology; ²Hanyang University*

Strain hardening behavior of ultrafine grained (UFG) dual phase (DP) steels via equal channel angular (ECA) pressing and subsequent intercritical annealing followed by water quenching was investigated at ambient temperature. A series of tensile tests were carried out for three distinct DP steels, i.e., CG-DP, UFG-DP and UFG-DPV steels. In contrast to conventional UFG steels with a lack of strain hardening, UFG-DPV steel showed significant strain hardening rate, resulting from uniform distribution of island-typed martensite as well as grain refinement of each constituent phase throughout the microstructure. Also, UFG-DPV steel containing 0.06% of vanadium exhibited the good combination of high strength and sufficient strain hardening, because initial microstructure of that was consisted of the fine martensite through equal channel angular pressing. Strain hardening behavior of these steels was discussed in relation to modified C-Janalysis based on Swift relationship.

Effect of Subsequent Annealing Treatment on Dynamic Deformation Behavior of Ultrafine Grain Al-Mg Alloy: *Young Gun Ko¹; Yang Gon Kim²; Dong Hyuk Shin²; Sunghak Lee²; Chong Soo Lee²; ¹Massachusetts Institute of Technology; ²Pohang University of Science and Technology; ³Hanyang University*

A study was made to investigate the dynamic deformation behavior of ultrafine grain Al-Mg alloy with subsequent annealing treatments at ambient temperature. By imposing an effective strain up to 8 via equal-channel angular pressing (ECAP), most grains were refined from to 300 nm with a non-equilibrium nature of grain boundaries. Upon several subsequent annealing treatments, the ultrafine microstructure was stable at temperature up to 473 K, whilst normal grain growth was found to take place above 523 K. In order to understand the effect of annealed microstructure (ultrafine grain with unstable grain boundary vs. fine grain with stable grain boundary) on dynamic deformation behavior, torsional tests were carried out for four samples i.e., as-ECAPed and 473, 523 and 573 K after ECAP process, using a Kolsky bar. Such mechanical response was discussed in relation to microstructure, tensile property and fracture mode associated with the occurrence of adiabatic shear bands.

Polymer Bonding Ultrafine Grained Al 6061-T6 Particulate Produced by Machining: *Boum-seock Kim¹; James Mann¹; Srinivasan Chandrasekar¹; Kevin Trumble¹; ¹Purdue University*

Plane-strain machining has been used to produce 20 to 200 μm size Al6061-T6 particulate having grain sizes less than 100 nm and 50% higher hardness than the bulk Al6061-T6. Several routes for low-temperature ($\sim 100^\circ\text{C}$) densification and bonding the particles using epoxy resins will be presented. Metal fractions greater than 90 vol % have been achieved with no loss of hardness (in the particulate) during the epoxy cure. Microstructure based modeling of composite hardness will be presented and tensile test results will be discussed. Potential structural applications for these composite materials will be elaborated.

Novel Microstructures from Severely Deformed Al-Ti Alloys Created by Chip Formation in Machining: *Jiazhaio Cai¹; Andreas Kulovits¹; M. Ravi Shankar¹; Jörg Wietzorek¹; ¹University of Pittsburgh*

We present some consequences of Severe Plastic Deformation (SPD) of Al-Ti alloys by chip formation in machining that can enable novel opportunities for creating materials with unprecedented properties. Chips cut from Al-6wt%Ti are composed of a refined dispersion of the fragmented remains of a hitherto coarse Al_3Ti embedded in a nanostructured matrix. This multi-phase nanostructured chip material demonstrates considerable resistance to coarsening owing to the thermally-stable dispersion of ultra-fine Al_3Ti precipitates and thus has promise in structural alloy applications. Furthermore, the Al-Ti machining chips are shown to possess excellent grain-refining characteristics, leading to microstructurally refined and homogeneous Al castings. This realization enables a low-cost route for enhancing the efficiency of the grain refiner Al(Ti) master alloy systems by exploiting SPD during chip formation.

Strain-Assisted Grain Refinement of Co-Fe Alloys upon Room-Temperature Compression: Lai-Chang Zhang¹; Mariana Calin¹; Flora Paturaud²; Jürgen Eckert¹; ¹Leibniz Institute for Solid State and Materials Research (IFW) Dresden; ²W.C. Heraeus GmbH

It is well-known that severe plastic deformation methods, including equal channel angular pressing and high-pressure torsion, have been widely used to produce bulk ultrafine- and/or nanoscale-grained metals and alloys. However, the mechanism of the deformation-induced grain refinement is strongly related to the crystal structure of the investigated metallic materials. In this work, instead of applying severe plastic deformation, pronounced grain refinement to ultrafine or nanoscale has been achieved upon the room-temperature conventional compression of initially coarse-grained single-phase bcc Co-xFe (x=25 and 35 wt%) alloys. These alloys exhibit large plasticity over 140% without fracture at room temperature. The grains refine with increasing of the deformation strains during compression. The possible mechanism for the strain-induced grain refinement under compression is a consequence of the shear deformation and dramatic deformation-enhanced atomic diffusion during deformation.

Thermal Stability of Ultrafine Grains Size of Pure Copper Obtained by Equal-Channel Angular Pressing: Nayar Lugo¹; Nuria Llorca²; Joan Suñol³; Jose Cabrera¹; ¹Universitat Politècnica de Catalunya; ²Universitat de Barcelona; ³Universitat de Girona

Ultrafine grains size of pure copper 99.98% have been obtained by severe plastic deformation using the Equal-Channel Angular Pressing (ECAP) method. Copper samples were ECAPped from 1 to 8 passes developing a finer microstructure showing grain sizes of 250 nm after the 8th pass through the die. Important enhancement in the mechanical strength properties was obtained in the material processed by this technique. Subsequent heat treatments were carried out to evaluate the grain size thermal stability of the ECAPped samples. Microstructure and mechanical properties together with Differential Scanning Calorimetric (DSC) tests were carried out in order to evaluate thermal recovery and recrystallization temperature as well as activation energy. Good correlation was obtained with the microstructure and the mechanical properties. Heat treatment produced significant changes in the behaviour of the material.

XRD Characterisation of Ultrafine Grained (UFG) Al-Mg Alloys: Markus Dinkel¹; Florian Pyczak¹; Mathias Göken¹; ¹University Erlangen - Nürnberg

The characterisation of ultrafine grained materials by X-ray diffraction (XRD) is a suitable and convenient method to acquire information about this material class. In this work examples from different areas of interest are covered. The effect of impurities on the crystallite sizes and dislocation densities of ECAP – processed AlMg alloys is studied. It can be shown that with increasing Magnesium content the achievable reduction in crystallite size with ECAP eventually reaches a saturation state and a further reduction of the structural size seems unlikely. Simultaneously the dislocation density increases to a plateau level with increasing Mg content. In annealing experiments the microstructural stability of AlMg0.5 and the resulting changes are determined by XRD. As a result it becomes evident that the annealing leads to a moderate increase in crystallite size up to a temperature where accelerated crystallite growth begins. Also XRD results prior and after fatigue testing are presented.

Solid State Amorphization of Cu+Zr Multi-Stacks by ARB and HPT Technique: Yufeng Sun¹; Yoshikazu Todaka²; Minoru Umemoto²; Nobuhiro Tsuji¹; ¹Osaka University; ²Toyoashi University of Technology

A series of CuZr binary alloys with wide composition range were fabricated through ARB and HPT technique using pure Cu and Zr metals as the starting materials. Bulk alloy sheets with thickness of about 0.8 mm after ARB process and alloy disks with 0.35mm in diameter and 10 mm in diameter after HPT process can be obtained respectively. The structures of all the alloys were found to be gradually refined with the increasing of ARB cycles or HPT rotations. As a result, nanoscale multiple-layered structure was formed for the 10 cycled ARBed specimens, which could partially transform into amorphous phase after low temperature annealing. While for the as-HPTed sample, the alloy will be completely amorphized after 20 rotations without any heat treatment. The thermal stabilities of the amorphous alloys were studied. The deformation behavior and the amorphization mechanism during the ARB and HPT process were put forward and discussed.

Creep Response and Deformation Processes in Nanocluster Strengthened Ferritic Steels: Taisuke Hayashi¹; Peter Sarosi¹; Joachim Schneibel²; Michael Mills¹; ¹Ohio State University; ²Oak Ridge National Laboratory

Mechanically alloyed Oxide Dispersion Strengthened (MA/ODS) ferritic alloys are considered as candidate structural materials for fission and fusion power plants applications because of their excellent creep strength at high temperature and good resistance to irradiation-induced swelling. An alloy designated 14YWT containing 100nm sized grains and nanometer sized clusters (Y and Ti containing oxides) was subjected to high temperature annealing followed by creep at 800°C. Microstructural characterization using scanning and transmission electron microscopy to understand the microstructure stability during annealing as well as the deformation processes during creep of the MA/ODS steel was performed. A detailed examination of the grain growth, nanocluster distribution and dislocation analysis will be discussed.

Evolution of Microstructure and Property of a Pure Iron during Equal Channel Angular Pressing: Yue Zhang¹; Jingtao Wang¹; Songming Wang¹; ¹Nanjing University of Science and Technology

Equal channel angular pressing (ECAP) was conducted on a pure iron up to 8 passes via route A and Bc. Evolution of microstructure and mechanical property during ECAP were characterized by tensile testing and TEM observation. While strong thin lamellae structure with an average thickness of 0.2–0.4 micrometer were observed after 8 pass of ECAP via route A, as one expected; similar structure is also observed, mixed with equiaxed fine grain structures in the sample after 8 pass of ECAP via route Bc. Immediate necking after yielding is observed in tensile test of all the samples after ECAP, although an obvious plastic deformation is observed before failure. A high tensile strength of ~880MPa could be achieved through ECAP by both route A and Bc.

Influence of Rolling Direction on Strength and Ductility of Aluminium and Aluminium Alloys Produced by Accumulative Roll Bonding: Irena Topic¹; Heinz Werner Höppel¹; Mathias Göken¹; ¹Friedrich-Alexander University of Erlangen Nürnberg

The accumulative roll bonding (ARB) process has been recognised as a successful severe plastic deformation method for production of ultrafine-grained (UFG) materials with superior mechanical properties compared to their conventionally grained counterparts. The biggest advantage of this process is that it can be easily adapted in industry to produce large scale UFG sheets, especially interesting for light weight construction in automotive industry due to high potential of cost reduction and energy savings. In this work, accumulative roll bonded AA1050 and AA6016 showed significantly increased specific strength paired with high ductility. Despite a strongly elongated grain structure, tensile testing of samples oriented 45° to the rolling direction (RD) revealed considerable improvement in elongation to failure compared to the samples parallel to RD. Hydraulic bulge testing showed a tendency to higher achievable burst pressures and strains indicating good formability. Friction stir welding proved to be a successful method for UFG sheet material.

Influence of SPD on the Magnetic Properties of Soft Magnetic Materials: Stephan Scheriau¹; Klemens Rumpf²; Siegfried Kleber³; Heinz Krenn²; Reinhard Pippan¹; ¹Erich Schmid Institute of Material Science; ²Karl-Franzens-University Graz; ³Böhler Edelstahl GmbH

Industrial available FeSi, FeCo and FeNi alloys with an initial grain size of 20–50µm were subjected to Severe Plastic Deformation (SPD) by high pressure torsion at both ambient temperature (293 K) and liquid nitrogen temperature (77 K). The strain levels were chosen in that way where a saturation of the microstructural refinement is observed. The microstructure of the severely deformed states is analysed by Back Scattered Electrons (BSE) micrographs captured in a SEM. Additionally samples that were deformed at 77 K are examined in a Transmission Electron Microscope (TEM). The magnetic properties were characterised by means of SQUID-magnetography providing information of the magnetic behaviour of the material in the as processed state. Depending on the deformation temperature the mean microstructural sizes in the SPD-state are about 120nm and 50nm at 293 K and 77 K, respectively. The microstructural size influences significantly the magnetic properties of these materials. The initial soft-magnetic behaviour of the coarse grained state shifts towards a hard-magnetic with decreasing crystallite size. By dropping below a crystallite size of ~50nm the magnetic properties become again soft-magnetic.

Microstructure Development Ultrafine Grained Tantalum Produced by Machining: Mert Efe¹; Hyun Jun Kim¹; Wilfredo Moscoso¹; W. Dale Compton¹; Srinivasan Chandrasekar¹; Kevin Trumble¹; ¹Purdue University

Severe plastic deformation (SPD) of pure tantalum and subsequent microstructure development in annealing has been studied. Bulk plates of 1- to 6-mm thickness with plastic strains of 1 to 4 have been achieved in a new process called Large Strain Extrusion Machining (LSEM), in which the imposed plastic strain and plate thickness can be controlled controlled independently in a single stage deformation process. Significant grain refinement and corresponding hardening of the tantalum has been measured. High vacuum annealing with and without zirconium gettering, and metallographic analysis were used to characterize the recrystallization and grain growth behavior of the UFG tantalum. The results are discussed relative to the corresponding behavior in conventional ingot Ta.

Nano-Grained Copper Strip Produced by Accumulative Roll Bonding Process: Mohammad Reza Toroghinejad¹; Mahnoosh Shaarbaf¹; ¹Isfahan University of Technology

Accumulative roll bonding (ARB) process is a severe plastic deformation process that has been used for pure copper (99.9%). The ARB process up to 8 cycles was performed at ambient temperature under unlubricated conditions. Microstructural characterizations were done by transmission electron microscopy and electron backscattered diffraction. It was found that continuous recrystallization resulted in microstructure covered with small recrystallized grains with an average diameter below 100 nm. The tensile strength and hardness of the ARB processed copper has become two times higher than initial value. On the other hand, the elongation dropped abruptly at the first cycle and then increased slightly. Strengthening in ARB processed copper may be attributed to strain hardening and grain refinement. In order to clarify the failure mode, fracture surfaces after tensile tests were observed by scanning electron microscopy. Observations revealed that failure mode in ARB processed copper is shear ductile rupture with elongated small dimples.

Precipitation Hardening and Grain Refinement in an Al-4.3wt%Mg-1.2wt%Cu Alloy Processed by ECAP: Vanessa Vidal¹; Zheng-Rong Zhang²; Bert Verlinden¹; ¹KULeuven; ²University of Electro-Communications

In this study the influence of severe plastic deformation on the microstructure and the properties of a precipitation hardenable Al-4.3wt%Mg-1.2wt%Cu alloy was investigated by room temperature compression tests, EBSD and TEM. Samples in under aged, peak aged and over aged condition were deformed in an ECAP die at 180°C. After four ECAP passes fine equiaxed grains with an average size of approximately 200 nm with some traces of remnant elongated grains were obtained. It was observed that peak aged and over aged samples lose much of their strength during ECAP due to fragmentation of the precipitates. The highest strength after four ECAP passes (route Bc) was obtained with samples in under-aged condition, although in this case dissolution of precipitates into the matrix occurred. Formation of new round precipitates with small size were detected during post-ECAP annealing at 180°C. However, this re-precipitation resulted in a softening of the severely deformed samples.

Cold and Hot Severe Plastic Deformation of an Al-3wt%Mg Alloy: Martin Hafok¹; Reinhard Pippan¹; ¹Erich Schmid Institute of Materials Science

In order to examine the effect of deformation temperature on materials processed by high pressure torsion, an Al-3wt%Mg alloy was chosen to analyse the evolution of microstructure and microtexture. By using a single phase aluminium alloy instead of pure aluminium the static recrystallization and recovery, which may occur in pure aluminium even at room temperature, is suppressed after quenching the sample from elevated temperatures or after heating the sample to room temperature from cryogenic temperatures. The characteristic development of microstructure and microtexture of the alloy deformed in a temperature range between -196°C and 450°C were investigated by SEM, EBSD and TEM technique in order to reveal the transition between cold working, dynamic recovery and dynamic recrystallization during HPT. In the experiments a characteristic microtexture and microstructure was found which is associated with the torsion deformation, the dynamic recovery and the dynamic recrystallization.

Crack Growth in Ultrafine-Grained AA6063T6 Produced by Equal Channel Angular Pressing: Lothar W. Meyer¹; Kristin Sommer¹; Thorsten Halle¹; Matthias Hockauf¹; ¹Chemnitz University of Technology

Crack growth behaviour of ultrafine-grained AA6063T6, processed by equal channel angular pressing (ECAP) via route E at room temperature, were evaluated with special emphasis on the effect of grain size distribution and work hardening. A bimodal, two times ECAPed state and a monomodal ultrafine-grained state after eight ECA-extrusions are compared with the coarse grained initial T6 state. Crack growth behaviour is investigated by using SE(N)B-specimens and described by a Paris-Erdogan-Ratwani-equation, covering crack growth behaviour from the threshold region up to the high rate region approaching the critical stress intensity. Depending on the number of ECA-extrusions, the ECAPed material shows significantly lower threshold values (ΔK_{th}) and higher crack growth rates (da/dN) than its coarse grained counterpart. SEM micrographs of crack propagation surfaces reveal reduced grain size as major key to increased crack growth rates of the ECAPed material, as it influences roughness-induced crack closure and crack deflections.

Grain Growth in Ultrafinegrained Aluminium Processed by Hydrostatic Extrusion: Malgorzata Lewandowska¹; Tomasz Wejrzanowski¹; Krzysztof Kurzydowski¹; ¹Warsaw University of Technology

Ultrafinegrained materials may be produced by a number of techniques involving severe plastic deformation. These materials are generally thermally unstable and undergo grain growth at elevated temperature driven by a large surface area of grain boundaries. The kinetics of growth at early stage of the process (in fine grain size range) depends on microstructural features, such as a high fraction of high angle grain boundaries and grain size uniformity. This implies a correlation between the SPD technique used for grain refinement and thermal stability of processed materials. In the present work, the changes in grain size and grain boundary characteristics during annealing at various temperatures were evaluated quantitatively for technically pure aluminium processed by hydrostatic extrusion. The experimental kinetics of grain growth have been analyzed in terms of the influence of initial fraction of high angle grain boundaries and grain size homogeneity and by simulation based on Monte Carlo method.

Mechanical Properties and Corrosion Behavior of Ultrafine-Grained AA6082 Produced by Equal Channel Angular Pressing: Matthias Hockauf¹; Lothar W. Meyer¹; Daniela Nickel¹; Gert Alisch¹; Thomas Lampe¹; Bernhard Wielage¹; Lutz Krüger²; ¹Chemnitz University of Technology; ²Technische Universität Bergakademie Freiberg

The mechanical properties and corrosion behaviour of AA6082 with ultrafine-grained (UFG) microstructure are investigated and compared with the coarse grained (CG) AA6056 with much higher Cu-content that has been increasingly used for automotive applications. The AA6082 was processed by equal channel angular pressing (ECAP) up to eight extrusions at room temperature in a die with an internal angle of 90° following Route E with active backpressure. Besides the peak-aged temper, which gave maximum strengths and strongly reduced ductility, the solution heat treated condition was considered as well. Combined with post-ECAP ageing, an optimum of high strength, ductility and toughness was achieved. Polarisation tests showed a slightly more positive corrosion potential for the UFG-conditions compared to the CG counterparts. The results indicate that UFG low-Cu Al-alloys like AA6082 are capable to replace Cu-containing Al-alloys like AA6056 for applications in automotive industry, for example in high strength screws.

Low Temperature Mechanical Properties of the Ultra-Fine Grained Zirconium: Elena Tabachnikova¹; Aleksey Podolskiy¹; Vladimir Bengus¹; Sergey Smirnov¹; Vladimir Azhazha²; Mikhail Tikhonovsky²; A. Velikodniy²; Natalia Andrievskaya²; ¹B.Verkin Institute for Low Temperature Physics and Engineering of the National Academy of Sciences of Ukraine; ²National Science Center Kharkov Institute of Physics and Technology

Mechanical behavior of the ultra-fine grained zirconium has been investigated in uniaxial compression at temperatures 300, 170, 77, and 4.2 K. Mechanical characteristics have been compared for the different structural states of Zr: initial coarse-grained state (CG) with grain size 20 µm; ultra-fine grained state (UFG) with grain size 0.5 µm, produced by extrusion, thermal treatment and wire drawing; and another ultra-fine grained state (UFG+Term), produced

analogously to state UFG, but with additional annealing (grain size 0.5 μm). It has been established that values of yield stress of ultra-fine grained Zr (UFG state) are 4-6 times larger at all temperatures in comparison with initial coarse-grained structural state. Additional annealing (UFG+Term state) leads to small decrease of strength values (3–20%) due to reduction of internal stresses in ultra-fine grained Zr. All structural states of Zr have rather large plasticity (10-20%).

Microstructural Refinement of Bismuth-Antimony Alloy by Severe Plastic Deformation Processing: K. Hartwig¹; Jae-Taek Im¹; Jeff Sharp²; ¹Texas A&M University; ²Marlow Industries, Inc.

Cast bismuth (Bi) antimony (Sb) alloy was deformed by equal channel angular extrusion (ECAE) to refine the microstructure. The material under study is used in thermoelectric cooling applications, and the objective of the study was to improve the thermoelectric figure of merit and mechanical properties by grain refinement. In the work reported, twelve millimeter diameter bars of Bi10Sb were encapsulated in square cross section aluminum 6061 alloy containers and heated to the processing temperature. The composite bars were then placed in a warm tool and extruded through a 90 degree angle die isothermally. Processing variables included punch speed, extrusion temperature, multipass route and exit channel area reduction ratio. Post extrusion material characterizations included optical microscopy, x-ray diffraction, energy dispersive spectroscopy, wavelength dispersive spectroscopy and scanning electron microscopy. Texture evolution was analyzed using the {006} reflection plane to identify the orientation of the basal poles. The cast microstructure was equiaxed, had a nominal grain size of one to three millimeters, and showed substantial microsegregation. Severe plastic deformation above the recrystallization temperature is shown to break down the cast grains into a bimodal microstructure consisting of fine-grained (5-30 micron) and coarse-grained (50-300 micron) regions. It is noteworthy that further grain refinement and the elimination of the bimodal microstructure do not progress rapidly beyond the first pass. Texture results show that route C processing gives a stronger texture than route A processing, and that in both cases, the basal-plane poles become aligned with the shear direction. Reducing the exit channel area is seen to encourage a much stronger texture than ECAE processing alone.

Processing and Ballistic Performances of Lightweight Armors Based on Ultra-Fine-Grain Aluminum Composites: Timothy Lin¹; Fei Zhou¹; Quan Yan¹; Chufu Tan¹; Bob Liu¹; Adolphus McDonald²; ¹Aegis Technology Inc.; ²U.S. Army Aviation and Missile Command

Over last few decades Al-based metal matrix composites (MMCs) have become a promising material of choice for lightweight armors in vehicles. Recent development in ultra-fine-grain (UFG) and nanostructured material technology provides a new opportunity for the substantial strength enhancement of MMCs unattainable with the conventional microstructure of microscale, leading to significant weight reduction in armor packages. In this paper, Aegis Technology will present its latest development of a novel class of nanostructured metal Matrix composites (NMMCs) based on submicron SiC particulates reinforced nanocrystalline Al alloys, which is sponsored through an U.S. Army Small Business Innovative Research (SBIR) project. In this project, Aegis has successfully demonstrated the fabrication of large-dimension NMMCs plates by using a cost-effective synthesis and consolidation process that can be scaled up for the mass production. In this presentation, Aegis will report the microstructure, processing, mechanical properties and their correlations of this class of NMMCs. Particularly Aegis will present a detail investigation of the ballistic behaviors of the NMMCs under high-speed bullets of rifle and machine guns, in which a physical model and the associated simulation have been also developed to predict the penetration depth and identify the key influential parameters.

NOTES

2008 Nanomaterials: Fabrication, Properties, and Applications: CNT

Sponsored by: The Minerals, Metals and Materials Society, TMS Electronic, Magnetic, and Photonic Materials Division, TMS: Nanomaterials Committee
Program Organizers: Seong Jin Koh, University of Texas; Wonbong Choi, Florida International University; Donna Senft, US Air Force; Ganapathiraman Ramanath, Rensselaer Polytechnic Institute; Seung Kang, Qualcomm Inc

Monday AM
 March 10, 2008
 Room: 274
 Location: Ernest Morial Convention Center

Session Chair: To Be Announced

8:30 AM Invited

Carbon Nanotubes - Related Technologies and Engineering Concepts:

*Pulickel Ajayan*¹; ¹Rice University

Carbon nanotube has an important place in nanotechnology. From nanoelectronics to high strength composites, these structures have shown promise and there is a large effort world-wide in research and development of these materials. Several start ups and newly initiated activities at large companies on nanotubes bear testimony to the importance of this material in the technologies to come. The focus in our laboratory over the last decade has been on the engineering of these materials through directed assembly and different approaches in synthesis and processing. The talk will present concepts that lead to the engineering of individual nanostructures as well as assembled architectures that might be used in applications, such as nanoelectronics and sensors, membranes, composites, thermal management and energy related products. The overall scope for this material and our approach in the near term emerging technologies will be briefly discussed.

9:00 AM

Controlled Single-Walled Carbon Nanotubes Growth for High Performance Electronic Devices: *Jun Huang*¹; Wonbong Choi¹; ¹Florida International University

Single-walled carbon nanotubes (SWNTs) have been proposed as the building blocks for future nanoelectronics due to their exceptional electronic and mechanical properties. However, the SWNT devices have often been fabricated by using individual nanotubes, positioned randomly on the substrate. For large scale applications, it is highly desired to control the SWNTs growth direction so that large arrays of nanotube devices can be fabricated in a reproducible way. We have demonstrated the aligned growth of SWNTs by varying different parameters, such as electric field, gas flow and substrate. In this presentation, we will discuss the effect of these parameters on the directional growth of SWNTs. The devices fabricated using these aligned SWNTs demonstrate high $I_{on/off}$ ratio, high mobility and no hysteresis effect. It is suggested that the aligned nanotubes can be used for large scale fabrication of SWNT devices for future integrated nanotube electronics.

9:15 AM

Mechanical Properties of Metal-Carbon Nanotube Composites: *Guangping Zheng*¹; ¹University of Hong Kong

Carbon nanotubes (CNTs) are promising in the producing of strong and light composite materials because of their unique mechanical properties such as exceptional elastic modulus, ultrahigh mechanical strength and large ultimate tensile strain. Although CNT-polymer and CNT-ceramic composites have been successfully fabricated and their mechanical properties have been extensively investigated in the past decade, the CNT-metal composites are still in their infancy. In this study, Multi-walled (MW) CNT metal-matrix composite is synthesized by electrodeposition. X-ray diffraction, transmission electron microscopy and Raman spectroscopy characterizations of the specimens show that MWCNTs are successfully embedded in the cobalt-nickel alloy matrix. The content of MWCNTs can be as large as 5 wt %. The hardness of the composite is larger than that of cobalt. In order to have a better understanding of the mechanical properties of CNT-metal matrix composite, we investigate the metal-CNT interaction using atomistic simulation.

9:30 AM Invited

The Evolution of Helical Forms in Nanotube and Nanofiber Growth: Thermodynamic Model and Experiment: *Prabhakar Bandaru*¹; Apparao Rao²; ¹University of California, San Diego; ²Clemson University

The synthesis of helical morphologies of nanotubes and nanofibers, through Chemical Vapor Deposition (CVD), has been widely reported and can be made practical for a wide variety of applications, e.g., nanoscale mechanical springs and electrical inductors. Coiled structures are also scientifically interesting in that helices abound in nature, e.g., DNA, proteins etc. and a connection is being made at the nanoscale between carbon based inorganic and organic structures. I will first briefly review the models, in vogue, for the growth of helical forms and point out their shortcomings. Second, a thermodynamic model, based on exclusion volume principles, common in chemical and biological systems, will be introduced to explain coiling. Third, specific predictions will be made for the rational synthesis of nano-coils/-helices. Finally, experimental results conforming to the above model, on the role of Indium catalyst particles and local temperature in influencing the coil pitch in nanotubes/fibers, will be presented.

10:00 AM

Deposition of Ultrathin Polymer Films on CNTs for Enhanced Dispersion and Interfacial Bonding by Plasma Polymerization in CNT-Alumina Composites: *Donglu Shi*¹; Yan Guo¹; Hoon Sung Cho¹; Jie Lian²; Yi Song¹; Jandro Abot¹; Bed Poudel³; Zhifeng Ren³; Rod Ewing²; ¹University of Cincinnati; ²University of Michigan; ³Boston College

Effects of nanoparticle/nanotube surface plasma coating on interfacial behaviors in single wall nanotubes (CNTs)-Al₂O₃ nanocomposites was studied by using high resolution transmission electron microscopy (HRTEM) and mechanical testing. A unique plasma polymerization method was used to coat the alumina nanoparticles and CNTs, which were precursors for the composites. The CNTs-Al₂O₃ nanocomposites were processed by both ambient pressure and hot press sintering. The HRTEM results showed ultrathin pyrrole films (~3 nm) on the surfaces of CNTs and Al₂O₃ nanoparticles. A distinctive stress-strain curve difference related to the structural interfaces and plasma coating was observed from the composites. The mechanism on the mechanical property enhancement due to nanoparticle surface plasma coating is discussed.

10:15 AM

Epoxidation of Carbon Nanotubes through Controlled Organic Acid Treatment: *Shiren Wang*¹; ¹Texas Technological University

Carbon nanotube (CNT) is the strongest fiber so far and has been regarded the most promising reinforcement for next generation multifunctional high-performance composites. However, the current fabrication challenges have seriously restricted these potential applications. In this research, we epoxidized carbon nanotubes with controlled organic acid treatment. Scanning Electron Microscope characterization indicated that dispersion of functionalized CNTs in the epoxy resin has been remarkably improved. It is also found that functionalized CNTs were well embedded in the polymer resin, suggesting improved interface bonding. With only 1wt% loading, epoxidized CNTs/Epoxy composites demonstrated a 50% increase in the Young's modulus, 32% improvement in the tensile strength while un-modified CNTs composites showed worse strength. Epoxy group can be converted into different kinds of functionalities through a ring-opening reaction. Therefore, epoxidation of CNTs significantly enriched the chemistry and facilitated their applications. This investigation provides a solid foundation for the further industrial application of CNTs.

10:30 AM

Fabrication and Mechanical Properties of Carbon Nanotube/Metal Nanocomposites Processed: *Kyung Tae Kim*¹; Seung Il Cha²; Yong Jin Jeong³; Thomas Gemming¹; Juergen Eckert¹; Soon Hyung Hong³; ¹IFW Dresden; ²NIMS; ³KAIST

The recent application of nanotechnologies to structural materials is a promising way to produce new strong materials that exceed current limitations. Grain size refinement is considered as one of the most effective strengthening method of materials. At the same time, the addition of carbon nanotubes (CNTs) in a material is known more effective than conventional reinforcements. Here, CNT/Co nanocomposites were fabricated by reinforcing the CNTs in nanocrystalline Co matrix using modified molecular level mixing process. The CNT/Co pearl-necklace-structured nanopowders, consisting of Co nanoparticles penetrated by

CNTs, were fabricated and then consolidated into CNT/Co nanocomposites using spark plasma sintering. The CNT/Co nanocomposite showed outstanding yield strength of 1.5 GPa, which is comparable to those of ceramics. This indicates that the synergistic strengthening mechanism of homogeneously dispersed CNTs in nanocrystalline metal matrix could extend the limitation of mechanical properties of materials.

10:45 AM Break

11:00 AM Invited

Solution-Processed Transparent and (Semi) Conducting Single Walled Carbon Nanotube Thin Films: *Manish Chhowalla*¹; ¹Rutgers University

Low-density random networks of SWNTs have received significant attention for applications such as transparent electrodes for solar cells and active layers in field-effect transistors. We will briefly review the optoelectronic properties of individual carbon SWNTs and networks. Secondly, we will show how the degree of bundling of SWNTs suspended in water can be determined as a function of the sedimentation time by monitoring their optical transmittance at different depth levels of the vessel. We discuss how the formation and aggregation of 1-200 nm-diameter nanotube bundles in suspension typically occurs on time scales of 0-20 hours and can be understood in the framework of the Mie theory of light scattering. Finally, morphology, optical properties and the electronic performance of solution-processed SWNT networks will be correlated to the type and age of the starting suspensions by means of spectroscopic ellipsometry and Raman spectroscopy combined with electrical transport measurements.

11:30 AM

Mechanical Properties of Well-Aligned Multi-Walled Carbon Nanotube Mats: *Christian Deck*¹; Jason Flowers¹; Brandon Reynante¹; Chi-nung Ni¹; Prabhakar Bandaru¹; Kenneth Vecchio¹; ¹University of California

Carbon nanotubes (CNTs) have been of interest in many fields, due to their exceptional mechanical properties and geometry. In this work, the mechanical properties of well-aligned CNT mats were investigated using two distinct methods. A stage was designed to allow in-situ scanning electron microscopy observation of compression, tension, and shear testing of CNT mats. Force measurements were taken and the elastic modulus of the CNT mats was measured. The flexural rigidity (the product EI) is also important in predicting mechanical response, and an optical method for measuring the flexural rigidity of CNT mats was developed. The deflection of CNTs was observed by introducing fluid flow over CNT mats; this deflection was correlated with measurements of transmitted laser intensity, where intensity drops were observed with increased velocity due to CNT bending. The fluid drag force was simulated, and the experimental and simulation results were used to determine the CNT flexural rigidity.

11:45 AM

Multi-Scale Tribology of Plasma Sprayed Carbon Nanotube Reinforced Aluminum Oxide Nanocomposite Coating: *Kantesh Balani*¹; Sandip Harimkar²; Narendra Dahotre²; Arvind Agarwal¹; ¹Florida International University; ²University of Tennessee

Our previous studies have revealed that carbon nanotube (CNT) reinforced plasma sprayed Al₂O₃ coating results in improved fracture toughness. In the present study, tribological properties of these coatings have been evaluated at multi-length scale. Owing to disparity of wear and friction at nanosurface contact and loss of material as a bulk, multi-scale tribological study becomes critical in bridging of the wear phenomenon. Pin-on-disc technique is utilized to calculate wear rate of the plasma sprayed coatings at a macro scale, whereas nanoscratch technique is adopted to describe the wear phenomenon at a nano scale. Role of CNT addition and dispersion has shown intriguing results in establishing the material loss of plasma sprayed nanocomposites. Scanning electron microscopy (SEM) has evinced pinning of wear debris by CNTs resulting in the reduced material loss.

12:00 PM Invited

Atomic and Molecular Nanostructures: From Assembly to Function: *Klaus Kern*¹; ¹Max-Planck-Institut für Festkörperforschung

A promising route toward the realization of functional nanosystems is the exploitation of nature's inherent drive to generate complexity. The transcription of the corresponding organization principles to artificial compounds and environments comprises intriguing perspectives. We emphasize the conductance

of self-organized growth processes at well-defined surfaces. The atomistic insight gained into the underlying mechanisms and interactions is used to control the formation of low-dimensional atomic and molecular architectures. This know-how opens up new avenues in engineering nanomaterials of well-defined shape, composition and functionality to be harnessed for future technological applications.

12:30 PM

Redox Synthesis of MnOx-CNT Composites for Supercapacitor Applications: Xianbo Jin¹; Shengwen Zhang¹; Wuzong Zhou²; *George Chen*¹; ¹University of Nottingham; ²University of St. Andrews

Direct reaction between solid carbon (graphite) and permanganate ion in aqueous solutions was first demonstrated recently by this group to be capable of coating the solid carbon with a thin layer of MnOx which exhibited highly satisfactory capacitive behaviour with high stability in cycle life tests. This presentation describes experimental findings in our extension of the previous work by replacing the graphite with carbon nanotubes (CNTs). By variation of the reaction conditions, it has been found through XRD, SEM and TEM that the reaction products can be composites of carbon nanotubes coated individually with MnOx with carbon/manganese ratio being controllable according to the redox reaction. The MnOx deposition mechanism has been proposed, based on experimental evidence, to include two steps: direct carbon-MnO₄⁻ reaction and the micro-electrochemical cell. The products are shown to be of ideal materials for supercapacitor applications with the electrode specific capacitance reaching beyond 5 F/cm².

12:45 PM

Studying on the Ce/Zr Oxide Coating on Carbon Nano-Tubes: *Zhi Guo Dong*¹; Yao Guangchun¹; ¹Northeastern University

Carbon nano-tube is a promising reinforcing material for its unique mechanical and physical properties, but the wetting property of metal-matrix and carbon nano-tube is poor. So, in this paper, a continuous Ce/Zr oxide layer was prepared on to the surface of carbon nano-tube to improve the wetting property with Al-matrix then improve the interfacial strength. As to carbon nano-tube, it is difficult to gain continuous Ce/Zr oxide layer because of lame proportion of longitudinal axis length and its diameter, weak reaction capacity, lame curvature of surface, small diameter. So, a series of way of optimization (oxidization, sensitization and activation) were used to increase the activated sites of carbon nano-tube before coating. The result of TEM, XPS, XRD showed that a continuous Ce/Zr oxide layer was successfully prepared onto the nanotube, which indicated a foreground of composite material of carbon nano-tube.

3-Dimensional Materials Science: ONR/DARPA Dynamic 3-D Digital Structure Program

Sponsored by: The Minerals, Metals and Materials Society, TMS Structural Materials Division, TMS: Advanced Characterization, Testing, and Simulation Committee
Program Organizers: Michael Uchic, US Air Force; Eric Taleff, University of Texas; Alexis Lewis, Naval Research Laboratory; Jeff Simmons, US Air Force; Marc DeGraef, Carnegie Mellon University

Monday AM
March 10, 2008

Room: 286
Location: Ernest Morial Convention Center

Session Chairs: Julie Christodoulou, Office of Naval Research; Alexis Lewis, Naval Research Laboratory

8:30 AM Invited

Dynamic 3-D Digital Structure: *Julie Christodoulou*¹; ¹Office of Naval Research

Launched in the spring of 2005, the Dynamic 3-D Digital Structure program is an ONR-DARPA jointly funded initiative that aims to establish a robust protocol for developing and extracting data, creating quantitative representation of salient materials features, and developing and linking modeling tools to enable a ten-fold increase in the efficiency by which materials science is developed and communicated. Within the program, we are developing both experimental and computational tools, recognizing the effectiveness of using physics-based and

statistical models to guide more rigorous experimentation. Three teams led by the Ohio State University, QuesTek LLC, and the Naval Research Laboratory are engaged in this effort. Their objectives and recent accomplishments will be introduced in this talk.

8:55 AM Invited

The Direct 3-Dimensional Characterization and Digitization of Complex Microstructures in Ti-Based Alloys across Length Scales: *Peter Collins*¹; Robert Williams¹; Hamish Fraser¹; ¹Ohio State University

There have been significant efforts at developing models relating composition, microstructure, and properties in a variety of Ti-based alloys. Until recently, the microstructural information has been estimated from two-dimensional images, resulting in descriptions of the average features determined using classical stereological methods. However, given the recent advent of direct three-dimensional characterization methods, it is possible to characterize the microstructural features without the a priori assumptions associated with stereology. This talk will focus on four novel techniques for the direct three-dimensional characterization of complex microstructures in Ti-based alloys for a range of length scales, from meso-scale (e.g., grain size), through micro-scale (e.g., α -lath thickness) and nano-scale features (e.g., secondary α in Ti-based alloys) to distributions of atomic species in ultra-fine clusters (e.g., athermal ω). These results will be related to those obtained using classical stereological approaches to show that many aspects of the microstructures cannot be accurately obtained using two-dimensional approaches.

9:20 AM Invited

Crystal Plasticity Models with Multi-Time Scaling for Cyclic Deformation of Polycrystalline Metals: *Somnath Ghosh*¹; Deepu Joseph¹; Pritam Chakraborty¹; ¹Ohio State University

The recent years have seen a paradigm shift towards the use of detailed micromechanical models to understand damage mechanisms leading to fatigue failure. Crystal plasticity theories with explicit grain structures are effective in predicting localized cyclic plastic strains. The recent years have seen significant efforts in modeling cyclic plasticity and fatigue with considerations of microstructural stress-strain evolution. Modeling cyclic deformation using conventional time increments can be an exorbitant task for crystal plasticity computations. Most simulations performed with 3D crystal plasticity are in the range of 100 cycles and the results are subsequently extrapolated for fatigue predictions. In modeling fatigue, it is however desirable to conduct simulations for a significantly high number of cycles to reach local states of damage initiation and growth. Conventional methods of time integration using semi discretization present numerous challenges due to the variation in time scales ranging from the scale of the entire process to the time resolution required by the damage evolution and crack propagation. A method of solution of crystal plasticity equations is developed in this paper using multiple time scaling that involves compression and rarefaction of time scales. The method enables large time scale homogenization in relatively benign periods of deformation, to very fine time scale simulations in temporal regions needing high resolution, e.g. with evolving localization. The multi time scaling formulation for polycrystalline materials is based on asymptotic expansion based homogenization method in the time domain. The comparison with the single time scale reference solution shows excellent accuracy while the efficiency gained through time compression can be enormous.

9:45 AM Invited

Dynamics of 3D Microstructures: *Erik Lauridsen*¹; ¹Riso National Laboratory

This talk will present highlights of studies of the dynamics of 3D microstructures conducted as part of the collaborative D-3D network funded by ONR/DARPA. Using non-destructive synchrotron X-ray based techniques such as 3D X-ray diffraction (3DXRD) microscopy and micro-tomography the microstructural evolution of selected titanium alloys have been monitored with a spatial resolution of a few micrometers. Results from studies of precipitation kinetics and grain growth in titanium alloys will be presented and the coupling of such evolving 3D experimental data with modeling efforts will be discussed.

10:10 AM Break

10:30 AM Invited

Morphological and Crystallographic 3D Reconstruction of β -Grains in Ti-21S: *David Rowenhorst*¹; Alexis Lewis¹; George Spanos¹; ¹Naval Research Laboratory

A large serial sectioning experiment was performed using 200 sections in Ti-21S, a β -stabilized Ti alloy, resulting in a three dimensional (3D) data set containing over 1000 grains. In addition to the morphological information, EBSD was used to determine the crystallographic orientation of each grain, which allows for the analysis of the grain boundary texture, nearest neighbor relationships, and exact morphological measurements of the structure such as grain sizes and interface curvature. The experimental results will be compared to grain growth theory and simulations.

10:55 AM Invited

Simulating Grain Growth in Three Dimensions: I. McKenna¹; M. Gururajan¹; M. Na²; Y. Wang²; *Peter Voorhees*¹; ¹Northwestern University; ²Ohio State University

There have been tremendous advances in the ability to collect experimental data on the three-dimensional microstructure of a multigrain material. To follow the evolution of a system of grains that have been measured experimentally, we have developed a single-order-parameter model that accounts for all five degrees of freedom that determine the grain boundary energy and a multiorder parameter model for grain growth. To insure that the computations using the multiorder parameter model are in the boundary-curvature-driven limit, we examine the dependence of grain growth kinetics on the boundary thickness. The single-order-parameter model for grain growth employs quaternions to account for the dependence of the grain boundary energy on the misorientation, a tensorial gradient energy coefficient to account for the change in grain boundary energy with boundary normal, and a singular diffusivity for the order parameter. A comparison of the multiorder and single order parameter models will be presented.

11:20 AM Invited

Atom-Probe Tomographic Characterization of Multicomponent Fe-Cu Based Steels: *David Seidman*¹; ¹Northwestern University

Atom-probe tomography (APT) is employed to characterize on a sub-nano scale multicomponent Fe-Cu based precipitation strengthening steels being developed for various applications. The three-dimensional (3D) characterization of the micro- and nano-structures is determined, for different thermal processing conditions, as a function of aging time. APT permits us to obtain a complete inventory of the different alloying elements of an area that approaches 200 x 200 nm² and a depth that can exceed one micrometer: copper-rich and metal carbide precipitates at disparate number densities are also studied. In parallel with the 3D characterization we are studying different mechanical properties: microhardness, yield strength, ultimate tensile strength, plasticity at failure, Charpy V-notch values, and blast resistance. All this information is used to determine the optimum thermal aging treatments that yield the desired values of the key mechanical properties. This research is supported by the Office of Naval Research, Dr. Julie Christodoulou, grant officer.

11:45 AM Invited

Computational Modeling of Ductile Failure of Steel: Direct Numerical Simulation and a Multi-Scale Micromorphic Constitutive Damage Model: *Brian Moran*¹; Wing Liu¹; Gregory Olson¹; ¹Northwestern University

We discuss recent advances in computational analysis of failure mechanisms in high strength steel (McVeigh et al., JMPS, 2007; Vernerey et al., JOM, 2006). Computational issues regarding modeling of the geometry, distribution and material behavior of the dispersed phases present in the microstructure of steel are described. The investigation of the failure mechanisms using computational cell model methodology in two and three dimension is then presented with an emphasis on microvoid-induced shear failure occurring at the scale of sub-micron grain-refining carbide precipitates. The failure of a 3D particle cluster extracted from tomographic analysis of an engineering alloy is simulated. A recently developed multi-scale micromorphic constitutive model (Vernerey et al., JMPS, 2007, submitted) which accounts for failure mechanisms at multiple scales is also discussed. Comparisons between the model and direct numerical simulation of microstructural failure are presented.

Advances in Roasting, Sintering, Calcining, Preheating, and Drying: Advances in Thermal Processing

Sponsored by: The Minerals, Metals and Materials Society, TMS Extraction and Processing Division, TMS: Pyrometallurgy Committee
Program Organizers: Jerome Downey, Montana Tech of the University of Montana; Guy Fredrickson, Idaho National Laboratory

Monday AM Room: 281
 March 10, 2008 Location: Ernest Morial Convention Center

Session Chairs: Jerome Downey, Montana Tech of the University of Montana; Guy Fredrickson, Idaho National Laboratory

8:30 AM Introductory Comments

8:35 AM

Pre-Cast Trifoil Heat Exchangers for Rotary Kiln Systems: *Joel Filius*¹; ¹LWB Refractories

LWB Refractories has developed and patented the design and installation of Internal Heat exchanger systems for rotary kilns. Installations to date total nearly 40 individual systems, installed primarily in Rotary Lime Kilns. These systems vary in installed length and orientation to maximize the thermal transfer of heat from the gas stream to the material burden. Internal Heat exchangers have demonstrated benefits of lowering fuel consumption through improved thermal transfer to the load, increasing production potentials and lowering inlet gas temperatures. This paper will explore the current benefits of these systems, with the direction towards application in Waelz or Calcining systems of the Zinc recovery systems. LWB's patent covers the production of 3, 4 and 5 leg internal systems.

9:05 AM

Investigation on Preparing Strontium Carbonate from Celestite Concentrate by Agglomeration-Reduction Roasting Process: *Mudan Liu*¹; *Jiang Tao*¹; *Guanghui Li*¹; ¹Central South University

An agglomeration-reduction roasting process leading to the preparation of SrCO₃ from celestite flotation concentrate was studied. A laboratory pelletization mill was used (18 to 20 min balling time) to produced 9% moisture green pellets with a high drop strength. Lignin xanthate binder improved the pellet formation and the pelletizing rate by enhancing the hydrophilicity of the concentrate particle surfaces. Under the optimal roasting conditions (i.e., between 30 and 50 min) at 1100 to 1150°C, 82 to 83% of the pelletized celestite (SrSO₄) was converted to strontium oxide when anthracite was used as reductant. This result was 10% higher than that attained by roasting celestite lumps under the same conditions. High-purity strontium carbonate (greater than 97% SrCO₃ containing less than 0.3% CaCO₃) was obtained by leaching, purifying, and carbonating the roasted pellets.

9:35 AM

The Simulation and Application of Spray Dryer Tower in Alumina Rotary Kiln Sintering: *Hongliang Zhang*¹; *Jie Lie*¹; *Xiangtao Chen*¹; ¹Central South University

The paper presents a new technology for alumina rotary kiln sintering, namely the spray dryer sintering. The process flow of the technology was as following: the raw slurries were ejected into the dryer tower, where they were heated and dehydrated by exhaust gases from the end of rotary kiln, and then they were transformed into dry solid particles, which were finally fed into rotary kiln. A 3-dimensional numerical model of the spray dryer tower was built using the CFD package Fluent. The distributions of the temperature, velocity, particles tracks and drying speed were analyzed. Industrial applications show that this technology can reduce the construction cost of rotary kiln, the energy consumption, and it is valuable for alumina plant.

10:05 AM Break

10:35 AM

Development and Application of Optimal Model for Iron Ore Sintering Process Parameters: *Dai fei Liu*¹; *Xiao hui Fan*¹; *Hong ming Long*¹; ¹Central South University

Input and output network optimization models were separately developed by analyzing the relationships between the iron ore mixing scheme, process parameters, yield, and quality indexes. Because the neural network modeling results favored the input network model, optimal process parameters were calculated using the input network model in conjunction with neural network and genetic algorithms. The model's effectiveness and practicability were demonstrated by a reduction in the sintering process energy consumption and improved sinter yield and quality.

11:05 AM

Induration Mechanism of Oxidized Pellets Prepared by Magnetite Concentrate and Hematite Concentrate Mixture: *Mudan Liu*¹; *Guanghui Li*¹; *Tao Jiang*¹; ¹Central South University

This investigation provides a theoretical basis for the establishing and optimizing the calcination of oxidized pellets prepared from a magnetite and hematite mixture. Strength formation mechanisms of Fe₂O₃ pellets were studied. Pellets were prepared by preheating and calcining mixtures of magnetite and hematite. The results indicate that the crystallite connection of Fe₂O₃ in hypo-hematite formed during the preheating process, is the main contributor to pellet strength. The strength of the Fe₂O₃ matrix in the hypo-hematite produced by oxidizing magnetite exceeded that of original hematite (from hematite concentrate). When calcined below 1250°C, pellet strength is mainly provided by the development of Fe₂O₃ crystals between hypo-hematite grains. When calcined above 1280°C, the Fe₂O₃ recrystallization in original hematite was well-developed, the grains within pellets were fully connected, and a strength approaching the theoretical maximum was obtained.

11:35 AM

A New Multi-Region Double Thresholds Segmentation and Its Application in Alumina Rotary Kiln Flame Image: *Hongliang Zhang*¹; *Jie Li*¹; ¹Central South University

Careful flame characteristics control is very important in the calcination stage of the alumina production process. This paper describes a multi-region double threshold segmentation algorithm, which is based on the kiln's "fire region" and the "material region." The algorithm iteratively calculates the corresponding region thresholds and segments the flame image with the two thresholds. In experimental evaluations, the flame image was initially sampled with a charge coupled device from an alumina rotary kiln, and then the single threshold, fuzzy c-means, and multi-region double threshold methods were applied to segment the flame image. The results indicated that multi-region double threshold method more rapidly achieved approximately the same result as fuzzy c-means method, and that both methods produced better results than the single threshold method. The research is of great significance for the flame pattern recognition and for the intelligent control of the rotary kiln.

Advances in Semiconductor, Electro Optic and Radio Frequency Materials: Silicon-Based Optoelectronics and Microelectronics

Sponsored by: The Minerals, Metals and Materials Society, TMS Electronic, Magnetic, and Photonic Materials Division, TMS: Thin Films and Interfaces Committee
Program Organizers: Nuggehalli Ravindra, New Jersey Institute of Technology; Narsingh Singh, Northrop Grumman Corporation ES; Choong-un Kim, University of Texas - Arlington; Yanfa Yan, National Renewable Energy Laboratory; Bhushan Sopori, National Renewable Energy Laboratory; Greg Krumbick, Argonne National Laboratory

Monday AM Room: 278
 March 10, 2008 Location: Ernest Morial Convention Center

Session Chairs: Narsingh Singh, Northrop Grumman Corporation ES; Choong-un Kim, University of Texas

8:30 AM Introductory Comments

8:40 AM Invited

Present Status of Silicon Photovoltaics: *Bhushan Sopori*¹; ¹National Renewable Energy Laboratory

Manufacturing and sales of photovoltaic (PV) cells and modules have been growing at rates exceeding 30% for the last several years. In 2006, PV production exceeded 2 GW and it is expected to surpass 3 GW in 2007. Silicon continues to be the dominant technology with > 90% market share. The position of Si-PV has been strengthened by many technological advances that have led to efficiencies > 16% and 20% for low-cost solar cells and for single-crystal, high-efficiency devices in commercial production. These advances include: improved as-grown material quality; cell processing techniques that include light trapping, impurity gettering, and hydrogen passivation; automation that has enabled high throughput; and newer diagnostics methods. The brisk growth in the market has resulted in a shortage of poly silicon feedstock. However, its impact has only been minor because the PV industry reacted fast to invest into new poly plants, some of which will cater solely to the PV industry. New approaches are needed to increase cell/module efficiencies, develop energy-efficient processing techniques, develop low-cost sources of feedstock, and minimize encapsulation costs. R&D efforts need to be extended into module technology to lower the module costs. This paper will review recent technical advances in Si-PV technology, discuss technical bottlenecks that limit efficiency of current solar cells, and describe potential approaches to overcome them.

9:10 AM Invited

Silicon Integrated Microplasma Optoelectronics: *Anthony Fiory*¹; Martin Lepselter²; Nuggehalli Ravindra¹; ¹New Jersey Institute of Technology; ²BTL Fellows Inc.

Microplasma devices are considered for illumination sources in silicon-based opto-microelectronics, owing to their high brightness and efficiency. A pressurized microplasma triode can optically pump microlasers on silicon chips for all-optic integrated systems. The plasma discharge optical pump comprises a microcavity plasma triode device that is fabricated with precision microbridge technology. Plasma elements utilize silicon hollow cathodes with regeneration chemistry for inhibiting erosion and enhancing operating lifetime. This technology enables fabrication of a massively parallel all-optical buss with microplasma microlasers (10^{13} bits/scm² at 1 W/cm² power dissipation). Miniature plasma displays can be implemented entirely in a silicon chip using microplasma illuminators. High system reliability derives from broad experience with the technology components of gas microplasma display devices, air bridges, silicon microelectronics and plasma display panels. Moreover, laser sources are built in silicon using materials and processing techniques that are integrable with optoelectronics in standard CMOS.

9:40 AM Invited

Characterization of Silicon Doped with Rare-Earth Metals: *Sufian Abedrabbo*¹; Asmaa Haddad¹; Qais Mohammed¹; Anthony Fiory²; Nuggehalli Ravindra²; ¹University of Jordan; ²New Jersey Institute of Technology

While silicon is intrinsically an inefficient light emitter, there is considerable interest in improving its optical emission efficiency through materials modification, owing to the inherent advantages of integrating silicon photonics with VLSI technology. In this work, rare-earth metals impurity centers in silicon are investigated. Erbium is co-evaporated with silicon on silicon substrates along with other proper dopants to yield improved emission efficiency. The processed samples are investigated optically by photoluminescence and structurally by Rutherford backscattering.

10:10 AM

Formation of a Ni-FUSI/HfO₂ Gate Stacks by a Novel Integration Process: *Shiang Yu Tan*¹; ¹Chinese Culture University

The low resistivity nickel fully silicided (FUSI) gate have received increasing attention over the past several years due to the simply integration scheme for implementation and ease of passivation of the underlying gate dielectric for sub-65 nm/45 nm CMOS devices. In order to obtain a thermally stable Ni-FUSI gate electrode, we developed a unique integration process to achieve NiSi phase stabilize at temperature 900°C and delay the agglomeration of NiSi. For the first time, we established an effective way to identify the phase transformations by some nondestructive techniques such as X-ray diffraction, sheet resistance measurement and AFM analysis. The correlations between its electrical and morphological changes during Ni-Si phase transformation were presented.

10:35 AM Break

10:45 AM Invited

Production of High Purity Silicon with Physical Metallurgical Method: *Liang Pang*¹; *Huimin Lu*¹; ¹Beijing University of Aeronautics and Astronautics

A physical metallurgical method has been used to purify industrial raw silicon to high pure silicon from 99.95% to 99.9999% purity. At present, polysilicon with 99.9999% purity has been used to solar battery. The traditional method of produce polysilicon is SIEMENS method. Current high-purity polysilicon technology is a combined technique of metallurgy and directional solidification method. The industrial raw silicon is crushed to 250µm firstly, and then acid dipping and placing processed silicon into a special refining furnace to purify with vacuum environment. The next step is directional solidification. Super high-purity polysilicon in excess of 99.9999% is produced.

11:15 AM

Mechanisms of Front Contact Formation in Si Solar Cells: *Vishal Mehta*¹; Bhushan Sopori²; Nuggehalli Ravindra³; ¹National Renewable Energy Laboratory, New Jersey Institute of Technology; ²National Renewable Energy Laboratory; ³New Jersey Institute of Technology

In commercial Si solar cell fabrication, the front and backside contacts are formed simultaneously in a one-step process. Because the front contact is formed on a rather shallow junction, its control is very critical. The front contact is typically screen-printed using a Ag-based ink and fired at about 800°C. The Ag-based ink also contains other constituents such as solvent metal(s), glass frit, and an organic binder, all of which help to achieve the desired properties of the contact. The reactions that occur during firing are quite complex. They include: (i) interaction of the solvent metal to lower the eutectic point of Si-Ag, (ii) fusion of various Ag particles to produce a laterally conducting bus, and (iii) formation of a Si-Ag alloy at the interface. To achieve the desired characteristics of the junction, one must understand various reactions and control them to minimize shunting and series resistance and to achieve high performance of the cell. We have studied contact formation in multicrystalline Si solar cells. Solar cells were screen-printed and fired under different processing conditions in a static optical furnace, and their solar cell parameters were measured. We measured other characteristics, such as Si-Ag contact fraction, sheet rho of the bus bar, and shunt resistance of the contact. Likewise, we also evaluated physical parameters of the front contact to investigate various aspects of contact formation. This paper will present results of our studies.

11:40 AM

Effect of Process-Induced Damage during SiN:H Deposition on the Surface Recombination of Silicon: Chuan Li¹; Bhushan Sopori²; Rene Rivero³; Nuggehalli Ravindra³; ¹National Renewable Energy Laboratory and New Jersey Institute of Technology; ²National Renewable Energy Laboratory; ³New Jersey Institute of Technology

Hydrogenated silicon nitride (SiN:H) is used in solar cell fabrication to provide bulk and surface passivation. However, SiN:H deposition is also known to produce a damaged region beneath the Si surface. Such surface damage can increase the effective surface recombination velocity (SRV) by introducing an extended region of interface state densities (Dit) in the space-charge region (SCR). Although the firing process can heal some of the surface damage, experimental results show that extended damage remains after annealing. To fully understand the effect of surface damage on surface recombination, we developed a model for calculating SRV of a wafer, which incorporates carrier recombination due to the distribution of Dit in the SCR. This paper describes the proposed model and discusses the results of calculations that relate SRV to the distribution of the damage. We will also describe the verification of the model from SRV measurements of unfired and fired samples, using lifetime data from the quasi-steady-state photoconductance decay technique.

12:05 PM

Edge Passivation in Small-Area N-P Junction Devices: Modeling and Experiments: Jesse Appel¹; Bhushan Sopori²; Nuggehalli Ravindra³; ¹National Renewable Energy Laboratory, New Jersey Institute of Technology; ²National Renewable Energy Laboratory; ³New Jersey Institute of Technology

A small-area mesa diode array, fabricated by chemical etching, is a very valuable technique for detailed characterization of photovoltaic substrates. These devices can be probed with an automatic probe to provide local solar cell parameters such as open-circuit voltage, short-circuit current, and fill factor, and other materials-related parameters such as resistivity, defect density, and minority-carrier diffusion length. Fabricating mesa diode arrays requires passivation of the diode edges, which occurs intrinsically during mesa etching with the Sopori etch by generating a H-saturated suboxide on the etched surface. However, the quality of the passivation is strongly controlled by the cleanliness of the fabrication process. This paper describes a computer model developed to study the influence of edge passivation on the measured cell parameters of the local device(s). We have developed a FE model, which includes generation-recombination at the diode edges. This model takes into account the charge accumulation at the suboxide layer and the loss of carriers that flow into the edge region as a function of the diode voltage. We discuss theoretical results of the model and describe its experimental verification.

Aluminum Alloys: Fabrication, Characterization and Applications: Development and Applications

Sponsored by: The Minerals, Metals and Materials Society, TMS Light Metals Division, TMS: Aluminum Committee

Program Organizers: Subodh Das, Secat Inc; Weimin Yin, Secat Inc

Monday AM
March 10, 2008

Room: 293
Location: Ernest Morial Convention Center

Session Chairs: Subodh Das, Secat Inc; Weimin Yin, Secat Inc; Zhong Li, Aleris International Inc

8:30 AM

Composition and Process Optimization of AA 5083 Aluminum Sheet for Quick Plastic Forming: Ravi Verma¹; Paul Krajewski¹; ¹General Motors Corporation

Sheet manufacturing data collected on approximately 175 coils of superplastic grade 5083 aluminum alloy was analyzed. Key alloy composition and processing variables affecting superplastic elongation of the 5083 sheet were identified. Of these variables, manganese and chromium contents of the alloy, and ingot homogenization time had the most effect on the sheet superplastic elongation, which improved with increasing manganese and chromium contents and longer

homogenization time. Significant improvement in material performance was achieved by implementing recommendations based on this study.

8:50 AM

An Aluminum Alloy Development Study to Investigate the Potential to Improve the Formability of the Alloys for Automotive Application: Kerry Border¹; Yansheng Liu²; Shridas Ningilieri²; ¹Toyota Technical Center; ²Secat Inc

Developing new aluminum alloys with formability comparable to steel will enable the existing tooling systems for steel to be used with minor modifications. The current investigation focuses on this topic and starts out by evaluating the current alloys and the effects of various alloying elements on the material characteristics. Several aluminum alloys are suggested as potential choices for development. Feasibility of various processes ranging from direct chill cast to strip casting as well as spray forming are discussed. Every step of the process starting from ingot casting through rolling process and heat treatment ending at stamping is reviewed based on potential costs. The paper also looks at certain technologies that can be applied at the fabrication shops to improve the materials ease of forming. The investigation also looks at the future prospects of aluminum alloy usage in automotive applications.

9:10 AM

Effects of Scandium and Thermal History on the Structure and Properties of Spray Formed Aluminum 7055 Alloys: Junyeon Hwang¹; John Whetten²; T.J. Eden³; A. Robinson³; W. Sharpe⁴; Michael Kaufman⁵; ¹University of North Texas; ²University of Idaho; ³Pennsylvania State University; ⁴U.S. Army Research Laboratory; ⁵Colorado School of Mines

7xxx series Al-Zn-Mg-(Cu) alloys are widely used in aerospace applications due to their excellent mechanical properties. In this study, the effects of small additions of scandium and the influence of conventional and novel, interrupted heat treatments on the precipitation hardening response of a spray-formed 7055 alloys have been investigated using microhardness, analytical electron microscopy and three-dimensional atom probe tomography. Specifically, single, two-step and multiple-step aging treatments were performed in order to gain insight into the influence of Sc and thermal history on the kinetics of the precipitation hardening response. It will be shown that the initial hardening rate of the alloy containing Sc at low aging temperatures is considerably higher than the Sc-free material. The results will be discussed with an emphasis on elucidating both the mechanism of the increased rate of hardening in the microstructural evolution as a function of the novel aging treatments.

9:30 AM

Development of Al-30%B4C Metal Matrix Composites for Neutron Absorber Material: X.-Grant Chen¹; Robert Hark¹; ¹Alcan Inc.

In recent years, aluminum boron carbide particulate-reinforced composites have been increasingly used as an excellent neutron absorber material in the nuclear industry. Alcan has developed a unique liquid mixing process to manufacture these metal matrix composites. The fabrication of durable and usable components with higher B4C content composites (up to 30%) is challenging in several aspects ranging from mixing, casting, extruding and rolling. In this paper, the results of development of Al-30%B4C metal matrix composites from raw material via semi-finished to finished products are presented. The casting processes as well as downstream processes (extrusion and rolling) are described. The micro-structural characteristics of Al-30%B4C composites at as-cast and deformed conditions are investigated. The mechanical properties of extruded and rolled components at different conditions are examined. Finally, the perspective of potential application and commercial production of these materials is outlined.

9:50 AM

Enabling Environmentally-Informed Materials Selection Decisions: Robustness of Early Stage Life-Cycle Assessment: Anna Allen¹; Subodh Das²; Frank Field¹; Jeremy Gregory¹; Randolph Kirchain¹; ¹Massachusetts Institute of Technology; ²Secat, Inc

This paper explores the robustness of materials selection decisions when using various life-cycle assessment methods. Improving the environmental performance of vehicles is a topic of growing concern met by today's designer. One approach to this goal is through vehicle mass reduction, enabled through the implementation of a growing array of material candidates. While LCA methods

are available to provide quantitative input into this selection decision, LCA applications are evolving and distinct. Specifically, this paper surveys the major analytical variations of LCA implementations and explores the implications of one major variant when applied to an automotive materials selection case study involving aluminum. This case study examines analytical variations in treatment of recycling by exploring allocation methods that affect product end-of-life. Preliminary results indicate that the choice of analytical method can have real impacts on individual metrics and there are sets of analytical variation over which strategic results are strongly affected.

10:10 AM

Impact of Mass Decoupling on Assessing the Value of Lightweighting: *Catarina Bjelkengren¹; Theresa Lee²; Richard Roth¹; Randolph Kirchain¹;* ¹Massachusetts Institute of Technology; ²General Motors

There is an increasing realization about the need for fuel efficient vehicles. An effective way to accomplish this is through mass reduction. Although primary mass reduction is often associated with additional costs, a decision to lightweight may, depending on when in the development process the decision is taken, result in secondary mass savings such that the value of lightweighting is increased. In this study, we develop a methodology to use regression analysis and vehicle development data to estimate the potential for secondary mass savings at different times in the development process. Subsequently, we employ performance data to estimate the value of the compounded savings in terms of fuel economy and acceleration improvements. Lastly, we utilize market data to estimate how much the improved performance is worth to the consumer. A case study of aluminum automotive closures will be adopted to assess the compounded value of lightweighting using the above methodology.

10:30 AM Break

10:40 AM

A Review of the Warpage Behavior of Aluminum Alloys: *E. Lee¹; Omar Es-Said²;* ¹Naval Air System Command; ²Loyola Marymount University

Extruded I sections of 7075-T6 aluminum were machined into four different sections shapes. Samples were solution treated and quenched in either a 30% polyalkylene Glycol solution or water. Points on the distorted samples were recorded before and after the solution treatment; the difference between the measurements indicated the extent of warpage. Structural components machined from aluminum forgings can exhibit distortion and poor dimensional quality due to residual stresses formed primarily during heat treatment. The purpose of this investigation was to characterize the influence of compressive strain on the mechanical properties achieved after subsequent aging treatment in aluminum alloy 7050 both by experiment and modeling.

11:00 AM

Ageing of Al-Zn-Mg-Cu Alloys with Minor Sc Additions: *Oleg Senkov¹; Marat Shaghiyev¹; Svetlana Senkova¹;* ¹UES Inc.

The effect of Sc additions on precipitation strengthening in an Al-Zn-Mg-Cu alloy was studied after natural and artificial aging. Microhardness, room temperature tensile properties, and microstructure of the alloy were determined after different steps of aging as a function of the Sc content and the strengthening mechanisms were discussed. Minor additions of Sc increase the strength of cast and solution heat treated Al-Zn-Mg-Cu alloys due to precipitation of fine coherent Al₃(Sc,Zr) particles. Sc has no effect on the natural aging, which is controlled by formation and growth of GP I zones. However, the Sc additions accelerate the aging process at 120°C and 150°C within a period of time of formation and growth of GP II zones and η' precipitates. At longer aging times at 120°C and 150°C, the aging response of the Sc-containing alloys slows down due to faster coarsening of the η' precipitates and their transformation into η particles.

11:20 AM

Characterizing Microstructural Alterations upon Retrogression and Reaging (RRA) Treatment in Al-Li-Cu-Mg Alloys: *Karuna Ghosh¹; K. Das¹;* U. Chatterjee¹; ¹Indian Institute of Technology - Kharagpur

Al-Li-Cu-Mg alloys of peak aged T8 tempers were subjected to retrogression and reaging (RRA) treatment. XRD, DSC, TEM techniques and electrochemical polarization studies have been used to evaluate the microstructural features of the T8, retrogressed, and RRA T77 tempers. Tensile testing studies have also been carried out to determine the mechanical properties of the alloy tempers.

Retrogression treatment has caused dissolution of matrix strengthening d' (Al₃Li) precipitates into solution resulting in decrease of strength, but, reaging the retrogressed state to peak aged temper resulted in regaining the initial T8 temper strength - attributed to the reprecipitation of the d' phase in the matrix. The investigation of microstructural features (such as the size, volume fraction and the distribution of d' (Al₃Li), d (AlLi), T1 (Al₂CuLi), S' (Al₂CuMg) phases etc.) of the RRA tempers reveal that the microstructures of the T77 tempers approach to that of the over aged T7 tempers.

11:40 AM

Effects of Heat Treating Aluminum Alloy 6061 in 8 T and 20 T Magnetic Fields: *Samuel Adedokun¹; Akin Fashanu²; Bayo Ogunmola²;* ¹Florida Agricultural and Mechanical University-Florida State University, College of Engineering; ²University of Lagos, Nigeria

Aluminum alloy 6061 has been used extensively for structural and other applications. Its properties is modified by various heat treatments ranging from solution heat treatment to aging processes. In this work, aluminum alloy 6061 of about 13 mm thickness was solution heat treated at 560C for 2 hours, then quenched in water at room temperature. The quenched piece was then cold rolled to about 2 mm thickness, that is about 85% severe deformation. Pieces were cut from the deformed aluminum alloy and heat treated at various periods of time at different temperatures in 8 T superconducting magnet and 20 T hybrid magnet. Texture measurements were carried using an x-ray diffractometer. It has been found that heat treatment in the 8 T magnetic field enhanced recovery and suppress recrystallization, whereas the 20 T field enhanced recrystallization.

11:55 AM

The Correlation between Deformation Conditions and Peripheral Coarse Grain Structure in Extrusion of AA7020 Aluminum Alloy: *Ali Reza Eivani¹; Hany Ahmed¹; Jie Zhou²; Jurek Duszczek²;* ¹Netherlands Institute for Metals Research; ²Delft University of Technology

In this investigation, a special heat treatment which resembled the actual conditions in the peripheral parts of an extrudate was applied after hot compression. The effects of deformation conditions and the subsequent heat treatment on the formation of coarse grain structure in the AA7020 aluminum alloy were investigated. The microstructure of the samples at two different cooling conditions, namely: (i) water quench and (ii) after the special heat treatment process, were studied in terms of the fraction recrystallized, average grain size and homogeneity. It was found that with increasing deformation temperature or decreasing strain rate, the recrystallized grain size increased. It was also observed that a homogeneous microstructure could be achieved by increasing strain rate. The coarse recrystallized grain structure was attributed to high temperature rather than strain rate.

12:10 PM

An Investigation of the Hot Deformation Behavior of AA7020 and AA7475 Aluminum Alloys: *Hany Ahmed¹; Ali Eivani¹; Jie Zhou²; Jurek Duszczek²;* ¹Netherlands Institute for Metals Research; ²Delft University of Technology

An extensive set of experiments, using a Gleeble 3500 thermo-mechanical simulator, was performed to investigate the hot deformation and subsequent recrystallization behavior of industrially significant AA7020 and AA7475 aluminum alloys during hot compression. A wide variety of deformation conditions along with different post-deformation heat treatments were employed in this investigation. The relationship between the deformation conditions and the resulting flow stresses, fraction recrystallized and the post-deformation heat treatments of both alloys was investigated. It was found that AA7475 has higher strength and a relatively higher fraction recrystallized compared to AA7020. It was also observed that steady state flow stress can only be achieved at higher temperatures in AA7020 whereas it is attained at all temperature range for AA7475, which may be attributed to the difference in their recrystallization behavior and in turn to the difference in their zirconium content and zinc to magnesium ratio.

12:30 PM

Development of Al-Si-P Master Alloy and Its Application in Al-Si and Al-Mg-Si Alloys: *Liu Xiangfa¹;* ¹Shandong University

A new type master alloy rich in phosphorus - Al-Si-P master alloy has been developed by melt reacting method. The master alloy contains pre-formed AlP particles, most of them enveloped in Si phases, this improves their distribution

remarkably. The new copper-free master alloy containing a high concentration of phosphorus (4-5 wt.%) is effective to refine primary Si particles for near eutectic and hypereutectic Al-Si alloys at lower temperature, addition rates, short contract times and without any composition contamination. Now the master alloy is widely applied in a lot of piston manufacturers and die cast factories. In addition, the master alloy can also be used in Al-12.67%Mg-10.33%Si alloy for the refinement and modification of Mg₂Si. The refinement mechanisms are also be researched for primary Si and Mg₂Si.

Biological Materials Science: Mechanical Behavior of Biological Materials I

Sponsored by: The Minerals, Metals and Materials Society, TMS Structural Materials Division, TMS: Biomaterials Committee, TMS/ASM: Mechanical Behavior of Materials Committee

Program Organizers: Ryan Roeder, University of Notre Dame; Robert Ritchie, University of California; Mehmet Sarikaya, University of Washington; Lim Chwee Teck, National University of Singapore; Eduard Arzt, Max Planck Institute; Marc Meyers, University of California, San Diego

Monday AM Room: 390
March 10, 2008 Location: Ernest Morial Convention Center

Session Chair: Ryan Roeder, University of Notre Dame

8:30 AM Keynote

How Really Tough is Human Cortical Bone?: *Robert Ritchie*¹; Kurt Koester¹; Joel Ager¹; ¹University of California

Human bone is more difficult to break than split. However, appropriate fracture-toughness measurements to break bone (in transverse directions) are rare. Most measurements focus on crack-initiation, whereas bone principally derives its toughness during crack-growth; moreover, the few crack-growth measurements are for longitudinal "splitting" orientations. Here we use nonlinear-elastic fracture mechanics to determine R-curves for both orientations in human cortical bone, using in-situ testing within an environmental SEM to simultaneously examine the salient damage/toughening mechanisms. We find that stress-intensities up to 5MPa^{1/2} are required to propagate large cracks along the bone long axis, whereas to propagate a crack only 500 microns in transverse directions requires stress-intensities some five times higher. Such toughnesses are far larger than previously thought, yet represent a truer depiction of conditions to break bone. Mechanistically, behavior results from microcracking at osteon/interstitial interfaces, which promotes gross crack deflections for transverse cracking and crack bridging for longitudinal orientations.

9:10 AM Invited

Post-Yield Energy Dissipation and Bone Quality: *Xiaodu Wang*¹; ¹University of Texas at San Antonio

A number of factors across multiple length scales may contribute to the toughness of bone, thus hindering a complete mechanistic explanation for bone fragility. Bone possesses a highly hierarchical structure, consisting of water, mineral, and collagen phases and showing a rather complex response to the mechanical loading. While previous research has investigated bone fracture mechanics, fatigue behavior, and load-induced damage accumulations, little is known about the progressive changes in the post-yield behavior of bone with increasing deformation (strain) levels. In this study, we investigated the progressive post-yield behavior of bone using a novel diagnostic loading scheme, so as to gain more information on the underlying mechanism of post-yield energy dissipation in bone. It was observed that two distinct modes exist in the post-yield behavior of bone and the major portion of energy dissipation is realized through an initial acute microdamage accumulation, followed by a mechanism dominated by a viscoplastic deformation.

9:40 AM

Bone Fracture Mechanisms under Dynamic Loading: *Robb Kulin*¹; Jiang Fengchun¹; Kenneth Vecchio¹; ¹University of California San Diego

Fracture of cortical bone in clinical situations for both human and animal subjects happens primarily under impact loading as experienced in crashes, falls or violence. However, despite this a full understanding of the fracture mechanisms

occurring under dynamic loading is lacking. Mechanical testing was therefore performed under dynamic and quasi-static loading conditions on equine femoral and third-metacarpal bones subjected to bending and compression loading conditions. Bending tests were performed using a four-point geometry on single and double notched samples. The double-notched samples facilitated an in-depth study of the fracture paths followed under both loading scenarios, and these were analyzed using confocal and electron microscopy techniques. Both bending and compression specimens were studied under loading parallel and transverse to the long axis of the bone in wet conditions, and represented horses ages 6 months to 28 years in order to study the age effects on dynamic response as well.

10:00 AM

Structure and Mechanical Properties of American Elk Antlers: *Po-Yu Chen*¹; Andrew Stokes¹; Joanna McKittrick¹; ¹University of California

We have examined structure and mechanical properties of the American elk antlers from the Cervidae family. Antlers are designed to be resilient, tough and able to sustain large bending loads, making them superior structural materials. Antlers have a similar structure to human bone apart from the higher collagen content and lesser degree of mineralization. Antlers were tested in bending to failure in both wet and dry state. The work of fracture and fracture toughness values were determined. The mechanical properties were highly anisotropic and correlated with the orientation of collagen fibers. Tensile and compressive tests were conducted in longitudinal and transverse directions. Compressive tests were further performed on interior cancellous and exterior compact bone. Correlation of mechanical properties with fracture surfaces was discussed along with fracture mechanism. Comparisons between antler and bone were made. This research is supported by the National Science Foundation Grant DMR 0510138.

10:20 AM Break

10:30 AM Invited

Biomechanical Design Lessons for Engineered Materials: *Mehmet Sarikaya*¹; Martha Somerman¹; Hanson Fong¹; ¹University of Washington

Hard tissue formation is controlled by proteins leading to complex and highly functional, hierarchical architectures. The inorganics include calcium carbonate polymorphs (CaCO₃) in mollusk shells and echinoderm spines/tests, silica-based (SiO₂) skeletal units of single-celled organisms, e.g., radiolarian, and spicules of sponges, magnetic (Fe₃O₄) nanoparticles in magnetotactic bacteria, and hydroxyapatite in bone and dental tissues of mammals. Proteins control nucleation, growth, and structural organization of inorganics and provide molecular scaffolds. In addition, proteins and other fundamental biomolecules, such as polysaccharides, form the soft component of hard tissues that are complex nano- and micro-composites. Here, we will describe nanostructure-nanomechanical function relationships of several biological composites, including: i. Nacre, "mother-of-pearl," ii. Enamel and cementum of teeth, and iii. Spicules of sponges and draw design lessons for practical materials. Guidelines will be drawn for potentially cell-free tissue engineering in medicine and peptide-assisted inorganic structures in practical nanotechnology. Supported by NSF-MRSEC, BioMat, and NIDCR Programs.

11:00 AM

Modeling Collective Effects in Nacre: *Mark Jhon*¹; Daryl Chrzan¹; ¹University of California, Berkeley and Lawrence Berkeley National Laboratory

Nacre is a hierarchically structured material with toughness greater than expected from the rule of mixtures. It consists of brittle aragonite platelets layered with a ductile organic phase. The inherent discreteness of this brick-and-mortar structure creates challenges for traditional continuum modeling techniques. Most existing models focus on identification of the dominant small scale structure and its impact on the deformation process. These studies, however, are incomplete in that they do not account for the large scale deformation patterns observed in nacre: deformation is not highly localized, but rather is spread over large volumes involving many platelets. Towards this end, a simplified spring-block model for the mechanical behavior of nacre, similar to the Burridge-Knopoff model for earthquakes, is introduced and analyzed via Monte Carlo simulations. This work was supported by the U.S. Department of Energy under Contract No. DE-AC02-05CH11231.

11:20 AM

Characterization of Sandwich Structures in Avian Materials: *Sara Bodde¹; Yasuaki Seki¹; Marc Meyers¹; ¹University of California*

Avian bills and feather rachises have been investigated as examples of sandwich structures in nature. Tensile strength at varied humidity and temperature conditions has been determined for the keratinous exterior of beaks and feathers rachises. The beak of toucan and hornbill is described as a keratinous shell (rhamphotheca) enclosing a closed-cell foam comprised of bony trabeculae as edges and lipid membranes as faces. The rhamphotheca of toucan and hornbill beaks have been imaged by electron microscopy. By TEM, filaments ranging in diameter from 7 nm to 12 nm were observed. The fiber-reinforcement may be correlated to anisotropic behavior observed in hornbill rhamphotheca. Foam geometry was characterized by SEM and computed tomography. Feather rachis consists of a keratinous sheath enclosing a honeycomb structure. The cells of the honeycomb, approximately 30 mm in diameter, are closed by surfaces comprised of fibers as observed by SEM and confocal microscopy techniques.

11:40 AM

Bioinspired Design of Dental Multilayers: Experiments and Models: *Nima Rahbar¹; Xinrui Niu²; Stephen Farias²; Wole Soboyejo²; ¹Princeton University, Department of Civil and Environmental Engineering; ²Princeton University, Department of Mechanical and Aerospace Engineering*

This paper explores the bioinspired design of dental multilayers within a combined computational/theoretical and experimental framework. Inspired by interfacial stress reductions associated with the almost linear gradation in moduli across the micron-scale dento-enamel junction (DEJ), this study explores the effects of graded architecture on the stress distributions and crack driving forces in model multilayered structures that are relevant to dental restorations. These are shown to result in: reduced maximum principal stresses; significant improvements in the critical crack lengths; a 30% increase in the critical loads to pop-in, and significant improvements in the number of fatigue cycles to failure over a wide range of clinically-relevant loading rates. The implications of the results are then discussed for the design of durable dental multilayers.

12:00 PM

3D Computer Graphic Modeling of Avian Beaks: *Yasuaki Seki¹; Sara Bodde¹; Falko Kuester¹; Marc Meyers¹; ¹University of California*

The internal structure of the beaks of selected species of Toucan and Hornbill has been investigated. The beak is a sandwich composite with an exterior consisting of staggered keratin tiles and a core consisting of a closed-cell foam. The edges of the closed-cell foam are bony trabeculae while the faces are lipid. Computed Tomography (CT) was employed for characterizing macrostructure of the network of osteal-trabeculae comprising the interior of the Toco Toucan and Wreathed hornbill bills. From CT image data, the internal foam structure was reconstructed by computer graphic imaging techniques. Visualization Tool Kit (VTK) was used to deal with CT images. Two different techniques, volume (Raycasting) and geometric rendering (Marching cube) techniques, were applied to visualize beak interior structure. The geometric rendering extracts the isosurface and creates the polygonal mesh. Delaunay tessellation was used for creating a finite element model.

Bulk Metallic Glasses V: Structures and Mechanical Properties I

Sponsored by: The Minerals, Metals and Materials Society, TMS Structural Materials Division, TMS/ASM: Mechanical Behavior of Materials Committee
Program Organizers: Peter K. Liaw, University of Tennessee; Wenhui Jiang, University of Tennessee; Guojing Fan, University of Tennessee; Hahn Choo, University of Tennessee; Yanfei Gao, University of Tennessee

Monday AM
March 10, 2008

Room: 393
Location: Ernest Morial Convention Center

Session Chairs: Peter K. Liaw, University of Tennessee; William Johnson, California Institute of Technology

8:30 AM Keynote

The Nature of Randomness in Metallic Glasses: *William Johnson¹; Marios Demetriou¹; ¹California Institute of Technology, Keck Laboratory of Engineering*

Variations in physical behavior among known metallic glasses and glass forming liquids can be broadly related to the liquid fragility as defined by Angell's parameter, m . In this talk, it is proposed that fragility is related to the degree of randomness in the properties Potential Energy Landscape (PEL) of the liquid. A simple 1-dim model PEL is proposed which consists of a finite sum of N sine waves of unit amplitude and random phase, and having a random distribution of wave-vectors, Q . Each sine wave represents a degree of freedom of a cluster of $N/3$ atoms within the liquid or glass. Randomness is characterized by the variance, σ_Q^2 , of the Q distribution compared with average squared wave-vector $\langle Q^2 \rangle$, and by the number terms in the sum (number of degrees of freedom). A dimensionless parameter, $\chi = \sigma_Q^2 / \langle Q^2 \rangle$ is introduced which characterizes landscape fragility. The thermodynamic and kinetic properties of this model can be computed. The relationship of this model to real BMG's and their landscapes is discussed. Results for the model are compared with experimental results on strong and fragile metallic glasses. The simple model reveals the microscopic origin of the properties of metallic glasses and liquids and shows that fragile liquids/glasses are characterized by a more disordered landscape compared with strong liquids.

9:00 AM Invited

Anelastic Deformation in an Al-Rich Metallic Glass: The Effect of Preexisting Shear Bands: *Michael Atzmon¹; Koteswararao Rajulapati¹; Dongchan Jang¹; Adam Gazuza¹; ¹University of Michigan*

In order to characterize the dependence of anelastic strain relaxation on the state of a metallic glass, macroscopic and microscopic bending experiments have been conducted in Al_{86.8}Ni_{3.7}Y_{9.5}. Cold rolling and/or annealing below the glass-transition temperature were used prior to bending in order to modify the state of the glass. At room temperature, time-dependent deformation is predominantly anelastic, whereas at higher temperatures, permanent deformation is also observed. The time constants for anelastic relaxation range from seconds to hundreds of hours. While relaxation anneals prior to bending do not result in significant changes in the subsequent response to bending, both cold rolling and subsequent annealing lead to significant changes. Trends in the dependence of anelastic deformation behavior on the extent of cold rolling will be discussed. Measurements of the time-dependent behavior of individual shear bands will be described. This work was supported by the National Science Foundation, Grant DMR-0605911.

9:20 AM Invited

Characterization and Control of Shear Band Propagation in Metallic Glasses: *Katharine Flores¹; Y. Jean²; Glenn Daehn¹; ¹Ohio State University; ²University of Missouri - Kansas City*

Bulk metallic glasses exhibit impressive mechanical properties and processing capabilities that make them attractive for structural applications. However, the formation and rapid propagation of shear bands present significant challenges for sub- T_g processing and structural applications. We discuss ongoing investigations of the glass structure and its evolution with deformation as well as potential processing techniques to enhance the utilization of metallic glasses. Positron

MONDAY AM

annihilation spectroscopy results for several glasses reveal that the open volume in the glass may be divided into three distinct size ranges and is redistributed after shear band propagation, with the sizes decreasing and concentration of large sites increasing with total strain. Because shear band propagation in tension typically leads to catastrophic failure, techniques for distributing flow under tensile conditions are of interest. A high velocity ring expansion experiment successfully generated numerous shear bands in the bulk metallic glass ring, resulting in approximately 3% plastic strain at failure.

9:40 AM Invited

Mechanical Properties and Electronic Structure of Fe-Based Structural Amorphous Metals: Gary Shiflet¹; S. Poon¹; ¹University of Virginia

The design and characterization of Fe-based structural amorphous metals (SAM) to obtain good plasticity and toughness while retaining the high fracture strength near 4 GPa and good glass forming ability is central to current work at the University of Virginia. This talk will focus on the synthesis, mechanical properties, and basic knowledge of Fe-SAM. The Fe-SAM undergoes a ductile-to-brittle transition. This ductile-to-brittle transition is suggested to correlate with the change of local atomic short-range order or bonding configurations. The local atomic electronic structures of Fe-Mo-C-B metallic glasses are investigated using electron energy loss spectroscopy (EELS). Working towards reducing the shear modulus, the variations of compressive plasticity and elastic properties with compositions are investigated, and the deformation and fracture features are examined. The present investigation underlines the role of local order and interatomic interactions in the elastic moduli and Poisson's ratio, and hence the ductility. Research sponsored by DARPA/ONR.

10:00 AM Invited

Probing the Nanoscale Strength Distribution in Metallic Glasses: Corinne Packard¹; Christopher Schuh¹; ¹Massachusetts Institute of Technology

The relationship between metallic glass structure and the process of deformation through shear banding has not yet been established. Using nanoindentation, we investigate plasticity in metallic glasses by characterizing the first shear band event under a local mechanical contact. We observe that the first shear band event is stochastic, and show that the strength distribution arises from local variations in the glass structure. By intentionally altering the glass structure through annealing, we observe subtle but consistent changes to the shape of the distribution. In addition, cyclic loading in the elastic range results in apparent strengthening, suggesting a mechanism of structural evolution during nominally elastic deformation. Implications of these results on the macroscopic properties of metallic glasses are discussed, as are potential connections to the modeling and simulation community.

10:20 AM Invited

Two-Glassy Phase Bulk Metallic Glass with Remarkable Plasticity: X. Du¹; Jacob Huang¹; K. Hsieh²; J. Jang³; P. Liaw⁴; ¹National Sun Yat Sen University; ²National Sun Yat Sen Univ; ³I-Shou University; ⁴University of Tennessee

By using the computational thermodynamic approach, the potential compositions of Zr-Cu-Ni-Al alloy system exhibiting the two-liquid miscibility phase equilibrium in the liquid temperature region have been identified. The resulting Zr base bulk metallic glasses exhibit a microstructure of two micro-scaled glassy phases mixed uniformly, i.e., the hard phases within some nanocrystals (Zr₂Ni) surrounded by the soft phases. The Zr base glasses possess a high compressive strength (~1.9 GPa), continuous "work hardening" and remarkable macroscopic plastic strain (~20%) before instable deformation at room temperature. The gain of mechanical properties is attributed to the unique deformation mode with microscale multistep shear bands originating from shear-induced breakage and coalescence of hard phases which have experienced nanocrystallization process under compression loading. This novel phenomenon provides a mechanism for strain hardening to offset the natural strain softening of the glass matrix and to assist delocalization of the plastic flow.

10:40 AM Break

10:45 AM Invited

Engineering Capabilities of Highly Porous Metallic Glass Foam: Marios Demetriou¹; William Johnson¹; Robert Conner²; Nikolaj Wolfson³; Aaron Wiest¹; ¹California Institute of Technology; ²California State University, Northridge; ³University of Southern California

Owing to their remarkably high plastic yield strengths, amorphous metals are thought to be attractive base materials for ultra strong foams. In addition, due to their ability to be processed thermoplastically above the glass transition, these materials are considered promising for high porosity foaming. In this presentation, a foam synthesis route will be introduced by which metallic glass foams with porosities as high as 92% are produced. The foams are capable of effectively inheriting the high plastic yield strength and low modulus of the parent amorphous metal under static as well as dynamic loading, and are able to deform plastically to full densification absorbing high amounts of energy. Potential applications for the foam will be discussed, and its engineering capabilities as an energy-absorbing cellular structure or a property-matched bone scaffold will be explored.

11:05 AM Invited

Influence of Free Volume on the Ductile-to-Brittle Transition in Rapidly Solidified Mg-Based Glasses: Jorg Loffler¹; Dirk I. Uhlenhaut¹; Florian H. Dalla Torre¹; Alberto Castellero¹; ¹ETH Zurich

Rapidly quenched Mg-Cu-Y glasses show ductility upon bending for a limited time at room temperature but then embrittle within a short time. This time-dependent embrittlement can be associated with a structural relaxation, which lowers the enthalpic content and increases the elastic constants of the metallic glass, as measured via acoustic excitation. Since the shear modulus increases faster than the Young's modulus, the Poisson ratio is found to decrease as the alloy ages and the ductile-to-brittle transition is observed at a critical value of 0.32. Using results obtained from synchrotron x-ray diffraction and positron annihilation experiments, we can relate this embrittlement to the amount and extent of free volume, which alters during room-temperature aging and also changes the Poisson ratio of the glass. Here we discuss the interrelation between the mechanical properties and the defect structure in the Mg-based glass.

11:25 AM Invited

Plasto-Hydrodynamic Deformation of Brittle Bulk Metallic Glass at Room Temperature: Fuqian Yang¹; John Nychka¹; Gongyao Wang²; Wenhui Jiang²; Brett G. Compton¹; Peter K. Liaw²; ¹University of Kentucky; ²University of Tennessee

The deformation of materials can be altered by the application of particular stress states. In this contribution we present results which offer a new approach to achieve high degrees of plastic deformation without catastrophic failure in brittle bulk metallic glasses (up to 36% plastic strain). The large strains are observed in uniaxial compression at room temperature with aid of a plastic layer at the fixed ends of the specimen. The result is of particular interest because the plastic deformation occurs in the presence of complex shear band formation on all surfaces without fracture or in situ crystallization. Implications of these findings suggest possible new strategies for deformation processing of bulk metallic glasses.

11:45 AM

Thermal and Elastic Response of Cu-Based Bulk Metallic Glasses to Cyclic Elastic Deformation: Rainer Hebert¹; Arif Mubarak¹; ¹University of Connecticut

It is well known that metallic glasses reveal structural relaxation or ageing when heated to temperatures near the glass transition or below. Little is known, however, about the effect of cyclic elastic deformation at room temperature on atomic rearrangements and the thermal behavior of the glasses during subsequent annealing. Suction-cast amorphous Cu-Zr and Cu-Ti-Hf rods were tested in compression-compression testing with strain amplitudes of 0.1%-0.3%, strain rates of about ten to the minus four and compression cycles ranging from 200 to 20,000. The thermal analysis reveals a decrease by approximately 80% of the enthalpy of crystallization for an amorphous Cu₅₀Zr₅₀ rod without a shift in the crystallization onset temperature and a decrease in the strength of the glass-transition signal. The results indicate that sustained elastic deformation can have a significant impact on the crystallization behavior or Cu-based metallic glasses.

12:00 PM

Deformation of an Annealed Zr₄₁Ti₁₄Cu_{12.5}Ni₁₀Be_{22.5} Bulk Metal Glass under Vickers Indenter: *Haowen Xie¹; Jianguo Lin¹; Yuncang Li¹; Peter Hodgson¹; Cui'e Wen¹; ¹Deakin University*

Zr₄₁Ti₁₄Cu_{12.5}Ni₁₀Be_{22.5} bulk metal glass (BMG) was annealed near the glass transition temperature, and the structure relaxation occurred. Vickers indentation was conducted on the annealed sample. The development of the shear band patterns was studied by using a bonded interface technique. The results indicated that the plastic deformation in the annealed sample was accommodated by the semicircular (primary) and radial (secondary) shear bands. Compared with the as-cast sample, the annealed sample exhibits the different distribution and patterns of shear bands due to the altered elastic-plasticity. The inter-band spacing of the semicircular shear bands at the variant angles was strongly dependent on the distribution of the stresses. The size of the deformation zone was measured, and the values are compared with the predictions by some theoretical models.

12:15 PM Invited

Effect of Coexistence of Alike Elements on Improving Glass-Forming Ability of Alloys: *Tao Zhang¹; ¹Beijing University of Aeronautics and Astronautics*

The effect of unlike component elements on GFA of alloys have been studied extensively and it is generally recognized that the main constituent elements of the alloys with high glass-forming ability (GFA) usually have large difference in atomic size and large negative heat of mixing among them. In the present work, we developed a series of rare-earth metal-based alloys with superior glass-forming ability (GFA) by using the approach of coexistence of alike elements in the alloys. Especially a La-Ce-Al-Co-Cu bulk metallic glass (BMG) with a diameter up to 32 mm can be synthesized by copper-mold casting, for which the GFA is significantly higher than that for ternary Ln-Al-TM alloys (Ln = La/Ce; TM = Co/Cu). This indicates that the coexistence of alike elements (elements with similar atomic size and chemical properties) has significant effect on GFA of alloys, which can also be observed in Zr-Al-(Ni-Cu), Cu-(Zr-Ti) and Pd-(Cu-Ni)-P glassy alloy systems, etc. Mechanism of coexistence of alike elements on improving GFA of alloys is also discussed. The Authors would like to acknowledge the financial supports from National Nature Science Foundation of China (No. 50631010), PCSIRT (IRT0512) and the Cultivation Fund of the Key Scientific and Technical Innovation Project, Ministry of Education of China (No. 705006).

12:35 PM

Relationship between Shear Displacement and Shear Band Spacing in Bulk Metallic Glasses: *Hongwen Zhang¹; Ghatu Subhash²; Spandan Maiti¹; Gerald Bourne²; ¹Michigan Technological University; ²University of Florida*

Bonded-interface technique is used to investigate the relationship between the shear band spacing and shear displacement in bulk metallic glasses. The vertical surfaces of the split-specimens were engraved with a set of lines at regular intervals (100 microns) and then bonded together for indentation test on the top surface along the interface. As the induced shear bands cut across the grid pattern, the resulting shear displacement along each shear band can be measured by the offset (displacement) of the different segments of an original straight line. It was revealed that widely spaced shear bands accommodate larger shear displacement and vice versa. To rationalize these observations, a thermo-micromechanical model that takes into account momentum diffusion mechanism at the core of shear band, free volume theory and heat diffusion analysis was developed. The model verifies that widely spaced shear bands indeed accommodate larger shear displacement.

12:50 PM

Stress-Induced Phase Transformation during In-Situ Compression Test of a Glass-Forming CuZr Alloy: *Feng Jiang¹; Yandong Wang²; Yang Ren³; James Morris¹; Peter Liaw¹; Hahn Choo¹; ¹University of Tennessee; ²Northeastern University of China; ³Argonne National Laboratory*

The in-situ compression test was applied on a glass-forming CuZr alloy, simultaneously, synchrotron X-ray is used to study the structure change. The results show that phase transformation occurs during in-situ compression test. The phase of martensite- (with the space group of P21/m) transforms to martensite α (with the space group of Cm) through twin mechanism.

Characterization of Minerals, Metals, and Materials: Emerging Characterization Techniques

Sponsored by: The Minerals, Metals and Materials Society, TMS Extraction and Processing Division, TMS: Materials Characterization Committee
Program Organizers: Jian Li, Natural Resources Canada; Toru Okabe, University of Tokyo; Ann Hagni, Intellection Corporation

Monday AM
March 10, 2008

Room: 284
Location: Ernest Morial Convention Center

Session Chairs: Jian Li, Natural Resources Canada; Donato Firrao, Politecnico di Torino

8:30 AM

Understanding the Effects of High Speed Orientation Mapping: *Matthew Nowell¹; Stuart Wright¹; John Carpenter¹; ¹EDAX-TSL*

The automated analysis of Electron Backscatter Diffraction (EBSD) patterns for orientation mapping has become an accepted microstructure characterization tool. Data acquisition speeds have increased by over two orders magnitude over the past decade. These increases are enabled primarily by digital CCD cameras capable of output frame rates greater than analog video rates. One feature of these cameras is the ability to group together adjacent pixels in a processes referred to as binning. This process reduces the pixel resolution of the output image and allows faster output frame rates. As CCD frame rates and binning options increase, understanding the effects of image resolution on EBSD pattern analysis is key to optimizing the quality of the orientation mapping data. In this work, the effects of camera resolution, coupled with band detection parameters, is examined. Indexing success rates and angular accuracy as a function of acquisition speed and camera resolution will be discussed.

8:50 AM

The Research Applications of Photoemission Electron Microscopy: *Mingdong Cai¹; J. Thomas Dickinson²; Wayne Hess³; ¹University of Houston; ²Washington State University; ³Pacific Northwest National Laboratory*

Photoelectron emission microscopy (PEEM) is a developing technique that images electrons emitted from conductor and semiconductor surfaces under UV, X-ray, or laser irradiation. Low energy PEEM can reveal surface morphology on a 10 nm scale and is sensitive material properties such as phase, adsorbed molecules, surface electronic structure, and other physical properties that affect work function and hence the photoelectron yield. We have used PEEM to study phase transformation in shape memory alloys, diffusion of Cu in Cu/Ru bilayers and laser-induced oxygen vacancy creation on TiO₂. In this talk, we will focus on using PEEM to study thermally-induced martensitic phase transformations in polycrystalline CuZnAl and thin-film NiTiCu shape memory alloys. In situ real-time PEEM images provide information on the spatial distribution of these phases and the evolution of the surface microstructure during transformation.

9:10 AM

Phase Identification and Quantification Utilizing QEMSCAN® Technology: *Ann Hagni¹; ¹Intellection Corporation*

Phase identification techniques such as optical microscopy (reflected light and transmitted light microscopy), X-ray diffraction (XRD), cathodoluminescence microscopy (CLM), and X-ray photoelectron spectroscopy (XPS) have been utilized by materials scientists for many years. Quantification of phases has generally been limited to Rietveld XRD and XPS. Elemental mapping and high magnification imaging of specific areas have been conducted by scanning electron microscopy (SEM), energy dispersive spectroscopy (EDS), and back-scattered electron imaging (BSI). An additional phase identification and quantification technique complements these older techniques. QEMSCAN® employs custom built SEM with EDS, BSI, and sophisticated software to identify and quantify inorganic phases, determine particle surface areas, particle shapes, phase associations, and statistics of phases. Automation of QEMSCAN® allows for analyses of large areas in an unattended mode of naturally occurring and synthetic raw materials, processed materials, and waste products. An overview of QEMSCAN® applications and techniques will be presented.

MONDAY AM

9:30 AM

Thermoreflexion Measurement of Thermal Conductivity of Glassy Polymeric Carbon Bombarded with MeV Proton: *Bangke Zheng*¹; Z. Xiao²; B. Chhay¹; A. Sharma³; D. Ila¹; ¹Alabama A&M University, Center for Irradiation of Materials; ²Alabama A&M University, Electrical Engineering School; ³Alabama A&M University, Department of Physics

Thermoreflexion is a suitable method for measurements of thermal conductivity of thin electrically conductive glassy polymeric carbon samples, which can not be measured by using 3 ω method. A layer of reflective metal film such as aluminum is deposited on the sample. When an Nd: YAG pulsed laser (with a pulse width of 5 ns, and a power of 1 mJ) radiates on the metal film, there is an increase in the reflection of probing laser (a diode laser) beam that is reflected by the surface of metal layer, the reflection of probing laser decays gradually. By measuring the decay time of reflection, which is related to thermal conductivity, the thermal conductivity of GPC with various MeV proton bombardment fluences can be obtained.

9:50 AM Break

10:10 AM

Application of Double Knudsen Cell Mass Spectrometry to Measurement on Thermodynamic Properties of Oxides: *Takashi Nagai*¹; Masao Miyake²; Hisao Kimura¹; Masafumi Maeda¹; ¹University of Tokyo; ²University of Illinois

Thermodynamic knowledge on alloys and oxides forms a scientific foundation for the development of new technologies for refining steel and alloys, and also for the development of new materials with required physicochemical properties. Double Knudsen cell mass spectrometry was developed as a method to measure thermodynamic properties of metals and alloys. This method was not often used to measure thermodynamic measurement on oxide and oxide system, since oxygen potential in measuring system can not be controlled easily, though control of oxygen potential in measuring system in thermodynamic measurement on oxide and oxide system is important. In this research, double Knudsen cell mass spectrometry equipment which has a system injecting gas, such as mixed gas carbon monoxide and carbon dioxide, into Knudsen cell to control oxygen potential was developed. And thermodynamic properties of calcium phosphates were investigated.

10:30 AM

Evaluation of the Influence of Median Rank Expression Selection and Location Factor over Weibull Modulus in Brittle Materials Characterization: *Eduardo de Carvalho*¹; Sergio Monteiro¹; ¹Universidade Estadual do Norte Fluminense

This work dealt with the influence of the location parameter and several expressions that may be used to define probability rank, over Weibull Modulus estimates for a sample analysis. A sample containing 71 red-ceramic specimens was used together with Probability Plot method to estimate distribution parameters. Sub-lots extracted from this major lot were created to evaluate sample size impact over factor estimations. For this lot a 15% difference was found for Weibull Modulus value when different rank expressions were used. The Location Parameter different from zero hypothesis drastically altered Weibull Modulus and Scale Parameter values and made necessary the introduction of other analytical elements to allow for a final valid conclusion.

10:50 AM

Electrostatic Levitation: An Emerging Materials Characterization Technique: *Jan Rogers*¹; Robert Hyers²; ¹NASA/Marshall Space Flight Center; ²University of Massachusetts

Electrostatic levitation (ESL) uses electrostatic fields to position samples between electrodes during processing and characterization studies. Because the samples float between the electrodes during studies, they are free from any contact with a container or test apparatus. This provides a high purity environment for the study of high-temperature (up to 3400°C), reactive materials, as well as access to deeply undercooled melts and metastable states. ESL can be used to process a wide variety of materials including metals, alloys, ceramics, glasses and semiconductors. Apparatus and techniques have been developed to use this technique to provide data for phase diagram determination, creep resistance, emissivity, specific heat, density/thermal expansion, viscosity, surface tension and triggered nucleation of melts. Scientific topics investigated using ESL include phase selection and the formation of quasicrystals and bulk metallic

glasses. Results from selected ESL-based characterization studies performed at NASA's Marshall Space Flight Center will be presented.

11:10 AM

Microstructure Evolution and Deformation in Low Solvus High Refractory (LSHR) Ni-Base Superalloy: *Vikas Sinha*¹; Patrick Martin²; Donna Ballard²; M. Scott¹; ¹UES Inc; ²US Air Force Research Laboratory

Low Solvus High Refractory (LSHR) is a high strength Ni-base superalloy, which has been patented by NASA-Glenn Research Center. Although developed primarily for disk applications, LSHR may be attractive for other applications in the sheet product form. In the current work, the microstructure evolution of LSHR at different times and temperatures (in the vicinity of the gamma prime solvus) has been examined. The microstructures have been characterized via Scanning Electron Microscopy (SEM) and Electron BackScattered Diffraction-Orientation Imaging Microscopy (EBSD-OIM) techniques. The compressive flow behavior at temperatures in both the sub-solvus and super-solvus regimes has been determined. The microstructural modifications resulting from the compression tests have also been examined. The results of the current work will be discussed in the context of hot rolling LSHR sheets.

Complex Oxide Materials - Synthesis, Properties and Applications: ZnO Nanostructures and Thin Films

Sponsored by: The Minerals, Metals and Materials Society, TMS Electronic, Magnetic, and Photonic Materials Division

Program Organizers: Zhiming Wang, University of Arkansas; Ho Nyung Lee, Oak Ridge National Laboratory

Monday AM

March 10, 2008

Room: 277

Location: Ernest Morial Convention Center

Session Chair: To Be Announced

8:30 AM Invited

Polar-Surface Induced Novel Growth Structures of ZnO Nanobelts: *Zhong Lin (Z.L.) Wang*¹; ¹Georgia Tech

The two important characteristics of the wurtzite structure are the non-central symmetry and the polar surfaces. The structure of ZnO, for example, can be described as a number of alternating planes composed of tetrahedrally coordinated O²⁻ and Zn²⁺ ions, stacked alternatively along the c-axis. The oppositely charged ions produce positively charged (0001)-Zn and negatively charged (000-1)-O polar surfaces, resulting in a normal dipole moment and spontaneous polarization along the c-axis. This polar surface gives rise a few interesting growth features. In this presentation, we will focus on the polar surface induced formation of nanospring, nanoring and nanohelix. ¹X.Y. Kong and Z.L. Wang, Nano Letters, 2 (2003) 1625. ²X.Y. Kong, Y. Ding, R.S. Yang, Z.L. Wang, Science, 303 (2004) 1348. ³P.X. Gao, Y. Ding, W.J. Mai, W.L. Hughes, C.S. Lao and Z.L. Wang, Science, 309 (2005) 1700. ⁴<http://www.nanoscience.gatech.edu/zlwang/>.

9:00 AM Invited

Catalyst-Free Selective Growth of ZnO Nanorods on Si Substrates: *Gyu-Chul Yi*¹; ¹Pohang University of Science and Technology

Position-controlled vertical arrays of semiconductor nanorods offer the ideal geometry for use as functional components in nanoscale integrated electronics and optoelectronics. Recently, a few well-controlled semiconductor nanorods have been prepared by either metal catalyst-assisted or catalyst-free methods. For metal catalyst-assisted methods, the selective growth of nanorods can be easily obtained by controlling metal catalyst sites. Meanwhile, for catalyst-free growth, the critical factors leading to the catalyst-free, selective growth of nanorods have yet to be established. Furthermore, there has been only a few reports on the selective growth of semiconductor nanorods on Si substrates although Si is the most important substrate for many device applications. Here I will present two different methods to grow ZnO nanorods at specific positions on Si substrates without using any metal catalyst: wet chemical solution growth and metal-organic chemical vapor deposition.

9:30 AM Invited

Controlled Growth ZnO Nanostructures by Thermal Evaporation: Zhengwei Pan¹; ¹University of Georgia

ZnO exhibits rich morphologies at the nanoscale, which are very sensitive to the growth techniques and growth conditions. In this talk, we show our effort on controlled growth of ZnO nanostructures with different morphologies by a thermal evaporation-based technique. The morphologies include nanorods, nanowires, nanobelts, combs and styluses. The growth mechanism will be discussed briefly. ¹Pan, Z.W., Dai, Z.R. and Wang, Z.L. *Science* 291, 1947-1949 (2001). ²Pan, Z.W. Mahurin, S.M., Dai, S. and Lowndes, D.H. *Nano Letters* 5, 723-727 (2005). ³Pan, Z.W., Rouleau, C.M., Dai, S. and Lowndes, H.L. *Angew. Chem. Int. Ed.* 44, 274 (2005).

10:00 AM Break

10:30 AM Invited

Atomically Controlled Heteroepitaxy of ZnO Enabling UV Emitting and Quantum Hall Devices: Atsushi Tsukazaki¹; Akira Ohtomo¹; Masashi Kawasaki¹; ¹Tohoku University, IMR

ZnO has been recognized as one of the key materials in Oxide Electronics enabling UV emitter, thin film transistor, self-organized nanostructures, spintronics, and so on. We have been focusing our effort for a decade on making ZnO epitaxy as perfect as possible. One of the breakthroughs was the development of high temperature annealed ZnO or Mg_xZn_{1-x}O buffer layer (HITAB) formed on lattice-matched ScAlMgO₄ substrate. During the regrowth of ZnO on such an atomically-smooth buffer layer, intensity oscillation of reflection high-energy electron diffraction persists and the point defect concentration can be minimized. Based on that technology level, we could demonstrate blue light-emitting pn junction diode and quantum Hall effect in high-mobility two-dimensional electron gases at abrupt heterointerfaces between ZnO and Mg_xZn_{1-x}O.

11:00 AM

Nanostructures in Thin Films of ZnO: Harish Bahadur¹; A. Srivastava¹; Rashmi¹; Sudhir Chandra¹; ¹National Physical Laboratory

Structure property co-relationship of thin films of ZnO grown by sol-gel spin process using zinc acetate and RF magnetron sputtering method has been studied. The films were crystalline in nature. The crystallite size for the film grown by using zinc acetate varied with the type of growth techniques and lay in the range of 15-145 in the c-axis direction of the growth. TEM exhibited that the film with uniform microstructure consisted of distribution of nanosized grains of the order of 5 nm. Selected area electron diffraction patterns have shown the presence of different rings corresponding to different planes of hexagonal ZnO crystal structure. The RF sputtered films have shown the formation of nanorods of ZnO which were found to have uniform distribution of crystallites of the size ~10 nm. Photoluminescence measurements also showed the quantum confinement of ZnO crystallites. The results would find application in nanoelectronic piezoelectric sensors.

11:20 AM

Effect of Defect Generation on Structural, Electrical and Optical Properties of ZnO Thin Films by Using Ar-Implantation: Sang Yeol Lee¹; Jung Kun Lee²; M. Nastasi²; ¹Korean Institute of Standards and Technology; ²Los Alamos National Laboratory

In order to investigate the effect of defects on the structural, electrical and optical properties of ZnO thin films, we have performed Ar ion implantation on ZnO thin films grown by pulsed laser deposition and sputtering. The variation of structural property has been observed before and after rapid thermal annealing on Ar implanted ZnO thin films. Ar implantation has been adopted to generate defects intentionally since Ar could not be doped into ZnO and the effect of defect on ZnO could be observed. We have changed the dose of Ar ions, the growth temperature of ZnO thin films and the deposition methods and compared the variation of structural, electrical and optical properties of ZnO thin films caused by the generation of defects due to Ar implantation.

Computational Thermodynamics and Kinetics: Defect Structure I

Sponsored by: The Minerals, Metals and Materials Society, TMS Electronic, Magnetic, and Photonic Materials Division, TMS Materials Processing and Manufacturing Division, ASM Materials Science Critical Technology Sector, TMS: Chemistry and Physics of Materials Committee, TMS/ASM: Computational Materials Science and Engineering Committee, TMS/ASM: Phase Transformations Committee

Program Organizers: Yunzhi Wang, Ohio State University; Long-Qing Chen, Pennsylvania State University; Jeffrey Hoyt, McMaster University; Yu Wang, Virginia Tech

Monday AM
March 10, 2008

Room: 288
Location: Ernest Morial Convention Center

Session Chairs: Meijie Tang, Lawrence Livermore National Laboratory; Yunzhi Wang, Ohio State University

8:30 AM Invited

Dynamic Complexity and Nanostructure Formation Due to Particle Irradiation: Chung Woo¹; ¹Hong Kong Polytechnic University

The evolution of irradiation damage accumulation is conventionally described by coupled rate equations, analogous to the description of diffusion-controlled chemical processes, the dynamic complexity of which is well known. However, to maintain the manageability of the calculation, a simplifying mean-field approximation is usually adopted. It has now been realized that important features of complex systems such as dynamic instabilities and bifurcations together with the accompanying phase-change-like behavior of the system may have been neglected. In this paper, ordering due to alignment of the microstructure along the crystallographic directions under irradiation is studied as an effect produced by one-dimensionally migrating self-interstitials on the post-bifurcation evolution of the system.

8:55 AM Invited

Quantitative Phase Field Model for Diffusion-Controlled Microstructural Evolutions in the Solid State: Pascal Bellon¹; Arnoldo Badillo¹; Robert Averback¹; ¹University of Illinois

Current phase field (PF) models for diffusion-controlled evolutions in the solid state are based on phenomenological kinetic equations. The lack of absolute time and space scale raises problems when applying PF models to alloys subjected to irradiation by energetic particles, since this external forcing introduces new length scales and time scales. We propose here a derivation of the phase field equations, by coarse graining in space and time a microscopic model. For a binary alloy with pairwise atomic interactions, in the framework of the cluster variation method, we derive the kinetic equation describing the evolution of its composition field. This derivation makes it possible to take into account important irradiation effects, namely the production and elimination of point defects and the forced chemical mixing. Examples of application of the model are given for spinodal decomposition in three dimensions, both in the absence and in the presence of irradiation.

9:20 AM Invited

Time-Evolution of Short-Range and Long-Range Ordering in Ni₄Mo Alloys during Isothermal Annealing and under Irradiation Studied by Monte Carlo Simulation: Syo Matsumura¹; Satoshi Hata¹; Tatsuro Takahashi¹; Christian Abromeit²; ¹Kyushu University; ²Hahn-Meitner-Institut, Berlin

The authors will give an overview of their achievements in study of time-evolution of short-range ordering (SRO) and long-range order (LRO) of D1_a type in Ni₄Mo alloys by means of Monte Carlo (MC) simulation. First, semi-quantitative high resolution TEM and MC simulation show that the SRO state consists of mixture of subunit cell clusters of D1_a, D0₂₂ and Pt₂Mo structures in the atomistic level of microstructure. The second part of the talk will mention the kinetics of disordering from D1_a-type LRO to SRO under particle irradiation. One can easily distinguish the disordering kinetics of LRO and the time-evolution of SRO in the MC simulations, owing to the characteristic feature that the two states show intensity maxima at different positions in the Fourier space.

The disordering behavior is discussed as a function of size of disordered zones due to particle collisions.

9:45 AM

Modeling the Effect of Particle Size Distribution on Platinum Surface Area Loss in PEMFC Cathodes: *Dane Morgan*¹; Edward Holby¹; Yang Shao-Horn²; Wenchao Sheng²; ¹University of Wisconsin; ²Massachusetts Institute of Technology

The long-term durability of platinum catalysts in Proton Exchange Membrane Fuel Cell (PEMFC) cathodes is an important issue in achieving the Department of Energy's 5000 hour PEMFC lifetime goal. Fuel cell efficiency is decreased as electrochemically active surface area (ECASA) of platinum is lost. A kinetic model has been used to explore the influence of particle size distribution on the loss of ECASA under both constant potential holds and cycled potentials for carbon supported Pt catalysts. It is shown that the thermodynamics of the nanoscale particles strongly impacts the Pt loss. It is found that the mean diameter and functional form of the initial particle size distribution are important considerations in the long-term loss of ECASA in PEMFCs. Also, it is confirmed that changes in the particle size distribution upon heat treatment help to explain the improved durability associated with heat-treating catalysts.

10:00 AM

First Principles Study of Point Defects in Uranium Dioxide and Cerium Dioxide: *Ying Chen*¹; Misako Iwasawa²; Yasunori Kaneta¹; Toshiharu Ohnuma²; Hua-Yun Geng¹; Motoyasu Kinoshita²; ¹University of Tokyo; ²Central Research Institute of Electric Power Industry

UO₂ is a widely used fuel in nuclear power generation, under its high burn-up, a characteristic fine grain structure is found to be formed. CeO₂ is used as simulation materials of UO₂ in the accelerator experiments due to their similar structural and thermodynamic properties. To get understanding on the fundamental properties and essential difference of these two substances, so as to clarify the origin of formation of the characteristic defective structure, the comprehensive first-principles calculations for two systems containing various types of point defects have been performed using the PAW-GGA+U. The electronic structure, the atomic displacement, and the defect formation energies are evaluated under lattice relaxation, the size effect of supercells on these properties is also investigated. Based on the results of electronic structures, the concentration of various types of point defects are further estimated in the framework of the point defects model.

10:15 AM Break

10:35 AM Invited

From Dislocation Dynamics to Continuum Modelling of Plastic Deformation in Ni-Base Superalloys: *Aurelien Vattré*¹; Arjen Roos¹; *Benoit Devincré*²; ¹ONERA; ²Centre National de la Recherche Scientifique

Understanding the plastic properties of alloys containing metallic precipitates of sub-micrometric size, such as Ni-based superalloys, is a difficult task. It has been emphasized many times that the plastic deformation of single crystalline superalloys depends in a complex manner on orientation. Three-dimensional simulations of dislocation dynamics dedicated to Ni-based superalloys have been developed, in which the boundary value problem is rigorously resolved through a coupled approach involving a FE and a DD code. These simulations aim at understanding the relation between the nature and number of activated slip systems and the macroscopic stress-strain behavior. In addition, they deliver a quantitative description of the microstructural mechanisms at the origin of strain localization in slip bands. The model results are found consistent with experimental observations and provide guidelines for the development of physically justified crystal plasticity models.

11:00 AM Invited

3D Dislocation Dynamics Simulations of the Deformation Behavior of Micrometer-Sized Crystals of FCC Ni and Superalloys: *Satish Rao*¹; Dennis Dimiduk²; Triplicane Parthasarathy¹; Meijie Tang³; Michael Uchic²; Christopher Woodward²; ¹UES Inc.; ²Air Force Research Laboratory/MLLM; ³Lawrence Livermore National Laboratory

We use large scale 3-dimensional dislocation simulations to study the deformation behavior of micron sized FCC single crystals as well as superalloys with initial dislocation source densities varying from 7x10¹¹/m² to 10¹³/m² and

specimen column diagonal sizes ranging from 0.5 to 20 micron. Mechanisms that are responsible for strengthening are identified through the use of dislocation dynamics (DD) simulations. The simulations reveal two size-sensitive hardening processes that are sufficient to produce the dimensional scaling of the flow stress and similar flow behavior observed experimentally. One mechanism, surface-mediated source-truncation hardening, is especially potent in micrometer-scale volumes and is attributed to the stress required to operate single-ended sources in such small micrometer volumes. Other mechanisms, termed 'exhaustion hardening', attributed to junction and debris formation, is a direct result of the paucity of mobile dislocations present in small crystals and the high stresses achieved during micro-plastic flow.

11:25 AM

Large Scale Dislocation Dynamics Simulations of Single Crystal Ta: A Realization of the Multi-Scale Modeling Strategy: *Meijie Tang*¹; Tom Arsenlis¹; M. Rhee¹; G. Hommes¹; Vasily Bulatov¹; Liming Yang¹; D. Orlikowski¹; R. Becker¹; ¹Lawrence Livermore National Laboratory

Over the years, we try to develop computational tools to carry out multi-scale modeling of mechanical properties of body-center-cubic single crystals in order to develop physics based predictive capabilities for materials mechanical behavior under a wide range of pressure/temperature/strain rate conditions. We have finally carried out the strategy by linking the data obtained at different length scales from the atomistic to the microscale, and to macroscale. This talk will present the multi-scale modeling work with a focus on the role of large scale dislocation dynamics (DD) simulations of single crystal Ta. Will discuss the inputs on dislocation mobilities obtained from first principle based atomistic simulations to the dislocation dynamics simulations, and to analyze the mechanical response obtained from the large scale DD simulations and the development of strength models based on the DD results for continuum level modeling of macroscopic behavior. The work is performed under the auspices of the U. S. Department of Energy by the University of California, Lawrence Livermore National Laboratory under Contract No. W-7405-Eng-48.

11:40 AM

Application of Fourier-Spectral Moving Mesh Method to Phase-Field Model of Dislocations: *Weiming Feng*¹; Peng Yu¹; Shenyang Hu²; Zi-Kui Liu¹; Qiang Du¹; Long-Qing Chen¹; ¹Pennsylvania State University; ²Los Alamos National Laboratory

We recently developed a new adaptive Fourier-spectral semi-implicit method (AFSIM) for domain and phase coarsening described by Allen-Cahn and Cahn-Hilliard equations. It combines the adaptive moving mesh method with the semi-implicit Fourier spectral algorithm. In this presentation, we report our recent progress in applying AFSIM to phase-field model of a multi-dislocation system with anisotropic elasticity. Accuracy and efficiency are analyzed by comparing with existing numerical algorithms. Numerical examples are presented for both two and three space dimensions.

11:55 AM

Investigation of Misfit Dislocation at Fe/Mo Interface: *Nirand Pisutha-Armond*¹; Bo Yang²; Mark Asta²; Katsuyo Thornton¹; ¹University of Michigan; ²University of California at Davis

We present a dislocation model based on Peierls-Nabarro's formulation to study dislocation structure during the epitaxial growth of Fe on Mo(110). The continuum model calculates the elastic field originating from the misfit dislocation array and network within a film of finite thickness. We use the stacking fault energy of the Fe/Mo system from an *ab initio* calculation as an input to the model. The interfacial energy stemming from the misfit dislocation is calculated using this model. The predicted dislocation structure within the thin film is compared to experimental observations, while the predictions for thick films and islands are compared to an experimental estimation of the dislocated interface in the Fe/Mo(110) system.

12:10 PM

Phase Field Modeling of the Electrochemical Interface: *Jonathan Guyer*¹; David Saylor²; James Warren¹; William Boettinger¹; Geoffrey McFadden¹; ¹National Institute of Standards and Technology; ²Food and Drug Administration

We previously developed a phase field model of the electrochemical interface [Phys. Rev. E 69, 021603 & 021604 (2004)] and demonstrated that a simple

set of assumptions gives rise to a rich set of behaviors. However, the need to resolve both the small charge separation distances (the Debye length) and large differences in concentrations placed severe limits on the time steps that could be taken. We have recently applied a variety of numerical techniques to this problem, including moving meshes and different discretizations, that have resulted in simulating larger domains, in higher dimensions, than previously achievable, while retaining the essential physics of the electrochemical interface. We have been able to increase the maximum stable time step by several orders of magnitude. We will present the approaches we have taken to make this problem tractable, as well as the results of simulations for a variety of applications.

Deformation Twinning: Formation Mechanisms and Effects on Material Plasticity: Experiments and Modeling: Twin Formation and Growth Mechanisms

Sponsored by: The Minerals, Metals and Materials Society, TMS Structural Materials Division, TMS/ASM: Mechanical Behavior of Materials Committee
Program Organizers: George Gray, Los Alamos National Laboratory; Subhash Mahajan, Arizona State University; Ellen Cerreta, Los Alamos National Laboratory

Monday AM Room: 383
March 10, 2008 Location: Ernest Morial Convention Center

Session Chair: Subhash Mahajan, Arizona State University

8:30 AM Introductory Comments

8:40 AM Invited

Properties of Twinning Dislocations in the HCP Metals Revealed by Computer Simulation: *David Bacon*¹; Hassan Khater¹; Anna Serra²; Yuri Osetskiy³; ¹University of Liverpool; ²Politechnic University of Catalunya; ³Oak Ridge National Laboratory

Deformation twin boundary motion occurs by stress-activation of sources of twinning disconnections, which are interfacial defects with step and dislocation character. The present work on the HCP metals uses topological theory to identify possible interfacial defects and atomic-scale computer simulation to study their properties. Motion of disconnections in otherwise planar boundaries and the influence of other interfacial defects on their mobility have been studied. The operation of a continuous source of disconnections has been demonstrated. A method to simulate the motion of twin boundaries over large distance has been developed and used to investigate the interaction of a moving {10-12} twin boundary with self-interstitial or vacancy clusters in α -zirconium. This has shown that the applied stress for boundary motion is raised by interaction with defect clusters, and moving boundaries can act as sinks or recombination centres for defects, thereby providing a means for removing defects from regions of radiation damage.

9:10 AM

Twinning as a Monatomic Phase Transformation: *John Gilman*¹; ¹University of California

Twinning is a particularly simple phase transformation because no change in chemical potential is involved; only a change in mechanical potential. Also, twinning is intrinsically athermal so changes in electronic structure determine its rate. Direct measurements have shown that twin interfaces can move at velocities up to, and possibly exceeding, elastic shear wave velocities in solids. Past estimates of the energies of twin nuclei have been excessive. A new estimate is presented. The onset of twinning is abrupt because it results from electron tunneling and the tunneling probability increases rapidly over a narrow range of applied stresses. The basic tunneling process is athermal but the rate is affected by temperature because the barrier to tunneling decreases with increasing temperature. The velocity of sound limits the rate because atoms as well as electrons must move in the process. Therefore, the tunneling attempt frequency is determined by atomic vibration frequencies.

9:30 AM

On the Formation and Evolution of Microtwins during Creep Deformation in Ni-Base Superalloys: *Raymond Unocic*¹; Libor Kovarik¹; Peter Sarosi¹; Chen Shen¹; Yunzhi Wang¹; Michael Mills¹; ¹Ohio State University

During high temperature creep deformation, microtwinning is a principle mode of deformation depending upon microstructure (γ' size, distribution, morphology, and γ channel width spacing), temperature and stress. In this TEM-based deformation mechanism study, the aim was to identify microtwin nucleation sources and track their evolution into fully developed microtwins as a function of increasing plastic deformation. Creep specimens were interrupted at different levels of plastic deformation. In the early stages of creep, deformation is highly localized around MC and $M_{23}C_6$ type carbides, which act as a dislocation source of $a/2\langle 110 \rangle$ matrix dislocations. Due to microstructural effects and low matrix stacking fault energies, the dislocations readily dissociate into Shockley partial dislocations. The detailed process by which these partials cooperatively shear both γ and γ' phases during the course of deformation will be discussed. The salient microstructural features that lead to the microtwinning mechanism will also be addressed.

9:50 AM

The Role of Interstitials on Slow Twin Growth in Alpha and Beta Titanium Alloys: *Paul Oberson*¹; Sreeramamurthy Ankem¹; ¹University of Maryland

Recent models for some of the twins in HCP and BCC materials show that the octahedral sites where interstitials reside are not conserved at the twin-matrix interface. If interstitial atoms such as oxygen in titanium are present, then these interstitial atoms must move away from the interface so that twin growth can proceed. Recent observations in regard to the low temperature creep of alpha and beta titanium alloys show that the twins grow very slowly due to the time factor involved in diffusion of oxygen atoms away from the twin-matrix interface. The activation energies measured from the twin growth were compared to that of oxygen diffusion in alpha and beta titanium alloys at room temperature and were found to be in good agreement. The details of the twin-growth and other details of the investigation will be presented. This work is supported by NSF under Grant Number 0513751.

10:10 AM

True Twin Formation in Gamma TiAl by $\langle 211 \rangle / (111)$ Pseudo-Twin Shear: *Dongsheng Xu*¹; Hao Wang¹; Rui Yang¹; Patrick Veyssi  re²; ¹Chinese Academy of Sciences, Institute of Metal Research; ²Laboratoire d'Etude des Microstructures, Centre National de la Recherche Scientifique-ONERA

A mechanism for true-twin growth resulting from the shearing of gamma TiAl along a $\langle 211 \rangle$ pseudo-twinning direction on a {111} plane was identified by extensive atomistic simulations. Twinned and perfect L10 lattices were shear-deformed under different hydrostatic pressures. It was found that under zero pressure or hydrostatic tension, true twins can grow by a dislocation-mediated mechanism even when the shear direction does not favor the deformation twinning. A twin thickens by one layer by a process involving five partial dislocations gliding on two adjacent atomic planes, with a total Burgers vector of $2/3[211]$. The strain thus provided, which is four times larger than that associated with a conventional twin or pseudotwin, is more effective in accommodating severe mechanical conditions. The dislocation substructure and critical conditions for this process to occur were studied using molecular dynamics and 'generalized' gamma surfaces were introduced to analyze the new twin growth process.

10:30 AM Break

11:00 AM Invited

The Double Cross-Slip Mechanism of Deformation Twinning: *Pirouz Pirouz*¹; ¹Case Western Reserve University

This talk reviews a twinning mechanism based on the different mobility of partial dislocations constituting a screw dislocation and the cross-slip of the latter. In most materials, the different mobility of partials arises from their different core structures. Thus, in compound semiconductors, a screw dislocation dissociates into two 30° partials each having a different atomic species at its core. A simple extension of the Frank-Read source, taking the different mobilities of partials into account, then accounts for twinning at low temperatures and high strain rates. On the other hand, the climb dissociation of screw dislocations and the operation of the same mechanism explains basal twinning in sapphire. A number of experiments in semiconductors and in sapphire in support of this

mechanism will be presented and the model will be compared with the classical pole mechanism proposed nearly half a century ago.

11:30 AM

Influence of Shockwave Obliquity on Deformation Twin Formation: *George Gray¹*; Ellen Cerreta¹; Robert Hixson¹; Larry Hull¹; ¹Los Alamos National Laboratory

Shock-loading of a material in contact with a high explosive (HE) experiences a complex loading path which evolves in both space and time. Energetic loading subjects a material to a "Taylor wave" (triangular wave) loading profile that as a function of obliquity experiences an evolving balance of hydrostatic and deviatoric stresses. While much has been learned over the past five decades concerning the propensity of deformation twinning in samples shock-loaded using "square-topped" profiles as a function of peak stress, achieved via flyer plate loading, considerably less quantitative information concerning direct in-contact HE-driven and sweeping detonation-wave loading on twinning propensity in materials is known. The influence of shock prestraining on various metals shock loaded via direct energetic loading on deformation twin formation was studied. Twinning propensity is shown to increase with increasing shock obliquity consistent with the increasing deviatoric shear stresses and decreasing peak shock stress with increasing shock obliquity.

11:50 AM

An Electron Microscope Study of Mechanical Twinning in Gamma-Based Titanium Aluminides: *Fritz Appel¹*; ¹GKSS Research Centre

Modern gamma-based titanium aluminide alloys are multiphase assemblies with complex constitution microstructure. Mechanical twinning in these alloys has been investigated by conventional and high-resolution electron microscopy. The major areas of the study are: twin nucleation and growth, effects of solid solution and precipitation hardening and the association of twinning and fracture. Particular emphasis is paid on the stress-induced transformation of the B₂ and orthorhombic phases, which are significant constituents in these alloys. These two phases are apparently unstable under mechanical distortion and transform into gamma phase by distinct shuffle operations. Thus, the product structure is not crystallographically identical to the matrix and the mechanism may be described as pseudo-twinning. Since such structures have been frequently observed in deformed and fatigued samples, it might be expected that this stress-induced transformation serves as a toughening mechanism.

12:10 PM

Formation Mechanism of Deformation Twinning in High-Nitrogen Austenitic Stainless Steel: *Tae-Ho Lee¹*; Chang-Seok Oh¹; Sung-Joon Kim¹; ¹Korea Institute of Materials Science

Formation mechanism of deformation twinning in high-nitrogen austenitic stainless steel was discussed based on the characteristics of dislocation configuration using dynamical two-beam theory. Deformation twinning showed strong orientation dependence: (i) primary and conjugate twinning system cooperated in <111>; (ii) only one twinning system was activated in <110>; (iii) no deformation twinning was observed in <100> orientation, respectively. At the early stage of deformation, fault pairs composed of stacking fault planes and bounding partials heterogeneously nucleated, and grew into overlapping stacking faults, resulting in the formation of deformation twinning. The dynamical two-beam analyses showed that the twinning partials were confirmed to be a Shockley dislocation with Burgers vector 1/6[1-21] and no other dislocation components such as Frank or stair-rod are found. The formation mechanism of deformation twinning could be accounted for by the three-layer twin model, and is discussed in comparison with other models.

Emerging Interconnect and Packaging Technologies: Pb-Free Solders: Fundamental Properties, Interfacial Reactions and Phase Transformations

Sponsored by: The Minerals, Metals and Materials Society, TMS Electronic, Magnetic, and Photonic Materials Division, TMS: Electronic Packaging and Interconnection Materials Committee

Program Organizers: Carol Handwerker, Purdue University; Srinivas Chada, Medtronic; Fay Hua, Intel Corporation; Kejun Zeng, Texas Instruments, Inc.

Monday AM
March 10, 2008

Room: 275
Location: Ernest Morial Convention Center

Session Chairs: Carol Handwerker, Purdue University; Darrel Frear, Freescale Semiconductor

8:30 AM Introductory Comments

8:35 AM Invited

Materials Characterizations of Sn-In Based Solders: *Fay Hua¹*; Yi He¹; Jim Maveety¹; Rajat Agarwal¹; Carl Deppisch¹; ¹Intel Corporation

Sn-Ag-Cu based solders have a number of limitations, such as a high melting point, being relatively stiff, etc. New alternative Pb-free solders are needed to meet both FLI (1st level, flip chip) and SLI (2nd level, BGA) applications. The requirements for the new solders are as follows: 1> highly deformable to absorb the thermo-mechanical strain caused by CTE mismatch of package and PCB materials during temperature cycling. 2> highly fatigue resistant to serve as electrical pass for products during operation under high stress. 3> Pb-free is a given requirement due to world wide ROHS requirements; 4> highly electro-migration resistant to avoid premature failure during operation at high current and temperature applications. In order to meet the requirements, detailed characterization on 2 to 15 wt.% of SnIn alloys were conducted. Very-small ~120°C peak observed in some of the high Sn SnIn solders from in DSC analysis likely due to macro segregation during solidification in current package assembly. Lab shear, creep and isothermal fatigue tests were also conducted for various SnIn solders. The mechanical behavior was optimized with smaller 3rd element doping. Lab scale solder joints electron migration was evaluated. The data shows superb current carrying capability of the SnIn based solder joints. SEM, EDX and other analytical tools were used in the evaluation. The paper summarizes all the material characterization of the materials series.

9:05 AM

A Novel Low-Temperature Solder Based on Intermetallic-Compound Phases with Superior High-Homologous Temperature Reliability: *Daewoong Suh¹*; Chi-won Hwang¹; Minoru Ueshima²; Jun Sugimoto²; ¹Intel Corporation; ²Senju Metal Industry Company

A novel low-temperature solder which consists entirely of two phases of intermetallic compounds is recently developed in an attempt to develop a highly reliable low-temperature solder for 125C reflow. The materials design, key properties and package-level reliability performance are presented in this article. The new solder can be reflowed at 125C and yet maintains high-temperature mechanical properties and reliability at homologous temperatures exceeding 0.9. Specifically, the new solder has creep resistance and high-temperature retention capability exceeding those of conventional low-temperature solders, and its strength even exceeds that of Sn-4%Ag-0.5%Cu (SAC405) at the same homologous temperatures. Accordingly, reliable temperature cycling performances up to 1000 cycles are demonstrated at the peak temperature corresponding to the homologous temperature exceeding 0.9. The new solder also exhibits ductility exceeding conventional solders at room-temperature, delivering drop reliability superior to SAC405.

9:20 AM

Oxidation Resistant Rare Earth-Containing Pb-Free Solders: *Martha Dudek¹*; Nikhilesh Chawla¹; ¹Arizona State University

Small additions of the Rare-Earth (RE) La to Sn-Ag-Cu alloys have been shown to significantly increase ductility, without significant loss in strength. Since most REs are prone to oxidation, this can severely affect the mechanical

performance of the solder. In this work, we have investigated the effect of the addition of Ce, La, and Y rare-earths on the oxidation behavior and shear strength of a Sn-3.9Ag-0.7Cu alloy. The degree of oxidation and oxidation mechanisms were studied by conducting experiments in air at 60°C, 95°C, and 130°C. The Ce-containing solders showed the highest oxidation resistance, approaching that of conventional Sn-Ag-Cu. Microstructure characterization of as-processed and reflowed samples was conducted to determine the influence of RE-containing phases on the mechanical properties and oxidation resistance. The oxidation mechanisms and their influence on mechanical performance will be discussed.

9:35 AM

Reaction Phases in the Sn/Ni-V Couples: *Chih-chi Chen*¹; *Sinn-wen Chen*¹; *Chih-hong Chang*¹; ¹National Tsing Hua University

Ni-V alloys are barrier materials in flip chip technology and Sn is the primary constituent of Pb-free solders. The interfacial reactions in the Sn/Ni-V are different from those in the Sn/Ni couples. A ternary T phase layer is formed at the early stage of the Sn/Ni-7wt.%V reaction couple at 200°C. After 48 hours reaction, a Ni₃Sn₄ phase layer is formed between Sn and T phase, the reaction path is Ni-V/T/Ni₃Sn₄/Sn. Periodic layers, Ni-V/T/Ni₃Sn₄/T/Ni₃Sn₄/Sn, are found in the couples after 72 hours reaction. The ternary T phase is examined by using transmission electron microscopy (TEM), grazing incident x-ray diffraction (GIXD) and electron probe microanalysis (EPMA). T phase composition varies with vanadium content which indicates T phase is with some amorphous characteristics. By TEM and GIXD analysis, T phase also shows some crystalline characteristics and it consists of fine grains. T phase is an amorphous phase with some ultra-fine crystalline grains.

9:50 AM Break

10:10 AM Invited

Sn/Co Interfacial Reactions: *Chao-hong Wang*¹; *Sinn-wen Chen*¹; ¹National Tsing Hua University

Interfacial reactions in the Sn/Co couples have been examined. The reaction temperature ranges from 150°C to 250°C and CoSn₃ phase is the dominant reaction phases. The growth rates of the reaction phases are very fast, and the layer thickness increases with linearly with the reaction time in the initial stage of the reaction. A very unique cruciform pattern is formed in the Sn/Co couple reacted at 200°C. The reaction phase layers are thick and uniform along the edges of the Co substrate, and there are no reaction phases at the corners. For the Sn/Co couple reacted at 180°C, a metastable CoSn₄ phase is formed at the corner in addition to the CoSn₃ phase formed along the edge of the Co substrate. The cruciform pattern of the reaction CoSn₃ phase layer is formed either by cracking or transformation to the CoSn₄ phase at the corners where stresses are most intensified.

10:40 AM

High Impact Strength Tin-Copper Based Lead-Free Solder Bump Alloys: *Keith Sweatman*¹; *Tetsuro Nishimura*¹; *Shoichi Suenaga*¹; ¹Nihon Superior Company, Ltd.

The advantages of the higher ductility of the Sn-Cu eutectic as a bumping alloy has previously been acknowledged but its use as a solder was initially limited its non-eutectic behaviour. With the success of an addition of Ni at a very specific level in promoting eutectic behaviour apparent in the very widespread use of a proprietary alloy in wave soldering consideration has been given to its application in BGA. In this paper we report the results of testing the impact strength of Sn-Cu-Ni BGA spheres soldered to ENIG and Cu/OSP substrates with pendulum hammer speeds of 10, 1000 and 4000mm/s. At the highest pendulum speed the energy to fracture Sn-Cu-Ni joint was consistently and significantly higher than that of similar Sn-Ag-Cu alloy spheres soldered to the same substrates. Study of the fracture surfaces confirmed the more ductile character of the failure in the Sn-Cu-Ni joints.

10:55 AM

The Effects of Minor Fe, Co, and Ni Additions to Lead-Free Solders on the Thickness of Cu₃Sn at the Interface: *Yi-Wun Wang*¹; *C. Robert Kao*¹; ¹National Taiwan University

The transition to lead-free solders in the microelectronics industry presents many reliability challenges. Examples include package compatibility, creep, and Kirkendall voids. It is widely accepted that the formation of the Kirkendall voids

is related to the growth of Cu₃Sn. The objective of this study is to investigate the effects of minor Fe, Co, and Ni additions on the soldering and aging reactions between lead-free solders and Cu. The experimental results show that the presence of minor elements can in fact reduce the growth rate of Cu₃Sn but increase the formation of Cu₆Sn₅. We find Kirkendall voids in the reaction between Sn₂.5Ag-xNi (x=0~0.1wt.%) and electroplated Cu at 160°C. However, we didn't find voids in the reaction between Sn₂.5Ag0.8Cu-xNi (x=0~0.1wt.%) and electroplated Cu. We consider that the Cu concentrations in the solders and the types of Cu substrate are two factors influencing Kirkendall voids formation.

11:10 AM

Wetting Kinetics of Eutectic Lead and Lead-Free Solders: Spreading over Cu Surface: *Hui Zhao*¹; *Dinesh Reddy Nalagatla*¹; *Dusan Sekulic*¹; ¹University of Kentucky

The main objective of this paper is to contribute to fundamental understanding of physical mechanisms of the kinetics of the triple line movement for solder systems over Copper substrates. This effort is devoted to a phenomenological and quantitative investigation of spreading of three representative, commonly considered lead-free solder systems, i.e., Sn, eutectic Sn-Ag, and an eutectic Sn-Cu, vs. an eutectic Pb - Sn solder over Cu substrates. Wetting kinetics was studied using a real time in situ monitoring of the triple line movement, facilitated by a hot-stage microscopy system under a controlled atmosphere. A significantly different kinetics of lead vs. lead-free solders is documented. In case of the eutectic lead solder, three characteristic spreading stages were identified. Spreading of lead-free solders features two stages with a sharp change of the spreading rate. SEM and EDX analysis of the re-solidified solder surface within the halo region is discussed.

11:25 AM

Surface Tension and Oxide Film Studies of Lead-Free Solders: *Kym Watling*¹; *Kazuhiro Nogita*¹; *Arne Dahle*¹; ¹University of Queensland

The relative surface tensions of a range of lead-free solders were determined on pyrex and copper substrates using the sessile drop method. Studies were performed under controlled atmospheres including air and protective gases. The formation of thin protective films was seen for some alloys, while bulk oxides showing interference colors were observed for others under the same atmosphere and temperature conditions. X-ray Photoelectron Spectroscopy was used to determine the chemical nature of the surface oxides and the thickness of thin protective films. The thickness of bulk films was studied using a spectral reflectance technique. Significant differences in the oxide film characteristics were observed between the different solders and for different atmospheres.

Emerging Methods to Understand Mechanical Behavior: Imaging Methods

Sponsored by: The Minerals, Metals and Materials Society, TMS Structural Materials Division, TMS Materials Processing and Manufacturing Division, TMS: Advanced Characterization, Testing, and Simulation Committee, TMS/ASM: Mechanical Behavior of Materials Committee, TMS: Nanomechanical Materials Behavior Committee
Program Organizers: Brad Boyce, Sandia National Laboratories; Mark Bourke, Los Alamos National Laboratory; Xiaodong Li, University of South Carolina; Erica Lilleodden, Forschungszentrum

Monday AM
March 10, 2008

Room: 285
Location: Ernest Morial Convention Center

Session Chair: Brad Boyce, Sandia National Laboratories

8:30 AM Invited

Elasticity and Large Strain Plasticity of Semiconductor Nanowires and Nanobelts: *Zhong Lin (Z.L.) Wang*¹; *Xiaodong Han*²; *Ze Zhang*²; ¹Georgia Tech; ²Beijing University of Technology

Covalence bonded materials are usually high strength and high hardness but with low temperature brittleness. However, lowering the dimension of the materials may result in dramatic change in their mechanical properties. In this talk, we will present mechanical characterization of individual oxide nanobelts

by AFM and Si and SiC nanowires by in situ nano-mechanical deformation in TEM. As for SiC nanowires (NWs), we demonstrated unusually large-strain plasticity of ceramics SiC nanowires (NWs) at temperatures close to room temperature that was directly observed. The continuous plasticity of the SiC NWs is accompanied by a process of increased dislocation density at early stage, followed by an obvious lattice distortion, and finally reaches an entire structure amorphization at the most strained region of the NW. These unusual phenomena for the SiC NWs are fundamental important for understanding the nano-scale fracture and strain induced band structure variation for high temperature semiconductors.

9:00 AM

In Situ Compression of Nanoparticles: Julia Nowak¹; William Mook¹; Joysurya Basu²; William Gerberich¹; C. Carter²; ¹University of Minnesota; ²University of Connecticut

The mechanical properties of nanoparticles are difficult to characterize because of the length scales which are inherently involved. With traditional nanoindentation methods, the crystallographic orientation of the particle usually cannot be determined, and it is impossible to definitively ascertain the presence of defects prior to deformation. These issues can be circumvented by compressing the nanoparticles in the transmission electron microscope (TEM), which is particularly sensitive to crystal structure. Previous studies on nanoparticles have shown length scale effects on particle flow stress, modulus and fracture toughness. This work uses a specially designed sample holder to compress individual nanoparticles *in situ*. The particles are compressed between a sapphire substrate and a diamond tip while quantitative load-displacement data is simultaneously acquired. By compressing the particles inside the TEM it is possible to observe the deformation events directly as they occur and correlate them to the particle's mechanical response.

9:20 AM

Nanomechanical Testing of Gum Metal: Elizabeth Withey¹; Miao Jin¹; Jia Ye²; Andrew Minor²; Shigeru Kuramoto³; Daryl Chrzan¹; John Morris¹; ¹University of California; ²Lawrence Berkeley National Laboratory, National Center for Electron Microscopy; ³Toyota Central Research and Development Laboratories, Inc.

"Gum Metal" describes a newly developed set of alloys with nominal composition Ti-24(Nb+V+Ta)-(Zr,Hf)-O. In the cold-worked condition these alloys have exceptional elastic elongation and high strength; the available evidence suggests that they do not yield until the applied stress approaches the ideal strength of the alloy, and then deform by mechanisms that do not involve conventional crystal dislocations. To clarify the mechanisms involved, in situ nanoindentation and microcompression experiments were performed in a TEM on electron transparent windows and pillars fabricated with a focused-ion beam. Results from these tests on solution-treated and cold-worked specimens were compared with TEM observations after ex situ nanoindentation, which revealed unusual patterns in the pits of the indents.

9:40 AM

In Situ Nanotension and Nanocompression Tests of Metallic Glasses in a TEM: Evan Ma¹; ¹Johns Hopkins University

For metallic glasses (MGs), the initial evolution of plastic strains in both time and space has not been resolved, because of strain localization in ~10 nm shear bands that propagates rapidly to failure. We discuss in situ tests, in tension and compression, of Zr-based and Cu-Zr-Al MGs in a TEM, employing samples with dimensions of the order of 100 nanometers. The tensile experiments were a collaboration with H. Guo and M.L. Sui at SYNLAB (H. Guo et al., Nature Mater. 2007), and the nanocompression was a joint project with Z.W. Shan of Hysitron/LBNL (Z.W. Shan et al., submitted, 2007). These tests show uniform deformation and extensive necking or slow shear displacement rate, i.e. deformation modes similar to their crystalline counterparts. The sample size effects revealed in these nanoscale in situ tests have implications for understanding the mechanical behavior of amorphous metals and their applications in thin films and micro-devices.

10:00 AM

In Situ TEM Nanoindentation of a 50nm Particle: Observed Deformation Mechanisms and Theoretical Analysis: Chris Carlton¹; Oleg Lourie²; Paulo Ferreira¹; ¹University of Texas at Austin; ²Nanofactory Instruments

Indentation of nanostructured materials is a very rapidly growing area of investigation. Many nanoindentation experiments have been performed on nanostructured materials to determine the fundamental effects of length scale constraints on their mechanical behavior. An in-situ deformation experiment was performed on a single crystal nanoparticle with a diameter of approximately 50nm. Evidence of dislocation nucleation and motion was observed during in-situ TEM nanoindentation, but upon unloading dislocations were no longer visible. The experiment provides insight into how nanomaterials behave under deformation. Because observed dislocations intersected the particle's surface, both the dislocation loop and image force only assumptions made by previous models explaining dislocation behavior are inadequate for addressing the situation observed. Additionally, dislocations are not seen to nucleate from Frank-Read sources, contrary to what is commonly assumed in models for nanoindentation. A new analytical model for explaining dislocation instability is introduced, and application of this model is considered.

10:20 AM Break**10:35 AM Invited**

3D Resolved in Situ Studies of Grain Dynamics and Plastic Strain: Henning Poulsen¹; ¹Risø National Laboratory

The status of two hard x-ray characterization techniques will be presented along with examples of applications: 1) 3DXRD microscopy is a diffraction method based on imaging/reconstruction principles. It enables fast and comprehensive characterization of the individual grains within thick specimens. 3D orientation maps can be acquired with a spatial resolution of currently ~ 5 µm, while diffracting units of size 20 nm can be observed. 3DXRD microscopy for the first time enables dynamic studies of the individual grains in polycrystals. Focus will be on recent extensions of the methodology to deformed specimens. 2) A universal method for 3D plastic strain characterisation has been developed based on displacement of markers and the use of x-ray tomography. The combination with FEM analysis will be illustrated.

11:05 AM Invited

Direct Observation and Measurement of Fundamental Deformation Mechanisms at the Nanoscale: Oden Warren¹; Zhiwei Shan¹; S.A. Syed Asif¹; Andrew Minor²; ¹Hysitron, Inc.; ²Lawrence Berkeley National Laboratory, National Center for Electron Microscopy

Nanoindentation has advanced sufficiently to become a routine technique, and is most commonly used to determine elastic modulus and hardness of small volumes of materials. However, there also is considerable interest in using nanoindentation to understand how material deformation proceeds at the nanoscale. But unfortunately, the often observed discontinuities in nanoindentation force-displacement curves do not represent unique fingerprints for specific deformation mechanisms. In order to directly observe and measure fundamental deformation mechanisms at the nanoscale, we have placed the nanoindentation technique into the transmission electron microscope (TEM). We have used this fully quantitative in situ TEM technique to correlate specific features of the nanoindentation force-displacement curve to the corresponding microstructure evolution, and to examine the response of individual nanostructures to compression or bending. Some in situ TEM results support conventional wisdoms whereas others do not, and it is the latter that will be the primary focus of this presentation.

11:35 AM

Design and Fabrication of In Situ Micro-Device to Study Mechanical Properties of One Dimensional Nanoscale Building Blocks: Y. Ganesan¹; Y. Lu¹; A. Minor²; Jun Lou¹; ¹Rice University; ²Lawrence Berkeley National Laboratory

This paper presents a simple micro-device that allows in situ quantitative mechanical characterization of one-dimensional nanoscale building blocks, such as metallic nanowires and carbon nanotubes, in scanning electron microscope (SEM) chamber equipped with a nanomanipulator, or transmission electron microscope (TEM) chamber equipped with a quantitative nanoindenter. The unique design of this device makes it possible to convert compression

from nanoindentation to uni-axial tension at the sample stages. Fabrication of the micro-device is successfully demonstrated using established micro-fabrication processes. Finite element analysis (FEA) is employed to model the device behavior under mechanical loading and compared with experiments. Finally, initial results from testing Ni nanowires and CNT bundles will also be discussed.

11:55 AM

Multistage Fatigue Model for an Extruded AZ31 Mg Alloy: *Yibin Xue*¹; Marcos Lugo¹; Mark Horstemeyer¹; Jim Newman¹; ¹Mississippi State University

Microstructure-fatigue properties relation is developed based on multiscale fatigue experiments and micromechanical simulations. The large inclusion particles at or near the surface are identified as the fatigue damage incubation sites. The shape and composition of the inclusion particles, as well as the bonding strength between the particle and alloy matrix, affects the fatigue incubation life as observed in micromechanical simulations in conjunction with the modified microscale Coffin-Manson law. The microstructurally and physically small crack growths were observed using in-situ SEM fatigue testing setup. The crack growth rate was directly quantified as a function of applied stress amplitude with a weight function of applied stress ratio. The fatigue long crack growth was modeled combining a generalized Paris law with the application of a strip-yield model at the crack tip. Finally, the multistage fatigue model was implemented to evaluate the fatigue life of a simple component in an automobile Mg-front end application.

12:15 PM

Application of Moiré Interferometry to Whole Field Strain Measurement in Thin Film Specimens: *Arash Tajik*¹; Hamid Jahed¹; ¹University of Waterloo

This paper presents the results of the application of Moiré interferometry to strain field measurements in thin films. For strain field measurements, gratings are milled directly on the film using Focused Ion Beam (FIB). The effect of FIB process parameters and the grating geometry on the mechanical property of the film, as well as on the quality and noise level of the Moiré interferogram is studied. Phase stepping and continuous wavelet ridge detection are used to enhance the sensitivity of the technique to 10nm displacements. This technique is potentially a versatile tool for investigation of the static and dynamic behavior of thin films. Tensile testing and the related results on free standing Aluminum thin films are also presented.

Enhancing Materials Durability via Surface Engineering: Residual Stress Effects on Durability

Sponsored by: The Minerals, Metals and Materials Society, TMS Structural Materials Division, TMS/ASM: Corrosion and Environmental Effects Committee, TMS: High Temperature Alloys Committee

Program Organizers: David Mourer, GE Aircraft Engines; Andrew Rosenberger, US Air Force; Michael Shepard, Air Force Research Laboratory/MLLMN; Bruce Pint, Oak Ridge National Laboratory; Brian Gleeson, Iowa State University

Monday AM Room: 388
March 10, 2008 Location: Ernest Morial Convention Center

Session Chair: Michael Shepard, Air Force Research Laboratory

8:30 AM

Advanced Residual Stress Inducing Surface Treatments: *Mike Shepard*¹; ¹Air Force Research Laboratory, Materials and Manufacturing Directorate

With the advent of processes capable of introducing deep, high magnitude residual compression into arbitrary geometries the use of engineered residual stresses has gained increased attention. Several processes, including laser shock processing (LSP) and low plasticity burnishing (LPB), have evolved and are entering common usage in fatigue critical applications. The chief characteristics and applications of these processes will be reviewed. The evolving suite of techniques used to successfully engineer stress distributions will also be described.

8:50 AM

Effects of Laser Shock Peening on the Microstructure and Residual Stress Distributions in Ti-6Al-4V Alloy: *Yixiang Zhao*¹; Seetha Mannava¹; Vijay Vasudevan¹; ¹University of Cincinnati

Laser shock peening (LSP) is a novel surface process that generates deep compressive residual stresses and microstructural changes and thereby dramatically improves fatigue strength of critical metal aircraft engine parts. The present study was undertaken to develop a basic understanding of the effects of LSP parameters on the residual stress distributions and microstructural changes in Ti-6Al-4V. Coupons of the alloy with and without a sacrificial/ablative layer were LSP-treated using the LSP system at GE and LSP Technologies, Inc. Depth-resolved characterization of the macro residual strains and stresses and was achieved using high-energy synchrotron x-ray diffraction. The near-surface and through-the-depth changes in strain, texture and microstructure were studied using EBSD/OIM and by TEM of thin foils fabricated from specific locations using the FIB method. Local property changes were examined using microhardness. The results showing the relationship between LSP processing parameters, microstructure, residual stress distributions and hardness are presented and discussed.

9:15 AM Invited

Bulk Residual Stress Measurements to Support Durability Enhancement:

*Michael Hill*¹; Adrian DeWald¹; ¹Hill Engineering, LLC

Residual stress measurement is a key technology for engineering of durability enhancement through surface treatment. The contour method is a new way to measure bulk residual stress fields in components that provides data useful for forecasting fatigue life. Relying on simple assumptions and straightforward experimental procedures, the method provides the two-dimensional spatial distribution of residual stress normal to a plane of interest within the component. When the method is applied at sections with high failure risk, the residual stress field determined may be used directly with standard methods for predicting fatigue crack initiation and growth. The paper provides a summary of the experimental details of the contour method and residual stress distributions measured in example surface treated components. The paper further provides a few case studies demonstrating the use of measured residual stress distributions in correlating the fatigue performance of surface treated coupons.

9:40 AM Break

9:50 AM

Modeling of Mechanical Surface Treatments: *Adrian DeWald*¹; ¹Hill Engineering, LLC

This presentation provides an overview of the methodology and a summary of capabilities for a model that predicts the effects of residual stress inducing surface treatments on foreign object damage (FOD) tolerance. The proposed model gives an efficient means for predicting the residual stresses (compressive and tensile) in complex 3D parts, which is useful for design calculations. In addition, the model is capable of predicting the effects of changes in the processing parameters and treatment zone, which provides an efficient means to iterate the process. Ultimately, the model is intended for use as a tool to help organizations adopt residual stress treatments with lower risk, lower cost, and reduced time to market.

10:15 AM

Fatigue Design Diagram (FDD) Code to Design Compressive Residual Stresses to Improve Performance of Damage-Limited Components and Structures: *Narayanan Jayaraman*¹; Paul Prevey²; Ravi Ravindranath³; Michael Shepard⁴; ¹Lambda Technologies; ²Lambda Research; ³NAVAIR; ⁴Air Force Research Laboratory

The Fatigue Design Diagram (FDD) is mainly used to design residual stresses to mitigate different damage conditions. It is also designed to take credit for beneficial residual stresses in components to achieve a required or optimal fatigue performance. The FDD code has been developed to interact with commercial finite element analysis (FEA) codes to determine the required residual stress distribution in a component or structure. Design features include determination of minimum, maximum and optimum residual stress distribution for fixed mean stress condition and fixed stress-ratio ($R = S_{min}/S_{max}$) condition. Other analytical features like prediction of fatigue life in the presence of known residual stress distributions will also be discussed. In this paper, the progress

made to date on the use of the FDD Code will be described. The paper will demonstrate the coupling of the FDD code with other standard commercial analytical tools with specific examples.

10:40 AM

Incorporating Residual Stress in Probabilistic Life Prediction of an $\alpha+\beta$ Titanium Alloy: *Sushant Jha*¹; Reji John²; James Larsen²; ¹Universal Technology Corporation; ²US Air Force Research Laboratory

The effect of surface residual stress (RS) on the fatigue lifetime variability of Ti-6Al-2Sn-4Zr-6Mo was studied at 260°C. The RS profiles induced by low stress grinding (LSG) and shot peening (SP) were considered. Particular focus was on relating the crack initiation mechanisms under these surface conditions to the mean vs. the life-limiting behavior. Deterministic and probabilistic life-prediction analyses, that incorporated the relaxation (upon exposure to temperature and cyclic loading) and variability in the RS profile, were developed. While SP provided a benefit in terms of the mean lifetime response when compared to the RS free condition, the lower-tail behavior was not significantly affected. The LSG treatment provided a greater benefit, both in the mean as well as the life-limiting behavior. These effects were related to the incidence of surface-crack-initiation mechanisms that occurred at a much smaller size scale under the LSG condition than the SP treated surface.

11:05 AM Break

11:15 AM

Relaxation of Shot-Peened Residual Stresses in a Nickel-Base Superalloy: *Dennis Buchanan*¹; Reji John²; Robert Brockman¹; ¹University of Dayton Research Institute; ²US Air Force

Creep tests on shot-peened nickel-base superalloy specimens, subject to applied stresses near yield, have been performed at 650°C on IN100 to characterize the residual stress relaxation behavior. Retained residual stress depth profiles show that yielding during the initial loading produces the largest change in the residual stress profile. For sustained loads above yield, a continual relaxation of residual stresses occurs with increasing exposure time. However, for stresses below yield the retained residual stress profiles are similar to specimens subject to thermal exposure alone. Baseline virgin samples subject to room temperature plastic deformation and tested under elevated temperature creep conditions display a creep rate dependency on prior plastic strain. These prestrain experiments simulate the deformation experienced by the material during shot-peening and form the basis of a coupled creep-plasticity constitutive model. The model successfully predicts the retained residual stress profiles of shot-peened IN100 specimens subject to elevated temperature loading histories.

11:40 AM Invited

Materials Development and Process Modeling for Engineered Surfaces – An Integrated Approach for Gas Turbine Engine Component Design: *Ann Bolcavage*¹; Kang Lee¹; Kong Ma¹; ¹Rolls-Royce Corporation

Modern gas turbine engines are required to provide increasing amounts of thrust and withstand severe environmental conditions. Resulting operational factors such as higher temperatures and loading for a given mission can be detrimental to the service life of the engine, and their effects are often manifested in the degradation or alteration of the component surface properties. To address these challenges to optimum performance, materials development and process modeling are increasingly coordinated during component definition and design. The benefits of an integrated approach include reduced part-to-part variability, increased component capability via the tailoring of surface-specific materials and mechanical properties, and better prediction of the effects of harsh environments on serviceable life. Examples include diffusion coating alloy optimization for oxidation resistance and peening process development and modeling.

Frontiers of Computational Materials Science

Sponsored by: The Minerals, Metals and Materials Society, American Physical Society, TMS Electronic, Magnetic, and Photonic Materials Division, TMS Materials Processing and Manufacturing Division, ASM Materials Science Critical Technology Sector, TMS: Chemistry and Physics of Materials Committee, TMS/ASM: Computational Materials Science and Engineering Committee, TMS: Global Innovations Committee, TMS: Nanomechanical Materials Behavior Committee, TMS/ASM: Phase Transformations Committee, TMS: Powder Materials Committee, TMS: Process Technology and Modeling Committee, TMS: Shaping and Forming Committee, TMS: Solidification Committee, TMS: Surface Engineering Committee
Program Organizers: Mark Asta, University of California; Giulia Galli, University of California, Davis

Monday AM
March 10, 2008

Room: APS Room, Hall A
Location: Ernest Morial Convention Center

Session Chair: To Be Announced

Program to be announced.

General Abstracts: Extraction and Processing: Session I

Sponsored by: The Minerals, Metals and Materials Society, TMS Extraction and Processing Division, TMS: Aqueous Processing Committee, TMS: Materials Characterization Committee, TMS: Process Technology and Modeling Committee, TMS: Pyrometallurgy Committee, TMS: Recycling and Environmental Technologies Committee

Program Organizers: Boyd Davis, Queens University; Michael Free, University of Utah

Monday AM
March 10, 2008

Room: 272
Location: Ernest Morial Convention Center

Session Chair: Boyd Davis, Queens University

8:30 AM

Study on AC Impedance Equivalent Circuit and Experimental Condition for Solution and Melts Electrical Conductivity Measurement by CVCC Technique: *Xianwei Hu*¹; Zhaowen Wang¹; Guimin Lu¹; Jianzhong Cui¹; Zhongning Shi¹; Xiaozhou Cao¹; Xingliang Zhao¹; ¹Northeastern University

Continuously varying cell constant(CVCC) technique is an advanced method for measuring the electrical conductivity of solution and melts. AC impedance spectroscopy of CVCC experimental conductivity cell system analyzed, and viewpoint error of former researchers was pointed out. So the AC impedance rational condition for electrical conductivity measurement by CVCC technique was determined. It was thought that the AC impedance course of the circuit researched was controlled by both of electrochemical polarization and concentration polarization. Warburg diffusion character was represented for AC impedance diffusion course of solution, meanwhile, melts' concentration polarization impedance was assumed to be Gerischer impedance. When electrical conductivity was calculated by CVCC equation, the best option of the circuit resistance was the sum of solution/melts resistance and electrode and line resistance gained by fitting the equivalent circuit. If fitting error was considered, the circuit high frequency resistance was also a good option.

8:55 AM

Improvements on the Process of Gold-Antimony Concentrate Smelting in China: *Liu Weifeng*¹; Yang Tianzu¹; *Dou Aichun*¹; Liu Yong¹; Chen Fangbin¹; ¹Central South University

On the basis of the brief introduction of the gold-antimony concentrate smelting process in China, the problems of some procedure in the original process were analyzed and the corresponding improvements were introduced in this paper, such as the treatment of antimony matte, the refinement of gold-silver alloys, the concentrating gold from gold-antimony alloys, the treatment of As-enriched slag, the pre-treatment of gold concentrate with high arsenic. The

roasting method that was used to treat the antimony matte was transferred to the ore dressing method. The solvent extraction was used to refine the gold alloys instead of the electrolytic method. The technology of selective chlorination leaching under controlling potential was applied to concentrate gold from the gold-antimony alloys and gold-lead alloys instead of the electrolysis method. As-enriched slag was recovered by the second reducing smelting method substituting for the method of compound of sodium arsenite. The pre-treatment roasting method was used for removing arsenic in gold concentrate with high arsenic.

9:20 AM

A Comparative Analysis of the Main Metallurgical and Mechanical Properties of Self-Reducing Pellets and Briquettes: *Jose Noldin¹; Jose D'Abreu²; Nivea Pimentel³; ¹Tecno-Logos S/A; ²Catholic University - PUC-Rio; ³Aços Villares*

The Tecno process is a new ironmaking technology based on the use of cold bonded self-reducing agglomerates both in the form of pellets and/or briquettes as the primary feedstock. The main characteristic of self-reducing agglomerates is the extremely fast reaction rates achieved due to the proximity of the reactants, their small size and inert gases free environment; almost complete reduction can be achieved within reaction times ranging from 5 to 10 minutes for temperatures between 1273K and 1423K. This paper discusses the main metallurgical and mechanical properties of both cold bonded self-reducing pellets and briquettes containing different types of raw materials, including mining and steelmaking residues.

9:45 AM Break

10:05 AM

Reduction Behavior of Lignite and Coke Fine Containing Composite Pellets: *Aliye Arabaci¹; Ercin Ersundu²; Süheyla Aydın²; ¹Istanbul University; ²Istanbul Technical University*

In the present investigation, an attempt has been made to study the reduction behaviour of composite pellets consisting of iron oxide fines and coke or lignite fines as reducing agents. The reduction experiments were carried out under isothermal conditions and constant flow rate of nitrogen gas in the temperature range of 900-1100°C. The variables investigated were the reduction temperature, Cfix/Fe₃O₄ ratio, reduction time and reductant type. In the experiments carried out at a temperature of 1100°C, for 40 min. and on the condition that Cfix/Fe₃O₄ ratio is 0.2, in which lignite and coke fines were used as reductant, degree of reduction was obtained as 91% and 86%, respectively. The highest degree of reduction was obtained by using lignite as reductant.

10:30 AM

Meeting the New Challenge in Smelter Gas Handling: *Erik Dupon¹; Rick Oliana¹; Travis Turco¹; Peter Klut¹; ¹Danieli-Corus BV*

New and stricter environmental and health regulations and specifications force Smelter operators to improve on their gaseous and particulate emissions from the potroom. A techno-economical overview is provided of available technologies to reduce emissions to the environment and health hazards inside the potroom. Special attention is given to reduction of emissions by the application of new technology developments such as GTC upgrading and boosted suction. Recent examples of application of these new technologies will be provided.

10:55 AM

Conceptual Design Criteria for Metallurgical Waste Heat Boilers and Electro Static Precipitators Downstream of Smelting- and Converting-Furnaces and Fluid Bed Reactors: *Kurt Westerlund¹; Jan Deisenroth²; Uwe Bock²; ¹Kamwest Oy; ²Alstom Energy Recovery GmbH*

The article deals with conceptual design originating from the reactors themselves; Gas temperature, Gas analyses, splashes, Dust carry over and exothermic dust gas reactions along the cooling path in the Waste heat boiler. Results and interpretations of Gas flow simulation and reactions are discussed.

The article also deals with dust smelting, softening temperatures and arrangement of cooling surfaces in the Waste heat boiler; cooling walls, screens, bundles and cleaning methods of these. The advantages and limitations in applying thermal siphons for cooling to avoid water leakages into the reactors are also outlined. Temperature operating windows for Waste heat boiler cooling surfaces are presented. Furthermore the article outlines the precipitation efficiency of different dusts at their optimal precipitation temperatures.

11:20 AM

Scrubbing: Development of a Technical Audit System for Process, Operation and Maintenance: *Mario Dion¹; Michel Meyer¹; ¹Alcan International Ltd*

Following the acquisition of Pechiney by Alcan, audit systems and expertise from both companies had to be integrated to take into account different equipment and practices. As part of this global approach, a team of experts was set up and created an audit system on gas scrubbing, covering four subjects: process, operation, maintenance and management, and based on the knowledge and best practices of both companies. This tool promotes the use of these Best Practices and gives a holistic picture of the status of a gas or fume treatment center, as well as a detailed action plan to improve the system performance. The new Alcan scrubbing audit system has been successfully tested through internal and external technology licensing projects.

General Abstracts: Materials Processing and Manufacturing Division: Solidification and Casting

Sponsored by: The Minerals, Metals and Materials Society, TMS Materials Processing and Manufacturing Division, TMS/ASM: Computational Materials Science and Engineering Committee, TMS: Global Innovations Committee, TMS: Nanomechanical Materials Behavior Committee, TMS/ASM: Phase Transformations Committee, TMS: Powder Materials Committee, TMS: Process Technology and Modeling Committee, TMS: Shaping and Forming Committee, TMS: Solidification Committee, TMS: Surface Engineering Committee

Program Organizers: Ralph Napolitano, Iowa State University; Neville Moody, Sandia National Laboratories

Monday AM

March 10, 2008

Room: 282

Location: Ernest Morial Convention Center

Session Chairs: Mark Jolly, University of Birmingham; Benjamin Hamilton, Miami University

8:30 AM

Austenite Grain Refining of As-Cast Bloom Surface by Reduction of Oscillation Mark Depth: *Yasuhide Ohba¹; Shin-ichi Kitade¹; Ichiro Takasu¹; ¹Sanyo Special Steel Company, Ltd.*

Austenite grain refining in the surface layer of as-cast bloom is effective for the reduction of surface cracks in steel production. This study was carried out to clarify the influence of cooling rate on the as-cast austenite grain size and its growth mechanism. The austenite grains at the bloom surface were refined under the oscillation conditions of higher frequency and shorter stroke. The average cooling rates were estimated to be 6-16K/s in austenite phase temperature. It was found that the austenite grain growth direction did not vary even when characteristics of oscillation mark changed. The austenite grain size below the surface layer was also determined by that of bloom surface.

8:50 AM

Quality Assessment of Casting Filling Method: *Carl Reilly¹; Mark Jolly¹; ¹University of Birmingham*

Cast component reliability is dependent on the quality of the casting process. This can be characterised by fluid flow characteristics within the running system. Prevention of free surface turbulence and oxide entrainment is critical to the mechanical integrity of the component. Past research highlighted that return waves were a major cause of free surface entrainment. These can be reduced by developing a quiescent flow regime. Using Flow 3D, the Froude number was extracted to allow the quantitative assessment of sumps at the end of the runner. The results showed the addition of a sump at the end of the running system can reduce the Froude number but increase the persistence and is therefore

detrimental to the cast component. Additionally, in-gate design is of utmost importance in controlling the back pressure and thus the persistence of the back wave which has a direct effect of the level of oxide entrainment.

9:10 AM

Phase Field Simulation of Irregular Eutectic Solidification: *Ruijie Zhang*¹; Mei Li¹; John Allison¹; ¹Ford Motor Company

The phase-field models have been originally developed for solidification of two phase system and then extended to multiphase system. In real multiphase alloy systems, facet phase often appears in the solidification process, such as Si in Al-Si alloy, Mg₂Si in Al-Mg-Si alloy. These facet phases are usually the highly anisotropic stoichiometric intermetallic compounds and solidify as a eutectic phase in solidification process. Their size, distribution and volume fraction are key factors which greatly affect the materials mechanical performance. So simulation of the growth of such phase will be very important for the alloy design and materials performance prediction. In this paper, the multiphase phase field model was extended to describe the solidification of irregular eutectic alloy. The strong anisotropy in interfacial energy and phase field mobility were considered. As an example, the simulation of irregular eutectic growth in Al-Si alloy was executed.

9:30 AM

Effect of Al Contents on Hot Crack Formation of the High-Manganese Steel: *Hyukjin An*¹; Yang-Mo Koo¹; ¹Pohang University of Science and Technology

The cracking condition near melting temperature during continuous casting of the high-manganese steel have been studied. During solidification, the peritectic solidification has been known to cause harm effects to the hot crack formation. The effects of Al contents on brittle temperature range for hot crack formation are analyzed by differential scanning calorimetry (DSC). To calculate the brittle temperature range, micro-segregation model and proper solidification model are used. To determine the proper Al contents for continuous casting, peritectic reaction range and brittle temperature range are calculated from heat flow graph during solidification with vary Al and Mn contents.

9:50 AM

A Numerical Scheme for Solving Microsegregation for Solidifying Metallic Alloys: *Salah Uddin*¹; Mainul Hasan¹; ¹McGill University

In this study, the microsegregation problem, which arises during solidification of an alloy, was analyzed for three different geometrical shapes namely, rectangular, cylindrical and spherical dendrite arms and for several pertinent parameters. A previously proposed numerical method for solidification/melting problems was extended in this study to deal with solute diffusion in both solid and liquid regions. An algorithm is proposed to solve the strongly coupled model transport equations. The algorithm is based on the control volume finite-difference scheme with an appropriately transformed grid system. In order to verify the accuracy of the present method with regard to tracking the solid/liquid interfaces in the microsegregation problem, the well-known analytical solution of the Stefan problem was used. A good agreement between the model predictions and the analytical solution was found. The developed computational procedure was also found to be stable for a wide range of values of the parameters.

10:10 AM Break

10:20 AM

Microstructural Characterization of Laser-Consolidated (LC) SS420 Stainless Steel: *Jiannin Chen*¹; Lijue Xue¹; ¹National Research Council Canada

Laser consolidation (LC) is a novel process that produces a net shape functional part layer by layer directly from a CAD model by using a laser beam to melt the injected powder and re-solidifying it on the substrate or previous layer. As an alternative to the conventional machining process, this computer-aided manufacturing (CAM) process can build complete parts or features on an existing part by adding instead of removing material. Due to the rapid solidification associated with this process, LC materials always show exceptionally fine dendritic microstructure, resulting in significantly improved mechanical properties as compared to the respective cast materials. In this paper, LC SS420 stainless steel was investigated. After various post-heat-treatments, the microhardness and residual stresses of the LC SS420 were measured. Their microstructure was examined by optical microscopy, SEM/EDS and XRD. The

implication of the post-heat-treatment on the microstructure and mechanical properties of LC SS420 was also discussed.

10:40 AM

Process Optimization in Laser Processing of Ceramics: *Anoop Samant*¹; Narendra Dahotre¹; ¹University of Tennessee

An integrated modeling technique based on modular approach is considered for the laser processing of the material. Heat transfer phenomenon during laser processing of alumina ceramic was modeled using COMSOL software. The macroscopic melt depth predicted using the software was enhanced by the Carman-Kozeny equations to analyze the effect of recoil pressure. Predicted residual stresses determined the range of laser fluence which doesn't cause failure of components. Taguchi method for the design of experiments identified a combination of process and materials parameters that will optimize any desirable material property. The estimated melt depths were substantially close to the measured values. For the laser processing conditions under study, the components did not fail in compression and in tension, majority of the stresses being compressive. Taguchi analysis gave a set of processing parameters that could optimize the grain size and porosity.

11:00 AM

Advances in NDT Techniques for Friction Stir Welding Joints of AA2024: *Telmo Santos*¹; Pedro Vilaca¹; Luis Reis¹; Luísa Quintino¹; Manuel Freitas¹; ¹Instituto Superior Técnico

Industrial applications of solid state welding technology have undergone a significant development with the advent of Friction Stir Welding (FSW). Although the good quality of FSW joints some defects may arise which are difficult or even impossible to detect with conventional NDT techniques. This work addresses an innovative NDT Eddy currents probe that was developed and tested for quality assessment of FSW joints of aeronautic aluminium alloy AA2024-T351. The influence of defects with different locations and morphology in joint mechanical efficiency are investigated under static and fatigue loads. The application potential of the new NDT Eddy currents probe in detecting the different defects is evaluated and compared with other NDT techniques. The results show a strong dependence between FSW parameters and defects formation and the feasibility in using the new NDT Eddy currents probe mainly concerning the detection of root defects which have a critical role in mechanical joint efficiency.

11:20 AM

A Thermal Model of Friction Stir Welding Applied to Aluminum 7136-T76511 Extrusions: *Benjamin Hamilton*¹; Stanislaw Dymek²; Marek Blicharski²; Isabella Kalembe²; ¹Miami University; ²AGH University of Science and Technology

A thermal model of friction stir welding is developed that utilizes an energy-based scaling factor to account for tool slip. The proposed slip factor is derived from an observed, empirical relationship between the ratio of the maximum welding temperature to the solidus temperature and energy per unit length of weld. The thermal model successfully predicts the maximum welding temperatures over a range of energy levels and supports the concept that the relationship between the temperature ratio and energy level is characteristic to aluminum alloys with similar thermal emissivities. The thermal model is applied to aluminum 7136-T76511 extrusions that were joined through friction stir welding at six different RPM and evaluated for residual properties. Residual mechanical properties of the alloy correlated with the energy per length of weld, i.e. the highest joint efficiency was achieved at the highest welding temperature.

11:40 AM

Purification of Cadmium from 4N (99.99%) to 6N (99.9999%) Level by Selective Vaporization Technique under Vacuum: *Gouni Rajkiran*¹; Rizwan Abdul Rahman Rashid¹; Siva Jyoth Reddy¹; Prasad Goud¹; ¹Mahatma Gandhi Institute of Technology

High purity (6N) cadmium is obtained through multiple vacuum distillation using 4N pure Cd as input material. The metal is purified by vapor phase condensation of cadmium on to a graphite collector. During the experiment, the process of selective vaporization of cadmium is carried out in a stainless steel retort under vacuum. The sample preparation procedure for chemical analysis using Inductively Coupled Plasma Optical Emission Spectrometry (ICP-OES) is studied and the results are explained with respect to their vapor pressures. The

vacuum and its effect on vapor pressure have also been observed. The detailed analysis of input as well as purified Cd was carried out by ICP-OES for 29 major elements. The final analysis shows the impurity content reduction from 190 to 1.8 ppm (6N) upon three consecutive vacuum distillations. The studies showed that the major impurities separated from the distilled cadmium are Zn, Cu, Ag, Sb, Pb, Bi, etc.

12:00 PM

Effect of Ultrasonic Vibration on Solidification Structure of TCS Stainless Steel: Jianping Liang¹; Lixin Wang¹; Changjiang Song¹; Lihua Liu¹; Fengmei Sun¹; Qijie Zhai¹; ¹Shanghai University

The effect of ultrasonic vibration on solidification structure of TCS steel was investigated in this present work. Ultrasonic power was injected into molten alloy along the horizontal direction. Experimental results show that when the ultrasonic vibration is imposed on the melt, the chill zone is extended, columnar crystals zone become narrow and dense and equiaxed crystal zone also is refined. Though ultrasonic attenuates very rapidly, the effect of refinement does not decrease markedly. Base on the experimental and theoretical deduction, it is confirmed that ultrasonic energy make the crystal accreting on the wall of mould desquamated, and the acoustic streaming make the desquamated crystal flowed into the liquid zone of cast. Desquamation of nucleus and acoustic streaming play an important role in metal structure refinement.

General Abstracts: Structural Materials Division: Mechanical Behavior of Metals and Alloys

Sponsored by: The Minerals, Metals and Materials Society, TMS Structural Materials Division, TMS: Advanced Characterization, Testing, and Simulation Committee, TMS: Alloy Phases Committee, TMS: Biomaterials Committee, TMS: Chemistry and Physics of Materials Committee, TMS/ASM: Composite Materials Committee, TMS/ASM: Corrosion and Environmental Effects Committee, TMS: High Temperature Alloys Committee, TMS/ASM: Mechanical Behavior of Materials Committee, TMS/ASM: Nuclear Materials Committee, TMS: Product Metallurgy and Applications Committee, TMS: Refractory Metals Committee, TMS: Superconducting and Magnetic Materials Committee, TMS: Titanium Committee

Program Organizer: Ellen Cerreta, Los Alamos National Laboratory

Monday AM
March 10, 2008

Room: 387
Location: Ernest Morial Convention Center

Session Chairs: Fang Cao, Los Alamos National Laboratory; Marian Kennedy, Clemson University

8:30 AM

A Comparative Study of the Tensile Response of Pure Mo and a Mo-Si-B Solid Solution Alloy: Padam Jain¹; S. Kumar¹; ¹Brown University

The Mo-Si-B solid solution matrix in multiphase Mo-Si-B alloys is thought to dominate low-temperature toughness and high-temperature creep resistance. Thus, it is important to understand the mechanical behavior of the solid solution phase in isolation. Uniaxial tension tests were performed on an extruded Mo-Si-B solid solution alloy between 400°C and 1200°C and nominal strain rates of 10⁻⁴ s⁻¹ and 10⁻⁶ s⁻¹. Dynamic Strain Aging (DSA) was observed in two different temperature and strain rate regimes. Tests were conducted on pure Mo in the recrystallized condition for comparison to isolate the possible role of B and Si on DSA in the solid solution alloy. In addition, constant load tensile creep tests were performed on the ternary solid solution alloy at 1000°C and 1200°C to evaluate the steady-state creep behavior. The deformed/fractured specimens were characterized to understand the underlying mechanisms. These observations will be presented and discussed.

8:50 AM

A Delta-Function Model for Three-Dimensional Axisymmetric Crystals: Ping Du¹; Harris Wong¹; ¹Louisiana State University

A surface energy polar plot contains two possible singularities: the cusps that give facets on an equilibrium crystal, and the circular arcs connecting the cusps that can lead to missing orientations. The common approach of specifying the surface energy usually cannot handle both singularities simultaneously. We

model the surface stiffness to avoid missing orientations. Furthermore, a facet is represented by the Dirac delta function with the weight of the delta function equal to the width of the facet. Thus, both singularities are treated precisely. This approach has been shown to work for two-dimensional symmetric¹ and axially symmetric² crystals. Here, we extend the delta-function model to three dimensions by modeling three-dimensional axisymmetric crystals. ¹Xin, T. and H. Wong "A δ -function model of facets," Surface Science 487, L529-L533 (2001). ²Du, P. and H. Wong "A delta-function model for axially symmetric crystals," Scripta Materialia 55, 1171-1174 (2006).

9:10 AM

Anisotropic Elastic/Plastic Model for Description of High Purity Alpha Titanium: M.E. Nixon¹; Oana Cazacu²; R.A. Lebensohn³; ¹Air Force Research Laboratory and University of Florida; ²University of Florida/REEF; ³Los Alamos National Laboratory

Accurate modeling of anisotropic hexagonal closed packed (hcp) polycrystals such alpha-titanium requires the description of the interplay between slip and twinning and its effects on texture evolution and hardening response. In this paper, an anisotropic model that captures the influence of evolving texture on the plastic response of hcp metals is proposed. Yielding is described using a new criterion which captures simultaneously anisotropy and compression-tension asymmetry associated with deformation twinning. The anisotropy coefficients as well as the size of the elastic domain are evolving with the plastic strain. Application of the model to the simulation of the three-dimensional deformation of high-purity alpha-titanium beams subjected to four-point bend tests along different directions is presented. Comparison between predicted and measured macroscopic strain fields and beam sections shows that the proposed model describes very well twinning and its role on evolving the material anisotropy.

9:30 AM

Blocking and Self-Locking of Superdislocations in Intermetallics: Bella Greenberg¹; M. Ivanov¹; ¹Russian Academy of Sciences

Superdislocations are carriers of plastic deformation in intermetallics. A large translation vector, different types of stacking faults and antiphase boundaries determine the diversity of dislocation configurations, both glissile and blocked ones. A significant point is that blocked superdislocations, which are formed due to re-splitting of glissile superdislocations or rearrangement of the superpartial dislocation core, have the lowest energy. A new concept about the possibility of thermally activated blocking of superdislocations in the absence of external stresses (self-locking) was proposed. A sufficiently general thermally activated process, which causes the extension of a dislocation in a preferred direction and constitutes a necessary step in dislocation transformations leading to blocking, was revealed. By its nature, this process represents the flip of a dislocation from a shallow valley to a deep valley of the potential relief. Reasons for the multivalley relief and the presence of preferred directions vary for dislocations of different types in different materials. Consecutive stages of this rearrangement of an initial dislocation with the direction approaching a preferred one: the formation of a double kink and its subsequent reorientation in a preferred direction. The driving force of the process was calculated and conditions for its realization in the cases of perfect, superpartial and partial dislocations were formulated. An experimental proof of the proposed concept was obtained: self-locking of dislocations, which were induced by preliminary deformation, was detected in Ni3(Al, Nb) and TiAl during no-load heating.

9:50 AM

Crack Growth across Grain Boundaries in Zinc Bicrystals: Experiments and Modeling: Dhiraj Catoor¹; Sharvan Kumar¹; ¹Brown University

Crack growth in polycrystalline materials prone to crystallographic cleavage is examined by studying fracture of bicrystals of zinc. Here, we will discuss the interaction of a crack with a grain boundary and its transmission across the boundary. In-situ fracture experiments were conducted using bicrystals, with the first grain oriented for mode I basal cleavage; the basal plane in the second grain is "twist-misoriented" w.r.t to the first. Three-dimensional finite element analysis incorporating crystal plasticity to account for anisotropy and cohesive zones to provide for crack growth is used to complement the experimental observations. Crack arrest, nucleation of secondary cracks, and extensive twinning and slip are observed in the vicinity of the grain boundary for misorientations of 10°

and 20°; for larger misorientations, the crack could not be transmitted across the boundary.

10:10 AM

Crack Growth on the Basal Planes in Zinc Single Crystals: Experiments and Modeling: *Dhiraj Catoor*¹; Sharvan Kumar¹; ¹Brown University

Although basal cleavage in zinc single crystals has been extensively studied, less is known on controlled crack growth, the nature of crack tip plasticity and its effects on crack propagation. To this end we have conducted in situ fracture tests on single crystal zinc specimens oriented for mode I fracture along the (0001) plane and along the <11-20> and <1-100> directions. Microstructural events such as twinning and slip that mediate crack propagation were recorded in real time along with the load-displacement curves. Basal slip, though unfavorable, was found to dominate crack tip plasticity; {10-12} <10-11> twinning was additionally noted. A 3-D finite element model incorporating crystal plasticity and a cohesive zone formulation to account for fracture has been developed to describe the crack growth process and assess stresses and strains in the vicinity of the crack tip; the results are in good agreement with experimental observations.

10:30 AM Break

10:50 AM

Deformation Behavior of Mg Single- and Bi-Crystals: *Badirujjaman Syed*¹; Sharvan Kumar¹; ¹Brown University

Single and bicrystals of pure Mg have been grown using the vertical Bridgman technique. Room-temperature compression and tension tests were conducted by loading chemically polished single crystal specimens along the [0001] and [10-11] directions in-situ under the optical microscope. Surface deformation markings were continuously recorded and observed slip and twinning systems were identified and were correlated with the resulting stress-strain curves. Higher temperature ex-situ tests were performed by loading along these orientations at multiple strain rates, and the deformation behavior was catalogued in tension and in compression to determine the effect of temperature and strain rate on the flow curves as well as operating deformation mechanisms. Isothermal constant load tests are being conducted on bicrystals of Mg in the temperature range 300C-450C to obtain an appreciation for the grain boundary sliding characteristics. These results will be presented and their implication for polycrystalline deformation at high temperatures will be discussed.

11:10 AM

Modeling of Grain Size Distribution Effect on Mechanical Properties of Ti Alloys: *Qizhen Li*¹; ¹University of Nevada, Reno

Due to their outstanding properties including high specific strength and light weight, Ti alloys are broadly used in aerospace industry. Since materials failures will cause the huge disasters environmentally and financially to the human world, a clear understanding of the relation between microstructure and mechanical properties is needed in materials selection and structural design. Extensive research was done to understand how the average grain size affects the mechanical behaviors of materials. This work will focus on studying the effect of grain size distributions with a fixed average grain size, since grain size fluctuation is a common phenomenon in the crystalline materials. Finite element modeling is applied to investigate the grain size distribution effect, and the results can guide the microstructure design to realize certain required property.

11:30 AM

Grain Size and Strain Rate Dependency of Flow Stress in FCC Metals: *Khaled Al-Fadhalah*¹; ¹Kuwait University

The effects of grain size and boundary structure on the flow stress of FCC metals were examined as a function of strain rate (less than 10⁻¹). Annealed samples of pure copper and aluminum were tested in tension at room temperature for grain size ranging from 5 µm to 50 µm. The resultant microstructure consists of grains with large population of annealing twin boundaries. By varying the strain rate, the dependency of flow stress on grain size and twin boundaries are modeled using polycrystal plasticity. Microstructure development during plastic deformation such as dislocation accumulation, and dislocation interaction at twin boundaries was accounted for in the model using the density of mobile and immobile dislocations. Computing both dislocation densities allows better simulation of the flow stress, showing good agreement with the experimental results.

11:50 AM

Effect of the γ/γ' Lattice Mismatch on the Creep Behaviour at 760°C of New Generation Single Crystal Superalloys: *Pierre Caron*¹; Frédéric Diologent²; ¹ONERA; ²Ecole Polytechnique Federale de Lausanne

We have analysed the creep behaviour at 760°C and 840 MPa of two new generation single crystal nickel-based superalloys. Both alloys exhibit similar amounts and sizes of γ' precipitates, but different values of γ/γ' lattice mismatch. The high lattice mismatch alloy exhibits a small primary creep strain and a long creep life, while a large extent of primary creep and a reduced creep life are obtained for the low lattice mismatch alloy. Transmission electron microscopy on the creep strained materials revealed different dislocation microstructures. Elevated coherency stresses due to the high lattice mismatch promote spreading of the matrix dislocations between the precipitates, resulting in homogeneous deformation and strong strain hardening. Moreover, decorrelation of matrix dislocations in two well-separated Shockley partials signs their low mobility. Shearing of the γ/γ' microstructure by heterogeneous <112>{111} slip in the alloy with a moderate lattice mismatch explains the high primary creep strain.

12:10 PM

High Temperature Oxidation of Alloy 617 in He-CO-CO₂ and He-H₂-H₂O Environments: *Deepak Kumar*¹; Gary Was¹; ¹University of Michigan

The helium coolant in the very high temperature gas cooled reactor (VHTR) contains CO, CO₂, H₂, H₂O and CH₄ as reactive impurities. Based on the oxidation and carburization potentials of the impurities, binary gas mixtures in helium have been selected to investigate the corrosion behavior of alloy 617; CO-CO₂, H₂-H₂O. Exposure experiments up to 750 hours were conducted in He-CO-CO₂ and He-H₂-H₂O environments at 900°C at similar oxidation potentials given by the CO/CO₂ and H₂/H₂O ratios. The nature and rate of gas/metal interactions occurring at the surface were determined by analyzing the gas mixtures at both the inlet and outlet of the reaction zone using a gas chromatograph and moisture analyzer. The microstructure stability and the surface scale on the exposed samples were analyzed using SEM. The oxidation behavior in the two different environments will be compared based on the TEM, XRD and EDX results.

Hael Mughrabi Honorary Symposium: Plasticity, Failure and Fatigue in Structural Materials - from Macro to Nano: Dislocations: Work Hardening, Patterning, Size Effects I

Sponsored by: The Minerals, Metals and Materials Society, TMS Structural Materials Division, TMS Materials Processing and Manufacturing Division, TMS: High Temperature Alloys Committee, TMS/ASM: Mechanical Behavior of Materials Committee, TMS: Nanomechanical Materials Behavior Committee
Program Organizers: K. Jimmy Hsia, University of Illinois, Urbana-Champaign; Mathias Göken, Universität Erlangen-Nürnberg; Tresa Pollock, University of Michigan - Ann Arbor; Pedro Dolabella Portella, Federal Institute for Materials Research and Testing; Neville Moody, Sandia National Laboratories

Monday AM

March 10, 2008

Room: 386

Location: Ernest Morial Convention Center

Session Chairs: K. Jimmy Hsia, University of Illinois, Urbana-Champaign; Mathias Göken, University Erlangen-Nürnberg

8:30 AM Introductory Comments

8:40 AM Keynote

Fatigue of Nanostructured Metals and Alloys: *Subra Suresh*¹; Ming Dao¹; ¹Massachusetts Institute of Technology

Nanoscale grain refinement is known to have a profound effect on the strength, hardening, rate sensitivity, ductility, toughness and tribological response. However, the resistance of fully nanocrystalline metals and alloys to cyclic deformation and fatigue crack initiation and growth is relatively poorly understood because of the paucity of experimental information. In this presentation, available experimental results, mechanistic models as well as information on the effects of structure and composition on cyclic strain hardening characteristics, stress-controlled fatigue, strain-controlled fatigue and fatigue

crack growth are examined for nanocrystalline and ultra-fine-grained metals and alloys. Effects of grain refinement on the resistance to contact fatigue are also discussed on the basis of experimental results available for nanocrystalline materials subjected to repeated indentation and frictional sliding contact fatigue. The results reveal competing effects of grain refinement on flaw nucleation and growth, and offer useful structural design guidelines for the surface and interior of fatigue-critical components.

9:10 AM Keynote

The Modeling of Plasticity: How Can Dislocation Dynamics Simulations Help?: *Ladislav Kubin¹; Benoit Devincere¹; Thierry Hoc²; ¹Centre National de la Recherche Scientifique-ONERA; ²Ecole Centrale Paris*

A major weakness of dislocation-based plasticity models resides in their inability to integrate the full complexity of the microscopic behavior at the scale of a single crystal or of the grain of a polycrystal. A few examples illustrate how dislocation dynamics simulations can help in establishing predictive models at the scale of a representative volume element, which can further serve as constitutive formulations in crystal plasticity codes. The first topic deals with the Hall-Petch relation in ultra-fine grained polycrystals and a critical comparison between simulated behavior and existing models. The second topic discusses experimentally known aspects of deformation stages in face-centered cubic crystals that have never been modeled like stage I mechanisms, the transition between stage I and stage II, the orientation dependence of stage II, multislip deformation and the orientation dependence of dynamic recovery. Current limitations of these approaches are discussed.

9:40 AM Invited

Dislocation Microstructure, Strain Localisation and Crack Initiation in Fatigue Studied by 3D Discrete Dislocation Simulations: *Marc Fivel¹; Christian Robertson²; Christophe Depres³; Chan Sun Shin⁴; ¹SIMaP-GPM2; ²Commissariat à l'Énergie Atomique/SRMA; ³Laboratoire Systèmes et Matériaux pour la Mecatronique; ⁴Korea Atomic Energy Research Institute*

First, 3D discrete dislocation simulations are performed in order to analyse the cyclic plasticity that occurs in surface grains of AISI 316L stainless steel. Simulations performed under various loading and boundary conditions show the crucial role played by cross-slip in the formation of the dislocation microstructure. As the cycling proceeds, slip bands exhibiting well organised dislocation arrangements progressively substitute to dislocation tangles. Calculations of the plastic steps printed on the free surface during the cycling give access to the surface relief which is found to be made of extrusion and intrusion profiles. Analyses of stress and distortion energy concentrations inside the slip bands reveals that a crack would most probably initiate at the surface when multipoles, driven by interfacial dislocations, will reach the surface. Finally, the fatigue behaviour of precipitate hardened materials is investigated and compared to the case of AISI 316L.

10:00 AM Invited

How Large are the Strains at Intersections of Slip Bands and What is Their Geometry?: *Peter Neumann¹; ¹Max-Planck Institute for Iron Research*

In slip bands, shear strains beyond 100% are quite common. The superposition of such large strains cannot be carried out linearly. In order to obtain correct results, either the displacement vectors have to be added or the non-linear terms in the strain tensors have to be taken into account exactly. The former leads to a differential equation, which can be solved easily, the latter leads to a non-linear matrix formula. The results are identical for both methods and show that extremely large strains can occur. It is shown in computer animations that drastic rearrangements of material or material separation can occur.

10:20 AM Break

10:30 AM Invited

Characterization of Lattice Defects by X-Ray Diffraction: *Tamas Ungar¹; ¹Eotvos University*

Plasticity, failure and fatigue in structural materials is in closest correlation with lattice defects, especially long-range internal stresses, dislocations, subgrain size and planar defects. X-ray line broadening is an alternative method to electron microscopy for characterizing the density and character of lattice defects. (i) Long-range internal stresses are revealed by characteristically asymmetric line broadening. (ii) Dislocation densities and Burgers vector analysis are provided

by the dislocation model of strain anisotropy. (iii) Subgrain size and size-distribution are given by the order independent part of line profiles. (iv) The frequency of stacking faults and twin boundaries is determined by specific line shifts and broadening. The four listed defect types can be separated since they follow different hkl dependences with limited correlations.

10:50 AM Invited

Professor Mughrabi's Strain Hardening Models as Applied to Transition Metals and Alloys: *David Davidson¹; ¹Southwest Research Institute*

Models based on dislocation interactions during tensile straining of fcc metals developed by Prof. Mughrabi in the 1980's have been found to be useful in describing the strain hardening behavior of straining single crystals in the series Nb-Mo-Re, which are bcc. Parameters used in these models must, therefore, be interpreted somewhat differently between the two systems, which will be the subject of this presentation.

11:10 AM Invited

Bulk Dislocation Microstructures Probed with Sub-Micrometer Spatial Resolution Using Synchrotron X-Rays: *Lyle Levine¹; Bennett Larson²; Jonathan Tischler²; Michael Kassner³; Peter Geantil³; Wenjun Liu⁴; ¹National Institute of Standards and Technology; ²Oak Ridge National Laboratory; ³University of Southern California; ⁴Argonne National Laboratory*

The existence and magnitude of long range elastic strains (and thus stresses) in dislocation cell interiors and walls in deformed metals have been the subject of extensive investigation for more than 20 years. Although numerous volume-averaged measurements have been used to infer their existence, direct measurements were not possible before the recent development of intense submicron X-ray beams. We have used submicron X-ray beams to directly measure the axial elastic strains within individual dislocation cells in copper single crystals deformed in both tension and compression. These spatially resolved measurements found large elastic strains that are consistent with Mughrabi's composite model. Moreover, the strains were found to exhibit large cell-to-cell variations. More recent experiments have studied the distributions of elastic strains within individual dislocation cell walls and looked at elastic strains within extended contiguous sample volumes containing numerous dislocation cells.

11:30 AM

Atomistic Simulations of Grain Boundary Dislocation Nucleation: *Mark Tschoopp¹; David McDowell²; ¹Air Force Research Laboratories/Universal Technology Corporation; ²Georgia Institute of Technology*

The objective of this research is to use atomistic simulations to investigate dislocation nucleation from asymmetric tilt grain boundaries in FCC copper and aluminum. The use of a 3D periodic bicrystal configuration enables the investigation of how the boundary degrees of freedom impact both boundary structure and dislocation nucleation from these boundaries. Simulation results show that dislocation nucleation from asymmetric tilt grain boundaries requires understanding of the structure and faceting of these boundaries. Deformation simulations under uniaxial tension and compression show entirely different nucleation mechanisms, i.e., nucleation of full dislocations in copper from the grain boundary under compression. The role of the grain boundary as a dislocation source is discussed in terms of a perfect source/sink model. Last, the resolved stress normal to the slip plane on which the dislocation nucleates plays an integral role in dislocation nucleation for single crystals and interfaces.

11:45 AM

Statistical Refinement of Mughrabi's Composite Model: *Wolfgang Pantleon¹; Tamas Ungár²; ¹Technical University of Denmark, Risø National Laboratory; ²Eötvös University Budapest*

For explaining yielding under stress reversal, the composite model was introduced by Hael Mughrabi distinguishing two phases of different strength: dislocation-rich walls and dislocation-depleted cell interiors. The asymmetry of radial x-ray diffraction profiles has been rationalized successfully by the composite model as superposition of two sub-profiles mutually shifted by internal stresses and broadened by the local dislocation content. The later has prompted criticism as the local dislocation density between the walls observed by transmission electron microscopy is much less than expected from profile analysis. Recent investigations by high angular resolution three-dimensional x-ray diffraction revealed nearly dislocation-free regions in deformed metals.

These dislocation-free regions experience quite different backward elastic strains and cause distinct sharp profiles at different radial positions. Consequently, the sub-profile associated with cell interiors is not broadened by the local dislocation content, but by shifts of several individual sharp profiles. A statistical refinement of the composite model is presented.

12:00 PM

On the Relevance of the Schmid's Factor to Analyse Cyclic Slip Activity and Crack Initiation in Polycrystals: *Patrick Villechaise*¹; José Mendez²; ¹Ecole Nationale Supérieure De Mécanique Et D'Aérotechnique/Centre National de la Recherche Scientifique

In metallic polycrystalline materials one of the most common fatigue crack initiation process involves localization of cyclic plasticity in slip bands. In this field, crystallographic orientation constitutes one of the main local characteristics to be considered. It determines some essential parameters in a mechanical point of view like the Schmid's factor and geometrical configuration of slip bands emergence at the free surface. The progress of electron back scattering diffraction technique permits now to investigate the influence of the crystallographic orientation taking into account a great number of grains. A quasi statistical approach of texture configuration that favour fatigue damage can be then developed. We propose to come back on the relevance or non relevance of the Schmid's factor to describe the local microstructure that favour slip activity and crack initiation. This will be illustrated from results obtained on a 316L stainless steel and on a Ti64 titanium alloy.

12:15 PM

Detection of Incipient Fatigue Damage with Scanning SQUID Microscopy: *John Morris*¹; Tae-Kyu Lee²; John Clarke¹; ¹University of California, Berkeley; ²Cisco Systems

The fatigue process can be detected and monitored in the earliest stages of high-cycle fatigue, by the increase in dislocation density and hardness, and in the final stages, through the direct observation of initiated cracks. But there are no probative, non-destructive techniques to follow incipient fatigue through the critical intermediate stage between dislocation saturation and prior to crack nucleation. In this study, we report initial success using SQUID microscopy for this purpose. The remanence fields of fatigued ferritic steel specimens were mapped using a high-resolution scanning magnetic microscope based on a high transition temperature Superconducting Quantum Interference Device (SQUID). The results of scans of fatigued specimens of ferritic steel show the development of local peaks in remanent magnetization prior to the development of visible fatigue cracking. Their spatial localization not only identifies incipient fatigue failure, but also identifies the specific locations where cracks will appear.

12:30 PM

Orientation Distributions in Plastically Deformed Copper Single Crystals: *Andras Borbely*¹; Claire Maurice²; René Fillard²; Julian H. Driver²; ¹Max-Planck Institut für Eisenforschung; ²Ecole des Mines de Saint Etienne

Local misorientation distributions developed in copper single-crystals deformed in tension and plane strain-compression were investigated experimentally by X-ray rocking curve (RC) analysis and by backscattered electron diffraction (EBSD). Based on the results obtained on the same samples with the two techniques, the applicability limit of the EBSD method for a statistical interpretation of orientation data was explored. It is shown that in spite of the very small penetration depth of the electrons into copper (of about 10-15 nm), large EBSD scans can provide a statistically-satisfactory characterization of deformation induced dislocation structures. Consequences of the limitations in angular resolution of the EBSD, but also the advantages of EBSD over the X-ray RC analysis are presented. A newly developed imaging method is made known, together with its successful application to the analysis of "geometrically necessary" and "incidental" dislocation boundaries developed during deformation of the investigated copper single crystals.

Hume-Rothery Symposium - Nanoscale Phases: Session I

Sponsored by: The Minerals, Metals and Materials Society, TMS Electronic, Magnetic, and Photonic Materials Division, TMS: Alloy Phases Committee
Program Organizers: Sinn-wen Chen, National Tsing Hua University; David Cockayne, University of Oxford; Seiji Isoda, Kyoto University; Robert Nemanich, Arizona State University; K.-N. Tu, University of California, Los Angeles

Monday AM

March 10, 2008

Room: 276

Location: Ernest Morial Convention Center

Session Chairs: King-Ning Tu, University of California, Los Angeles; Robert Nemanich, Arizona State University

8:30 AM Introductory Comments

8:35 AM Keynote

Nanoscale Metal Silicides: *L. J. Chen*¹; ¹National Tsing Hua University

Metal silicides have been introduced into microelectronics devices in late 1970s as gates, contacts and interconnects. In the 1980s, almost all transition metal silicides were found to grow epitaxially on silicon to some extent. In the 1990s, amorphous interlayers of a few nm in thickness were observed to occur in all refractory metal/Si and a number of rare-earth metal and platinum group metal and crystalline silicon systems. As the integrated circuits (IC) industry moves into the nano era, scaling down the metal silicide contacts and gates have become an important issue. A large number of epitaxial and free-standing silicide nanowires were grown. In this talk, a historical account of evolving roles of metal silicides will be presented. Epitaxial growth of silicides on silicon and formation of amorphous interlayers in the metal/Si systems will be reviewed. Synthesis and applications of silicide nanowires will be described. Future outlook will be addressed.

9:25 AM Invited

In Situ Studies of Reactions in Metal Silicides and Metal Oxides: *Robert Sinclair*¹; ¹Stanford University

In future integrated circuit devices, metal silicides and oxides are becoming increasingly important. However any reactions which occur during processing can adversely influence the designed properties. This article reviews the study of this behavior for some metal-silicon systems (e.g. Ni-Si, Ti-Si) and some metal oxides (e.g. Ta oxide, Hf-Si-O). The processes range from silicidation and metal mediated crystallization in the former, to crystallization and spinodal decomposition in the latter. In situ TEM has proved to be very profitable for such investigations.

9:50 AM Invited

Nucleation and Growth Kinetics of Semiconductor Nanowires: *Frances Ross*¹; ¹IBM Research

The exciting applications of semiconductor nanowires are best realised through a detailed understanding of the crystal growth processes that take place during wire formation. For this it is important to quantify both the nucleation of wires from their catalyst particles and their subsequent steady-state growth. We have therefore examined both processes using time-resolved environmental microscopy, growing Si and Ge wires from Au catalysts in situ in a TEM. We firstly discuss a simple model for nucleation which explains the time at which nuclei appear and their immediate growth rate. For nanowire heterostructures, we show how nucleation determines the morphology at the heterojunction. Subsequently, the dependence of growth rate on conditions allows us to determine the rate limiting step, while direct observations of the catalyst structure show unexpected features of growth, such as the existence of a liquid phase far below the eutectic temperature that is stabilised by growth-driven supersaturation.

10:15 AM Break

10:30 AM Invited

Silicide Formation: Bulk vs. Thin Films vs. Nanowires: *King-Ning Tu¹; Kuo-Chang Lu¹; Yi-Chia Chou¹; ¹University of California, Los Angeles*

Owing to the applications of thin film silicide as contacts and gates in microelectronic Si devices, the interfacial reaction between metal film and silicon have been studied systematically. Single silicide phase formation in the thin film reactions has been found and has been explained by a competing growth model combining diffusion-controlled and interfacial-reaction-controlled processes. In comparison, a diffusion-controlled growth of multiple silicide phases is obeyed in bulk diffusion couples of metal and Si. Recently, in the point contact reaction between a nano metal wire and a nano Si wire, a supply-controlled growth of nano silicide is found. In this talk, a comparison among the three kinds of reactions; diffusion-controlled, interfacial-reaction-controlled, and supply-controlled growth will be given.

10:55 AM Invited

Transition Metal Silicide Nanowires: *Song Jin¹; ¹University of Wisconsin-Madison*

We report general synthetic approaches to transition silicide nanowires (NWs), their properties and applications in nanoelectronics, nanophotonics, spintronics, and thermoelectric energy conversion. We utilize chemical vapor deposition (CVD) of metal carbonyl-silyl single source organometallic precursors without any catalyst seeds on silicon substrates covered with a thin (1-2 nm) layer of silicon oxide to produce FeSi and CoSi NWs. We have also developed a complementary method of chemical vapor transport (CVT) to prepare NWs of silicides for which analogous precursors can not be readily made, such as CrSi₂, Ni₂Si and Ni₃Si. We discovered a new and general nanowire growth mechanism that is different from the typical vapor-liquid-solid NW growth and critically depends on the oxide thickness. The nanophase formation rules and nanophases of some Nowotny Chimney Ladder phases will be discussed. The physical properties of these silicide NWs were investigated using electrical transport, thermal transport, X-ray spectroscopy, and magnetometry.

11:20 AM Invited

A Global Perspective of New Paradigm and Challenges of Semiconductor Industry in the Nano/Tera Scale Integration Era: *Chih-Yuan Lu¹; ¹Macronix International Company, Ltd.*

After more than fifty years rapid evolution of semiconductor devices from ZSI to GSI, the linewidth scaled down to nanometer and thus the transistor integration up to multi-giga bit scale, this scaling power totally changed the human daily life in the world. First we will review the roadmap and discuss the possibility of continuous scaling from technological point of view, and how could keep its pace by close cooperation among academia, consortium, and industrial labs. In addition to technology evolution, the investment scale and economics of semiconductor industry has dramatically changed due to its minimum barrier for the R&D resources threshold level and manufacturing critical mass. We will illustrate these facts by reviewing historical data and possible future roadmap, and some visionary scenarios will be suggested.

Magnesium Technology 2008: Magnesium Plenary Session

Sponsored by: The Minerals, Metals and Materials Society, TMS Light Metals Division, TMS: Magnesium Committee

Program Organizers: Mihriban Pekguleryuz, McGill University; Neale Neelameggham, US Magnesium LLC; Randy Beals, Chrysler LLC; Eric Nyberg, Pacific Northwest National Laboratory

Monday AM
March 10, 2008

Room: 291/292
Location: Ernest Morial Convention Center

Session Chair: Mark Verbrugge, General Motors Research and Development

8:30 AM Introductory Comments

Automotive Programs in Materials Engineering: *Mihriban Pekguleryuz¹; ¹McGill University*

8:45 AM

Integrated Computational Materials Engineering (ICME) for Magnesium: An International Pilot Project: *John Allison¹; Baicheng Liu²; Kevin Boyle³; Randy Beals⁴; Louis Hector, Jr.⁵; ¹Ford Motor Company; ²Tsinghua University; ³CANMET Materials Technology Laboratory; ⁴Chrysler Corporation; ⁵General Motor Corporation*

Integrated Computational Materials Engineering (ICME), a new paradigm within the materials profession, offers a means to unify analysis of manufacturing, design and materials into a holistic system. A central component of ICME is the development and utilization of advanced material models which capture our quantitative knowledge of processing-structure-property relationships in a form which can be used by the broader engineering community. This talk will provide an overview of a recently initiated international collaborative project to develop an ICME infrastructure for magnesium for use in automotive body applications. The work will be conducted at leading universities, national labs and industrial research facilities in the US, China and Canada. This project is sponsored by the U.S. Department of Energy, the U.S. Automotive Materials Partnership (USAMP), Chinese Ministry of Science and Technology (China) and Natural Resources Canada (Canada).

9:15 AM

Magnesium Front End Research and Development: A Canada-China-USA Collaborative Program: *Alan Luo¹; Eric Nyberg²; Kumar Sadayappan³; Wenfang Shi⁴; ¹General Motors Corporation; ²Pacific Northwest National Laboratory; ³Canmet Materials Technology Laboratory; ⁴China Magnesium Center*

The Magnesium Front End Research & Development (MFERD) Program is a jointly sponsored effort by the United States Department of Energy, the United States Automotive Materials Partnership (USAMP), the Chinese Ministry of Science and Technology and the Natural Resources Canada to demonstrate the technical and economic feasibility of a magnesium intensive automotive body structure. The MFERD program started in early 2007 by initiating R&D in the following areas: crashworthiness, NVH, fatigue and durability, corrosion and surface finishing, extrusion and forming, sheet and forming, high-integrity body casting, as well as joining and assembly. In addition, the MFERD program is also connected to the Integrated Computational Materials Engineering (ICME) program that will investigate the processing/structure/properties relations for various magnesium alloys and manufacturing processes.

9:45 AM

The Chrysler Magnesium Alloy Development Program: *Randy Beals¹; ¹Chrysler LLC*

The Chrysler Magnesium Alloy Development (CMAD) program used a Design of Experiments (DOE) approach to create several new high pressure die cast creep resistant magnesium alloys. The goal of this approach was to find the optimum combination of the following alloy characteristics; good corrosion resistance, good castability, creep resistance, high strength and elongation that can be produced at a reasonable cost. A dynamic computer program was developed in order to control the DOE of various chemical compositions (ratio

of elements, etc.) during the high pressure die casting of the specimens. A total of seven alloy groups were produced and investigated (series 0 to 6) that had differing amounts of following alloying elements; Al, Zn, RE, Sr, Ca and Sn. Data will be presented comparing the cost effective performance of these materials to other commercially available magnesium and aluminum alloys.

10:15 AM

Performance of Creep-Resistant Magnesium Alloys in Dynamometer and Component Testing of the USAMP Magnesium-Intensive V6 Engine: *Bob Powell*¹; William Miller¹; Larry Ouimet¹; Joy Hines²; John Allison²; Randy Beals³; Robert McCune⁴; Lawrence Kopka³; Peter Ried⁵; ¹General Motors Corporation; ²Ford Motor Company; ³DaimlerChrysler; ⁴Robert C. McCune and Associates LLC; ⁵Ried and Associates LLC

In 2007 the US Automotive Materials Partnership- and US Department of Energy-supported Magnesium Powertrain Cast Components project team completed all support aspects of this six year project and began engine dynamometer and component testing the V6 engine with its four Mg components (cylinder block, oil pan, front engine cover, and rear seal carrier). A full array of dynamometer testing was conducted, including hot scuff, cold scuff, global durability, high speed durability, thermal cycle and deep thermal shock. The purpose of these tests was to validate the predictions of the engine design and to identify any critical areas for further work in bringing the mass reduction potential of Mg into major powertrain applications. Engine test results to date, lessons learned, and other project accomplishments will be presented.

10:35 AM Panel Discussion

Materials in Clean Power Systems III: Fuel Cells, Hydrogen-, and Clean Coal-Based Technologies: Plenary Session

Sponsored by: The Minerals, Metals and Materials Society, TMS Structural Materials Division, TMS/ASM: Corrosion and Environmental Effects Committee
Program Organizers: Zhenguo "Gary" Yang, Pacific Northwest National Laboratory; Michael Brady, Oak Ridge National Laboratory; K. Scott Weil, Pacific Northwest National Laboratory; Xingbo Liu, West Virginia University; Ayyakkannu Manivannan, National Energy Technology Laboratory

Monday AM
March 10, 2008

Room: 392
Location: Ernest Morial Convention Center

Session Chair: Ayyakkannu Manivannan, National Energy Technology Laboratory

8:30 AM Introductory Comments

8:40 AM Keynote

DOE Perspectives of Materials for Advanced Power Systems: *Robert Romanosky*¹; ¹National Energy Technology Laboratory
Abstract not available.

9:25 AM Keynote

"Near Zero" Emissions Solid Oxide Fuel Cell (SOFC) Power Generation Systems for Operation on Hydrocarbon and Coal Derived Fuels: Technology Review: *Prabhakar Singh*¹; Nguyen Minh¹; ¹Pacific Northwest National Laboratory

Intermediate to high temperature (600-1000°C) operation and novel electrode processes in solid oxide fuel cells (SOFC) enable efficient utilization of hydrocarbons and coal derived fuels. SOFC's also show tolerance to higher levels of fuel impurities (compared to low temperature fuel cells), utilizes a much simpler balance of plant and offer the potential to develop "near zero emissions" power systems architecture. This presentation will review recent advances in SOFC technology including materials of construction, electrode processes, and long term degradation. Cell and stack designs will be reviewed with emphasis on structural analysis and thermal management. Systems requirements for stationary, mobile and portable applications will be presented. Key challenges will be examined and discussed and current research trends will be presented.

10:10 AM Invited

CO₂-Selective Membranes for Hydrogen Purification and CO₂ Capture: He Bai¹; W.S. Winston Ho¹; ¹Ohio State University

This talk covers carbon dioxide-selective membranes for applications in hydrogen purification for fuel cells and in carbon dioxide capture for the greenhouse gas sequestration. We have synthesized new membranes for the removal of carbon dioxide from hydrogen-containing synthesis gas by incorporating amino groups into polymer networks. The membranes are selective to carbon dioxide preferentially versus hydrogen since the acid gas permeates through the amine-containing membranes via the facilitated transport mechanism due to its reversible reaction with the amine. The membranes synthesized have shown high carbon dioxide permeability and selectivity vs. hydrogen or carbon monoxide. This type of membranes has the potential for hydrogen purification for environmentally friendly fuel cells, including the use of the membrane in the membrane reactor configuration to enhance water gas shift (WGS) reaction. Results from WGS membrane reactor experiments have shown carbon monoxide conversion/reduction to 10 ppm as well as significant hydrogen enhancement via carbon dioxide removal. The data have been in good agreement with modeling prediction. The carbon dioxide captured on the permeate side had a dry concentration of greater than 98% by using steam as the sweep gas. Hydrogen sulfide has much higher reaction rate with the amine than carbon dioxide as the former reacts with the amine via proton transfer and the latter reacts with the amine via carbamate formation primarily. Thus, hydrogen sulfide can permeate through the membrane much faster than carbon dioxide. Our initial membrane data have shown hydrogen sulfide with about 3 times permeability of carbon dioxide. In addition, our initial experiments with a limited membrane area have shown a nearly complete removal of hydrogen sulfide from 50 ppm in the synthesis gas feed to about 10 ppb in the hydrogen product, which is good for fuel cell applications.

Materials Processing Fundamentals: Solidification and Deformation

Sponsored by: The Minerals, Metals and Materials Society, TMS Extraction and Processing Division, TMS: Process Technology and Modeling Committee
Program Organizer: Prince Anyalebechi, Grand Valley State University

Monday AM
March 10, 2008

Room: 283
Location: Ernest Morial Convention Center

Session Chair: Prince Anyalebechi, Grand Valley State University

8:30 AM

Bicrystalline Silicon Growth in Si-Al: Principles of Morphological Selection: *Ralph Napolitano*¹; ¹Iowa State University

Low velocity gradient-zone growth from Si-Al melts gives rise to a primary structure consisting of very large bicrystalline domains, with each comprised of a 210/310 twin pair sharing a common <001> axis aligned in the growth direction. Strong morphological selection of this primary structure is investigated with respect to (i) mechanisms of lateral propagation for the array, (ii) high mobility coherent twin configurations within the primary cores, and (iii) diffusion-based selection principles. Based on detailed morphological and compositional measurements and high resolution TEM analysis, the observed morphology is attributed to a hybrid primary/coupled growth mode, where the persistent defect structure at the front is the critical feature, affording a substantial kinetic advantage for strong selection. The diffusional component of this mode selection is investigated using a phase field approach, accounting for high anisotropy. Scaling rules for selection are compared with the more common diffusion-based selection observed in nonfaceted dendritic growth.

8:50 AM

Rapid Freeze Prototyping of Investment Cast Thin-Wall Metal Matrix Composites I – Pattern Build and Molding Parameters: *Von Richards¹; Edward Druschitz¹; Sriram Isanaka¹; Ming Leu¹; Matt Cavins¹; Tim Hill¹*; ¹University of Missouri

Rapid Freeze Prototyping (RFP) is a novel solid freeform fabrication technology that creates parts by depositing water droplets and freezing them rapidly to form layers. An investigation into the smallest thickness that can be achieved by the RFP process was conducted. The factors that could significantly affect the thickness of the part built by this process including substrate temperature, volumetric feed rate, table velocity, nozzle frequency, nozzle standoff distance, and head pressure were considered. A shell building technique for use with the RFP system has been developed. Thin wall ice patterns have been invested using production shell building techniques and an alcohol-based slurry. The finished shells were quantitatively evaluated by inspecting their total shell thickness, mold cavity dimensional reproducibility and shell strength.

9:10 AM

Solidification Cracking of Allvac 718Plus: *Joel Andersson¹; Göran Sjöberg¹; Anssi Brederholm²; Hannu Hänninen²*; ¹Volvo Aero Corporation; ²Helsinki University of Technology

Weldability is a broad term used to explain how a material behaves when it is welded. There is an increasing demand for weldable superalloys since fabricated components or several castings are joined together to add up to the final component. Allvac 718Plus is a newly developed superalloy and has a high potential in terms of fabricated structures. Transvarestraint testing has been employed when testing the weldability or susceptibility to solidification cracking.

9:30 AM

Thermal Study and Metallographic Characterization of Zn-20%Al and Zn-20%Al-10%Si-3%Cu Alloys Directionally Solidified: *Alicia Ares¹; Sergio Gueijman¹; Carlos Schvezov¹*; ¹CONICET/University de Misiones

The present investigation was undertaken to investigate the directional solidification of Zn-20%Al and Zn-20%Al-10%Si-3%Cu alloys under different conditions of heat transfer at the metal/mould interface. The type of structure obtained in both cases is analyzed and related to the solidification thermal parameters such as cooling rate, growth rate, thermal gradient and recalescence which were determined from the temperature versus time curves. These parameters were correlated with the structure-like length of columnar grains and size of equiaxed grains. The metallographic analyses were done performing quantitative metallography and composition analysis of the different alloying elements along the cast samples were done by SEM (Scanning Electron Microscopy) and EDXA (Energy Dispersive X-Ray Analysis). Correlations between properties, structures and compositions were found.

9:50 AM

Effect of Cross-Hatched Mold Surface Topography on Shell Morphology in the Solidification of an Aluminum Alloy: *Prince Anyalebechi¹*; ¹Grand Valley State University

The effects of a mold surface topography consisting of cross-hatched grooves and casting speed on the morphology of solidifying shells of an aluminum alloy 3003 have been characterized by a series of immersion tests. The cross-hatched grooves were 0.232 mm deep with wavelength or spacing between 1 mm and 15 mm. The shells solidified at casting speed of less than 10 mm/s on a 1 mm spaced cross-hatched grooved mold surface were fairly uniform with little or no localized variations in thickness. However, the propensity for non-uniform shell growth morphology was exacerbated by increase in casting speed, melt superheat, and the wavelength of the cross-hatched grooves. This is provisionally attributed to the effects of the casting conditions and the cross-hatched grooves on interfacial heat transfer and wetting of the mold surface by the molten metal.

10:10 AM Break

10:20 AM

Effects of Silicon, Iron, and Chromium on the Response of Aluminum Alloy 3004 Ingots to Homogenization: *Prince Anyalebechi¹*; ¹Grand Valley State University

The effects of Si (0.19-0.52 wt.%), Fe (0.20 wt.%-0.44 wt.%), and Cr (0-0.10 wt.%) on the response of ingots of aluminum alloy 3004, solidified at different rates (0.10 K/s to 30 K/s), to homogenization heat treatment have been investigated. Response to homogenization was determined by quantifying the following microstructural parameters: (i) amount of Mn retained in solid solution; (ii) types, relative amounts, sizes, size distributions, shapes, and chemical compositions of second phases; (iii) extent of the alpha-transformation reaction; (iv) interparticle spacing; (v) dispersoid formation; and (vii) alleviation of dendritic microsegregation. Of the three alloying elements investigated, Si had the greatest effect on the response of aluminum alloy 3004 to the homogenization heat treatment. Increase in Si content, fineness of cast microstructure, and homogenization temperature facilitated alpha-transformation reaction, dissolution of Mg₂Si, loss of Mn supersaturation, and formation of Al₁₂(Fe,Mn)₃Si and Mg₂Si dispersoids.

10:40 AM

Effect of Interfaces on Melting and Solidification Behavior of Lead, Bismuth and Tin Embedded in Icosahedral Quasicrystalline Phase: *Alok Singh¹; AnPang Tsai²*; ¹National Institute for Materials Science; ²Tohoku University

Novel interfaces were created by embedding lead, bismuth or tin nanoparticles in an Al-Cu-Fe matrix. By heat treatment, three states of matrix phase were obtained, altering the nature of interfaces. Interface structures were studied by TEM and melting and solidification behavior was studied by differential scanning calorimetry (DSC). Each of the embedded elements showed a different melting and solidification behavior. Lead shows a lowering of melting temperature in quasicrystalline matrix and no clear solidification peak. Bismuth shows superheating in quasicrystalline matrix but a significant lowering of temperature in the microcrystalline matrix. Tin shows no change of melting temperature in either matrix, and clear solidification peaks in both. Through a crystallographic analysis and a study of the interfaces, it is shown that melting and solidification of heavily dependent of the crystallographic match between the two phases and consequently the interface structure.

11:00 AM

Effect of Oxygen Content on Type of Inclusion Precipitated during Unidirectional Solidification of Steel: *Huigai Li¹; Shaobo Zheng¹; Liwei Wang¹; Qijie Zhai¹*; ¹Shanghai University

The fine titanium oxide inclusions precipitated during solidification are favorable for intragranular ferrite nucleation. The oxygen content before solidification affects the type and size of inclusions. The type of the precipitated inclusions in Mn and Ti alloyed steel was studied by means of thermodynamic calculation and experiment in this paper. The micro-segregation of Mn, Ti and O during solidification was considered in the calculation. The unidirectional solidification apparatus was employed in the experiment to ensure that the alloy elements diffused along the solidification direction. The results showed that, the inclusions are mainly Ti₂O₃ when the oxygen content is in 10ppm; they are Ti₂O₃ and MnTiO₃ when it is in 20ppm and MnTiO₃ in 30ppm. With the increase of the oxygen content, the size of the inclusions increases.

11:20 AM

Influence of Chemical Composition on Bake Hardening Effect for Hot Rolled Multiphase Steels: *Heinz Palkowski¹; Mehdi Asadi¹; Goran Kugler¹*; ¹Technical University of Clausthal

Recent trends in the automotive industry lead to increasing interest in advanced high strength steels (AHSS). Beside good ductility and high strength, those steels have a high bake hardening effect (BH), giving additional contribution to the strength of structural parts, subjected to the paint baking process. For hot rolled AHSS, namely dual phase and martensitic steels, the effect of process conditions on mechanical properties had been investigated by the authors. However, the study of the influence of chemical composition on BH ability of the AHSS is not been investigated sufficiently and published in literature. In the current research, samples of different chemical compositions within the characteristic interval for industrial production had been studied under different pre-load conditions, simulating the thermo-mechanical production process. The samples were then

subjected to BH process. Tensile tests were performed to study the varying chemical composition on the BH effect.

11:40 AM

Microstructure and Texture Evolution of Pure Gold in Intense Torsion Straining: *Jong Soo Cho*¹; Jeong Tak Moon¹; Seok-Hoon Gang²; Kyu-Hwan Oh²; ¹MKE; ²Seoul National University

The microstructure development of pure gold wire (99.99 wt.%) deformed at low temperature (usually less than 0.4 Tm) in intense torsion straining was studied here. Gold rod(100mm dia.) deformed by torsion straining was drawn through dies to 25um dia. Samples of pure gold wire were characterized by FIB (Focused Ion Beam), EBSD (Electron Back Scattered Diffractometer), and mechanical properties of samples were measured by tensile tester. The effect of grain size, mechanical properties and strain rate was also investigated, compared with non-torsion process. The torsion process of gold rod increased considerably mechanical properties, and It also were examined and discussed that substantial grain refinement, texture evolved from initial (100) fiber to (111) fiber in the center part especially, an large amount of low angle grain boundary.

Mechanical Behavior, Microstructure, and Modeling of Ti and Its Alloys: Processing: Design, Control and Optimization

Sponsored by: The Minerals, Metals and Materials Society, TMS Structural Materials Division, TMS: Titanium Committee

Program Organizers: Ellen Cerreta, Los Alamos National Laboratory; Vasisht Venkatesh, TIMET; Daniel Evans, US Air Force

Monday AM
March 10, 2008

Room: 384
Location: Ernest Morial Convention Center

Session Chair: Vasisht Venkatesh, TIMET

8:30 AM Introductory Comments

8:40 AM Keynote

Models for Mill Processing of Alpha/Beta Titanium Alloys: *S. Semiatin*¹; Perikles Nicolaou²; Ayman Salem³; Michael Glavicic²; ¹Air Force Research Laboratory; ²UES, Inc.; ³Universal Technology Corporation

Models for the mill processing of alpha/beta titanium alloys will be reviewed. Attention will be focused on coarsening, spheroidization, and cavitation during the breakdown of colony microstructures and on texture evolution during plate rolling. The mechanisms and kinetics of the coarsening of lamellar microstructures, which impacts the ease of spheroidization, will be summarized. An approximate diffusion analysis is used to model this coarsening process. Second, models to treat the growth and shrinkage of cavities formed during multi-step hot working sequences involving strain-path changes will be presented. The cavitation phenomena have been interpreted in the context of concurrent dynamic spheroidization. Last, the effect of hot working variables (preheat temperature, reheating/cooling practice) on the evolution of deformation and transformation alpha-phase textures during plate rolling will be discussed. The effect on texture of strain partitioning between the alpha and beta phases during rolling and preferential alpha-variant selection during cooldown will be highlighted.

9:20 AM

Design of High Formable and Strong Titanium Alloys through Plasticity Induced Transformation: *Suresh Neelakantan*¹; Pedro E.J. Rivera-Díaz-del-Castillo¹; Sybrand van der Zwaag¹; ¹Delft University of Technology

Preliminary works show the existence of Plasticity induced Transformation in metastable β -Titanium alloys (PiTTi), similar to TRIP steels. Extensive studies have been carried out to understand the defining parameters of PiTTi effect in β -metastable Ti-10V-2Fe-3Al (wt.%) and β -Cez alloys. Mechanical testing results show that the microstructures, which depend on heat treatment temperature and time, have a significant effect on the PiTTi properties. Optimizing PiTTi effect would aid in achieving improved strength-ductility relation in existing Ti-alloys or new alloy sets. A model was developed to estimate the M_s temperature (a

critical optimizing parameter for PiTTi) of Ti-base systems incorporating Fe, Al, V, Nb, Mo, Cr, Zr and Sn. The chemical inhomogeneities in β phase are employed to predict its ability to transform into martensite. The model is based on a modified version of Ghosh and Olson theory for martensite nucleation, [*Acta. Met. Vol. 42, pp. 3361, 1994*].

9:40 AM

Fabrication Method of SCS-6/Ti-6-4 Titanium Alloy Matrix Composite: *Chitoshi Masuda*¹; ¹Waseda University

The new fabrication method was proposed in order to obtain the homogenous fiber arrangement and the fabrication method and the microstructure and interfacial reaction layer were examined. The bulk composite was foil/sheet/foil method and hot press method at 900°C revealed that the SCS-6 fibers have been arranged homogeneously and the fiber spacing was about 100um. The interfacial reaction layer was also observed and the layer thickness was about 0.6mm and the grain size was about 10 micro-m. On the other hands, the same foil/sheet/foil was consolidated by Spark Plasma Sintering method at various temperatures and the composite were good consolidated from 700 to 900°C. As the interfacial reaction layers were also observed, the layer thickness was thinner than those for hot press method. Tensile strength was examined and the effect of hot press and SPS methods on the tensile strength was discussed.

10:00 AM

Innovative Direct Powder Rolling Process for Producing Titanium and Titanium Alloy Flat Products from Hydrogenated Titanium Powder: *Jane Adams*¹; Volodymyr Duz²; Vladimir Moxson²; ¹Army Research Laboratory; ²ADMA Products Inc

Titanium alloys exhibit attractive mechanical properties, good corrosion resistance and low density, but they are expensive. This paper is related to use of low cost direct powder rolling (DPR) processes to produce titanium and titanium alloy flat products (plates, sheets, foils) from hydrogenated Titanium powder. A blended elemental (BE) approach is used in this study in which hydrogenated titanium powder produced by a modified Kroll process is alloyed with a master alloy to achieve the required chemistry. Direct roll-compacting to form flat products of near final thickness and subsequent vacuum sintering produces near full density Titanium alloys with optimized microstructures and properties equivalent to those of the ingot metallurgy. This article reviews the general DPR process, microstructures, properties and ability to produce the Titanium alloy flat product in a cost-effective manner. Heat treatments performed on sintered alloys demonstrated that it is possible to achieve refined microstructures with the resulting improved combination of mechanical properties.

10:20 AM Break

10:40 AM Invited

Novel Heat-Treatments for the Production of Refined Microstructures in α/β Ti Alloys: Jonathan Orsborn¹; Peter Collins¹; Michael Loretto²; *Hamish Fraser*¹; ¹Ohio State University; ²University of Birmingham

High strength α/β Ti alloys often involve sub-solvus thermo-mechanical processing to effect a duplex, equiaxed alpha/transformed beta, microstructure. There are, however, significant advantages to be accrued from effecting such high strengths in alloys with a microstructure consisting either of Widmanstätten alpha plates in either the colony or basketweave forms. The coarseness of the microstructural features and the significant volume fraction of allotriomorphic alpha phase precipitated along prior beta grain boundaries limit the strength that can be achieved in these alloys with these microstructures when conventionally processed, i.e., solution heat-treatment in the beta phase field followed by cooling to room temperature followed by a sub-solvus annealing/aging treatment. This paper describes a new heat-treatment process that produces a refined distribution of Widmanstätten alpha plates with minimal grain boundary alpha phase which results in very high strengths (e.g., yield strengths ~1200MPa) in alloys such as Ti-6-4 and Ti-6-2-2-2.

11:10 AM

Interaction between NiTi SMA and Graphite Mold in Unidirectional Solidification Process: *Chonghe Li¹; Ming Zhu¹; Leyou Wang²; Xiemin Mao¹; ¹Shanghai University; ²General Research Institute for Nonferrous Metals Beijing*

One unidirectional solidification equipment based on Bridgman method with high temperature gradient was designed, and used to fabricate NiTi single crystal SMA (shape memory alloy) together with a selective growing zigzag-shaped crystallizer and a steady growth container that were made of electro graphite. The results show that this special shape crystallizer can enhance that only one crystal/(or 2-3 grain) survived at the exit of the selective growing crystallizer. Although the carbon dissolves into the melt and reacts with molten Ti to form TiC duo to the long time contact between the liquid melt and graphite container at 1450°C, this TiC particles can not become the nucleus of new grain, thus almost have no influence on the further direction solidification growth of crystal grain at the exit of the selective growing crystallizer.

11:30 AM

Oxygen Diffusion Dramatically Improves Tribological Characteristics for Titanium by Enabling Anti-Wear Surface Boundary Film Formation: *Jun Qu¹; Peter Blau¹; Jane Howe¹; Larry Walker¹; ¹Oak Ridge National Laboratory*

Titanium alloys have poor wear-resistance and cannot be efficiently lubricated because of their incompatibility with common anti-wear lubricant additives, such as zinc-dialkyl-dithiophosphate (ZDDP). This paper describes a surface engineering process, oxygen diffusion (OD), which has demonstrated great potential for improving the tribological characteristics of titanium by increasing surface hardness (from 3.7 to 12-14 GPa (HK)) and enabling tribochemical tractions with ZDDP to form an anti-wear boundary film. The OD treated Ti-6Al-4V demonstrated a 70% friction reduction and a remarkable six orders of magnitude wear reduction compared to untreated Ti-6Al-4V in an engine oil-lubricated, piston ring-on-flat bench test. The composition of the anti-wear boundary film was analyzed and the mechanisms of the tribochemical tractions between an oxygen-diffused titanium surface and ZDDP are discussed. Relative to more sophisticated surface treatment methods, oxygen diffusion offers much lower cost, few geometric restrictions, and no spallation of the treated layer.

11:50 AM

Processing of Ti Alloys by ECAE: Process Scale-up, FEM Simulation and Experimental Validation: *Shankar Sastry¹; Gian Colombo¹; ¹Washington University*

Equal channel angular extrusion (ECAE) is a processing method during which large amounts of plastic strain are induced in a material through simple shear deformation. This is done by forcing the material through a die consisting of two channels of equal cross-sectional area that intersect. Current studies on ECAE processing have used billets in the size range of 0.5 inches to 1 inch. Promising results for grain refinement and property improvement for billets of this size have been reported, but these small size billets have limited industrial use. In order for industry to take advantage of the beneficial aspects of ECAE, the billet sizes must be increased for them to be suitable for subsequent working and fabrication of structural components. In the present investigation, the feasibility of scaling up the ECAE process for producing 2.0 in diameter Ti-6Al-4V billets was demonstrated. FEM simulation and experimental results will be presented.

12:10 PM

Viscosity of Slags for High Titanium Ferroalloy by Vacuum Refining: *Lina Jiao¹; Ting'an Zhang¹; Jianming Yao¹; Jianming Yao¹; ¹Northeastern University*

Viscosity of CaO-Al₂O₃-CaF₂-TiO₂ and CaO-Al₂O₃-CaF₂-SiO₂ quaternary system was researched by internal-rotating cylinder method for their use as refining slag to remove oxygen and inclusions in crude high titanium ferroalloy produced by aluminothermy reduction process. It was showed that the viscosity of CaO-Al₂O₃-CaF₂-TiO₂ and CaO-Al₂O₃-CaF₂-SiO₂ system was below 0.4 Pa·S, when the temperature is up to 1520°C and 1495°C, respectively. Viscosity of the two systems both decreased with the increasing content CaF₂ content at a constant basicity. XRD results has showed that the major phases of molten CaO-Al₂O₃-CaF₂-TiO₂ were 3CaO·Al₂O₃, 12 CaO·7Al₂O₃, Ca₁₂Al₁₄O₃₂F₂, Ca₃(AlO₃)₂ and CaTiO₃ and the major phases of the melted slags were Ca₁₂Al₁₄O₃₂F₂, Ca₃SiO₄, Ca₂SiO₂F₂, Ca₃Al₂(SiO₄)₃, 5CaO·3Al₂O₃ and Al₂(SiO₄)O.

Mechanics and Kinetics of Interfaces in Multi-Component Materials Systems: Mechanics of Adhesion, Friction and Fracture

Sponsored by: The Minerals, Metals and Materials Society, TMS Electronic, Magnetic, and Photonic Materials Division, TMS Structural Materials Division, TMS/ASM: Composite Materials Committee, TMS: Thin Films and Interfaces Committee
Program Organizers: Bhaskar Majumdar, New Mexico Tech; Rishi Raj, University of Colorado, Boulder; Indranath Dutta, US Naval Postgraduate School; Ravindra Nugehalli, New Jersey Institute of Technology; Darrel Frear, Freescale Semiconductor

Monday AM
March 10, 2008

Room: 279
Location: Ernest Morial Convention Center

Session Chairs: Indranath Dutta, US Naval Postgraduate School; John Lewandowski, Case Western Reserve University

8:30 AM Keynote

Adhesion of Interfaces in Hierarchical Layered Structures for Emerging Technologies: *Reinhold Dauskardt¹; ¹Stanford University*

Understanding the mechanics and kinetics of debonding of interfaces in layered structures remains a crucial challenge for the integrity and reliability of layered structures in a wide range of technology areas including microelectronic devices and high-performance metal laminates. The layered structures are frequently engineered over a range of length scales, producing a hierarchical structure with selected compositions and structures at length scales ranging from the atomic to macroscale dimensions. We review understanding of the mechanics and kinetic aspects of adhesion and time dependent delamination in blanket and patterned layered structures representative of some of the above technologies. Particular attention is given to micromechanical characterization of properties under complex loading and chemically active environmental conditions. The effects of interface parameters and thin-film composition and porosity will also be considered including novel strategies to strengthen and toughen nanostructured materials. Implications for device reliability and integration of new materials are considered.

9:10 AM

Adhesion of Rough Curved Surfaces and Applications in Nanotribology: *Bing Ye¹; Bhaskar Majumdar¹; Somuri Prasad²; ¹New Mexico Tech; ²Sandia National Laboratory*

Adhesion of surfaces, as influenced by topology and texture, is central to the understanding and manipulation of phenomena at the micron and nanometer length scales, including biological and micro-electro-mechanical systems. Here, we analyze the general adhesion of initially rough curved surfaces and show that the pressure distribution over the region of contact does not contain any singularity, unlike the case of JKR singularity for smooth curved surfaces. Most significantly, we show a simple universal form for the adhesive pull-off load, which decreases with elastic modulus, increases with initial effective curvature, and is nearly inversely proportional to the surface roughness. The results suggest methods by which adhesion/de-adhesion could be actively manipulated, and may actually be exploited by insects and geckos for adhesion and locomotion. Applications of the results in nano-contact and adhesion at interfaces will be presented.

9:35 AM

Sliding at Metal-Ceramic Interfaces at Elevated Temperatures: *Rishi Raj¹; ¹University of Colorado*

Measurement of sliding viscosity at metal-ceramic interfaces, measured by the periodic cracking method will be presented. Two unexpected results deriving from two systems, copper-silica and aluminum-spinel, are: i) the activation energy for sliding is significantly lower than for grain boundary diffusion in the polycrystalline metals, and ii) the sliding behavior is always linear viscous, that is, the power law creep seen in polycrystals is absent. These results suggest that dislocation creep may not play a significant role in accommodating sliding at such interfaces. Possible reasons for this interpretation will be discussed.

10:00 AM Break

MONDAY AM

10:15 AM Invited

On the Role of Interfacial Layers and Shear Accommodation in the Frictional Behavior of Solid Lubricants: *Somuri Prasad*¹; Thomas Scharf²; ¹Sandia National Laboratories; ²University of North Texas

Friction coefficient is generally regarded as independent of applied load, as predicted by Amontons' law of friction. However, in many instances involving contact with polymeric materials, or whenever a liquid or solid lubricating film is used to mitigate friction, load dependency on the coefficient of friction (COF) has been observed. For the case where the contact is purely elastic, the data fit the general trend that the COF is proportional to the inverse of the mean Hertzian contact stress, $COF = (S_o/P) + \alpha$, where S_o is the interfacial shear strength of the lubricating layer separating the surfaces. Numerous examples from literature involving lamellar solids (e.g., graphite, MoS_2 , WS_2), diamond and diamond-like carbon, and polymers (e.g., PTFE) that exhibit non-Amontonian friction behavior are analyzed. The role of environmental reactions and tribochemistry influencing shear accommodation of friction-induced interfacial layers will be presented with examples from our recent work on diamond-like nanocomposite coatings.

10:45 AM Invited

Interface Effects on Fracture and Fatigue of Laminated Aluminum Composites: *John Lewandowski*¹; H. Hassan¹; ¹Case Western Reserve University

The effects of interface changes on the fracture and fatigue behavior of Laminated Aluminum Composites will be presented. Laminates were prepared via diffusion bonding or adhesive bonding with various aluminum alloys and DRA composites to systematically vary the interfacial strength. These laminated aluminum composites were tested in the crack divider and crack arrestor orientations under both quasi-static and fatigue crack growth conditions. The significant effects of changes in interfacial character and layer thickness on the toughness and fatigue crack growth behavior of these systems will be demonstrated and compared to non-laminated materials of similar chemistry.

11:15 AM Invited

Grain Boundary Fracture Initiation Parameter for Creep of a Co Based Superalloy: *Thomas Bieler*¹; Sara Longanbach¹; Carl Boehlert¹; ¹Michigan State University

Surface deformation of grain boundary engineered Udimet alloy 188 was examined in a scanning electron microscope during in-situ creep at 760°C and 220MPa. Grain boundary cracking was followed using surface imaging and EBSD mapping. Careful observation was needed to distinguish cracks from ledges that developed from grain boundary sliding. EBSD pattern quality (image quality) maps were inadequate to positively identify crack locations. Cracking occurred preferentially along general high-angle grain boundaries and less than 15% of the cracks were found on low angle grain boundaries and coincident site lattice boundaries. A fracture initiation parameter analysis was performed to identify the role of slip system interactions at the grain boundaries and their impact on crack nucleation. This analysis was successful in separating the population of intact random grain boundaries from cracked random grain boundaries at lower levels of strain, but not after crack coalescence dominated the grain boundary fracture process.

Micro-Engineered Particulate-Based Materials: Session I

Sponsored by: The Minerals, Metals and Materials Society, TMS Materials Processing and Manufacturing Division, TMS: Powder Materials Committee
Program Organizers: Khaled Morsi, San Diego State University; Iver Anderson, Iowa State University

Monday AM
March 10, 2008

Room: 271
Location: Ernest Morial Convention Center

Session Chairs: Iver Anderson, Iowa State University; Khaled Morsi, San Diego State University

8:30 AM

Phase Transformations in Reactive Gas Atomized Stainless Steel Powders That Promote an Oxide Dispersion Strengthened Microstructure: *Joel Rieken*¹; Iver Anderson²; M. Kramer²; D. Shechtman¹; M. Besser²; ¹Iowa State University; ²Ames Laboratory

A novel processing technique employing gas atomization reaction synthesis (GARS) has been used to produce stainless steel powders that are encapsulated with a thin chromium oxide shell. This paper will investigate the reactions involved with transformation from as-atomized Fe-(12.5-15.0)Cr-(0.3-1.0)Y powders (wt.%) to a consolidated isotropic oxide dispersion strengthened microstructure. A series of heat treatment studies were conducted in an effort to understand and control the oxygen exchange reaction occurring between chromium oxide and yttrium at elevated temperatures. Scanning electron microscopy and transmission electron microscopy were used to evaluate post heat treatment microstructures. Phase transformations associated with volume fraction changes were tracked using x-ray diffraction analysis. Initial high temperature tensile strength analysis was performed to assess the effectiveness of the resulting heat treatment procedure. Support from the DOE-FE (ARM program) through Ames Laboratory contract no. DE-AC02-07CH11358 is gratefully acknowledged.

8:55 AM

Tailored Oxide Films on Precursor Powders for Isotropic ODS Ferritic Stainless Steels: *Iver Anderson*¹; Joel Rieken¹; ¹Iowa State University

Innovation is needed to exploit the benefits of a new type of precursor alloy powder for simplified processing of oxide dispersion strengthened (ODS) stainless steels. While the heat treatment of consolidated forms of such Fe-Cr-Y powder is under extensive study, the options for liquid state, mushy state, or solid state oxidation processes also are being explored to tune the starting balance of Cr and Y oxides associated with the powders. Because of the competition for oxidation between Cr and Y that is designed into the Fe-Cr-Y system, detailed characterization by SEM, XPS, and AES is needed to understand the oxide phase development on the powders. This is critical to the quest for an ideal state where the ODS microstructure consists only of nano-metric dispersoids without remnants of the oxide supply phase due to a completed exchange reaction. Supported by USDOE-FE-ARM Program through Ames Laboratory contract no. DE-AC02-07CH11358.

9:20 AM

Analytical Electron Microscopy of Mechanically Alloyed 12YWT and 14YWT Nano-Structured Ferritic Alloys for Structure-Property-Processing Correlations: *James Bentley*¹; David Hoelzer¹; Larry Walker¹; ¹Oak Ridge National Laboratory

The contributions of analytical (transmission) electron microscopy (AEM) to understanding structure-property-processing correlations in nano-structured ferritic alloys that include prototypical 12YWT (12%Cr) and ORNL-developed 14YWT (Fe-14.2%Cr-1.95%W-0.22%Ti-0.25%Y₂O₃) will be described. Beyond conventional AEM methods (e.g. for grain-size measurements and x-ray microanalysis of second-phase particles), energy-filtered transmission electron microscopy (EFTEM) methods have been emphasized for reliably revealing the oxide nano-clusters (typically with diameters less than 4 nm and concentrations exceeding 10²³ m⁻³) that are responsible for the exceptional mechanical properties of these materials. Material processing steps include mechanical alloying of base-alloy and yttria powders followed by extrusion. Supplemented by electron

probe microanalysis (EPMA) measurements, correlations of AEM results with ball-milling parameters and extrusion temperatures identified undesirable processing conditions and aided the selection of more optimum protocols. AEM characterization of tensile- and creep-tested specimens allowed an assessment of the nano-cluster contribution to yield strength and revealed the remarkable high-temperature stability of the nanoclusters.

9:45 AM

Characterization of Al-TiC Composites Produced via Mechanical Alloying: *Elif Can Özgün¹; Mustafa Lütfi Öveçoglu¹; ¹Istanbul Technical University*

The microstructural and mechanical evolution of TiC reinforced aluminium metal matrix composites in three different weight fractions were investigated. The TiC particles were dispersed in aluminium matrix using powder metallurgy technique via mechanical alloying (MA) using five different MA times for every weight fraction. The powders were consolidated and sintered under argon atmosphere. Both mechanical alloyed powders and sintered samples were characterized using optical microscope, XRD, SEM with EDS unit, BET and hardness tests. After sintering at 630°C, needle like intermetallic phases were observed.

10:10 AM Break

10:30 AM

In Situ Aluminum Based Nanocomposites Produced by Friction Stir Processing: *I. S. Lee¹; S. H. Lee¹; C. F. Chen¹; P. W. Kao¹; ¹National Sun Yat-Sen University*

In this study, friction stir processing (FSP) is applied to produce aluminum based nanocomposites from powder mixtures of Al-10at%Fe and Al-2mol%Fe₂O₃. Billet of powder mixtures was prepared by the use of conventional press and sinter route. It was then subjected to multiple passages of FSP. This technique has combined the hot working nature of FSP and the exothermic reaction between Al and Fe or Al and Fe₂O₃. The composites produced were fully dense with high strength. Transmission electron microscopy (TEM) showed that the second phase particles (~100 nm in size) were distributed uniformly, and the grain size of aluminum matrix was ~1 µm. The particles were identified as Al₁₃Fe₄ in Al-Fe, and Al₁₃Fe₄ and Al₂O₃ in Al-Fe₂O₃. The fine structure of these composites can be attributed to the severe deformation in FSP. The mechanical properties of these nanocomposites were evaluated by using microhardness, tensile and compressive tests.

10:55 AM

Research of Electrodeposited RE-Ni-Fe-P-PTFE Composite Coating: *Jinhui Li¹; Xinhai Li¹; ¹Central South University*

Composite coating is a very important part in new materials because it has special excellent physical and chemical properties. PTFE(polytetrafluoroethylene) is a special particle with some excellent properties. Experiment of electrodeposited RE-Ni-Fe-P-PTFE composite coating is proceeded and the effect of surfactant, PTFE, and the ion of rare earth on the coating's content of PTFE were researched. The results shows that the optimum process parameters are that the conc. of rare earth La is 3g/L, the conc. of PTFE solution is 50ml/L, temperature is 55°C, current density is 10 ampere per square decimeter. And that the coefficient of friction of the coating is decreased, and the lubricating property is improved.

11:20 AM

Properties of Silver-Doped Titania Antibacterial Powder Coating with Alumina: *Wei Shunwen¹; ¹Central South University*

The life of silver doping antibacterial powder was related to the release rate of silver ion from powder in water. In order to improve the life of silver-doped titania antibacterial material, the composite antibacterial powder was prepared by coating silver-doped titania core with a layer of alumina. Analysis results shown that the shape of particle was spherical with a diameter of about 200-600nm, and the coating γ-Al₂O₃ film was observed at the surface of the silver-doped titania particle and the thickness of the alumina shell was approximately 30-40nm. The Ag⁺ release rate of the composite powder was decreased with increasing annealed temperature. A direct deposition of alumina onto the surface of silver-doping titania particles was proved to control the release of silver ion effectively, it suggested that coating process was help to lengthen the life of the materials.

Minerals, Metals and Materials under Pressure: New Experimental and Theoretical Techniques in High-Pressure Materials Science

Sponsored by: The Minerals, Metals and Materials Society, TMS Structural Materials Division, TMS: Chemistry and Physics of Materials Committee

Program Organizers: Richard Hennig, Cornell University; Dallas Trinkle, University of Illinois; Ellen Cerreta, Los Alamos National Laboratory

Monday AM
March 10, 2008

Room: 385
Location: Ernest Morial Convention Center

Session Chairs: Ellen Cerreta, Los Alamos National Laboratory; Eric Brown, Los Alamos National Laboratory

8:30 AM Introductory Comments

8:35 AM Invited

Atomistic and Mesoscale Modeling of the Response of Molecular Crystals to Dynamical Loading: *Alejandro Strachan¹; ¹Purdue University*

We use large scale molecular dynamics (MD) with an accurate, first principles-based interatomic potential to characterize the atomic level mechanisms that govern inelastic deformation of the molecular crystal α-HMX under dynamical loading along the [100] direction. We find that for weak shocks plastic deformation is governed by dislocations with Burgers vector $b = \frac{1}{2}a$ and $b = \frac{1}{2}a$. As the shock strength is increased we observe a gradual transformation to a regime governed by shear bands characterized individual molecular events that cluster in thick bands and do not show a well defined crystallographic slip. I will also describe a new approach for coarse-grain simulations that leads to a thermodynamically accurate description of materials. The new method, denoted dynamics with implicit degrees of freedom (DID), shows excellent agreement with all-atom MD simulations when parameterized with using classical statistics but also enables the incorporation of quantum thermal effects that are critical in molecular materials.

9:05 AM

High Rate Plasticity under Pressure Using an Oblique-Impact Isentropic-Compression Experiment: *Jeffrey Florando¹; David Lassila¹; Grant Bazan¹; Tong Jiao²; Stephen Grunschel²; Rodney Clifton²; ¹Lawrence Livermore National Laboratory; ²Brown University*

An experimental technique has been developed to study the strength of materials under conditions of moderate pressures and high strain rates. The technique is similar to the traditional pressure-shear experiments except that window interferometry is used to measure both the normal and transverse particle velocities at the sample-window interface. Additionally, the sample is impacted with a graded density impactor, which imposes a near isentropic compression ramp wave and controls the strain rate to between 10⁴–10⁶. Both simulation and experimental results on copper samples with a sapphire window will be presented to show the utility of the technique to measure the strength properties under dynamic loading conditions.

9:25 AM Break

9:40 AM Invited

Quantum-Based Atomistic Simulation of Metals at Extreme Conditions: *John Moriarty¹; ¹Lawrence Livermore National Laboratory*

First-principles generalized pseudopotential theory (GPT) provides a fundamental basis for bridging the quantum-atomistic gap from density-functional quantum mechanics to large scale atomistic simulation in metals and alloys. In directionally-bonded bcc transition metals, advanced generation *model* GPT or MGPT potentials based on canonical *d* bands have been developed for Ta, Mo and V and successfully applied to a wide range of thermodynamic and mechanical properties at both ambient and extreme conditions of pressure and temperature, including multiphase equation of state; phase transitions, melting and solidification; thermoelasticity; and the atomistic simulation of point defects, dislocations and grain boundaries needed for the multiscale modeling of plasticity and strength. Recent algorithm improvements have also allowed an MGPT implementation beyond canonical bands to achieve increased accuracy,

extension to *f*-electron actinide metals, and high computational speed. A further advance in progress is the development of temperature-dependent MGPT potentials that subsume important electron-thermal contributions to high-temperature properties. This work was performed under the auspices of the U.S. Department of Energy by the University of California Lawrence Livermore National Laboratory under contract No. W-7405-Eng-48.

10:10 AM

First-Principles Phonon Approach to the Equation-of-States of Al, Cu, Ta, Pt, and Au: *Yi Wang*¹; *Zi-Kui Liu*¹; *Long-Qing Chen*¹; ¹Pennsylvania State University

The main objective of this work is to make the equation-of-state standard for the diamond-anvil-cell experiment. Calculated 300-K isotherms and Hugoniot at pressures up to shock-wave melting points for the five reference metals Al, Cu, Ta, Pt, and Au are reported using the first-principles phonon approach. With these data, shock-reduced 300 K isotherms are derived for these metals by subtracting the calculated thermal volume expansion from the experimental shock-wave data.

10:30 AM Break

10:45 AM

Acoustic Properties of Fluoropolymers at High Pressure: *Dana Dattelbaum*¹; *Muhtar Ahart*²; *Russell Hemley*²; ¹Los Alamos National Laboratory; ²Geophysical Laboratory

Fluoropolymers are a class of polymers that are used extensively in engineering applications because of their favorable properties that include chemical inertness, thermal stability, low coefficients of friction, and high densities. For the first time, the acoustic properties of a series of semi-crystalline fluoropolymers have been measured from ambient pressure to >12 GPa using Brillouin spectroscopy. From the measured acoustic properties, elastic constants, moduli, and Poisson's ratios were calculated as a function of pressure. P-V isotherms were also constructed, and fit to a range of empirical/semi-empirical isothermal equation-of-state (EOS) forms. From this analysis, the isothermal bulk modulus and its pressure derivative were obtained for the polymers interrogated, and the static results were compared to available shock wave compression data. The Brillouin data also show sensitivity to crystalline phase transitions and non-linear compressibility at low pressures.

11:05 AM

Plasticity, Spall Damage and Microstructure Interactions in Shock Loaded Copper Multicrystals: *Pedro Peralta*¹; *Shima Hashemian*¹; *Stephan DiGiacomo*¹; *Heber D'Armas*²; *Shengnian Luo*³; *Eric Loomis*³; *Dennis Paisley*³; *Robert Dickerson*³; *Darrin Byler*³; *Ken McClellan*³; ¹Arizona State University; ²Universidad Simon Bolivar; ³Los Alamos National Laboratory

Correlations among plasticity, damage and local microstructure were investigated in copper via impact tests conducted with laser-driven plates at low pressures (3-6 GPa). The copper samples had a large grain size as compared to the thickness, which was either 200 or 1000 μm , to isolate the effects of microstructure on the local response. Velocity interferometry was used to measure the bulk response of the free-surface velocity of the samples to monitor traditional spall tensile failure. Electron Backscattering Diffraction (EBSD) was used to relate crystallography to plasticity and to the presence of porosity around defects. A transition between transgranular and intergranular damage was observed as the grain sized was reduced from 230 μm to 150 μm in thin samples, whereas both modes were observed in thick specimens (450 μm grain size). Potential sites for preferred damage nucleation were identified in terms of their crystallography via statistical sampling in serial sectioned specimens.

Neutron and X-Ray Studies for Probing Materials Behavior: Resolving Local Structure

Sponsored by: National Science Foundation, The Minerals, Metals and Materials Society, TMS Structural Materials Division, TMS: Advanced Characterization, Testing, and Simulation Committee

Program Organizers: Rozaliya Barabash, Oak Ridge National Laboratory; Yandong Wang, Northeastern University; Peter K. Liaw, University of Tennessee

Monday AM

Room: 391

March 10, 2008

Location: Ernest Morial Convention Center

Session Chairs: Rozaliya Barabash, Oak Ridge National Laboratory; Judy Pang, Oak Ridge National Laboratory

8:30 AM Keynote

Spatially-Resolved Polychromatic Neutron and X-Ray Microdiffraction: *Gene Ice*¹; ¹Oak Ridge National Laboratory

Polychromatic microdiffraction is an emerging materials-characterization tool made practical by powerful x-ray and neutron sources, and by advanced optics and software. With polychromatic techniques, local crystalline properties including phase, texture (orientation), elastic strain and defect density can be mapped with good spatial resolution in 3 dimensions. The evolving ability to nondestructively map local crystal structure in three dimensions, addresses long-standing issues of inhomogeneous grain-growth, deformation, fracture, and elastic strain. Applications impact virtually all materials including electronic, solar, and LED materials, nanomaterials, structural materials and joining materials. In addition the ability to focus small beams on small samples dramatically increases signal-to-noise and greatly reduces the cost of extreme environmental chambers required for high-pressure, high temperature, high magnetic field or corrosive environments. These techniques efficiently use source brilliance and minimize the required sample volume, which is essential for hard-to-make materials, irreplaceable materials, and for radioactive, toxic or otherwise dangerous materials.

9:05 AM Invited

Structural Characterization by Three Dimensional X-Ray Diffraction Microscopy: *Wenjun Liu*¹; *Gene Ice*²; *Bennett Larson*²; *Jonathan Tischler*²; *Paul Zschack*¹; ¹Argonne National Laboratory; ²Oak Ridge National Laboratory

The principle research activities in the beamline 34-ID-E at the Advanced Photon Source involve development of exciting new micro/nano-diffraction techniques for characterization and microscopy in support of material sciences and condensed matter physics. With high-brilliance, third generation synchrotron X-ray source, advanced focusing mirrors, and the newly developed depth profiling techniques, spatially resolved diffraction measurements can be made in all three dimensions with submicron resolution. Properties that can be measured include local crystallographic orientations, orientation gradients and strains. This capability enables detailed studies of fundamental deformation processes, basic grain-growth behavior, and meoscale structures. The performance of the beamline facility and future development plan are discussed.

9:30 AM

X-Ray Microbeam Probing the Inhomogeneous GNDs Distribution near the Boundary of a Ni Bicrystal: *Rozaliya Barabash*¹; *J. Pang*¹; *G. Ice*¹; *Tetsuya Ohashi*²; ¹Oak Ridge National Laboratory; ²Kitami Institute of Technology

In this study we report on inhomogeneous plastic deformation in a natural Ni bicrystal after uniaxial pulling. A focused, polychromatic synchrotron X-ray microbeam together with orientation imaging microscopy, scanning electron microscopy, and finite element simulations were used to characterize the physics of geometrically necessary dislocation formation and their collective behavior during plastic deformation. The local crystallographic orientation of subgrain volumes were characterized to determined the plastic response during deformation. Finite element simulations were used to understand the influence of grain orientation and the initial structural inhomogeneities on the evolution of geometrically necessary dislocations arrangement and distribution. Strain in both grains increases in the vicinity of the coherent boundary.

9:50 AM Invited

Studying Complex Materials Using Submicron-Resolution Laue X-Ray Microdiffraction: *John Budai*¹; W. Liu²; J.Z. Tischler¹; D.D. Sarma³; G. Shenoy²; B.C. Larson¹; G.E. Ice¹; S.-W. Cheong⁴; ¹Oak Ridge National Laboratory; ²Argonne National Laboratory; ³Indian Institute of Science; ⁴Rutgers University

We have developed a polychromatic, scanning synchrotron microbeam capability with 3D submicron spatial resolution. White-beam Laue diffraction patterns are analyzed with automated software, yielding real-space maps of the local crystal structure, lattice orientation, and strain tensor. Polychromatic scanning x-ray microdiffraction has been used to investigate a variety of complex materials, and this talk will illustrate with examples from 1D, 2D and 3D systems. 1D nanostructures mounted on TEM grids make convenient samples, and we have mapped the crystal perfection along individual 200nm ZnO nanorods. In 2D studies of thin films, microdiffraction studies revealed atomic-level mechanisms for local crystallographic tilting in epitaxial oxide buffer layers for superconducting applications. In 3D, structural investigations have included nondestructive studies of thermal grain growth in polycrystalline aluminum and local eutectic phase separation in complex manganite crystals. Support by DOE-BES, DMS&E at ORNL; UT-Battelle; UNI-XOR by ORNL and APS by DOE-BES.

10:15 AM Break

10:20 AM Invited

A Synchrotron X-Ray Diffraction Method for Measuring the Micromechanical Response of Multiphase Alloys: *Matthew Miller*¹; Jun Park¹; Alexander Kazimirov¹; Martin Mataya²; ¹Cornell University; ²Colorado School of Mines

Diffraction is a powerful tool for understanding deformation partitioning with a multiphase alloy. This talk describes a powder diffraction method developed to measure lattice strain pole figures during in-situ loading. The pole figures are used to calculate the distribution of crystal stresses over orientation space. The inversion method for reduction of the pole figure data is motivated by quantitative texture analysis. Issues that are particular to multiphase experiments include peak overlap and detection of extreme ranges of x-ray intensity. Results from experiments conducted at the Cornell High Energy Synchrotron Source (CHESS) on a number of alloys including iron/copper, aluminum/beryllium and titanium are presented.

10:45 AM Invited

In-Situ Observations of Subgrain Dynamics by High Energy X-Ray Diffraction: *Wolfgang Pantleon*¹; Christian Wejdemann¹; Ulrich Lienert²; Bo Jakobsen¹; Henning Poulsen¹; ¹Risoe National Laboratory; ²APS Argonne National Laboratory

By means of high angular resolution three-dimensional X-ray diffraction, individual subgrains can be identified within a single grain in the bulk of a polycrystalline, macroscopic specimen. Each broadened Bragg reflection constitutes of individual sharp peaks superimposed on a broad cloud of enhanced intensity. The sharpness of the peaks in all directions of reciprocal space and their integrated intensity allows their identification with almost dislocation-free subgrains. In this manner, the evolution of the dislocation structure can be monitored during in-situ loading: Intermittent subgrain dynamics is observed during in-situ tension with individual subgrains emerging and disappearing in the course of deformation, indicating a rather volatile dislocation structure. On the other hand, no significant changes are observed in the subgrain structure during stress relaxation or unloading; the individual subgrains survive, but redistribute their internal stresses. During strain path changes, dissolution and re-building of the entire subgrain structure is observed.

11:10 AM Invited

X-Ray Imaging of Phonon Interaction with Dislocations: *Emil Zolotoyabko*¹; ¹Technion-Israel Institute of Technology

Unique characteristics of synchrotron radiation are used for ultra-fast time-resolved measurements of structural dynamics in crystals. For example, by exploiting the pulsed structure of synchrotron radiation combined with the stroboscopic mode of data acquisition, the periodic processes with frequencies up to a few GHz can be probed with temporal resolution down to 50 ps. By using this technique we studied high-frequency dislocation dynamics in brittle crystals induced by interaction with acoustic waves (phonons). Stroboscopic topographs

taken from acoustically excited LiNbO₃ crystals exhibited well-resolved individual acoustic wave fronts as well as their distortions due to dynamic deformation fields related to vibrating dislocation segments. The dislocation dynamics is characterized by very high velocities (in significant parts of the speed of Rayleigh waves) and extremely low viscosity coefficients, 2-3 orders of magnitude lower than measured in ductile materials. Such low viscosity in dislocation motion can be hardly probed by the established characterization techniques.

11:35 AM Invited

Local Dislocation Properties and Diffraction Methods: *Patrick Veyssiere*¹; ¹LEM, Centre National de la Recherche Scientifique-ONERA

The aim of this contribution is chiefly to review transmission electron microscopy (TEM) methods used to establish local dislocation properties and their relation with the plastic behaviour of materials. Several TEM operation modes are reviewed with their potential and limitations critically assessed. Special emphasis is placed on the so-called weak beam method whose unique capability to provide information not only on the core of dislocations but also on the organization of these, are demonstrated from studies on metallic systems. It will be shown that weak-beam observations can help uncover local dislocation mechanisms controlling plasticity. An attempt will be made to place TEM, X-ray (or neutrons) into perspective will be made.

12:00 PM

Slip System - Dependent Calculations of Dislocation Density and Dislocation-Wall Spacing from In-Situ Neutron Measurements: *E-Wen Huang*¹; Rozaliya Barabash²; Björn Clausen³; Yandong Wang⁴; Yang Ren⁵; Peter Liaw¹; Hahn Choo¹; ¹University of Tennessee; ²Oak Ridge National Laboratory; ³Los Alamos National Laboratory; ⁴Northeastern University; ⁵Argonne National Laboratory

Monotonic-tensile experiments were conducted to observe diffraction-profile evolutions at room temperature. The pseudo-Voigt function had been applied to distinguish the diffractions from Gaussian to Lorentzian distributions. The randomly-distributed dislocations and non-uniform dislocation walls diffracted neutrons in Gaussian and Lorentzian distributions, respectively. The calculations of the distributions accompanying with the contrast factor determine the dislocation density and the dislocation-wall spacing as a function of the strains. As a result, the slip system -dependent calculated dislocation density and dislocation-wall spacing of the annealed HASTELLOY® C-22HSTM nickel-based superalloy were examined by the in-situ neutron-diffraction experiment. The stress evolutions as a function of strains are compared with the evolution of the dislocation density and the dislocation walls spacing in light of the activation from different slip systems during the monotonic-tension experiments.

12:15 PM

Neutron and X-Ray Microbeam Diffraction Studies around a Fatigue Crack after Overload: *Sooyeol Lee*¹; Rozaliya Barabash²; Jin-Seok Chung³; Yinan Sun¹; Hahn Choo¹; Peter Liaw¹; Donald Brown⁴; Gene Ice²; ¹University of Tennessee; ²Oak Ridge National Laboratory; ³Soongsil University; ⁴Los Alamos National Laboratory

Fatigue-crack-growth experiments were performed on a compact-tension specimen of a Type 316 LN austenitic stainless steel. A single overload was applied during fatigue tests and a retardation period was observed, showing a temporary decrease in crack growth rates. Neutron diffraction and X-ray microdiffraction techniques were used to study crack-tip deformation behaviors in millimeter and submicrometer spatial resolutions, respectively. From neutron diffraction, elastic lattice strain profiles and dislocation densities were measured as a function of the distance from crack tip. Furthermore, Laue diffraction patterns obtained from polychromatic X-ray microdiffraction at different locations near the crack tip showed alternating regions with high and low dislocation densities. Authors acknowledge the financial supports from the National Science Foundation, the International Materials Institutes Program (DMR-0231320). The research is sponsored in part by the Division of Materials Sciences and Engineering Office of Basic Energy Sciences, U.S. Department of Energy, under Contract DE-AC05-00OR22725 with UT-Battelle, LLC.

Particle Beam-Induced Radiation Effects in Materials: Metals I

Sponsored by: The Minerals, Metals and Materials Society, American Nuclear Society, TMS Structural Materials Division, TMS/ASM: Nuclear Materials Committee

Program Organizers: Gary Was, University of Michigan; Stuart Maloy, Los Alamos National Laboratory; Christina Trautmann, Gesellschaft für Schwerionenforschung; Maximo Victoria, Lawrence Livermore National Laboratory

Monday AM
March 10, 2008

Room: 389
Location: Ernest Morial Convention Center

Session Chairs: David Jenkins, CSIRO; Stuart Maloy, Los Alamos National Laboratory

8:30 AM

Materials Research at the Paul Scherrer Institute for Developing High Power Spallation Targets: Yong Dai¹; Friedrich Groeschel¹; Werner Wagner¹; ¹Paul Scherrer Institut

For the R&D of high power spallation targets, one of key issues is the understanding of behaviors of structural materials in severe irradiation environments in spallation targets. At PSI, several experiments have been conducted in the targets of the Swiss spallation source (SINQ) for studying radiation damage effects induced by high energy protons and spallation neutrons. Meanwhile, experiments have been performed to investigate liquid lead-bismuth (LBE) corrosion and embrittlement effects on the T91 steel under irradiation of 72 MeV protons. In this presentation, an overview will be given to show the main outcome of these experiments and the inspection of spent SINQ targets as well, which will cover the mechanical properties and microstructure of structural materials such as T91, SS316L, Zircaloy-2, and AlMg₃ irradiated to doses ever obtained from irradiations in spallation environment, and the behaviors of T91 irradiated with 72 MeV protons in contact with flowing LBE.

9:10 AM

Novel Characterization Methods for Ti-6Al-4V Implanted with High Energy Ions: Kale Stephenson¹; Kip Findley¹; Michael Carroll¹; Vaithiyalingam Shutthanandan²; ¹Washington State University; ²Environmental Molecular Sciences Laboratory; Pacific Northwest National Laboratory

Titanium alloys are valuable in structural and biomedical applications because of their high strength-to-weight ratio and biocompatibility. With the demand for titanium alloys in these critical areas, it is important to develop surface treatments that can improve fatigue, wear, and corrosion resistance. Ti-6Al-4V was implanted with nitrogen, gold, and aluminum ions with energies of 1-5 MeV. Nanoindentation experiments were conducted to determine the surface hardness and modulus gradient for each of the implantation conditions; additionally, electron backscatter diffraction (EBSD) was used to assess the extent of lattice damage as a function of distance from the implanted surface in each condition. These results were correlated to Rutherford Backscatter Spectrometry measurements of the implantation depths and TRIM calculations of ion projected ranges and displacement events. The specimens implanted with aluminum ions were heat treated to determine if Ti-Al intermetallics could be produced with the experimental dose rates and their subsequent surface hardness.

9:30 AM

A Description of Stress Driven Bubble Growth and Gas Release of Helium Implanted Tungsten: Shahram Sharafat¹; Akiyuki Takahashi²; Koji Nagasawa²; Nasr Ghoniem¹; ¹University of California Los Angeles; ²Tokyo University of Science

Low energy (< 100 keV) helium implantation of tungsten has been shown to result in the formation of unusual surface pore morphologies, following annealing over a large temperature range. We developed and employed a space-dependent Kinetic Rate Theory code to model spatial distributions of defect concentrations as well as stable helium-bubble nuclei and a Kinetic Monte Carlo simulation code to model helium bubble migration and coalescence. In this work, we describe bubble growth and gas release during annealing of implanted helium including the influence of stress fields. First, the spatial profile of stable bubble nuclei and defect concentrations are calculated. Next, effects of matrix

strain caused by pressurized bubbles are included. The influence of near-surface stress fields on bubble migration is also modeled. Surface pore densities and size distributions are compared with experimental results and the role of stress fields on bubble and surface-pore evolution is compared with stress-free simulations.

9:50 AM

High Temperature Surface Effects of He+ Implantation in ICF Fusion First Wall Materials: Samuel Zenobia¹; Gerald Kulcinski¹; ¹University of Wisconsin, Madison

The first wall armor of Inertial Confinement Fusion (ICF) reactor chambers must withstand high temperatures and significant radiation damage from ICF target debris and neutrons. The resilience of multiple materials to one component of the target debris has been investigated using energetic (20-40 keV) helium ions generated in the UW Inertial Electrostatic Confinement (IEC) device. Studied materials include: single-crystalline, polycrystalline, and powder metallurgy prepared tungsten, tungsten coated TaC and HfC "foams," tungsten-rhenium alloy, CVD SiC, carbon-carbon velvet (CCV), and tungsten coated CCV. Steady-state irradiation temperatures ranged from 750–1250°C with helium fluences between 5×10^{17} – 1×10^{20} He⁺/cm². The crystalline, rhenium alloyed, carbide foam, and powder metallurgical tungsten specimens each experienced pore formation after irradiation. Flaking and pore formation occurred on CVD SiC samples after He⁺ implantation. Individual fibers of CCV specimens sustained erosion and corrugation, in addition to roughening and rupturing of tungsten coatings after He⁺ implantation.

10:10 AM Break

10:30 AM

Displacement Rate Effects in Nucleation Processes: Kenneth Russell¹; ¹Massachusetts Institute of Technology

Nucleation in solids depends crucially on the concentrations and mobilities of point defects, in particular vacancies, self-interstitials, and impurity interstitials. These defects provide solute mobility and may also act as nucleus components. Changes in displacement rate give changes in defect concentrations that are reflected in the kinetics of nucleation. This paper analyzes the effects of displacement rate on the nucleation rates of the voids that give rise to swelling and the Cu-rich precipitates that contribute to pressure vessel embrittlement. The resulting equations are intended to be of use in designing radiation resistant materials.

10:50 AM

Amorphization at Grain Boundaries in Zr-Ti-Ni-Cu Alloys by 300 MeV Kr Ions: Gerhard Schumacher¹; Stefan Mechler²; Siegfried Klaumünzer¹; Nelia Wanderka¹; Michael Macht¹; Christian Abromeit¹; ¹Hahn-Meitner-Institut Berlin; ²Harvard University

Structural changes in quasicrystalline Zr_{64.5}Ti_{11.4}Ni_{13.8}Cu_{10.3} alloy (V4-0) during room temperature irradiation with 300 MeV Kr ions were studied ex-situ by means of XRD and TEM. XRD measurements revealed a continuously decreasing amount of the volume fraction V(qc) of the quasicrystalline phase up to a fluence of about $1 \cdot 10^{15}$ Kr/cm². Above this fluence V(qc) levelled off approaching a value of about 25% compared to the initial value. TEM investigation showed that the regions near the grain boundaries had transformed to the amorphous state while the cores of the quasicrystals remained stable. The influence of the nuclear and electronic energy loss on amorphization of the highly defective grain boundaries is discussed. The interior of the quasicrystals may serve as nuclei for subsequent crystallization which promotes the stability of the grain interior.

11:10 AM

Enhanced Catalytic Structures by Beam Irradiation: Claudiu Muntele¹; Liviu Popa-Simil²; ¹Center for Irradiated Metals-Alabama Agricultural and Mechanical University; ²LAVM LLC

The thin layer deposition of catalytic layers offers low porosity, high density and adhesion, while making a fluffy deposition in controlled atmosphere the porosity and surface is becoming good but mechanical properties are weakened. The usage of a compact deposition with beam based treatment using implantation in order to create volume controlled structure by generating wide range of defects-dislocations. The dislocations-voids inside make surface very rough allowing the catalytic process to cover the entire surface and get volume. Tests have been

made for the reactivity modifications of Pa, Pt and Ni thin layers. Relationship between the thickness on silicon wafer support of the catalyst deposition and absorbed micro-dose is traced as function of chemical reactive composition. The experiment shows the capability of the ion beam processing of the catalyst layers to create a more suitable structure for catalytic depositions that to mitigate the high reactivity and good adhesion resulting in an extended life product.

11:30 AM

Swelling Measurements Using an Ion Beam Accelerator and Nanoscale Measurements: *Peter Hosemann*¹; *Stuart Maloy*¹; *Richard Greco*¹; ¹Los Alamos National Laboratory

Radiation induced swelling can be a major concern for designing systems operating in a radiation environment. Swelling experiments on materials are in general very time consuming and costly material tests. Accelerator experiments on the other hand in combination with nanoscale techniques such as atomic force microscopy, micro machining, interferometry and nano indentation allow one to perform fast and relatively inexpensive experiments where radiation induced swelling can be studied in great detail. This study shows results of a study where μm scale structures are created in tungsten and tantalum and their size and shape accurately measured before exposing them to irradiation. Next, a He⁺ beam was used to create the radiation induced swelling. Post analysis of the structures was done using atomic force microscopy. The shape and size change of the structures allows accurate measurement of void swelling and can be compared to swelling from fission reactor irradiations.

Recent Developments in Rare Earth Science and Technology - Acta Materialia Gold Medal Symposium: Session I

Sponsored by: The Minerals, Metals and Materials Society, TMS Electronic, Magnetic, and Photonic Materials Division, TMS: Superconducting and Magnetic Materials Committee

Program Organizers: Vitalij Pecharsky, Iowa State University; Ashutosh Tiwari, University of Utah; James Morris, Oak Ridge National Laboratory

Monday AM Room: 280
March 10, 2008 Location: Ernest Morial Convention Center

Session Chairs: Thaddeus Massalski, Carnegie Mellon University; Vitalij Pecharsky, Iowa State University

8:30 AM Opening Remarks: Recognition of Karl Gschneidner, Jr, the Acta Materialia Gold Medal Award recipient.

8:45 AM Keynote

The Magnetocaloric Effect, Magnetic Refrigeration and Ductile Intermetallic Compounds: *Karl Gschneidner, Jr.*¹; ¹Iowa State University

The magnetocaloric effect (MCE) is the ability of a magnetic material, particularly near its Curie temperature, to heat up when a magnetic field is applied (magnetization) and to cool when the field is removed (demagnetization). A number of new materials, especially $\text{Gd}_5(\text{Si}_{1-x}\text{Ge}_x)_4$, have outstanding MCE properties, significantly better than the well known standard, Gd metal. The giant MCE effect observed in the $\text{Gd}_5(\text{Si}_{1-x}\text{Ge}_x)_4$ alloys for $x \geq 0.5$ is due to a coupled magnetostructural transformation. The coupled transformation also accounts for several other interesting phenomena – giant magnetoresistance; colossal magnetostriction; spontaneous generation of voltage; unusual training, dynamical and thermal phenomena; acoustic emissions; and a novel glass-like kinetically retarded state. Extension of the work on the MCE has led to the near commercialization of magnetic refrigeration as a viable cooling technology, and to the discovery of ductile RM (R = rare earth, T = transition metal) B2 cesium chloride-type intermetallic compounds.

9:15 AM Invited

Strongly Correlated Electron Phenomena in Filled Skutterudite Compounds: *M. Brian Maple*¹; ¹University of California, San Diego

The filled skutterudite compounds MT_4X_{12} (M = alkali metal, alkaline earth, lanthanide, actinide; T = Fe, Ru, Os; X = P, As, Sb) display a wide variety of

strongly correlated electron phenomena and are candidates for thermoelectric applications. The strongly correlated electron phenomena include conventional BCS superconductivity, unconventional superconductivity, magnetic order, quadrupolar order, valence fluctuation behavior, heavy fermion behavior, non-Fermi liquid behavior, and hybridization gap insulator behavior. When M is a lanthanide or actinide atom, the localized f-states hybridize with the ligand-states of the surrounding pnictogen atoms that form atomic “cages” within which the M atoms reside. The ground states are determined by a delicate interplay between the hybridization of the f- and ligand-states, crystalline electric field splitting of the f-electron energy levels, magnetic and quadrupolar interactions, and electron band structure. Examples of the strongly correlated electron phenomena found in filled skutterudite compounds are reviewed in this talk.

9:45 AM Invited

Progress in Understanding the High Ductility of Rare Earth B2 (CsCl-type) Intermetallics: *Alan Russell*¹; *Karl Gschneidner, Jr.*¹; *S. Biner*¹; *L. Chumbley*¹; *Sujing Xie*¹; *Andrew Becker*¹; *Qian Chen*¹; *Andrew Frerichs*¹; *Scott Williams*¹; ¹Iowa State University

In recent years, several rare earth intermetallic compounds with the B2 (CsCl-type) structure have been reported to exhibit high tensile ductility and high KIC fracture toughness at room temperature; these materials retain considerable ductility even at 77K. These are noteworthy findings because most intermetallics possess poor room temperature ductility and low fracture toughness unless one or more special “contrivances” are applied (e.g., doping with small additions of interstitial elements, off-stoichiometric compositions, testing in ultra-dry atmospheres, etc.). This presentation will summarize recent findings on rare earth B2 intermetallics’ active slip systems; their strain rate sensitivities and yield strength maxima at elevated temperatures; the search for possible twinning and stress-induced phase transformations; ab initio calculations on their defect energies and the anisotropy of dislocation line tension; the potential applications of these materials; and the possibilities that their study may suggest ductilizing strategies for other intermetallic compounds.

10:10 AM

Magnesium Rare Earth B2 Intermetallics: Brittle Behaviors in a Family of Ductility: *James Wollmershauser*¹; *Sean Agnew*¹; ¹University of Virginia

Intermetallics with B2 (CsCl) structure, comprised of a rare earth metal and a late transition metal have recently been shown to be a new family of ductile compounds. The present study was initiated to determine if rare earth metal – magnesium compounds would exhibit a similar effect. However, polycrystalline MgCe and MgNd are revealed to exhibited brittle transgranular cleavage fracture. SEM-based stereology plus electron backscatter diffraction (EBSD), has been used to determine the cleavage plane present. All of the intermetallics presently under investigation are line compounds MgY, MgCe, MgNd, and MgDy possess the B2 structure, verified by x-ray diffraction. It is hoped that by further defining the qualifications for ductility in B2 intermetallics, more complete theories can be realized and their applications can be expanded.

10:20 AM

A Comparative Neutron Diffraction Study of B2 Intermetallics: *James Wollmershauser*¹; *Sean Agnew*¹; ¹University of Virginia

Intermetallic alloys with fully-ordered B2 (CsCl) structures were examined by in-situ neutron diffraction. The alloys under investigation (NiAl, CoZr, AgCe, and CuZn) exhibit a wide range of ductility. It is important to note that, depending upon the operative dislocation slip modes, many materials with the B2 structure fail to satisfy the Taylor criterion requiring 5 independent slip systems and, therefore, should not be ductile. Of the selected alloys, only the brass is known to satisfy the Taylor criterion, and should arguably be the only ductile alloy in the study. Indeed, NiAl is known to exhibit brittle behavior at room temperature. However, CoZr and some rare-earth containing compounds similar to AgCe, have recently been shown to sustain approximately 20% room temperature elongation. The experiments are designed to determine if the internal strain and Bragg peak intensity evolutions of the B2 compounds correlate with distinctions in their propensities to exhibit appreciable ductility.

10:25 AM Break

10:40 AM Invited**X-Ray Magnetic Circular Dichroism (XMCD) for Rare Earth Magnets: Toward Quantitative Analysis:** *Bruce Harmon*¹; ¹Iowa State University

In 1992 and 1993 sum rules for x-ray magnetic circular dichroism (XMCD) were derived, and have since been employed with great benefit for studies involving magnetic materials containing 3d-transition elements. The great utility of these sum rules applied to XMCD spectra stems from their ability to extract element and orbital specific information (spin and orbital magnetic moments) for highly complex alloys and compounds. Unfortunately these sum rules break down when applied to rare earth elements. Since rare earths are often constituents for the best permanent magnets, there is strong motivation to develop XMCD into a quantitative analytical tool for analysis. This talk will focus on the physics of rare earth magnetism and the odyssey of unraveling the intricacies of why the XMCD spectra disobey the sum rules. Emphasis will be on recent examples of first principles electronic structure calculations in concert with precise experiments on rare earth containing magnetic materials.

11:10 AM Invited**Research on 5f Electron Systems: Surprises at the End of the Periodic Table:** *Gerard Lander*¹; ¹European Commission, JRC, Institute for Transuranium Elements

Experiments on the transuranium elements are difficult, time consuming, require special facilities, and deal with material that is actually changing during the experiment. Despite this, new effects can be found in this little explored part of the periodic table that are relevant to some of the important questions in condensed-matter physics. Although the heavier actinide elements show behavior reminiscent of their 4f analogs, the lighter actinide elements (U, Np, Pu) are quite different. Recent experiments, mainly involving the application of pressure, have shown how these two different aspects are connected. This talk will make comparisons between the physics of the 4f and 5f systems and will focus mainly on the elements but include also some discussion on the recently discovered 18 K superconductor, PuCoGa₈.

11:40 AM Invited**Optimization of Ionic Conductivity in Doped Ceria:** *Borje Johansson*¹; ¹Royal Institute of Technology and Uppsala University

Oxides with the cubic fluorite structure, e.g., ceria (CeO₂), are known to be good solid electrolytes when they are doped with cations of lower valence than the host cations. The high ionic conductivity of doped ceria makes it an attractive electrolyte for solid oxide fuel cells, whose prospects as an environmentally friendly power source are very promising. In these electrolytes, the current is carried by oxygen ions that are transported by oxygen vacancies, present to compensate for the lower charge of the dopant cations. Ionic conductivity in ceria is closely related to oxygen-vacancy formation and migration properties. A clear physical picture of the connection between the choice of a dopant and the improvement of ionic conductivity in ceria is still lacking. Here we present a quantum-mechanical first-principles study of the influence of different trivalent impurities on these properties. Our results reveal a remarkable correspondence between vacancy properties at the atomic level and the macroscopic ionic conductivity. The key parameters comprise migration barriers for bulk diffusion and vacancy-dopant interactions, represented by association (binding) energies of vacancy-dopant clusters. The interactions can be divided into repulsive elastic and attractive electronic parts. In the optimal electrolyte, these parts should balance. This finding offers a simple and clear way to narrow the search for superior dopants and combinations of dopants. The ideal dopant should have an effective atomic number between 61 (Pm) and 62 (Sm), and we elaborate that combinations of Nd/Sm and Pr/Gd show enhanced ionic conductivity, as compared with that for each element separately.¹ ¹D. Andersson et al. PNAS | March 7, 2006 | vol. 103 | no. 10 | 3518-3521.

12:10 PM Invited**Electrochemical Single Crystal Growth by Electrolyzing Rare Earth Ion Conducting Solids:** *Nobuhito Imanaka*¹; ¹Osaka University

In general, for the single crystal growth, the starting materials should be heated above the melting temperature of the target compounds by the conventional procedures such as Czochralski, Verneuil methods. Accordingly, the operating temperature is high if the compounds are refractory oxides. In this presentation, however, single crystals of the high refractory rare earth oxides such as Sc₂O₃,

Y₂O₃ were grown by dc electrolyzing the Ln₂(MoO₄)₃ solid electrolytes at elevated temperatures. Here, solid electrolytes (ion conducting solids) are the solid materials that only single ion species can conduct in solids. In addition, single crystals of the intermediate oxide phases of Tb_nO_{2n-2m} were also successfully grown for the first time by the electrolysis.

Recent Industrial Applications of Solid-State Phase Transformations: Superalloys and TRIP Steels/Automotive Steels

Sponsored by: The Minerals, Metals and Materials Society, TMS Materials Processing and Manufacturing Division, TMS/ASM: Phase Transformations Committee
Program Organizer: Milo Kral, University of Canterbury

Monday AM

March 10, 2008

Room: 287

Location: Ernest Morial Convention Center

Session Chair: Milo Kral, University of Canterbury**8:30 AM Introductory Comments****8:35 AM Keynote****Is Phase Transformation Research Still Important?:** *Morris Fine*¹; *Sungho Jin*²; ¹Northwestern University; ²University of California at San Diego

Does further research on solid-state phase transformations have a high probability of being scientifically important and industrially useful at this time? This Symposium's answer is a strong yes! The large number of presentations in this Symposium's program is proof to that answer. All processes for making materials (sintering, mechanical working, thermal treatment, microstructural manipulations, self-assembly, etc) are basically accomplished by phase transformations. Degradation of materials (corrosion, mechanical failure, overaging of the microstructure, etc) occurs by phase transformations. Nanotechnology is becoming a subject of great interest to the scientific and industrial community these days. Achieving desired structures down to the sub-nano scale often depends on phase transformations and their control. Examples of recent important developments will be given for a variety of materials such as biological materials, electronic materials and magnetic materials.

9:25 AM Invited**Precipitation Simulation of Nickel Alloys:** *Fan Zhang*¹; *Kaisheng Wu*¹; *Y. Chang*²; ¹CompuTherm LLC; ²University of Wisconsin

The mechanical properties of a material depend on its microstructure which is determined by the alloy chemistry and processing conditions. To achieve desired microstructure and mechanical properties, alloy chemistry and processing parameters need to be carefully selected and optimized. This optimization process, normally accomplished by a slow and labor-intensive series of experiments, is significantly sped up due to the modeling efforts currently being undertaken. In this presentation, we will present efforts in the modeling of U720 alloy, which includes both thermodynamic calculation and kinetic simulation. Thermodynamic calculation is based on the Calphad approach, while kinetic simulation of γ' precipitation is based on the mean-field approximation. This modeling tool allows the simulation of the amount of γ' precipitate, its average size and size distribution change with heat treatment conditions for U720 alloy. It can also be applied to other nickel alloys and integrated with other models.

9:50 AM Invited**Development of Microstructure Modeling Tools for Industrial Applications Using Phase Field Approach:** *Ning Ma*¹; *Billie Wang*¹; *Yunzhi Wang*¹; ¹Ohio State University

Phase transformations in solid state are usually dominated by long-range elastic interactions among different defects and produce extremely complicated microstructures with strong spatial correlation and anisotropy. The traditional constitutive models representing microstructural features by their average values may not be sufficient to quantitatively define the microstructure. In this presentation we review our recent efforts in developing quantitative microstructure modeling tools for industrial applications using the phase field approach that has proven to be able to handle realistic microstructural

patterns. In particular we show the synergy of coupling phase field simulations to experimental characterization in developing fundamental understanding of the mechanisms that govern microstructural evolution during solid state phase transformations, upon which fast-acting models could be formulated for direct industrial applications. Critical issues related to modeling nucleation and interaction among different extended defects will be addressed. Examples of applications will be given for Ni-base superalloys and alpha/beta Ti alloys.

10:15 AM

Prediction of Microstructure Evolution of Ni-Base Superalloy Bond Coats: *Carelyn Campbell*¹; ¹National Institute of Standards and Technology

The high temperature performance of many superalloys depends on a thermal barrier coating (TBC). A bond coat is placed between the superalloy and the TBC to act as a diffusion barrier and to accommodate large difference in thermal expansion between the TBC and the superalloy. Understanding the microstructure evolution at the substrate/bond coat interface is a critical step to predicting the life of the TBC system. Diffusion simulations, using multicomponent thermodynamics and diffusion mobilities, predict the microstructure evolution of various Ni-base superalloys and bond coat compositions. The Ni-base superalloy consists of a γ (fcc) matrix with γ' (L_{12}) and various carbide precipitates. The bond coat compositions considered are either single phase B2 (ordered BCC) or a B2 matrix with γ' precipitates. 1-D diffusion simulations that predict the composition and phase fraction profiles to optimize the bond coat composition are presented and discussed.

10:40 AM Break

10:50 AM Invited

Transformation Behaviors of Intercritically Annealed and As-Hot Rolled TRIP Steels: *John Jonas*¹; *Youliang He*²; ¹McGill University; ²Cornell University

TRIP steels can be prepared by intercritical annealing followed by transformation into bainite or else employed directly after hot rolling and transformation. The textures formed by following these two contrasting processing routes are presented and compared. Another aspect of importance is whether hot rolling is carried out above or below the T_{nr} or recrystallization-stop temperature. In the former case, the austenite microstructure is equiaxed prior to transformation, whereas in the latter case, it is flattened or "pancaked". This aspect of hot rolling also affects the transformation texture. The austenite texture components responsible for the principal features of the as-hot rolled bainite textures are described. In a similar manner, the ferrite texture components responsible for the principal features of the intercritically processed material are also presented. The role of variant selection in accentuating some of the features of the final textures is also considered.

11:15 AM Invited

Orientation Relationships and Variant Selection during Phase Transformations in Ultra High Performance Steels: *Stephane Godet*¹; *Arnaud Péteín*²; *Pascal Jacques*²; ¹Université Libre de Bruxelles; ²Université Catholique de Louvain

In recent years, TRIP steels have drawn the attention of many researchers, mainly because of their exceptional mechanical properties that render them very attractive to the automotive industry. Their large ductilities and high work-hardening rates originate from the dynamic transformation of austenite in martensite (TRansformation Induced Plasticity). Specimens were deformed at various temperatures. The orientation relationships holding during the different phase transformations (i.e. the transformation of austenite into bainite and epsilon or alpha' martensite) were characterised using high-resolution orientation imaging and EBSD techniques. The results are presented in the fundamental zones of Rodrigues-Frank space corresponding to the different phase transformations under consideration (cubic to cubic or cubic to hexagonal transformations). Rodrigues-Frank space enables a straightforward comparison with the various orientation relationships proposed in the literature. The variant selection taking place during these transformations is also analysed.

11:40 AM Invited

Recent Development in Transformation Hardening Steel Sheets for Automobile: *Hiroshi Takechi*¹; ¹Fukuoka Institute of Technology

For reducing fuel consumption and CO₂ emission, weight saving of car should be promoted by using high strength steel sheets (HSS). Many kinds of HSS have been developed, in which transformation hardening HSS such as DP (Dual Phase) steel and TRIP (TRansformation Induced Plasticity) steel are highly evaluated on the relationship among strength, formability and energy absorption during car crashing. Metallurgical features of the transformation hardening HSS are presented as well as a new mechanism for controlling deep drawability of TRIP steel by transformed components. Another recent technology called hot stamping is compared with the application of transformation hardening HSS to produce stronger automobile parts.

12:05 PM Invited

Strategy and Application of Bar Steels Development for Future Automotive Components: *Hyounsoo Park*¹; ¹Hyundai Motors

A major trend of automotive components development has been practically focused on maximizing the fatigue strength while minimizing the production cost. To achieve this goal, a combined approach should be considered both in alloy design and process optimization. Microalloy steels, mainly for the application of engine and chassis components, have been widely used to eliminate additional quenching-tempering heat treatment after forging process. Traditional ferritic-pearlitic microalloy steels have been widely used for crankshafts and connecting rods. Due to the needs for higher endurance limit for heavy-duty engine performance, needs for higher strength steels has been raised while fulfilling affordable machinability and cost saving. This paper will introduce recent development in next generation microalloy steels for the essential parts of engines and chassis. Regarding development of the transmission gear and shaft steels, a new approach has been carried out to achieve both high strength and cost saving. Vacuum carburizing at higher temperature exhibits the best results. This treatment should be accompanied by special alloy design application for the best results. In this presentation, details of new application and development of innovative alloys along with the controlled forging, state of art carburizing process.

Structural Aluminides for Elevated Temperature Applications: Applications

Sponsored by: The Minerals, Metals and Materials Society, TMS Structural Materials Division, TMS: High Temperature Alloys Committee, TMS/ASM: Mechanical Behavior of Materials Committee

Program Organizers: Young-Won Kim, UES Inc; David Morris, Centro Nacional de Investigaciones Metalúrgicas, CSIC; Rui Yang, Chinese Academy of Sciences; Christoph Leyens, Technical University of Brandenburg at Cottbus

Monday AM

March 10, 2008

Room: 394

Location: Ernest Morial Convention Center

Session Chairs: Dennis Dimiduk, US Air Force; Wilfried Smarsly, MTU Aero Engines GmbH

8:30 AM Opening Remarks

8:40 AM Invited

Gamma TiAl Applications at GE Aviation: *Michael Weimer*¹; *Thomas Kelly*¹; ¹GE Aviation

Overview of the implementation status of GE alloy 48Al-2Nb-2Cr applications in aircraft engines. This will be an update of the presentation made in Bamberg in May of 2006.

9:10 AM

Refractory Crucible Melting and Related Mechanical Properties of Nb-Containing TiAl Alloys: *Antonin Dlouhy*¹; *Katerina Docekalova*¹; *Ivo Dlouhy*¹; *Ladislav Zencik*²; ¹Academy of Sciences; ²Brno University of Technology

Aiming at a cheaper processing technology, the present study focuses on a vacuum induction melting and related mechanical properties of Nb-containing

TiAl intermetallic cast parts. The attention is mainly given to a cost-effective melting process in which a primary alloy ingot is re-melted in a ceramic crucible and cast into a ceramic shell mould. Besides standard Al₂O₃ coated crucibles, a new type of crucible (based on Y₂O₃) is considered. Depending on the refractory type and the coating strategy, there is a potential for chemical reactions between the molten intermetallic and the crucible wall. Results suggest that the wall attack can be considerably limited by either using the Y₂O₃ (with no SiO₂-type binder) or by a suitable wall coating. Mechanical properties of the Nb-containing alloys were investigated before and after remelting in the refractory crucibles. Results show that a limited impairment of alloy strength may occur due to remelting.

9:30 AM

The Development of a Tranquil Tilt Pouring Process for Casting Titanium Aluminides: *Richard Harding*¹; Michael Wickins¹; Hong Wang²; Georgi Djambazov²; Koulis Pericleous²; ¹University of Birmingham; ²University of Greenwich

Reactive alloys such as gamma TiAl are commonly melted in water-cooled crucibles using processes such as Induction Skull Melting (ISM). The limited superheat is compensated for by rapid mold filling, but the resulting surface turbulence readily entrains gas bubbles which often persist as defects in the solidified casting. The present research has developed a novel quiescent casting process for TiAl which combines clean melting in an ISM with the well-established Durville tilt casting method. The potential of this process has been explored using a combination of practical trials and a novel computer model of mold filling, heat transfer and solidification. This paper will describe the equipment used to evaluate the feasibility of this process, and show examples of its use to produce TiAl turbine blades up to 300 mm long. Numerical results will be included which highlight the importance of rotation control, vent location and superheat retention on defect elimination.

9:50 AM

Refractories as Mould Face Coatings for Investment Casting TiAl-Based Alloys: *Qing Jia*¹; Yuyou Cui¹; Rui Yang¹; ¹Institute of Metal Research CAS

Interfacial reactions between Ti-46Al (at.%) casting and ceramic shell mould made of ZrO₂ and Al₂O₃ were compared using a range of techniques. On the surface of the TiAl casting, a reaction layer as thick as 230µm was found in the case of the zirconia mould, whereas there was no visible reaction layer for the alumina mould. Electron probe microanalysis indicated that elements of the two kinds of shell moulds diffused into the alloy melt during casting but to different extents. Metallographic analysis, microhardness measurements and composition analysis showed that alumina was stable and suitable for use as shell moulds when casting TiAl based alloys. In the case of zirconia however Al₂Zr formed at the dendrite boundaries of gamma TiAl constituting the reaction layer. It is concluded that zirconia-based face coat, while suitable for casting titanium alloys, is not suitable for casting TiAl although the latter is generally regarded less reactive.

10:10 AM Break**10:20 AM Invited**

Current Status of Mass Production of Gamma Titanium Aluminide Alloy Turbine Rotors in Turbochargers and Future Challenges: *Toshiharu Noda*¹;

¹Daido Steel Company, Ltd.

Gamma titanium aluminide alloys have a great potential for use in aircraft engine and automobile engine components. Since we demonstrated the potential of gamma titanium aluminide as a turbocharger turbine wheel in 1987, a great effort has been paid in order to put the gamma titanium aluminide turbine wheel to practical use. Through successful development of a gamma titanium aluminide alloy and of processes of casting and joining between the turbine wheel and an alloy steel shaft, we got into mass production of titanium aluminide turbine rotors of turbochargers for passenger car application in 2003. Current automobile companies compete fiercely to develop more fuel-efficient car in order to reduce CO₂ emission. Turbocharger is focused on as one of the key technologies to downsize engines. In this paper, current status of mass production of cast gamma titanium aluminide turbine rotors in turbochargers is discussed along with future challenges.

10:50 AM

Development of the Cost-Affordable TiAl Alloy Based Turbo-Charger Rotor: *Si Young Sung*¹; Myoung Gyun Kim²; Sang Ho Noh¹; Beom Suck Han¹; Young Jig Kim³; ¹Korea Automotive Technology Institute (KATECH); ²RIST/ New Metallic Materials Research Team; ³Sungkyunkwan University

A turbo-charger rotor has been focused on the increment of both the power efficiency and the fuel reduction in an automotive internal combustion engine. However, the "turbo-lag" which delays the steady state operation of turbo-charger under 2,000 rpm is a fatal disadvantage. The simplest way to improve the performance of them is to substitute the lightweight materials the turbine wheel for steels and Ni-based superalloys. TiAl alloys could be a substantial alternative since they have the combination of high specific strength, excellent mechanical properties, and heat resistance. In our study, as a feasible approach for the economic net-shape forming of TiAl turbocharger, the alpha-case formation, fluidity, alloy design for the improvement of oxidation resistance, and welding. The results of the investment casting of TiAl alloys confirm that the casting route can be an effective approach for the economic net-shape forming of TiAl alloys.

11:10 AM

Properties of Cast Al-Rich Ti-Al Alloys: *Michael Paninski*¹; Anne Drevermann¹; Georg Schmitz¹; Martin Palm²; Frank Stein²; Nico Engberding²; Martin Heilmair³; Holger Saage³; Klemens Kelm⁴; Stephan Irsen⁴; ¹ACCESS Materials and Processes; ²Max-Planck-Institut für Eisenforschung GmbH; ³Otto-von-Guericke-Universität Magdeburg; ⁴Caesar Research Center

Gamma TiAl alloys with a lamellar TiAl + Ti₃Al microstructure are on their way into industrial application but oxidation at operating temperatures exceeding 900°C still poses a problem. Titanium alloy systems with an increased aluminum content are expected to reveal a higher oxidation resistance and provide a significant additional weight reduction up to 20 percent. Casting processes like ISM (Induction Skull Melting), Investment Casting and Bridgman Solidification will be presented. Furthermore the temperature dependant mechanical properties and a characterization of the microstructure by combined TEM imaging techniques of Al-rich TiAl + Al₂Ti alloys will be discussed, as well as the influence of alloy modifications with Nb and Cr.

11:30 AM

The Solidification Feature of TiAl Alloy with Different Boron Addition: *Kui Liu*¹; Bo Chen¹; Yingche Ma¹; Ming Gao¹; Weidong Wang¹; Yiyi Li¹; ¹Institute of Metal Research

The behavior during solidification process of Ti₄₅Al₈Nb with different boron addition from 0.2at% to 0.7 at.%B has been studied by high temperature heating the sample at L+beta phase zone and quickly quenched it to preserve the solidified feature method. Optical microscope and SEM analysis show B addition really affected Ti₄₅Al₈Nb initial solidified temperature but not effect on the final solidified temperature. Boride has begun precipitating in the liquid phase at more boron addition, but low content it just appeared at low temperature, in L+beta phase zone. Solidified structure of Ti₄₅Al₈Nb with different boron content gives the results that big beta grain formed at low boron addition, and small beta grain in the high boron alloy. Beta grain refinement by added certain amount of boron in Ti₄₅Al₈Nb alloy in this study on its solidification process may be benefited to clarify boron refining mechanism to TiAl alloys.

11:50 AM

Development of a Cost-Effective Recycling Process for Titanium Aluminides: *Bernd Friedrich*¹; Jan Reitz¹; Claus Lochbichler¹; ¹IME Process Metallurgy and Metals Recycling

An innovative recycling concept for scraps from intermetallic titanium alloys has been developed and successfully proved at laboratory and semi-pilot scale at the IME. It is based on vacuum induction melting (VIM) for melt-down and homogenization of the scraps, using ceramic crucibles and thus accepting a significant oxygen pick up at first-hand. Subsequently VIM and electroslog remelting (ESR) are used for deoxidization. In a last step vacuum arc remelting (VAR) is applied for final refining and consolidation. The process allows the treatment of various scrap types (flexibility) and for correcting the initial melt composition. Careful investigations on the origin of non-metallic inclusions (NMI) have been conducted particularly with regard their subsequent removal in VAR, along with other impurities from the desoxidation step. With 95% of TiAl

being scrapped along present processing routes, this recycling process promises substantial cost-reduction.

Sustainability, Climate Change and Greenhouse Gas Emissions Reduction: Responsibility, Key Challenges and Opportunities for the Aluminum Industry

Sponsored by: The Minerals, Metals and Materials Society, TMS Light Metals Division
Program Organizer: Halvor Kvande, Hydro Aluminium AS

Monday, 8:30 AM Room: 295/296
March 10, 2008 Location: Ernest Morial Convention Center

Session Chair: Halvor Kvande, Hydro Aluminium

Presentations by the world's leading aluminum companies, including:

Dick Evans, Rio Tinto Alcan

Bernt Reitan, Alcoa Inc

Eivind Reiten, Norsk Hydro

Chalco (tentative)

United Company Rusal (tentative)

Program will conclude with a panel discussion by the presenters. There will be an opportunity for the audience to ask questions of the panelists.

Ultrafine-Grained Materials: Fifth International Symposium: Modeling, Theory, and Property

Sponsored by: The Minerals, Metals and Materials Society, TMS Structural Materials Division, TMS Materials Processing and Manufacturing Division, TMS: Shaping and Forming Committee, TMS: Nanomechanical Materials Behavior Committee
Program Organizers: Yuri Estrin, Monash University and CSIRO Melbourne; Terence Langdon, University of Southern California; Terry Lowe, Los Alamos National Laboratory; Xiaozhou Liao, University of Sydney; Zhiwei Shan, Hysitron Inc; Ruslan Valiev, UFA State Aviation Technical University; Yuntian Zhu, North Carolina State University

Monday AM Room: 273
March 10, 2008 Location: Ernest Morial Convention Center

Session Chairs: Yuri Estrin, Monash University; Vesselin Yamakov, National Institute of Aerospace; Florian Dalla Torre, Swiss Federal Institute of Technology; Suveen Mathaudhu, US Army Research Laboratory

8:30 AM Introductory Comments

8:35 AM Invited

On the Role of Diffusion Creep in the Deformation of Nanocrystalline Materials: Paul Millett¹; Tapan Desai¹; Dieter Wolf²; ¹Idaho National Laboratory

We have previously demonstrated by means of molecular-dynamics simulation that for the very smallest grain sizes, nanocrystalline silicon and nanocrystalline fcc metals deform via grain-boundary diffusion creep, provided the applied stress is low enough to avoid microcracking and dislocation nucleation from the grain boundaries. Here we review recent MD simulations that show that in the absence of grain growth both, a nanocrystalline model bcc metal (Mo) and a model metal oxide (UO₂) also deform via diffusion creep. However, in the case of Mo both grain-boundary and lattice diffusion are observed to contribute to the creep rate; i.e., the deformation mechanism involves a combination of Coble and Nabarro-Herring creep. Moreover, in the case of UO₂ chemical diffusion of both ionic species through the grain boundaries represents the rate-controlling process that governs the intricate interplay between grain-boundary sliding and grain-boundary diffusion during the Coble creep.

8:55 AM

Multiscale Modeling of Fracture in Ultrafine Grained Aluminum: Constitutive Relation for Interface Debonding: Vesselin Yamakov¹; Erik Saether²; Dawn Phillips³; Edward Glaesgen²; ¹National Institute of Aerospace; ²NASA/Langley Research Center; ³Lockheed Martin Space Operations

Intergranular fracture is a dominant mode of failure in ultrafine grained materials. In the presented study, the atomistic mechanisms of grain-boundary debonding during intergranular fracture in aluminum are modeled using a coupled molecular dynamics – finite element simulation. Through a developed statistical procedure, a series of constitutive traction-displacement relationships characterizing the load transfer across a growing edge crack at different loading conditions are extracted from atomistic simulations and then recast in a form suitable for inclusion within continuum finite element models. A cohesive zone model, which incorporates the atomistic aspects of the elasto-plastic processes at the crack tip is created. The sensitivity of the extracted cohesive zone models on the conditions of the simulation, system size and temperature, is discussed for the example of a high-angle S99 symmetric tilt grain boundary in aluminum. The study is a step towards relating atomistically derived decohesion laws to macroscopic predictions of fracture.

9:10 AM

Atomistic Simulations of Diffusional Creep in Nanocrystalline BCC Molybdenum: Paul Millett¹; Vesselin Yamakov²; Tapan Desai¹; Dieter Wolf¹; ¹Idaho National Laboratory; ²National Institute of Aerospace

As grain sizes are reduced to ultra-fine and nanocrystalline dimensions, the role of diffusional creep as a dominant deformation mechanism becomes important. In this work, molecular dynamics (MD) simulations are used to study diffusion-accommodated creep deformation in nanocrystalline molybdenum, a body-centered cubic metal commonly used as structural cladding. The microstructures are subjected to constant-stress loading at levels below the dislocation nucleation threshold and at high temperatures (i.e., $T > 0.75T_{\text{melt}}$) thereby ensuring that the overall deformation is indeed attributable to atomic diffusion. Remarkably, the results show that both GB diffusion in the form of Coble creep and lattice diffusion in the form of Nabarro-Herring creep contribute to the overall deformation. Visual analysis confirms that the GB's serve as sources for lattice vacancies that form within the GB's and subsequently emit into the grain interiors thus enabling lattice diffusion.

9:25 AM

Molecular Dynamics Simulations of Dislocation Nucleation from Special and General Grain Boundaries in Fcc Metal Bicrystals: Yvonne Ritter¹; Alexander Stukowski¹; Karsten Albe¹; ¹Technische Universität Darmstadt

Plastic deformation of nanostructured metals is determined by an intricate interplay between dislocation motion and grain boundary (GB) processes. Although it is well established that grain boundaries in nanocrystalline materials serve as sources for dislocations, the fundamental mechanisms of dislocation nucleation are still not understood. In this contribution we investigate detail mechanisms of dislocation nucleation from grain boundaries of elemental fcc metals by molecular dynamics simulations. Rather than simulating the deformation of nanocrystalline microstructures, we are studying well defined bicrystal geometries. Special tilt and twist GBs as well as general GBs are considered under various loading conditions and the influence of materials parameters, loading and grain boundary structure are discussed.

9:40 AM

Intrinsic Microstrain in Nanocrystalline Metals: Jürgen Markmann¹; Vesselin Yamakov²; Alexander Stukowski³; Karsten Albe³; Jörg Weissmüller⁴; ¹Universität des Saarlandes; ²National Institute of Aerospace; ³Technische Universität Darmstadt; ⁴Forschungszentrum Karlsruhe in der Helmholtz-Gemeinschaft

Determination of the grain size and microstrain by x-ray diffraction is an important characterisation technique when investigating nanocrystalline materials. Interestingly, the observed microstrain in nanocrystalline metals exceeds the one measured in even heavily deformed conventional materials. To investigate this, defect-free nanocrystalline 3-dimensional microstructures containing between 16 and 1024 grains were thermally relaxed at 300 K by molecular dynamics simulation. X-ray diffractograms were calculated and the x-ray peak broadening was analysed to determine the average grain size and

microstrain. The evaluated grain size is in excellent agreement with the grain size of the starting microstructure. Nevertheless there is a large amount of microstrain in the relaxed samples. The lack of extrinsic sources for microstrain in these "samples" supports an intrinsic nature of microstrain in nanocrystalline metals. Investigation of atomic stress levels were used to localise the microstrain and to determine the underlying mechanism of its occurrence.

9:55 AM Invited

Modeling Microstructure and Mechanical Properties of Polycrystalline Materials that Deform by Multiple Slip and Twinning Modes under Severe Plastic Deformation: *Irene Beyerlein*¹; ¹Los Alamos National Laboratory

This talk will present recent results from our theoretical and experimental program focused on texture and substructure evolution and plastic deformation after severe plastic deformation. In our previous work, we developed a multi-scale model for equal channel angular extrusion including the macroscale extrusion [Mat. Sci. Engng. 380 (2004) 171], polycrystal deformation, and individual crystal hardening [Int. J. Plast. 23 (2007) 640]. For materials that deform by one slip mode, such as Cu and Al, the model could reasonably predict texture evolution and mechanical behavior in subsequent reloading of the processed material [J. Mat. Sci. 42 (2007) 1733]. The mechanisms leading to important features, such as anisotropy, work softening, and tension-compression asymmetry, could be studied. Using the same basic framework, we extend our application to materials that deform by multiple slip and twinning modes. In this case, the model must accurately find their relative contributions and treat appropriately their interactions.

10:15 AM Break

10:30 AM Invited

On the Derivation of the Cottrell-Stokes Law for Very Small Grain Size Metals: *Yannick Champion*¹; ¹Centre National de la Recherche Scientifique

In large grain sized ductile metals, multiplication and interactions between mobile dislocations leads to an inverse dependence between the activation volume and the stress; this behaviour is known as the Cottrell-Stokes law. When the grain size is refined to fine grain and nanoscale domains, a linear dependence is observed up to a non-dependence of the activation volume with stress at low strain rate and/or high temperature. This behaviour was observed on nanostructured copper with grain size of 90 nm. Activation volume was measured by jump test and stress relaxation technique from RT to 120°C. Derivation of the Cottrell-Stokes law is proposed for small grain size metals starting with the Orowan relation and taking into account the contribution of grain-boundaries in the mechanism of plasticity.

10:50 AM

Role of Microstructural Inhomogeneity on Stress Concentration during Grain-Boundary-Controlled Creep Deformation in Polycrystals: Lucian Zigoneanu¹; Jijun Lao¹; *Dorel Moldovan*¹; ¹Louisiana State University

Grain boundary diffusion and grain boundary sliding are widely accepted as the main plastic deformation mechanisms in fine-grained polycrystalline metals and ceramics at high homologous temperatures. Mesoscopic simulations are used to elucidate the effects of grain size distribution and of heterogeneity in grain boundary diffusivity and grain-boundary sliding resistance on creep deformation and stress concentration in polycrystals. Considering two-dimensional model microstructures we investigate the stress distribution around various topological and grain boundary inhomogeneity (i.e., distributions in grain boundary diffusivities and sliding resistances) at the onset of creep and during the steady state regime. Our simulations indicate that at higher strains the mechanism of grain boundary migration plays a critical role in mediating various topological transformations crucial for maintaining the equiaxed character of the microstructure.

11:05 AM

Finite Element Modeling and Experimental Validation of Equal Channel Angular Pressing: *Venkata Nagasekhar Anumalasetty*¹; Tick-Hon Yip²; ¹University of Queensland; ²Nanyang Technological University

Equal channel angular pressing (ECAP) is the most promising severe plastic deformation (SPD) for fabrication of bulk nanostructured materials, compaction of powders nearer to theoretical density, and property enhancement of tubular materials. In current study, single pass ECAP finite element modeling was carried

by using tool angles of 90 and 10 deg by considering the strain hardening behavior of pure copper. In order to validate the FEM results, pure copper is subjected to single pass ECAP at room temperature. Hardness measurements were carried in the flow plane of single pass ECAP copper. The effective strain variations are compared with the flow plane hardness measurements. Experimental and simulated load-stroke curves and peak load calculations are also compared. The results showed that FEA strain homogeneity has good conformity with hardness measurements, and peak load calculations.

11:20 AM

Effect of Strain on "Hardening by Annealing and Softening by Deformation" Phenomena in Ultra-Fine Grained Aluminum: *Daisuke Terada*¹; Hironobu Houda¹; Nobuhiro Tsuji¹; ¹Osaka University

Ultra-fine grained (UFG) metals fabricated by severe plastic deformation (SPD) sometimes exhibit peculiar mechanical properties. For example, it was reported that the strength increased by an annealing and decreased by deformation in UFG aluminum, which was totally opposite to the behaviors of conventional coarse grained materials. In this study, an effect of SPD strain on the peculiar phenomena was investigated. The UFG aluminum was fabricated by various cycles of the accumulative roll-bonding (ARB) process with lubrication. The specimen ARB processed by 10 cycles certainly showed the "hardening by annealing and softening by deformation" phenomena. On the other hand, the 6-cycle specimen did not show the phenomena, but was softened by annealing and hardened by deformation normally. The results will be discussed on the basis of microstructural differences.

11:35 AM

The Effect of the ECAP Induced Microstructure on Tensile Properties of an Al6082 Alloy: *Ilchat Sabirov*¹; Yuri Estrin²; Matthew Barnett¹; Ilana Timokhina²; Peter Hodgson¹; ¹Deakin University; ²Monash University

Aluminium alloy 6082 was subjected to 8 passes of equal channel angular pressing (Route B₁) at 100°C, which resulted in an ultra-fine grained (UFG) microstructure with an average grain size in the range of 0.2-0.4 µm. A pronounced effect of this extreme grain refinement on the strain rate sensitivity of the flow stress and the uniform tensile elongation was found. The classical Hart criterion of tensile necking fails to explain the observed enhanced ductility of the UFG material in the low strain rate regime. The mechanisms underlying plastic deformation of the UFG alloy were studied in detail by SEM and AFM analysis. The higher-than-expected uniform elongation is discussed in terms of the active deformation mechanisms.

11:50 AM

Grain Growth in Nanocrystalline Materials: Effect of Non-Linear Interface Kinetics: *Moneesh Upmanyu*¹; Paul Martin¹; Anthony Rollett²; ¹Colorado School of Mines; ²Carnegie-Mellon University

Grain growth in polycrystalline materials is based on a linear gradient approximation for the underlying interface migration (IM) rates, wherein the migration fluxes at the interfaces vary linearly with the driving force. Recent experimental studies have shown that coarsening of nanocrystalline interface microstructures is unexpectedly stable compared to conventional parabolic coarsening kinetics. Here, we show that during early stage coarsening of these microstructures, IM rates can develop a non-linear dependence on the driving force, the mean interface curvature. We derive the modified mean field law for coarsening kinetics. Molecular dynamics simulations of individual grain boundaries reveal a sub-linear curvature dependence of IM rates, suggesting an intrinsic origin for the slow coarsening kinetics observed in ultra-fine grained metals.

12:05 PM

Rate Dependent Characteristics of Pure Magnesium and ZK60 Alloy: *Shailendra Joshi*¹; Bin Li¹; Evan Ma¹; Kalpat Ramesh¹; Toshiji Mukai²; ¹Johns Hopkins University; ²National Institute for Materials Science

In the quest for light weight structural materials, nanostructured magnesium (Mg) and its alloys have generated tremendous interest as the potential candidates for strong structural components. Whereas the microstructural underpinnings of the mechanical behavior for both coarse-grained (CG) pure and alloyed Mg (e.g. ZK60) are reasonably well explored, the impact of ultrafine grain size on the mechanical properties remains elusive especially due to the strong influence of the texture. In this work, our goal is to articulate this relationship and

understand the pertinent deformation mechanisms. We perform strain controlled experiments on pure Mg and ZK60 over a wide range of strain rates (10⁻⁴ -10⁺⁴ s⁻¹) under compression. The corresponding microstructural characterization of the deformed microstructures as a function of the imposed strains provides insight in to the deformation mechanisms in the CG and fine-grained Mg alloys and its relation with the observed mechanical response.

2008 Nanomaterials: Fabrication, Properties, and Applications: Nanomaterials Synthesis

Sponsored by: The Minerals, Metals and Materials Society, TMS Electronic, Magnetic, and Photonic Materials Division, TMS: Nanomaterials Committee
Program Organizers: Seong Jin Koh, University of Texas; Wonbong Choi, Florida International University; Donna Senft, US Air Force; Ganapathiraman Ramanath, Rensselaer Polytechnic Institute; Seung Kang, Qualcomm Inc

Monday PM
 March 10, 2008
 Room: 274
 Location: Ernest Morial Convention Center

Session Chair: To Be Announced

2:00 PM Invited

Nanoprobes and Applications Based on Carbon Nanotubes: *Sungho Jin*¹; ¹University of California

The key component of the AFM is the probe tip, the size and properties of which determine the resolution and reliability of nanoscale imaging. We have fabricated an extremely sharp probe based on carbon nanocone structure directly grown on an AFM cantilever at a predetermined tilt angle by orientation-controlled DC plasma CVD process. The high-aspect-ratio yet thermal-vibration-resistant geometry, together with excellent mechanical strength of the carbon nanocone AFM probes offer many advantages for nanoscale imaging in nanotech and biotech applications. We have also fabricated MFM probes for analysis of magnetic nanostructures, and special AFM probes with extremely low modulus, about three orders of magnitude reduced, for imaging of soft matters, living cells or delicate components. Stresses and Si cantilever beam bending introduced during CVD growth of carbon nanotubes, and techniques to prevent such undesirable geometry changes are also discussed.

2:30 PM

Nanotechnology in Early Disease Detection and Diagnostics: *Matt Trau*¹; ¹University of Queensland

Diagnostics that detect diseases such as cancer at an early stage, when the disease is most responsive to contemporary therapies, provide the greatest social and economic benefits to society. This has been demonstrated in early disease detection programs such as the PAP smear cervical cancer test and colonoscopy for colon cancer. Unfortunately, current diagnostic protocols typically depend on a complicated variety of tests based on a wide range of different, and often expensive, technological platforms. Each different platform requires significant investment in single-use equipment and training. Despite this investment, results can be ambiguous and require multiple, different tests to produce a confirmed result for a single pathogen. Nanotechnology offers the promise of miniaturized, inexpensive, flexible and robust "plug-and-play" molecular reading systems which can be effectively deployed in the field. In this talk we will present several platforms which our Centre is currently developing for such applications.

2:45 PM

Quantum-Dot-Activated Luminescent Carbon Nanotubes via a Nano Scale Surface Functionalization for In Vivo Imaging: *Donglu Shi*¹; Yan Guo¹; Zhongyun Dong¹; Jie Lian¹; Wei Wang¹; Guokui Liu²; Lumin Wang³; Rodney Ewing²; ¹University of Cincinnati; ²Argonne National Laboratory; ³University of Michigan

A critical challenge for biomarking, based on luminescent materials, has been the development of nano structures with highly visible or characteristic near infrared emissions for precise imaging, combined with nanoscale cavities for drug storage and delivery. The design of such materials requires complex nanostructures that have both the intense emissions and appropriate storage geometries. We report here a scheme for the use of novel nanostructures designed

to satisfy both of these important requirements. Hypodermal and *in vivo* organic imaging from quantum dot conjugated carbon nanotubes has been realized in mice for the first time. The coupling of quantum dots on carbon nanotubes was materialized based on a novel plasma nanotube surface polymerization. The quantum dot activated carbon nanotubes exhibited intense visible light emissions in both fluorescent spectroscopy and *in vivo* imaging. These experimental results can be extended to the development of new techniques for early cancer diagnosis.

3:00 PM

Synthesis CuO Nanowire Array for Gas-Sensor Applications: *Kai Wang*¹; Zhongming Zeng¹; Weilie Zhou¹; ¹University of New Orleans

CuO nanowires, a typical p-type oxide semiconducting nanostructures, can enhance the selectivity of gas sensor array using opposite resistance variation to n-type semiconductors when exposed to the gases. We present a synthesis of high density CuO nanowires and measurement of the electrical properties of a single nanowire. Large quantities of CuO nanowires have been synthesized by heating the copper foil in air. The as-synthesized nanowires are characterized by scanning electron microscopy (SEM) and transmission electron microscopy (TEM). The nanowires grow vertically on the foil and the diameter ranges from 50 nm to 120 nm with a length of tens micrometers. The nanowires were patterned by e-beam lithography. I-V characteristic of a single CuO nanowire indicates the resistance of CuO nanowire is in the order of 10⁸ohm, which is a good for selective gas sensor fabrication. The nanowire array can be potentially used to build three-dimensional hybrid nanostructures for gas sensors.

3:15 PM

Electrospun Vanadium Oxide Fibers for Gas Sensor Applications: *Kevin Stokes*¹; Christopher Lomatayo²; Jaijun Chen¹; ¹University of New Orleans; ²South Dakota School of Mines

We have fabricated vanadium oxide ultra-thin fibers from a simple organometallic vanadium precursor using electrospinning. Fibers with diameters ranging from 700 nanometers to 3.0 microns were fabricated from a solution of vanadium oxytriisopropoxide (VOTIP), acetic acid and polyethylene oxide (less than 1% polymer by weight). As the clear precursor solution exits the spinneret, the VOTIP reacts with the moisture in the air resulting in a partially hydrolyzed orange fiber. The fibers are left overnight to completely hydrolyze, then collected and calcined at 400°C. The fiber morphology was characterized using field emission scanning electron microscopy (FESEM) before and after calcination. Electrical conductivity of collections of fibers deposited onto microelectrode arrays is also presented.

3:30 PM

GaN and ZnO-Based Nanowire Sensors for Bio and Chemical Detection: *Stephen Pearton*¹; F. Ren¹; B. Kang¹; H. Wang¹; B. Gila¹; D. Norton¹; L. Tien¹; T. Chancellor¹; T. Lele¹; Y. Tseng¹; J. Lin¹; ¹University of Florida

In this talk we will give examples of using ZnO nanorods and nitride nanowires and High Electron Mobility Transistors (HEMTs) for pH sensing in the range of interest for human blood (7-8 pH), detection of DNA hybridization and detection of Hg. In all of these sensor systems, integrating the resulting sensors with modern GPS and wireless communication systems in a convenient module is important for ease of use and monitoring applications.

3:45 PM

SnO₂/GeO₂ Bicrystalline Nanowires: Synthesis, Characterization, Photoluminescence and Sensing Properties: *Ying Li*¹; Jiajun Chen¹; Weilie Zhou¹; ¹University of New Orleans

Bicrystalline structure has unique optical and mechanical properties due to its grain boundary, which not only includes two combined single crystals in same materials, but also can be formed by different materials. We report a synthesis of SnO₂/GeO₂ bicrystalline nanowires by thermal evaporation with the mixture of metal Sn and Ge powders. The as-synthesized products have been characterized by scanning electron microscopy, energy-dispersive X-ray spectroscopy and selected-area electron diffraction. The diameters of the nanostructures range from 20 to 200 nm, and lengths are up to several hundreds of micrometers. Microstructure characterization indicates the orientation relationship between two crystals is [001]GeO₂//[001]SnO₂, (110)GeO₂//(110)SnO₂. The PL spectrum of the bicrystalline nanowires shows some difference compared with pure SnO₂ and GeO₂ nanostructure which are associated with interface defects in SnO₂/

GeO₂ bicrystalline nanowires. In addition, the sensing properties of the SnO₂/GeO₂ bicrystalline nanowire to CO and H₂ will also be discussed.

4:00 PM Break

4:15 PM Invited

Atomic Layer Deposited Thin Films and Their Applications: *Hyeongtag Jeon*¹; Seokhoon Kim¹; ¹Hanyang University

Recently thin film deposition technology has been developed extensively due to the great needs in many application areas especially in the fields of semiconductor, nanomaterials and nanorelated technologies. There are many deposition methods introduced and actually applied in the real thin film processes. However, in these days thin films with nanoscale thickness are needed for research and development for many different areas. Therefore the deposition method to control nanoscale thin film is focused to develop and atomic layer deposition (ALD) technique is one of promising choices. ALD method provides to grow high quality thin film by a layer-by-layer fashion, and to deposit thin films with large area uniformity and low impurity content in nanoscale devices. There are many different ALD methods are already introduced such as thermal, plasma and other reactive ALDs. In this presentation, different types of ALD methods and application areas will be presented.

4:40 PM Invited

Nanoheteroepitaxy: An Approach toward a Monolithic Phosphor-Free White LED: *Timothy Sands*¹; ¹Purdue University

The global energy challenge will be addressed in part by the development of more efficient energy conversion devices, from solid-state lighting to solid-state refrigerators and generators. Materials limit the performance of each of these devices. For example, the luminous efficiency of white LEDs is limited by the so-called "green gap" – i.e., the low internal quantum efficiency of LEDs that emit at wavelengths near 555 nm, the peak of the photopic vision sensitivity spectrum. In this talk, I will describe our approach to utilize nanostructured (In,Ga)N to bridge the green gap. The free surfaces of nanorod heterostructures allow elastic relaxation of lattice misfit strain, thereby altering the kinetics of InN incorporation. Thus, (In,Ga)N nanorods can incorporate higher InN mole fractions without the introduction of the dislocations that limit the internal quantum efficiency. Challenges remaining on the path toward a monolithic nanostructured phosphor-free white LED will be highlighted.

5:05 PM

Atomic-Scale Features of Dislocation Dynamics in Thin Films: *Yuri Osetsky*¹; Roger Stoller¹; Yoshitaka Matsukawa¹; ¹Oak Ridge National Laboratory

Atomistic modelling has demonstrated that the dynamic interactions of dislocations in thin films have a number of remarkable features. A particular example is the interaction between a screw dislocation and a stacking fault tetrahedron (SFT) in Cu which can be directly compared with in situ observations of quenched or irradiated fcc metals. If the specimen is thin, the dislocation is slow and the temperature is high enough, a segment of the original SFT can be transported towards the surface via a double cross-slip mechanism and fast glide of an edge dislocation segment formed during the interaction. The particular mechanism depends on the stress distribution in the film for it affects the screw dislocation dissociation and reactions with an SFT. The mechanisms observed in the simulations provide an explanation for the results of in situ straining experiments and the differences between bulk and thin film experiments.

5:20 PM

Structure and Properties of Al/TiN Nanoscale Multilayers: *Dhriti Bhattacharyya*¹; Nathan Mara¹; Patricia Dickerson¹; Richard Hoagland¹; Amit Misra¹; ¹Los Alamos National Laboratory

Nano-scale multilayers of Al/TiN have been deposited with Al:TiN ratio equal to 9:1 and 1:1, using reactive sputter deposition, with TiN layer thickness varying from 50 nm to 1 nm. The structure of these nano-scale multilayers has been studied using Transmission Electron Microscopy (TEM), high resolution TEM, and X-Ray diffraction. Nano-indentation experiments have been performed on these multilayered thin films to measure their hardness. This work clearly demonstrates that these multilayers are definitely stronger (hardness ~ 4 GPa) than a simple rule of mixtures would suggest (hardness ~ 1 GPa). It is shown that the hardness varies with bilayer thickness λ with a Hall-Petch behavior to a λ value of 20 nm, below which the hardness value drops below that predicted by

the Hall-Petch equation. The effect of volume fraction of the two components is also demonstrated in terms of variations in hardness.

5:35 PM

Fabrication and Characterization of Single Stand-Alone TiO₂ Nanotube Devices: *Dongkyu Cha*¹; Kyungmin Lee¹; Bongki Lee¹; M. J. Kim¹; Hyunjung Shin²; Jaegap Lee²; Jiyoung Kim¹; ¹University of Texas at Dallas; ²Kookmin University

TiO₂ nanotubes have great potential to enhance performance for sensor applications and dye sensitized solar cell applications, primarily due to increased surface area to volume ratio. However, the nanotubes are very fragile, so it is still challenging to fabricate single stand-alone nanotube devices. We successfully fabricate devices with single stand-alone TiO₂ nanotubes using a process which combines Focused Ion Beam with photolithography. This process provides several advantages over previously published methods, including freedom of structural geometry, shorter fabrication time, and higher throughput. This rapid prototyping method enables the direct measurement of single nanotubes under ambient conditions. In this study, we will present the electrical characteristics and potential gas sensor applications of single TiO₂ nanotubes. This research was supported by a grant (code #: M105KO010026-05K1501-02611) from 'Center for Nanostructured Materials Technology' under '21st Century Frontier R&D Programs' of the Ministry of Science and Technology, Korea.

5:50 PM

Low Temperature Growth of ZnO Nanorods and Nanotubes by Atomic Layer Deposition for the Application of Field Emission: *Yung-Huang Chang*¹; Chih Chen¹; ¹National Chiao Tung University

Self-organized ZnO nanorods and nanotubes are grown on Si substrates by using AAO as a template and ALD to deposit ZnO. With the aid of the ALD, the deposition temperature can be lowered down to as low as room temperature, and no any metal catalysts or seed layers are needed. Each individual nanorod or nanotube is perpendicular to the Si substrate. We controlled the diameter and thickness of AAO template to modify the morphology of ZnO nanorod arrays. The screening effect and field enhancement were investigated to obtain the best parameters for the application of field emission. In addition, the nanorods and nanotubes were annealed at 700°C for one hour under oxygen ambient, and their average grain size grew up from 11 nm to 15 nm. The results of photoluminescence, TEM, and the performances of field emission for the ZnO nanorods and nanotubes arrays will be presented in the conference.

3-Dimensional Materials Science: Large Datasets and Microstructure Representation I

Sponsored by: The Minerals, Metals and Materials Society, TMS Structural Materials Division, TMS: Advanced Characterization, Testing, and Simulation Committee
Program Organizers: Michael Uchic, US Air Force; Eric Taleff, University of Texas; Alexis Lewis, Naval Research Laboratory; Jeff Simmons, US Air Force; Marc DeGraef, Carnegie Mellon University

Monday PM
March 10, 2008

Room: 286
Location: Ernest Morial Convention Center

Session Chairs: Marc DeGraef, Carnegie Mellon University; Jeff Simmons, Air Force Research Laboratory

2:00 PM Invited

Towards the Incorporation of Realistic Microstructures in Computational Models: A Framework for Automated 3D Microstructure Analysis and Representation: *Michael Groeber*¹; Michael Uchic¹; Dennis Dimiduk¹; Somnath Ghosh²; ¹Air Force Research Laboratory; ²Ohio State University

Over the past five years there have been significant advances in developing serial-sectioning methods that provide quantitative data describing the structure and crystallography of grain-level microstructures in three dimensions (3D). Subsequent analysis and representation can provide modeling and simulation efforts with a highly-refined characterization of specific microstructural features. For example, the structure of an engineering alloy could be characterized and then translated directly into a 3D volume mesh for Finite Element (FE) analysis.

However, this approach requires a multitude of data sets in order to sample the heterogeneity observed in typical microstructures. One way to circumvent this issue is to develop computation tools that create synthetic microstructures that are statistically-equivalent to the measured structure. This presentation will discuss the development of software programs that perform a robust statistical analysis of a material's 3D microstructure as well as generate a host of synthetic structures which are analogous to the real material.

2:30 PM

Spectral Representation and Reconstruction of 3-D Materials: *David Fullwood*¹; Steven Niezgoda²; Surya Kalidindi²; ¹Brigham Young University; ²Drexel University

Representation of 3-D material data using correlation functions is a key statistical technique for material analysis. Reconstruction of large 3-D material realizations from such statistical data has historically been too computationally intensive to attempt with traditional reconstruction techniques (such as simulated annealing). We present a newly developed approach to reconstruction based upon phase retrieval methods from the signal processing industry. Rapid reconstruction of 3-D datasets from 2-point statistical data is demonstrated. We also investigate the space of 2-point statistics correlating to physically meaningful material realizations, and the issues of generating full sets of statistics from partial data.

2:50 PM

Moment Invariant Shape Descriptors for Microstructure Representation: *Jeremiah MacSleay*¹; Jeff Simmons²; Marc DeGraef¹; ¹Carnegie Mellon University; ²Wright Patterson Air Force Base

In this contribution we show how moment invariants (combinations of second order shape moments that are invariant w.r.t. affine or similarity transformations) can be used as sensitive shape discriminators in 2-D and 3-D. After defining the invariants, we introduce moment invariant space, and illustrate how all possible shapes reside within a finite region in this space. Then we provide applications of invariants, such as the quantitative representation of shapes and shape changes of precipitates that develop in real 3-D microstructure observations as well as in microstructure evolution simulations. Since particle shapes are characteristic of microstructures, this technique can be used to quantify the "closeness" of two microstructures by the statistics of their moment invariants. As an example of 3-D moment invariants, we show that the shapes of complex precipitates in a Rene-88DT alloy lie along a curved surface in moment invariant space.

3:10 PM Invited

Collecting, Segmenting and Analyzing Large Serial-Section Materials Data Sets: *David Rowenhorst*¹; Alexis Lewis¹; George Spanos¹; ¹Naval Research Laboratory

As the field of 3-D Materials Science advances, the ability to collect large data sets has consistently grown, which has lead to new problems in the analysis, and representation of these data sets. We will present methods for collecting large serial sectioning data sets, addressing using image montaging, robust fiducial marks and image alignment. We will primarily as an example, a serial sectioning data set of β -Ti grains, containing 200 sections, and resulting in more than 1000 grains in the microstructure. We will also present how this data set is segmented using an adapted Watershed Algorithm. Finally will show different techniques for visualizing, analyzing and representing the data contained in such data sets.

3:40 PM Break

4:00 PM Invited

Statistical Methods for Segmentation of 3-D Microstructural Image Data with Minimal Supervision: *Mary Comer*¹; Peter Chuang¹; Jeff Simmons¹; ¹Purdue University

3-D materials science is fueled simultaneously by the integration of computer controls with microscopes and by the increase in collection rates. Image data rates are expanding exponentially. To utilize all of this information, features must be extracted from images. Conventional image processing is currently used for this extraction, but is heavily labor intensive, often requiring manual segmentation of each frame. Developing minimally supervised algorithms for making these segmentations is the goal of this work. Segmentation seeks to classify pixels into regions, corresponding to Different objects or textures. We will describe a method we have developed for finding the segmentation that minimizes the expected number of misclassified pixels, with minimal supervision. Parameters

of the statistical models used for the image data are automatically estimated during the segmentation procedure, reducing the amount of human interaction required. Preliminary results on serial section stacks of Ni-base alloys and carbon foam images will be presented.

4:30 PM

Applications of Active Contours in Microstructural Analysis: *Aleks Ontman*¹; Gary Shiflet¹; ¹University of Virginia

Edge detection is a widely used technique regularly employed as an intermediate step in microstructure analysis. Having an outline of region of interest enables the user to extract data about the region or use it in reconstruction of 3-D models. Since traditional edge detection relies on a user selected threshold value the results often are subjective. Furthermore, traditional edge detection frequently results in outlines that are incomplete, requiring additional processing steps, such as, edge linking and spur removal, and it is a very noise sensitive technique. Active contouring (AC) is an edge detection based technique that typically yields results superior to that of a traditional edge detector. High noise tolerance and built-in flexibilities of AC make the technique desirable to use across a broad range of applications with increasing automation. Several uses of AC are presented to demonstrate robustness and the range of applications that can employ AC.

4:50 PM

An Eigenvalue-Based Method for Characterizing Plastically Deformed Surfaces: *Mark Stoudt*¹; Joseph Hubbard¹; Lyle Levine¹; ¹National Institute of Standards and Technology

Since real surfaces evolve and interact in three dimensions, it is essential that surface morphology be characterized in three dimensions with tools that maximize fidelity with the original surface. However, spatial analysis of plastically deformed polycrystalline surfaces in three-dimensions is problematic due to inadequate numerical tools. Moreover, mathematical artifacts such as boundary discontinuities or periodic extrapolations introduced by two-dimensional numeric parameters are exacerbated in three-dimensional analysis. We have developed a representation-independent, non-interpolated spatial analysis protocol that does not utilize conventional time series analysis methods. Because it exclusively examines the behavior of eigenvalue spectra calculated directly from a topographic image, this protocol eliminates the need for a priori assumptions about surface character. The eigenvalue spectra change systematically with plastic strain and correspond to correlations in the surface morphology at all length scales. The capabilities of this protocol and results of initial analyses shall be presented and discussed.

5:10 PM

Image Registration Using Neural Networks: *Aleks Ontman*¹; Gary Shiflet¹; ¹University of Virginia

Image Registration (IR) is a process of transforming images in a dataset into one common coordinate system. The original method, developed by Mangan and Shiflet, relied on hardness indentations to align serial images in the dataset. However, as the sample is continuously sectioned, the marks and the microstructure change and an appropriate 'hands-on' registration method is required to locate the marks for IR. Feature and area based algorithms fail to perform adequately when marks are scaled or rotated. A Neural Network can be trained to discriminate shapes of interest which can then be used to assist and automate the IR process. We will present a NN that can successfully isolate indentation squares that are rotated, scaled and located among other microstructural features and then use the information to automatically register a set of synthetic and optical microscope images.

9th Global Innovations Symposium: Trends in Integrated Computational Materials Engineering for Materials Processing and Manufacturing: Session I

Sponsored by: The Minerals, Metals and Materials Society, TMS Materials Processing and Manufacturing Division, TMS/ASM: Computational Materials Science and Engineering Committee, TMS: Global Innovations Committee, TMS: Nanomechanical Materials Behavior Committee, TMS/ASM: Phase Transformations Committee, TMS: Powder Materials Committee, TMS: Process Technology and Modeling Committee, TMS: Shaping and Forming Committee, TMS: Solidification Committee, TMS: Surface Engineering Committee

Program Organizers: Corbett Battaile, Sandia National Laboratories; Amit Misra, Los Alamos National Laboratory; Joy Hines, Ford Motor Company; James Sears, South Dakota School of Mines and Technology

Monday PM
March 10, 2008

Room: 281
Location: Ernest Morial Convention Center

Session Chair: To Be Announced

2:00 PM Introductory Comments

2:05 PM Invited

CAE in Product Development and the Role of Computational Materials:

*Gerould Young*¹; ¹Boeing Phantom Works

CAE is an indispensable part of the product development cycle for Boeing. Computational fluid dynamics and computational structural analysis are used via general purpose tool sets to develop and certify products. As we look to further improve the performance of our products, we look to advanced alloys and composite materials, to speed the development of these new materials and associated manufacturing processes and to understand in service behavior. This leads us to look to the use computational materials run on high speed computing platforms. The challenge is to make these new tools systemic within a discipline which has traditionally not used the "perfect laboratory" offered by high speed computing, but instead relied on experiment and laboratory development. Furthermore, there's a challenge to develop general purpose tools for the materials engineer at each appropriate scale to simulate specific material behaviors and to link these tools across scales to other computational disciplines.

2:35 PM Invited

Application of ICME in the Air Force's Materials Research and Development Program:

*Charles Ward*¹; ¹US Air Force

Strides in the physical understanding of materials behavior coupled with advances in both modeling techniques and computing power are leading to the increasing application of integrated computational materials engineering to provide solutions to materials development, processing and life prediction problems. While the structural materials community is still quite some time off from having a truly integrated capability across all length and time scales, progress is clearly being made in linking descriptions of material behavior across several orders of magnitude in scale. This talk will present the current focus of the Air Force ICME efforts for propulsion materials, and will highlight several examples of ICME application.

3:05 PM Invited

An Automotive Perspective on Integrated Computational Materials Engineering:

*Matthew Zaluzec*¹; ¹Ford Motor Company

In the automotive industry, ICME has been a key enabler for "up-front" component and vehicle design and has provided savings in cost and timing in an era of increased competition and "just-in-time" manufacturing. Ford Motor Company's Research and Advanced Engineering Laboratory has been an innovator in the area of ICME for aluminum powertrain components for several years and has worked to expand that expertise into other areas of the vehicle requiring other materials and/or processing paths such as steel stampings, virtual paint and plastics processing used in the design and manufacturing of automotive components. This talk will focus on Ford's efforts in the area of ICME in a number of different applications as well as some of the collaborative efforts in ICME through its participation in the FreedomCAR/USAMP programs.

3:35 PM Break

3:55 PM Invited

Structural Materials in Advanced Nuclear Energy Systems: The Need for Revolutionary Research:

*Ronald Gibala*¹; *Steven Zinkle*²; ¹University of Michigan; ²Oak Ridge National Laboratory

We present a partial overview of key findings of the DOE-sponsored BES Workshop on *Basic Research Needs for Advanced Nuclear Energy Systems* held in August, 2006. The focus is on topics from our panel on structural materials and their performance under extreme environments. The recommendations and goals, although including dozens of specific questions to be answered, are generically three-fold: (1) discover mechanisms that render materials impervious to the interacting extreme conditions of irradiation, temperature, stress and environmental surroundings; (2) achieve seamless integration of novel experimental techniques with advances in the methodology of computational materials science; (3) bring fundamental design of materials to a new level of accomplishment that includes expanded development of functionalized interfaces for optimization of materials properties. We will also discuss related recommendations from other panels of the Workshop and give a brief 'scorecard' on how the Workshop recommendations have affected DOE program initiatives and funding.

4:25 PM Invited

Multiscale Modeling and Materials Design:

*David McDowell*¹; ¹Georgia Institute of Technology

Engineering design has historically been taught using the paradigm of selecting materials on the basis of tabulated databases of properties (mechanical, physical, electronic, etc.). Recent trends have moved towards concurrent design of material composition and microstructure together with the component/system level, moving through the process-structure-property-performance hierarchy. The goal is to tailor materials to meet specified ranges of performance requirements of the overall system, rectifying the aforementioned hierarchy of design with hierarchy of scales of structure that affect properties. Materials design falls under the general category of simulation-based design, in which computational materials science and multiscale modeling modeling play key roles in evaluating performance metrics necessary to support design decision-making. The interplay of hierarchical, multi-level systems-based design of materials with methodologies for multiscale modeling is core to materials design.

4:55 PM Panel Discussion

Advances in Semiconductor, Electro Optic and Radio Frequency Materials: Compound Semiconductors and Beyond

Sponsored by: The Minerals, Metals and Materials Society, TMS Electronic, Magnetic, and Photonic Materials Division, TMS: Thin Films and Interfaces Committee

Program Organizers: Nugehalli Ravindra, New Jersey Institute of Technology; Narsingh Singh, Northrop Grumman Corporation ES; Choong-un Kim, University of Texas - Arlington; Yanfa Yan, National Renewable Energy Laboratory; Bhushan Sopori, National Renewable Energy Laboratory; Greg Krumbick, Argonne National Laboratory

Monday PM
March 10, 2008

Room: 278
Location: Ernest Morial Convention Center

Session Chairs: Yanfa Yan, National Renewable Energy Laboratory; Greg Krumbick, Argonne National Laboratory

2:00 PM Introductory Comments

2:10 PM Invited

Effect of Growth Conditions on the Morphology of Nanodots:

*Narsingh Singh*¹; *Sean McLaughlin*¹; *Anthony Margarella*¹; *David Kahler*¹; *David Knuteson*¹; *Andre Berghmans*¹; *Brian Wagner*¹; ¹Northrop Grumman Corporation

We have developed Germanium (Ge) nanodots and arrays of nanodots on Silicon (Si) wafers with etched trenches. We used Silicon trenches to study the effect of planar silicon with high energy interfaces. Several growth experiments were carried out and growth conditions were varied to study the nucleation and

growth of dots. The morphologies of the nanodots were very much dependent on the growth conditions. We observed that the germanium grew as nanodots in the field of edges and trenches. Larger Ge dots grew along high energy interfaces. We used diborane and arsine for doping. The growth rates for nanodots are slower for an arsine atmosphere in comparison to the case of diborane. Our experiments indicated that using oxides on Si wafers, growth of Ge nanodots can be grown on the desired area.

2:40 PM Invited

Medical Applications of Advanced Semiconductors: *Roger Narayan*¹; Robin Brignon²; Shaun Gittard¹; Christopher Berry²; ¹University of North Carolina and North Carolina State University; ²Savannah River National Laboratory

Medical device infection is associated with significant morbidity, mortality, and associated healthcare costs. Microorganisms colonize the medical device surface and form sessile communities known as biofilms. These biofilms contain 5-50 micrometer thick glycoprotein matrices that protect the bacteria through a diffusion limitation process, and increase their resistance to antibodies, macrophages, and antibiotics. The sustained delivery of antimicrobial agents into the medical device microenvironment may prevent biofilm formation and avoid systemic side effects associated with oral or intravenous antimicrobial administration. For example, coating a medical device with a ceramic thin film may impart antimicrobial properties. Structural studies and microbial studies were performed on diamondlike carbon-silver nanocomposite films, diamondlike carbon-platinum nanocomposite films, diamondlike carbon-silver-platinum nanocomposite films, and zinc oxide thin films prepared using pulsed laser deposition. These materials may provide unique biological functionalities and improved lifetimes for next generation cardiovascular, orthopaedic, biosensor, and implantable microelectromechanical systems.

3:10 PM

Lithium Phthalocyanine: An Overview: *Sushil Sikha*¹; Trishla Kanthala²; Raymonde Jean-Charles³; Shanakey Cupidon³; Nuggehalli Ravindra¹; ¹New Jersey Institute of Technology; ²New York Institute of Technology; ³East Orange Campus High School

Lithium Phthalocyanine is a narrow bandgap semiconductor with an energy gap of 0.2 eV and a high frequency dielectric constant equal to 6. In recent years, this material has gained notoriety, both as bulk and in thin film form on various substrates, as an oxygen sensor for biological applications. An overview of the various electrical, optical, structural and magnetic properties of Lithium Phthalocyanine (LiPc) is presented in this study. The study concludes with the chemical and environmental stability of LiPc.

3:30 PM Break

3:40 PM Invited

Chemical-Mechanical Methods for Making Quality Compound Semiconductor Nanocrystals: *Nancy Michael*¹; Choong-Un Kim¹; ¹University of Texas

Synthesis of high quality compound semiconductor nanoparticles has been a topic of research interest as advances in nanoparticle manipulation and device structure have enabled many exciting applications. In order to achieve the needed high quality, most of these synthesis methods are bottom-up, that is, building the particles atom by atom, and involve expensive precursor chemicals and equipment. In this paper we present an inexpensive top-down method by which a larger particles are chemically/mechanically broken down to high quality nanosized particles. This method is applicable to compound semiconductors as well as semiconductor alloys, enabling nanocrystals with tunable properties.

4:10 PM

Synthesis and Characterization of Ga and N Incorporated ZnO Films: *Sudhakar Sheri*¹; Kwang-Soon Ahn¹; Yanfa Yan¹; Todd Deutsch¹; Muhammad Huda¹; Nuggehalli Ravindra²; Mowafak Al-Jassim¹; John Turner¹; ¹National Renewable Energy Laboratory; ²New Jersey Institute of Technology

Ga and N incorporated ZnO thin films (ZnO:N:Ga) were synthesized by reactive RF magnetron sputtering in N₂/O₂ gas ambient. All the films were deposited on F-doped tin oxide-coated glass. The gas ambient was mixed N₂ and O₂ gas with a gas ratio of O₂/(N₂+O₂) = 5%. Structural properties, optical absorption and PEC responses for ZnO:N:Ga films were investigated. The influence of the varying Ga concentration in the ZnO:N:Ga films on the

bandgap and resulting photoelectrochemical properties has been studied. The n-type conductivity in these films was confirmed by analysis of Mott-Schottky plots and current voltage characteristics under illumination.

4:30 PM

Novel Cu-Doped ZnO Diluted Magnetic Semiconductors for Spintronics Applications: *Deepayan Chakraborti*¹; John Prater²; Jagdish Narayan¹; ¹North Carolina State University; ²Army Research Office

Recently transition metal doped ZnO based diluted magnetic semiconductors have drawn a lot of attention for use in spintronics applications where charge as well as spin of an electron can be utilized for device functionality. Here we present the systematic studies on epitaxial growth and properties of Cu-doped ZnO thin films grown on (0001)-Al₂O₃ single crystals by PLD. The Cu-doped ZnO system has shown near 100% spin polarization making them an attractive candidate for efficient injection of spin polarized carriers in spin-based devices. The effect of free carriers and intrinsic point defects like oxygen vacancies on the long range ferromagnetic ordering of localized Cu²⁺ spins has been investigated to develop a clear understanding of the origin of ferromagnetism in ZnO based DMS systems. Finally we have fabricated a spin valve type device structures to study the injection of spin polarized carriers across a non-ferromagnetic layer sandwiched between two ferromagnetic layers.

4:55 PM

The Photocatalytic Oxidation of Water to O₂ over Vanadium-Dopant of Rutile TiO₂: *Daixin Wu*¹; Qiyuan Chen¹; ¹Central South University

Vanadium doped rutile TiO₂ with different Vanadium doping concentration were prepared by low temperature hydrolysis using Tetrabutyl titanate. Powers were characterized by XRD, PL, DRS, BET. With Fe³⁺ as electron acceptor at pH=2.0 under UV irradiation and visible radiation. Results show that with appropriate concentration, Vanadium was doped into rutile TiO₂ lattice without causing any change in rutile TiO₂ crystal structure. Therefore, surface oxygen vacancies and the donor energy level near the bottom of the conduction band lead to easier departure of photoinduced electrons from holes to achieve stronger photocatalytic activity. The highest photocatalytic oxygen evolution and PL Spectra intensity were achieved with the O₂ evolution speed of 473 μmol.L⁻¹.h⁻¹ and 88 μmol.L⁻¹.h⁻¹ under UV irradiation and visible radiation when the Vanadium concentration was 1.0 mol%, which demonstrated certain relationship between photoluminescence performance affected by Vanadium concentration and the photocatalytic activity. The best initial concentration of Fe³⁺ is 8.0 mmol.L⁻¹.

5:15 PM Invited

New Phenomena in Luminescence of Gallium Phosphide: *Sergei Pyshkin*¹; John Ballato²; Michael Bass³; Giorgio Turri³; ¹Academy of Sciences of Moldova; ²Center for Optical Materials Science and Engineering Technologies, Clemson University; ³University of Central Florida

We discuss the phenomena in luminescence of pure and doped GaP as the result of over 40 years ordering of impurity and host atoms. Data obtained between the last TMS conferences confirms the conclusions presented earlier on formation of a crystal lattice where periodically disposed impurities modify, improve and essentially change crystalline properties. The latter will be used as the basic element for new generation of optoelectronic devices. We demonstrate that spectra of bright "hot" luminescence in pure and N doped ordered GaP have deep analogy in origin, shape and position with those obtained in GaP nanocrystals. Unique ordered GaP:N:Sm at the uniformly intermixed impurities generates with high efficiency the luminescence, which depending on intensity of excitation is switched between green (N bound excitons) and yellow-red (Sm activators). These results well correlate with the data obtained from the same crystals in investigations on Raman light scattering and microhardness.

5:40 PM

Bandgap Narrowing of ZnO Films by Cu and In Incorporation: *Sudhakar Sheri*¹; Kwang-Soon Ahn¹; Yanfa Yan¹; Todd Deutsch¹; Muhammad Huda¹; Nuggehalli Ravindra²; Mowafak Al-Jassim¹; John Turner¹; ¹National Renewable Energy Laboratory; ²New Jersey Institute of Technology

ZnO thin films with significantly reduced bandgaps were synthesized by co-doping of Cu and Cu and In at room temperature and followed by post-deposition annealing at 500°C in air for 2 hours. All the films were synthesized by RF magnetron sputtering in O₂ gas ambient on F-doped tin oxide-coated glass. Structural properties, optical absorption and PEC responses for ZnO:

Cu and ZnO:Cu:In films were investigated. ZnO:Cu and ZnO:Cu:In films with various bandgaps were realized by varying RF power and In concentration respectively. The band gap reduction and photoresponse with visible light for Cu and In incorporated ZnO thin films were investigated. The ZnO:Cu films exhibited higher total photocurrent when RF power was increased to 200 W. The n-type conductivity was confirmed for ZnO:Cu:In film by Mott-Schottky plots and illuminated I-V analysis.

Alumina and Bauxite: HSEC

Sponsored by: The Minerals, Metals and Materials Society, TMS Light Metals Division, TMS: Aluminum Committee

Program Organizers: Sringeri Chandrashekar, Rio Tinto Aluminium Limited; Peter McIntosh, Australus Management Services

Monday PM
March 10, 2008

Room: 296
Location: Ernest Morial Convention Center

Session Chair: Benoit Cristol, Rusal Australia, United Company Rusal

2:00 PM Introductory Comments

2:05 PM

Alunorte Safety Performance: *Jorge Lima*¹; ¹Alunorte

Alunorte have started-up the first two of its 5 production lines in July 1995, with a designed nominal capacity of 1.1 mi t/y. Considering that the project was in slow down for ten years, it was necessary to review and establish new policies and standards for operational training and others. Among those it was very much decisive the commitment with Safety. During the last eleven years the production has increased more than four times. Now Alunorte has five lines in full operation with a nominal capacity of 4.3 mi t/y and around 800 new employees, comprising around 160 operators with no former experience, hired through a CSR program. This paper aims to present the strategies implemented to reduce the Serious Accident Frequency Rate from 22,83, in the first year of operation 1995, down to 1,43 in the last year 2006, when the production reached 3,94 mi t/y.

2:30 PM

Sustainable Development of Chinese Alumina Industry: *Jibo Liu*¹; Wangxing Li¹; ¹Aluminum Corporation of China Limited

China has the second largest annual output of alumina in the world, however, the bauxite resources in china are relatively scarce with main content of diaspore which require higher energy consumption and more complex process in alumina production compared with other bauxite. How to produce alumina with low energy consumption and high efficiency resource utilization is an important issue for sustainable development of Chinese alumina industry. In this article, the latest features of bauxite resources and alumina production were introduced; the most important improvement of sustainable development including the aspects of bauxite resources utilization, energy consumption reduction, product quality improvement and environmental protection were illustrated, as well as the future strategy of sustainable development of alumina production in China was described.

2:55 PM

Tailings Impoundment Life Extension at Sherwin Alumina Company: Success Breeds Its Own Challenges: Thomas Ballou¹; Ed Peterson¹; ¹Sherwin Alumina, L.P.

In the mid-1990s, Sherwin Alumina, realizing that traditional dilute slurry storage of their 3300mt/day of Bauxite residue solids could not be sustained. Sherwin explored dense slurry "stacking" as the apparent least cost/most feasible life extension alternative. Laboratory testing of the residue showed that significant gains were feasible to achieve both objectives, minimal cost and life extension. Initially, stack slope results appeared disappointing; however core analysis of the highly plastic material demonstrated the stacking was achieving consolidation of not only the newly deposited material, but also of the underburden, well in excess of the expected values. As stacking proceeded, new issues arose with stormwater management, internal dike stability, leachate recovery and episodic

fugitive dust. Ultimately, stack stability analysis and surface tilling, has allowed Sherwin to manage both placement and crust conditions for optimum life with minimum fugitive dust. The consolidated material exhibits permeability in the 10-8cm/sec range and when treated with simple amendments such as treated effluent it can be directly vegetated.

3:20 PM

Proposed Mechanism for the Formation of Dust Horizons on Bauxite Residue Disposal Areas: *Craig Klauber*¹; Nicole Harwood¹; Renee Hockridge¹; Campbell Middleton²; ¹CSIRO Minerals; ²Billiton Aluminium Australia Pty Ltd

Without some form of mitigation control bauxite residue disposal areas in Mediterranean climates can be subject to large-scale dust lift-off events during summer, with significant environmental impact. Intuitively dust formation relates simply to the process of drying. However, whilst wet solids will not produce dust, the converse is not always true. Both the rate of drying and the composition of the bauxite residue are critical factors in determining whether a potential dust horizon will form. In this work a dust formation mechanism is proposed in which caustic salts transport and effloresce along with a changing phase composition in the brine solids from sodium bicarbonate through to trona and then to carbonate monohydrate. The efflorescence leads to a white dust event, but the carbonate phase change and the associated reduction in sodium molar volume critically breaks inter-particulate bonding between the residue particles leading to a more severe red dust event.

3:45 PM Break

4:00 PM

Waste into Wealth: *Balasubramaniam Subbaian*¹; Vasanthakumar Rangasamy¹; ¹Madras Aluminium Company

Red mud generated from Bayer's Process for Alumina production is a high volume solid waste with 60 to 70% solids, doesn't have any wide industrial application. Though valuable elements like Alumina and Silica are available in Red Mud, presence of soda makes it a waste. But presence of Alumina, Silica and Iron Oxide in Red mud compensates for the deficiency of the same components in Limestone which is the primary raw material for Cement production. What makes Red Mud special in cement manufacturing is the presence of soda which neutralizes the sulfur content in pet coke that is used for burning clinker enroute cement production and adds to the cement's setting characteristics. This paper details MALCO's efforts in turning Red Mud considered a Waste into Wealth which otherwise would be lying in the back yards of Alumina Plant requiring special care and attention in storing and handling it.

4:25 PM

Short- and Long-Range Order in Smelter Grade Alumina – Development of Nano- and Microstructure during the Calcination of Bayer Gibbsite: *Linus Perander*¹; Zoran Zujovic²; Margaret Hyland¹; Mark Smith³; Luke O'Dell³; James Metson¹; ¹Light Metals Research Centre; ²University of Auckland, Department of Chemistry; ³University of Warwick, Department of Physics

The development of structural features during the calcination of Bayer Gibbsite to produce Smelter Grade Alumina (SGA) is a complex process that involves both a dehydroxylation reaction and a rearrangement of the crystal lattice. The disorder and the co-existence of the transition alumina phases complicate structural and quantitative analysis. In order to evaluate a wider range of structural ordering both XRD and high-field solid-state MAS-NMR were applied on a variety of industrial and laboratory prepared alumina samples. Quantitative information was obtained by simulating the NMR spectra and assigning the peaks to various alumina phases and by Rietveld analysis of the XRD data. Although the thermodynamically stable alpha alumina content can be accurately monitored, the results clearly demonstrate some of the limitations of XRD, especially for quantifying the transition aluminas. An amorphous component, with aluminium in pentahedral coordination, detectable by NMR but not XRD, accounts for part of the observed differences.

4:50 PM

Start-up of the Lines 4 and 5 at Alunorte: Pre-Operational Strategy, Commissioning and Ramp-up: *Anderson Amaral¹; Jorge Lima¹; Joaquim Filho¹; ¹Alunorte*

Alunorte began its operation in 1995 with two production lines and a designed nominal capacity of 1.1 mi t/y. Trough process improvements and minor investment this capacity was increased up to 1.6 mi t/y in 2000. In 2003 the third line was started-up increasing this capacity to 2.5 mi t/y. In 2006 the capacity of 4.3 mi t/y was reached, after the start-up of the lines 4 and 5. This paper aims to present the strategies implemented for the pre-operational, commissioning and ramp-up stages for the lines 4 and 5, allowing Alunorte to achieve the nominal daily production capacity in only 20 and 12 days respectively, emphasizing that this excellent result was achieved with the low index of 1.43 for Serious Accident Frequency Rate and that 50% of the operators were hired with no previous experience.

Aluminum Alloys: Fabrication, Characterization and Applications: Processing and Properties

Sponsored by: The Minerals, Metals and Materials Society, TMS Light Metals Division, TMS: Aluminum Committee

Program Organizers: Subodh Das, Secat Inc; Weimin Yin, Secat Inc

Monday PM
March 10, 2008

Room: 293
Location: Ernest Morial Convention Center

Session Chairs: Subodh Das, Secat Inc; Weimin Yin, Secat Inc; Gyan Jha, ARCO Aluminum Inc

2:00 PM

Press Formability of Twin Roll Cast Aluminum Alloys for Automotive Applications: *SooHo Kim¹; Anil Sachdev¹; ¹General Motors Research and Development Center*

This study characterizes the material properties of low-cost twin roll cast (TRC) aluminum alloys, AA3005, AA5052 and AA5754. Tensile properties and forming limit curves of TRC AA5754 are comparable to those of AA5052, due to its lower limit of Mg content (2.6%), coarser grain structure and higher degree of centerline segregation with Fe-rich intermetallic particles. The grain size of TRC AA3005 is much larger than those of the other TRC 5xxx materials, but its plane strain limit is higher than the others, indicating its higher formability. The press formability tryout of all three TRC materials in actual stampings will be demonstrated.

2:20 PM

Forging of Long Flat Pieces of Aluminium with a Precise Mass Distribution Operation: *Malte Stonis¹; ¹Institute of Integrated Production Hannover*

In the automotive forging industry parts made of aluminum alloys are used more often due to the favorable strength to mass relationship and their high ductility. A possibility for preform processes for long flat pieces is a multi-directional forging operation in partly closed dies. In a current project a multidirectional forming operation with three main axial directions is analyzed using FEM simulations. During the forging process, every two of three directions are combined with the third forming direction inactivated. The simulations are evaluated and analyzed regarding the form filling, the formation of flash and the development of temperature and fiber orientation. It was shown that with some combinations it is possible to realize a successful forming operation with the advantage of decreasing the quota of flash in comparison to conventional preforming processes. The detected optimal combination will be verified in a real forging process.

2:40 PM

Hemispherical Bubbles Growth on Electrochemically Charged Aluminum with Hydrogen: *Paul Rozenak¹; ¹Hydrogen Energy Batteries Company*

The formation of surface bubbles (blisters) in aluminum during electrochemical charging by hydrogen was studied. The experiments reveal that, in aluminum samples, a wide distribution of hydrogen bubbles on the surface (blisters) were produced during electrochemical charging. A wide variety in density, distribution

and geometrical shape of the surface bubbles was obtained, with sizes ranging from large (tens of micrometers in the diameter) to very small (nanometers in the diameter). Bubble growth in a various shapes is controlled by hydrogen diffusion to the surface layer of the aluminum, from the defects region below it together with separation of cohesive atomic bonds between the hydroxide layer and the aluminum matrix. In such electrochemically charged aluminum the various hydrogen bubble structures formed during the growth process in the hydroxide layer, can be developed mathematically by the principles used in obtaining the shapes of the grains-boundaries in the polycrystalline microstructures of material.

3:00 PM

Mechanical Properties of Various Aluminum Alloys by Powder Metallurgy: *Antonyraj Arockiasamy¹; Seong Park¹; Randall German¹; ¹Mississippi State University*

Complex aluminum alloy components economically fabricated by powder metallurgy (P/M) offer high strength-to-weight ratio, which meets the demands of the automotive sector. This paper describes die compaction and sintering behavior as well as mechanical properties of various aluminum alloy powders, containing Mg, Cu, Ti, Si and SiC, produced by conventional mixing based on a rapidly solidified 6061 alloy matrix. Three-point bending test, hardness test, dilatometer, TGA/DSC, and SEM/EDS were extensively employed for this study. Comparisons are based on density, flexural strength, and hardness, complimented by microstructure analysis. The overall consolidation is modeled using 3D finite element simulation for optimization of process conditions.

3:20 PM

Formability of Work Hardenable and Heat Treatable Aluminum Alloy Periodic Cellular Metals: *Eral Bele¹; Lily Cheng¹; Brandon Bouwhuis¹; Glenn Hibbard¹; ¹University of Toronto*

Periodic Cellular Metals (PCMs) are open cellular lattices which have a greater structural efficiency than conventional metallic foams. They can be fabricated using perforation stretching methods, in which the nodes of a perforated starting sheet are displaced above and below the plane to form three-dimensional architectures. This approach offers the advantage of being able to tailor the properties of the cellular core by a combination of architectural design, material selection and thermo-mechanical treatments. The focus of this study is the perforation stretching formability of aluminum alloy PCMs. A finite element model is used to investigate the mechanisms that control the load-displacement forming curves of pyramidal cores fabricated from both work-hardenable (AA3003) and heat treatable (AA6061) aluminum alloys.

3:35 PM

The Welding Behaviours of Hot and Cold Rolled AL 5754 Alloys and Residual Stress Analysis: *Firat Esit¹; Özgül Keles¹; I. Yilmaz Taptik¹; ¹Istanbul Technical University*

Comparison to steels, aluminum is one over three times lighter on the contrary some aluminum alloys have the strength as high as steels. Furthermore, some of these aluminum alloys have application areas in automobile, shipbuilding, food processing and aviation industries because of their good corrosion resistance. Especially, Al 5000 (Al-Mg-Mn) alloys became the most popular metal in shipbuilding, food and chemical processing areas to meet the need of developing technology. Joint by welding has lots of defects which cause many serious damages in weldments in service conditions. Particularly, loss of strength and residual stress after welding are common problems in aluminum welding. In this work, welding behaviors of hot and cold rolled Al 5754 alloys are worked out. The aim of the study is analyzing the weldability features between two different alloys depend on the manufacturing methods, and the relations between welding parameters and weldability.

3:50 PM Break

4:00 PM

The Ablation Casting Process: *John Grassi¹; John Campbell¹; ¹Alotech Limited*

A new casting process is described, based on a precision aggregate mold, bonded with a water-soluble binder. For the first time the functions of the mold (i) defining shape and (ii) providing cooling have been successfully separated. Thus thin-walled castings can be filled without the loss of significant temperature,

MONDAY PM

allowing the production of extensive thin castings. Because solidification is separately controlled by the application of water a number of advantages follow immediately. The mold is ablated (i.e. eroded) away by the water without fume or dust, and the 'air gap' is eliminated by direct water contact with the cooling casting enhancing the rate of solidification to levels normally unattainable, resulting in significantly enhanced properties. The process is currently proving itself in commercial operation, having the additional advantages of modest costs of capital equipment and low piece part costs because of the use of low cost and recycling of consumables.

4:20 PM

Study of the Effects of Heating Rate on 7000 Series Aluminum Alloys: Courtney Nowill¹; Mohammed Maniruzzaman¹; Satya Shivkumar¹; Richard Sisson¹; ¹Worcester Polytechnic Institute

The quench sensitivity of various alloys has been studied with the use of the Jominy end quench test. Some studies have shown that heating rates also have an effect on mechanical properties, but data is scarce in the literature. A methodology has been developed in order to study the effects of heating rates. The apparatus designed is for a type of "reverse" Jominy test and results in one dimensional heating throughout the specimen, and therefore, a distribution of heating rates. Two 7000 series alloys, AA7075 and AA7136, were heated using this method to study the effects of heating rate on both solution and aging heat treatments. The effects of a rapid heat up by immersion in a salt bath were also studied versus the effects of a slow air furnace heat up. This study provides a better understanding of the effects of heating rate on 7000 series aluminum alloys.

4:40 PM

Strength-Toughness Optimization Scenarios through Interrupted Ageing in AA6061 and AA2024: Doty Risanti¹; Pedro Rivera Diaz del Castillo²; Sybrand van der Zwaag²; ¹Netherlands Institute for Metals Research; ²Delft Technical University

Aimed at maximisation of strength-toughness relationships in aluminium alloys, interrupted ageing has been proposed as a means to combine these properties. Such processing schedule initiates with a T6 short underageing (177°C for up to 1 hour) followed by a dwell period at a lower temperature for periods up to two weeks and re-aged to the T6 temperature. By combining DSC with hardness, tensile and Kahn-tear testing in studied alloys, the present work studies several heat treatment scenarios and their impact in strength-toughness improvements. Dwell temperatures above 65°C result in a hardness increase whereas those below 45°C decrease it in comparison to the standard T6. DSC scans of AA6061 reveal that dwell temperatures above 65°C lead to an increase in the dissolution of clusters which cannot evolve into GP-zones and β''-precipitate, while in AA2024 it leads to the formation of GPB2-zones. Toughness behaviour for different heat treatment scenarios is presented.

5:00 PM

The Evolution of Microstructure in Rapidly Solidified Al-Si Powders: Eren Kalay¹; Scott Chumbley¹; Iver Anderson¹; ¹Ames Laboratory/Iowa State University

Increasing demand for lightweight materials has helped Al-Si alloy to become a key alloy systems in many industrial applications. In this study, the as-quenched microstructures of Al-Si produced by high pressure gas atomization at eutectic (12.6 wt% Si) and a hypereutectic composition (18 wt% Si) were investigated using scanning electron microscopy (SEM) and transmission electron microscopy (TEM) with respect to particle size. The interface growth velocities and undercooling values were estimated from Jackson-Hunt (JH) and Trivedi-Magnin-Kurz (TMK) solidification models. TEM studies showed that the particle size at which JH and TMK predicts a divergence is consistent with the appearance of microcellular growth morphology. High amount of solute trapping was observed with the evolution to microcellular microstructure. Enhanced solute trapping was determined using energy dispersive spectroscopy and x-ray diffractometry and it was compared with the results obtained from Cu block melt spinning experiments at similar compositions.

5:15 PM

Preparation of Al-Sr Alloys with High Concentration by Molten Salt Electrolysis: Jidong Li¹; Mingjie Zhang¹; Tingan Zhang¹; Dan Li¹; ¹Northeastern University

Al-Sr alloy was prepared by molten salt electrolysis in electrolyte system of SrCl₂-2-SrF₂-BaF₂. Back electromotive force was measured by continuous pulse-computer and the influencing factors for back electromotive force and current efficiency were studied in detail. The result is as follows: the back electromotive force increases with the cathodic current density increasing; when the electrode distance raising, the back electromotive force also increases in a little; with the increase of electrolysis duration, the back electromotive force increases gradually whereas the current efficiency decreases gradually after reaching 73.2%; as the increase of electrolysis duration, the current intensity increasing and the amount of aluminium master alloy decreasing, a high strontium content of 34.8% (mass fraction) in Al-Sr alloy can be obtained.

5:35 PM

Preparation of Al-Li Alloy by Molten Salt Electrolysis: Jidong Li¹; Mingjie Zhang¹; Tingan Zhang¹; Zhuo Zhang¹; Dan Li¹; ¹Northeastern University

Al-Li alloy was prepared with Li₂CO₃ as raw material by using liquid aluminium cathode and a mixture of LiF-KF-BaF₂ as the molten salt electrolysis in a laboratory electrolyte cell. The back electromotive force was measured by the monitoring apparatus of molten salt electrolysis. The factors effecting on back electromotive force, current efficiency, period of feeding and lithium content of Al-Li alloy were studied in detail. Finally, at 770°C, the lithium content of 9.6% (mass fraction) in Al-Li alloy can be obtained by electrolyzing for 5h in the cathodic current density of 0.5A/cm², which the current efficiency can reach 74%. It is affirmed by SEM that the distribution is uniform.

5:55 PM

The Preparation of Al-Sc Alloy by Molten Salt Electrolysis: XiuJing Zhai¹; Yan Fu¹; Junfu Li¹; Mingjie Zhang¹; ¹Northeastern University

The paper was studied on the preparation of Al-Sc alloy by molten salt electrolysis with LiF-ScF₃-ScCl₃ as the electrolyte. ScCl₃ and Sc₂O₃ were used as raw material. And the processing condition of the preparation of Al-Sc alloy which include the influence of current density, the composition of the electrolyte and the electrolysis time were carefully studied respectively. As electrolysis time prolonged, the current efficiency increases gradually and can reach to 73% as the maximum. The content of Sc in alloy can reach to 5.86%. In this experiment condition, the period of adding material is 1g /20 min. It was proved that the current from 2A to 4A and temperature of 850°C is feasible.

Aluminum Reduction Technology: Sustainability and Environment

Sponsored by: The Minerals, Metals and Materials Society, TMS Light Metals Division, TMS: Aluminum Committee

Program Organizers: Martin Iffert, Trimet Aluminium AG; Geoffrey Bearn, Rio Tinto Aluminium Tech

Monday PM

March 10, 2008

Room: 298

Location: Ernest Morial Convention Center

Session Chair: Nancy Jorunn Holt, Hydro Aluminium AS

2:00 PM

Innovative Solutions to Sustainability in Hydro: Hans Petter Lange¹; Lene Solli¹; Nancy Jorunn Holt¹; Hogne Linga¹; ¹Hydro

Sustainability represents challenges for the Aluminium industry but also opportunities. Innovation is essential in meeting these challenges. By being innovative and by having a sustainable approach to the whole value chain, there are large potential for improvements both environmentally as well as financially. Hydro have an innovative approach looking at the value chain from power production to the end user of aluminium products which is improving Hydro's environmental footprint as well as it is generating value for Hydro. The two main challenges the industry is facing today is climate change and energy consumption. In this paper we will show how Hydro systematically have worked

to reduce energy consumption as well as share with you what Hydro is working on for future improvements. Main focus on GHG was AE reduction. Today we are talking about CO₂ capture on the energy production side as well as from the reduction process itself.

2:20 PM Invited

Smelters in the EU and the Challenge of the Emission Trading Scheme: Heinrich Kruse¹; ¹Corus Aluminium Voerde GmbH

The majority of scientists believe that the increasing amounts of CO₂ emitted into the atmosphere by mankind will have severe impacts on the world's climate. The Kyoto protocol was one of the first attempts to reduce CO₂ emissions all over the world significantly. To enforce the protocol's intention within the EU, the commission had introduced the so called "Emission Trading Scheme" (ETS). This brought the EU into a leading position regarding the reduction of CO₂ emissions. For those parties, who are already affected by the ETS, the emission of CO₂ is no longer free of charge. Although the aluminium smelting industry in the EU is exempted from the ETS, it is indirectly – but significantly – affected due to the increasing prices for electrical energy. This paper will give a brief overview about the impacts of ETS and of the national schemes for the competitiveness of the EU aluminium smelters.

2:40 PM

Wireless Measurement of Duct Temperatures on Aluminum Smelting Pots: Correlation to Roofline HF Concentration: Daniel Steingart¹; James Evans²; Andrew Redfern¹; Paul Wright²; Neal Dando³; Weizong Xu³; Michael Gershenzon³; Henk Van der Meyden³; ¹Wireless Industrial Technologies; ²University of California; ³Alcoa Inc

Previous papers described wireless devices (motes) for measuring the temperature of the gas in ventilation ducts from smelting pots, and the heat flux through the pot shells. This paper describes more extensive, longer measurements of duct temperature carried out on ten pots at a smelter in 2006. Measurements were carried out for 43 days and 1.3 million temperatures were recorded, along with simultaneous real-time measurements of roofline HF concentration. The duct motes were self-powered using thermoelectric generators operating off temperature differences between the duct gasses and the surrounding air. Temperatures measured by the motes reflected all pot-work such as removal of cover panels or opening of end doors. Temperature measurements showed a good correlation with roofline measurements of HF above the pots. Even after elimination of temperatures when the pot were clearly being worked, significant variations in duct temperature were observed, both from pot-to-pot and from day-to-day on individual pots.

3:00 PM

Hard Gray Build-Up: Neal Dando¹; Stephen Lindsay¹; ¹Alcoa Inc

The dry scrubbing and secondary alumina handling systems for pre-bake cell technologies are hampered by accumulations of hard gray build-up, or HGB. These mineral-like deposits are dependant upon a number of factors that control the rate of scale formation. If not systematically addressed with cleaning and maintenance procedures HGB can: greatly reduce the removal efficiency of gaseous fluoride in dry scrubbers, reduce the capability to convey alumina in sufficient quantities, reduce filter life and alter the concentration of fluoride on secondary alumina. This paper will define the chemical structure of HGB, propose a mechanism for HGB formation, identify the key areas of concern in a smelter and discuss practical alternatives to control the rate of formation.

3:20 PM Break

3:30 PM

Comparison of PFC Emission Rates for Operating and Newly Started Pots at a Horizontal Stud Soderberg Smelter: Neal Dando¹; Weizong Xu¹; Steven Rusche¹; ¹Alcoa Inc

Anode effect durations are commonly described as "total time above 8 volts," wherein the total pot operating time above 8 volts is integrated and used to estimate perfluorocarbon (PFC) emissions. Soderberg smelting pots are known to exhibit sustained periods of time where operating voltage may exceed 8 volts (commonly 8-10 volts), however the pots do not exhibit ore starvation, nor do they exhibit "typical" anode effect behavior (i.e. rapid voltage spikes to 20-50 volts). This behavior is observed during pot startups, as well as during "normal" pot operations. Continuous PFC monitoring studies of individual horizontal stud

Soderberg pots were performed during startup and during normal operation to show that Soderberg pots exhibiting sustained elevated operating voltages (8-10V) in the absence of ore starvation do not generate PFC emissions. These observations suggest that an anode effect (AE) definition of "time > 8 volts" would overestimate true AE durations at Soderberg smelters.

3:50 PM

Reduced Emissions from the Elkem Aluminium Lista Soderberg Smelter: Tor Pedersen¹; Marianne Jensen¹; Kjell Kalgraf¹; Willi Larsen¹; Arnt Olsen¹; ¹Elkem Aluminium ANS

Elkem Aluminium Lista has worked on developing its Soderberg Technology for many years. Dry paste was introduced in the early eighties. In 1986 Elkem Aluminium decided to develop a closed point feeding technology and improve the pot gas collection system. It was also decided to develop a technology to collect and clean the fumes from the Soderberg anode tops. These technologies are now developed and installed at the smelter. The point feeding technology comprises a complex of elements such as feeding locations, pot signal filtering, alumina feed algorithm, design of the point feeding system, equipment and not at least the standard operating practices. The technology has resulted in a substantial drop in the anode effect frequency, giving an according reduction in the emission of climate gases. The technology has also led to big reductions in fluoride, particulate and PAH emissions. Low emissions can be obtained even with an increased production.

4:10 PM

Comparison of PFC Emission Coefficients for Operating and Startup Pots at a Side Work Prebake Smelter: Weizong Xu¹; Neal Dando¹; David Sedlacek¹; ¹Alcoa Inc

Tier 3b perfluorocarbon (PFC) emission coefficients are determined by performing ventilation duct PFC measurements under normal potline operation and used to estimate plant-specific PFC emissions based upon integrated anode effect duration. To-date, little information exists regarding the PFC emission of newly started pots relative to those under normal operation. In addition, the practice of including or excluding anode effect data from newly started pots is not uniform between aluminum smelters. Two PFC monitoring campaigns were performed during a side work prebake (SWPB) potline restart at an Alcoa smelter in 2007. The measured PFC slope terms agreed well (< 10%) from these two tests, and were also consistent with 2006 benchmarked data, suggesting that no significant difference exists between new and "old" pot PFC emission coefficients. This data also suggests that anode effect data from newly started prebake pots should be included in the plant's PFC reporting inventory.

4:30 PM

Study on the Anode Effect Reduction at Zhengzhou Research Institute of CHALCO: Wangxing Li¹; Qingyun Zhao¹; Shilin Qiu¹; Hengwei Yan¹; ¹Zhengzhou Research Institute of CHALCO

In order to cope with environment limits, many aluminum smelters are being forced to adapt their operations to reduce the emission of greenhouse gas. The anode effect plays an important role in PFC emission. So reducing the anode effect is an emergency task for primary aluminum smelters. Zhengzhou Research Institute of CHALCO (ZRIC) has achieved a substantial improvement on anode effect rate reduction in the prebaked cells with point-feeders. Those achievements mainly based on some initiatives in cell control and management. As a result of industrial experiment on some real life pots, the anode effect rate has dropped from 0.35 to 0.03 anode effects per cell day (AE/C/D), which is an excellent result. This paper mainly presents the basic research on AE and some experiences on AE reduction, as well as the implementation of AE quenching techniques.

Biological Materials Science: Implant Biomaterials I

Sponsored by: The Minerals, Metals and Materials Society, TMS Structural Materials Division, TMS: Biomaterials Committee, TMS/ASM: Mechanical Behavior of Materials Committee

Program Organizers: Ryan Roeder, University of Notre Dame; Robert Ritchie, University of California; Mehmet Sarikaya, University of Washington; Lim Chwee Teck, National University of Singapore; Eduard Arzt, Max Planck Institute; Marc Meyers, University of California, San Diego

Monday PM

Room: 390

March 10, 2008

Location: Ernest Morial Convention Center

Session Chairs: Ryan Roeder, University of Notre Dame; Albert Lin, University of California, San Diego

2:00 PM Invited

Phase-Separated Hydrogels Comprised of Both Hydrophilic and Hydrophobic Segments: *James Mason*¹; Brian Thomas¹; Mike Wallick¹; Don Yakimicki¹; ¹Zimmer Inc.

Typical hydrophilic hydrogels lack the required mechanical properties to be useful as articulating and weight bearing mediums. Therefore, hydrogels were developed which incorporated both a hydrophilic and a hydrophobic segment. These new hydrogels behave like semi-crystalline polymers utilizing both crystalline regions and amorphous regions. The hydrophilic segments (amorphous regions) provide the water absorption, fluid flow, and lubricious properties. The hydrophobic segments (crystalline regions) provide the strength, tear, shear and creep resistance. The initial focus of the work presented here was to provide a material with higher strength, ease of processing, and better shear resistance that can be injection molded. Therefore, efforts focused on utilizing polymer blends and reactive compounding. When tested, the new hydrogels show improved mechanical properties without loss of lubricity.

2:30 PM

Evaluation of a Synthetic Vertebral Body Augmentation Model for Rapid and Reliable Cyclic Compression Testing of Materials for Balloon Kyphoplasty: *Gladius Lewis*¹; Jeffrey Schwardt²; Thomas Slater²; ¹University of Memphis; ²Kyphon, Inc.

A validated synthetic vertebral body augmentation model — a cube (26 mm sides) of low-density polyurethane foam with a centrally-located through-thickness cylindrical hole completely filled with a bolus of augmentation material — was used to compare two balloon kyphoplasty (BKP) augmentation materials with very different chemistries (a high-viscosity acrylic bone cement (PMMA) and a calcium phosphate bone substitute (CP)) in cyclic compression tests. The model was immersed in PBS, at 37°C; the frequency was 3 Hz; and the maximum load was either 1150 N or 2300 N. Clear demarcation was seen in the qualitative results (fracture patterns) and the quantitative results (Kaplan-Meier survival analysis of the number of cycles to failure) obtained with the two materials tested. Thus, the use of this model for rapid and reliable ex vivo screening of BKP augmentation materials was considered both valid and appropriate (that is, clinically relevant to BKP).

2:50 PM

Rapid Prototyping of Biological Materials: Aleksandr Ovsianikov¹; Boris Chichkov¹; Anand Doraiswamy²; Roger Narayan²; ¹Laser Zentrum Hannover; ²University of North Carolina and North Carolina State University

Recent studies have shown that rapid prototyping techniques may be used to create patient-specific medical devices and artificial tissues. In this presentation, recent advances in the use of laser direct writing and two-photon polymerization to fabricate microstructured medical devices and scaffolds for tissue engineering will be discussed. For example, we have used two-photon polymerization for rapid prototyping of microneedles and middle-ear bone replacement prostheses. In addition, we have developed differentially adherent surfaces using laser direct writing process. In this work, 60-400 micrometer-wide diameter channels were micromachined onto agarose surfaces using an ArF excimer laser and filled with extracellular matrix solution. Muscle-like and nerve-like cells were then allowed to proliferate on the surfaces of these micromachined channels. Our

results demonstrate that laser-based rapid prototyping techniques may be used to fabricate medical devices with a larger range of sizes, shapes and materials than conventional microfabrication techniques.

3:10 PM

Microstructures and Mechanical Properties of Electron Beam – Rapid Manufactured Ti-6Al-4V Biomedical Prototypes Compared to Wrought Ti-6Al-4V: *L. Murr*¹; E. Esquivel¹; S. Quinones¹; S. Gaytan¹; M. Lopez¹; E. Martinez¹; D. Hernandez¹; E. Martinez¹; J. Martinez¹; T. Hoppe²; W. Meyers²; S. Stafford¹; R. Wicker¹; F. Medina³; U. Lindhe³; ¹University of Texas; ²Stratasys; ³Arcam AB

This study represents an exploratory characterization and comparison of electron-beam manufactured (EBM) or rapid-prototype (RP) manufacturing of Ti-6Al-4V components (from nominal 30 µm diameter powder) with wrought products. Acicular α and β microstructures observed by optical metallography and electron microscopy (SEM and TEM) are compared along with corresponding tensile test and hardness data; including the initial powder particles where the Vickers microindentation hardness averaged 5.0 GPa in comparison with the fully dense, EB manufactured product with an average microindentation hardness ranging from 3.6 to 3.9 GPa. This compares with wrought products where the Vickers microindentation hardness varied from 3.4 to 5.4 GPa. Biomaterials/biomedical applications of EBM prototypes in direct prosthesis or implant manufacturing from CT or MRI data are reviewed in the context of this work, especially prospects for the tailoring of properties through EB control to achieve customized implant and prosthetic products direct from CT-scans.

3:30 PM Break

3:40 PM Short Oral Presentations for the Student Poster Contest

Bulk Metallic Glasses V: Structures and Mechanical Properties II

Sponsored by: The Minerals, Metals and Materials Society, TMS Structural Materials Division, TMS/ASM: Mechanical Behavior of Materials Committee

Program Organizers: Peter K. Liaw, University of Tennessee; Wenhui Jiang, University of Tennessee; Guojing Fan, University of Tennessee; Hahn Choo, University of Tennessee; Yanfei Gao, University of Tennessee

Monday PM

Room: 393

March 10, 2008

Location: Ernest Morial Convention Center

Session Chairs: A. L. Greer, University of Cambridge; Jürgen Eckert, IFW Dresden

2:00 PM Keynote

Effects of Shear Banding on the Structure and Properties of Metallic Glasses: *A. L. Greer*¹; ¹University of Cambridge

It is well known that under ambient conditions, metallic glasses show plasticity in the form of shear bands. The localization of deformation in bands as little as 10 nm thick implies extreme conditions of high shear rate, high shear, high heating rate and cooling rate. The consequences of these conditions for the structure of the glass after shear will be reviewed, taking account of recent structural and calorimetric studies. The possibilities for using shear banding to tailor properties will be considered.

2:30 PM Invited

How to Improve the Deformability of Bulk Metallic Glasses: *Jürgen Eckert*¹; ¹IFW Dresden

Metallic glasses have mechanical properties that make them attractive candidates for a variety of structural and functional applications. One drawback still limiting such applications is their tendency for shear localization upon deformation. To circumvent such limitations, concepts of creating heterogeneous materials with different type and length-scale of phases have been followed to control the mechanical properties by proper alloy and microstructure design. The recent developments along this line will be summarized and new results for different types of bulk metallic glasses and composites will be presented

to illustrate how the mechanical properties can be tuned by appropriate phase and microstructure control. In all these cases the details of the metastable phase formation are closely linked with optimized processing conditions required to form the desired microstructure. The possible mechanisms that govern the deformation behavior will be discussed and linked with the overall plastic deformability and the fracture of the material.

2:50 PM Invited

Size Effect in the Deformation and Failure of Metallic Glasses: *Ju Li*¹; ¹Ohio State University

Recent experimental and theoretical work have suggested possible size effect in the plasticity and failure resistance of metallic glasses. While bulk metallic glasses manifest negligible tensile ductility, nanoscale metallic glasses show significant ductility under tension (PNAS 104, 11155). Nanopillar compression experiments also show intriguing behavioral differences sensitive to pillar size. Multiple reasons could contribute to this size dependence: (a) proliferation of amorphous-crystal interfaces or surfaces that directly mediate plasticity, as well as indirectly alter the glass structure, (b) Weibull-like statistics for the nucleation of a runaway flow defect from the condensation of shear transformation zones in a finite volume, and (c) intrinsic thermomechanical lengthscales, such as the glue zone width in the aged-rejuvenation-glue-liquid model of a runaway shear band (Acta Mater. 54, 4293). A “Hall-Petch” like relationship may exist with respect to the metallic glass sizescale, but for the useful ductility (tensile and compressive) instead of strength.

3:10 PM Invited

Size Dependence of Compressive Strength of a Zr-Based BMG: *W.F. Wu*¹; *Yi Li*¹; ¹National University of Singapore

A sample size dependence of the compressive strength has been established for a Zr-based bulk metallic glass (BMG) with a statistical method. Two competing factors, namely, free volume effect and flaw-sensitivity effect were found to affect the apparent strength of BMGs with different specimen sizes. As a result, there was a critical size with which the strength of BMG reached a maximum. In addition, a size dependence of Weibull modulus was observed which is attributed to the fact that the resulted BMG samples possessed various structural configurations due to the different size dependence cooling rate. The decrease in Weibull modulus as the sample size increases indicates a deterioration of mechanical reliability for larger-sized BMG component.

3:30 PM Invited

Studies of Shear Band Propagation Using Spatially and Temporally Resolved Measurements of Strain During Compression of a Bulk Metallic Glass: *Wendelin Wright*¹; *Jeffrey Florando*²; *Mary LeBlanc*²; *Todd Hufnagel*³; ¹Santa Clara University; ²Lawrence Livermore National Laboratory, Engineering Technologies Division; ³Johns Hopkins University

As a shear band rapidly deforms during constant displacement rate compression testing of bulk metallic glasses, the displacement rate of the material in the band exceeds the displacement rate imposed on the sample. Consequently, the load drops, and the load train and the bulk of the sample elastically recover. Previous work has recorded some features of these serrations, but typically only the sample average displacement is measured. Strain gages were applied to each side face of rectangular parallelepiped specimens which were then subjected to quasi-static uniaxial compression. The data indicate the existence of a latent period between the onset of strain events as recorded on opposing faces of the sample. The results also show that strain gages on opposing sides of the sample record strain events of opposite sign (tensile vs. compressive). The implications of this data for shear band initiation and propagation in bulk metallic glasses will be discussed.

3:50 PM Break

3:55 PM Invited

The Amorphous to Crystalline Massive Transformation in Al-10 at%Sm: *Jason Hadorn*¹; *Gary Shiflet*¹; ¹University of Virginia

Melt-spun amorphous Al90Sm10 ribbon has been previously documented to crystallize via massive transformation. In this study, the crystallization of this material was studied and analyzed using XRD, TEM, and EDS in order to determine whether or not this phase transformation met the requirements for a massive transformation. Crystallization was observed to be a single-phase to single-phase phenomenon and to occur without any chemical partitioning,

both requirements for such a transformation. Additionally, the growth of the crystallized product phase was observed to be linear, a property also characteristic of a massive transformation. From analysis of the growth rate, an activation energy for growth of a precipitate was calculated. In addition to crystallization, subsequent phase transformations were observed en route to the equilibrium state. These other transformations were analyzed via similar methods, and an isothermal TTT curve was consequently constructed.

4:15 PM Invited

Mechanical Properties and Fracture Behaviors of Bulk Amorphous Alloys: *Jun Shen*¹; ¹Harbin Institute of Technology

In this presentation, we will report on the observation of elastic-wave patterns on nano-scale that form in the compressive fracture process of a Ni-based amorphous alloy. The formation of nano-waves is evidenced via the creation of microbranching instability as well as the interaction of a crack front with the material inhomogeneities, i.e., micro-cracks. We will also report on the dramatic effect of sample size on the plastic deformation capability of a Ti-based bulk metallic glass. Compared with the larger one, the smaller size glassy alloy with the same chemical composition exhibits significantly enhanced plasticity, suggesting a “smaller is softer” trend of metallic glasses. The phenomenon is attributed to the fact that the smaller size alloy, which experienced a faster cooling rate during solidification, contains a larger number of soft regions - free volume sites, favoring the preferential nucleation of shear bands and thus allowing enhanced plasticity upon compressive loading.

4:35 PM

Effect of Temperatures on Plastic Flow and Shear Bands in a Zr-Based Bulk-Metallic Glass: *Wenhui Jiang*¹; *Fengxiao Liu*¹; *Peter K. Liaw*¹; *Hahn Choo*¹; *Ran Li*²; *Tao Zhang*²; ¹University of Tennessee; ²Beijing University of Aeronautics and Astronautics

The recent development of bulk-metallic glasses (BMGs) makes the applications of metallic glasses as structural materials become reality. However, the poor ductility and subsequent premature fracture, which are imputed to the highly-localized inhomogeneous deformation, still limit their applications. In spite of intensive studies on the inhomogeneous deformation of metallic glasses, there are still inconsistent understandings on inhomogeneous-deformation behavior. It is known that strain rate and temperature are two important external factors affecting deformation behavior of BMGs. While some research focuses on effect of strain rate, little work has been done on effect of temperature. In this talk, we will present our recent work on the inhomogeneous deformation of a Zr-based BMG at various temperatures and strain rates. Based on the shear-banding spatiotemporality that we observed, we can explain strain-rate- and temperature-dependences of shear-banding operations and serrated plastic flows. The work provides new insights into the inhomogeneous-deformation behavior of bulk-metallic glasses.

4:50 PM

Rate Dependence of Shear Banding in a Mg-Based Bulk Metallic Glass Characterized by Nanoindentation: *Shuangxi Song*¹; *J.S.C. Jang*²; *T.G. Nieh*¹; ¹University of Tennessee; ²I-Shou University

Nanoindentation behavior of Mg57Cu31Y6.6Nd5.4 bulk metallic glass was characterized at different loading rates. The load-displacement curves exhibit significant displacement serrations, apparently associated with discrete shear-band emission, at low loading rates but disappear at high rates. Analyses based on displacement serration, strain rate oscillation and hardness serration were carried out to determine the critical strain rate at which the transition from inhomogeneous to homogeneous deformation takes place. It was concluded that hardness serration analysis probably provides the most reasonable result as the other two were limited by the instrument noises. From a shear band nucleation model the critical nucleus size was also estimated to be a sphere of about 25 nm in diameter.

5:05 PM

Rate- and Temperature-Dependent Shear Band Initiation and Implications on Ductile to Brittle Transition: *Yanfei Gao*¹; *T. Nieh*¹; *Takeshi Egami*¹; ¹University of Tennessee and Oak Ridge National Laboratory

Shear banding behavior in amorphous alloys is very sensitive to the environmental temperature, the applied strain rate, and the geometric constraints. The competition between cleavage fracture and crack tip blunting

in the amorphous alloy is studied by numerically determining the responses of a crack subjected to a history of applied stress intensity factor. The brittle fracture is modeled by a traction-separation law in the crack plane. The amorphous alloy is modeled by a viscoplastic constitutive law in which the viscosity depends on the free volume, while the free volume evolution equation is driven either by shear or by hydrostatic tension. Because of the strain softening and strain rate hardening behavior, it is found that at low loading rate, the initiation of shear bands will reduce the stress concentration, while the fracture behavior is brittle at high loading rate. A preliminary assessment of ductile fracture is also presented.

5:20 PM

Ductilization of Brittle Bulk Metallic Glass by Deformation at Room Temperature: *Min Ha Lee*¹; Kwang Seok Lee¹; Jayanta Das¹; Uta Kühn¹; Jürgen Eckert¹; ¹IFW Dresden

Metallic glasses, especially bulk metallic glasses (BMGs) are well-known interesting for their exceptional properties, including high strength, relatively low Young's modulus, and perfect elastic behavior. However, in the case of typical glassy metallic alloys, there are no well-defined atomic planes or slip systems, and it is well established that at temperatures below the glass transition temperature (T_g), inhomogeneous plastic deformation occurs, during which localized narrow shear bands are formed and plastic flow is confined to these shear bands resulting in catastrophic failure. As a result BMGs show little macroscopic room temperature plasticity. To understand the plasticity in BMGs based on a comparative study between as-quenched state and the severely deformed state in typical brittle monolithic BMG, in the current study, we compare the physical and thermo-mechanical properties between the as-quenched state and the severely deformed state (structurally relaxed state) of typical monolithic BMG.

5:35 PM

Comparison of Formability between Zr-Based Monolithic Bulk Metallic Glass and Bulk Metallic Glass Composite in Supercooled Liquid Region: *Hyun-Joon Jun*¹; Kwang Seok Lee²; Young Won Chang¹; ¹POSTECH; ²IKM

The deformation behaviors of a monolithic Cu_{47.5}Zr_{47.5}Al₅ (at. %) bulk metallic glass (BMG) and Zr_{76.11}Ti_{4.20}Cu_{4.51}Ni_{3.16}Be_{1.49}Nb_{10.53} (at. %) bulk metallic glass composite were studied through a series of compression tests in supercooled liquid region (SLR). In the homogeneous flow regime, a transition from the Newtonian to non-Newtonian flow was observed to take place depending upon both the strain rate and temperature. These two flow modes were then described by applying the Newtonian viscous flow theory and the transition state theory, respectively. On the basis of a dynamic materials model, a processing map could successfully be constructed to estimate the feasible forming conditions for these monolithic BMG and BMG composite alloys. Formability of the alloys through a processing map was compared with extrusion simulation results, and BMG composite was harder to deform compared to a monolithic BMG due to the hindrance of dendrite requiring strength for a viscous flow in the SLR.

5:50 PM

Relationship between the Viscous Deformation of Bulk Metallic Glasses and the Diffusional Creep of Polycrystalline Materials: *Young-Sang Na*¹; Jong-Hoon Lee¹; ¹Korea Institute of Materials Science, Korea Institute of Machinery and Materials

Viscous deformation of bulk metallic glass around glass transition temperature was analyzed based on the diffusional creep model. Viscous flow behaviors of 2 Zr-based BMG alloys and 1 Fe-based BMG alloy were employed. Viscous flow behaviors of the selected alloys in the supercooled-liquid state were obtained both from the literature and from a series of isothermal compression tests. Amorphous matrix of bulk metallic glasses was assumed to behave similar to the grain boundary in polycrystalline metals to approximate the diffusivity of major constituent elements. In spite of rough approximation of the parameters in Nabarro-Herring creep equation, the reasonable value of the diffusion path could be obtained from the experimentally-obtained metal flow data. By comparing the calculated average diffusion path with the shear bands observed, new viscous deformation model based on the atomic diffusional motion via free volume or nano-voids will be proposed.

6:05 PM

Effects of High Pressure Treatment on the Structural Relaxation and the Deformation of a La-Base Bulk Metallic Glass: *Jianguo Lin*¹; Fenghua Wang²; Haowen Xie¹; Cui'e Wen¹; Peter Hodgson¹; ¹Deakin University; ²Xiangtan University

In the present study, a La-based, La_{62.0}Al_{15.7} (Cu, Ni) 22.3, BMG was annealed at room temperature under the high pressure up to 5 GPa, and the structures of the samples treated at the different pressures were characterized by X-ray diffraction (XRD) and differential scanning calorimetry (DSC). It was found that the structural relaxation occurred in the BMG during HP treatment, and the extent was strongly dependent on the applied pressure. The glass transition temperature (T_g) and the onset temperature of the first crystallization (T_{x1}) of the BMG display a nonmonotonic increasing function of pressure. The effects of HP treatment on the mechanical properties and deformation of the BMG were also investigated by using indentation and compression tests.

Cast Shop Technology: Sustainability in the Casthouse

Sponsored by: The Minerals, Metals and Materials Society, TMS Light Metals Division, TMS: Aluminum Committee

Program Organizers: Hussain AlAli, GM Casthouse and Engineering Services, Aluminium Bahrain Company (ALBA); David DeYoung, Alcoa Inc

Monday PM
March 10, 2008

Room: 295
Location: Ernest Morial Convention Center

Session Chair: Subodh Das, Secat Inc

2:00 PM Keynote

Melting Furnaces, Technical Developments Reviewed and Thoughts for the Future: *Barry Houghton*¹; ¹Solios Thermal

Over the last 20 years or so, melting furnace technology, has seen a few significant developments affecting efficiency, melt rate and reliability. The basic heat transfer technology is well understood, and small improvements to performance are now generally through incremental changes and optimisation. Compared to some other technologies however, there is still much scope for further development outside of the basic performance criteria. This paper looks at many of the improvements to date but then goes on to compare it to where other technologies are now positioning themselves. Are they relevant to the casthouse situation and can we learn from them? We believe so and this will be discussed in relation to environmental impact, safety, automation, service intervals and of course value for money. This is the big challenge, we all expect much more for our money than previously, can we achieve it?

2:20 PM

Metal Treatment Update: Bruno Maltais¹; Dominique Privé¹; *Martin Taylor*¹; Marc-André Thibault¹; ¹STAS

There have been significant improvements in the last few years to operating procedures and equipment in treating molten aluminium. It is now recognised that reducing bath from pot room crucibles with siphoning and/or skimming can reduce contaminants in cast house furnaces. The TAC (Treatment of Aluminium in a Crucible) is a well-known equipment to reduce sodium but there have been significant improvements in design. Furnace treatment in the cast house using an RFI (Rotary Flux Injector) to both efficiently stir the metal and remove alkalines and inclusions, can contribute to a chlorine free environment. In-line treatment with degassers can remove hydrogen, alkalines and inclusions. There have been significant advances to the operating procedures for the use of chlorine gas in degassers to enable cleaner metal, attaining high levels of cleanliness. Salt additions into the degassers have also been shown to significantly reduce inclusions, even with a chlorine free degasser.

2:40 PM

Highest Efficiency and Economic Burner Concepts: *Michael Potesser*¹; Burkhardt Holleis²; Davor Spoljaric³; Helmut Antrekowitsch¹; Adrianus Hengelmolen⁴; ¹University of Leoben; ²Messer Austria GmbH; ³LLC Elme Messer Gaas; ⁴Hengelmolen Furnace Systems

The efficiency of industrial combustion processes can be raised in two ways, either by preheating the fuel and combustion air or by adding oxygen. The most important issue of the usage of oxygen burners is the substantially increasing melting rate by lowering the specific production costs because of the higher combustion efficiency and lower investment costs. The diluted or flameless combustion (internal offgas recirculation) and the external offgas recirculation solves the problem with the high flame temperature and leads to cold combustion and lower dross formation. The Oxipyr®-Air combines the technology of diluted combustion during air and oxygen usage decreasing the emission of pollutants. Constitutive of the Oxipyr®-Air development a fuel-oxygen-burner, Oxipyr®-Flex, was designed for a maximum of flexibility for the customer. The Oxipyr®-Air and Oxipyr®-Flex have been developed for the specific needs of melting and recycling companies for all non ferrous metals.

3:00 PM

Increase of the Productivity in an Aluminum Slug Plant Using Porous Plugs: *Klaus Gamweger*¹; ¹RHI

Gas purging systems are well established in the non ferrous metallurgy at multiple steps in the metal production, including melting, converting, alloying and cleaning. The kinetics of all of these process steps are influenced positively by using gas purging systems. In the aluminum industry, inert or reaction gases are blown into the melt using porous plugs to achieve improved metal qualities and a higher productivity. To enable the best possible efficiency of the applied process gases a complete package was developed that includes porous plugs, refractory expertise, gas supply technology and gas control equipment. This paper discusses the technological and economical advantages of this system. The benefits in fuel reduction, gas consumption, service live, maintenance and most notably the potential time savings were shown on the basis of an aluminum slug plant in Austria.

3:20 PM

Minimizing Potroom Bath Transfer to the Casthouse: *Edward Williams*¹; David DeYoung¹; Robert Levesque¹; ¹Alcoa, Inc

Transfer of electrolytic bath from potroom smelting cells to casthouse furnaces causes many problems in casting facilities. Bath that gets transferred collects in casthouse furnaces, reducing furnace capacity and refractory life. Bath transferred can also react in the furnace to release alkalis to the melt, which must be removed, typically by fluxing with some form of chlorine. These fluxing requirements lead to significant cost, cycle time and EHS issues. Measurement of the actual amount of bath transferred from the smelter has been difficult in the past. A method for evaluating the amount of bath transferred into an ingot has been developed. This method has been used to show a reduction in bath transfer by holding crucibles to a temperature where any bath present is solidified and is less likely to be transferred into the furnace.

3:40 PM Break

3:50 PM

Understanding of the Mechanisms of Bath Carryover with Molten Aluminium in Smelters: *Vincent Goutière*¹; Claude Dupuis¹; ¹Alcan International Limited, Arvida Research and Development Centre

Tapping of Hall-Héroult cells has always been associated with the simultaneous uncontrolled aspiration of a significant amount of electrolytic bath with the molten aluminium. The bath carried over with the molten metal has numerous negative impacts on tapping tube blockage, crucible cleaning and on downstream metal processing steps such as metal pre-treatment and furnace operations and costs. Over the years, few research works to understand the mechanisms responsible for bath aspiration during tapping were published. This paper presents the experimental work done at the Arvida Research and Development Centre. Physical modelling was used to develop an understanding of the key parameters and the mechanisms responsible for bath aspiration. The importance of integrating metal circulation patterns in the cell will be exemplified. The effect of the key operating parameters such as the tapping flowrate and tapping

tube positioning will be presented and the correlation with industrial results will also be discussed.

4:10 PM

Furnace Energy Saving Myths: *David White*¹; ¹Schaefer Group, Inc.

This will be a presentation on the true ROI for some of the more popular energy saving ideas out there. For example: (1) Recuperation, (2) Regenerative Burners, (3) Fixed Heat Loss (refractory construction), (4) Pre-heating, (5) Circulation, (6) Doors, (7) Thermocouple placement. Discussion about the best way to save money with each of these items. To do's and not to do's when trying to save energy.

4:30 PM

Salt Injection to Replace Chlorine in A622 In-Line Degassers: *Corleen Chesonis*¹; David DeYoung¹; ¹Alcoa Inc

Rotating impeller degassers like the Alcoa A622 typically inject a mixture of argon and chlorine to treat the metal as it flows from the furnace to the casting pit. The use of gaseous chlorine represents a significant environmental and industrial hygiene issue. Storage, piping, safety, and training requirements can be stringent. Eliminating the use of chlorine requires the development of alternative methods to remove alkali and alkaline earth impurities and to maintain metal cleanliness. Static and dynamic tests were conducted to evaluate the feasibility of using solid salts containing MgCl₂ to replace chlorine in an A622 degasser. This paper will present comparisons between chlorine injection and salt injection for Na, Ca, and hydrogen removal, utilization efficiency of the injected reactant, metal cleanliness measured by LiMCA and PoDFA, and emissions of particulate, chlorine, and HCl. The effects of salt chemistry, particle size, and feed rate will also be discussed.

4:50 PM Panel Discussion

Characterization of Minerals, Metals, and Materials: Characterization of Extraction and Processing

Sponsored by: The Minerals, Metals and Materials Society, TMS Extraction and Processing Division, TMS: Materials Characterization Committee
Program Organizers: Jian Li, Natural Resources Canada; Toru Okabe, University of Tokyo; Ann Hagni, Intellection Corporation

Monday PM

March 10, 2008

Room: 284

Location: Ernest Morial Convention Center

Session Chairs: Tzong Chen, CANMET-MMSL; Junji Shibata, Kansai University

2:00 PM

In-Situ Monitoring and Validation of a Uranium Mill Tailings Management Facility Design Using X-Ray Absorption Near-Edge Structure (XANES) Spectroscopy: *Jeff Warner*¹; John Rowson Rowson²; ¹Canadian Light Source Inc.; ²Areva Resources Canada Inc.

Uranium ore containing elevated concentrations of arsenic (up to 2 wt %) are processed at the McClean Lake Operation in the Athabasca Basin of northern Saskatchewan. This region of northern Saskatchewan is responsible for 33% of the world production of uranium. A major concern of AREVA Resources Canada Inc. (AREVA) as well as provincial and federal regulators is the potential long term risk that significant amounts of arsenic may pose to surrounding lakes and waters after their disposal in the JEB Tailings Management Facility (TMF). This article is concerned primarily with the geochemical monitoring of arsenic in sediments obtained from bore holes in the JEB TMF. Sample depth in the TMF corresponded to the time of disposal and the age of the sediments in the TMF. The evolution of arsenic oxidation states was investigated by X-ray Absorption Near-Edge Structure (XANES) spectroscopy.

2:20 PM

Characterization of Gold in a Conventional Copper Refinery Anode Slimes Treatment Circuit: *Tzong Chen*¹; John Dutrizac¹; ¹CANMET-MMSL

During the electrorefining of copper anodes, gold shows a strong affinity for selenium. In the raw anode slimes, gold occurs mainly as tiny metallic gold

MONDAY PM

particles which show a strong affinity for the selenide phases. Decopperizing of the anode slimes generates mostly metallic gold, but also promotes the incorporation of Au in silver selenide. A greater fraction of the gold is converted to $(\text{Ag,Au})_2\text{Se}$ or Ag_3AuSe_2 when high-Se and high-Ag anode slimes are decopperized at elevated temperatures and pressures. After pelletization and roasting of the slimes, the gold is converted to a (Ag,Au) -alloy and Ag_3AuSe_2 . Smelting of the roasted products eliminates the selenium and converts the gold to an Ag-rich (Ag,Au,Pd) -alloy in the Dore metal. In the subsequent silver refining process, gold collects as a gold-rich (Au,Ag,Pd) -alloy in the gold mud.

2:40 PM

Copper Release Velocity from Copper Vermiculite in Aquatic Environment: Bowen Li¹; *Jiann-Yang Hwang*¹; ¹Michigan Technological University

The lifespan of antimicrobial materials is an important factor for applications. Copper vermiculite is a new material with excellent antimicrobial ability. In this study, the antibacterial durability of copper vermiculite in static and shocked aquatic environments has been investigated. The release velocity of copper ions from copper vermiculite grains is demonstrated. The diffusion mechanism of copper from vermiculite structure and the testing method for discharge of metallic ions are also discussed.

3:00 PM

Characterization of Wastes from Water Treatment Plant: *Carlos Maurício Vieira*¹; Jhonatas Vitorino¹; Rubén Sánchez¹; Sergio Monteiro¹; ¹State University of the Northern Fluminense

This work has for objective the characterization by XRD, XRF, DTA/TG, SEM and sedimentation techniques of three types of waste from water treatment plant for incorporation into clayey ceramics for civil construction. The plasticity of the waste was evaluated by the Atterberg limits. The wastes were collected at different points: the sand collector, the decantation stage and the filter stage in the water treatment plant of the county of Campos dos Goytacazes, Rio de Janeiro State, Brazil. The results indicated that the sludges from decantation and filter stages are mainly formed by clay mineral. The waste from sand collector is basically quartz sand material. Both types of wastes can be used into clayey ceramic according to the characteristics of the clays used in the body formulation.

3:20 PM Break

3:40 PM

Measurement of Leaching Rate of Heavy Metals from Copper Tailing: Bowen Li¹; *Jiann-Yang Hwang*¹; Rick Nye²; Domenic Popko²; Peter O'Dovero³; ¹Michigan Technological University; ²Lesktech Ltd.; ³Westwood Lands, Inc.

The copper tailing piles in the Western Upper Peninsula of Michigan State is a significant concern for environment protection both for local land and Lake Superior. This study investigated the measurement of leaching rates of heavy metals including copper, arsenic, chromium, cobalt, barium, iron, titanium, and zinc from copper tailings piled on Lake Superior shore. The characteristics and compositions of copper tailing, and leaching mechanism are also discussed.

4:00 PM

Field-Emission Properties of Sulfide Minerals under High-Power Nanosecond Electromagnetic Pulses: *Igor Bunin*¹; Valentin Chanturiya¹; ¹Russian Academy of Sciences

The mechanism of absorption of the energy of high-power electromagnetic nanosecond pulses (HPEMP) due to the field emission from the surface of natural semiconductors is considered. The limitations and possibilities of implementing this mechanism in sulphide minerals (pyrite and arsenopyrite) are demonstrated. The effect of HPEMP on the physicochemical properties and surface state of sulphide minerals, as well as on the technological properties of resistant gold-(PGM)-containing ores and beneficiation products was investigated. The results of the SEM/EDX (LEO 1420VP scanning electron microscope equipped with an Oxford INCA Energy EDX detector) investigations of a pyrite and a pyrrhotite samples testify that the irradiation with a series of nanosecond HPEMP produced prebreakdown state of the mineral surfaces, with numerous microcracks and neoformations. The influence of HPEMP irradiation on composition change and oxidation process of a mineral surface, together with sorption and flotation activity of sulphide minerals was studied.

4:20 PM

Characterizations of Halloysite Clay as Functions of Temperature: *Dan Rutman*¹; Joe Hutchins¹; Eric Peterson¹; Morgan Reed¹; Donald Mencer²; Gary Beall³; Jewel Gomes¹; David Cocke¹; ¹Lamar University; ²Wilkes University; ³Texas State University

Halloysite, a natural kaolinitic clay mineral, has hollow nanotubular structure with diameters typically smaller than 100 nanometers and lengths ranging from about 500 nanometers to 5 microns. This unusual structure is spurring interesting modifications for novel applications. This warrants a thorough chemical and physical examination as a function of temperature since thermal treatments are requisite for future applications. The Halloysite was examined over the range from room temperature to 1000C by FTIR, XRD, DSC, TGA, and SEM. Particular attention was given to chemical changes that have been correlated with structural and physical alterations in properties associated with these clays to be used as a possible catalyst. Analytical SEM with EDAX provided detailed morphological information that has been correlated with size and structural data provided by XRD. Insights into the best approaches to perform ASEM have been gleaned from these comparative characterization methodologies which are outlined in this work.

4:40 PM

Study of the Leaching Kinetic of Low Grade Zinc Oxide Ores: *Feng Linyong*¹; ¹Kunming University of Science and Technology

Low grade powdery zinc oxide ores (5.17% Zn, < 2 mm) are mixed with cement 5% (wt), pelletized and solidified. The diameters of the pellets obtained are between 5 mm to 8 mm. When the pellet solidification periods are 3 days, 10 days and 45 days respectively, the alkaline leaching rates of zinc in the pellets are up to 92.2%, 87.3% and 72.9% respectively. Decreasing the solidification time can reduce reaction time, increase dissolution of zinc in pellets and lower the effect of initial zinc concentration on leaching rate. The experiment results show that the minimum solidification time is three days, and the kinetic study indicates that alkaline leaching of the low grade zinc oxide pellets is controlled by the diffusion of the leach liquor through the gangue layer in the whole leach process, and the apparent rate constants are $3.51 \times 10^{-2} \text{ day}^{-1}$, $8.09 \times 10^{-3} \text{ day}^{-1}$, $4.74 \times 10^{-3} \text{ day}^{-1}$ respectively.

Complex Oxide Materials - Synthesis, Properties and Applications: Novel Functionality from Complex Oxide Heterointerfaces

Sponsored by: The Minerals, Metals and Materials Society, TMS Electronic, Magnetic, and Photonic Materials Division

Program Organizers: Zhiming Wang, University of Arkansas; Ho Nyung Lee, Oak Ridge National Laboratory

Monday PM

March 10, 2008

Room: 277

Location: Ernest Morial Convention Center

Session Chair: To Be Announced

2:00 PM Invited

Dielectric and Magnetic Anomalies at Oxide Interfaces: *Harold Hwang*¹; ¹University of Tokyo

The electrostatic, magnetic, and physical boundary conditions at oxide interfaces can lead to unusual non-bulk-like interface states, which have been the subject of much recent interest. We present investigations of rectifying Schottky junctions, which we have used as a probe of the near interface electronic structure. Using Nb:SrTiO_3 as an n-type semiconductor, the strong internal electric field across the junction induces significant dielectric nonlinearities, giving rise to a strongly temperature and bias dependent depletion barrier profile. Junctions formed by using manganites as the Schottky metal exhibit a magnetic field dependent shift of the current-voltage characteristics, resulting in an exponentially-enhanced differential magnetoresistance and junction magnetocapacitance. These features arise from a magnetic field dependent Schottky barrier height and depletion width, reflecting the large charge-spin coupling arising from the double-exchange mechanism at the interface.

2:30 PM Invited

Novel Physical Phenomena in $\text{LaTiO}_3/\text{SrTiO}_3$ and $\text{LaTiO}_3/\text{LaAlO}_3$ Oxide Superlattices Investigated by Optical Spectroscopy: *Tae Noh*¹; ¹Seoul National University, ReCOE, Department of Physics and Astronomy

Recent advances in atomic-scale control and fabrication techniques of oxide multilayers have triggered extensive investigations on artificial oxide superlattices. LaTiO_3 is a well known d1 Mott-insulator, where correlation plays important roles. We fabricated $\text{LaTiO}_3/\text{SrTiO}_3$ and $\text{LaTiO}_3/\text{LaAlO}_3$ superlattices, both of which are composed of the d1 Mott-insulator and a band insulator. In $\text{LaTiO}_3/\text{SrTiO}_3$ superlattices, we found novel metallic behaviours at the interface due to electron spill-over effects. We carefully excluded the possibility of oxygen vacancy as a cause for the conducting interface. On the other hand, in $\text{LaTiO}_3/\text{LaAlO}_3$ superlattices, we obtained experimental evidences for strong confinement of the Ti 3d electronic states at the TiO_2 sheet, suggesting a sharp 2D Mott insulating state. In this talk, we will present some intriguing optical spectroscopy results in combination with the first-principle calculation results. We will also address why transport properties of the similar material systems (with LaTiO_3 layers) behave so differently.

3:00 PM Invited

Magnetic Effects at the Interface between Non-Magnetic Oxides: *Guus Rijnders*¹; ¹University of Twente/ MESA+ Institute for Nanotechnology

The discovery of conduction caused by electronic reconstruction at oxide interfaces has attracted a lot of interest. A heterointerface between perovskites (ABO_3) introduces polarity discontinuities when both elements A and B on either side of the interface have different valence states. Recently, a different electronic behavior for thin LaAlO_3 films on either SrO - or TiO_2 -terminated SrTiO_3 substrates was found, the former interface being insulating and the latter interface being an n-type conductor. Here we show how, in analogy to this remarkable interface-induced conductivity, magnetism can be induced at the interface between the otherwise non-magnetic insulating perovskites SrTiO_3 and LaAlO_3 . A large negative magnetoresistance of the interface is found, together with a logarithmic temperature dependence of the sheet resistance. At low temperatures, the sheet resistance reveals magnetic hysteresis. The conducting oxide interface now provides a versatile system to induce and manipulate magnetic moments in otherwise non-magnetic materials.

3:30 PM Invited

Engineering High-Mobility in SrTiO_3 -Based Structures: *Gervasi Herranz*¹; Mario Basletic²; Olivier Copiel¹; Manuel Bibes³; Cécile Carrétero¹; Emil Tafra²; Eric Jacquet¹; Karim Bouzehouane¹; Cyrille Deranlot¹; Amir Hamzic²; Agnès Barthélémy¹; Albert Fert¹; ¹Unité Mixte de Physique CNRS/Thales; ²University of Zagreb, Department of Physics, Faculty of Science; ³Centre National de la Recherche Scientifique Université Paris-Sud, Institut d'Electronique Fondamentale

The development of electronic devices based on oxide requires materials with high carrier mobility. In this regard, SrTiO_3 (STO) is intensively investigated due to the dramatic sensitivity of its electronic properties to extrinsic impurity doping. Stoichiometric STO is a band insulator, but an insulator-to-metal transition is induced when STO is doped with extrinsic impurities. We have demonstrated that this doping is achieved by oxide thin film deposition on STO substrates,¹ providing promising ways to generate controlled high-mobility conduction. We have analyzed the mechanisms of oxygen vacancy formation and diffusion in STO to provide accurate protocols to control the electronic properties. We have also explored alternative methods for the generation of high-mobility carriers in STO, with the objective of achieving two-dimensional conduction. We discuss the relevance of these results for all-oxide electronic devices. ¹G. Herranz et al., Phys. Rev. B 73, 064403 (2006); Phys. Rev. Lett. 98, 216803 (2007).

4:00 PM Break

4:30 PM Invited

Interface Electronic and Magnetic States in Nanoscale $\text{CaRuO}_3/\text{CaMnO}_3$ Superlattices: *John Freeland*¹; Jerald Kavich¹; Jacques Chakhalian²; A. Boris³; P. Yordanov³; B. Keimer³; H. Lee⁴; ¹Argonne National Laboratory; ²University of Arkansas; ³Max Planck Institute for Solid State Physics; ⁴Oak Ridge National Laboratory

By creating an atomically abrupt boundary between two different complex oxide systems, one can explore how strong electron correlations are modified in

proximity to the interface. Here we present results on the mixing of a G type anti-ferromagnetic insulator (CaMnO_3) and a paramagnetic metal (CaRuO_3). Using pulsed laser deposition, high-quality (100) oriented ultra-thin superlattices were grown with the structure $[\text{CaRuO}_3(\text{N u.c.})/\text{CaMnO}_3(10 \text{ u.c.})] \times 6$ on LaAlO_3 . Our results show the formation of a canted anti-ferromagnetic state at the interface, which is attributed to weakening of the antiferromagnetic interactions by leakage of the metallic state into the insulating CaMnO_3 layer. This strong interface magnetism gives rise to a large magneto-resistance resulting from interface spin scattering of carriers in the metallic CaRuO_3 layers. Work at Argonne is supported by the U.S. Department of Energy, Office of Science, under Contract No. DE-AC02-06CH11357. JC is funded by U.S. DOD-ARO under Contract No. 0402-17291.

5:00 PM Invited

Recent Theoretical Progress on Correlated-Electron Interface: *Satoshi Okamoto*¹; ¹Oak Ridge National Laboratory

Correlated-electron systems have been providing a variety of functionalities including high-TC superconductivity in cuprates and colossal-magnetoresistance in manganites. Therefore, studies of interfaces involving such materials are indispensable for realizing electronic devices utilizing novel properties of these materials. Further, interfaces involving these systems may become an alternative route to explore further interesting phenomena because one can control carrier concentration and lattice parameters of constituent materials without introducing chemical disorder. In this talk, I will describe recent theoretical progress on correlated-electron interface problem along with these issues including (1) transport and optical properties of a metal/Mott insulator/metal junction, (2) possible carrier injection and superconductivity at a cuprate/manganite interface, (3) novel quantum phases at correlated interfaces. This work is supported by the Division of Materials Sciences and Engineering, Office of Basic Energy Sciences, U.S. Department of Energy, under contract DE-AC05-00OR22725 with Oak Ridge National Laboratory, managed and operated by UT-Battelle, LLC.

5:30 PM Invited

Material Design and Application Based on Magnetic Oxide Interfaces: *Hiroyuki Yamada*¹; ¹National Institute of Advanced Industrial Science and Technology

Extensive studies of magnetic oxide superstructures have revealed the crucial roles of interface effects, such as spin exchange, charge transfer or orbital degree of freedom [H. Yamada, et al., APL 81, 4793 (2002), APL 89, 052506 (2006)]. Atomic scale control and observation of interfaces actually lead to some interesting discoveries. For example, $(\text{La,Sr})\text{MnO}_3$ -based junction with engineered interfaces shows huge tunneling magnetoresistance (TMR) [H. Yamada et al., Science 305, 646 (2004)]. Or we have found enhanced nonreciprocal directional birefringence (optical magneto-electric effect) originating from polar and ferromagnetic interfaces, which were realized in a form of 'tricolor' superlattice composed of LaMnO_3 , SrMnO_3 , and LaAlO_3 . Those novel functionalities, from TMR to multiferroics, demonstrate the potential of the correlated electron magnetic interfaces for future devices. This work was done in collaboration with Tokura multiferroics and spin superstructure projects, ERATO, Japan Science and Technology Corporation (JST), and partly conducted in CREST, JST.

Computational Thermodynamics and Kinetics: Defect Structure II

Sponsored by: The Minerals, Metals and Materials Society, TMS Electronic, Magnetic, and Photonic Materials Division, TMS Materials Processing and Manufacturing Division, ASM Materials Science Critical Technology Sector, TMS: Chemistry and Physics of Materials Committee, TMS/ASM: Computational Materials Science and Engineering Committee, TMS/ASM: Phase Transformations Committee

Program Organizers: Yunzhi Wang, Ohio State University; Long-Qing Chen, Pennsylvania State University; Jeffrey Hoyt, McMaster University; Yu Wang, Virginia Tech

Monday PM

Room: 288

March 10, 2008

Location: Ernest Morial Convention Center

Session Chairs: Yu Wang, Virginia Tech; William Curtin, Brown University

2:00 PM Invited

Modeling of Dynamic Strain Aging in Solid Solutions: Part I: Single Strengthening Mechanism: *William Curtin*¹; Monica Soare¹; ¹Brown University

The aim of this work is to propose a robust, physically-based constitutive model for aging mechanisms in various technologically important metal alloys. The study is motivated by the need to explain quantitatively the stress-strain rate-temperature regime of material instabilities that often arise in material processing. The first part of the study describes the general framework of the rate dependent theory and addresses a single rate-dependent mechanism: solute strengthening by dislocation pinning at favorable random static solute configurations followed by solute diffusion toward temporarily-arrested mobile dislocations. The analysis shows that such a single mechanism cannot produce a regime of negative strain rate sensitivity but it reduces this parameter (SRS). The model predicts the transient stress behavior occurring upon imposition of an instantaneous change in strain rate, qualitatively consistent with the ad-hoc model of McCormick. Multiple competing strengthening mechanisms necessary for negative SRS are considered in the second part of our study.

2:25 PM

Dislocation Pinning by Impurities and Obstacles: A Level-Set Simulation Study: Zi Chen¹; Kevin Chu¹; Mikko Haataja¹; Jeffrey Rickman²; David Srolovitz³; ¹Princeton University; ²Lehigh University; ³Yeshiva University

A basic understanding of the mechanical behavior of advanced metallic systems utilized in the aerospace community is essential for the design of robust structures to ensure their performance under a variety of loads and under extreme thermal environments. In particular, in systems that are solution and/or precipitation hardened, such as γ -TiAl and Al-Mg-Cu alloys and reinforced MoSi₂, interactions among defects lead to a complex plastic response that is difficult to capture in empirical constitutive relations. Here, we employ a parallel three-dimensional level-set code to simulate the complex motion of dislocation lines and loops in an obstacle-rich environment. Specifically, we have extracted the effective dislocation mobility as a function of solute concentration and mobility, spatial obstacle distribution, misfit strain, and external stress. These studies will guide the development of coarse-grained dislocation dynamics models which have the capability to provide a better microstructurally-informed description of the continuum mechanics of plastically deformed metals.

2:40 PM

Interaction Energy between Carbon Solutes and Dislocation in BCC Iron: Y. Hanlunyuang¹; P. Gordon²; N. Thirumalai²; D. Chrzan¹; ¹University of California, Berkeley; ²ExxonMobil Research and Engineering

The interaction energy between a carbon atom and an edge dislocation in BCC iron is computed using three approaches: (1) an anisotropic elastic model wherein the chemical contribution is ignored, (2) an open-system thermodynamics model with both anisotropic elastic and chemical contributions incorporated, and (3) an *ab initio* electronic structure based total energy method. In the *ab initio* approach, the segregation energy is computed within a local strain approximation that neglects strain gradients. The results of the three methods are compared, and the importance of electronic and magnetic effects assessed. This research is supported by ExxonMobil Research and Engineering.

2:55 PM

Computing Solute Drag Stresses in Al-Mg: Fan Zhang¹; William Curtin¹; ¹Brown University

In solute-strengthened alloys, dynamic strain aging could be associated with solute drag caused by diffusion of solute atoms around moving dislocations. Drag stresses predicted by classical theories using a singular core are much larger than experiments. Here, the drag stress is computed numerically, as in Yoshinaga et al. (Phil. Mag. 23, 1367 (1971)), but using a more-realistic dislocation core structure and literature atomistic data on energy barriers for Mg diffusion in Al. In the 700K-750K range typical of Al processing, the maximum drag stress is much smaller than analytic estimates (43 MPa vs. 3.4 GPa). Using the Orowan relationship, the predictions for drag stress versus strain rate are in the range of experimental data. But, a power-law behavior emerges with in contrast to data suggesting, which is accounted for by considering the stress dependence of the mobile dislocation density.

3:10 PM

Interface Properties from Their Equilibrium Fluctuations: Moneesh Upmanyu¹; Zachary Trautt¹; Branden Kappes¹; Alain Karma¹; ¹Colorado School of Mines

The thermodynamic and kinetic properties of interfaces play a central role in the interplay between growth and form of interfacial microstructures. Due to the limitations associated with accessible spatio-temporal scales in experiments and in atomic-scale simulations, extracting these properties has been challenging. In this talk, I will present our recent work on theoretical frameworks and associated computational techniques aimed at extracting equilibrium interface properties from their fluctuations. The main focus is on grain boundaries; the capillarity fluctuation method allows us to extract grain boundary stiffness, which the random walk of the mean interface position directly yields its absolute mobility. Comparisons with previous studies on driven grain boundaries will also be made. The misorientation dependence of these grain boundary properties in pure aluminum show that these properties are structurally coupled. Finally, I will also discuss extensions of this methodology to alloy systems, in particular on quantifying the solute drag effect.

3:25 PM

Toward Predicting the Properties of All Grain Boundaries in a Material: David Olmsted¹; Stephen Foiles¹; Elizabeth Holm¹; ¹Sandia National Laboratories

Microstructural evolution depends on both the energy and mobility of the constituent grain boundaries. Because grain size and texture are key microstructural parameters that contribute to material properties, mesoscopic simulations of grain evolution that provided accurate predictions for specific materials would be of great value. Such simulations require detailed properties, including energy and mobility, for individual grain boundaries. The large crystallographic space of grain boundaries, with five macroscopic degrees of freedom, has always posed a challenge for general analysis of these properties. The focus on this work is on studying the properties of a large and general set of fcc grain boundaries. Our ultimate goal is to verify existing models, or develop novel models, which provide reasonably simply ways to predict these properties. We report on our studies of the zero-temperature energy and the finite temperature mobility of several hundred non-equivalent fcc grain boundaries in nickel and aluminum.

3:40 PM Break

4:00 PM Invited

Grain Growth of Metallic Nanocrystals: Insights from Molecular Dynamics: Stephen Foiles¹; Elizabeth Holm¹; David Olmsted¹; ¹Sandia National Laboratories

Understanding the structural evolution of nanograin metals is important for both the processing of these materials and to ensure their stability during use. In this talk, the evolution of the grain structure of nanograin Ni will be studied using molecular dynamics simulations of both model grain structures and random grain structures. The results will be compared to predictions based on models of grain growth developed for conventional polycrystalline materials. The goal of these comparisons will be to determine how grain growth in nanocrystalline metals differs from grain growth in more conventional polycrystalline metals. Sandia is a multi-program laboratory operated by Sandia Corporation, a Lockheed Martin

Company, for the United States Department of Energy's National Nuclear Security Administration under contract DE-AC0494AL85000.

4:25 PM

Quantitative Phase Field Simulations of Anisotropic Grain Growth in Columnar Thin Films with a Fiber Texture: *Nele Moelans*¹; Frans Spaepen²; Bart Blanpain¹; Patrick Wollants¹; ¹Katholieke Universiteit Leuven; ²Harvard University

Many thin films have a columnar grain structure in which all crystals have nearly identical orientation in the axial direction or the direction perpendicular to the film, but nearly random radial or planar orientation. We simulated the evolution of the grain structure of such films with a generalized phase field model. The model allows quantitative specification of the grain boundary energy and mobility for each interface individually. A Read-Shockley orientation dependence of the grain boundary energy was assumed. The dependence on the boundary inclination was assumed negligible. The presence of special high-angle misorientations with lower energy was considered as well. In this presentation we will discuss how the fraction of low-angle and low-energy grain boundaries evolves in time and how the misorientation-dependence of the grain boundary energy affects the grain growth exponent. Our findings will be compared with those from mean field theories and previous mesoscale simulation studies.

4:40 PM

Phase Field Models of Grain Growth in Cubic Crystalline Materials: *Mogadala Gururajan*¹; Ian McKenna¹; Peter Voorhees¹; ¹Northwest University

We present a phase field model for grain growth based on quaternions; we show that by a proper ordering of the quaternion components, the grain orientations related by cubic point group operations can easily be identified, and the grain boundary energy can be made to depend only on the smallest angle (consistent with cubic symmetry) that is needed to rotate one grain to orient it with the neighbouring grain. Further, we also indicate how the anisotropic grain boundary energies due to the cubic symmetry of the underlying lattice can be incorporated into the phase field models by including a higher order fourth rank gradient energy coefficient tensor. Finally, we also discuss a multiple order parameter grain growth models implemented using a sparse matrix algorithm, and compare it with the quaternion based model in terms of computational efficiency.

4:55 PM

Multi-Phase Field Study of Grain Boundary/Particle/Solute Interaction: *Seth Wilson*¹; J. Gruber¹; A.D. Rollett¹; ¹Carnegie Mellon University

We utilize a multi-phase field model to study the interaction between grain boundaries, solute, and second-phase particles. We first verify via simulation that our model correctly incorporates each pair of interactions (boundary-particle, solute-particle, and solute-boundary) in the absence of the third. We then study shape and volume change during boundary traversal as a function of global solute concentration and local misorientation-dependant boundary-solute interaction strength. The effect on particle drag is discussed.

5:10 PM

Simulation and Theory of Interface Texture Development: *Jason Gruber*¹; Herbert Miller¹; Anthony Rollett¹; Gregory Rohrer¹; ¹Carnegie Mellon University

The distribution of internal interface types in a polycrystal is often non-random. We discuss results from several computational models that show how interface texture results from grain growth with anisotropic interface properties. A quantitative theory that agrees with our simulated results is presented. We demonstrate that the qualitative features of our simulations and theory closely match a number of real materials.

5:25 PM

The Effect of Nb and Austenite Grain Size on γ/α Transformation in Nb Added Steels: *Jong Min Choi*¹; Jong Hun Kim¹; Kyung Sub Lee¹; Kyung Jong Lee¹; ¹Hanyang University

It was generally accepted that γ/α transformation in Nb added steels was strongly retarded by solute drag effect when most of Nb were not precipitated. When they were precipitated, the transformation was much faster than they were soluble since the pinning effect of coarse precipitates on γ/α transformation was

negligible. However, when the prior austenite grain was smaller, this solute drag effect nearly disappeared. In this study, the combined effect of prior austenite grain size and solute drag effect on γ/α transformation was studied. The classical nucleation and growth theory was adopted considering solute drag effect. The results including CCT diagram were compared with the observed.

Deformation Twinning: Formation Mechanisms and Effects on Material Plasticity: Experiments and Modeling: Twin Effects on Material Deformation I

Sponsored by: The Minerals, Metals and Materials Society, TMS Structural Materials Division, TMS/ASM: Mechanical Behavior of Materials Committee

Program Organizers: George Gray, Los Alamos National Laboratory; Subhash Mahajan, Arizona State University; Ellen Cerreta, Los Alamos National Laboratory

Monday PM
March 10, 2008

Room: 383
Location: Ernest Morial Convention Center

Session Chairs: Rodney McCabe, Los Alamos National Laboratory; Ian Robertson, University of Illinois

2:00 PM Invited

Texture, Twinning and Hardening Evolution during Deformation of Hexagonal Zr and Mg: *Carlos Tome*¹; ¹Los Alamos National Laboratory

Hexagonal materials deform plastically activating diverse slip and twinning modes. The relative contribution to deformation of such modes depends on their critical stresses and the orientation of the crystals with respect to the loading direction. For a constitutive description of these materials to be reliable, it has to account for the dislocation-twin interaction and for twin creation and reorientation. This talk discusses the connection between twinning and the mechanical response of two HCP metals - Zr and Mg - and presents a model for their mechanical response based on the active crystallographic mechanisms. Information from TEM, OIM, neutron diffraction, and mechanical testing is used for developing a model of the grain which is, in turn, incorporated into our Visco-Plastic Self-Consistent (VPSC) polycrystal plasticity code. We apply this model to the challenging problem of reproducing the results of strain-path-change tests done in pure Zr and AZ31 Mg.

2:30 PM

Temperature and Rate Effects in the Deformation of Pure Zirconium: *Irene Beyerlein*¹; Carlos Tome¹; Gwenaelle Proust¹; George Kaschner¹; ¹Los Alamos National Laboratory

In this work, we develop a dislocation density-based constitutive law for slip and twinning in hcp materials that accounts for temperature and rate effects within the thermal activation regime. The evolution law for slip covers Stages II through IV, by including temperature-dependent terms for recovery and debris formation. The hardening law for twin propagation accounts for temperature effects through interactions with slip dislocations. In turn, slip dislocations interact with twin boundaries through a Hall-Petch relationship, including a temperature-dependent coefficient. When implemented in a VPSC model which contains a micromechanical model for twin reorientation, the constitutive law effectively predicts the plastic anisotropy of ultra-pure polycrystalline Zr over a wide range of temperatures, 76K to 450K, and strain rates, 10⁻³ 1/s and 10³ 1/s. The model considers the four deformation modes observed previously via microscopy analyses in this Zr: prismatic slip, pyramidal <c+a> slip, tensile twinning {10-12}{10-11}, and compressive twinning {11-22}{11-2-3}.

2:50 PM

Effect of Twining on Deformation Behavior of Zirconium Alloys: *Young Suk Kim*¹; Tae Ook Oh¹; Yong Moo Cheong¹; ¹Korea Atomic Energy Research Institute

Tensile tests were conducted from RT to 400°C on the tensile specimens taken from the tangential direction (TD) and the longitudinal direction (LD) of a Zr-2.5Nb tube with a strong tangential texture. When the tensile stresses were applied to the TD with the tensile axis normal to the basal plane, the {10 2} twinning was activated. With the tensile stress applied to the LD with the tensile axis parallel to the {10 0} plane, however, slip only was activated. The

operation of the twinning caused the tensile properties of the Zr-2.5Nb tube to be anisotropic, leading to higher yield strengths and lower tensile elongations in the TD when compared to those in the LD. Furthermore, it promoted necking soon after yielding only in the TD while slip on the prism plane facilitated strain hardening after yielding. The role of twinning in tensile properties of the Zr-2.5Nb tube is discussed.

3:10 PM

Hardening from Plastically Deformable Twins in a CPFEM Framework: *Luc Hantcherli¹; Philip Eisenlohr¹; Franz Roters¹; Dierk Raabe¹; ¹Max-Planck-Institut für Eisenforschung*

A statistical model of mechanical twinning in fcc metals is formulated for inclusion in a CPFEM framework. Growth rate of the twin volume fraction is phenomenologically linked to the resolved shear stress on each twin system by a power law. Twins are first considered to be impenetrable to matrix dislocations. The resulting contributions of hardening due to increasing volume fraction of plastically non-deformable twins and due to extra storage of dislocations largely exceed experimental reference. We present a feasible way of how to account for the thus required — end experimentally confirmed — dislocation penetration through twins.

3:30 PM

Internal Stress Development Due to Deformation Twinning: *Bjorn Clausen¹; Carlos Tome¹; Donald Brown¹; Sean Agnew²; ¹Los Alamos National Laboratory; ²University of Virginia*

Most metals with hexagonal crystal structure exhibit deformation twinning due to the limited number of available slip systems. In the case of magnesium, tensile twinning is easily activated, and depending on the initial texture and the loading path it can be a primary mode of plastic deformation. In the present work we have focused on the development of the local stress state in grains that twin. In-situ bulk diffraction measurements have been employed to determine the development of elastic lattice strains and crystallographic texture during compressive loading of extruded magnesium and during unloading after various levels of applied plastic strain. De-twinning is observed during unloading following a large percent of plastic deformation consistent with the development of strong internal stresses in twinned grains. Correlating the measured data with predictions of the elastic-plastic self-consistent polycrystal deformation model shows that the developed stress state is consistent with an initial twinning overshoot.

3:50 PM

Interfacial Plasticity Governs Strain Rate Sensitivity and Ductility in Nano-Twinned Metals: *Ting Zhu¹; Ju Li²; Amit Samanta³; Hyoun Gyu Kim²; Subra Suresh³; ¹Georgia Institute of Technology; ²Ohio State University; ³Massachusetts Institute of Technology*

Nano-twinned copper exhibits an unusual combination of ultrahigh strength and high ductility, along with increased strain-rate sensitivity. We develop a mechanistic framework for predicting the rate sensitivity and elucidating the origin of ductility in terms of the interactions of dislocations with twin boundaries. Using atomistic reaction pathway calculations, we show that slip transfer reactions mediated by twin boundary are the rate-controlling mechanisms of plastic flow. We attribute the relatively high ductility of nano-twinned copper to the hardening of twin boundaries as they gradually lose coherency during plastic deformation. These findings provide new insights into possible means of optimizing strength and ductility through interfacial engineering.

4:10 PM Break

4:30 PM Invited

Deformation Twinning and Transformation Plasticity in Rare Earth Orthophosphates: *Randall Hay¹; Pavel Mogilevsky²; Emmanuel Boakye²; ¹Air Force Research Laboratory; ²UES Inc.*

Rare earth orthophosphates are refractory materials that are thermochemically stable in a wide range of environments and are relatively soft. Their mechanical and physical properties make them attractive for use as oxidation resistant fiber-matrix interfaces in ceramic composites. They are also of interest as phosphors and as nuclear waste hosts. Deformation twinning modes in monazite (monoclinic) and xenotime (tetragonal) rare earth orthophosphates (ABPO₄) are identified from TEM of indented polycrystalline and single crystal samples.

Five modes are active in monazite, and one in xenotime. These modes all have very small shuffles for the rare earth cation and the PO₄ group. Methods for predicting twin modes in complex oxides, and their relative abundance, based on analysis of atom shuffles and other considerations are discussed. Indentation of some xenotimes can cause transformation to monazite and softening by transformation plasticity. Conditions under which this occurs are described, and possible applications are discussed.

5:00 PM

On the Role of Deformation Twinning in Work Hardening Behavior of FCC Polycrystals: *Farzad Hamdi¹; Siros Asgari¹; ¹Sharif University of Technology*

Results of an investigation on the evolution of microstructure during simple compression testing of some FCC polycrystals are reported. It is found that, in contrast to the current belief, deformation twinning may not be the sole cause of linear hardening in low SFE FCC polycrystals. It is suggested that, due to the requirement of slip system change prior to twinning, only FCC crystals with sufficiently low twinning stress are expected to form mechanical twins. In other FCC polycrystals that show linear hardening behavior, competitive mechanisms such as formation of dislocation locks may be dominant hardening mechanism. The effectiveness of these slip barriers is expected to increase with the tendency of the material to slip planarity. Therefore, parameters such as SFE, temperature, Peierls stress and short range ordering are expected to have a contribution to the linear hardening response of FCC polycrystals.

5:20 PM

Kinematic Hardening Arising from Grain Size and Twinning in TWIP Steels: *Olivier Bouaziz¹; Colin Scott¹; Sebastien Allain¹; Chad Sinclair²; ¹Arcelor Research; ²University of British Columbia*

While the role of deformation twinning in modifying the work hardening rate of TWIP steels is well appreciated, less well appreciated is the fact that this is accompanied by significant kinematic hardening. In this talk, experimental results from two different austenitic TWIP steels will be presented that reveal a large Bauschinger effect developed during straining. These results will be discussed in light of a new physically based model that is capable of capturing both isotropic and kinematic components of the work hardening rate.

5:40 PM

Mechanical Response of High Purity Alpha Titanium Orthotropic Plate: Role of Deformation Twinning on Anisotropy and Its Evolution with Deformation: *M.E. Nixon¹; R.A. Lebensohn²; Oana Cazacu³; M.L. Lovato²; G. Proust²; C. Liu²; C.N. Tome²; ¹Air Force Research Laboratory and University of Florida; ²Los Alamos National Laboratory; ³University of Florida/REEF*

An experimental investigation on high-purity, polycrystalline alpha-titanium plate was performed. Quasi-static tests at room temperature were conducted in monotonic tension and compression. The response is orthotropic and highly dependent on the orientation of the loading direction with respect to the predominant orientation of the <c> axis of the grains. Furthermore, four-point bending tests were performed on beams cut from the same plate, along different in-plane directions, for two mutually perpendicular bending planes. A digital image correlation technique was used to analyze the distribution of deformation. Due to the plate anisotropy and directionality of twinning qualitative differences in response were observed between the response of the upper and lower fibers of the different bent beams. The results indicate the need to use a constitutive description that accounts for the interplay between slip and twinning and its effects on texture evolution and hardening response when simulating the inhomogeneous deformation of Ti.

Electrode Technology Symposium (formerly Carbon Technology): Carbon Sustainability and Environment Aspects

Sponsored by: The Minerals, Metals and Materials Society, TMS Light Metals Division, TMS: Aluminum Committee
Program Organizers: Carlos Zangiacomi, Alcoa Aluminum Inc; John Johnson, RUSAL Engineering and Technological Center LLC

Monday PM Room: 299
 March 10, 2008 Location: Ernest Morial Convention Center

Session Chairs: Trygve Foosnas, Norwegian University of Science and Technology; Neal Dando, Alcoa Inc

2:00 PM

Triple Low–Triple High, Concepts for the Anode Plant of the Future: Wolfgang Leisenberg¹; Dragan Dojic²; Detlef Maiwald¹; ¹Innovatherm; ²Anotec

For the next generation of anode plants six main goals should be achieved. Three of them, summarized in Triple Low, represent the targets of the process technology: Low Energy, Low Emissions, Low investment and running Costs. The three others, summarized as Triple High, stand for the product: High Quality, High Quality Consistency and High Density. And this should be governed under the umbrella of maximum operational safety and efficiency. Different concepts of anode plants are on the market, which only cover parts of the defined goals. This paper deals with technologies to achieve all of these partly contradicting goals which are available today or in the near future. Especially technologies with environmental impact like minimization of energy consumption and emissions will be spotlighted.

2:20 PM

New Environmental Approach at Baking Furnace: Felipe Navarro¹; Francisco Figueiredo¹; Helio Truci¹; Hélio Oliveira¹; Raimundo Reis¹; Fabiano Mendes¹; Marcos Silva¹; ¹Alumar

Consorcio de Alumínio do Maranhão is one of the largest aluminium smelters of Latin America producing 450'000 tons of primary metal. The plant has three baking furnaces with capacity to produce 700 anodes/day. The furnaces are operated with diesel oil due to the lack of natural gas distribution in the Northeast of Brazil. Alcoa Inc. started in 2006 an effort to reduce the green house gases emission worldwide, increasing the sustainability of their business and allowing Alcoa to apply for carbon credits. Alumar's Baking Furnace started using in September a mix of light oil and biodiesel as standard fuel. The development presented in this paper presents a new environmental approach where the main targets have been: 1)Reduce CO₂ generation with lower cost impact; 2)Implement an environmental fuel in the baking furnace with no impacts in anode quality, fuel efficiency and baking furnace operations.

2:40 PM

Pneumatic Transfer of Fine Carbon Residues at Albras – A Case Study at the Carbon Plant: Paulo Douglas Vasconcelos¹; André Mesquita²; ¹Albras Alumínio Brasileiro S.A.; ²Federal University of Pará

Albras Alumínio Brasileiro S.A has upgraded the carbon plant to capture and transport the fugitive dust emissions from the operations of butt cleaning, crushing and grinding of butts and reject anodes, and the anode baking furnace tending cranes to elevate environmental pollution in the work place and to the environment. Originally, the residual dusts, mostly carbon were conveyed by a screw conveyor for loading into a bulk solids truck for subsequent disposal. The rest of the paper describes the development, design, and implementation of a pneumatic conveying system developed at past of a Masters dissertations to resolve the environmental issues, eliminating the coke contamination from the residual dusts while reducing annual maintenance and labour expenditures.

3:00 PM Break

3:10 PM

Towards Fully Automated Cast-Iron Sealing of Anode Rods: Barry Woodrow¹; ¹Stimir hf.

Cast-iron sealing of anode rods is one of the few areas in the rodding shop which remains to be fully automated. Today's semi-automatic casting machines are a considerable improvement on manually poured ladles but still require the operator to engage in accurate and repetitive work in a potentially unhealthy and dangerous environment. This paper examines recent developments and the application of automation technologies to the anode rod sealing process. Automation of repetitive tasks is examined. Health and safety considerations - hot metal, fumes, operator posture, eyestrain - are addressed. Remote sensing devices are proposed to enable relocation of the operator away from the danger area. In conclusion, a fully automatic anode rod casting machine is described.

3:30 PM

Development In Situ of a Semi-Automated System in the Casting Station: A Case Study at Albras: Emerson Santos¹; Dourivaldo Dias¹; Antônio Ivan Arruda¹; Marco Antônio Reis¹; Luis Carlos Carvalho Costa¹; ¹Albras

The work in the Casting Station is very risky, because the flying sparks of molten cast iron are a safety hazard for operators. The objective of this work is present an automation project of the casting station developed by Albras team. The Semi-automated System it consists of: The static cabins with air-conditioner control and a large open view, for maximum operator comfort; automation metal emptying device operation with electronic-hydraulics drive, using Control Proportional Valves, controlled by electronics joysticks. Finally, the gains of productivity, casting quality, ergonomics and safety obtained by the project are showed.

3:50 PM

Chemical Stability of Fluorides Related with Spent Potlining: Xiping Chen¹; Wangxing Li²; ¹Zhengzhou Research Institute of Chalco; ²Chalco

Chemical stability of fluorides related with spent potlining was studied. Experiments were carried out under conditions of exposure to air and exposure to active calcium oxide or limestone. Results from exposure to air at high temperature of 700~950°C showed that most of aluminum fluoride changed into Al₂O₃ or volatilized when the temperature was over 800°C and the weight loss of aluminum fluoride surpassed 60%, sodium fluoride did not volatilize or alter when heated up. Na₃AlF₆ and Al₂O₃ generated when the mixture of aluminum fluoride and sodium fluoride was heated up, NaAl₁₁O₁₇ formed when cryolite and sodium fluoride were heated up together. When foregoing fluorides were heated up exposure to active calcium oxide or limestone, CaF₂ formed easily.

Emerging Interconnect and Packaging Technologies: Pb-Free and Sn-Pb Solders: Electromigration

Sponsored by: The Minerals, Metals and Materials Society, TMS Electronic, Magnetic, and Photonic Materials Division, TMS: Electronic Packaging and Interconnection Materials Committee

Program Organizers: Carol Handwerker, Purdue University; Srinivas Chada, Medtronic; Fay Hua, Intel Corporation; Kejun Zeng, Texas Instruments, Inc.

Monday PM Room: 275
 March 10, 2008 Location: Ernest Morial Convention Center

Session Chairs: John Osenbach, Agere Systems Inc; K. Subramanian, Michigan State University

2:00 PM Invited

Effect of Current Crowding on Electromigration Induced Damage in Flip Chip Solder Joints: King-Ning Tu¹; ¹University of California at Los Angeles

Owing to the line-to-bump configuration in flip chip solder joints, current crowding occurs when electric current enters into or exits from the solder bump. At the cathode contact where electrons enter into the bump, current crowding induced pancake-type void formation has now been recognized widely to be the unique mode of electromigration failure. On the other hand, at the anode contact, the effect of current crowding induce electromigration failure has rarely been studies. We report here that hillock and whisker formation occurs respectively

in eutectic SnPb and SnAgCu as the mode of electromigration failure at the anode. The effect of current crowding induced stress concentration at the anode on whisker and hillock growth will be analyzed.

2:30 PM

Basic Studies on Electromigration in Electronic Solders: *K. Subramanian*¹; Andre Lee¹; Cheng-En Ho¹; ¹Michigan State University

Electromigration studies on electronic solders, present in a joint configuration with minimal current crowding, were carried out with a current density. These studies were aimed at identifying the migration of individual atomic species, evolution of microstructure, interface intermetallics layer stability, extents of surface undulations etc. Effects of joint thickness, temperature were also evaluated. These studies provided a possible scenario for hillock formation in the anode region of multi-phase solder alloy joints. Synergistic influences of temperature and electrical stressing were evaluated by comparing the microstructure development with and without current stressing under isothermal condition. To gain a better understanding the roles of alloying and presence of multiple phases on the electromigration behavior, results obtained with eutectic Sn-Pb solder joints are compared to the electromigration induced changes in a solder joint made with pure tin.

2:45 PM

Failure of SnAgCu Solder Joints Under Current and Mechanical Load: *Christopher Kinney*¹; Tae-Kyu Lee¹; J.W. Morris¹; ¹University of California, Berkeley

The work reported here investigated the failure of Pb-free SnAgCu solder joints under the simultaneous action of electrical current and mechanical load. The solder joints were made in a simple planar configuration with Cu on both sides. They were tested to failure in an apparatus that permitted the application of creep loads to samples that were subjected to known electrical current at controlled temperature. The results show a strong symbiotic effect between load and current density. The samples failed much more quickly under both stress and current than under either alone. The evolution of microstructure was monitored and the temperature profile was measured for various operating conditions to help clarify this behavior.

3:00 PM

Electromigration Failure Mechanism in SnAg Flip-Chip Solder Joints during Lateral Current Stressing: *Ming-Hui Chu*¹; Chih Chen¹; Yung-Ching Hsu¹; ¹National Chiao Tung University

Many studies have been performed on how the current crowding has affected the electromigration failure in flip-chip solder bumps. But the effect the lateral current stressing has not been studied. In this study, electromigration of Sn3.5Ag solder bumps with 5- μ m-thick Cu UBM is investigated when the solder joints were stressed by a lateral current of 0.9 A at 100°C, that is, the current was applied through two Al traces on the chip end. The microstructure analysis and the measurement of the resistance reveal that the occurrence of electromigration failure occurs during the lateral current stressing, and the failure mode is quite different from that stressed through the chip and the substrate ends. Kelvin probes were employed to monitor the resistance change due to electromigration damage. The consumption of UBM and void formation occurred in solder bumps, and the resistance of bumps may increase to 50% of its original values.

3:15 PM Break

3:30 PM

Design Limitations Related to Conductive Anodic Filament (CAF) Formation in a Micro-World: *Laura Turbini*¹; Antonio Caputo²; ¹Research In Motion; ²University of Toronto

The drive toward more compact, highly functional and portable electronic devices has forced a reduction in conductor spacing. A direct reliability concern of reduced pitch designs is an electrochemical failure mode in printed wiring boards known as conductive anodic filament (CAF) formation. CAF test coupon designs must take into account a number of factors in the board manufacturing process which will affect the reproducibility of the coupons. These include glass fiber style, resin type and content, as well as the drilling parameters such as drill bit wear, speed, diameter, and drilling sequence. Cracking between barrels can occur during the drilling process, especially for more brittle laminate materials. During the plating process, residues can accumulate in the cracks. Subsequent

testing under humidity and bias conditions will lead to shorts which can be mistaken for CAF. This paper will identify the limitations in designing a PWB for CAF reliability testing.

3:45 PM

Effect of Al Trace Width on Electromigration Failure Time of Flip-Chip Solder Joints: *Shih-Wei Liang*¹; Chih Chen¹; ¹National Chiao Tung University

The effect of Al-trace width on electromigration of flip-chip solder joints was investigated in this study. Two thicknesses of Al trace adopted for lead-free SnAg solder with 5- μ m Cu under bump metallization (UBM) were 40 μ m and 100 μ m. For the same stressing condition, 0.5 A on a 165°C hotplate, the solder joints with larger width has longer electromigration lifetime. As predicted by Black equation, the two factors, current density and temperature, will affect the lifetime of the solder joint. A higher current crowding effect occurs in the solder joints with a 40- μ m Al trace than that with a 100- μ m Al trace. Also, large resistance of 40- μ m Al trace caused more serious Joule heating effect to increase the temperature in the solder bump. By these two reasons, the solder joint with a 100- μ m Al trace have 2.6 times of failure time than the solder joint with 40- μ m Al trace.

4:00 PM

Effects of Bump Height on Electromigration Failure Time and Failure Modes of Pb-Free Solder Joints: *Min-Feng Ku*¹; Chih Chen¹; ¹National Chiao Tung University

Effects of bump height on electromigration failure time and failure modes have not been studied for Pb-free SnAg solder joints. In this study, we fabricated two kinds of solder joints with different bump heights: the low bump height (LBH) of 25 μ m, and the high bump height (HBH) of 75 μ m. Both sets of solder joints were subjected by electromigration tests by 0.9A at 150°C. We measured the changes of bump resistance with Kelvin bump probes. It is found that when the bump resistance increased to 20% of its initial value, the failure time of LBH solder joints was about 80 hours and the HBH solder joints was about 300 hours. According to Joule heating results measured by infrared microscope, we found the different temperature increase in the two solder joints, which may be responsible for the difference in failure time. The failure mechanism will be presented in the conference.

4:15 PM

Electromigration Induced Microstructure and Morphological Changes in Eutectic SnPb Solder Joints: *Andre Lee*¹; Cheng-En Ho¹; K. Subramanian¹; ¹Michigan State University

Simultaneous direct current stressing with thermal aging accelerates the migration of conducting species resulting in significant microstructural coarsening. Due to the synergistic influences of these fields such coarsening begins from the anode and propagates towards cathode. Prolonged current stressing with 10⁴ A/cm² at 150C causes the inter-lamellar SnPb eutectic morphology to become a two-layer structure, with Pb-rich layer adjacent to the anode and Sn-rich layer adjacent to the cathode. This mass movement causes hillock/valley formation and the extents of such surface undulations increase with increases in the time duration of current stressing as well as with the joint thickness. In thinner solder joints these events occur sooner, although the extents of surface undulations depend on the thickness of joints. In addition Cu present in the substrate and in the intermetallic layer at the cathode migrates to form Cu₆Sn₅ within the Sn-rich layer, in a region close to the Pb-rich layer.

4:30 PM

Current Density Effect on the Interfacial SnAg/Cu Reaction: *Yeh Yu-Ting*¹; Liu Cheng-Yi¹; ¹National Central University

Current density effects on the interfacial reaction between Sn₃Ag solder and Cu were investigated. Firstly, we found that IMC formation and Cu pad consumption highly depends on the current density under EM test. A critical current density was determined to define the growth behavior of interfacial IMC. Above the critical current density, IMC thickness increases with EM time. On the contrary, below the critical current density, IMC remains constant thickness with time. We also examine how does 5% Ag content response with EM. It seems that Ag₃Sn IMC formation at the Sn₃Ag/Cu interface will also depend on the current density. Depending on the values of current density, different interfacial Ag₃Sn IMC formations were observed: (1) mixed CuSn and SnAg compounds or (2) distinguish CuSn and SnAg compound layers at Sn₃Ag/Cu interface.

4:45 PM

Electrothermal Effect on the Impression Creep of a Pb40Sn60 Alloy: *Rong Chen¹; Fuqian Yang¹; ¹University of Kentucky*

Solder joints provide electrical and mechanical interconnections in microelectronic circuits and devices. The mechanical behavior of the solder joints plays an important role in determining the reliability and lifetime of microelectronic devices. In this work, we studied the electrothermal effect on the creep behavior of a Pb40Sn60 alloy using the impression technique in the temperature range of 50 to 130°C and under the punching stress of 6.9 to 110 MPa. During the test, a constant DC electric current passed through the sample, which introduced electrothermal interaction through Joule heating. It was observed that there exists a stage of steady state creep when subjected to electrothermal interaction. The steady state impression velocity increased with the increase in electric current; and the stress dependence of the impression velocity followed the Eyring hyperbolic relation.

5:00 PM

Diffusion Mechanisms of Electromigration in Eutectic Solder Reaction Couples: *Guangchen Xu¹; Hongwen He¹; Fu Guo¹; ¹Beijing University of Technology*

Electromigration is a well known threat to the reliability of flip chip solder joint in recent years. The formation of hillocks and valleys were regarded as diffusion of atoms/ions propelled by electron wind. Temperature is a key factor to influence the diffusion mechanics of electromigration in eutectic binary solder alloy. Few researchers provided the discussions on diffusion mechanisms of electromigration in eutectic solder materials both at room temperature (<30°C) and high temperatures (>90°C) in one study. In this study, a newly designed solder reaction couple which could effectively minimize current crowding effect and remove the influence of thermomigration was introduced to electromigration experiment. Through in-situ observation, the material migration of alpha-rich and beta-rich phases present in the inter-lamellar morphology will produce purer phases with less solute contents under different temperature, which could provide the explanations of diffusion mechanisms in eutectic solder alloy under high current densities.

Emerging Methods to Understand Mechanical Behavior: Digital Image Correlation

Sponsored by: The Minerals, Metals and Materials Society, TMS Structural Materials Division, TMS Materials Processing and Manufacturing Division, TMS: Advanced Characterization, Testing, and Simulation Committee, TMS/ASM: Mechanical Behavior of Materials Committee, TMS: Nanomechanical Materials Behavior Committee
Program Organizers: Brad Boyce, Sandia National Laboratories; Mark Bourke, Los Alamos National Laboratory; Xiaodong Li, University of South Carolina; Erica Lilleodden, Forschungszentrum

Monday PM Room: 285
March 10, 2008 Location: Ernest Morial Convention Center

Session Chair: To Be Announced

2:00 PM Invited

On the Digital Image Correlation (DIC) Technique and Its Applications: *Cheng Liu¹; ¹Los Alamos National Laboratory*

Different techniques for determining various components of surface displacement field have been developed in the past, techniques like geometric moire, holography, moire interferometry, speckle shearing interferometry, to just name few. All these techniques involve either delicate sample surface preparation or complicated optical instrumentation. Also the outcome of these techniques is some kind of fringe patterns and their interpretation is sometimes tedious and difficult. The digital image correlation (DIC) technique has gained popularity for deformation measurement applications recently due to the advances of personal computer and software engineering. In this talk, I will present some of our recent applications of the DIC technique to different materials and specimen designs. The materials and specimen designs can be categorized as unconventional so that the conventional deformation measurement techniques are difficult to apply.

The applications include polymeric foams, syntactic foam, high explosives and their mocks, and large deformation of some metallic materials.

2:30 PM Invited

Micro-Bending Experiments to Characterize the Elastic Properties and Interfacial Toughness of Yttria Stabilized Zirconia Thermal Barrier Coatings: *Christoph Eberl¹; Daniel Gianola¹; Ming He²; Anthony Evans²; Kevin Hemker³; ¹Forschungszentrum Karlsruhe; ²University of California Santa Barbara; ³Johns Hopkins University*

Multilayered thermal barrier systems offer tremendous technological advantages but must remain attached to the substrate to be effective. Important phenomena that affect delamination occur in each layer and at the interfaces between the different materials. This talk will detail the development and use of micro-bending experiments undertaken to measure the elastic modulus of physical vapor-deposited (PVD) 7-YSZ thermal barrier coatings. Digital image correlation (DIC) used to measure the spatial displacement fields associated with the application of point loads will be coupled with a detailed finite element (FE) model of the micro-bending specimen and used to deduce the strain dependence of the in-plane modulus. DIC also allows for observation of crack nucleation and propagation and determination of the crack tip for different applied loads. Comparisons with FE simulations allow for determination of the inter-columnar YSZ fracture strength and the interfacial toughness between the YSZ and the underlying thermally-grown oxide.

3:00 PM

Digital Image Correlation – Strain Evaluation Made Easy: *Carl Cady¹; Cheng Liu¹; Billy Taylor¹; ¹Los Alamos National Laboratory*

Digital image correlation (DIC) technique was used in conjunction with standard loading techniques. The deformation on the surface of the samples was obtained using a series of random speckle images acquired during the loading and unloading of a sample. The strength of the DIC technique for measuring strains in samples that have unusual geometries, joints, and/or size limitations will be demonstrated in this presentation. The unique adaptability of this technique to measure overall strain as a standard extensometer can, or to measure local strains like a strain gage gives this technique the unique ability to re-evaluate a test multiple times. This ability to re-evaluate tests can bring insight into the failure process of different classes of materials. One strength of this technique is the ability to analyzing the deformation characteristics of welded materials. Evaluation of sub-sized samples, welded materials and constrained two phase materials will be discussed in this presentation.

3:20 PM

Digital Image Correlation in Materials Deformation Studies: From Fuel Cell Membranes to Advanced High Strength Steels: *Louis Hector, Jr.¹; ¹General Motors R&D Center*

We present a survey of recent applications of digital image correlation (DIC) to deformation measurement in automotive materials. We begin our survey with a look at measurement of drying-induced strain fields in perfluorosulfonic acid membrane and membrane electrode assembly materials in fuel cells. We continue with a discussion of the measurement of strain fields in Portevin-LeChatelier (PLC) bands during deformation of an Al-Mg alloy with high speed digital photography. Next, we examine deformation and fracture of spot welds in a dual-phase steel and lap welds in Al alloys generated with a high power CW Nd:YAG laser. We complete our survey with plastic deformation behavior of press hardened boron steel and two grades of martensite steel. These materials belong to a new class of ultra-high strength steels that holds great promise for automotive applications. We conclude with a summary of potential future applications for DIC.

3:40 PM

Drift and Spatial Distortion Elimination in Atomic Force Microscopy Images by Digital Image Correlation Technique: *Zhi-Hui Xu¹; Xiaodong Li¹; Michael Sutton¹; Ning Li¹; ¹University of South Carolina*

The characterization of nanomaterials and nanostructures at the nanoscale has been a tremendous challenge to many existing testing and measurement techniques. With the rapid development of micro/nanofabrication technologies, the development of appropriate and accurate tools for nanometrology and nanomechanical testing is greatly needed. In this study, a recently developed methodology for scanning electron microscopy (SEM) image correction has been

successfully adapted to correct the drift and spatial distortions of atomic force microscopy (AFM) images. The errors in AFM images have been significantly reduced down to 0.015% with a standard deviation of 0.13% for an AFM sample stage and 0.02-0.03% with a standard deviation of 0.1% for a close loop sample stage.

4:00 PM Break

4:15 PM Invited

Strain Fields in Thin Metal Films for MEMS Subjected to Various Strain Rates: Ioannis Chasiotis¹; Krishna Jonnalagadda¹; John Lambros¹; Jeff Pulskamp²; Ron Polcawich²; Madan Dubey²; ¹University of Illinois at Urbana-Champaign; ²Army Research Laboratory

An optical method to obtain local deformations in rate sensitive films for MEMS was developed. A speckle pattern is generated with silicon nanoparticles on freestanding films. Digital Image Correlation (DIC) is used to resolve elastic/plastic deformations from high magnification optical images. In the reported study, the average gauge size of the test samples was 1x100x1000 microns, while the strain rates were 10-6 to 10-1 s-1. The strain resolution was 0.01%, which is equivalent to 1/10 of the pixel size. Two materials were investigated. The first were 0.4-micron Pt films, and the second were 2.0-micron Au films. The former showed significant strain rate sensitivity in terms of proportional limit (600-1000 MPa) and ultimate strain (3% - 4.3%) but their elastic modulus (175 GPa) and strength (1.8-2.0 GPa) were rate independent. On the other hand, Au films showed significant sensitivity in their strength and ductility especially at rates faster than 10-3 s-1.

4:45 PM

Strain Mapping of Al-Mg Alloy with Multi-Scale Grain Structure Using Digital Image Correlation Method: Byungmin Ahn¹; Steven Nutt¹; ¹University of Southern California

Al-Mg alloy powder was mechanically milled in liquid N₂ (cryomilling) to produce thermally stable powder with nanocrystalline microstructure for the manufacture of high-strength alloys. A multi-scale microstructure was achieved by blending unmilled coarse-grained powder with the cryomilled powder and subsequently consolidating. The final bulk alloy was comprised of nanocrystalline regions separated coarse-grained bands. In-situ observations of tensile deformation of the alloy were made using a micro-straining stage attached to a light microscope. Interactions between ductile coarse-grain bands and nanocrystalline regions were investigated. Special emphasis was given to the distinct displacements between adjoining regions during the deformation, and these displacements were measured by digital image correlation (DIC).

5:05 PM

Full Field Strain Measurement of Resistant Spot Welds Using 3D Image Correlation Systems: Hong Tae Kang¹; German Reyes-Villanueva¹; Zhenzhen Lei¹; Ilaria Accorsi²; ¹University of Michigan-Dearborn; ²DaimlerChrysler

This paper describes the local strain measurement of resistant spot welds for three sheet stack-ups of DP600 and Mild steel under quasi-static and fatigue loading. The experiments were designed to investigate the effects of electrode tip types, surface indentation levels, and base metal strengths on local strain distributions at vicinity of spot welds. The used electrode tip types were B-nose and E-nose for DP600 and surface indentation levels were 10%, 30% and 50% of the sheet thickness. To obtain the goal, geometric factors were precisely controlled, especially the diameters of spot welds. Welding schedules varied to obtain a proper surface indentation levels while keeping the same weld sizes for the different materials and electrode tip types. Local strains at critical locations in resistant spot welds were measured using 3D image correlation systems (ARAMIS) during quasi-static and fatigue testing. The measured local strains were also compared with finite element analysis results.

5:25 PM

Using 3-Dimensional Digital Image Correlation to Map Deformation Fields in Bovine Cornea: Brad Boyce¹; J. Mark Grazier¹; Thao Nguyen¹; Reese Jones¹; ¹Sandia National Laboratories

Understanding the mechanical behavior of cornea tissue has implications to several ocular diseases and to corrective procedures such as LASIK. As a physiologically-relevant alternative to tensile-strip testing, intact ocular globes have been pressurized to observe the pressure-dependent response of

cornea tissue. In our approach, the corneo-scleral junction is constrained as a fixed boundary condition, so all deformation occurs solely in the cornea. Digital image correlation analysis of the anterior cornea is enabled by imaging graphite speckles with transmission-illumination to prevent glare. A two-camera arrangement permits dynamic 3-dimensional mapping of the deformation field during pressure- or volume-controlled inflation and subsequent time-dependent creep/relaxation. To interpret observed displacement fields, we have developed a microstructurally-based viscoelastic fiber-composite model of the cornea accounting for multiple viscous-relaxation modes and an inhomogenous, anisotropic collagen fibril distribution. Discussion will focus on the observed viscoelastic properties of the cornea as well as the capabilities and limitations of the technique.

5:45 PM

New Techniques for the Characterization of Expansion in Thermal Barrier Coating Bond Coat Alloys: Robert Thompson¹; Ji-Cheng Zhao²; Kevin Hemker¹; ¹Johns Hopkins University; ²General Electric Company

Thermal barrier coatings (TBCs), commonly used in modern gas turbines and jet engines, are dynamic multi-layered structures. Understanding the disparate thermal expansion behavior of the coating is essential to improving the overall performance of the system. Various components of the TBC, however, are incapable of actuating pushrods that commercial dilatometers use to determine the coefficient of thermal expansion (CTE). This paper outlines a non-contact digital image correlation technique for measuring the thermal strain and CTE of various bond coat and superalloy materials from room temperature to 1100°C. Results from well-characterized superalloys are used to validate the experimental and data processing methodologies. Temperature-dependent CTE results for 50 to 100 µm thick (Ni,Pt)Al and NiCoCrAlY coatings will be presented as well. The influence of other important properties, such as elevated temperature strength, creep, and phase transformations will also be discussed with regards to the system-level mechanical behavior of the TBC.

Enhancing Materials Durability via Surface Engineering: Steel and Other Alloys Surface Durability

Sponsored by: The Minerals, Metals and Materials Society, TMS Structural Materials Division, TMS/ASM: Corrosion and Environmental Effects Committee, TMS: High Temperature Alloys Committee

Program Organizers: David Mourer, GE Aircraft Engines; Andrew Rosenberger, US Air Force; Michael Shepard, Air Force Research Laboratory/MLLMN; Bruce Pint, Oak Ridge National Laboratory; Brian Gleeson, Iowa State University

Monday PM

Room: 388

March 10, 2008

Location: Ernest Morial Convention Center

Session Chair: Bruce Pint, Oak Ridge National Laboratory

2:00 PM Introductory Comments

2:05 PM

Low-Temperature Aluminide Coating Synthesized via Pack Cementation on Ferritic/Martensitic Alloys: Brian Bates¹; Ying Zhang¹; Yongqing Wang¹; Bruce Pint²; ¹Tennessee Technological University; ²Oak Ridge National Laboratory

Aluminide coatings synthesized at elevated temperatures showed good long-term oxidation protection in the water vapor environment. To prevent potential damage to the mechanical properties of the ferritic/martensitic alloys and also make the coating process more compatible with the heat treatment cycle of these alloys, efforts were made to fabricate coatings at lower aluminizing temperatures (~700°C). Thermodynamic calculations carried out for packs containing NH₄Cl activator and binary Al-Cr masteralloys indicate that the partial pressure of metal halide vapors depends on both the pack composition and aluminizing temperature. Binary Cr-Al masteralloys containing 15 and 25 wt.% Al were used to lower the Al activity in the aluminization and therefore to reduce the tendency to form brittle Al-rich phases (e.g. Fe₂Al₃) in the coating.

2:25 PM

Evolution of Steel Surface Compositions with Heating in Vacuum and Air:

Colin Doyle¹; Bryony James¹; ¹University of Auckland

The surface composition of mild steel and 304 and 316 austenitic stainless steels have been monitored using X-Ray photoelectron spectroscopy (XPS) whilst the steels were heated to 600°C. The bulk elemental compositions determined by OES are compared with the XPS data. The heating experiments were conducted under ultrahigh vacuum (UHV) and oxidizing conditions (6×10^{-6} Torr air). Before heating, the major elements at the steel surfaces were iron, oxygen, carbon, and manganese, along with chromium and nickel for the two stainless steel samples. The iron present at the surface was predominantly iron(III), with a small amount of zero-valent iron. UHV heated steel surfaces all showed zero-valent iron at temperatures greater than 450°C. Both stainless steels showed progressively decreasing iron content, with the surfaces becoming enriched with chromium oxides. Under oxidizing conditions the iron at the surface is converted to a mixture of Fe(II) and Fe(III).

2:45 PM

The Performance of Al-Rich Oxidation Resistant Coatings for Fe-Base Alloys: Bruce Pint¹; Ying Zhang²; Sebastien Dryepondt³; ¹Oak Ridge National Laboratory; ²Tennessee Technological University; ³University of California at Santa Barbara

Oxidation resistant Al-rich coatings are being investigated for applications such as ultra-supercritical fossil-fuel plants. The presence of water vapor accelerates the environmental degradation of chromia-forming ferritic and austenitic steels but has little effect on coatings able to form an Al-rich surface oxide. Long-term (=10,000h) diffusion and oxidation experiments are being conducted to determine the rate of Al loss from the coating by oxidation and interdiffusion. Based on these data, a coating lifetime model is being developed. Creep experiments were conducted to assess the effect of the coating on substrate mechanical properties.

3:05 PM

Surface Treatment of Metals by Electro Plasma Technology: Pratheesh George¹; Greg Tenhundfeld¹; Edward Daigle¹; Danila Ryabkov¹; ¹CAP Technologies LLC

Electroplasma technology is a patented surface engineering technology developed by CAP Technologies LLC. The application of this technology includes surface cleaning, modification, alloying and coating of metal surfaces for corrosion resistance and wear resistance applications. The main advantages of this process are the environmentally friendly technology, cost effectiveness, unique surface profile for better coating adhesion and a fast deposition of nanocrystalline coatings with deposition rates as high as 1 μm per second with excellent corrosion resistance. The mechanism behind the electroplasma technology and its main characteristics will be presented. Different coatings such as Zn-Ni, Zn-Ni-Mo and Zn-Ni-P have been applied and are being considered as an alternative for the hazardous cadmium and chromium plating, especially in the aerospace industry. The processing and properties of these coatings will be also presented. The effect of this process on the fatigue and hydrogen embrittlement properties of the substrate materials will be discussed.

3:25 PM

A Functionally Graded Design Study for Boron Carbide and Boron Carbonitride Thin Films Deposited by Plasma Enhanced DC Magnetron Sputtering: Tolga Tavsanoglu¹; Michel Jeandin²; Okan Addemir¹; ¹Istanbul Technical University; ²Ecole des Mines de Paris

The B-C-N system is characterized by short bond lengths and includes the hardest known materials, c-BN and boron carbide (B_4C), as well as other materials with remarkable tribological properties such as h-BN. Despite these good properties, adhesion problems were observed for B_4C and boron carbonitride (BCN) thin films on steel and Si substrates when the film thickness exceeds 500 nm. To enhance the adhesion, three functionally graded designs; surface boronizing of the steel substrate before deposition ($\text{B}/\text{B}_4\text{C}$), Ti/TiC/ B_4C and Ti/TiN/BCN structures were discussed. Cross-sectional FE-SEM examinations and elemental depth profiling by Secondary ion mass spectrometry were revealed the graded structure of the films. The elemental film composition was measured by EPMA. The mechanical properties were determined by nanoindentation and the tribological properties by pin-on disc measurements. The results demonstrated

the possibility of growing well adherent boron carbide and boron carbonitride films with thicknesses in the μm range.

3:45 PM Break

3:55 PM

Enhancing Adhesive Fatigue Life of Wear Resistant HVOF Coating: Ashwin Hattiangadi¹; Ram Krishnamurthy¹; Jibin Han¹; ¹Caterpillar Inc.

HVOF coatings consisting of ceramic carbides in metallic matrix are increasingly considered for use as wear resistant coatings, in machine applications such as tractor undercarriage sealing joints. Coating delamination, cracking and failure are critical considerations for their use and can limit overall benefits of wear life increase. Here, we examine post-processing heat-treatments that promote coating adhesion. Adhesion depends upon the post processing temperature, and adhered coatings develop a periodic array of through-thickness cracks or not depending upon the prescribed heat-treatment. The appearance of the periodic array of cracks and crack spacing conforms to elastic fracture analysis. FEM simulation with cohesive zone capability was developed to help predict fatigue life performance and S-N curve. It was calibrated with simple experiments to estimate the coating, interface energies and their dependence on the post processing method. Our findings have interesting implications for the production of crack-free bonded wear-resistant HVOF coatings.

4:15 PM Invited

High Performance Wear Materials for Earthmoving Applications: M. Beardsley¹; Jason Sebright¹; ¹Caterpillar Inc.

Sacrificial wear materials applied to buckets, blades and ground engagement tools represent a high maintenance cost of operation of earthmoving equipment. Improved wear materials can result in lower operating costs by reducing replacement intervals. New materials and processes to improve the surface durability of components have been developed and are currently under evaluation to demonstrate two times the wear life of standard heat treated steels.

4:35 PM

Pulsed Laser Treatment of 4Cr/2Mn/0.25C Steel: Greg Kusinski¹; Jan Kusinski²; ¹Clemson University, School of Materials Science and Engineering; ²AGH University of Science and Technology

The aim of this research was to experimentally verify the possibility of improvement of wear properties of 4Cr/2Mn/0.25C steel, used in automotive engine parts, by laser hardening and laser re-melting. A high power CO₂ pulsed laser treatment was applied and the microstructure-property-relationship was studied as a function of both laser power and pulse duration. Advanced analytical techniques (SEM and TEM microscopy, and EDS microanalysis) were used to study structural details in the laser hardened layer, as well as to show fine differences in comparison with conventionally hardened steel. It was shown, that high wear resistance of the laser hardened layer (microHV65 > 2000) was due not only to the grain refinement caused by rapid laser heating but also to the high stresses induced during rapid cooling of the surface layer, both creating essentially fine, highly dislocated and internally twinned martensite with some amount of stable, interlath retained austenite.

4:55 PM

Reduced Wear and Friction Losses by DLC Coating of Piston Pins: Roman Morgenstern¹; Frank Dörnenburg¹; Wolfgang Kiessling¹; Simon Reichstein¹; ¹Federal-Mogul Nürnberg GmbH

Diamond like carbon coatings are well known to offer superior friction and wear behaviour. To evaluate the potential of DLC coatings applied to piston pins in internal combustion engines, linearly reciprocating sliding wear examinations have been performed on uncoated and DLC coated piston pin segments versus different counter part materials. The tests have been investigated with respect to friction and wear performance of typical pin - piston material combinations. The analysis of the results show the enormous potential of DLC coatings to reduce wear and friction for each of the different counter part materials. Examined engine tests confirm the results of the non-engine wear test rig, showing that the specific engine output increases and the fuel consumption decreases if DLC coatings are applied to the piston pin.

MONDAY
PM

5:15 PM

Re-Melt – Improved Durability for Aluminum Diesel Pistons by Local Surface Microstructure Modification: *Simon Reichstein*¹; Scott Kenningley¹; Peter Konrad¹; Frank Dörnenburg¹; ¹Federal Mogul

Driven by the customers request for increasing fuel efficiency and reduced CO₂ emission solutions, pressure and temperature in internal combustion Diesel engines has rapidly increased during the last 15 years. Operated at maximum temperatures of up to 420°C in series production engines (which is equivalent to a homologous temperature of 0.92!) at complex thermo-mechanical loading conditions, Diesel pistons in modern passenger vehicles are probably today's most challenging Aluminium high temperature application. To meet these requirements, Federal Mogul has developed the process of local remelting for critical piston regions. In this paper a microstructure based model is discussed, showing how the modified (Re-melted) local microstructure can be directly attributed to an improvement in piston durability. The model is derived from surface crack initiation observations and quantified by microstructure modeling FE analysis. For validation the models predictions are compared to results from superimposed TMF-HCF rig testing and to engine testing results.

5:35 PM

Effect of Hot-Dip 55%Al-Zn Alloy Coating on Properties of Un-Hardened and Tempered N80 Steel: *Ming Jiang*¹; Guoxi Li¹; Changsheng Liu¹; Yiran Zheng¹; ¹Northeastern University

In this paper, the hot-dip 55%Al-Zn alloy coating was performed on the un-hardened and tempered N80 steel by two-step flux method, to prevent severe corrosion in oil field. The microstructure of hot-dip 55%Al-Zn alloy coating was analyzed by metalloscope, SEM, X-ray diffraction instrument and EDS. The corrosion resistance of the alloy-coated steels in NaCl solution was studied by means of laboratory immersion testing and EIS. And the comparison of the mechanical properties of N80 steel before-and-after coating was carried out, using tension machine and shock test machine. The results showed that the microstructure of 55%Al-Zn coating was composed of two layers: an Al-Zn alloy overlay and an intermetallic compound layer between overlay and substrate. Hot-dip 55%Al-Zn coating could improve the corrosion resistance of un-hardened and tempered N80 steel obviously in NaCl solution. After hot dipping 55%Al-Zn alloy, the strength and plasticity of the alloy-coated steels could also been greatly improved.

General Abstracts: Extraction and Processing: Session II

Sponsored by: The Minerals, Metals and Materials Society, TMS Extraction and Processing Division, TMS: Aqueous Processing Committee, TMS: Materials Characterization Committee, TMS: Process Technology and Modeling Committee, TMS: Pyrometallurgy Committee, TMS: Recycling and Environmental Technologies Committee

Program Organizers: Boyd Davis, Queens University; Michael Free, University of Utah

Monday PM

Room: 272

March 10, 2008

Location: Ernest Morial Convention Center

Session Chair: Joe Ferron, VP Metallurgical Technology for Recapture Metals

2:00 PM

Electrochemical Reduction of Beryllium Oxide from CaCl₂ Melts Saturated with CaO: *Joel Katz*¹; ¹Los Alamos National Laboratory

Work to electrochemically reduce beryllium oxide to beryllium using the FFC Process will be reported on. Several samples underwent reduction for periods of up to two weeks in calcium chloride melts, which were held between 930 and 950°C. Experiments were performed using a graphite crucible and anode. Calcium oxide additions to the calcium chloride melt varied from a few percent to saturation. Cells were maintained between 2.6 and 3.2 V, which is sufficient to allow the electrolysis of calcium oxide to occur as follows. $\text{CaO} = \text{Ca}^{2+} + \text{O}^{2-}$. Calcium ions are thought to be responsible for the actual reduction. The overall reduction reaction is thought to be: $\text{BeO} + \text{Ca} = \text{Be} + \text{CaO}$. Experimental evidence of reaction layers and intermediate reaction products will be discussed.

2:25 PM

Solid Oxide Membrane Process for Calcium Production Directly from Its Oxide: *Soobhankar Pati*¹; Marko Suput¹; Rachel Delucas¹; Uday Pal¹; ¹Boston University

Solid oxide membrane (SOM) technology has been successfully employed for the production of high energy metals such as magnesium, titanium and tantalum by directly reducing their oxides. This paper reports on the recent investigation for calcium production from CaO dissolved in fluoride and chloride based fluxes by the SOM process. This process employs an inert oxygen-ion-conducting stabilized zirconia membrane to separate the cathode in the flux from the anode. When the applied electrical potential between the electrodes exceeds the dissociation potential of CaO, oxygen ions are driven out of the melt and through the zirconia membrane to the anode where they are oxidized. Reduced calcium metal deposits or evolves at the cathode depending on the operating temperature. The SOM cell has been electrochemically characterized. Key concepts related to CaO dissociation, solubility of calcium in the flux and hygroscopic nature of the flux relevant to the SOM process has been explained.

2:50 PM

Studies on Coal in Pressure Leaching of Marmatite Concentrates: *Zhifeng Xu*¹; Dingfan Qiu²; Haibei Wang²; ¹Jiangxi University of Science and Technology; ²Beijing General Research Institute of Mining and Metallurgy

Pressure leaching of a Yunnan marmatite concentrates with adding coal as the elemental sulfur disperser was investigated. The experimental results showed that the coal with carbon content higher than 70% was incapable of dispersing the elemental sulfur from mineral and could not improve the leaching of zinc. The coal with low carbon content (lignite coal) could act as excellent sulfur-disperser in the pressure leaching at 423 K. The mechanism of the lignite coal as the sulfur-disperser was further discussed by ultraviolet, infra-red spectrum and mass spectrum.

3:15 PM Break

3:35 PM

Sulfurization Behavior of Cerium Doped Uranium Oxide by CS₂: *Nobuaki Sato*¹; Motohiro Komura¹; Shintaro Kato¹; Akira Kirishima¹; Osamu Tochiyama¹; ¹Tohoku University

A new recycle process of uranium from spent fuel by sulfide reprocessing process, which consists of voloxidation for decladding and sulfurization for FP separation, has been developed. During the voloxidation procedure, it was found that cerium doped UO₂ solid solution as well as the U₃O₈ phase was formed by the reaction of U₃O₈ and cerium dioxide at 1000°C in air. Then the sulfurization of the cerium doped uranium oxide was examined at temperatures lower than 500°C, and found that U₃O₈ was reduced to form UO₂. However, sulfurization of the cerium containing UO₂ solid solution phase was suppressed compared with those for pure UO₂ and CeO₂ cases. The conditions for selective sulfurization were also discussed.

4:00 PM

Titanium Dioxide Potential of the Montecristi Region, Dominican Republic (Hispaniola Island): *Francisco Longo*¹; ¹Xstrata

Titanium dioxide (ferrotitaniferous) sands deposits have been discovered and are presented as widely spread as beach sands along the Northwest coast of the Dominican Republic, close to actual shoreline, located on the Montecristi region, Dominican Republic (Hispaniola Island). Potential for these resources are now object of this study, taking in account the potential of the area, strategic location (close to a major Marine Port and on an inhabited area) and on a region declared by the DR State as of free taxes to promote and to incentivate investments.

General Abstracts: Light Metals Division: Session I

Sponsored by: The Minerals, Metals and Materials Society, TMS Light Metals Division, TMS: Aluminum Committee, TMS: Reactive Metals Committee, TMS: Recycling and Environmental Technologies Committee

Program Organizers: Neale Neelameggham, US Magnesium LLC; Anne Kvithyld, Norwegian University of Science and Technology

Monday PM
March 10, 2008
Room: 297
Location: Ernest Morial Convention Center

Session Chairs: Anne Kvithyld, Norwegian University of Science and Technology; Mike Powers, Agilent Technologies Inc

2:00 PM

Possibilities of Aluminium Dross Treatment and Application of Dross

Residue: *Helmut Antrekowitsch*¹; Bernd Prillhofer¹; ¹University of Leoben

Concerning the different European and world wide ecological regulations, as well as economic reasons the necessity of dross treatment will increase in future. Due to the processes of the secondary aluminium metallurgy the amount of impurities, the metallic aluminium and the chlorine content of the produced dross vary in a wide range. In the most cases landfilling of the treated dross or even of the whole dross is usual. A defined treatment as a function of the process and the composition leads to different applications without disposal. Furthermore old waste sites can also be treated. This paper characterises the dross in dependence on the processes and the parameters for the treatment and usage in the industry are discussed.

2:20 PM

An Optimization Study for Efficient Hydrogen Removal during Twin Roll Casting: *Aziz Dursun*¹; Beril Corlu¹; Murat Dundar¹; Rasim Erdogan¹; ¹Assan Aluminium

The efficiency of hydrogen gas removal from liquid metal depends mainly on operational parameters. Inert gas flow rate and rotational speed of the rotor are among those for the systems employing injection and shearing of the gas bubbles for gas removal mechanism. In this study we aimed at determining the optimum argon flow rate and rotor speed for the SNIF system which will result in the most efficient hydrogen removal rate within the liquid metal. The measurements were conducted during 1050 and 3003 aluminium alloy castings. Nine different gas flow rate-rotor speed combinations determined from Design of Experiments(DOE), were applied during castings. A mathematical equation estimating the hydrogen content as a function of flow rate and rotor speed has been developed using a statistical software. The optimum flow rate/rotor speed combinations were determined for the most effective hydrogen gas removal and implemented in real scale production.

2:40 PM

Methods of Aluminium Alloying and Their Impact on Melt Quality: *Volker Ohm*¹; Reiner Bauer¹; ¹HOESCH Metallurgie GmbH

Various alloying additions are used in primary or secondary smelters to adjust the chemical composition of aluminium based alloys of all kinds. Due to cost reasons those alloying additions are used as pure metals, where applicable. However, there are close limits for a series of metals used as alloying components. Metals like Mn are thus added either in form of cast low concentrated master alloys, as high concentrated powder metallurgically produced compacts and some are available as high concentrated cast master alloys. This article sets a special focus on the melt quality affected by application of the different products. Laboratory scale trials were carried out to determine the effects under reproducible and controlled conditions. The melt quality was monitored applying AlScan and Prefil. The resulting alloy composition was checked chemically by spectrometer and/or by ICP-OES.

3:00 PM

Manufacture and Characterization of Al-3Mg-Nb: *Noe Lopez P.*¹; Xochitl Rodriguez G.¹; Sandra Domínguez M.¹; Lucio Vazquez B.¹; V. J. Cortés S.¹; Marco Domínguez²; Gabriel Lara³; Manuel Vite⁴; Joel Aguilar⁴; Silvia Buenavista⁵; ¹Universidad Autónoma Metropolitana; ²Instituto Mexicano del Petróleo; ³Universidad Nacional Autónoma de México, Instituto de Investigación en Materiales; ⁴Unidad Adolfo López Mateos, Sección de Posgrado en Ingeniería, ESIME; ⁵Unidad Adolfo López Mateos, ESQIE

Ingots of Al-3Mg-Nb alloys, were prepared in an electrical induction furnace using a 1/100 Torr vacuum, they were homogenized for 14 h in a box furnace in an argon atmosphere to avoid oxidation. The ingots were preheated and rolled to a final 20 mm thickness. The plates were annealed and samples were machined for tensile, wearing and corrosion tests and for metallography, as well. Yield stress, tensile stress, fracture stress, wearing resistance and corrosion resistance increased with niobium content. Crystalline subgrain size decreases as niobium increases. Results are presented by using graphs.

3:20 PM

An Investigation of Hexavalent-Free Chromate Conversion Coatings for Test and Measurement Instrumentation: *Mike Powers*¹; ¹Agilent Technologies Inc

Test and Measurement (T&M) products represent a very high performance subset of the monitoring and control product category. These products are characterized by highly sensitive electrical systems that must perform at levels well beyond the conventional products they test. This is an investigation to define and develop a cost effective production process for application of a trivalent (Cr3+) chromate conversion coating (CCC) to replace the hexavalent (Cr6+) CCC that has been employed for aluminum alloy shields, waveguides and other aluminum components used in high frequency T&M instruments. Testing and characterization included surface contact resistivity, corrosion resistance and paint adhesion. It was found that several trivalent chromate conversion coating products demonstrate electrical performance and corrosion resistance that is essentially equivalent to the traditional Cr6+ CCC, while mitigating the toxicological and environmental concerns associated with the use of hexavalent chromium.

3:40 PM Break

3:50 PM

Cryomilled SiC Reinforced Aluminum Nanocomposites: *Timothy Lin*¹; Fei Zhou¹; Quan Yan¹; Chufu Tan¹; Bob Liu¹; Adolphus McDonald²; ¹Aegis Technology Inc.; ²U.S. Army Aviation and Missile Command

At present, metal matrix composites (MMCs) typically based on Al alloys are the materials of choice for many lightweight structural applications. Recent development in nanostructured material provides a new opportunity for the substantial strength enhancement of materials (e.g. over 50% improvement) unattainable with conventional approaches, leading to significant weight reduction in structures. In this paper, Aegis will present the development of lightweight, high strength, and impact shielding SiC reinforced Al-based NMMCs (Nanostructured Metal Matrix Composites), with a focus on microstructure design, processing repeatability/consistency, as well as preliminary impact and high-temperature performance. Aegis will also demonstrate the production of large-dimension NMMCs billets and plates by using a cost-effective synthesis and consolidation process that can be scaled up for the mass production.

4:10 PM

Comparative Analysis of the Influence of Inhibitor Concentrations on the Corrosion Susceptibility of Al - 1.0%Zn Alloy in Acidified Vernonia Amegdalina, Pipernigrum and Telferia Occidentalis: *Ndubuisi Idenyi*¹; *Chinedu Ekuma*¹; Simeon Neife²; ¹Ebonyi State University; ²Enugu State University of Science and Technology

The influence of varying concentrations of extracts of vernonia amegdalina, pipernigrum and telferia occidentalis on the corrosion behaviour of Al - 1.0%Zn alloy in varying molarities of HCl has been investigated. Pre-weighed samples of the alloy were subjected to 0.5M and 1.0M HCl, each containing 50 cm³ and 100 cm³ of the extracts separately. The set-ups were allowed to stand for 28 days with a set of samples withdrawn weekly for corrosion rate characterization. The results obtained showed the usual corrosion behaviour of initial steep increase in corrosion rate followed by a gradual decline over exposure time, characteristic

of most passivating metals. Expectedly, the vegetable extracts showed inhibition traits with pronounced effects at lower acid molarities with higher extract concentrations. When compared, *telferia occidentalis* showed the best manifestations, *vernonia amegdalina* the worst and *pipernigrum* in-between.

4:30 PM

The Impact of Corrosion on the Deformation Behaviour of Al-Zn Alloys in 0.1M HCl and Seawater: Ndubuisi Idenyi¹; Israel Owate²; Cajethan Okeke³; Simeon Neife⁴; ¹Ebonyi State University; ²University of Port Harcourt; ³University of Nigeria; ⁴Enugu State University of Science and Technology

An investigation into the deformation characteristics of Al-Zn alloys exposed to corrosion environments has been carried out. Tensile specimen samples of four (4) different grades of aluminium alloys with varying percentages of zinc were prepared and immersed in baths containing 0.1M HCl and seawater separately and allowed to stand for 30 days. At expiration of the exposure time, the samples were withdrawn and rinsed with distilled water and acetone before being subjected to tensile loading until fracture occurred. The results showed that all the samples obeyed the stress-strain relationship for a relatively ductile material with those exposed to acid showing more brittle fracture than those exposed to seawater, a behaviour that is possibly attributable to hydrogen embrittlement necessitated by the diffusion of hydrogen into the alloy samples from the acidic media.

4:50 PM

Nitrocarburization of Tool Steels for High Temperature Aluminum Forming: M. David Hanna¹; James G. Schroth¹; ¹General Motors

Forming of aluminum at elevated temperatures requires wear-resistant tool surfaces. The effects of nitrocarburizing temperature and time on the compound layers developed on different low and medium carbon tool steels for use in high temperature forming processes were investigated. The surface layers were analyzed by optical and scanning electron microscopy, microhardness measurements, and X-ray techniques. AISI P20 tool steel was found to be suitable for nitrocarburization and for use as an elevated temperature tool material due to its relative stability and durability, its availability in large block sizes, and also its functional properties in the forming environment. A non destructive method of relating the hardness of the nitrocarburized AISI P20 steel tool surface with the depth of the compound layer was used to evaluate tool durability with time to provide a means to monitor and estimate the compound layer thickness in the plant environment.

5:10 PM

Development of Ductility-Limited Local Yield Strength Model for High Pressure Die Cast A380 Alloy: Mei Li¹; Jake Zindel¹; John Allison¹; Larry Godlewski¹; ¹Ford Motor Company

In recent years there has been an increasing need for robust simulation methods and tools to accelerate the optimization of process and product design of cast aluminum components in automotive industry. High pressure die casting process provides tremendous cost saving opportunities in manufacturing cast components. Development of Virtual Casting tools for HPDC aluminum will lead to fast prototyping and tooling, thus fast final products with reduced cost. This work describes the development of yield strength model for HPDC A380 alloy. It was found that the yield strength of HPDC aluminum alloy depends not only on the amount of eutectic and precipitation phases, but also strongly on the porosity level present in the casting. High level porosity reduces the ductility property which results in lower yield strength. The prediction can be used to design and optimize casting component and process.

5:30 PM

Effects of Different Annealing Processes on Microstructural Features of Twin Roll Cast 3003 Aluminum Alloy: Beril Corlu¹; Aziz Dursun¹; Murat Dündar¹; Canan Inel¹; ¹ASSAN Aluminium

Twin roll casting (TRC) can be used to produce aluminum sheets by direct solidification from the melt. Rapidly solidified (upto 800 OC/sec) outer skin has a supersaturated microstructure with very fine grains. Application of prescribed processing routes of TRC cast material, like soft annealing to produce H1X tempers, to the TRC 3003 and 8006 alloys, results in the formation of very large surface grains after recrystallization which causes unwanted surface features called "orange peel" after bending or deep drawing processes. In the present work, annealing processes were carried out in a salt bath in order to see the

effect of high heating rate on recrystallized grain size. In addition, the effect of high temperature rapid annealing process prior to the rolling operation on microstructural features were also demonstrated. Surfaces and through thickness microstructures of the specimens were investigated under optical microscope and the mechanical properties have been discussed accordingly.

General Abstracts: Materials Processing and Manufacturing Division: Composition Structure Property Relationships I

Sponsored by: The Minerals, Metals and Materials Society, TMS Materials Processing and Manufacturing Division, TMS/ASM: Computational Materials Science and Engineering Committee, TMS: Global Innovations Committee, TMS: Nanomechanical Materials Behavior Committee, TMS/ASM: Phase Transformations Committee, TMS: Powder Materials Committee, TMS: Process Technology and Modeling Committee, TMS: Shaping and Forming Committee, TMS: Solidification Committee, TMS: Surface Engineering Committee

Program Organizers: Ralph Napolitano, Iowa State University; Neville Moody, Sandia National Laboratories

Monday PM

March 10, 2008

Room: 282

Location: Ernest Morial Convention Center

Session Chairs: Michael Miles, Brigham Young University; Mohammed Maniruzzaman, Worcester Polytechnic Institute

2:00 PM

Acoustic Cavitation Assisted Improvement of Solidified Structure: Mamoru Kuwabara¹; ¹Nagoya University

Ultrasound is applied before or during solidification of metals. SEM observations show improved refinement of crystal structure and/or entrapment of micro-voids in the matrices of the solidified materials. The results is attributed to micro-multibubble emerged during acoustic cavitation. Not only by vigorous agitation of melt due to micro-jets during solidification but also by a great many nano-bubbles entrapped in the melt before solidification may both contribute to the improved crystal structures. Cold model experiments using water and low melting point metals have been carried out. High speed photography of acoustic multibubble in water and SEM images of many indentations on aluminum foils dipped into the melts with ultrasound verifies the proposed mechanism. The effects of various operating parameters on the solidified structures of metals are discussed based on the experimental results. Many micro-voids acoustically entrapped in the materials are attractive to produce innovative foamed materials with different physical properties.

2:20 PM

Grain Refinement and Grain Boundary Character Distribution of Commercially Pure Molybdenum Produced by Equal Channel Angular Pressing (ECAP): Seng-Ho Yu¹; Dong Hyuk Shin²; Sun-Keun Hwang¹; ¹Inha University; ²Hanyang University

Commercially pure Mo was grain-refined by ECAP at 500°C. A total of 8 passes of ECAP was conducted and the resulting microstructure and texture were studied. In the as-deformed state, the development of the microstructure and texture was influenced by the strain paths during repetitive ECAP. With four passes of ECAP, lamellar grains of 300 nm in thickness and equiaxed grains of 500 nm were obtained via route A and C, respectively. The grain refinement achieved by the ECAP was attributed to the evolution of low angle boundaries into high angle boundaries with increase in the number of pressing. Like other bcc metals, a strong fiber texture consisting of $\langle 111 \rangle_0$ and $\{110\}_0$ components was generated in Mo by ECAP. The characteristics of the texture strongly implied that the $\{110\}\langle 111 \rangle$ slip systems were in operation, which is thought to be the main mode of deformation during the severe plastic deformation.

2:40 PM

Effect of Sn Content on the Magnetic Properties and Recrystallization Behaviors of Grain-Oriented Electrical Steels: *Chun-Chih Liao*¹; Chun-Kan Hou¹; ¹National Yunlin University of Science and Technology

Fe-3% Si with a sharp Goss orientation has a good magnetic property suitable for the core material of transformers. In order for secondary recrystallization to occur, the growth of other primary grain must be restrained. Sn is easy to segregates at grain boundary and on the surface that pinning the grain boundary mobile. This study was changing the Sn content ranging from 0 to 0.31wt%, and investigating the effects of SRT (secondary recrystallization annealing temperature) on the recrystallization behaviors and magnetic properties of oriented electrical steel sheets. It was found that the pinning effect of Sn was very strong as the SRT below to 900 degree. The specimens containing 0wt% and 0.05wt% Sn reached secondary recrystallization completing at 900 and 1100 degree, respectively. As Sn content was higher than 0.5wt%, the specimen has pool secondary recrystallization. Specimen containing 0.05wt% Sn has maximum flux density and minimum iron loss.

3:00 PM

Effects of Alloying Elements on the Properties of Mechanical Alloying Processed Cu-Cr Alloys: *Seung Hoon Yu*¹; Kwang Seon Shin¹; ¹Seoul National University

The mechanical alloying process has been widely used to refine the microstructure and obtain homogeneous distribution of second phases for the high strength and high conductivity Cu alloys. In powder metallurgy, contamination from the milling media, chamber and process control agent is unavoidable in the process. The electrical conductivity of Cu can be seriously affected by these contaminants, particularly by Fe and O. In this study, minor alloying elements were added to the initial charges of the Cu-Cr powders to form stable second phases. After mechanical alloying, the consolidated products were fabricated by canning, degassing and hot extrusion. The mechanical properties and electrical conductivity were evaluated. It was found that the addition of minor alloying elements improved the mechanical properties and conductivity of the Cu-Cr alloys. They are thought to have had scavenging effects on the contaminants and formed stable second particles which increased the strength of the Cu-Cr alloys.

3:20 PM

Microstructural Effects on Corrosion Behavior of ZnAl Alloy at Different Ag Addition: *S. Valdez*¹; M. Flores²; Said R. Casolco³; ¹Universidad Nacional Autónoma de México, Instituto de Ciencias Físicas; ²Universidad de Guadalajara, Departamento de Ingeniería de Proyectos, CUCEI; ³University of California, Riverside, Department of Mechanical Engineering

The effect of electrochemical corrosion behavior and microstructure of ZnAl alloy with Ag addition has been investigated using Scanning electron microscopy (SEM), X-ray diffraction (XRD), EDX, Cyclic voltammetry and Corrosion potential measurements in 3.5 wt% NaCl. Surface examination and analytical studies showed that the corrosion behavior of α -Al, η -Zn and ϵ phases was significantly influenced by Ag additions. ZnAl-0.5 wt.% Ag alloyed exhibited a high corrosion resistance than the 4, 2, 1 wt. % Ag alloyed. Potentiodynamic polarization measurements showed higher icorr values of ZnAl-4 wt.% Ag alloyed. Experimental results revealed that precipitation of ϵ as a result of reaction between ZnAl alloy and Ag has a beneficial effect on corrosion resistance due to interruption of the continuity of the matrix.

3:40 PM Break

3:50 PM

Mechanical Properties and Microstructure of Friction Stir Welded High-Strength Automotive Steel: *Michael Miles*¹; Eric Olsen¹; Tracy Nelson¹; Matthew Gallagher²; ¹Brigham Young University; ²Mittal Steel

Friction stir welding (FSW) was used to weld high strength automotive steels, including TRIP 590 and DP 590, 780, and 980. Various processing conditions were used to weld these alloys, resulting in different levels of formability, weld hardness, and various weld microstructures. The relationship between welding conditions and resulting properties and weld microstructures will be discussed and compared to laser welded blanks.

4:10 PM

Prediction of Mechanical Strength Evolution during Aging Heat Treatment of Al-Si-Mg-Cu Based Cast Aluminum Alloy: *Mohammed Maniruzzaman*¹; Boquan Li¹; Richard Sisson¹; ¹Worcester Polytechnic Institute

Age hardening of aluminum alloys is done to improve the alloy strength and other mechanical properties of interest. To optimize the properties, the aging schedule, i.e. aging time and temperature, is often chosen empirically. A more efficient way for optimizing the properties would be a model capable of predicting the microstructure and the properties as a function of aging schedule and the alloy compositions. A micromechanical model has been developed to predict the yield strength evolution of Al-Si-Mg-Cu based cast aluminum alloy as a function of time and temperature during aging heat treatment process. The model also predicts the size and volume fraction of the plate-shaped precipitates and incorporates various strengthening mechanisms describing the interaction between precipitates and the motion of dislocation as well as solid-solution strengthening and intrinsic strength of matrix. A set of experiments has been performed to verify the model predictions.

4:30 PM

Integrated Fabrication of Functionally Graded Ti_3SiC_2 -TiC Binary Phase Rod by Traveling Zone Sintering Method: *Shuji Tada*¹; Keizo Kobayashi¹; ¹National Institute of Advanced Industrial Science and Technology

Ti_3SiC_2 -TiC binary phase material was synthesized from raw powder compound of Ti, Si and TiC at molar ratios of 1:1:x ($x = 1.8-7.0$) with the aim of developing a new hard product. The product obtained by the sintering of the above compound was single phase Ti_3SiC_2 when x was 2.0 or less, while a Ti_3SiC_2 -TiC binary phase structure was synthesized from the powder compound with larger x and the mass fraction of TiC in this structure increased with increasing x. Ti_3SiC_2 single phase structure was well densified at up to 1673 K, whereas higher temperature was required to densify the binary phase structure. Functionally graded Ti_3SiC_2 -TiC binary phase rod was produced by the traveling zone sintering method which enabled integrated sintering of materials at variable temperatures. The synthesized structure was successfully graded and TiC mass fraction in the product varied from 0 to 50%.

4:50 PM

Influence of Small Amounts of Zn, Ni, Fe, Cr and Ti as Quaternary Additions on Shape Memory Characteristics of Cu-Al-Mn Shape Memory Alloys: *U.S. Mallik*¹; Sampath Vedamanickam²; ¹Siddaganga Institute of Technology; ²Indian Institute of Technology Madras

Quaternary alloying elements Zn, Ni, Fe, Cr and Ti were added to ternary Cu-Al-Mn shape memory alloy in quantities of 1 to 3 wt.% each. The Cu-12.5 wt.% Al-5 wt.% Mn- wt.% Quaternary element, alloys were prepared by melting pure metals in an induction furnace under an argon atmosphere. The Al and Mn concentrations were maintained constant and amount of quaternary element was varied. Ingots were then homogenized and step quenched to obtain martensitic structure. The alloys were characterized using XRD, DSC and microstructural examination. The shape memory effect and superelasticity were determined by bend and tensile tests. Quaternary elements Zn and Ni are completely soluble, forming solid solution, whereas quaternary elements Fe, Cr and Ti have low solubility and form precipitates. Addition of Zn and Ni increases transformation temperatures, whereas Fe, Cr and Ti decrease. Addition of these quaternary elements increases shape memory effect by 4%, whereas decreases superelasticity by 2%.

5:10 PM

Study on Deformation of Large-Scale Hydraulic Turbine Blade during the Casting Process: *Jiafeng Zhang*¹; Jinwu Kang¹; Baicheng Liu¹; ¹Tsinghua University

Deformation is one of the most common defects during the casting process of large-scale hydraulic turbine blade because of the complex curved 3-D surface geometry. To finally obtain the exact surface contour, anti-deformation is given to wooden pattern in many factories. Numerical simulation is carried out to calculate the deformation of a blade casting used for Three Gorges Power Station. And the calculation is iterated by adjusting the anti-deformation values to finally realize even and appropriate machining allowance. By using ECDS (Electronic Coordinate Determination System), the surface of the casting is measured and machining allowance of each measurement point is given. The calculated results and the measured are in good agreement.

MONDAY PM

5:30 PM

A Research Study on the High Strength API Steel Production for Sour Gas Pipelines: *Shahrokh Pourmostadam*¹; ¹Mobarakeh Steel Company

With regard to the achievement of the latest global Technologies for Pipe transportation of natural gas, containing substantial amounts of H₂S (sour gas) is becoming increasingly common. Transportation of sour gas through HSLA pipelines can lead to failure from two mechanisms, hydrogen induced cracking (HIC) and sulfide stress corrosion cracking (SSCC). Over the years, suitable measures in alloy design, steelmaking technology and downstream processing has resulted in sour gas resistant linepipe steels. In line with these efforts MSCO, with the utilization of the latest technologies in production trends and suitable design has initiated the trial production of API steels. In this study, efforts are made to present the chemical analysis and mechanical properties of the coils produced in the trial running in addition to the characteristics of API steels for sour gas services.

General Abstracts: Structural Materials Division: Mechanical Behavior of Materials

Sponsored by: The Minerals, Metals and Materials Society, TMS Structural Materials Division, TMS: Advanced Characterization, Testing, and Simulation Committee, TMS: Alloy Phases Committee, TMS: Biomaterials Committee, TMS: Chemistry and Physics of Materials Committee, TMS/ASM: Composite Materials Committee, TMS/ASM: Corrosion and Environmental Effects Committee, TMS: High Temperature Alloys Committee, TMS/ASM: Mechanical Behavior of Materials Committee, TMS/ASM: Nuclear Materials Committee, TMS: Product Metallurgy and Applications Committee, TMS: Refractory Metals Committee, TMS: Superconducting and Magnetic Materials Committee, TMS: Titanium Committee

Program Organizer: Ellen Cerreta, Los Alamos National Laboratory

Monday PM

Room: 387

March 10, 2008

Location: Ernest Morial Convention Center

Session Chairs: Rajan Vaidyanathan, University of Central Florida; Veronica Livescu, Los Alamos National Laboratory

2:00 PM

Investigation of the Oxidation Behavior of High Strength NiAl Alloys:

*Arthur Brown*¹; *Michael Bestor*¹; *Mark Weaver*¹; ¹University of Alabama

Cast model alloys were prepared to investigate the effects of combinations of alloying elements on the oxidation behavior of prospective high strength overlay bond coatings for Ni-base superalloys. Additions of Ti, a potent solid solution strengthener, were studied along with additions of Hf, a Heusler forming element, and Cr. For the investigated compositions, NiAl-1.0 at.% Ti was found to be single phase whereas those containing either higher Ti concentrations, i.e., 5 or 10 at.% Ti, or multiple alloying additions were found contain Heusler-phase and/or alpha Cr precipitates. Single and multi-phase alloys were examined following isothermal and cyclic exposures at 1100°C to determine the influence on the oxide growth rate and the propensity for scale spallation. Alloys containing multiple alloying elements were generally found to oxidize more rapidly and to form thicker oxide scales than single phase alloys. The results are discussed relative to those for binary and microalloyed NiAl.

2:20 PM

Oxidation Behavior of Mo-Si-B Alloys Produced by Reaction Synthesis:

*Michael Middlemas*¹; *Joe Cochran*¹; ¹Georgia Institute of Technology

The oxidation behavior of Mo-Si-B alloys produced from the reaction of molybdenum, Si₃N₄ and BN powders was investigated. This powder metallurgy processing method yields finer grained microstructures than is achieved from melt processing. Specimens of composition 97Mo-3Si-1B (wt%), which lie in the phase field consisting of bcc-Mo and the intermetallics Mo₃Si and Mo₃SiB₂, were studied. During oxidation Mo-Si-B alloys undergo an initial period of high weight loss due to evaporation of MoO₃, followed by parabolic oxidation kinetics due to the formation of a protective borosilicate layer. The formation of borosilicate glass layers was examined under reduced P₂O₅. Oxidation resistance in air was examined between 700°C and 1300°C. The small spacing of the intermetallic phases significantly reduces the transient weight loss during the

initial stages of oxidation. Using powder metallurgy processing allows the addition of aluminum to the alloy. The effect of aluminum additions on oxidation resistance was also examined.

2:40 PM

Martensitic Transformation Paths of NiTi: *Nicholas Hatcher*¹; *Oleg Kontsevoi*¹; *Arthur Freeman*¹; ¹Northwestern University

Despite intensive investigations of NiTi shape memory alloy, the detailed microscopic mechanisms governing its structural evolution during the martensitic transformation is not fully understood. Using first-principles DFT calculations with the highly precise FLAPW method, we have studied the transition paths between the B2, R, B19, and B19' phases of NiTi to identify the governing processes of the transformation by means of calculations of total energies, electronic and band structures, elastic moduli, and shear and generalized stacking fault energetics. We also investigated a new transition path between the B2 and B19' phases via a transformation that involves shuffles of atomic layers followed by a monoclinic angle relaxation. We show the role of electronic topological transitions, Fermi surface nesting and band structure evolution in the stability of the corresponding phases, and the effect of the doping on the electronic structure and transformation paths. Supported by the AFOSR (grant No. FA9550-07-1-0013).

3:00 PM

Mechanical Behavior of Electrodeposited Nanocrystalline Nickel: *Hsiao-Wei Yang*¹; ¹University of California

In the present investigation, the mechanical behavior of bulk electrodeposited (ED) nanocrystalline nc-Ni having average grain size of 100 nm was investigated at temperatures, T, lower than 445 K (T < 0.25 T_m, where T_m is the melting point of the material) where there is limited grain growth and as a function of varying strain rate. The results show that for constant strain rate, the ductility of nc-Ni increases with increasing temperature, but the opposite is true for the ultimate tensile strength; and that for constant temperature, ductility decreases with increasing strain rate. The results are discussed with reference to findings recently reported for nc-materials.

3:20 PM

Pile-up/Sink-in in Nanoindentation Rate Sensitive Creeping Solids: *A. Elmustafa*¹; ¹Old Dominion University

We use FEM to simulate materials of variable hardness, work hardening exponent, χ of 0.1-0.3 and a strain rate sensitivity of von Mises stress, ν_σ of 0.08-0.16 to estimate pile-ups and sink-ins during indentation creep. We report that materials pile-up for $\nu_H/\nu_\sigma \geq 1.0$ and sink-in for $\nu_H/\nu_\sigma \leq 1.0$, ν_H is the strain rate sensitivity of the hardness. This is consistent with the fact that ν_H/ν_σ approaches 1 for small H/E*, i.e., soft materials and deformation is intimately dominated by pile-up. On the other hand when ν_H/ν_σ approaches 0 for high H/E* it corresponds to purely elastic deformation and is apparently dominated by sink-in in a manner prescribed by Herizian contact mechanics.

3:40 PM

Irradiated Mechanical and Microstructural Properties of a Nano-Structured Ferritic Alloy for Nuclear Applications: *David McClintock*¹; *David Hoelzer*²; *Mikhail Sokolov*²; *Randy Nanstad*²; ¹University of Texas/Oak Ridge National Laboratory; ²Oak Ridge National Laboratory

Advanced nano-structured ferritic alloys (NFAs) containing a high density of ultra-fine (2-5 nm) nanoclusters enriched in Y, Ti, and O are considered promising candidates for structural components in future nuclear systems. The microstructure of a NFA is composed of nanometer sized regions rich in Y-Ti-O uniformly distributed in a ferritic matrix. The high number density of nanoclusters in NFAs are responsible for their superior tensile strengths compared to conventional ODS ferritic alloys and may provide effective trapping centers for point defects and transmutation products produced during neutron irradiation. This paper summarizes the mechanical and microstructural properties of an advanced NFA, designated 14YWT, currently being developed at Oak Ridge National Laboratory. An identical alloy to 14YWT, designated 14WT, was produced without nanocluster dispersions in order to quantify the effect of the nanoclusters on mechanical properties. Microstructural characterization, tensile, and fracture toughness data for the irradiated and unirradiated condition will be presented.

4:00 PM Break

4:20 PM

Modeling of Hollow Particle Filled Functionally Graded Composites: Maurizio Porfiri¹; Nikhil Gupta¹; ¹Polytechnic University

Functionally graded composites are generally made by creating a particle volume fraction gradient along the material thickness. However, such composites have several inherent limitations, e.g. non-uniform coefficient of thermal expansion. A composite is analyzed in this work, which is based on creating a gradient of wall thickness of hollow particles in the material microstructure rather than the volume fraction gradient. A differential scheme is applied to estimate effective elastic modulus of such composites containing high volume fraction of particles. The modeling scheme extends the existing mathematical models applicable for dilute suspension of particles in a matrix material to account for the particle-particle interaction. The model can be used to prepare materials selection charts given the properties of the constituent materials and their volume fractions in the composite material.

4:40 PM

Modeling of Viscoelastic Properties of Syntactic Foams: Gabriele Tagliavia¹; Maurizio Porfiri¹; Nikhil Gupta¹; ¹Polytechnic University

Glass hollow particle filled polymeric composites, called syntactic foams, are widely used in marine applications. The damping capabilities of syntactic foams are of major interest in marine structural applications. The objective of this analysis is to develop relations between the viscoelastic properties of syntactic foams in terms of the properties and the volume fractions of their constituents. Therefore, a new model for the complex dynamic Young's modulus is developed. The elastic-viscoelastic correspondence principle is applied to obtain the viscoelastic relation for an infinitely dilute dispersion of hollow particles. The differential effective medium approach (DEMA) is then used to extrapolate the solution for a concentrated dispersion. The developed model is validated with the data obtained with an in-house experimental setup.

5:00 PM

On Equations of Fatigue Crack Propagation (or FCG) of Materials: Ngo Van Quyet¹; ¹Hanoi LeQuyDon University of Technology

After presenting overview on Equations of Fatigue Crack Propagation, the new equation of Fatigue Crack Propagation with load frequency and based on theory on analysis misuse of Sedov L.I. and experimental data of some the other researchers has been being suggestion by author. That new non-measure equation had been testing and its application in the practice (reinforced Frame of meter-gauged locomotive of type D19E.

5:20 PM

Bending Analysis of Functionally Graded Hollow Particle Filled Composites: Nikhil Gupta¹; Maurizio Porfiri¹; ¹Polytechnic University

Particle reinforced functionally graded composites (FGCs) are analyzed for bending properties. The FGCs are based on filling hollow particles in a matrix material. Hollow particle filled composites are used in marine and aerospace structural applications. Hollow particle filled FGCs have potential to be used in a variety of additional applications. The bending performance is compared for FGCs having gradient of wall thickness and volume fractions. The tensile and compressive moduli values of hollow particle filled composites are different. Hence, the neutral axis of the composite is determined and then appropriate tensile or compressive modulus values are applied for the analysis. Results show that the variation in wall thickness provides better opportunities for tailoring the properties of such composites.

5:40 PM

Modeling Ductile Fracture Using the Discontinuous Velocity Domain Splitting Method: Ioan Ionescu¹; ¹University Paris 13

We present a new method and its application to modeling ductile fracture of heterogeneous materials. This method considers a special class of velocities fields constructed as follows. The body is split into two subdomains: one subdomain is at rest and on the other the velocity corresponds to a rigid motion. Thus, the discontinuous velocity field is determined only by the shape of one subdomain and by a rigid motion. The deformation is localized at the boundary of this subdomain. The problem is thus reduced to the minimization of a mesh free plastic dissipation functional depending on shapes. For discretization

we make use of the Bezier interpolation and genetic algorithms are used to minimize the plastic energy. Computational tests, performed for benchmarks related to the in-plane flow of a Von-Mises material, gives excellent results at a very low computational cost. Other examples involving plastic yield surfaces characterizing geo-materials are also presented.

Hael Mughrabi Honorary Symposium: Plasticity, Failure and Fatigue in Structural Materials - from Macro to Nano: High-Temperature Mechanical Properties: Creep, Fatigue and Thermomechanical Fatigue

Sponsored by: The Minerals, Metals and Materials Society, TMS Structural Materials Division, TMS Materials Processing and Manufacturing Division, TMS: High Temperature Alloys Committee, TMS/ASM: Mechanical Behavior of Materials Committee, TMS: Nanomechanical Materials Behavior Committee
Program Organizers: K. Jimmy Hsia, University of Illinois, Urbana-Champaign; Mathias Göken, Universitaet Erlangen-Nuernberg; Tresa Pollock, University of Michigan - Ann Arbor; Pedro Dolabella Portella, Federal Institute for Materials Research and Testing; Neville Moody, Sandia National Laboratories

Monday PM
March 10, 2008

Room: 386
Location: Ernest Morial Convention Center

Session Chairs: Tresa Pollock, University of Michigan; Hans-Juergen Christ, University of Siegen

2:00 PM Keynote

Fatigue of Austenitic Stainless Steel under Isothermal and Thermomechanical Conditions: Hans Christ¹; Valerij Bauer¹; ¹University of Siegen

One of the first studies in the newly formed research group of Hael Mughrabi in Erlangen dealt with thermomechanical fatigue (TMF) behavior of an austenitic stainless steel. The results obtained at that time were broadly supplemented in the present work by means of isothermal and thermomechanical fatigue tests carried out at temperatures ranging from room temperature to 800°C. The tests were conducted both in air and vacuum applying plastic-strain control at constant plastic strain rate and amplitude. The test results in combination with microstructural findings regarding dislocation arrangement and damage evolution were used for an advancement of life prediction models. Three models published in literature were selected, since they were found to be suitable for isothermal fatigue conditions. The models were extended to non-isothermal conditions and applied to TMF. By means of tests comprising dwell times within the loading cycle, the predictive capability of the models were analysed.

2:30 PM Invited

Extending the Flow Behavior in High-Temperature Creep to Materials with Ultrafine Grain Sizes: Terence Langdon¹; ¹University of Southern California

The characteristics of creep in conventional materials are now understood reasonably well. However, a considerable interest has developed in the last decade in the processing of materials with submicrometer or nanometer grain sizes. Many of these materials are fabricated using various techniques based on the application of severe plastic deformation. This presentation describes the principles of these techniques and examines the significance of extending the conventional creep mechanisms to materials with exceptionally small grain sizes. Special emphasis is placed on the role and significance of superplasticity in deformation at elevated temperatures and the possibility of achieving grain boundary sliding at relatively low homologous temperatures.

2:50 PM

Formation of a Braid Structure during Cyclic Deformation a Heat-Treated PM Ti-48Al-2Cr-2Nb Alloy at 500°C: Gilbert Henaff¹; Mustapha Jouiad¹; Marc Thomas²; Olivier Berteaux²; ¹Ecole Nationale Supérieure De Mécanique Et D'Aérotechnique; ²ONERA

The present paper addresses the relation between the stress-strain behaviour, cyclic deformation mechanisms and the microstructures produced by various heat treatments applied to hipped Ti-48Al-2Cr-2Nb powder compacts. More precisely, it is shown that, at room temperature, the cyclic strain hardening is

directly related to the rate of formation of a vein-like structure. The influence of microstructural parameters such as grain size, volume fraction of different phases, lamellar spacing, etc. on this relation has been examined. At 500°C, a vein-like structure is also observed, even in microstructures that do not exhibit this type of substructure at room temperature. Furthermore the superior fatigue resistance and limited strain hardening exhibited by a fine fully lamellar microstructure at 20°C still holds at 500°C, where the vein-like structure is changed into a braid-like structure due to the longer fatigue life.

3:05 PM

Point-Defect Mediated Dislocation Nucleation in Nanoindentation: *Amit Samanta*¹; Ju Li¹; Ting Zhu²; ¹Ohio State University; ²Georgia Institute of Technology

We examine the conditions for heterogeneous nucleation of dislocations beneath an indenter in copper, aided by vacancies and interstitials near the surface. Atomistic calculations are performed to assess the stress-dependent formation and migration energies of point defects in the bulk and near the surface, which are used to predict the realistic kinetics of point-defect motion under the indenter due to the large stress gradient. The reaction pathways and activation energy barriers for dislocation nucleation near these point defects are computed using a modified nudged elastic band method, and compared with those of homogeneous nucleations. The activation volumes of point-defect mediated dislocation nucleations are also compared with homogeneous nucleation. A deformation mechanism map is drawn as a function of temperature and indentation load. Our results indicate the presence of a diffusive regime for small indentation loads while for higher loads dislocation-nucleation and defect migration govern the kinetics of the process.

3:20 PM

Effect of Particle Strengthening on the Very High Cycle Fatigue Behavior of Two Nickel-Base Alloys: *Martina Zimmermann*¹; Christian Stoecker¹; Hans-Juergen Christ¹; ¹University of Siegen

Fatigue behaviour in the VHCF regime is dominated by crack initiation rather than long crack propagation. Due to heterogeneously distributed plastic deformation the correlation between microstructure and damage mechanism is widely discussed. Fatigue tests were carried out on two nickel-base alloys (solid-solution hardened Nimonic 75 and precipitation hardened Nimonic 80A) in order to characterize the damage evolution in the VHCF range. Fatigue failure still occurred beyond 10⁷ cycles. An adjustment of the microstructure for the precipitation-hardened alloy Nimonic 80A showed surprisingly for the fatigue life that the overaged condition behaves more beneficial as compared to the peak-aged condition in the VHCF range. This result could not be rationalized by means of fracture surface analysis and, hence, seems to be a result of slip homogeneity. Transmission electron microscopy was carried out, in order to characterize the influence of microstructure, the resulting dislocation slip behaviour and the relevant dislocation particle interaction mechanism.

3:35 PM Break

3:45 PM Invited

Interfacial Dislocations and Creep in Ru-Containing Superalloy Single Crystals: *Tresa Pollock*¹; Laura Carroll²; Shuwei Ma¹; ¹University of Michigan; ²General Electric Aviation

Ruthenium additions to Ni-base single crystals permit new alloying domains to be explored within these superalloy systems. Creep deformation and the development of interfacial dislocation networks have been investigated in alloys with wide variations in Ru, Cr and Co. Additions of Ru and Cr strongly influence partitioning of elements between the matrix and precipitate phases and therefore strongly influence misfit and the development of interfacial dislocation networks. The spacing of dislocations in interfacial nets following high temperature aging and after creep deformation at 950°C has been characterized. Additionally, the density of dislocations within "rafted" precipitates has been measured. Creep rates do not directly scale with interfacial network spacing and the density of dislocations in excess of that needed to relax misfit varies with alloy composition. The implications for creep modeling and for alloying to increase creep resistance will be discussed.

4:05 PM Invited

Interfacial Structure and Mechanical Properties of Al₂O₃ Long Fiber Reinforced NiAl Composites: *Günter Gottstein*¹; Weiping Hu¹; Hao Chen¹; Yunlong Zhong¹; ¹RWTH Aachen University

The intermetallic compound NiAl has excellent potential for high temperature structural applications but suffers from low temperature brittleness and insufficient high temperature strength. One way to remove these deficiencies is the reinforcement by high strength ceramic fibers. Such intermetallic matrix composites can be conveniently fabricated by hot pressing of matrix coated fibers. Al₂O₃ single crystal fibers show excellent chemical stability with the NiAl matrix, but the residual thermal compressive stresses during cool down dramatically degrades the fiber strength and thus, renders the composite useless for structural applications. We report on an experimental and computational study to mitigate this problem and to fabricate Al₂O₃/NiAl composites with sufficient high temperature strength. Analytical TEM, mechanical testing and push-out tests were employed to characterize chemistry, microstructure and mechanical properties of the composites. It will be shown that a processing window exists that allows producing intermetallic matrix composites with promising mechanical properties.

4:25 PM

Mechanisms of Crack Propagation in TiAl-Alloys Observed by In-Situ Testing in the Atomic Force Microscope (AFM): *Florian Pyczak*¹; Farasat Iqbal¹; Mathias Göken¹; ¹University Erlangen-Nuernberg, Institute General Materials Properties

TiAl-alloys, especially the variants with high niobium content, are attractive light weight high temperature materials. Nevertheless, a deeper understanding of crack nucleation and propagation in these materials is desirable. AFM is an interesting technique to study crack propagation in-situ in TiAl-alloys. AFM is not only able to picture the crack path itself but also elastic and plastic deformation in the vicinity of the crack. Here AFM was employed to investigate the crack tip and the elastic and plastic deformation zone near it. Many TiAl-alloys have a lamellar microstructure, where boundaries between the gamma-TiAl and alpha2-Ti₃Al lamellae act as favorable sites for crack propagation mixed with sections of the crack path running more or less perpendicular to the lamellar interfaces along twins or deformation bands. Nucleation of new cracks was often preceded by deformation in the respective area visible as significant local elevations and depressions of the surface in an AFM.

4:40 PM

Characterization of Crystallographic Crack Initiation Sites in René 88DT at 593°C: *J. Miao*¹; T.M. Pollock¹; J.Wayne Jones¹; ¹University of Michigan, Ann Arbor

The very high cycle fatigue behavior of a polycrystalline nickel-base superalloy René 88 DT has been studied by using ultrasonic fatigue testing instrumentation at 593°C. All fatigue failures initiated internally. Nearly all initiation sites consist of large crystallographic facets. Crystallographic facets at crack initiation sites can be divided into two groups according to their 3D geometric shape: single plane facets or chevron-shaped facets. The microstructure associated with crystallographic crack initiation was examined by combining metallographic serial sectioning, EBSD and fractographic analysis. Facets at crack initiation sites were formed by fatigue crack initiation and crack growth in large grains. The crystallographic planes of these facets are of {111} type and oriented close to the orientation for maximum shear stress. Clusters of grains with similar orientations exist at crack initiation sites. The mechanisms of fatigue crack initiation and early small crack propagation in this alloy are described.

4:55 PM

Interaction of Fatigue Crack Propagation with Grain Boundary Networks: *Yong Gao*¹; *Mukul Kumar*²; James Stolken²; Robert Ritchie¹; ¹University of California; ²Lawrence Livermore National Laboratory

Grain boundary engineering has lead to performance improvements where intergranular degradation is operative. Such processing to improve the HCF properties of a Ni-base superalloy through modification of the grain-boundary distribution is considered. Fatigue properties at ambient and elevated temperatures for microstructures with varying proportions of crystallographically "special" vs. "random" boundaries are considered. We shall also examine the interaction of propagating (~10–900 µm) surface cracks with grain boundaries (and their

networks) of known character, with respect both to deflections in crack trajectory and local changes in crack-growth rates that occur at or near the boundary. In addition, FEM calculations are performed to evaluate the effective driving force and plastic-zone profile for such small-crack propagation, incorporating information from both the local microstructure (from EBSD scans) and the surface crack-path profile. This work was performed under the auspices of the U.S. DOE by University of California, LLNL under contract No. W-7405-Eng-48.

5:10 PM

Plasticity Size-Effects and Dislocation Substructures in Two Titanium Alloys: *Dave Norfleet*¹; Peter Anderson¹; Dennis Dimiduk²; Michael Uchic²; Michael Mills¹; ¹Ohio State University; ²Air Force Research Laboratory

Using current micromechanical fabrication and testing methods, micron-sized compression samples (Ti-6Al and single colony Ti-6Al-2Sn-4Zr-2Mo-0.1Si) were tested at room temperature. The results of these experiments are compared to recent Ni and Au microcrystal experiments under the context of obstacle vs. kink-mode dislocation mechanisms. Nickel and gold, obstacle controlled materials, display strong size effects with a marked increase in strength as the sample volumes were reduced. In comparison, the titanium alloys, kink-mode materials, exhibit a much less dramatic strengthening effect. Subsequent FIB-based TEM foil preparation was performed on the titanium microcrystals, utilizing an in-situ micromanipulator. Foils were prepared along active slip bands to study the dislocation dynamics of the slip system. Using a variety of TEM imaging conditions, such as Bright Field STEM, dislocation analysis was performed on each of these materials to gain an understanding as to the micro-mechanisms that control plasticity at this size scale.

5:25 PM

3D Modeling of Size Scaling Aspects of Plastic Flow in Single Crystal Ni-Based Superalloys: Jaafar El-Awady¹; Akiyuki Takahashi²; *Nasr Ghoniem*¹; ¹University of California, Los Angeles; ²Tokyo University of Science, Faculty of Science and Technology

Here we utilize large scale 3-dimensional Parametric Dislocation Dynamics (PDD) simulations coupled with the Boundary Element Method (BEM) to study the deformation behavior of cylindrical micron sized single crystal Ni-based superalloys. The BEM is used to calculate the image fields due to the interaction of dislocations with precipitates and the finite dimensions of the crystal. The solution is then superimposed on the elastic field resulting from dislocation ensembles in an infinite medium as calculated from the PDD. Statistical analysis are performed on cylindrical samples have diameters in the range 0.25 to 5 μm and the range of initial dislocation densities in the simulations are varied from 10^{11} m^{-2} to 10^{13} m^{-2} . The fundamental aspects of size scaling aspects of plastic flow in a precipitation-strengthened material are identified through the use of these simulations and the simulated results of dimensional scaling of the flow stress agree well with experimental findings.

5:40 PM

Microscopic Examination of Fatigue Behavior in a Monocrystalline Ni-Based Superalloy: *Clarissa Yablinsky*¹; Katharine Flores¹; Michael Mills¹; James Williams¹; ¹Ohio State University

Historically, the critical design parameter for Ni-based superalloy turbine blades has been creep resistance. Recently, because of modern airfoil designs, the focus has broadened to include fatigue resistance, resulting in the need to better understand fatigue behavior. In this study, compact tension specimens of monocrystalline Ni-based superalloy René N5 were tested under cyclic loading conditions. Test temperature, frequency (0.5 Hz/10 Hz), and environment (air/vacuum) were varied in order to examine the effects of recovery, plastic zone size, oxidation, etc. on crack growth. Fracture surfaces and microstructures were characterized using a scanning electron microscope in order to examine crack path selection and changes to the γ/γ' morphology within the crack wake and in the far-field. Dislocation arrangements were characterized via transmission electron microscopy using conventionally prepared and site-specific foils prepared by focused ion beam techniques in order to understand the damage mechanisms active during cyclic loading.

Hume-Rothery Symposium - Nanoscale Phases: Session II

Sponsored by: The Minerals, Metals and Materials Society, TMS Electronic, Magnetic, and Photonic Materials Division, TMS: Alloy Phases Committee
Program Organizers: Sinn-wen Chen, National Tsing Hua University; David Cockayne, University of Oxford; Seiji Isoda, Kyoto University; Robert Nemanich, Arizona State University; K.-N. Tu, University of California, Los Angeles

Monday PM

March 10, 2008

Room: 276

Location: Ernest Morial Convention Center

Session Chairs: Robert Nemanich, Arizona State University; King-Ning Tu, University of California, Los Angeles

2:00 PM Invited

Controlling Metal/Compound Semiconductor Interfacial Phase Formation at the Nanometer Scale through the Interplay of Thermodynamics and Kinetics: *Chris Palmstrom*¹; ¹University of California at Santa Barbara

Determination and understanding phase formation sequences and reaction kinetics is of utmost importance for controlling thin films and interfaces at the nanoscale. In-situ and ex-situ atomic scale structural and chemical characterization in combination with molecular beam epitaxial growth and post growth reaction studies have been used to make predictions of phase diagrams and reaction kinetics at the nanometer scale to form stable films and interfaces in these systems. This presentation will emphasize approaches for controlling the interfacial and bulk structural and electronic properties of epitaxial ferromagnetic metal/compound semiconductor heterostructures for Spintronic and shape memory applications. Material systems will include elemental transition metals, transition metal-group-III compounds, rare-earth-group-V compounds and Heusler alloys grown on III-V semiconductor surfaces.

2:25 PM Invited

Coaxial Metal-Oxide-Semiconductor(MOS) Au/Ga₂O₃/GaN Nanowires: *Li-Jen Chou*¹; ¹National Tsing-Hua University

Coaxial metal-oxide-semiconductor (MOS) Au-Ga₂O₃-GaN heterostructure nanowires were successfully fabricated by in-situ two-step process. The Au-Ga₂O₃ core-shell nanowires were first synthesized by the reaction of Ga powder, mediated Au thin layer and SiO₂ substrate at 800°C. Subsequently, these core-shell nanowires were nitridized in ammonia ambient to form GaN coating layer at 600°C. An atomic flat interface between oxide and semiconductor which warrant the high quality of the MOS device is achieved. The crystal structure of the GaN was characterized by field-emission transmission electron microscope (FETEM) indicated the single crystalline nature. These novel 1-D nitride based MOS nanowires would not only enrich a well-established bank of nanostructure morphologies, but also may have a promise for the building block to the future vertical high power and high frequency logic nanoelectronics.

2:50 PM Invited

Fabrication of Hollow Nanostructures: *Ulrich Goesele*¹; ¹Max Planck Institute of Microstructure Physics-Halle

Various approaches will be discussed to fabricate hollow nanostructures including those based on nanoporous templates and those based on the nanoscale Kirkendall effect. The presentation will concentrate on one-dimensional nanostructures but will also touch on zero-dimensional nanostructures. Experimental as well as theoretical aspects will be presented

3:15 PM Invited

Employment of Oriental Philosophy in the Establishment of Framework for Probing Nano-Scale Science and Technology: *Jeng-Gong Duh*¹; ¹National Tsing Hua University

Nano technology is not only scale-down of feature size for things of interest, but also envisages it as functional set of conceptual and spiritual essence. This study is aimed to demonstrate striking identity between nano-world and oriental philosophy. The theory of Yin and Yang in Yi-Jing describe system of cosmology and philosophy on the ideas of dynamic balance, and evolution of events. Being and non-being are two special aspects of Taoism by Lao-Tzu and Chuang-Tzu.

MONDAY PM

The spirit of Zen in Buddhism and Confucianism reflect internal constancy and wisdom to identify order and inevitability of change. It will be revealed that development of nano-science and technology is indeed originated from Yi-Jing, Taoism, Buddhism and Confucianism. Take the diffusion process as an example, and "vacancy" and "matrix atom" in material can be considered as "non-being" and "being" in Taoism. Especially, phase transformation encountered in materials seems like chance events in Yin-Ching.

3:40 PM Break

4:00 PM Invited

Silicide Nanostructure Evolution during Coarsening Processes: *Robert Nemanich*¹; *Matthew Zeman*²; *Anderson Sunda-Meya*²; ¹Arizona State University; ²North Carolina State University

The real time coarsening phenomena involving rare earth (Dy, Er) and transition metal (Ti, Zr, Hf) silicide nanostructures is studied with UV-PEEM. The measurements are obtained with the samples at ~1100C, and that in both cases larger islands grow at the expense of smaller islands. The process is characteristic of surface diffusion driven ripening of 3d nanostructures on a 2d surface. Inspection of individual islands shows significant differences between the two groups of materials. The transition metal silicides show unfaceted structures and smoothly curved edges, while the rare earth silicides show faceted island structures some of which are elongated into nano wires. During the process the transition metal silicides show significant displacement and often are seen to attractively migrate and coalesce, while the transition metal islands do not show significant displacement. These differences are discussed in terms of the attachment and detachment of silicide clusters near edges of the islands.

4:25 PM Invited

Interplay of Nanoscale Phases in Some Ferroelectric Oxides: *Haydn Chen*¹; ¹Tunghai University

The ever growing micro-to-nano electroic industries called for investigation of materials system in many aspects, not limiting to the scaling down technologies of devices but also the understanding of nanoscale phases or domains or other entities by which the system behaviors. In the past decades, our group has been engaged in a range of studies focusing on the interplay of structure and properties in dielectrics and ferroelectrics. Our works encompassed ferroelectric, anti-ferroelectric as well as relaxor materials in many bulk and thin-film complex oxides. Further, we have pursued investigation into the nontraditional behaviors including nonlinear, temporal and coupled interactions. This paper highlights our recent research and presents a systematic view of the interplay among dipoles in multi-phase systems.

4:50 PM Invited

Stabilization of Nanometer-Thick Subsolidus Quasi-Liquid Interfacial Films: *Jian Luo*¹; *Haijun Qian*¹; *Xiaomeng Shi*¹; *Vivek Gupta*¹; ¹Clemson University

Recent observations of two classes of impurity-based, nanometer-thick, quasi-liquid interfacial films are presented. First, vanadia-based, surficial amorphous films are stabilized on anatase (101) surfaces (APL 91, DOI: 10.1063/1.2768315 (2007)). Second, impurity-based disordered grain boundary films are stabilized in Ni-doped W and other refractory metals (APL 87, 231902 (2005); Acta Mater. 55, 3131(2007)). These films exhibit an "equilibrium" thickness, which corresponds to the Gibbsian excess of solutes/adsorbates and is a function of the equilibration temperature and chemical potential(s). Both classes of films are stabilized well below the bulk eutectic/solidus temperatures; yet they exhibit large structural disorder (being quasi-liquid) in HRTEM, where analogies to prewetting and premelting phenomena are made. They can be considered as free-surface and metallic counterparts to the well-known equilibrium-thickness intergranular films (IGFs) in ceramics, respectively. Unified thermodynamic models are envisioned (Crit. Rev. Solid State Mater. Sci. 32, 67 (2007)). Acknowledgements: NSF CAREER and AFOSR Young Investigator awards.

Magnesium Technology 2008: Primary Production

Sponsored by: The Minerals, Metals and Materials Society, TMS Light Metals Division, TMS: Magnesium Committee

Program Organizers: Mihriban Pekguleryuz, McGill University; Neale Neelameggham, US Magnesium LLC; Randy Beals, Chrysler LLC; Eric Nyberg, Pacific Northwest National Laboratory

Monday PM

March 10, 2008

Room: 292

Location: Ernest Morial Convention Center

Session Chair: Neale Neelameggham, US Magnesium LLC

2:00 PM

Effects of KCl on Density and Liquidus of $\text{MgF}_2\text{-BaF}_2\text{-LiF}$ Electrolyte:

*Ying Nie*¹; *Shaohua Yang*¹; *Zhaowen Wang*¹; *Linzhi Ma*¹; *Xingliang Zhao*¹; ¹Northeastern University

This paper studies on the preparation of Mg-Al alloys from MgO by molten salt electrolysis method. $\text{MgF}_2\text{-BaF}_2\text{-LiF}$ is taken as electrolyte. The experimental results indicated that KCl as additive can obviously improve the physical and chemical properties of electrolyte. The research is focused on density and liquidus. The density and liquidus of the electrolyte are decreased with the increase of KCl content. The density of electrolyte reduces from 3.250g/cm³ to 2.793g/cm³ with the mass percentage of KCl from 0 to 11% under 850°C temperature, the difference is about 0.457g/cm³. The liquidus of electrolyte decreases gradually from 807°C to 790°C with the mass percentage of KCl from 0 to 11%, the decreased value is 17°C.

2:20 PM

Electrodeposition of Magnesium from $\text{BaF}_2\text{-LiF-MgF}_2$ Electrolyte: *Shaohua Yang*¹; *Zhaowen Wang*¹; *Ying Nie*¹; *Xingliang Zhao*¹; ¹Northeastern University

Electrodeposition of magnesium from molten salts was studied by electrochemical techniques. $\text{BaF}_2\text{-LiF-MgF}_2$ was electrolyte system with magnesium oxide as raw material. It was proved Mg^{2+} was deposited more prior than other ions during cyclic voltammetry and potential step measurement at 850°C. There is difference of deposited potential on different electrode, such as glassy carbon, platinum and graphite. The determined concentration of diffusing species, as well as the fact that Mg^{2+} are the only cation to deposit on electrode, indicate that the process in diffusion of dissolved metal from the electrode interface to the electrolyte.

2:40 PM

Preparation of Al-Mg Alloys from MgO through Molten Salt Electrolysis

Method: *Shaohua Yang*¹; *Zhaowen Wang*¹; *Ying Nie*¹; *Jidong Li*¹; ¹Northeastern University

Aluminum-magnesium alloys were prepared from magnesium oxide through molten salt electrolysis method. $\text{MgF}_2\text{-BaF}_2\text{-LiF}$ was taken as electrolysis, and its density is higher than aluminum liquid, so upload cathode, which was aluminum liquid, was carried through in test. Current efficiency is more than 80%, the maximum comes up to 87.7%. Some amount of MgO was flowed into electrolytic cell every some time. The content of Mg in alloys increases gradually and up to 18.6% with lengthening electrolyzing time. It was revealed that addition of KCl can improve the physical-chemical property of the electrolyte.

3:00 PM Break

3:20 PM

The Application of Pattern-Recognition and a Back Propagation Artificial Neural Network Model in Mg Electrolysis Current Efficiency: *Bing Li*¹;

*Jiangning Liu*¹; *Ze Sun*¹; *Jianguo Yu*¹; ¹East China University of Science and Technology

The effects of current density, electrode distance and temperature on the current efficiency for magnesium electrolysis have been investigated in laboratory cell. Pattern-recognition method was used to analyze current efficiency data of the industrial magnesium cell. The current efficiency sort plot in planar main component space has been obtained and data points of current efficiency more than 85% can be centralized and the distinct optimizing region was obtained. The relationship between current efficiency and multifactors presents non-linear,

a back propagation artificial neural network model(BPANN) has been applied for magnesium electrolysis. The results has indicated that BPANN is suitable for setting up model between non-linear relationship current efficiency and multifactors with higher imitation definition, and it can be served to conduct practical application in industry by accurately predicting the current efficiency.

3:40 PM

The Reverse Effects of MgO on Magnesium Electrolyte Properties and Measure to Improve MgO Solubility: *Bing Li¹; Jun Li¹; Jian Guo Yu¹; Jiangning Liu¹; ¹East China University of Science and Technology*

In this paper MgO as impurity was added to the traditional quadribasic magnesium electrolyte, namely MgCl₂(12%)-CaCl₂(18%)-NaCl(40%)-KCl(30%). The effects of MgO on electrolyte physicochemical properties such as conductivity, density and interface tension and the liquid Magnesium aggregation state on cathode during Magnesium electrolysis have been studied. LaCl₃ was used as additives to the above electrolyte to improve MgO solubility and the electrolyte composition has been evaluated by current efficiency.

4:00 PM

Electrochemical Co-Deposition of Magnesium Based Alloy from Molten Salts: *Ninglei Sun¹; Jialin Ren¹; Hongmin Zhu¹; ¹Beijing University of Science and Technology*

Magnesium based alloys with aluminum and zinc were obtained through electrochemical co-deposition from LiCl-NaCl-MgCl₂ melt. The possibility of electrochemical co-deposition was discussed in detail by electro-analytical methods. The co-deposition happens when the concentration of aluminum and zinc ions were kept at low value and the current density is high enough. The components of alloy elements can be controlled by fixing the components of the feeding salts with the expected component and consistent with the current. A laboratory test of the co-deposition was also performed and certain compositions of the Mg-Al, and Mg-Zn were obtained. The alloys obtained from the co-deposition show a typical microstructure.

4:20 PM

Magnesiothermic Reduction of TiO₂ for the Production of Titanium Metal Using the Solid Oxide Membrane Process: *Rachel De Lucas¹; Soobhankar Pati¹; Uday Pal¹; ¹Boston University*

Solid Oxide Membrane (SOM) Electrolysis is a revolutionary environmentally-sound new process for synthesis of metals from their oxides, which can potentially produce titanium metal at a small fraction of its current cost. This multi-phase process uses electrical and optionally chemical energy to reduce titanium oxide dissolved in a molten salt, producing either powder metal or dense solid ingot or billet product at the cathode. Previous experiments have found that during electrolysis the presence of multi-valence oxides of titanium (Ti²⁺, Ti³⁺ and Ti⁴⁺) in the flux imparts electronic conductivity, leading to lower current efficiency and SOM degradation. A novel metallothermic reduction process was investigated wherein the Mg(g) generated from the SOM electrolysis of magnesium oxide was employed to reduce the oxidation state of TiO₂. The resulting Ti₂O can be utilized in the Ti-SOM process to address the problem of the electronic conductivity resulting from the presence of multi-valence oxides of titanium.

Magnesium Technology 2008: Wrought Alloys I

Sponsored by: The Minerals, Metals and Materials Society, TMS Light Metals Division, TMS: Magnesium Committee

Program Organizers: Mihriban Pekguleryuz, McGill University; Neale Neelameggham, US Magnesium LLC; Randy Beals, Chrysler LLC; Eric Nyberg, Pacific Northwest National Laboratory

Monday PM

March 10, 2008

Room: 291

Location: Ernest Morial Convention Center

Session Chair: To Be Announced

2:00 PM

Baseline Ballistic Performance of AZ31B-H24 for Armor Applications: *Tyrone Jones¹; Matthew Burkins¹; William Gooch¹; ¹US Army Research Laboratory*

The Army Research Lab is developing a ballistic specification for the use of magnesium alloy AZ31B-H24 as armor on Army platforms. Data were generated for a range of thicknesses of magnesium, 0.25 to 4 inches, using five different projectiles. The magnesium performance is parametrically quantified on an equivalent areal density to 5083 Aluminum because it is a mature well quantified, low density metal with a baseline specification performance. The results show the performance of magnesium to be dependent on the diameter of the threat. This research sets a baseline ballistic performance for magnesium for quality control purposes and for use in developing and evaluating improved alloys.

2:20 PM

Deformation Mechanisms of AZ31 Magnesium Alloy: *Timo Ebeling¹; Torsten Laser¹; Christian Hartig¹; Rüdiger Bormann¹; ¹Hamburg University of Technology*

A detailed investigation of the deformation mechanisms plays an important role for a better understanding of texture evolution and anisotropic behaviour of magnesium wrought alloys. Therefore, room temperature deformation tests of AZ31 hot rolled sheets and extruded bars have been performed. The experimental tensile textures of the rolled sheets show a reorientation resulting in a {0001}<10-10> main component. The results were compared with simulations using a viscoplastic self-consistent model to gain further information about deformation mode activities, texture evolution and mechanical properties. Thereby three simulation sets were executed: The first set included the results of both the rolled sheets and the extruded bars, while the others considered the results separately. Based on the simulations, it will be demonstrated that the activity of the basal, prismatic, pyramidal slip and the twinning mode is required to achieve comprehensive results for the mechanical properties as well as for the texture evolution.

2:40 PM

Effect of Coiling on Hot Bulge Testing of AZ31 Magnesium Sheet: *Jon Carter¹; ¹General Motors Corporation*

The effect of coiling of AZ31B magnesium alloy sheets on subsequent hot blow formability was studied on lab scale. This work was undertaken largely to increase the formability of the softer ("O" temper) sheet, which is less than that of the harder ("H24" temper) sheet. Coiling the softer sheet increased the maximum dome height by 14%, increased the forming rate by 55%, and greatly increased the surface smoothness. Coiling the harder sheet decreased the maximum dome height by 5%, increased the forming rate by 9%, and had no effect on surface finish, which was always smooth. Although coiling greatly improved the bulge behavior of the soft sheet, the results were still worse than those of the hard sheet. The poorer behavior of the soft sheet is explained by the very large grains which form on the surface during the bulge test.

MONDAY PM

3:00 PM

Effect of Pre-Ageing Treatment on Hot Compression Behavior of AZ31 Magnesium Alloy: *Lihong Shang*¹; Stephen Yue¹; Elhachmi Essadiqi²; Javid Amjad²; Verma Ravi³; ¹McGill University; ²CANMET Materials Technology Laboratory; ³General Motors Research and Development Center

The effect of second phase precipitates on the hot working behavior of cast AZ31 magnesium alloy was investigated. A series of cast AZ31 samples were solution treated at 450°C, quenched, and then aged at 150-350°C for one hour to produce precipitates with different amounts and size distributions. The aged samples were heated to the test temperature of 350°C at a heating rate of 1°C s⁻¹, and compression tested at a true strain rate of 0.01 s⁻¹, to a true strain of 0.6. The results show that the lower the aging temperature, the higher is the compression flow stress. This is explained in terms of the second phase characteristics observed in the aged samples.

3:20 PM

Finite Element Modeling of the Thermo-Mechanical Behavior of an AZ31 Magnesium Alloy during Hot Rolling: *Fady Elsayed*¹; Hany Ahmed²; Mary Wells³; Gary Lockhart³; Daan Maijer³; ¹German University in Cairo; ²Netherlands Institute of Metals Research (NIMR); ³University of British Columbia

A finite element model was developed using the commercial software package ABAQUS to predict the thermo-mechanical behavior of AZ31 magnesium alloy during hot rolling. Specifically, a 2-D model was employed to predict the distribution of temperature, and strain through the thickness of the strip, as well as the rolling loads. The model predictions were validated for a wide range of hot rolling conditions by comparison to experimental data obtained on a pilot rolling facility located at the CANMET Materials Technology Laboratory in Canada. The model predictions are in reasonable agreement with the experimental values. A sensitivity analysis was performed to quantify the influence of changing the heat transfer coefficient and friction coefficient between the roll and the strip on the predicted results. A study was performed to examine the effect of changing various rolling parameters including the strip entry temperature, the strain and strain rate on the predicted rolling loads.

3:40 PM

Flow Stress Modelling of Magnesium AZ31 Alloy Based on High Strain Plane Strain Compression Data: *Rahul Bhattacharya*¹; Brad Wynne¹; Mark Rainforth¹; Bruce Davis²; ¹University of Sheffield; ²Magnesium Elektron

Plane strain compression testing of commercial magnesium alloy AZ31 under commercial deformation conditions to equivalent tensile strains of 0.7 has been undertaken. The temperature of deformation varied from 350°C to 450°C and the strain rates for all the tests were between 0.5-50s⁻¹. The stress-strain curves at all temperatures and strain rates showed the alloy follows dynamic recrystallization behaviour. Quantitative metallography revealed the microstructure shows a dependence on the Zener-Hollomon (Z) parameter and decreases as the Z increases which produces fine equiaxed grains (~7µm at highest Z; 2.42 x 10¹¹s⁻¹). Equations correlating flow stress and Zener-Hollomon parameter (Z) at fixed strain levels are obtained and continuous flow stress curves with the effect of dynamic recrystallization are derived. These computed flow stress curves show good match with the experimental flow curves.

4:00 PM

Grain Structure and Its Effect on the Deformation Behavior of AZ31 Magnesium Alloy at Room Temperature: *Li Jin*¹; W. Ding¹; X. Zeng¹; D. Lin¹; ¹Shanghai Jiaotong University

This paper investigates the grain structure and its effect on the deformation behavior of AZ31 Magnesium alloy at room temperature. Experiments were conducted on conventionally extruded AZ31 rod with grain size of 20µm and typical extrusion texture of ND//0001, and the AZ31 rod after Equal Channel Angular Extrusion (ECAE) with fine grain size of 2µm and texture of. The slip traces and the crystal orientation transformation during tensile deformation were characterized by in-situ Scanning Electron Microscopy (in-situ SEM) and in-situ Electron Back-Scattered Diffraction (in-situ EBSD), respectively. The results indicated that the deformation mechanisms of magnesium alloy were different with different grain size, texture and grain boundary structures in the alloy samples. The contribution of twinning would decrease and grain boundary sliding (GBS) would contribute more to the strain of magnesium alloy with the grain size decreased during deformation at room temperature.

4:20 PM

Investigating the Effect of Strain Rate and Temperature on the Deformability and Microstructure Evolution of AZ31 Magnesium Alloy: *Ismael Abdel Maksoud*¹; Hany Ahmed²; Johannes Rödel¹; ¹German University in Cairo; ²NIMR, Delft University of Technology

Magnesium, being one of the lightest available structural materials, is one of the primary candidates in automotive industries; however, the difficulty of deforming magnesium is a limiting factor. This research work aims to investigate the deformability of AZ31 magnesium alloy under different deformation conditions. Tensile testing experiments were applied to determine the constitutive behavior of AZ31 magnesium alloys. The effect of changing the deformation conditions on the resulting microstructure is examined and quantified by measuring the volume fraction and size of the dynamically recrystallized grains, to account for the material softening during deformation. It was found that as the strain rate decreases by a factor of 10, the peak stress is reduced by 23% while an increase in deformation temperature by 50°C results in a change in the fraction of dynamic recrystallization by 30%. Further correlations were developed to optimize the deformation behavior.

4:40 PM

Mechanical Behavior of AZ31 Sheet Materials at Room and Elevated Temperature: *Jon Carter*¹; Ravi Verma¹; Paul Krajewski¹; ¹General Motors Corporation

Magnesium sheet is increasingly being considered for light-weighting of automotive body structures. In this paper, AZ31 magnesium sheets produced by both the current industrial direct-chill (DC) casting process and the developmental twin-roll continuous casting (CC) process are compared for potential use in hot forming of automotive body panels. The paper compares microstructure, texture, tensile properties both at ambient and elevated temperatures, and biaxial bulge forming of two DC and two CC materials. They exhibit significant, but different, anisotropies in tensile properties in the sheet plane. Both types of material show high tensile elongation-to-failure (~300%) under typical QPF (quick-plastic forming) conditions, but the DC materials show more necking. Both can form tall domes in hot pneumatic bulge tests, but, for the same inflation rate, the CC material requires less gas pressure. Recrystallization is critical during hot-forming of magnesium sheet, as it can enhance or reduce formability.

5:00 PM

Microstructure Refinement of AZ31B Alloys Processed with an Electromagnetic Vibration Technique: *Kenji Miwa*¹; Mingjun Li¹; Takuya Tamura¹; ¹National Institute of Advanced Industrial Science and Technology (AIST)

Electromagnetic vibrations, which are generated by simultaneous imposition of a static magnetic field and an alternating electric field, are considered to lead to the formation and collapse of cavities even in a molten metal, and then achieve the refinement of solidified structure. In order to refine the microstructure of AZ31B magnesium alloy, the electromagnetic vibration (EMV) process has been applied. Fine equiaxed grains can be obtained when AZ31B alloys are solidified at a frequency interval of ca. 500 up to 2000 Hz. The difference in electrical resistivity between the solid and liquid in mushy zone originates uncoupled motion, which breaks dendrite into fragments, destroys the crystallographic orientations, and yields deformation twins. Effective refinement occurs when the leading solid is driven to move out the operation scope of solute redistribution area where the solute cannot be piled up to generate a constitutionally undercooled region that always destabilizes.

Materials in Clean Power Systems III: Fuel Cells, Hydrogen-, and Clean Coal-Based Technologies: Gas Separation and CO₂ Capture

Sponsored by: The Minerals, Metals and Materials Society, TMS Structural Materials Division, TMS/ASM: Corrosion and Environmental Effects Committee
Program Organizers: Zhenguo "Gary" Yang, Pacific Northwest National Laboratory; Michael Brady, Oak Ridge National Laboratory; K. Scott Weil, Pacific Northwest National Laboratory; Xingbo Liu, West Virginia University; Ayyakkannu Manivannan, National Energy Technology Laboratory

Monday PM
 March 10, 2008
 Room: 392
 Location: Ernest Morial Convention Center

Session Chairs: Henk Verweij, Ohio State University; Wei Liu, Pacific Northwest National Laboratory

2:00 PM Invited

Critical Material and Process Issues for CO₂ Separation from Coal-Powered Plants: Wei Liu¹; ¹Pacific Northwest National Laboratory

Coal is a viable alternative energy source to petroleum, since other renewable energies such as biomass and solar can only supply a fraction of energy consumption in US. However, coal is one major source of air pollutants, CO₂, SO₂, NO_x, Hg, particulates. Among those pollutants, CO₂ capture costs the US power industry a few hundred billion dollars per year if the regulation is implemented. It is imperative to develop cost-effective CO₂ capture technologies and replace the oil import with indigenous coal reserve. Concentrating CO₂ from the dilute coal combustion or gasification gas stream to a level suitable for sequestration presents a very challenging separation problem in Chemical Engineering and Materials Science disciplines. This is largely due to huge gas volume, complex and dirty gas compositions, and low value of CO₂ credit. Major innovations in separation materials and processes are required. A critical review on different separation technologies, absorption, adsorption, membrane, distillation, will be presented for respective flue gas and gasification application. As a result, important material issues and their impacts to the process viability will be identified. Finally, the author will share the latest research results on zeolitic adsorbent and membrane materials as potential, step-out separation technologies.

2:30 PM

Oxygen Transport Membrane Materials Development for Oxyfuel Firing of Coal Power Plants with CO₂ Capture: G.M. Christie¹; B. vanHassel¹; J. R. Wilson¹; ¹Praxair

Praxair, in cooperation with The United States Department of Energy is developing an oxygen transport membrane (OTM) based oxycombustion process for carbon dioxide (CO₂) capture from coal power plants. Oxycombustion, or burning fuel in oxygen to generate flue gas consisting of primarily CO₂ and H₂O, is established as a credible means to facilitate CO₂ capture from coal power plants. The economics of conventional oxycombustion processes are currently limited by the parasitic power that is required for cryogenic oxygen production in conventional air separation units (ASU). Praxair has developed novel OTM technology that when integrated directly in a coal fired boiler has the potential to reduce the parasitic power consumption required for oxygen production by 70-80% as compared to cryogenic ASU. This paper describes the materials requirements for oxygen transport membranes designed for integration in a coal fired power boiler. The Praxair OTM materials development strategy will be discussed along with recent results from the development program.

3:00 PM Invited

Oxygen Production Using Ion Transport Membranes: Phillip Armstrong¹; Michael Carolan¹; Alexander Makitka¹; VanEric Stein¹; Richard Underwood¹; Lori Vratsanos¹; Charles Lewinsohn²; ¹Air Products and Chemicals, Inc.; ²Ceramatec Inc.

Air Products, in partnership with the U.S. Department of Energy, is leading a team to develop Ion Transport Membranes (ITM) to separate oxygen from air. When operated at elevated temperature, these dense, ceramic membranes selectively permeate oxygen from a pressurized air stream to produce a pure

oxygen permeate. Integrating the high temperature and pressure non-permeate stream from the membrane with a gas turbine allows the co-production of oxygen, power and steam. Consequently, the ITM Oxygen technology is ideally suited to advanced power generation processes such as integrated coal gasification combined cycle (IGCC) that require oxygen as a feedstock. The project is currently in the third phase of a three-phase program. During the first and second phases, the ITM Oxygen team designed and fabricated planar membrane modules. These membranes were then used to demonstrate the feasibility of air separation using ceramic membranes. During the current Phase 3, a prototype facility capable of producing 5 tons-per-day of oxygen is operating. This paper will present an overview of some of the key features and advantages of the microchannel ceramic membranes used in this technology, along with economic benefits of using ITM Oxygen technology to produce oxygen. This abstract was written with support of the U.S. Department of Energy under Contract No. DE-FC26-98FT40343. The Government reserves for itself and others acting on its behalf a royalty-free, nonexclusive, irrevocable, worldwide license for Governmental purposes to publish, distribute, translate, duplicate, exhibit and perform this copyrighted paper.

3:30 PM

Effect of Pd Addition on Hydrogen Permeability and Microstructures of Nb₄₉Zr₁₅Ni₃₆ Alloy: Huixiang Tang¹; Kazuhiro Ishikawa¹; Kiyoshi Aoki¹; ¹Kitami Institute of Technology

Effect of Pd addition on hydrogen permeability and the microstructure of as-cast Nb₄₉Zr₁₅Ni₃₆ (mol%) alloy prepared by arc melting has been investigated. Hydrogen permeability of Nb₄₉Zr₁₅Ni₃₆ and Nb₄₉Zr₁₅Ni₃₀Pd₆ alloys at 673K is 3.79 and 6.58×10⁻⁸ [mol H₂ m⁻¹ s⁻¹ Pa^{-0.5}], respectively. The former consists of the primary body-centered-cubic (bcc), rod-like and eutectic phases. On the contrary, the latter is composed mainly of the primary (bcc), plate-like (bcc) and ZrNi phases and the primary phase is connected by the plate-like phase. Activation energy E_a for hydrogen permeation of the Nb₄₉Zr₁₅Ni₃₆ alloy decreases with 6 mol % Pd addition. The changes in the microstructure and activation energy because of Pd addition may be the main causes for increment of hydrogen permeability, which make hydrogen atoms diffuse more easily in this metal membrane. It is expected that a small amount of Pd addition is effective to tune Nb-Zr-Ni alloys properties.

3:55 PM

Optimization of Supported Membrane Structures for Energy Conversion Technology: William Chiu¹; Matthew Mottern¹; Melissa Schillo¹; Krenar Shqau¹; Henk Verweij¹; ¹Ohio State University

Supported inorganic membranes consist of a thin film of permselective material on top of a graded support structure with increasing pore size in the direction away from the membrane. The requirements for the membrane materials, in brief, are that they are <1 μm thick with a molar permeance of >10⁻⁶ mol/(m²·s·Pa) for the permeable gas, or a mechanical permeance of >10⁻¹² m for the permeable liquid and a separation factor >50. These requirements make that the supporting structure must have a smooth, fine-porous deposition surface with a flexure strength >100 MPa and a permeance higher than the membrane permeance. The supported membrane structures are expected to allow for thousands of hours uninterrupted operation, and their manufacturing costs should stay well below \$500/m² at a surface to volume ratio of >100 m. The presentation will discuss progress in the integrated approach to optimize practical supported membrane structures for energy conversion technology.

4:20 PM Break

4:30 PM Invited

Thermodynamic Properties of the Pd-H, Pd-D, and Pd-T Systems: Ricardo Schwarz¹; Douglas Safarik¹; Stephen Paglieri¹; ¹Los Alamos National Laboratory

The pressure-composition isotherms of metal-hydrogen systems often show hysteresis. A recent model¹ attributes the hysteresis to the coherence elastic strains that must be overcome (by a macroscopic change in the hydrogen chemical potential) to nucleate the coherent hydride phase (on absorption) and the coherent hydrogen solid solution (on desorption). The model predicts the hysteresis decreases as 1/T and vanishes, by definition, at the crossing of the van't Hoff lines (log of chemical potential plotted vs. 1/T). This suggests that the crossing can be used to accurately measure the critical pressure and temperature

for the two phase decomposition. We have used this method to accurately measure the critical points for the Pd-hydrogen, Pd-deuterium and, for the first time, the Pd-tritium system. These measurements are used to derive the entropy and enthalpy of hydride, deuteride and tritide formation. ¹R. B. Schwarz and A. G. Khachaturyan, *Acta Mater.* 54 (2006) 313.

5:00 PM Invited

Palladium Based Membranes for Hydrogen Permeation – A First-Principles Modeling Study: *Ole Lovvik*¹; *Susanne Opalka*²; ¹University of Oslo; ²United Technologies Research Center

Dense, hydrogen permeable metal membranes may find future applications in membrane reactors for hydrogen production from hydrocarbons and in systems requiring hydrogen purification, for example hydrogen fuel cells. Among the most promising materials for such membranes are palladium based alloys, which exhibit both very high selectivity and high hydrogen permeability. This study focuses on fundamental properties of such alloys, including surface segregation, hydrogen diffusion, and adsorption of various gases. The principal tool is modeling based on density functional theory, but links are close to experimental studies.

5:30 PM Invited

Self-Supporting Pd-Cu Alloy Membranes for Production of Coal-Derived Hydrogen: *Kent Coulter*¹; ¹Southwest Research Institute

Thin self-supported permeable membranes of palladium alloys such as Pd₆₀Cu₄₀ have many applications in which hydrogen separation is required. High permeability membranes have been fabricated by magnetron sputtering onto a pretreated silicon substrate followed by lift-off to form free standing high quality films of controllable alloy composition down to 3 microns in thickness. Using these methods, Pd₆₀Cu₄₀ membranes 12 inches in diameter have been made with thicknesses ranging from 2 to 15 microns. The highest flux recorded was 242 SCFH/ft² with a 2 μm thick Pd₅₃Cu₄₇ at 400°C and 20 psig feed pressure which when extrapolated is over twice the 2010 Department of Energy pure H₂ flux target. Several membranes have been made with the same permeability, but with different thicknesses and these membranes are highly selective. The fabrication process, hydrogen separation performance and physical property characteristics of these vacuum deposited palladium alloys for hydrogen separation will be discussed.

6:00 PM Invited

Modeling of B2 Phase PdCuTM Alloy Hydrogen Selective Membrane Performance: *Susanne Opalka*¹; *Thomas Vanderspurt*¹; *Sean Emerson*¹; *Weiming Huang*²; *Da Wang*³; *Ted Flanagan*³; *Ying She*¹; ¹United Technologies Research Center; ²QuesTek Innovations, LLC; ³University of Vermont

The production of fuel cell grade H₂ and sequestration grade CO₂ from coal or other resources will be facilitated by a high permeability, sulfur resistant, thermally stable hydrogen separation membrane. A Pd-Cu-TM B2 phase alloy with commercially attractive permeability and sufficient thermal and chemical stability for practical application to H₂ production from an Advanced Water-Gas Shift Membrane Reactor (AWGSMR) has been identified through combined first principles atomic predictions, thermodynamic modeling, and H solubility measurements. AWGSMR operation at reduced steam to carbon ratios could lead to increased efficiency and decreased implementation costs. However, these conditions may induce metal-catalyzed carbon formation, which could compromise membrane integrity, H permeability, or active surface area. Atomic modeling of CO reactions on the new alloy surface was used to evaluate possible impact of C solubilization and coke and carbide formation on H permeation performance.

Materials Processing Fundamentals: Process Modeling

Sponsored by: The Minerals, Metals and Materials Society, TMS Extraction and Processing Division, TMS: Process Technology and Modeling Committee
Program Organizer: Prince Anyalebechi, Grand Valley State University

Monday PM

March 10, 2008

Room: 283

Location: Ernest Morial Convention Center

Session Chair: Prince Anyalebechi, Grand Valley State University

2:00 PM

Use of SEM Fractography to Guide Thermo-Mechanical Process (TMP) Optimization for Cu-Ni-Si-Cr Alloys: *Mark Hashiguchi*¹; *John Kuli*¹; ¹Brush Wellman Inc.

Examination of tensile and Charpy bar surfaces shortly after destructive testing was conducted to search for clues that would aid in optimization of mechanical properties, especially tensile strength, yield strength and elongation to fracture. Cu-Ni-Si-Cr alloy bars in the as-cast, forged, rolled and extruded conditions were examined. Low ductility bars (<4% Elongation) showed dramatically different features than the fracture surfaces of high strength -high ductility bars (7 to 10% Elongation). Analysis of the fracture surfaces at 10X to 1500X and use of Energy-Dispersive X-Ray Spectroscopy (EDS) identified Ni-Si and Ni-Si-Cr precipitates of varying sizes and morphologies. TMP techniques to control the size and distribution of these precipitates show promise in improving the properties and performance of this alloy system and appear to correlate with improvements in the fracture surface morphology.

2:20 PM

Microstructural Analysis of Sticking Phenomenon Occurring during Hot Rolling of Two 430J1L Ferritic Stainless Steels: *Daejin Ha*¹; *Chang-Young Son*¹; *Joon Wook Park*²; *Jong Seog Lee*³; *Yong Deuk Lee*³; *Sunghak Lee*¹; ¹Pohang University of Science and Technology; ²Hyundai Steel Company, Ltd.; ³Pohang Iron and Steel Company

Sticking phenomenon occurring during hot rolling of two STS 430J1L ferritic stainless steels were analyzed in this study. Hot-rolling simulation tests were conducted by using a high-temperature wear tester. The modified 430J1L steel had a smaller number of sticking nucleation sites and slower growth rate than the conventional 430J1L steel because of higher high-temperature hardness, thereby leading to less serious sticking. When the simulation test was conducted at 1070°C, chromium oxides were formed on the surface of the rolled materials, and thus the sticking was drastically reduced because of the increased surface hardness of the rolled materials. According to these findings, in order to prevent or minimize the sticking, it was suggested to improve high-temperature properties of stainless steels in the case of hot rolling at 900°C~1000°C, and to promote the formation of oxides in the case of hot rolling at temperatures higher than 1000°C.

2:40 PM

Numerical and Experimental Study of Constrained Solidification through Parallel Planar Channels: *Rui Shao*¹; *Matthew Krane*¹; *Kevin Trumble*¹; ¹Purdue University

To understand the development of microstructure and microsegregation in constrained solidification, growth of Al-4.5wt%Cu through parallel planar channels of different widths is simulated using a 2-D CA-FV model. Experiments of dendrites growing through channels are also conducted. As the channel width decreases below the primary dendrite spacing, lateral solute diffusion is constrained, and thus the secondary arms become shorter and even disappear as channel width decreases. When the channel width decreases further, the solute diffusion in front of the dendrite tip is also constrained and the growth of the dendrite tip is suppressed. As a result, the dendrites grow at lower undercoolings than in wider channels, leading to higher and more uniform solute concentration in the primary phase and lower eutectic fraction in the alloy. The change of dendrite morphology and eutectic fraction with channel width obtained through experiments matches the numerical results.

3:00 PM

Fluid Flow, Heat and Mass Transfer in the Molten Pool of LENS® Processes: *Hebi Yin¹; Sergio Felicelli¹; Liang Wang¹; ¹Mississippi State University*

A two-dimensional finite element solidification model was developed to simulate the transport phenomena occurring during laser deposition of AISI 410 stainless steel during the Laser Engineered Net Shaping (LENS®) process. The molten pool geometry and the distribution of temperature, solute concentration and velocity were calculated during deposition of a thin wall plate. An analysis revealed the importance of heat transfer by both conduction and convection as well as the roles of the driving forces for convection in the molten pool. The heat transfer and the flow pattern in the molten pool are considerably dependent on the travel speed of the laser beam. For the alloy and process parameters in the simulations, no significant macrosegregation was observed. The temperature-dependent properties and thermodynamic variables involved in solidification modeling were calculated using Thermo-Calc software. The simulation results contribute to the current understanding of transport phenomena in the molten pool of laser deposition processes.

3:20 PM

Effect of Boundary Heat Flux Transients on the Solidification Behavior and Microstructure of Al-Cu Alloys: *K.V. Sreenivas Rao¹; G. Phanikumar¹; T.S. Prasanna Kumar¹; ¹Indian Institute of Technology*

A serial solution of the inverse heat conduction problem (IHCP) is extended for determining multiple heat fluxes at the metal mould interface during casting of Al-Cu alloys in permanent molds. The temperature history of the casting and the mold during solidification is recorded using mineral insulated K-type thermocouples. Computer interfaced data logger is used for temperature data acquisition. The measured temperatures are used as input to the IHCP algorithm for simulating multiple heat fluxes at the boundary. The obtained heat fluxes are used as boundary conditions for the casting simulation. It is observed that the measured heat flux is a function of alloy composition and thermo-physical properties of the mold material. The effect of heat diffusivity of the mold on interfacial heat flux and cooling rate is analyzed. The cooling rate decreases with increase in interfacial thermal resistance at the metal/mold interface and affects macrosegregation and microstructure formation.

3:40 PM Break

3:50 PM

Modeling and Simulation of a Large Composite Casting: *Autumn Fjeld¹; Andreas Ludwig¹; ¹University of Leoben*

The filling and solidification of an industrial scale composite casting has been simulated to investigate the remelting of the outer shell material of the casting. A composite casting requires a multi-step casting process which, in this investigation, includes casting of a high alloy cast iron outer material and subsequent conventional ingot casting of a nodular steel core material into the mold assembly. During casting of the nodular-steel, a thin layer of the high alloy material re-melts and mixes with the core material producing a bonding layer of intermediate composition. The present numerical model employs the volume of fluid method and an enthalpy-porosity technique to couple the filling of the core material and re-melting of the shell material. The interface between the solid and liquid phases is tracked and can be used as a guide to examine the extent of remelting and, to some degree, mixing of the two fluids and species diffusion.

4:10 PM

Model Studies on Slag Droplet Generation in Gas-Stirred Ladles: *Krishnakumar Krishnapisharody¹; Gordon Irons¹; ¹McMaster University, Steel Research Centre*

The phenomenon of slag droplet formation under the action of gas-stirring in steel ladles has been analyzed with the help of experiments conducted in a thin-slice room-temperature model using water and mineral oils as the working fluids. Visual and video investigations have been performed on the interface behaviour along with measurements of liquid velocities in both phases, using the Particle Image Velocimetry (PIV) technique. The measured velocity data and observations on the interface break-up establish that the droplet formation results primarily from an instability mechanism at the interface.

4:30 PM

Numerical Evaluation of the Performance of a BOF Steelmaking Lance: *Miguel Barron¹; Cesar Lopez¹; Isaias Hilerio¹; ¹Universidad Autonoma Metropolitana*

Recently, a new lance design for BOF steelmaking has been proposed by Sambasivam et. al. (2007). This lance, in addition to six peripheral inclined supersonic nozzles, contains a vertical centered nozzle whose oxygen flow is independent from the main oxygen supply. The above authors affirm that their lance maximizes the droplet generation without causing spitting. In this work, the performance of a lance with four peripheral nozzles and one vertical centered nozzle is numerically modeled by means of Computational Fluid Dynamics (CFD) software. Transient 2D CFD computer simulations were carried out considering two phases, namely molten steel and gaseous oxygen. Numerical results confirm that bath agitation and droplet generation are enhanced as a result of the vertical centered nozzle; however a proper performance of this lance, related to a conventional one, strongly depends on lance height and Mach number of the oxygen jets.

4:50 PM

Numerical Simulation of Droplet Generation of the Buoyant Phase in Two-Phase Liquid Baths: *Krishnakumar Krishnapisharody¹; Gordon Irons¹; ¹McMaster University, Steel Research Centre*

A mathematical model has been developed to predict the interface dynamics and droplet generation of the buoyant phase in a two-fluid system. The model employs the well-known SIMPLE algorithm for obtaining flow fields and the Volume of Fluid (VOF) method, for interface tracking. The implementation of the model in water-oil systems, where the oil layer is placed above a recirculating water bath, is discussed. It is demonstrated that the evolution of the water-oil interface leading to the formation of oil droplets is predicted realistically. The model can be extended to include a third phase (gas) to simulate the generation of slag droplets in a gas-stirred ladle.

5:10 PM

CFD Simulation of a Copper Converter with Bottom Air Injection: *Jesus Gonzalez¹; Cesar Real¹; Manuel Palomar¹; Luis Hoyos¹; Marco Gutierrez¹; ¹Universidad Autonoma, Metropolitana*

Peirce-Smith converters (PSC) are long cylindrical chemical reactors where copper matte reacts with air. Traditionally, air is injected laterally through submerged tuyeres at different subsonic velocities. However, the accumulated experience in steelmaking, particularly in the basic oxygen furnace (BOF) process, shows that the gas bottom injection may improve the mixing efficiency of a liquid pool. The aim of bottom injection is to maximize the copper kinetic energy meanwhile avoiding excessive reactor splashing. When gas is injected from a single orifice at the bottom of a liquid pool, two main gas flow regimes can be identified, bubbling and jetting. In this work, a PSC with bottom air injection is studied by means of multiphase 3D CFD numerical simulations considering multiple air velocities. Special attention is paid to the bubbles and jet formation mechanism. The mixing efficiency is measured by calculating the turbulent kinetic energy of the copper matte.

MONDAY PM

Mechanical Behavior, Microstructure, and Modeling of Ti and Its Alloys: Phase Transformation and Microstructure Development I

Sponsored by: The Minerals, Metals and Materials Society, TMS Structural Materials Division, TMS: Titanium Committee

Program Organizers: Ellen Cerreta, Los Alamos National Laboratory; Vasishth Venkatesh, TIMET; Daniel Evans, US Air Force

Monday PM
March 10, 2008

Room: 384
Location: Ernest Morial Convention Center

Session Chair: Daniel Evans, US Air Force

2:00 PM Invited

Application of Thermodynamic Modeling to Multicomponent Titanium Alloys: Fan Zhang¹; Shuanglin Chen¹; Weisheng Cao¹; Kaisheng Wu¹; Ying Yang¹; Y. Chang¹; ¹CompuTherm LLC

To achieve desired microstructures and mechanical properties, alloy chemistry and processing conditions need to be carefully selected and adjusted. Traditionally, these improvements have been made by a slow and labor-intensive series of experiments. Today, with the help of models and simulation tools, significant amount of experimental work can be reduced. These modeling tools will accelerate the development of new alloys and the improvement of the existing ones. In this presentation, we will discuss the thermodynamic modeling tool we have developed at CompuTherm LLC, and its application to multicomponent titanium alloys. With this modeling tool, beta transus temperatures, beta approach curves, phase compositions can be calculated for Ti64, Ti6242, Ti17 and so on, which are critically needed in the selection of processing parameters. Integration of thermodynamic calculations with phase field modeling for the simulation of microstructure evolution will be discussed via the concept of pseudo-ternary system.

2:30 PM

Deoxidization Mechanism of In-Situ Electro-Deoxidization of TiO₂ to Titanium: XiuJing Zhai¹; Zhuo Zhang¹; Jidong Li¹; Mingjie Zhang¹; ¹Northeastern University

Molten salt electrolysis monitoring and controlling instrument (DD-A) had been used in this research. Electrolysis process of in-situ electro-deoxidization of TiO₂ to titanium was measured. The change trend of back electromotive force indicated that the decomposition reaction of CaCl₂ was first happened during normal decomposition, then TiO₂ was deoxidized to titanium by calcium which was from the decomposition reaction, the reaction equation is 2Ca₂++TiO₂=Ti+2CaO.

2:50 PM

Investigating Macrozones in Titanium Billet using Electron Backscattered Diffraction: Bradley Wynne¹; Peter Davies¹; Mark Rainforth¹; ¹University of Sheffield

The use of orientation image maps (OIMs) obtained from electron backscattered diffraction has led to significant improvement in our knowledge of titanium billet microstructure. Most significantly, OIM studies have shown that on a global scale the crystallographic texture is relatively weak but on the meso-scale can be composed of regions with strong local textures which are often referred to as macrozones. These strongly textured regions are inherited from the ingot forging process and are at least an order of magnitude greater than the apparent grain size. Most work to date, however, has investigated relatively small areas of billet, making it difficult to determine the average size and size and shape distribution of the macrozones. In this work we report on a large scale investigation of a slice of 200mm diameter Timetal@834 billet with the aim being to determine what amount of material is required for a statistical confident analysis.

3:10 PM

Kinetics of Elevated Temperature Phase Transformations in TIMETAL LCB: Henry Rack¹; Basak Yazgan Kokuzo¹; ¹Clemson University

This investigation has examined the phase transformations occurring during isothermal aging of TIMETAL LCB. Three differing alpha phase morphologies were considered, i.e grain boundary alpha heterogeneously forming at prior beta grain boundaries, side-plate alpha growing and/or forming in the vicinity of the aforementioned grain boundary alpha and intragranular alpha precipitating within the matrix. The beta-to-alpha phase transformation kinetics were found to be controlled by the kinetics of grain boundary alpha formation at the early stages of reaction, irrespective of aging temperature. Increased transformation successively included formation of side-plate and intragranular alpha. The overall transformation kinetics can be explained by considering the individual effects of the different morphologies on the variation of the total alpha phase volume fraction, the overall kinetics approaching that for intragranular alpha at lower aging temperatures and that for grain boundary alpha at increased aging temperatures.

3:30 PM Break

3:50 PM Invited

Phase Field Modeling of Phase Transformation and Microstructure Development in Alpha/Beta Titanium Alloys: Ning Ma¹; Chen Shen¹; Yunzhi Wang¹; ¹Ohio State University

Phase transformations in alpha/beta Ti-alloys are dominated by strong coupling among different extended defects and produce extremely complicated microstructures with strong spatial variation, correlation and anisotropy. The traditional constitutive models representing microstructural features by their average values may not be sufficient to quantitatively define the microstructure and allow for establishing a robust microstructure-property relationship. We discuss recent development and applications of the phase field method to quantitative modeling of microstructural evolution during solid state phase transformations in alpha/beta Ti-alloys. The model accounts explicitly for anisotropy in interfacial energy and mobility, orientation relationship and lattice- and modulus-misfit between the parent and product phases and misfit dislocation structures at the alpha/beta interfaces. Applications of the model to globular alpha growth, development of sideplates from grain boundary alpha and formation of basketweave structures in three-dimensions will be presented. Variant selection during nucleation and growth of the colony and basketweave structures will be addressed.

4:20 PM

Nano-Structured Ti-6Al-4V Alloy by Severe Deformation Processes and Rolling: Ike Su-Chi¹; Xiang Li¹; Rick Lee¹; Yi Liu¹; Amit Ghosh¹; ¹University of Michigan

Severe deformation was imparted into Ti-6Al-4V alloy by compression and die pressing at around 400C under superposed hydrostatic pressure. Nanocrystalline microstructure has been obtained with grain size in the range of 100nm although a small fraction of beta phase exists as in the original microstructure before it was heat treated and transformed by quenching from the beta phase. TEM observations indicated that there exists a high density of dislocations in the severe deformed samples. Dislocation dipoles are frequently observed by HREM. Microhardness measurements indicated extremely high strength of the severely deformed sample. Texture evolution showed enhancement of basal texture. Low temperature processing to sheet by rolling of the fine grain material is possible by this approach, and small size nanograin titanium sheet was demonstrated to have highly superplastic properties at 600-700°C. (Work supported by US Air Force).

4:40 PM Invited

Recent Advances and Challenges in Solidification and Microstructure Modeling of Titanium Alloys: Laurentiu Nastac¹; ¹Concurrent Technologies Corporation

Modeling and simulation of microstructure evolution requires complex multi-scale computations, from computational fluid dynamics (CFD) macroscopic modeling through mesoscopic to microscopic modeling, as well as strategies to link various length-scales emerged in modeling of microstructural evolution. The presentation will cover numerical approaches able to predict the solidification structure evolution in large and complex casting geometries as well as relevant examples of the microstructure modeling in commercial casting technologies

including investment casting and remelting processes. The presentation will also discuss relevant techniques for controlling the structure formation during the solidification processes of Ti alloys and to identify means to improve quality of the castings (e.g., improvement of mechanical properties through the microstructure development and control to eliminate the casting factor, in particular in aerospace applications). Recent developments on ultrasonic technology modeling and integration efforts at CTC for grain refinement/modification for improved Ti ingot/casting quality will also be covered.

5:10 PM

Microstructural Development in near Beta Titanium Alloy Ti-5Al-5V-5Mo-3Cr: *Nicholas Jones¹; Martin Jackson¹; David Dye¹; Richard Dashwood¹*; ¹Imperial College London

The selection of the near beta alloy Ti-5Al-5V-5Mo-3Cr (Ti-5-5-5-3) for use in the latest landing gear assemblies has lead to an increase in interest in relevant processing parameters. Previous work has suggested that Ti-5-5-5-3 offers benefits over the more established Ti-10V-2Fe-3Al, through higher strength, a shallower β approach curve and less microstructural sensitivity to forging temperature. Through the use of in-situ x-ray synchrotron experiments and more traditional electron microscopy new insights into the behaviour and timescale of microstructural development in Ti-5-5-5-3 have been obtained; particularly with regards to flow softening during hot working, the α dissolution kinetics and the α to ω to α transformation. The effect on subsequent thermomechanical processing and final properties has also been considered.

5:30 PM

Research on Inclusion in High Titanium Ferroalloy: *Lina Jiao¹; Ting'an Zhang¹; Jianming Yao¹; Changce Xing¹*; ¹Northeastern University

Microstructure of inclusion and occurrence state of oxygen in high titanium ferroalloy was examined against the problem of large-mount inclusion and high-content oxygen in high titanium ferroalloy production by aluminothermy reduction process of rutile. And then formation mechanism of oxygen-containing phase was discussed. It was assumed that there were four phases in high titanium ferroalloy. XRD, SEM and EPMA results showed that the main forms of inclusion were Al_2O_3 and titanoxane solid solutions. It was thought that Al_2O_3 was formed by incomplete metal-slag separation and Ti_2O , Fe_2TiO_4 , TiO_2 and titanoxane solid solutions were the incomplete products of reduction reaction.

Mechanics and Kinetics of Interfaces in Multi-Component Materials Systems: Nanoscale Structures and Simulations

Sponsored by: The Minerals, Metals and Materials Society, TMS Electronic, Magnetic, and Photonic Materials Division, TMS Structural Materials Division, TMS/ASM;

Composite Materials Committee, TMS: Thin Films and Interfaces Committee

Program Organizers: Bhaskar Majumdar, New Mexico Tech; Rishi Raj, University of Colorado, Boulder; Indranath Dutta, US Naval Postgraduate School; Ravindra Nuggahalli, New Jersey Institute of Technology; Darrel Frear, Freescale Semiconductor

Monday PM
March 10, 2008

Room: 279
Location: Ernest Morial Convention Center

Session Chairs: Rishi Raj, University of Colorado; Mingwei Chen, Tohoku University

2:00 PM Keynote

The Ultra-Hardness of Nano-Structured Composite Ceramic Coatings of nc-TiN/a-Si₃N₄: *Ali Argon¹; Stan Veprek²; Ruifeng Zhang²*; ¹Massachusetts Institute of Technology; ²Technical University of Munich

The superior hardness of nano-structured ceramic composite coatings of nc-TiN/a-Si₃N₄ with hardnesses in the range of 100 GPa, exceeding that of polycrystalline diamond, can now be fully explained thanks to very recent first principles computations of the plastic shear resistances of the amorphous Si₃N₄ layers of atomic thickness separating the non-deformable nano-sized grains of TiN. This, and appropriate spacial averaging of the effects of the latter, as well as accounting for their substantial strength differential effects has permitted bridging the gap between atomic level and macro properties.

2:40 PM Invited

Influence of Interfaces on the Deformation Behavior of Materials at Small Length Scales: *Gerhard Dehm¹*; ¹Erich Schmid Institute for Materials Science

Interfaces and surfaces can impose mechanical size-effects on materials. The deformation mechanisms become constrained when microstructural and/or geometrical dimensions decrease. This effect can improve, e.g. the strength of a bulk lamellar material, but it may cause failure for a miniaturized material component due to high internal stresses. Several dislocation mechanisms causing size-dependent flow stresses are addressed and the current understanding of size-effects in miniaturized and bulk materials is reviewed.

3:10 PM Invited

Stress-Induced Grain Boundary Migration: "Cold" Grain Growth in Nanocrystalline Metals: *Mingwei Chen¹*; ¹Tohoku University

Stability of nano-grains is of great importance in technological applications of nanocrystalline materials because coarsening of nano-grains results in the loss of the advanced properties solely owned by the nanostructures. In polycrystalline materials, the elimination of GBs via grain growth is a thermodynamically favorable process, but controlled by the kinetics of atomic mobility at GBs. Thus, grain coarsening generally takes place at high temperatures where GB atoms have enough thermal energy. Nevertheless, recent observations suggested that grain growth in nanocrystalline metals can occur at room temperature during plastic deformation. The "cold" nanograin growth reveals an interesting new phenomenon arising from nanosize effect. Our recent results demonstrated that the "cold" nanograin growth is rate-dependent and can be described by a power law equation. The measured activation volume for the nanograin growth is well consistent with MD predications, suggesting that the nanograin growth is motivated by the stress-enhanced mobility of GB atoms.

3:40 PM Break

3:50 PM Invited

First Principles Calculations of Interfacial Boundaries in Ni-Ni₃Al and Al-Al₃Sc: *Christopher Woodward¹; Axel Van De Walle²; Mark Asta³*; ¹US Air Force Research Laboratory; ²California Institute of Technology; ³University of California, Davis

Solute and precipitation strengthening are often used to optimize the properties of structural materials used in aerospace applications. A great deal can be learned about these alloys by studying the model binary and ternary systems. Here Ni-Ni₃Al and Al-Al₃Sc are used as model systems for the Ni-based superalloys and Sc strengthened Al alloys in order to estimate interfacial boundaries (IFB) properties. The thermodynamic properties of these IFB's strongly influence growth and coarsening rates of precipitates and are used in models of precipitation strengthening and microstructural evolution. Cluster expansion methods and lattice gas methods are used to study composition profiles and free energies of IFB's in these materials. In Al-Al₃Sc a lattice gas model is used to predict Mg impurity segregation to the Al side of the (100) IFB. This result has recently been verified by atom probe tomography.

4:20 PM Invited

Arbitrary Sharp-Diffuse Interface Computational Modeling of Phase Evolution in Multi-Component Systems: *Ganesh Subbarayan¹*; Kaushik Setty¹; ¹Purdue University, School of Mechanical Engineering

In this paper, we describe a computational procedure for arbitrary sharp-diffuse interface modeling through either explicit (geometrical) or implicit (material) descriptions of interfaces. The approach is based on iso-parametric descriptions of geometrical, material and behavioral fields over primitive domains, which in turn are hierarchically composed to describe complex domains. The process is philosophically similar to the Constructive Solid Geometry procedure of CAD. The compositions are constructed so that the basis functions used to approximate the fields obey the mathematical notion of partitions of unity thereby ensuring convergence of the approximations over the complex domain. Such a scheme avoids the complexity of representing multiple phases in phase field models, and the mesh density required to adequately resolve interfaces in phase field simulations. We demonstrate the computational scheme through simulations of solidification in the presence of heterogeneities (holes, inclusions), and through simulations of secondary phase evolution in solder alloys.

4:50 PM

Searching for the Low Energy Interfaces in β -Mg₂Si/ α -Al: Yi Wang¹; Zi-Kui Liu¹; Chris Wolverton²; Long-Qing Chen¹; ¹Pennsylvania State University; ²Northwestern University

The main objective of this work is to search for low energy interfaces between the β -Mg₂Si precipitate and the α -Al matrix from a first-principles approach. Extensive calculations were performed to examine the effects of interfacial termination, atomic alignment and intermixing, and interfacial orientations. We have calculated interfacial energies, strain energies, and lattice mismatches for the interfacial system β -Mg₂Si/ α -Al. Our study involved three types of interfacial orientations between β -Mg₂Si and α -Al, namely, (130)_{Al}/(100) _{β} , (001)_{Al}/(010) _{β} , and (-320)_{Al}/(001) _{β} . In each case, we find that the low-energy interfaces possess two key attributes in common: a large amount of Al-Si bonds, and an alignment across the interface with a pre- β /fcc topology.

5:15 PM

Atomistic Simulation of Dislocation Nucleation from Homogeneous and Doped Copper Grain Boundaries: Douglas Spearot¹; Rahul Rajgarhia¹; Ashok Saxena¹; ¹University of Arkansas

Recently published simulation results have indicated that high temperature grain growth in nanocrystalline copper can be prevented by introducing dopant atoms, which segregate to the grain boundaries. Unfortunately, the impact of grain boundary dopant atoms on inelastic deformation mechanisms, such as dislocation nucleation, is unclear. Thus, the objectives of this work are to use molecular dynamics simulations (i) to capture the influence of interface structure on the strength required to nucleate a dislocation from homogeneous copper grain boundaries and (ii) to study the role of antimony dopant atoms at the interface on dislocation emission. It is shown that homogeneous grain boundaries with certain structural features are particularly susceptible to dislocation activity at low applied tensile stresses. It is expected that dopant atoms will have an analogous effect on the dislocation nucleation stress, depending on their position within the grain boundary and the conformation of nearby structural units.

Micro-Engineered Particulate-Based Materials: Session II

Sponsored by: The Minerals, Metals and Materials Society, TMS Materials Processing and Manufacturing Division, TMS: Powder Materials Committee
Program Organizers: Khaled Morsi, San Diego State University; Iver Anderson, Iowa State University

Monday PM
March 10, 2008

Room: 271
Location: Ernest Morial Convention Center

Session Chairs: Khaled Morsi, San Diego State University; Iver Anderson, Iowa State University

2:00 PM

Controlled Transformations in Laser Multi-Deposited Alloy Steel: Nathan Smelser¹; Hailam El Kadiri¹; John Berry¹; ¹Mississippi State University, Center for Advanced Vehicular Systems

The Laser Engineering Net Shaping (LENS®) technology has not yet yielded suitable control of deposited steel microstructures. Rather, the constraints implied by the need for defect-free deposits impose a very specific material microstructure. To facilitate broadening LENS® microstructural capabilities, researchers contend to correlate the obtained microstructure to the imposed thermal history. In this study, we generate different microstructure gradients while varying cooling rates and minimal temperatures of the last melting cycle (CT cycle) associated with each layer. The cooling properties of the CT cycle are varied thru varying the geometry of coupons deposited in the form of single thin walls. The microstructure evolution in these steel deposits is examined with electron and optical microscopy, and the mechanical properties are appreciated thru multi-scale depth sensing indentation and standard static tests. The thermal history associated with each condition is modeled using a user LENS® suitable subroutine for the process implemented in Sysweld.

2:25 PM

Corrosion Behavior of Hot-Pressed TiB₂ in Metallic Neodymium and Nd₂O₃-NdF₃-LiF System: Xudong Luo¹; Zhaowen Wang¹; Zhongning Shi¹; Xianwei Hu¹; Kaiyu Zhang¹; Bingliang Gao¹; Ganfeng Tu¹; ¹Northeastern University

TiB₂-based composite ceramics were sintered by vacuum hot-pressing furnace. Matrix materials were titanium diboride. Molybdenum powder and nickel powder were used as sintering additives, respectively. Corrosion resistant properties of the cermet materials at high temperature were studied in this paper. The experiments were carried out in metallic neodymium and Nd₂O₃-NdF₃-LiF system. Corrosion temperature was 1150°C and the holding time was 24h. The cermet materials and corrosion products were characterized by XRD and SEM, respectively. Effect of the sintering additives on sintering process and mechanism of corrosion process were discussed in paper. The results showed that hot-pressing TiB₂ ceramics is a kind of promising material for neodymium electrolysis.

Minerals, Metals and Materials under Pressure: Shock-Induced Phase Transformations and Microstructure

Sponsored by: The Minerals, Metals and Materials Society, TMS Structural Materials Division, TMS: Chemistry and Physics of Materials Committee
Program Organizers: Richard Hennig, Cornell University; Dallas Trinkle, University of Illinois; Ellen Cerreta, Los Alamos National Laboratory

Monday PM
March 10, 2008

Room: 385
Location: Ernest Morial Convention Center

Session Chairs: Eric Brown, Los Alamos National Laboratory; Ellen Cerreta, Los Alamos National Laboratory

2:00 PM Invited

The Role of Crystalline Instabilities in Shock-Induced Plasticity and Melting: Ramon Ravelo¹; ¹University of Texas El Paso

Large-scale atomistic simulations of shock-wave propagation in single crystals exhibit large anisotropies in the elastic-plastic and solid-liquid transitions. Characteristic of this type of simulations are the large strains at which the crystal yields plastically, regardless of crystal orientation. At these large strains, uniaxial deformations, such as those produced in planar shock loading can generate dynamical instabilities, which compete with defect nucleation mechanisms. At larger compressions near the melt transition, shear instabilities at the shock front enhance lattice amorphization and melting. We will review the criteria, which explain how these instabilities develop and discuss recent large-scale atomistic simulations of plastic deformation and melting in Cu and Al single crystals.

2:30 PM

Microstructural Modifications after Small Charge Explosions in Aluminum and Copper Targets: Donato Firrao¹; Paolo Matteis¹; Chiara Pozzi¹; Giorgio Scavino¹; Graziano Ubertalli¹; Maria Rosa Pinasco²; Maria Giuseppina Ienco²; Paolo Piccardo²; Gabriella Pellati²; Girolamo Costanza³; Roberto Montanari³; Maria Elisa Tata³; Giovanni Brandimarte⁴; Santo Petralia⁴; ¹Politecnico Di Torino; ²Università di Genova; ³Università di Roma Tor Vergata; ⁴Marina Militare Italiana

Metals exposed to explosions undergo several macro and micro changes. At the microstructural level slip bands or mechanical twins, caused by the pressure and temperature wave, can be detected. Twinning or slip occurs depending on the metal stacking fault energy, the blast wave pressure and the deformation rate. An experimental campaign was performed on different FCC metals. Results concerning OFHC copper and AA 2014 aluminum alloy are presented herein and compared with previous results concerning AISI 304Cu stainless steel and a 18 carat gold alloy. Specimens exposed to small charge explosion (50 or 100 g of plastic explosive) were analyzed by optical microscopy and by X-ray diffraction. Microstructural plastic deformation marks were detected and their possible attribution either to mechanical twinning or to cross slip is discussed on the basis of the X-ray diffraction patterns. The detectability target-to-charge distance limit, and hence the critical stress for microstructural changes, are evaluated.

2:50 PM Break

3:05 PM Invited

Direct Shock-Density Measurements Using Plate Impact and Proton Radiography: *Paulo Rigg¹; Cynthia Schwartz²; Robert Hixson¹; Alexander Saunders¹; Frank Merrill¹; Chris Morris¹; ¹Los Alamos National Laboratory*

Proton radiography (pRad) is a powerful new diagnostic with the potential of producing accurate (1%) direct density measurements from dynamically loaded materials. Experiments have been performed to investigate the feasibility of using proton radiography (pRad) to obtain dynamic radiographs of shock-compressed materials during plate impact experiments. This work has involved the design, manufacturing, and testing of a new 40mm single-stage, powder driven gun, the development of methods to synchronize the shock event generated with the gun to proton output, and initial proof-of-principle experiments in Area C at the Los Alamos Neutron Science Center (LANSCE). The method used to attain synchronization of the shock event to proton beam output will be discussed and the results of our initial experiments will be presented.

3:35 PM

Plastic Deformation and Phase Transformations in Cyclotrimethylene Trinitramine (RDX) under Shock Loading: Theory and Experiment: *Marc Cawkwell¹; Tommy Sewell¹; Von Whitley¹; Kyle Ramos¹; Dan Hooks¹; ¹Los Alamos National Laboratory*

The response of the secondary explosive RDX, and organic molecular crystals in general, to shock loading involves mechanisms that cannot reliably be extrapolated or inferred from those seen under quasi-static conditions. We employed non-equilibrium molecular dynamics simulations (NEMD), first-principles calculations and laser and flyer-plate generated shock waves in the study of (111) and (010) oriented single crystals. Shock waves propagating normal to (111) above a threshold particle velocity result in the homogeneous nucleation of partial dislocation loops on (001). The stacking faults generated by these dislocations are obstacles for the glide of perfect dislocations and hence give rise to an anomalous hardening. NEMD simulations of (010) oriented crystals predict that a phase transformation takes place for particle velocities > 750 m/s. Experimental validation of this result can be obtained from measurements of the Hugoniot locus and refractive index during flyer-plate and laser-driven shocks compared with NEMD and first-principles calculations.

3:55 PM Break

4:10 PM

Shock Damage Quantification and Modeling: *Veronica Livescu¹; John Bingert¹; Scott Dillard²; Daniel Worthington²; Davis Tonks¹; ¹Los Alamos National Laboratory; ²University of California, Davis, Materials Design Institute*

The characterization and quantification of damage in polycrystalline materials is an important component toward understanding mechanisms controlling failure processes. The effect of microstructural variables is of particular interest. This work is concerned with damage processes resulting from shock impact events. Incipient damage quantification in specimens from plate impact experiments was performed using a three-dimensional characterization technique. Important damage statistics needed for the validation of damage models were obtained from the three-dimensional reconstruction of the true shock-induced damage field. Reconstruction of grain vertices, edges and facets, and crystallographic orientation information from integrated optical and electron backscattered diffraction data provided quantitative information on the damage nucleation process. This characterization reveals the effect of high-pressure, high-rate loading on microstructural evolution, and the interplay between microstructure and damage processes. Results are applied to the development and validation of a mesoscale micromechanical damage model to reproduce the development and evolution of damage in shocked materials.

4:30 PM

Shock Induced Polycrystallization and Residual Tension in Tantalum Single Crystals: *Jikou Zhou¹; Luke Hsiung¹; Ricky Chau¹; Cheng Saw¹; ¹Lawrence Livermore National Laboratory*

In this presentation, we report shock-induced lattice orientation changes and residual lattice tension in tantalum single crystals. The single crystals with orientations in [001], [011], [111], and [123] directions are shock loaded at ~ 55 GPa in gas gun under the almost identical conditions. The crystal

orientation changes at macroscale and microscale are revealed by a combination of x-ray diffraction analysis and microscopic examination. Rather than lattice compression that is frequently probed by in situ x-ray diffraction technique, we find significant residual lattice tension in the recovered tantalum crystals. Such residual lattice tension is attributed to the dislocation cells and their deformation. The dislocation cells are accordingly estimated to be greater than 100 nm from broadening of x-ray diffraction peak.

4:50 PM

Microstructural Investigation of Very High Strain Rate Deformation of DP 600: *Brian Hamburg¹; Judy Schneider¹; ¹Mississippi State University*

High gasoline prices and increasing safety regulations have forced the automotive industry to look beyond conventional steels to advanced high strength steels such as dual phase (DP) steels. Previous researchers have tested DP 600 up to strain rates order of 10^3 1/s and have found some very interesting properties which have been further investigated in this study. The object of this study is to gain an understanding of the microstructural changes occurring in DP 600 at very high strain rates. The method selected to produce the very high strain rates was normal impact of a hardened steel penetrator into a piece of DP 600 steel. The average strain rates produced from this method with the test set-up used are on the order of 10^5 1/s. The micro-structure has been observed with several different methods to study the micro-structural changes of DP 600 under high strain rate deformation.

Neutron and X-Ray Studies for Probing Materials Behavior: Diffraction at Small Dimensions

Sponsored by: National Science Foundation, The Minerals, Metals and Materials Society, TMS Structural Materials Division, TMS: Advanced Characterization, Testing, and Simulation Committee

Program Organizers: Rozaliya Barabash, Oak Ridge National Laboratory; Yandong Wang, Northeastern University; Peter K. Liaw, University of Tennessee

Monday PM
March 10, 2008

Room: 391
Location: Ernest Morial Convention Center

Session Chairs: Vaclav Holy, Charles University; Sunil Sinha, University of California, San Diego

2:00 PM Invited

Studies of Structure and Dynamics of Surfaces and Interfaces with X-Rays and Neutrons: *Sunil Sinha¹; ¹University of California San Diego*

In the last decade or so there has been increased attention paid to diffuse and off-specular scattering at grazing incidence from surfaces and interfaces, as a means of obtaining in-plane structural information about properties such as roughness, wetting phenomena, film growth morphologies, in-plane ordering and phase transitions, nanoparticle assemblies, mineral surfaces, dynamical surface fluctuations, thin film magnetism, domain morphology and dynamics, etc. Modern synchrotron and neutron sources have developed beamlines specially equipped for such studies. We shall discuss the development of the technique and the methods for analyzing such scattering, and illustrate with some examples of recent studies, including the extension to slow dynamics of films near the glass transition.

2:25 PM Invited

X-Ray Scattering Studies of Inhomogeneous Length Scales in Correlated Electron Systems: The Case of High-Tc Cuprates: *Zahirul Islam¹; ¹Argonne National Laboratory*

High-temperature superconductors are electronically "inhomogeneous" on various length scales, which may be due to distortions modulating both pair potential and exchange interactions. X-ray scattering studies of cuprates reveal lattice modulations and superstructures on various length scales comparable to superconducting coherence lengths. These modulations can be one, two, or three dimensional in nature. In YBCO, modulations characterized by $q=(qx, 0, 0)$ correspond to correlated atomic displacements due to relaxation effects caused by O-vacancy ordered "nanopatches". These nanopatches form well above room temperature and persist well into the superconducting state. Furthermore,

"bowtie"-shape Huang scattering in YBCO and LSCO indicates characteristic long-range strain, which makes the lattice intrinsically inhomogeneous at all doping levels. Structural modulations are also present in BSCCO and HBCO. An inter-play between electronic inhomogeneities and lattice modulations seems inevitable in cuprate superconductors. [APS is supported by the DOE, Office of Science, under Contract No. DE-AC02-06CH11357.]

2:50 PM

X-Ray Microscopic Studies on Electromigration in Electronics Solder Joints: *Andre Lee*¹; K. Subramanian¹; Cheng-En Ho¹; Wenjun Liu²; ¹Michigan State University; ²Argonne National Laboratory

Synchrotron X-ray investigations on a two-phase Sn-Pb alloy solder joint subjected to current stressing have provided significant insight on the events that take place under electromigration in a multi-phase alloy. X-ray fluorescence studies indicated that different conducting species move at different rates during electromigration. X-ray micro-diffraction, with sub-micrometer spatial resolution, facilitated the characterization of 2- and 3-dimensional crystallographic orientations and strain fields at different regions of the joint with respect to the direction of electron flow as a function of time. In the joint configuration, the continuous build-up of slow moving dominating species just behind the fast moving species causes significant compressive deformation in the anode region to push out the fast moving species towards the free surface to form the hillock. The non-destructive micro-beam X-ray techniques employed provided an effective means for the continuous monitoring of the microstructural evolution and development of surface features resulting from current stressing.

3:10 PM Invited

X-Ray Investigation of the Structure of Magnetic Semiconductor Epitaxial Layers: *Vaclav Holy*¹; Vit Novak²; Tomas Jungwirth²; Guenther Bauer³; Rainer Lechner³; ¹Charles University; ²Institute of Physics; ³Kepler University

The main goal of the structural studies of magnetic semiconductor epitaxial layers such as GaMnAs or GeMn is to determine the lattice positions of the magnetic ions, since only substitutional positions of the ions give rise to a ferromagnetic ordering of their magnetic moments. Several x-ray methods are used for this task. X-ray diffraction precisely determines the lattice parameter of a magnetic semiconductor layer, however its connection with the density of the magnetic ions in substitutional and interstitial positions is not completely understood yet. A direct information on the positions of the magnetic ions in the lattice can be obtained by x-ray standing wave method or x-ray fluorescence holography; using these techniques the densities of the ions in different lattice positions were studied in non-annealed and annealed magnetic layers.

3:35 PM

Structural Characterization of SrTiO₃ Thin Films on Sr Terminated (100) Si Substrates by X-Ray Measurements: *Hong Ji*¹; Xiaoyuan Zhou²; ¹University of Electronic Science and Technology of China; ²Hong Kong Polytechnic University

X-ray diffraction is a very powerful tool for the structural characterization of thin films and heterostructures. In this work, a detailed structure analysis on the heterostructure of SrTiO₃(STO)/Sr using a variety of X-ray scattering techniques (2θ/ω, ω scan, φ-scan, pole figure and XRR) is demonstrated. The sample was prepared by laser molecular beam epitaxy under optimized conditions of substrate temperature and oxygen pressure. Symmetrical 2θ/ω scan indicates a high crystallization quality and epitaxial grown of STO. φ-scans over STO (101) and Si (202) reflections have further revealed the in-plane orientation relationship between STO and Si. The α- and c-lattice parameters of the STO thin film were found to be 0.3898, and 0.3901 nm, respectively, suggesting a slight lattice distortion. To better understand the role of the buried interface, further characterizations by pole figure and XRR have been carried out and will be reported in the conference presentation.

3:55 PM Break

4:05 PM Invited

Complex X-Ray Characterization of Magnetron Deposited TiO₂ Thin Films - Growth, Crystallization and Thermal Stability: *Radomir Kuzel*¹; Lea Nichtova¹; Zdenek Matej¹; Jan Sicha²; Jindrich Musil²; ¹Charles University, Faculty of Mathematics and Physics; ²University of West Bohemia, Faculty of Applied Sciences

Sets of amorphous and nanocrystalline titanium dioxide thin films with different thickness were studied after deposition, after annealing and also by in-situ measurements during the heating. Phase analysis and X-ray line broadening were studied by PXRD in parallel beam optics; the residual stresses and textures were measured with the Eulerian cradle and evolution of the surface roughness determined by X-ray reflectivity measurement. Microstructure parameters were extracted by peak profile fitting and by whole powder pattern modelling. Crystallization temperature of about 250°C for thicker films was found for amorphous films. The crystallite size immediately after crystallization was larger than 100 nm. Thin nanocrystalline films consisted mainly of about 7 nm rutile crystallites while thicker films (> 500 nm) were composed of mainly anatase crystallites of similar size. Depth profiling measurements indicated transformation of the rutile phase into anatase with increasing distance from the substrate.

4:30 PM Invited

Adaptive Diffraction Phenomenon of Nanodomain Materials: *Yu Wang*¹; ¹Virginia Tech

A nanodomain diffraction theory is developed. It reveals drastically different diffraction phenomenon in nanodomain materials from that in coarse-domained materials, and a conventional interpretation of the diffraction data leads to identification of erroneous phases. Since the nanodomain sizes are significantly smaller than the coherence length of diffraction radiation, e.g., X-ray and neutron, the scattered waves from individual nanodomains coherently superimpose in diffraction, which produces significant interference effects and must be taken into account. Our analysis reveals an adaptive diffraction phenomenon peculiar to nanodomain materials, where fundamental Bragg peaks disappear while new reflection peaks appear, whose positions are determined by a lever rule according to twin domain volume fractions. The criterion for transition between adaptive diffraction and conventional diffraction is derived. Brillouin zone-dependent diffraction behaviors are discussed. Experimental confirmation of the adaptive nanodomain diffraction phenomenon is presented.

4:55 PM

Monitoring the Deformation Mechanism Evolution over a Large Range of Grain Sizes by In-Situ Diffraction: *Xun-Li Wang*¹; *Alexandru Stoica*¹; Sheng Cheng²; Jon Almer³; Yang Ren³; Don Brown⁴; ¹Oak Ridge National Laboratory; ²University of Tennessee; ³Argonne National Laboratory; ⁴Los Alamos National Laboratory

The in-situ high-energy X-ray and neutron diffraction techniques were used to study the deformation of nickel under monotonic and cyclic tensile loading. The diffraction data evidenced a dramatic change in the deformation mechanisms as the grain size is reduced from microns to nanometers range. The classical dislocation-mediated plasticity induces in the coarse-grained nickel characteristic grain orientation dependent residual strains (intergranular strains), which are also visible in the ultrafine-grained material. However, the evolution of the preferential grain orientation relative to the loading direction indicates that the deformation mechanism for the grain sizes ranging from 100 to 1000 nm includes the twinning as an essential component. Under further grain refinement, down to the grain size of 20 nm, no intergranular strains develop during the plastic deformation and the texture remains unchanged. This behavior leads to the conclusion that the grain boundaries control the plastic deformation of nano-grained nickel.

5:15 PM

Wear Properties and Strain Distribution Analysis of Ti-Based Biomedical Alloy with Different Types of Microstructure: *Eri Fujiwara*¹; Eliot Specht²; Gene Ice³; Kunihiro Hisatsune¹; ¹Nagasaki University; ²Oak Ridge National Laboratory

Effect of heat treatment on wear and frictional properties in Ti-6Al-7Nb was investigated by powder diffraction method. The frictional test between Ti and Ti-alloy was carried out using a pin-on-disk type method in artificial saliva at

310 K. Surface deformation and stress distribution were determined for the wear surface of a fine-grained $\alpha + \beta$ phase Ti-6Al-7Nb biomedical alloy with lamellar or lamellar + equiaxed α structures from peak broadening observed in powder diffraction with a scanning X-ray microbeam probe. Broadening of powder diffraction peaks was observed, especially for the β phase. Integrated diffraction spectrum suggested that crystalline orientation of the α phase occurred, and besides, the lattice parameter of the β phase increased. A peak broadening analysis revealed that broadening was caused by deformation or faulting, and that higher strain was induced in the β phase than in the α phase.

5:35 PM

Plasticity in Nanoscale Metallic Multilayers with In-Situ Synchrotron X-Ray Diffraction: *Cahit Aydinler*¹; Don Brown¹; Amit Misra¹; Jon Almer¹; Nathan Mara¹; ¹Los Alamos National Laboratory

Free-standing Cu-Nb multilayer thin films (nominally 20 micrometers thick) have been tensile loaded as elastic strain sensors in both phases are determined in-situ by high-energy synchrotron X-ray diffraction (SXRD). This immiscible system with incoherent, weak interfaces has been studied heavily to investigate size effects in plasticity as the layer thicknesses are reduced to the nanometer scale. Typically, at tens of nanometers, single dislocation glide substitutes the dislocation pile-up at the interfaces, signifying a fundamental change in plasticity mechanism. We use in-situ SXRD to further our understanding of these mechanisms, by quantifying the load sharing between the two phases, texture, residual stress and unloading behavior. Samples of 5, 27, 40 and 100 nanometers layer thicknesses have been used to span the length scales of interest. The experimental data is interpreted by an adaptation of elasto-plastic self-consistent model that reflects dislocation mechanisms at the nanoscale.

Particle Beam-Induced Radiation Effects in Materials: Metals II

Sponsored by: The Minerals, Metals and Materials Society, American Nuclear Society, TMS Structural Materials Division, TMS/ASM: Nuclear Materials Committee
Program Organizers: Gary Was, University of Michigan; Stuart Maloy, Los Alamos National Laboratory; Christina Trautmann, Gesellschaft für Schwerionenforschung; Maximo Victoria, Lawrence Livermore National Laboratory

Monday PM Room: 389
March 10, 2008 Location: Ernest Morial Convention Center

Session Chairs: Yong Dai, Paul Scherrer Institut; Maximo Victoria, Paul Scherrer Institut

2:00 PM

Dynamic Observations of Microstructural Evolution in Fe and Fe-Cr Alloys under Heavy-Ion Irradiation: *Michael Jenkins*¹; Zhongwen Yao¹; Mercedes Hernandez-Majoral²; Mark Kirk³; ¹University of Oxford; ²Centro de Investigaciones Energeticas, Medioambientales y Tecnologicas; ³Argonne National Laboratory

Thin foils of Fe-0-11%Cr alloys were irradiated with 100-150 keV Fe⁺ and Xe⁺ ions at 20C and 300C. Dynamic TEM observations followed the evolution of damage over doses 0-1dpa. Small 2-4nm dislocation loops with $\langle 100 \rangle$ and $\frac{1}{2} \langle 111 \rangle$ Burgers vectors first appeared at about 0.001-0.01dpa. Loop motion and loss of loops to the surface was induced by the electron beam. In iron the number of loops retained was strongly dependent on the foil orientation; less loop loss occurred in FeCr alloys. At doses > 0.1 dpa complex microstructures developed in thicker regions of foils, involving cooperative alignment and interaction of smaller loops. In UHP Fe irradiated at 300C the damage took the form of interstitial loops with $b = \frac{1}{2} \langle 111 \rangle$. Large finger-shaped loops developed by the growth and coalescence of smaller loops. Similar damage structures developed in UHP Fe at 20C and in Fe8%Cr at both 20C and 300C.

2:40 PM

The Effect of Cr and Ni Content on the Irradiated Microstructure of High Purity Austenitic Alloys: *Zhijie Jiao*¹; Gary Was¹; ¹University of Michigan

The mechanical properties of irradiated materials heavily depend on irradiation-induced microstructures. The effect of Cr and Ni content on the

irradiated microstructure in iron-based austenitic alloys has been widely discussed but rarely studied in a systematic way. To isolate the effect of Cr and Ni from possible impurities, six high purity austenitic alloys with Cr and Ni content ranging from 13-22% and 12-32%, respectively, were selected and irradiated to 1 and 5 dpa at 360°C using 3.2 MeV protons. Irradiated microstructure consisting of dislocation loops and voids was characterized by transmission electron microscopy. The dependence of microstructure on Cr and Ni content by proton irradiations was compared to available data from neutron irradiations at similar doses and temperatures. The similarity and discrepancy between these two types of irradiations will be discussed.

3:00 PM

Self-Organization Processes in Metals by Low-Energy Ion Irradiation: I. Tereshko¹; V. Abidzina¹; I. Elkin²; V. Glushchenko¹; A. Tereshko¹; ¹Belarusian-Russian University; ²"NANTES - Systemy Nanotechnologii" Plc.

The goal of this paper is to study self-organization processes that cause nanostructural evolution in nonlinear crystal media. The computer simulation was used to investigate the interaction between low-energy ions and nonlinear crystal lattices. A molecular dynamics method has been applied for calculating the evolution of atom ensembles in lattices of different dimensions using the equations of classical dynamics. The subjects of investigation were nonlinear homogeneous and heterogeneous (with embedded clusters) atoms chains. We showed that nonlinear oscillations become excited in the chains after low-energy ions irradiation and as a result of them the whole atoms become stabilized in new positions, which results in the formation and development of new metastable atomic groups (nanoclusters). We showed that in homogeneous atom chains critical energy needed for self-organization processes development is less than for nonlinear atom chain with embedded clusters. In this case nanocluster becomes active zone that determine further self-organization processes.

3:20 PM

Mechanical Properties of Ferritic/Martensitic Steels Irradiated in Spallation Target Environments: *Yong Dai*¹; Bin Long¹; Zhenfeng Tong¹; ¹Paul Scherrer Institut

Comparing to neutron irradiation, irradiation of high energy protons can produce not only displacement damage, but also helium and hydrogen at high rate, which may result in severe embrittlement in FM steels. For developing advanced spallation targets, it is essential to understand the behaviors of FM steels under such an irradiation condition. For this reason, thousands of specimens of FM steels have been irradiated in the SINQ (the Swiss Spallation Neutron Source) target irradiation program (STIP). Since 1998 five large irradiation experiments have been carried out and samples of different FM steels such as T91, EM10, F82H, Optifer, Eurofer 97 have been irradiated up to 20 dpa in a wide temperature range. In this presentation, an overview will show the main interesting results obtained from mechanical testing on the FM steels irradiated in STIP with a comparison to results published in the literature after neutron irradiation.

3:40 PM Break

4:00 PM

Microstructural and Mechanical Effects of He Ion Implantation on Ultra Fine Grain Steel: *David Foley*¹; K. Hartwig¹; Engang Fu¹; Stuart Maloy²; Peter Hoseman²; Ning Li²; Xinghang Zhang¹; ¹Texas A&M University; ²Los Alamos National Laboratory

The commercial viability of advanced nuclear reactor designs is currently limited by the radiation damage tolerance of structural steel components. Recent works have demonstrated that increasing the layer interface density of multilayer films can lead to an improvement in radiation damage tolerance. Several levels of microstructural refinement have been achieved in ferritic-martensitic steel via severe plastic deformation (SPD) using equal channel angular extrusion by varying processing temperature and plastic strain level. Room temperature helium ion implantation was carried out on the as-received and processed materials. Microstructural and mechanical properties of these materials were studied via transmission electron microscopy, x-ray diffraction and microhardness. The affects of SPD on the microstructure and resulting post-implantation properties will be discussed.

4:20 PM

Heavy-Ion Irradiation Damage in Bulk Fe-Cr Alloys: *Michael Jenkins¹; Sen Xu¹; Zhongwen Yao¹; ¹University of Oxford*

Bulk Fe-0-12%Cr alloys have been irradiated with 1.5 MeV Fe⁺ ions at a temperature of 300C. The irradiation produces buried damage with the peak damage region at a depth of about 400 nm. A TEM specimen preparation technique has been developed to access this damage peak. Preliminary TEM experiments have been carried out on pure Fe, Fe-8%Cr and Fe-11%Cr. In all materials the damage took the form of interstitial dislocation loops with sizes ranging up to a few tens of nanometres. Loops with Burgers vectors $b = \langle 100 \rangle$ and $b = \frac{1}{2}\langle 111 \rangle$ were both present with the majority of the loops having $b = \langle 100 \rangle$. A full analysis is now underway. Loop Burgers vectors, nature, size distributions and number densities will be determined as a function of the Cr content of the alloys. Comparisons will also be made with in-situ experiments in which ion irradiations are performed on thin foils.

4:40 PM

Influence of Ion Irradiation Dose Rates on the Mechanical Properties in HT-9: *Richard Greco¹; Peter Hosemann¹; Yongqiang Wang¹; Stuart Maloy¹; Marcus Cappiello¹; John Swadener¹; ¹Los Alamos National Laboratory*

Materials irradiation experiments in nuclear reactors or spallation sources are essential for understanding the change of the materials properties due to irradiation. In a thermal reactor only ~12 dpa per year is possible and the specimen can become radioactive, making testing difficult. In order to save time a faster way to study the property changes in materials due to irradiation needs to be established. Particle accelerators using energetic particles can cause much higher radiation damage in a shorter time. A few studies performed previously have shown that these types of experiments produce comparable results to reactor irradiations. In this study HT-9, a candidate material for nuclear reactors, was irradiated to 7 dpa using He⁺ particles at three different dose rates. After irradiation, the samples were tested using nano-indentation to investigate the changes in mechanical properties. The data was compared to experiments from the literature and to the Dispersed Hardening Model.

5:00 PM

Irradiation-Induced Precipitation Modelling of Ferritic Steels: *Roy Faulkner¹; Zheng Lu¹; ¹Loughborough University*

Ferritic steels are the leading structural materials for nuclear reactor applications due to their excellent swelling resistance. Previously, phase-transformations under irradiation had only been treated in a semi-quantitative fashion (Nolfi 1983). Until this current work was undertaken, no attempts had been made to accurately alter the thermodynamics of phases present as a function of neutron irradiation effects. In principle this should be straightforward, so long as the additional energy input to the system coming from the neutron irradiation is known. It is shown in this paper that this accommodation of the additional energy can be introduced to the model and that the model output reflects well the real situation for phase-transitions and second-phase particles in irradiated steels. The model considers formation of irradiation-induced inter- and intra-granular carbide-precipitation in reactor-pressure-vessel steels (C-Mn/MnMoNi). Predicted differences in carbide-distribution as a function of Ni/Cu ratio and absolute Ni-concentration will be highlighted and confirmed well experimental data.

5:20 PM

Nanoscale Mechanical Testing on Ion Irradiated Steels: *Peter Hosemann¹; Christiane Vieh¹; Stuart Maloy¹; Richard Greco¹; ¹Los Alamos National Laboratory*

Radiation induced mechanical property changes are a major difficulties in designing systems operating in a radiation environment. Testing various materials in an irradiation environment is a costly and time consuming activity. Ion beam accelerator experiments have the advantage of allowing relatively fast and inexpensive materials irradiations without activating the sample but do in general not allow large beam penetration depth. In this study, many different ferritic/martensitic steels (e.g. T91 and HT-9) were exposed in an ion beam and tested after irradiation using micro pillar testing and nano indentation in combination with a focused ion beam (FIB) instrument to investigate the changes on mechanical properties. Microstructural changes were evaluated using TEM. The results show good agreement with similar testing after irradiation in a fast neutron flux.

Recent Developments in Rare Earth Science and Technology - Acta Materialia Gold Medal Symposium: Session II

Sponsored by: The Minerals, Metals and Materials Society, TMS Electronic, Magnetic, and Photonic Materials Division, TMS: Superconducting and Magnetic Materials Committee

Program Organizers: Vitalij Pecharsky, Iowa State University; Ashutosh Tiwari, University of Utah; James Morris, Oak Ridge National Laboratory

Monday PM
March 10, 2008

Room: 280
Location: Ernest Morial Convention Center

Session Chairs: James Morris, Oak Ridge National Laboratory; Ashutosh Tiwari, University of Utah

2:00 PM Invited

Case Compounds of the Rare-Earth Metals: Interplay of Chemistry and Physics: *Grin Yuri¹; ¹Max-Planck-Institut fuer Chemische Physik Fester Stoffe*

Intermetallic clathrates (e.g. $\text{Eu}_8\text{Ga}_{16-x}\text{Ge}_{30+x}$), clathrate-like compounds (like EuSi_6) and skutterudites (like $\text{RE}_x\text{TM}_4\text{E}_{15-12}$, TM - transition metal, E15 - element of the group 15 of the Periodic Chart), with rare-earth (RE) cations attracted the worldwide attention, e.g., as promising thermoelectric materials. For the case of the covalent intra-network bonding with RE cations as bonding-balance medium in sense of the Zintl concept, a low charge carrier concentration should be expected. Application of the real space bonding analysis showed indeed the covalent 2c-2e interactions within the network and the charge transfer from the cations to the network. Deviations from the Zintl-like electronic balance or the d states of the TM participating in the bonding lead to the low-charge-carrier behaviour, favourable, e.g., for the thermoelectric applications. The question, how far the picture of the chemical bonding may be used for development of the new cage compounds, is still open.

2:30 PM Invited

Rare Earth Zintl Phases: From Power Generation to the Anomalous Hall Effect: *Brian Sales¹; ¹Oak Ridge National Laboratory*

Zintl phases contain both ionic and covalent bonds, tend to be narrow gap semiconductors or low carrier concentration metals, and often have open crystal structures. In rare earth Zintl phases, the strongly electropositive rare earth atoms donate electrons to other atoms in the structure to form covalent bonds. Examples of rare earth Zintl phases are the filled skutterudites (e.g. $\text{CeFe}_4\text{Sb}_{12}$), Eu clathrates (e.g. $\text{Eu}_8\text{Ga}_{16}\text{Ge}_{30}$) as well as more complex phases such as $\text{Yb}_{14}\text{MnSb}_{11}$. As will be discussed, many of these phases are good thermoelectric materials and can be used in devices to directly convert heat into electricity. In addition, the magnetic properties of the rare earth ions, coupled with the diversity in bonding inherent in Zintl compounds, often leads to unusual ground states and new physics. Two examples of unusual ground states will be discussed. A ferromagnetic compound where the Eu atoms tunnel among four equivalent sites at a frequency of ~500 Mhz, and an underscreened ferromagnetic Kondo compound that exhibits a highly anisotropic anomalous Hall effect. Research at Oak Ridge was sponsored by the Division of Materials Sciences and Engineering, Office of Basic Energy Sciences, U.S. Department of Energy, under contract with Oak Ridge National Laboratory, managed and operated by UT-Battelle, LLC.

3:00 PM Invited

Recent Developments in Geometrically Frustrated Magnetic Materials: Rare Earth Pyrochlore Oxides: *John Greedan¹; A. Diego Lozano¹; Shahab Derakhshan¹; Delphine Gout²; Thomas Proffen²; ¹McMaster University; ²Los Alamos National Laboratory*

Rare earth oxides with the pyrochlore structure, $\text{Ln}_2\text{M}_2\text{O}_7$, where M is a tetravalent element and Ln is a trivalent lanthanide have played a major role in research on geometrically frustrated magnetic materials. This arises from the topology of both the Ln^{3+} and M^{4+} sublattices which consist of three dimensional arrays of corner-sharing tetrahedra and the local, strongly axial, symmetry of the rare earth site. The role of the rare earth in determining the ground magnetic state will be reviewed. As well, the long standing puzzle of the

spin glass behavior of Y₂Mo₂O₇ will be addressed using results from neutron diffraction and neutron pair distribution function analysis. These show the absence of evidence for a phase transition driven by frustration and a disorder model is proposed involving one of the oxygen positions. Earlier results from EXAFS and Y nmr are discussed in light of these new findings.

3:30 PM

Structure-Property Correlations in Rare Earth Based Manganites: *Nori Sudhakar*¹; G. Trichy¹; J. Narayan¹; ¹North Carolina State University

The important physical phenomena exhibited by manganites, namely, metal-insulator transition (MIT), colossal magnetoresistance (CMR) and para to ferromagnetic phase transition are highly sensitive to the growth conditions. For lattice relaxation in thin films dislocations mostly nucleate at the film surface and propagate to the interface. Due to the difficulty in nucleation and propagation of dislocations in LCMO or oxides in general, only a small fraction of strain is reduced in low misfit systems and the remaining strain builds up with the thickness of the film. However, under a large misfit such as in LCMO on MgO, most dislocations nucleate at the steps and get set at the interface, so that the rest of the film can give relatively strain free with properties similar to bulk crystals. The structural and physical properties of the thin films are correlated and interpreted within the theoretical framework of the domain matching epitaxy. The field and temperature dependent magnetization data in the critical region is probed with the aid of Arrott analysis.

3:45 PM

Thermodynamic and Elastic Properties of La(TM)₅ Hydrides (TM = Fe, Co, Ni) from First Principles Density Functional Theory: *Louis Hector, Jr.*¹; Jan Herbst¹; ¹General Motors Research and Development Center

Thermodynamic and elastic properties computed with state-of-the-art density functional theory are presented for La(TM)₅H₈ materials with TM one of the magnetic transition metals Fe, Co, or Ni. We specifically focus on calculating 0K and 298 K formation enthalpies, ΔH , for all compounds. Room temperature ΔH values are obtained from phonon calculations based upon the direct method. Our phonon calculations for LaCo₅ and LaCo₅H₈ yield new information on their crystal structures. While no La-Fe compounds exist, we find $\Delta H(\text{LaFe}_5) > 0$, and hence its formation under experimentally attainable pressures may be possible. LaFe₅ hydrides are predicted to form for several prototype crystal structures. Some issues that arise between experiment and theory will be addressed.

4:00 PM Break

4:15 PM Invited

Synthesis and High-Temperature Thermoelectric Properties of the Rare Earth Containing Compounds of the Ca₁₄AlSb₁₁ Structure Type: *Shawna Brown*¹; Catherine Cox¹; *Susan Kauzlarich*¹; Franck Gascoin²; Teruyuki Ikeda³; Eric Tobler³; G. Snyder¹; ¹University of California; ²Jet Propulsion Laboratory, California Technical Institute; ³California Institute of Technology

Thermoelectric devices are becoming increasingly useful in a wide range of applications. Increasing the efficiency of these devices would boost the development of clean energy technologies; however, over the last two decades, even with new materials development, there has been a lack of high-temperature, high-efficiency materials, thus limiting the attainable effectiveness of thermoelectric devices. Existing thermoelectric data on Yb₁₄MnSb₁₁ show an improved figure of merit of at least 67% over the current material, SiGe. Our aim is to further improve this value and further increase device efficiency by optimizing the electronic and thermal parameters of the materials. Here, we present the synthesis and high-temperature thermoelectric properties of the Yb₁₄Mn_{1-x}Zn_xSb₁₁ solid-solution (with x = 0.00, 0.17, 0.33, 0.50, 0.67, 0.83, and 1.0). Single crystal diffraction, microprobe analysis, differential scanning calorimetry, thermogravimetry, resistivity, Seebeck coefficient, and thermal conductivity results will be presented.

4:45 PM Invited

Structures and Physical Properties of Ternary Rare-Earth Intermetallic Phases in the RE-M-Ge and RE-M-Sb Systems: *Haiying Bie*¹; Andriy Tkachuk¹; Oksana Zelinska¹; *Arthur Mar*¹; ¹University of Alberta

The wide variety of magnetic properties displayed by intermetallic compounds containing rare-earth (RE) and transition metals (M) arises from differing interactions between the localized f-electrons of the RE atoms, through the

possible intermediary of the d-electrons of the M atoms. Because Ge and Sb have similar electronegativities and atomic radii, we have been interested in extending our longstanding work on ternary rare-earth antimonides to germanides. New phases have been identified in these systems containing an early transition metal: RECr_{1-x}Ge₂, REMGe₃ (M = V, Cr), RE₂Ti₉Sb₁₂, and RE₂Ti₉Sb₁₅. In the Cr-containing phases, strong magnetic exchange interactions between the f and d electrons lead to relatively high ferromagnetic ordering temperatures (e.g. T_c = 155 K for SmCrGe₃) that coincide with prominent transitions in the electrical resistivity. Band structure calculations have been performed to draw insight into the bonding and properties of these compounds.

5:15 PM Invited

The Role of Rare-Earth Atoms in Polar Intermetallic Compounds: *Gordon Miller*¹; ¹Department of Chemistry, Iowa State University

Polar intermetallic compounds involve combinations of electropositive, active metals and electronegative, late- or post-transition metals. Their structures are typically governed by optimized orbital interactions within the network of electronegative metals with an electron count achieved by formally donating the valence electrons of the active metals to the electronegative components. When rare-earth metals serve in place of the active metals, potentially interesting chemistry and physics can arise, phenomena that are related to the combination of valence 5d orbitals for chemical bonding and 4f orbitals with localized electron character at the rare-earth metals. This seminar will summarize these characteristics in polar intermetallics ranging from heavy fermion-like Ce-Ni-Al phases to the magnetic refrigerants (Gd_{1-x}Y_x)₃Ge₄ and (Gd_{1-x}Y_x)₃Si₄.

5:45 PM

Effect of Fluoride Coating on Mechanical Properties of Polymer-Bonded Rare Earth Magnets: *Nathaniel Oster*¹; Peter Sokolowski¹; Iver Anderson²; Wei Tang²; Y. Wu²; Kevin Dennis²; Matthew Kramer²; R. McCallum²; ¹Iowa State University; ²Ames Laboratory (US Department of Energy)

Mixed rare earth (MRE) magnetic alloy particulate of the MRE2Fe14B type readily form a brittle, non-protective oxide layer. Efforts have been made to passivate MRE magnet alloy powders through the creation of a fluoride surface layer. This study is an investigation of the effect of a fluoride coating on the mechanical properties of polymer-bonded magnets made from MRE magnetic particulate. Surface chemistry, particle geometry, and mixing ratios were among the factors considered in this study. High-pressure gas atomized MRE2Fe14B spherical powder and crushed MRE2Fe14B melt spun ribbon were used in the study. Nitrogen trifluoride was used at elevated temperatures to passivate the powders. The powders were mixed with polyphenylene sulfide and compression molded at elevated temperature to form the bonded magnets. Mechanical strength was measured with a four point bend test and the findings will be reported. Support from DOE-EERE-FCVT Office through Ames Lab contract DE-AC02-07CH11358.

Recent Industrial Applications of Solid-State Phase Transformations: Alloy Design, Microstructure Prediction and Control

Sponsored by: The Minerals, Metals and Materials Society, TMS Materials Processing and Manufacturing Division, TMS/ASM: Phase Transformations Committee
Program Organizer: Milo Kral, University of Canterbury

Monday PM
March 10, 2008

Room: 287
Location: Ernest Morial Convention Center

Session Chair: Milo Kral, University of Canterbury

2:00 PM Introductory Comments

2:05 PM Invited

Design Applications of Transformation Theory: *Gregory Olson*¹; ¹Northwestern University and QuesTek Innovations LLC

The new industry of Computational Materials Science is built on a foundation of predictive phase transformation theory. In the parametric design of new alloys, the Langer-Schwarz framework for precipitation at high

supersaturations allows control of length and time scales through transformation driving forces and coarsening rate constants employing the ThermoCalc/DICTRA multicomponent thermokinetic system, with unstable equilibrium trajectory models giving accurate control of peak hardness, dispersed phase transformation toughening, and Zener-Smith grain refinement. Accelerated process optimization at the component/device level and prediction of property variation in multistage manufacturing under the DARPA-AIM methodology employs explicit simulation of multimodal precipitation with the PrecipiCalc software. Under the ONR/DARPA "D3D" Digital Structure initiative, a company-led university consortium addresses integration of multiscale tomographic characterization with high fidelity simulation of the spatial distribution of precipitate dispersions in processing and service for the accurate design and AIM qualification of high performance steels combining strength, toughness and fatigue resistance.

2:30 PM

Phase Transformation Theory, a Powerful Tool for the Design of Advanced Steels: From Macro to Nano: *Francisca Caballero*¹; Michael Miller²; Carlos Garcia-Mateo¹; Carlos Capdevila¹; Carlos Garcia de Andrés¹; ¹CENIM-CSIC; ²Oak Ridge National Laboratory (ORNL)

An innovative design procedure based on phase transformation theory alone has been successfully applied to design steels with a microstructure consisting of a mixture of bainitic ferrite, retained austenite and some martensite. An increase in the amount of bainitic ferrite is needed in order to avoid the presence of large regions of untransformed austenite, which under stress, decompose to brittle martensite. Therefore, the maximum amount of bainite that can be obtained at any temperature is limited by the T₀ curve. The design procedure addresses this difficulty by adjusting the T₀ curve to greater carbon concentrations using substitutional solutes such as Mn and Cr. With this design procedure, bainitic microstructures with strengths in the range of 1600-1700 MPa and toughness values of 130 MPa m^{1/2} were obtained. The concepts of bainite transformation theory can be exploited even further to design steels with a strength in excess of 2.5 GPa and considerable toughness (30 MPa m^{1/2}). Research at the Oak Ridge National Laboratory SHaRE User Facility was sponsored by Basic Energy Sciences, U.S. Department of Energy.

2:55 PM

Microstructure Prediction of Hot-Rolled Sheet during Continuous Cooling Using Phase Field Method: *Katsumi Nakajima*¹; Yasushi Tanaka¹; Yoshihiro Hosoya¹; Markus Apel²; Ingo Steinbach²; ¹JFE Steel Corporation; ²RWTH-Aachen

A precise prediction of microstructure during continuous cooling after hot-rolling is very important for steel engineers. Each sheet product has each controlled cooling history in order to get an ideal microstructure. Phase field simulation has proved to be a useful tool for not only solidification, but also solid-state transformation. In this paper, we applied phase field method to gamma-alpha transformation of low carbon steel which has various kinds of continuous cooling histories and compared them to experimental data. At first, we tried simulations without strain energy effect during transformation in the case of constant continuous cooling rate and also in the case of a few types of commercial cooling. In the presentation, a simulation with strain energy effect will be discussed.

3:20 PM Invited

Design and Development of Mg-Gd-Zn Based Alloys for Elevated Temperature Applications: *Jian-Feng Nie*¹; Xiang Gao¹; Laure Bourgeois¹; Keiichi Oishi²; Kazuhiro Hono²; ¹Monash University, ARC Centre of Excellence for Design in Light Metals; ²National Institute for Materials Science

Lightweight magnesium alloys have attracted increasing interest in recent years for potential applications in the automotive and aircraft industries. One important group of magnesium alloys is those strengthened by precipitation hardening. Unfortunately, the age hardening response achievable in these magnesium alloys is substantially lower than that obtained in aluminium alloys. Further improvement in strength of magnesium alloys requires better understanding of precipitate microstructures and microstructural factors that are important in controlling the strength of the alloys. This presentation will show recent results on the design and development of Mg-Gd based alloys for elevated temperature applications. It shows that Zn additions to dilute Mg-Gd alloys result in a substantial enhancement in precipitation hardening and creep resistance.

The strengthening precipitates in these Mg-Gd-Zn alloys are characterised using TEM and 3D atom probe, and results will be discussed in the context of previous work on other Mg-RE-Zn alloys of similar compositions.

3:45 PM Break

3:55 PM Invited

Phase Transformations during Friction Stir Welding: *Richard Fonda*¹; Keith Knipling¹; ¹Naval Research Laboratory

Friction stir welding has become an established and commercially-viable joining technique for aluminum alloys. This welding technique is a solid-state joining process which uses a rotating tool to heat the surrounding material such that it can be "stirred" and then consolidated in the wake of the tool. This presentation discusses the phase transformations that occur during the friction stir welding process and relates those phase transformations to the thermal and deformation history of different regions within the weld. The presentation will focus primarily on aluminum alloys, although friction stir welding of higher-strength alloys such as titanium and steel, both of which undergo a high temperature allotropic phase transformation, are also discussed. This presentation also examines the benefits, and limitations, of using friction stir welding in an industrial environment.

4:20 PM Invited

Controlling the Microstructure of CF8C-Plus and CF8C-Plus+Cu/W Alloys to Improve High Temperature Strength and Creep Properties: *Neal Evans*¹; Philip Maziasz¹; John Shingledecker¹; Michael Pollard²; ¹Oak Ridge National Laboratory; ²Caterpillar Inc.

CF8C-Plus cast austenitic stainless steel (Fe-19Cr-12Ni-0.07C-0.7Nb-0.4Si-4Mn-0.25N; Wt%) is a new cost-effective material upgrade for improved performance, durability, and temperature capability relative to current heavy-duty diesel engine exhaust components made from SiMo ductile cast iron and other creep resistant stainless steels. The improved tensile and creep properties observed in both centrifugally cast and thin-section castings of CF8C-Plus and CF8C-Plus+Cu/W alloys will be discussed in terms of the scientifically designed microstructures, which have been revealed by electron microscopy, that develop during high-temperature exposure or creep-rupture testing. These include the formation of nano-scale dispersion-strengthening precipitates of MX and a Cu-rich precipitate phase, and interdendritic regions that are stabilized with M₂₃C₆ carbides.

4:45 PM Invited

Mechanical Design with Low Temperature Carburization: *Sunniva Collins*¹; P. Williams¹; ¹Swagelok Technology Services Company

Fluid systems in a variety of industries use tube fittings to readily install leak free connections. Robust tube fitting performance depends on both an adequate differential hardness gripping element to tube, and a guided plastic deformation of the tube gripping components. Low-temperature carburization technology hardens the surface of austenitic stainless steel. For many years, this treatment has been applied to the ferrules of the Swagelok tube fitting, ensuring tube grip, gas-tight seal, and vibration resistance in hundreds of millions of fluid system connections around the world. The process involves activation of the surface followed by a gas phase treatment, performed at temperatures low enough to avoid the formation of carbides, for a sufficient time to allow carbon diffusion to occur. The result is a hardened conformal case on the treated parts, without distortion or change to dimension. The treated case remains austenite (with verified carbon concentrations over 12 atomic percent at the surface) and retains its ductility. This presentation will discuss the design features and performance characteristics of tube fittings enabled by low temperature carburization. Examples of other mechanical designs in wear, fatigue, and corrosive applications will also be given.

5:10 PM

Alloying Effects on Precipitation and Microstructural Evolution in Self-Shielded Ferritic Weld Metal: *Badri Narayanan*¹; Peter Sarosi²; Marie Quintana¹; Michael Mills²; ¹Lincoln Electric Company; ²Ohio State University

The effect of alloying additions on the morphology and composition of nitride/oxide precipitates and subsequent effect on the austenite to ferrite phase transformation has been studied in a high strength ferritic weld metal deposited with a self-shielded arc welding process. Aluminum, titanium and zirconium

are intentional additions to protect the weld metal during solidification. The complex precipitates and coarse ferritic microstructures resulting from the unique alloying additions, prevents achieving acceptable strength and toughness of the weld. The precipitates are characterized in the TEM using energy dispersive spectroscopy and electron energy loss spectroscopy techniques to differentiate the effect of titanium and zirconium on the morphology of the complex precipitates. Orientation microscopy utilizing electron backscattered diffraction has been used to characterize the effect of alloying on the austenite-ferrite phase transformation. This work focuses on understanding the link between the microstructural features to strength and toughness of the weld metal.

5:35 PM Invited

Phase Transformation in Meteorites: The Effect of Cooling under 'Equilibrium' Conditions: John Jonas¹; Youliang He²; ¹McGill University; ²Cornell University

The microstructures of the Gibeon and other meteorites were examined by means of optical microscopy and EBSD techniques. The orientations of the bcc lamellae formed from a single prior-austenite grain were determined and found to lie between the Kurdjumov-Sachs (K-S) and Nishiyama-Wassermann (N-W) correspondence relations. These can all be characterized as 'co-planar' variants. Measurements carried out in the plessite regions indicated that the variants were continuously distributed around the Bain circles and included both the co-planar and 'co-directional' variants. Thus the crystallographic data support the view that somewhat different mechanisms are involved in the formation of the Widmanstätten and plessitic structures in meteorites. The above observations obtained from materials cooled at such low ('equilibrium') rates are compared with those pertaining to steels cooled in industrial rolling mills to indicate that the very much higher industrial rates do not influence the orientations of the transformation products in a significant way.

Sloan Industry Centers Forum: Techno-Management Issues Related to Materials-Centric Industries: Session I

Sponsored by: The Minerals, Metals and Materials Society
Program Organizers: Subodh Das, Secat Inc.; Diran Apelian, Worcester Polytechnic Institute

Monday PM Room: 397
March 10, 2008 Location: Ernest Morial Convention Center

Session Chair: Diran Apelian, Worcester Polytechnic Institute

2:00 PM Introductory Comments by Diran Apelian and Subodh Das

2:10 PM Invited

Overview of Sloan Industry Studies: Gail Pesyna¹; ¹Alfred P. Sloan Foundation

Sloan's Industry Studies program was founded in 1990 on the belief that industries are sufficiently different from one another that they individually deserve rigorous and deep academic study grounded in direct observation. Industry studies research requires close cooperation between academics and industry, and supports the integration of observation-based research with appropriate theory and analysis. There are 26 Industry Centers at U.S. universities, consisting of groups of faculty and students who study a specific industry, plus nearly 1,000 affiliated researchers working in many other university and scholarly settings around the world. Opportunities for participation in this unique program will be described.

2:30 PM Invited

Robustness of Materials Selection Decisions Using Various Life-Cycle Assessment Methods: A. Allen¹; Subodh Das²; F. Field¹; Jeremy Gregory³; Randolph Kirchain⁴; ¹Massachusetts Institute of Technology, Materials Systems Laboratory; ²Secat Inc.; ³Massachusetts Institute of Technology, Materials Systems Laboratory, Laboratory for Energy and the Environment; ⁴Massachusetts Institute of Technology, Materials Systems Laboratory, Department of Material Science and Engineering, Engineering Systems Division

The use of alternative materials to reduce vehicle mass is a tactic often promoted as improving the fuel efficiency and environmental performance of vehicles. However, a growing array of materials candidates confronts today's designer. While life-cycle assessment methods are available to provide quantitative input into this selection decision, their implementations are evolving and distinct. This paper explores the robustness of materials selection decisions when using different LCA methods. Specifically, this paper surveys the major analytical variations of LCA implementations and explores the implications of several of these variants when applied to an automotive materials selection case study. This case study examines analytical variations in: valuation method, secondary weight savings, and treatment of recycling. Preliminary results indicate that, although the choice of analytical method can have real impacts on individual metrics, there are sets of analytical variation over which strategic results are not strongly affected.

2:50 PM Invited

Material Change in Automotive: Enablers and Obstacles: Glenn Mercer¹; ¹International Motor Vehicle Program

The amount of steel, aluminum, and polymer in a modern car is only exceeded by the weight of the engineering studies published by advocates of one or the other material as to their relative merits. Despite all the solid scientific work, material choices in cars remain mystifyingly capricious to the outside observer. This talk will cover some of the real-world enablers of and obstacles to changes in automotive materials, with a focus on the nuances that tilt the balance, as in: "not just price... but price volatility over time", "not just weight... but weight class", and "not just performance... but performance in context". This paper will draw upon two decades of field experience in OEMs and suppliers sectors of the automotive material selection business. Further more, recommendations will be made on how material suppliers can advance their own practical solutions more efficiently and effectively.

3:10 PM Break

3:20 PM Invited

Identification, Development and Commercialization of Recycling – Friendly Aluminum Alloys: Subodh Das¹; John Kaufman¹; John Green²; Frank Field³; Randolph Kirchain³; ¹Secat Inc.; ²JASG Consulting; ³Massachusetts Institute of Technology

Today's commercial aluminum alloys have largely been designed for production from primary aluminum with pure alloying elements added. However, the changing aluminum supply situation, in which the US has become primarily a fabricator of aluminum products comprising imported primary aluminum and domestically recycled secondary aluminum, means that new, recycle-friendly aluminum alloys must be identified, developed and commercialized to sustain the industry's economic and environmental strengths. In addition to suggesting several recycling friendly compositions, this paper examines the issues associated with rapid commercialization of aluminum alloys, and suggests several strategies and paths forward that may expedite early adoption. Furthermore, this paper also discusses several mathematical modeling techniques and methodologies, such as chance constraint modeling, that can be used to refine the composition of starting and finished products to maximize benefits over the entire supply chain.

3:40 PM Invited

An Overview of Global Aluminum Industry: Challenges and Opportunities: Ed Hoag¹; ¹Aleris International

World aluminum industry has experienced steady growth and significant structural changes in the past years aligning with booming global economy. Fueled by globalization and consolidation in the world materials industry, the aluminum industry is going through a period of hyper changes in mergers and acquisition. Great efforts have been made to develop novel process and product to maintain and enhance the sustainability of the aluminum industry. The understanding, development and implementation of recycling friendly-industry is a key component to sustain the aluminum industry. This paper will overview the trends of aluminum industry and examines the complex forces in leading to these changes. Additionally, this paper will also discuss lessons learned including an attempt to suggest some paths forward.

4:00 PM Invited

Wood Products - What Does the Consumer Want?: *Al Landers*¹; ¹Huber Engineered Woods LLC

Driven primarily by the domestic residential housing market, the annual value of wood products manufactured in the US is nearly \$165 billion. The wood products industry has evolved into a highly fragmented supply chain that has been designed and continues to operate using the mass production model that is most efficient at moving high volumes of only a limited few commodities or standard products. However, on the consumer side of the wood supply chain, this business model is no longer sufficient to address the emerging needs of customers. In addition to new product designs, new capabilities are also needed to install, maintain, interface, integrate, service, and recycle these wood products in ever more diverse ways. This presentation describes the emerging needs of the consumer and opportunities for restructuring the wood products supply chain that can better match and balance material needs and production capability with demand.

4:20 PM Invited

Demand Driven Materials Management: From the "Woods" to the Consumer: *Earl Kline*¹; ¹Virginia Tech

The wood products supply chain, with many independently operating segments, has become very "detached" from the final customer. To compensate for this detachment the supply chain relies on traditional strategies such as demand forecasting and holding excessive inventories "just-in-case". Today, these strategies are creating costly "feast or famine" variations in wood materials and their associated products. Dealing with such supply variations has led to monumental infrastructures, policies, and regulations that are negatively impacting supply chain effectiveness and competitiveness. This presentation presents a "forest to consumer" benchmarking study that maps the flow of wood materials with respect to final consumer demand. Key metrics benchmarked are those related to inventory levels, product quality, demand amplification, transportation, lead times, and information availability/quality. Systems modeling analyses results are presented to identify and prioritize potential areas for improved material and product flow through the supply chain.

Structural Aluminides for Elevated Temperature Applications: Mechanical Behavior

Sponsored by: The Minerals, Metals and Materials Society, TMS Structural Materials Division, TMS: High Temperature Alloys Committee, TMS/ASM: Mechanical Behavior of Materials Committee

Program Organizers: Young-Won Kim, UES Inc; David Morris, Centro Nacional de Investigaciones Metalurgicas, CSIC; Rui Yang, Chinese Academy of Sciences; Christoph Leyens, Technical University of Brandenburg at Cottbus

Monday PM
March 10, 2008

Room: 394
Location: Ernest Morial Convention Center

Session Chairs: Thomas Bieler, Michigan State University; Antonin Dlouhy, Academy of Sciences

2:00 PM Invited

Durability Assessment of TiAl Alloys: *Susan Draper*¹; *Bradley Lerch*¹; *Young-Won Kim*²; ¹NASA; ²UES Inc

This paper will present a summary of durability issues for TiAl alloys, particularly impact and environmental resistance. Various gamma alloys, including a TNB alloy (Ti-45Al-5Nb-B-C) and a new beta-gamma TiAl alloy (Ti-44Al-4Nb-2Cr-2V-B-C), along with some more traditional TiAl alloys were ballistically impacted. Variables such as impact energy, projectile hardness and impact location were related to the resulting damage. The goal was to produce damage that was similar to the domestic object damage found in low pressure turbine blades. Damaged samples were subsequently tested under high cycle fatigue loading using the step-test method. The fatigue strength of each alloy was characterized as a function of initial crack size and modeled using a threshold-based fracture mechanics approach. Differences among the various alloys will be discussed, particularly with respect to their microstructure, manufacturing

process, and tensile properties. The effect of environmental exposure on impact resistance and resulting fatigue strength will be discussed.

2:30 PM

Influence of Impact on the Mechanical Behaviour of a Cast and a Forged Gamma Based TiAl Alloy: *Susanne Gebhard*¹; *Piet Peters*¹; *Dan Roth-Fagaraseanu*²; *Heinz Voggenreiter*¹; ¹German Aerospace Center; ²Rolls-Royce Deutschland

One of the main problems representing a barrier for TiAl gas turbine applications is its low resistance against impact. For this reason, the influence of high-speed impact on the mechanical behaviour of a cast TiAl alloy and a more ductile, forged alloy has been investigated. Impact tests are performed and the caused damage has been evaluated as a function of the impact speed, the particle weight (the impact energy) in relation to the specimen thickness and location of the impact. Impact near the specimen edge produces a severer damage than an impact in the centre. This is shown with the aid of residual strength and fatigue experiments. The residual strength could be described on the basis of a linear elastic fracture mechanics analysis and a fracture toughness of 15 to 17MPa(m)^{1/2}. Fatigue experiments were performed to determine the threshold for crack growth as a function of the impact damage size.

2:50 PM

Effect of Heat Treatment on Microstructures and Properties of Y-Bearing TiAl Alloy: *Yuyong Chen*¹; *Baohui Li*²; *Fei Yang*¹; *Fantao Kong*¹; *Shulong Xiao*¹; *Zhiguang Liu*¹; ¹Harbin Institute of Technology; ²Harbin Institute of Technology, Institute of SAST

In this article, the microstructure controls and properties for various microstructures of Ti-45Al-5Nb-0.3Y have been studied using relatively large forged pancake. The canned forging pancake was successfully gained. The effect of processing and heat treatment on microstructure and properties was studied using X-ray diffraction, optical microscopy, scanning electron microscopy (SEM) and transmission electron microscopy (TEM). Results showed that the microstructure of forged pancake consisted of major curved lamellar, broken lamellar and minor dynamic recrystallized grains (DRX) with the size of about 1-2µm and the YAl₂ phase at grain boundaries. Three different microstructures, duplex, nearly lamellar and fully lamellar, have been obtained through heat treatment, respectively. And the microstructure evolution was also analyzed. The alloy with duplex microstructure owed the best ductility, the elongation reached 1.9%, and which with fully lamellar microstructure took on better strength, yield strength and fracture strength were 557.1MPa and 715MPa, at room temperature, respectively.

3:10 PM

Effect of Surface Condition and Thermal Exposure on the Fracture Mechanisms on a Gamma-TiAl Alloy: *Maria Perez-Bravo*¹; *Iñaki Madariaga*¹; *Koldo Ostolaza*¹; ¹Industria de Turbo Propulsores

The use of gamma-TiAl alloys in the aeronautical market has been a long during wish. Developments carried out up to now are close to allow their exploitation. Although several processing routes have been considered for manufacturing turbine components, casting would be the preferred one. Current casting technology might require going through various machining stages up to the final shape. Hence, it is relevant to consider the effect of the resulting surface condition of a cast gamma-TiAl alloy after different machining routes as ECM and grinding. The nature of this condition will be assessed through metallurgical and fractographic analysis on specimens tested under various LCF and HCF test conditions. This research will focus on identifying the acting fracture mechanisms and their contribution to the macroscopic mechanical behaviour. Specimens will be investigated in the as-machined and in the as-exposed condition, aiming at capturing temperatures and exposure times representative of engine working conditions.

3:30 PM

Predicting Microcrack Nucleation Due to Slip-Twin Interactions at Grain Boundaries in Duplex Near Gamma-TiAl: *Thomas Bieler*¹; *Philip Eisenlohr*²; *Deepak Kumar*¹; *Martin Crimp*¹; *Franz Roters*²; *Dierk Raabe*²; ¹Michigan State University; ²Max-Planck-Institut für Eisenforschung

A fracture initiation parameter (fip) based upon the geometry of the Burgers vector interactions as they are related to slip transfer across the grain boundary is described. The fip is expressed as a probability statement consisting of factors,

which when multiplied together, allow weak boundaries to be identified in the context of a state of stress. In addition to Burgers vectors, the misorientation between slip planes in the grain boundary and differences in elastic properties in adjoining grains are considered. Boundaries are characterized to identify tilt and twist character and whether they are low SIGMA value boundaries. There is no definite preference for crack initiation based on SIGMA values or tilt and twist character of the boundary, implying that these are not critical parameters affecting crack nucleation at the grain boundary in duplex near- γ TiAl. Incorporation of this parameter in finite-element crystal plasticity simulations for predicting optimal microstructures is discussed.

3:50 PM Break

4:00 PM

Heat Treatment Response of Forged Powdered Metal 03k near Gamma Titanium Aluminide Disks of Nominal Composition Ti-45.5Al-1.0Cr-3.0Nb-0.2W-0.2B-0.2Si-0.4C (at%): Ray Simpkins¹; ¹Williams International

The attractive density corrected strength of gamma titanium aluminides for use in aerospace applications has led to extensive alloy and process development over the few past decades. This research has led to the development of a powdered metal (PM) processing technique that yields repeatable chemistries and avenues to forgable pre-forms. A PM TiAl alloy with a nominal composition of Ti-45.5Al-1.0Cr-3.0Nb-0.2W-0.2B-0.2Si-0.4C (at%) was evaluated as a compressor rotor material. The PM preforms were varied in size to scale up the fabrication process to replicate component size forgings. Mechanical testing was performed to measure the response to heat treatment of the PM forgings. These results were compared to a cast/HIP + forged version of a similar chemistry. Forging defects were detected during post PM forging ultrasonic inspection. Microscopic analysis of the defects was also performed. The resultant mechanical properties and microstructural relationships will be presented along with forging defect analysis.

4:20 PM

Effect of Al Content on Microstructure/Phase Distribution and Strength/Ductility in a PM Gamma Alloy: Young-Won Kim¹; Stephan Russ²; Christopher Woodward³; Charles Yolton³; ¹UES Inc; ²US Air Force; ³Crucible Materials Corporation

The dependency of strength and ductility of TiAl alloys to microstructure and variations in chemistry are quite complicated, and possible interaction effects exist. For example, Al is known to affect strength and the volume fraction of gamma and alpha-2 phases have been credited with the effect. However, the impact of chemistry versus phase has not been satisfactorily quantified. In an effort to understand such effects, four billets of gamma alloy 03K, nominal composition of Ti-45.5Al-3Nb-1Cr-0.2W-0.2B-0.4C-0.2Si (at%), were produced from gas atomized powder. The realized Al content varied between 44.8 and 47.4 at%. The forgings were heat treated to develop three microstructure variants: fully lamellar, nearly lamellar and duplex. The microstructure and Rockwell hardness were analyzed on all samples, and room temperature tensile testing was conducted on the fully lamellar materials. The resulting strength and ductility as a function of Al content and microstructure will be discussed.

4:40 PM

Determination of the Creep Rate in Gamma Titanium Aluminide by Stress Relaxation Tests: Jonathan Paul¹; Roland Hoppe¹; Michael Oehring¹; Fritz Appel¹; ¹GKSS Research Centre

In high temperature applications the creep behaviour of TiAl components can be an important issue. In this respect alloy composition and processing are important factors which need to be optimised so that a proper balance of mechanical properties can be obtained. To obtain a large creep property database requires many tests to be performed at different stress levels and temperatures which of course is both time consuming and expensive. To overcome this requirement during alloy and processing development, a method of obtaining the minimum creep rate at a single temperature but at a series of stress levels from a single short term tensile test including repeated stress relaxations has been developed. The experimentally measured minimum creep rates are in quite good agreement with those predicted from the stress relaxation tests.

5:00 PM

Axial-Torsional Thermo-Mechanical Fatigue Behavior of Ti-45Al-5Nb-0.2B-0.2C: Stephen Brookes¹; Hans- Kühn¹; Birgit Skrotzki¹; Hellmuth Klingelhöffer¹; Rainer Sievert¹; Janine Pfitzing²; Gunther Eggeler²; ¹BAM; ²Ruhr-University Bochum

Structural components in aeronautical gas turbine engines typically experience large variations in temperatures and multiaxial states of stress under non-isothermal conditions. Therefore, the uniaxial, torsional and axial-torsional thermo-mechanical fatigue (TMF) behavior was studied. TMF tests were performed at 400-800°C and with mechanical strain amplitudes from 0.15%-0.7%. The tests were conducted axially thermo-mechanically in-phase (IP) and out-of-phase (OP). For the same lifetimes, IP tests required the highest strain amplitudes, while OP test conditions were most damaging and needed the lowest strain amplitudes. The Mises equivalent mechanical strain amplitudes of pure torsional tests are found in between uniaxial IP and OP tests for the same lifetimes. As a result, for the same equivalent mechanical strain amplitude uniaxial IP tests showed also significantly longer lifetimes than pure torsional TMF tests. The non-proportional multiaxial OP test showed the lowest lifetime at the same equivalent mechanical strain amplitude compared to the other types of tests.

5:20 PM

Tensile Impact Behavior of Duplex Ti-46.5Al-2Nb-2Cr at Elevated Temperatures: Xiang Zan¹; Yang Wang¹; Yuehui He¹; Yuanming Xia¹; ¹University of Science and Technology of China

The tensile behavior of Duplex Ti-46.5Al-2Nb-2Cr intermetallics (DP TiAl) is studied at strain rates ranging from 0.001 to 1350 s⁻¹ and temperatures from room temperature to 840°C, in which tensile impact tests are conducted on a self-designed rotating disk indirect bar-bar tensile impact apparatus at University of Science and Technology of China (BTIA at USTC). Results show obvious effects of temperature and strain rate. The strength under dynamic loading is higher than that under quasi-static loading. The Brittle-to-Ductile Transition Temperature (BDTT) rises with elevated strain rates. The fractographic analysis shows that below BDTT the fracture mode changes from planar cleavage fracture to intergranular fracture with increased test temperatures and voids are found on the colony boundaries at elevated temperature.

Ultrafine-Grained Materials: Fifth International Symposium: Processing and Materials

Sponsored by: The Minerals, Metals and Materials Society, TMS Structural Materials Division, TMS Materials Processing and Manufacturing Division, TMS: Shaping and Forming Committee, TMS: Nanomechanical Materials Behavior Committee
Program Organizers: Yuri Estrin, Monash University and CSIRO Melbourne; Terence Langdon, University of Southern California; Terry Lowe, Los Alamos National Laboratory; Xiaozhou Liao, University of Sydney; Zhiwei Shan, Hysitron Inc; Ruslan Valiev, UFA State Aviation Technical University; Yuntian Zhu, North Carolina State University

Monday PM
March 10, 2008

Room: 273
Location: Ernest Morial Convention Center

Session Chairs: Ruslan Valiev, UFA State Aviation Technical University; David Alexander, Los Alamos National Laboratory; Cheng Xu, University of Southern California; Laszlo Kecskes, US Army Research Laboratory

2:00 PM Invited

Experimental Attempts to Manage Both High Strength and Adequate Ductility in Ultrafine Grained Metals: Nobuhiro Tsuji¹; ¹Osaka University

It has been recognized that the ultrafine grained metals usually perform very high strength but limited ductility. However, there are several ways to overcome this trade-off relationship through microstructure control: for example, bimodal nanostructures, ultrafine grained dual phase, ultrafine grains including fine dispersoids, transformation induced plasticity, etc., are expected to result in managing strength and ductility. In this presentation, results of several experimental attempts to manage both high strength and adequate ductility in ultrafine grained metals, which have been carried out in the author's group

by using severe plastic deformation processes and other thermomechanical processing techniques, will be introduced.

2:20 PM

Role of Strain Reversal in Grain Refinement by Severe Plastic Deformation: *Dmitry Orlov¹; Yoshikazu Todaka²; Minoru Umemoto²; Nobuhiro Tsuji¹; ¹Osaka University; ²Toyohashi University of Technology*

Most of severe plastic deformation processes involve strain reversal. Till now quite big number of researches has been done on indirect study of its role, which discusses the effect of loading path in ultra-fine grained structure formation. The present work was aimed to study directly the role of the strain reversal in grain refinement by severe plastic deformation. A 99.99% purity aluminum was processed by High Pressure Torsion up to 96° rotation (average equivalent strain $\epsilon \approx 4$) with two deformation modes: monotonic and reversal deformation with a step of 12° rotation (average equivalent strain $\epsilon \approx 0.5$). It was shown that strain reversal retards the grain refinement in comparison with (quasi)monotonic deformation. This explains less effectiveness of SPD schemes that involve full strain reversal after each consequent processing step.

2:35 PM Invited

Application of ECAP in Tailoring the Mechanical Property of Magnesium Alloys: *Jingtao Wang¹; Jinqiang Liu¹; Jun Tao¹; Ping Huang¹; Deliang Yin¹; ¹Nanjing University of Science and Technology*

An approach of combination of processing by grain refinement via equal channel angular pressing, conventional extrusion and/or age hardening was applied to a new Mg-12Gd-3Y-0.5Zr aging hardening alloy and an AZ31 alloy respectively. Four passes of ECAP of the alloy at elevated temperature effectively refined their grains effectively, and improved ductility significantly in both alloy. Additional conventional extrusion with an extrusion ratio of 9 after 4 passes of ECAP improved obviously their strength, especially yield strength, without obvious loss of ductility. Subsequent ageing of the aging hardening alloy Mg-12Gd-3Y-0.5Zr significantly increased its yield and tensile strength further, nevertheless, its ductility was substantially decreased. These results indicate the effectiveness of the influences of these processing, individually or in combination on the mechanical properties of the experimental magnesium alloy. And good combination of strength and ductility could be obtained by optimizing the processing parameter of this approach.

2:55 PM

Effect of Shear Strain in an Al-6061 Alloy Processed by HPT: *Cheng Xu¹; Terence Langdon¹; ¹University of Southern California*

It has been established that High Pressure Torsion (HPT) is capable of producing exceptional grain refinement, often even to the nanometer level for some materials. This is attributed to the large shear strain which is introduced during the torsional straining. This paper examines the effect of shear strain using an Al-6061 alloy subjected to HPT for 1 and 5 turns under a pressure of 4 GPa and with the alloy pressed under the same pressure for the same time spans as 1 and 5 turns. The Vickers microhardness was recorded on the surface of the as-processed disks and plotted in contour form to give microhardness distributions on the samples.

3:10 PM Invited

Property Optimization of Nanostructured Metals by Post-Process Deformation: *Xiaoxu Huang¹; Naoya Kamikawa¹; Niels Hansen¹; ¹Riso National Laboratory*

Nanostructured metals produced by high strain deformation typically have high strength and low elongation when deformed in tension. In a recent study it has however been found for nanostructured aluminum processed by accumulative roll bonding (ARB) that a slight post-process deformation may have a beneficial effect on the elongation followed by a slight decrease in strength (X. Huang, N. Hansen and N. Tsuji, Science, 312 (2006) 249). This effect has been explored for aluminum and IF steel representing fcc and bcc metals, respectively. These metals have been produced by ARB to an ultrahigh strain and afterwards cold rolled to thickness reductions from 5 to 50%. For both metals it has been found that only a small strain is required to obtain the beneficial effect of post-process deformation. This finding is underpinned by a structural characterization carried out by transmission electron microscopy.

3:30 PM Invited

Mechanical Properties and Microstructure Evolutions of ECAPed Ultrafine Grained Al during Low Temperature Annealing: *Yonghao Zhao¹; Andrea Danglewicz²; Peiling Sun²; Xiaozhou Liao³; Yuntian Zhu²; Yizhang Zhou¹; Enrique J. Lavernia¹; ¹University of California at Davis; ²Los Alamos National Laboratory; ³University of Sydney*

Ultrafine grained (UFG) metals processed by severe plastic deformation usually exhibit strain softening in tensile testing. To overcome the strain softening, the easiest way is to introduce recovery or recrystallization/grain growth by annealing. Usually annealing elevates ductility by lowering strength. We will report results obtained with UFG Al by equal-channel angular pressing (ECAP) with routes A, Bc and C. It was found that the strength of the UFG Al by all routes increases first and then decreases with isothermal annealing. With increasing annealing time, the ductility increases first and then is unchanged for UFG Al by route A, and decreases first and then increases for UFG Al by route Bc, while remaining unchanged for UFG Al by route C. The different mechanical responses versus isothermal annealing of the UFG Al by different ECAP routes will be explained by their different microstructural evolutions during annealing.

3:50 PM Break

4:05 PM Invited

Dynamic Plastic Deformation: A Novel Approach for Processing Bulk Nanostructured Metals: *K. Liu¹; N. R. Tao¹; ¹Chinese Academy of Sciences, Institute of Metal Research*

The minimum grain sizes obtained in metals and alloys subjected to severe quasi-static plastic deformation at ambient temperature are usually in the submicrometer regime. In this talk, we will present a novel approach to further refine grains of bulk metals into the nanometer regime. The process, referred to as Dynamic Plastic Deformation (DPD), is to deform bulk metals dynamically at high strain rates and/or at cryogenic temperatures. During dynamic deformation, the recovery or recrystallization kinetics (of dislocation structures) is suppressed and meanwhile twinning tendency is enhanced. Combination of the two effects leads to a substantial change in grain refinement mechanism. We will demonstrate a twinning-dominated grain refinement mechanism in the nanometer regime. For DPD-Cu, the average grain size is reduced down to about 50 nm and the tensile strength is elevated above 620 MPa. Perspectives on development of DPD processes and their applications in other engineering alloys will be addressed.

4:25 PM

Application of ECAP for Ferritic Stainless Steel Sheets to Control Texture and Alleviate Ridging: *Hirofumi Miyamoto¹; Masaharu Hatano²; Takuro Mimaki¹; ¹Doshisha University; ²Nippon Steel and Sumikin Stainless Steel Corporation*

Equal-channel angular pressing (ECAP) has been applied to ferritic stainless steel sheets with 17wt% Chromium in order to control texture and alleviate ridging. The hot rolled and annealed sheets of 4 mm thickness were ECAP-pressed only for one pass, followed by cold rolling and final annealing. Microstructures were fragmented by heterogeneous plastic deformation such as shear bands during ECAP, and they appear to remain after cold rolling. When the final sheets were strained by 20%, they exhibited alleviated ridging as compared with the counterpart fabricated by conventional process. Local orientational change due to shear bands formation during ECAP may disconnect colonies of grains with similar orientations such as {001}<110> texture, which are otherwise hard to be recrystallized and frequently regarded as the cause of the ridging.

4:40 PM Invited

Ultrafine-Grained Ni and Ti with High Ductility: *Yonghao Zhao¹; Enrique J. Lavernia¹; ¹University of California at Davis*

The limited ductility of nanocrystalline/ultrafine-grained materials has emerged as a singular issue in the study and application of this novel class of materials. Numerous investigators have addressed this issue, with varying degrees of success, via a variety of approaches, most of which can be grouped into two general categories: microstructural design and introduction of alternative deformation mechanisms. In this talk, we will report results obtained with ultrafine-grained Ni prepared by cryo-milling and subsequent forging. The consolidated Ni has a yield strength of 480 MPa, and a ductility of 40%. Similarly, an ultrafine-grained (UFG) Ti was prepared by equal-channel angular

(ECAE) and subsequent rolling. Following annealing the UFG-Ti at 350°C for 6 h, the ductility increased from 5% to 10%, the ultimate strength increased from about 1100 MPa to 1400 MPa. The microstructural origins for such combinations of good strength and high ductility are discussed in the present paper.

5:00 PM

Processing of Copper by Flat Plate Equal Channel Angular Extrusion:

David Alexander¹; ¹Los Alamos National Laboratory

Flat plate samples of copper have been processed by equal channel angular extrusion (ECAE). Processing was performed at room temperature, for die angles of both 120 and 90°, for up to 4 passes, by route C. The mechanical properties have been measured in both tension and compression, in 3 orthogonal directions. The processed material showed mechanical anisotropy, depending on testing orientation, and also showed a tension/compression asymmetry. The tooling for flat plate ECAE will be described, and the problems associated with scaling up to larger sizes will be considered.

5:15 PM

Consolidation of Cu and Al Nanoparticles via Equal Channel Angular Extrusion (ECAE) and the Effect of Post-ECAE:

Mohammed Haouaoui¹; Cathleen Hutchins¹; Ibrahim Karaman¹; Hans Maier²; Enrique Lavernia³; ¹Texas A&M University; ²University of Paderborn, Lehrstuhl f. Werkstoffkunde; ³University of California, Davis

Ultrafine grained (UFG) and nanocrystalline (NC) materials are of interest due to their high strength, compared with coarse grained counterparts. In the present work, Equal Channel Angular Extrusion (ECAE) is used to consolidate microcrystalline and nanocrystalline Cu and Al particles into bulk samples with relatively large dimensions (all dimensions in cm range). The effects of ECAE route, extrusion temperature, and post-ECAE processing such as swaging and wire drawing on microstructure and mechanical behavior are investigated. The main objective of the study is to determine the optimum processing parameters to increase the ductility of the consolidates, while maintaining relatively high strength. The preliminary results showed UTS levels as high as 800 MPa with fracture strains up to 10% for consolidated Cu nanoparticles. The ability of ECAE for the consolidation of cryomilled Al-10.5Mg microparticles and pure Al nanoparticles are demonstrated. The effect of post-ECAE processing on the consolidate will be presented.

5:30 PM

Hall-Petch and Recrystallization Behavior of Heavily Worked Tungsten:

Suveen Mathaudhu¹; Armand deRosset¹; Qiuming Wei²; Laszlo Kecskes¹; Ted Hartwig³; ¹US Army Research Laboratory; ²University of North Carolina-Charlotte; ³Texas A&M University

We investigated the recrystallization behavior and Hall-Petch relationship of large-grained, commercial purity tungsten (W) processed by ECAE to obtain UFG microstructures. Extrusions were performed to strains of ~4.6 with a 90 degree tool, up to 1200C. Subsequent 60 min annealing up to 1600C of the worked W allowed to determine the recrystallization temperature. Light, scanning electron, and transmission electron microscopy, Vickers microhardness, and quasi-static (~10⁻³ s⁻¹) uniaxial compression testing were used to examine the properties of the W extrudates. The ECAE-processed W showed 100-300 nm grain size in the fully worked state, ~10 µm equiaxed grains in the recrystallized state, and grains >500 µm after the onset of grain growth. The range of grain size was used to determine the Hall-Petch relationship for W. The recrystallization behavior, along with the interdependence between quasi-static yield strength, microhardness, and grain size and are to be discussed.

5:45 PM

Plane-Strain Machining for Studying Severe Plastic Deformation in Metals

and Alloys: Srinivasan Swaminathan¹; M. Ravi Shankar¹; W. Dale Compton¹; Alex King¹; Srinivasan Chandrasekar¹; Kevin Trumble¹; ¹Purdue University

Large plastic strains up to ~15 can be imposed by plane-strain machining of metals and alloys. In addition to achieving a wide range of well-defined strains in a single-pass, continuous process, the strain rate and temperature also can be controlled over large ranges. The deformation field in plane-strain machining is compared with other methods of severe plastic deformation (SPD) such as equal channel angular extrusion. The paper focuses on the application of machining to study microstructure refinement by SPD in a wide range of metals and alloys, including copper and its solid solution alloys, CP titanium, precipitation-

hardenable aluminum alloys, and a nickel-based superalloy. The capabilities and limitations of developing bulk structural materials through machining are also discussed.

2008 Nanomaterials: Fabrication, Properties, and Applications: Device

Sponsored by: The Minerals, Metals and Materials Society, TMS Electronic, Magnetic, and Photonic Materials Division, TMS: Nanomaterials Committee

Program Organizers: Seong Jin Koh, University of Texas; Wonbong Choi, Florida International University; Donna Senft, US Air Force; Ganapathiraman Ramanath, Rensselaer Polytechnic Institute; Seung Kang, Qualcomm Inc

Tuesday AM
March 11, 2008

Room: 274
Location: Ernest Morial Convention Center

Session Chair: To Be Announced

8:30 AM Invited

From Nanogenerators to Nano-Piezotronics: *Zhong Lin (Z.L.) Wang*¹; ¹Georgia Tech

Developing novel technologies for wireless nanodevices and nanosystems are of critical importance for in-situ, real-time and implantable biosensing. It is essential to explore innovative nanotechnologies for converting mechanical energy (such as body movement, muscle stretching), vibration energy (such as acoustic/ultrasonic wave), and hydraulic energy (such as body fluid and blood flow) into electric energy that will be used to power nanodevices without using battery. We have demonstrated an innovative approach for converting nano-scale mechanical energy into electric energy by piezoelectric zinc oxide nanowire (NW) arrays.^{1,2} We have recently developed DC nanogenerator driven by ultrasonic wave, which is a gigantic step towards application in practice. A field of nano-piezotronics has been proposed.³ ¹Z.L. Wang and J.H. Song, Science, 312 (2006) 242-246. ²X.D. Wang, J.H. Song, J. Liu, and Z.L. Wang, Science, 316 (2007) 102-105. ³Z.L. Wang "Nano-piezotronics", Adv. Mater., 19 (2007) 889.

8:55 AM Invited

Nanomaterials for Energy Conversion and Storage: *Ryne Raffaele*¹; ¹Rochester Institute of Technology

We will review some of the exciting new developments in the use of nanomaterials in energy conversion and storage for space power applications. In particular, we will present results on synthesis, purification, and characterization of single- and multi-wall carbon nanotubes and their use in lithium ion batteries, as well as other potential space power applications. We will also discuss how these materials are being used in concert with a variety of other nanomaterials to further improve device efficiencies and performance. Finally, we will also review some of the work we have been engaged with recently concerning the use of epitaxially grown InAs quantum dots on GaAs for use in multi-junction space solar cells. A particular focus in this talk will be given to the potential improvements to specific power and ancillary behavior of power devices which is beneficial to space application, such as thermal stability and radiation tolerance, afforded through the use of nanomaterials.

9:20 AM

Hyperbranched Nanowires of PbS and PbSe and Their Applications in Photovoltaics: *Song Jin*¹; ¹University of Wisconsin-Madison

The discovery of multiple exciton generation in nanocrystals of semiconducting PbS and PbSe promises a 800% quantum efficiency limit and 65% theoretical photovoltaic conversion efficiency. We report a chemical vapor deposition synthesis of hyperbranched single-crystal nanowires of PbS and PbSe. Multiple levels of nanowires nucleate perpendicularly from the previous generation of nanowires in an epitaxial fashion to produce a dense cluster structure of a complex nanowire network. No intentional catalyst was employed for the nanowire synthesis, but it is suggested that lead itself might serve as a vapor-liquid-solid (VLS) catalysts for the anisotropic growth of PbS/PbSe. The flow rate and duration of a hydrogen co-flow are found to have significant effect on the PbS/PbSe nanowire nucleation and growth. We will explain the formation mechanism of these intricate network structures and other complex exotic PbS/PbSe nanostructures, and explore these nanostructures in high performance photovoltaic applications.

9:35 AM Invited

Monodisperse Anatase TiO₂ Nanotubes: Template-Directed Synthesis and Applications for High - Efficient Solar Energy Conversion: Changdeuck Bae¹; Hyunjun Yoo¹; Sihyeong Kim¹; Kyungeun Lee¹; *Hyun Jung Shin*¹; ¹Kookmin University, National Research Laboratory for Nanotubular Structures of Oxides and School of Advanced Materials Engineering and Center for Materials and Processes of Self-Assembly

Template-directed synthesis strategy is an ideal tool to fabricate oxide nanotubes in that their physical dimensions can be precisely controlled and monodisperse samples can be harvested in large quantity. Wall thickness of the oxide nanotubes is controllable with a high precision by varying the deposition cycles of atomic layer deposition (ALD), and the length and diameter can be tailored in accordance with the templates used. A wealth of functional oxide materials with the controlled polymorphs can be deposited to be nanotubular structures by various synthesis methods. Here we present our recent progress made in the template synthesis and applications of anatase TiO₂ nanotubes. (i) We first discuss the template synthesis strategy that combines porous membrane templates and ALD techniques, addressing the processing issues associated with coating inside nanoscale pores, selectively etching of oxide nanotubes from the templates, and dispersion against the formation of nanotubes' bundle-up. (ii) We then report on bamboo-like self-organization of the anatase grains along the axis during the amorphous-anatase transitions at 400-500°C being responsible for their transport properties. (iii) We also studied electrical transport properties of both individual and bundle anatase nanotubes on the basis of conventional thermionic emission model and found that they have a superior conductivity (over three orders of magnitude) to that of bulk. (iv) Toward solar energy conversion applications, we explored their surface defect structures, which are strongly related to harvesting efficacy of photo-oxidized electrons, based on photoluminescence measurements. (v) Finally, we constructed dye-sensitized solar cells (DSSCs) devices consisting of our anatase TiO₂ nanotubes and preliminarily came by high conversion efficiency (~ 8%) of the devices. (vi) Their potential for other applications such as drug delivery systems, (bio)sensors, and photocatalysts are introduced based on our preliminary results.

10:00 AM Invited

Nanomaterials in Space Power Generation: *John Merrill*¹; ¹Air Force Research Laboratory

Photovoltaics continue to be the primary source for electric power for space missions. The need for ever higher power, specific power, areal power density, and radiation resistance continues to push development of novel solar cell technologies. To meet present and future space power requirements, conventional crystalline multijunction solar cells, next generation thin-film solar cells, and novel technologies are being pursued. In the near term, III-V based multijunction solar cell efficiencies are being increased through incorporation of new materials and metamorphic structures. These efforts are expected to result in AM0 solar cell efficiencies of 33-35%, however, theoretical efficiency limits for such structures are typically less than 40%. For significantly increased efficiency and radiation hardness, so-called "third generation" technologies are being pursued by many. These approaches have theoretical efficiencies around 70%; practical efficiencies well in excess of 40% are possible. Third generation concepts include intermediate band structures, hot carriers, multi-exciton, and nanocomposite approaches. These technologies will be discussed in relation to space military and commercial needs as well as the unique requirements attributable to the harsh space environment.

10:25 AM

The Usage of Nano-Structure for Direct Harvesting of the Nuclear Particles Energy as Electricity: *Liviu Popa-Simil*¹; *Claudiu Muntele*²; ¹LAVM LLC.; ²AAMU

Most of the exothermic nuclear reactions transfer the mass defect or binding and surplus energy into kinetic energy of the resulting particles. These particles are traveling through material lattices, interacting by ionization and nuclear collisions. Placing an assembly of conductive-insulating layers in the path of such radiation, the ionization energy is transformed into charge accumulation by polarization. The result is a super-capacitor charged by the moving particles and discharged electrically. Another more promising solution is to use bi-material nanoparticles organized such as to act like a serial connection and add the voltage. A spherical symmetry fission products source coated in several nano-

layers is desired for such structures. The system may operate as dry or liquid-immersed battery, removing the fission products from the fissile material. There is a tremendous advantage over the current heat flow based thermal stabilization system allowing a power density up to 1000 times higher.

10:40 AM

Continuous Manufacturing and Novel Coating Technologies of Photocatalytic Nanoparticles: *Christian Wögerer*¹; Nils Stelzer²; Humbert Noll³; ¹Profactor Research and Solutions GmbH; ²Austrian Research Center Seibersdorf - ARC; ³University for Applied Science Wiener Neustadt

A continuous manufacturing technology by high pressure mixing reactors, the HPMN reactor, is a production method for Nanoparticles with the Possibility of functionalization and aftertreatment in one step and he will open the door for the Industries to a cost efficient mass production of functionalized Nanoparticles and Nanoproducts. The HPMN-reactor combines the flexibility of precipitation with the possibilities of controlling the particle characteristics and the ability of continuous processing. Combined with new photocatalytic particles and coating technologies in the same plant it is possible to realize the production from materials to a ready product with new photocatalytic properties in only one equipment. In a two year common research project 5 Austrian research institutes and 9 companies from different markets develop new photocatalytic materials, production equipment and photocatalytic applications.

10:55 AM Break

11:10 AM Invited

Functional Wide Bandgap Semiconductor Nanowire Devices: *Stephen Pearton*¹; D. Norton¹; B. Kang¹; F. Ren¹; H. Wang¹; L. Tien¹; J. Lin¹; ¹University of Florida

We have fabricated many types of ZnO and GaN nanowire devices, including MOSFETs, diodes, UV sensors and pH sensors. ZnO has been effectively used as a gas sensor material based on the near-surface modification of charge distribution with surface-absorbed species. The large surface area of the nanorods makes them attractive for gas and chemical sensing, and the ability to control their nucleation sites makes them candidates for high density sensor arrays.

11:40 AM

Large-Scale Fabrication of Single Electron Devices: *Vishva Ray*¹; Ramkumar Subramanian¹; Pradeep Bhadrachalam¹; Seong Jin Koh¹; ¹University of Texas at Arlington

Fabrication of single electron devices requires defining source-drain electrode gap in the range of 10 nm as well as precise positioning of Coulomb island between the electrode gap. Achieving these nanoscale geometrical requirements over a large area for large-scale device fabrication is a formidable task. Here we present new single electron device architecture and its large-scale fabrication using CMOS technology. This has been possible by employing vertical electrode configuration as well as spontaneous and precise positioning of Coulomb islands between vertically placed electrodes. We demonstrate Coulomb staircases at room temperature using 10 and 20 nm Au nanoparticles as Coulomb islands. The voltage intervals of the Coulomb staircases were ~55 and ~25 mV for 10 and 20 nm Au nanoparticles, respectively, which is in good agreement with calculated single electron charging energies. The current demonstration implies that practical fabrication of integrated systems of single electron devices is now quite feasible.

11:55 AM

Electron-Phonon Interaction in Nanodevices: *Karel Kral*¹; ¹Institute of Physics, Academy of Science of Czech Republic

Theory of the nanotransistor will be presented with the effect of the electronic multiple scattering on LO phonons included. The electronic transport part of the theory will be based on the well-known simple model, in which the quantum dot-contact coupling will be expressed with help of the electronic energy level broadening in a zero-dimensional nanostructure. The effect of the up-conversion of electronic level occupation will be included in the transport equations.

12:10 PM Invited

Nanoscale Heterojunction Engineering and Selective Growth of High-Quality Ge on Si by Molecular Beam Epitaxy: *Sang Han*¹; ¹University of New Mexico

Growing a lattice-mismatched, dislocation-free epitaxial film on Si has been a challenge for many years. Herein, we exploit nanoscale heterojunction engineering to grow high-quality Ge epilayer on Si. A 1.2-nm-thick chemical SiO₂ film is produced on Si in a H₂O₂ and H₂SO₄ solution. When the chemically oxidized Si substrate is exposed to Ge molecular beam, relatively uniform nanoscale seed pads form in the oxide layer and "touchdown" on the underlying Si substrate. Upon continued exposure, Ge selectively grows on the seed pads rather than on SiO₂, and the seeds coalesce to form an epilayer. The resulting density of threading dislocations is ≤ 1E5 per square cm. In this presentation, we will discuss the reasons behind the selective growth as well as reduction in strain density near the Ge-Si heterojunction, leading to high quality Ge epilayer.

12:40 PM

Microstructure and Magnetic Properties of Nickel Nanorod Arrays on Silicon Substrate: *Chien-Ming Liu*¹; Chih Chen¹; ¹National Chiao Tung University

In this work, Ni nanorod arrays were grown on Si substrate using anodized aluminum oxide (AAO) as a template. The Ni nanorods were formed in the nanopores of the AAO film by electroless plating. The microstructure and magnetic property of Ni nanorod arrays on Si were examined by field emission scanning electron microscopy, transmission electron microscopy (TEM), and superconducting quantum interference device. The results show that the Ni nanorod is nanocrystalline, about 70 nm in diameter. It is found that these Ni nanorods appear to be superparamagnetic after they were deposited. However, after annealing at 400°C for few minutes, their magnetic properties changes from superparamagnetism to ferromagnetism. TEM results shows that grain growth occurred during the annealing process and thus change their magnetic properties.

12:55 PM

Influence of Fast Neutron Irradiation on Nanocrystalline Materials: *Walid Mohamed*¹; K. Murty¹; ¹North Carolina State University

The aim of this study is to investigate the influence of fast neutron irradiation on both mechanical properties and microstructure of nanocrystalline materials. Nanocrystalline materials are expected to have high resistance to radiation damage since the large volume of grain boundaries would act as sink for the dislocations produced by irradiation. Mechanical properties of irradiated nanocrystalline samples will be measured using a miniature tensile tester designed specially for that purpose. Developed microstructures of the irradiated samples will be studied by TEM. The samples have been already irradiated and currently under cooling to be ready for handling at lab.

3-Dimensional Materials Science: Large Datasets and Microstructure Representation II

Sponsored by: The Minerals, Metals and Materials Society, TMS Structural Materials Division, TMS: Advanced Characterization, Testing, and Simulation Committee
Program Organizers: Michael Uchic, US Air Force; Eric Taleff, University of Texas; Alexis Lewis, Naval Research Laboratory; Jeff Simmons, US Air Force; Marc DeGraef, Carnegie Mellon University

Tuesday AM

March 11, 2008

Room: 286

Location: Ernest Morial Convention Center

Session Chairs: David Rowenhorst, Naval Research Laboratory; Anthony Rollett, Carnegie Mellon University

8:30 AM Invited

Design and Implementation of an Interactive Repository for Materials Microstructural Data: *Paul Dawson*¹; *Donald Boyce*¹; ¹Cornell University

We discuss the concepts underlying the design of a repository for data related to the structure and properties of structural alloys. The design follows from the intended functionality of the repository, allowing for access by parties

that store data in the repository and by parties that view or work with the data. The organization of data mimics the nature of the material, beginning with its constituent elements to define an alloy and branching to domains that reflect its state in terms of the attributes of its microstructure. The design anticipates that new motivations for accessing the data will emerge once the system is implemented and can facilitate a wide array of applications via an interface for application plug-ins. We will discuss the software for organizing the data (a relational database) and for storing the data (the repository) as well as the graphical user interfaces for communicating with these.

9:00 AM

Development of a Methodology for the Prediction of 3D Grain Structure from 2D Measurements: *Michael Groeber*¹; Michael Uchic¹; Dennis Dimiduk¹; Somnath Ghosh²; ¹Air Force Research Laboratory; ²Ohio State University

Currently, there remains a disconnect between the ability to investigate microstructure in 3D and its widespread use. Though many tools have matured to allow for robust data collection, availability continues to be limited to much of the community. Thus, it is still a reality to investigate materials in 2D and infer 3D characteristics. Stereological relationships have provided 3D information with limited data collection. However, there are microstructural descriptors that cannot be inferred from 2D measurements. In addition, many stereological relationships yield only average quantities to describe features. These limitations provide areas for improvement in predicting 3D structure from 2D measurements. Advances in collection of 3D microstructural data offer insight into the quality of stereological methods. True 3D microstructures serve as an answer key to stereological approaches, highlighting shortcomings in various techniques. This presentation will develop new, more robust, prediction tools using the true 3D structure as a validation tool.

9:20 AM

Reconstructing 3D Polycrystals: *Anthony Rollett*¹; S. Lee¹; S. Sintay¹; ¹Carnegie Mellon University

Three-dimensional polycrystals can be assembled or reconstructed from statistical information on grain shape by packing ellipsoids into a representative volume element (RVE). A specified distribution of size and shape of ellipsoids can be used as input, from which the packing algorithm selects a subset according to an objective function that minimizes gaps and overlaps. The set of packed ellipsoids is converted to a space filling polycrystal by operating a cellular automaton in which each grain is grown from the ellipsoid center using its axes to specify (anisotropic) growth rates. The resulting polycrystal typically has a slightly different size distribution than the input and the junctions between boundaries do not conform to local equilibrium. Relaxation of the microstructures with a Monte Carlo grain growth model is used to examine the potential for generating realistic polycrystals with specified size distributions.

9:40 AM Break

10:00 AM Invited

A Data Driven Approach for Generating Reduced-Order Stochastic Models of Random Heterogeneous Media: *Nicholas Zabaras*¹; Baskar Ganapathysubramanian¹; ¹Cornell University

Stochastic analysis of random heterogeneous media provides information of significance only if realistic input models of the property variations are used. We will review a framework for constructing such input stochastic models using a data-driven strategy. This problem is analogous to the problem of manifold learning encountered in image processing and psychology. We showcase the methodology by constructing low-dimensional input stochastic models to represent property variations in two-phase and polycrystalline 3D microstructures. We will show how this model is used to model physical processes on the random microstructure. This framework has direct applicability to problems where working in high-dimensional spaces is computationally intractable, for instance, in visualization of property evolution, extracting process-property maps in low-dimensional spaces, among others. Furthermore, the generation of a low-dimensional surrogate space has major ramifications in the optimization of properties-processes and structures, making complicated operations like searching, contouring and sorting computationally feasible.

10:30 AM

Vectorized 3D Microstructure for Finite Element Simulations: *Asim Tewari*¹; Vijayalakshmi Swamydhas¹; Pinaki Biswas¹; Raja Mishra²; Sooho Kim²; Anil Sachdev²; ¹General Motors Research and Development, India Science Laboratory; ²General Motors Research and Development, Materials and Processes Laboratory

A technique to perform finite element analysis on a vectorized 3D microstructure is developed and applied to intermetallic particles found in continuous cast (CC) AA5754 and AA3005 sheets. CC sheets have particles of several phases (Al(FeMnSi), Al₃MnFe, etc) in different shapes and sizes (from 0.2μm to 10 μm) and heterogeneously distributed in stringers and centerline segregations. The technique consists of 3D reconstruction of the true microstructure through serial-sectioning and conversion of the 3D raster image to vector image. The vector image is constructed by union set operation of closed quadratic surfaces of tri-axial ellipsoids capable of approximating a wide range of shapes. This results in a 3D mesh generated automatically using Unigraphics and Hypermesh from real microstructural measurements, which can be imported to any FE code. Extension of this approach to create a composite input file combining particle distribution with EBSD measurement of grain orientations and morphologies will be discussed.

10:50 AM

Some Implications of Microstructure Representation below the Homogenization Limit: *Jeff Simmons*¹; Dennis Dimiduk¹; Marc De Graef²; ¹Air Force Research Laboratory; ²Carnegie Mellon University

Statistical representation of microstructural information is becoming an important area of research, particularly with exponentially increasing volumes of experimental information becoming available. Synthetic microstructures are often generated with statistical properties consistent with the representation and used for physics-based simulations. This allows property scatter to be estimated by using multiple synthetic inputs. Local features such as particles generally are not symmetrical, but in the infinite limit, must be distributed to reproduce the macroscopic symmetry. Arbitrarily chosen statistical functions can be combined to reproduce the macroscopic symmetry, but will generally result in excessive variability at the local scale, resulting in an over-estimate of the property scatter. Recent work towards developing unbiased microstructure feature representations that bridge the homogeneous and local scales will be presented. Unbiased representations developed from Principal Component Analysis of sets of particle and particle neighborhood features will be presented, along with progress towards correctly matching the local scale variability.

11:10 AM

Mean Width Evaluation of Digital Microstructures in Relation to 3-D Grain Growth Theory: *Fatma Uyar*¹; Seth Wilson¹; Jason Gruber¹; Anthony Rollett¹; ¹Carnegie Mellon University

Mean width is an important measure for computational materials science, not only for grain shape representation but also for verification of 3-D von Neumann grain growth relation. Two methods have been employed for calculation of mean width of digital microstructures in a finite element mesh. Grains are composed of tetrahedral volume elements and grain boundaries are represented by interface triangles. The first method for mean width calculation uses the additivity rule on volume elements. The second method uses the flat surface rule. Measurements of net mean width and volume change rate are then compared to predictions of the theory of MacPherson and Srolovitz [Nature 446, 1053–1055(2007)] in a moving finite elements model of isotropic grain growth.

9th Global Innovations Symposium: Trends in Integrated Computational Materials Engineering for Materials Processing and Manufacturing: Session II

Sponsored by: The Minerals, Metals and Materials Society, TMS Materials Processing and Manufacturing Division, TMS/ASM: Computational Materials Science and Engineering Committee, TMS: Global Innovations Committee, TMS: Nanomechanical Materials Behavior Committee, TMS/ASM: Phase Transformations Committee, TMS: Powder Materials Committee, TMS: Process Technology and Modeling Committee, TMS: Shaping and Forming Committee, TMS: Solidification Committee, TMS: Surface Engineering Committee

Program Organizers: Corbett Battaile, Sandia National Laboratories; Amit Misra, Los Alamos National Laboratory; Joy Hines, Ford Motor Company; James Sears, South Dakota School of Mines and Technology

Tuesday AM Room: 281
March 11, 2008 Location: Ernest Morial Convention Center

Session Chair: To Be Announced

8:30 AM

Integrated Thermo-Magneto-Hydrodynamic Control of Bridgman Growth of Semiconductor Single Crystals: Nicholas Zabaras¹; Baskar Ganapathysubramanian¹; ¹Cornell University

The manufacturing of a semiconductor single crystal through the Bridgman process is a complex thermo-mechanical phase transition process. There have been significant advances in terms of enhancing the quality of the crystal by controlling the thermal and hydrodynamic processes during solidification. We will illustrate an integrated computational approach for the design and control of the solidification processes for producing high quality single crystals. This is based on a 3D simulator of the crystal growth process in the presence of an imposed magnetic field and varying thermal gradients. A 3D optimization problem is posed to design the temporal variation of the magnetic field and/or the imposed thermal gradients in order to achieve certain goals. These goals include maximizing the pulling rate, minimizing the thermal gradient imposed, as well as controlling the shape of the melt-solid interface.

8:55 AM

Application of a Multi-Physics Computational Model to the Casting of Actinide Metal: Paula Crawford¹; Deniece Korzekwa¹; Franz Freibert¹; Tarik Saleh¹; ¹Los Alamos National Laboratory

The casting of high purity plutonium metal is a process that is not well understood even after several years of study. The application of modern computer modeling and simulation techniques to materials processes can aid in providing valuable insight into the effects of process variables and mold design variations on the final casting product. Following this concept, a plutonium casting was prepared to produce parts of various thicknesses. The plutonium parts were examined and characterized in terms of microstructure, density, experimental cooling rates, etc. A computer model was developed to simulate the casting process using a multi-physics computational modeling package. Combining the results of the simulation with the experimental casting results should provide a better understanding of the effect of process variables on the casting of plutonium metal.

9:20 AM

Thermo-Mechanical Analysis of Continuous Casting with Reduction by Using Meshless Methods: Lei Zhang¹; Yiming Rong¹; ¹Worcester Polytechnic Institute

Meshless method can solve large deformation problem without re-meshing. An integrated analysis model of heat transfer and thermal stress based on meshless methods has been developed for continuous casting with mechanical reduction. The Finite Point Method is employed to build a thermal module. Solutions of the non-linear material properties and heat latent are given. The stress-strain analysis module is established based on the meshless Local Petrov-Galerkin method. The large deformation stress-strain is presented by Total Lagrange formulation, simultaneously the non-linear and contact problems are solved. Finally, the model is applied in the simulation of continuous casting slab.

Temperature distribution and cooling history of the slab was calculated. Thermal stress evolution in the mold and the mechanical reduction regions are evaluated. The result predicted is consistent with the values obtained by theoretical analysis. Successful solution of large deformation problem also shows the potential benefits of meshless methods to continuous casting simulation.

9:45 AM

Simulation-Based Integration of Rapid Solidification to Fatigue Prognostic Predictions Using Laser-Deposited High Strength Materials as an Example:

Paul Wang¹; Haitham El Kadiri¹; Mark Horstemeyer¹; Liang Wang¹; Gabriel Potirniche²; Sergio Felicelli¹; ¹Mississippi State University; ²University of Idaho

The goal of this research is to develop a set of simulation tools integrating thermal/solidification processes with fatigue prognostic models to demonstrate that predictive plasticity and ductility behavior of metallic materials shall be history dependent of upstream process steps. High strength materials made by laser engineering net-shaped (LENSTM) process were used as an example. To understand and be able to virtually predict the service performance of LENSTM components, i.e., ductility, fatigue, and fracture strength, three-dimensional computer-assisted X-ray tomography (CT), nano-indentor, EBSD and estimates of dislocation network become a set of vital characterization tools for measuring initial and as-deformed states of materials. At the macro-scale, an internal state variable constitutive theory representing plasticity and hardening behavior is adopted for its ability of tracing deformation history and incorporating structure-property relationships. Results of integration schemes through rapid thermal/solidification, the resulting microstructure state of phase transformation, and its connection to prognostic modeling are discussed.

10:10 AM Break

10:20 AM

Atomistic Scale Study on Effect of Pressure on Densification during Sintering Nano Scale Tungsten Powder: Amitava Moitra¹; Sungho Kim¹; Seong-Gon Kim¹; Seong Jin Park¹; Randall German¹; Mark Horstemeyer¹; ¹Mississippi State University

Pressure assisted sintering is a well-known metrology to enhance densification by increase in the contact pressure of particles and thus the driving force for sintering, compared to pressureless solid state sintering. The effect of pressure is getting more important during sintering of nano scale particles with electrical field. In this study, atomistic simulation is used to gain insight into the fundamental characteristics of atomic movement with and without pressure before sintering and during sintering. The presentation will focus on particle deformation before sintering, material softening at elevated temperatures, temperature and pressure sensitivities, and particle size effect. The findings have a potential for nanoscale processing modeling and its optimization.

10:45 AM

Modeling Methods to Guide Recycling Friendly Alloy Design: The Impact of Compositional Data Structure: Gabrielle Gaustad¹; Ray Peterson²; Randolph Kirchain¹; ¹Massachusetts Institute of Technology; ²Aleris International, Inc.

Recyclability is a context dependent materials property that has proven challenging to evaluate. However, previous studies by the authors have shown that certain modeling techniques, specifically chance constrained optimization, can provide a quantitative evaluation of recyclability. This information can be used to accelerate the evaluation and design of alloys (as well as products and operations) for improved recycling. One assumption in this work, however, is that the compositional variability of materials would be normally distributed. Previous work would indicate this may not be the case for all recycled materials. Performance, in terms of recyclability, may then be heavily influenced by the structure of the compositional data used. To test this, specific case studies involving several recycled material streams were investigated including both metals and non-metals. Results indicate that the underlying structure/distribution of the compositional data can have a profound effect on alloy design decisions to encourage usage of recycled materials.

11:10 AM

Heat Transfer Coefficient Study for Quenching by Experiment and CFD Modeling: Gang Wang¹; Lei Zhang¹; Qigui Wang²; Bowang Xiao¹; Yiming Rong¹; ¹Worcester Polytechnic Institute; ²Powertrain Engineering

Heat transfer coefficient is a key issue in quenching process, and the HTC values obtained directly from experiments are limited to evaluate/predict the quenching ability of real production due to the complicated flow and workpiece geometry. In this paper, CFD method is employed to simulate the heat transfer and flow in the loaded experimental apparatus, which is used to test the temperature and the heat transfer coefficient. The experimental local HTC values are verified and modified for the whole workpiece by studying the details of the simulated temperature, velocity and pressure from CFD modeling. The HTC database is furthermore generated, and extended to include more values calculated by CFD modeling of quenching experiment design under the adjustable variables, e.g. temperature and velocity, but without experiments. Finally, the HTC database is applied to simulate heat transfer in real quenching production and verified by the measurement.

11:35 AM

A Microstructure-Sensitive Design Approach for Controlling Properties of HCP Materials: Babak Kouchmeshky¹; Nicholas Zabarav¹; ¹Cornell University

A model reduction technique based on the proper orthogonal decomposition method is presented for modeling the microstructure evolution of HCP polycrystals including slip and twinning. The polycrystal is represented by an orientation distribution function using the Rodrigues parameterization. This model can be used for representation and fast exploration of process/structure/property relations in HCP polycrystals. Using this model, a number of microstructure-sensitive deformation design problems are addressed for the control of texture-dependent properties. A continuum sensitivity-based gradient optimization framework is introduced for computing the variability of the microstructure evolution induced by perturbations on the macroscale velocity gradient. Design of both single and multiple stage processes is considered. Finally, integration of the material point design simulator with a multiscale design framework will be shown demonstrating the design of macro-process parameters for the control of microstructure-sensitive properties.

Alumina and Bauxite: Equipment

Sponsored by: The Minerals, Metals and Materials Society, TMS Light Metals Division, TMS: Aluminum Committee

Program Organizers: Sringeri Chandrashekar, Rio Tinto Aluminium Limited; Peter McIntosh, Australus Management Services

Tuesday AM
March 11, 2008

Room: 296
Location: Ernest Morial Convention Center

Session Chair: Gajendra Singh, Alcan Engineering Party Ltd.

8:30 AM Introductory Comments

8:35 AM

Advanced Filtration Methods for Pregnant Liquor Purification: Reinhard Bott¹; Thomas Langeloh¹; Juergen Hahn¹; ¹Bokela GmbH

A new generation of backflush filters offers the possibility of improved pregnant liquor filtration. BOKELA have developed a continuous pressure filter of advanced mechanical and process design. The new designed and the specially arranged filter elements provide for high specific performance and large filtration area per vessel volume which exceeds status quo values. The new filter runs completely automated due to automatic and complete cake discharge and compared to the status quo technologies it provides for improved filter performance and operation with higher specific performance, improved filtrate clarity, higher concentrated solids discharge, improved mounting and lifetime of filter bags and lower idle times. Thus, the new filter offers the possibility of pregnant liquor filtration with improved performance, lower invest and operating cost. The lecture highlights modern demands on pregnant liquor filtration and presents design characteristics of the new backflush filter. Furthermore, future options of pregnant liquor filtration are discussed.

9:00 AM

Delivering World Class Digestion Energy Consumption at RTA Yarwun Alumina Refinery: Samantha Parry¹; ¹Rio Tinto Aluminum Yarwun

Community and shareholder awareness around environmental sustainability has increased industries accountability to deliver significant improvements in utilising energy more efficiently. The Greenfields development of the RTA Yarwun alumina refinery, commissioned in 2004, provided the opportunity to be world class in the alumina industry with respect to energy consumption through an innovative Digestion design. The Digestion tube design has demonstrated to be the most energy efficient for processing Weipa grade bauxite which is typically high in boehmite. The benefit of reduced water ingress, by eliminating the need for direct steam injection, translates to reduced plant evaporation requirements and boiler makeup water. The use of single stream also has the benefit of achieving a tighter balance between the energy required for slurry heating and energy generated by the flash vapour which sees very little excess steam generated by the blowoff system.

9:25 AM

Operational Experience with a Brownfield Expansion Project in Russia: Andreas Wolf¹; Peter Hilgraf¹; Arne Hilck¹; ¹Claudius Peters Projects GmbH

This paper describes the installation, experience and operational improvements made after one year of operation for a full scale installation at an aluminium Brownfield expansion project in a Russian Aluminium Smelter. The operational conditions and challenges on the equipment of the so-called "FLUIDCON" pneumatic conveying system, mass flow: 135 tph, conveying distance: 400m, feeding device: screw feeder, will be described in detail. The alumina pot-feeding system ADS (Aerated Distribution System) is engineered and installed for feeding alumina into two pot rooms with 168 electrolysis cells 300kVA each. This paper concludes technical papers presented on earlier TMS Annual Meetings: ¹New Aerated Distribution (ADS) and Anti Segregation (ASS) Systems for Alumina 2002. ²FLUIDCON - A New Pneumatic Conveying System for Alumina 2006. ³A New Alumina Distribution and Feeding System for Aluminium Reduction Cells 2007.

9:50 AM

MAX HT™ Sodalite Scale Inhibitor: Plant Experience and Impact on the Process: Donald Spitzer¹; Owen Chamberlain¹; Calvin Franz¹; Morris Lewellyn¹; Qi Dai¹; ¹Cytec Industries Inc

Development of a reagent to prevent sodalite scale formation in the Bayer process was presented at the 2005 TMS. Since that time this product has been run on many plants across the globe under various operating conditions and has demonstrated that it completely eliminates sodalite scale. This paper will cover the application experience gained and the benefits derived at the plants.

10:15 AM Break

10:30 AM

How to Achieve High Availability with Large Calciners and Avoid Unforeseen Downtime: Pekka Hiltunen¹; Cornelis Klett¹; Michael Missalla¹; Hans-Werner Schmidt¹; ¹Outotec GmbH

In the last 15 years, the largest available capacity for a new calciner has significantly increased. Large size calciners are being selected to both increase total refinery output and also to replace rotary kiln capacity. Factors that influence the decision to install these larger size calciners include reduced investment cost, operating costs and plant footprint per tonne of capacity. On the other hand, unforeseen downtime, particularly for large calciners can significantly jeopardize these anticipated savings and result in completely different economic outcomes: operating cost overruns and lost production. Parameters such as availability, operating factor, in relation to calciner capacity together with the hydrate filtration facility are identified. Operating data and the impact on production cost of unforeseen downtime based on existing calcination units are presented. Measures in areas such as design, construction, control, operation and maintenance are described to avoid unforeseen downtime during operation of the calcination facility.

10:55 AM

Customized Descaling Robots – Improving Worker's Health and Safety, Increasing Alumina Production Capacity: Éloïse Harvey¹; Antonio Pucci²; Claude Caya¹; Don Puxley²; ¹Mecfor; ²Alcan International

It is a fact that alumina production capacity decreases as residue builds up on a reservoir's shell; nevertheless, descaling operations are often delayed because of the necessary downtime required to perform this maintenance operation. The purpose of this paper is to highlight the many advantages of descaling a reservoir, such as a bauxite digester, with a remotely controlled descaling robot, rather than by installing scaffolding and having workers manually remove the scale with jackhammers. Through real-life case studies in Alcan's plants, we will establish that a descaling robot dramatically improves the worker's working conditions, considerably reduces the downtime required to perform this critical operation, and greatly improves production capacity. Furthermore, it will be demonstrated that the Alcan/Mecfor descaling robot is highly adaptable to a variety of reservoir configurations and sizes, and is designed to work with many descaling methods.

11:20 AM

Bauxite Filtration and Red Mud Filtration: New Challenges - Good Solutions: Reinhard Bott¹; Thomas Langeloh¹; Juergen Hahn¹; ¹Bokela GmbH

The continuous pressure filtration or hyperbaric filtration offers new solutions for bauxite and red mud filtration. When bauxite is transported to the refinery via pipeline and or when diasporic bauxite has to be treated before digestion it is milled and slurried with water for enabling pipeline transport or treatment. It has then to be dewatered to a moisture content below 14 wt%. Filter presses and belt filters need long cycle times and large filter areas to attain the required cake moisture. Continuous pressure filtration achieves the required cake moistures with large specific throughput what keeps filter area small. A first filter plant for dewatering of pipeline-transported bauxite has now started operation in Brazil. Red mud is washed and dried with Hi-Bar steam pressure filtration - the most modern variant of continuous pressure filtration - to moisture content of 21-23% which makes re-usage possible.

Aluminum Alloys: Fabrication, Characterization and Applications: Modeling

Sponsored by: The Minerals, Metals and Materials Society, TMS Light Metals Division, TMS: Aluminum Committee

Program Organizers: Subodh Das, Secat Inc; Weimin Yin, Secat Inc

Tuesday AM
March 11, 2008

Room: 293
Location: Ernest Morial Convention Center

Session Chairs: Subodh Das, Secat Inc; Weimin Yin, Secat Inc; Zhengdong Long, University of Kentucky

8:30 AM

Numerical Simulations of Texture Evolution in Polycrystalline Al during Channel Die Compression and Uniaxial Tensile Straining: Fan Zhang¹; Allan Bower¹; Raj Mishra²; ¹Brown University; ²General Motors Corporation

Finite element simulations are used to study the evolution of local and global texture during uniaxial tensile straining and channel die compression of a polycrystalline pure Al. The simulations predict the overall texture in the crystal as well as to track the evolution of the orientation of individual grains. Results are obtained as functions of relevant loading and material parameters, as well as temperature, and the predicted texture and orientation evolution are compared with published experimental data. The simulations predict overall texture evolution that is in agreement with experiment, but the rotation of individual grains in the specimen does not match experimental observations. To explore this discrepancy, we study the influence of material parameters, the initial orientation of the grain, and the orientation of surrounding grains on the evolution of orientation within a particular grain in the specimen.

8:50 AM

Numerical Simulations of Void Growth by Coupled Grain Boundary Sliding, Diffusion and Dislocation Creep During Elevated Temperature Deformation of Al AA5083: Ningning Du¹; Allan Bower¹; Paul Krajewski²; Eric Taleff³; ¹Brown University; ²General Motor Research and Development Center; ³University of Texas at Austin

Finite element simulations are used to calculate void growth rates in Al alloy AA5083 during uniaxial tensile straining at elevated temperature. The finite element model incorporates grain interior dislocation creep, grain boundary diffusion and grain boundary sliding mechanisms. The simulations are used to predict the influence of applied strain rate, grain size, void volume fraction and stress triaxiality on the void growth rate. In particular, we contrast the cavitation behavior in the grain boundary sliding and dislocation creep regimes. The results are found to be in good agreement with experimental observations of cavitation in AA5083.

9:05 AM

The Use of Experimentally-Based Material Models in Simulating High-Temperature Forming of Aluminum and Magnesium Sheet: Eric Taleff¹; Louis Hector, Jr.²; Ravi Verma²; John Bradley²; Paul Krajewski²; ¹University of Texas; ²General Motors R&D Center

High-temperature deformation of aluminum and magnesium sheet materials was investigated through experiments and simulations. Sheet materials were subjected to tensile tests and gas-pressure bulge tests at temperatures in the range of 450 to 500°C. Tensile test data over a range of strain rates were used to construct constitutive models of material behavior. Bulge tests were then simulated using a finite element methodology and these constitutive models. The results of the simulations were compared with bulge experiments. An experimentally-derived, two-term constitutive model based on creep phenomenology and experimental data was found to provide good agreement between simulations and experiments.

9:25 AM

Effect of Fe on Texture Evolution and Microstructures of the Cold Rolling AA5052 Alloy Sheets from Continuous Cast Processing after Anneal at Different Temperatures: Xiyu Wen¹; Yansheng Liu¹; Lirong Tong²; Tongguang Zhai²; Zhong Li³; Subodh Das¹; ¹Secat Inc.; ²University of Kentucky; ³Aleris International Inc.

Texture characters of the cold rolling AA5052 alloy with the two Fe levels were determined and studied by use of the orientation distribution function method. The microstructures were observed by use of optical and scanning electronic microscopes. The effect of Fe on texture and microstructures of the alloy from continuous cast processing after anneal at temperature from 450F to 900F was analyzed and discussed. It was found that Fe influence recrystallization texture components and microstructures of the aluminum alloy. When Fe is low level, the Cube component is more.

9:45 AM

Aluminum Plate Hot Rolling Process Modeling: Zhengdong Long¹; Yansheng Liu²; Randall Bowers²; Weimin Yin²; Shridas Ningilieri²; ¹University of Kentucky; ²Secat, Inc.

The hot rolling process plays a vital role in the microstructure, texture and tensile properties determination of the aluminum plate and sheet products. A multi-passes hot rolling process was simulated using the ABAQUS/Explicit algorithm. The heat transfer from the ingot to its environment and to the rollers as well as friction between the ingot and the rollers were defined. Industrial rolling parameters of ingot temperature, work roll rotation velocity, reduction rate, and initial ingot velocity were set as boundary conditions. A thermally coupled plain strain mesh type was used for the model. The flow stress as a function of plastic strain, strain rate and temperature was used in the material model. Temperature, plastic strain and stress evolution during the rolling process and its distribution along the through thickness direction were evaluated. The results indicate that the explicit dynamics approach produces a reliable solution for hot rolling simulations.

10:05 AM

Influence of Microstructure and Material Variables on Hemmability of Aluminum Alloys: *Rajesh Raghavan*¹; Pinaki Biswas¹; Raja Mishra¹; ¹General Motors Research and Development

The influence of material and microstructure on hemmability of aluminum sheets are investigated using finite element analysis. First, the three separate steps of flanging, prehemming and hemming along with springback analysis after each of the steps are performed using a homogeneous material model. Macroscopic stress-strain data as the only input failed to discriminate materials for their hemmability. Next, a substructure modeling is performed wherein second phase intermetallics are added as a microstructural input. It is shown that even single subsurface elastic particle alters local stress distribution dramatically. Large particles located close to the surface or a string of particles have the largest effect. Different materials with similar particles exhibit different local stress enhancements. Since particles can crack when the local stress exceeds a threshold value leading to micro-cracking, this points to the need for simultaneous optimization of material properties and microstructure to improve hemmability.

10:25 AM Break

10:35 AM

Calculating Behavior of 5xxx in Marine Service: *Catherine Wong*¹; ¹Naval Surface Warfare Center

5xxx aluminum alloys have long been used in Navy decks and bulkheads. Although the material is restricted to routine service below 65°C, deck temperatures on sunny days in southern latitudes can exceed this temperature. Thermocoupled 5xxx test specimens were situated on the flight deck and interior of the ONR research ship Seafighter in order to record the thermal profile seen by the material. 5xxx samples were thermally treated in furnaces with varying time and temperature followed by corrosion testing using ASTM G67 in order to develop the sensitization rates. The thermal profile and sensitization rates were combined to estimate the amount of sensitization to be expected on the Seafighter exposed specimens.

10:55 AM

Effect of Asymmetric Rolling on Texture and Anisotropy of AA6016 Alloy for Automotive Applications: *Linzhong Zhuang*¹; Menno van der Winden¹; ¹Corus Research, Development and Technology

Asymmetric rolling (ASR) was applied to aluminium alloy AA6016 with various circumferential velocity ratios between the top and bottom rolls. This gives rise to intense plastic shear strains, and in turn the shear deformation textures through the sheet thickness. The developed texture in asymmetrically rolled materials is weaker in comparison to that developed during conventional rolling. The recrystallization texture in asymmetrically rolled materials is also considerably weaker than that in conventionally rolled materials. With proper design of the ASR parameters, the shear deformation textures are still stable in recrystallized materials after SST. The presence of shear texture orientations significantly improves both the minimum r value and Δr value. Furthermore, with 25% ASR reduction and annealing, an average grain size is about 3 times smaller in comparison to that observed in conventionally rolled material.

11:15 AM

The Residual Stress Investigation in Al, Using β Particles Penetration Method: *Behrooz Salehpour*¹; H. Pirhoseinloo¹; M. Taheri Hashjin¹; ¹University of Tabriz

Investigation of residual stress, RS, in a work-piece of industrial equipments is one of the very important test to finding out the lifetime and reliability of that device. In this work we tried to trace-out RS in the industrial Aluminium (99.5%) by means of measuring the penetration range, R_p and absorption coefficient (μ) of energetic β particles in the samples. Where plates of Al with different thickness were exposed to thermo-mechanical induced stresses and amount of R_p and μ of β particles were determined using a conventional nuclear instrumentation way. Hence the values of μ and R_p for the stressed samples were compared with that of the stress free (annealed) samples. Experimental results show increasing of the penetration range, and/or lowering the absorption coefficient μ of β particles for the cases of stressed samples.

11:35 AM

Numerical Simulations of a New Local Hot Forming Process for Making Imprints in Aluminium Extrusions: *Hallvard Fjær*¹; Børge Bjørneklett²; ¹Institute for Energy Technology; ²Hydro Aluminium

A local hot forming method to fabricate imprints in closed aluminium extrusions has been developed. This forming method involves an interplay between an induction coil heating a defined region for a few seconds, and a ceramic tool pressed subsequently into the profile. The process combines high formability with low forming loads and it allows forming of profiles without internal tools. The shape of the work piece is determined both by the movement of the tools and by local variation in flow stress resulting from large thermal gradients. Simulating this process requires a thermomechanical model incorporating the effects of temperature, microstructure and strain rate on the flow stress. Numerical simulations can be applied to assess the feasibility of a local hot forming process and to identify improved design of tools and forming procedures. Results from numerical simulation of forming of triggers in crash boxes of aluminium are compared with measurements.

11:55 AM

Orientation Gradient Evolution in Precipitation Hardening Aluminum Alloys: *Reza Shahbazian Yassar*¹; Mark Horstemeyer²; David Field³; ¹Michigan Technological University; ²Mississippi State University; ³Washington State University

Development of sound physics-based plasticity models in precipitation hardening materials requires better understanding of the interaction between the nano-scale precipitates and orientation evolution of the individual grains. This investigation is concerned with characterization of in-grain orientation gradient as a function of precipitate characteristics. Several polycrystals of 6xxx series aluminum alloys containing hardening precipitates with different morphologies and characters were subjected to tensile deformation and dislocation structure evolution was investigated using high resolution electron backscatter diffraction and transmission electron microscopy. Local misorientation and geometrically necessary dislocation content were studied for various grains as a function of precipitate characteristics. It is found that precipitate characters affect the density and distribution of geometrically necessary dislocations as well as the misorientation boundaries within the grains.

12:15 PM

An Internal Variable Approach on Load Relaxation and Creep Transition Behavior of an Extruded Al-6061 Alloy: *Min Soo Kim*¹; Young Won Chang¹; ¹Pohang University of Science and Technology

The high temperature deformation behavior of an extruded Al-6061 alloy has been studied by using the load relaxation test and constant load creep test at temperature ranging from 300°C to 500°C. A series of load relaxation test has been carried out to obtain the flow curves. The change of strain rate sensitivity and creep transition of dispersion strengthened Al alloy were analyzed by using the internal variable theory proposed by Chang et al. The framework of the theory is built on the basis of well known dislocation dynamics to provide the concept of an internal strain tensor as the most fundamental deformation state variable. In addition, the constant load creep test was performed and the creep resistance of an extruded Al-6061 alloy was observed to enhance at the range of low strain rate and stress.

12:30 PM

Simulation of PLC-Effect in Al6061/Al₂O₃-Alloy: *Galina Lasko*¹; Ye. Ye. Deryugin²; S. Schmauder³; ¹Institut für Materialprüfung, Werkstoffkunde und Festigkeitslehre, Universität Stuttgart; and Institute of Strength Physics and Material Science, SB RAS; ²Institute of Strength Physics and Material Science, SB RAS; ³Institut für Materialprüfung, Werkstoffkunde und Festigkeitslehre, Universität Stuttgart

The instability of plastic flow in aluminium alloys in the form of PLC-Bands has attracted attention of scientific and metallurgical society. This is very extensively investigated and still less understood phenomenon. In the present contribution the attempt was made to investigate the mechanism of jerky flow in aluminium alloys by simulation of the evolution of the localized plastic deformation on mesoscopic scale level. The approach is based on the recently introduced and little known Relaxation element method. The unambiguous connection between the stress drop in the local volume of solid and plastic

deformation in it is on the basis of this method. Based on this method the model of evolution of plastic deformation operates on principle of cellular automata, where each grain is considered as a proper hexagon, which can be in two states-plastically and elastically deformed. The influence of the following parameter on the patterns of the plastic strain localization has been investigated: externally applied strain rate, rigidity of the machine, the value of Young's modulus of the material. The results of simulations are accompanied by experimental findings. The ways of further improvement of the model are discussed.

Aluminum Reduction Technology: Cell Development Part I and Operations

Sponsored by: The Minerals, Metals and Materials Society, TMS Light Metals Division, TMS: Aluminum Committee

Program Organizers: Martin Iffert, Trimet Aluminium AG; Geoffrey Bearne, Rio Tinto Aluminium Tech

Tuesday AM
March 11, 2008

Room: 298
Location: Ernest Morial Convention Center

Session Chair: Paul Hemburrow, NZAS - New Zealand Aluminium Smelters Limited

8:30 AM

Image Analysis for Estimation of Anode Cover Material Composition: *Jayson Tessier*¹; Carl Duchesne¹; Claude Gauthier²; Gilles Dufour²; ¹Laval University; ²Alcoa, Inc

Anode cover material, a mixture of secondary alumina and electrolytic bath, is used to cover newly set anodes and to fill crust holes following crust meltdown. However, maintaining a constant composition over time is difficult since bath mass balance, from a potroom point of view, must be respected. Alumina and bath, particulate products with different properties, are mixed together and delivered to pot-tending-machines or hoppers. Hence, uneven mixing and segregation are frequently encountered, resulting in important deviations from target composition. To follow these variations, a few grabbed samples are analyzed on a daily basis which is not enough to capture the composition variations. Nevertheless, this composition plays an important role in keeping a good crust integrity ensuring good productivity and low gas emissions. Image analysis is presented in this paper, to extract features from anode cover material images that are related to alumina composition. Methodology and monitoring results are presented.

8:50 AM

Impact of Alumina Fines Content on Potline Performance Ouro Preto Smelter: *Thiago Simões*¹; João Martins¹; Márcio Guimarães¹; João Costa¹; ¹Novelis

On the present paper we discuss the influence of alumina fines on pot performance and stability on HS Soderberg pots. The environment aspects are also taken into account; we discuss the challenge of compliance with the local environment agency requirements. Alumina size is an essential characteristic to be analyzed in the raw material of the primary aluminum production process. The presence of considerable quantity of fine particles – 325# screen undersize – generates a series of problem in potlines. Alumina fines play an important role in order to achieve process performance; operational results and environment can be seriously charged by changes in alumina fines. Supported by statisticals tools an evaluation is done to better understand the influence of alumina fines in the process.

9:10 AM

Expansion of the Potline in Svalco: *Marvin Bugge*¹; Milos Koniar²; Kamil Skladan²; Milan Stas²; ¹Hydro Aluminium; ²Svalco

The reduction technology in Svalco, HAL230, was developed in the 80's. The potline was started at 230 kA in 1995. The amperage in the potline was gradually increased to 250 kA before the start up of the expansion in July-August 2003. The 54 expansion pots were started in 5 weeks at 250 kA. In the expansion several technical changes were introduced. The busbar system was improved, a new potshell was designed and new pot control, HAL3000, was applied. New

types of cathode blocks were selected in cooperation with the cathode block suppliers. After 4 years of operation the expansion pots show good results with high current efficiency, low energy consumption and low anode effect frequency. The amperage in the potline has been increased to 258 kA. No expansion pot has been relined so far.

9:30 AM

FECRI Approach and the Last Development of AP3X Technology: *Serge Despinasse*¹; Claude Ritter¹; Renaud Santerre¹; Thierry Tomasino¹; *Oliver Martin*¹; ¹Alcan

More than 3800 AP30 cells are presently operating in the world, 1500 additional AP30 cells will start in the coming years. In order to continuously improve the AP30 technology, Alcan has launched an intensive technology development program. The aim of the program is to push the amperage in the range 350-400 kA and to reduce specific energy consumption below 13000 kWh/t. In addition Alcan has started in January 2005 an internal project targeting a significant reduction of the full economic cost for a new smelter: the Full Economic Cost Reduction Initiative (FECRI). This article describes the operational tests allowing bringing the AP3X above 350 kA and the last improvements made in the modelling of the AP30 cell, especially the coupling between thermic and MHD. It shows great economical benefits resulting from FECRI for the future smelters.

9:50 AM

The Alcan's P155 Technology Cells Now Operating at 195 Ka. a Successful Asset Optimization Strategy: *Patrice Desrosiers*¹; Louis Lefrançois¹; Bruno Gaudreault¹; *Claude Richard*¹; ¹Alcan

Alcan started up its first Alcoa P155 technology potlines in 1980. During the 80's and 90's, Alcan improved both operational practices and computer control logic at its three P155 smelters resulting in a current efficiency increase of 3 % as well as a significant decrease of the anode effect frequency, therefore the PFC emissions. With a much more robust cell operation and benchmark performances, Alcan undertakes in 2001 an intensive technology development program aiming at increasing the amperage as well as reducing the specific energy consumption while maintaining excellent current efficiency and low emissions performances. This article describes the operational tests allowing the amperage increase up to 195 kA as well as the main results at this amperage level. In addition to provide excellent technical performances, the P155 HALE program (High Amperage Low Energy) was a successful low cost creeping program resulting in a low investment and operating cost project.

10:10 AM Break

10:20 AM

An Automated Metal Purity Optimization System for Enhanced Revenue Capture: *Jason Lodzik*¹; Doc Murdoch²; Michael Van Hauwermeiren³; ¹Century Aluminum; ²Crystal Ball (Oracle); ³Vose Consulting

A project recently undertaken at the Century Aluminum reduction facility in Hawesville will increase metal sales revenue with a more efficient capture and sale of premium grade metal. Crystal Ball was utilized because of its optimization and adaptability capabilities. The project required a user-friendly automated application that could satisfy several constraints while easily altering goals based on changing market or plant conditions. Tests have proven a more consistent and optimal use of available purity metal has increased the premium metal stream from the potroom. Opportunities gained by an automated optimization tool come from eliminating human error, inaccurate inputs, and paper work. The optimization strategy must operate with a large number of physical constraints which creates a considerable level of discontinuity when compared to basic linear problems. The automated blending system has been developed and implemented in four purity lines. Key issues and findings from this project are described in detail.

10:40 AM

Design Enhancements to GP320 Technology at Balco: *J. Ramaswamy*¹; C. Sukumaran¹; Gude Narendra Kumar¹; ¹Bharat Aluminum Company

Bharat Aluminium Company Ltd (BALCO) is part of the Vedanta Resources Plc. BALCO, located in Korba district of Chhattisgarh State, India has enhanced its production capacity from 135000 tpa to 385000 tpa by constructing a state of art 320 kA prebaked pot line with 288 cells. In GAMI technology, if the

Anode Beam-to-Beam aluminium welding plates for distribution of current or compensating bus bar gets damaged, the pot is cut off from the pot line circuit. To avoid this authors have designed a temporary bus bar connections, which can be fitted in the pots without cutting out the pot, till the rectification is done. In GAMI technology, to cut out a pot, complete power outage is required. The authors have developed a technical procedure, by which the pots are being cut out at full line load, without any reduction in the line current.

11:00 AM

Improvement in Pot Life by Operational Stability at MALCO VSS Smelter:

Vasanth Kumar Rangasamy¹; Muthukumar Ponnusamy¹; ¹Madras Aluminium Company (MALCO) Ltd.

Cell house life decides both Primary Aluminum production and quality in any Smelter worldwide and in particular VSS technology, which in nature is prone to many operational difficulties. At MALCO with VSS technology, we have improved the pot life from 1470 days to 2300 days over a period of years, by continuous improvement in operating parameters and practices. Also we are running Line-1 pots without any stoppage for the past 400 days. With this increased pot life, a substantial gain in productivity is obtained which ultimately reduced our COP. This paper describes the changes made in Pot operating parameters, MHD study implementation, Electronic pot controller (EPC) and cathode material selection, which altogether have contributed for the increase in pot life.

11:20 AM

The Continuous Development of Sami's SY300 Technology:

Zhu Jia Ming¹; Yang Xiao Dong¹; Liu Ya Feng¹; ¹Shenyang Aluminum and Magnesium Engineering and Research Institute (SAMI)

The first SY300 potline began operation in June 2002 in HeNan province. Today, there is a total of thirteen SY300 potlines in operation in China. In the past five years, SAMI has made vast improvement and continuously optimizing its SY300 technology. This paper describes features of the SY300 technology with focus on cell design, pot data and process control. Major developments made in the technology and the performance of a SY300 potline operating at 335kA will also be discussed.

11:40 AM

Increase of Amperage at Sayanogorsk Aluminum Smelter:

Alexander Krasovitsky¹; Oleg Burkatsky¹; Victor Buzunov¹; Victor Mann¹; ¹United Company «Russian Aluminum»

In order to increase metal production in an operating area starting in 2001 until 2006 specialists of RUSAL Company's Sayanogorsk Aluminum Smelter and The Engineering and Technology Center have successfully realized a package of measures which facilitated an increase in the smelter's average amperage from 208.3 to 248.5 kA. Among these measures are: 1. mathematical modeling of the feasibility of an amperage increase for operating cell designs and finding ways to stabilize heat balance and MHD stability, 2. improved practice of forming and maintaining the anode carbon cover, 3. altered anode setting patterns, 4. evaluation of process capability of the potrooms to increase amperage, 5. upgrading of busbar of potline 4, and several other measures. The Amperage increase resulted in an increased output of the Sayanogorsk Smelter from 405,800 tons to 521,600 tons per year.

12:00 PM

Anode Signal Analysis: The Next Generation in Reduction Cell Control:

Jeffrey Keniry¹; Eugene Shaidulin²; ¹Alumination Consulting Ltd; ²Russian Engineering Company, Engineering and Technology Centre

Reduction cells have achieved excellent control capability over the past 20 years by improved acquisition and treatment of the cell resistance signal, which provides the basis for regulation of alumina feeding, thermal balance and cell stability. As cells become larger in size however, there is an increasing need for control sensors that can recognize and react to spatial variation in the cell both in terms of anode performance and alumina feed control. Monitoring of individual anode current signals can provide the 'next generation' control capability that will be necessary to ensure that very large cells can deliver the same process efficiencies as their smaller predecessors. Coincidentally, anode signals can now be acquired, stored and processed with far greater convenience and lower cost than was possible in the past, making an enhanced control capability within practical reach.

Biological Materials Science: Bioinspired Design and Processing

Sponsored by: The Minerals, Metals and Materials Society, TMS Structural Materials Division, TMS: Biomaterials Committee, TMS/ASM: Mechanical Behavior of Materials Committee

Program Organizers: Ryan Roeder, University of Notre Dame; Robert Ritchie, University of California; Mehmet Sarikaya, University of Washington; Lim Chwee Teck, National University of Singapore; Eduard Arzt, Max Planck Institute; Marc Meyers, University of California, San Diego

Tuesday AM

March 11, 2008

Room: 390

Location: Ernest Morial Convention Center

Session Chair: Marc Meyers, University of California, San Diego

8:30 AM Keynote

Designing Hard Tissue by Genetic Knock-In Approaches:

Malcolm Snead¹; Y. P. Lei¹; W. Luo¹; P. Bringas, Jr.¹; S. N. White²; M. L. Paine¹; ¹University of Southern California, Center for Craniofacial Molecular Biology; ²University of California, Los Angeles

Enamel covers the teeth. Enamel is the hardest tissue in the vertebrate body, containing the longest biologically produced HAP crystallites. Enamel is the only ectoderm-derived tissue to biomineralize and unlike bone, contains no collagen and does not remodel. Enamel must be formed properly for it to survive a lifetime of mastication, in a wet, bacterial-laden environment. Ameloblasts are the cells that fabricate the enamel tissue, producing a tissue with unique materials properties under conditions amenable to life. Amelogenin is the dominant protein of forming enamel. Enamel tissue starts life during late gestation as a 100% protein matrix that undergoes self-assembly in the extracellular space to form a device capable of directing its own replacement by the mineral phase. Amelogenin contains highly conserved domains, suggesting their role during enamel biomineralization. Using protein engineering in vitro, we show the importance of these domains to self-assembly. We use homologous recombination technique to eliminate the native amelogenin gene, replacing it with engineered protein confirming the importance of these conserved domains to enamel biomineralization in vivo. We reduce the complexity of amelogenin protein isoforms used to biosynthesize a suitable enamel extracellular matrix, suggesting strategies for producing an enamel biomimetic. Supported by NIH, National Institute for Dental and Craniofacial Research.

9:10 AM Invited

Enzymatic Control of Biomineralizing Interfaces: Structuring of Mollusc Shells via Myosin-Dependent Chitin Synthesis:

Ingrid Weiss¹; ¹University of Regensburg

The multifunctional transmembrane structure of the mollusc myosin chitin synthase opens new horizons to explain various mollusc shell microtextures. Chitin self-assembly provides a dynamic extracellular biomineralization interface. Phase transitions that the chitin undergoes during enzymatic polymerization are likely to be monitored by the shell forming epithelial cells of the mollusc mantle tissue via their cytoskeleton. The mollusc myosin chitin synthase is thus identified as an outstanding key player in the cross-talk between mechano-chemical cell signaling, extracellular polymer self-assembly, mineralization, and the control of biomineralization related gene expression. Our current research indicates that supramolecular myosin chitin synthase arrays provide an effective and highly sensitive trans-cellular control mechanism. It can be speculated that the mollusc chitin synthase also bears a tremendous potential to contribute in both ways, enzymatically and via signaling pathways to the implementation of hierarchical patterns into chitin mineral-composites such as prismatic, nacre, and crossed-lamellar shell types.

9:40 AM

Mimicking Bone Formation via a Polymer-Induced Liquid-Precursor (PILP) Process:

SangSoo Jee¹; Laurie Gower¹; ¹University of Florida

The intrafibrillar mineralization that is achieved during bone formation has eluded scientists who seek to duplicate this nanostructured architecture using conventional synthetic techniques. We have been able to achieve intrafibrillar

mineralization using a polymer-induced liquid-precursor (PILP) process, in which acidic polypeptides transform the solution crystallization process into a precursor process by sequestering ions and generating liquid-liquid phase separation within the crystallizing medium. This fluidic mineral precursor can be drawn into the gaps of the collagen fibrils by capillary forces. Once the collagen is infiltrated with mineral precursor, the amorphous phase crystallizes, leaving the collagen fibrils embedded with HA nanocrystals. SAED and DF-TEM and selective etching studies reveal the interpenetrating structure of the mineral-collagen composite, which has a strikingly similar appearance to natural bone. We are currently examining biomaterials applications for the fabrication of synthetic bone graft substitutes which can replace the need for autograft and cadaver bone substitutes.

10:00 AM

Peptide Hydrogels for Cell Delivery: Lisa Haines-Butterick¹; Daphne Salick¹; Darrin Pochan²; Joel Schneider¹; ¹University of Delaware, Department of Chemistry and Biochemistry; ²University of Delaware, Department of Material Science and Engineering

Hydrogels are hydrated materials finding use in tissue regeneration efforts. The design of "smart" peptides that undergo sol-gel phase transitions in response to biological media enable minimally invasive delivery of extracellular matrix substitutes in-vivo. Towards that goal, we have designed a family of peptides that undergo triggered self-assembly to form a rigid hydrogel. When dissolved in aqueous solutions, these peptides exist in an ensemble of random coil conformations rendering them fully soluble. The addition of an exogenous stimulus results in peptide folding into β -hairpin conformation. This folded structure undergoes rapid assembly into a highly crosslinked hydrogel network whose nanostructure is defined and controllable. Peptides can be designed to fold and assemble in response to changes in pH or ionic strength, the addition of heat or even light. In addition to these stimuli, cell culture media is able to initiate gelation. When hydrogelation is triggered in the presence of cells, gels become impregnated with cells. A unique characteristic of these gels is that when a shear stress is applied, the gel will shear-thin. However, after the application of shear has stopped, the low viscosity gel quickly self-heals producing a gel with a mechanical rigidity nearly identical to the original hydrogel. This attribute allows gel/cell constructs to be delivered to target tissues via syringe where they quickly recover complementing the shape of the tissue defect. Gels are cytocompatible towards NIH 3T3 murine fibroblasts, mesenchymal stem cells, chondrocytes, osteoblasts and hepatocytes. As an added bonus, MAX1 hydrogels possess broad spectrum antibacterial activity suggesting that adventitious bacterial infections that may occur during surgical manipulations can be greatly reduced.

10:20 AM Break

10:30 AM Invited

Molecular Design of Peptides for Materials Assembly Using Genetic Engineering: Candan Tamerler¹; Mehmet Sarikaya²; ¹Istanbul Technical University; ²University of Washington

High selectivity and precise organization in biological systems lead to control of functions, in particular mechanics. Biological molecular building blocks, in particular proteins, in addition to lipids and polysaccharides, play a major role in biological design for controlled assembly of materials from the nanometer to the macroscale. In a cross-disciplinary approach at the confluence of materials and molecular biology, we utilize peptides as molecular building blocks in synthesizing, assembling, and fabricating materials systems for applications in engineering and medicine. Here, we first genetically select and then tailor inorganic binding peptides towards specific functions, as molecular linkers, couplers and growth modifiers. Using computational and experimental tools we study peptide molecular recognition of solids, kinetics of their binding and assembly. Here we describe molecular mechanical stability of engineered polypeptides in nano/nanobiotechnology with examples that include: i. Inorganic biofabrication through synthesis; ii. Molecular thin films iii. Molecular couplers. Supported by NSF/MRSEC-BioMat, TR-SPO programs.

11:00 AM Invited

Biomimetic Materials Processing: Osamu Takai¹; ¹Nagoya University

Living organisms produce a wide variety of materials at room temperature and atmospheric pressure. Moreover, each material produced plays a key role in each function in biological systems. Biomimetic materials processing

(BMMP) is defined as the design and synthesis of new functional materials by refining knowledge and understanding of related biological products, structures, functions, and processes. Hence BMMP is not a simple imitation of biological materials processes, but is advanced materials processing for bionics, electronics, photonics, mechanics, magnetism, medicine, and so on. BMMP, therefore, is closely related to nanotechnology and by using BMMP we can make a new nanotechnology named "biomimetic nanotechnology" which is based on lessons from nature. We are developing transparent ultra water-repellent surfaces imitating lotus leaves, three-dimensional cell cultures using ultra water-repellent surfaces, site-selective cell cultures using hydrophobic-hydrophilic patterning, and SAM (self-assembled monolayer) processing for nano/micro fabrications.

11:30 AM

A Paradigm for the Integration of Biology into Materials Science and Engineering: Ryan Roeder¹; ¹University of Notre Dame

The integration of biology and disciplines such as materials science can be complicated by the lack of a common framework and language for synthesizing the diversity of thought and expertise of those trained in otherwise disparate disciplines. History may offer a valuable lesson as modern materials science and engineering itself resulted from the integration of traditionally disparate disciplines that were delineated by classes of materials – metals, ceramics and polymers. The integration of metallurgists, ceramists and polymer scientists into materials science was facilitated in large part by a unifying paradigm based upon processing-structure-property relationships that is now well accepted. Therefore, a common paradigm might also help unify the vast array of perspectives and challenges present in the field of biomaterials. The traditional materials engineering paradigm was modified to account for the adaptive and hierarchical nature of biological materials. Various examples of application to research and education will be considered.

11:50 AM Invited

Biomaterials Funding at NSF (DMR Biomaterials Program): David Brant¹; ¹National Science Foundation

The NSF Division of Materials Research (DMR) initiated a new Biomaterials program (BMAT) in 2006 to support fundamental research on bio-derived, bio-inspired, biomimetic, and biocompatible materials. This talk will describe the kinds of proposals BMAT received and funded during the initial (2007) funding cycle. Any trends or changes in the BMAT program evident at the time of the Symposium will be reported.

12:20 PM Question and Answer Period

Bulk Metallic Glasses V: Structures and Modeling I

Sponsored by: The Minerals, Metals and Materials Society, TMS Structural Materials Division, TMS/ASM: Mechanical Behavior of Materials Committee

Program Organizers: Peter K. Liaw, University of Tennessee; Wenhui Jiang, University of Tennessee; Guojang Fan, University of Tennessee; Hahn Choo, University of Tennessee; Yanfei Gao, University of Tennessee

Tuesday AM
March 11, 2008

Room: 393
Location: Ernest Morial Convention Center

Session Chairs: Takeshi Egami, University of Tennessee; Brett Conner, US Air Force, Office of Scientific Research

8:30 AM Keynote

Atomistic Mechanism of Relaxation and Deformation in Metallic Glasses:

Takeshi Egami¹; ¹University of Tennessee

The mechanism of mechanical deformation and relaxation will be discussed from the atomistic point of view. The majority of the experimentalists working on metallic glasses use the free-volume theory. In the field of liquids and glasses, on the other hand, the main-stream theory today is the energy landscape theory. Both of them are essentially phenomenological theories, in the sense that the parameters in the theory cannot be directly computed from the first-principles. Thus the connection of these theories to the microscopic reality is not totally clear. What we need is a theory for the intermediate steps that link these theories

to atomistic processes. While this is a challenging problem since metallic glasses are atomic glasses, they may be simple enough to allow some progress. We discuss the theory of topological fluctuations in the atomic connectivity network that may shed some light into this difficult problem.

9:00 AM Invited

Anomalies in the Thermophysical Properties of Undercooled Glass-Forming Alloys: *Robert Hyers*¹; Jan Rogers²; Kenneth Kelton³; Anup Gangopadhyay³;

¹University of Massachusetts; ²NASA Marshall Space Flight Center; ³Washington University

The surface tension, viscosity, and density of several bulk metallic glass-forming alloys have been measured using non-contact techniques in the electrostatic levitation facility (ESL) at NASA Marshall Space Flight Center. All three properties show unexpected behavior in the undercooled regime. Similar deviations were previously observed in titanium-based quasicrystal-forming alloys, but the deviations in the properties of the glass-forming alloys are much more pronounced. New results for anomalous thermophysical properties in undercooled glass-forming alloys will be presented and discussed.

9:20 AM Invited

Shear Banding in Metallic Glasses as Investigated through Atomic-Scale Simulation: *Michael Falk*¹; ¹University of Michigan

Recent simulations of shear banding in metallic glasses reveal the structural changes that accompany plastic deformation and localization. We have simulated 2D and 3D systems in nanoindentation,^{1,2} uniaxial tension³ and compression⁴ in plane strain. The degree of localization depends on the quench rate, with localization only arising in more gradually quenched samples. A systematic analysis of simulated systems in simple shear geometries⁵ reveals a Boltzmann-like relationship between strain rate and structure over eight orders of magnitude in strain rate. The consequences of this scaling for constitutive models of glass plasticity will be discussed. ¹Y. Shi and MLF, App. Phys. Lett., 86, 011914 (2005). ²Y. Shi and MLF, Acta Mat., 55, 4317 (2007). ³Y. Shi and MLF, PRL, 95, 095502 (2005). ⁴Y. Shi and MLF, PRB, 73, 214201 (2006). ⁵Y. Shi, M.B. Katz, H. Li and MLF, PRL, 98, 185505 (2007).

9:40 AM Invited

Shear Band Thermal Profiles in Metallic Glasses: *Daniel Miracle*¹; Yi Zhang²; Lindsay Greer²; Reza Yavari³; ¹US Air Force; ²University of Cambridge; ³Institut National Polytechnique de Grenoble

The characteristic temperatures, times and spatial dimensions of a moving shear band are expected to exert a profound influence on the mechanical behaviour of metallic glasses, and are a topic of active debate. Only limited experimental measurements are available, which typically suffer from spatial and temporal resolution that masks important features. The results of a thermal diffusion analysis for the calculated thermal profile behind a moving shear band will be presented and discussed, along with the importance of the boundary conditions used for the calculations. These profiles will be compared with recent experimental measurements. Relevant microstructural and sample length scales arise from coupling of characteristic dimensions of the thermal profiles. These length scales will be introduced and discussed.

10:00 AM

Correlations between Nearest Neighbor Bond Energy and Glass Forming Ability in Metallic Glass Forming Systems: *James Dahlman*¹; Daniel Miracle¹;

¹Air Force Research Laboratory

Experimental evidence has demonstrated the tendency for metallic glass systems to form structures with a high degree of short range order. Ordering amongst nearest neighbors indicates the presence of an underlying thermodynamic criteria, as interatomic bond strength largely governs nearest neighbor interactions. In particular, earlier empirical guidelines suggest that the heat of mixing exerts a strong influence on glass stability. However, previous work has failed to show a correlation between the heat of formation and glass forming ability. This work seeks to establish a connection between nearest neighbor bond energy and glass-forming ability through evaluation of bond energies and the heat of formation for a range of metallic glass forming systems.

10:15 AM Invited

Entropic Contribution to Glass Stability Based on the Pair Distribution Function: *Donald Nicholson*¹; ¹Oak Ridge National Laboratory

Increased entropy is frequently cited as one of the reasons that bulk metallic glasses are usually multicomponent. However, competing phases such as solid solutions would seem to have identical entropic contributions based on the regular solution model thus undermining the entropic argument for improved glass stability. The Wallace formula for the entropy in terms of the pair distribution function shows that there are terms beyond regular solution theory that can contribute to stability. Although experimental and calculated pair distributions decline in reliability as a function of distance the short range contributions to the entropy can indicate entropic contributions to stability. These contributions will be described for FeZrB, CuZrPd, and AgGa systems. Research sponsored by the Division of Materials Sciences and Engineering, Office of Basic Energy Sciences, U.S. Department of Energy, under Contract DE-AC05-00OR22725 with UT-Battelle, LLC.

10:35 AM Break

10:40 AM Invited

Nucleation Issues in Metallic Glasses: *James Morris*¹; ¹Oak Ridge National Laboratory

A key issue in glass formation is the competing process of crystal nucleation. Metallic glasses are ideal systems for examining this process, and for testing theory and simulation. These issues will be reviewed, including recent work on nucleation simulations and the comparison with classical nucleation rates. In metallic glasses, the role of chemical composition is particularly of interest. When the nucleating phase has a different composition than the amorphous matrix, classical nucleation theory is shown to be inapplicable, as diffusive dynamics must be considered. Nevertheless, calculations based on critical nuclei energetics may be useful. Even when the stable phase has the same composition as the amorphous matrix, metastable phases may form during devitrification; again, chemical flow plays an important role. This research has been sponsored by the Division of Materials Sciences and Engineering, Office of Basic Energy Sciences, U.S. Department of Energy under contract with DE-AC05-00OR-22725 with UT-Battelle.

11:00 AM Invited

Atomic Level Characterization of the Devitrification Path of a Zr_{52.5}Cu_{17.9}Ni_{14.6}Al₁₀Ti₅ Bulk Metallic Glass: *Michael Miller*¹; Xun-li Wang¹; David Larson²; Robert Ulfig²; ¹Oak Ridge National Laboratory; ²Imago Scientific Instruments

Atomic level characterization methods are required to establish the earliest stages of devitrification of bulk metallic glasses. The application of laser-assisted field evaporation has enabled zirconium-based bulk metallic glasses to be reliably characterized in the three-dimensional atom probe. The recent introduction of energy compensation to wide field-of-view three-dimensional atom probes has significantly improved the mass resolving power and lowered the background noise. A new local electrode atom probe equipped with these improvements in conjunction with small angle X-ray scattering experiments and differential scanning calorimetry have been used to study the initial stages of the devitrification path of a Zr_{52.5}Cu_{17.9}Ni_{14.6}Al₁₀Ti₅ bulk metallic glass. Research at the Oak Ridge National Laboratory SHaRE User Facility was sponsored by Basic Energy Sciences, U.S. Department of Energy.

11:20 AM Invited

Molecular Dynamics Simulation of Mechanical Properties of Cu-Zr Amorphous Alloys: *Mikhail Mendelev*¹; David Rehbein¹; Ryan Ott¹; Matthew Kramer¹; Daniel Sordet¹; ¹Ames Laboratory

We will present a new many-body potential for simulating the structure and mechanical properties of Cu-Zr amorphous alloys. As a first test of the potential we determined the bulk and Young's moduli of the Cu-Zr alloys for comparison with values found from ultrasound measurements. While the simulation underestimates the acoustic velocities by ~10%, it does correctly predict that this quantity increases with increasing Cu concentration. Analysis of the structural changes reveals that Zr-Zr pair-correlations are affected by an applied stress more strongly than the Cu-Cu and Cu-Zr pair-correlations. Additionally, we simulated the elastic-plastic response for a bi-axially deformed Cu-Zr amorphous alloy. The obtained stress – strain relationship was found to be consistent with our

experimental data. The structural changes accompanying this deformation will be discussed in the end of the talk. Work at Ames Laboratory was supported by Department of Energy, Office of Basic Energy Sciences, under Contract No. DE-AC02-07CH11358.

11:40 AM

Experimental and Computational Investigations of Structural Changes Associated with Deformation of Bulk Metallic Glasses: *Ashwini Bharathula*¹; Weiqi Luo¹; Katharine Flores¹; Wolfgang Windl¹; ¹Ohio State University

Bulk metallic glasses exhibit a number of unique capabilities, including excellent mechanical behavior combined with unusual processability in the supercooled liquid regime. In the present study, we examine the structural changes associated with the homogeneous flow of Zr_{58.5}Cu_{15.6}Ni_{12.8}Al_{10.3}Nb_{2.8} (nominal at%) bulk metallic glass over a range of strain rates at temperatures above and below the glass transition. Mechanical testing was performed on a high resolution electro-thermo-mechanical test frame, and structural changes were investigated via SEM, TEM, DSC, and positron annihilation spectroscopy. Experimental results for this complex alloy are discussed in light of a molecular dynamics study of deformation in a simpler binary glass subjected to simulated mechanical loading modes including tension, compression and shear. Based on the fluctuations of the electron density distribution in the structure, evolution of low atomic density regions with flow is analyzed. These results are compared and contrasted with a hard-sphere model.

11:55 AM

First-Principles Calculations of Shear Bands in Zr-Based Bulk-Metallic Glasses: *Ning Ma*¹; Bruce Kang¹; G. Wang²; Peter Liaw²; ¹West Virginia University; ²University of Tennessee

Bulk-metallic-glass (BMG) materials, due to their great strength and corrosion resistance, have attracted much research interest. However, these materials are usually brittle because they lack the dislocation-flow systems and only respond to the external stress by forming and propagating shear bands. The understanding of the mechanisms and characteristics of shear banding is of crucial importance to plasticity-improvement efforts. Shear bands are areas of high local stresses where the chemical environment is vastly different from their bulk amorphous counterparts. Empirical potential methods are, therefore, inadequate to describe the complicated structures and the chemical complexity within the shear bands. Using a first-principles tight-binding package, we simulated shear-band formation in Zr-based BMGs. Structural, thermal, and mechanical properties are analyzed within and outside shear bands. In addition, we studied the electronic structures and properties of chemical bonds, which may provide a mechanistic understanding of shear-band formation and the associated mechanical properties.

12:10 PM Invited

Novel Applications of Metallic Glass Composites Using Their Functional Properties: *Nobuyuki Nishiyama*¹; Nozomu Togashi¹; Yasunori Saotome²; Akihisa Inoue³; ¹Research and Development Institute of Metals and Composites for Future Industries; ²Tohoku University, Institute for Materials Research; ³Tohoku University

Metallic glasses (MGs) generally exhibit superior mechanical properties such as high-strength, low Young's modulus and high elastic elongation limit. These excellent mechanical properties are used for production of prototype industrial products. For instance, precision MG gear parts for micro geared motor and MG diaphragms for pressure sensor are successfully developed and these products exhibit an outstanding performance due to unique mechanical properties. In a few years, some applications will be on the market. This fact encourages further progress of fundamental researches and industrial developments. Unfortunately, there are several issues that have to solve among industries. That is, lack of plastic elongation under tensile load, high electrical resistivity or only exhibiting soft magnetic properties. If the issues could be solved, applications of MG will be drastically broadened. In this paper, we propose the way to solve the issues by applying MG composites and novel applications of MG composites will be discussed.

12:30 PM Invited

Alloy Design for Zr-TM-Al (TM: Co, Ni, Cu) Bulk Glassy Alloys: *Y. Yokoyama*¹; T. Yamasaki²; Peter K. Liaw³; A. Inoue¹; ¹Tohoku University, Institute for Materials Research; ²University of Hyogo, School of Engineering; ³University of Tennessee

With the aim to locate the key for designing useful bulk glassy alloys, the mechanical and thermal properties were examined in different component and composition of ternary Zr-TM-Al (TM: Cu, Ni or Co) alloys. The intrinsic mechanical-properties change with the component and composition, which result in the glass structural or atomic-bonding change, shows high correlation coefficients with some thermal-properties change. As a result, the glass-transition temperature has large positive correlation coefficients with Young's modulus and Vickers hardness. The liquidus surface temperature has large negative correlation coefficients with the Charpy impact value, fracture strain, and volume-change ratio due to the structural relaxation. Based on the systematic analyses between the thermal and mechanical properties, we found that the relationship between the Young's modulus and volume-change ratio reveals the suitable guide for the design of glassy alloys. By using this guide, we suggested that hypoeutectic bulk-glassy alloys exhibit significant resistance against the structural-relaxation embrittlement, and noble-metal-added Zr-Cu-Al bulk-glassy alloys exhibit extremely high fatigue limits.

Carbon Dioxide Reduction Metallurgy: Mechanisms

Sponsored by: National Materials Advisory Board, Metallurgical Society of the Canadian Institute of Mining Metallurgy and Petroleum, The Minerals, Metals and Materials Society, American Iron and Steel Institute, TMS Light Metals Division, TMS Extraction and Processing Division, TMS: Reactive Metals Committee, TMS: Recycling and Environmental Technologies Committee
Program Organizers: Neale Neelameggham, US Magnesium LLC; Masao Suzuki, Al Tech Associates; Ramana Reddy, University of Alabama

Tuesday AM
March 11, 2008

Room: 294
Location: Ernest Morial Convention Center

Session Chairs: Ray Peterson, Aleris International Inc.; Mahesh Jha, US Department of Energy

8:30 AM Introductory Comments by Neale Neelameggham, Organizer

8:35 AM Keynote

From the Manhattan Project to Global Warming: *Meyer Steinberg*¹; ¹Brookhaven National Laboratory (Retired)

Some early experiences of a Cooper Union Chemical Engineer on the Manhattan project and his latest studies on CO₂ Greenhouse Gas Mitigation Technologies will be presented. Mitigating the Global Greenhouse effect while maintaining a fossil fuel economy, requires improving the efficiency of conversion and utilization of fossil fuels, use of high hydrogen content fossil fuels, decarbonization of fossil fuels and sequestration of carbon and CO₂, applied to all energy consuming sectors of the economy including electric power generation, materials production, transportation and industrial domestic heating. Decarbonization means removal of carbon as C or CO₂ either before or after fossil fuel utilization and sequestration means long term disposal of C or CO₂. The review will cover the principles of removal and recovery from power plant stacks, the geologic and geological disposal of CO₂ and the conversion of CO₂ to gaseous and liquid transportation fuels. The global economic aspects of CO₂ mitigation technologies will be touched upon.

9:20 AM

Chemical Utilization of Sequestered Carbon Dioxide as a Booster of Hydrogen Economy: *Michael Moats*¹; Jan Miller¹; Włodzimierz Zmierzczak¹; ¹University of Utah

For many, hydrogen in a pure hydrogen economy would be like natural gas in today's energy economy. Unfortunately, hydrogen's physical properties are unsuited to the energy market's requirements in terms of packaging, storage, transfer, and delivery. In this paper, a hybrid energy economy that packages hydrogen chemically on carbon atoms from various sources including recycled

carbon dioxide is introduced and discussed. For this new hybrid energy economy to become a sustainable reality, the ability to recycle carbon dioxide and attach hydrogen to create a usable energy product, such as dimethyl ether (DME), is needed. DME is recognized as a potential next generation, "beyond-petroleum", environmentally benign commodity for energy storage and distribution. To maximize the sustainability of the proposed hybrid energy economy, "green" hydrogen will be utilized. The "green" hydrogen would be created by the electrolysis of water powered by renewable energy sources, such as solar, wind or geothermal heat.

9:40 AM

Methods for Reducing CO₂ Emissions Using Ceramic Membranes with Oxygen Ion/Electronic Conductivity: *John Gordon*¹; ¹Ceramtec Inc.

Let's examine the opportunity to reduce CO₂ emissions from metallurgical production by employing mixed conductive ceramics, in particular, ceramics conductive to oxygen ions and electrons. These mixed properties enable three types of process opportunities. 1) Oxygen can be co-generated with power. First, heat and compress air to form a high PO₂ stream. Ceramic structures can be constructed resulting in generation of pure tonnage quantity oxygen useful in various metallurgical processes without the inefficiency of conventional cryogenic approaches. 2) Combustion with pure oxygen results in much higher CO₂ concentration in offgas enabling efficient sequestration. 3) Exposure of the CO₂ stream to a mixed conductive ceramic membrane opposite a reductant results in partial stripping of oxygen from the CO₂ stream to create CO. Developing processes to efficiently separate CO from the CO₂ further provides advantages. The benefit is further increased when reductant is selected requiring controlled partial oxidation.

10:00 AM Break

10:15 AM

CO₂ Reduction by Dry Methane Reforming over Hexaaluminates: A Promising Technology for Decreasing Global Warming in a Cost Effective Manner: *Maria Salazar-Villalpando*¹; *Todd Gardner*¹; ¹National Energy Technology Laboratory

Efficient utilization of CO₂ can help to decrease global warming. Methane reforming using CO₂ has been of interest for many years because CO₂ provides a source of clean oxygen. Coal power or metallurgical plants have wasted heat streams that can be utilized in CO₂ reduction. The product of this reaction is syngas, which could generate electrical power in a SOFC or used in the production of synthetic fuels. Hexaaluminate catalysts prepared at NETL may represent a product that can be utilized for the conversion of CO₂ to syngas. A series of BaNi₁₂Al₁₂-yO_{19-z} catalysts were prepared by co-precipitation followed by calcination at 1400°C. Reactions were carried out to determine catalyst performance and catalyst characterization was conducted to determine surface area, pore size, catalyst phases and structures. Moreover, catalyst characterization analysis of three samples (y = 0.2, 0.6, and 1.0 in BaNi₁₂Al₁₂-yO_{19-z}) was performed by EXAFS and temperature programmed reduction.

10:35 AM

A Proposal for a Reduction Method of Global Atmospheric CO₂: Isolation of Surplus CO₂ from Biosphere by the Fixation as an Insoluble Mineral onto a Sea Bottom: *Katsuyoshi Tatenuma*¹; ¹Kaken Inc.

In order to mitigate the effect of global warming by preventing the accumulation of atmospheric CO₂, a permanent fixation method of surplus CO₂ as an insoluble mineral onto a sea bottom is proposed. As a new and practical reduction method of atmospheric CO₂, a concrete concept of this method is that an insoluble carbonate mineral (CaCO₃) formed by direct electrolysis of the seawater, $\text{Ca}^{2+} + 2\text{HCO}_3^- + \text{OH}^- \rightarrow \text{CaCO}_3(\text{insoluble}) + \text{CO}_3^{2-}(\text{soluble}) + \text{H}^+ + \text{H}_2\text{O}$ (not coral reef reaction), is directly disposed by itself onto a sea bottom. By this treatment, a concentration of carbonate is reduced at the section of superficial seawater, and the absorption capacity of atmospheric CO₂ is therefore increased as a result of chemical equilibrium between the superficial ocean and atmosphere. The proposed method without any additives, generation of secondary wastes and CO₂ itself, and disturbance of the environmental balance as a green-orientated method has an ability to resolve fundamentally the problem of global warming.

10:55 AM

CO₂ Capture and Sequestration – Implications for the Metals Industry:

*Mark Berkley*¹; *Jim Sarvinis*¹; *Jason Berzansky*¹; *David Clarry*¹; ¹Hatch

Technologies developed to sequester CO₂ or use CO₂ for enhanced fossil fuel recovery are currently in operation. Taxation regimes and CO₂ credit trading are becoming drivers for a number of projects. Some mining companies have also identified an opportunity to sequester CO₂ in their by-products; recent work by Alcoa is a prime example. In addition to process plant emissions, mining companies are becoming increasingly aware of their overall carbon footprint, including CO₂ generated during the production of power they use. New power plant designs, in various stages of development, include CO₂ separation and sequestration techniques. This paper summarizes the state-of-the-art for these technologies, including integrated gasification combined cycle (IGCC power plants. A concept to use the gasification products as reductant in metallurgical processes is also described. The relevance of technology from power plant designs with post-combustion capture to the processing of off-gas generated in metallurgical facilities is also reviewed.

11:15 AM Panel Discussion

Cast Shop Technology: Casthouse Operation

Sponsored by: The Minerals, Metals and Materials Society, TMS Light Metals Division, TMS: Aluminum Committee

Program Organizers: Hussain AlAli, GM Casthouse and Engineering Services, Aluminium Bahrain Company (ALBA); David DeYoung, Alcoa Inc

Tuesday AM

March 11, 2008

Room: 295

Location: Ernest Morial Convention Center

Session Chairs: Ghyslain Dube, Centre de Recherche et de Développement Arvida; Barbara Rinderer, Rio Tinto Aluminium Technology

8:30 AM Keynote

ICON: Sodium Removal: *Erik Aspen*¹; *Bjarne Heggset*¹; *Jo Vaagland*¹; ¹Heggset Engineering

A new process for sodium removal has been developed. The technology is based on direct injection of AlF₃ into the melt while tapping metal from potcells. The ICON technology makes sure AlF₃ is injected directly into the melt and ensures excellent mixing of AlF₃ with the melt causing good conditions for the chemical reaction. Preliminary results from testing indicate total sodium removal down to a level of 5-10 ppm(90%), before casting. The technology can be installed at several locations; integrated in the tapping vehicle and integrated in the crantapping system. ICON is flexible, easy to install and can be fitted to any tapping system, no limitations on crucible size. Furthermore ICON can be characterized by low installation and operation cost, very low maintenance, no rotor system, no extra crucible handling systems, minimal metal temperature drop in the crucible, dust extraction to existing plant systems, fully automated and operator friendly.

8:50 AM

Gas Fluxing of Molten Aluminum: An Overview: *Geoffrey Sigworth*¹; *Eddie Williams*¹; *Corleen Chesonis*¹; ¹Alcoa Inc

The aluminum industry is under continual pressure to improve metal quality, while at the same time reduce costs. Although a reasonably mature technology, there has been a continual evolution in degassing equipment over the years. A detailed review and theoretical analysis is given of the chemical and kinetic factors which control the metal quality after gas fluxing, and the evolution of degassing technology in Alcoa is summarized. Particular emphasis is placed on hydrogen removal, minimization of chlorine use, reduced operating costs and minimization of environmental emissions. Considerations related to inclusion removal are also discussed briefly.

9:10 AM

Monolithic Refractory Furnace Linings Designed for Rapid Commissioning:

Andrew Brewster¹; Zena Carden¹; ¹Vesuvius

Monolithics are widely used for lining aluminium melting and holding furnaces and have many advantages in performance and security. One major disadvantage is the time taken to fully cure and dry out the structure. The use of high cost pre-cast and dried pieces can reduce this down-time but unless all the furnace is built in pre-cast pieces the need to cure and dry the in-situ installed monolithics prevails. New materials have been developed with a different bonding system such that the lining does not require any curing time and all the water can be removed quickly at low temperatures. Savings of several days can result. These new products are very versatile with the option to install the same material by casting, pumping or shotcreting. They have excellent aluminium penetration resistance and are well proven in service. The paper describes the product development principles and gives examples of application.

9:30 AM

Design Considerations for Holding and Casting Furnaces:

Jan Migchielsen¹; Tom Schmidt¹; Hans-Walter Gräb¹; ¹Thermcon Ovens BV

Holding and casting furnaces are common tools in aluminium cast houses. This paper addresses the aspects to be considered for selecting the most appropriate furnace design. The differences in design are discussed between holding/casting furnaces, melting furnaces and combined melting-holding furnaces. The paper addresses the main consideration in designing a holding furnace with respect to mechanical, thermal-process and control aspects. The last part of the paper considers the choice to be made for using a combined furnace versus a separate casting furnace.

9:50 AM

Producing Bright Shining Products for Special Applications-Experience from Practice:

Jana Dressler¹; Dietmar Bramhoff¹; Hubert Koch¹; C. Deiters¹; ¹Trimet Aluminium AG

The TRIMET/GERHARDI gloss alloy is a high purity aluminium extrusion alloy. It is characterized by an extremely homogenous micro structure without internal defects or inclusions. This material composition and the special processing know-how allow a considerably higher productivity. Due to optimal polishing and brightness properties as well as an excellent bending quality the gloss alloy is especially appropriate for the production of surface sensitive components like trim parts, roof racks, decorative fittings, door handles, cover plates for automotive application and power train or design elements for high end audio equipment or the lighting industry. This gloss alloy allows any surface treatment from anodizing to coating. The paper covers the production of this special extrusion alloys including quality requirements, qualifying of the alloying material, and process parameters, as well as latest results from laboratory examinations covering podfa analysis and inclusion identification. Finally examples of applications are shown and discussed.

10:10 AM Break

10:20 AM Keynote

Almex Minicast™ Casthouse Philosophy Helps Southern California Extrusion Company Meet Their Billet Demand Requirement and Optimize Turnaround Scrap Economics:

Shaun Hamer¹; Ravi Tilak¹; ¹Almex USA Inc

Universal Molding Company Inc. started up a new casthouse in Southern California in the third quarter of 2007 designed and empowered by Almex's Minicast™ series of equipment and technology. Minicast™ has been developed by Almex specifically for extrusion companies to cast billet from their in-house scrap. Minicast™ is a single source supply of the entire casting line from melting to homogenization furnaces, configured specifically for this application. UMC, a well respected, privately owned extrusion company, in operation since 1944, recognized the benefits of the system and, on an available 1 acre (0.288 hectare) site, decided to install the Minicast™ system. This paper describes the installation of the 28,000 ton per year facility, and touches on some of the specific design, technology and environmental technologies in use.

10:40 AM

Nonmetallic Inclusions in the Secondary Aluminium Industry for the Production of Aerospace Alloys:

Bernd Prillhofer¹; Helmut Antrekowitsch¹; Holm Böttcher²; Phil Enright³; ¹University of Leoben; ²AMAG Rolling GmbH; ³N-Tec Limited

Due to the enormous growth of the secondary aluminium industry and the higher content of impurities in the input materials, the development of methods for inclusion removal has become highly important. To produce high quality aerospace alloys with very low inclusion contents, casthouses must analyse and optimise their production processes from the beginning to the end. Nowadays there are several methods available for process evaluation to determine the inclusion level from one step to another. Furthermore the most important parameters for control of the final inclusion level have to be investigated. This paper characterises the change of the inclusion content for the alloy AA 7075 during standard casthouse processing. Additionally, possibilities for the improvement of the melt quality are discussed.

11:00 AM

Effect of Temperature and Charge Borings in the Fluidity of an Aluminum-Silicon Alloy:

Eulogio Velasco¹; Guillermo Ruiz²; ¹Nemak; ²Facultad de Ingeniería Mecánica y Eléctrica-Universidad Autónoma de Nuevo León

In the processing of secondary alloys, mixed of different aluminum scrap grades are typically used in the melting furnace charges. Turnings and borings are materials with high availability to in the metal market with competitive price compare with others aluminum scrap grades, the drawbacks with turnings are related with melting practices and the cost of devices and equipment to obtain a high yields and avoid possible contamination by fine aluminum oxide particles. Molten Aluminum-Silicon alloy was prepared in a crucible gas furnace and several percentages of chips were added during melting, after each addition, fluidity test at different temperatures and PreFilÖ samples were taken in order to evaluate the effect of temperature and cleanliness of metal in the fluidity of the alloy.

11:20 AM

Production of Aluminium-Silicon-Magnesium Wrought Alloy Rod with Applications in the Manufacture of Extra-High Conductivity AAAC for Overhead Electrical Transmission Lines:

Mohamed Rafea¹; ¹Midal Cables

Aluminium-Silicon-Magnesium (Al-Si-Mg) wrought alloy rods have been used extensively in the manufacture of wires stranded into conductors used in high voltage transmission lines. Midal Cables has modified the productions process of this type of rod for use in the manufacture extra-high conductivity AAAC for applications as overhead transmission line conductors. These have low DC Resistance thus in turn have higher current carrying capacity. With modifications in the chemical composition, casting and hot rolling parameters Midal has developed a rod which respond differently to heat treatment after wire drawing resultig to a product that has a higher electrical conductivity than conventionally manufactured Al-Si-Mg alloy wires for the same application. This paper discusses the various production parameters used in the manufacture of Al-Si-Mg alloy rods and establish the mechanisms that effect the extra-high conductivity property after wire drawing and heat ageing.

11:40 AM Panel Discussion

TUESDAY AM

Characterization of Minerals, Metals, and Materials: Characterization of Microstructure and Properties of Materials I

Sponsored by: The Minerals, Metals and Materials Society, TMS Extraction and Processing Division, TMS: Materials Characterization Committee
Program Organizers: Jian Li, Natural Resources Canada; Toru Okabe, University of Tokyo; Ann Hagni, Intellection Corporation

Tuesday AM Room: 284
March 11, 2008 Location: Ernest Morial Convention Center

Session Chairs: Sergio Monteiro, State University of the Northern Rio de Janeiro - UENF; Jeongguk Kim, Korea Railroad Research Institute

8:30 AM

Characterization of Aging in U-Nb Martensites: Robert Hackenberg¹; Amy Clarke¹; Robert Field¹; Heather Volz¹; Don Brown¹; Dave Teter¹; Dan Thoma¹; Michael Miller²; Kaye Russell²; ¹Los Alamos National Laboratory; ²Oak Ridge National Laboratory

Artificial aging at temperatures <300C gives rise to strengthening accompanied by undesirable ductility loss in U-5.6wt.%Nb and U-7.7wt.%Nb. Two hypotheses have been suggested to account for this phenomenon: 1) diffusional decomposition of Nb-supersaturated thermoelastic martensite into Nb-rich and Nb-lean clusters or phases, and 2) Nb or impurity segregation to twin boundaries. X-ray and neutron diffraction and transmission electron microscopy (TEM) could not unambiguously discern microstructural changes to support either hypothesis. Thus, atom probe tomography was performed to show Nb and impurity atom distribution as a function of aging time and temperature at T=200C, forcing a reevaluation of the accepted aging mechanisms in U-Nb alloys. Research at the Oak Ridge National Laboratory SHaRE User Facility was sponsored by Basic Energy Sciences, U.S. Department of Energy.

8:50 AM

Mechanical Characterization of Ramie Fiber Reinforced Polyester Composites: Sergio Monteiro¹; Luiz Fernando Santos¹; Frederico Margem¹; ¹State University of the Northern Rio de Janeiro - UENF

Lignocellulosic natural fibers have been used as reinforcement for polymeric composites as low cost type of biodegradable and renewable materials. For this purpose, sisal, jute, hemp, coir and flax are successful examples of reinforcement fibers in composites, which are currently applied as components in building construction and automobiles. Among these fibers, ramie (*Boehmeria nivea*) has received less attention. The objective of this work was to evaluate the mechanical behavior of ramie reinforced polyester matrix composites. Rectangular specimens with up to 30wt.% aligned ramie fibers were embedded in polyester resin and the cured at room temperature. Bend tests were performed in an Instron machine. The results showed that a sensible improvement in strength occurs with the introduction of ramie fibers into the polyester matrix. SEM analysis revealed that the surface cellular structure of the ramie fiber contribute to a better adherence to the matrix and to a higher fiber/matrix interfacial resistance.

9:10 AM

Surface Characterization in Aluminium 6063 by Mecano-Chemical Treatment: Isaías Hilerio¹; Miguel Barrón¹; ¹Universidad Autonoma Metropolitana Azcapotzalco

The principal objective of finishing surfaces is protected and/or decorates them. This can be obtained by adding or removing material of the work surface. In this work it is important to develop the improvement of surfaces by removal of material. Between these are used Barreling or Polishing. The pieces are at first sandblasted and arranged in the barrel with a natural or synthetically abrasive and an additive (water or a tensioactive). When the abrasives passes against the surfaces of the pieces to treat, produces an action of rubbing and impact that clean the surface of the pieces. In this work are studied evolution surfaces in aluminum 6063 by this method. The process was carried out in 5 samples with the following dimensions: 35 x 100 x 8 mm. It has been done micro hardness

study, MEB and Ray X diffraction. It has been founded higher hardness values in samples treated.

9:30 AM

On the Determination of Compositional Gradients at Interfaces in Alloys and Multilayered Materials: Arda Genc¹; Soumya Nag¹; Rajarshi Banerjee²; Peter Collins¹; Hamish Fraser¹; ¹Ohio State University; ²University of North Texas

It is important to be able to determine quantitatively the compositional gradients about interfaces in various types of materials. Such measurements have been made in Ti alloys and Nb/Cu multilayered materials. Use has been made of both the tomographical atom probe (Imago's LEAP) and analytical electron microscopy (FEI Titan 80/300 S/TEM with monochromator (0.15eV) and spherical aberration corrector for the probe and both an electron energy loss spectrometer (0.15eV) and energy dispersive x-ray spectroscopy. Emphasis has been placed on optimizing and assessing the quality and reliability of data from both instruments, and comparing the results of measurements of the same gradients in both machines. The results from the study of the multilayers are very promising, where similar results from both techniques have been obtained. However, the Ti alloys studied have been quite complex, e.g., Ti-5-5-5-3, and work has been focused on assessing and optimizing the quality of the data obtained.

9:50 AM Break

10:10 AM

Influence of Weave Damage on the Strength of Composites Reinforced with Jute Fabric: Amanda Lima¹; Sergio Monteiro¹; Luis Augusto Terrones¹; ¹State University of the Northern Rio de Janeiro - UENF

Jute fabric detached from sackcloth is being considered as reinforcement of polymeric matrix composites. Discarded sackcloth usually has weave damages, which affect the fabric mechanical resistance and could impair its reinforcement effect in composites. The objective of this work was to investigate the effect of pre-existing weave damage in the fabric, cut from jute sackcloth and used as reinforcement, on the strength of polyethylene composites. Fabrics were obtained from either new or already damaged sackcloth. Composites were fabricated by 160°C compression molding interlayer fabric pieces together with either new or recycled polyethylene pellets. The composite strength was evaluated by bend test and the fracture analyzed by SEM. The consideration of Godfrey and Rossetos model has shown that the discarded jute fabric has a significant lower tolerance to damage. This results in a comparative decrease in the strength of the composites reinforced with fabrics from discarded jute sackcloth and recycled polyethylene.

10:30 AM

The Effect of Hydrostatic-Testing on Pipeline SCC Propagation: Jian Li¹; ¹Natural Resources Canada

Stress corrosion cracking (SCC) is an important failure mechanism for oil and gas pipelines. In the past, hydrostatic testing has been frequently used to assess and mitigate stress corrosion cracking. It is commonly agreed that an effective hydrostatic test not only eliminates critical crack-like flaws, but also blunts the sub-critical crack tip thereby suppressing further SCC propagation. However, little study has been done on the plastic deformation that results from the high stress intensity at the crack tip due to hydrostatic testing pressure and its possible role in subsequent SCC propagation. In this study, microstructural details were examined of an API 5L X52 SCC-containing pipe removed from field service. Plastic deformation generated by the hydrostatic testing pressure was revealed by using high-resolution focused ion beam (FIB) microscope. The existence of the microscopic plastic zones around some crack tips suggests that caution should be taken when setting up pipeline hydrostatic tests.

10:50 AM

Damage Evolution and Fracture Behavior of Ceramic Matrix Composites during Monotonic Loadings: Jeongguk Kim¹; ¹Korea Railroad Research Institute

Ceramic matrix composites (CMCs) have been identified as potential candidates for high-temperature structural applications, such as aircraft structures, fusion reactors, and heat management systems due to their high-temperature strength, lightweight, and excellent corrosion and wear resistance.

In this paper, damage evolution and failure mechanisms of CMCs during tensile loadings were investigated using nondestructive evaluation (NDE) techniques and microstructural characterization. The CMCs used for this investigation is continuous fiber reinforced ceramics matrix composites. NDE techniques were employed to characterize defect information before and during mechanical testing. Microstructural characterizations using scanning electron microscopy (SEM) were performed to investigate fracture modes and failure mechanisms of CMC samples. In this investigation, the NDE technique and SEM characterization were employed to facilitate a better understanding of damage evolution and progress of Nicalon/CAS composites during monotonic and cyclic loadings.

11:10 AM

Dynamic Thermo-Mechanical Characterization of Coir Fiber Reinforced Polymeric Composites: *Sergio Monteiro*¹; Rubén Sanchez¹; Helvio Santafé¹; Lucas da Costa¹; ¹State University of the Northern Rio de Janeiro - UENF

The fibers extracted from the coconut fruit, also known as coir fibers are being applied as reinforcement in polymeric composites. In the present work, a study on the temperature variation of the dynamic-mechanical parameter of polymeric matrix composites incorporated with continuous coir fibers was carried out. Thermoset polymers were mixed with different amounts of coir fibers and then press-molded cured for 24 hours at room temperature. DMA tests permitted to obtain the storage modulus and the tangent delta for each studied condition. The results revealed that the incorporation of coir fiber decreases the viscoelastic stiffness of the polymeric matrix. Moreover, modifications in the glass transition temperature and in the alpha relaxation peak could be associated with the incorporation of coir the fiber into the matrix. The interaction of the coir fiber with the polymeric matrix, which reduces the molecular mobility, is the proposed mechanism for these experimental results.

Complex Oxide Materials - Synthesis, Properties and Applications: Functionally Cross-Coupled Heterostructures

Sponsored by: The Minerals, Metals and Materials Society, TMS Electronic, Magnetic, and Photonic Materials Division

Program Organizers: Zhiming Wang, University of Arkansas; Ho Nyung Lee, Oak Ridge National Laboratory

Tuesday AM March 11, 2008 Room: 277 Location: Ernest Morial Convention Center

Session Chair: To Be Announced

8:30 AM Invited

Correlated Oxide Heterostructures: *Ramamoorthy Ramesh*¹; ¹University of California

Complex perovskite oxides exhibit a rich spectrum of functional responses, including magnetism, ferroelectricity, highly correlated electron behavior, superconductivity, etc. The basic materials physics of such materials provide the ideal playground for interdisciplinary scientific exploration. At Berkeley, we are exploring the science of such materials (for example, colossal magnetoresistance, ferroelectricity, etc) in thin film form by creating epitaxial heterostructures and nanostructures. Among the large number of materials systems, there exists a small set of materials which exhibit multiple order parameters; these are known as multiferroics. Using our work in the field of ferroelectric and ferromagnetic oxides as the background, we are now exploring such materials, as epitaxial thin films as well as nanostructures. Specifically, we are studying the role of thin film growth, heteroepitaxy and processing on the basic properties as well as magnitude of the coupling between the order parameters. A new development has been the discovery of the formation of spontaneously assembled nanostructures consisting of a ferromagnetic phase embedded in a ferroelectric matrix that exhibit very strong coupling between the two order parameters. This involves 3-dimensional heteroepitaxy between the substrate, the matrix perovskite phase and spinel phase that is embedded as single crystalline pillars in this matrix. In this talk I will describe to you some aspects of such materials as well as the scientific and technological excitement in this field.

9:00 AM Invited

In Pursuit of Strongly Coupled Multiferroic Oxides: *Craig Fennie*¹; ¹Argonne National Laboratory

To realize novel electrically controlled magnetic devices based on multiferroic oxides - materials that are simultaneously ferroelectric and magnetic - an external electric field is required to strongly couple to a switchable magnetization. Given the known challenges simply to synthesize and to measure the properties of new strongly coupled multiferroics, a theory-driven, first-principles search for new candidates will greatly advanced the discovery of such structurally and chemically complex materials. In this talk we discuss our recent identification of a new class of multiferroic oxides. Combining density-functional calculations with group-theoretic arguments we elucidate the interplay between the electrical polarization and the spins to show how the direction of the magnetization can be switched between symmetry equivalent states with an applied electric field.

9:30 AM

Non-Linear Modulation of Transport Properties in Magnetic-Ferroelectric Bilayers: *Zolt Marton*¹; Ho Nyung Lee²; Takeshi Egami³; ¹University of Pennsylvania, Department of Materials Science and Engineering; ²Oak Ridge National Laboratory, Materials Science and Technology Division; ³University of Tennessee, Department of Materials Science and Engineering/Physics and Astronomy

In doped manganites, strong correlation between structural, electronic and magnetic properties leads to fascinating phenomena such as metal-insulator transition and colossal magnetoresistance. We utilize the ferroelectric polarization to modulate the charge carrier density in high quality $\text{La}_{1-x}\text{Sr}_x\text{MnO}_3$ (LSMO) ($x = 0, 1/8, 1/5, 1/3$, and $1/2$) epitaxial films by using highly-polar ferroelectric $\text{PbZr}_{0.2}\text{Ti}_{0.8}\text{O}_3$ (PZT) films with $P_r \approx 80 \mu\text{C}/\text{cm}^2$. All epitaxial LSMO/PZT heterostructures on (001) SrTiO_3 with epitaxial SrRuO_3 electrodes were grown by pulsed laser deposition. We will present a systematic study on the screening and transport/magnetic properties of the doped manganites under the influence of ferroelectric polarization of PZT. The role of thickness, strain, and composition of the manganite film, besides the effect of external magnetic field, on the magnetoelectric properties will be also discussed. Research sponsored by the LDRD Program of ORNL, managed by UT-Battelle, LLC for the U.S. Department of Energy and by NSF DMR-0404781.

9:50 AM Invited

Exploiting Oxide Interfaces to Generate New Functionalities: *Nicola Spaldin*¹; ¹University of California Santa Barbara, Materials Department

Recent developments in thin film growth techniques have enabled the production of oxide heterostructures with interfaces of unprecedented quality. A range of unusual behaviors have been reported at such interfaces, including electrical conductivity between oxides that are insulating in their bulk form, and ferromagnetism between non-magnetic bulk oxides. Here we describe first-principles computational explorations of functionalities that exploit the fact that interfaces break space-inversion symmetry. We demonstrate computationally a novel linear magnetoelectric effect at the interface between a non-magnetic, non-polar dielectric and a metal with spin-polarized carriers at the Fermi level. We show that an electric field induces a linear change in magnetization in the metal at the interface, with the magnetic response mediated by the accumulation of spin-polarized charge at the interface. As a result of the magnetoelectric response, magnetism and dielectric polarization coexist in the interfacial region, suggesting a route to a new type of interfacial multiferroic.

10:20 AM Break

10:50 AM Invited

Magnetism and Electronic Structure at the Interfaces of Complex Magnetic Oxides: *Jak Tchakalian*¹; ¹University of Arkansas

Atomically controlled interfaces between two materials can give rise to novel physical phenomena and functionalities not exhibited by either of the constituent materials alone. Modern synthesis methods have yielded high-quality oxide heterostructures with competing order parameters. Magnetic correlations at the interface are expected to be important in determining the macroscopic properties of such nanosystems, but quantitative determination of the interfacial magnetic structure in oxides has thus far been very limited. Here we examine superlattices composed of the half-metallic ferromagnet $\text{La}_2/3\text{Ca}_{1/3}\text{MnO}_3$ and the high-temperature superconductor $\text{YBa}_2\text{Cu}_3\text{O}_7$ by polarized soft x-rays and

by diffuse neutron reflectometry. The resulting data yield microscopic insight into the interplay of spin and orbital degrees of freedom at the interface. The data also reveal an extensive rearrangement of the magnetic domain structure at the superconducting transition temperature. The combination of techniques establishes an incisive probe of the interplay between competing order parameters in complex oxide heterostructures.

11:20 AM Invited

Piezoelectric Strain Control of Thin Film Magnetism: Kathrin Dorr¹; Diana Rata¹; Andreas Herklotz¹; Orkidia Bilani¹; ¹IFW Dresden

Multiferroic (magnetic and ferroelectric) nanofabricated composites principally offer the “magnetoelectric” functionality of controlling magnetization by electric voltage. In recent years, intense research has been devoted towards the search for thin film (nano)structures being capable of efficient coupling of the components. In most composites, magnetoelectric coupling originates from joined elastic strain in the components. Here, the approach of epitaxial growth of strain-sensitive magnetic oxide films on a single-crystalline piezoelectric substrate (PMN-PT(001), with 28% PbTiO₃ and 72% PbMg_{1/3}Nb_{2/3}O₃) is discussed. Application of an electric voltage to the rhombohedral pseudocubic substrate allows one to reversibly cycle the biaxial in-plane strain of substrate and film. In this way, the impact of (uniform) biaxial strain on the magnetization of epitaxially grown films of ferromagnetic manganites (La,A)MnO₃ and cobaltates (La,Sr)CoO₃ has been quantitatively studied. The immense strain sensitivity of manganites is reflected in the observation of large magnetoelectric coupling at ambient temperature (PRB 75, 054408).

11:50 AM

Theoretical Modeling of Bifunctional Multilayer Systems: Donald Ellis¹; Norman Tubman¹; Daniel Wells¹; ¹Northwestern University

Crystalline multilayer systems with structure ABABA... offer the possibility of combining functional properties of two distinctly different materials, and of exploiting the interfaces to couple functionality of one component to the other. The multilayer environment permits the amplification of interface properties as would be important for device applications. The roles of interfacial strain and orientation, chemical variability at the interface, and film thickness are explored, taking as a starting point the classic BaTiO₃||Fe₃O₄ ferroelectric||ferrimagnetic interactions. First principles band structure calculations are used to determine relaxed interface structures and residual stresses, as well as the underlying electronic distributions. Embedded cluster methods are then used to extract local chemical bonding characteristics and hyperfine properties, including contact spin densities, anisotropic spin distributions, and electric dipolar and quadrupolar fields. Mixed composition interfaces involving cation substitution; e.g., (Fe,Co) and (Ti,Pd), are examined as a means to enhance coupling between functional slabs.

12:10 PM

The Origin of Photovoltaic Effect in Heterophase Ferroelectric M/PZT/M Structure: Liubov Delimova¹; Valentin Yuferev¹; Anatolii Petrov²; Valentin Afanasjev²; Igor Grekhov¹; ¹Ioffe Physicotechnical Institute of the Russian Academy of Sciences; ²St. Petersburg Electrotechnical University “LETI”

A steady-state short-circuit photocurrent is measured in polycrystalline Pt/Pb(ZrTi)O₃(PZT)/Ir structures with Pb excess. It is found that although the photocurrent is directed opposite to ferroelectric polarization and defined by the magnitude of the polarization, it is not the depolarization current of the ferroelectric. To explain this, we assume that Pt/PZT/Ir capacitor is heterophase medium, which consists of PZT grains and semiconductor PbO phase segregated on PZT grain boundaries during the PZT formation. The PZT and PbO phases are connected in parallels between the electrodes, and the PbO phase forms conducting channels. The uncompensated polarization charge of PZT grains generates an electric field in the PbO channels, which is directed opposite to the ferroelectric polarization and is responsible for the observed photocurrent in the film. Using this concept, we describe the experimental dependence of photocurrent on polarization and can study a contribution of polarization charge into current-voltage characteristics of M/PZT/M structures.

Computational Thermodynamics and Kinetics: Phase Field Crystal

Sponsored by: The Minerals, Metals and Materials Society, TMS Electronic, Magnetic, and Photonic Materials Division, TMS Materials Processing and Manufacturing Division, ASM Materials Science Critical Technology Sector, TMS: Chemistry and Physics of Materials Committee, TMS/ASM: Computational Materials Science and Engineering Committee, TMS/ASM: Phase Transformations Committee
Program Organizers: Yunzhi Wang, Ohio State University; Long-Qing Chen, Pennsylvania State University; Jeffrey Hoyt, McMaster University; Yu Wang, Virginia Tech

Tuesday AM
March 11, 2008

Room: 288
Location: Ernest Morial Convention Center

Session Chairs: Jeff Hoyt, McMaster University; Ken Elder, Oakland University

8:30 AM Invited

Phase Field Modeling from Atomic Mesoscopic Scales: Ken Elder¹; ¹Oakland University

Understanding the formation and characteristics of non-equilibrium structures has been greatly enhanced by the use of continuum or ‘phase’ field models. Such models typically describe phenomena on mesoscopic length and time scales. More recently an extension to this approach, known as phase field crystal modeling, has been introduced to describe processes on atomic length and diffusive time scales. This approach has the advantage of incorporating elastic and plastic deformations in a natural and simple fashion. In this talk I would like to discuss the connection between standard microscopic descriptions, phase field crystal and standard phase field models. Emphasis will be placed on the physical significance and microscopic origin of the parameters and fields that enter phase field models.

8:55 AM Invited

Phase-Field-Crystal Modeling of Interface Coalescence: Jesper Mellenthin¹; Mathis Plapp²; Alain Karma³; ¹Ecole Polytechnique and Northeastern University; ²Ecole Polytechnique; ³Northeastern University

Crystal cohesion during the late stages of solidification, and its failure often described as “hot tearing”, depends critically on the coalescence of crystal grains impinging upon each other. In metallic systems, crystal density waves decay slowly into the liquid over several atomic layers. Therefore crystal-melt interfaces interact when the envelopes of density waves from nearby grains start to overlap. This interaction is studied as a function of temperature and misorientation in a pure material using a phase-field crystal approach. This method provides a natural description of crystal density waves, is computationally efficient, and allows for a precise determination of the excess free energy due to the interaction of the interfaces. The nature of this interaction, whether attractive or repulsive, is found to depend both on misorientation and separation between interfaces. Results shed light on the physics of coalescence and are compared to the predictions of sharp-interface theories and multi-phase-field models.

9:20 AM Invited

Multi-Scale Modeling of Solidification: Connecting Density Functional Theory to Phase Field Crystals and Phase Field Models: Nikolas Provatas¹; Sami Majaniemi¹; ¹McMaster University

The connection of phase field crystal modeling in pure materials and alloys to density functional theory (DFT) is reviewed. We discuss new approaches for using higher order correlation functions, critical to modeling complex crystal structures in phase transformations. We then move up in length scale and discuss new coarse graining strategies for projecting out anisotropic phase field models, the form and coefficients of which are more fundamentally connected to first principles than their phenomenological counterparts used traditionally. Outstanding challenges for modeling interface kinetics in two-sided phase field crystal (or DFT) models –akin to those that plagued traditional phase field models— are discussed.

9:45 AM Invited

Incorporating Mechanics into Phase Field Models: *James Warren*¹; Daniel Wheeler¹; William Boettinger¹; ¹National Institute of Standards and Technology

The addition of hydrodynamics to diffuse interface models of phase transformations has now been well studied in some relatively simple systems. However, properly coupling such flows to a description of an elastic solid remains an area where the models need substantial improvements. In recent years we have been interested in the problem of reactive wetting, where a droplet dissolves the substrate upon which it spreads. Describing this system mathematically, for realistic materials (such as Sn-Bi) in a manner that admits numerical solution in reasonable time scales is the focus of this work. We will also discuss related approaches, including phase field crystal models, of the same phenomenon.

10:10 AM

Molecular Dynamics Validation of Phase Field Modeling: *James Belak*¹; Patrice Turchi¹; Milo Dorr¹; Bryan Reed¹; David Richards¹; Jean-luc Fattebert¹; Michael Wickett¹; Fred Streitz¹; ¹Lawrence Livermore National Laboratory

Recently, phase field models have been introduced to model the crystallography during polycrystal microstructure evolution^{1,2}. Here, we assess these models with molecular dynamics and phase field simulations that overlap in time and space. Large parallel computers have enabled MD simulations of sufficient scale to observe the formation of realistic microstructure³. We compare the two methods by calculating the phase field order parameter (quaternion) from the atomic coordinates and drive the evolution with the MD. Results will be presented for the solidification of tantalum. ¹ R. Kobayashi and J.A. Warren, *Physica A*, 356, 127-132 (2005). ² T. Pusztai, G. Bortel and L. Granasy, *Europhys. Lett.*, 71, 131-137 (2005). ³ F. H. Streitz, J. N. Glosli, and M. V. Patel, *Phys. Rev. Lett.* 96, 225701 (2006). This work was performed under the auspices of the U.S. Department of Energy by University of California, LLNL under Contract W-7405-Eng-48.

10:25 AM Break

10:45 AM Invited

The Phase Field Crystal Model: Atoms, Defects and Nonlinear Elasticity: Pak Yuen Chan¹; *Nigel Goldenfeld*²; Zhi Huang¹; Badrinarayan Athreya¹; Jon Dantzig¹; ¹University of Illinois at Urbana-Champaign

The phase field crystal (PFC) model describes the local atomic density in a material as the solution of a sixth order partial differential equation in space and time. The periodic solutions represent crystalline materials, but as with real materials, approach to the true equilibrium is kinetically-limited, resulting in the full plethora of microstructural phenomena found in real materials. Here we show how our multiscale representation of the PFC leads naturally to a way to represent the full nonlinear elasticity of materials. We use the PFC to simulate the dynamics of dislocations, observing a variety of avalanche, scaling and intermittent acoustic phenomena that strongly resemble observations of plastic flow in pure materials. Thus, the PFC model provides a unified description of materials from the atomic scale up to continuum mechanics.

11:10 AM Invited

Phase-Field Crystal Model: Deformation and Ferroelectric Phenomena at the Nanoscale: *Mikko Haataja*¹; ¹Princeton University

Traditionally, the spatio-temporal evolution of morphologies during phase transformations has been modeled through numerically solving either a set of physically-based sharp-interface or diffuse-interface ("phase-field") models. While such approaches have proven to be very useful in elucidating the physics behind the evolving morphologies in, e.g., phase transformations and thin film growth, incorporating plastic effects and other atomistic features in these models becomes quite cumbersome. The so-called "phase-field crystal" method introduces a continuous atomic mass density field in which fast atomic vibrations have been integrated out. The free energy functional of the system supports spatially periodic states, and naturally incorporates elastic and plastic effects, grain boundaries, free surfaces, and arbitrary crystal orientations. Dissipative dynamics can be constructed to govern the temporal evolution of the density field at diffusive time scales, inaccessible by direct Molecular Dynamics simulations. In this talk I will discuss recent efforts in incorporating ferroelectric phenomena within the PFC formalism.

11:35 AM Invited

Diffusive Molecular Dynamics: *Ju Li*¹; William Cox¹; Thomas Lenosky¹; Ning Ma¹; Yunzhi Wang¹; ¹Ohio State University

Starting from the variational Gaussian approach of LeSar et al. to approximate the vibrational entropy in solids, we develop a method called diffusive molecular dynamics (DMD) to overcome the timescale limitation of MD. Akin to the phase field crystal model, DMD has atomic spatial resolution but evolves at diffusion timescale. We assign fractional occupation to Gaussian basis to represent diffusion. The occupation on a Gaussian site evolves according to the chemical potential differences with its nearest neighbors. The DMD model can be shown to be equivalent to the regular solution model in treating configurational entropy. Gradient thermodynamics, long-range elastic stress and short-range interaction effects are all taken into account automatically. We have applied DMD to model dislocation climb and sintering.

12:00 PM

Phase-Field Crystal Model for Epitaxial Growth: *Kuo-An Wu*¹; Dong Hee Yeon²; Katsuyo Thornton²; Ken Elder³; Peter Voorhees¹; ¹Northwestern University; ²University of Michigan; ³Oakland University

The original phase-field crystal model by Elder has successfully modeled various non-equilibrium systems. We present here a modified phase-field crystal approach to simulate epitaxial growth in which the vapor phase is introduced by a new phase field. This model extends the original phase-field crystal model which describes liquid and solid phases to a model that can be used to model vapor, liquid and solid phases. This model is used to investigate step flow dynamics, island formation and growth, and the effects of stress generated by a lattice misfit between the film and substrate on the dynamics of film growth.

12:15 PM

Phase Field Method on a Discrete Lattice: *Tetsuo Mohri*¹; Munekazu Ohno¹; Ying Chen²; ¹Hokkaido University; ²University of Tokyo

Phase Field Method (PFM) has been attracting broad attentions. PFM, however, is basically a phenomenological method in a sense that the length scale and time scale are not determined self-consistently. Cluster Variation Method (CVM) and Path Probability Method (PPM) were devised as the approximate schemes to calculate phase equilibria and time evolution kinetics on a discrete lattice. By combining with electronic structure calculations, one is able to derive various thermodynamic quantities including a phase diagram from the first principles. We combined PFM with CVM+PPM to fix the length and time scales, and first principles calculation of microstructural evolution is attempted.

Deformation Twinning: Formation Mechanisms and Effects on Material Plasticity: Experiments and Modeling: Twinning and Associated Defect Structures

Sponsored by: The Minerals, Metals and Materials Society, TMS Structural Materials Division, TMS/ASM: Mechanical Behavior of Materials Committee

Program Organizers: George Gray, Los Alamos National Laboratory; Subhash Mahajan, Arizona State University; Ellen Cerreta, Los Alamos National Laboratory

Tuesday AM
March 11, 2008

Room: 383
Location: Ernest Morial Convention Center

Session Chair: David Bacon, University of Liverpool

8:30 AM Invited

Constitutive Modeling of the Slip-Twinning Transition and Its Applications to the High Strain Rate Regime: *Marc Meyers*¹; Hussam Jarmakani¹; Eduardo Bringa¹; ¹University of California

Slip and twinning are presented as competing deformation mechanisms. This concept, originally proposed by G. Thomas, is applied to different situations and successfully rationalizes the differences in microstructure and behavior. 1. Effect of Grain Size, Temperature, Stacking-Fault Energy, and Strain Rate: the model is applied to FCC, BCC, and HCP metals and the effects are predicted and compared with observations. 2. Shock and Isentropic Compression: results from gas gun and laser experiments are analysed in conjunction with molecular dynamics simulations. The Zerilli-Armstrong and Swegle-Grady relations are

used to predict the critical twinning pressure as a function of grain size in shock and isentropic compression of Ni. The grain size is varied from the conventional to the nanocrystalline regime. 3. Martensitic Transformation: the criterion is applied to steel and successfully explains and predicts the transition from lath to twinned martensite at a critical carbon content.

9:00 AM

Dislocation Nucleation at the Vicinal Coherent Twin in FCC Cu and Al: *Mark Tschopp*¹; Douglas Medlin²; David McDowell³; ¹Air Force Research Laboratories/University Transportation Center; ²Sandia National Laboratories; ³Georgia Institute of Technology

We have used atomistic simulations to investigate dislocation nucleation from the $\Sigma 171$ vicinal coherent twin boundary. Simulation results show that in copper, this symmetric tilt boundary structure is composed of alternating $1/3\langle 111 \rangle$ disconnections that possess a dissociated structure. Deformation simulations of the bicrystal configuration under uniaxial tension and compression show very different nucleation mechanisms. For instance, our simulations of copper under compression predict that full crystal lattice dislocations nucleate from the $1/3\langle 111 \rangle$ disconnections. The lattice dislocation emits from one $1/3\langle 111 \rangle$ disconnection leaving a glissile $1/6\langle 112 \rangle$ type defect on the boundary plane that glides to react with the adjacent $1/3\langle 111 \rangle$ defect, forming a second lattice dislocation that also emits into the lattice, thereby restoring a perfect coherent twin boundary. Furthermore, the analysis of the dislocation reactions that occur during dislocation nucleation from the vicinal twin may provide insight into the behavior of twin boundaries during the plastic deformation of polycrystalline materials.

9:20 AM

Localized Twin Shear at Grain Boundaries Leading to Fracture Nucleation: *Thomas Bieler*¹; Philip Eisenlohr²; Deepak Kumar¹; Marty Crimp¹; Franz Roters²; Dierk Raabe²; ¹Michigan State University; ²Max-Planck-Institut Für Eisenforschung

In gamma-TiAl, certain mechanical twins interact with a grain boundary to nucleate fracture, which can be accounted for with a fracture initiation parameter based upon the geometry of the Burgers vectors as they are related to slip transfer across the grain boundary and the global stress state. The fracture initiation parameter is able to separate cracked and intact boundary populations. Whether the intense shear will cause cracking depends on elastic anisotropy, primary twin (slip) systems vs. secondary slip systems. Cracked and intact boundaries were also characterized to assess tilt and twist character and whether they are low SIGMA (or coincident site lattice) boundaries, but these did not strongly influence crack nucleation at the grain boundary. Finite-element crystal plasticity simulations are used to assess heterogeneous deformation that accounts for observed microcrack nucleation in one of the characterized microstructures. This approach is also examined for its application in other metals.

9:40 AM

MD Simulation of Dislocation Slip and Twinning in Tensile Deformation of Single Crystal Magnesium: *Bin Li*¹; En Ma¹; Kalliat Ramesh¹; ¹Johns Hopkins University

The mechanism for plastic deformation of HCP magnesium is rather complex. We present molecular dynamics (MD) simulations on the dislocation structure and twinning in single crystal magnesium, in which external strain was applied perpendicular and parallel to the c axis, respectively. Prismatic slip with type $\langle a \rangle$ screw dislocation, twinning and detwinning of (10-12) tension twins was obtained when the strain was perpendicular to the c axis [0002], whereas when parallel to the c axis, a new mechanism of pyramidal slip on the (10-12)[10-1] was obtained. This pyramidal slip was composed of alternate slips on the two intercepting slip systems $1/3(30-34)1/6[20-2-3]$ and $1/3(30-38)1/6[40-4-3]$ with a stable stacking fault. The simulations show that this new dislocation slip mechanism can nucleate the (10-12) tension twinning, hence properly associate the dislocation slip with the (10-12) twinning in HCP Mg.

10:00 AM

$1/3\langle 111 \rangle$ Dislocations at FCC Twin Boundaries: *Douglas Medlin*¹; E. Marquis¹; F. Léonard¹; S. Foiles¹; ¹Sandia National Laboratories

We discuss experimental observations and theoretical analysis of the structure and interactions of $1/3\langle 111 \rangle$ dislocations at twin boundaries in face-centered-cubic metals. These defects can arise at twin boundaries in several ways: as

dissociation products of crystal lattice dislocations; via the clustering of point defects; or to accommodate deviations from the exact twin misorientation. We have studied $1/3\langle 111 \rangle$ dislocations at twins in both aluminum and gold by high-resolution transmission electron microscopy and atomistic modeling. Depending on the sign of the Burgers vector, the defect can dissociate by emitting a Shockley partial dislocation and stacking fault into the matrix and leaving a stair-rod dislocation at the interface. The availability of this dissociation path allows for some novel interactions of the defect. Specifically, we discuss how the interaction of the $1/3\langle 111 \rangle$ dislocation with $\{111\}/\{112\}$ twin junctions can stabilize an extended fault that bridges two closely spaced twin lamellae.

10:20 AM

Neighbor Effects on Deformation Twinning in Hexagonal Materials: *Erin Barker*¹; Carlos Tome¹; Ricardo Lebensohn¹; ¹Los Alamos National Laboratory

Elasto-plastic and visco-plastic self-consistent polycrystal deformation models have been utilized to simulate the mechanical response of hexagonal materials. These models represent grains as ellipsoidal inclusions within a homogeneous equivalent medium. By using an average neighborhood, all grains within a sample with the same orientation respond the same. This results in over predicting quantities such as the twin volume fraction. The approach discussed herein is a local finite element simulation that explicitly represents the grain geometry. Each grain is assigned its own elastic, visco-plastic material properties and lattice orientation in order to investigate the influence of a grain's neighborhood on its response. Multiple analyses are conducted on varying the grain orientations to observe the impact on the stress state of the overall sample and the central grain which is held constant and allowed to twin. Such investigation can produce statistical information about twinning and improve the fidelity of averaged polycrystal models.

10:40 AM Break

11:00 AM Invited

Twinning and Twin Interactions in Uranium and Uranium-Niobium Alloys: *Robert Field*¹; Rodney McCabe¹; Amy Clarke¹; ¹Los Alamos National Laboratory

Alpha-U (orthorhombic, Cmcm) displays a plethora of twinning modes, including Type I, Type II, and Compound systems. Interactions between these different twins also are varied and unique. As a result, investigations of uranium and its alloys have often led to new understanding of deformation twinning. Early works by R. Cahn and A. Crocker not only provide insight into twinning mechanisms in this material, but also are considered standard references in twinning theory, including the crystallography of twin crossings and the role of shuffle processes in multiple lattice structures. Similar twinning mechanisms are observed in alloys, particularly U-14at.%Nb, which forms a monoclinically distorted, thermoelastic martensite and displays the shape-memory effect (SME). SME deformation modes display even more interesting and complex twin interactions than those observed in the pure metal. In this talk, twinning systems and interactions will be discussed along with results from recent investigations of both U and U-Nb alloys.

11:30 AM

EBSD Analysis of Deformation Twinning in Alpha-Uranium: *Rodney McCabe*¹; David Alexander¹; Robert Field¹; Donald Brown¹; George Gray¹; Carl Cady¹; ¹Los Alamos National Laboratory

The contribution of twinning to the deformation and fracture of alpha-uranium was examined using electron backscatter diffraction (EBSD). Twinning fractions were measured for quasi-static deformation of textured, fine grained samples for tension and compression in several orientations. Similarly, twinning fractions were measured as a function of depth in a shock loaded uranium plate with the same initial grain size and texture. In both cases, $\{130\}$ twins are the dominant twinning mode with smaller numbers of $\{172\}$ and $\{112\}$ twins. Interestingly, while the $\{130\}$ twins make a significant contribution to deformation, they have a minor effect on the overall texture. For large grained uranium, $\{172\}$ twinning is the dominant twinning mode during tensile loading with smaller numbers of the other twinning modes.

11:50 AM

Study of Dislocations and Twins in Zr Compressed at Liquid Nitrogen Temperatures: *Dhriti Bhattacharyya*¹; Ellen Cerreta¹; Rodney McCabe¹; Amit Misra¹; Carlos Tome¹; ¹Los Alamos National Laboratory

Zirconium undergoes extensive twinning during deformation at low temperatures. In this study the activity of dislocations within twins in Zr has been investigated. Clock-rolled and annealed samples of Zr were compressed at 76 K in the through-thickness direction. The deformation microstructure was examined using Electron Backscatter Diffraction and Transmission Electron Microscopy. The twins formed were mainly hcp compressive twins, with $K1 = \{11\cdot22\}$ and $\eta1 = \langle 11\cdot2\cdot3 \rangle$. Both 'a' and 'c' type dislocations were found inside the twins. A fraction of the 'c' type dislocations were visible as elongated loops inside the twins, and others terminated at the twin boundary and are probably sessile products of twin formation. The 'a' and 'c' dislocations were found to be elongated parallel and perpendicular to the twin boundaries, respectively. Crystallographic analysis showed that the dislocations were formed within the twins, implying that the twins themselves were deforming through a dislocation mechanism involving the 'a' dislocations.

12:10 PM

Mechanical Twinning of TWIP-Steels from Scattering Data Using the Pair Distribution Function: *Jae Suk Joong*¹; Yang Mo Koo¹; Il-Kyoung Jeong²; ¹POSTECH; ²Pusan University

The good mechanical properties of TWIP austenitic steels are mainly due to mechanical twinning (stacking faults). Therefore, it is important to find correlations between planar-defects and strain, and between planar-defects and constitutions quantitatively. In order to study the correlation, we increased mechanical twinning using tensile tests. In the tests, the strain rate and the temperature (298K) was constant while the degree of strain varied in specimens with different constitutions. The formation of twins and dislocation cells during the plastic deformation was confirmed by microscopic methods. The mechanical twinning was quantitatively identified by a (X-ray, neutron) diffraction line profile analysis for the defects study. The local structure of TWIP-steels was determined by a direct interpretation of the peaks observed in the pair distribution function (PDF). The function was Fourier-transformed the scattering data from neutron scattering experiment performed up to high momentum transfer.

Electrode Technology Symposium (formerly Carbon Technology): Anode Raw Materials and Properties

Sponsored by: The Minerals, Metals and Materials Society, TMS Light Metals Division, TMS: Aluminum Committee

Program Organizers: Carlos Zangiacomi, Alcoa Aluminum Inc; John Johnson, RUSAL Engineering and Technological Center LLC

Tuesday AM
March 11, 2008

Room: 299
Location: Ernest Morial Convention Center

Session Chairs: Abdulmunim Binbrek, DUBAL; Stephen Whelan, Alcoa Inc; Charles Mark Read, Bechtel Corporation

8:30 AM

Coke Blending and Fines Circuit Targeting at the Alcoa Deschambault Smelter: *Michel Gendron*¹; ¹Alcoa Deschambault Smelter

The continued increase of the demand for Aluminium metal combined with the fluctuations in the quality of aluminium grade coke makes it more challenging for the anode manufacturing plants to deliver steady quality anodes. The low sulphur coke material is becoming less available on the market and the price is steadily increasing. Environment regulations are aiming at reducing sulphur emissions, while the coke suppliers are offering higher sulphur material. The use of low sulphur material as feed stock increases anode CO₂ reactivity and therefore making the product less attractive for the downstream process. An attempt was made to use only the high sulphur material in the fines fraction, in order to optimise CO₂ reactivity while respecting sulphur emissions limit and coke supplier agreements. This paper presents the detailed results of this test, which later became a process flowsheet modification.

8:50 AM

Design Criteria for Petcoke Calciners: *Ravindra Narvekar*¹; Jose Botelho²; Arun Kumar Mathur¹; ¹Goa Petcoke Consultancy Services; ²Baltin Metal Ltd.

Goa Petcoke Consultancy Services provides comprehensive consultancy services and solutions in the field of petroleum coke calcination. During the course of working on various assignments, we probed into fundamental principles underlying design of rotary kiln systems for petcoke calcination, resulting into evolution of this paper. The important process criteria in calciner design are retention time, heating up rate and operating drafts. These factors depend on kiln dimensions, slope, heat transfer rate and air injections. To understand this well, we have worked out mass and heat balance across kiln, cooler and incinerator. The mechanical design should consider load factors, thermal expansions and strength of materials at elevated temperatures to ensure mechanical soundness and protection against flexing and distortion of kiln shell. The refractory design should take into account differential thermal expansion coefficients, ability to withstand high temperatures, resistance to spalling, chemical attack, abrasion and good coatability.

9:10 AM

Understanding the Calcined Coke VBD- Porosity Paradox: *Bernard Vitclus*¹; Frank Cannova¹; Randall Bowers²; Shridas Ningiler²; ¹BP Coke; ²Secat, Inc.

Carbon plants use either calcined coke bulk density or porosity analysis to predict pitch content and anode density. However, there is a calcined coke VBD-porosity paradox. That is, high bulk density calcined coke often has higher porosity while low porosity coke tends to make more dense anodes. Understanding why this paradox exists should help lead to consistent high density anodes. Mercury porosimetry and novel techniques were used to characterize calcined coke's shape, internal porosity and packing characteristics. Calcined cokes sieved to a mesh size of -30+50um from different coke sources were analyzed in the natural, jaw crushed, and roll crushed states. For particle shape analysis, calcined coke particles were suspended in a moving fluid and analyzed with a high speed camera to determine aspect ratios. Internal porosities were investigated by cross-sectioning particles, using optical microscopy techniques, and image analysis to determine area fraction per particle and pore morphology.

9:30 AM

Structural Evaluation of Petroleum Coke and Coal Tar Pitch for the Elaboration of Anodes for the Aluminum Industry: *Rafael Tosta*¹; Evelyn Inzunza¹; ¹CVG Alcasa

The present work shows a microstructure's evaluation and changes during the thermal treatment of two types of cokes and three types of Coal Tar Pitch. The objective was to establish the applicability of the optic and electronic microscopy technique, as well as XRD to determine the grade of calcinations of the coke and pitch through the Lc, as a source of additional information and quality control to select cokes and pitches for desirable anode properties. The investigation was carried out at laboratory scale; for the analysis both coke and pitch were calcined and then evaluated at different temperatures and times. The results showed that with the application of technical microscopic and XRD, it was possible to select better raw materials quality and made the necessary process adjustments to tackle with different raw materials quality.

9:50 AM

Coke and Anode Desulfurization Studies: Les Edwards¹; Lorentz Lossius²; ¹CII Carbon LLC; ²Hydro Aluminium

The sulfur level of high sulfur cokes used by the calcining industry for blending is increasing. During calcination, petroleum coke partially desulfurizes and the rate of sulfur loss is dependent on both the sulfur level and final temperature. Desulfurization negatively affects coke properties such as real density and porosity and additional desulfurization during anode baking can negatively affect anode properties. This paper is a follow-up to a 2007 TMS paper on desulfurization and presents the results of additional studies on anode and coke desulfurization versus equivalent baking level and discusses the effect of the level of calcination of high sulfur cokes on anode reactivity. The results indicate that the coke calcination levels must be set with coke sulfur levels in mind. It also shows that blending with high sulfur cokes need not be detrimental to most anode properties.

10:10 AM Break

TUESDAY AM

10:20 AM

New Analytical Methods to Determine Calcined Coke Porosity, Shape, and Size: *Randall Bowers*¹; Shridas Ningileri¹; David Palmund²; Bernard Vitchus³; Frank Cannova³; ¹Secat, Inc.; ²Fluid Imaging Technologies, Inc.; ³BP Coke

Carbon Anode properties especially density are dependent on the structure and porosity of calcined coke used to fabricate the anode. Optimum anode density is produced from blending together natural, rolled, and crushed calcined coke with their inherent structure and porosity characteristics. Two tests were developed to characterize the particle shape including internal and between particle porosity. The first method is a novel technique developed by Fluid Imaging of suspending particles in a moving fluid during which a high speed camera is used to obtain a silhouetted outline of the particle shape and size. Secondly, using traditional optical microscopy techniques and image analysis, internal porosity of the calcined coke was determined. The results of the two methods are presented and compared with evaluation techniques found in literature. These techniques were used to obtain a better understanding of the Calcined Coke VBD - Porosity Paradox presented in a subsequent paper.

10:40 AM

Evaluation of the Necessary Amount of Quinoline Insolubles in a Binder Pitch: *John Baron*¹; Robert Wombles¹; Stacey McKinney¹; ¹Koppers Industries Inc

The role of quinoline insolubles in a binder pitch has long been a topic of discussion and disagreement. A review of the technical literature shows a variety of opinions regarding the importance and role of quinoline insolubles in binder pitch. This paper will present the results of a study designed to shed light on the importance and desirable amount of quinoline insolubles in a binder pitch. The paper will report the results of a laboratory anode study using coal tar pitches with quinoline insolubles contents of 1 wt. %, 2 wt. %, 4 wt. %, and 6 wt. %.

11:00 AM

The Use of Blended European Coal Tar and Petroleum Pitches as Anode Binder: *John Jones*¹; ¹Anglesey Aluminium Metal Limited

Uncertainty about the security of supply of traditional coal tar binder pitches led to the need to consider alternatives. The paper describes an industrial scale trial of a blend of European pitches through the green anode production process to cellroom performance.

11:20 AM

Study on Quality of Chinese Modified Pitch: *Fengqin Liu*¹; Yexiang Liu²; ¹Zhengzhou Research Institute of Chalco; ²Central South University

The properties and quality of 5 kinds of heat treated Chinese modified pitch and one vacuum distilled pitch are analyzed, compared and investigated in this paper. The content and particle sizes of mesophases in the pitch samples are observed and tested by optical microscopic photography. The study results show that the TI and QI content in the Chinese modified pitch produced by heat treatment are quite higher than that of the vacuum distilled pitch. And the Chinese modified pitch has greater coke value and higher viscosity, which is about 3 to 5 times as high as that of the vacuum distilled pitch at 150°C. There exist about 2-6% of mesophase in Chinese modified pitch, the size range of which is 2-20 micrometer, whereas there is no mesophase in vacuum distilled pitch.

Emerging Interconnect and Packaging Technologies: Advanced Interconnects

Sponsored by: The Minerals, Metals and Materials Society, TMS Electronic, Magnetic, and Photonic Materials Division, TMS: Electronic Packaging and Interconnection Materials Committee

Program Organizers: Carol Handwerker, Purdue University; Srinivas Chada, Medtronic; Fay Hua, Intel Corporation; Kejun Zeng, Texas Instruments, Inc.

Tuesday AM

March 11, 2008

Room: 275

Location: Ernest Morial Convention Center

Session Chairs: Kejun Zeng, Texas Instruments Inc; Srinivas Chada, Medtronic

8:30 AM Introductory Comments

8:35 AM Invited

Advances in Electronic Packaging Technologies: *Darrel Frear*¹; ¹Freescale Semiconductor

The trend for advanced packages for microelectronics is towards smaller feature size, faster speeds, more complexity, higher power and lower cost. With the tremendous growth of wireless telecommunication, RF, Analog and Sensor applications are beginning to drive many areas of microelectronics packaging traditionally led by the development of the microprocessor. An increasingly dominant factor in RF, Analog and Sensor packaging are the materials in the package because they have an increasing dominant affect performance. Trends in Advanced Packaging technology will be highlighted including the revolutionary Redistributed Chip Package (RCP) that offers a one third reduction in size and cost over the best current packages solutions. This presentation will also discuss key materials processing and reliability issues that must be overcome to enable all advanced packages. This includes interconnect (including solder), substrate, and encapsulation materials (metals, polymers and ceramics) with a focus on interfacial behavior in the package.

9:05 AM Invited

Interconnection Alternatives - Is Nanotechnology the Solution?: *Alan Rae*¹; ¹Nanodynamics Inc

In the electronics industry we are between a rock and a hard place. As more complex devices exhibit a decreased tolerance to process temperatures we have increased the soldering temperature due to the adoption of SAC (tin-silver-copper). Not only that, but in an attempt to reduce the cost of the alloy we reduce the silver content at the same time as we are soldering more complex boards, both of which increase the reflow temperature further! iNEMI has initiated a "warm assembly" program aimed at reducing the process temperature back to tin-lead temperatures or even lower by using nano-sized solder and carbon nanotube arrays. Others are using novel build-up techniques, microsprings and other concepts to enable "room-temperature assembly. This paper outlines some of the promising technology solutions with examples.

9:35 AM Invited

An Overview on Pb-Free, Flip-Chip Wafer Bumping Technologies: *Sung Kang*¹; Peter Gruber¹; Da-Yuan Shih¹; ¹IBM Corporation

To meet the RoHS guidelines and the demand for lower costs, finer pitch and higher quality, considerable work is going on in electronic industry to develop Pb-free solutions for flip chip technology. In this paper, various solder bumping technologies developed for flip-chip applications are reviewed with an emphasis on a new wafer bumping technology called C4NP (controlled collapse chip connect new process). Several inherent advantages of C4NP technology are discussed over other technologies. This paper will also discuss the recent development and implementation of Pb-free C4 interconnections for 300 mm wafers demonstrated at IBM. In addition, some metallurgical issues associated with C4NP technology are discussed.

10:05 AM Break

11:20 AM

Thermal Degradation of Al/Ni(V)/Cu-UBM in Flip Chip Solder Joints: John Osenbach¹; ¹LSI/Package Development

The resistance-time behavior of flip chip solder joints made with Al/Ni(V)/Cu-UBM, eutectic Pb-Sn solder bumps on substrates with either Electroless Ni(P)-Immersion Gold (ENIG) or Cu surface finish was determined at temperatures between 150C and 175C. Degradation of the ENIG based devices was well characterized by a single Arrhenius expression with an effective activation energy, E_a , of approximately 1.57eV and a pre-exponential constant, A_t , of approximately 1×10^{-16} /hour. In contrast the resistance remained essentially constant over the entire aging time interval for the device made on Cu independent of aging temperature. The stability at 175C of solder joints made on Cu was found to be more than 50 time greater than equivalent joints made on ENIG. The detailed degradation mechanism based on detailed microstructural studies will be reported in a companion paper "Microstructural Changes in Al/Ni(V)/Cu-UBM Resultant From High Temperature Induced Degradation of Flip Chip Solder Joints."

10:35 AM

Microstructural Changes in Al/Ni(V)/Cu-UBM Resultant from High Temperature Induced Degradation of Flip Chip Solder Joints: John Osenbach¹; ¹LSI/Package Development

The time dependent microstructural and chemical characterization of flip chip solder joints made with Al/Ni(V)/Cu-UBM and eutectic Pb-Sn solder bumps on either Electroless Ni(P)-Immersion Gold (ENIG) or Cu aged at 150C to 175C are reported. The microstructure and chemical composition of these joints were determined with a combination of techniques including Scanning Electron Microscopy (SEM), Energy Dispersive Spectroscopy (EDS), Focused Ion Beam Microscopy (FIB), and Transmission Electron Microscopy (TEM). The microstructural characterization clearly showed that electrical degradation of the ENIG devices was a direct result of the conversion and interfacial oxidation of the as deposited Ni(V)-barrier UBM layer into a porous layer that contained a web like fine grain V3Sn IMC. This conversion was driven by the Au from the ENIG surface finish. No such conversion was observed for the devices assembled on Cu-SOP surface finish substrates.

10:50 AM

Lead Free Solder Using TRIP Effect: Kyu-Oh Lee¹; John Morris¹; Fay Hua²; ¹University of California, Berkeley; ²Intel Corporation

The research reported here explored the use of transformation induced plasticity effect to enhance stress relaxation in lead free solder. The materials tested were Sn-In solders with 9-15 wt. per cent indium, with either Cu:Cu or Ni:Ni metallization. Samples were tested in simple shear at various temperatures to measure the deformation-induced martensite transformation temperature and study creep and stress relaxation behavior. Deformation-induced martensitic transformations were observed in this set of alloys. The transformation is characterized by a significant increase in elongation to failure, and by the appearance of lens-shaped martensite plates in the microstructure. The potential uses of TRIP behavior in solder joints is discussed on the basis of these results.

11:05 AM

Direct Observation of Hot Spots in Flip-Chip Solder Joints under Current Stressing Using Infrared Microscopy: Hsiang-Yao Hsiao¹; Chih Chen¹; ¹National Chiao Tung University

The temperature and hot spot in the SnAg3.5 solder joints were directly obtained using thermal infrared microscope in this study. Previous simulation results indicate that there exists a hot spot. However, there are no experimental results to verify it. In this study, a hot spot is observed when the applied current is higher than 0.4A. The horizontal thermal gradient near the chip side of the bump with a 5- μ mCu UBM can be as high as 571°C/cm when 0.4A was applied at 100°C. As the applied current increased, the difference between the hot spot and the average temperature continue to increase. It may be as large as 29°C when the solder joint was powered by 0.6A. In addition, the hot spot and average temperature decrease with a thicker UBM consisting 5- μ mCu/3- μ mNi UBM. This hot spot may play an important role in predicting the MTTF of solder joints and the failure mode of electromigration failure.

11:20 AM

Interfacial Reactions of Die Attached AlN-DBC Module Using Zn-Sn High Temperature Solders: Seongjun Kim¹; Keun-Soo Kim²; Do-seop Kim²; Katsuaki Suganuma²; ¹Osaka University; ²Osaka University, Institute of Scientific and Industrial Research

For the higher thermal dissipation and operating temperature, power modules in a hybrid car employ the AlN-DBC substrate, which has an excellent thermal conductivity. And the high temperature solder for this application must be used beyond 150°C. In spite of the RoHS regulation, however, very few attempts have been made for developing an alternative high temperature solder which can replace the high Pb solders. In the previous study, we suggested Zn-xSn(x=20, 30, 40wt%) solders as one of the best candidates. To evaluate the possibility of this alloy further, we have investigated the interfacial reactions of the die attached AlN-DBC module by using Zn-xSn solders. Through the microstructural analysis, the effect of soldering condition and the alloying contents were evaluated. Thermal conductivity of solder alloys were examined using a Xe-flash measurement. And the reliability of joint was evaluated by using the reflow test and thermal cycling test.

11:35 AM

The Microstructure Changes, Diffusion Mechanism and Kinetics of the Intermetallics Growth in Ag/Ag Interconnections: Pawel Zieba¹; Joanna Wojewoda¹; Anna Wierzbicka¹; ¹Polish Academy of Sciences

Application of the diffusion soldering technology with transient presence of liquid indium or tin solder allowed to obtain stable Ag/Ag interconnections. Three different techniques were verified where the solder was: sputter deposited on the substrate surface, electrochemically deposited or clamp as the thin foil between silver pads. Comprehensive description of the joint microstructure and interfaces was performed using optical, scanning and transmission electron microscopy. Moreover, the chemical composition and the sequence of appearance of the intermetallic phases was determined. On the other hand, the intermetallic growth kinetics study resulted in evaluation of the diffusion mechanism and diffusivity values.

Emerging Methods to Understand Mechanical Behavior: Indentation and Dynamic Methods

Sponsored by: The Minerals, Metals and Materials Society, TMS Structural Materials Division, TMS Materials Processing and Manufacturing Division, TMS: Advanced Characterization, Testing, and Simulation Committee, TMS/ASM: Mechanical Behavior of Materials Committee, TMS: Nanomechanical Materials Behavior Committee
Program Organizers: Brad Boyce, Sandia National Laboratories; Mark Bourke, Los Alamos National Laboratory; Xiaodong Li, University of South Carolina; Erica Lilleodden, Forschungszentrum

Tuesday AM
March 11, 2008

Room: 285
Location: Ernest Morial Convention Center

Session Chair: To Be Announced

8:30 AM

Quasi-Static and Dynamic Testing of Wear Tested Single Crystal Nickel: Neville Moody¹; Megan Cordill²; Somuri Prasad¹; William Gerberich²; ¹Sandia National Laboratories; ²University of Minnesota

Nanoindentation is often the test chosen for measuring mechanical properties of small volumes. It is the test we use to measure properties of materials for MEMS applications. However, properties can differ significantly depending on the use of quasi-static or dynamic test methods. As a consequence, we used both test methods to measure mechanical properties in wear tested single crystal nickel. The results show that hardness values from quasi-static tests exhibit the same effect of load and number of cycles used to generate wear patterns as those from dynamic tests but are consistently higher. More importantly, when bulk baseline hardness values are subtracted from the measured values the values superimpose. In this presentation, we will show that both techniques accurately describe the effects of wear on properties and discuss the factors that lead to

differences in measured values. This work was supported by Sandia National Laboratories under USDOE contract DE-AC04-94AL85000.

8:50 AM

Study on the Indentation Size Effect in CaF_2 : Dislocation Structure and Hardness: *Karsten Durst*¹; *Peiman Sadrabadi*¹; *Mathias Göken*¹; ¹University Erlangen-Nürnberg

Understanding size effects in indentation testing requires the analysis of the underlying dislocation structure. In this study nanoindentations have been performed on a cleaved CaF_2 crystal. The deformation during indentation is first purely elastic until dislocations are created, observable in a pop-in the load displacement data. After pop-in a relatively high hardness is observed, which gradually decreases, until a nearly constant hardness is found. This behavior is modeled from 50 nm to 3500 nm indentation depth using a modified Nix/Gao model, where geometrically necessary dislocations and statistically stored dislocations are considered. The dislocation structure is quantified using a "nano" dislocation etch pit technique in conjunction with AFM. By using polishing and sequential etching and imaging, the dislocation structure is studied in three dimensions around and underneath the indented material. The observed 3D dislocation structure will be discussed within the Taylor dislocation hardening model.

9:10 AM

Mechanical and Electrical Properties of Sputtered Single Crystal Cu Films with Nanoscale Growth Twins: *Osman Anderoglu*¹; *Amit Misra*²; *Vibhor Jain*¹; *Haiyan Wang*¹; *Filip Ronning*²; *Michael Hundley*²; *Richard Hoagland*²; *Xinghang Zhang*¹; ¹Texas A&M University; ²Los Alamos National Laboratory

We have synthesized single crystal Cu thin films via magnetron sputtering technique onto Si substrates with different orientations. Single crystal Cu films grown on Si (110) substrate possess high density {111} type growth twins. Single crystal Cu films with nanotwins have a hardness of 2.5 GPa with electrical resistivity comparable to that of bulk Cu. Single crystal Cu of {100} type grown on Si (100) substrate has a hardness of 1.2 GPa with bulk Cu resistivity. The influence of deposition parameters on the electrical and mechanical properties of polycrystalline Cu films will also be discussed.

9:30 AM

Improvement of Extracting Material Properties by Sharp Nanoindentation with Valid Reduced Modulus for Elasto-Plastic Materials: *Insuk Choi*¹; *Yanping Cao*²; *Ruth Schwaiger*¹; *Oliver Kraft*¹; ¹Forschungszentrum Karlsruhe; ²Max-Planck-Institut für Eisenforschung GmbH

Recent computational parametric studies have developed reverse algorithms to extract material properties of elasto-plastic materials using experimental sharp nanoindentation. These methods used reduced modulus in their parameters to include the effect of indenter compliance. To investigate the validity of using reduced modulus, we performed a finite element study for sharp indentation of a wide range of sample materials with rigid, diamond, and sapphire indenters. Then, we conducted experimental indentation of several representative cases. Both computational and experimental results indicate that the usage of reduced modulus is invalid for a certain material regime. For example, the indentation loading responses of Ni are identical for all three tips, whereas the previous predictions using reduced moduli generated deviation of 8%. This difference can cause a substantial error in extracting material properties by reverse algorithms. We will provide comprehensive and systematic study of using reduced modulus so as to improve reverse algorithms.

9:50 AM

Nanoindentation Analysis as a Two-Dimensional Tool for Mapping the Mechanical Properties of Complex Surfaces: *Nicholas Randall*¹; *Jill Powell*¹; ¹CSM Instruments

Nanoindentation has now become established for the single point characterization of hardness and elastic modulus of both bulk and coated materials. This makes it a very good technique for measuring mechanical properties of homogeneous materials. However, many composite materials comprise material phases that cannot be examined in bulk form ex-situ (e.g., carbides in a ferrous matrix, calcium silicate hydrates in cements, etc.). The requirement for in-situ analysis and characterization of chemically complex phases obviates conventional mechanical testing of large specimens representative of these material components. This paper will focus on new developments in the

way that nanoindentation can be used as a two-dimensional mapping tool for examining the properties of constituent phases independently of each other. This approach relies on on large arrays of nanoindentations and statistical analysis of the resulting data. Examples will be presented ranging from soft polymer blends to metal-matrix composites.

10:10 AM

Temperature Dependent Viscoelastic Properties of Polymers Investigated by Nanoscale Dynamic Mechanical Analysis: *Yuebin Lu*¹; *Douglas Shinozaki*²; ¹University of Kentucky; ²University of Western Ontario

The viscoelastic properties of polymers are investigated by nanoscale dynamic mechanical analysis (DMA) in the temperature range of -100 – +200°C. The polymers tested range from glassy polymer (atactic polystyrene), semicrystalline polymer (high density polyethylene), to rubbery polymer (polyisobutylene). The nanoscale DMA is performed with a flat-tipped microindenter by imposing a sinusoidal displacement of amplitude of less than 40 nm into the specimen and then measuring the responses of load and phase angle. The storage modulus, loss modulus and loss tangent are calculated and found to be independent upon the sample size (thickness). The results from nanoscale DMA are consistent with those from conventional dynamic mechanical analysis by testing the bulk materials in bending mode.

10:30 AM Break

10:45 AM

Nano-Mechanical Analysis of Mechanical Characteristics of a Ultra High Strength Pipeline Steel: *Byoung-Wook Choi*¹; *Jung-Eun Jung*¹; *Byung-Gil Yoo*¹; *Jae-il Jang*¹; *Dong Seo*²; ¹Hanyang University; ²Pohang Iron and Steel Company

The mechanical characteristics in micro-phases of two different-typed API X-100 pipeline steels (ultra high strength steels recently developed for the transmission of crucial oil and natural gas) were evaluated by using nanoindentation technique. The steels' microstructures mainly consist of equiaxed/acicular ferrite and bainite. Nanoindentation experiments were made on each phase, and the hardness impressions were analyzed by scanning electron microscopy (SEM) and atomic force microscopy (AFM). The results are discussed in terms of the microstructural effects on the deformation and hardening mechanisms in the steels. This work was supported by Pohang Iron and Steel Company.

11:05 AM Invited

Dynamic Testing: In Situ Diagnostics and Post Test Recovery: *Carl Trujillo*¹; *G.T. Gray III*¹; *Shuh-Rong Chen*¹; *Philip Rae*¹; ¹Los Alamos National Laboratory

Developing innovative dynamic experimental techniques has enhanced our understanding of mechanical behavior of materials. Various techniques such as velocity interferometer system for any reflector (VISAR) and high speed imaging provide in situ observation of numerous high rate phenomena such as failure, incipient damage, and pressure induced phase transformations. In addition, multiple experimental techniques have been designed to capture and soft recover these specimens for post test analysis. Recovery methods using momentum trapping allow a dynamic test to be arrested for either post test characterization and/or further mechanical testing. This allows for in situ diagnostics to be coupled with post test characterization of specimens via electron backscattered diffraction (EBSD), neutron diffraction, or transmission electron microscopy. The aim of this talk will be to give an overview of the capabilities and recent innovations in dynamic test diagnostics and recovery techniques within the dynamic test facilities in MST-8 at Los Alamos National Laboratories.

11:35 AM

Investigation of Inter and Intramolecular Deformation within Energetic Molecular Single Crystals: *Kyle Ramos*¹; *Von Whitley*¹; *Daniel Hooks*¹; *Marc Cawkwell*¹; *Thomas Sewell*¹; *David Bahr*²; ¹Los Alamos National Laboratory; ²Washington State University

Multiple materials testing and characterization techniques have been employed in tandem with molecular dynamics simulations in order to investigate inter and intramolecular deformation occurring within brittle molecular single crystals, both for energetic (RDX) and inert systems (sucrose). Nanoindentation coupled with scanning probe microscopy was used to measure hardnesses and reduced

moduli while recording deformation features within pile-up zones around indentation impressions to determine deformation mechanisms within these brittle crystals. The onset of plastic deformation has been identified using this technique. Laser-driven shock experiments were used to recover samples for post shock microstructural characterization and were compared to deformation from quasistatic tests, while intramolecular deformation was mapped with confocal Raman microscopy. Plate impact experiments were conducted using a linear resolved optical recording velocity interferometry system (Line ORVIS) to record the spatial homogeneity of orientation dependent impact responses. Molecular dynamics simulations suggest microstructural responses associated with the nanoindentation and plate impact experiments.

11:55 AM

Electromagnetic Ring Expansion for High Strain Rate Tensile Testing: Glenn Daehn¹; Jason Johnson²; Gregg Fenton³; ¹Ohio State University; ²Michigan State University; ³Applied Research Associates, Inc.

The electromagnetically driven expanding ring has been proposed as a test for high strain rate tensile and was highly developed by Gourdin in 1988. This is a very elegant test in that it provides true uniaxial tension and can drive to strain rates over 10⁴ s⁻¹. It is also a very useful test in studying high strain rate ductility and fragmentation behavior. This test never became widely used because the instrumentation was rather expensive and cumbersome and to boundary conditions very simple, rings of very slender cross-sections were used, limiting the strain rates that could be achieved. Here we will detail new attempts to build upon this framework using modern developments in instrumentation and numerical analysis. This efficient test can provide constitutive behavior, as well as ductility and fragmentation data in one straightforward test. Here construction, use and information available from this test will be discussed.

12:15 PM

Growth of Voids during Dynamics Fracture: James Belak¹; Mukul Kumar¹; John Kinney¹; Lyle Levine²; Jan Ilavsky³; ¹Lawrence Livermore National Laboratory; ²National Institute of Standards and Technology; ³Argonne National Laboratory

Samples of high purity single and polycrystal Al and Cu were brought to incipient spallation fracture under dynamic loading conditions. X-ray, electron and neutron scattering were used to quantify the nucleation and growth of voids inside at the spall plane. The samples were first analyzed using x-ray tomography to reveal the 3D spatial distribution of porosity. Both small angle x-ray and neutron scattering experiments were performed on the same samples resulting in a dataset spanning four decades in lengthscale. The scattering as calculated from the tomography is compared to the neutron scattering at overlapping length scales. Finally, the samples were sectioned and EBSD was used to characterize the plastic zone surrounding the voids and the microstructural processes of nucleation and growth. This work was performed under the auspices of the U.S. Department of Energy by University of California, LLNL under Contract W-7405-Eng-48.

Enhancing Materials Durability via Surface Engineering: Superalloy Surface Durability

Sponsored by: The Minerals, Metals and Materials Society, TMS Structural Materials Division, TMS/ASM: Corrosion and Environmental Effects Committee, TMS: High Temperature Alloys Committee

Program Organizers: David Mourer, GE Aircraft Engines; Andrew Rosenberger, US Air Force; Michael Shepard, Air Force Research Laboratory/MLLMN; Bruce Pint, Oak Ridge National Laboratory; Brian Gleeson, Iowa State University

Tuesday AM

Room: 388

March 11, 2008

Location: Ernest Morial Convention Center

Session Chair: Andrew Rosenberger, US Air Force

8:30 AM Introductory Comments

8:35 AM

Mechanisms of Lifetime Improvement in Thermal Barrier Coatings with Hf and/or Y Modified CMSX-4 Superalloy Substrates: Jing Liu¹; Kenneth Murphy²; Yong-ho Sohn¹; ¹University of Central Florida; ²Howmet Corporation

Superior thermal cyclic lifetime was observed for thermal barrier coatings (TBCs) with (Ni,Pt)Al bondcoat and Hf- and/or Y-modified CMSX-4 superalloy, where each thermal cycle consisted of 10-minute heat-up, 50-minute dwell at 1135°C, and 10-minute forced-air-quench. Microstructural degradation and failure of TBCs were examined by scanning and transmission electron microscopy. Distribution of Hf in the thermally grown oxide (TGO) scale was examined by secondary ion mass spectroscopy. While rumpling and ratcheting of the TGO-bondcoat interface were observed to be the main damage characteristic for TBCs on CMSX-4, the same interface remained flat for durable TBCs with modified CMSX-4. For TBCs with superior lifetime, monoclinic HfO₂ was observed as fine precipitates along the grain boundaries of TGO scale, the parabolic growth constant of the TGO scale was slightly lower, the columnar diameter of the TGO scale was smaller, and Hf and/or Y were observed to segregate to the TGO-bondcoat interface.

8:55 AM

Microstructural Investigation of Multiphase NiAl-Hf Bond Coats on Nickel-Base Superalloys: Michael Bestor¹; Arthur Brown¹; Richard Martens¹; Mark Weaver¹; ¹University of Alabama

It has been reported that NiAl overlay bond coatings containing Hf or Zr concentrations well above their solubility limits can exhibit oxidation resistance that is comparable to state-of-the-art platinum aluminide coatings. In this study, a microstructural investigation has been conducted at UA via tomographic atom probe and transmission electron microscopy of precipitation/strengthened NiAl-Hf coatings deposited via DC magnetron sputtering onto single crystal superalloy substrates. Post-deposition annealing of NiAl-1.0 at.% Hf at 1000°C for 1 to 4 hours resulted in the formation of nanometer-sized Hf-rich precipitates. Longer pre-oxidation annealing times resulted in smaller mass gains during isothermal oxidation with values approaching those of model NiAl-0.05 at.% Hf coating alloys. Results suggest that suitable oxidation resistance can be obtained in "over-doped" alloys by optimizing the coating chemistry, grain structure and precipitate distribution.

9:15 AM

Opportunities in YbO_{1.5}-TiO₂-ZrO₂ for Application in Thermal Barrier Systems: Rafael Leckie¹; Tobias Schaedler¹; Anthony Evans¹; Carlos Levi¹; ¹University of California at Santa Barbara

Co-doping of yttria stabilized zirconia (YSZ) with rare earth (RE) oxides has provided a promising variety of next generation thermal barrier oxides with low thermal conductivity. However, the advantages offered by these novel compositions typically carry penalties regarding durability which have been broadly associated with a loss of toughness concomitant to the decline in tetragonality of the structure with increasing dopant addition. Ti additions have shown to be beneficial in enhancing toughness in t' zirconias by increasing the tetragonality of the structure. This paper discusses opportunities in the

YbO_{1.5}-TiO₂-ZrO₂ system regarding the effects of chemical composition on toughness, phase stability, and thermal conductivity and compares it with previous experiences in the Y and Gd systems. The connection between chemical composition, phase equilibria, microstructure and potential toughening mechanisms will be discussed.

9:35 AM

Microstructure and Thermo-Mechanical Properties of CMAS-Penetrated APS Thermal Barrier Coatings: *Sabine Faulhaber*¹; *Anthony Evans*¹;

¹University of California Santa Barbara

A new extrinsic failure mechanism of thermal barrier coatings becoming more relevant with higher engine operating temperatures is infiltration with molten calcium-magnesium-alumino-silicate (CMAS) deposits. Thermo-mechanical stresses during cooling can lead to delamination and spallation of the coating. The determination of changes in thermo-mechanical properties due to infiltration and solidification is important for the assessment of "safe" cooling scenarios. Isothermal experiments have been conducted to replicate the infiltration characteristics of thick air-plasma sprayed (APS) yttria-stabilized zirconia (YSZ) coatings found in engine hardware. The microstructure of these coatings has been characterized by scanning electron microscopy (SEM), energy-dispersive x-ray analysis (EDS) and transmission electron microscopy (TEM). Young's modulus and fracture toughness have been characterized by indentation methods. A laser setup has been used for infiltration experiments in thermal gradients as well as for measurement of the thermal conductivity. Combination with different cooling scenarios can confirm the validity of proposed delamination mechanics.

9:55 AM Break

10:05 AM

The Effects of Hot Corrosion Attack on the Fatigue Resistance of a Disk Superalloy: *Timothy Gabb*¹; *Jack Telesman*¹; *Brian Hazel*²; *David Mourer*²;

¹NASA Glenn Research Center; ²General Electric Aircraft Engines

Recently developed powder metallurgy nickel-base superalloys can be employed in gas turbine engines at temperatures approaching 700°C. Hot corrosion attack could occur at such temperatures, if corrosive species are present. The effects of high temperature salt exposures were investigated for the disk superalloy ME3/Rene 104. Fatigue specimens were machined from a full scale turbine disk. The gage sections were coated with a salt-containing mixture and exposed at 704°C in air. Fatigue tests were subsequently performed at 427 and 704°C on exposed specimens. The salt mixture produced localized pitting damage, with sulfides forming below outer oxide layers there. Fatigue life was reduced up to 90% by this hot corrosion damage.

10:25 AM

Evaluating Stability and Erosion Wear Behavior of HVOF Sprayed Cr3C2-20%(Ni20Cr) Coatings at Elevated Temperatures: *Prajina Bhattacharya*¹; *Anand K.*¹; *T. Shalini*¹; *T. Kluge*¹; ¹General Electric

HVOF processed Cr3C2-20%(Ni20Cr) coating is deposited with GTW of 6 and 10 inches. XRD and SEM characterization reveals Cr3C2 presence with Ni-Cr and Ni-Cr-C solid-solutions. XRD peak sharpness, carbide size and volume fraction vary slightly in the two samples. The coating thermal behavior is studied with DTA coupled with TGA. Coating stability is assessed under exposure to extended aging at 700°C and 800°C. Cr7C3 is prominent after aging. At 700°C, fine carbide distribution increases and at 800°C, pores are evident. Jet erosion of the samples with silica show that the erosion rate decreases after 700°C aging and increases back to the as-deposited value after 800°C aging. Ploughing and compaction are identified as erosion mechanisms. The ploughing effect is more pronounced with elevated temperature aging. The erosion mechanism is investigated with single particle erosion. Samples are subjected to hard quartz and soft magnetite to understand the effect of erodent hardness on the erosion behavior.

10:45 AM

Grain Boundary Engineering of Superalloys for Aerospace Engine Applications: *Peter Lin*¹; *Virgil Provenzano*¹; *Robert Heard*¹; *Herbet Miller*¹; *Tim Gabb*²; *Jack Telesman*²; ¹Integran Technologies USA Inc.; ²NASA Glenn Research Center

Grain Boundary Engineering (GBE) involves microstructural optimization via the strategic application of thermo-mechanical metallurgical processing and fabrication steps which increase the fraction of special, low-energy, and degradation-resistant grain boundaries (i.e., structurally ordered low grain boundaries) in the microstructure. By elevating the fraction of special grain boundaries in a metal or alloy either in the bulk or in the near-surface region, a commensurate improvement in the material properties is achieved owing to the intrinsic degradation-resistance (sliding, cracking, corrosion) of the "special" grain boundaries. Alloys that can benefit from this treatment include nickel-based superalloys that are used in the hot sections of gas turbine engines. Under increasingly demanding operating conditions, these materials can be vulnerable to grain boundary-related elevated-temperature degradation processes including creep, fatigue, solute segregation, precipitation embrittlement, and intergranular environmental attack.

11:05 AM

Effects of Surface Orientation on High-Temperature Oxidation Behavior: *Louis Bonfrisco*¹; *Megan Frary*¹; ¹Boise State University

Surface orientation plays an important role in oxidation behavior; studies of single crystals suggest that {111} surfaces are most resistant to oxidation. However, most materials are polycrystalline and contain numerous orientations which contribute to the oxidation process. Here we determine the effect of orientation on oxidation behavior of metals over all surface orientations. The microstructure is characterized with electron backscatter diffraction (EBSD). After high temperature oxidation, the oxide topography is characterized using optical profilometry (OP). By correlating results from EBSD and OP, the oxide height can be determined for each orientation. The data suggests that as the surface normal deviates from the <111> direction, the oxide thickness increases. The oxidation rate may depend on not only the surface orientation, but the character of the grain boundaries. This technique allows a thorough understanding of the role of surface orientation on oxidation and may provide insight to the production of oxidation-resistant surfaces.

11:25 AM Invited

Directed Vapor Deposition of Advanced Coatings for Aerospace Applications: *Derek Hass*¹; ¹Directed Vapor Technologies International

Alternative coatings and coating approaches are required to improve the performance of components used in aerospace applications including those in gas turbine engines and aircraft landing gear. Such coatings include thermal barrier coatings used to increase the durability and thermal resistance of hot-section engine components, environmental coatings for oxidation and hot corrosion protection and wear and corrosion protection coatings for landing gear components. Directed Vapor Technologies International (DVTI), is currently investigating the use of an advanced electron beam vapor deposition approach, Directed Vapor Deposition (DVD), as a method for applying high quality coatings at high rates onto aerospace components. The DVD process operates in a novel processing environment that employs a supersonic gas jet to "direct" vapor atoms onto components resulting in highly efficient deposition of complex coating structures and compositions. Here, the use of this approach to deposit advanced coatings for aerospace applications will be discussed.

Frontiers in Process Modeling: Metallurgical Reactors

Sponsored by: The Minerals, Metals and Materials Society, TMS Extraction and Processing Division, TMS Materials Processing and Manufacturing Division, TMS: Process Technology and Modeling Committee
Program Organizers: Andrew Campbell, WorleyParsons; Adam Powell, Opennovation

Tuesday AM Room: 287
March 11, 2008 Location: Ernest Morial Convention Center

Session Chair: Andrew Campbell, WorleyParsons

8:30 AM Introductory Comments

8:50 AM

A New Multi-Scale Modelling Approach for Metallurgical Reactors: Mark Schwarz¹; Tom Liu¹; Graeme Lane¹; Peter Koh¹; Yuqing Feng¹; ¹CSIRO Minerals

Metallurgical process reactors generally involve complex turbulent multi-phase flow phenomena, and one of the characteristics of such systems is that there are physical and chemical processes occurring at a wide variety of different length scales. One implication of this scale hierarchy is that standard Computational Fluid Dynamics (CFD) models of such systems require significant empirical input to describe the effect of phase interactions at the small scales, limiting the predictive capability of such models. A new multi-scale modelling methodology has been developed to overcome this deficiency. Unlike most multi-scale methods which depend on domain decomposition, the new method is based on process or phenomenological decomposition. This new method promises much faster simulation than methods that operate in the domain space. The method is described and two examples of applications of the method will be described, namely inclusion flotation and aluminium electrowinning.

9:10 AM

Modelling Metal Powder Production by the Gas Atomisation Process: Claudio Lena¹; Georgi Djambazov¹; Koulis Pericleous¹; ¹University of Greenwich

Metal powder in the range of 10-100 microns is widely employed in the production of Raney nickel type catalysts for hydrogenation reactions and hydrogen fuel cell manufacture. In this presentation we examine the modelling of powder production in a gas atomisation vessel using CFD techniques. In a fully coupled Lagrangian-Eulerian two phase scheme, liquid metal particles are tracked through the vessel following atomisation of a liquid nickel-aluminium stream. There is full momentum, heat and turbulence transport between particles and surrounding argon gas and the model predicts the position of solidification depending on particle size and undercooled condition. Maps of collision probability of particles at different stages of solidification are computed, to predict the creation of satellite defects, or to initiate solidification of undercooled droplets. The model is used to support experimental work conducted under the ESA/EU project IMPRESS.

9:30 AM

Simulating Morphology of Electrochemical Deposits in Shear Flow: Adam Powell¹; ¹Veryst Engineering LLC

Electrodeposition often takes place in shear flow, either to promote mixing in the aqueous or ionic electrolyte, or sometimes to sweep away deposited powder. Modeling such a system requires solving coupled equations for mass transfer of ions, electric field, moving metal-electrolyte interface, and fluid-structure interactions across that interface. Phase field is a robust thermodynamics-based methodology for mass transfer and phase change, particularly when the interface topology changes. For this reason, several researchers have published phase field models of electrodeposition including dendritic growth. However, the method's diffuse interface complicates fluid-structure interaction modeling. The model presented here uses the mixed stress method to model fluid dynamics in the liquid electrolyte coupled with elastic behavior of solids, including solid particles which break off and float away. While presenting results for electromigration-controlled deposition of an isotropic material in 2-D, this presentation will also discuss extension to 3-D, anisotropy, and charge transfer resistance.

9:50 AM

Simulation of the Dual Cooling Rates of Oil-Quenched Alloy Droplets Produced by the Uniform-Droplet Spray Process: Suresh Kumar Pillai¹; Teiichi Ando¹; Tatsuya Shoji²; ¹Northeastern University; ²Hitachi Metals Ltd.

A model was developed to simulate the thermal history of mono-size alloy droplets produced by the uniform-droplet spray (UDS) and quenched in oil. The model adopts a metallographic approach to account for the dual-phase heat transfer that the droplets experience in the oil. Model predictions are analyzed with the help of experimental data obtained with a glass-forming Fe45Ni22.5Co7.5Mo3B14Si8 alloy. The ability to predict the droplet cooling in liquid medium allows for the use of smaller spray chambers and inexpensive chamber gases.

10:10 AM Break

10:20 AM

Boundary Element Modeling of Solid Oxide Membrane Process: Rachel De Lucas¹; Adam Powell²; Uday Pal¹; ¹Boston University; ²Veryst Engineering LLC

Mathematical modeling is a useful tool for design of electrochemical systems such as the magnesium solid-oxide membrane process (Mg-SOM). In this study, the Boundary Element Method (BEM) was particularly suited to the 3-dimensional modeling of the Mg-SOM process. BEM modeling allows one to change the geometry without remeshing, a useful feature for parametric optimization. After benchmarks demonstrated the accuracy of the program, the resulting model calculated electric current density and heat generation rates for both single YSZ membrane and three YSZ membrane geometries of this process. The model then provided a platform for optimization of electrode placement, first to minimize total resistance of the system, and second to maximize current density uniformity at the anode.

10:40 AM

CFD Simulation of Mixing in Stirred Reactor: Xiaochang Cao¹; Ting'an Zhang¹; Qiuyue Zhao¹; ¹Northeastern University

Stirred reactors are widely used in mineral and metallurgy industries. Computational Fluid Dynamics (CFD) provides a tool for determining detailed information on fluid flow inside stirred reactors. A new-style stirred reactor was designed for digestion process of minerals. This paper is a preliminary study to demonstrate the CFD simulation of fluid flow in an impeller stirred reactor using Multiple Reference Frames (MRF) impeller rotation model and the standard k-ε turbulence model. The computational model is solved using commercial CFD code FLUENT 6.3 (FLUENT Inc.). Simulations are achieved at various values of initial rotating speed and flux, and the influences of swirl motion has also been investigated. The residence time distributions (RTD) curves predicted by CFD model show good agreement with experimental data. The information would be useful for optimizing stirrer's design and enlarging multiphase flow in stirred reactor.

General Abstracts: Light Metals Division: Session II

Sponsored by: The Minerals, Metals and Materials Society, TMS Light Metals Division, TMS: Aluminum Committee, TMS: Reactive Metals Committee, TMS: Recycling and Environmental Technologies Committee

Program Organizers: Neale Neelameggham, US Magnesium LLC; Anne Kvithyld, Norwegian University of Science and Technology

Tuesday AM
March 11, 2008

Room: 297
Location: Ernest Morial Convention Center

Session Chairs: Jean-Jacques Grunspan, Brochot SA; Chitoshi Masuda, Waseda University

8:30 AM

Microstructure and Properties of Gas-Atomised and Ingot-Route Burti: Hui Jang¹; Michael Loretto¹; Dawei Hu¹; Xinhua Wu¹; Francesco Paster²; Michael Preuss²; Phillip Withers²; ¹University of Birmingham; ²University of Manchester

The response to imposed tensile deformation of hot isostatically pressed (HIPped) powder BurTi, the burn-resistant Ti alloy, Ti25V15Cr2Al0.2C (wt%), has been compared with that of extruded ingot-route material. Both gas-atomised powder and PREP powder have been used. Some powder HIPped samples were heat treated at a temperature above the HIPping temperature before testing. Acoustic emission, synchrotron radiation and transmission electron microscopy have been used to assess the response to strain up to failure. The importance of any porosity in the powders has been assessed and detailed observations will be reported on the influence of process-route on behaviour.

8:50 AM

Prefabricated Materials Preforms in Al and Ti Using Friction Welding: Philip Threadgill¹; Bradley Wynne²; ¹TWI; ²Sheffield University

Many complex aerospace components are machined from expensive large blocks of materials which often have long lead times. Many of these materials, especially titanium alloys, are difficult to machine, and since the fly/buy ratios can be below 10%, this is a financially and environmentally unattractive approach. Many machining preforms can be easily manufactured from smaller pieces of materials for relatively low cost. Several approaches are available, but this presentation will consider the benefits of friction welding and friction stir welding. Examples will be given of recent work which highlights the possibilities for aluminium and titanium alloys, using various friction based approaches. The presentation will also include detailed microstructure analysis of welded samples via optical and scanning electron microscopy as well as orientation image maps obtained by electron backscattered diffraction, which demonstrate the excellent microstructures which can be obtained.

9:10 AM

High Temperature Oxidation Studies of Ti₃Al-4.0at%Mo in Pure Oxygen: Christopher Williams¹; ¹University of Alabama

Ti₃Al-4.0at%Mo samples were oxidized under pure oxygen atmosphere at temperatures ranging from 1023-1223 K in a Thermogravimetric Analysis (TGA) apparatus. Effective activation energy of 294 kJ/mol was determined from the weight gain data. This composition oxidizes more rapidly than binary Ti₃Al alloy of comparable composition as well as alloys containing smaller concentrations of Mo found in the literature. Reaction products consisted of rutile and alumina particles.

9:30 AM

Fabrication of Carbon Fibers Reinforced Aluminum Matrix Composites: Chitoshi Masuda¹; Yu-suke Nishimiya¹; ¹Waseda University

Carbon fiber reinforced aluminum matrix composites were expected for the application of automobile engine parts such as radiator, piston head, and engine wall due to the high strength and high heat exchange rate. Composites were fabricated by powder metallurgy method. The aluminum powder were blended in to the carbon fibers and mixing with the ball mill in alcohol solutions. After milling the solutions were heated at low temperature for 24 hours. The mixed powders were consolidated by Spark Plasma Sintering machine at

maximum temperature of 585°C for 1 hour. The microstructures were examined and thermal conductivity was measured using laser flash method and DSC method. The chopped carbon fibers were homogenously distributed up to about the volume fraction of 50wt%. On the other hand, the CNT was not so homogenous distribution up to about the volume fraction of 30wt%. Carbon nano-fibers(VGCF) were almost homogenously distributed after ball milling.

9:50 AM

Effect of Oil-Soluble Additive on the Gibbsite Precipitation from Sodium Aluminate Solution with Seeds: Chen Feng¹; Xie Zhihui¹; Zhang Baoyan¹; Bi Shiwen¹; Li Yue¹; ¹Northeastern University

The effect of an oil-soluble additive which contained a gemini surfactant and a common anionic surfactant on the seed precipitation from sodium aluminate solution had been studied. We researched the two conditions which were the additive's concentration and the additive's injecting time, the results showed that when the additive's concentration in sodium aluminate solution was 60 mg.L⁻¹ and the injecting time was 15th hour, the precipitation ratio was improved by about 1.5% and the granularity of Al(OH)₃ didn't become badly, the granularity distributing of Al(OH)₃ centralized at 45-75µm. It made improving the precipitation ratio come true under the condition that the mass fraction of Al(OH)₃(≤45µm) didn't increased.

10:10 AM Break

10:20 AM

Influence of Cooling Rate on the Structure of Closed-Cell Aluminium Foams: Manas Mukherjee¹; Francisco Garcia-Moreno¹; John Banhart¹; ¹Hahn-Meitner-Institute

We present the influence of cooling rate on both the morphology and the microstructure of closed-cell aluminium foams produced by the powder metallurgical method. Precursors were prepared by uni-axial hot compaction of metal and blowing agent powder blends and were foamed in a second step by heating to above the melting point. Foam evolution and shrinkage were studied in-situ by X-ray radiography. A specially designed furnace was used to have a wide range of cooling rates. X-ray computed tomography was conducted on these foams to study their three-dimensional macrostructure and to quantify pore size distribution. In addition the microstructure was studied by metallography and microscopy. Some selected mechanical properties of these foams were measured. It was found that the microstructure as well as the macrostructure vary with cooling rate. The influence of cooling rate on cell wall coalescence during solidification was found to be the main mechanism causing the differences.

10:40 AM

Low Temperature Electrochemical Synthesis of Ti-Al Alloys Using Ionic Liquid Electrolytes: Debabrata Pradhan¹; Ramana Reddy¹; ¹University of Alabama

The synthesis of Ti-Al alloys were carried out using AlCl₃-1-butyl-3-methyl imidazolium chloride (BmimCl) electrolyte at different temperature between 70°C and 125±3°C. The alloy was deposited on titanium cathode at various voltages between 1.5V and 3.0V. The molar ratio of AlCl₃ and BmimCl is 2:1 for all experiments. Titanium sheet (>99.99 wt%) was used as anode. Morphology and composition of electrodeposited Ti-Al alloy were characterized using SEM/EDS and ICP-OES respectively. Also, the effect of applied voltage and temperature on cathode current density, current efficiency, composition and morphology of electrodeposit were investigated. The Ti-Al alloys containing 26-37 wt% Ti were produced with a current efficiency of about 80-85%.

11:00 AM

Residual Life Extension of Aged Transformers in Aluminium Smelters: Santhosh Kumar Rajamoorthy¹; Muralidharan Kesavan¹; Saravanan Krishnamoorthy¹; ¹Madras Aluminum Company Ltd.

The modern world is increasingly dependent on electricity for economic prosperity. Without doubt the single most important piece of equipment in electrical networks in Aluminium Smelters is the Power transformer. However the average age of transformers around the world is increasing rapidly with transformer failures rising exponentially, and to replace all of the aged power transformers at risk would be prohibitively expensive. This paper focuses on the extension of residual life of these aged transformers through online reclamation

of oil a process through which the quality of oil is renewed better than the new oil meeting the standards of a new oil thereby the life.

11:20 AM

Revamping of Rodding Shop Worldwide: *Jean-Jacques Grunspan*¹; ¹BROCHOT SA

The decision to revamp a rodding shop after 20 or 30 years use is a strategic decision for an aluminium smelter in view of its potential threat to the continuity of supply of rodded anodes to the potrooms. BROCHOT has undertaken the revamping of 3 rodding shops in 3 different smelters (PNL Netherlands, Lynemouth UK and DUBAL in UAE). In this article, it shares its experience by highlighting those factors which must necessarily be considered before undertaking any such revamping project so as to prevent major problems.

11:40 AM

Expert System on Properties of Molten Electrolytes: *Alexander Redkin*¹; Anatoly Shurygin¹; Olga Tkacheva¹; ¹Institute of High Temperature Electrochemistry

Development of new electrochemical technologies requires new electrolytes. Every change in the electrolyte composition leads to property change. Experimental investigation of molten electrolytes properties, such as density, electrical and thermal conductivity etc. takes much time. The physical model connecting above mentioned parameters is needed in order to evaluate the properties. We propose empirical model that allows describing the most of electrolyte properties as a function of molar volume and temperature. This model is used in our expert system "Molten Salt Properties" which makes possible to describe existing experimental data or evaluate some unmeasured properties for new electrolytes. The work is based on experience, knowledge and experimental results that have been collecting at the Institute of High Temperature Electrochemistry during 50 years of molten salts investigations.

General Abstracts: Materials Processing and Manufacturing Division: Composition Structure Property Relationships II

Sponsored by: The Minerals, Metals and Materials Society, TMS Materials Processing and Manufacturing Division, TMS/ASM: Computational Materials Science and Engineering Committee, TMS: Global Innovations Committee, TMS: Nanomechanical Materials Behavior Committee, TMS/ASM: Phase Transformations Committee, TMS: Powder Materials Committee, TMS: Process Technology and Modeling Committee, TMS: Shaping and Forming Committee, TMS: Solidification Committee, TMS: Surface Engineering Committee
Program Organizers: Ralph Napolitano, Iowa State University; Neville Moody, Sandia National Laboratories

Tuesday AM Room: 282
 March 11, 2008 Location: Ernest Morial Convention Center

Session Chairs: Bryony James, University of Auckland; Christopher Roberts, Carnegie Mellon University

8:30 AM

Towards Single Crystals Using Strain Induced Grain Growth Part I: Experimental Results with Pure Iron: *Benjamin Fell*¹; Tien Tran¹; Corentin Guebels¹; Jean-Pierre Delplanque¹; Joanna Groza¹; ¹University of California at Davis

Experimental results from creep tests on pure iron are presented in the context of static (SRX) and dynamic recrystallization (DRX). The aim of the experiments are to, first, provide necessary recrystallization and grain growth data across various strain rates and maximum strain values to calibrate DRX simulation models and, second, produce abnormal grain growth (AGG) through strain assisted recrystallization. Producing single crystals with solid state techniques has been shown to be advantageous for allotropic materials such as molybdenum and uranium. The results show that grain growth is a function of strain rate and that abnormal grain growth initiates in the neck region across all strain rates. The experimental program investigates strain rates in the creep regime (10⁻⁴ to

10⁻⁵ /s) at temperatures ranging from 800 to 900°C (~0.6T_m) to determine the sensitivity of these parameters in initiating AGG.

8:50 AM

Towards Single Crystals Using Strain Induced Grain Growth Part II: Monte Carlo Simulations and Physical Time Predictions: *Corentin Guebels*¹; Benjamin Fell¹; Tien Tran¹; Joanna Groza¹; Jean-Pierre Delplanque¹; ¹University of California, Davis

The microstructural evolution and kinetics of thermal and strain-induced grain growth were analyzed using a two dimensional Monte Carlo Potts (MCP) model. MCP simulations have captured various grain growth behaviors; however, the stochastic nature of the MCP time-step limits its verification with physical data. An energy-controlled relationship between MCP and physical time-steps was established using thermal grain growth simulations and published experimental data. The case of static strain-induced growth is considered next. The modeling strategies for the strain-induced energy, recovery and nucleation and their implementations are discussed in connection with experimental evidence.

9:10 AM

Elevated Temperature Uniaxial Compression Testing of Sintered ZrN and (Zr, Ti)N Pellets as Surrogate for PuN and (Pu,Zr)N Fuel Pellets: *Kirk Wheeler*¹; Pedro Peralta¹; Kenneth McClellan²; ¹Arizona State University; ²Los Alamos National Laboratories

In this work, ZrN and (Zr,Ti)N were studied as possible surrogates for PuN and (Pu, Zr)N under the Global Nuclear Energy Partnership (GNEP) program. The mechanical properties of sintered ZrN and (Zr, Ti)N pellets were examined to investigate the effects that sintering temperatures and material segregation have on structural integrity at various working temperatures. Uniaxial compression testing was performed on ZrN and (Zr,Ti)N pellets sintered at various temperatures. Testing was performed in an ultra-high purity Argon atmosphere at various temperatures (25°C, 800°C, 1200°C). Post-Mortem fractography was performed using optical and electron microscopy (SEM) and energy dispersive x-ray spectroscopy (EDS). The failure modes of the pellets and their mechanical properties are evaluated in terms of the initial microstructure. Applicability of the results to the understanding of the elevated strength properties of multi-element transmutation fuel pellets is discussed. Work supported under DOE/NE Agreement # DE-FC07-05ID14654.

9:30 AM

Mesh-Insensitive Analysis of Dynamic Shear Banding in Metal Alloys: *X. Poulain*¹; *Amine Benzerga*¹; ¹Texas A&M University

The cost performance of various manufacturing processes requires accurate prediction of shear band formation and propagation. Conventional finite-element simulations of shear banding and subsequent ductile failure in metallic alloys suffer from pathological mesh sensitivity due to the softening character of constitutive equations. Incorporation of material rate-sensitivity reduces this pathological dependence and can eliminate it. However, there are circumstances where significant mesh size effects remain, which complicates the interpretation of shear band induced fracture. Here, we develop a computational framework that aims at regularizing the boundary-value problem solutions by the introduction of a material length scale. To this end, a new ductile damage model is used with strain gradients over distances comparable with void spacing included along with work-conjugate higher-order stresses. After presenting the numerical methods used for implementation in finite element code, fully transient analysis of shear banding and shear-induced failure will be presented.

9:50 AM

Variations in Plasticity and Fracture with Respect to Crystallographic Orientation in Individual Grains of Sintered ZrN Pellets: *Kirk Wheeler*¹; Pedro Peralta¹; Kenneth McClellan²; ¹Arizona State University; ²Los Alamos National Laboratories

ZrN was studied as a possible surrogate material for PuN under the Global Nuclear Energy Partnership (GNEP) program. In particular, this work addresses variability on mechanical properties of ZrN sintered at 1600°C on a sub-micron scale as a result of grain crystallographic orientations. Nano-indentation using Berkovich and Cube Corner indenters are used to determine plasticity variations and to induce cracking in different grains of a dense ZrN sample. Seven different crystallographic orientations were selected via Electron Backscattering Diffraction (EBSD) and isolated with fiducial markings using a Focused Ion

Beam (FIB) and nano-indenters are examined using Atomic Force Microscopy (AFM). Post indentation characterization and indent cross sectioning are performed using a FIB to correlate surface topography, cracking behavior and indentation shape to local crystallography. The implications of the results for multiscale simulations of structural reliability in ceramic nuclear fuels are discussed. Work supported under DOE/NE Agreement # DE-FC07-05ID14654.

10:10 AM Break

10:20 AM

Zener Pinning of a Nickel-Base Alloy: A Computational and Experimental Investigation: *Christopher Roberts*¹; *S. Lee Semiatin*²; *Anthony Rollett*¹; ¹Carnegie Mellon University; ²Air Force Research Laboratory

The role of low volume fraction (0.2%) second phase particles in grain boundary pinning was examined. The wrought material, Waspaloy, was annealed isothermally at 1100C for various times to permit grain growth and pinning. A transition from normal grain growth to abnormal grain growth occurred at late times (>1h.) and was evident in the pinned microstructure which contained a bimodal grain size distribution. The fraction of particles located on the grain boundaries was found to be higher than the random case while a nonrandom correlation with grain boundary type was measured in the initial state; however, this correlation diminished after a one hour soak. Potts-based Monte Carlo grain growth simulations were conducted to evaluate the significance of the particle placement on the limiting grain size attained and subsequently compared to the original Zener prediction.

10:40 AM

A New Yield Criterion for Porous HCP Metals: *Oana Cazacu*¹; *J.S. Stewart*²; ¹University of Florida/REEF; ²Air Force Research Laboratory and University Florida/REEF

Hexagonal closed packed (hcp) polycrystals (e.g. Zr, Sn, Ti and their alloys) display plastic anisotropy and strong asymmetry between tension and compression, which is the result of the operation and interaction between crystallographic slip and deformation twinning. Despite recent progress, modeling damage of such materials remains a challenge. In this paper, we address modeling the effects of the tension-compression asymmetry of the matrix on void growth. A new plastic potential for porous randomly oriented hcp polycrystals is developed. It is shown that this criterion reduces to Gurson (1977) criterion if the matrix doesn't display strength differential effects (i.e. is described by the Von Mises yield criterion). The accuracy of the analytical criterion is assessed through comparison with results derived from numerical minimization procedure.

11:00 AM

Microstructural Analysis of the Chip Formation during Cutting of AISI 1045 by Nanoindentation: *Mahdi Saket Kashani*¹; *Viswanatha Madhavan*¹; ¹Wichita State University

The microstructure of the AISI 1045 is studied before, during and after cutting occurs. Ferrite and pearlite grains are identified by etching and their mechanical properties are characterized by nanoindentation. The existence of some undeformed pearlite grains in the chip and the observation of greater work hardening of ferrite grains lends support to other observations that indicate that the deformation is preferentially concentrated in the ferrite phase as opposed to the pearlite phase.

11:20 AM

The Effects of High-Intensity Ultrasonic Treatment on the Phase Morphology of Mg-9.0wt.%Al Binary Alloy: *Zhiqiang Zhang*¹; ¹Key Laboratory of Electromagnetic Processing of Materials, Ministry of Education

Phase morphology is one of the most important microstructural characteristics determining the mechanical properties and therefore the application and service performance of metal components. The effects of ultrasonic treatment on the β -phase(Mg17Al12) morphology of Mg-9.0wt.%Al alloy are investigated in this paper. The results show that the β -phases in Mg-9.0wt.%Al alloy are significantly refined and discontinuously distributed throughout the sample when it was treated by high-intensity ultrasonic field during the solidification. After applying the ultrasonic field, spherical β -phases were observed in the sample.

11:40 AM

Effect of Electric Current Pulse on Solidification Structure of Bearing Steel with Low Voltage and High Discharging Frequency: *Jie Li*¹; *Yulai Gao*¹; *Jianhong Ma*¹; *Qijie Zhai*¹; ¹Shanghai University

An experiment with respect to the influence of electric current pulse (ECP) on solidification structure of bearing steel with low voltage and high discharging frequency during solidification has been carried out. The results show that with the constant voltage and the pulse current peak, the primary dendritic arm shortened and the rate of equiaxed crystal increased with increasing the discharging frequency, but the secondary dendritic arm gets coarse. It is suggested that the transverse temperature gradient of ingot is reduced attributed to the the broadened mushy zone by the agitation of ECP, and meanwhile the distribution of solutes gets more homogeneous in virtue of interaction on electric and magnetic field, which also result in refinement of structure. In addition, the refined dendritic grains and the increased rate of equiaxed grain will obviously improve the central carbon segregation.

12:00 PM

Mechanical and Wear Properties of Copper-Lead Alloy Prepared by PM Processing: *Priyanka Dash*¹; *Anish Upadhyaya*¹; ¹Indian Institute of Technology - Kanpur

Cu-Pb alloys have no solubility in each other when they are in the solid state. However powder metallurgy processing techniques produces a more stable and homogeneous microstructure. In this work, water atomized Cu and premixed Cu-12Pb alloy powder were compacted and sintered at 500°C, 700°C and 900°C and further characterized to evaluate their mechanical and tribological properties. The effect of sintering temperature on pore morphology and dimensional shrinkage were also investigated. It was observed that shrinkage in the direction of sintering was generally higher than that of the radial direction. There was a significant reduction in wear as Pb was added to Cu. Wear Test conducted at room temperature reveal that with increasing load the mechanism of wear also changes from oxidative to abrasive. At higher loads the wear is due to the rupture of the lead film resulting from plastic deformation, whereas at lower loads this film served as a lubricating layer to reduce the wear rate.

General Abstracts: Structural Materials Division: Structure/Property Relations

Sponsored by: The Minerals, Metals and Materials Society, TMS Structural Materials Division, TMS: Advanced Characterization, Testing, and Simulation Committee, TMS: Alloy Phases Committee, TMS: Biomaterials Committee, TMS: Chemistry and Physics of Materials Committee, TMS/ASM: Composite Materials Committee, TMS/ASM: Corrosion and Environmental Effects Committee, TMS: High Temperature Alloys Committee, TMS/ASM: Mechanical Behavior of Materials Committee, TMS/ASM: Nuclear Materials Committee, TMS: Product Metallurgy and Applications Committee, TMS: Refractory Metals Committee, TMS: Superconducting and Magnetic Materials Committee, TMS: Titanium Committee

Program Organizer: Ellen Cerreta, Los Alamos National Laboratory

Tuesday AM

March 11, 2008

Room: 387

Location: Ernest Morial Convention Center

Session Chairs: Lisa Dougherty, Los Alamos National Laboratory; Subhadarshi Nayak, Intel Corporation

8:30 AM

Research Concerning the Structural Characterization of Hybrid Composite Materials: *P. Moldovan*¹; *Gabriela Popescu*¹; *C. Popescu*¹; *Brandusa Ghiban*¹; *Oana Bajenaru*¹; ¹Polytechnic University of Bucharest

This paper's aim is to present the processing and characterization of some hybrid composite materials. The hybrids composite were realized using aluminum alloys as matrixes and silicon carbide and aluminum oxide particles as reinforcements. The ceramic particles were used in composite materials in different rates. Were analyzed the processes that take place at the interface between matrix and reinforcements, as well as the wettability of ceramic particles by the melt. Structural analyses of hybrid composites were realized using

electron microscopy. The matrix nature and compounds have been investigated using an electron-probe microanalyzer.

8:45 AM

Quantitative Evaluation of Creep Curve of Alloy-Type and Metal-Type Creep in Magnesium-Aluminum Binary Alloys at around 0.6Tm: *Hirokyu Sato*¹; ¹Hirosaki University

Evaluation of creep curve is an important subject for life prediction of materials used in severe environment. Minimum creep rate is one of the major parameter used for characterization of deformation behavior of materials, but the values are evaluated from a part of creep curve. In this report, author propose new parameter that reflects shape of creep curve, analyze its stress dependence and compare with creep characteristics based on the minimum creep rates. Magnesium-aluminum alloys are one of the alloys whose creep characteristics are investigated and divided into classes with its stress dependence of minimum creep rates. The magnitude of strain-rate change before and after minimum strain rates are quantitatively evaluated and opposite stress dependence of the parameter in Alloy-type regime and Metal-type regime has been found. It is expected to improve precision of predicted lifetime of materials used in severe environment.

9:00 AM

The Influence of the External Force on the Value of Energetical Barrier of the Atomic Migration in Alloy NiAl: *Evgeniya Dudnik*¹; *Ludmila Popova*¹; *Mikhail Starostenkov*²; *Dmitry Khoroshilov*¹; ¹Rubtsovsk Industrial Institute; ²Altai State Technical University

The research in alloy NiAl was made by the method of Monte Carlo. The calculated block of crystal of anisotropic structure was presented by the 3-Dimensional crystal of L10 superstructure. The crystal spread by the appliance of periodical grain conditions outside the calculated block. The interactions between different pairs of atoms in NiAl intermetallide were given by symmetric Morse potential. A single vacancy was introduced in the crystal. The atom, situated close to the vacancy was moved to one of the vacant sites. It was established, that the value of the energetical barrier of the atomic migration changed in the dependence on the deformation of hydrostatic compression and a tension. Deformation of an all-round tension results in decrease of value of the energetical barrier and deformation of all-round compression raises value of the energetical barrier migration of atom to the place of vacancy.

9:15 AM

The Research Structure-Energetical Transformations in Alloy Ni₃Al with Antiphase Boundaries: *Evgeniya Dudnik*¹; *Mikhail Starostenkov*²; *Nikita Sinitsa*²; *Alexander Yashin*²; ¹Rubtsovsk Industrial Institute; ²Altai State Technical University

The research was made by the method of molecular dynamics. The calculated block of crystal was presented by the 3d crystal of L12 superstructure. The crystal spread by the appliance of periodical grain conditions outside the calculated block. The interactions between different pairs of atoms in Ni₃Al intermetallide were given by symmetric Morse potential. The features of changes of domain structure of alloy Ni₃Al were investigated. It was established, superstructural microdomains near to antiphase borders till high temperatures was formed. Clusters in the disorder phase of alloy were observed with raises temperature. Parameters of long-rang order were designed; free energy of alloy in the dependence on the temperature was designed.

9:30 AM

Microstructures, Thermodynamic Modeling and Mechanical Properties in the Ti-Si-Sn Ternary System: *Jean-Claude Tedenac*¹; *Yaoyan Ma*¹; *Nicolas Pradeilles*¹; *Marina Bulanova*¹; *Suzana Fries*¹; ¹Institut C. Gerhardt-Universite de Montpellier 2

The determination of phase equilibria and microstructures of the alloys in the Ti-Si-Sn system were studied in as-cast and long-term annealed conditions by means of imaging with back scattered electrons (BSE) in a scanning electron microscope (SEM), energy dispersive X-ray spectroscopy (EDS) and X-ray diffraction (XRD). The isothermal sections at Ti-rich part in 25°C, 700°C and 1000°C have been experimentally established. Based on the present experimental results and the reliable literature data, a consistent set of thermodynamic parameters was obtained by means of CALPHAD method. The ternary interactions for Ti, Ti₃Sn, Ti₂Sn, Ti₃Sn₃ and Ti₅Si₃ phases were introduced

in order to model the large solubility of Si in Ti-Sn alloys and Sn in Ti-Si alloys. The isothermal sections and the liquidus surface calculated from the present thermodynamic description are in agreement with experiments. some results on mechanical properties have been obtained for titanium high content alloys.

9:45 AM

Structure-Property Correlations in Low Modulus Ti-Nb-Zr-Ta Alloys - the Role of Mechanical and Thermal History on Observed Macroscopic Properties: *Srini Rajagopalan*¹; *Gopal Viswanathan*¹; *Rajarshi Banerjee*²; *Soumya Nag*¹; *Hamish Fraser*¹; ¹Ohio State University; ²University of North Texas

Recently developed Ti-Nb-Zr-Ta alloy systems exhibit several interesting mechanical properties, including low elastic moduli and high tensile strengths, of particular interest in biomedical and other structural applications. One particular aspect observed in these alloy systems is their ability to sustain significant amounts of deformation while experiencing a decrease in modulus. This paper explores the possible microstructural factors governing such observed mechanical behavior in two specific Ti-Nb-Zr-Ta based alloys. The role of prior mechanical history, such as cold-rolling, is discussed, in light of the apparently anomalous deformation behavior in certain compositions. The effect of thermal history, such as solutionizing heat treatments, on alloy microstructure, and correspondingly, deformation mechanisms, is also studied. Finally, an attempt is made to correlate these microstructural observations to observed macroscopic mechanical properties.

10:00 AM

Properties of Titanium Oxide Films Deposited by the Sol-Gel Technique: *Pablo Favilla*¹; *Miguel Alterach*²; *Mario Rosenberger*²; *Alicia Ares*²; *Carlos Schvezov*²; ¹CEDIT/University de Misiones; ²CONICET/University De Misiones

In the development of new material for use in mechanical heart valves there are conditions that must be satisfied. In particular for the present report the focus is in good surface quality, mechanical and corrosion resistance and biocompatibility for the intended period of use. The material object of this investigation is titanium oxide deposited on a substrate of Ti-6Al-4V. The oxide films were deposited by the sol-gel technique by dip-coating, withdrawing at a constant velocity, drying and thermal treatment. The films were characterized by optical and scanning microscopy observations and test of adherence. The adherence of the films were determined as a function of the number of layers deposited and also in relation with the surface morphology. The results show that the mono-layer films have much better adherence than the multilayer films and also, that the multilayer films presented small cracks during the different processing steps.

10:15 AM

Microstructural and Mechanical Properties of Alumina Coatings Produced by Microarc Oxidation Technique on 7039 Aluminum Alloy Substrate: *Aytekin Polat*¹; *Juhi Baxi*²; *Yusuf Kar*²; *Metin Usta*¹; *Murat Makaraci*³; *Hong Liang*²; *Ahmet Ucisik*⁴; ¹Gebze Institute of Technology; ²Texas A&M University; ³Kocaeli University; ⁴Bogazici University

Aluminum alloy (7039) was coated using a microarc oxidation (MAO) process in an alkali solution. To vary the coating's microstructure and thickness, various current densities and duration were used. The microstructure was studied using a scanning electron microscope and X-Ray Diffraction. Surface roughness was measured using a surface profilometer. Microhardness measurements on the coated layer, and tribological investigation in biofluids were also performed. The results showed that the coating consists of α -Al₂O₃, γ -Al₂O₃, and δ -Al₂O₃, and mullite phase. It was found that the high hardness and thickness are associated with the high concentration of α -Al₂O₃ resulted from the increased current density. MAO coatings typically exhibit micro hardness gradient across the coating thickness. Results also showed that the thicker the coating, the higher the surface roughness. Tribological experiments indicated that this coating is table and relatively wear resistant in synthetic biofluids.

10:30 AM Break

TUESDAY AM

11:00 AM

Effect of Lattice Defects Induced by Hydrogen and Strain on Environmental Degradation: *Kenichi Takai*¹; ¹Sophia University

Hydrogen absorbed during corrosion causes environmental degradation for mechanical properties. The principal factor of the degradation has been investigated using Inconel 625 for fcc metal and pure iron for bcc metal. Hydrogen content of Inconel 625 and pure iron applying constant strain with hydrogen is larger than that applying constant strain without hydrogen. This result suggests that hydrogen and strain induced formation of lattice defects in metals. When Inconel 625 and pure iron were applied constant strain with hydrogen and released hydrogen at 303 K and 473 K, the ductility does not recover at 303 K regardless of no hydrogen, in contrast, recovers at 473 K. This result suggests that the principal factor of hydrogen degradation is not hydrogen, but vacancy and vacancy cluster induced by hydrogen and strain.

11:15 AM

Micro-Structural Characterization and Fatigue Life Variability of a Ni-Base Single Crystal PWA1484: *Kezhong Li*¹; William Porter¹; Ryan Morrissey¹; ¹University of Dayton Research Institute

Research has shown that fatigue life variability is closely associated with material response in the presence of small (<100 micron) fatigue cracks. In this project, the effect of elemental segregation on fatigue variability in the cast, single crystal superalloy PWA1484 is of interest. To that end, quantitative Electron Probe Micro Analysis (EPMA) and x-ray mapping were employed to determine the extent of elemental segregation in the dendrite core and interdendritic region in the hot isostatically pressed castings. The location of fatigue initiation sites and adjacent material relative to the EPMA maps was investigated to understand the effect of elemental segregation on variability in fatigue behavior.

11:30 AM

Microstructural Stability in Grain Boundary Engineered Materials: *Scott Schlegel*¹; Megan Frary¹; ¹Boise State University

Grain boundary engineering (GBE) is a thermomechanical process in which sequential straining and annealing cycles are used to increase the fraction of special, low-energy grain boundaries (with $\Sigma \leq 29$ according to the coincidence site lattice model). In the present work, two cubic face-centered materials, pure copper and Inconel 617, were processed by GBE. In addition, a conventionally-processed sample was processed with a single strain step, equal to the total strain in the GBE sample. The thermomechanically-processed samples were subjected to elevated temperatures for varying times. The GBE samples exhibited a resistance to change in the fraction of special boundaries and grain size (as determined by Orientation Imaging Microscopy (OIM)), while the conventionally-processed samples experienced abnormal grain growth. Monte Carlo grain growth simulations on the OIM-determined microstructures confirm the increased microstructural stability of the GBE samples. Therefore, GBE processing can produce more stable and predictable microstructures than can conventional processing.

11:45 AM

Microstructure and Strengthening Processes of Alloys for Next Generation Nuclear Plants: *Liu Liu*¹; Deepak Kumar¹; Raghav R. Adharapurapu¹; Chris Torbet¹; Gary Was¹; Tresa Pollock¹; J. Wayne Jones¹; ¹University of Michigan, Material Science and Engineering

Structural materials for the next generation nuclear power plant will require microstructure stability, creep resistance and corrosion/oxidation resistance in impure helium environments at temperatures as high as 1000°C. Here, a preliminary alloy development study is described, based on modifications to Alloy 617. Compositional modifications were made that provide potential for enhanced solid solution strengthening and lower interdiffusion rates for improved creep resistance. Elevated temperature deformation behavior and environment attack in various impure helium environments is described. Creep behavior, including damage accumulation processes in candidate alloys in impure helium environments that promote carburization/decarburization or oxidation is also described. Microstructure stability under long time and its influence on long time creep resistance are examined.

12:00 PM

Brittle Crack Susceptibility of Low Temperature Separator Vessel Material: *Ahmad Nawaz*¹; ¹GIK Institute

Low temperature separator vessel made from HSLA steel grade A516-70, is used in gas sector following the JT valve or the turbo-expander. Being at very low temperature (-7°F to -13°F), it is susceptible to brittle fracture due to ductile to brittle transition. The influence of temperature on the failure behavior of this material has been studied. Moreover, since the low temperature separator is manufactured from welded sheets, therefore, affect of temperature on the failure behavior on the post weld heat treated (PWHT) sample have also been carried out. In particular, SEM examination revealed the type of fracture that occurred in the parent metal as well as PWHT sample. A significant increase in the impact toughness of the PWHT samples as compared to the parent metal was observed which was explained by optical micrographs as well as SEM examination.

Hael Mughrabi Honorary Symposium: Plasticity, Failure and Fatigue in Structural Materials - from Macro to Nano: Dislocations: Work Hardening, Patterning, Size Effects II

Sponsored by: The Minerals, Metals and Materials Society, TMS Structural Materials Division, TMS Materials Processing and Manufacturing Division, TMS: High Temperature Alloys Committee, TMS/ASM: Mechanical Behavior of Materials Committee, TMS: Nanomechanical Materials Behavior Committee
Program Organizers: K. Jimmy Hsia, University of Illinois, Urbana-Champaign; Mathias Göken, Universität Erlangen-Nürnberg; Tresa Pollock, University of Michigan - Ann Arbor; Pedro Dolabella Portella, Federal Institute for Materials Research and Testing; Neville Moody, Sandia National Laboratories

Tuesday AM
March 11, 2008

Room: 386
Location: Ernest Morial Convention Center

Session Chairs: Michael Kassner, University of Southern California; Ladislav Kubín, Centre National de la Recherche Scientifique-ONERA

8:30 AM Keynote

A New Model for Dynamic Recovery in Stage III Deformation of FCC Metals: *Ali Argon*¹; ¹Massachusetts Institute of Technology

In the Seeger model of 1956, dynamic recovery in Stage-III deformation of FCC metals is controlled by massive cross slip of screw dislocations, circumventing linear LC dislocation barriers and resulting in decreasing strain hardening rates. There is little evidence for this mechanism which is also quite inconsistent with the cellular dislocation microstructure of Stage- III strain hardening. In a proposed new mechanism dynamic recovery results from the systematic removal of LC locks in cell walls under the repeated impingement of dislocation fluxes that, trigger associated collapse events in the pinned, redundant cell wall dislocation microstructure. This, permits the flow-noise-induced cell refinement process of Haehner and Zeiser, to develop unhindered, forming dislocation cells with fractal characteristics. The model correctly predicts the onset of dynamic recovery, its temperature dependence, as well as the temperature and stress dependence of the decreasing strain hardening rate of Stage-III, commonly referred to as the Voce Law.

9:00 AM Invited

Plastic Flow in Confined Volumes: *Nasr Ghoniem*¹; ¹University of California, Los Angeles

Characteristics of plastic deformation of metals are strongly dependent on the underlying microstructure. Moreover, when dislocations are confined to move in small volumes, the yield strength and hardening rate in monotonic deformation and the fatigue strength under cyclic loading can be significantly different from corresponding conditions where dislocations are not confined. In this talk, we discuss results of dislocation dynamics simulations of plasticity in small and confined volumes. This includes plastic deformation in nano-scale anisotropic multi-layered structures, where confinement is achieved through elastic modulus mismatch, plastic flow in micron-size single crystals, where confinement is attained through free surfaces, and the confined motion of dislocations in

Persistent Slip Band (PSB) channels, where confinement is determined by dislocation interaction with dipolar arrays under cyclic loading conditions.

9:20 AM Invited

Plastic Shear Stress-Strain Behaviour of Oriented Microstructures: *Javier Gil-Sevillano*¹; Isabel Gutiérrez¹; ¹CEIT and TECNUN, University of Navarra

The torsional stress-strain response of several disparate axially oriented two-phase materials displays peculiar plastic transient behaviours. The response can be rationalised on account of the superposition of effects of both the instantaneous structural orientation of the material during the test and the relative strength of the two phases and their interface. Understanding this torsional behaviour provides hints for explaining observations of the behaviour of layered materials in plane strain modes easily accommodated by a composition of simple shears (shear kinking).

9:40 AM Invited

Size-Affected Exhaustion Hardening and the Correlation Length for Glide Resistance in Nickel Microcrystals: *Dennis Dimiduk*¹; Michael Uchic¹; Michael Mills²; Satish Rao³; David Norfleet⁴; Triplicane Parthasarathy³; ¹US Air Force; ²Ohio State University; ³UES Inc; ⁴Ohio State Univ

Modeling the strength of small material volume elements that deform plastically by dislocation glide implicitly brings the question: what is the correlation length for the glide resistance of the dislocation ensemble (i.e. the characteristic dislocation length for which the intrinsically-stochastic mobile dislocation segment lengths act locally independently to defeat the strongest obstacles to glide)? A related question is what minimum number of locally-independent dislocation features must be sampled over the deforming volume to represent continuum behavior for the dislocation ensemble? There are historical deficiencies in addressing these questions which, in part, lead to the current active interest in strain-gradient plasticity mechanics, the statistical mechanics of dislocation ensembles, intermittency of flow and the myriad "size-effects" on plastic flow. Our studies of the effect of sample size on flow stress of single crystals show a systematic change in the transition from elastic to plastic flow with decreasing sample size. Analysis of those results suggest both a dislocation source-hardening effect and, a period of plastic straining that exhibits an unusually high strain-hardening rate called exhaustion hardening. This study reports results from both discrete dislocation simulations and TEM examinations of deformed microcrystals. In both studies efforts have been made to tie dislocation micromechanisms to the phenomenology found in small-strain flow of nickel microcrystals. The results are discussed in the context of a correlation length for glide resistance and its influence on size effects.

10:00 AM

Fracture of Edge Dislocation Cores during Fatigue Failures: *John Gilman*¹; ¹University of California - Los Angeles

Since numerous materials obey Coffin's Law of fatigue failure not only during cyclic stressing, but also for the initial quarter cycle (tension test), the intrinsic cause of failure seems to be only secondarily associated with repeated cycling. If this conjecture is true, something that is present during the initial plastic deformation must lead to the final fracture. The only culprits present are individual dislocations, dipoles, and higher multipoles; i.e., dislocations themselves. In fact, the cores of edge dislocations are sources of weakness. The author has shown this in: bubble rafts; prestrained LiF crystals; and bent zinc crystals. Others have demonstrated the weakening effect of plastic torsion on fracture. The local weakening effect is estimated to be about 30%. Griffith's fracture condition demands a high stress to convert these incipient cracks into running cracks, but as dislocations accumulate in persistent glide bands, the critical stress progressively decreases.

10:15 AM Break

10:25 AM Invited

Recent Experimental Developments in Examining Long Range Internal Stresses: *Michael Kassner*¹; Lyle Levine²; Ben Larson³; Jon Tischler⁴; Peter Geantil¹; ¹University of Southern California; ²National Institute of Standards and Technology; ³Oak Ridge National Laboratory; ⁴Argonne National Laboratory

Hael Mughrabi was pioneering in advancing the concept of long-range internal stresses (LRIS) in deformed microstructures. Evidence for such long-range internal stresses included the famous dislocation pinning by neutron

irradiation experiments by Mughrabi, and x-ray line broadening by Mughrabi and colleagues. Experiments by others, including some relatively recent dipole-separation observations and convergent beam electron diffraction experiments in connection with LRIS, will be described as well. Most recently, the concept and the interpretation of long-range internal stress was investigated using advanced x-ray microbeam diffraction on a synchrotron source; axial strains within individual cell interiors have been measured and measurements of strain in individual cell walls are in progress. These were accomplished using oriented monotonically deformed Cu single crystals. The results demonstrate that long-range internal stresses are consistent with the earlier findings of Professor Mughrabi. These recent synchrotron experiments are discussed in greater detail in another talk in the Symposium.

10:45 AM Invited

Slip Circle Constructions for Plasticity of Polycrystals: *Lawrence Brown*¹; ¹University of Cambridge

Patterns of plastic flow around undeformable particles, and at hardness indenters, can be understood by rotational flow which transfers matter from where it is in excess to where it is in deficit. Such slip-circle constructions are a simple way of treating the operation of antisymmetrical combinations of slip systems. The constructions predict lattice rotations, geometrically necessary dislocation densities, and any size effects. Applied to flow in polycrystals, they predict a Hall-Petch law dependent upon the root-mean-square dispersion of Schmidt factors for the array of grains. They also predict residual stresses, and allow an estimate to be made of the maximum uniaxial flow stress sustainable by the polycrystal without loss of cohesion at the grain boundaries. In all cases, there should be a transition from laminar to rotational flow at small plastic strains and at small grain sizes, particularly in nanocrystalline materials.

11:05 AM Invited

Properties of Dislocations under Single Slip: *Patrick Veyssiere*¹; ¹Laboratoire d'Etude des Microstructures, Centre National de la Recherche Scientifique-Onera

Dislocations of a given slip system engender obstacles to their own propagation forming entanglements. This property, essential in fatigue, has received renewed interest with the development of computer simulation experiments and with investigations of single crystal pillars but little is known on local mechanism. The talk concentrates on selected aspects related to self-organization. Namely: 1 – Some properties of dislocation contrast are re-visited. 2 – The model for the formation of loops and the further sweeping of these by mobile dislocations is confirmed experimentally by dislocation dynamics and MD simulations. 3 – Properties of dipoles are analyzed under isotropic and anisotropic elasticity in cubic systems. The passing stress under constrained deformation conditions, such as fatigue, is discussed.

11:25 AM

Local Shear Strain Amplitude and Half-Cycle Slip Activity of Persistent Slip Bands in Cyclically Deformed Polycrystals: *Anja Weidner*¹; Wolfgang Tirschler¹; Christian Blochwitz²; Werner Skrotzki¹; Jiri Man²; Tomas Kruml²; ¹Technical University of Dresden; ²Academy of Science of Czech Republic

The local slip activity of persistent slip bands (PSBs) was studied after half-cycle deformation on a well-polished specimen surface at different stages of fatigue life using atomic force microscopy (AFM) and scanning electron microscopy (SEM). In-situ deformation experiments were carried out in order to investigate both the formation of slip steps during half-cycle loading as well as the development of extrusions with increasing number of cycles. It is shown that during half-cycle loading the slip steps do not develop proportionally to the applied plastic strain and not the whole accumulated PSB volume is active. Additionally, the half-cycle slip activity of PSBs depends on the stages of fatigue life. The local shear strain amplitudes of PSBs in polycrystals are comparable to those for single crystals and are nearly independent on the stage of fatigue life. PSBs in polycrystals have a development history which is characterized by active and inactive periods.

11:40 AM

Relationship between Dislocation Microstructure and Flow Stress during Cyclic Deformation in Al and Al-Mg Alloy Single Crystals: Toshiyuki Fujii¹; Shizuma Uju¹; Hiroyuki Tanaka¹; Chihiro Watanabe²; Susumu Onaka¹; Masaharu Kato¹; ¹Tokyo Institute of Technology; ²Kanazawa University

Al single crystals with a multiple slip orientation and Al-0.7mass%Mg solid-solutioned alloy single crystals with a single slip orientation were cyclically deformed under constant plastic-strain amplitudes at room temperature. A sequential change, i.e. initial hardening, intermediate softening, and secondary hardening, was obtained in cyclic hardening curves for Al. The dislocation microstructure for Al was characterized by the labyrinth structure, which consists of two sets of mutually perpendicular {100} walls. On the other hand, cyclic hardening to saturation was obtained in the Al-Mg single crystals, and the cyclic stress-strain curve (CSSC) showed a plateau with the stress of 26MPa. At strain amplitudes within the plateau region of the CSSC, persistent slip bands with ladder structure were formed. The relationship between the macroscopic cyclic flow stress and the dislocation microstructure can be explained in both the materials by an analysis based upon Mughrabi's composite model.

11:55 AM

Microstructural Modeling of Large Strain Failure Modes in Crystalline Aggregates: Omid Rezvanian¹; Jibin Shi¹; Mohammed Zikry¹; ¹North Carolina State University

The objective of this research is predict failure modes and scenarios at different physical scales that occur due to a myriad of microstructural factors, such as texture, grain size and shape, grain subdivision, heterogeneous microstructures, and grain boundary misorientations and distributions. The microstructurally-based formulation for inelastic deformation is based on coupling a multiple-slip crystal plasticity formulation to three distinct dislocation densities, which pertain to statistically stored dislocations (SSDs), geometrically necessary dislocations (GNDs), and grain boundary dislocations (GBDs). This dislocation density based multiple-slip crystal plasticity formulation is then coupled to specialized finite-element methods to predict how scale-dependent microstructural behavior and the evolving heterogeneous microstructure can contribute to failure initiation. Furthermore, a clear understanding of how GB strength changes due to microstructural evolution is obtained as a function of microstructural heterogeneities and dislocation-density transmission, blockage, and absorption.

12:10 PM

An Analysis of Geometrically Necessary Dislocation Evolution and Plasticity Size Effects in Micro-Crystals: P. Guruprasad¹; A. Benzerga¹; ¹Texas A&M University

Mechanism-based discrete dislocation dynamics is used to study the plastic behavior of micron scale single crystals under compression. Calculations were carried out for initially high (HSD) and low (LSD) dislocation source density. The results for both cases predict strengthening upon scale reduction. Significant work hardening was seen only in the HSD case. This was attributed to the emergence of a GND density locally, aided by lattice rotations associated with dislocation pattern formation. The net build-up of GND density leads to a strong Bauschinger effect in the smallest specimens. By way of contrast, strengthening in the LSD case was related to the dislocation source length distribution. Occasionally, a yield-strength asymmetry between tension and compression was observed and attributed to the initial dislocation structure. In addition, strain-rate sensitivity analyses indicate a significant size effect in the HSD case down to a strain rate of 10/s.

Hume-Rothery Symposium - Nanoscale Phases: Session III

Sponsored by: The Minerals, Metals and Materials Society, TMS Electronic, Magnetic, and Photonic Materials Division, TMS: Alloy Phases Committee

Program Organizers: Sinn-wen Chen, National Tsing Hua University; David Cockayne, University of Oxford; Seiji Isoda, Kyoto University; Robert Nemanich, Arizona State University; K.-N. Tu, University of California, Los Angeles

Tuesday AM
March 11, 2008

Room: 276
Location: Ernest Morial Convention Center

Session Chairs: David Cockayne, University of Oxford; Sinn-wen Chen, National Tsing Hua University

8:30 AM Invited

Structure and Composition Effect of (Co, Fe) Electrode on the Tunneling Magnetoresistance of AIO_x Based Magnetic Tunnel Junction: Y. Chang¹;

¹University of Wisconsin

A direct experimental evidence of the crystal structure effect on the tunneling magnetoresistance (TMR) was observed. The TMR of AIO_x based magnetic tunnel junction (MTJ) with (Co, Fe) electrodes increased from 32.1% to 46.7% when the crystal structure of the Co₈Fe₁₃ bottom electrode is altered from fcc to bcc by using Cu and Cr buffer, respectively. This increase was attributed to the electronic structure change of the FM electrodes, as confirmed by *ab initio* calculation that spin polarization of bulk bcc is greater than bulk fcc. A compositional dependence of TMR was performed for AIO_x and (Co, Fe) based MTJs. The experimental results combined with *ab initio* calculations suggest that TMR is mainly determined by the s-like electron spin polarization values associated with different compositions and crystal structures. By further optimizing the crystal structure, interface roughness of the bottom electrode, more than 70% TMR was achieved at room temperature.

8:55 AM Invited

The Structure and Composition of Au/Pd Nanoparticles: Miguel Yacaman¹; Domingo Ferrer¹; Sergio Mejia²; Eduardo Perez-Tijerina²; Ubaldo Ortiz²;

¹University of Texas; ²Universidad Autonoma de Nuevo Leon

The study of bimetallic nanoparticles is of great interest in nanotechnology. The physics of phase transitions is still not well understood. The system of Au/Pd is a very interesting case. In the bulk, the system is totally miscible. However, in form of nanoparticles it shows a very interesting structure. When the particles are prepared by wet chemistry methods, they show a three-layer structure with a core rich in Pd, a second layer rich in gold, and a surface rich in Pd. When the particles are produced by evaporation, an alloy is produced with an icosahedral shape. The structure of the Au/Pd is studied in detail using STEM-HAADF, HREM, Energy Filtering, and Electron Diffraction. Models that simulate that particle structure are presented.

9:20 AM Invited

The Structure of Amorphous Nanovolumes: David Cockayne¹; Konstantin Borisenko¹; Guoqiang Li¹; Yixin Chen¹; ¹University of Oxford

The structure of amorphous materials is traditionally investigated using neutron or X-ray diffraction, including refining models against the diffraction data. However these techniques are not able to study nanovolumes of amorphous material, such as in thin films, rapid phase change "bits", intergranular films and insulating layers in devices. We have developed electron diffraction techniques which enable model structures to be refined against the experimental data for both elemental and alloy amorphous nanovolumes.

9:45 AM Invited

d-States in Complex Metallic Alloys: Jean-Marie Dubois¹; Esther Belin-Ferré²;

¹Institut Jean Lamour; ²Centre National de la Recherche Scientifique

Many complex alloys exist in metal systems like Al-Mg and Al-Mg-Zn or Al-Metal and Mg-Metal systems. Their electronic structure was investigated using X-ray emission spectroscopy technique, which provides separately the energy distribution of electronic states around each of the chemical species in the solid, averaging the data over their various sites. In this talk, we examine and discuss

the Al 3s,d and Mg 3s,d electronic distributions of several complex alloys in comparison to the pure metals as well as to other simpler structures. In complex systems, the contribution of Al and (or) Mg d-like states is important at the Fermi level and in its close vicinity. By comparison to simple alloys containing a transition metal, it is suggested that Al or Mg d-like states play a significant role in the formation of a pseudo-gap at the Fermi level and therefore contribute to select and stabilize the complex structures.

10:10 AM Break

10:30 AM Invited

Shape Controlled Nanocrystals of Ceria and Platinum—Synthesis and Growth Mechanism: *Zhong Lin (Z.L.) Wang*¹; ¹Georgia Tech

Two examples will be presented about shape control of nanocrystals. The first example is about the formation of spherical ceria nanocrystals. For chemical-mechanical planarization of advanced integrated circuits, the polyhedral shaped nanoparticles scratch the silicon wafers and increase defect concentrations. We present here an innovative approach for large-scale synthesis of single-crystal ceria nanospheres,² which can reduce the polishing defects by 80% and increase the silica removal rate by 50%. The second example is about shape controlled Pt nano nanocrystals.³ Platinum NCs of very unusual tetrahedral (THH) shape were prepared at high yield by an electrochemical treatment of Pt nanospheres supported on glassy carbon by a square-wave potential, which has a much improved catalytic properties. ¹X.D. Feng, D.C. Sayle, Z.L. Wang et al., Science, 312, 1504 (2006). ²Na Tian, Zhi-You Zhou, Shi-Gang Sun, Yong Ding, and Zhong Lin Wang, Science, 316, 732 (2007).

10:55 AM Invited

Nanocrystallization of Bulk Amorphous Alloys in a Magnetic Field: *James Li*¹; ¹University of Rochester

For equilibrium in an externally applied magnetic field, the work done by the magnetic field should be considered. As a simple mechanical example, let a dead weight W be hung at the end of a vertical spring of length l (original length l_0) with the other end fixed. The equilibrium is described by minimizing a free energy function $(k/2)(l-l_0)^2 - W(l-l_0)$ where k is the spring constant. The term Wl is similar to PV (pressure, volume) in the Gibbs free energy for equilibrium under constant pressure. So we need a term BH in the free energy expression for equilibrium under externally applied magnetic field H where B is the magnetic flux. This term has been neglected in the literature. By using this free energy expression, the enhancement or retardation of the nucleation or growth of crystals from amorphous solids in a magnetic field can be understood.

11:20 AM Invited

Properties of ZnO/SnO₂-Cosubstituted In₂O₃ Thin Films: *Robert Chang*¹; M. Zhang¹; D. Buchholz¹; ¹Northwestern University

In indium tin oxide (ITO), indium is present as the In^{3+} ion, thus two atoms of indium can be replaced by a zinc atom, which forms a Zn^{2+} ion and a tin atom, which forms a Sn^{4+} ion. In this manner up to 40% of the indium can be replaced by co-substitution of zinc and tin to form a new and less expensive TCO, zinc-indium-tin-oxide (ZITO). $Zn_{0.3}In_{1.4}Sn_{0.3}O_{3-\delta}$ (ZITO) thin films were grown by computer-controlled pulsed laser deposition (PLD) on (0001) Al_2O_3 substrate both at room temperature and at high temperatures ($>700^\circ C$). The room temperature grown samples were found to be amorphous. Electrical measurements indicate that conductivities for room temperature and high temperatures were 1500 S/cm and 4000 S/cm respectively. Cross-section and plan-view transmission electron microscopy (TEM) revealed that the ZITO films grown at high temperatures were composed of twin-related domains with a lattice mismatch of approximately 2.8%.

IOMMS Global Materials Forum 2008: Creating the Future MS&E Professional

Sponsored by: The Minerals, Metals and Materials Society, International Organization of Materials, Metals and Minerals Societies

Program Organizer: Robert Shull, National Institute of Standards and Technology

Tuesday AM

Room: 272

March 11, 2008

Location: Ernest Morial Convention Center

Session Chairs: Robert Shull, National Institute of Standards and Technology; Yoshimasa Kajiwara, Japan Institute of Metals

8:30 AM Introductory Comments by Dr. Robert Shull, TMS President and Dr. Yoshi Kajiwara, JIM, and Chair of IOMMS

8:40 AM Keynote

International Perspectives on the Creation of Engineers for the 21st Century: *Norman Fortenberry*¹; ¹National Academy of Engineering

Concerns about the quality and quantity of engineers to meet the needs of the 21st Century have emerged in multiple countries. These concerns are driven by increased competition in tightly coupled global economies as well as concerns about maintaining and enhancing domestic standards of living in increasingly technological societies. In more industrialized economies there are also concerns about being able to maintain the competitiveness of engineering as a career field when other avenues for personal and social progression are presenting themselves to tradition entrants into the field. This presentation summarizes the global context for engineering practice, reviews commonly cited global requirements for 21st Century engineers, and suggests nationally collaborative effort that might be pursued in order to enhance their attainment. The suggested collaborations are grounded in the formal educational preparation of engineers, but take advantage of emerging uses of information technologies as well as better utilization of existing collaborative mechanisms.

9:10 AM Invited

Requirement of Technical Professionals in the Indian Steel Industry over the Next Two Decades: *Amit Chatterjee*¹; ¹Tata Iron and Steel Company Ltd

The Indian steel industry is going through a complete metamorphosis. Though only 40 million tonnes of capacity has been added in 60 years after Independence, it is foreseen that at least 150 Mt, if not 175 Mt additional capacity will be created in India before 2020. In fact, the projects that have already been announced envisage production of around 200 Mt by this time. Given this background, it is important that India prepares for meeting the requirements of the steel industry as far as Engineering Graduates and other professionals like Diploma holders and Trade Apprentices are concerned. The supply position is extremely bleak going by the present trend. Skilled and trained personnel are difficult to find. Diploma holders of the right quality are also not available. In the case of Engineering Graduates, even if the total number is satisfactory, they are not keen to join the steel industry and are attracted by lucrative options like the IT sector. Hence, innovations are required to attract professionals to the steel industry in future. Time is running out and an immediate action plan is called for. The paper will focus on these issues.

9:30 AM Invited

The Constitution and Practice for Training the Comprehensively Qualified Students in the Field of Materials Science and Engineering: *Xinxin Zhang*¹; ¹University of Science and Technology

The discipline of materials science and engineering is developed on the basis of the mutual overlapping and integration from all those disciplines such as chemical metallurgy, physical metallurgy and mechanical metallurgy. The development started since the 60s of last century. The most obvious change is the research orientation transformation from the traditional focus on iron, steel, ceramics and plastics to the preparation and synthesis of advanced materials. Especially in the last 20 years, with the investigation and application of magnetic materials, high temperature superconductors, hydrogen storage materials, as well as nano materials and bulk glasses which are drawing more and more attention since last 10 years, many inherent concepts and ideas are broken through. The

revolutionary progresses and the epoch-making achievements are appearing in the field of materials science and engineering. All these accomplishments are obtained and promoted by the scientists stepping into the materials field from physics and chemistry, and even working together with those in the fields of mining and metallurgy, chemical engineering and machinery fabrication etc. Under this new situation, we are trying to adapt teaching principles and improve courses offered. A new education system is established preliminarily for training such students with solid basis, self-study independency, practicing ability and innovative consciousness so that to meet the need of the development of society, economy, science and technology.

9:50 AM Invited

Materials Science and Engineering Education: Indian Perspectives: *Srinivasa Ranganathan*¹; ¹Indian Institute of Science

The first university of the world was founded at Taxila closely followed by another in Nalanda in India. They had an international character drawing students from China and other nations. Due to historical forces there was a long decline over the past five hundred years in the educational sector, reversed only in the past century with the establishment of national universities in Bangalore and Varanasi. Metallurgical education began in 1923, materials science courses were started in 1964 and nanoscience courses were started in the early years of this century. A dichotomy has arisen as the demands of the Indian industry with explosive growth in steel and aluminium production are not responded to by the education sector. Globalization has had its own impact. Some prescriptions for addressing the gap in supply and demand of human resources will be advanced, as the Indian economy continues its onward march.

10:10 AM Break

10:25 AM Invited

Some Effective and Innovative Educational Efforts for Materials Engineers: *Chester Van Tyne*¹; ¹Colorado School of Mines

The measure of an effective engineering education is the ability of graduates to perform well as engineers upon completion of their degree program. ABET is the accrediting agency in the US that evaluates engineering programs to determine if this goal is being achieved. ABET accrediting activities are often viewed with apprehension and skepticism by faculty and universities. One of the reasons that these reviews are perceived negatively is that the focus is often on the shortcomings that exist within the engineering program being accredited. The ABET review also provides an opportunity for the evaluator to comment on the program strengths. These strengths encompass a number of innovative and effective methods for educating future materials engineers. A summary of the strengths found in materials program over the last four years will be presented. Additionally, several unique educational opportunities that have been introduced by programs and universities will also be briefly described.

10:45 AM Invited

Education for Non-Ferrous Metallurgy in Japan—The Present Issues and the Future: *Takahiko Okura*¹; *Susumu Okabe*²; *Takashi Nakamura*³; ¹Akita University; ²The Mining and Materials Processing Institute of Japan; ³Tohoku University

Japanese non-ferrous industry is producing environmental-soundly 9% of the world copper production, 6% of zinc, and 3% of lead, which account some 0.5% of GDP. The industry is receiving approximately 25 new graduates from universities per year these days, but it needs more in order to sustain its business in Japan as well as to develop it in the global market. However, the industry is faced with the crisis of less-educated graduates and its less supply. Since the aging of the society in this field is going on and the mind of professors and students tend to decline into so-called high technology, the lectures and researches in the field are becoming less and less in Japanese universities. It will be difficult to change these diverse challenges and to again increase the lectures and research themes as same as in the old days. In the presentation, such situations in Japan are reported in detail, and the recent countermeasure for the new century, developed and operated by universities, the industry, and the government collaboratively, will be discussed, including 3 subjects, (1) continuing education program (2) donated chair at a university, (3) Collaborative educations for Japanese and Asian engineers in non-ferrous metallurgy and recycling.

11:05 AM Invited

Current Topics on Continuous Education and Training of Professional Material Engineers in Japan: *Shu Yamaguchi*¹; ¹University of Tokyo

Recent development of education and training of professional and experienced engineers at academic society, university, and other organizations in Japan will be reviewed and summarized in addition to the recent Governmental policy and support in cultivation of experienced engineers to support industry.

11:25 AM Invited

Online Materials Education Communities: Transforming More Than Just Content Delivery: *Adam Powell*¹; ¹Veryst Engineering LLC

The World-Wide Web provides educators with much more than a means for delivering educational content. It has facilitated new types of visual and interactive content for improved educational effectiveness. It has changed the culture of distribution, from a profit motive to an ethic of sharing everything with everyone, from Wikipedia to MIT Open CourseWare. And it has facilitated collaboration in content development: on the web, everyone has thousands of proforeaders and a hundred potential collaborators. The resulting overwhelming cacophony of opportunities and resources requires new means of sorting and evaluating them for classroom use. Toward that end, Materials Technology@TMS provides a sorted collection of nearly 300 links to pre-screened resources, along with discussion forums where educators can share experiences on using resources and developing curricula. While centered around the MT@TMS Education Community, this talk hopes to provoke thoughts and discussion on the production and dissemination of educational content in general.

Magnesium Technology 2008: Thermodynamics and Phase Transformations

Sponsored by: The Minerals, Metals and Materials Society, TMS Light Metals Division, TMS: Magnesium Committee

Program Organizers: Mihriban Pekguleryuz, McGill University; Neale Neelameggham, US Magnesium LLC; Randy Beals, Chrysler LLC; Eric Nyberg, Pacific Northwest National Laboratory

Tuesday AM

March 11, 2008

Room: 292

Location: Ernest Morial Convention Center

Session Chairs: Rainer Schmid-Fetzer, Technische Universität Clausthal; Zi-Kui Liu, Pennsylvania State University

8:30 AM

Elastic Constants of Magnesium Compounds from First-Principles Calculations: *Swetha Ganeshan*¹; *Hui Zhang*¹; *Shunli Shang*¹; *Yi Wang*¹; *Zi-Kui Liu*¹; ¹Pennsylvania State University

The deformation behaviors of second phases are important in understanding the mechanical properties of Magnesium alloys. In the present work, the elastic constants of Mg based binary compounds have been predicted from first principles calculations using the stress strain method¹. The Mg-X systems that have been investigated in the present work include Mg-As, -Ba, -Ca, -Cd, -Cu, -Dy, -Ga, -Ge, -La, -Lu, -Ni, -Pb, -Sb, -Si, -Sn and -Y. A comparative study between the results obtained in the current work and the available experimental data has been made. The accuracy in the calculated data sets off a landmark to use the same for any future work incorporating the design of Mg based alloys. ¹S. Shang, Y. Wang, and Z. K. Liu, "First-principles elastic constants of α - and θ -Al₂O₃", Appl. Phys. Lett., Vol. 90, 2007, 101909.

8:50 AM

The Role of Solutes for Grain Refinement by (SiC)₂: Experiment and Theoretical Calculation: *Robert Günther*¹; *Christian Hartig*¹; *Okechukwu Anopuo*²; *Norbert Hort*²; *Rüdiger Bormann*¹; ¹Hamburg University of Technology; ²GKSS Research Centre

Grain refiners for Al-containing Mg-alloys are still deficient and under investigation. To clarify the mechanisms of grain refinement by inoculation a simulation method for heterogeneous nucleation has been used, allowing the prediction of the grain size for a given particle size distribution, volumetric content of inoculants, cooling rate and alloy constitution. To proof the

model, grain refinement efficiency of $(\text{SiC})_p$ in Mg3wt%Al was examined experimentally. It was found that $(\text{SiC})_p$ results in significant grain refinement. Experiments with $(\text{SiC})_p$ in Al-free Mg-alloys have shown that additionally to the low lattice misfit of SiC, solutes play an important role for effective grain refinement. While the grain refinement via $(\text{SiC})_p$, inoculation of pure Mg is negligible, a distinct effect has been achieved in Mg3wt%Zn. The model makes quantitatively correct predictions for the grain size and its variation with cooling rate. Relevant aspects for the consideration of particle-specific properties and solutes will be discussed.

9:10 AM

Thermodynamic Database of Mg-Al-Ca-Sr: A Resource for Alloy Development and Improvement: *Hongbo Cao*¹; Jun Zhu¹; Chuan Zhang²; Y. Chang¹; ¹University of Wisconsin; ²University of Wisconsin

We developed a thermodynamic database of Mg-Al-Ca-Sr, an important base system for a number of current magnesium alloys such as AXJ530. Our database focuses primarily on the Mg-rich phase equilibria. Using the Scheil model, the calculated solidification paths of several Mg-Al-Ca-Sr alloys are in accord with the reported data on the as-cast microstructure. Since the database was obtained from the constituent key ternaries modeled in terms of data and other ternaries obtained via extrapolation from the binaries, we believe that it is equally valid for other Mg-rich alloys containing Al, Ca and Sr. Additionally, we have calculated the equilibrium state of AXJ530 alloy at low temperature and found that the stable phases calculated agree with literature data. More importantly, the predictive nature of the calculation using either only thermodynamic database or coupled with kinetic model makes it possible to exploit new alloy compositions where experimental investigation has not been attempted.

9:30 AM

Thermodynamic Investigation of Alkali-Metal-Induced High Temperature Embrittlement in Mg-Li Alloys: *Shengjun Zhang*¹; Qingyou Han²; Zi-Kui Liu³; ¹Northwestern University; ²Oak Ridge National Laboratory; ³Pennsylvania State University

Alkali metals are undesirable impurity elements in magnesium-lithium alloys. Despite their trace amount, they lead to high temperature embrittlement (HTE) due to intergranular fracture which is prone to edge cracking during thermal processing. In the present work, the results of a thermodynamic investigation are presented to elucidate its mechanism and compared with available experimental data. It is demonstrated that HTE arises from an intergranular alkali-metal-rich liquid phase that segregates into grain boundaries from the matrix and significantly weakens their strength. In order to suppress HTE, a proper processing temperature should be chosen to locate an alloy in the HTE safe zone, according to the alloy composition. There exists a maximum alkali-metal content above which HTE cannot be avoided for a given Mg-Li alloy. A new model is developed to describe the tendency of HTE, which shows grain refinement can decrease the tendency.

9:50 AM

Thermodynamic Modeling of Porosity Formation during Non-Equilibrium Solidification in Magnesium Alloy Castings: *John Li*¹; Jeff Wood¹; John Auld²; Gerry Wang³; ¹University of Western Ontario; ²Meridian Technologies Inc.; ³Meridian Technologies Inc

Casting properties are mainly controlled by filling and solidification related defects. Due to the complex nature of flow and thermal process, the ability to accurately predict the solidification porosity is limited. Although commercial solvers are available to predict solidification hot spots, there is no established math model able to quantitatively predict the solidification porosity for magnesium alloy castings. This is because commercial solvers for porosity prediction are only based on the classic Niyama Criteria. In this research project, a new porosity model for magnesium alloy casting has been developed. The model uses combined pressure drops of inter-dendritic feeding, volumetric shrinkage, surface tension and gas evolution during the solidification stage. It also considers the non-equilibrium solidification process by using the Scheil Equation to predict the solute (Al) redistribution at the mushy zone. A series of step-shaped magnesium alloy plate castings have been produced and investigated to validate this new porosity model.

10:10 AM Break

10:30 AM

Aging Behavior of Die-Cast MRI230D: *Jessica TerBush*¹; J. Wayne Jones¹; Tresa Pollock¹; ¹University of Michigan

The aging behavior of die-cast MRI230D magnesium alloy has been investigated. Samples were aged for times ranging from 10s to 500h for temperatures between 175 and 350°C. The hardness of the aged specimens was measured using a micro-Vickers test with 500 gf load. After aging for 100h at 250°C, the hardness increased from 68.7 Hv in the as-cast state to 74.7 Hv. Microstructure of the aged specimens was examined using transmission electron microscopy (TEM). Precipitates were observed in the as-cast and aged conditions lying parallel to the basal plane. The results will be compared to a similar study previously conducted on die-cast AXJ530.

10:50 AM

Effect of Pre-Aging on Age Hardening and Microstructure in Mg-Zn and Mg-Zn-Al Alloys: *Keiichiro Oh-ishi*¹; Kazuhiro Hono¹; Kwang Seon Shin²; ¹National Institute for Materials Science; ²Seoul National University

Mg-Zn alloys are well known as an age-hardenable alloy. The tensile strength of Mg-Zn alloys were found to increase further by Al additions and two-step aging. The age-hardening response and microstructural variation of Mg-Zn and Mg-Zn-Al alloys were examined by hardness test, transmission electron microscopy (TEM) and three-dimensional atom probe. The two-step aged samples exhibit enhanced age hardening response at an earlier stage compared to the single-aged ones. TEM observations exhibited that the peak aged Mg-Zn samples had rods along the c-axis of the matrix phase and plates lying on the basal plane. The Mg-Zn-Al samples had rods and cuboidal precipitates. After two-step aging, the microstructure becomes finer for both the Mg-Zn and Mg-Zn-Al alloys. Atom probe analyses for the samples pre-aged at 70°C clearly showed the formation of Zn-rich zones.

11:15 AM

The Influence of Zn on the Precipitation Path in Mg-Sn Alloys: *Shaul Avraham*¹; Tomer Leviatan¹; Yael Maoz¹; Alex Katsman¹; Menachem Bamberger¹; ¹Technion, Israel Institute of Technology

Intermetallic phases in Mg alloys determine the elevated temperature mechanical properties. Dissolved alloying elements at low temperatures and thermally stable intermetallics can hinder plastic deformation mechanisms (dislocation sliding). The presence of Sn in Mg alloys can result in the high melting Mg₂Sn intermetallic. Zn is a common alloying element in Mg alloys, it can form several Mg-Zn intermetallics. This work is focused on the mechanisms by which Zn modifies the age hardening response of Mg-Sn alloys. A binary Mg-Sn and a ternary Mg-Sn-Zn alloys were designed according to computational thermodynamic simulations. The two alloys were solution treated and aged ($t < 32$ days, 175°C). Micro hardness measurements were used to follow microstructural changes. Thermal analysis and electron microscopy methods were used to analyze the influence of Zn on the Mg₂Sn precipitation.

11:35 AM

Age Hardening Response and Precipitate Microstructures of ZK60 Alloy Containing Trace Additions of Ag and Ca: *Chamini Mendis*¹; Keiichiro Oh-ishi¹; Kazuhiro Hono¹; ¹National Institute for Materials Science

Mg-Zn based ZK60 alloy is a widely used wrought magnesium alloy that has a good combination of strength and ductility but only minor increments in strength is achieved through precipitation hardening due to the very limited hardening response. The low hardening response has been attributed to formation of coarse precipitates of MgZn₂. Trace additions of 0.1at.% Ag and 0.1at.% Ca to Mg-2.4Zn and Mg-2.4Zn-0.16Zr (at.%) alloys have been shown to increase the peak hardness in the temperature range 160-200°C. With the combined additions of Ag and Ca the hardening response doubles that observed in the Mg-2.4Zn and Mg-2.4Zn-0.16Zr (at.%) alloys. The transmission electron microscopy examinations revealed that the increment in hardening response was achieved by refining the precipitate distribution observed in the binary alloy. In the presence of Zr, these alloys also show significant refinement of grain structures in addition to the fine scale distribution of precipitates within the grains.

11:55 AM

Local-Electrode Atom-Probe Tomographic Investigation of Strengthening Precipitates in a Mg-7Zn-3Al Alloy at Peak: *Shengjun Zhang*¹; Gregory Olson¹; ¹Northwestern University

The precipitates in a Mg-7Zn-3Al (in wt. %) alloy aged to peak hardness at 150°C have been characterized by local-electrode atom-probe (LEAP) tomography. The chemical compositions of the matrix and the precipitates were measured and compared with the results calculated using the COST2 database by the Thermo-Calc software. Ternary nanoscale precipitates have been found consistent with the predicted ϕ phase demonstrating a metastable composition. The measured particle size at peak hardness, corresponding to an equivalent sphere radius of 17 nm, provides an important calibration point for quantitative modeling of precipitation strengthening for alloy design. The interfacial energy is also determined based on the capillarity effect.

Magnesium Technology 2008: Wrought Alloys II

Sponsored by: The Minerals, Metals and Materials Society, TMS Light Metals Division, TMS: Magnesium Committee

Program Organizers: Mihriban Pekgulyuz, McGill University; Neale Neelameggham, US Magnesium LLC; Randy Beals, Chrysler LLC; Eric Nyberg, Pacific Northwest National Laboratory

Tuesday AM

Room: 291

March 11, 2008

Location: Ernest Morial Convention Center

Session Chair: To Be Announced

8:30 AM

Direct Chill Casting and Plastic Deformation of Magnesium Alloys: *Gady Rosen*¹; Menachem Bamberger²; Galia Harel²; Enrico Evangelista³; Mohamad El Mehtedi³; Sandrine Sereni⁴; ¹Alubin Ltd; ²Technion Israeli Institute of Technology; ³Università Politecnica Delle Marche; ⁴Centro Ricerche Fiat-Società Consortile Per Azioni

Magnesium alloys stimulate growing interest for use in structural and functional components (aeronautics, automotive, electronics, etc.). Due to their attractive mechanical properties the market share of wrought products is rapidly increasing. In order to produce sound extruded products, high quality billets (feed stock) are required. Therefore, in-depth understanding of the influence of casting conditions on the production quality, and on micro-structure, properties and workability are of high importance. Efficiency of the production can be improved by utilizing advanced process-simulation. Modelling the underlying physics aspects so that process improvement variables can be identified and controlled, resulting in significant benefits. Thus, modelling the solidification of a casting yields: Temperature profiles for a more accurate solidification analysis. Predict solidification time and the effect of cooling system on the solidification. Estimate billets micro-structure, and, mechanical properties in as cast state. Complimentary work is conducted on torsion tests to produce constitutive constants for FEM models.

8:50 AM

Effect of Reheating and Warm Rolling on Microstructure and Mechanical Properties of Twin Roll Strip Cast Mg-4.5Al-1Zn-0.3Mn-0.3Ca Alloy Sheet: *Suk-Bong Kang*¹; Hongmei Chen¹; Hyoung Wook Kim¹; Jae Hyoung Cho¹; ¹Korea Institute of Materials Science

Twin roll strip cast magnesium sheet was prepared to evaluate the characteristic of microstructure induced by relatively higher cooling rate. The segregation of aluminum elements was hardly seen to exist after more than 60 % rolling reduction at 300°C. In order to study the effect of reheating and warm rolling on twin roll strip cast magnesium alloy sheet, the thickness of sheet was reduced from 3.2 mm to 0.6 mm through 5 sequential reheating at 350°C for 10 min and warm rolling at about 300°C. Tensile test was performed after each warm rolling pass and following reheating. The microstructure was also observed along the through thickness of cast and rolled sheets together with following reheated ones. The grain refinement during reheating and warm rolling is attributed to

the formation of heavy shear band partly from the micro-sized precipitates of Al₂Ca and/or Al₆Mn.

9:10 AM

Forming Characteristics of Mg Sheet with Variation of Temperature: *Yong Nam Kwon*¹; Y-S Lee¹; J-H Lee¹; ¹Korea Institute of Materials Science

Mg alloys are the lightest alloys among the industrially applicable engineering alloys. Wrought alloys are superior in terms of mechanical properties and reliability to casting. A lot of efforts has given to establish an optimum forming condition for the industry uses, since wrought Mg alloy has a limited applications due to the poor formability. Most wrought Mg parts are fabricated under the elevated temperature condition of around 250°C where more slip systems are activated with temperature rise. Superplastic forming is another way to get over the low formability of Mg alloys. In the present study, formability of AZ31 sheet was investigated in terms of forming temperature with differing forming speed. For this purpose, both experimental and computational studies were carried out.

9:30 AM

Grain Refinement Studies in Two Different Mg Alloys by Severe Deformation Process and by Rolling: *Bilal Mansoor*¹; *Amit Ghosh*¹; Raymond Decker²; ¹University of Michigan; ²Thixomat, Inc.

Significant grain refinement of Mg alloys has been achieved to produce low temperature superplastic forming capability in these alloys. Severe plastic deformation is imparted to two different magnesium alloys, AZ31C and AM60. The AZ31C Mg alloy plate is processed via alternate biaxial reverse corrugation (ABRC) process followed by flattening and hot rolling. The initial bimodal grain structure is progressively subdivided during repeated deformations followed by flattening at 250°C and hot rolling at 350°C to nearly uniform microstructure of average size 1.5 micron. Thixomolded AM60 samples showed some cracking under the ABRC processing regime and was processed in by hot rolling at 350°C. It was shown that ultrafine grain size structure could be obtained for AZ31C and AM60 magnesium alloys. Comparison of mechanical properties and formability properties of the two alloys is provided in this article (work supported under grant from NSF).

9:50 AM

High Strength Mg Alloy Sheet Derived from Thixomolding: *Raymond Decker*¹; *Amit Ghosh*²; *Bilal Mansoor*²; *Stephen LeBeau*¹; *Sanjay Kulkarni*¹; ¹Thixomat, Inc.; ²University of Michigan

The inherent fine-grain microstructure, low macrosegregation and isotropy of Thixomolded Mg alloys are advantageous in starting stock for vigorous thermal mechanical processing to high strength/density Mg alloy sheet. Thus it is possible to further refine the grain size to micron size by continuous dynamic recrystallization. Twinning and related crack initiation and texturing are minimized with this fine grain approach. Coarse intermetallic eutectic phases are subdivided to then serve as dispersoids and as grain growth inhibitors. Furthermore, both strength and ductility are increased by this process, which also fosters improved formability. The effect of variables in Thixomolding, alloy content, deformation temperatures and reductions and annealing will be related to microstructure and properties.

10:10 AM

Microstructure, Mechanical Properties and Bendability of AM60 and AZ61 Magnesium Alloy Extruded Tubes: *Yingxin Wang*¹; *Alan Luo*²; *Xiaoqin Zeng*¹; *Anil Sachdev*²; *Li Jin*¹; *Raj Mishra*²; *Wenjiang Ding*¹; ¹Shanghai Jiao Tong University; ²General Motors Corporation

Microstructure, mechanical properties and bendability of AM60 and AZ61 magnesium alloy tubes have been investigated. The AM60 tubes were successfully extruded at the temperatures of 370°C and 420°C and average strain rates of 0.1 s⁻¹ and 0.6 s⁻¹; while the AZ61 tubes were extruded at 410°C and 0.1 s⁻¹. The lower extrusion temperatures resulted in higher yield strength for the AM60 tubes, and the strain rate had no significant effect on the mechanical properties. The bendability of both AM60 and AZ61 alloy tubes improved at elevated temperatures. For AM60 alloy tubes, a moderate temperature range (100 - 200°C) was sufficient since twinning and possible non-basal slip enhanced the formability. Higher bending temperatures (200 - 250°C) were needed for bending AZ61 alloy tubes where extensive non-basal slip was facilitated by the CDRX (continuous dynamic recrystallization) mechanism.

10:30 AM

Study of Deformation Modes at 77K in an AZ80 Magnesium Alloy: *Jayant Jain*¹; Warren Poole¹; Chad Sinclair¹; ¹University of British Columbia

This work represents an effort to examine the basic deformation modes in high aluminium bearing magnesium alloy (AZ80, 8 wt% Al) at low temperature with the motivation being that these results will provide insight into room-temperature deformation mechanisms. The alloy was deformed in solution-treated condition where the material had a grain size of 32 μm and there was a random orientation of grains. Uni-axial compression was applied at 77K by immersing the compression rig in liquid nitrogen. The deformed surface of the sample was examined for slip and twin identification using Nomarski interference microscopy and electron backscattered diffraction, respectively. The activation of different slip modes (basal, prismatic, pyramidal ($[a]$ type) and second order pyramidal ($[c+a]$ type)) and twin modes ($\{10-12\}$, $\{10-11\}$, $\{10-11\}-\{10-12\}$) were considered during trace analysis. Preliminary results suggest the importance of non-basal slip (both $[a]$ and $[c+a]$) and tensile twinning ($\{10-12\}$) during low-temperature deformation behaviour of AZ80.

10:50 AM

Texture Modification to Reduce Yield Anisotropy in Wrought Mg Alloys: *Toshiji Mukai*¹; Hidetoshi Somekawa¹; Alok Singh¹; Tetsuya Shoji²; Akira Kato²; ¹National Institute for Materials Science; ²Toyota Motor Corporation

As is well known from previous literatures, wrought magnesium alloys often show yield anisotropy; the yield stress in tension shows a higher value than that in compression. This yield anisotropy results from the formation of strong basal texture in wrought magnesium alloys. In this study, texture modification has been carried out to reduce the yield anisotropy. For a conventional AZ31 alloy, the basal texture was modified to make it relatively random by applying ECAE which can change the texture by reiterative shear loading. Another method used for texture modification was by changing the recrystallization behavior with a combination of adding a rare earth element and severe plastic working. Microstructure analysis by SEM/EBSD revealed that both the examined alloys possessed a relatively random texture. Yield stress in compression was found to be comparable to that in tension in a wide range of strain rate. The deformation mechanism will be also addressed.

11:10 AM

Texture Randomization of Rare Earth Containing Magnesium Alloys: Sean Agnew¹; *Jeremy Senn*¹; ¹University of Virginia

Rare earth (RE) element-containing Mg alloys were thermomechanically processed and characterized to understand the mechanisms by which their deformation texture is randomized during recrystallization. Two conventional Mg-Zn-Zr alloys were analyzed in the same fashion, because they are known not to randomize. The deformation textures of all the alloys examined were similar to one another after plane strain compression. However, the texture radically decreased during recrystallization and subsequent grain growth in the Mg-RE alloys. It was found that these alloys generate randomly oriented nuclei during recrystallization in shear bands, and further reduced their textures during subsequent grain growth. For the Zn-containing materials, grain boundary nucleation and bulging were observed during recrystallization, and the textures actually increased during grain growth. It is believed that the texture increases in these conventional alloys due to an oriented growth mechanism, which may be shut down in the case of Mg-RE alloys due to solute drag.

11:30 AM

Constitutive Behavior of Four Wrought Magnesium Alloys under Warm Forming Conditions: *Sean Agnew*¹; Cyrus Dreyer¹; John Polesak III¹; William Chiu¹; Charles Neil; Marcos Rodriguez²; ¹University of Virginia; ²Universidad Pltécnica de Madrid, Ciencia de los Materiales, Centro Nacional de Investigaciones Metalúrgicas-Consejo Superior de Investigaciones Científicas

The constitutive response of traditional wrought magnesium alloys, AZ31 and ZK10, is compared with two new rare earth element-containing alloys. The alloys were tested in tension over a range of strain rates and temperatures relevant to warm forming technology. The alloy denoted ZW41, which contains 4 wt% Zn and 1 wt% Y, exhibits superior elongation to failure within specific rate and temperature regimes. A proprietary alloy designated 'X' was shown to exhibit superior strength, particularly at the highest temperatures explored. All the alloys exhibited a temperature regime over which their elongation to

failure decreased or at least remained constant with temperature and this was understood in terms of their strain hardening and rate hardening responses

11:50 AM

Weld-Seam Quality of Hollow Magnesium Alloy Extrusions: *Wim Sillekens*¹; Daniël van der Linden¹; Andrew den Bakker²; ¹TNO Science and Industry; ²Nedal Aluminium

Extrusion technology for wrought magnesium alloys is still maturing, with research efforts being directed to bringing production efficiency as well as product quality to a level matching up to aluminum. For hollow extrusions, one particular aspect concerns the mechanical integrity of the so-called longitudinal weld seams (that form when the metal streams flowing around the mandrel in the die are rejoined through a process of solid-state bonding). This paper presents the results of laboratory trials in which tubular extrusions were produced using a porthole die. Several magnesium alloys (ZM21, AZ31, AZ61, ZE10) were investigated along with some corresponding aluminum alloys (AA6060, AA6082). Tube expansion tests and light-optical microscopy were carried out to study the quality of the weld seams in relation to the parent material. The results show that weld-seam quality in magnesium alloys is much less critical than in aluminum alloys (notably AA6082).

Materials in Clean Power Systems III: Fuel Cells, Hydrogen-, and Clean Coal-Based Technologies: Solid Oxide Fuel Cells: Metallic Interconnects

Sponsored by: The Minerals, Metals and Materials Society, TMS Structural Materials Division, TMS/ASM; Corrosion and Environmental Effects Committee

Program Organizers: Zhenguo "Gary" Yang, Pacific Northwest National Laboratory; Michael Brady, Oak Ridge National Laboratory; K. Scott Weil, Pacific Northwest National Laboratory; Xingbo Liu, West Virginia University; Ayyakkannu Manivannan, National Energy Technology Laboratory

Tuesday AM
March 11, 2008

Room: 392
Location: Ernest Morial Convention Center

Session Chairs: James Rakowski, Allegheny Ludlum; Richard Smith, Montana State University

8:30 AM **Invited**

Evaluation of a Ferritic Stainless Steels for SOFC Interconnect Application: *Paul Jablonski*¹; Christopher Cowen¹; David Alman¹; ¹National Energy Technology Laboratory

Ferritic stainless steels have many characteristics that are attractive for application as an interconnect in SOFC. These characteristics include low cost, good thermal expansion matching with the ceramic components and slow growth of adherent oxide scales in service. We have developed a surface treatment which greatly enhances the oxidation resistance of this class of alloys in SOFC relevant conditions. We report on the performance of this surface treatment on several stainless steels. We also discuss a probable mechanism for the enhanced performance and the likelihood for long term effectiveness of treated stainless steels.

9:00 AM **Invited**

Metallic Alloys for Solid Oxide Fuel Cell Interconnects: *James Rakowski*¹; ¹Allegheny Ludlum

Ferritic stainless steels are viable candidates for solid oxide fuel cell interconnect substrates due to attractive elevated temperature properties. Commercially available alloys with 16-30 wt. % chromium have been used as interconnects with varying degrees of success. Commonly encountered issues include oxide scale resistivity, spallation, and evaporation. Fe-Cr alloys with optimized compositions have been melted, processed, and tested in environments simulating SOFC operating conditions, with the results compared to those obtained for commercially available ferritic stainless. In addition to alloy development efforts, novel surface modifications applied to off-the-shelf materials have been investigated with promising results.

TUESDAY
AM

9:30 AM

Investigation and Development of Cost-Effective Ferritic Stainless Steel Interconnects for SOFC Applications: *Zhenguo "Gary" Yang*¹; Guanguang Xia¹; Zimin Nie¹; Joshua Templeton¹; Sharri Li¹; Jeff Stevenson¹; Prabhakar Singh¹; James Rakowski¹; ¹Pacific Northwest National Laboratory

Ferritic stainless steels are among the most promising candidate materials for interconnect applications in intermediate-temperature planar SOFC stacks due to their good oxidation resistance and excellent thermal expansion match to the cell components. In particular newly developed compositions demonstrate improved properties relevant to the interconnect applications over traditional ones. However there is still a need of further reduction of chromium volatility, long term-stability and foremost cost-reduction. Thus efforts have been initiated to search and develop ferritic stainless steel interconnects that are made from more cost-effective ferritic substrates, while being protected with conductive oxide coatings. This paper will present details of this work and discuss the suitability of the developed interconnects.

9:55 AM

The Glass-Metal Joint Strength Improvement in SOFC Interconnect Stacks by Reactive Air Coating Process: *Sung-tae Hong*¹; Jung Pyung Choi¹; K. Scott Weil¹; ¹Pacific Northwest National Laboratory

One of the keys to making glass-ceramic sealants viable as a long-term sealing solution for SOFCs is to control their reactivity with the metal components. For example, the barium aluminosilicate class of sealants generally adhere well to YSZ with little chemical interaction, but tend to form interfacial reaction products such as barium chromate (BaCrO_3) and monocelsian ($\text{BaAl}_2\text{Si}_2\text{O}_8$) with the oxide scales of the various candidate stainless steel alloys. With long-term exposure at the stack operating temperature, it has been previously shown that these phases thicken and become porous yielding interfaces that are often weak and susceptible to thermomechanically induced cracking. This correlates with observations of the glass-ceramic failures along the metal/sealant interface observed in full-scale stacks operated for 1000hrs or longer. The study presented here examined a new process to modify the surface of the metal component. Simple mechanical tests performed to quantitatively evaluate the effect of modification on the joint strength showed an improvement of 350% relative to conventional glass joints. The reasons for this can be explained in part based on findings from microstructural analysis, which will also be presented and discussed.

10:20 AM Break

10:30 AM

The Catalytic Property of Ni-Fe Alloys towards Methane Oxidation in SOFC: *Xiaochuan Lu*¹; Jiahong Zhu¹; ¹Tennessee Technological University

SDC + Ni-Fe composites have been investigated as anode for SOFC running on both H_2 and methane. Single cell with $\text{Ni}_{0.8}\text{Fe}_{0.2}$ + SDC anode and Pt current collector possessed the highest maximum power density of 1.43 and 1.03 W/cm^2 in wet H_2 and CH_4 at 800°C, respectively. Only 3.3 % loss in power density was observed during 100 hours operation in methane at 800°C. To eliminate the possible contribution of Pt towards methane oxidation, the same single cell with Au current collector was also run in H_2 and methane. The cell exhibited a maximum power density of 0.94 W/cm^2 in H_2 and a much lower power density of 0.36 W/cm^2 in methane. To clarify the catalytic property of Ni-Fe alloys towards methane oxidation, composite anodes of YSZ + $\text{Ni}_{1-x}\text{Fe}_x$ were exposed to methane at 800°C for 10 h. Additional single-cell testing with the anodes was conducted to confirm the results.

10:50 AM

Microstructure Modeling and Design of Solid Oxide Fuel Cells: *Kei Yamamoto*¹; *Edwin Garcia*¹; ¹Purdue University

With soaring oil prices and diminishing fossil fuel reserves, the development of new ways to produce electricity has become a priority. One such technology is Solid Oxide Fuel Cells (SOFC), whose elevated operating temperatures allow them to use a wide variety of fuels. Fuel cell performance is intricately related to material properties and thus a correctly engineered microstructure will increase the efficiency of the device. In this paper, the effect of particle size, crystallographic orientation, morphological anisotropy, porosity, etc., are engineered to maximize the delivered power density of the device. Moreover, the details and spatial distribution of triple phase boundaries are

tailored by implementing a novel numerical approach that accounts for the local electrochemical particle-particle interactions. Alternate, non-conventional device architectures are proposed.

11:15 AM

Performance Evaluation of SOFC with Different Interconnect Alloys/Coatings: *John Batey*¹; ¹Tennessee Technological University

The performance stability of a solid oxide fuel cell (SOFC) was studied with different interconnect materials. The cell configuration included a porous Ni/YSZ anode substrate as support, a Ni/YSZ anode interlayer, a thin YSZ electrolyte layer, a LSM/YSZ cathode interlayer, and a LSM cathode, and a Pt layer for cathode-interconnect contact, and a channeled alloy interconnect. The cell testing was conducted at 1073K using $\text{H}_2 + 3\% \text{H}_2\text{O}$ gas as fuel and the current density of the cell was monitored as a function of time at a fixed cell voltage of 0.7V. Several alloy interconnects, such as Crofer 22 APU and low-Cr Fe-Ni-Co alloys, were selected for evaluation. The spinel coatings evaluated included both thermally-grown spinel phases and spinel layers synthesized via electroplating. The effectiveness of surface spinel composition/quality on mitigating Cr migration from the interconnect to the cathode was assessed.

11:40 AM Invited

Carbon Tolerant Electrocatalysts Based on Ni/YSZ Modified with Au or Ag: *Stelios Neophytides*¹; Ilias Gavrielatos¹; Dario Modinaro²; Nicos Triantafylopoulos³; ¹Institute of Chemical Engineering and High Temperature Processes; ²SOFCpower S.r.l.; ³ADVENT Technologies

Carbon tolerant Ni/YSZ anode modified with 1%at Au or Ag with respect to Ni was tested under methane rich steam reforming conditions. The electrodes had shown high tolerance to C deposits, even at methane to water ratios as high as 3, at temperatures ranging between 700°C-900°C. The Ni based bimetallic anodes were prepared by combustion synthesis at 600°C and sintered under air at 850°C. The SEM images have shown that the Au or Ag modified Ni/YSZ electrode were nanostructured with particle size ranging between 50-100nm. XRD and XPS measurements provide a strong evidence for the formation of surface alloy. Temperature programmed reaction experiments, kinetic and electrokinetic measurements, under CH_4 steam reforming conditions in combination to physicochemical characterization of the electrocatalysts, had shown that the presence of Au or Ag plays a vital role in the tuning of CH_4 sequential dehydrogenation and oxidation rates of the hydrogenated adsorbed carbon species.

12:05 PM

Interdiffusion in γ (Face-Centered Cubic) Fe-Ni-Cr-X (X = Al, Si or Ge) Alloys at 700°C and 900°C: *Narayana Garimella*¹; Michael Brady²; Yong-ho Sohn¹; ¹University of Central Florida; ²Oak Ridge National Laboratory

Effect of minor alloying additions on the interdiffusion behavior of quaternary Fe-Ni-Cr-X (X = Al, Si or Ge) alloys were investigated using solid-to-solid diffusion couples. Fe-Ni-Cr-X alloys (fcc γ -phase) having compositions of Fe-25wt.%Ni-20wt.%Cr-3 wt.%Al, Fe-25wt.%Ni-20wt.%Cr -2.0wt.%Si and Fe-25wt.%Ni-20wt.%Cr -2wt.%Ge were arc-melted and chill-cast. Solid-to-solid diffusion couples were assembled in Invar steel jig, encapsulated in Ar after several hydrogen flushes, and annealed at 700° and 900°C in a three-zone tube furnace for 168 and 720 hours, respectively. Experimental concentration profiles were determined by using electron probe microanalysis with pure standards. Interdiffusion fluxes of individual components were determined directly from the experimental concentration profiles, and integrated to determine average interdiffusion coefficients. Effects of alloying additions on the diffusional behavior of Fe-Ni-Cr-X alloys are examined in the light of the formation and the growth kinetics of protective Cr_2O_3 scale.

Materials Informatics: Enabling Integration of Modeling and Experiments in Materials Science: Informatics and Materials Property Design

Sponsored by: The Minerals, Metals and Materials Society, TMS Materials Processing and Manufacturing Division, TMS/ASM: Computational Materials Science and Engineering Committee

Program Organizer: Krishna Rajan, Iowa State University

Tuesday AM
March 11, 2008

Room: 271
Location: Ernest Morial Convention Center

Session Chair: To Be Announced

8:30 AM

Advanced Computational Modeling of Titanium Alloys: Jaimie Tiley¹; ¹US Air Force

Three dimensional analysis of titanium alloys using new electron microscopy techniques provides incredible potential for incorporating texture information into mechanical behavior models. The use of crystallographic data provides vital information on slip lengths and three dimensional shapes of Widmanstätten alpha and beta structures that is used in property-microstructure models including fuzzy logic and neural network models. Results using the slip length data are compared to more traditional regression models to determine relationships between microstructure features and properties. In addition, probability distribution functions are used in place of mean values to improve accuracy and determine interparameter relationships between features.

9:10 AM

Application for Pre-Calculation Global Cost of Heat Treatment: Szota Michal¹; Jozef Jasinski¹; Grzegorz Walczak¹; ¹Czestochowa Technical University

At present, different thermo-chemical techniques are used in the thermo-chemical treatment practice. One of this is heat treatment in fluidized bed. This is characterized by high heat and mass transfer. These techniques are very often used in the research institutes and small industrial plants. In this processes is very important predicted global cost. These research are conducted in order to introduce analysis cost of thermo-chemical process, before it will be lead. Special prepared software connected with this system may be using in pre-calculated process cost. The cost pre-calculation is very important for process designer, because at present prices of every thing rise continuously every day. The customer usually wants get to know of heat treatment, before he commissions workmanship of it.

9:35 AM

Application of Measuring Electrical Conductivity of NaNO₂-KNO₃-NaNO₃ Melts by CVCC Technique: Zhang Kaiyu¹; Zhaowen Wang¹; Yungang Ban¹; ¹Northeastern University

The continuously varying cell constant (CVCC) technique was verified to be feasible by measuring the electrical conductivity of standard KCl aqueous solutions and molten salts. It was found that the error due to polarization resistance is very small if using CVCC technique to determine the electrical conductivity of liquid, and no deduction of lead and electrode resistance value from read out value required, thus the experimental procedure is simplified. Then the electrical conductivity of NaNO₂-KNO₃-NaNO₃ melts was measured by CVCC technique, and the results show that the electrical conductivity of the melt was varied by concentration of melts which has been influenced by the concentration of melt substances.

9:55 AM

Computational Design and Prototype Evaluation of Aluminide-Strengthening bcc-Based Superalloys for Elevated Temperature Applications: Zhenke Teng¹; Shenyang Huang¹; Peter K. Liaw¹; Chain T. Liu¹; Morris E. Fine²; Gautum Ghosh²; Mark D. Asta³; Gongyao Wang¹; Daniel Worthington³; ¹University of Tennessee; ²Northwestern University; ³University of California, Davis

Strengthening through a homogeneous distribution of a second phase is widely employed in the design of high-temperature materials. Nickel-based γ/γ'

superalloys owe their excellent creep strength to the presence of a high volume fraction of coherent-coplanar ordered fine γ' precipitates. Like γ/γ' systems, the body centered cubic (bcc) Fe-matrix with NiAl-type precipitates exhibit a cube-on-cube orientation relationship. However, ferritic steels with β/β' phases are brittle at room temperature and they are only used at temperatures below 893K due to the limited creep resistance. In our study, computational thermodynamic modeling is employed for the phase-stability study and microstructure design. Prototype Fe-based alloys with microstructures analogous to the classical Ni-based γ/γ' superalloys are obtained. The creep resistance can be improved by adding small amounts of alloying elements. This project is acknowledged by the Department of Energy (DOE) Office of Fossil Energy Program, Dr. Patricia Rawls.

10:20 AM

Estimation and Measurement on Conductivity of NaNO₂-KNO₃ Melts System: Zhang Kaiyu¹; Zhaowen Wang¹; Yungang Ban¹; ¹Northeastern University

The calculation models for conductance estimation have been established in this paper, and the mixed model can give approximation on conductivity of NaNO₂-KNO₃ system which has been measured by using the continuously varying cell constant (CVCC) technique. Two factors changes experiments were applied to study the effect of temperature and substance composing on conductivity of the melts. The results show that the data of the conductivity of melt has been influenced by concentrations of several melt substance and the temperature.

10:45 AM

Neural Networks Modeling Used for Improving Mechanical Property of Cars Elements after Heat Treatment in Fluidized Bed: Szota Michal¹; Jozef Jasinski¹; ¹Czestochowa Technical University

This paper presents neural network model used for improving mechanical property of cars elements after heat treatment in fluidized bed. Thermo-chemical process in fluidized bed is very complicated and difficult. The multi-parameters changes during this process are non linear characteristic. This fact and lack of mathematical algorithms complex describing processes in fluidized bed makes modeling by traditional numerical methods difficult or even impossible. In this case it is possible to try using artificial neural network. Such prepared neural network model, after putting expected values of mechanical property of steel in output layer, can give answers to a lot of questions about leading thermo-chemical process in fluidized bed. Neural network simulation allowed to carried out heat treatment with suitable process parameters, which allowed to obtain better mechanical property of cars elements after heat treatment.

11:10 AM

Scaling Techniques as Part of the Materials Informatics Toolbox: Patricio Mendez¹; ¹Colorado School of Mines

Scaling is a proven technique for the synthesis, generalization, and extrapolation of knowledge across systems in physics, applied mathematics, and many engineering disciplines. Judging by the impact of scaling on those other disciplines, their application to the field of materials science and engineering holds enormous potential. Paradoxically, scaling techniques are seldom applied in the materials field, and the results in those cases are occasionally unreliable. This presentation will discuss the reasons behind this paradox, promising efforts and techniques aimed at overcoming the challenges, and the type of results that could be accomplished by using scaling techniques as a tool of materials informatics.

11:50 AM

Titanium Based Alloy Chemistry Optimization for Maximum Strength, Minimum Weight and Minimum Cost Using JMatPro and IOSO Software: George Dulikravich¹; Amit Kumar¹; Igor Egorov²; ¹Florida International University; ²IOSO Technology Center

Chemical concentrations of Ti-Al-Cr-V alloys were predicted computationally so that they maximize Young's modulus of elasticity while minimizing alloy density and cost of raw materials. JMatPro software calculated the properties and IOSO software performed multi-objective evolutionary optimization. The method was applied at temperatures up to 1500°C. The intention was to demonstrate a possibility to computationally create alloys having multiple superior properties without a need for expensive experimental verifications. The

resulting alloys at each temperature had significantly reduced cost and lower density while increasing the Young's modulus. This method is applicable to alloys with a large number of alloying elements and significantly more properties. The accuracy of the method depends on the accuracy of the software packages used. ¹<http://www.jmatpro.com> ²I.N. Egorov, "Indirect Optimization Method on the Basis of Self-Organization," Proceedings of Optimization Techniques and Applications (ICOTA'98), Curtin University of Technology, Perth, Australia, 2 (1998), 683-691.

Materials Processing Fundamentals: Powders, Composites, Coatings and Measurements

Sponsored by: The Minerals, Metals and Materials Society, TMS Extraction and Processing Division, TMS: Process Technology and Modeling Committee
Program Organizer: Prince Anyalebechi, Grand Valley State University

Tuesday AM
March 11, 2008

Room: 283
Location: Ernest Morial Convention Center

Session Chair: Prince Anyalebechi, Grand Valley State University

8:30 AM

Preliminary Investigation into the Effect of Composite Reinforcement Particle Size on the Sintering of Ti-Titanium Boride Dual Matrix Composites: *Khaled Morsi¹; V.V. Patel¹; Kee Moon¹; Ahmed El-Desouky¹; Javier Garay²; ¹San Diego State University; ²University of California-Riverside, Department of Mechanical Engineering*

Titanium-titanium boride whisker (TiBw) composites are emerging as strong candidate materials for advanced applications within the automotive, aerospace and defense industries. Although increasing TiBw volume fraction improves the specific stiffness and wear resistance of titanium, it is usually on the expense of fracture toughness and ductility especially at the higher volume fractions of reinforcements where whiskers interlock. This research addresses strategies for microstructural design that may overcome these shortcomings, by generating titanium composites that are locally reinforced with TiBw through in-situ reaction in segregated regions of the microstructure and separated by ductile Ti matrix. The effect of varying composite reinforcement particle sizes (i.e. size of the reinforced regions) on the pressure-less sintering of these dual matrix composites is discussed. Electric current activation was also used to generate high density dual matrix composites and a new simultaneous imaging and modulus mapping technique was used to characterize these unique microstructures.

8:50 AM

Biomorphic Cellular TiC/C Ceramics from Woods: *Sutham Niyomwas¹; ¹Prince of Songkla University*

Biomorphic Cellular TiC/C ceramics were produced by vacuum-infiltrating carbon preforms with TiO₂ sol and subsequently synthesized by carbothermal reduction process. Carbon preforms were pyrolyzed from para-rubber wood, sadao-chang wood and coastal pine wood. The effect on holding infiltrated time of TiO₂ sol to the TiC/C products was analyzed. By observing the resulted products by SEM and XRD found that TiC/C was formed with retaining morphology of the original template structure.

9:10 AM

An Investigation of TiB₂ Synthesis Using TiO₂/B₄C Powder Mixture: *Filiz Sahin¹; Kutluhan Kurtoglu¹; Bora Derin¹; Onuralp Yucel¹; ¹Istanbul Technical University*

This paper presents a synthesis of TiB₂ via carbothermal reduction method using a mixture of TiO₂, B₄C and C prepared in molar ratio of 2:1:3. Reduction experiments were carried out in a high temperature Tammann Nernst furnace in a graphite crucible under argon atmosphere at different time (0-15-30-60 min.) and temperatures (1400-1500-1600-1700°C). The products were ground and investigated using XRD, SEM and BET techniques. Results were also compared with the literature about the carbothermally produced TiB₂ using mixture of TiO₂, B₂O₃ and carbon black powder.

9:30 AM

Periodic Technique for Measurement of the Thermal Properties of Nanocomposite Materials: *Garrett May¹; Donald Swart¹; Kevin Stokes¹; ¹University of New Orleans*

We present a periodic technique for measuring the thermal conductivity of thin, disk-shaped samples. In samples of this type, temperature measurements must be made across the sample faces and are therefore subject to large error due to the interface resistance between the temperature sensor and the sample. The technique uses measurements of the amplitude and phase of the periodic temperature across both a reference sample and the unknown material at several different frequencies. Modeling of the heat flow in the sample allows the simultaneous determination of the thermal parameters of the sample as well as the interface resistance. The technique is demonstrated on nanocomposite samples less than 1.0 mm thick.

9:50 AM

Preliminary Investigations into the Aqueous Processing of Alumina-Carbon Nanotube Composites: *Roberto Angulo¹; Khaled Morsi¹; ¹San Diego State University*

Carbon nanotubes (CNTs) have recently emerged as materials with outstanding properties. This has promoted their consideration as reinforcements for other material systems, such as ceramics. However, one of the fundamental problems with producing CNT-reinforced ceramics is the effective dispersion of CNTs during processing. This has been successfully carried out recently using organic solvents, albeit with negative implications for the environment. This paper investigates the rheological behavior of aqueous CNT-alumina slips, with the objective of producing an environmentally friendly aqueous tape casting process for the production of alumina-CNT composites. The effect of CNT (and surface modified CNT) addition on the rheology of the slip and tape casting is presented.

10:10 AM Break

10:20 AM

Titanium Diboride Synthesis by Carbothermal Reduction of TiO₂ and B₂O₃: *Kutluhan Kurtoglu¹; Bora Derin¹; Filiz Sahin¹; Onuralp Yucel¹; ¹Istanbul Technical University*

The synthesis of titanium diboride (TiB₂) by carbothermal reductions of TiO₂ and B₂O₃ mixed with carbon black was investigated. For this aim, TiO₂, B₂O₃ and carbon black powders were dried, weighed out in stoichiometric proportions, ball-milled, and then charged into graphite crucibles. The experiments were carried out in a graphite resistance furnace (Tammann furnace) in argon media using different range of temperature (1400-1700°C) and time (0-60 min). The phase analyses and the microstructural observation of the products were examined by using XRD and SEM. Results were also compared with the TiB₂ products previously obtained with self-propagating high-temperature synthesis (SHS) method using mixture of TiO₂, B₂O₃ and Mg followed by acid leaching.

10:40 AM

Activity Measurement of REs and Their Alloy System Using Multi-Knudsen Cell Mass Spectrometry: *Woong-hee Han¹; Masao Miyake²; Hisao Kimura¹; Masafumi Maeda¹; ¹University of Tokyo; ²University of Illinois*

Although development of the production process with rare earth (RE) metals requires thermodynamic data of alloys, available experimental and theoretical data in the literature aren't sufficient yet. Those can be attributed to the experimental difficulties brought by the high reactivity of rare-earth metals. In this study, vapor pressure of RE metals and activities of RE in alloys were determined by Knudsen cell mass spectrometry. The Knudsen cell method was developed to measure vapor pressure of species by weight loss per evaporated unit area. After then, combination of a single Knudsen cell with mass spectrometry could determine activity in metal alloy by measured ion current of evaporated species from a substance. In this study, Multi Knudsen cell was used. The method of multi Knudsen cells mass spectrometry allow measurement of ion currents of evaporated species from substances, which are pure metal taken as reference, and RE alloy, in a single experiment.

11:00 AM

Transportation of a Liquid Droplet on a Substrate Having a Spatial Gradient: Itaru Jimbo¹; Minehiro Arai¹; Norimasa Okada¹; ¹Tokai University

A surface having a spatial gradient in its surface free energy is promising for its applicability. The transportation of a liquid droplet on such surfaces does not need complicated mechanisms or energy sources. This kind of surface can be applied to form various shapes to transport liquid or even bubbles. The idea was first documented in the study of immunochemistry by Swedish scientists in 1984, where a spatial gradient of surface free energy was made on a silicon substrate by using methylsilane. In this study, the concept and various schemes of droplet and bubble transportation will be reviewed and the capability of the surface properties to realize the motion of a droplet will be discussed on several key parameters such as advancing and receding contact angles and surface free energy gradient. Microscopic observation will also be introduced in order to clarify the relationship with the surface wettability.

11:20 AM

Synthesis of Nanosized Tungsten Carbide Powder by Thermal Plasma: Taegong Ryu¹; Kyu Sup Hwang¹; Hong Sohn¹; Zhigang Fang¹; ¹University of Utah

Thermal plasma has been applied to the preparation of nanosized tungsten carbide powder. The reduction and carburization of the vaporized tungsten chloride by methane-hydrogen mixtures produced nanosized WC_{1-x} powder, which sometimes contained the WC, W₂C and/or W phase. The products were characterized using XRD, carbon analyzer, and TEM. The effects of plasma torch power, flow rate of the primary plasma gas (Ar) to generate plasma flame, CH₄/WCl₆ molar ratio, and H₂/CH₄ molar ratio on the product composition were investigated. The tungsten carbide (WC_{1-x}) powders showed particle sizes of less than 30 nm. The powder was treated under hydrogen atmosphere to fully carburize the WC_{1-x}, W₂C and W and to remove excess carbon, from which essentially pure WC powder was obtained.

11:40 AM

Rapid Synthesis of Ultrafine WC-Co Cemented Carbides by In-Situ Reactions and Spark Plasma Sintering: Xiaoyan Song¹; Jiuxing Zhang¹; Wenbin Liu¹; Kai Wang¹; Shixian Zhao¹; Mingsheng Wang¹; Xuemei Liu¹; ¹Beijing University of Technology

A novel route for rapid synthesis of ultrafine WC-Co cemented carbides with homogeneous binder phase distribution is reported. The composite powder is produced by in situ reduction-carbonization reactions by using WO₃, Co₃O₄ and carbon black as raw powders. The reaction equilibrium and phase stability are studied by thermodynamic calculations. The WC-Co composite powder is condensed by spark plasma sintering (SPS) to obtain the cemented carbides bulk. The sintering temperature is lower than that in the conventional sintering methods by 150-300°C, while the sintering time is remarkably reduced by 3-5 times. The high performances of the hardness and the fracture toughness are obtained. The experimental results confirm that the present processing scheme of *in situ* reduction-carbonization reactions and subsequent SPS sintering is an efficient way to prepare WC-Co cemented carbides, and is apparently superior to the conventional long-period techniques of preparing composite powder and cemented carbides bulk.

Mechanical Behavior, Microstructure, and Modeling of Ti and Its Alloys: Phase Transformation and Microstructure Development II

Sponsored by: The Minerals, Metals and Materials Society, TMS Structural Materials Division, TMS: Titanium Committee
Program Organizers: Ellen Cerreta, Los Alamos National Laboratory; Vasishth Venkatesh, TIMET; Daniel Evans, US Air Force

Tuesday AM
March 11, 2008

Room: 384
Location: Ernest Morial Convention Center

Session Chairs: Ellen Cerreta, Los Alamos National Laboratory; Michael Mills, Ohio State University

8:30 AM Invited

Constitutive Based Modelling of the Alpha Phase Lath Width and Spheroidisation in Titanium-6-4: Jeffery Brooks¹; M. Mulyadi²; M. Rist²; ¹Qinetiq Ltd; ²Open University

The control of alpha lath width during hot working and the subsequent formation of a uniform spherodised alpha structure during thermo-mechanical processing are essential for the development of the properties required for Titanium-6-4 critical aero-engine parts. A quantitative description of the evolution of flow stress and microstructure is used to predict the alpha lath width and degree of spheroidisation of the alpha phase during the hot deformation of Titanium-6-4. The approach is validated using quantitative metallographic analysis data obtained from uniaxial compression tests carried out in the alpha-beta temperature range (850-1000°C) for strains (0-1) and strain rates (0.003-1/s) relevant to primary processing. The validation of the models is dependent on the quality of the microstructural data and as a consequence a number of approaches to the quantification of the structures are discussed together with the errors that are associated with the different measurement techniques and assumptions.

9:00 AM

Characterization of Ti-TiC and Ti-TiN Composites Produced by "Reactive LENS®": Junyeon Hwang¹; Anantha Puthucode¹; Alderson Neira¹; Rajarshi Banerjee¹; Michael Kaufman²; ¹University of North Texas; ²Colorado School of Mines

Ti-TiC and Ti-TiN composites were prepared by a reactive LENS® (laser engineered net shaping) process. It is shown that the as-deposited structures contain primary TiC and primary TiN dendrite cores surrounded by α -Ti grains. Further the TiC and TiN dendrite cores are shown to contain α -Ti precipitates in the form of Widmanstätten plates that lie on {111} planes. In all cases, the α -Ti grains and precipitates have an orientation relationship with the TiC and TiN where the close-packed planes and directions: $\{111\}_{\text{TiC}} // (0001)_{\alpha\text{-Ti}}$ and $\langle 011 \rangle_{\text{TiC}} // \langle 1120 \rangle_{\alpha\text{-Ti}}$. In the case of the Ti-TiN composite material, the precipitation of metastable α -Ti precipitates instead of Ti₃N in the primary TiN appears to be related to the mechanism of nucleation of this phase on stacking faults in the TiN. Finally, the similarities and differences in these two systems will be discussed and related to the potential of using reactive LENS for producing structural Ti-matrix composites.

9:20 AM

Effect of Initial Structure on Dynamic Recrystallization in a Ti-Fe Alloy: Tadashi Furuhashi¹; B. Poorganji¹; G. Miyamoto¹; M. Yamaguchi²; Y. Itsumi³; K. Matsumoto³; T. Tanaka³; Y. Asa³; ¹Tohoku University; ²Sumitomo Titanium Corporation; ³Kobe Steel, Ltd.

Deformation behavior and microstructure evolution of a Ti-1.5Fe alloy in (alpha+beta) two-phase region is studied with focusing on effect of initial microstructure at different deformation temperatures and strain rates. Quenching to room temperature after beta solutionizing and reheating to the deformation temperature causes a fine interlamellar spacing and colony size in the (alpha+beta) lamellar microstructure whereas direct cooling to the deformation temperature results in a coarser lamellar structure. Decrease in interlamellar spacing of initial microstructure results in promotion of DRX at a given deformation condition. At a high temperature where alpha volume fraction is lower, dynamic recovery is a major deformation mechanism while at a lower temperature, i.e., a higher fraction

TUESDAY AM

of alpha phase, DRX of alpha phase occurs predominantly. It is concluded that critical needed strain for initiation and completion of dynamic recrystallization is decreased by refining the initial microstructure.

9:40 AM

Finite Element Analysis of the Primary Processing of TIMETAL 555: *Manish Kamal*¹; Vasisht Venkatesh¹; ¹Titanium Metals Corporation

TIMETAL 555 (Ti-5Al-5Mo-5V-3Cr), a near beta titanium alloy, is currently under evaluation for several major airframe applications. TIMET has recently started processing Ti-5553 as production heats. Being a relatively new material the understanding of forging routes and their effects on material properties is still in the early stages. Numerical modeling techniques were used to study the cogging process to evaluate the hot workability of Ti-5553. Finite element analysis codes were used to determine the local state of stress, strain, strain rate, and temperature within the workpiece. These variables were then utilized to predict damage within the workpiece using an appropriate ductile fracture criterion. Cogging routes for the primary processing of TIMETAL 555 were designed based on the model. Simulation results show that strain induced porosity should not be an issue with the proposed forging route. However, pass schedules need to be optimized to yield a more uniform final structure.

10:00 AM Invited

Some Aspects of Phase Transformations in Ti and TiAl-Based Alloys: *Michael Loretto*¹; H. Saage¹; D. Hu¹; H. Jiang¹; N. Wain¹; J. Mei¹; X. Xu¹; ¹University of Birmingham

Some factors which affect the precipitation of alpha in Ti-15-3 and Ti5553 have been investigated with the aim of understanding the factors that control the extent and the nature of the alpha which is precipitated from solution. The influence of ageing temperature and of the addition of small additions of carbon on both grain boundary alpha and of the scale of the alpha precipitated in the matrix in Ti-15-3 has been investigated. These results will be discussed in terms of the role of oxygen in enhancing precipitation of alpha. Recent work has shown that the amount of alpha which is precipitated during heat treatment of TiAl-based alloys in the two phase field can be strongly influenced by the pressures used during HIPping and similar results have been obtained in Ti5553. These observations will be discussed in terms of the control of phase transformations by HIPping and by post-HIP heat treatments.

10:30 AM Break

10:50 AM Invited

Phase Formation and Decomposition in IMI 550 during Cooling from Elevated Temperature: *Henry Rack*¹; L. Allred²; J. Hudson¹; Javid Qazi³; ¹Clemson University; ²Oak Ridge National Laboratory; ³KEMET Electronics Corporation

This investigation has examined the formation and decomposition of phases formed during cooling from elevated temperature in IMI550. Decomposition at the fastest cooling rate examined is initially controlled by the solution treatment temperature, i.e the composition of the parent beta phase, higher temperatures within the alpha plus beta and beta phase field resulting in alpha prime martensite, with lower solution treatment temperatures, where the parent beta phase becomes increasing higher in beta stabilizing content, resulting in orthorhombic martensite formation. Reduction in cooling rate have been found to result in short range diffusion within both the martensitic platelets and increasing within the retained beta matrix. The mechanisms of the alpha phase formation at slower rates will be discussed and related to the commonly observed Widmanstätten, basketweave and colony microstructures observed in titanium alloys after cooling from elevated temperature.

11:20 AM

Modeling and Experimental Validation of Hot Rolling Ti-6-4 Plates: *Vasisht Venkatesh*¹; ¹TIMET

DEFORM-3D, a commercial finite element analysis (FEA) software, was used to model multi pass hot rolling of Ti-6-4 plates. In order to validate the FEA model appropriately designed small scale rolling experiments were conducted, at alpha+beta temperatures, on 2-high rolling mill using 25 mm thick plates. The effect of key rolling parameters such as temperatures, heat transfer coefficient, friction and pass line on mill load, strain distribution and final plate shape were

investigated. In addition, predictions from relevant alpha spheroidization models were compared to final rolled microstructures.

11:40 AM

Residual Stresses in Flowformed Ti-6Al-4V: *Ibrahim Ucak*¹; Gabriel Hostetter¹; Mehmet Gungor¹; Joseph Pickens¹; Wm. Tack¹; ¹Concurrent Technologies Corporation

Flowforming is a novel processing method for the manufacture of near-net-shape structural metallic tubes. Flowforming is generally performed at room temperature with a wall thickness reduction between 50% and 80%. This large amount of cold work generates significant residual stresses that may cause problems during final manufacturing processes, such as machining, cutting and welding. In this study, Ti-6Al-4V tubes in the as-flowformed and stress-relieved conditions were subjected to residual stress measurement by X-ray method. In addition, optical microscopy, transmission electron microscopy, and tensile testing were conducted on both types of materials. The effect of stress-relief treatment on the magnitude of residual stresses, microstructure and tensile properties were presented and discussed. This work was conducted by the Navy Metalworking Center, operated by Concurrent Technologies Corporation, under Contract No. N00014-00-C-0544 to the Office of Naval Research as part of the U.S. Navy Manufacturing Technology Program. Approved for public release; distribution is unlimited.

12:00 PM Invited

Probing the Early Stages of Phase Separation and Second Phase Nucleation in Complex Beta Titanium Alloys: *Rajarshi Banerjee*¹; Soumya Nag²; Anantha Puthucode¹; Arda Genc²; Hamish Fraser²; ¹University of North Texas; ²Ohio State University

The solid-state decomposition of the beta phase of titanium alloys is a rather complex phenomenon involving multiple competing compositional and structural instabilities including, phase separation in the beta phase and precipitation of the omega and alpha phases. The influence of these beta phase instabilities on the microstructural evolution and resultant mechanical properties of these alloys are rather poorly understood. Furthermore, recent developments in advanced characterization techniques such as high-resolution scanning transmission electron microscopy and 3D atom probe tomography allow for unprecedented insights into the true atomic scale structure and chemistry changes associated with the instabilities in the beta phase of these complex alloys. Such detailed studies are being carried out on two different beta titanium alloys, the Ti-5Al-5Mo-5V-3Cr-0.5Fe (TIMETAL-5553 or Ti-5553) alloy, used in aerospace applications, and the Ti-35Nb-7Zr-5Ta (or TNZT) alloy, used in orthopedic implant applications, and will form the basis of this presentation.

Mechanics and Kinetics of Interfaces in Multi-Component Materials Systems: Mechanical Properties of Interfaces

Sponsored by: The Minerals, Metals and Materials Society, TMS Electronic, Magnetic, and Photonic Materials Division, TMS Structural Materials Division, TMS/ASM: Composite Materials Committee, TMS: Thin Films and Interfaces Committee
Program Organizers: Bhaskar Majumdar, New Mexico Tech; Rishi Raj, University of Colorado, Boulder; Indranath Dutta, US Naval Postgraduate School; Ravindra Nuggeshalli, New Jersey Institute of Technology; Darrel Frear, Freescale Semiconductor

Tuesday AM
March 11, 2008

Room: 279
Location: Ernest Morial Convention Center

Session Chairs: Darrel Frear, Freescale Semiconductor; Carl Boehlert, Michigan State University

8:30 AM Keynote

Ductile-to-Brittle Transition in Solder Joints Measured by a Mini Charpy Impact and Drop Machine: *King-Ning Tu*¹; Yuhuan Xu¹; Alan Wang¹; Masaru Fujiyoshi²; ¹University of California, Los Angeles; ²Hitachi Metals

The most frequent failure of wireless, handheld, and portable consumer electronic products is an accidental drop to the ground. The impact may cause interfacial fracture of ball-grid-array solder joints. In this talk, a mini impact and

drop tester based on the classic Charpy impact machine was built and utilized to measure the impact toughness and to characterize the impact reliability of both eutectic SnPb and SnAgCu solder joints. The annealing effect on the impact toughness was investigated and the fractured surfaces were examined. A ductile-to-brittle transition for the Pb-free solder joints has been observed. By cross-sectional SEM analysis, it is found that the annealing has allowed more growth of intermetallic compound at the interface, which may have contributed to the ductile-to-transition of the SnAgCu solder joints.

9:10 AM Invited

Characterizing Interfacial Delamination in Layered Thermal Barrier Coatings: Kevin Hemker¹; ¹Johns Hopkins University

Multilayered thermal barrier systems offer enhanced temperature capabilities but are susceptible to interfacial delamination and global spallation. Important phenomena that affect delamination occur in each layer and at the interfaces, and mechanics-based models of these events require a detailed understanding of the properties of each layer. The system investigated in the current study is comprised of: a EBPVD 7YSZ top coat, a thermally grown oxide (TGO), a low-pressure plasma sprayed NiCoCrAlY two-phase bond coat and a Ni-base superalloy substrate. This talk will outline experimental techniques developed to capture the salient material properties of these disparate layers and introduce the physics-based model developed to describe delamination in this system.

9:40 AM

The Strength of Adhesive Joints as Influenced by the Interface Structure and Stress States: Bhaskar Majumdar¹; Michael Kent²; Earl Reedy²; ¹New Mexico Tech; ²Sandia National Laboratory

The strength of adhesive joints depends strongly on the interface, with failure shifting from ductile cohesive failure inside the adhesive to brittle interfacial failure, depending on the local chemistry and interface morphology. In this work, self assembled monolayers (SAMs) were used to alter the interface conditions between the substrate and an epoxy based adhesive. Results show a highly non-linear dependence of joint strength on the concentration of interacting sites, where weak sites were obtained with methyl terminated SAMs and strong sites were obtained with bromine terminated SAMs. The non-linear behavior is shown to depend on yielding of the polymer, as also influenced by local stress states. Lap shear tests as well as toughness tests exhibited slightly altered behavior, and the roles of stress concentration and stress states are discussed. These results highlight the importance of developing appropriate design parameters to characterize the strength and durability of joints.

10:05 AM Break

10:20 AM

Complementary Testing Techniques for Mechanical Properties in Metal-Polymer Systems: Peter McNabb¹; John Yeager¹; David Bahr¹; Marian Kennedy²; ¹Washington State University; ²Clemson University

Testing the mechanical properties and fracture resistance of metal-polymer systems is important for reliability in flexible electronics. Using a model system of Au/Kapton, this study focuses on the development of a method to measure interfacial fracture energy using bulge testing, and the toughness is compared to previous four point bending results. Initial results show that this technique, combined with nanoindentation, can be used to study interfacial fracture energies, fatigue lifetimes and creep of metal-polymer systems. Fracture within the metals films was shown to occur during tensile strain of the film system with tensile stress. The interfacial energies can then be predicted as the substrates is depressurized and the film delaminates due to compression. These fracture energies are shown to be a function of both interlayer chemistries, TiW and W, as well as interphase regions formed by reactive ion etching within the kapton substrate.

10:45 AM

Thermocompression Bonding of Gold Coated Carbon Nanotube Turfs for Heat Transfer Applications: Ryan Johnson¹; David Bahr¹; Cecilia Richards¹; Robert Richards¹; Jeong-Hyun Cho¹; Ali Zbib¹; Amer Hamdan¹; Devon McClain²; Jun Jiao²; ¹Washington State University; ²Portland State University

Vertically aligned carbon nanotubes turfs (VACNTs), grown using chemical vapor deposition, have been proposed as heat transfer media in thermal applications. Mechanical contact allows conduction, making the thermal

resistance of the interface between the VACNTs and the contact surface a critical parameter. To normalize the contact surfaces for heat transfer measurements, VACNTs were coated in a thin layer of sputtered gold and then mechanically transferred to a gold film on silicon using thermal compression bonding. Controlling the applied pressure allows clean transfer while avoiding CNT buckling, incomplete transfer, or transfer of the catalyst. A stress of 0.5 MPa has produced a clean transfer of 200 micrometer tall turfs. Electron microscopy and mechanical measurements of interfacial strength are used to characterize the structural implications for thermal conductivity applications. We present a discussion of bonding mechanisms between the separate materials in the structure: the gold, CNTs, and the oxide containing the catalyst.

11:10 AM

Debond Strength Comparisons of Microscopic Evaluations of Ti-24Al-17Nb-0.66Mo (at%), Ti-24Al-17Nb-1.1Mo and Ti-24Al-17Nb-2.3Mo SiC Fiber-Reinforced Composites: Jeffrey Quast¹; Carl Boehlert¹; ¹Michigan State University

The debond strength is a critical design parameter for continuously-reinforced metal matrix composites (MMCs) as the use of such materials is dependent on the ability of the interface to transfer load from the matrix to the fiber. Research on MMCs containing first generation orthorhombic-based matrix alloys based on Ti-25Al-17Nb-xMo(at.%) has shown promising results. Powder-processed and tape cast four-ply, unidirectional-reinforced MMC samples, possessing Ti-24Al-17Nb-xMo(at.%) matrices with Ultra SCS-6 continuous fibers (approximately 36% vol. pct.), were room-temperature tensile tested with the fibers transverse to the loading direction using a cruciform specimen geometry, which has been previously used for transverse interfacial property evaluation of high volume fraction MMCs. The effects of processing conditions and small Mo additions (0.66, 1, and 2.3at.%) on the debond strength of Ti-24Al-17Nb-xMo(at.%) MMCs were investigated. Debonding events were captured by the stress-strain curves along with metallographic examination. The greatest debond strengths were observed in the Ti-24Al-17Nb-1.1Mo MMC.

11:35 AM

Evaluation of Variability on the Thermomechanical Response of Nitride Nuclear Fuels through Microstructurally Explicit Models: Manuel Parra Garcia¹; Sung-Ho Park²; Kirk Wheeler¹; Pedro Peralta¹; Ken McClellan³; ¹Arizona State University; ²Gyeongsang National University; ³Los Alamos National Laboratory

A two-dimensional (2D) thermo-mechanical finite element model of a cylindrical fuel pellet seen from the longitudinal plane has been run to investigate variability of the thermo-mechanical response (stress field, strain field, grain boundary interaction, temperature distribution) due to microstructure heterogeneity within a Representative Volume Element (RVE). Microstructural information was obtained from sintered ZrN, as a surrogate for PuN, processed under conditions similar to those used in actinide bearing fuels. The 2-D RVE obtained from the microstructural characterization, which includes pore and grain geometry as well as grain orientation, was surrounded by "effective material" and was located at different positions in the model to evaluate the effect of stress and temperature gradients on the local fields. This effort is directed towards the formulation of a framework that can be translated into characterization and modeling of actual fuels to improve simulations of fuel performance. Work supported under DOE/NE Agreement # DE-FC07-05ID14654.

Minerals, Metals and Materials under Pressure: Electronic, Magnetic and Optical Properties of Materials under High Pressure

Sponsored by: The Minerals, Metals and Materials Society, TMS Structural Materials Division, TMS: Chemistry and Physics of Materials Committee
Program Organizers: Richard Hennig, Cornell University; Dallas Trinkle, University of Illinois; Ellen Cerreta, Los Alamos National Laboratory

Tuesday AM
March 11, 2008
Room: 385
Location: Ernest Morial Convention Center

Session Chairs: Richard Hennig, Cornell University; Dallas Trinkle, University of Illinois

8:30 AM Invited

Exotic Pressure Effects in Silane to 75 GPa: *Arthur Ruoff*¹; Chandrabhas Narayana¹; Raymond Greene²; ¹Cornell University; ²Corning, Inc.

Two groups of theorists have calculated the crystal structures of silane at high pressures and have predicted that those present at the highest pressure will become metallic. Their lowest enthalpy structures (infinite mass approximation) do not agree with each other or with experiment. It has also been suggested that metallic silane may be a high T_c superconductor. Our experimental work finds that at pressures from 7 to 40 GPa silane has a monoclinic structure (point group 14). Silane at 298K is thermodynamically unstable with ΔG super zero = 56,900 J/mole. We have obtained $\Delta G(P)$ which becomes negative at 4 GPa but reverts to being positive at 16 GPa. When using stainless steel gaskets the samples become black beginning next to the gasket at 20 GPa (with no raman signal of H₂). No Si-H or H₂ vibrons are present. This phase is an excellent shiny metal based on reflectivity studies.

9:00 AM Invited

Theoretical Aspects of Light-Element Alloys under Pressure: *Ji Feng*¹; Richard Hennig²; Neil Ashcroft²; Roald Hoffmann²; ¹Cornell University, Harvard University; ²Cornell University

Nothing is more fundamentally chemical than compound formation. Yet some elements are quite reluctant to bind, at least under normal conditions of temperature and pressure. An archetypical example is the beryllium (Be) and lithium (Li) system; these two lightest of all metallic elements in the condensed state are immiscible, and form no binary alloy. Here we report a computational study indicating that the reactivity of Be and Li can be fundamentally altered by pressure, leading to the formation of ordered alloys. We also show that in these compounds, the valence electrons reside in unexpected and quite striking 2-dimensional free-electron-gas-like states embedded in a 3-dimensional crystalline environment. Along with other examples, a general electronic structure viewpoint, which unifies some important aspect of the reactivity, electronic structure and geometric structure concerning light-element alloys under pressure, will be discussed.

9:30 AM Break

9:45 AM Invited

Recent Studies in Superconductivity at Extreme Pressures: *James Schilling*¹; ¹Washington University

High pressure experiments play an important role in the field of superconductivity in three primary ways:¹ (a) increase the number of known superconductors and enhance their transition temperatures to record values, (b) serve as a guide in the synthesis of materials with superior superconducting properties at ambient pressure, and (c) give information on the pairing interaction and allow a quantitative test of theory. In this talk I will discuss recent experimental results on the alkali metals, Y, CaC₆, and high-temperature superconductors which illustrate these possibilities. For example, the number of elemental superconductors has been increased by 22 through the application of high pressure from 30 to 52, including Li, Y, Fe, O, and Si. Recently the transition temperature of Y metal has been pushed by 1.2 Mbar pressure to 20 K and that of Ca by 1.6 Mbar to 25 K, a record value for an elemental superconductor. Such enormous pressures are sufficient to even destroy the free-electron character of the conduction electrons

in the alkali metals, as predicted by Neaton and Ashcroft,² which is why both Cs and Li become superconducting. Comparison of parallel studies on the trivalent d-electron elements Sc, Y, La, and Lu reveals an interesting correlation between T_c and the free volume available to the conduction electrons outside the ion cores, as suggested many years ago by Johansson and Rosengren.³ ¹J. S. Schilling, Ch. 11 in "Handbook of High Temperature Superconductivity: Theory and Experiment", editor J. R. Schrieffer, associate editor J. S. Brooks (Springer Verlag, Hamburg, 2008), p. 427-462. ²J. B. Neaton and N. W. Ashcroft, Nature 400, 141 (1999); *ibid.*, Phys. Rev. Lett. 86, 2830 (2001). ³B. Johansson and A. Rosengren, Phys. Rev. B 11, 2836 (1975).

10:15 AM

First-Principles Calculations of High-Coordinated Group IV Metal Dioxides: *Varghese Swamy*¹; Barry Muddle¹; ¹Monash University

High-coordinated Ti, Zr, and Hf dioxides have received significant attention as potential ultrastiff/ultrahard substances. Cotunnite-TiO₂ with nine-fold metal-oxygen coordination synthesized at ~60 GPa represents the stiffest and hardest of the oxides identified to date. Other proposed high-density structures (stable at high-pressures) include an orthorhombic phase, a pyrite phase, and a fluorite phase. Good agreements have been obtained between experimental and ab initio results on the elastic properties of most of the phases; however, a major discrepancy has emerged between the available experimental and theoretical elastic data on pure and Zr-substituted cubic TiO₂. Here we present the results of our first-principles calculations with a focus on the elastic properties of the cubic phases. We used density-functional and hybrid density-functional -Hartree-Fock approaches. A detailed comparison of the effects of the functionals used on the computed elastic properties as well as that between the theoretical and experimental data will be presented.

10:35 AM Break

10:50 AM Invited

Ex Nihilo Determination of Structures by Random Searching: Richard Needs¹; Chris Pickard²; ¹University of Cambridge; ²University of St. Andrews

We introduce a search strategy for predicting structures based on relaxation of randomly chosen structures under the forces and stresses obtained from ab initio density functional theory (DFT) computations. By starting from random structures we aim to obtain a wide coverage of the "structure space", which allows for the possibility of finding radically new structures which have not been considered previously. Our search strategy is remarkably straightforward and does not require the selection of highly-system-specific parameter values. Tests indicate that our strategy works very well for systems with up to of order 10 atoms, which allows us to address many interesting problems. We illustrate the performance of the method with applications to various systems under high pressures, including solid hydrogen¹ where we find a new candidate structure for phase III,² silane where we find electron deficient bonds at high pressures, and aluminium hydride where we find high-pressure insulating and metallic phases.³ ¹"Structure of phase III of hydrogen", C. J. Pickard and R. J. Needs, Nature Physics 3, 473 (2007). ²"High-pressure phases of silane", C. J. Pickard and R. J. Needs, Phys. Rev. Lett. 97, 045504 (2006). ³"Metallisation of Aluminium Hydride at High-Pressures", C. J. Pickard and R. J. Needs, submitted for publication.

11:20 AM Invited

Superconductivity in Hydrogen Dominant Materials: Silane: *Mikhail Erements*¹; I. Trojan¹; S. Medvedev¹; ¹Max Plank Institute fuer Chemie

The fundamental problem of metallization of hydrogen requires currently experimentally inaccessible pressures of $P > 400$ GPa. The dense group IVa hydrides has recently attracted considerable attention because hydrogen in these compounds is chemically precompressed. We report experimental observation of the transformation of SiH₄ to the metallic state with P63 structure with high density of hydrogen atoms likely creating a three-dimensional network. In addition, we found that silane becomes superconducting with $T_c = 17$ K at 96-120 GPa. These findings support the idea of modeling metallic hydrogen by hydrogen-rich compounds.

Neutron and X-Ray Studies for Probing Materials Behavior: Phase Transitions and Beyond

Sponsored by: National Science Foundation, The Minerals, Metals and Materials Society, TMS Structural Materials Division, TMS: Advanced Characterization, Testing, and Simulation Committee

Program Organizers: Rozaliya Barabash, Oak Ridge National Laboratory; Yandong Wang, Northeastern University; Peter K. Liaw, University of Tennessee

Tuesday AM
March 11, 2008
Room: 391
Location: Ernest Morial Convention Center

Session Chairs: Yang Ren, Argonne National Laboratory; Donald Brown, Los Alamos National Laboratory

8:30 AM Keynote

Dynamic PDF Method: A Novel Technique to Study Local Dynamics: Takeshi Egami¹; Wojtek Dmowski¹; ¹University of Tennessee

Neutron scattering is a powerful method to study excitations in solids, such as phonons and spin waves (magnons). But when the solid is disordered, as in liquids and glasses, these excitations are scattered by the structure, and have short coherence. Thus the peaks in the dynamic structure factor, $S(Q, E)$, become broad, and it is difficult to determine their dispersion. We propose a new technique of dynamic pair-density function (DPDF), which is obtained by Fourier-transforming $S(Q, E)$ over Q . DPDF is a two-dimensional function of r (atomic distances) and E (frequency), and registers only localized or semi-localized phonons and magnons, while propagating phonons and magnons are not observed. Thus it is a complementary technique to the conventional approach. Using the Pharos spectrometer of Los Alamos NL to obtain $S(Q, E)$, we demonstrate how the DPDF method captures the saddle-point phonons in nickel, and local phonons in relaxor ferroelectric $\text{Pb}(\text{Mg}_{1/3}\text{Nb}_{2/3})\text{O}_3$ (PMN).

9:00 AM Invited

High-Energy Synchrotron X-Ray Study of Magnetic-Field-Driven Structural Transformation and Its Role in the Colossal Magneto-Electric, -Elastic and -Caloric Effects: Yang Ren¹; Yandong Wang²; Sergio Gama³; Feng Ye⁴; Peter Liaw⁵; Dennis Brown⁶; ¹Argonne National Laboratory; ²Northeastern University; ³University of Campinas-UNICAMP; ⁴Oak Ridge National Laboratory; ⁵University of Tennessee; ⁶Northern Illinois University

One of the emerging features of many materials with interesting properties, like high temperature superconductivity, relaxor ferroelectricity, colossal magneto-resistivity, magnetic shape-memory effect, and multiferroics, is a propensity to form inhomogeneous structures on a variety of length scales, due to micro- or macro-scopic phase separation. It is of fundamental importance to study those structural inhomogeneities and their real-time responses to the external stimuli. Exploiting advantages of synchrotron high-energy photons, we have been developing experimental facilities for high-energy x-ray study of structural changes of samples under multiply environments combining high/low temperature, high pressure, high magnetic field and electric field. In this talk, we will present some recent results on the high-energy synchrotron x-ray study of materials under high magnetic field. We demonstrate that the magnetic-field-driven structural transformation plays a key role in the physical and mechanical properties of the materials including correlated electron systems, inter-metallic compounds, and magnetic shape memory alloys.

9:25 AM

In-Situ Study on Pressure-Induced Microstructure Evolution of Ferromagnetic Shape-Memory Alloys: Gang Wang¹; Yandong Wang¹; Yang Ren²; Yandong Liu¹; Liang Zuo¹; ¹Northeastern University; ²Argonne National Laboratory, X-Ray Science Division

Full information on crystallographic aspects during the phase transformation is essential for understanding the 'memory' characteristics in the ferromagnetic shape-memory alloys (FSMA) related to texture and stress. In the present paper, the detailed local information of microstructure of Ni_2MnGa alloy under different pressure was observed in-situ on the high energy synchrotron beam line 11-ID-C of APS. The transformation between parent phase and martensite phase was traced by means of the instantaneously recorded 2D images of diffraction

results. The characteristics of orientation variation are analyzed to give a detailed description of the pressure-induced phase transformation process of Ni_2MnGa . According to these results, the mechanism of phase transformation of Ni_2MnGa induced by pressure is illuminated, which can enrich our knowledge for controlling the microstructure and performances of FSMA.

9:45 AM Invited

X-Ray Scattering Studies of Semiconductor Nanoclusters in Zeolites: A. M. Milinda Abeykoon¹; Miguel Castro-Colin²; M. N. Iliev¹; W. Donner¹; A. J. Jacobson¹; S. C. Moss¹; ¹University of Houston; ²University of Texas

When electrons and holes in a semiconductor are confined to ultra-small regions of space (typically 1-25 nm), the optical and electronic properties become strongly size-dependent. Such structures are called quantum dots, nanowires or nanoclusters, depending upon their shape and dimensionality. These nanostructures are of great interest for a variety of potential electronic, photochemical and nonlinear optical applications and are necessary for an analysis of the transition from molecular to bulk semiconductor properties. This talk will discuss the structure of HgSe and Se semiconductor nanoclusters encapsulated in both Nd-Y (spherical pore) and LTL (tubular pore) zeolites. The molecular structure of these systems was modeled by performing a Rietveld refinement on X-ray Bragg data. A remarkable feature in our X-ray diffraction patterns, continuous diffuse scattering under the Bragg peaks, will also be discussed along with forthcoming PDF results. We use the results of optical studies to complement our X-ray structural work.

10:10 AM

Conversion of a First-Order Bulk Phase Transition in V_2H to a Tricritical Transition in the Presence of Defects: A. Korzhenevskii¹; Rozaliya Barabash²; J. Trenkler³; K. E. Bassler⁴; G. F. Reiter⁴; S. Moss⁴; ¹Russian Academy of Science, Institute of Problems of Mechanical Engineering; ²Oak Ridge National Laboratory; ³Carl Zeiss SMT AG; ⁴University of Houston, Department of Physics and Texas Center for Superconductivity

In our pursuit of the "two-length-scale" issue measured in a single domain single crystal of V_2H , a conversion from a strong 1-st-order phase transition in the bulk to a continuous transition in a defective near-surface region ("skin layer") we have employed high- and low-energy x-ray diffraction in transmission and reflection geometry, respectively. The conversion appears to be driven by the depth-dependent change in the mosaic spread associated with the surface-enhanced dislocation walls, which act to nucleate an ordered phase, yielding a depth-dependent decay of the correlation length and effective local critical temperature TC. Related aspects of the data were also measured, such as strongly anisotropic diffuse scattering in the defective "skin layer" but isotropic scattering in the bulk, and a "crossover behavior" from mean field (tricritical) exponents (susceptibility and correlation range) closer to TC, to larger, non-universal values, further from TC. Supported in Houston by the DOE/BES—DMS.

10:30 AM Break

10:40 AM

Strain-Induced Phase Transformation in a Cobalt-Based Superalloy during Different Loading Modes: Michael Benson¹; Peter K. Liaw¹; Hahn Choo¹; Don Brown²; Mark Daymond³; Dwaine Klarstrom⁴; ¹University of Tennessee; ²Los Alamos National Laboratory; ³Queens University; ⁴Haynes International Inc

The strain-induced face-centered-cubic (FCC) \rightarrow hexagonal-close-packed (HCP) phase transformation in a cobalt-based superalloy was investigated with four in-situ loading neutron-diffraction experiments: monotonic tension, monotonic compression, high-cycle fatigue, and low-cycle fatigue. The experiments revealed relevant characteristics about the phase transformation. The transformation onsets for the four respective cases were 685 MPa, 700 MPa, 1 cycle, and 3 cycles. The accumulation rates for the tension and compression cases were 0.1 g-MPa⁻¹ and 0.05 g-MPa⁻¹, respectively, throughout the experiment. For the cyclic-loading cases, the accumulation rates were found to be inversely proportional to the number of fatigue cycles. A criterion of tensile plastic work is proposed to describe the observed results.

10:55 AM

New Strain Path to Inducing Phase Transition in PTFE Measured by Neutron Diffraction: *Eric Brown*¹; Philip Rae¹; Dana Dattelbaum¹; Donald Brown¹; Bjorn Clausen¹; ¹Los Alamos National Laboratory

A novel application of in situ neutron diffraction under applied uniaxial strain is presented; measuring the crystalline domain evolution in a semi-crystalline polymer under bulk deformation. PTFE is shown to respond to uniaxial deformation by undergoing a crystalline phase transition previously believed to occur only at very high hydrostatic pressure. Discovery of this phase transition under applied uniaxial-strain fundamentally changes our understanding of the deformation mechanisms in semi-crystalline polymers and how they need to be modeled. Under compression parallel to the basal plane normal (i.e., parallel to the molecular axis) the modulus is $\sim 1000\times$ bulk dominated by intra-polymer chain compression, providing experimental validation of theoretical predictions. Deformation parallel to the pyramidal plane normal exhibit both axial and transverse strains of the opposite sign as the applied load, suggesting the crystalline lattice is accommodating deformation by shearing along the prismatic planes.

11:15 AM

Analysis of Chemical Segregation in Nickel Based Super Alloys Using Neutron Diffraction: *Jaimie Tiley*¹; ¹US Air Force

Neutron Diffraction techniques were used to determine chemical segregation and crystal parameters in several nickel super alloys. The results validate crystal models used for determining occupancy sites and amounts within both gamma and ordered gamma prime systems with as many as 8 elements. Combining the techniques with advanced three dimensional analysis tools including atom probe tomography and transmission electron microscopy provides powerful tools for characterizing microstructures and atomic behavior. In addition, neutron diffraction techniques were used to determine volume fractions, thermal expansion terms and chemical segregation/phase changes for ordered gamma prime as a function of temperature.

11:35 AM

Texture Evolution in the Ni-Mn-Ga Ferromagnetic Shape-Memory Alloys Studied by Neutron Diffraction Technique: *Z.H. Nie*¹; Y.D. Wang¹; G.Y. Wang²; J.W. Richardson³; G. Wang¹; Y.D. Liu¹; P.K. Liaw²; L. Zuo¹; ¹Northeastern University, Key Laboratory for Anisotropy and Texture of Materials (MOE); ²University of Tennessee, Department of Materials Science and Engineering; ³Argonne National Laboratory, Intense Pulsed Neutron Source

The initial and transformation textures in the as-cast Ni-Mn-Ga ferromagnetic shape-memory alloys were studied by the time-of-flight (TOF) neutron diffraction technique. The neutron diffraction experiments were performed on General Purpose Powder Diffractometer (Argonne National Laboratory). Inverse pole figures were extracted from the neutron data for determining the orientation distributions of polycrystalline Ni-Mn-Ga rods before and after the uniaxial compression deformation. Texture analysis reveals that the initial texture in the as-cast Heusler state composed of $\{110\}<001>$ and $\{110\}<011>$, which was weakened after the deformation. Moreover, a strong preferred selection of martensitic variants ($\{110\}<001>$ and $\{100\}<001>$) was observed in the transformed martensite after a compression stress was imposed along the axial direction on the Heusler phase. The preferred selection of martensitic variants can be well explained by considering the grain/variant-orientation-dependent Bain distortion energy under the stress field applied during the phase transition.

11:50 AM

Texture Development in Transformation-Induced Plasticity (TRIP) Steels Studied by Neutron and X-Ray Diffraction: *Sheng Cheng*¹; X.-L. Wang²; Z. L. Feng²; Y. D. Wang¹; S. Vogel³; J. J. Wall¹; H. Choo¹; P. K. Liaw¹; X. Sun⁴; ¹University of Tennessee; ²Oak Ridge National Laboratory; ³Los Alamos National Laboratory; ⁴Pacific Northwest National Laboratory

Complete texture studies by in situ neutron diffraction in two commercial C-Mn-Si TRIP steels with different amount of retained austenite were conducted at High-Pressure Preferred Orientation Neutron Diffractometer (HIPPO) of Los Alamos Neutron Science Center (LANSCE). The texture evolution as a function of plastic strain will be analyzed and compared with other typical steels. The effect of retained-austenite fraction on texture evolution will be discussed. The texture of these commercial TRIP steels will also be compared to that of stainless

TRIP steels, and their implications will be discussed. This work was supported by the National Science Foundation Major Research Instrumentation (MRI) Program (DMR-0421219) and International Materials Institutes (IMI) Program (DMR-0231320), respectively. Research sponsored by the U.S. Department of Energy, Assistant Secretary for Energy Efficiency and Renewable Energy, Office of Freedom CAR and Vehicle Technologies, as part of the Automotive Light weighting Materials Program, under Contract DE-AC05-00OR22725 with UT-Battelle, LLC.

12:10 PM

In Situ Neutron Diffraction Study of B₂ Ordered FeCo under Compressive Loading: *Saurabh Kabra*¹; Donald Brown¹; Easo George²; ¹Los Alamos National Laboratory; ²Oak Ridge National Laboratory

FeCo magnetic alloys are limited in their applicability because of brittleness under tensile stress. The brittleness of B₂ ordered alloys in general and ordered FeCo in particular is an unexpected phenomenon given the high symmetry of the B₂ crystal structure and the abundance of $\langle 111 \rangle$ type directions and $\{110\}$ type planes for $\frac{1}{2} \langle 111 \rangle \{110\}$ slip. In order to study the deformation mechanism in these alloys, *in situ* neutron diffraction experiments were performed at the SMARTS diffractometer at Los Alamos Neutron Science Center. The diffraction pattern showed many anomalous changes during loading. Along with unusual changes in peak positions, the most notable changes occurred in the intensities of FeCo peaks. As a general trend, the fundamental peaks increased in intensity while the superlattice peaks decreased. These intensity changes along with supporting experiments (texture on HIPPO diffractometer and metallography) show that APB induced disorder is introduced as the sample is loaded.

Particle Beam-Induced Radiation Effects in Materials: RIS and Multilayers

Sponsored by: The Minerals, Metals and Materials Society, American Nuclear Society, TMS Structural Materials Division, TMS/ASM: Nuclear Materials Committee
Program Organizers: Gary Was, University of Michigan; Stuart Maloy, Los Alamos National Laboratory; Christina Trautmann, Gesellschaft für Schwerionenforschung; Maximo Victoria, Lawrence Livermore National Laboratory

Tuesday AM

Room: 389

March 11, 2008

Location: Ernest Morial Convention Center

Session Chairs: Todd Allen, University of Wisconsin-Madison; Gary Was, University of Michigan

8:30 AM

Tomographic Atom Probe Analyses of Grain Boundaries in Ion Irradiated Nanostructured Austenitic Stainless Steels: *Auriane Etienne*¹; Bertrand Radigue¹; Philippe Pareige¹; ¹Rouen University

The irradiation-assisted stress corrosion cracking of austenitic stainless steel is linked to radiation induced segregation at grain boundaries. Thus an atomic scale observation of these segregation is of primary importance to the understanding of the mechanism of segregation under irradiation and to give experimental data to be compared to computer simulation. In this work, austenitic steels have been nanostructured (grain size of few nanometres) and ion irradiated at 350°C. The segregation and depletion of solute at grain boundaries were characterized at the atomic scale with the Tomographic Atom Probe and are compared to simulation and experimental (with other technique) results. This work focused on grain boundary studies and the joint paper (same session) dedicated to dislocation loops and associated solute segregation give an atomic scale description of irradiation induced segregation in austenitic steels.

9:10 AM

Radiation Induced Segregation in 304 and 316 Austenitic Stainless Steels: Study by Tomographic Atom Probe, Transmission Electron Microscopy and Rate Theory Modelling: *Auriane Etienne*¹; Philippe Pareige¹; Bertrand Radigue¹; ¹Rouen University

The internal structures of pressure water reactor made of Austenitic Stainless steels and are submitted to a high neutron flux. This irradiation induces a degradation of mechanical properties of these materials due to a change

of the microstructure under irradiation. A study the evolution of the point defect population and the intragranular induced segregation of solute species under irradiation has been performed. Tomographic Atom Probe (TAP) and Transmission Electron Microscope (TEM) were performed on 304 and 316 steels samples that have been irradiated with 160 keV Fe⁺ ions at different doses at 350°C. At the same time a rate theory model has been used to predict the evolution of the point defect population under irradiation. A correlation between point defects clusters and solute clusters will be discussed.

9:30 AM

Ab Initio-Based Radiation-Induced Segregation Modeling in Fe-Ni-Cr Alloys: Julie Tucker¹; Todd Allen¹; Dane Morgan¹; ¹University of Wisconsin

High concentrations of point defects, such as those created in radiation environments, can cause severe material degradation as they migrate and cluster. Radiation induced segregation (RIS), the process by which the local composition of an alloy is altered near point defect sinks, is a phenomenon that has concerned the nuclear industry for decades. While substantial progress has been made in the area of RIS prediction by empirical fitting, many questions remain about the diffusion mechanisms of point defects and how they are affected by local environment changes in multi-component alloys. This research uses *ab initio* methods to determine diffusion coefficients associated with both vacancy and interstitial migration in Ni rich fcc Fe-Ni-Cr alloys. We find that the alloy kinetics differs significantly from that predicted by simple extrapolation of empirical fits to high-temperature data. The calculated diffusion coefficients are used to parameterize a rate theory type RIS model.

9:50 AM

Understanding Oversized Solute Effects on Radiation-Induced Segregation in Austenitic Alloys: Micah Hackett¹; Jeremy Busby²; Gary Was¹; ¹University of Michigan; ²Oak Ridge National Laboratory

The addition of oversized solutes to austenitic stainless steels reduces radiation-induced segregation (RIS) of chromium. Zr or Hf was added to 316-type stainless steels and then irradiated with 3.2 MeV protons at temperatures of 400 and 500°C to several different doses. Measurements of the grain boundary RIS show Zr to be more effective than Hf at reducing RIS. The relative effectiveness of Zr vs. Hf is associated with a difference in vacancy binding energy as determined by *ab initio* calculations. Rate theory modeling demonstrates that the difference in RIS results is accounted for by the change in vacancy binding energy. The oversized solute effect disappears at higher doses due to a loss of solute for the trapping and recombination of point defects, which are responsible for the reduction in RIS.

10:10 AM Break

10:30 AM

Incoherent Interface Structure and the Fast Recombination of Irradiation-Induced Frenkel Pairs in Cu/Nb Multilayer Composites: Michael Demkowicz¹; R. Hoagland¹; A. Misra¹; ¹Los Alamos National Laboratory

In contrast to vacancies or interstitials in single crystals of Cu or Nb, point defects that have been absorbed at a Cu/Nb interface do not remain compact and well-localized. Instead, they spread out within the interface by transforming the interface structure in the neighborhood of the site at which they were absorbed. Since the effective size of such interfacial defects is notably larger than that of the corresponding defects in single crystal Cu or Nb, the critical distance for Frenkel pair recombination is significantly increased at Cu/Nb interfaces. Random walk simulations are used to demonstrate that this phenomenon predicts a reduction of radiation damage accumulation in Cu/Nb multilayer composites, in agreement with experimental findings. This work was supported by the Los Alamos National Laboratory Directed Research and Development Program (LDRD) and the Los Alamos National Laboratory Director's Fellowship Program.

10:50 AM

Evolution of Microstructure and Mechanical Properties of Cu/V Nanolayers Subjected to Helium Ion Irradiation: Engang Fu¹; Jesse Carter¹; Michael Martin¹; Lin Shao¹; Haiyan Wang¹; Stuart Malay²; Ning Li²; Xinghang Zhang¹; ¹Texas A&M University; ²Los Alamos National Laboratory

Sputter-deposited Cu/V nanolayer films with individual layer thickness varying from 1 to 100 nm have been subjected to 50 keV helium ion irradiation at room temperature with a dose of 6x10¹⁶ He ions/cm². The evolution of microstructure

and mechanical properties after ion irradiation has been investigated. Significant hardness enhancement has been observed in Cu/V with individual layer thickness of 10 nm or greater, whereas hardnesses barely change in radiated Cu/V with smaller layer thickness. Helium bubbles, 1-2 nm in diameter, induced by ion irradiation, were observed both within the layers and along layer interfaces. Dependence of radiation hardening on layer thickness will be discussed based on the evolution of microstructures (He bubbles), and interaction of radiation induced defects with layer interfaces.

11:10 AM

Nanostructure Fe/W Multilayers Subjected to Helium Ion Irradiation: Nan Li¹; Engang Fu¹; Haiyan Wang¹; Amit Misra²; Richard G. Hoagland²; Jesse J. Carter¹; Michael Martin¹; Lin Shao¹; Xinghang Zhang¹; ¹Texas A&M University; ²Los Alamos National Laboratory

We report on the evolution of microstructure and mechanical properties of Fe/W multilayers, with incoherent bcc/bcc interface, subjected to helium ion irradiation. Fe/W multilayer films with individual layer thickness, ranging from 1 nm to 200 nm, were deposited by magnetron sputtering technique, followed by helium ion-irradiations. Peak helium concentration approaches a few atomic percent with 5-7 displacement-per-atom in Fe or W. He bubbles, 1-2 nm in diameters, were observed with helium bubbles aligned along layer interfaces. Film hardness varies after ion implantation and the magnitude of hardness variation depends on the layer thickness of multilayer films. He bubbles and the interfaces may play an important role in hardness enhancement.

Phase Stability, Phase Transformations, and Reactive Phase Formation in Electronic Materials VII: Session I

Sponsored by: The Minerals, Metals and Materials Society, TMS Electronic, Magnetic, and Photonic Materials Division, TMS: Alloy Phases Committee

Program Organizers: Sinn-wen Chen, National Tsing Hua University; Srinivas Chada, Medtronic; Chih-Ming Chen, National Chung-Hsing University; Hans Flandorfer, University of Vienna; A. Lindsay Greer, University of Cambridge; Jae-Ho Lee, Hong Ik University; Kejun Zeng, Texas Instruments Inc; Katsuaki Suganuma, Osaka University

Tuesday AM
March 11, 2008

Room: 278
Location: Ernest Morial Convention Center

Session Chairs: Katsuaki Suganuma, Osaka University; Sinn-wen Chen, National Tsing Hua University

8:30 AM Invited

The Growth of Semiconductor Nanowires for Research or Industrial Purposes: Djamilia Hourlier¹; Patricia Lefebvre-Legry¹; Pierre Perrot¹; ¹National Center of Scientific Research

Silicon or germanium-based nanowires are the leading candidates for the building-blocks in next generation nanoelectronic devices. The growth of these nanowires is commonly described either by the Vapor-Liquid-Solid (VLS) or Solid-Liquid-Solid (SLS) processes. In this study a new approach to the problem of nanowire formation which does not violate thermodynamic principles is presented. We will show that many aspects of the growth mechanisms, such as the surface curvature of the solid phase (nano or microscopic range), in equilibrium with the liquid phase are of extreme interest. With the variety of cases encountered in this study, we are now in a position to treat any size liquid alloy (Au-Si or Au-Ge) in equilibrium with any solid (nano or macroscopic size). By using a method to date neglected, and by choosing the SLS process rather than the VLS process, we succeeded in answering the thorny question of the size limit of nanowires.

8:50 AM

Effect of Interface Structures on Melting and Solidification Behavior of Bismuth Nano-Particles Embedded in an Icosahedral Phase Matrix: Alok Singh¹; AnPang Tsai²; ¹National Institute for Materials Science; ²Tohoku University

Effect of interfaces on stability of nano-particles has been brought out by creating novel interfaces of bismuth nano-particles in an Al-Cu-Fe matrix. By heat treatment, three states of matrix phase were obtained, altering the nature

of interfaces. Interface structures were studied by TEM and melting and solidification behavior was studied by differential scanning calorimetry (DSC). Earlier studies on bismuth nano-particles embedded in crystalline matrices such as aluminum and zinc have reported a lowering of melting temperature of bismuth. We show that, when embedded in the icosahedral phase, a superheating is possible. This is because, as we show, bismuth has a better lattice match with icosahedral phase than with any crystalline phase, and therefore makes matching interfaces.

9:05 AM

Controlled Growth of Atomic-Scale Si Layer with Huge Strain in the Nano-Heterostructure NiSi/Si/NiSi through Point Contact Reaction between Nano-Wires of Si and Ni: *Kuo-Chang Lu¹; Wen-Wei Wu²; Han-Wei Wu²; Carey Tanner¹; Jane Chang¹; Lih Chen²; K. N. Tu¹*; ¹University of California, Los Angeles; ²National Tsing Hua University

The point contact reaction between a Si nanowire and a Ni nanowire is reported where the Si nanowire is transformed into a bamboo-type grain of single crystal NiSi from both ends. The reaction was investigated in-situ in an ultra-high vacuum transmission electron microscope. It is proposed that the epitaxial growth of the NiSi is limited by the dissolution rate of Ni into Si at the point contact interface and assisted by interstitial diffusion of Ni atoms within the Si nanowire. Based on the point contact reaction, single crystal NiSi/Si/NiSi heterostructures have been fabricated, in which more than 12% of strain was found in the middle Si layer, the dimension of which can be controlled down to 2 nm, overcoming the limit of conventional patterning process. This study is expected to support the realization of nanoscale electronic devices.

9:20 AM

Formation of the $\langle -1010 \rangle / \{ -12-10 \}$ Side Bands-Modulated Structures Due to a Periodic Modulation in the Composition of Mn in Ilmenite-Mn₂O₃ Alloys: *Mohammad Shamsuzzoha¹; Chandan Srivastava¹; Pranoti Kale¹; Padmini Periaswamy¹; Raghavendra Pandey¹*; ¹University of Alabama

Conventional and analytical transmission electron microscopy techniques have been applied to study the microstructure, phase transition and chemical composition of the ilmenite-Mn alloys containing 0-40wt % of Mn and prepared by standard ceramic processing. Bright field electron microscopy revealed that the alloy nominally containing 35-wt% of Mn (an electronic material) exhibits a side bands-modulated structure. Electron diffraction patterns of the modulated structure revealed that the side bands in the sample have the $\langle -1010 \rangle / \{ -12-10 \}$ growth habit, and are formed due to the variation in contrast resulted by a periodic but unidimensional variation of interplanar spacings. TEM/EDS line profiles across and normal to these side bands showed a sinusoidal variation in the composition of Mn. The modulated structure is suggested to be caused by a decomposition in the supersaturation of the solid solution of Mn in the lattices of hexagonal ilmenite structure.

9:35 AM

Improvement of against Oxidation and Electrical Properties of Cu-Hf Thin Film: *Jau-Shiung Fang¹; Y. Chen¹*; ¹National Formosa University

A Cu thin film with high conductivity can be used in advanced electronic devices and thin-film transistors. However, its poor oxidation resistance must be solved. This study investigates the feasibility of using a self-forming passive layer to prevent copper oxidation in Cu_{1-x}Hf_x (x = 0.6-7.9 at.%) thin films. The resistivity of the studied film declined slowly as the film was annealed at an elevated temperature because of the formation of HfO₂ passive layer on the Cu film. A high Hf-content copper film exhibited a superior passive property, but it showed high resistivity because of its high Hf content. A 0.6 at.% Hf-doped Cu film had the lowest resistivity of 2.17 μΩcm when the film was annealed at 600°C, which exhibited a superior passive property in oxygen ambient. The electrical and passivation properties of Hf-doped Cu film demonstrated that the film can be adopted for future interconnection and thin-film transistors.

9:50 AM

Cu with Insoluble MoN for Advanced Barrier-Free Metallization: *Jinn P Chu¹; Chon-Hsin Lin²; V.S. John¹*; ¹National Taiwan University of Science and Technology; ²Chin-Min Institute of Technology

As a diffusion barrier is required for copper metallization in microelectronics, searching a new and reliable barrier material with thickness less than 5 nm becomes very challenging when the device feature size continues to shrink beyond 45 nm.

Thus, advanced barrier-free Cu metallization is proposed. In this study, a copper seed layer was generated by doping an insoluble MoN, which can improve the thermostability of copper and further inhibit the crystal growth. In addition, this seed has a barrier property that restrains the inter-diffusion between Cu and Si. The seed layer has been characterized using X-ray diffraction, focused ion beam, secondary ion mass spectroscopy, transmission electron microscope, film resistivity and current-voltage (I-V) measurements. The results indicate notable thermal stability enhancements up to 730°C without any apparent interactions with Si. The detail of the results will be further discussed.

10:05 AM Break

10:15 AM Invited

Phase Transitions in the BiVO₄-nPbO System: Structural-Electrical Properties Relationships: *Jean Pierre Wignacourt¹; Michel Drache¹; Pascal Roussel¹; Olfa Labidi¹*; ¹University of Sciences and Technologies of Lille

In a general survey of nPbO-BiVO₄ compounds, interesting phases corresponding to n=2 (Pb₂BiVO₆) are showing several successive structural transitions $\alpha \rightarrow \beta \rightarrow \delta$. Structures of α and δ forms have been previously described from powder diffraction data (X-rays, neutrons). In this work, we have refined these structures from single crystal data, and the resolution of the intermediate β form, so far unsolved, was possible through a stabilisation thermal cycle; its complete structural understanding required a 4D formalism. Two new polymorphic phases, α' and δ' were obtained by substituting Mn or P for V; their structures are closely related to respectively the α phase at room temperature, and the δ phase at 680°C. Electrical conductivities of all structurally characterized compositions were investigated, and correlations were drawn between their conduction properties and structural characteristics. Conductivity properties measured under variable O₂ partial pressures for Pb₂Bi(V_{0.75}P_{0.25})O₆ were interpreted as mixed ionic-electronic (p type) conduction mechanism.

10:35 AM Invited

Degradation of Ag-Epoxy Conductive Adhesive/Sn Interface in Humid Atmosphere: *Sun Sik Kim¹; Keun Soo Kim¹; Katsuaki Suganuma¹*; ¹Osaka University

Isotropic conductive adhesives, such as Ag-epoxy pastes, have been continuously studied as ecological alternatives to lead-bearing solders. Ag-epoxy conductive adhesive is known to possess excellent heat-resistance against severe thermal exposure during the reflow process. However, regarding joint reliability, Ag-epoxy conductive adhesive has significant drawbacks under the high temperature and humidity exposure. This exposure causes interfacial degradation of the joints, resulting in higher electrical resistance and reduction of joint strength. There have been several arguments on the degradation mechanism, but no definitive explanation has been achieved yet. The present study focuses on microstructural characterization of the interface between the Sn plating and Ag-epoxy conductive adhesive under 85/85%RH condition. The degradation mechanism is considered through microstructural variation of the interface with exposure time. As a result of HREM and AEM, a nano-scaled tin oxide layer, one of the phases detrimental to joint reliability, was found to be partially formed at the interface.

10:55 AM

Active Evaluation of Solder Joint Microstructures by Noise Spectrum Analysis: *Iver Anderson¹; David Rehbein¹; Joel Harringa¹*; ¹Iowa State University

High power audio equipment with optimum sound quality depends on uncompromised performance from all components and from the solder joints used in their assembly. Analysis of the noise spectrum generated by a single frequency continuous wave signal is being developed for detecting alloy differences in as-solidified solder joints and for "real time" tracking of microstructural evolution, e.g., during thermal aging. Each experiment utilized a standard (AFPB) Cu shear test specimen that was joined with a SAC or SAC + X solder, with testing of as-soldered or thermally aged (150C, up to 1000h) joints. Shifting of characteristic noise peaks was detected from different solder alloys and after each thermal aging treatment, along with stable peaks due to the sample apparatus and specimen geometry. Initial results will be verified and identification of microstructural differences causing peak shifts will be attempted. Supported by Nihon-Superior, Inc., through Ames Lab contract no. DE-AC02-07CH11358.

11:10 AM

A Reliability Test Study of the VFBGA Sn-Ag-Cu Solder Joints: *Huann-Wu Chiang*¹; Ting-Yu Liu¹; Yi-Shao Lai²; ¹I-Shou University; ²Advanced Semiconductor Engineering, Inc.

The interfacial reactions of the lead-free Sn-3.0Ag-0.5Cu and Sn-37Pb solder joints bonded on electroplated Ni/Au/Cu pads under multi-reflowed and high temperature storage tests were investigated in this study. Metallurgical evolutions of the intermetallic compounds (IMCs) were scrutinized by scanning electron microscopy/energy dispersive x-ray spectroscopy (SEM/EDS) and electron probe microanalysis (EPMA) mapping. Ball shear and ball impact tests (BIT) were performed to examine strengths of these solder joints as functions of multi-reflow and thermal aging times. The relationship between the interfacial microstructure and the joint strength as well as the failure mode of the fractured joints were then analyzed and discussed.

11:25 AM

Reliability of Rigid PCB/Flexible PCB Joint Bonded Using Ultrasonic Vibration: *Jong Bum Lee*¹; Ja Koo¹; Seung Jung¹; ¹Sungkyunkwan University

Rigid printed circuit board (RPCB) has been broadly used because of its advantages such as low-cost, high reliability and excellent processability. The demand for flexible printed circuit board (FPCB), which has light, high glass transition temperature (Tg) and flexibility, continues to expand with market growth of portable electronics. Electrodes between the RPCB and FPCB have been electrically and mechanically connected by anisotropic conductive adhesive (ACA) and non-conductive adhesive (NCA). However, these bonding methods have disadvantages such as high contact resistance and low reliability. The interest in ultrasonic bonding method is growing to connect the electrodes, because of its higher electrical property, higher reliability, shorter processing time and lower processing temperature than adhesive bonding methods. Therefore, the long-term reliability of RPCB-to-FPCB joint bonded using ultrasonic vibration was investigated with different surface finish. The microstructural observation, contact resistance evaluation and peel test were conducted to investigate the failure behavior of the joints.

11:40 AM

Reliability of 3-D Chip Stacked Package with Through-Chip Interconnects: *Jong-Woong Kim*¹; Young-Chul Lee¹; Seung-Boo Jung¹; ¹Sungkyunkwan University

The 3-dimensional (3-D) chip stacking technology is a leading technology to realize a high density and high performance system in package (SiP). There are several kinds of methods for chip stacking such as die attachment with wire bonding, solder through wafer interconnect technology and via formation and filling technology employing flip chip bonding, etc. Among them the interconnection through Cu filled through-via and die stacking with flip chip technology are considered to be one of the most advanced 3-D packaging technology. Therefore, we have tried to optimize the process of through-via formation and Cu electroplating process for Si die stacking. A Pb-free solder was additionally deposited on the electroless-Ni immersion-Au (ENIG) under bump metallization (UBM) to be used for bonding with another carrier. Finally, the Si die was flip chip bonded with another die, and thermal shock testing was conducted to evaluate the reliability of the final stacked package.

Recycling: Electronics Recycling

Sponsored by: The Minerals, Metals and Materials Society, TMS Extraction and Processing Division, TMS Light Metals Division, TMS: Recycling and Environmental Technologies Committee

Program Organizers: Christina Meskers, Delft University of Technology; Greg Krumdick, Argonne National Laboratory

Tuesday AM
March 11, 2008

Room: 280
Location: Ernest Morial Convention Center

Session Chair: Greg Krumdick, Argonne National Laboratory

8:30 AM Introductory Comments

8:35 AM

Recycling of Electronic Wastes: Degradation and Combustion: *Xiangjun Zuo*¹; *Lifeng Zhang*¹; ¹Norwegian University of Science and Technology

Firstly, recycling methods of Printed Circuit Boards (PCBs) were summarized. PCBs mainly contains 72% organic substance and 28% metals in mass. Then PCB materials from a waste printer named were combusted and pyrolysed in TG/DTA and MS machines with the aim of separating and recovering the organic and metallic materials. The current PCB waste materials were combusted at 700°C, 800°C, 900°C under 50ml/min, 100ml/min, 150ml/min with synthetic air atmosphere respectively. The sample was also heated at 800°C under 50ml/min, 100ml/min, 150ml/min under argon gas atmosphere. The mass loss, conversion fraction with the temperature, activation energy etc. are investigated. The main compositions of organic substance are found to be the ethoxylene resin bromide or ethoxylene resin chloridate, and the metals in PCB are mainly copper, solder, iron(ferrite), nickel, silver, gold, and palladium, etc.

8:55 AM

Degradation of Plastics to Liberate Metals from Electronic Waste: *Anne Kvithyl*¹; Scott Shuey²; Sean Gaal³; Patrick Taylor⁴; ¹Norwegian University of Science and Technology; ²Phelps Dodge Corporation; ³SINTEF Materials and Chemistry; ⁴Colorado School of Mines

Printed circuit boards contain considerable metal values. In this study the decomposition of common plastics used in printed circuit boards were studied. Teflon (PTFE), polyvinyl chloride (PVC) and polyethylene (PE) were heated in both CO₂ and argon atmospheres using a thermo-gravimetric furnace (TGA) coupled to a mass spectrometer. Soda ash Na₂CO₃ and baking soda NaHCO₃ were used as reactants. The degradation temperatures and evolved gases are presented from single plastics and mixtures. Mixed plastics are shown to be an overlap of the individual plastics. The mass loss temperature is the same in CO₂ and argon. However, less residue is formed when heated in CO₂. The possibilities and difficulties of detecting dioxin and furan formation are also presented.

9:15 AM

Decomposition Process for Polychlorobiphenyl Containing 1 to 5 Chlorine by Using Basic Molten Salts as Reaction Field: *Osamu Takeda*¹; Takeshi Handa¹; Masayoshi Kimura¹; Yasufumi Yokka¹; Yuzuru Sato¹; ¹Tohoku University

In order to establish a safe, highly efficient, and simple decomposition process for poly chlorinated biphenyls (PCBs), a decomposition process for PCBs by using basic molten salts as a reaction field was investigated. PCBs containing 1 to 5 chlorine (e.g. 2,2',4,4'-tetrachlorobiphenyl), dissolved in n-nonane solution, was supplied into basic molten salts (NaOH-Na₂CO₃ or KOH-K₂CO₃) maintained at 500-700°C together with the carrier gas (N₂-21 vol% O₂) through an injection tube. The injected PCBs in a bubble were decomposed by the reaction with the molten salts and oxygen during rise in the molten salts. The decomposition efficiency of PCBs increased with increasing temperature and was achieved to be higher than 99.999% in a certain condition. From a series of systematic study, the effectiveness of the decomposition process for PCBs by using molten salts was demonstrated.

9:35 AM

Establishment of Complete Treatment System of Recyclable Materials Generating from Home Appliance Recycling Plants at Mitsubishi Materials Corporation: Tetsuro Sakai¹; Syogo Yamaguchi¹; ¹Mitsubishi Materials Corporation

Home appliance recycling law was put into force in April 2004 in Japan. Specified kinds of home appliances, such as air conditioners, television sets, refrigerators and washing machines, should be recycled according to the law. Mitsubishi Materials Corporation (MMC) in cooperation with home appliance manufacturers is operating five home appliance recycling plants in Japan. MMC established complete treatment system of recyclable materials generating from home appliance recycling plants, which is formed by unique collaboration among home appliance recycling plants, copper smelter and refinery, and cement plants. Recyclable materials containing copper and precious metals are only handled and treated within the MMC group. By using this lock-in system, safe treatment and traceability of materials are guaranteed as 100% materials recycle.

9:55 AM

Recovery of Copper from Printed Circuit Boards (PCBs) Scraps by Mechanical Pre-Treatment and Hydrometallurgical Routes: Manis Jha¹; Jinki Jeong¹; Jae-chun Lee¹; Min-Suck Kim¹; Byung-Su Kim¹; ¹Korea Institute of Geoscience and Mineral Resources

In respect to conventional pyro-metallurgical process to recycle waste PCBs in copper smelter, a feasible hydrometallurgical copper recycling process following pre-treatment, acid-leaching and solvent-extraction has been proposed. The 99.2% of copper was liberated from the PCBs by pre-treatment consisted of shredding, iron separation by hand magnet, stamp milling, air-classification of metallic / resin particles and the separation of fine metallic particles by corona electrostatic separator. The copper was leached from the beneficiated particles of PCBs with 6M H₂SO₄ at 90°C in 1 hr. The leach liquor was then processed to recover copper using 20% LIX 84I diluted in kerosene. Almost total copper was extracted to organic phase at O/A ratio 1, pH 1.75 and mixing time 5 minutes leaving nickel in the raffinate. The loaded copper from the organic phase could be completely stripped with strong sulphuric acid to recover copper as metal or salt by electrolysis or crystallization, respectively.

10:15 AM Break

10:25 AM

Recycling of Copper and Precious Metals Containing Waste: Helmut Antrekowitsch¹; Thomas Messner¹; Stefan Konetschnik¹; Bernd Prillhofer¹; ¹University of Leoben

Nowadays, the secondary copper metallurgy is the commonly used process for the recycling of copper and precious metals containing waste especially electronic scrap. Due to the high amount of impurities and plastic the process optimisation becomes more important. The decrease of slag and dust and the increase of the metallic yield depend on the physical and chemical properties of the input material. An agglomeration and a reduction of the plastic by using a pre-treatment step lead to a process optimisation of the secondary metallurgy of copper. Besides the experimental work thermodynamic calculations of the element distribution is necessary. The paper discusses the different possibilities and the results of the pre-treatment of the input material to optimise the process material flow. Furthermore, the thermodynamic calculations support these investigations.

10:45 AM

Dissolution Rates of Precious Metal Compounds in Acid: Hideaki Sasaki¹; Masao Miyake²; Hisao Kimura¹; Masafumi Maeda¹; ¹University of Tokyo, Institute of Industrial Science; ²University of Illinois at Urbana-Champaign

A precious metal recovery process utilizing active metal vapor was proposed previously. In the process, scraps are treated with the vapor prior to acid leaching in order to make contained precious metals to form compounds that dissolve easily. In this study, dissolution rates of precious metal compounds were measured electrochemically using channel flow double electrode method aiming to inquire what compounds should be formed by the vapor pretreatment. It was revealed that the apparent dissolution rate of Pt was about 100 times higher from Pt-75%Zn than from pure Pt. The dissolution rate of Au-Zn was studied and compared to that of Pt-Zn. Dissolved surfaces of Pt-Zn and Au-Zn compounds were examined by SEM and XRD to consider their dissolution behaviors.

11:05 AM

Treatment of Gold-Containing Technogenous Wastes Tailings by Electrochemical Method, in Condition of "Slight" Oxidation Regime: Tsisana Gagnidze¹; Teimuraz Royva¹; Tamaz Lejava¹; Manana Mamforia¹; ¹R. Agladze Institute of Inorganic Chemistry and Electro Chemistry

A processing of technogenous wastes, which involve a gold-containing sulphide minerals, is a potential source to supplement the gold reserves. Hence, searching of ecologically safe and economically reasonable methods for processing of gold-containing technogenous wastes is a topical problem. To increase a parameters of gold extraction and to simplify a technology of the processing of above-mentioned wastes of sulphide minerals, an investigations have been carried out in the direction of the use of the method of electrochemical leaching without any preliminary processing of the mineral. It was established experimentally that an introduction of nitrogen-containing organic additive into chloride solution favours to reduce a Red/Ox potential of the solution from 0.8/1.2 V to 0.350/5V, which permits to conduct the process of direct electrochemical leaching at "soft" oxidation regimes at temperatures 20-30°C without an environmental contamination by molecular chlorine and with a high degree of a gold extraction up to 80-90%.

11:25 AM

Adsorption of Copper from the Effluents of Electronic Industry Using the Cation Exchange Resin Amberlite IR-120 (Na): Nguyen Van Nghiem¹; Jae-chun Lee¹; Manis Jha¹; Jae-Min Yoo¹; Kyoungkeun Yoo¹; Taek Sung Hwang²; ¹Korea Institute of Geoscience and Mineral Resources; ²Chungnam National University

Copper is widely used as interconnecting material in the electronic industry, inevitably resulting in the generation of large amount of copper bearing waste streams during different processing steps viz. electroplating, etching, rinsing, and chemical and mechanical polishing (CMP) etc. Ion exchange (IX) studies with the solutions containing 300 to 700 ppm copper have been carried out using the cationic exchanger Amberlite IR-120 (Na). Various process parameters viz. contact time, solution pH, resin dose, and acid concentration of eluant were investigated for recovering copper from the effluents. Complete adsorption of copper was achieved at equilibrium pH 2.5 and aqueous/resin (A/R) ratio 100 mL/g in 14 minutes contact time. The mechanism of adsorption of copper was found to follow the Langmuir isotherm and second order reaction rate. The copper was eluted effectively from loaded resin with dilute sulphuric acid to produce copper-enriched solution.

Sloan Industry Centers Forum: Techno-Management Issues Related to Materials-Centric Industries: Session II

Sponsored by: The Minerals, Metals and Materials Society

Program Organizers: Subodh Das, Secat Inc; Diran Apelian, Worcester Polytechnic Institute

Tuesday AM
March 11, 2008

Room: 397
Location: Ernest Morial Convention Center

Session Chair: Subodh Das, Secat Inc

8:30 AM Introductory Comments by Diran Apelian and Subodh Das

8:40 AM Invited

Technology Management in the Global Steel Industry: Strategy and Organization Models: Ravi Madhavan¹; ¹University of Pittsburgh

As the globalization of the steel industry gathers pace, steel producers are faced with unprecedented strategic and organizational challenges and opportunities, with an emphasis on the creation of multinational structures and processes reflective of the global basis of competition. In particular, developing a technology strategy that is consistent with the global distribution of resources and markets is an important concern for the newly multinational steel company. This presentation will provide an overview of some of the current challenges

and opportunities in technology management, as well as suggest appropriate strategic and organizational models for thinking about them.

9:00 AM Invited

Winds of Change and Management Challenges in the Global Steel Industry: Sanak Mishra¹; ¹Mittal Steel India Ltd

The Apparent Steel Use (ASU) in the World is projected at 1.251 billion metric tons in the year 2008, at a healthy growth rate of 6.1%. This is back to back with an estimated growth of 5.9% in 2007 and 8.5% in 2006. In fact the steel industry has had a boom time for about five years now. What is more significant, there have been dramatic changes in the characteristics of the industry, following the emergence of China as largest steel producer as well as consumer, the impact of consolidation processes piloted by large mergers and acquisitions and the attention received by the so-called BRIC countries (Brazil, Russia, India, China), as happening places. Consequent upon these changes, management challenges in the industry are more demanding than ever before and these will be explored in this presentation.

9:20 AM Break

9:30 AM Invited

Powder Metallurgy: The Challenges of a Rapidly Changing Global Industry: Chickery Kasouf¹; ¹Worcester Polytechnic Institute

Powder metallurgy (P/M) produces components for many OEM and higher tier suppliers. As manufacturing growth shifts away from the United States into other economies, especially Asia, North American companies are faced with significant challenges. For example, GKN, the world's largest producer of P/M parts, recently closed four US plants as part of a consolidation in response to the contraction of the US automotive industry. On the other hand, there is tremendous growth in China resulting in many start-ups. Moreover, despite the inhospitable U.S. market, and the requirement for global capabilities, there is still start-up activity in the U.S. due to the low entry barriers in the industry. The challenges for P/M will be discussed in light of the implications for other metal processing industries.

9:50 AM Invited

Techno-Management Issues Facing Metal Processing Industries: Anne Stevens¹; ¹Carpenter Technology

Abstract not available.

10:10 AM Invited

North American Paper Industry - Impacts of Evolutionary and Revolutionary TechnoBusiness Developments: Jacquelyn McNutt¹; ¹Georgia Institute of Technology

Looking back ~ The North American Paper Industry experienced a major technical overhaul during the 20th Century ~ largely driven by a focus on technical research. These efforts transformed the industry into a highly efficient, environmentally compliant, and high product quality oriented sector. But sustained business success has still been very elusive in spite of this major technical transformation. Looking Out ~ The North American Paper Industry ~ must find a more successful business platform to avoid major disruptions and dislocations in the years ahead. Yet while the industry is trying to look within to find that internal transformation solution, there are major factors going on in parallel outside the industry that will cause the industry to face a "TechnoBusiness" Evolution if not Revolution in the first part of the 21st Century ~ with our without their own efforts. The noted major new factors both inside and outside the Industry that will drive this agenda, include ~ Global Warming/Dimming, Bio-energy/Bio-fuels, Sustainability, Nanotechnology, Cross Industries/Global/Societal Issues. The purpose of this presentation is to provide a broad overview of both the historical and the looking out factors that have and will shape this vital industry sector.

10:30 AM Invited

North American Paper Industry: Transforming to the Forest Biorefinery: Paul Stuart¹; ¹Abitibi-Consolidated Inc. and Ecole Polytechnique, Department of Chemical Engineering Chair

Commodity industries such as pulp and paper are characterized by a low R&D intensity, which have migrated from process innovation research to enterprise efficiency research (achieved for example through analysis of the supply chain following the implementation of ERP and other systems). Investments in this kind

of enterprise efficiency naturally "align" to existing products. Thus commodity industries and especially those that are capital intensive create inertia against a model of "punctuated equilibrium" (where punctual innovations result in new products which add significant value to company performance). The forest biorefinery is a concept being increasingly considered by forestry companies as a strategy to diversify their basic business model; however the implications of this transformation go beyond a requirement for significant capital spending in a cash-limited industry. It is far from obvious how the forestry industry might quickly jump from a manufacturing-centric culture to a product-centric culture. The objective of this presentation will be to summarize some of the key driving forces and barriers to successful commercial implementation of the forest biorefinery.

Structural Aluminides for Elevated Temperature Applications: FE and Other Aluminides

Sponsored by: The Minerals, Metals and Materials Society, TMS Structural Materials Division, TMS: High Temperature Alloys Committee, TMS/ASM: Mechanical Behavior of Materials Committee

Program Organizers: Young-Won Kim, UES Inc; David Morris, Centro Nacional de Investigaciones Metalúrgicas, CSIC; Rui Yang, Chinese Academy of Sciences; Christoph Leyens, Technical University of Brandenburg at Cottbus

Tuesday AM
March 11, 2008

Room: 394
Location: Ernest Morial Convention Center

Session Chairs: Haruyuki Inui, Kyoto University; David Morris, Centro Nacional de Investigaciones Metalúrgicas, CSIC

8:30 AM Invited

The Role of Stable Nanoparticles on Improving the Creep Resistance of Iron Aluminides: David Morris¹; Maria Muñoz-Morris¹; Ivan Gutierrez-Urrutia¹; ¹Centro Nacional de Investigaciones Metalúrgicas Consejo Superior de Investigaciones Científicas

The high-temperature creep strength of iron aluminides is relatively low and can be improved by alloying additions and processing improvements, especially those that lead to large numbers of stable and fine particles. The high temperature creep behaviour has been examined at temperatures of 700°C and above in a precipitation-strengthened Fe-Al-Zr cast alloy and in an oxide dispersion-strengthened Fe-Al-yttria mechanically-alloyed material. In the first, precipitates of an Fe-Zr intermetallic form during preliminary heat treatments or during creep itself. The distribution of the precipitates is modified by the dislocations present during creep, which affects the creep behaviour. The oxide dispersion provides good strengthening up to above 800°C. At 700°C these particles create threshold stresses that lead to very low creep rates. At higher temperatures, general climb allows dislocations to overcome the small obstacles and no threshold stresses are noted.

9:00 AM

In-Situ TEM Analysis of Deformed FeAl-Ni-B (B2) Alloy: Anna Fraczkiewicz¹; Brigitte Decamps²; David Colas¹; Olivier Calonne¹; Francois Louchet³; ¹Ecole Nationale Supérieure des Mines; ²Laboratoire de Chimie Métallurgique des Terres Rares, UPR 209 Centre National de la Recherche Scientifique; ³Laboratoire de Glaciologie et Géophysique de l'Environnement, Centre National de la Recherche Scientifique

Room temperature brittleness of B2-ordered FeAl remains their main flaw. Different origins of this lack of ductility are considered: hydrogen embrittlement, a high value of the DBTT, as well as superdislocation reactions, leading to the presence of sessile <100>. This work deals with dislocation reactions in a Fe40Al-5Ni-B (at. %) single crystal, in situ TEM strained at 600°C. Specific dislocation configurations were observed: two short, "fork-shaped" segments associated with a straight-lined and highly contrasted segment. These configurations are only partially glissile: only the short segments move under the stress. Still, their evolution is observed, through expansion of individual loops from "fork-shaped" segments. These configurations are formed by reactions between two different <111> superdislocations, gliding on different {112} planes. This mechanism is

somewhat similar to that observed previously in FeAl by Munroe and Baker. The possible effects of such dislocation reactions on brittle cleavage fracture of FeAl will be discussed.

9:20 AM

Exothermic Reactions in Cold-Rolled and Physical-Vapor-Deposited Ni/Al Multilayer Foils: *Laszlo Kecskes*¹; Xiaotun Qiu²; Jesse Grater²; Jiaping Wang²;

¹US Army Research Laboratory; ²Louisiana State University

The exothermic reaction pathways in cold-rolled and physical vapor deposited Ni/Al reactive multilayer foils were investigated. To understand the conditions approaching self-propagating high-temperature reactions, Ni/Al foils were heated to 1000°C in a differential scanning calorimeter. During thermal explosion, in both types of foils multiple (three to four) exothermic peaks were noted, corresponding to a multi-step reaction process. Determined by a reduced interlayer spacing in the PVD foils, the peak positions were found to sharpen, separate, and shift to lower temperatures. Subsequent to obtaining the total calorimetric heat output for a given heating rate, samples were also heated to each peak temperature to allow identification of the intermediate reaction product and evolution of the microstructure from reactants to steady state products. XRD and SEM showed that lower temperature peaks corresponded to formation of Al₃Ni, while the higher temperature peaks corresponded to conversion of Al₃Ni to the nominal stoichiometric AlNi.

9:40 AM

Fatigue Crack Growth Resistance of a Fe-40Al Alloy Prepared by Mechanical Alloying and Forging: *Gilbert Henaff*¹; Naziha Berramdane¹; Guillaume Benoit²; Yannick Girard³; Sebastien Launois⁴; ¹Ecole Nationale Supérieure De Mécanique Et D'Aérotechnique; ²Ecole Nationale Supérieure De Mécanique Et D'Aérotechnique; ³European Aeronautic Defense and Space Company IW; ⁴Atomic Energy Commission

The FeAl 40 grade 3 alloy strengthened by oxide dispersion introduced by mechanical alloying presents attractive performances for application in aircraft components at elevated temperature. However several issues relative to its damage tolerance still need to be addressed. The present study tackles this issue, with a special attention paid to the influence of load ratio, temperature, environment and load history. It comes out that the FCG behaviour is only slightly affected when the load ratio is changed in relation with a limited crack closure effect. The relevance of water vapour adsorption, identified on the same alloy tested in the as-hipped condition as the environmentally-assisted mechanism controlling FCG in air, is also analysed. Finally, it is also shown that a periodic overload in a baseline loading at R=0.1 induces a significant retardation effect on crack growth. However this beneficial effect cannot be accounted for by closure effects enhanced by overloads.

10:00 AM

The Yield Strength Anomaly in Fe₂MnAl Single Crystals: *Yifeng Liao*¹; Ian Baker¹; ¹Dartmouth

A [411]-oriented single crystal Fe₃₅Mn₁₉Al₂₆ was grown using a modified Bridgman technique and its mechanical behavior investigated as a function of temperature. Specimens were strained under compression over the temperatures range 300-900K at a range of strained rates. A yield strength anomaly was observed in which the yield strength peak was ~180 MPa at 600 K, with the yield strengths ranging from 170 MPa at 300K to 70 MPa at 900K. The yield peak appeared to be little affected by the strain rate. Microstructural analysis in the TEM showed that the compound adopted the L2₁ structure at room temperature, but that it transformed to the B2 structure at ~900K. In the L2₁ state the superdislocations were four-fold dissociated with the outer partials separation being 4 nm while that of the inner partials was 15nm. The interaction of the gliding dislocations with the thermal anti-phase boundaries was studied by *in-situ* straining.

10:20 AM Break

10:30 AM

First-Principles Prediction of Site Preference of Transition-Metal Elements in B2 NiAl: *Chao Jiang*¹; ¹Los Alamos National Laboratory

B2 NiAl intermetallic compound is a promising material for high temperature structural applications due to its high melting temperature and excellent oxidation resistance. However, its application is limited by the poor room temperature ductility. One approach to improve the ductility of B2 NiAl is through alloying.

A precise knowledge of the site occupancy behavior of ternary elements is thus required to understand their roles in modifying the mechanical properties of NiAl. In this study, we combine first-principles calculations with the Wagner-Schottky model to predict the site preference of 3d, 4d, and 5d transition-metal elements in B2 NiAl. Model calculations indicate that such a preference can be a strong function of both alloy composition and temperature. It is our hope that our study can stimulate further experimental investigations and provide a guide for future development of NiAl-based alloys.

10:50 AM

Oxidation Behavior and Thermal Stability of Ni-20Al-20Pt Refractory Alloy at High Temperature Exposure: *Rabindra Mahapatra*¹; ¹Naval Air Systems Command

The isothermal oxidation behavior of Ni-20Al-20Pt (in at.%) refractory alloy was investigated up to a period of 312 hr in air from 1200 to 1400°C. A comparison of the oxidation behavior of this alloy with a conventional Ni-base superalloy (Inconel 713) shows an order of magnitude oxidation resistance. This experimental alloy oxidizes by forming Al₂O₃ and a trace of PtO with Al₂O₃ oxide layer in contact with air. Optical and Scanning Electron Microscopy (SEM) were used to study the microstructure, morphology, and composition of scale formed after oxidation. The thermal stability of the alloy after extended periods of exposure in air at 1200, 1300, and 1400°C was studied using Transmission Electron Microscopy (TEM). The microstructure of the alloy observed to be stable at 1300°C for 312 hr exposure in air.

11:10 AM

Physical Properties of Single Crystals of Co₃(Al,W) with the L12 Structure: *Haruyuki Inui*¹; Katsushi Tanaka¹; Kyosuke Kishida¹; Takashi Ohashi¹; ¹Kyoto University

The recent discovery of the stable L12-ordered intermetallic compound, Co₃(Al,W) coexisting with the solid-solution based on Co with a fcc structure has opened up a pathway to the development of a new class of high-temperature structural material based on cobalt, 'Co-base superalloys'. However, almost nothing is known about mechanical properties of these Co-based two-phase alloys, especially of the constituent L12 phase, Co₃(Al,W). We have investigated some physical properties (elastic constants, thermal conduction, thermal conductivity and plastic deformation behavior) of single crystals of Co₃(Al,W) with the L12 structure. The values of all the three independent single-crystal elastic constants and polycrystalline elastic constants of Co₃(Al,W) experimentally determined are considerably smaller than those previously calculated by others. When judged from the values of Poisson ratio, Cauchy pressure and Gh/Bh, the ductility of Co₃(Al,W) is expected to be sufficiently high so that Co₃(Al,W) can be practically used as the constituent phase of 'Co-base superalloys'.

11:30 AM

The Influence of Cr and B Additions on the Mechanical Properties and Oxidation Behaviour of L21-Ordered Fe-Al-Ti-Based Aluminides at High Temperature: *Ronny Krein*¹; Martin Palm¹; ¹Max-Planck-Institut für Eisenforschung GmbH

Several Fe-25Al-Ti-X (X = Cr, B) alloys with 15 or 20 at.% Ti and varying Cr and B contents have been investigated with respect to their mechanical properties and their oxidation behaviour at elevated temperatures. The mechanical properties have been characterized by means of high-temperature compression tests, 4-point-bending tests and creep tests at 750, 800 and 850°C. The oxidation behaviour has been examined using thermogravimetric analyses at 800°C in synthetic air. The addition of Cr and B are both beneficial for the creep resistance and has no influence to the still excellent oxidation behaviour. The alloys exhibit two flow stress anomalies at around 550 and 800°C, a phenomenon which has been observed for the first time. The appearance of the additional flow stress maximum at around 550°C can be suppressed by aging and by increasing the deformation rate.

11:50 AM

From Nanometric Ni/Al Multilayers to Intermetallic Thin Films: *T. Vieira*¹; *J. Noro*²; *A. S. Ramos*²; ¹University of Coimbra; ²Instituto de Ciência e Engenharia de Materiais e Superfícies

Ni aluminides are potential candidates for practical applications as thin films, which can be formed by thermal annealing of alternate layers of Ni and Al that react exothermically at rather low temperatures. The aim of this work is to

produce nanometric Ni/Al multilayer thin films and to evaluate their structural and mechanical properties (H, E and $\sigma_{0.2}$) having in mind its application for joining microparts. Thin films of the B2-NiAl ordered intermetallic phase were produced after thermal annealing of Ni/Al multilayers deposited by d.c. magnetron sputtering from pure nickel and aluminium targets. The substrates' holder was a copper block to avoid intermixing and reaction during deposition. The multilayers were designed in order to have an overall atomic composition of 50Al:50Ni and modulation periods, λ , ranging from 5 to 120 nm. Depending on the multilayer period, the formation of the NiAl equilibrium phase could be preceded by NiAl₃ and/or Ni₂Al₃ phase(s).

Ultrafine-Grained Materials: Fifth International Symposium: Stability, Technology, and Property

Sponsored by: The Minerals, Metals and Materials Society, TMS Structural Materials Division, TMS Materials Processing and Manufacturing Division, TMS: Shaping and Forming Committee, TMS: Nanomechanical Materials Behavior Committee
Program Organizers: Yuri Estrin, Monash University and CSIRO Melbourne; Terence Langdon, University of Southern California; Terry Lowe, Los Alamos National Laboratory; Xiaozhou Liao, University of Sydney; Zhiwei Shan, Hysitron Inc; Ruslan Valiev, Ufa State Aviation Technical University; Yuntian Zhu, North Carolina State University

Tuesday AM Room: 273
 March 11, 2008 Location: Ernest Morial Convention Center

Session Chairs: Yuntian Zhu, North Carolina State University; Günter Gottstein, RWTH Aachen; Qiuming Wei, University of North Carolina; Yinmin Wang, Lawrence Livermore National Laboratory

8:30 AM Invited

Stabilization of Nanocrystalline and Ultrafine Grain Sizes by Solute Additions: *Carl Koch*¹; Ronald Scattergood¹; Kristopher Darling¹; Jonathan Semones¹; ¹North Carolina State University

Nanocrystalline and ultrafine grained microstructures offer improved mechanical behavior. However, they are subject to coarsening due to the driving force from the large grain boundary area, and therefore energy, that the small grains provide. While some nanocrystalline metals exhibit grain growth, usually abnormal grain growth, even at room temperature, there are many examples of the stabilization of grain sizes to significant fractions of the material's melting point. Both kinetic (reduction of grain boundary mobility), and thermodynamic (reduction of the specific grain boundary energy), approaches have been used. This talk will present evidence for the stabilization of grain sizes in nanocrystalline materials from the literature and from recent research from the authors' laboratory. Reduction of the specific grain boundary energy by solute segregation will be emphasized.

8:50 AM

Mechanical and Biological Properties of Nanostructured Titanium: *X. Zhang*¹; Yinmin (Morris) Wang²; ¹Shanghai Jiao Tong University; ²Lawrence Livermore National Laboratory

Nanostructured titanium is known to have high strength (~1GPa) and decent useful ductility. Because of its excellent biocompatibility, nanostructured titanium is also considered as one of the top candidates for bio-implant type of applications. In this work, we will present some of our recent progresses on improving the biomechanical properties of the nanostructured titanium. Our focus will be on the reduction of Young's modulus and enhanced adhesion properties between nanostructured titanium and animal tissues. This work was supported by the Nano Foundation of Shanghai, China, and was also partially performed under the auspices of the US Department of Energy by University of California, Lawrence Livermore National Laboratory under contract of No. W-7405-Eng-48.

9:05 AM Invited

Effect of Isothermal Annealing on the Microstructure of Nanocrystalline: *Indranil Roy*¹; Hsiao-Wei Yang¹; Linh Dinh¹; Farghalli Mohamed¹; ¹University of California

Bulk nanocrystalline (nc) Ni specimens having an average grain size of 100 nm were subjected to isothermal annealing at 573 K for different holding times. The microstructure developed in nc-Ni following annealing was examined by means of transmission microscopy (TEM). Also, electron backscatter diffraction (EBSD) was used to generate orientation maps. The results show the presence of a large volume of annealing twins. Post deformation TEM micrographs reveal that dislocations are blocked at the nano-twinned boundaries resulting in dislocation accumulation and entanglement.

9:25 AM

Mechanical Properties of Ti-6Al-4V Titanium Alloy with Submicrocrystalline Structure Produced by Severe Plastic Deformation: *Gennady Salishchev*¹; Sergey Zhrebtsov¹; Svetlana Malysheva¹; Anatoliy Smyslov²; Eduard Saphin²; Nailya Izmailova³; ¹Institute for Metals Superplasticity Problems; ²Ufa State Aviation Technical University; ³JSC Ufa Engine Industrial Association

A comparative investigation of mechanical properties of Ti-6Al-4V titanium alloy with microcrystalline (10 μ m) and submicrocrystalline (0.4 μ m) structures in the temperature range of 20–600°C has been carried out. The submicrocrystalline structure was obtained by multiple isothermal forging. The alloy with the microcrystalline structure has been additionally subjected to a heat-strengthened treatment. The structure refinement of the alloy results in increase in both strength and fatigue limit at room temperature by about 20%. The strength of the submicrocrystalline alloy is higher than that of the microcrystalline alloy up to 400°C. However, the creep strength of the submicrocrystalline alloy is slightly lower than that of the heat-strengthened microcrystalline alloy already at 250°C. The impact toughness in submicrocrystalline state is lower especially in the samples with introduced cracks. Processing advantages of practical application of submicrocrystalline titanium alloys for producing aero-space articles have been evaluated using isothermal forging.

9:40 AM

Production, Properties and Application Prospects of Bulk Nanostructured Materials: *Radik Mulyukov*¹; Renat Imaev¹; Ayrat Nazarov¹; ¹Russian Academy of Sciences, Institute for Metals Superplasticity Problems

Principles of the method of multiple isothermal forging for the production of bulk nanostructured materials will be formulated. The method was pioneered and has been widely used at the Institute for Metals Superplasticity Problems. The common features and distinctions of this method with severe plastic deformation methods such as high-pressure torsion and equal-channel angular pressing will be analyzed. It will be demonstrated that multiple isothermal forging is a versatile method allowing for the production of bulk and sheet nanostructured semi-products with the grain size down to about 50 nm and is applicable to various metals and alloys including heat-resistant, hard-to-deform and intermetallic ones. Novel mechanical properties of bulk nanostructured materials produced by this method will be presented. The prospects of their structural and functional applications will be outlined.

9:55 AM Invited

Grain Refinement and Mechanical Properties of Two-Phase Cu-Zn Alloys Subject to Constrained Groove Pressing: *Leon Shaw*¹; Kaiping Peng²; Ying Zhang²; K.-W. Qian²; ¹University of Connecticut; ²Fuzhou University

The applicability of constrained groove pressing (CGP) for grain refinement and improvements in mechanical properties of two-phase Cu-Zn alloys is demonstrated in this study. It is shown that the grain size and volume fraction of the beta-prime phase in the Cu-Zn alloy should be kept small through proper heat treatment, and the die design with wider groove can reduce stresses at the most severely loaded region of the workpiece, all of which allow more numbers of pressing to attain grain refinement. The hardness and tensile strength increase with the number of the CGP cycle. The improved tensile properties are related to microstructural evolution induced by CGP.

10:15 AM Break

10:30 AM Invited

Thermal Stability of Nanostructured Metals: *Niels Hansen*¹; Xiaoxu Huang¹; Roy Vandermeer¹; ¹Risoe National Laboratory

Common to metals deformed to high strains is a very fine microstructure, high strength and limited ductility. Structure and property optimization by annealing after deformation must therefore be explored. In the present study commercial purity aluminium has been annealed after cold rolling to ultrahigh strains up to $\epsilon_M=6$ and the annealing process has been analyzed in terms of recovery and conventional recrystallization. The recovery kinetics has been analyzed for specimens annealed in the temperature range 140-220°C and it is found that increasing strain has no effect on the activation energy of recovery but the more highly deformed metal does have recovery rate much larger than the less deformed material. Deformation and annealing conditions must therefore be balanced when property optimization is sought through a recovery anneal of metals deformed to ultrahigh strains.

10:50 AM

Quasi-Static and Dynamic Mechanical Properties of Commercial-Purity Tungsten (W) Processed by ECAE below the W Recrystallization Temperature: *Z. Pan*¹; Suveen Mathaudhu²; L. Kecskes²; K. Hartwig³; Q. Wei¹; ¹University of North Carolina at Charlotte; ²US Army Research Laboratory; ³Texas A&M University

Thermo-mechanical processing tungsten (W) has proved to be difficult due to its poor workability. Particularly, commercial purity polycrystalline W exhibits a very high ductile to brittle transition temperature (DBTT). Recently, severe plastic deformation (SPD) has been used to refine the W grain size of. Previous experiments have reported the quasi-static (QS) and dynamic mechanical behavior of the SPD W showing unique results. However, the processing, particularly equal-channel angular extrusion (ECAE) was performed at relatively high temperatures to avoid cracking of the work piece. Recent developments in ECAE processing allowed us to process W at lower temperatures. In this work, we have processed commercial purity W via different ECAE routes at temperatures well below the nominal recrystallization temperature of 1400°C. We have systematically evaluated the QS and dynamic compressive behavior of the processed W. Quasi static compression tests were performed using an MTS machine at room temperature. It was observed that, with decreasing temperature, the ECAE samples showed higher yield and flow stresses than those processed near the recrystallization temperature; no obvious strain hardening was observed in the QS stress strain curves below a certain temperature. Quasi static strain rate jump tests show that the strain rate sensitivity of the ECAE W is in the range of 0.02-0.04, about half the value for coarse grained W. Uni axial dynamic compressive tests were also performed on a Kolsky bar (or split Hopkinson pressure bar) system. Scanning electron microscopy was used to observe the post loading surfaces of the deformed samples to understand the deformation and failure mechanisms under quasi static and dynamic compression.

11:05 AM Invited

Recent Development in Nanometals by Hydrostatic Extrusion: *Krzysztof Kurzydowski*¹; ¹Warsaw University of Technology

Hydrostatic extrusion is an efficient method of grain refinement down to nanometer scale in metallic materials. The paper shows, that it can be directly used to obtain a mean grain size smaller than 100 nm and a significant fraction of high angle grain boundaries in aluminium alloys, titanium or iron. It is also demonstrated that grain size reduction to this level in some other materials, e.g. nickel, requires combination HE, as a final operation, with of some other SPD methods.

11:25 AM

Effect of ECAP Deformation on the Thermal Stability of an Aluminum Alloy 3103: *Xenia Molodova*¹; Günter Gottstein¹; ¹RWTH Aachen University

Studies of the annealing behavior of severely plastically deformed materials are rare compared to other features of such processed materials. As shown recently, discontinuous recrystallization is the governing phenomenon during heat treatment of severely deformed materials. In the present study the microstructure evolution of an aluminium alloy 3103 subjected to ECAP applying route Bc was investigated after deformation and subsequent heat treatment. The isothermal annealing was carried out at 330°C. The deformed and annealed states were analyzed by EBSD, TEM and microhardness tests. It

will be demonstrated that the ECAP deformed material exhibited an increased stability against discontinuous recrystallization with growing number of passes. This superior thermal stability is desirable for many applications of UFG alloys. In addition, the ECAP deformed material was subjected to a low temperature annealing prior annealing at 330°C. The effect of this precedent recovery treatment on the thermal stability will be discussed.

11:40 AM

Formation of Ultrafine-Grained Microstructure in HSLA Steel Profiles by Linear Flow Splitting: *Tilman Bohn*¹; Enrico Bruder¹; Clemens Müller¹; ¹Technische Universität Darmstadt, Department of Materials Science, Division Physical Metallurgy

Linear flow splitting is a new cold forming process for the production of branched sheet metal structures in integral style. The process induces extremely high deformation degrees without formation of cracks in the split sheets due to hydrostatic compressive stresses. Investigations on a HSLA steel (ZStE 500) show the formation and fragmentation of a dislocation cell structure in the severely deformed regions of the steel sheet. This results in ultrafine-grained microstructures and improved mechanical properties, similar to SPD processes as ECAP or HPT. EBSD measurements reveal a gradient in grain size with an increase in direction perpendicular to the surface whereas micro hardness decreases in the same direction. Based on these results, basic principles of the linear flow splitting process and its expected potential are discussed.

11:55 AM

Effect of Stacking Fault Energy on the Mechanical Behavior of Nanostructured Co-Ni Alloys: *Pei-Ling Sun*¹; Yonghao Zhao²; Jason Cooley³; Michael Kassner⁴; Yuntian Zhu⁵; ¹Feng Chia University; ²University of California at Davis; ³Los Alamos National Laboratory; ⁴University of Southern California; ⁵North Carolina State University

Co-Ni alloy has very small solution-hardening effect and is, therefore, perfect for studying the effect of stacking fault energy on the mechanical properties. Nanostructured Co-Ni alloy samples were processed by high-pressure torsion. The addition of cobalt to nickel reduces the stacking fault energy (SFE) in nickel. These nanostructured Co-Ni alloys were then tested under tension. It was found that increasing SFE reduces the tensile stress in Co-Ni alloys. The related microstructures will be examined in TEM and compared with experiments in the literature.

2008 Nanomaterials: Fabrication, Properties, and Applications: Application

Sponsored by: The Minerals, Metals and Materials Society, TMS Electronic, Magnetic, and Photonic Materials Division, TMS: Nanomaterials Committee
Program Organizers: Seong Jin Koh, University of Texas; Wonbong Choi, Florida International University; Donna Senft, US Air Force; Ganapathiraman Ramanath, Rensselaer Polytechnic Institute; Seung Kang, Qualcomm Inc

Tuesday PM Room: 274
 March 11, 2008 Location: Ernest Morial Convention Center

Session Chair: To Be Announced

2:00 PM Invited

Sculpture and Properties of Functional Nanostructures and Nanolayers for Applications: *Ganapathiraman Ramanath*¹; ¹Rensselaer Polytechnic Institute

Harnessing nanostructures for many applications requires the sculpture of nanoscale building blocks with control over atomic-level structure, surface chemistry, and their assembly into controllable configurations. This talk will describe three different examples from our recent works in on directing the growth and assembly of assemblies of nanostructures of magnetic and thermoelectric materials, and novel properties of molecular nanolayers. Our approaches open up new possibilities for a variety of applications, e.g., data storage, power generation and refrigeration, and nanodevices. I will first illustrate the synthesis and assembly of nanoparticles of magnetic and thermoelectric materials with control over crystal structure, shape and surface chemistry. We have devised entirely new strategies to obtain high-coercivity FePt-silica core-shell nanomagnets with simultaneous control over size, dispersity, composition and phase stability, by using surfactant-stabilized water nanodroplets, and to realize low temperature chemical ordering by impurity incorporation. The nanoparticles can be assembled into chains of desired length and diameter, or ordered films by exploiting molecular coupling agents as braidors and spacers. Directed synthesis of molecularly braided magnetic nanoparticle chains using molecular couplers, *Adv. Mater.* (2007). Accepted. A new dynamic templating method to obtain rod-shaped assemblies by synergistic growth of two phases will be presented. Rod-shaped assemblies of FePt-PtTe₂ through dynamic templating, *Adv. Mater.* (2007) accepted.. I will then describe a new surfactant-mediated technique to obtain single-crystal nanorods of chalcogenides with and without branching. Low-temperature templateless synthesis of single-crystal bismuth telluride nanorods, *Adv. Mater.* 18, 496-500 (2006)., by manipulating surfactant type, concentration and temperature. I will finally demonstrate the use of organosilane and polyelectrolyte nanolayers to enhance the chemical integrity, electrical device reliability and mechanical toughness of metal-dielectric thin film interfaces and porous materials. Self assembled nanolayers as adhesion enhancers and diffusion barriers, *Appl. Phys. Lett.* 83, 383 (2003)., Suppression of chemical and electrical instabilities in mesoporous silica films by molecular capping, *J. Appl. Phys.* 100, 114504 (2006)., Cu diffusion and mechanical toughness at Cu-silica interfaces glued with polyelectrolyte nanolayers, *J. Appl. Phys.* 101, 084505 (2007)., Molecular-nanolayer-induced suppression of in-plane Cu transport at Cu-silica interfaces, *Appl. Phys. Lett.* 90, 163507 (2007)., Annealing-induced interfacial toughening using a molecular nanolayer, *Nature* 447, 299 (2007). . I will highlight the use of a sub-nm-thick molecular layer as an adhesive that can bond interfaces of disparate materials at temperatures higher than previously envisioned.

2:30 PM

Damping of Hybrid Surface Plasmon Modes in Ag Nanoparticles; Application to Vapor Sensing: *Sriharsha Karumuri*¹; *Kaan Kalkan*¹; ¹Oklahoma State University

The present work demonstrates ultra-fast sensing of Hg vapor by a novel sensing mechanism: nonradiative damping of hybrid dipolar surface plasmon modes in metal nanoparticles. Although, the Mie theory predicts Hg adsorption can lower the plasmon extinction in Ag nanoparticles, previous work has only shown its increase due to a different competing mechanism: electron transfer from Hg. The investigators show that once the intrinsic damping on the surface

of a silver nanoparticle is reduced significantly, additional damping due to adsorption becomes the dominant mechanism for sensing. Further, a dramatic gain in response speed is observed. An 8% change in plasmon extinction is recorded in the first 30 s of exposure to few ppm of Hg. The investigators will report on: their plasmon damping model where Hg atoms serve as electron scattering centers; Ag nanoparticle reduction on Si substrates and subsequent plasmon damping-reduction process; as well as various AFM, SEM, and EDX characterizations.

2:45 PM

Fabrication and Characterization of Laser Drilled Vias in SiO₂ Nanofluidic Devices: *Xiaoxuan Li*¹; *William Hofmeister*¹; ¹University of Tennessee

Nanofluidics is used to study fluid flow in nanometer sized structures or objects. Biomolecules can be confined and trapped in nanospace in nanofluidics in separation science and single molecule detection in life science, biophysics, and analytical chemistry. In this paper, electron beam photolithography was used to fabricate nanochannels in fused silica (SiO₂) and nanochannel patterned glass chip was bonded with blank SiO₂ chips to fabricate nanofluidics. The nanofluidics device was used in laser fluorescence spectroscopy to study single molecules in nanochannels. Fabrication and characterization of nanochannels in SiO₂ was reported. The vias in SiO₂ nanofluidics devices were manufactured by a CO₂ laser in "superpulse" mode and their microstructure was studied. The laser drilling parameters including number of laser pulses, laser pulse-on time, laser beam size, thickness of SiO₂ glass were evaluated for the optimization of access hole morphology.

3:00 PM

Fabrication and Microstructure Characterization of Graded Anisotropy Media: *Robb Morris*¹; *Gregory Thompson*¹; *Yuki Inaba*¹; *J. Harrell*¹; ¹University of Alabama

The superparamagnetic limit poses a fundamental barrier that threatens to limit further increases in magnetic storage density. Attempts to increase the thermal stability by making the grains "magnetically harder" have failed because they have also made them impossible to write. One solution to this conundrum is to use exchange coupled composites, in which one end of the grain is magnetically soft (low Ku) and the other end magnetically hard (high Ku). To date, most of the work has focused on composites with discrete layered interfaces. This talk will address the use of a graded compositional profile to achieve a gradient in Ku. Our proof-of-principle study has used a graded CoPt film. The technical fabrication challenges, performance and stability of different gradient profiles will be addressed in terms of the films' microstructure, which has been characterized by TEM, XRD, LEAP and AGM analysis.

3:15 PM

Faceting and Surface Energy Effects on the Self-Assembly of Epitaxial Quantum Dots: *Lawrence Friedman*¹; ¹Pennsylvania State University

Epitaxial self-assembled quantum dots (SAQDs) will allow breakthroughs in electronics and optoelectronics. SAQDs result from Stranski-Krastanow growth whereby epitaxial 3D islands form spontaneously on a planar thin film. Common systems are Ge_xSi_{1-x}/Si and In_xGa_{1-x}As/GaAs. SAQDs are typically grown on a (001) surface. The formation and evolution of SAQDs is determined by the interaction of surface energy and elastic strain; however, there are competing theories of the nature of the planar (001) surface: (1) It is a stable non-facet. (2) It is a stable crystal facet. (3) It is an unstable anti-facet. The first theory appears most often in modeling literature, but the second two theories take explicit account of the discrete nature of a crystal surface. Here, the impact of the three theories on SAQD formation is discussed along with the possibility of a phase transition. Can they all three be correct?

3:30 PM

Formation of Metallic Nanoparticles through Colloid-Induced Spontaneous Metallization: *Tzy-Jiun Luo*¹; ¹North Carolina State University

We report a room temperature synthesis of metallic nanoparticles that is based on spontaneous metallization induced by colloidal solution of silane that contains methanol. Metallic ions (e.g. Sn⁴⁺, Ag⁺) have been successfully reduced in the presence of organically modified silane colloids while the same reaction was not observed in a polymer solution that contains similar functional groups. Metallic nanoparticles with diameters around 5 ~ 7 nm were identified using TEM. Kinetic studies were conducted using UV-Vis spectroscopy. Nanoparticle containing

silica colloids can be easily transformed into monolith sol-gel materials, and have been examined using XRD and electrochemical methods. The results have shown that nanoporous silica materials doped with metallic nanoparticles exhibit enhanced electrochemical properties and stability. Currently, study of this nanocomposite for electrochemical sensing is underway.

3:45 PM

Electrophoretic Phenomena of Fine Particles in Aqueous and Non-Aqueous Solvents: *Junji Shibata*¹; Daisuke Yamashita¹; Masato Tateyama¹; Norihiro Murayama¹; ¹Kansai University

The electrophoretic phenomena of fine polystyrene particles in aqueous and non-aqueous solvents were investigated in the electric field. The spherical polystyrene particles of 0.03, 0.1, 1.0, 4.3 and 9.6 μm were used as a sample particle, and water-alcohol mixtures such as methanol, ethanol, etc. were also used as a solvent of suspension. The electrophoretic mobility of fine particles is decreased with a decrease in volume percent of water in water-alcohol mixtures. These tendencies of the decrease in electrophoretic mobility can be expressed by the Smoluchowski equation. The forces acting the particles in electric field are considered to be electrical force, friction force and the other forces like asymmetric effect and electrophoretic retardation effect which appear in ionic behavior. The behavior of fine polystyrene particles in non-aqueous solvents can be explained by the forces acting the particles in the electric field.

4:00 PM Break

4:15 PM Invited

Direct Writing: How Can We Leverage Nature's Directed Self-Assembly to Create Novel Constructs?: *Douglas Chrisey*¹; David Corr¹; Cerasela Dinu¹; ¹Rensselaer Polytechnic Institute

The rapidly growing fields of nanoscience and nanotechnology have stimulated considerable interest in methods for building structures that have nanometer dimensions. As a result, there is interest in patterning techniques that offer nanometer resolution using experimentally simple set-ups as well as in systems which can mimic cellular self-assembly to direct patterning on engineered environments. We describe two different strategies for building structures on a substrate. The first approach involves CAD deposition of controlled patterns of cells to direct the formation of tissue constructs while the second approach relates to the possibility of using the evolutionary machineries of the cell, microtubules, and the kinesin molecular motor to direct the bottom-up patterning at the nanoscale level.

4:45 PM

Large-Scale Placement of Single Nanoparticles with Nanoscale Precision: *Hong-Wen Huang*¹; Vishva Ray¹; Seong Jin Koh¹; ¹University of Texas at Arlington

Nanoparticles have drawn a lot of attention due to their unique and size-dependent electrical, optical, and magnetic properties. Practical devices utilizing nanoparticles, however, require techniques that enable precise placement of single nanoparticles on targeted substrate locations. Here, we present a large-scale and precise placement of nanoparticles, where single nanoparticles are electrostatically guided and placed on the centers of circular patterns, one nanoparticle per one circular pattern. The electrostatic guiding structure was formed using self-assembled monolayers (SAMs) with pattern diameter of ~ 130 nm. We demonstrate placement of single 20 nm Au nanoparticles onto centers of the circular patterns with precision of ~ 7 nm. Out of 400 patterns, more than 70% of the circular patterns were occupied by exactly one Au nanoparticle. We envision that this method could be applied for fabrication of single electron devices, photonic devices, biological/chemical sensors, and other devices that require precise nanoparticle placement.

5:00 PM

Position Controlled Fabrication of Metal Nanostructures with Focused Electron Beam: *Kazuo Furuya*¹; Masaki Takeguchi¹; Minghui Song¹; Kazutaka Mitsuishi¹; Miyoko Tanaka¹; ¹National Institute for Materials Science

Electron beam induced deposition (EBID) is one of the promising techniques, because of short wavelength which results in the resolution limit less than several 10 nm. We have been using FE-SEMs and FE-TEMs for the fabrication of position and size controlled metal nanostructures. A gas introduction system with a nozzle of 0.1 mm was developed. The flux of the gas for EBID was

estimated to be approximately 2×10^{-4} Pa l s⁻¹. The position and size control was carried out careful manipulation of electron beam. The diameters of the nanostructures were ranged from 4 to 20 nm. Magnetic nanostructures were also obtained with iron containing precursor gas, Fe(CO)₅. Free-standing iron nano-antennas were examined by FE-TEM with electron holography. The magnetic field produced an electron hologram for the nanostructures. It is found that magnetic fields were leaked from the nanostructure body and the whole was likely to be one "nano-magnet".

5:15 PM

Phase Field Modeling of Nansocale Island Dynamics: *Zhengzheng Hu*¹; Shuwang Li¹; John Lowengrub¹; Steven Wise²; ¹University of California, Irvine; ²University of Tennessee

In this talk, a Burton-Cabrera-Frank (BCF) island dynamics model is used to analyze the epitaxial growth of a circular island. We show that there exists a critical deposition flux for which a single-mode perturbation remains unchanged and this flux together with other parameters may be exploited to control the shape of the island. To demonstrate the idea, a phase-field model that accounts for Ehrlich-Schwoebel effect and surface diffusion, is used to simulate the dynamics of the island. A block-structured adaptive mesh refinement method and an efficient numerical method is developed using a second order accurate fully implicitly time discretization together with a second order accurate finite difference spatial discretization. We close by demonstrating the nonlinear evolutions of islands to show the extent of applicability of our ideas on shape control at the nanoscale.

5:30 PM

Temperature, Thickness and MeV Si Ions Bombardment Effects on the Thermoelectric Generator from ErFe₄Sb_(6-y)Ge_y Thin Films: *Satilmis Budak*¹; Sadik Guner¹; Claudiu Muntele¹; Daryush Ila¹; ¹Alabama A&M University

We have grown monolayers of ErFe₄Sb_(6-y)Ge_y (y = 2,4) thin films on silica substrates with varying thickness between 200-1000 nm using ion beam assisted deposition (IBAD). MeV Si ions bombardments have been performed on samples with varying fluences. The Seebeck coefficient, electrical and thermal conductivity measurements were carried out before and after bombardment to calculate the figure of merit, ZT. MeV Si ions bombardment caused changes on the thermoelectric properties of films. Rutherford Backscattering Spectrometry (RBS) was used to analyze the elemental composition of the deposited materials and to determine the layer thickness of each film. Research sponsored by the Center for Irradiation of Materials, Alabama A&M University and by the AAMURI Center for Advanced Propulsion Materials under the contract number NNM06AA12A from NASA, and by National Science Foundation under Grant No. EPS-0447675.

5:45 PM

Photonic Curing for Low Temperature Sintering of Printed Nanoparticulate Materials: *James Sears*¹; Michael Carter¹; Jeffery West¹; ¹South Dakota School of Mines and Technology

Photonic Curing is being developed to cure or sinter metal nano-particle based films by exposing them to a brief, intense pulse of light from a xenon flash lamp. This photonic curing technology allows for rapid and selective heating that fuses nano-scale metallic ink particles into functional components. This technology allows the curing or sintering of nanoscale metallic ink patterns on low-temperature substrates including flexible circuit boards, flat panel displays, interconnects, RFID tags, and other disposable electronics without the use of heat. This paper reports on the results obtained after sintering conductive, magnetic, and dielectric nano-particle inks. Sintering was performed with the photonic curing technique developed by NovaCentrix, 2W frequency doubled Nd:YAG CW laser, and a conventional muffle furnace. Sample thickness, microstructural details, resistivity, and sintering characteristics are also examined and compared for the sintering techniques.

3-Dimensional Materials Science: Modeling and Characterization across Length Scales I

Sponsored by: The Minerals, Metals and Materials Society, TMS Structural Materials Division, TMS: Advanced Characterization, Testing, and Simulation Committee
Program Organizers: Michael Uchic, US Air Force; Eric Taleff, University of Texas; Alexis Lewis, Naval Research Laboratory; Jeff Simmons, US Air Force; Marc DeGraef, Carnegie Mellon University

Tuesday PM Room: 286
 March 11, 2008 Location: Ernest Morial Convention Center

Session Chairs: Andrew Geltmacher, Naval Research Laboratory; Dennis Dimiduk, US Air Force

2:00 PM

Construction of Simplified Three-Dimensional Grain Boundary Surfaces from Serial Section Micrographs: *Scott Dillard*¹; John Bingert²; Dan Thoma²; Bernd Hamann¹; ¹University of California, Davis; ²Los Alamos National Laboratory

A method is presented for extracting 3D grain boundary surfaces from serial sections of polycrystalline materials comprising a mixture of electron backscatter diffraction (EBSD) data and light-optical micrographs. This method relies on a constrained Potts model to interpolate grain boundaries between segmented section images, allowing for greater sectioning thickness and more spacing between EBSD micrographs. The result is a segmented volume from which a triangulated boundary surface is extracted, complete with topological information about the connectivity of grain faces, edges and vertices. A method to reduce the number of triangles in this surface without introducing error is also described. The application of these methods to an actual 3D data set will be demonstrated through the analysis of a shocked tantalum polycrystal.

2:20 PM

Integration of Focused Ion Beam Serial Sectioning and Orientation Imaging Microscopy for 3-D Microstructure Reconstruction: Suk-Bin Lee¹; Emine Gulsoy¹; Michael Groeber²; Gregory Rohrer¹; Anthony Rollett¹; Michael Uchic¹; Jeff Simmons³; *Marc DeGraef*¹; ¹Carnegie Mellon University; ²Ohio State University; ³US Air Force

A new method for reconstructing a 3D microstructure using the focused ion beam-orientation imaging microscope (FIB-OIM) is introduced. The method was applied to the IN100 superalloy, and results cross-sectional ion-induced secondary electron (ISE) images and corresponding electron back-scattered diffraction (EBSD) maps. Both data series show small translational misalignments. For the EBSD map alignments, we developed a procedure based on the expectation that good alignment will result in minimal average disorientation between pixels in adjacent layers. After alignment of all ISE images using a convolution-based algorithm, the images were brought in coincidence with the orientation data. The final grain boundaries were obtained by employing an eroded orientation data volume combined with the 3-D Euclidean distance map of the image data volume as the starting input for a 3-D watershed algorithm. We will discuss the experimental and numerical methods developed for this approach.

2:40 PM

3D Visualization of Solid Phase Morphology during Solidification of Al-Cu Alloys in Unconstrained and Constrained Growth Conditions: *Demian Ruvalcaba-Jimenez*¹; Dmitry Eskin¹; Laurens Katgerman²; ¹Netherlands Institute for Metals Research; ²Delft University of Technology

Microstructure development during solidification has been studied in post-solidified samples and samples quenched during solidification. Visualization of microstructure has been done over 2D images. 2D images can accurately represent the structure if the morphology of phases is geometrically simple e.g. spheres. However, during solidification, growth and coarsening occur simultaneously developing complex morphologies of phases. Moreover, thermo-solutal gradients can be imposed asymmetrically during unconstrained growth solidification conditions affecting dendritic growth. Therefore, accurate representation of the microstructure under these conditions may only be archived by reconstructing it in 3D. In the present study, 3D visualization of microstructure development

during solidification is presented for unconstrained and constrained growth conditions. Quenching, serial sectioning and 3D rendering in the reconstruction of unconstrained growth (in Al-7 wt% Cu alloy) is discussed. Finally, partial 3D visualization is demonstrated by image processing for images taken in-situ during constrained growth of columnar dendrites (in Al-20 wt% Cu alloy).

3:00 PM

On the Direct Three Dimensional Characterization of Microstructural Features in α/β and β Ti-Alloys Using Robo.Met-3D and FIB: *Robert Williams*¹; Peter Collins¹; Hamish Fraser¹; ¹Ohio State University

Two techniques for the direct three dimensional characterization of microstructures, the Robo.Met-3D and the small dual-beam Focused Ion Beam (DB-FIB), have been used to characterize features present in α/β and β Ti-based alloys. The further development and expansion of these types of techniques is important, as many details of the microstructures are either misinterpreted or not observed when only considering classical two-dimensional projections. Examples at both length scales illustrating such cases will be shown, and compared with traditional stereological methods. As these techniques are seeing increased usage, it has become important to develop descriptions of the scale of features best observed using certain techniques, and how best to relate features observed using one technique (e.g., α -lath thicknesses in FIB) to features observed using the other (e.g., colony sizes using Robo.Met-3D). Finally, a direct comparison between reconstructions made of the same types of features using the different techniques will be presented.

3:20 PM Break

3:40 PM Invited

Application of 3D Microstructural Characterization to Dynamic Deformation and Damage: *John Bingert*¹; Veronica Livescu¹; Scott Dillard²; Lisa Dougherty¹; Daniel Worthington²; Pat Dickerson¹; Davis Tonks¹; ¹Los Alamos National Laboratory; ²University of California, Davis

The evolution of damage in polycrystalline materials from high-rate, dynamic deformation processes is a function of both the applied stress state and the material's microstructure and properties. Three-dimensional interrogation and quantification of damaged microstructures provides insight toward understanding the interaction between microstructure and the damage evolution process. This work investigates damage and deformation in materials under different conditions, including shocked, incipiently spalled tantalum and dynamically sheared 1018 steel. Serial sectioning by mechanical polishing and ion-beam milling were performed in order to reconstruct microstructures over a range of length scales. Electron backscatter diffraction was applied to investigate the relative levels of induced plasticity, revealing surprisingly contiguous and complex plastic linkages. The primary motivation of quantifying damage is to provide realistic input for, and validate, predictive damage models. Tantalum microstructural data were thus incorporated into a polycrystal plasticity finite element calculation, for which preliminary simulation results will be presented.

4:10 PM

Three-Dimensional Mesoscale Mechanical Modeling of a Beta Titanium Alloy: *Andrew Geltmacher*¹; Muhammad Qidwai²; Alexis Lewis¹; ¹Naval Research Laboratory; ²SAIC

The three-dimensional (3D) microstructure of a beta-Ti alloy (beta-21s) was characterized using serial sectioning and computerized 3D reconstruction. The reconstructed volumes, comprising hundreds of beta-Ti grains, provide information on grain morphology and crystallography. These 3D volumes contain experimental data derived from optical microscopy and Electron Backscatter Diffraction (EBSD). This data is input into 3D Image-Based Finite Element Models to analyze the spatial evolution of state variables, such as stress, strain and local plasticity in the microstructure under mechanical loading conditions. These models incorporate anisotropic elasticity, von Mises plasticity and/or crystalline plasticity to simulate the interactions between different microstructural features and mechanical behavior, and to determine which microstructural features serve as initiation sites of deformation and failure.

4:30 PM

Identifying Critical Features in a Beta-Ti Microstructure Using Image-Based Finite Element Modeling: Alexis Lewis¹; Muhammad Qidwai²; David Rowenhorst¹; George Spanos¹; Andrew Geltmacher¹; ¹Naval Research Laboratory; ²Science Applications International Corporation

Three-dimensional image-based finite element models were used to analyze stress and strain evolution in a 3D beta-Ti microstructure (beta-21s), obtained using serial sectioning. The simulation outputs and data from the reconstructed microstructures, including grain volume, true 3D grain shape, crystallographic orientation, 3D grain boundary networks, and distributions of grain boundary crystallographic normals are used to interrogate correlations between microstructural features and mechanical response. In this beta-Ti microstructure, high stresses and strains were observed at grain boundaries, and the morphological and crystallographic properties of these boundaries were analyzed to determine which factor(s) contribute to high local strains under a variety of loading condition.

4:50 PM

Full-Field Modeling of the Elastic Behavior of Foams Using Direct Input from Their Measured 3-D Structure: Ricardo Lebensohn¹; Anthony Rollett²; ¹Los Alamos National Laboratory; ²Carnegie Mellon University

A formulation based on Fast Fourier Transforms (FFT) for the calculation of the micromechanical behavior of heterogeneous materials has been adapted to predict the local elastic fields and the effective elastic properties of foams using direct voxelized input from their actual 3-D structure. In this presentation we show an application of the FFT-based model to prediction of the elastic behavior of carbon foams of about 90% porosity under uniaxial tension. The 3-D microstructure used as input was obtained by serial sectioning and light microscopy. The model predicts local stress concentrations along ligaments oriented longitudinally with respect to the applied load and an effective Young modulus consistent with experimental measurements.

5:10 PM

Three-Dimensional Reconstruction of Metallic Microstructures for Uncertainty Representation and Propagation in Finite Element Simulations of Local Mechanical Behavior: Andrea Keckl¹; ¹Arizona State University

Prediction of scatter on the mechanical behavior of metallic materials due to microstructural heterogeneity is quite important in a variety of scientific and technological applications. Three-dimensional (3D) representations of microstructures of 2xxx Al alloys are created via a combination of dual-scale serial sectioning techniques, with a smaller scale for particles and a larger scale for grains, and available microstructure reconstruction software. Basic statistics are measured from the 3D reconstructions, which are also used to create finite element meshes. Comparisons are made between statistics obtained from 2D and 3D reconstructions and criteria to find the smallest RVE needed for an example application are addressed. In addition, stochastic homogenization methodologies to propagate the uncertainty from the micro- to the meso-scale based on these reconstructions are discussed. Work funded by a Structural Health Monitoring MURI, Department of Defense AFOSR Grant FA95550-06-1-0309, Victor Giurgiutiu program manager.

5:30 PM

Three-Dimensional (3D) Microstructure Visualization and Finite Element Modeling of Deformation and Crack Growth in Particle Reinforced Metal Matrix Composites: Nikhilesh Chawla¹; ¹Arizona State University

The mechanical behavior of materials is inherently controlled by micro-structure. In particular, composite materials, consisting of two or more components or phases, have highly complex microstructures. This makes modeling of the mechanical behavior a challenge. We have developed a three dimensional (3D) approach to (a) construct a "virtual microstructure" in 3D by serial sectioning technique, and (b) finite element modeling using the 3D microstructure as a basis. In this talk the fundamentals of the 3D virtual microstructure modeling methodology will be explored. This methodology was used to study the deformation behavior of SiC particle reinforced metal matrix composites. The role of second phase fraction, morphology, and aspect ratio on deformation was quantified and will be discussed. The 3D crack growth behavior of the composites was modeled using finite element modeling. Results from the microstructure-based 3D simulations were found to be in good agreement with experimental observations.

Alumina and Bauxite: Bauxite

Sponsored by: The Minerals, Metals and Materials Society, TMS Light Metals Division, TMS: Aluminum Committee

Program Organizers: Sringeri Chandrashekar, Rio Tinto Aluminium Limited; Peter McIntosh, Australus Management Services

Tuesday PM

Room: 296

March 11, 2008

Location: Ernest Morial Convention Center

Session Chair: Everett Phillips, Cytec

2:00 PM Introductory Comments

2:05 PM

Chinese Bauxite and Its Influences on Alumina Production in China: Songqing Gu¹; ¹Zhengzhou Research Institute of Chalco

It is shown in this paper that the main bauxite deposit in China is located in such central and south-west provinces as Shanxi, Henan, Guizhou and Guangxi provinces etc. The chemical and mineralogical composition of various Chinese bauxites is reviewed to present the characteristics of the Chinese bauxites, which have great influences on the alumina production process, key technology and equipment applied in China.

2:30 PM

Alunorte Bauxite Dewatering Station - A Unique Experience: Ayana Oliveira¹; Juarez De Moares¹; Jorge Lima¹; ¹Alunorte-Alumino Do Norte Do

Alunorte concluded the expansion 2 project increasing the installed production capacity from 2.5 for 4.3 mi t/y in 2006, through new 2 lines. Bauxite supplying for the new lines was conceived using pipeline from the mine to the refinery. With a length of 242 km and a diameter of 24", the pipeline carries bauxite slurry with 50% solid concentration and a density of 1.45 Kg/dm³. This slurry is received in a distribution station and pumped for the dewatering station, where this slurry is dewatered through five hyperbaric filters, aiming to reduce the moisture content to about 12 to 14%. This paper aims to present the start-up and the process improvement at the hyperbaric filters, which made possible the operational conditions for the first unit of bauxite dewatering in the world that is being replicated in the next expansion, scheduled to start-up in 2008.

2:55 PM

A New Method Using Hydraulic Excavator and Tractor on Paragominas Bauxite Mine: Octávio Guimarães¹; Henrique Santos¹; Hildegundes Silva¹; ¹Companhia Vale do Rio Doce

The Paragominas bauxite mine (CVRD) started its operation in 2007 and has 303.000.000 metric tones of dry washed bauxite. It's the first bauxite mine that uses an ore pipe (pipeline) in the world. The continuous flat tabular bauxite deposit, averaging 1.59 m thick, under an overburden that averages 11.45 m, characterizes the geometry of the operation. The mining sequence consists of deforestation, waste stripping, excavation, loading and transporting the bauxite. The mining operation has two major conditions to consider: a high stripping ratio (7.6 in volume) and a high rainfall, thus it is necessary to have a mining system that is conducive to waste stripping and ore selectivity. This paper describes the system developed to achieve these goals using hydraulic excavators and bulldozers for waste stripping, and hydraulic excavators and trucks for ore production.

3:20 PM

Design and Operation of the World's First Long Distance Bauxite Slurry Pipeline: Ramesh Gandhi¹; Michael Weston¹; Maru Talavera¹; Geraldo Brittes²; Eder Barbosa²; ¹Pipeline Systems Incorporated; ²Companhia Vale do Rio Doce

Mineração Bauxita Paragominas (MBP) is the first long distance slurry pipeline transporting bauxite slurry. Bauxite had developed a reputation for being difficult to hydraulically transport using long distance pipelines. This myth has now been proven wrong. The 245-km- long, 10 MT/y capacity MBP pipeline was designed and commissioned by PSI for CVRD. The pipeline is located in the State of Para, Brazil. The Miltonia bauxite mine is in a remote location with no other efficient means of transport. The bauxite slurry is delivered to Alunorte Alumina plant located near Barcarena. This first of it's

kind pipeline required significant development work in order to assure technical and economic feasibility. This paper describes the technical aspects of design of the pipeline. It also summarizes the operating experience gained during the first year of operation.

3:45 PM Break

4:00 PM

Bauxite to Gallium - The Electronic Metal of the Twenty-First Century: Chitta Mishra¹; M. Nair¹; ¹National Aluminium Company Limited

Alumina is produced from Bauxite using Bayer Process where alumina present in Bauxite reacts with aqueous caustic soda to form sodium aluminate. The sodium aluminate solution, or Bayer liquor, is continuously recycled; this results in equilibrium concentration of 100ppm to 125ppm Gallium in the liquors. A bleed stream is separated from the liquor for extraction of Gallium. Gallium is a strategic metal and has been gaining world wide importance by virtue of its application in the electronic industries. NALCO have plans for setting up of a 7TPA Gallium Extraction Plant (99.99%/99.999% purity) from Bayer liquor of its Alumina Refinery utilizing the eco-friendly Ion-exchange Resin technology of Nippon Light Metal, Japan. Extraction of Gallium from NALCO's Bayer liquor containing 120ppm of Gallium have been successfully completed both in the laboratory and pilot plant scales and preparation of Techno- Economic Feasibility Report for commercialization of the technology is underway.

4:25 PM

Behaviour of Beryllium in Alumina Production from Bauxites by Bayer Process and Development of Reliable Method of Its Determination: Andrey Panov¹; Alexander Suss¹; Irina Paromova¹; Olga Shipova¹; Natalia Kutkova¹; ¹Russian National Aluminium-Magnesium Institute

The matter of beryllium have been raised recently with the aim to toughen beryllium standards in aluminium smelting area. Now the work group of the International Aluminium Institute is engaged in investigation of this problem and developing reliable method for Be determination. In the way of the study optimum conditions of beryllium determination in bauxite by mass spectrometry (ICP MS) method have been found. Principle possibility beryllium determination by spectrophotometry has been shown with the detection limit of about 0.1 ppm. Two methods of bauxite and red mud decomposition for mass-spectrum analysis for reliable beryllium determination and two methods of bauxite and red mud decomposition for spectrophotometric analysis have been developed. During investigation of beryllium behavior in Bayer process, effect of temperature, digestion time and presence of impurities on solubility of beryllium has been checked that give us possibility to forecast behavior of Be in Bayer process.

4:50 PM

Impact of Jamaican Bauxite Mineralogy on Plant Operations: Desmond Lawson¹; Lawrence Andermann²; Austin Mooney¹; Ab Rijkeboer³; ¹West Indies Alumina Company; ²SNF Holding Company; ³Rinalco B. V.

Over the period 2003 to 2006 the bauxite feed to the Kirkvine refinery has undergone a dramatic change in composition with severe impact on plant performance. Surprisingly, the change in composition is not directly evident from the XRF analysis of the major elements, which showed that the total Al₂O₃, Fe₂O₃ and LOI contents of the bauxite remained largely unchanged. A more detailed examination however, shows a remarkable change in Al₂O₃ distribution over the various minerals, indicative of a substantial change in bauxite mineralogy. Over the same period significant changes in plant behaviour were experienced with respect to, notably alumina recovery, mud settling and liquor chemistry.

Aluminum Alloys: Fabrication, Characterization and Applications: Alloy Characterization

Sponsored by: The Minerals, Metals and Materials Society, TMS Light Metals Division, TMS: Aluminum Committee

Program Organizers: Subodh Das, Secat Inc; Weimin Yin, Secat Inc

Tuesday PM

Room: 293

March 11, 2008

Location: Ernest Morial Convention Center

Session Chairs: Subodh Das, Secat Inc; Weimin Yin, Secat Inc

2:00 PM

Crystallographic Texture Development of Aluminum Alloy Sheet under Single and Multipass In-Plane Stretching: Stephen Banovic¹; Mark Iadicola¹; Tim Foecke¹; ¹National Institute of Standards and Technology

Increasing gas mileage has been one of the driving forces to reduce overall automotive vehicle weight. By replacing conventional steel sheet metal with lightweight materials, specifically aluminum alloys, this objective can be realized. Towards achieving this goal, research has been initiated to measure the multiaxial flow curves of commercially available aluminum sheet. An important aspect to understanding the mechanical behavior of the sheets is the associated microstructural description of the deformed materials. This talk will focus on the microstructural evolution of various aluminum alloys using x-ray diffraction techniques, to discern crystallographic texture, on single and multipass in-plane stretchings. The observed changes in texture, as a function of plastic strain level and strain state, will be discussed with respect to plastic constraint and compared to measured multiaxial flow surfaces.

2:20 PM

Formation of P Orientation {011}<566> in Cold Rolled Continuous Cast Al-Mn-Mg Alloy with and without Pre-Heat Treatment Followed by Annealing: Qiang Zeng¹; Xiyu Wen¹; Tony Zhai¹; ¹University of Kentucky

The development of microstructure and crystallographic macrotexture of the cold rolled continuous cast Al-Mn-Mg alloy hot band with different pre heat treatment conditions after annealing was investigated. It was found that the intensity of P orientation depends on the size and density of precipitates and the cold rolling reduction. The specimen with the very fine and well distributed precipitates can generate strong P orientation in high cold rolling reduction. TEM observation showed that the very fine precipitates exert a very effective pinning effect on dislocation and subgrain boundaries, which would be the reason for the strong P orientation. The samples with the higher volume fraction of P orientation yielded an inferior mechanical property. EBSD results revealed that P orientated grains were coarser and more elongated. The higher volume fraction of P component, the more coarse and elongated grains were generated, which would be the reason for the inferior mechanical property.

2:40 PM

Effect of Alloying Elements on the Segregation of Complex Phases in A356 Alloy Adding Mg, Cu, Ni and Sr as Modifier, Using Thermal Analysis and Characterization Microstructural: Aline Hernandez-Garcia¹; Alejandro García-Hinojosa¹; ¹National Autonomus University of Mexico

The properties in cast conditions could be increased if adequate alloying elements are added and also treatment in liquid phase (modification) is applied. This will turn the base alloy in multicomponent with the formation of new and complex phases. The fraction, morphology and distribution of these new phases control of the microstructure will have an important impact in the development of new mechanics properties. This work studied the effect of the Cu, Mg and Ni alloying elements add to A356 alloy and modified with Sr. The complex alloys were analyzed using thermal analysis, metallographic etching qualitative-quantitative, with support of image analysis and scattering electron microscopy (SEM.EDS). The metallographic analysis was confronted with the predicted by the commercial software Thermocalc. Finally tensile properties and hardness were evaluates to explain the effect of the alloying elements. The better properties were reached for the Al-7Si-1.5Cu-1Mg-0.5Ni cast alloy modified with Sr.

2:55 PM

Investigation into Phase Relations in the Aluminum-Boron System:*Dominick Bindl*¹; ¹University of Minnesota

This research project was conducted with the aims of placing thermal constraints on the stabilities of both aluminum diboride and aluminum dodecaboride phases for use as reinforcements in aluminum MMCs. DTA, TGA, XRD and optical microscopy analysis techniques were utilized to track phase changes through thermally varied isothermal castings. From this project it was seen that there is a transition tentatively identified as the formation of gamma-AlB₂-12 with an onset ~ 900°C as identified with Muffle Furnace heating and observed at 1010°C when seen in DTA trials. AlB₂ was observed to oxidize preferentially over dodecaboride phases with a hexagonally configured Al₂O₃ oxide. This research serves to anticipate further research into targeted aluminum dodecaboride formation and stabilization for use as aluminum MMC reinforcement.

3:10 PM

Subgrain Coarsening of Aluminum Alloy AA 5005 by In-Situ EBSD*Observations: Shengyu Wang*¹; Anthony Rollett¹; ¹Carnegie Mellon University

The subgrain structure of hot rolled aluminum alloy AA 5005 has been characterized on as-received samples using Electron Backscatter Diffraction (EBSD). However, to observe the actual microstructural evolution during recrystallization at elevated temperatures, hot stage EBSD has been implemented to capture in-situ development of the subgrain structure at the initial recrystallization stage. The in-situ results will be compared with current Monte Carlo simulation results, which are based on experimental data fitted 3D microstructure and textures with anisotropic grain boundary properties discriminating high angle grain boundaries, low angle grain boundaries and some special grain boundaries. The main objective of this study is to understand the circumstances under which we can expect abnormal (sub-)grain growth leading to nucleation of recrystallization. Therefore the results are compared to simulations of subgrain coarsening with initial (unrecrystallized) structures obtained by statistical reconstruction.

3:25 PM Break

3:35 PM

Fatigue of Extruded AA6063: *Nick Nanninga*¹; Calvin White¹; ¹Michigan Technological University

The effect of orientation as well as of extrusion seam and charge welds on the fatigue life of specimens from a hollow AA6063 alloy extrusion profile have been characterized in the form of S-N curves. Specimen orientation with respect to the extrusion direction has a large effect on fatigue life. Transverse specimens exhibit only a fraction of the high cycle fatigue life exhibited by longitudinal specimens. At lower stress levels, transverse specimens with seam and/or charge welds oriented transverse to the loading direction exhibited less than half the fatigue life of transverse specimens not containing welds. Specimens, with and without welds present, loaded 45 degrees with respect to the extrusion direction, display only moderate reductions in fatigue life. The variations in fatigue life are explained by surface roughness and variations in microstructure.

3:55 PM

Effect of Die Line Roughness on the Fatigue Life of Extruded AA6082: *Nick Nanninga*¹; Calvin White¹; ¹Michigan Technological University

To better understand the relationship between extrusion die line features and fatigue behavior, the fatigue life of polished and as-extruded specimens taken from a hollow extruded AA6082 profile have been characterized in the form of S-N curves. As-extruded specimens, taken transverse to the extrusion direction, i.e. containing die lines transverse to the loading direction, exhibit fatigue lives that are less than ten percent of those for longitudinal specimens at low stress levels. Transverse specimens containing seam welds show even slightly shorter fatigue lives. Transverse specimens that have been polished to remove die lines exhibit fatigue lives comparable to longitudinal specimens. Surface roughness of specimens with and without seam welds was characterized with standard profilometry techniques. Actual profilometer surface scans were used to create FEA models for evaluating stress concentrations associated with die lines, which appear to largely explain the reduced fatigue life of as-extruded transverse specimens.

4:15 PM

Effect of Si Distribution on the Fracture Toughness of A356 Aluminum Alloys: *Yong Nam Kwon*¹; Kyuhong Lee²; Sunghak Lee²; J.-H. Lee¹; ¹Korea Institute of Materials Science; ²Pohang University of Science and Technology

Correlation of microstructure with mechanical properties of cast A356 alloys was investigated in this study. Three processes used for this study were low-pressure-casting, rheo-casting and casting-forging. Their mechanical properties and fracture toughness were analyzed in relation with microfracture mechanisms. All the cast A356 alloys contained eutectic Si particles segregated along solidification cells. Distribution of Si particles could be modified by casting-forging processes. Microfracture observation results showed that eutectic Si particles were cracked first, but that the aluminum matrix played a role in blocking crack propagation. Tensile properties and fracture toughness of the cast-forged alloy were superior to those of the low-pressure-cast or rheo-cast alloy according to the matrix strengthening and homogeneous distribution of eutectic Si particles due to forging process.

4:35 PM

Effect of Si on the Particle Structure in Mn-Containing Aluminium Alloys:*Tanja Pettersen*¹; Yanjun Li¹; Trond Furu¹; ¹Hydro Aluminium

During casting and homogenisation of aluminium the microstructural fundament for further processing is made. Particle structure (dispersoids and primary particles), grain structure and level of elements in solid solution govern the mechanical and annealing properties of the material. The chemical composition, casting and homogenisation of the material constitute the first part of the processing chain and are crucial in controlling the properties of the material. In 3xxx-alloys, Mn in solid solution and Mn-bearing dispersoids formed during homogenization has an important impact both on grain size and texture of the rolled material. Other elements, such as Si, will have an influence on the formation of dispersoids.^{1,2} In the present investigation, a 3xxx-alloy, and modified versions of this alloy, have been investigated. The content of Mn, Si and Fe has been varied, various homogenisation procedures have been performed and the resulting material has been studied. Electrical conductivity and hardness have been measured and microstructural investigations have been undertaken. The results include the effect of Si on the solid solution level of Mn, and the effect of Si on the precipitation of dispersoids. A microstructural homogenisation model^{3,4} has also been applied to predict the development with temperature and time. ¹A. Dons, Y.Li, C. Marioara, C. Simensen, A. Johansen, S. Benum, Aluminium, Vol. 80 (2004) pp 583-587. ²G. Hausch, P. Furrer, H. Warlimont, Z. Metallkunde, 69 (1978) p. 174. ³A. Håkonsen, D. Mortensen, S. Benum, T. Pettersen, T. Furu, Light Metals 2002, pp 793-800. ⁴Y.J. Li, A. Håkonsen, D. Mortensen, T. Pettersen, T. Furu, Material Science Forum Vols. 519-521 (2006) pp 297-302.

4:55 PM

Fatigue Behavior of Cast A319-T7 Aluminum Alloy: *Younghwan Jang*¹; Sangshik Kim¹; Jeonghwan Roh²; Gyejeong Lee²; Yoo In Jeong³; ¹Gyeongsang National University; ²ACK Company, Ltd; ³Korea Aerospace Industries, Ltd

The casting process inevitably produces defects, such as porosity and trapped oxide films, which are detrimental to the fatigue life. In this study, the effect of casting defects on fatigue behavior of cast A319-T7 aluminum alloy was investigated. Staircase fatigue test up to 10⁷ cycles was conducted at an R ratio of -1 and at room temperature and 150°C, respectively. The characteristics of casting defects on the fracture surface of fatigue tested specimens, particularly at the initiation sites, were quantitatively identified by using SEM and image analyzer. It was found that the fatigue life was greatly influenced by the size of casting defects. The fatigue endurance limit for A319-T7 alloy specimen appears to be controlled by maximum stress intensity factor encompassing casting defect area. The effect of casting defects on fatigue behavior of cast A319-T7 aluminum alloy was discussed based on the fractographic analysis.

5:10 PM

Effect of Pin Tool Geometry on Material Flow in Friction Stir Welding:*Joseph Querin*¹; Judy Schneider¹; ¹Mississippi State University

In this study AA2219-T87 panels were welded with three different pin tools. The pin tools were tapered and included 0 degree (straight cylinder), 30 degree, and 60 degree angles on the frustum. Friction stir welding (FSW) process parameters for each of the pin tool geometries were optimized to eliminate

internal defects. The affects of heat, strain, and strain rate were investigated by maintaining a constant heat input while varying the process parameters of spindle speed and travel speed. This was performed in an attempt to maintain a constant heating for the weld panels while altering the strain rate. Variations in the material flow were investigated by use of microstructural analysis including optical microscopy (OM), scanning electron microscopy (SEM), and orientation image mapping (OIM).

Aluminum Reduction Technology: Process Control

Sponsored by: The Minerals, Metals and Materials Society, TMS Light Metals Division, TMS: Aluminum Committee

Program Organizers: Martin Iffert, Trimet Aluminium AG; Geoffrey Bearn, Rio Tinto Aluminium Tech

Tuesday PM Room: 298
March 11, 2008 Location: Ernest Morial Convention Center

Session Chair: Geoffrey Bearn, Rio Tinto Aluminium Tech

2:00 PM Invited

Common Behavior and Abnormalities in Aluminium Reduction Cells: *Marco Stam*¹; Mark Taylor²; John Chen²; Albert Mulder¹; Renuka Rodrigo³;

¹Aluminium Delfzijl; ²University of Auckland; ³Heraeus Electro-Nite Company

The requirement of operating reduction cells at or beyond known performance limits is a new challenge for the aluminium industry. Most existing control systems are based on compensatory control actions with a short-term focus to move the controlled variable(s) back into the optimum region, and have independent strategies for alumina feeding and bath chemistry control. In order to incorporate natural cell behaviour into the control philosophy this paper investigates not only common cell behaviour, but also frequent cell abnormalities and failure mechanisms were studied. Statistical multivariate control surfaces, including alumina feeding, are presented for operating cells using three dimensional Hotelling T2 statistics. This approach allows a holistic decision making process on feeding, heat supply, compositional regulation and on troubleshooting cells. The liquid bath volume is an essential parameter control in control decisions, as is the bath superheat and liquidus temperature. These medium term state variations will be discussed as well.

2:20 PM

New Method of Measuring the Liquidus and Bath Temperature of Hall-Héroult Cells: *Hans Bohner*¹; V. Arora²; T.K. Nasipuri²; ¹K&T Engineers Ltd;

²Hamilton Research and Technology Pvt Ltd.

A procedure and equipment for measuring the liquidus and bath temperature of Hall-Héroult cells was developed and tested in PFPB pots at 65 and 185kA. Inconel-sheathed, reusable K-type thermocouples were inserted into stainless steel cups and immersed into the electrolyte for bath temperature measurement and withdrawn to obtain cooling curves. Undercooling was prevented by moving the thermocouple tip forth and back using a magnetically shielded electromotor. The liquidus temperature was determined electronically using the inflection point of the cooling curves or the "Noise" at the inflection point. The results in function of time and alumina feed rate indicate +/- 1°C temperature variation and were valid in 90% of all measurements (min. 16 pots and 120 measurements in each smelter). The cost of thermocouples is minimal as they can be used normally 100 times without deterioration.

2:40 PM

Analysis of a Potroom Performance Drift, from a Multivariate Point of View: *Jayson Tessier*¹; Carl Duchesne²; Gary Tarcy³; Claude Gauthier³; Gilles Dufour³; ¹Alcoa Deschambault; ²Laval University; ³Alcoa Inc

Analysis of reduction cells performance could be a hard task for process engineers. One has to handle many highly correlated variables, where time lags and missing values must be covered. Performing an efficient analysis of complex potroom data does not always lead to good answers, for example; when an important production drift occurs. It is often necessary to include anode and alumina quality, which makes the analysis harder. The complications associated with the analysis of such database have limited engineers to analyze few

variables at a time using univariate SPC charts, underutilizing the information hidden in extensive databases. In this paper, multivariate statistical analysis techniques are used to perform a combined analysis of potroom process data, anode and alumina quality. In this case study, the analysis is set up to investigate a specific drift in potroom performances, where time lag, anode residence time and correlation between many variables are encountered.

3:00 PM

Experimental Designs for Use in the Aluminium Industry: *Stephen Rutledge*¹;

¹Boyne Island Smelters Ltd

The use of designed experiments for process improvement has been well understood since Sir Ronald Fisher's "The Designs of Experiments" published in 1935. However the application of these designs in the aluminium smelter reduction process has proven to be difficult. This paper details the problems that are relevant to the reduction environment. It also puts forward two techniques to improve the chances of obtaining statically valid results from process improvement trials. The use of these techniques has allowed the rapid deployment of process changes in a variety of reduction lines and lead to significant improvements in performance, by destroying many of the myths that are common in the black art that is Aluminum smelting.

3:20 PM

Practical Applications of the Continuous Measurement of Individual Anode Currents in Hall-Héroult Cells: *Roald Hvidsten*¹; Ketil Rye¹; ¹Elkem Aluminium

Traditionally, the anode current distribution is found by manual measurement of voltage drops across a fixed length of the anode rods. These measurements take time and are normally performed once per day or less. Anode currents change rapidly however, due to anode burnoffs, spikes and deformations, instable metal pad or incorrect anode setting height. These deviations will normally not be discovered until the next routine measurement. An instrument for continuous monitoring and display of individual anode currents has been developed and used at Elkem Aluminium Mosjøen for some years. The instrument removes the need for manual measurements and a signal feed into the computer control enables incorporation of the anode current distribution in the pot control system. Some practical applications of the continuous measurement of anode currents are presented in this paper.

3:40 PM Break

3:50 PM

Experiments on Wireless Measurement of Anode Currents in Hall Cells: Daniel Steingart¹; *James Evans*²; Paul Wright²; Donald Ziegler³; ¹Wireless Industrial Technologies, Inc; ²University of California; ³Alcoa, Inc

The currents of individual anodes provide information on Hall cells, e.g. the occurrence of "metal roll". These currents are usually measured by voltage drops along anode rods but this is inconvenient for routine monitoring of pots because of the need to change anodes, plus the hazards of draping signal wires around. Experiments have been carried out on wireless measurement anode currents. Hall effect probes measured magnetic fields, reflecting mostly the current in the nearby rod. Signals were relayed wirelessly to a laptop some distance from the pot. Measurements have been carried out on both pots with pair-controlled anodes and pots with anodes on a fixed bridge. For the former, comparison with independent measurement is possible (from voltage drop along the anode flex). Although at the experimental stage, this investigation has served to show that wireless measurements agree roughly with other measurements; wireless measurements reveal metal roll and incipient anode effects.

4:10 PM

Smart Feeders at Alumar Plant: *Haroldo Ferreira*¹; Nilton Nagem¹; Antonio Coimbra¹; Camões Pereira¹; Roberta Camili¹; Pedro Leite¹; Merval Aguiar¹; Eliezer Batista¹; Elisio Bessa¹; Joel Camara¹; ¹Alumar

Alcoa is searching continuously for alternatives to eliminate or reduce the environmental impact caused by operations. Alumar, an Alcoa unit in Brazil has implemented a new project to reduce anode effects. This project is based on the change from the current point feeder to smart point feeder technology. This change in technology is based on the anode effect frequency root cause, which is feeder plunger (more than 85%). The smart feeder is more than a sensor on the feeders, there is a computer routine that alarms failures and compensates if

a feeder is not working properly. The test is on six pots and this group of pot shown around 50% anode effect frequency reduction. Other gains such as air consumption and noise reduction were archived.

4:30 PM

Breakthrough in Analysis of Electrolytic Bath Using Rietveld-XRD Method: Frank Feret¹; ¹Alcan Inc

A standardless Rietveld-XRD method was devised for quantification of crystalline phases in bath electrolyte specimens. The phases present in the bath material are: cryolite, chiolite, fluorite, NaCa1.5AlF7, NaCaAlF6, corundum and diaoyudaoite. Two commercial software were employed in Rietveld quantification. Numerous advantages of the Rietveld method are compared with the traditional calibration approach. Departure from the need for calibration curves improves determination reliability and accuracy of all mineralogical phases. 38 Alcan bath standards were quantified for the phase composition by the new method. The CaF2 concentrations were calculated using fluorite, NaCa1.5AlF7 and NaCaAlF6 and compared with CaF2 measured directly. The ExAlF3 concentrations were calculated using chiolite, NaCa1.5AlF7 and NaCaAlF6. The Rietveld-XRD determined ExAlF3 concentrations agree to within $\pm 0.35\%$ with corresponding concentrations determined by wet chemistry. As a primary and universal method for determination of the phase composition in electrolytic bath the Rietveld-XRD method is replacing existing methodology in plant laboratories.

4:50 PM

Model Predictive Control of Superheat for Prebake Aluminum Production Cells: Zeng Shuiping¹; Li Jinhong¹; ¹North China University of Technology

Model Predictive Control (MPC) of superheat was investigated for 300kAprebake aluminum production cells. The control includes a predictive model, error feedback, and timely optimisation actions. The mathematical model was set up based on previous work and industrial experiments. It can predict bath temperature and bath liquidus temperature from the AlF3 additions, aluminum tapping magnitude and cell voltage set-point. The superheat in the production is measured and the difference between the measurement and prediction and its change rate are used to correct the parameters in the predictive model. If the average error and error change rate within a period are above a set value, the optimum program activates. This method has been used in the Hope Aluminum Company in Inner Mongolia for 3 months. Both current efficiency and DC energy consumption have visibly improved.

5:10 PM

The Application of Data Mining at the National Aluminum Test Base: WangXing Li¹; QingYun Zhao¹; ShiLin Qiu¹; Qiang Li¹; ¹ZhengZhou Research Institute of CHALCO

At the National Aluminum Test Base (NATB, which is subordinate to Zhengzhou Research Institute of CHALCO), we have used data mining technology to settle some problems and achieved many improvements. In this paper, the application of this technology to lengthening the life of the cell, intensifying current, lowering cell voltage, reducing AE and increasing CE is described. So far, we have gained many achievements: current is intensified by 7%, energy consumption decreased by 500 kW.h/t-Al, the anode effect rate below 0.03 AE/cell.day, and the CE enhanced by 1% at least. There are many other data mining methods, but in this paper we just use some clear figures and tables to show you the usage and effectiveness of data mining. The use of data mining, combined with the good operating practice, can provide guidance for the optimizing of technical parameters.

5:30 PM

Re-Discussion of Alumina Feeding Control Strategies: Qi Xiquan¹; ¹Northeastern University Engineering and Research Institute, Company, Ltd.

Abstract: For alumina feeding control, many strategies have been adopted to keep a reasonable content range for high current efficiency and low anode effect frequency. Meanwhile, control strategies should be reflected by the historical curve on the supervising computer, which can be used to diagnose and analyze cell condition. In our opinion, a better control strategy should be characterized with lower daily RC times and reasonable feeding cycle duration. Based on this, some new ideas are incorporated into newly upgraded systems which showed rather better results. In this paper, new control philosophies are

described systematically. Criteria to judge pot stability and control results as well as optimal daily RC times are put forward too.

5:50 PM

The Importance in Keeping the Pots on the Bath Ratio Target for Pot Line Stability: Thiago Simões¹; João Alberto Martins¹; Marcio Guimarães¹; João Reis¹; ¹Novelis

The potline performance is completely dependent on pots stability that can be evaluated by pot resistance variation. Talk about pot stability is to think in reduce process parameters deviation. In the present case we tried to reduce pot resistance oscillation having in mind that to reduce variation of the output response it is necessary to reduce the variation of the inputs variables. Focusing on only one input factor of this process, the present paper has the objective to discuss the importance in keeping the pots on bath ratio target range for the potline stability. It is a practical work that shows a discussion on Novelis process team experience based on statistical analyses and using the Six Sigma concepts.

Aqueous Processing - General Session: Aqueous Processing General Abstracts

Sponsored by: The Minerals, Metals and Materials Society, TMS Extraction and Processing Division, TMS: Aqueous Processing Committee
Program Organizer: Michael Free, University of Utah

Tuesday PM

March 11, 2008

Room: 281

Location: Ernest Morial Convention Center

Session Chair: Shijie Wang, Kennecott Utah Copper Corporation

2:00 PM

Alternative Leaching Processes for Cobalt Oxide Minerals: Cesare Ferroni¹; Philippe Henry²; ¹HydroProc; ²Hydrometal

Acidic dissolution of cobaltic oxide minerals require reducing conditions. Typically, reducing conditions are generated by using sulphur dioxide in a gaseous form or equivalent. The use of SO2 compounds can lead to serious health/safety issues, and can affect the recovery of other metals, namely copper. Alternative processes to dissolve cobaltic oxide minerals are presented here that overcome these two issues. The first alternative consists in using ferrous iron as the reductant, while the second process involves cathodic reduction of the cobaltic ion in a special design cell. Examples are provided for both alternatives.

2:25 PM

Continuous Circuit Production and Accelerated Ageing of Iron(III)-Arsenic(V) Coprecipitates - Probing Process-Stability Relationships: Richard De Klerk¹; George Demopoulos¹; ¹McGill University

The standard industrial method of arsenic removal from acidic aqueous processing effluents involves coprecipitation of arsenic with ferric iron (Fe/As>3) by lime neutralization in continuous circuits. To better understand current industrial practice, continuous circuit coprecipitation experiments were performed to identify industrially relevant process parameters and admixtures that contribute to improved arsenic removal and retention. The coprecipitated solids were subjected to accelerated ageing at 20°, 40° and 70°C and arsenic behavior was monitored and modeled. Staging and the presence of calcium ions were found to have the most significant impact on arsenic retention. In this paper the techniques used and major results obtained are discussed.

2:50 PM

Field-Deployable Aqueous Lead Analysis Using Nanoband Electrode System and Use of Green Rust for Its Removal: Jewel Gomes¹; David Cocke¹; Manohar Miryala¹; Hector Moreno¹; Eric Peterson¹; Dan Rutman¹; ¹Lamar University

Lead has long been an USEPA priority pollutant and an important environmental and health concern because of its toxicity at ppb levels. In light of health and exposure data for lead, the EPA has set standards for Maximum Contaminant Level (MCL) and MCL Goal (MCLG) as 15 ppb and 0 ppb, respectively. An accurate and rapid measurement of lead in the field remains still a technical challenge. In this work, a relatively new method deploying a nanoband electrode

system using anodic stripping voltammetry has been optimized by changing deposition potential, electrolyte, and plating time used for the measurement of Pb(II) in water samples. Green rust has been proven to be an efficient intermediate matrix for removal of lead contaminants. We also reported here the removal efficiency of lead using green rust produced by electrocoagulation directly and indirectly. Lead containing floc was also characterized through XRD, SEM, and EDAX techniques.

3:15 PM Break

3:35 PM

The Influence of Chloride Ion to the Biooxidation of Arsenic Bearing Gold Concentration: *Dawen Wang*¹; Hongying Yang¹; Changliang Zhu¹; Huanjie Jiang¹; ¹Northeastern University

During the process of arsenic bearing gold concentration biooxidation, the content of chloride ion in water is a very important factor to the activity of bacteria and the oxidation of sulfide minerals. In this paper, the influence of underground mine water with different chloride ion content to the biooxidation of arsenic bearing gold concentration and the limit of chloride ion content to bacteria were summarized. These results indicated if the content of chloride ion was less than 1.2g/L, the bacteria's ability to oxidize sulfide minerals was little affected, and if the content of chloride ion were increased to 2g/L or more, the activity of bacteria was seriously restrained, and if the content of chloride ion were increased to 4g/L, the activity of bacteria was absolutely restrained.

4:00 PM

Hydrochloric Acid Leaching of Panzhihua Ilmenite for Preparation of Synthetic Rutile: *Jilai Xue*¹; Zengjie Wang¹; Haibei Wang²; Xunxiong Jiang²; ¹University of Science and Technology; ²Beijing General Research Institute of Mining and Metallurgy

Investigation on hydrochloric acid leaching of the ilmenite from Panzhihua, China was carried out to prepare synthetic rutile. Various leaching parameters were optimized to obtain high content of TiO₂ in the products. The experimental data suggest that an optimum leaching can be realized with 30% acid, a solid/liquid ratio of 1/4 at 95°C, and ore ground for -400 mesh size. Kinetic data of the leaching was found to follow the spherical model $f(a)=1-(1-a)^{1/3}$, and the apparent activation energy was calculated as 47.21 KJ/mol. After the acid leaching, an additional alkaline leaching process using hot NaOH solution was performed, and then the products was heat treated at 900°C in order to extract Si and increase the particle size of synthetic rutile. The final product has a high content of TiO₂ (about 95%), a low content of chlorine consuming elements (total CaO+MgO =0.07%) and a suitable particle size distribution for chlorination process.

Biological Materials Science: Scaffold Biomaterials

Sponsored by: The Minerals, Metals and Materials Society, TMS Structural Materials Division, TMS: Biomaterials Committee, TMS/ASM: Mechanical Behavior of Materials Committee

Program Organizers: Ryan Roeder, University of Notre Dame; Robert Ritchie, University of California; Mehmet Sarikaya, University of Washington; Lim Chwee Teck, National University of Singapore; Eduard Arzt, Max Planck Institute; Marc Meyers, University of California, San Diego

Tuesday PM
March 11, 2008

Room: 390
Location: Ernest Morial Convention Center

Session Chair: Roger Narayan, University of North Carolina and North Carolina State University

2:00 PM Invited

Composites and Scaffolds for Calcified Tissue Regeneration: *Antoni Tomsia*¹; ¹Lawrence Berkeley Laboratory

Despite extensive efforts in the development of fabrication methods to prepare porous ceramic scaffolds for osseous tissue regeneration, all porous materials have a fundamental limitation - the inherent lack of strength associated with porosity. Shells (nacre), tooth and bone are frequently used as examples for how nature achieves strong and tough materials made out of weak components. The

objective of this study was to mimic the architecture of natural materials in order to create a new generation of strong hydroxyapatite-based porous scaffolds. The porous inorganic scaffolds were fabricated by the controlled freezing of water-based hydroxyapatite slurries. The scaffolds obtained by this process have an ordered and homogeneous lamellar architecture that exhibits striking similarities with the meso- and micro- structure of the inorganic component of nacre. These biomimetic scaffolds could be the basis for a new generation of porous and composite biomaterials.

2:30 PM Invited

Novel Scaffolds for Bone Tissue Engineering: *Fergal O'Brien*¹; Matthew Haugh¹; Claire Tierney¹; ¹Royal College of Surgeons in Ireland

Tissue engineering relies extensively on the use of porous scaffolds to provide the appropriate environment for the regeneration of tissues and organs. Collagen-GAG scaffolds have shown excellent potential as a scaffold on which to culture cells and produce extracellular matrix. However, the scaffolds have limitations for bone tissue engineering, most notably, the mechanical properties of the scaffold are currently not suitable for use as a bone graft. In this study we sought to develop the optimal scaffold for bone tissue engineering by varying: (i) the crosslinking density to improve the mechanical properties of the scaffolds and (ii) the collagen and GAG content to investigate their effect on osteoblast viability. The results indicate that the use of crosslinking leads to a substantial increase in scaffold modulus while a 1% collagen and 0.2% GAG scaffold composition provides the best environment for osteoblast proliferation and bone formation. Acknowledgements: Science Foundation Ireland.

3:00 PM

Porous PLLA:PGA:PVA Scaffolds for Tissue Engineering: *Mayur Uttwarwar*¹; Ashwin Nair¹; Liping Tang¹; *Pranesh Aswath*¹; ¹University of Texas at Arlington

In this study highly porous scaffolds were prepared by emulsion freeze dry method. PLLA:PGA (85:15) in chloroform solution was blended with PVA in a water solution. Four combinations of the scaffolds were obtained by varying blender speed and PVA concentration. The resultant scaffolds exhibited highly porous, interconnected structure with porosity more than 90%. The viability of scaffolds for cells attachment and growth was studied in vitro by culturing mouse 3T3 fibroblast cells for one week. The cells were quantitatively determined by following MTT assay. The attachment and location of the cells on the scaffolds was determined by florescent microscopy and SEM. The study gave important information about the pore size, porosity, pores distribution and the relative effect of these variables on cells behavior with scaffolds. The potential use of scaffolds fabrication method for tissue engineering with emphasis on growth factor release and controllable design is also discussed.

3:20 PM

Hydroxyapatite Whisker Reinforced Polyetherketoneketone for Bone In-Growth Scaffolds: *Gabriel Converse*¹; Ryan Roeder¹; ¹University of Notre Dame

Porous scaffolds are of interest for orthopaedic implant fixation. The scaffold should have porosity that promotes bone in-growth and mechanical properties sufficient to withstand physiological loads. Additionally, the scaffold biomaterial should be biocompatible, bioactive and amenable to providing osteoinductive growth factors. In order to meet these criteria, polyetherketoneketone (PEKK) was reinforced with 20-40 vol% hydroxyapatite (HA) whiskers. 40 vol% reinforcement resulted in an elastic modulus (17.9 GPa) and ultimate tensile strength (82.0 MPa) within the ranges reported for human cortical bone. Composites were loaded in four-point bending fatigue to 30 MPa for one million cycles without failure. Finally, HA whisker reinforced PEKK scaffolds with 75-90% porosity and 0-40 vol% HA whiskers were prepared using a particle leaching technique. HA whiskers were embedded within the polymer struts to act as reinforcement and were also exposed on the surface of polymer struts to promote growth factor retention and tissue attachment.

3:40 PM Break

3:50 PM Invited

Novel Polymer-Reinforced Calcium Phosphate Cement as Mesenchymal Stem Cell Carrier: Daniel Alge¹; W. Goebel²; Tien-Min Chu²; ¹Purdue University; ²Indiana University

Novel hydroxyapatite-based calcium phosphate cements reinforced with PLLA-based monomers have shown significant improvements in mechanical properties. In this study, we investigated the feasibility of using polymer-reinforced calcium phosphate cement (PRCPC) as a potential carrier for mesenchymal stem cells (MSCs). Rat MSCs were isolated from the femur bone marrow of Sprague-Dawley rats. CPC with starting ceramic powder ratio of hydroxyapatite: monocalcium phosphate monohydrate = 2:0.5, 2:1, 2:3, and 2:5 were reinforced with 5% PLLA and were seeded with MSCs. The cell proliferation profiles of the MSCs on the CPC with and without reinforcement were characterized. Three-dimensional PRCPC cubes with interconnected channels were seeded with MSCs and implanted subcutaneously on the backs of Sprague-Dawley rats for two weeks. The in vitro characterization through MTT assay and in vivo characterization by histology and micro-CT will be presented. The potential of using three-dimensional PRCPC as scaffold for MSC carrier will be discussed.

4:20 PM

Porous Chitosan Scaffolds and Chitosan-Clay Nanoparticle Carrier for Advanced Drug Delivery Systems: Wah Thein-Han¹; Y. Kitiyanant¹; Devesh Misra²; ¹Mahidol University, Institute of Science and Technology; ²University of Louisiana

In the advanced drug delivery and in tailored tissue engineering, modified chitosan nanoparticles and porous biodegradable three dimensional chitosan scaffolds are potential biomaterials for the improvement of drug and cell delivery systems. Chitosan nanoparticles incorporated with medical clay, montmorillonite (MMT) and chitosan scaffolds of different degree of deacetylation (DD) were prepared by emulsion/solvent evaporation approach and combination of freezing and lyophilization methods, respectively. We describe here the physico-chemical analysis of nanoparticles and scaffolds. The studies suggest that the properties of chitosan-MMT nanoparticles and chitosan scaffolds have potential for drug delivery system.

4:40 PM

Resorbable Polymer Nanocomposites as Structural Tissue Engineering Constructs and Bone Graft Substitutes: Kevin Baker¹; Rangaramanujam Kannan²; ¹William Beaumont Hospital; ²Wayne State University

The development of biocompatible scaffolds is an area of intense research as tissue engineering-based solutions to orthopaedic surgical procedures gain popularity. Several techniques, including thermal induced phase separation, particulate leaching and gas foaming have been used to create porous polymer constructs. However, the maximum compressive strengths reported by researchers, render these constructs unsuitable for most load bearing applications. Addition of bioceramic fillers to the scaffolds have resulted in only modest gains in mechanical strength. Utilizing a supercritical-CO₂ (scCO₂) process, we have synthesized a novel, resorbable polymer nanocomposite (RPN), which consists of nanostructured Montmorillonite clay particles dispersed in a resorbable polymer matrix. Synthesis by the scCO₂ process imparts a porous architecture to the RPN constructs with a bimodal distribution of pore sizes (100-250µm, 10-50µm). The uniform dispersion of nanostructured clay particles achieved by scCO₂ processing reduces polymer chain mobility, leading to enhanced static and dynamic mechanical properties.

5:00 PM

Biological and Physicochemical Study of Tricalcium Phosphate-Silicone Rubber Composite: An Implantable Biomaterial System: Qiang Yuan¹; Devesh Misra¹; ¹University of Louisiana

We describe here the processing routes to successfully develop a new tricalcium phosphate-silicone rubber composite system that can be reliably used as an implantable biomaterial system. The objective here is to uniquely combine the chemical stability of silicone rubber with the superior biological characteristic of new bone formation by self degradation property of the tricalcium phosphate. A relative comparison of biological and physicochemical functions is made with silicone rubber to evaluate the viability of the implantable biomaterial.

5:20 PM

Monotonic and Cyclic Compression Properties of Titanium-Niobium Foams for Biomedical Applications: Jianguo Lin¹; Yuncang Li¹; Peter Hodgson¹; Cui'e Wen¹; ¹Deakin University

Porous titanium alloys, as implant materials, possess new bone tissue ingrowth ability, thus ensuring long-term biological fixations. The porous titanium alloys may be subjected to cyclic loading after implantation. However, there have been relatively few studies on the fatigue failure in titanium alloy foams. In the present study, Ti-35Nb (wt.%) foams were fabricated by a powder metallurgical process. The pore size, porosity and mechanical properties of the titanium alloy foams closely resemble to those of cancellous bone. The compressive fatigue tests were conducted under sinus-wave loading on the foams, and the S-N curves were determined. The deformed and fractured samples were observed by means of scanning electron microscopy (SEM). The fatigue fracture mechanism was discussed.

5:40 PM

Fabrication of Porous Titanium Materials for Orthopedic Implant Applications: Xing Yang Liu¹; Jianfeng Wang¹; Ben Luan¹; ¹IMTI, NRC

Titanium has been widely used in orthopedic implants due to their good biocompatibility, corrosion resistance, and mechanical properties. However, the elastic modulus of titanium alloys is still too high as compared with human bones. It is desired to further reduce the elastic modulus of the titanium alloys so as to minimize the stress-shielding effect of the implants. This paper presents the research work on the mechanical properties and microstructures of porous titanium produced by a powder metallurgy method so as to produce titanium materials with bone-matching modulus and good mechanical strength. The effect of porosity, particle size and impurity content on the bending strength and elastic modulus is discussed.

Bulk Metallic Glasses V: Structures and Mechanical Properties III

Sponsored by: The Minerals, Metals and Materials Society, TMS Structural Materials Division, TMS/ASM: Mechanical Behavior of Materials Committee

Program Organizers: Peter K. Liaw, University of Tennessee; Wenhui Jiang, University of Tennessee; Guojiang Fan, University of Tennessee; Hahn Choo, University of Tennessee; Yanfei Gao, University of Tennessee

Tuesday PM

Room: 393

March 11, 2008

Location: Ernest Morial Convention Center

Session Chairs: T.G. Nieh, University of Tennessee; Y. Yokoyama, Tohoku University

2:00 PM Invited

On the Interpretation of Ductility Improvement in Bulk Metallic Glasses: T. G. Nieh¹; Shuangxi Song¹; ¹University of Tennessee

Reports on the ductility improvement in bulk metallic glasses (BMGs) will be reviewed first. The commonality of mechanical and structural characteristics will be noted and summarized. We will then present our recent results on the deformation of several bulk metallic glasses (BMGs). Some mechanical features such as yielding, flow serration, strain hardening, and perfectly plastic flow will be carefully analyzed and described. Several artifacts which can cause data misinterpretation will be especially pointed out. Finally, we will discuss the dominant deformation mode that occurs in the case of "ductility improvement".

2:20 PM Invited

Evolution of Large Plastic Strains in Metallic Glasses: In Situ Monitoring in a TEM: Evan Ma¹; ¹Johns Hopkins University

For metallic glasses (MGs), the initial evolution of plastic strains in time and space has not been resolved. Here I discuss in situ tests, in tension and compression, of monolithic Zr-based and Cu-Zr-Al MGs in a TEM, employing samples with dimensions of the order of 100 nanometers. The tensile experiments were carried out in collaboration with H. Guo and M.L. Sui at SYNLAB (H. Guo et al., Nature Mater. 2007), and the nanocompression work was a joint project with Z.W. Shan of Hysitron and LBNL and J. Li at OSU (Z.W. Shan et al.,

submitted, 2007). Large ductility was observed, including uniform deformation and extensive necking or slow growth of the shear offset. The MGs deformed in a manner similar to their crystalline counterparts, without deflection/branching of shear bands or nanocrystallization. The sample size effects have implications for the application of MGs in thin films and micro-devices.

2:40 PM Invited

Modeling the S-N Behavior of Bulk-Metallic Glasses: *D. Harlow*¹; Gongyao Wang²; Peter Liaw³; ¹Lehigh University; ²University of Tennessee

Modeling the S-N behavior of bulk-metallic glasses (BMG) is critical for their acceptance in engineering applications as the material for structural members. Typically the S-N response of materials is characterized through empirically based statistical analyses of experimental data. This approach requires extensive amounts of data, and frequently laboratory testing does not adequately reflect long-term performance required of service conditions. Because of the inherent microstructural properties of BMG, experimental testing cannot identify all of the key sources and the extent of their contributions to the randomness in fatigue life, especially for the very high cycle regime. The primary sources of variability arise from the microstructure, environment, and loading. An approach for modeling the S-N response using standard fatigue crack growth modeling is proposed. The model captures the variability in fatigue lives by relating it to key material variables, both deterministic and random, that are readily identified in the proposed model. The identification and significance of these variables are paramount for predicting fatigue crack growth and the subsequent damage evolution. Variability associated with manufacturing and material variables are considered. The effectiveness of this approach is demonstrated with an amalgamated set of S-N data for bulk-metallic glasses. Further consideration is given to three classes of BMG, *i.e.*, Zr, Cu, and Fe based BMG, in order to evaluate the effect of the different microstructural materials. Adoption of the proposed approach is recommended for sound scientific and probabilistic life prediction.

3:00 PM Invited

Fatigue of Zr-Based Bulk Metallic Glass: *Yoshikazu Nakai*¹; ¹Hyogo University

Fatigue tests of smooth specimens and sharp-notched specimens of Zr-based BMG were conducted. The fatigue notch factor was identical to the stress concentration factor. In either specimen, shear step was formed just before fatigue crack initiation. The fatigue crack propagation tests were also conducted, and it was found that the fatigue crack propagation in air was cycles dependent and the rate was controlled by the stress intensity range or its effective component, independent of the stress ratio and the loading frequency. The crack growth rate in deionized water was almost identical to that in air. The rates in NaCl solutions, however, were much higher than that in air. In NaCl solution, the time-based crack propagation rate was determined by the maximum stress intensity factor independent of the loading frequency and the stress ratio, and the growth rate was almost identical to that of environment-assisted cracking under a sustained load.

3:20 PM

Microstructural Investigation and Mechanical Behavior of a Zr-Based Bulk Metallic Glass: *Matthew Freels*¹; Y. Wang¹; J. Jang²; D. Du³; K. Hsieh³; J. Huang³; Peter Liaw¹; ¹University of Tennessee; ²I-SHOU University; ³National Sun Yat-Sen University

The microstructure of a (Zr_{53.1}Cu_{29.8}Ni₉Al_{8.1})_{99.75}Si_{0.25} bulk metallic glass (BMG) was investigated by x-ray diffraction (XRD), synchrotron high-energy x-ray diffraction (HEXRD), and transmission electron microscopy (TEM). XRD patterns showed a broad maximum, with no evidence of any obvious peaks. HEXRD patterns, however, exhibited distinct crystalline peaks. Thermodynamic calculations can predict the type of crystalline phase. Moreover, uniaxial compression and cyclic compression tests were performed. After failure, fracture surfaces were investigated via scanning electron microscopy (SEM). Proposed deformation mechanisms are discussed. The present work is supported by the National Science Foundation (NSF), the Combined Research-Curriculum Development (CRCD) Program, under EEC-9527527 and EEC-0203415, the Integrative Graduate Education and Research Training (IGERT) Program, under DGE-9987548, and the International Materials Institutes (IMI) Program, under

DMR-0231320, with Ms. M. Poats, and Drs. P. W. Jennings, L. S. Goldberg, L. Clesceri, and C. Huber as contract monitors.

3:35 PM

Study on the Metallic-Glass Coatings for Fatigue-Resistance Enhancements: *F. X. Liu*¹; F. Q. Yang²; Y. F. Gao¹; W. H. Jiang¹; J. P. Chu³; P. D. Rack¹; P. K. Liaw¹; ¹University of Tennessee; ²University of Kentucky; ³National Taiwan Ocean University

Multicomponent metallic-glass coatings were deposited on structural substrates by magnetron sputtering. X-ray diffraction and high-resolution transmission electron microscopy were utilized to study the structure of the coatings. Mechanical properties of the coatings were investigated by nanoindentation and microscratch tests. Four-point-bend fatigue tests were performed on the coated materials. It was shown that the application of the metallic-glass coatings could improve the fatigue life and fatigue-endurance limit of the substrates. The high hardness and strength of the amorphous coatings, and the good adhesion to the substrates are the beneficial factors for the enhancement. The effects of various films, and different film thicknesses on the fatigue resistances of different substrates were discussed by a hypothetical micromechanical model. It was suggested that the suppression of the slip offset by the metallic-glass film (with the enhanced ductility by shear-band confinement) may delay fatigue-crack-initiation process, and therefore extend the fatigue life.

3:50 PM

Effects of Partial Crystallization on Bending Fatigue Behavior of Zr-Based Bulk Metallic Glasses: *Gongyao Wang*¹; Peter Liaw¹; Y. Yokoyama²; Matt Freels¹; A. Inoue²; ¹University of Tennessee; ²Tohoku University

Zr₅₀Cu₄₀Al₁₀, Zr₅₀Cu₃₀Al₁₀Ni₁₀, and Zr₅₀Cu₃₇Al₁₀Pd₃ (in atomic percent) are arc-melt tilt-casting bulk-metallic glasses (BMGs). Plate and rod specimens are fabricated. However the cooling rate of plate specimens was lower than that of rod specimens. Thus, the X-ray diffraction results exhibited that the rod specimens are fully amorphous alloys, but the plate specimens could be subjected to the partial crystallization. Four-point-bend fatigue experiments were performed on these zirconium (Zr)-based BMGs in air. The experiments were conducted at a frequency of 10 Hz, using an electrohydraulic machine with a R ratio of 0.1, where $R = \sigma_{\min} / \sigma_{\max}$, σ_{\min} , and σ_{\max} are the applied minimum and maximum stresses, respectively. The fatigue-endurance limits of these BMGs with the partial crystallization were much lower than those of fully-amorphous alloys. These results suggested that the fatigue behavior of a bulk-metallic glass is very sensitive to the microstructure. A mechanistic understanding of the fatigue behavior is suggested.

4:05 PM Break

4:10 PM

Mechanical Behavior of a Cu-Zr-Al-Ag Bulk Metallic Glass: *Matthew Freels*¹; Peter Liaw¹; Gongyao Wang¹; W. Zhang²; A. Inoue²; ¹University of Tennessee; ²Tohoku University

The mechanical behavior of a Cu₄₅Zr₄₅Al₅Ag₅ bulk metallic glass (BMG) was investigated under both uniaxial compression and compressive cyclic loading. The effect of frequency on fatigue behavior was studied. The fatigue experiments were performed using an electrohydraulic machine under a load control mode at frequencies of 10 and 25 Hz (sinusoidal waveform) with $R = 0.1$. Preliminary results show a high compressive strength and a fatigue endurance limit as high as 1550 MPa. Fracture surfaces were examined via scanning electron microscopy (SEM). Proposed deformation mechanisms are discussed. The present work is supported by the National Science Foundation (NSF), the Combined Research-Curriculum Development (CRCD) Program, under EEC-9527527 and EEC-0203415, the Integrative Graduate Education and Research Training (IGERT) Program, under DGE-9987548, and the International Materials Institutes (IMI) Program, under DMR-0231320, with Ms. M. Poats, and Drs. P. W. Jennings, L. S. Goldberg, L. Clesceri, and C. Huber as contract monitors.

4:25 PM

Temperature and Strain-Rate Dependence of Shear Band Propagation in Zr-Based Bulk Metallic Glasses: *Florian Dalla Torre*¹; Alban Dubach¹; Jörg Löffler¹; ¹Swiss Federal Institute of Technology

In this study the inhomogeneous flow behavior of Zr-based bulk metallic glasses (BMGs) is investigated as function of strain rate and temperature. In

contrast to other BMGs the plastic strain exceeds 5% in these materials, which makes possible accurate measurement of the flow behavior under various conditions. At low temperatures the deformation kinetics is characterized by a positive strain rate sensitivity and smooth yielding, while above a critical temperature and strain rate the flow becomes serrated and the strain rate sensitivity is negative. A constitutive strain rate equation is proposed, which accounts for this flow behavior. Here serrated flow is understood to result from structural relaxation which occurs within shear bands; the propagation speed of the shear bands is strongly related to the applied temperature. TEM observations of samples deformed at various temperatures are also presented.

4:40 PM

Probe the Tensile Plasticity in Nanoscale Metallic Glasses: *Yinmin (Morris) Wang*¹; J. Li²; A. Hamza¹; T. Barbee¹; ¹Lawrence Livermore National Laboratory; ²Ohio State University

We present the experimental evidence that nanoscale metallic glasses may sustain appreciable tensile plasticity under certain confined conditions. We observe such phenomenon in tensile deformations of crystalline-amorphous nanolaminates with nanometer-sized (<10nm) Cu/Zr glass layers sandwiched between nanoscale copper crystalline layers. The appreciable amount of tensile plasticity developed in nanoscale amorphous layers and unusual overall high tensile ductility observed in nanolaminates are discussed in terms of the suppression of shear-banding mechanisms in nanometer-sized amorphous layers and the unique capability of amorphous phases that help to sink dislocations evolved from large plastic deformations. This work was performed under the auspices of the US Department of Energy by University of California, Lawrence Livermore National Laboratory under contract of No. W-7405-Eng-48.

4:55 PM

Nanoscale Heterogeneity Correlated with Shear Initiation in Monolithic Metallic Glasses: *Yongqiang Cheng*¹; Hongwei Sheng¹; En Ma¹; ¹Johns Hopkins University

Monolithic glasses are usually considered homogeneous. However, on nanoscale, they may exhibit obvious heterogeneity, in terms of both structure and dynamics. This heterogeneity originates from the diversified configurations and spatial correlations of atoms at this scale. We discuss the impact of the nanoscale heterogeneity on the mechanical properties of amorphous materials. By computer simulation, we study the nanoscale heterogeneity of model metallic glasses by structural and dynamic analysis. Typical length-scale of heterogeneity, effect of cooling rate on the degree of heterogeneity, and fertile sites consisting of extraordinarily mobile atoms are investigated and characterized. To establish statistic correlations between shear initiation and structural/dynamic heterogeneity, we simulate early stage of plastic deformation with difference loading configurations. Triggering events, shear transformations, and collective excitation of shear transformation zones are observed and illustrated. Analytical models regarding shear initiation in monolithic metallic glasses are proposed and discussed.

5:10 PM

Evolution of Shear Bands in Ductile Bulk Metallic Glasses: *Mingwei Chen*¹; ¹Tohoku University

Room-temperature plastic deformation of metallic glasses has been known to accomplish through shear bands in which plastic flow driven mainly by shear stresses is localized within a nano-scale zone. Due to strain softening, these bands are preferential sites for further plastic flow and lead to the final failure that typically breaks a sample along a single shear band. It has been widely recognized that the mechanical properties of bulk metallic glasses depend on the formation and evolution of shear bands. In this study, we systematically characterized shear band evolution in ductile BMGs by high resolution electron microscopy combining with micro-/nano-mechanical measurements. Our results well explain the extraordinary plasticity that was recently observed in some bulk metallic glasses and also reveal the underlying micromechanisms on localized shearing in metallic glasses.

5:25 PM

The Effect of Hydrogen Charging on Ln-Based Amorphous Materials: *ChihPin Chuang*¹; P. Liaw²; R. Kuo³; J. Huang¹; G. Yu¹; W. Dmowski⁴; R. Li⁵; Tao Zhang⁵; R. Yang⁶; ¹National Tsing-Hua University, Department of Engineering and System Science; ²Department of Materials and Engineering, University of Tennessee; ³Division of Nuclear Fuels and Materials, Institute of Nuclear Energy Research; ⁴University of Tennessee, Department of Materials and Engineering; ⁵Beijing University of Aeronautics and Astronautics, Department of Materials and Engineering; ⁶Argonne National Laboratory, Advanced Photon Source

In the present work, the effects of hydrogen charging on Ln-based amorphous alloys had been studied. The (La_{0.5}Ce_{0.5})₆₅Al₁₀Co₂₅ bulk metallic glasses (BMG) were charged with hydrogen by an electrochemical method in an alkali solution. The hydrogen concentration in the sample after a 36-hours charge can reach as high as 1,904 ppm. With the presence of hydrogen atoms, the hardness of Ln-based BMGs increased 80% comparing with the as-cast samples. The structural evolution of the amorphous matrix due to the high fugacity of hydrogen gas during the hydrogen-uptake process was investigated by the high-energy synchrotron X-ray scattering technique. The sample surface was crystallized after hydrogen charging. X-ray diffraction (XRD) measurements revealed broad crystalline peaks superimposed on an amorphous-scattering pattern. The crystalline phase grew through the surface to several hundred microns deep into the amorphous matrix. The atomic arrangements of both amorphous and crystalline phases were described by the atomic pair-distribution-function (PDF).

5:40 PM

The Effects of Surface Nanocrystallization and Hardening Process on the Mechanical Behaviors of Zr-Based Bulk-Metallic Glasses: *J. W. Tian*¹; L. L. Shaw²; Y. Yokoyama³; P. K. Liaw¹; ¹University of Tennessee; ²University of Connecticut; ³Tohoku University

A surface-treatment process, which can generate severe plastic deformation in the near-surface layer of crystalline materials, is applied on the Zr50Cu40Al10 bulk metallic glasses (BMGs). The experiment is implemented using twenty high-speed WC/Co balls to bombard the surface of the samples in an argon atmosphere. Plastic-flow deformation in the unconstrained sample edge was observed, which exhibits the good intrinsic ductility of the BMG materials in this experimental condition. Differential-scanning-calorimetry tests on the specimens show that possible crystallization may occur during the process. Surface hardness was improved by about 15% after three hours of the treatment, which may be attributed to the partial crystallization in the material and/or the reduced free volume. Four-point-bending fatigue behavior has been characterized and related to the modified surface structure and the compressive residual stress induced by the surface treatment. This work is support by the NSF combined research-curriculum development (CRCD) program under DGE-9987548.

5:55 PM

Instrumented Spherical Indentation of Bulk Metallic Glasses: *Byung-Gil Yoo*¹; Byung-Wook Choi¹; *Jae-il Jang*¹; ¹Hanyang University

To analyze the unique low-temperature deformation in bulk metallic glasses (BMGs), here we performed the instrumented spherical indentation tests on BMGs using the various spherical indenters (having different tip radii from 1 to 250 μ m). Unlike indentation with a geometrical self-similar sharp indenter (such as Berkovich and Vickers indenters), spherical indentation can induce the sequential development of stresses and strains in a material under the indenter, which means that one might observe the flow behavior by single indentation experiment. The results are discussed in terms of the evolution of plasticity during spherical indentation. This research was supported by the Korea Research Foundation Grant funded by the Korean Government, MOEHRD (Grant # KRF-2006-331-D00273).

Carbon Dioxide Reduction Metallurgy: Ferrous Industry

Sponsored by: National Materials Advisory Board, Metallurgical Society of the Canadian Institute of Mining Metallurgy and Petroleum, The Minerals, Metals and Materials Society, American Iron and Steel Institute, TMS Light Metals Division, TMS Extraction and Processing Division, TMS: Reactive Metals Committee, TMS: Recycling and Environmental Technologies Committee

Program Organizers: Neale Neelameggham, US Magnesium LLC; Masao Suzuki, AI Tech Associates; Ramana Reddy, University of Alabama

Tuesday PM Room: 294
March 11, 2008 Location: Ernest Morial Convention Center

Session Chairs: Lawrence Kavanagh, American Iron and Steel Institute; Kanchan Mondal, Southern Illinois University, Department of Mechanical Engineering and Energy Processes

2:00 PM

CO₂, the Steel Industry and the ULCOS Program: *Jean-Pierre Birat*¹; ¹Arcelormittal Research

The European Steel Industry has been engaged since 2004 in an extensive, 5-year and 50M€+ program to develop breakthrough process technologies to produce Steel with a reduction of specific CO₂ emissions by at least a factor 2. This program, called ULCOS (Ultra Low CO₂ Steelmaking), will deliver a few process route concepts that meet this target and are ready for scaling up to a commercial size pilot by 2009. After screening a large number of potential routes in an extensive future studies, the program now focuses on 5 concepts: the oxygen blast furnace with top gas recycling and CCS, a bath smelting reduction process, also using pure oxygen and CCS, a new direct reduction, also oxygen and CCS-based, and two processes to carry out the electrolysis of iron ore; they will now be tested at fairly large scales. The approach may be of interest to other metallurgies than steelmaking.

2:20 PM

Recent Developments in Technology Management for Reduction of CO₂ Emissions in Metal Industry: *Malti Goel*¹; ¹Department of Science and Technology

Ferrous and Non-ferrous industry in India is undergoing a transition to meet the growing demand and a new thrust to Research and Development (R&D) is mounting. On one hand, to meet the target laid by the policy in the Iron and Steel sector for 110 million tones production by 2020; on the other, innovations taking place in light metal production technology; both have necessitated greater attention to development of industrial ecological framework. Industrial ecology provides a number of new challenges as well as opportunities for the industry. The development and growth in a particular industry should have a trend towards reduced energy consumption, reduced resource consumption, thereby reducing the cost of production. Technology management strategies will have a key role in achievement of these targets. The paper describes recent developments in technology management, importance of R&D and case studies on adoption of energy efficient and CO₂ reduction technologies in metal industry in India. In the end suggestions for future are made. * The views expressed here do not represent organization's viewpoint.

2:40 PM

Impact on Greenhouse Gas Emissions of a Switch from Carbon to Hydrogen as the Principal Reducing Agent in Producing Metals: *James Evans*¹; Brian Wildey²; ¹University of California; ²Pacific Consolidated Industries

Carbon has been the principal reducing agent in producing metals for centuries. Carbon is an inexpensive reducing agent, but also an effective one, as any undergraduate who knows her Ellingham diagrams is aware. Even in the production of aluminum, an electrolytic process, carbon consumed at the anodes serves to reduce the voltage of the Hall-Héroult cell. The interest in reducing the amount of anthropogenic CO₂ has led to this examination of whether a switch to hydrogen as a major reductant is feasible and economic. The main source of hydrogen is natural gas and its production entails the generation of CO₂; however, that CO₂ is more easily captured than, say, the CO₂ leaving an iron

blast furnace. Calculations and speculations lead to conclusions about whether there is significant benefit to be obtained from such a radical change in our way of producing metals and the approximate cost of such change.

3:00 PM

Sequestration of Carbon Dioxide by Steelmaking Slag: Process Phenomena and Reactor Study: *Von Richards*¹; Simon Lekakh¹; Charles Rawlins¹; Kent Peaslee¹; ¹University of Missouri

Steel-making processes generate carbon dioxide air emissions and a slag co-product. The aim of this project was to develop a functional sequestration system using steelmaking slag to permanently capture carbon dioxide emitted in steelmaking offgas. A possible parallel benefit of this process would be rapid chemical stabilization of the slag minerals with reducing swelling or leaching. This paper summarizes the original results of the project, including mineralogical and structural features of carbon sequestration with steel making slag, mathematical modeling of reaction phenomena using a modified shrinking core model, METSIM modeling of several possible industrial applications, a thermo-gravimetric study of the reaction between slags and different gases, and design and testing for a lab scale apparatus consisted of two reactors.

3:20 PM Break

3:35 PM

Carbon Dioxide Separation for Fuel Utilization for Coal Gasification: *Fawzy Abdelmalek*¹; ¹Abdelmalek and Associates Inc.

This paper presents the Abdelmalek processes for the separation of carbon dioxide gas emitted through a flue gas stream. The flue gases emitted will separate through a thermodynamic liquefaction process. The paper provides technical information and data for a new generation of a Ultra Low Emission-High Efficient coal burning plant that will economically reduce carbon dioxide emissions 25% to 35% without additional energy penalty. Liquid carbon dioxide and sulfur dioxide will be removed from the flue gas stream as by-products for industrial use. The carbon dioxide separated from the flue gases will be utilized for commercial and industrial purposes. The gas product produced will be utilized for the gasification of coal to produce carbon monoxide-rich synthesis gas where a part of the synthesis gas is burned for increased fuel utilization and power generation, and the remaining part is catalytically converted to a by-methanol product.

3:55 PM

Canadian Green Steel: Adopting Best Practices – Reaps Impressive Results: *Jon Feldman*¹; ¹Hatch

In 2006, Canadian independent steel maker, Algoma Steel Inc. embarked on an ambitious initiative to become “Best in Class in Energy Management”. The initiative focussed on identifying energy/GHG management improvements leading to low-cost savings. The key components of the approach were: [1] Review site energy management practices and benchmark internationally. [2] Review best technical practices and benchmark against public energy intensity data. [3] Conducted a site-wide Energy Assessment and physical review of operating areas. [4] Facilitation of on site-workshops with staff to prioritise savings opportunities, identified and removed implementation barriers. [5] Development of Energy Management Action Plan for implementation of improvements. Most organisations can produce, with relative ease, a list of ideas for saving energy, implementing them is the challenge. This paper addresses these issues as well as the profitability of the energy efficiency improvements and the consequences for GHG emissions.

4:15 PM

Reduction of Ti-V-Magnetite with Microwave: *Chenguang Bai*¹; Liangying Wen¹; Feng Xia¹; ¹Chongqing University

The situation of the Ti-V-Magnetite samples reduced with microwave has been investigated in lab. scale. The relationship between carbon consumption and microwave energy consumption for magnetite reducing processing has been studied. In different microwave power level the carbon usage for unit ore is different. While the output of power increase and irradiation time increase the carbon consumption will decrease. The result approve that microwave is a good energy resource that can be used in magnetite extractive procedure in order to reducing carbon dioxide emission.

4:35 PM Panel Discussion

Cast Shop Technology: Melt Handling and Treatment

Sponsored by: The Minerals, Metals and Materials Society, TMS Light Metals Division, TMS: Aluminum Committee

Program Organizers: Hussain AlAli, GM Casthouse and Engineering Services, Aluminium Bahrain Company (ALBA); David DeYoung, Alcoa Inc

Tuesday PM
March 11, 2008

Room: 295
Location: Ernest Morial Convention Center

Session Chair: Jonathan Prebble, Euroservice, Pyrotek Engineering Materials Ltd.

2:00 PM Keynote

Melt Treatment - Evolution and Perspectives: *Pierre Le Brun*¹; ¹Alcan Inc

The use of aluminium alloys is increasingly oriented towards high quality end products, where aluminium enters into competition with other materials on a property/quality/cost basis. The aluminium industry has developed several technologies to provide the required quality of the aluminium alloy as function of the end application. Furnace treatment, in line treatment, and filtration are mainly used to tailor the quality. This paper summarises the evolution of these technologies in the last years, and illustrates the link with quality and product properties. The following aspects are integrated in the discussion: environment, productivity, recycling, flexibility, quality measurement. Finally some areas were developments are required or would be beneficial are discussed.

2:20 PM

Optimization of the Melt Quality in Casting/Holding Furnaces: *Bernd Prillhofer*¹; *Helmut Antrekowitsch*¹; *Holm Böttcher*²; ¹University of Leoben; ²AMAG Rolling GmbH

There are several criteria which characterize melt cleanliness, e.g. hydrogen, alkali metal and the non-metallic inclusion content. According to the increasing quality demand of materials for high end applications (e.g. the aerospace industry) melt cleanliness has to be improved. Beside the in-line melt treatment, which is a very important step for rising melt quality, the content of impurities in casting/holding furnaces have to be reduced in front of for enhanced efficiency of in-line operations. This paper describes the optimisation possibilities for the casting furnace process. Based on CFD-calculations a methodology for melt treatment of AA 7075 has investigated and applied to the real process. Out of this, key factors can be derived and will be discussed.

2:40 PM

Variations in Aluminium Grain Refiner Performance and the Impact on Addition Optimization: *Rein Vainik*¹; ¹Opticast Aluminium AB

A prerequisite for the optimization of the use of aluminium grain refiners is that the refiners exhibit a constant efficiency. Differences in efficiency will have a large impact on the possibility to optimize the use of grain refiners and will therefore lead to high costs for grain refinement. Furthermore, the risk of unwanted cast defects, e.g. cracking of ingots and billets, is greatly increased. A large number of aluminium grain refiners of different compositions have been investigated and the results show that there are large variations in performance, even if the nominal composition is the same. The test procedures used today are not discriminative enough and a new technique has been developed which can differentiate a good grain refiner from a bad one. The new procedure has been developed as an integral step in the implementation of the Opticast technology for grain refiner addition optimization.

3:00 PM

Improved Understanding of the Melting Behavior of Fused Magnesium Chloride-Potassium Chloride Based Refining Fluxes: *John Courtenay*¹; ¹Melt Quality Partnership Limited

Fused magnesium chloride-potassium chloride refining fluxes have become widely adopted as a more environmentally acceptable means for removing alkali metals and oxides from molten aluminium than injection of chlorine gas. Refining fluxes were initially designed based on the binary system magnesium chloride-potassium chloride which exhibits two low melting point eutectics; one at 60% and one at 40% magnesium chloride. In a further development products

containing 25% magnesium chloride have found widespread adoption exhibiting equal removal efficiencies and satisfactory melting behaviour. The objective of the current work was to investigate the effect of fluoride additions and to reconcile the observed performance with the phase equilibria by conducting differential thermal analysis on industrial compositions and relating data collected to known binary and ternary systems. The findings indicate a significant beneficial effect from fluoride addition and the existence of a third low melting point eutectic in industrially produced compositions at 30 mole %.

3:20 PM

Development of an Improved System for the Filtration of Molten Aluminium Based on a Three Stage Reactor Employing a Cyclone as the Final Stage: *John Courtenay*¹; *Frank Reusch*²; *Andrey Turchin*³; *Dmitry Eskin*³; *Laurens Katgerman*⁴; ¹Melt Quality Partnership Limited; ²Drache Umwelttechnik GmbH; ³Netherlands Institute for Metals Research; ⁴Delft University of Technology

The development of a new prototype multi stage filter is described in which a ceramic foam filter is applied in the first chamber operating in cake mode; grain refiner is added in a second chamber and in a final chamber a cyclone is deployed to ensure removal of any oxides or agglomerates arising from the grain refiner addition or release events from the ceramic foam filter. The concept of using a cyclone has been verified as an effective means of flow modification and inclusion removal in a flow modelling study presented separately by A.N. Turchin et al. The first industrial prototype has been installed at Trimet Aluminium in Essen in Germany and the initial trial results with respect to inclusion removal efficiency and operational performance are reported.

3:40 PM Break

3:50 PM

Furnace Flux Additions for Reduction of Sodium: *Malcolm Couper*¹; *John Spranklin*²; *Robert Bridi*³; *Rio Tinto Aluminium Ltd.*; ²Boyne Smelters Limited; ³Pyrotek Inc.

Crucible and/or casthouse processes are required to reduce sodium content in primary aluminium to appropriate levels. Chlorine and/or fluxes are commonly used to control sodium, which adds process complexity and requires careful management of OHS&E issues and costs. Na is an important factor linked to generation of dross and at high levels can have a negative impact on hot tearing susceptibility. In this work, the sodium levels have been characterised at different stages of casthouse processing from crucible transfer through furnace preparation and in-line melt treatment. This included looking at the effect of furnace charge make-up, furnace preparation sequence and in-line degasser performance. The impact of manual furnace flux additions (MgCl₂/KCl) on sodium reduction has been investigated. Factors considered included furnace preparation sequence, flux addition amount, flux composition and flux particle size.

4:10 PM

Mechanisms of Inclusion Removal from Aluminum through Filtration: *Lucas Nana Wiredu*¹; *Lifeng Zhang*¹; ¹Norwegian University of Science and Technology

Alumina Ceramic Foam Filters (CFF) are used to remove inclusions from aluminium in laboratory experiments. Morphology and composition of inclusions in aluminium are identified using before and after filtration using optical microscope, SEM, XRD and EPMA. Qualitative analysis of results from various filtration experiments indicates that CFF filtration is an effective process to remove inclusions from molten aluminium. Interaction between inclusions and filter materials is theoretically investigated, which includes the effects of surface energy change before and after attachment, inclusion size, and fluid flow. Mechanisms of inclusion removal through filtration are then proposed.

4:30 PM

The Effect of Solid Particles on Foaming Process of Aluminum Melt: *Hongjie Luo*¹; *Yihan Liu*¹; ¹Northeastern University

The effects of endogenous or introduced solid particles on bubble nucleation and its Stabilization was studied in this paper in producing aluminum foam by directly foaming in the melt. It was also analyzed the state of solid particles in aluminum melt and their distribution remained in foam block. The results show that the existence of solid particles, which are generated by adding Ca into aluminum melt and introduced through using TiH₂ particles as foaming agents, provides necessary conditions of heterogeneous nucleation of bubbles. These

solid particles can be suspended in the melt and be trapped in the course of bubble nucleation. The solid particles that can't act as nucleating agent may adhere to the generated bubble surface spontaneously and increase its stabilization in aluminum melt. In the interior of obtained foam block, solid particles are mainly concentrated in foam layer and few of them appear in bubble-free layer.

4:50 PM

Predicting of Effect of Delivery System Configuration on Flow and Solidification in the Pool of Twin-Roll Strip Casting: *Bo Wang*¹; Jieyu Zhang²; ¹Inner Mongolia University of Science and Technology; ²Shanghai University

A wedge type metal delivery system has been designed for the twin-roll strip casting process. In this study, a three-dimensional mathematical model has been developed for the coupled analysis of fluid flow, heat transfer and solidification in the pool using finite difference method. The effect of difference delivery system configuration on flow pattern and solidification was predicted. The simulation results showed that it was desirable for the wedge metal delivery system to not only gain the uniform of flow and temperature in the pool, but also improve strip quality and ensure casting process.

5:10 PM Panel Discussion

Characterization of Minerals, Metals, and Materials: Characterization of Microstructure and Properties of Materials II

Sponsored by: The Minerals, Metals and Materials Society, TMS Extraction and Processing Division, TMS: Materials Characterization Committee
Program Organizers: Jian Li, Natural Resources Canada; Toru Okabe, University of Tokyo; Ann Hagni, Intellection Corporation

Tuesday PM
March 11, 2008
Room: 284
Location: Ernest Morial Convention Center

Session Chairs: Jiann-Yang Hwang, Michigan Technological University; Tetsuya Uda, Kyoto University

2:00 PM

FSP Induced Structure Evolution in the HAZ/TMAZ of the Ni-Based IN738 Superalloy: *Oleg Barabash*¹; Zhili Feng¹; Stan David¹; Rosa Barabash¹; ¹Oak Ridge National Laboratory

The range of the application of the FSP is fast expanding to include IN738 superalloy strengthened by 50 vol % Ni₃AlTi-particles. By means of X-ray microbeam, OM, SEM and OIM structural transformations in the HAZ and TMAZ of this alloy due to FSP were studied. In the HAZ the dendrite orientation remains same. In the TMAZ rotation and bending of the dendrites take place. The character of Laue patterns changes from spot-like in the HAZ to the streaked ones in the TMAZ. In the immediate vicinity of the SZ (within 100 microns) recovery with the formation of the cellular substructure with low angle boundaries takes place. Partial coagulation of Ni₃AlTi-particles takes place in both zones. These processes increase approaching the boundary with SZ. At the boundary the complete dissolution of the Ni₃AlTi-particles takes place resulting to the transition of the alloy into ductile state.

2:20 PM

Laser Shock Peening of IN718 Superalloy: *Amrinder Singh Gill*¹; Vijay Vasudevan¹; S. R. Mannava¹; ¹University of Cincinnati

LSP enhances service lifetimes of critical metal parts like aircraft engine fans and compressor blades. LSP dramatically improves fatigue strength, life and crack propagation resistance with shock wave-induced generation of deep compressive residual stress and microstructural changes. This study aims to understand effects of LSP parameters on residual stress distributions and microstructural changes in an important aero-engine material, IN718. Coupons of alloy with and without sacrificial layer were LSP-treated with varying energy densities using the GENIV system at GE Aircraft Engines. Depth-resolved characterization of macro residual strains and stresses and degree of cold work in peening direction and transverse to it was achieved using high-energy synchrotron x-ray diffraction at the Advanced Photon Source. Property changes

were also studied using EBSD in SEM and TEM. Local property changes were examined using micro and nano-indentation measurements. Results showing the relationship between LSP processing parameters, microstructure, residual stress distributions and hardness are presented.

2:40 PM

Characterization of δ -Phase in the Nickel Based Alloy Allvac 718 Plus™: *Christof Sommitsch*¹; Christoph Stotter¹; Harald Leitner¹; Julian Wagner²; Stephan Mitsche²; Martin Stockinger³; ¹University of Leoben; ²Austrian Centre for Electron Microscopy; ³Boehler Schmetedetechnik GmbH

Aerospace gas turbine disks operate in an environment of relatively high stresses caused by centrifugal forces and elevated temperatures. These severe conditions necessitate the need for materials with high temperature strength and good low cycle fatigue resistance. A new nickel based alloy Allvac 718 Plus™ shall further enhance the high temperature properties and is characterized. During hot forming, the grain structure development is strongly influenced by plate-like δ -phase (Ni₃Nb) with orthorhombic β -Cu₃Ti structure. These plates look different from δ -Ni₃Nb investigated in Inconel 718. The phase appearance and fraction as a function of temperature was predicted both by thermodynamical calculations measured by DSC. The detailed phase identification was conducted by FIB, EBSD as well as TEM technique to investigate its morphology, volume fraction, crystallography and chemical composition.

3:00 PM

Microstructural Evolution and Mechanical Properties of IN740 Superalloy: *Hyojin Song*¹; Quanyan Wu¹; Manuj Nahar²; John Shingledecker³; Vijay Vasudevan¹; ¹University of Cincinnati, Department of Chemical and Materials Engineering; ²Indian Institute of Technology; ³Oak Ridge National Laboratory

The IN740 Ni-base superalloy is a relatively new alloy that is being evaluated as a potential boiler material for ultra supercritical steam power systems under a ultra-supercritical condition Steam Boiler Consortium composed of industry, government laboratories and academia. In this study, microstructural evolution during aging of this alloy between 700 to 800°C for times to 3000 h and corresponding changes in tensile mechanical properties and fracture behavior are reported. Aging leads to rapid and substantial increase in strength, whose magnitude depends strongly on the aging temperature and time. Microstructure evolution was studied principally using SEM and TEM and the observations indicated that the strengthening is related to the formation of γ' precipitates. The fine structure of defects and their interactions with the γ' precipitates were characterized by TEM to disclose the deformation mechanisms and these results, together with the size and volume fraction data, was used to model strength.

3:20 PM Break

3:40 PM

Mechanical Behavior of Epoxy Matrix Composites Reinforced with Piassava Fibers: *Sergio Monteiro*¹; Regina Coeli Aquino²; Denise Cristina Nascimento¹; Luiz Fernando dos Santos¹; ¹State University of the Northern Rio de Janeiro - UENF; ²Centro Federal de Educação Tecnológica - CEFET-Câmpus

Natural fibers are being considered as reinforcement for polymeric composites owing to low cost, as compare to synthetic fibers, as well as environmentally correct renewable and biodegradable characteristics. This work investigates the mechanical behavior of epoxy composites reinforced with piassava fibers. These are stiff lignocellulosic fibers obtained from a Brazilian tropical palm tree, scientifically designated as *Attalea funifera* Mart. Composites with up to 40wt.% of piassava fibers embedded in epoxy matrix with different percentages of hardener were bend tested after 24 hours cure at room temperature. The fracture was analyzed by SEM. The results showed that the piassava fibers significantly increase the strength of the composite. A relatively strong fiber/matrix interface is partially responsible for the performance of the composite.

4:00 PM

Texture Transformation in Annealed Wire-Drawn OFHC Copper: *Daudi Waryoba*¹; Ana Erb¹; Peter Kalu¹; ¹Florida A&M University-Florida State University College of Engineering

It is well documented that the texture of medium to high stacking fault energy (SFE) fcc materials, such as copper, consists of strong<111>+weak<100> fiber texture when deformed by wire drawing. The texture transformation on annealing, however, is not as clear. Although it is recognized that at low

annealing temperature the wire-drawn texture evolves during recrystallization to a strong $\langle 100 \rangle$ + weak $\langle 111 \rangle$, which later changes to a dominant $\langle 111 \rangle$ texture at higher temperatures, the effect of both annealing temperature and time on this transformation is not well understood. The objective of this investigation is to present a quantitative temperature-time-dependence of texture transition in annealed wire drawn OFHC copper. Two annealing procedures were performed: the first involves variable temperature at constant time, and the second involves constant temperature at variable time. Microtexture results from both experiments show that indeed the strong $\langle 100 \rangle$ + weak $\langle 111 \rangle$ is a metastable recrystallization texture, whereas the $\langle 111 \rangle$ texture is the stable orientation.

4:20 PM

Microstructural and Hardness Evolution of Roll-Bonded Cu-Nb Composite that Undergoes Annealing: Chao Voon Samuel Lim¹; Anthony Rollett¹; ¹Carnegie Mellon University

A metal-metal composite of Cu and Nb was made using the roll-bonding technique with layer thicknesses as small as 200 nm. Samples were annealed at temperatures of 300°C to 800°C and characterized with high resolution EBSD scans. This study reports the microstructural evolution with particular focus in the Cu layers and the hardness of the composite as a function of layer thickness and annealing temperature. The elongated grain structures observed in the as-deformed state were found to evolve into “bamboo-like” structures with increasing annealing temperature. No evolution was evident in the Nb layers below 600°C, although recovery may well take place. The growth of the grains in the thin layers was also found to be restricted by the phase boundaries. The hardness of the composite decreased with increasing annealing temperature but the total softening was the least for the composite with the thinnest layers, about 200 nm.

4:40 PM

Properties and Microstructural Characterization of Synthesized Brazilian Carbonado Diamond: Guerold Bobrovitchii¹; Sergio Monteiro¹; Ana Lucia Skury¹; Alan Monteiro¹; ¹State University of the Northern Rio de Janeiro - UENF

Carbonado is the original denomination of a polycrystalline natural diamond found in Brazil and in the Central Republic of Africa. Carbonado-like diamonds can be synthesized at high pressure and high temperature from bulk graphite transformation in the presence of a molten solvent/catalyst metallic alloy. In the present work, the properties and microstructure of the first synthetic carbonado produced in Brazil were evaluated. The carbonado was transformed from Brazilian graphite inside a toroidal anvil chamber of a 6300 ton press at 1800°C and 7 GPa of pressure. The properties were evaluated by Raman spectroscopy, X-ray diffraction and microhardness determination. The microstructure was analyzed by SEM. The results showed typical properties of diamonds with a non-uniform distribution of hardness, which is a consequence of a temperature gradient inside the high pressure chamber. The microstructure was associated with metallic segregation at the grain boundaries in addition to polyhedral-shaped diamond crystals.

Complex Oxide Materials - Synthesis, Properties and Applications: Epitaxial Oxides: Ferroelectric, Dielectric, and (Electro-)Magnetic Thin Films

Sponsored by: The Minerals, Metals and Materials Society, TMS Electronic, Magnetic, and Photonic Materials Division
Program Organizers: Zhiming Wang, University of Arkansas; Ho Nyung Lee, Oak Ridge National Laboratory

Tuesday PM
March 11, 2008

Room: 277
Location: Ernest Morial Convention Center

Session Chair: To Be Announced

2:00 PM Invited

Effect of Strain and Crystal Structure on the Ferroelectric Properties of BiFeO₃: Chang-Beom Eom¹; ¹University of Wisconsin-Madison

With a spontaneous polarization (Ps) over 100 $\mu\text{C}/\text{cm}^2$ and its lead-free ferroelectric nature, BiFeO₃ has made it an extremely important material for non-volatile memory applications. Its simultaneous magnetism puts it in the rare class of magnetic ferroelectrics. Since the discovery of its incredible properties in thin-film form, the question of how strain and crystal structure affect the ferroelectric properties of BiFeO₃ still remains unclear, considering that bulk BiFeO₃ yields relatively small Ps values. Here we answer this question through measurements on the same epitaxial (001) BiFeO₃ thin-film capacitors before and after releasing them from the underlying Si substrate to which they are strained. Our measurements reveal that the Ps of BiFeO₃ is intrinsically large and the remanent polarization (Pr) has a strong strain dependence for strain in the (001) BiFeO₃ plane.

2:30 PM Invited

Stability of the Ferroelectric Polarization in Strained BiFeO₃ and Related Materials: Hans Christen¹; ¹Oak Ridge National Laboratory

In epitaxial films of many ferroelectrics (BaTiO₃, KNbO₃), epitaxial in-plane strain results in a fundamental modification of the polar behavior (such as increases in the transition temperature). However, in this presentation we show results confirming theoretical predictions that this behavior is far from being universal. In fact, in BiFeO₃, the magnitude of the polarization changes only insignificantly over a very wide range of epitaxial strain (achieved by varying the thickness of the films on a given substrate), similar to the behavior in PbZr_{0.2}Ti_{0.8}O₃ [Lee et al., PRL v98 p217602 (2007)]. To further investigate this surprising stability of the A-site driven ferroelectricity, alloys between BiFeO₃ and the antiferroelectric BiCrO₃ were grown. In these BiFe_{1-x}Cr_xO₃ films, the ferroelectric phase remains stable even at x = 7/8. Research sponsored by the Division of Materials Sciences and Engineering and the Division of Scientific User Facilities (MDB), BES, US-DOE.

3:00 PM

Thermodynamic Stability and Electronic Structure of LaMnO₃ and La_{0.875}Sr_{0.125}MnO₃ (001) Surfaces: First-Principles Calculations by Means of Hybrid Density-Functional Theory: Sergei Piskunov¹; Eckhard Spohr¹; Timo Jacob²; Eugene Heifets³; Eugene Kotomin⁴; Donald Ellis⁵; ¹Universitaet Duisburg-Essen; ²Fritz-Haber-Institut der Max-Planck-Gesellschaft; ³California Institute of Technology; ⁴University of Latvia, Institute of Solid State Physics; ⁵Northwestern University, Materials Research Center

Surface properties of La_{1-x}Sr_xMnO₃ and its parent compound LaMnO₃ are of high scientific and technological interest due to potential application of these materials in magnetoresistive devices, spintronics, and high-temperature fuel cells. Using the hybrid Hartree-Fock/density functional theory approach, we calculated the electronic structure for a wide range of (001) surfaces of both LaMnO₃ and La_{1-x}Sr_xMnO₃ at low doping x = 1/8. In agreement with experiment, we predict a layered antiferromagnetic ground state for insulating bulk LaMnO₃ while La_{0.875}Sr_{0.125}MnO₃ in both the low temperature orthorhombic and the high temperature pseudo-cubic phases is found to be ferromagnetic and shows half-metallic spin states in the band gap. With respect to surfaces, the layered antiferromagnetic structure is found to be most stable for both LaMnO₃

and $\text{La}_{1-x}\text{Sr}_x\text{MnO}_3$ perovskites. Stability of the surfaces considered has been calculated by means of an *ab initio* thermodynamic approach and found strongly dependent on La or Mn chemical potentials.

3:20 PM

Ab Initio Study of Surface and Surface Oxygen Diffusion Properties of LaMnO_3 : *Dane Morgan*¹; Yueh-Lin Lee¹; ¹University of Wisconsin

The rate of the oxygen reduction reaction on $(\text{La,Sr})\text{MnO}_3$ is a major limitation in developing lower temperature solid oxide fuel cells (SOFCs). To understand the relationship between surface structure and oxygen reduction we use *ab initio* methods to study the energetics of surfaces, near surface vacancies, and oxygen transport in LaMnO_3 (LMO). Vacancy formation energies near the most stable (100) surface are found to deviate dramatically from their bulk values, leading to orders of magnitude differences in vacancy concentrations between bulk and surface. The oxygen vacancy and surface binding energetics have been incorporated into a thermokinetic model to predict the oxygen coverage on the surface, near surface vacancy concentrations, and oxygen diffusivity on the surface and in near surface layers.

3:40 PM

Field-Assisted Reaction Sintering and Magnetic Properties of FeCr_2S_4 : *Dat Quach*¹; Veaceslav Zestrea²; Vladimir Kodash¹; Vladimir Tsurkan²; Joanna Groza¹; ¹University of California, Davis; ²Academy of Science of Moldova

The novel Field-Assisted Sintering Technique (FAST) was successfully utilized to prepare bulk FeCr_2S_4 from a mixture of FeS and Cr_2S_3 powders. This technique significantly reduces the processing time from days in conventional solid-state synthesis to 10 minutes in FAST. FAST samples have high density (almost fully dense) compared to more porous ones synthesized by the conventional technique. Even though both types of samples have some similar magnetic properties, residual structural disorder in FAST specimens has a pronounced impact on the ferrimagnetic-paramagnetic transition and the orbital ordering at low temperatures.

4:00 PM Break

4:30 PM Invited

Materials Design for Piezoelectric Thick Films from Study on MOCVD-Grown Epitaxial Films: *Hiroshi Funakubo*¹; Shintaro Yokoyama¹; Satoshi Okamoto¹; Keisuke Saito²; Takashi Iijima³; Ken Nishida⁴; Takashi Katoda⁵; Joe Sakai⁶; Takashi Yamamoto⁷; Hirotake Okino⁷; ¹Tokyo Institute of Technology; ²Bruker AXS; ³Advanced Institute of Science and Technology; ⁴National Defence Academy and Kouchi University of Technology; ⁵Kouchi University of Technology; ⁶Japan Advanced Institution of Science and Technology; ⁷National Defence Academy

Epitaxial $\text{Pb}(\text{Zr}_{1-x}\text{Ti}_x)\text{O}_3$ [PZT] and $(1-x)\text{Pb}(\text{Mg}_{1/3}\text{Nb}_{2/3})\text{O}_3$ - $x\text{PbTiO}_3$ [PMN-PT] films, above 2 μm in thickness, were grown on (100) cSrRuO_3 /(100) SrTiO_3 substrates by MOCVD. PbTiO_3 content (x) dependencies of the crystal structure, dielectric and piezoelectric properties were systematically investigated for these films. The longitudinal electric-field-induced strain Δx_{33} and transverse piezoelectric coefficient $e_{31,f}$ for PZT films were also maximum at the mixed phase region, on the other hand, that for PMN-PT films were maximum at larger x edge of rhombohedral (pseudocubic) region. Almost the same order of Δx_{33} was observed under applied electric fields up to 100 kV/cm, while larger $e_{31,f}$ was observed in PMN-PT films compared with the case of PZT films. $e_{31,f}$ coefficients of ~ 8.9 C/m² and ~ 11.0 C/m² were calculated for the PZT film with $x=0.46$ and for the PMN-PT film with $x=0.39$, respectively. Based on these research, we discuss on the material design concept of piezoelectric thick films.

5:00 PM Invited

Combinatorial Discovery of a Morphotropic Phase Boundary in a Lead-Free High Tc Piezoelectric Perovskite: *Shige Fujino*¹; *Nagarajan Valanoor*²; Makoto Murakami¹; Sung Hwan Lim¹; Anbusathaiah Varatharajan²; Lourdes Salamanca-Riba¹; Manfred Wuttig¹; Ichiro Takeuchi¹; ¹University of Maryland; ²University of New South Wales

The lead (Pb) content of Pb-based piezoceramics has recently raised environmental concern, and has created motivation to find a Pb-free replacement with comparable characteristics and simple perovskite structure. Though some guidelines which predict the presence of MPBs do exist, comprehensive mapping

of compositions requires synthesis of an enormously large number of individual samples. We overcome this challenge by implementing a combinatorial synthesis strategy, where we have identified a property enhancing morphotropic phase boundary (MPB) in the $(\text{Bi,Sm})\text{FeO}_3$ system, whose electromechanical properties represent substantial enhancement over those of simple BiFeO_3 . We show a rhombohedral to triclinic to orthorhombic structural transition which exhibits a ferroelectric (FE) to antiferroelectric (AFE) transition at the MPB with piezoelectric properties comparable to those of PZT. Thus the newly discovered MPB sits at an interesting ferroelectric/antiferroelectric transition, and as a consequence we also demonstrate characteristics of a new Pb-free antiferroelectric.

5:30 PM

Comparison of the Atomic and Electronic Structure of Single F Centers in Cubic PbZrO_3 , PbTiO_3 , and SrTiO_3 Perovskites: *Yuri Zhukovskii*¹; Sergei Piskunov¹; Eugene Kotomin¹; Donald Ellis²; ¹University of Latvia, Institute of Solid State Physics; ²Northwestern University

Hybrid DFT-LCAO calculations were performed using $3 \times 3 \times 3$ supercells of defective cubic perovskites. Outward displacements of Zr and Ti atoms nearest to oxygen vacancy (F center) are 1% (PbZrO_3) vs. 3% (PbTiO_3). Inward relaxation of next-nearest oxygens is larger in zirconate (10 vs. 2%), similarly to inward shift of following leads (12 vs. 5%). Strontium relaxation around F center is almost negligible. F center formation energy is larger in SrTiO_3 (8.75 eV) relatively to PbZrO_3 and PbTiO_3 (7.25 vs. 7.82 eV). O vacancies in PbZrO_3 , PbTiO_3 and SrTiO_3 trap 0.7, 0.9, and 1.2 e. Band structures show different defect level location. For zirconate, it lies 1.72 eV below bottom of conduction band, with small dispersion over Brillouin zone (0.14 eV). For PbTiO_3 vs. SrTiO_3 , this level is closer to CB, with larger dispersion (0.97, 0.21 vs. 0.69, 0.25 eV). Thus, different chemical nature of cations results in considerable variation of properties.

Computational Thermodynamics and Kinetics: Functional Materials

Sponsored by: The Minerals, Metals and Materials Society, TMS Electronic, Magnetic, and Photonic Materials Division, TMS Materials Processing and Manufacturing Division, ASM Materials Science Critical Technology Sector, TMS: Chemistry and Physics of Materials Committee, TMS/ASM: Computational Materials Science and Engineering Committee, TMS/ASM: Phase Transformations Committee
Program Organizers: Yunzhi Wang, Ohio State University; Long-Qing Chen, Pennsylvania State University; Jeffrey Hoyt, McMaster University; Yu Wang, Virginia Tech

Tuesday PM
March 11, 2008

Room: 288
Location: Ernest Morial Convention Center

Session Chairs: Long-Qing Chen, Pennsylvania State University; Gunther Eggeler, Ruhr University

2:00 PM Invited

Domain Mechanisms in Giant Magnetostrictive Materials: *Yongmei Jin*¹; Yongxin Huang¹; ¹Texas A&M University

A phase field micromagnetic microelastic model is employed to study the domain mechanisms in giant magnetostrictive materials. The model explicitly treats magnetic-elastic domain microstructures, takes into account various magnetization-strain coupling mechanisms (intrinsic direct coupling through magnetostriction and extrinsic indirect coupling through magnetocrystalline anisotropy), and calculates multiple thermodynamic driving forces (magnetostatic, elastostatic, magnetocrystalline, exchange, chemical, twin boundary, applied magnetic and mechanical loading). Simulations of the coupled magnetic and elastic domain microstructure evolution are performed for two distinct giant magnetostrictive materials, namely, ferromagnetic shape memory alloy Ni-Mn-Ga and magnetostrictive Terfenol-D. The results identify domain mechanisms in these two types of materials and clarify their respective advantages and disadvantages, providing insight for new giant magnetostrictive materials development.

2:25 PM Invited

The Effect of Microstructure on the Local and Macroscopic Ferroelectric Switching of Polycrystalline Ferroelectric Films: *R. Edwin Garcia*¹; ¹Purdue University

Ferroelectric Lead Zirconate Titanate (PZT) films display physical behavior that makes them an important candidate for several device applications. In such devices, polarization domains are locally switched by the application of an electric field, and the microstructural features are very important. In particular, large spatial variations of the fields arise as a combined result of the stresses that develop due to the thermal expansion and lattice mismatch of the film-substrate system, the anisotropy of the properties, and the processing conditions. Simulations show that in-plane electromechanical interactions electrically shield some of the grains, while enhancing the polarization response in others. Additionally, grain corners and boundaries become domain nucleation sites as well as domain pinning locations. The local phenomenology observed in these simulations agrees macroscopically with the observed experimental behavior, and is used as a basis to propose microstructural mechanisms that explain the local in-plane and out-of-plane ferroelectric switching behavior.

2:50 PM

Computer Simulations of Ferroelectric Domains and Switching Using Phase-Field Approach: *Samrat Choudhury*¹; Yulan Li²; Long Chen¹; ¹Pennsylvania State University; ²Los Alamos National Laboratory

Application of ferroelectrics in information storage devices, involves switching of ferroelectric domains by an applied electric field. Conventional thermodynamic approach to describe switching behavior typically assume a material to be a perfect crystal while a real ferroelectric material is generally inhomogeneous and contains defects such as domains and domain walls, surfaces, grain boundaries, dislocations and dipolar defects. In this work, we developed a three-dimensional (3-D) phase-field model for predicting the domain structures and ferroelectric properties in presence of structural inhomogeneities. The model takes into account realistic polycrystalline grain structures as well as various energetic contributions including elastic energy, electrostatic energy, and domain wall energy. It is shown that the defects such as existing domain walls and grain boundaries play a critical role in domain switching and the magnitude of coercive field. It will be demonstrated that ferroelectric properties obtained from phase-field simulation are in excellent agreement with experimental measurements.

3:10 PM

Phase Field Modeling of Morphotropic Phase Boundary Ferroelectrics: *Weifeng Rao*¹; *Yu Wang*¹; ¹Virginia Tech

Phase field model is employed to study some fundamental aspects of morphotropic phase boundary (MPB) ferroelectrics. MPB ferroelectrics offer the best electromechanical properties among all ferroelectric and piezoelectric materials. This talk will present some new insights into the underlying mechanisms responsible for the advanced piezoelectric behaviors around MPB. The new findings are domain wall broadening mechanism for domain size effect of enhanced piezoelectricity, bridging domain mechanism for phase coexistence, ferroelectric shape memory effect, composition-induced inter-ferroelectric phase transition, nanodomain microstructures of coherent ferroelectric phase decomposition, and adaptive diffraction phenomenon peculiar to nanodomains. Application of the gained understanding to other ferroic functional materials is also discussed.

3:30 PM Break

4:00 PM Invited

On the Role of Microstructure on the Martensitic Transformation of NiTi Shape Memory Alloys: *Gunther Eggeler*¹; ¹Ruhr-University Bochum

NiTi shape memory alloys show fascinating properties like the one way effect and pseudoelasticity. These rely on thermally or mechanically induced martensitic transformations. Many atomistic, crystallographic and micromechanic aspects of the martensitic transformations are reasonably well understood. But this is not enough for making good shape memory alloys. There is a need to understand the role of microstructure during the martensitic transformation. Microstructures of shape memory alloys evolve during processing and consist of crystal defects including vacancies, dislocations, internal boundaries and particles which can all interact with each other and with the martensitic transformation. The first part

of this overview presentation will recall some shape memory basics. It will then be shown how individual defects can interact with the martensitic transformation and what implications this has for shape memory properties. Challenges for modellers in view of experimental results will finally be highlighted.

4:25 PM

Effect of Ni₄Ti₃ Precipitation on Martensitic Transformations in Ti-Ni Based Shape Memory Alloys: *Ning Zhou*¹; Chen Shen¹; Martin Wagner²; Gunther Eggeler²; Yunzhi Wang¹; ¹Ohio State University; ²Ruhr-University Bochum

Precipitation of Ni₄Ti₃ plays a critical role in determining the martensitic transformation path and Ms temperature in Ni-Ti based shape memory alloys. In this study the concentration and stress fields around growing Ni₄Ti₃ precipitates are simulated quantitatively using the phase field method. Experimental data for lattice parameters of the parent and precipitate phases, precipitate/matrix orientation relationship, elastic constants and thermodynamic database are used as model inputs. Simulation predictions of the concentration and stress fields as function of precipitate size and spatial distribution are compared with experimental observations. The effects of the concentration and stress fields on subsequent martensitic transformations are investigated using a combination of the phase field method and the nudged elastic band method. These quantitative simulation results could be used for designing alloy composition and heat treatment schedule to precisely control the martensitic transformation temperature through manipulation of the size and density of Ni₄Ti₃ precipitates.

4:45 PM Invited

A Comparative Phase Field and Lagrangian Analysis of the Dynamics of the Martensitic Transition: *Alphonse Finel*¹; Umut Salman²; ¹ONERA; ²CNRS

When slowly driven by an external force, a martensitic transition is often characterized by a random sequence of burst or avalanches whose amplitudes display power-law distributions over several decades. This indicates that the martensitic volume fraction evolves without characteristic length and time scales, which is the signature of criticality. We present a comparative investigation of this critical dynamics in athermal martensite using both a Time-Dependent Ginzburg-Landau modeling and a lagrangian method that takes into account inertial effects.

5:10 PM

Phase-Field Study of Size Effects in Nanoscale Shape-Memory Materials: *Mathieu Bouville*¹; Rajeev Ahluwalia¹; ¹Institute of Materials Research and Engineering

The microstructure of martensite is well known and well understood. Twins form along habit planes set by elastic compatibility. In the case of thin films or nanograins there exists an extra constraint, geometry, which affects martensite formation: the usual habit planes are altered to accommodate the geometry. Size, shape, and orientation of the grains all have an impact on the nanostructures, even giving rise to domain patterns not found in bulk martensite. Stress can also play a role by stabilizing austenite and thus giving rise to martensite-austenite structures; these nanostructures are different from what is observed in bulk systems. We will use the phase-field method, which has been extensively used to study martensitic transformation in bulk systems, to study the impact of geometrical constraints and of stress on pattern formation in nanoscale martensite.

5:30 PM

Calculation of Impurity Free Energies by Ab-Initio Molecular Dynamics: *Chris Retford*¹; Mark Asta¹; Ben Haley²; Niels Gronbech-Jensen¹; Michael Manley³; Christopher Woodward⁴; Dallas Trinkle⁵; ¹University of California, Davis; ²Purdue University; ³University of California, Davis/Lawrence Livermore National Laboratory; ⁴Northwestern University/Air Force Research Laboratory; ⁵University of Illinois, Urbana-Champaign

In first-principles calculations of the thermodynamic properties of solids, vibrational contributions are typically calculated within the framework of quasi-harmonic theory. This talk discusses approaches for calculating vibrational thermodynamic properties of solids when the quasi-harmonic theory is not applicable, namely for crystalline solids which are harmonically unstable at zero temperature. We discuss in particular an application to the calculation of site preference for ternary additions in the austenitic phase of the shape-memory NiTi compound. The formation free energy for Fe additions to NiTi alloys are computed employing a semigrand-canonical-ensemble relation, implemented

within the framework of ab-initio molecular dynamics, which includes naturally electron-phonon coupling. The results of these calculations are discussed in the context of recent experimental studies of the effect of Fe additions on structural transitions in the NiTi(Fe) system.

Deformation Twinning: Formation Mechanisms and Effects on Material Plasticity: Experiments and Modeling: Twin Effects on Material Deformation II

Sponsored by: The Minerals, Metals and Materials Society, TMS Structural Materials Division, TMS/ASM: Mechanical Behavior of Materials Committee

Program Organizers: George Gray, Los Alamos National Laboratory; Subhash Mahajan, Arizona State University; Ellen Cerreta, Los Alamos National Laboratory

Tuesday PM Room: 383
March 11, 2008 Location: Ernest Morial Convention Center

Session Chair: Ellen Cerreta, Los Alamos National Laboratory

2:00 PM Invited

The Influence of Deformation and Microstructure on Twinning Processes: *Ian Robertson*¹; Bryan Miller¹; Cynthia Smith¹; ¹University of Illinois Urbana-Champaign

Dislocation slip and twinning are the two common modes of deformation in metals. The latter is more common in metals with limited slip system availability, and under quasi-static loading rates at low temperature or high strain rate loading at higher temperature. In addition, deformation twinning has been reported to occur in high stacking-fault energy face-centered cubic metals with a nanometer grain size, although it does occur in large grains of these same materials in regions of high stress. Deformation twinning can also occur after extensive dislocation slip, which raises the question of how the twinning dislocations penetrate the existing dislocation structure. In this talk, the different conditions under which twinning occurs in face-centered cubic metals, the effectiveness of twins as dislocation sources and dislocation sinks, and a new mechanism for twinning in the presence of extensive slip will be presented and discussed.

2:30 PM

A Simple Non-Hardening Rate-Independent Constitutive Model for HCP Polycrystals Deforming by Slip and Twinning: *Babak Kouchmeshky*¹; Nicholas Zabarav¹; ¹Cornell University

A continuum approach is presented for predicting the constitutive response of HCP polycrystals using a simple non-hardening constitutive model incorporating both slip and twinning. A physically based methodology is introduced for restricting the amount of the twinning activity. A continuum approach is used for modeling the texture evolution that eliminates the need for increasing the number of discrete crystal orientations to account for new orientations created by twinning during deformation. The polycrystal is represented by an orientation distribution function using the Rodrigues parameterization. Numerical examples are used to show the application and accuracy of the methodology for modeling deformation processes.

2:50 PM

Microscopic Phase Field Modeling of Microtwinning in Ni-Base Superalloys during Creep Deformation: *Chen Shen*¹; Ju Li¹; Michael Mills¹; Yunzhi Wang¹; ¹Ohio State University

Recent investigations of creep deformation of Ni-base superalloys have demonstrated clearly the importance of twinning and reordering in determining dislocation-precipitate interactions and the corresponding kinetic pathways of the deformation process. Guided by concurrent experimental characterization we apply phase field modeling at different length scales to study the motion of dislocations in the g/g' microstructure and the formation of various planar faults in both precipitate and matrix under different loading conditions. In combination with ab initio calculations of generalized stacking fault (GSF) energy and the nudged elastic band (NEB) method, the effects of key material parameters and microstructural features on the minimum energy paths and activation energies

of various deformation modes including microtwinning and isolated faulting are investigated. This work is supported by AFOSR through the MEANS program.

3:10 PM

Twinning during Low-Temperature Deformation of Sub-Microcrystalline Pulsed-Electrodeposited Nickel: *Lutz Hollang*¹; Klemens Reuther¹; Werner Skrotzki¹; ¹Dresden University of Technology

Pure sub-microcrystalline nickel was produced by pulsed electro-deposition without additives for grain refinement. The average grain size of the material is $d_{\text{EBSD}} = 150$ nm and $d_{\text{XRD}} = 25$ nm if determined by electron backscatter diffraction (EBSD) and by X-ray diffraction (XRD), respectively. Tensile tests between 4 K and 320 K reveal that the material is ductile in the whole temperature range. Above a characteristic temperature $T^* = 7$ K the stress-strain curves are parabolic and the stress reaches its maximum after about two percent plastic strain, with the ultimate stress strongly increasing with decreasing temperature. However, during deformation below T^* , at a stress level of 2400 MPa the deformation mode suddenly changes to twinning. The twinning events are characterized by substantial stress drops accompanied by acoustic emissions. The microstructural changes connected with twinning will be discussed on the basis of results obtained by scanning and transmission electron microscopy.

3:30 PM

Size-Effects in Materials Deforming by Mechanical Twinning: *Javier Gil-Sevillano*¹; Jon Alkorta¹; Jon Molina¹; ¹University of Navarra, CEIT and TECNUN

Size-effects associated to plastic strain gradients in materials deforming by dislocation-mediated slip have been thoroughly discussed in the recent past. By contrast, similar effects in materials deforming by mechanical twinning have been up to now ignored, despite the technological importance of some advanced twinning-deforming materials. This paper is a first attempt to analyze such effects both theoretically and experimentally. Results of the indentation size effect (ISE) in a high-Mn low stacking-fault energy TWIP will be presented.

3:50 PM Break

4:20 PM Panel Discussion with Carlos Tome, Moderator

Electrode Technology Symposium (formerly Carbon Technology): Anode Manufacturing and Developments

Sponsored by: The Minerals, Metals and Materials Society, TMS Light Metals Division, TMS: Aluminum Committee

Program Organizers: Carlos Zangiacomi, Alcoa Aluminum Inc; John Johnson, RUSAL Engineering and Technological Center LLC

Tuesday PM Room: 297
March 11, 2008 Location: Ernest Morial Convention Center

Session Chairs: Markus Meier, R&D Carbon Ltd; Alan Tomsett, Rio Tinto Aluminium

2:00 PM

Anode Butts Automated Visual Inspection System: *Jean-Pierre Gagne*¹; Marc-André Thibault¹; Gilles Dufour²; Claude Gauthier²; Michel Gendron²; ¹STAS; ²Alcoa, Inc

Anodes consumed in the smelting process for the production of primary aluminium need to be replaced regularly. Inspecting anode butts properties can be helpful to optimize the electrolysis process, reduce the anode cycle and optimize anode fabrication. In most of the aluminium smelters, manual measurements are taken on a sampling basis in order to obtain minimum feedback information. STAS-Alcoa's R&D team has been working to develop an automated inspection system; the intention was to design a low cost solution to automatically obtain a series of measurements on 100% of the anode butts. The prototype has been implemented at "Alcoa, Aluminerie de Deschambault", Canada, on May 2006. The inspection system, based on artificial vision is integrated within the existing conveyor system of the rod plant. All anode butts are inspected in line while they are transported on the conveyor. This paper presents some of the results obtained.

2:20 PM

New Rodding Shop Solutions: *Nicolas Dupas*¹; ¹ECL

With more than 25 years of experience in rodding shop equipment design and commissioning, ECL is the leading supplier for modern smelters. All types of technology (2, 3, 4, or 6 stubs) are catered for, from individual machines to turnkey solutions: - Overhead conveyors, - Loading/unloading stations with unique centering mechanism, - Bath breaking and removal stations, - New hot-bath cleaning solutions, - Shot Blasting stations, - Butt stripping machines, - Thimble press, new simultaneous breaking design, - New butt stripping and thimble combination, - Stem control and preparation stations, - Casting stations: standard carriage, articulated carriage, casting crane, mating tables and carousels. "Level 2" solutions allow a centralized computer control of the rodding shop to increase productivity, efficiency and facilitate maintenance. As for all of the smelter's equipment range, environment, health and safety are the top priorities in the design and commissioning of the rodding shop.

2:40 PM

Safe Operation of Anode Baking Furnaces: *Inge Holden*¹; ¹Hydro Aluminium AS

The baking of anodes is a process in which combustible substances are released. Ring main fires do occur and even explosions in the ring main or fume treatment plant have happened in carbon plants. The risks associated with different process deviations and the possible consequences of these, can be evaluated for both existing and new furnaces to be built. European and IEC safety standards give useful guidelines for the design of process control and safety systems applicable to the baking process. This paper will present and discuss methods for evaluating the risks and consequences, and give examples for how operational procedures and the design of safety systems can reduce the occurrence of unwanted events for open as well as closed top furnaces.

3:00 PM

Baking Furnace Optimisation: *Amer Al Marzouqi*¹; *Tapan Sahu*¹; *Saleh Rabba*¹; ¹Dubai Aluminium Company Limited

Dubai Aluminium Company Limited (Dubal) began its operation in 1979 as a 135 000 tons/annum of primary aluminium smelter. The electrode requirements for its three pot lines were supplied by two closed-top baking furnaces. Today, Dubal is a 890 000 tons/annum producer of primary aluminium operating four open top Alcan-Alesa baking furnaces beyond their design capacity, to meet its continuously expanding anode requirements. Recent increases in pot line amperage have demanded the use of larger anodes of varying configuration which has made the furnace operation extremely complicated. For the past three years Dubal has optimised its baking furnace operations to improve baked anode quality and increase productivity, with the support of R&D Carbon. This paper describes the improvement measures taken during these three years, through systematic implementation of various innovations in baking furnace practices, which have resulted in increased production and improved anode quality at Dubal.

3:20 PM Break

3:30 PM

New Concept for a Green Anode Plant: *Michael Kempkes*¹; *Werner Meier*¹; ¹Buss ChemTech AG

Buss ChemTech, the leading supplier for anode production since 1950's producing about 80% of world's anodes with individual machines to turnkey solutions. Moreover, with increasing smelter capacity from 50'000 t/a to today's smelters reaching above 1 million t/a the throughput of anodes increased while quality of raw materials steadily decreases requiring higher attention in production to archive stable results. Success of any smelter depends on the performance of carbon, green carbon and anode baking from start-up through its operation. Furthermore, future changes in all regulations need to be incorporated into new designs to reduce construction time, assure safe, efficient and stable operation, address present and future environmental regulations while still being most cost effective. This paper outlines the future green anode plant design build around highly reliable equipment, avoidance of unneeded equipment and simplification of process steps to formulate the concept for producing the perfect quality anodes.

3:50 PM

Finite Element Modeling of Baked Anodes: *Odd Einar Frosta*¹; *Trygve Foosnaes*¹; *Harald Øye*¹; ¹Norwegian University of Science and Technology

Carbon anodes used in the aluminium reduction process are consumed and replaced with new ones. The new anode is exposed to a severe thermal shock as it is submerged in the molten bath. The thermal shock induces thermal stress that sometimes initiates cracks in the carbon anode. Temperatures and stresses in a carbon anode have been modelled using three-dimensional finite element methods through the modeling program ANSYS. The first model grid was based on a homogeneous anode. Inhomogeneity was introduced stepwise by giving the grid varying properties according to analyses of core samples drilled throughout industrial anodes. Modeling gradients of several material properties through the anode can now be done. The result is an anode model in which certain parameters can be altered in order to determine optimal thermal shock resistance (TSR).

4:10 PM

Characteristic and Development of Production Technology of Carbon Anode in China: *Guanghui Lang*¹; *Rui Liu*¹; *Kangxing Qian*¹; ¹Sunstone Carbon

With rapid developments in Chinese aluminium industry, technology in carbon anode production has quickly improved. Sunstone construction project reflected the characteristics and development of Chinese technology in carbon anode production. The main characteristics are shown as following: Pot - type calcining furnaces for petroleum coke are widely used in China with a steady quality, low investment and long service life; Weigh batchers used in blending procedure; mixer used in kneading procedure and vibratory compaction make the green anode with composition of high precision, good effect in kneading and high density; anode quality is closed to international level. The main technique developments are shown as following Emphasis on quality of raw materials; Development of large size in pot - type calcining furnaces; Emphasis on environmental protection and utilization of waste heat; More attentions on homogenization of anode quantity.

4:30 PM

Discussion of Production Quality of Slotted Carbon Anode: *Guanghui Lang*¹; *Rui Liu*¹; *Lin Tang*¹; *Kangxing Qian*¹; ¹Sunstone Carbon

Advantages of slotted anode were recognized in laboratory. An aluminium smelter with 800,000 t/a.p. in Middle East used the slotted anodes made by Sunstone in 2006. It shown a example of normal use in industrial smelters. There are two kinds of process to product slotted anode: forming before baking or cutting forming after baking. Based on technical and the economical analysis including its benefit in electrolysis, the process of forming before baking is used in Sunstone. The process of forming before baking will produce itself weakness, one of them is thermal stress which is easy to cause crack in slotted part. Based on measuring crack position, depth and expansion, analyzing impact factors from raw materials, component, forming and baking, a optimum process is selected. In this article, improvement in baking process is focused on due to its important and problematic, other processes will be discussed subsequently.

Electrode Technology Symposium (formerly Carbon Technology): Cathodes Raw Materials and Properties

Sponsored by: The Minerals, Metals and Materials Society, TMS Light Metals Division, TMS: Aluminum Committee

Program Organizers: Carlos Zangiacomi, Alcoa Aluminum Inc; John Johnson, RUSAL Engineering and Technological Center LLC

Tuesday PM
March 11, 2008

Room: 299
Location: Ernest Morial Convention Center

Session Chairs: Alexander Proshkin, Rusal; Claude Gauthier, Alcoa Inc

2:00 PM

ISO Standards for Testing of Cathode Materials: *Harald Oye*¹; ¹Norwegian University of Science and Technology

ISO/TC 226 (Materials for the Production of Primary Aluminium) recently published a CD with 109 ISO Standards and 2 ISO Technical Specifications. covering the materials: Alumina, Pitch, Coke, Anodes, Cathodes and Ramming

Paste. All standards are easily accessed from the CD. In addition to the test procedures for common room temperature properties, methods which characterizes the cathode materials at operational conditions has been developed. Examples are: Sodium expansion of cathodes with and without external pressure, rammability of paste and expansion and shrinkage of ramming paste. Additional studies of cathode property changes as function of temperature and time enables room temperature ISO standards to be extrapolated to operational conditions. The standards are not only useful for material evaluation, but also important for development of more reliable mechanical-thermal-electrical models.

2:20 PM

Test and Analysis of Nitride Bonded SiC Sideline Materials: Typical Properties Analyzed 1997-2007: *Egil Skybakmoen*¹; Jannicke Kvello¹; Ove Darell¹; Henrik Gudbrandsen¹; ¹SINTEF Materials and Chemistry

During the last ten years, SINTEF has tested a large number of different commercial nitride bonded SiC sideline materials produced world-wide. The following properties will be summarized in the paper: Apparent porosity, density, mineral phase analyses (α -Si₃N₄, β -Si₃N₄, Si₂ON₂, Si, and SiC), chemical analyses (level of Al, Fe, Ca and Ti), LECO analyses (total oxygen and total nitrogen), bending strength, hot modulus of rupture (HMOR), cold crushing strength, thermal expansion, thermal conductivity, oxidation resistance, and chemical resistance. Some comparisons between blocks with good and bad properties will be given, as well as some examples of variation in properties within the same block.

2:40 PM

A Laboratory Evaluation of Cathode Blocks from Different Well-Known Suppliers: *Galina Vergazova*¹; ¹Rusal, Engineering and Technology Center Ltd.

Development of reduction cell technologies and the cathode design largely depends on the cathode blocks quality. Furthermore the cathode blocks can be a reason in early failures of cells. A lot of cathode blocks types and qualities are available on the market. To choose cathode blocks for powerful reduction cells we have tested a number of cathode blocks of different quality from several well-known suppliers. The cathode blocks studied were selected by references from other aluminium smelters, publications and product specifications. Results of the tests shall be used in product specifications and new cell designs.

3:00 PM

High Swelling Cold Ramming Paste for Aluminum Reduction Cell: *Galina Vergazova*¹; ¹Rusal, Engineering and Technology Center Ltd.

Life and energy efficiency of a reduction cell largely depend on the sealing efficiency of the ramming paste that determines the extent and rate of electrolytic penetration into the cell bottom. The problem of the ramming paste quality and its densification in the joints is especially acute for more and more widely used graphitic and graphitized cathode blocks with their very low sodium swelling index and heat expansion factor. High swelling capacity of ramming pastes can be an avenue of attack on the problem. The work presents a study to control the swelling capacity and caking with ramming paste blocks based on typical electrically and gas-calcined anthracite and pitch binder by selection of size distribution and liquid and solid additives.

3:20 PM Break

3:30 PM

Wear Mechanism Study of Silicon Nitride Bonded Silicon Carbide Refractory Materials: *Ron Etzion*¹; James Metson¹; ¹University of Auckland, Light Metals Research Centre

Unused Silicon Nitride Bonded Silicon Carbide (SNBSC) bricks from different manufacturers were studied using x-ray powder diffraction (XRD), SEM-EDS, XPS and Solid state NMR. Powder XRD analysis reveals that the ratio of α to β Si₃N₄ varies significantly in different samples and in different zones of the brick. In samples which contain higher β Si₃N₄ its concentration decreases from the core to the exterior. The high β Si₃N₄ content in the core of some bricks could be attributed to poor temperature control and the exothermic nature of the nitridation reaction. This would account for the higher internal temperatures conducive to β Si₃N₄ formation. Core samples with high β Si₃N₄ content show higher corrosion rates compared to samples with high α Si₃N₄ content. The corrosion test reveals that the degradation mechanism consist of a combination of bath penetration into the sample followed by gas attack.

3:50 PM

Chemical Resistance of Sideline Refractory Based on Si₃N₄ Bonded SiC: *Richard Laucouret*¹; Didier Lombard¹; Abdellatif El Bakkali²; Catherine Bessada²; Jacques Poirier²; Veronique Laurent¹; ¹Alcan; ²Centre de Recherche sur les Matériaux à Haute Température

The state of art for the sidewall lining in modern electrolysis cells is Si₃N₄ bonded SiC refractories. The chemical resistance of sidewall materials is one the key factors of the pot lifetime. ALCAN intends to improve its electrolysis technology by identifying and selecting the most chemical resistant materials to the oxidation and chemical dissolution by the cryolithe. The present study is aimed at improving our knowledge of corrosion mechanism of Si₃N₄ bonded SiC materials and determining the key parameters of materials structure which impact on the behaviour of these refractories in operation conditions. The chemical resistance in cryolithe of SiC and Si₃N₄ powders was investigated by XRD, the behaviour of some Si₃N₄ bonded SiC samples was studied in two oxidizing atmospheres: dry and wet air and the influence of the permeability of materials on their oxidation was established.

4:10 PM

Sodium Vapour Degradation of Refractories Used in Aluminium Cells: *Asbjørn Solheim*¹; Christian Schoning²; ¹SINTEF; ²SINTEF Materials and Chemistry

The bottom lining in aluminium cells can be degraded by several mechanisms. In the present work, reaction with sodium vapour that diffuses through the cathode was studied ("dry attack"). The reaction paths depend on the oxygen level. At reducing conditions, metallic Si is formed, whereas the presence of oxygen gives Na₂O. Based on available thermodynamic data for the compounds present in the system SiO₂-Al₂O₃-Na₂O, each alkemade triangle in the phase diagram could be supplied with numbers for the equilibrium pressure of sodium (or sodium and oxygen), as well as lines showing the change in composition during attack. The calculations show that chamotte bricks normally end up as a mixture of nepheline and albite. This is in accordance with practical observations. The reducing nature of sodium was verified through laboratory experiments, and autopsies of old linings have revealed the presence of Si-metal particles due to the reduction of SiO₂-containing compounds.

4:30 PM

The Effect of Current Density on Cathode Expansion during Start-Up: *Arne Ratvik*¹; Anne Støre¹; Asbjørn Solheim¹; Trygve Foosnæs²; ¹SINTEF; ²Norwegian University of Science and Technology

During start-up of aluminium cells, sodium penetration causes expansion in the carbon cathode, which may influence the lifetime of the cathode lining. Traditionally, the sodium expansion has been measured up to cathode current densities up to 0.75 A/cm². However, it is well known that the current distribution in the cathode is non-uniform, and high local current densities may be experienced close to the sideledge, which commonly is associated with the W wear pattern. Hence, the Na expansion may cause both local stresses in the cathode blocks, as well as in the total cell lining. The aim of this study is to determine the sodium expansion in a wider range of current densities. Typically, it is found that the sodium expansion starts to increase again above 0.7 A/cm², after the plateau reached at 0.2 A/cm². Apparently, this second increase continues outside the range of 1.5 A/cm² applied in this work.

4:50 PM

Change of Electrical Resistivity of Graphitized Cathode Block during and after Electrolysis in Alumina Molten Salt: *Chihiro Ozaki*¹; Hiroshi Imagawa¹; *Yoshinori Sato*¹; Noboru Akuzawa²; Manabu Hagiwara²; ¹SEC Corporation; ²Tokyo National College of Technology

It is considered the intercalation between graphitized carbon and sodium in molten salt is one of causes of erosion of graphitized cathode used in aluminium reduction cell. The objective of research is to obtain knowledge about deterioration of graphitized cathode by measuring changes of electrical resistivity (ER) during/after electrolysis. As a result of research, it was found when graphitized sample is used as cathode, ER of sample rapidly decreases from start of electrolysis and reaches the lowest after 30 to 50 minutes, and then increases gradually. Upon interruption of electrolysis, lower ER suddenly increases and return to value of pre electrolysis after reaching the plateau area. The behavior of ER change differs by material and heat treatment temperature

of sample. Further, the change of ER obtained by repetitive cycle of ER measurement at electrolysis and its interruption and analysis results of samples after the electrolysis is reported in this paper.

5:10 PM

Potshell Heaving: Thermal Effects on Potshell Geometry during Startup and Shutdown: Wang Yu¹; David Shifflet²; ¹Guiyang Aluminium-Magnesium Design and Research Institute; ²Consultant

Report the measuring of the heaving of aluminium potshell bottom right after the pot start-up. Give some analysis and calculation to investigate possible reasons for the heaving. Describe the effects of the heaving on the reduction cell and suggest some methods to prevent damage from the heaving.

Emerging Interconnect and Packaging Technologies: Pb-Free Solder: Tin Whisker Formation and Mechanical Behavior

Sponsored by: The Minerals, Metals and Materials Society, TMS Electronic, Magnetic, and Photonic Materials Division, TMS: Electronic Packaging and Interconnection Materials Committee

Program Organizers: Carol Handwerker, Purdue University; Srinivas Chada, Medtronic; Fay Hua, Intel Corporation; Kejun Zeng, Texas Instruments, Inc.

Tuesday PM
March 11, 2008

Room: 275
Location: Ernest Morial Convention Center

Session Chairs: Thomas Bieler, Michigan State University; Indranath Dutta, US Naval Postgraduate School

2:00 PM Invited

Tin Whisker Formation: Relationship between Intermetallic Formation, Stress and Whisker Nucleation: Eric Chason¹; K.S. Kumar¹; Nitin Jadhav¹; Lucine Reinbold¹; ¹Brown University

Whiskers in pure tin platings limit the reliability of lead-free electronics. To understand the fundamental mechanisms controlling whisker formation, we have made simultaneous measurements of the intermetallic (IMC) growth kinetics, stress evolution and whisker density. We find that the IMC initially grows rapidly and then slows down as the growing layer blocks diffusion of copper into the tin. The corresponding stress saturates after a small amount of IMC is formed and the whiskers start to grow only after the stress saturates. We interpret these results in terms of a model in which the volumetric strain around the growing IMC particles leads to dislocation and diffusional creep processes. Cross-sectional TEM measurements show that plastic relaxation around the precipitating IMC leads to the formation of subgrain boundaries. The presence of the surface oxide is thought to play a critical role in the stress evolution by preventing relaxation at the surface.

2:30 PM Invited

Sn-Whiskers: What Do We Know: John Osenbach¹; ¹LSI Corporation

Although a number of significant improvements in Sn-plating bath chemistry and process have been developed to reduce the probability of Sn-whisker growth on electronic components with a pure Sn surface finish, Sn-whiskers remain a concern for the electronics industry. This talk will focus on what is known and unknown about Sn-whisker nucleation and growth, the effectiveness of mitigation strategies, and the current state of understanding on how to predict when and under what conditions whisker growth induced field failures may occur.

3:00 PM

Thermo-Electromigration Induced Sn Whisker Growth in Pb-Free Flip Chip Solder Joints: Fan-Yi Ouyang¹; K.N. Tu¹; ¹University of California, Los Angeles

In-situ Sn whisker growth in flip chip solder joints of Pb-free 96.5Sn-3Ag-0.5Cu has been studied at temperature of 150°C. Voids were found to form on the cold side in the neighboring un-powered bump, which means thermomigration drives Sn atoms to the hot end (silicon side). Also, electromigration pushes Sn atoms to the anode side. This combined effect of thermomigration and electromigration,

which we defined as thermo-electromigration, pushed Sn atoms to move in the same direction in the bump with upward electron flow from the substrate to the silicon chip, thus produced a concentration of compressive stress near the exit where the current leaves the solder bump. The stress results in the accelerated growth of Sn whisker in the current crowding region.

3:15 PM Break

3:30 PM

Prevention of Sn Whisker Formation by Surface Treatment of Sn Plating Part II: Keun-Soo Kim¹; Sun-Sik Kim¹; Seong-Jun Kim¹; Katsuki Suganuma¹; Masanobu Tsujimoto²; Isamu Yanada²; ¹Osaka University, Institute of Scientific and Industrial Research; ²C. Uyemura and Company, Ltd.

Establishment of lead-free plating technology and whisker countermeasures is one of the critical problems remaining to be solved for lead-free electronics packaging. Recent researches have revealed the mechanisms of Sn whisker formation and growth. However, more researches are required to find acceptable methods to prevent Sn whisker formation. We propose a new approach to prevent the Sn whisker by surface treatment on pure Sn plating. Ni, Au and Pd layer with the thickness of 0.05µm or 0.2µm was deposited on typical Sn plating by flash-coating process. These samples and pure Sn plating samples were stored in room ambient environment. Comparing with pure Sn plating, Ni/Sn, Au/Sn and Pd/Sn plating is much stable against Sn whisker formation in room ambient environment. Ni/Sn, Au/Sn and Pd/Sn plating samples significantly suppressed the Sn whisker formation under the compressive stress condition.

3:45 PM

Numerical Simulations of Stress Relaxation, Including Whisker Nucleation and Growth, in Mechanically Stressed Sn Films: Eric Buchovecky¹; Allan Bower¹; Eric Chason¹; Sharvan Kumar¹; ¹Brown University

Three-dimensional finite element simulations are used to study the mechanisms of stress relaxation, including the nucleation and growth of whiskers, in a polycrystalline Sn film under compressive loading. Our simulations explicitly model long-range, stress-driven diffusion of Sn through Sn-Sn grain boundaries, as well as anisotropic elasticity and dislocation plasticity within Sn grains. Within a textured, columnar microstructure typical of electroplated Sn films, we examine the role of anomalously oriented grains and non-vertical grain boundaries in producing stress concentrations capable of nucleating a whisker grain (fracturing the native oxide; inducing sliding along vertical grain boundaries). After a whisker nucleates, the rate of whisker growth and the relaxation of stress in the surrounding grains are measured. The results of our study are compared with recent experimental measurements of stress gradients surrounding individual whiskers.

4:00 PM

Effect of Aging on High Strain Rate Deformation and Fracture Behavior of Sn3.8Ag0.7Cu Solder Joints: P. Kumar¹; Indranath Dutta¹; V. Sarihan¹; D. Frear¹; M. Renavikar¹; ¹US Naval Postgraduate School

With the proliferation of mobile electronic devices, solder joints are frequently subjected to loading under high strain rates. This paper studies the influence of microstructural coarsening on (i) the flow behavior of Sn-3.8Ag-0.7Cu under compression over strain rates ranging from 0.1 to 30s⁻¹, and (ii) the fracture behavior of Sn-3.8Ag-0.7Cu joints at nominal strain rates of 1-100s⁻¹. Yield strength and work hardening rate were observed to increase substantially with increasing strain rate, with the strain rate sensitivity at higher temperatures being greater. Low temperature aging (25-50°C) appeared to enhance yield strength slightly, but decreased the work hardening rate. With aging at higher temperatures, both yield strength and work hardening rate decreased dramatically. Associated with the alteration of flow behavior, transitions in fracture behavior and joint toughness were noted. Correlations between joint microstructure and the observed fracture mechanisms will be highlighted. Supported by NSF-DMR-0705734, Freescale and SRC.

4:15 PM

Strain-Rate-Dependant Mechanical Properties for SnAgCu and SnAgCu-X Solder Alloy: Luhua Xu¹; John H.L. Pang²; ¹University of California, Los Angeles; ²Nanyang Technological University

SnAgCu solders have limited mechanical strength and are within the creep range. Their properties of solders are highly dependent on test temperature

and strain rate. The elastic modulus and yield strength of Sn3.0Ag0.5Cu and Sn3.0Ag0.5Cu-X (X=200ppm Ni, Ce) solder alloys were studied at 25, 75, 125°C and a comprehensive range of strain rate from low strain rate (10E-5~10E-2 1/sec) using uni-axial tensile test and extremely high strain rate (104-105 1/sec) by employing Hopkins bar test. The intermediate strain rate test (10E-3~10E1) were conducted by using Nano-indentation continuous stiffness measurement. A statistical method was employed to quantify the strain-rate-dependent mechanical properties. For all the tests conducted, the higher the strain rate the higher the elastic modulus and yield stress of the solder; the higher the temperature the lower the elastic modulus and yield stress. The modulus and yield stress of SnAgCu-X solders are larger than those of the SnAgCu solder.

4:30 PM

Mechanical Properties of Lead-Free Solder Joints – The Size Effect: Peter Zimprich¹; Usman Saeed¹; Brigitte Weiss¹; *Herbert Ipsen*¹; ¹University of Wien

It has been known for some time that various mechanical properties of solder joints depend critically on their size, especially on the gap to thickness ratio. This can have serious effects on brittleness and ductility of these joints and, as a consequence, on their long time stability. Thus it was the aim of this study to investigate the influence of decreasing gap size on tensile, shear, and stress relaxation behavior of solder joints, and to find possible variations with changes in the solder and/or substrate material. The model solder joints were prepared from Sn-3.5Ag and Sn-10.0In-3.2Ag solders using both Cu and Ni substrates. They were of rectangular form with gap sizes varying from 850 down to 25 µm, and they were obtained by a reflow soldering procedure in order to achieve near-industrial process conditions. The microstructure and the complex fracture and crack propagation modes were characterized by scanning electron microscopy.

4:45 PM

Measurement of Impact Toughness of Eutectic SnPb and SnAgCu Solder Joints in Ball Grid Array by a Micro-Impact Tester: Yuhuan Xu¹; Shengquan Ou¹; King-Ning Tu¹; *Kejun Zeng*²; Rajiv Dunne²; ¹University of California, Los Angeles; ²Texas Instruments Inc.

The most frequent failure of wireless, handheld, and portable electronic products is an accidental drop to the ground. The impact may cause interfacial fracture of BGA solder joints. Existing metrology, such as ball shear and ball pull tests, cannot characterize the impact induced high speed fracture failure. In this study, a micro-impact tester was utilized to measure the impact toughness and to characterize the impact reliability of both SnPb and SnAgCu solder joints. The annealing effect at 150°C on the impact toughness was investigated. The impact toughness of SnAgCu solder joints with the plating of electroless Ni/immersion Au (ENIG) became worse after annealing, decreased from 10 or 11 mJ to 7 mJ because of a ductile-to-brittle transition. On the other hand, an improvement of the impact toughness of eutectic SnPb solder joints with ENIG was found after annealing, increased from 6 or 10 mJ to 15 mJ.

5:00 PM

Microstructural Modification of Thick Copper Films to Optimize Chemical-Mechanical Planarization of Through-Wafer Interconnects: *Patrick Andersen*¹; Mariela Bentancur¹; Megan Frary¹; ¹Boise State University

Large through-wafer interconnects may be required for high current applications or novel devices like backside connected solar cells. The electroplated copper film required to fill large vias is typically much thicker than conventional films and has a much different microstructure. Previous work has shown films with smaller, more equiaxed grains tend to have lower removal rates and different topography after chemical mechanical planarization (CMP). Here we alter the plating parameters (bath chemistry and current density) and thermal treatments in order to create different microstructures and measure their effects on CMP outputs. Electron backscatter diffraction is used to quantify microstructural parameters such as grain size and crystallographic texture. We find that annealing thick copper films after complete room-temperature relaxation has a significant impact on CMP outputs such as removal rate and surface roughness. The results of this work could be applied to optimize CMP of thick copper films and through-wafer interconnects.

Emerging Methods to Understand Mechanical Behavior: Subscale Methods

Sponsored by: The Minerals, Metals and Materials Society, TMS Structural Materials Division, TMS Materials Processing and Manufacturing Division, TMS: Advanced Characterization, Testing, and Simulation Committee, TMS/ASM: Mechanical Behavior of Materials Committee, TMS: Nanomechanical Materials Behavior Committee
Program Organizers: Brad Boyce, Sandia National Laboratories; Mark Bourke, Los Alamos National Laboratory; Xiaodong Li, University of South Carolina; Erica Lilleodden, Forschungszentrum

Tuesday PM

Room: 285

March 11, 2008

Location: Ernest Morial Convention Center

Session Chair: To Be Announced

2:00 PM Invited

Size Effects in Metal Deformation and the Role of Stress Concentrations:

*Cynthia Volkert*¹; Daniel Gianola²; Reiner Moenig²; ¹Institute of Materials Physics, University of Goettingen and Institute of Materials Research II, Forschungszentrum Karlsruhe; ²Institute of Materials Research II, Forschungszentrum Karlsruhe

A wide range of studies on the strength of polycrystalline and single crystalline metals support the idea that “smaller is stronger”. In this presentation, an explanation for this trend will be proposed that is based on requiring critical stress concentrations in a critical sized volume for dislocation nucleation. This will be discussed in detail for micro-compression specimens, where the stress concentrations are attributed to sticking between the sample and the punch. Possible extensions to the case of bulk and thin film polycrystals will also be presented and used to provide a justification for Hall-Petch behavior. Such a picture calls into question the existence of size effects in homogeneously loaded, micrometer-size specimens. Tensile testing of single crystal metal nanowires by in-situ manipulation in a dual beam SEM/FIB is proposed as a method to distinguish between size effects from homogeneous and inhomogeneous stress states.

2:30 PM

Microtensile Testing of Nanocrystalline Thin Films for MEMS: *Timothy Rupert*¹; John Sharon¹; Daniel Gianola²; Kevin Hemker¹; ¹Johns Hopkins University; ²Forschungszentrum Karlsruhe, Institute for Materials Research II

Microtensile testing techniques have been employed to characterize the scale-specific mechanical behavior of materials for MEMS through the study of nanocrystalline thin films. The challenges and opportunities associated with these techniques will be reviewed and case studies involving micro-scale specimens presented. MEMS structures are often deposited far from microstructural equilibrium and the mechanical properties of these materials will be shown to be strongly dependent on processing, structure, and temperature. The mechanical behavior of nanocrystalline thin films has been shown to be dependent on microstructural stability. Of particular interest is the extended plasticity that occurs as a result of discontinuous grain growth, where grain boundary pinning and stress-assisted grain boundary migration appear to be important. Experiments to probe the stress dependence of this mechanism will be highlighted and the fact that the mechanical behavior appears to not only be different than that of microcrystalline metals, but also dynamic, will be discussed.

2:50 PM

Mini-Tensile Experiments of Clock-Rolled Zirconium Plate: *George Kaschner*¹; Manuel Lovato¹; Michael Stout¹; Gwénaëlle Proust¹; Irene Beyerlein¹; Carlos Tomé¹; ¹Los Alamos National Laboratory

We present our efforts to measure the tensile strength of clock-rolled pure zirconium in the through-thickness direction of the plate. Such measurements are relevant to benchmarking our constitutive models of hardening and texture evolution. We have designed a fixture and sample to perform tensile tests on our 9mm thick plate. The sample is a double-legged mini-tensile sample: 8mm x 8mm x 1mm overall; each leg has a gage section of 1mm x 1mm x 3mm. In contrast, our standard “macro” tensile sample is a flat dogbone with a gage section of 3mm x 1.5mm x 25mm. We validate our design by comparing the

results of meachanical tests performed on samples of both geometries. Although the hardening response is nearly identical, the flow stress of the miniature samples is offset by +25 MPa at the onset of plastic yield. We present our efforts to resolve the origin of this offset.

3:10 PM

Tensile Testing with the Double Ligament Specimen: *David Alexander¹; Cheng Liu¹; ¹Los Alamos National Laboratory*

The double-ligament (DL) tensile specimen has been used to measure the tensile properties of 6061-T651 aluminum plate. These results have been compared to conventional tensile tests. The DL specimen can be used to measure through-thickness tensile properties in plates as thin as 0.25 in. The strain fields in the DL specimen have been measured during the test by using full-field digital image correlation methods for strain mapping. The effects of sample geometry on the strain distribution in the DL specimen, and the resultant effects on the stress-strain data from the DL test are discussed.

3:30 PM

Room and Elevated Temperature Validation of a Novel Sub-Scale Electromechanical Tester: *Benjamin Peterson¹; Daniel Huber¹; Peter Collins¹; Hamish Fraser¹; ¹Ohio State University*

The Electrothermomechanical Tester (ETMT) is a fully instrumented load frame with software to control direct resistive heating of subscale coupons during thermomechanical excursions and mechanical testing. This talk will focus on the determination of the mechanical properties of alpha/beta and beta processed Ti64 that were heat-treated to produce an extended range of properties. The tests were conducted at several temperatures, including room temperature, and the results compared to identical conventional tensile testing. A size scale exists that is dependent upon the microstructure, and will be discussed. Digital image correlation is employed to measure strain. This has been used to characterize the local and macro strain distribution due to inherent temperature variations along the length of the samples. The statistical variation between samples is also discussed. Once validated, this method offers an attractive alternative to conventional testing for the population of databases relating composition, microstructure, and properties.

3:50 PM

Tension-Tension Cyclic Testing of Sub-Micrometer Copper Freestanding Thin Films: *Ming-tzer Lin¹; Kai-Shiang Shiu¹; Chi-Jia Tong¹; ¹National Chung Hsing University*

A specially designed apparatus to carry out a series of tension-tension cyclic testing of submicron freestanding copper films attached on electroplated frame integrates pin holes, spring and load sensor beam is demonstrated. The sample fabrication involves three steps of lithography and two steps of electroplating to hold a dog bone freestanding copper thin film. The gage section of films is 600x100µm with a thickness of 300–900nm. The remaining thin film outside the gage section maintained good adhesion to the frame that would subsequently be gripped for tensile testing. It was then loaded by performing monotonic and tension-tension fatigue experiments at 10Hz up to 10⁷ cycles. Loading was applied by piezoelectric actuator and loads were measured by capacitor load cell. All samples tested here passed 10³ cycles under constant stress amplitude below yielding and a trend of decreasing cycles to failure with increasing loading amplitude and increasing mean stresses has been noted.

4:10 PM Break

4:25 PM Invited

Mechanical Behavior/Microstructure Relationship in Cu/Nb Multilayers Tested via Micropillar Compression: *Nathan Mara¹; Dhriti Bhattacharyya¹; Pat Dickerson¹; Richard Hoagland¹; Amit Misra¹; ¹Los Alamos National Laboratory*

Mechanical testing of nanoscale multilayers has been largely limited to nanoindentation, with few studies carried out to examine bulk mechanical behavior, such as tensile testing of freestanding samples or micropillar compression testing. In this work, the mechanical behavior of Cu/Nb multilayers are evaluated using three test methods: micropillar compression, nanoindentation, and tensile testing of freestanding samples. Through the use of Focused Ion Beam (FIB) milling, post-deformed microstructures are examined via Transmission Electron Microscopy (TEM). Individual layer thicknesses

tested range from 100 nm to 5 nm, with flow stresses ranging from ~1.1 GPa to nearly 3 GPa, respectively. Remarkable deformability is demonstrated in these materials during micropillar testing, with 40 nm Cu/Nb exhibiting 30% strain to failure and 5 nm Cu/Nb exhibiting strains in excess of 20%. The unique behavior of these materials will be discussed in terms of interfacial effects on dislocation motion.

4:55 PM

Characterization of Damage of Ferritic ODS Alloys with Advanced Micro-Sample Methods: *Wolfgang Hoffelner¹; Manuel Pouchon¹; Jiachao Chen¹; Johann Michler²; Maria Samaras¹; ¹Paul Scherrer Institute; ²Swiss Federal Laboratories for Materials Testing and Research (EMPA)*

Oxide dispersion strengthened (ODS) steels are candidate materials for advanced electric energy and heat generation plants (nuclear, fossil). Understanding the degradation of mechanical properties of these alloys as a result of service exposure is very important. For advanced nuclear applications combination of temperature, irradiation and stress are important damage conditions which are preferentially studied with subsized samples like nano-indentation, micro-pillar or thin strip testing due to size constraints given by irradiation. Irradiation hardening, thermally and/or irradiation induced phase reactions and creep (irradiation induced, thermal) deformation were investigated with these methods. The results were linked with transmission electron microscopic investigations. Ferritic ODS steels with 16 to 20% chromium were investigated. The materials were studied in qualities differing in grain sizes and in sizes of the dispersoids. Irradiation was performed in an accelerator using He ions and protons. The interpretation of the results with multiscale modeling will be discussed.

5:15 PM

A Micro-Compression Study of Shape-Memory Deformation in U-6wt%Nb: *Amy Clarke¹; Robert Field¹; Patricia Dickerson¹; Rodney McCabe¹; John Swadener¹; Robert Hackenberg¹; Donald Brown¹; Dan Thoma¹; ¹Los Alamos National Laboratory*

Quenching U-6wt%Nb results in a martensitic phase transformation from the high temperature, bcc γ phase to a monoclinic α' structure. This material has been shown to display the shape-memory effect (SME), where deformation proceeds by twinning and twin rearrangement via boundary migration within the SME regime. A theoretical single crystal analysis, which incorporates the Bain strain and the parent γ phase orientation relationship with the product martensite, successfully predicts polycrystalline deformation structures and texture evolution within the SME regime. In the current study, micro-compression samples from single γ grains of a polycrystalline sample have been fabricated using focused ion beam milling and tested in a nano-indentation instrument to directly investigate the single crystal behavior and determine the influence of orientation on stress-strain behavior. Microstructure characterization was performed using orientation imaging microscopy (OIM) and transmission electron microscopy (TEM).

5:35 PM

Size Effects during Compression of Passivated Micropillars: A Comparison between Dislocation Dynamics and Experiments: *Lucia Nicola¹; Erik Van der Giessen²; Alan Needleman³; ¹Delft University of Technology; ²University of Groningen; ³Brown University*

Several experiments have shown a size dependent flow strength of micropillars under compression. The size effect is even more pronounced when the pillars are passivated. The aim of this study is to attain a better understanding of the size effect in the pillars by modeling their plastic deformation using two dimensional discrete dislocation plasticity and comparing the results to experimental findings. To capture the size effect, we rely on the length scales intrinsic in the model, i.e. the dislocation Burgers vector and the average spacing between dislocation sources. Additional length scales that may appear during evolution of the dislocation structure, like the length of dislocation pile-ups, will also play a role. By changing not only the pillar diameter but also its height (and therefore volume) some insight can be gained in issues like nucleation controlled hardening and dislocation starvation.

5:55 PM

Fabrication and Mechanical Properties of Miron-Sized Nip Amorphous and Composite Pillars: Xiao Qiang Zhang¹; Yi Li²; ¹Singapore-MIT Alliance; ²National University of Singapore

The array of micro-sized pillars of NiP amorphous alloy and its composite are fabricated by electro-plating into the UV-lithography defined photoresist mask. This method offers a batch of pillar samples with various shapes for the investigation of the mechanical behavior of amorphous and its composites in micro-size under compressive load. The mechanical properties of the amorphous alloy were studied by micron-compression conducted in a nanoindenter. The effects of samples' geometry and microstructure on the compressive mechanical properties are reported.

Enhancing Materials Durability via Surface Engineering: Novel Surface Durability Approaches

Sponsored by: The Minerals, Metals and Materials Society, TMS Structural Materials Division, TMS/ASM: Corrosion and Environmental Effects Committee, TMS: High Temperature Alloys Committee

Program Organizers: David Mourer, GE Aircraft Engines; Andrew Rosenberger, US Air Force; Michael Shepard, Air Force Research Laboratory/MLLMN; Bruce Pint, Oak Ridge National Laboratory; Brian Gleeson, Iowa State University

Tuesday PM
March 11, 2008

Room: 388
Location: Ernest Morial Convention Center

Session Chair: Brian Gleeson, Iowa State University

2:00 PM Introductory Comments

2:05 PM

Diffusion Alloying of Thin Stainless Steel Foils by Simultaneous Addition of Al and Reactive Elements: Daniela Pilone¹; Ferdinando Felli¹; Umberto Bernabai¹; ¹Sapienza Università di Roma

Automotive catalytic converter lifetime is linked to the amount of aluminum present in the base alloy that promotes the formation of a protective alumina layer. The process involving cold rolling and annealing allows to produce ferritic stainless steel containing more than 7 wt.% of Al. Unfortunately many α -Al₂O₃ scales tend to spall particularly during thermal cycling with consequent revelation of the bare alloy. Small additions to the ferritic stainless steel of oxygen reactive elements are known to improve the adhesion of α -Al₂O₃ scales. In this work reactive elements were added to the aluminum foil before roll bonding and their behavior during the diffusion bonding was evaluated. This novel process, that appears really promising, allows to overcome problems related to steel alloying with reactive elements and reduces the quantity of expensive reactive elements that needs to be added per square meter of catalyst carrying foil.

2:30 PM

Effects of Copperize Graphite to the Properties of Graphite-Copper Metal Matrix Composites: Liu Wei¹; Guangchun Yao¹; Yihan Liu¹; ¹Northeastern University, School of Materials and Metallurgy

The interface between graphite and copper as well as distributed form is a very important factor to affect the properties of graphite-copper metal matrix composites (MMC). We used copper sulfate as main salt, zinc powder as reducer to copperize graphite. The graphite-copper MMC made with Cu-coated graphite and graphite are prepared by powder metallurgy. The results show that the properties of graphite-copper MMC are remarkably increased after graphite is copperized. The electrical conductivity increased 6.4%, impact toughness increased 61%, friction coefficient reduced 5.6%.

2:55 PM

Novel Surface Modification of Steel Using High-Density Infrared Heating: Ryan Haase¹; Brian Gleeson¹; ¹Iowa State University

High-density infrared heating is a surface heating technique capable of producing wear-resistant coatings over a considerably larger processing area than currently available techniques (e.g. lasers). The focus of this study was to establish plasma arc-lamp processing parameters for the production of

carbon-enriched, wear-resistant coatings on a 1018 steel substrate. The phase transformations involved were found to be in accordance with what occur in a fast-cooled hypoeutectic Fe-C system. The resulting structures contained a significant amount of Fe₃C near the surface present as discrete plates and with the ledeburite (i.e., eutectic microconstituent). A large fraction of carbide and the fine scale of the structures resulted in high hardnesses, reaching 750 HV 0.1 and 980 HV 0.1 for the graphite-only and Fe-Mo-C surface-modified regions, respectively. The high hardness and carbide fraction resulted in a significant improvement in two-body sliding wear-resistance over a standard carburized-and-hardened microstructure.

3:20 PM

Preparation of Trivalent-Chrome Chemical Conversion Coatings on 6061 Aluminum Alloy and Its Electrochemical Studies: Huicheng Yu¹; Baizhen Chen¹; ¹Central South University

The environmental laws in many countries have imposed severe restrictions on chromate (Cr6+) use due to its high toxicity and consequent environmental hazards. Many attempts have been made to find alternatives to chromate (Cr6+) chemical conversion coatings, little attention has been paid to Chromate (Cr3+) conversion coatings. In this work, Chromate (Cr3+) conversion coatings on 6061 aluminum alloy were prepared using trivalent-chrome compound (KCr(SO₄)₂·H₃PO₄ and additive. The influence of six different variables (trivalent-chrome compound (KCr(SO₄)₂ and pH and H₃PO₄ concentration, time and temperature of immersion, and drying temperature) were studied using potentiodynamic polarization curves and AC impedance spectroscopy (EIS) in 3.5 wt% NaCl at room temperature. We found out the optimized range of process parameters evaluating the potentiodynamic polarization curves and AC impedance spectroscopy (EIS) data. Probable mechanisms are proposed to explain the polarization curves and EIS results for the six treated conditions tested.

3:45 PM Break

4:00 PM Invited

The Use of Copper to Prevent High Temperature Surface Attack by Carbon: David Young¹; Jianqiang Zhang¹; ¹University of New South Wales

Carbon-rich reducing gases can attack heat resisting alloys by internal carburisation and/or metal dusting. Both processes involve alloy supersaturation by carbon, followed by precipitation of either carbides or graphite at or near the surface. The addition of copper to pure nickel largely suppresses dusting at 680°C. This benefit is also achieved for 304 and 316 stainless and Alloy 800, but is limited by copper solubility in these alloys. The basis of the copper effect is discussed in terms of nucleation and growth of the precipitating species, together with the accompanying permeation of carbon through the alloy matrix. Carburisation rates measured for model Ni-Cu-Cr alloys are used to assess the effect of copper on carbon permeability in austenite.

4:25 PM

Interdiffusion Behavior of "Simple" Pt-Enriched $\gamma+\gamma'$ Coatings on Ni-Based Superalloys: Justin Stacy¹; Ying Zhang¹; Bruce Pint²; Allen Haynes²; Brian Hazel³; Ben Nagaraj³; Lirong Lui¹; ¹Tennessee Technological University; ²Oak Ridge National Laboratory; ³General Electric Aircraft Engines

"Simple" Pt-enriched $\gamma+\gamma'$ coatings (16-19 at.% Al, ~18 at.% Pt) were synthesized on René 142 and René N5 Ni-based superalloys by electroplating ~7 μ m Pt followed by an anneal treatment in vacuum at 1175°C. The interdiffusion experiments were carried out in the temperature range of 900-1100°C with different periods of time for investigation of coating compositional and microstructural evolutions. After 1000h at 1000°C, the 30- μ m coating diffused into the substrate to a depth of ~65 μ m. At 1050°C, the coating became ~120 μ m after 1000h. The changes in the compositional profiles after the diffusion experiments were determined by electron probe microanalysis, and a diffusion model was used to predict the Pt content at the coating surface.

4:50 PM

Cold Roll Bonding and Annealing Process to Produce an Intermetallic Layer on Ti Substrate: Daniela Pilone¹; Ferdinando Felli¹; ¹Sapienza Università di Roma

Titanium is characterized by poor resistance against oxidation at high temperature. Surface modification by formation of titanium aluminide coatings would be effective to improve oxidation resistance. In this study, a 100 μ m

TUESDAY
PM

aluminum foil was initially bonded with a 1 mm Ti sheet by means of cold roll bonding. The aluminum clad Ti foil was heat treated over the temperature range 600-1000°C in order to form an outer TiAl₃ layer protecting the substrate from high temperature oxidation. Al and Ti concentration profiles, as well as microhardness profiles, were determined in order to investigate the relationship between heat treatment conditions and formation of intermetallic compounds. The morphology and the structure of TiAl₃ layer formed at different temperatures were studied by means of SEM/EDS and X-ray diffraction.

5:15 PM Break

National Academies Corrosion Education Study Community Town Hall Meeting

Sponsored by: The Minerals, Metals and Materials Society, TMS Structural Materials Division, TMS/ASM: Corrosion and Environmental Effects Committee
Program Organizer: Michael Moloney, National Academies

Tuesday, 5:30 PM Room: 388
March 11, 2008 Location: Ernest Morial Convention Center

Session Chair: Michael Moloney, National Academies

Frontiers in Process Modeling: Casting and General Modeling

Sponsored by: The Minerals, Metals and Materials Society, TMS Extraction and Processing Division, TMS Materials Processing and Manufacturing Division, TMS: Process Technology and Modeling Committee
Program Organizers: Andrew Campbell, WorleyParsons; Adam Powell, Opennovation

Tuesday PM Room: 287
March 11, 2008 Location: Ernest Morial Convention Center

Session Chair: Adam Powell, Opennovation

2:00 PM

A Closed Form Simulation of Coarsening Analog System: *Vaughan Voller*¹; ¹University of Minnesota

If a froth of soap bubbles is held between two closely spaced parallel plates it will coarsen-over time, the number of bubbles will decrease and the average area of bubbles will increase. This system has often been used as an analog system for grain growth in metals. In this paper a simple simulation for froth bubble dynamics is developed. This simulation is based on a random walk process for removing bubbles coupled to a Voronoi diagram visualization to track geometric changes in the froth. This simple approach can be reduced to a closed form expression for the bubble dynamics that produces the correct long time scaling and follows the form of the classic Mullins-Neumann growth law. Predictions from the model are validated against available experimental data. The possible application of the simulation to grain growth is discussed.

2:20 PM

A Generic Enthalpy Based Approach to Incorporate the Kinetics of an Equiaxed Eutectic Microstructure Formation in Castings – A Concept: *Suresh Sundarraj*¹; ¹General Motors Corporation

This work summarizes the development of a new Generic Enthalpy Model (GEM) to describe the macroscopic heat transfer during solidification in binary equiaxed eutectic alloy system. For the first time, this model simultaneously accounts for the kinetics and thermodynamics of the solidification process in a seamless manner. The GEM approach accurately predicts the macroscopic cooling curve in a casting region. It has the potential to provide a framework for readily adapting to multi-component alloy systems.

2:40 PM

A Nouvelle Thermo Physical Solution to Casting Deformation Problem in DC Casting of Light Metals: *Dimitry Sediako*¹; *Olga Sediako*²; ¹National Research Council of Canada; ²Renfrew County District School Board, Ministry of Education, Ontario

3D model development has become a common place in process computational analysis and technology optimization in DC casting of light metal alloys. The computational systems are usually based on traditional formulation of 3D equation of thermal conductivity coupled with a set of boundary and initial conditions. A problem exists however in calculation of shrinkage/contraction of metal during casting and accommodating this deformation in the dynamically changing boundary conditions. A nouvelle solution has been developed to calculate and account for various types of deformation that are taking place during bloom/billet formation in the DC casting process: shrinkage and contraction, as well as swell and bow type deformation of the butt of the DC castings. The solution offers a new approach to designing the 3D system architecture and extends practical application of the models in the casting process analysis and optimization.

3:00 PM

The Development of Flexible Hot Rolling Technology Based on Through-Process Modeling: *Priya Manohar*¹; ¹Robert Morris University

A new paradigm is proposed in this paper that underpins the development of flexible rolling technology in industrial processing of C – Mn and Low C – microalloyed steels. Scientific knowledge of industrially-significant processes for these materials is presently fragmented and scattered in published literature. This results in impediments to process optimization and new technology development. In the current work, it is demonstrated that new process sequences could be developed by breaking down existing process routes in to key elements and then by recombining them to generate novel alternative and more efficient hot processing sequences. The proposed methodology establishes a platform for a more realistic assessment of existing process routes and the development of new hybrid process routes that combine ideas from alternative processes. This enables the identification of an optimal process sequence for specified steel compositions that also satisfies simultaneous design criteria such as process feasibility and property maximization.

3:20 PM

Using Computational Techniques to Determine Aluminum Cast House Equipment's Environmental Carbon Contribution at the Design Stage: *Prptal Sandhu*¹; ¹Technology Innovation Centre

This paper looks at using computational design to determine the carbon content of cast house equipment. Reviewing current methods used in industry in evaluating carbon footprints and applying these before the production stage. By providing mathematical modeling techniques, which can be applied through software to determine the equipments carbon contribution as part of a Knowledge Based Engineering program. Using computer design simulations to evaluate the changes made towards energy requirements, for purpose of carbon labeling compliance. By automating this information the capturing of carbon footprints and embodied energy information at the design stage, engineers can determine its environmental effects and included them in the products specification. Allowing the end users of the equipment to make informed choices over what cast house products they plan to use.

3:40 PM

Overview: Modeling Material Properties Critical for Process Simulation: *Zhanli Guo*¹; *Nigel Saunders*¹; *Peter Miodownik*¹; *Jean-Philippe Schille*¹; ¹Sente Software, Ltd.

Process simulation requires reliable data for a wide variety of material properties, ranging from thermal conductivity to flow stress curves. Traditionally such data are gathered from experimentation, which can be time-consuming and costly. This presentation describes the development of computer models that can provide in situ calculations of many material properties, such as solidification properties and high temperature stress-strain curves. The solidification properties are affected by changes in composition within the specification range of an alloy; such changes in properties then also affect casting simulation itself. The mechanical properties are calculated by considering two competing deformation mechanisms (dislocation glide or dislocation climb), with automatic selection of the dominant mechanism. These models have been integrated into the computer

software package JMatPro, which can then be used to export data files directly to FE/FD based packages used for casting, forging and deformation simulation.

4:00 PM Break

4:10 PM Panel Discussion

An open forum to discuss the latest developments in modeling and areas where further advancement would assist industry.

General Abstracts: Materials Processing and Manufacturing Division: Films, Coatings, and Surface Treatments

Sponsored by: The Minerals, Metals and Materials Society, TMS Materials Processing and Manufacturing Division, TMS/ASM: Computational Materials Science and Engineering Committee, TMS: Global Innovations Committee, TMS: Nanomechanical Materials Behavior Committee, TMS/ASM: Phase Transformations Committee, TMS: Powder Materials Committee, TMS: Process Technology and Modeling Committee, TMS: Shaping and Forming Committee, TMS: Solidification Committee, TMS: Surface Engineering Committee
Program Organizers: Ralph Napolitano, Iowa State University; Neville Moody, Sandia National Laboratories

Tuesday PM Room: 282
March 11, 2008 Location: Ernest Morial Convention Center

Session Chairs: Jun Qu, Oak Ridge National Laboratory; Arthur Heuer, Case Western Reserve University

2:00 PM

Advanced Polymer Coatings Produced by High Velocity Thermal Spray: *Bryony James*¹; Margaret Hyland¹; Krishal Patel¹; ¹University of Auckland

Coatings of Poly-ether-ether-ketone (PEEK) have been deposited on stainless steel substrates using high velocity air fuel (HVOF) thermal spray. One essential parameter that dictates the performance of any coating is the adhesion of the coating to the substrate. In this case, of PEEK coatings on metal, adhesion occurs between an organic molecule and the surface oxide/hydroxide layer of the metals and as such can be altered by surface pretreatments of the metal. Surfaces of stainless steel were modified by degreasing, using proprietary etchants, and bead blasting with a variety of media. These surface pretreatments altered both chemistry and morphology of the metal as shown by analysis using X-Ray Photoelectron Spectroscopy (XPS) and Atomic Force Microscopy (AFM). Single sput studies of PEEK wetting on the substrates were used to determine optimum conditions to promote wetting and good sput morphology, and these conditions were subsequently used to produce well adhered PEEK coatings.

2:20 PM

Optical Property of Thermal Barrier Coating at High Temperature: *Geunsik Lim*¹; Aravinda Kar¹; ¹University of Central Florida

A radiative component in thermal barrier coatings and other ceramic oxides becomes significant at high temperature. Low radiative absorption and high scattering properties of thermal barrier coating play in reducing the temperature gradient. The dielectric constant, refractive index, and extinction coefficient are determined for improvements in turbine blade performance at high temperature. Optical properties of zirconia containing 7wt% Y_2O_3 will be discussed both for the conductive and the radiative components in the temperature range 1000–1873 K. The effect of various influencing parameters, i.e., radiation-conduction parameter, surface emissivity, single scattering albedo and optical thickness has been illustrated.

2:40 PM

Anodizing Steel for Corrosion Protection: T. Burleigh¹; Samuel Gabay¹; Taylor Dotson¹; Keenan Dotson¹; Trista Sloan²; Shannon Ferrell¹; ¹New Mexico Institute of Mining and Technology; ²Vibrant NDT

A novel process has been developed to protect steel from corrosion by anodization. Steel was anodized in a simple two-electrode cell in a concentrated NaOH or KOH solution. The steel grew a thick oxide surface film and was more resistant to corrosion than bare steel. Different ranges of anodizing

voltage, time and temperature were found that produced varying thicknesses, adhesion, and color. Analysis of the oxides revealed that they were primarily magnetite. A follow-up heat treatment increased the corrosion protection beyond either anodizing or heat-treating alone. Anodizing steel could help address the economic problem of corrosion of steel while providing an alternative to costly or toxic coatings. This paper describes what steps researchers have made in anodizing steel, what future improvements are needed, and how anodizing steel can benefit different industries.

3:00 PM

Synthesis and Characterization of Boron Carbonitride (BCN) Thin Films by Plasma Enhanced DC Magnetron Sputtering: *Tolga Tavsanoglu*¹; Michel Jeandin²; Okan Addemir¹; ¹Istanbul Technical University; ²Ecole des Mines de Paris

In the last few years, thin films with composition within the ternary system B–C–N have attracted much attention as they are expected to combine some specific properties of c–BN, h–BN and B_4C , such as, high hardness, low friction coefficient. In this study B_4C was used as target material and BCN films with different composition were obtained by varying the N_2/Ar proportion in the sputtering gas (0–100%). A negative bias voltage was applied V_b to the substrates (0–250 V). The microstructure and crystallinity of the films were characterized by cross-sectional FE-SEM and XRD analysis. The film composition was measured by EPMA. The elemental depth profiles of the coatings were obtained using a Secondary ion mass spectrometer. The bonding characteristic of the films were investigated by Fourier transform infrared spectroscopy. The mechanical properties were determined by nanoindentation and the tribological properties by pin-on-disc measurements.

3:20 PM

Forming a Wear-Resistant Nanocomposite Surface Using Friction Stir Processing: *Jun Qu*¹; Hanbing Xu¹; Zhili Feng¹; D. Alan Frederick¹; Brian C. Jolly¹; Rick Battiste¹; Peter Blau¹; Stan David¹; ¹Oak Ridge National Laboratory

Aluminum alloys would have much wider usage in bearing applications if their wear-resistance could be significantly improved. In this study, friction stir processing was used to stir and mix nano-sized Al_2O_3 particles into an aluminum surface to form a nanocomposite layer to improve the hardness, strength, and wear-resistance without sacrificing the bulk ductility and conductivity. Compared with a non-processed aluminum surface, the nanocomposite surface demonstrated increased hardness (by 3X) and yield strength (by 8X), and reduced friction coefficient (by 55%) and wear rate (by 200X). Major challenges encountered in process development include the low densities of nano-powders and the high wear of conventional FSP tools. Solutions to these challenges are proposed. Unlike most other surface engineering techniques, this process can form very thick layers, up to centimeters in thickness, with delamination avoided because of the inherent material continuity.

3:40 PM Break

3:50 PM

Fatigue of Surface-Treated Austenitic Fe-Base and Ni-Base Alloys: *Arthur Heuer*¹; Gary Michal¹; Frank Ernst¹; Hal Kahn¹; Yindong Ge¹; ¹Case Western Reserve University

A low-temperature gas-phase carburization process has been developed that allows surface concentrations up to 15 at% carbon in austenitic stainless steels and Ni-base alloys without carbide formation, and with no decrease in ductility. Fatigue lifetimes under fully reversed loading ($R = -1$) are significantly enhanced, due to the extremely high strength and tough surface region, which contains residual compressive stresses of ~2 GPa generated by the carburization process. The increase in fatigue performance is associated with the absence of surface fatigue crack nucleation. Virtually all fatigue cracks nucleate in the interior of the sample. Several stainless steels have been investigated and will be discussed, including the 316L, 304, AL-6XN, and A286 grades, in addition to Ni-base IN718. The microstructural features responsible for crack initiation are described and the role of surface modification on fatigue life is discussed.

4:10 PM

Optimization of Gas Carburizing Process in Batch Furnaces with Endothermic Carburizing Atmosphere: Olga Karabelchchikova¹; Md. Maniruzzaman¹; Richard Sisson¹; ¹Worcester Polytechnic Institute

The paper addresses the current industrial issues with the gas carburizing process control and carburizing time/cost optimization. The optimization strategy is based on 1) understanding the effect of process parameters on the mass transfer coefficient and carbon diffusivity in austenite; 2) functional correlation of the observed variations in the process parameters on the kinetics of carburizing; and 3) developing a robust optimization technique to achieve the desired case depth with minimum cost and processing time. The index of performance for the process optimization involves both the surface carbon concentration and the case depth. While the first parameter depends on accurate control of the atmosphere and the carbon potential in the furnace, the case depth is primarily influenced by the temperature in the furnace and the duration of the carburizing process. Application of this optimization technique will result in significant energy reduction by shortening cycle time and thereby enhanced furnace capacity.

4:30 PM

Enhanced Corrosion Resistance of Austenitic Stainless Steels Due to Low-Temperature Carburization: Arthur Heuer¹; Gary Michal¹; Frank Ernst¹; Hal Kahn¹; Farrel Martin²; Ted Lemieux³; Theresa Newbauer³; Bob Bayles³; Paul Natishan³; ¹Case Western Reserve University; ²SAIC/Naval Research Laboratory Operations; ³U. S. Naval Research Laboratory

A low-temperature (~460°C) gas-phase carburization process has been developed that allows surface carbon concentration up to 15 at% in austenitic stainless steels without carbide formation. The carburization occurs under paraequilibrium conditions. The corrosion resistance of the steels after carburization is significantly enhanced – for example, pitting corrosion of 316L stainless steel is essentially suppressed, breakdown potential is increased by 850 mV, and crevice corrosion resistance can be greater than some Ni-base alloys such as Inconel 625. The carburized samples re-passivate ~150 mV below the breakdown potential, and the increased corrosion resistance is also evident in slow-strain-rate experiments performed in saltwater, particularly when the samples contain a crevice former. Possible mechanisms involved in the improved corrosion resistance are discussed, as are results for other carburized alloys.

4:50 PM

Experimental and Numerical Study of Flame Load Heat Transfer in an Experimental Furnace: Ashwini Kumar¹; Raj Venuturumilli¹; Laszlo Kiss²; Geza Walter²; ¹Fluent Inc.; ²University of Quebec

Flame impingement on solid objects is a routinely encountered phenomenon in metallurgical operations. This was studied in an experimental furnace in order to obtain heat transfer data. In this paper, the same is simulated using Computational Fluid Dynamics (CFD) approach and the resulting temperature, velocity and chemical composition distributions were compared to the experimental data. This comparative analysis demonstrates the potential of mathematical modeling not only in complementing the experiments but also in providing a cost-effective framework for obtaining the data after proper validation with the experimental data. Examples with different burner and flame types used in the industry are given.

5:10 PM

Evaluation of Braze-Bonding Mechanism of Ternary Boride Based Cermet on to Ferrous Alloy Substrates for Improved Performance: Barath Palanisamy¹; Anish Upadhyaya¹; K. Anand²; ¹Indian Institute of Technology; ²GE India Technology Centre

Materials possessing good wear resistance also possess high hardness and strength. Boride based cermets (C50, V30) are a new class of materials and aim to improve wear resistance of ferrous alloy substrates. The current work focuses on studying a unique surface modification process, Sinter-bonding. The process of sintering of the cermet, the substrate and the bonding between them occur simultaneously thereby rendering it economic. A range of ferrous alloy substrates were used with significant change in bonding mechanism owing to the change in composition of the base material. Bonding was carried out at 1250°C and it was observed that the atmosphere used affects the surface appearance and densification of the bonded cermet. The study was performed using SEM,

EDS, XRD characterization tools and the mechanical properties were evaluated using micro-hardness, transverse rupture strength and tribological tests and it is observed that the material is competitive with other prevalent hard coatings.

5:30 PM

A Model of Thermo-Induced Processes during Particle Cooling in the Component-Coating System in Plasma Spraying Processes: Niu Liping¹; Zhang Ting-an¹; Dou Zhihe¹; ¹Northeastern University

The temperature distributions on coating are analyzed in the component-coating system in plasma spraying processes. This process can be considered a thermo-mechanical treatment and with respect to other treatments, such as shot-peening in which the target is hit by metal or ceramic spheres, the biggest difference is the thermo effects. Temperature change is a source of stresses in target and the purpose of this analysis is to evaluate the stress by some numerical methods. A model of thermo-induced processes is obtained by calculation-experimentation during the particle cooling between elastic limit and temperature of the particle material.

General Abstracts: Structural Materials Division: Novel Issues in Materials Processing

Sponsored by: The Minerals, Metals and Materials Society, TMS Structural Materials Division, TMS: Advanced Characterization, Testing, and Simulation Committee, TMS: Alloy Phases Committee, TMS: Biomaterials Committee, TMS: Chemistry and Physics of Materials Committee, TMS/ASM: Composite Materials Committee, TMS/ASM: Corrosion and Environmental Effects Committee, TMS: High Temperature Alloys Committee, TMS/ASM: Mechanical Behavior of Materials Committee, TMS/ASM: Nuclear Materials Committee, TMS: Product Metallurgy and Applications Committee, TMS: Refractory Metals Committee, TMS: Superconducting and Magnetic Materials Committee, TMS: Titanium Committee

Program Organizer: Ellen Cerreta, Los Alamos National Laboratory

Tuesday PM

Room: 387

March 11, 2008

Location: Ernest Morial Convention Center

Session Chair: Pietro Navarra, Hatch

2:00 PM

A Comparison of Resistance Brazing and Adhesive Bonding as Joining Methods for Periodic Cellular Metals: Eral Bele¹; Ian Stewart¹; Glenn Hibbard¹; ¹University of Toronto

Periodic Cellular Metals (PCMs) are frames of beams, wires or hollow tubes arranged to create a three dimensional architecture. Due to the fact that only the structurally efficient part of the total mass is retained, they exhibit improved strength-to-weight and stiffness-to-weight ratios compared to conventional metallic foams. Bulk PCM structures can be fabricated using perforation stretching methods that produce single layers of micro-truss frames, which are successively stacked and joined. However, conventional brazing methods that are typically used to join aluminum alloy PCMs can reduce the strength of work hardened cores by as much as 50%, since the brazing temperature is significantly above the typical recrystallization temperature. This study evaluates two alternative joining methods: adhesive bonding and resistance brazing. Compression tests show that the resultant structures have significantly improved properties compared to their conventionally brazed counterparts. The results are also used to establish design guides for each joining method.

2:20 PM

Bonding and Adhesion at the Fe/TiC Interface: Theoretical Strength and Misfit Dislocations: Oleg Kontsevoi¹; Yuri Gornostyrev²; Arthur Freeman¹; Gregory Olson¹; ¹Northwestern University; ²Institute of Metal Physics

The dispersed inclusions of TiC were shown to provide superior fracture toughness and increased strength for steels. To obtain a fundamental understanding of their effect, we calculated the work of adhesion for two kinds of Fe/TiC interfaces with the first-principles FLAPW method. For the coherent <100>{001}Fe//<110>{001}TiC interface, a theoretical strength of 3.89 J/m² was obtained. Within the framework of the Peierls-Nabarro model with ab-initio generalized stacking fault energetics, we estimated that the misfit dislocations,

which may form due to 6.4% Fe-TiC lattice mismatch, would decrease the interface strength by 0.8 J/m². The second, <110>{110}Fe/<010>{100}TiC semicoherent interface contains one primary misfit dislocation per unit cell. Despite that, it shows a surprisingly high strength of 3.24 J/m², and the dislocation energy is estimated at 0.6 J/m². We discuss the electronic origins of strong interfacial bonding based on electronic structure and charge densities analyses. Supported by the ONR through Dynamic Microstructure Design Consortium.

2:40 PM

An Investigation on the Chemical Stability of Inert Anodes during Electro-Reduction of TiO₂: Xiaobing Yang¹; Abhishek Lahiri¹; Animesh Jha¹; ¹University of Leeds

The direct electrochemical reduction process to electro-win Ti metal has a potential for reducing the production cost. Carbon anodes in the FFC cell reduce the current efficiency by producing carbon soot, which also acts as an impurity in the metal. In the present investigation we have analysed the chemical stability of intermetallic anodes, based on Al-Ti-Cu alloys in the CaCl₂ bath for the electro-reduction of TiO₂. In this investigation we have measured the cell resistance, current efficiency and performed detailed microstructural and phase analyses for both the anodes in the cell and the metallic/oxide phases present at the cathode. In particular, we have examined the phase stability of perovskite phase which limits the metallization of TiO₂ to Ti metal. The anodic reaction has also been analysed for phases present which are essential for reducing the corrosion rate.

3:00 PM

Direct Production of Super-Grade Materials in Nano-Particle Based Fuels: Liviu Popa-Simil¹; Claudiu Muntele²; ¹LAVM LLC; ²AAMU

Nuclear transmutation reactions are based on the absorption of a smaller particle as neutron, proton, deuteron, alpha, etc. The resulting compound nucleus gets out of its initial lattice mainly by taking the recoil, also with help from its sudden change in chemical properties. The recoil implantation is used in correlation with thin and ultra thin materials mainly for producing radiopharmaceuticals and ultra-thin layer radioactive tracers. In nuclear reactors, the use of nanoparticulate pellets could facilitate the recoil implantation for breeding, transmutation and partitioning purposes. Using enriched 238U or 232Th leads to 239Pu and 233U production while using other actinides as 240Pu, 241Am etc. leads to actinide burning. When such a lattice is immersed into a radiation resistant fluid (water, methanol, etc.), the recoiled product is transferred into the flowing fluid and removed from the hot area using a concentrator/purifier, preventing the occurrence of secondary transmutation reactions.

3:20 PM

Simulation Study on Dynamics of Femtosecond Laser Ablation of the CMSX-4 Ni-Based Superalloy: Mousumi Das¹; Katsuyo Thornton¹; ¹University of Michigan

We have studied the dynamics of femtosecond-pulsed-laser ablation of the CMSX-4 Ni-based superalloy by hydrodynamics simulations. Simulation results qualitatively describe time-resolved pump-probe shadowgraphic images obtained experimentally. In the experiment, a jet-like feature formed by ablated material propagated perpendicularly to the sample surface within an envelope of the air-shock that expanded in both perpendicular and parallel directions. The simulation was performed using two- and three-dimensional hydrodynamics code (FLASH), with initial condition provided by one-dimensional radiation-hydrodynamics (HYADES) simulation. The simulated density profile matches well with pump-probe shadowgraphs, providing insights into the origin of the contrast obtained by shadowgraphic imaging.

3:40 PM Break

4:10 PM

Rapid Manufacturing of Ti64 Components Using Net Shape Hot Isostatic Pressing: Xinhua Wu¹; Junfa Mei¹; Wayne Voice²; Martin Bache³; ¹University of Birmingham; ²Rolls Royce; ³University of Wales

Manufacturing large Ti64 components using Net Shape HIPping is introduced. Recent work on Net Shape HIPping has shown that the shape control, after one iteration is comparable with that found in investment casting. The mechanical properties are generally similar to those found in thermomechanically processed samples although the fatigue properties of Net Shape HIPed samples are slightly lower but the fracture toughness of the as-HIPed samples much higher than

that of thermomechanically processed samples. The factors which control the properties of as-HIPed samples will be reviewed and methods to increase the cost-effectiveness of the process will be discussed.

4:30 PM

Alpha Case Formation in Titanium Alloy IMI834: Martin Jackson¹; Trevor Lindley¹; ¹Imperial College London

Titanium alloys are widely used for compressor components for aeroengine gas turbines. However, during exposure in oxidising atmospheres at temperatures up to 900K, inward diffusion of oxygen can result in the formation of an all alpha surface layer - 'alpha case'. The depth of the alpha case increases with increasing exposure time and temperature. This alpha layer is brittle and mechanical properties can be significantly degraded. This paper presents investigations to understand the formation kinetics of alpha case and the subsequent effects on mechanical performance in IMI834. The results of a parametric study to determine the effects of temperature, time and degree of surface deformation (i.e. intensity of shot peening) on alpha case formation will be discussed. Mechanical performance has been assessed by a sequence of room temperature tensile loading to determine the nature of crack nucleation/growth and to quantify the cracking size/density in the alpha case and subsurface region.

4:50 PM

Extraction of Titanium Dioxide from Ilmenite Ore by Alkali Roasting Followed by Leaching: Abhishek Lahiri¹; Animesh Jha¹; ¹University of Leeds

Titaniferous minerals have impurities (Fe, Cr, Al, Si, Ca, Ce, La, Nd, etc), which must be removed for achieving complete whiteness in TiO₂ pigments. It is difficult and expensive to remove minor and trace impurities from titaniferous minerals using the conventional processes, currently operating worldwide. In this paper we describe a new beneficiation process which comprises of two main steps: the roasting of ores with alkali to form water soluble alkali ferrite and the formation of insoluble alkali titanate. In the second step leaching of roasted mineral is carried to concentrate titanium rich part of mineral. For both steps, the reaction chemistry, phase formed and their analysis were carried out in detail by using the XRD, XRF, SEM and EDX techniques. From the chemical and phase equilibria analysis, we explain the applicability of the new process for the production of better than 95% pure synthetic rutile for chlorination.

5:10 PM

Synthesis of Bulk Mo-Ta Multilayers with Accumulative Roll Bonding: Rainer Hebert¹; Girija Marathe¹; ¹University of Connecticut

Metallic multilayers with a nanoscale layer thickness reveal extraordinary strength levels. While thin-film techniques are limited in synthesizing bulk samples for structural applications, accumulative rolling and folding can provide bulk samples with individual layer thicknesses of less than 100 nm. Rolling and folding experiments with multilayers of tempered Mo and Ta foils lead to a codeformation behavior and layer thicknesses of approximately 200 nm at a strain of -10. The codeformation behavior is rationalized based on microhardness measurements of the multilayers and on micro- and nanoindentation measurements of the individual layers, complemented by cross-sectional SEM and TEM analysis. The rule of mixture is examined for the hardness of the layers and the multilayer throughout the deformation range. The codeformation behavior is furthermore rationalized based on the ratio of the hardness of the Mo and Ta layers. The support of the NSF (CMMI-0700377) is gratefully acknowledged.

5:30 PM

Synthesis and Microstructure of Si₃N₄-TiN Nanocomposites: Mei Yang¹; Mingli Lv¹; Hongmin Zhu¹; ¹Beijing University of Science and Technology

Si₃N₄-TiN nanocomposite was prepared by in situ coating in liquid ammonia using TiCl₄ and Si₃N₄ as starting materials. The reduction reaction of TiCl₄ by sodium in liquid ammonia was performed and resulted TiN nano-powders which nuclei and grew on the surface of Si₃N₄. The composite powder was consolidated though Spark Plasma Sintering (SPS) at 1600°C and dense compact (>98% of theoretical) with a mean grain size of 100~300 nanometers was obtained. The electronic conductivity value (3.1×10³Ω⁻¹cm⁻¹) enough for electrical discharge machining (EDM) was reached by compositing 20vol% TiN to Si₃N₄. The relationship of microstructure and conductivity was discussed.

Hael Mughrabi Honorary Symposium: Plasticity, Failure and Fatigue in Structural Materials - from Macro to Nano: Cyclic Deformation and Fatigue of Metals I

Sponsored by: The Minerals, Metals and Materials Society, TMS Structural Materials Division, TMS Materials Processing and Manufacturing Division, TMS: High Temperature Alloys Committee, TMS/ASM: Mechanical Behavior of Materials Committee, TMS: Nanomechanical Materials Behavior Committee

Program Organizers: K. Jimmy Hsia, University of Illinois, Urbana-Champaign; Mathias Göken, Universität Erlangen-Nürnberg; Tresa Pollock, University of Michigan - Ann Arbor; Pedro Dolabella Portella, Federal Institute for Materials Research and Testing; Neville Moody, Sandia National Laboratories

Tuesday PM Room: 386
March 11, 2008 Location: Ernest Morial Convention Center

Session Chairs: Pedro Portella, Federal Institute for Materials Research and Testing (BAM); Petr Lukas, Czech Academy of Sciences

2:00 PM Keynote

Fatigue Behavior of Nano-Twinned High Purity Copper Films: *Julia Weertman*¹; *Andrea Hodge*²; *Troy Barbee*²; *Mark Seniow*¹; *Anthony Escudro*¹; ¹Northwestern University; ²Lawrence Livermore National Laboratory

The response of high purity, nano-twinned ultra-fine grained Cu thin films to tension-tension fatigue is examined. The 5-9s purity copper samples studied are from sputter deposited free standing 175 micrometer thick films fabricated in a manner eliminating damage occurring during removal from the (100) single crystal silicon substrates or as a result of specimen preparation. Thus, the properties reported are characteristic of the nano/micro structure of these thick copper films. The films' fatigue endurance is determined and compared to coarse-grain as well as UFG Cu produced via cold-rolling. The films are also characterized by changes in surface features and internal microstructure that develop during cyclic loading. This work was partially performed under the auspices of the U.S. Department of Energy by the University of California, LLNL under Contract No. W-7405-ENG-48 and at Northwestern University by US DOE grant DE-FG02-02ER46002.

2:30 PM Invited

Cyclic Deformation Behavior and Fatigue Life of Ultrafine-Grained Metals: *Heinz Werner Höppel*¹; ¹Institute General Materials Properties WWI

Sufficient or improved fatigue properties are one of the key-features for a successful use of bulk nanostructured materials for potential technological applications. Consequently, a detailed understanding of the cyclic deformation behaviour and fatigue life plays a very significant role. Due to the significantly smaller grain size in UFG materials, the grain size becomes the dominating microstructural length scale and hence strongly affects the (dominating) cyclic deformation mechanisms. Hence, the cyclic mechanical properties of UFG materials cannot simply be explained by the well known Hall-Petch relationship. Other key features, like microstructural stability, strain rate dependence of the deformation behaviour, effect of the grain size and potential changes in the mechanisms of localization of plastic deformation compared to conventionally grained materials have to be considered. The addressed aspects on the deformation mechanisms as well as on the fatigue life will be reviewed in the talk.

2:50 PM Invited

On the Influence of Biaxiality on Fatigue Deformation and Microstructure: *Horst Biermann*¹; *Sebastian Henkel*¹; *Juliane Fischer*¹; *Tamas Ungar*²; ¹Technical University Bergakademie Freiberg; ²Eötvös University, Institut für General Physics

The LCF behaviour of the metastable austenitic stainless steel AISI 304 was investigated in monoaxial and biaxial strain-controlled fatigue tests. Constant amplitude, incremental step and load enhancement tests, respectively, were performed on monoaxial, hourglass-shaped specimens and on planar biaxial cruciform samples. In biaxial strain control, different strain paths, i.e. different strain axis ratios and phase angles were studied. The microstructure evolution depending on the different strain paths was investigated by scanning

and transmission electron microscopy and x-ray line profile analysis. The percentage of deformation-induced martensitic phase was measured using a magneto-inductive ferrite-sensor and gives a correlation to the applied total strain amplitude. In addition, crack initiation and crack growth were studied using surface replicas. Based on the experimental results, the influence of the biaxiality is discussed. The von Mises equivalent strain can be applied for proportional load cases. The biaxial IST gives a better understanding of real multiaxial load cases.

3:10 PM

Biaxial Cyclic Stress-Strain Response of Ultrafine Grain Nickel: *Ntirelang Batane*¹; *David Morrison*¹; *John Moosbrugger*¹; ¹Clarkson University

The biaxial cyclic stress-strain response of ultrafine grain (UFG) nickel produced by an electrodeposition process was studied by performing proportional and 90° out-of-phase nonproportional axial-torsional fatigue experiments at room temperature. For comparison purposes, identical experiments were also accomplished on conventional grain (CG) nickel. The grain sizes of the UFG and CG metals were on the order of 100 nm and 50 µm respectively. Axial-torsional tests were performed at constant effective plastic strain amplitudes of 1.0×10^{-4} and 1.0×10^{-3} . In addition, multiple step tests were accomplished at selected effective plastic strain amplitudes between 1.0×10^{-4} and 1.0×10^{-3} . The effects of grain size, loading path, and strain amplitude on cyclic stress-strain response will be discussed in terms of cyclic hardening behavior, cyclic stress-strain curves, and the evolution of dislocation structures.

3:25 PM

Damage Evolution during Low-Cycle Fatigue Testing of Ultra-Fine Grained Interstitial-Free Steel: *Thomas Niendorf*¹; *Hans Maier*²; *Ibrahim Karaman*²; ¹University of Paderborn; ²Texas A&M University

In the present study damage evolution in bcc UFG IF steel under cyclic loading is investigated. We focus on microstructural aspects such as fractions of high-angle and low-angle grain boundaries. ECAE processing following route A leads to high fractions of LAGBs and processing along routes C' and E leads to high fractions of HAGBs. We link the different kinds of boundaries with crack nucleation on the specimens' surfaces. The experiments used for this investigation included LCF tests at room temperature and EBSD measurements in a SEM. EBSD measurements conducted on the same surface area before and after fatigue testing showed that LAGBs are not stable under cyclic loading, as indicated by a rearrangement of boundaries in areas that are dominated by LAGBs and a high density of surface extrusions in these areas. The rearrangement of the LAGBs causes the observed softening and localized damage of route A UFG materials.

3:40 PM Break

3:50 PM Invited

Mechanisms of Cyclic Plastic Deformation in Ultrafine-Grained Copper Produced by Severe Plastic Deformation: *Petr Lukas*¹; *L. Kunz*¹; *M. Svoboda*¹; ¹Czech Academy of Sciences

Fatigue properties and microstructure of UFG coppers of different purities produced by ECAP technique were studied in a broad region of stress amplitudes. While the fatigue strength of low purity UFG copper is by a factor of about 2 higher than that of conventional-grain-size copper in the broad region of fatigue lives from 6×10^3 to 2×10^{10} cycles, the high purity UFG copper is superior to CG UFG copper only at high stress amplitudes. For both low purity and high purity UFG copper the grain structure is stable and undergoes only very marginal changes during cycling. Two mechanisms of cyclic plastic deformation are taken into consideration: (i) bulk mechanism consisting of irreversible movement of dislocations within the grains and (ii) surface mechanism operating in the surface layer consisting of GB sliding along the trace of the last ECAP pass. The later mechanism depends strongly on purity and on temperature.

4:10 PM Invited

Structural and Functional Fatigue of NiTi Shape Memory Alloys: *Gunther Eggeler*¹; ¹Ruhr-University Bochum

Cyclic loading characterizes present and potential future applications of NiTi shape memory alloys which exploit mechanical (pseudo elasticity) or thermal shape memory (one and two way effect). It is associated with structural and functional fatigue, which both limit the service life of shape memory

components. Structural fatigue describes microstructural damage accumulation that eventually leads to failure. Functional fatigue indicates that the intensity of shape memory effects like the working displacement in a one way effect (1WE) actuator or the dissipated energy in a loading-unloading cycle of a pseudo elastic (PE) damping application decreases during cycling. This is due to a gradual change in microstructure. In both cases it is important to know how fatigue cycling affects microstructure and shape memory properties. The present paper provides an overview and highlights some new microstructural results from shape memory fatigue research within the collaborative research center SFB 459 (shape memory technology).

4:30 PM Invited

On the Analysis of the Rate of Fatigue Crack Propagation: *Arthur McEvily*¹; ¹University of Connecticut

Although fatigue of metals has been a subject of importance since the early nineteenth century, interest in the details of the fatigue crack propagation aspect of fatigue failure did not develop until after the crashes of Comet aircraft in 1953. Prior to that time the approach to fatigue design had been largely based solely upon the work of Wöhler and the use of S/N curves. Since the 1950's advances in the fracture mechanics, computers, testing equipment and techniques, and in transmission and scanning electron microscopy have all contributed to a tremendous growth in the understanding of the fatigue crack growth process and of its role in the overall fatigue process. The object of this presentation will be to review some of the advances that have made to provide the basis for the quantitative analysis of fatigue crack propagation.

4:50 PM

Fatigue Behavior of Homogeneous-Microstructure and Mixed-Microstructure Steels: *Donato Firrao*¹; Paolo Matteis¹; Giovanni Mortarino¹; Pasquale Russo Spena¹; Maurizio Chiarbonello¹; Giuseppe Silva²; Barbara Rivolta²; Riccardo Gerosa²; Andrea Ghidini³; ¹Politecnico di Torino; ²Politecnico di Milano; ³Lucchini Sidermeccanica

Molds for plastic automotive components such as bumpers and dashboards are usually machined from large pre-hardened steel blocks. Due to the dimensions, the heat treatment of these blocks produces mixed microstructures, continuously varying with the distance from the quenched surface. The fatigue behavior of these mixed microstructures is not well known, and peculiar results stemmed from previous tests. Such a theme has been examined through experimental tests on two different plastic mold steels, the traditionally used ISO 1.2738 steel and a quenched and tempered microalloyed steel recently proposed for the purpose. The threshold and fatigue crack growth behavior has been investigated. Moreover, in order to clarify the correlations between the microstructural features and the fatigue behavior, fatigue crack growth tests have been performed on re-heat-treated samples with homogenous microstructures (pearlite, or tempered martensite, or bainite), and have been compared with the results obtained while testing mixed microstructure samples.

5:05 PM

Microstructural Effects on Length Scales for Plastic Blunting of Stage II Fatigue Cracks in Metallic Materials: *Pedro Peralta*¹; Rikki Teale¹; Andrea Keck¹; Seon-Ho Choi¹; ¹Arizona State University

A length scale has been recently proposed for plastic blunting of stage II fatigue cracks in metals that is proportional to the product of the cyclic plastic zone radius and the average shear strain ahead of the crack tip. This quantity is measured via in-situ loading experiments in compact tension specimens of Al 2024-T351 and Ti-6Al-4V, where the strain fields ahead of the crack tip are quantified using Digital Image Correlation (DIC) for several values of applied load. Microstructure at the tip is characterized using Electron Backscattering Diffraction (EBSD) and correlations between local microstructure, cyclic strain fields and the plastic blunting length scales are sought. Results are compared to similar measurements in pure polycrystalline nickel and the effects of microstructure are discussed in terms of differences and similarities between the results for the engineering alloys and pure nickel. Funding by Department of Defense AFOSR Grant FA95550-06-1-0309, Victor Giurgiutiu program manager.

5:20 PM

Microtexturing Effects on the Fatigue Lifetime Variability of an Alpha + Beta Ti Alloy: *Christopher Szczepanski*¹; Sushant Jha²; James Larsen³; J. Wayne Jones¹; ¹University of Michigan; ²Universal Technology Corporation; ³US Air Force

Ultrasonic fatigue was used to characterize the fatigue behavior of Ti-6%Al-2%Sn-4%Zr-6%Mo in the very high cycle fatigue regime. Observed lifetimes ranged from 10⁶ – 10⁹ cycles. The initiation mechanism was crystallographic and the facets at the site of crack initiation resulted from fracture of the equiaxed alpha grains along the basal plane. Additionally, the initiation sites were located within microtextured regions where a majority of the alpha phase material was oriented for basal <a> or prismatic <a> type slip modes. OIM analysis indicated that these microtextured regions are generally larger than 1mm in size. The presence of these microtextured regions is believed to promote crack initiation and small crack growth. A computational model has been developed for probabilistic analysis of the size and spatial distributions of these microtextured regions. These results will be presented to highlight the relationship of microtexturing to the variability in fatigue crack initiation and associated lifetimes.

5:35 PM

Crystal Plasticity and Failure at Metal/Ceramic Interfaces: From Nano to Macro: *Siegfried Schmauder*¹; A. Siddiq¹; ¹University of Stuttgart/Institute for Material Testing, Materials Technology and Strength Theory

Deformation and fracture at metal/ceramic interfaces are related to local processes at the crack tip. Internal interfaces play a prominent role in metal/matrix composites between ceramic (such as Al₂O₃) particles and a metallic matrix, e.g. Al. Despite their widespread use, a basic understanding of these interfaces is still underway. The deformation behaviour of niobium single crystals is simulated using crystal plasticity theory. Good agreement between experiment and simulation results was found. The second part provides results on effects of the different niobium single crystalline material orientations on crack initiation energies. Crack propagation analyses of niobium/alumina bicrystal interface fracture are performed using a cohesive modelling approach for three different orientations of single crystalline niobium. Parametric studies are presented. The results show that cohesive strength has a stronger effect on the macroscopic fracture energy as compared to the work of adhesion. In the last part, a correlation among the macroscopic fracture energy, cohesive strength, work of adhesion and the yield stress of niobium single crystalline material will be derived.

Hume-Rothery Symposium - Nanoscale Phases: Session IV

Sponsored by: The Minerals, Metals and Materials Society, TMS Electronic, Magnetic, and Photonic Materials Division, TMS: Alloy Phases Committee

Program Organizers: Sinn-wen Chen, National Tsing Hua University; David Cockayne, University of Oxford; Seiji Isoda, Kyoto University; Robert Nemanich, Arizona State University; K.-N. Tu, University of California, Los Angeles

Tuesday PM
March 11, 2008

Room: 276
Location: Ernest Morial Convention Center

Session Chairs: Sinn-wen Chen, National Tsing Hua University; Seiji Isoda, Kyoto University

2:00 PM Invited

Grain Size Refinements in Al-Mg and Cu-Mg Alloys by Hydrogen Heat Treatment: *Atsunori Kamegawa*¹; Masuo Okada¹; ¹Tohoku University

We have investigated the hydrogen heat treatment of the so-called hydrogenation disproportionation desorption recombination (HDDR) process applied to alloys that contain some amounts of elements with a strong affinity for hydrogen, for example Mg, even though the major constituent of these alloys are mostly elements with a weak affinity for hydrogen. Upon the hydrogenation of the Al-Mg alloys, a disproportionation reaction occurred in the formation of MgH₂ embedded in the Al matrix phase. In the subsequent hydrogen-desorption of the alloys, MgH₂ was decomposed and Mg was resolved into the Al matrix

phase, thereby resulting in the original solid solution alloys, and the Al grain size of about 10nm was observed. This indicates that HDDR phenomena occurred in the Al-Mg alloys. In addition, it was found that the Cu-Mg alloys also exhibit HDDR phenomena and that the grain size was refined.

2:25 PM Invited

Formation of Hexagonal Close Packing at Grain Boundaries in Gold:

Douglas Medlin¹; J. Hamilton¹; O. Uche¹; G. Lucadamo¹; ¹Sandia National Laboratories

Grain boundaries in metals that possess low stacking fault energies can reconstruct into three-dimensional configurations by the emission of stacking faults. An important question is how the arrangement of these faults, and hence the phase of the interfacial layer, depends on the orientational parameters of the interface. Here, we present electron microscopic observations and modeling of two boundary misorientations in gold that both reconstruct to form a nanometer-scale layer of hexagonal-close-packed (HCP) material. In both cases, the HCP layer and its relationship to the grain misorientation is directly explained and predicted by the arrangement of Shockley partial dislocations at the interface. A comparison of the two boundary structures, one of which has partials paired as full lattice dislocations and other which does not, provides insight concerning the formation of other stacking arrangements, such as 9R, that have been observed at other grain misorientations in low SFE FCC metals.

2:50 PM Invited

Application of Microscopy to Nanoscale Organic Materials: Seiji Isoda¹;

Hiroki Kurata¹; ¹Kyoto University

There is an awareness among scientists and technologists that organic materials offer considerable potential for application in many diverse areas. Recent advances in organic materials are found in electrically conducting materials, superconductors, non-linear optical materials, organic electroluminescence devices, organic solar cells, organic field-effect transistors (FETs) and molecular electronic devices. In these innovations, novel system performance could be recognized through nanostructuring as well as molecular property itself. As the dimensions of the structures approach the nanometer level, it becomes increasingly important to characterize materials properties at nanometer scale. Much of information on such nanoscale phases is being obtained by electron microscopy and this method is also an area of rapid progress. In the presentation, structural aspects of nanoscale phases in organic FETs will be discussed in relation with their properties, in which the phases are analyzed using various recent techniques in electron microscopy.

3:15 PM Invited

Bioactivity of Nanostructured and Plasma-Treated Biomaterials: Paul Chu¹;

¹City University of Hong Kong

The biological properties of biomaterials are influenced by their micro- and nano-structures and can be improved by surface treatment. Nano-TiO₂ and ZrO₂ coatings have been produced using plasma spraying and plasma immersion ion implantation. The structure is evaluated by TEM, SEM, Raman and XRD and their bioactivity and biocompatibility are assessed using simulated body fluid soaking test and cell culturing. The nanostructured surfaces treated with the proper plasma processes exhibit excellent bioactivity and biocompatibility. The bioactivity of the films depends on a nanostructured surface composed of enough small particles, as reflected by the ability of the nano films to induce bone-like apatite formation on their surfaces after immersion in a simulated body fluid for a certain period of time. The plasma treatment is believed to provide the nanostructured surfaces have a high density of negative charges that influence the adsorption of molecules and ions from the simulated body fluids.

3:40 PM Break

4:00 PM Invited

An EDX-Based Oxidation Test for Evaluating Cu Out-Diffusion in Pre-Plated Cu-Alloy Leadframes: Lilin Liu¹; Ran Fu²; Deming Liu²; Tongyi Zhang¹;

¹Hong Kong University of Science and Technology; ²Assembly Automation Ltd.

An EDX-based oxidation test is developed to study the Cu out-diffusion and oxidation in pre-plated Cu-alloy leadframes. A model is established to determine the diffusion coefficients of copper in nickel barrier platings and copper in an in-situ formed Sn-based intermetallic compound(IMC) nano-barrier-layer.

The calculated diffusion coefficient is $(1.56 \times 10^{-10} \text{ cm}^2/\text{s}) \exp(-0.736 \text{ eV}/kT)$ for copper in the IMC nano-layer at the temperature 150°C~400°C, and $(1.59 \times 10^{-9} \text{ cm}^2/\text{s}) \exp(-0.602 \text{ eV}/kT)$ for copper in the nickel plating at the temperature 260°C~300°C, indicating that the in-situ formed Sn-based IMC nanolayer is a more effective diffusion barrier than the Ni layer. Discussion on the EDX-based oxidation test is given in details, thereby results in that the developed EDX-based oxidation test proves to be a simple and effective way for quantitative analysis of diffusion and oxidation at the nanometer scale.

4:25 PM Invited

Metal Phase Formation and Interaction in Electronic Packaging: C Robert

Kao¹; ¹National Taiwan University

An intriguing materials interaction problem arising from the metallurgical bonding in advanced electronic packages will be discussed. We report the strong cross-interaction between Sn-based solders and two common substrate materials, Cu and Ni. The interaction of Cu and Ni causes many problems. Nevertheless, this cross-interaction may also offer us opportunity to design a longer lasting UBM. The effect of Ni on the solders/Cu reactions is to be reviewed first. The effect of Cu on the solders/Ni reactions is then introduced. A slight variation in Cu concentration can change the reaction product from one phase to another. The knowledge gained from the Cu and Ni effects is applied to explain the recently discovered intermetallic massive spalling. It is pointed out that the massive spalling is caused by the shifting of the equilibrium phase as more and more Cu is extracted out of the solder by the growing intermetallic.

4:50 PM Invited

Size Effects in the Electronic Solder Joints: Sinn-wen Chen¹; Yu-chih Huang¹;

Kuan-hsien Wu¹; ¹National Tsing Hua University

With the emerging of flip chip technology and the trend of higher integration density in electronic products, sizes of electronic solder joints are shrinking. Solder joints in the electronic products are of various sizes, and more importantly there are solder joints which are very small. Melting temperature ranges of solders and interfacial reactions are the primary issues in the electronic soldering. Different interfacial reactions have been observed in the electronic solder joints of different sizes. Smaller solder volumes result in less supply of atoms, and the time frames of reaction sequences change significantly. With even smaller sizes of electronic solder joints in the future, the melting and interfacial reaction will be affected as well. Solders of nano-size are of lower melting points, and then the reflowing temperatures should be lower. Size effects in the electronic solder joints are certainly an important and challenging issue needs to be addressed.

5:15 PM Concluding Comments

Magnesium Technology 2008: Casting

Sponsored by: The Minerals, Metals and Materials Society, TMS Light Metals Division, TMS: Magnesium Committee

Program Organizers: Mihriban Pekguleryuz, McGill University; Neale Neelameggham, US Magnesium LLC; Randy Beals, Chrysler LLC; Eric Nyberg, Pacific Northwest National Laboratory

Tuesday PM

March 11, 2008

Room: 292

Location: Ernest Morial Convention Center

Session Chair: To Be Announced

2:00 PM

Carbonate Inoculation and Grain Refinement of Magnesium Alloys: Young

Min Kim¹; Chang Dong Yim¹; Sung Soo Park¹; Bong Sun You¹; ¹Korea Institute of Materials Science

While low cost grain refiners have been developed for castings of aluminum alloys, there are no commercial inoculants for magnesium alloys, especially Mg-Al alloys. Although hexachloroethane is a very effective inoculant for grain refinement of Mg-Al alloys, the emission of toxic gases gives rise to detrimental problems in environment and workshop, resulting in the restriction of its use. Therefore many alternative grain refiners being more effective for Mg-Al alloys than hexachloroethane without any environmental problem have

been investigated. In this study, the effect of carbonate inoculation on grain refinement of Mg-Al base alloys was investigated. The results show that MgCO_3 and MnCO_3 have excellent grain refining efficiency in Mg-Al base alloys, of which average grain size is less than $70\mu\text{m}$. This is because inoculation of carbonates causes the formation of heterogeneous nucleant in a melt as well as the agitation of melt by the generation of carbon dioxide gas.

2:20 PM

Castability of Magnesium-Aluminum Alloys: Shezad Khan¹; Norbert Hort¹; Ingo Steinbach²; Siegfried Schmauder³; ¹GKSS Research Center; ²Access e.V.; ³Universität Stuttgart

Research and development of magnesium alloys depends largely on the metallurgist's understanding and ability to control the microstructure of the as-cast part. This work comprises the determination of experimental input parameters to run a successful and vast informative simulation using state of the art software. Various thermodynamic analyses have been used to study the thermo physical properties of binary magnesium-aluminum alloys, and the resultant microstructures have been simulated and then compared with the experimental output. The calculated heat distributions have been used to simulate the resulting microstructure using the phase-field method. This paper presents an overview of a range of ideas that have been undertaken to improve our understanding on the gravity die-casting behavior and solidification characteristics of Mg-Al alloys. It follows the solidification process of binary alloys Mg-Al, beginning with the nucleation and grain refinement. The simulated and the experimental results are compared and used for validation.

2:40 PM

Characterization of AM60B Magnesium Castings Using a Counter Gravity (Hitchiner) Lost Foam Casting Process: Kenneth Currie¹; Qingyou Han²; ¹Tennessee Technological University; ²Purdue University

Utilizing a Taguchi Design of Experiments (DOE), the results reported in this paper help to identify preferred parameters when using a Counter Gravity (Hitchiner) process for lost foam casting of magnesium alloys. Contrary to most other casting studies, a complex "widget" pattern was used as the test article with foam type, temperature, coating type, and pressure as the key parameters. Cast patterns were analyzed by volumetric and gravimetric standards as well as hardness and tensile strength. Statistical results from the DOE will be reported along with other general conclusions.

3:00 PM

Grain Refinement and Grain Morphology Evolution in Magnesium Castings Investigated by Phase-Field Simulations: Janin Eiken¹; Ingo Steinbach¹; ¹RWTH-Aachen

The role of the composition of a quaternary Mg-Al-Zn-Ca-Mn alloy on the nucleation and growth morphology of equiaxed grains is investigated by phase-field simulations. A model for heterogeneous nucleation on particles with a prescribed size distribution is used to investigate the interplay between growth, solute redistribution and latent heat release in the solidifying mush. The morphology evolution of the individual grains is characterized by their volume to surface ratio and studied in its dependence on the alloy composition. The results are compared to experimental results from laboratory castings.

3:20 PM

Hot Tearing in Castings of Mg-Al-Sr Alloys: Sindu Kou¹; Guoping Cao¹; ¹University of Wisconsin

Ternary Mg-Al-Sr alloys are the base of a few new creep-resistant, light-weight Mg alloys for automobiles. Hot tearing in Mg-Al-Sr alloys was studied, including Mg-(4,6,8)Al-1.5Sr and Mg-(4,6,8)Al-3Sr, by constrained rod casting (CRC) in a steel mold. The hot tearing susceptibility was determined based on the widths and locations of the cracks in the rods. With Mg-(4,6,8)Al-1.5Sr alloys, the hot tearing susceptibility decreased significantly with increasing Al content. With Mg-(4,6,8)Al-3Sr alloys, the trend was similar but not as significant. At the same Al content, the hot tearing susceptibility decreased significantly with increasing Sr content. The onset of hot tearing was detected by instrumented CRC, in which the rising tension in the bottom rod was measured with a load cell and the temperature near the crack site was measured with a thermocouple. The results of instrumented CRC were correlated with those of CRC.

3:40 PM

Mould Thermal Analysis in DC Casting of Magnesium Alloys: Dimitry Sediako¹; William Macdonald²; Stephen Hibbins²; ¹National Research Council of Canada; ²Timminco Metals

This study was performed to evaluate the major thermal parameters in the areas of primary and secondary cooling in magnesium DC casting process. The analysis included comprehensive experimental study of the major thermal parameters of the process, as well as 3D computer simulation of the casting process and its verification based on the experimental data. Three segments of primary cooling were clearly identified along the mould, length of these segments depends greatly on mould cooling arrangement and casting speed. The results included evaluation of thermal conditions of the process that might cause casting defects, such as surface folding and radial cracking. Neutron diffraction studies were performed to evaluate crystallographic texture of the as-cast metal depending on the cooling rates for the specimens taken from the centre and surface of an as-cast bloom. The outcome of the study has been discussed from the point of view of further "optimal" mould development.

4:00 PM

Strengthening of Cast Mg Alloys by Friction Stir Processing: Taiki Morishige¹; Masato Tsujikawa¹; Sachio Oki²; Tomotake Hirata³; Kenji Higashi¹; ¹Osaka Prefecture University; ²Kinki University; ³Technology Research Institute of Osaka Prefecture

Cast magnesium alloys were processed by friction stir processing (FSP) to acquire fine grain and high strength. FSP is a novel grain refinement method for light metal alloys. By using FSP, the microstructure was refined by dynamic recrystallization (DRX) and second phase particles could be finely dispersed. Moreover, for casting products, FSP is effective process to eliminate cast defects like micro porosities. Thick plate of commercial Mg alloy for die-casting AZ91D or Mg-Y-Zn alloys of two different chemical compositions have been prepared for FSP. Changes in the FSP-ed microstructures that affect mechanical properties were not only grain size refinement, but also the distributions of second phase particles. As-cast Mg-2at.%Y-2at.%Zn alloy, differs from Mg-2at.%Y-1at.%Zn, has icosahedral quasi-crystalline phase in grain boundaries. It has higher elevated temperature stability than inter-metallic compound of $\text{Al}_{12}\text{Mg}_{17}$. The distribution of fine second phase particles and mechanical properties were discussed.

4:20 PM

Study on Solidification Process of Squeeze-Cast AZ91D Alloy: Yanling Yang¹; Liming Peng¹; Wenjiang Ding¹; ¹Shanghai Jiaotong University

This study aims to investigate solidification process of squeeze-cast AZ91D alloy. By the contrast of gravity-cast AZ91D alloy, it can be known that the microstructure of squeeze-cast AZ91D alloy has four zones, from brim to core, they are rapid cooling zone, segregation zone, crystallization area under pressure and hot spot. In crystallization area under pressure, from external to inside, dendrite is thin and having no directivity, developed and having evidence directivity which is parallel with thermal flow, developed and having no evidence directivity, cracked dendrite in turn.

4:40 PM

The Behaviors of Second Phase and Hardness of Rheo-Die Cast AZ91D during Solid Solution Heat Treatment: Yongfeng Jiang¹; Yefeng Bao¹; ¹Hohai University

Solid solution heat treatment of AZ91D die cast is performed at from 300°C to 420°C in from 2h to 32h to improve strength and result in maximum toughness and shock resistance, the behaviors of second phases and hardness are investigated by optical microscopy and microhardness meters. It is indicated that at from 300°C to 450°C , the second phases precipitated are dispersed in variation of from matrix to grain boundary, which have effects on microhardness, from 2h to 32h at same temperature, the hardness is increased firstly to peak value, and then decrease; from 300°C to 450°C peak values and valley is in advance at from 300°C to 450°C ; The grain size is also varied according to temperature and time.

5:00 PM

Development of a Strip-Rolling Technology for Mg Alloys Based on the Twin-Roll-Casting Process: Rudolf Kawalla¹; Matthias Oswald¹; Madlen Ullmann¹; Christian Schmidt¹; Hans-Peter Vogt²; Nguyen Duc Cuong²; ¹Freiberg University of Mining and Technology; ²MgF Magnesium Flachprodukte GmbH

The Institute of Metal Forming, Freiberg and the MgF, Freiberg are currently working on a new production technology for magnesium strip, based on twin-roll-casting and strip rolling. By means of this economic method it is possible to produce strips in deep drawing quality with good forming properties in order to satisfy the request for low cost Mg sheets in the automotive and electronic industry. Strips of magnesium wrought alloy AZ21 and AZ31, which have been produced by twin-roll-casting technology, feature a good forming ability. In order to develop an optimal strip rolling technology it is important to discover the influence of the different technological factors. Therefore, the project aims at determining the property development depending on several influencing factors. Consequently, conclusions regarding the technology can be made. Besides, fundamental research in terms of microstructure and texture development of twin-roll-casted and rolled magnesium strips has been conducted.

5:20 PM

The Effect of Different Direct-Chill Casting Process on Microstructures, Macroseggregation and Mechanical Properties of ϕ 200mm AZ31 Billets Obtained: Zhiqiang Zhang¹; ¹Key Laboratory of Electromagnetic Processing of Materials, Ministry of Education

AZ31 alloy billets of ϕ 200mm diameter have been produced by three different process of conventional direct chill (DC) casting, low frequency electromagnetic casting (LFEC) and low frequency electromagnetic vibration casting (LFEVC), respectively. The effect of LFEC and LFEVC on the microstructures, macroseggregation and mechanical properties in AZ31 billets was investigated. In conventional DC casting, the AZ31 billets exhibited coarse grains (about 370 μ m) and severe segregation of Al and Zn. In the presence of a solo low frequency alternating magnetic field(LFEC) or a low frequency electromagnetic vibration field(LFEVC) applied during DC casting of F200mm AZ31 billets, the grains of the AZ31 billets was effectively refined (about 210 μ m) and the macroseggregation of Al and Zn in the billets was greatly decreased. Furthermore, there was a significant increase in tensile strength, fracture elongation and hardness of the as-cast AZ31 billets obtained by LFEC and LFEVC relative to that cast by conventional DC casting.

Magnesium Technology 2008: Wrought Alloys III

Sponsored by: The Minerals, Metals and Materials Society, TMS Light Metals Division, TMS: Magnesium Committee

Program Organizers: Mihriban Pekguleryuz, McGill University; Neale Neelameggham, US Magnesium LLC; Randy Beals, Chrysler LLC; Eric Nyberg, Pacific Northwest National Laboratory

Tuesday PM
March 11, 2008

Room: 291
Location: Ernest Morial Convention Center

Session Chair: To Be Announced

2:00 PM

Effect of Texture on the Damping Capacity of Mg-0.4Zn-0.6Zr (ZK01) Alloy: Liming Peng¹; Lin Du¹; Li Jin¹; Wenjiang Ding¹; ¹Shanghai Jiaotong University

Improve damping capacity of metal and alloy is an effective approach to solve the vibration and noise problems for some special apparatus. The Mg-Zn-Zr alloy will be a potential material due to the light weight and high damping capacity by controlling its microstructure, and the effect of texture on the damping capacity of Mg-0.4Zn-0.6Zr (ZK01) was investigated in this study. The textures were observed by X-ray diffraction (XRD), the results show that there is typical rolling texture ND//{0001} fiber texture in this Mg-0.4Zn-0.6Zr (ZK01) alloy sheet and the damping capacity are different in these specimens which have the included angles relationship, 0°, 45° and 90° with the rolling plane along the rolling direction (RD) and the transverse direction(TD), respectively. The

higher damping capacity can be ascribe to the higher dislocation slip possibility in grains.

2:20 PM

Effect of Twinning on the Mechanical Behavior of Mg-Zn-Y Alloys: Ju Youn Lee¹; Hyun Kyu Lim¹; Do Hyung Kim¹; Won Tae Kim²; Do Hyang Kim¹; ¹Yonsei University; ²Department of Nanoscience, Chongju University

The effect of twinning on the mechanical behavior of Mg-Zn-Y alloys was investigated by controlling process parameters and alloy chemistry. To study the effect of process parameters, Mg-6Zn-1.2Y sheets were prepared by changing rolling speeds. DRXed-grains are developed under a lower rolling speed while twinned-grains are obtained under a higher rolling speed. The uniform elongation increases from 5.3% to 7.3% with increasing rolling speed from 32 to 64 mm/s. To study the effect of alloy chemistry, Mg-xZn-0.6Y (x= 3~7) sheets consisted of α -Mg and quasicrystalline particles were prepared. Strength and elongation-to-failure increase with increasing Zn despite of similar grain size and volume fraction of particles. Interrupted tensile tests showed that larger fraction of twinned-region developed in Mg-7Zn-0.6Y than in Mg-3Zn-0.6Y. EBSD analysis shows that extension twins are developed. It is suggested that twinning leads to reorientation of basal-plane to more favorable orientations, improving the elongation in Mg-Zn-Y alloys.

2:40 PM

Effect of {10-11} Contraction and {10-11}-{10-12} Double Twins on the Subsequent Deformation Behavior of Two Mg Alloys: Lan Jiang¹; John Jonas¹; Raj Mishra²; ¹McGill University; ²General Motors

Mg alloy tubes are frequently bent prior to hydroforming. As a result, such metals are subjected to reversals of strain path. Therefore, it is useful to know the effects of changing strain path as well as of twinning on the stress-strain response after a change in strain path. In this study, experiments were designed and conducted to introduce contraction and double twins during prestraining; these prestrained samples were subsequently compressed at a strain rate of 0.1/s and at ambient temperature as well as at 200°C. It shows that the initial compressive deformation is slip-dominated, which is then followed by extension twin-dominated deformation. In addition, an annealing treatment (heat at 300°C for one hour) was performed on some prestrained tensile samples. The heat treatment of heavily extended material containing contraction and double twins displays an effective method of refining the grain size and modifying the texture.

3:00 PM

Effects of Zn on the Mechanical Properties of Wrought Magnesium Alloys: Jong Doo Ju¹; Jung Woo Choi¹; Ji Hoon Hwang¹; Kwang Seon Shin¹; ¹Seoul National University

In order to improve the poor ductility and the anisotropic mechanical properties of magnesium alloys which limit their applications as structural parts, new Mg-Zn based wrought magnesium alloys were developed. The billets of Mg-Zn-Al and Mg-Zn-Sn alloys with different compositions were fabricated by gravity casting and extruded after the homogenization heat treatment. The amount of each phase present in the alloys was predicted from thermodynamics and solidification kinetics, and the theoretical value was compared with that determined by microstructure observation using optical and scanning electron microscopy. The mechanical properties of the extruded magnesium alloys were evaluated at different orientations with respect to the extrusion direction, and the texture evolution was determined by X-ray diffraction using the Schulz reflection method. The effect of Zn content on the mechanical properties of the extruded magnesium alloys was examined. The effects of subsequent heat treatments were also identified.

3:20 PM

Influence of Cerium on Texture and Ductility of Magnesium Alloy Extrusions: Raja Mishra¹; Anil Gupta²; P. Rao³; Anil Sachdev¹; Arun Kumar⁴; Alan Luo¹; Li Jin⁵; ¹Materials and Processes Laboratory, General Motors Research and Development; ²National Physical Laboratory; ³International Advanced Research Centre for Powder Metallurgy and Advanced Materials; ⁴General Motors India Science Laboratory; ⁵Shanghai Jiaotong University

Ce-containing Mg alloys were extruded as solid rounds at 400°C in a 500 ton vertical extrusion press at 10 mm/sec. Careful EBSD analysis of the recrystallized extrudate was conducted. This paper will discuss the tensile properties and

texture evolution of these alloys following extrusion and recrystallization, and also a detailed microstructural evaluation of the polished cross-section close to the fracture surface as well as the fracture morphology.

3:40 PM

Mechanical Properties and Microstructures of Extruded Mg-2.4at%Zn Alloys Containing Ag and Ca: *Chamini Mendis*¹; Keiichi Oh-ishi¹; Yoshiaki Kawamura²; Tomoyuki Honma²; Shigeharu Kamado²; Kazuhiro Hono¹; ¹National Institute for Materials Science; ²Nagaoka University of Technology

Mg-Zn based ZK60 (Mg-2.4at%Zn-0.16at%Zr) are used widely as wrought magnesium alloys due to the good combination of strength and ductility. Recently we reported that addition of Ag and Ca in trace quantities (0.1at% each) to Mg-2.4at%Zn alloys has shown significant increments to the precipitation hardening response. Examination of the mechanical properties of extruded Mg-2.4at%Zn(-0.16at%Zr) with trace additives of Ag and Ca has shown to significantly improve tensile properties. Tensile yield stress of 290MPa, UTS of 350MPa and an elongation of 17% has been realized for as extruded Mg-2.4at%Zn-0.1at%Ag-0.1at%Ca-0.16at%Zr alloy. Following extrusion these alloys may be precipitation hardened by ageing at 160°C. The mechanical properties of these alloys may be further improved with heat treatments subsequent to the extrusion processing. The microstructures observed following processing have been characterized with the use of optical and transmission electron microscopy and show that there is significant refinement of both grain size and precipitates.

4:00 PM

Microstructural Investigation of Twins under the Fracture Surface in AZ31 Mg Alloys: *Daisuke Ando*¹; Junichi Koike¹; ¹Department of Materials Science, Tohoku University

Magnesium alloys form many types of twins which play important roles on deformation and failure. Reed-Hill and others suggested that double twins are the origin of poor ductility. Recently, we experimentally showed that double twins accompany large surface relieves and cracks. However, the current knowledge does not provide an undisputable evidence of the double twins being the major reason for premature failure. In this work, we performed detailed observation and analysis of the underlying microstructure on fractured surface. The sample was a rolled AZ31 sheet. Tensile test was performed at room temperature. A number of facets were observed on fractured surface. Cross-sectional TEM samples were prepared by FIB from these facets. TEM observation showed the formation of double twins underneath the facet. The presence of fine recrystallized grains indicates substantial dislocation activity related to the double twins. These results indicate the relation between localized large deformation and macroscopically brittle failure.

4:20 PM

Study of Microstructure and Texture in an AZ31 Magnesium Alloy Deformed in Tension at Elevated Temperatures: *Emilie Hsu*¹; Faramarz Zarandi¹; Ravi Verma²; Jerzy Szpunar¹; Steve Yue¹; ¹McGill University; ²General Motors Research and Development Center

A commercial AZ31 magnesium alloy was deformed in tension at temperatures 300, 400, and 450°C and strain rates 0.001, 0.01, and 0.1s⁻¹. At low temperature and high strain rate, failure is associated with a pronounced necking which occurs after a limited elongation. On the other hand, at high temperature and low strain rate, a diffuse neck leads to a significant uniform elongation. Texture analysis indicates that the initial basal texture persists during tensile deformation. However, distribution of non-basal planes varies depending on the deformation condition. At low temperature, the distributions of {1-100} and {11-20} poles are rather uniform, whereas, at high temperature, they tend to rearrange as they are in the hcp single crystal. Such a difference in texture indicates distinct slip mechanisms activation. Additionally, examination of microstructure shows that GBS also contributes to the flow accommodation, especially at low strain rates. These observations will be discussed in this paper.

4:40 PM

The Effect of Solute Atoms on the Recrystallization Texture of Mg Alloys: In-Situ Annealing Experiments: *Reza Shahbazian Yassar*¹; Sean Agnew²; Peter Kalu³; ¹Michigan Technological University; ²University of Virginia; ³National High Magnetic Laboratory

At room temperatures, the ductility of Mg alloys is limited ascribed to their hexagonal close-packed (HCP) crystal structure and the shortage of independent slip systems. Several researchers have reported the dramatic improvement of Mg ductility using rare-earth solute atoms. The present research work aims to understand the effect of the rare-earth solute atoms on recrystallization texture of Mg alloys by means of the in-situ heating experiments in scanning electron microscopy along with electron backscatter diffraction technique. Several specimens with different concentration of solute atoms were subjected to deformation and the subsequent recrystallization behavior was tracked in the microscope. A study of both boundary motion and texture development as a function of plastic strains and solute atoms concentration is presented.

5:00 PM

The Flow Stress during Hot Compression Deformation of Mg-Gd-Y-Zr Magnesium Alloy: Tests and Numerical Simulations: *Xinping Zhang*¹; *J. Wang*¹; ¹Department of Materials Science and Engineering, Nanjing University of Science and Technology

The hot deformation behaviour of Mg-Gd-Y-Zr alloy was investigated by compression test and Finite Element analysis method. Compression tests were conducted in the temperature range 350 to 500°C and strain rate range 0.1 to 0.4 per second. The load-displacement data obtained from the compression tests were used to obtain stress-strain data for hot compression by inversed Finite Element method. As expected, the flow stress increases with the increase of strain rate, and decreases with the increase of the deforming temperature. The flow stress of the Mg-Gd-Y-Zr magnesium alloy during hot compression deformation can be described by using Zener-Hollomon parameter including Arrhenius item, and the deformation activation energy is estimated to be 230.098kJ/mol.

5:20 PM

The Influence of Calcium and Cerium Mischmetal on the Microstructural Evolution and Mechanical Properties of Mg-3Al-1Zn during Extrusion: *Torsten Laser*¹; *Christian Hartig*¹; *Timo Ebeling*¹; *Marcus Nürnberg*²; *Dietmar Letzig*²; *Rüdiger Bormann*²; ¹Technical University Hamburg-Harburg; ²GKSS Research Centre

The role of calcium and rare earth rich intermetallic particles in magnesium alloys during extrusion is studied by mechanical tests and texture measurements. After extrusion a reduction of the final grain size mainly caused by the influence of these intermetallic particles is observed, which becomes more distinct for higher alloying contents and low extrusion temperature. The extruded rods exhibit typical extrusion fibre-textures (c-axes in radial direction) with a high tension-compression asymmetry of the yield stress in the extrusion direction. Differences in mechanical properties are related to changes of the texture development. The influence of the intermetallic particles on the texture evolution are discussed in view of the activation of non basal slip modes at higher temperatures and mechanisms of dynamic recrystallization.

Materials for Infrastructure: Building Bridges in the Global Community: Session I

Sponsored by: The Minerals, Metals and Materials Society, Indian Institute of Metals, Chinese Society for Metals

Program Organizer: Brajendra Mishra, Colorado School of Mines

Tuesday PM

Room: 272

March 11, 2008

Location: Ernest Morial Convention Center

Session Chair: Brajendra Mishra, Colorado School of Mines

2:00 PM Introductory Comments by Brajendra Mishra

2:10 PM Keynote

The Geology of the Katrina Disaster in New Orleans: *Stephen Nelson*¹; ¹Tulane University

A combination of historical and geological factors combined with inadequate design of levees and floodwalls resulted in a series of levee overtoppings and catastrophic levee failures in the New Orleans area during the passage of Hurricane Katrina on August 29, 2005. Early in the morning of August 29, levees along the Mississippi River Gulf Outlet and Intracoastal Waterway were overtopped by the storm surge generated by Katrina resulting in the flooding of eastern New Orleans and St. Bernard Parish. Later in the morning storm surge entering New Orleans' Inner Harbor Navigational Canal overtopped levees and floodwalls on both sides of the canal, eventually resulting in the catastrophic failure of the floodwalls and the destruction of the Lower 9th Ward. Three drainage canals in New Orleans, originally constructed in the mid-1800s to drain rainwater from the city into Lake Ponchartrain to north, then became subject to storm surge entering from the Lake. The excess pressure of the surge combined with the weak geological material underlying the levees and floodwalls resulted in two levee breaches on the London Avenue Canal and one on the 17th St. Canal by mid-morning on August 29. These breaches resulted in flooding of about 80% of the city of New Orleans. The failures of levees on these drainage canals did not result from overtopping the floodwall system, but apparently from weaknesses in the design of the system that failed to adequately account for the underlying geologic conditions.

2:40 PM Invited

The Application of Steel in a New Residential Structural System: *Zigang Li*¹; ¹Baoshan Iron and Steel Company, Ltd.

Baosteel, as a member company of Living Steel Project organized by IISI, aims at extending the use of steel in house buildings, and exerts deep research on the application of steel materials and components in new type residential structural systems. A new structural system with roll formed shape steel columns and high frequency welding H-section steel beams was studied through finite element analysis method and was testified with experiments.

3:10 PM Break

3:30 PM Invited

Emerging Role of Non-Ferrous Metals in Public Utilities and Infrastructural Projects: *L. Pugazhenth*¹; ¹India Lead Zinc Development Association

After the economic liberalization in 1991, India's focus shifted to the infrastructural sector that covers national highways, power, telecom, aviation, ports, etc. In view of the consistent and impressive GDP growth rates, substantial funds have been spent on these sectors and the results are yielding. For instance, the rate of telecom subscriber growth – 8 million a month – is almost twice the population of Finland. The Planning Commission of India proposes to invest about US \$500 billion during the Eleventh Five Year Plan period (2007–2012) in the infrastructural segment. In one sector alone ie., power, it is proposed to add 80,000 MW of electric power during the same period. Similar would be the growth in the other infrastructural sectors. The thrust on infrastructural projects in the country has given a great boost in demand for steel, non ferrous metals etc. Base metals like aluminium, copper, zinc and lead are used in a wide variety of applications in power generation and transmission, transportation, building, construction, irrigation, telecom, agriculture, public health etc. As a result of

the growth trends in these areas, the non ferrous metals have been witnessing double digit growth rates in their usage every year. Zinc has been growing at a rate of 15% per year. After China, it is India that has been galloping in the demand for non ferrous metals. Accordingly metal producers, both primary and secondary, have been expanding their capacities. Each of the two industrial groups involved in Aluminium, Zinc, Copper has been planning to set up 1.0 million tonne smelters for these three metals. In order to achieve the targeted production levels, the non ferrous metal manufacturers are also acquiring mines in Zambia, Australia etc., so that there is an uninterrupted flow of input materials. The metal producers are also investing huge sums of money in survey, exploration and mining so as to find new resource bases. The Indian government has also been fine-tuning appropriate policies for domestic investment, foreign direct investment, taxation, environment protection so as to accelerate the pace of activity in the metals sector.

4:00 PM Invited

Opportunities for Aluminum Alloys in Restoration of Aging Bridge Decks: *Subodh Das*¹; J. Randolph Kissell²; John Kaufman¹; ¹Secat Inc; ²TGB Partnership

Thousands of steel and concrete highway bridges in North America are deteriorating. Many have been load-limited due to this deterioration and because traffic and loads now exceed original designs. Yet replacing these spans is often slow, costly, and done at great inconvenience to drivers, including those of emergency vehicles. Aluminum alloys, with their 75 year record of successful use in bridges, offer the opportunity to address this challenge. Aluminum bridge decks have a high strength-to-weight ratio and can be prefabricated offsite and installed quickly with minimum disruption to traffic. In addition, because of their excellent corrosion resistance, aluminum decks do not have to be painted and require very little maintenance. This paper addresses how aluminum bridge decks might be developed and deployed.

4:30 PM Invited

Research and Development of a Ultra-Fine Grained Steel Rebar with Low Cost and High Performance: *Zhongmin Yang*¹; ¹Division of Structural Materials, Central Iron and Steel Research Institute

In the past decade, "Ultra-fine grain" (UFG) has been paid more and more attention to seek for low cost high strength steels. People in Chinese steel academy and industry have devoted many of their efforts on the investigation to the ways to refine grains in steels and the mechanisms. Also, to make great efforts on develop to the industrial and application technology of ultra-fine grain steel products. Grain refinement has been as one of the effective ways of microstructure control to improve the performances of steel products. Compare with original steels, due to the increased strength, improved toughness and ductility, the ultra-fine steels has been gradually taken broad application. We have developed the DIFT (Deformation Induced Ferrite Transformation) rolling technology to refine ferrite grains in low carbon steel rebar. Plain low carbon steel rebars of 400MPa grade, with ferrite grains in the range of 4 – 8µm, have been developed. According to test results, ultra-fine steel rebars can be as the candidate to replace microalloyed steel rebars of 400 MPa grade. Therefore, it can be saving a great deal of microalloying elements (V, Nb, Ti. etc). In recent years, DIFT Technology has been applied in wide range of long-product lines with very economic production costs and the annual product of ultra-fine steel rebars was achieved 100 million ton.

Materials in Clean Power Systems III: Fuel Cells, Hydrogen-, and Clean Coal-Based Technologies: Metallic Interconnects in SOFCs: Oxidation, Protection Coatings

Sponsored by: The Minerals, Metals and Materials Society, TMS Structural Materials Division, TMS/ASM: Corrosion and Environmental Effects Committee
Program Organizers: Zhenguo "Gary" Yang, Pacific Northwest National Laboratory; Michael Brady, Oak Ridge National Laboratory; K. Scott Weil, Pacific Northwest National Laboratory; Xingbo Liu, West Virginia University; Ayyakkannu Manivannan, National Energy Technology Laboratory

Tuesday PM Room: 392
 March 11, 2008 Location: Ernest Morial Convention Center

Session Chairs: Xingbo Liu, West Virginia University; Paul Gannon, Montana State University

2:00 PM Invited

The Effect of Substrate Impurities on Coated Metallic Interconnect Materials for Solid Oxide Fuel Cell Interconnects: *Christopher Johnson*¹; Nina Orlovskaya²; Anthony Coratolo³; Caleb Cross¹; Xingbo Liu⁴; Junwei Wu⁴; Randall Gemmen¹; ¹National Energy Technology Laboratory; ²University of Central Florida; ³Drexel University; ⁴West Virginia University

Substrate impurities can affect the performance of coated metallic interconnect materials used in solid oxide fuel cells (SOFC) applications. Impurities, such as silicon and aluminum can lead to increased area specific resistance (ASR), and a number of typical low level additives used in metallurgy to enhance the properties of the bulk materials for other applications can interact in detrimental ways when these substrates are coated to prevent chromium migration in SOFC. Coatings discussed in this work are applied by magnetron sputtering and by DC and pulsed plating techniques. Substrates are ferritic alloys with varying amounts of silicon, aluminum and other additives, and having CTEs that are relatively similar to that for typical SOFC (Crofer APU 22, and SS430) Samples are characterized by ASR measurements, X-ray Diffraction (XRD), scanning electron microscopy (SEM), and by energy dispersive X-ray analysis (EDX) before and after long term annealing under simulated cathode conditions.

2:30 PM Invited

Large Area Filtered Arc Deposited Coatings for SOFC Metallic Interconnects: *Paul Gannon*¹; Vladimir Gorokhovskiy²; Max Deibert¹; Preston White¹; Richard Smith¹; Hui Chen¹; W. Priyantha¹; ¹Montana State University; ²Arcomac Surface Engineering

Thin film (<5µm) MCrAlY oxide coatings were deposited on ferritic steels using large area filtered arc deposition (LAFAD) technology (M = Ti, Co and/or Mn). Coated and uncoated specimens were characterized as-received, and as a function of solid oxide fuel cell-interconnect (SOFC-IC) relevant exposures. Significant improvement of simulated SOFC-IC performance was observed in coated vs. uncoated specimens, including lower and more stable area specific resistance (ASR) and reduced Cr volatility. TiCrAlY oxide coatings exhibited the best high-temperature stability, while coatings containing Co and/or Mn exhibited the lowest ASR. Coating thickness and substrate steel surface finish were also observed to influence high-temperature corrosion behavior. Coating deposition processes, characteristics and SOFC-IC applicability are presented and discussed.

3:00 PM

Ceramic Coatings for Metallic SOFC Interconnects: *Jeffrey Fergus*¹; ¹Auburn University

The two approaches for SOFC interconnect materials – ceramics and metals – each have advantages, but neither is ideal. Metallic chromia-forming alloys are most commonly used, but the formation of chromium-containing vapor species can lead to poisoning of the cathode after long operation times. The resistance to this degradation can be improved through a combination of the two approaches by coating the metallic interconnect with a ceramic. The coating serves three functions – it must i) limit the inward diffusion of oxygen to reduce the growth of the scale, ii) limit the outward diffusion of chromium to reduce

chromium poisoning, and iii) transport electrons from the interconnect to the cathode. Performing all these functions, while simultaneously satisfying other requirements, such as chemical stability/compatibility and thermal expansion match, is a significant challenge. In this paper, the approaches used in the development of ceramic coatings for metallic SOFC interconnects will be reviewed.

3:25 PM

Novel Coatings for Stainless Steel Interconnects Utilized in SOFCs: *Douglas Ivey*¹; Weifeng Wei¹; Nima Shaigan¹; Weixing Chen¹; Anthony Wood²; Sofiane Benhaddad²; ¹University of Alberta; ²Versa Power Systems

Intermediate temperature SOFCs operate at temperatures <800°C, permitting the use of ferritic stainless steels as interconnects. Long term SOFC operation is limited, however, by the resistivity and volatility of the protective chromia scale that forms on the steel surface. To overcome these limitations, two novel methods of applying protective coatings are studied in this work. In the first approach, Mn-Co spinel oxides are anodically electrodeposited from aqueous solutions containing Mn and Co divalent ions. By controlling the solution composition and deposition parameters, dense and crack free deposits are obtained. Oxidation tests show significantly improved oxidation resistance compared with uncoated steels. In the second approach, composite coatings consisting of dispersed conductive lanthanum chromite particles in a Ni matrix are electrodeposited onto ferritic stainless steel substrates. Upon oxidation in air, a bilayer oxide scale forms, with NiO covering a protective chromia embedded with conductive chromite particles.

3:45 PM Break

4:00 PM Invited

Micro/Nanomechanical Characterization of Coatings and Its Applications to Fuel Cell Systems: *Xiaodong Li*¹; ¹University of South Carolina

Reliability study is the key for practical applications and commercialization of today's advanced full cells. Coatings of different materials are structural and functional components in full cell systems. The mechanical failure of these coatings may cause malfunction or even break down of the full cells. Precise characterization of the mechanical properties of the coatings is required for proper design and structural integration of full cell systems. In this presentation, recent progress in micro/nanoscale mechanical characterization of coatings is briefly reviewed. Emphasis is placed on nanoindentation techniques and how they are used to study hardness, elastic modulus, scratch resistance, fracture toughness, fatigue, friction and wear properties of different coatings, especially those designed for use in full cell systems. The presentation ends with a discussion on directions for future research.

4:30 PM Invited

Thermal Stability and Oxidation Resistance of Protective Metal Oxide Coatings on Steel SOFC Interconnects: *Richard Smith*¹; H. Chen¹; W. Priyantha¹; M. Kopczyk¹; J. Lucas¹; C. Key¹; M. Finsterbusch²; P. Gannon¹; P. White¹; M. Deibert¹; V. Gorokhovskiy³; V. Shutthanandan⁴; P. Nachimuthu⁴; ¹Montana State University; ²Technical University Ilmenau; ³Arcomac Surface Engineering; ⁴Pacific Northwest National Laboratory

The requirements of low cost and high-temperature corrosion resistance for interconnects in SOFC stacks have directed attention to the use of steel plates with electron conducting, oxidation resistant coatings. We studied coatings from the MCrAlYO family (where M = Co, Mn, or Ti) deposited on 430 steel coupons using filtered arc deposition technology at Arcomac Surface Engineering. Ion beam analysis, x-ray diffraction, and electron microscopy were used to characterize the thermal stability, composition, and structure of the coatings before and after high temperature annealing. Significant reductions in oxidation rates as well as reduced Cr volatility were seen for these coatings as contrasted with bare steel surfaces. To better understand the reduced Cr volatility for the CrAlO system, we studied volatility as a function of alumina content in chromia/alumina solid solutions. Supported through HiTEC, funded by DOE (PNNL) No.DE-AC06-76RL01830. Work in EMSL supported by OBER (DOE) DE-AC06-76RL01830.

5:00 PM

Investigation of Thin Film Mn-Co-Fe Spinel Oxide Coatings Deposited by RF-Magnetron Sputtering on Metallic Interconnects for SOFC Applications: *Cezarina Mardare*¹; Michael Spiegel¹; Alan Savan²; Alfred Ludwig²; ¹Max-Planck Institut fuer Eisenforschung; ²Centre for Advanced European Studies and Research

In order to improve the properties (i.e. oxidation resistance, conductivity) of ferritic stainless steels created for SOFCs applications, thin metallic films from the Mn-Co-(±Fe) system were deposited by RF-magnetron sputtering on the metal surface. The depositions were followed by a heat treatment for converting the metallic coatings (300 or 1000nm) to (Mn,Co,±Fe)₃O₄ spinel oxides, and by long-term annealing in cathodic-like atmospheres for assessing the stability of the coatings. The samples were analyzed by GIXRD and SEM/EDX to confirm the presence of the spinel structure on top of the steel, and by ToF-SIMS to investigate and characterize the evolution and growth of internal oxides at the steel/coating interface after the long time exposure. For the thin (300nm) coatings after 500h, Cr penetration was observed. The evolution of Cr diffusion profiles in thicker coatings (1000nm) together with ASR measurements at high temperature for the coated steels is currently under investigation.

5:20 PM

Structure and Stability of Surface Coated UNS 430 Ferritic Steel for SOFC Interconnect Application: *Hui Chen*¹; Chih-Long Tsai¹; Weerashinge Prithantha¹; Richard Smith¹; Paul Gannon¹; Max Deibert¹; ¹Montana State University

The development of intermediate temperature solid oxide fuel cells enable ferritic stainless steels as possible candidates for interconnects. Those SOFC interconnect should be stable both in oxidizing and reducing atmosphere. The thermal stabilities of UNS 430 stainless steels coated with dense and well adherent Ni or Cu protecting layers were studied in air and hydrocarbon fuel gases. Scanning electron microscopy was utilized to characterize the microstructure of the coated steels before and after oxidizing and carburizing. XRD was used to characterize the evolution of crystal structure. Rutherford backscattering with He⁺ and non-Rutherford scattering with H⁺ were used to characterize the composition and the interdiffusion of the coatings. The chromium volatility of the coated steel plates at 800°C was measured using ion beam analysis. Significant reductions in oxidation rates as well as reduced Cr volatility were observed for the coated alloys.

5:40 PM

Pulse Plating of Mn/Co Alloys for SOFC Interconnects Application: Junwei Wu¹; Christopher Johnson²; Yinglu Jiang¹; *Xingbo Liu*¹; ¹West Virginia University; ²National Energy Technology Laboratory

(Mn,Co)3O₄ spinel is a promising coating for SOFC interconnect application due to its high conductivity. Besides, Mn_{1.5}Co_{1.5}O₄ spinel demonstrated a good thermal expansion match to ferritic stainless steels such as AISI 430, as well as the cathode compositions such as LSM, LSF, Slurry coating and PVD has been reported to apply the (Mn,Co)3O₄ spinel for SOFC interconnect application. Electroplating and following oxidation offers another cheaper option. In this research, the effects of three parameters of pulse plating, namely peak current density, on-time and off-time, on the composition and morphology of Mn-Co coatings were investigated. By varying the parameters, Mn/Co alloys was deposited successfully, whose surface and cross section was characterized by SEM/EDX and XRD. Further on-cell tests prove pulse plating Mn/Co is an alternative cheap option for interconnects coatings

Materials Informatics: Enabling Integration of Modeling and Experiments in Materials Science: Informatics and Combinatorial Experiments and Materials Characterization

Sponsored by: The Minerals, Metals and Materials Society, TMS Materials Processing and Manufacturing Division, TMS/ASM: Computational Materials Science and Engineering Committee

Program Organizer: Krishna Rajan, Iowa State University

Tuesday PM

March 11, 2008

Room: 271

Location: Ernest Morial Convention Center

Session Chair: To Be Announced

2:00 PM

Combinatorial Approach to the Synthesis of Carbon Nanotubes: *Pablo Caceres-Valencia*¹; ¹University of Puerto Rico-Mayaguez

Carbon Nanotubes are synthesized with the aid of a catalyst via the VLS mechanism. The relationship between the catalyst composition and the characteristics of the carbon nanotube is not known. This can be study using composition spreads. Three well known catalyst such as Fe, Co and Ni have been studied using composition spreads. These elements were deposited using a magnetron sputtering technique at an angle. The chemical composition was determined using EDS-SEM and a GMS-program. Before the exposure to a carbon gas, the sample was annealed in the CVD and in selected samples the particle size was measured as a function of particle composition. The carbon nanotubes were synthesized using acetylene as a carbon source. Carbon nanotubes were formed preferentially at the Fe corner. Small additions of Co to Fe increase the deposition rate.

2:40 PM

Informatics and High Throughput Screening of Thermophysical Properties: *Robert Hyers*¹; Jan Rogers²; ¹University of Massachusetts; ²NASA Marshall Space Flight Center

The combination of computer-aided experiments with computational modeling enables a new class of powerful tools for materials research. A non-contact method for measuring density, thermal expansion, and creep of undercooled and high-temperature materials has been developed, using electrostatic levitation and optical diagnostics, including digital video. These experiments were designed to take advantage of the large volume of data (many gigabytes/experiment, terabytes/campaign) to gain additional information about the samples. For example, using sub-pixel interpolation to measure about 1000 vectors per image of the sample's surface allows the density of an axisymmetric sample to be determined to an accuracy of about 200 ppm (0.02%). A similar analysis applied to the surface shape of a rapidly rotating sample is combined with finite element modeling to determine the stress-dependence of creep in the sample in a single test. Details of the methods for both the computer-aided experiments and computational models will be discussed.

3:20 PM

Informatics for Imaging and Spectroscopy Databases: *H. Meco*¹; M. Heying¹; K. Boysen¹; M. Stukowski¹; W. Qin¹; W. Hu¹; Krishna Rajan¹; ¹Iowa State University

Quantitative interpretation of large amounts of spectroscopy and imaging data is challenging due to very large amounts of data. Informatics provides techniques that not only help to manage data but also to track correlations in a systematic way, and also identify subtle features that otherwise are difficult to see. In this presentation we provide examples using a variety of material characterization techniques including electron microscopy, 3D atom probe tomography and diffraction. The integration of informatics with spectroscopy data in is shown as a means of significantly accelerating the interpretation of complex high dimensional data.

4:00 PM

Modeling of Titan Oxidation Process in Fluidized Bed: *Szota Michal¹; Jozef Jasinski¹; Tomasz Mrozinski¹; ¹Czestochowa Technical University*

This paper presents neural network model used for designing leading of titan oxidation processes in fluidized bed. In this case the neural network structure is designed and prepared by choosing input and output parameters of process. The method of learning and testing neural network, the way of limiting nets structure and minimizing learning and testing error are discussed. Such prepared neural network model, after putting expected values of for example assumed microhardness curve and thickness of surface layer in output layer, can give answers to a lot of questions about running oxidizing process in fluidized bed. The neural network model can be used to build control system capable of on-line controlling leading process and supporting engineering decision in real time.

Materials Processing Fundamentals: Smelting and Refining

Sponsored by: The Minerals, Metals and Materials Society, TMS Extraction and Processing Division, TMS: Process Technology and Modeling Committee
Program Organizer: Prince Anyalebechi, Grand Valley State University

Tuesday PM
March 11, 2008

Room: 283
Location: Ernest Morial Convention Center

Session Chair: Prince Anyalebechi, Grand Valley State University

2:00 PM

Precipitation Rate of Hematite in Sulfate Media: *Maria Ruiz¹; Daniel Castillo¹; Rafael Padilla¹; ¹University of Concepcion*

Hematite precipitation is a convenient alternative for the removal of iron from leaching circuits because of its chemical stability, high density and high iron content. The precipitation of hematite from ferrous sulfate solutions was studied in an autoclave. The precipitation occurs by two sequential steps: oxidation of the ferrous to ferric ions followed by hydrolysis of the ferric to hematite. The objective of this study was to determine the effect of operating variables on the two-step rate of hematite precipitation. The variables included: stirring speed (100 to 600 rpm), temperature (160 to 200°C), acid concentration (1 to 10 g/L), initial iron concentration (1 to 15 g/L), and oxygen overpressure (1 to 6 atm). The sulfur content and the particle size of the precipitates were also determined. The results showed that the rate of oxidation of Fe²⁺ to Fe³⁺ is the controlling step of the overall process.

2:20 PM

A New Molten CaCl₂ Electrolysis Process for Titanium from High Titanium Slag: *Fanke Meng¹; Huimin Lu¹; ¹Beijing University of Aeronautics and Astronautics*

A new method for direct reduction of high titanium slag in molten CaCl₂ is studied in this paper. High titanium slag is made as cathode; an inert material is used as anode, and CaCl₂ as electrolyte. During the electrolysis, oxygen ion from high titanium slag cathode is reduced to oxygen on the surface of the anode; titanium is obtained on the cathode sinking underneath molten high titanium slag. The gas released on the anode is oxygen rather than carbon oxides and the cathode used is molten high titanium slag rather than solid titanium oxide, the electrolysis temperature is about 1700°C. This process is environment-friendly, low energy consumption and high current efficiency.

2:40 PM

Pressure Leaching of Enargite in Sulfate-Oxygen Media: *Rafael Padilla¹; Cristian Rivas¹; ¹University of Concepcion*

Enargite (Cu₃AsS₄) occurs normally associated with copper sulfides, mainly chalcopyrite. When the enargite content in chalcopyrite concentrates is high, direct smelting of the concentrate presents problems related to environmental pollution and contamination of the final metallic copper. Leaching processes are viable alternatives to treat copper concentrates with high content of enargite. Consequently, in this paper, the pressure leaching of enargite in sulfuric acid-oxygen system is discussed. The leaching rate was studied at 160 to 220°C and

partial pressures of oxygen of 74 to 200 psi. The enargite dissolution increased substantially with temperature increase. Complete dissolution of enargite was obtained at 220°C, and 100 psi of oxygen pressure in 90 min. The shrinking core model controlled by surface reaction was used to analyze the kinetics of enargite dissolution. Activation energy of 70 kJ/mol was obtained for the temperature range 160 to 220°C.

3:00 PM

In-Situ Analysis of the Effect of Other Oxides for the Reduction Process of Wustite by Carbon in TEM: *Ishikawa Nobuhiro¹; Takeshi Aoyagi¹; Takashi Kimura¹; Kazuo Furuya¹; Nayuta Mitsuoka²; Takashi Inami²; ¹National Institute for Materials Science; ²Ibaraki University*

The reduction of iron oxides has been one of the most frequently studied topics in iron smelting. We developed the in-situ observation of the reduction of iron oxides by solid state carbon in transmission electron microscope (TEM). The pure wustite (FeO) was used in the previous study as an iron oxide. But many kinds of additive is used to promote the reduction efficiency. The purpose of this study is to analyze the effect of additive during the reduction. We prepared several wt % of lime (CaO) and alumina (Al₂O₃) including wustite. Then the reaction between wustite and carbon was observed in TEM at about 800-1100K. The results were completely different from using pure wustite. Lime suppressed the reaction and Alumina promoted the reaction.

3:20 PM

Development of a Static Model for COREX Process: *Wang Chen¹; ¹Northeastern University*

COREX process is briefly introduced. A static model combining a set of mass and heat balance equations has been developed. Taking the specified inputs from the graphical user interfaces, the model is capable of calculating the consumption of raw materials and fluxes, the volume and composition of the slag and the volume and composition of the generator gas. The model enables the examination of the changes of materials and energy flows induced by the variations of operational parameters and raw materials chemical analysis. The model allows a detailed process analysis and adjustment of the plant operation and can thus be used to improve plant operation.

3:40 PM Break

3:50 PM

Thermal Stability of Nano-Twins in Pulse Electrodeposited Cu: Experimental and Calculations: *Di Xu¹; Luhua Xu¹; King-Ning Tu¹; Vidvuds Ozolins¹; ¹University of California, Los Angeles*

Cu with high density of nano-twins has excellent mechanical strength and electrical properties at the same time. It has potential to improve the reliability of Cu interconnects for very-large-scale-integration of circuits in the near-future Si microelectronic technology. The thermal stability of nano-twinning structure is of concern for large scale production and its future application. The annealing of pulse-electroplated Cu films shows that the thermal stability of nano-twins depends on the stability of {112} incoherent twin boundaries which are perpendicular to the {111} coherent twin planes. First principle calculations and MD simulations are used to study the twin boundary energy and mobility of twin planes. The simulations show a considerable mobility of {112} twin boundary while a near-zero mobility of {111} twin boundary, which is consistent with the experimental results.

4:10 PM

Thermodynamic and Kinetic Studies of Hydrochloric Acid Leaching Process of Panzhihua Ilmenite for Rutile Synthesis: *Jilai Xue¹; Zengjie Wang¹; Haibei Wang²; Xunxiong Jiang²; ¹University of Science and Technology Beijing; ²Beijing General Research Institute of Mining and Metallurgy*

Thermodynamic and kinetic studies of hydrochloric acid leaching of Panzhihua ilmenite from China are presented. The Eh-Ph diagram for system Fe-Ti-Cl-H₂O has been constructed, where a reaction medium of high acidity is of necessity to make iron into solution as Fe²⁺. The leaching process is found to follow the spherical model $f(a)=1-(1-a)^{1/3}$ and the apparent activation energy is calculated as 47.21 KJ/mol. The studies reveal different dissolving behaviors in various kinetic stages of the acid leaching. At the beginning stage the dissolved amount of both Fe and Ti increased monotonically with time of leaching, while about 30 minutes later the dissolved Ti in the form of TiOCl₂ began hydrolyzed into TiO₂

TUESDAY
PM

solid powder that reunited on the surface of ilmenite ore, as observed by SEM. The leaching process can end 4h later when most of Fe and other impurities have been dissolved and the hydrolyzing of TiOCl_2 almost finished.

4:30 PM

Thermodynamic Analysis and Its Application to Preparing Sm-Fe Alloy Oxide Precursor by Wet-Chemical Co-Precipitation: Ping Xue¹; Xueyi Guo¹; Qinghua Tian¹; Rongquan Jiang¹; ¹Central South University

$\text{Sm}_2\text{Fe}_{17}$ alloy is an important precursor for the preparation of $\text{Sm}_2\text{Fe}_{17}\text{N}_x$ magnet, which possesses a higher Curie temperature, larger anisotropy field, better resistance to oxidation and thermal stability. In this paper, the wet chemical co-precipitation was developed for synthesis of the Sm-Fe alloy oxide precursor. Based on the principles of simultaneous equilibrium and mass balance, a series of thermodynamic equilibrium equations of $\text{Sm}(\beta)\text{-Fe}(\alpha)\text{-NH}_3\text{-C}_2\text{O}_4\text{-H}_2\text{O}$ system at ambient temperature were deduced theoretically and the thermodynamic diagrams of $\lg[M2+]\text{-T}$ ($M=\text{Sm, Fe}$) versus pH at different solution compositions were drawn. Then, the experiments were done to address the various effects on the wet chemical process, including solution pH value, reactant concentration, reaction temperature and aging time, etc. It is found that by precise control of the process, the Sm-Fe alloy oxide precursor was synthesized with fine crystallization and special size and size distribution.

4:50 PM

Thermodynamic Modelling and Control of High MgO Copper Smelting Slag: Pengfu Tan¹; ¹Xstrata Copper

The control of liquidus temperature of high MgO copper smelting slag has played an important role in smelting high MgO copper concentrate. A thermodynamic model has been developed to predict the liquidus temperature of high MgO copper smelting slag $\text{FeO-Fe}_2\text{O}_3\text{-SiO}_2\text{-MgO-CaO-Al}_2\text{O}_3$. The effect of oxygen potential, matte grade, SiO_2/Fe in slag, SiO_2/CaO in slag, MgO and Al_2O_3 contents in slag on liquidus temperature of copper smelting slag has been modeled and discussed. The solid fraction below the liquidus temperature of the slag is also predicted and potential industrial applications are discussed.

Mechanical Behavior, Microstructure, and Modeling of Ti and Its Alloys: Microstructure/Property Correlation I

Sponsored by: The Minerals, Metals and Materials Society, TMS Structural Materials Division, TMS: Titanium Committee

Program Organizers: Ellen Cerreta, Los Alamos National Laboratory; Vasisht Venkatesh, TIMET; Daniel Evans, US Air Force

Tuesday PM
March 11, 2008

Room: 384
Location: Ernest Morial Convention Center

Session Chairs: Charles Ward, US Air Force; Patrick Martin, US Air Force

2:00 PM Invited

Low-Temperature Tensile and Creep Deformation Behavior of Grade 7 Commercially Pure Titanium Alloy: Paul Oberson¹; S. Ankem²; Kuang-Tsan Chiang³; Luis Ibarra⁴; ¹U.S. Nuclear Regulatory Commission; ²Ankem Technologies Inc.; ³Southwest Research Institute; ⁴Center for Nuclear Waste Regulatory Analyses (CNWRA)

The drip shield design considered by the U.S. Department of Energy includes Titanium Grade 7 (Ti-0.2wt%Pd-0.13wt%O) components. The tensile and creep behavior of Grade 7 Titanium alloy was independently investigated by the Center for CNWRA at low temperatures (25 to 250°C). The tensile behavior exhibited flow stress drops that increased with an increase in temperature. This behavior was attributed to a rise in the mobile dislocation density. In regard to creep deformation, there was no change in the amount of creep strain with an increase in temperature at 85% of the respective yield stress. This behavior was attributed to a change in the deformation mechanisms from slip and twinning at low temperatures (25 to 50°C) to solely slip at higher temperatures. Disclaimer: This abstract is an independent product of the CNWRA and does not necessarily reflect the view or regulatory position of the NRC.

2:30 PM

Application of Thermodynamic Modeling Tools in the Prediction of Titanium Alloy Properties: Manish Kamal¹; Vasisht Venkatesh¹; ¹Titanium Metals Corporation

Thermodynamic modeling tools are becoming increasingly important in materials development and processing. However, the use of these tools in the Titanium industry is still in its early phase. This study details the validation study at TIMET of PANDAT, a thermodynamic modeling tool. PANDAT was used to generate beta transus and alpha approach curves for production billets. Validation of the thermodynamic model was carried out with experimental techniques using digital image analysis and manual point count method. Model predictions were compared for alpha-beta alloy (Ti-64) and a near alpha, alpha-beta alloy (Ti-6242). Effects of interstitial elements, ingot chemistry and product chemistry and top and bottom ingot chemistry on the approach curve will be discussed.

2:50 PM

Characterization and Neural Network Models of a Creep-Resistant β -Titanium Alloy Based on Ti Metal-21S: Benjamin Peterson¹; Peter Collins¹; Hamish Fraser¹; ¹Ohio State University

Ti metal 21S has been selected as a baseline composition for the development of a new high temperature β -Ti alloy. A combinatorial approach employing directed laser deposition has been used to produce test coupons with different compositions. In addition to variations in the amounts of the elements present in the unmodified alloy (Ti, Mo, Nb, Al, and Si), the alloys contain varying amounts of Zr, Sn, W, B, C, and Ge. Subsequently, the creep properties (minimum creep rate) have been assessed and the microstructures characterized and quantified. This data is used to populate databases and subsequently train and test Bayesian Neural Network models for the prediction of creep properties. Advanced characterization techniques and computation tools are employed to identify the creep rate-limiting features. For example, SEM and TEM studies show a critical dependence of the size of a denuded β regions on the creep properties in these β -Ti alloys.

3:10 PM

Correlating Fracture Topography and Underlying Microstructure in α/β Ti Alloys: Adam Pilchak¹; Robert Williams¹; Andrew Rosenberger²; Mary Juhas¹; James Williams¹; ¹Ohio State University; ²US Air Force

High strength titanium alloys contain two ductile phases, the hcp α -phase and the bcc β -phases. The size and spatial distribution of these two constituents largely influence the strength and fracture related properties of these alloys. Consequently, the resulting fracture topography can be complex, even confusing. We have been developing or refining several methods for interpreting the fracture topography of Ti alloys. For example, using a focused ion beam to reveal underlying microstructure then using EBSD to determine constituent crystallographic orientation beneath particular fracture features. This talk will present and describe some examples of these methods for specimens fatigued to fracture under a variety of conditions and lifetimes. For example, it will be demonstrated that care must be taken to not confuse low ΔK fatigue fracture with traditional cleavage fracture observed in bcc metals. This work is sponsored by ONR under Project # N00014-06-1-0089, Dr. Julie Christodoulou, Manager.

3:30 PM

Effect of Microstructure on the Elevated-Temperature Low-Cycle Fatigue Behavior of Boron-Modified Ti-6Al-4V: Wei Chen¹; Carl Boehlert¹; Sesh Tamirisa²; Daniel Miracle³; ¹Michigan State University; ²FMW Composite Systems, Inc.; ³Air Force Research Laboratory

This study investigated the effect of boron addition on the low-cycle fatigue behavior of Ti-6Al-4V (wt.%) at elevated-temperature (455°C) for stresses between 200-550MPa ($R=0.1$; frequency=5Hz). The boron concentration of alloys was 0wt.%, 0.1wt.% and 1wt.% respectively, and alloys in two different processing conditions, as-cast and cast plus extruded, were tested. The results indicated that the boron additions improved the fatigue properties of Ti-6Al-4V. The cast-plus-extruded alloys exhibited significantly greater fatigue lives than the as-cast alloys. This was attributed to the microstructural changes caused by extrusion. S-N curves and the microstructure of each alloy will be presented, and the fracture and deformation behavior of the Ti-6Al-4V-xB alloys will be compared.

3:50 PM Break

4:10 PM Invited

Microstructure Development, Mechanics and Behaviour of Near-Beta and Beta-Titanium Alloys: *David Dye*¹; Richard Dashwood¹; Martin Jackson¹; Seema Raghunathan¹; Russell Talling¹; Nicholas Jones¹; ¹Imperial College

Near-beta and beta titanium alloys are of current interest from a practical point of view because of their using in landing gear and biomedical applications. Theoretically they are also interesting because of (i) the ability to form fine-scale (20nm) alpha, (ii) the vulnerability to omega formation and (iii) because of the tailorability of the single crystal elastic moduli with alloying. We will present recent results, chiefly from synchrotron x-ray diffraction, on the mechanics of these alloys. These show that (i) the elastic constants of the beta phase change dramatically when the beta is enriched by fine-scale alpha precipitation, (ii) that the single crystal elastic constants of GUM metal alloys can be characterised using synchrotron diffraction, (iii) that the dynamics of omega precipitation and subsequent alpha formation can be characterised, in situ, with ~2 second time resolution. In addition, some observations on the grain behaviour during hot working will be shown.

4:40 PM

Microstructural Investigation of Crack Initiation During Dwell Fatigue in Alpha/Beta Titanium Alloys: *Amit Bhattacharjee*¹; S. Rokhlin¹; M. Mills¹; S. Ghosh¹; J. Williams¹; ¹Ohio State University

Several near alpha titanium alloys are used widely by various aero-engine manufacturers in the lower temperature and pressure region of an aircraft engine both as discs and blades. These alloys are prone to micro/macro texturing which causes debit in the dwell (where load is held at a constant value) time fatigue life and are also detrimental to other mechanical properties. A combination of X-ray radiography, orientation imaging microscopy (OIM) in a scanning electron microscope and polarized light microscopy has been utilized to characterize the local microtexture around internal secondary and primary fatigue cracks. This information is being used to generate image-based, finite element models of local strain and stress development, with the ultimate goal of determining a local crack initiation criteria for dwell fatigue.

5:00 PM

Multiscale and Multistage Characterization of Fatigue Damage in Ti-6Al-4V: *Rikki Teale*¹; Andrea Keck¹; Manuel Parra¹; Pedro Peralta¹; ¹Arizona State University

Fatigue damage on notched and "smooth" specimens of Ti-6Al-4V was monitored to account for effects of local microstructure on nucleation and propagation of short and long. Grain/colony sizes and crystallographic orientations around nucleation sites and along the potential fatigue crack propagation paths are characterized using Electron Backscattering Diffraction (EBSD) in the test specimens. The geometry of short cracks is examined using serial sectioning and correlated to the local crystallographic environment. In addition, in-situ loading experiments were performed under optical and scanning electron microscopes to obtain strain fields beyond the crack tip via digital image correlation (DIC). These tests will provide data to quantify the effects of local microstructure on crack nucleation and crack propagation. These data, in turn, will be used to build a progressive damage model of crack growth at the microscale. Work funded by a Structural Health Monitoring MURI, Department of Defense AFOSR Grant FA9550-06-1-0309, Victor Giurgiutiu program manager.

5:20 PM

Mechanical Behavior and Microstructure of Ti-6Al-4V-0.25O Rich Oxygen Titanium Alloy: *Hui Wang*¹; *Huimin Lu*¹; ¹Beijing University of Aeronautics and Astronautics

Self-propagating High-temperature Synthesis (SHS) with reduction process was used to fabricate the Ti-6Al-4V-0.25O powder from TiO₂-V₂O₅-Al-CaH₂ system. In this process, there was no chlorine and the oxygen content in the powder was about 0.2% ~0.3%. The Ti-6Al-4V-0.25O alloy material was prepared by powder injection method from the rich oxygen titanium alloy powder. Some mechanical behavior and microstructure of the rich oxygen titanium alloy material was superior to Ti-6Al-4V titanium alloy. This process for producing the rich oxygen titanium alloy material is environment-friendly and low-cost.

5:40 PM

Thermophysical and Structural Properties of a Gamma-TiAl Alloy in the Temperature Range of 50-900°C: *Rainer Wunderlich*¹; Taishi Matsushita¹; Robert Brooks¹; Seshadri Seetharaman¹; Hans-Jörg Fecht¹; ¹Ulm University

Gamma-TiAl alloys offer great promise as a turbine blade material in jet engines because of increased specific strength and good creep resistance while issues like embrittlement at elevated temperature still need to be solved. Characterization of the material microstructure, its thermophysical properties and their temperature dependence is an important aspect in product development. Within the framework of the EC-FP6 IMPRESS project the thermophysical and microstructural properties of a Ti-45.5at% Al-8at% Nb have been investigated. The thermal diffusivity exhibited a pronounced maximum at T=750°C which could not be explained by the temperature dependence of the specific heat capacity or that of the electrical resistivity. A temperature dependent XRD-investigation revealed a change in the intensities of the γ-phase (111), (200), and (222) reflections as a function of temperature which otherwise would be typical for texture. This observation is interpreted as a temperature dependent reorientation of γ-lamellae resulting from twinning and the release of internal stress.

Mechanics and Kinetics of Interfaces in Multi-Component Materials Systems: Interfacial Microstructures and Effects on Mechanical and Physical Properties

Sponsored by: The Minerals, Metals and Materials Society, TMS Electronic, Magnetic, and Photonic Materials Division, TMS Structural Materials Division, TMS/ASM: Composite Materials Committee, TMS: Thin Films and Interfaces Committee
Program Organizers: Bhaskar Majumdar, New Mexico Tech; Rishi Raj, University of Colorado, Boulder; Indranath Dutta, US Naval Postgraduate School; Ravindra Nugehalli, New Jersey Institute of Technology; Darrel Frear, Freescale Semiconductor

Tuesday PM
March 11, 2008

Room: 279
Location: Ernest Morial Convention Center

Session Chairs: Nugehalli Ravindra, New Jersey Institute of Technology; Corbett Battaile, Sandia National Laboratories

2:00 PM Invited

Effect of Rare-Earth Additions to Al-Sc Alloys on Precipitate Composition and Resistance to Dislocation Motion: *David Seidman*¹; Richard Karnesky¹; Marsha van Dalen¹; David Dunand¹; ¹Northwestern University

Al-Sc alloys display a high number density of nanosize trialuminide L₁₂ precipitates with coherent interface with the Al matrix. The rare-earth (RE) elements Y, Sm, Gd, Dy, Er and Yb were found to partition to the precipitates. Local Electrode Atom Probe was used to follow the evolution of the RE concentration in the precipitates as a function of aging time at 300°C. RE segregate towards the center of the Al₃(Sc,RE) precipitates, minimizing lattice mismatch with the matrix. Hardness and creep measurements were used to assess the effect of Sc replacement by RE within the precipitates. RE do not increase hardness of the alloys, as expected from the fact that matrix dislocation bypass precipitates by the Orowan mechanism at ambient temperature. RE however improve creep resistance of the alloy, which is explained by the increased matrix/precipitate lattice mismatch resulting in enhanced elastic interactions with matrix dislocations.

2:30 PM

Stress Effects on Hydrogen Trapping in the Proximity of TiC-Fe Interfaces: Masato Enomoto¹; *Jong Lee*²; ¹Ibaraki University; ²Michigan Technological University

In steels, the interfacial region between ferrite matrix and TiC inclusions is suspected of a major trapping site for hydrogen, but the trapping nature is unknown. Due to the lattice misfit, fine TiC particles (< 20 nm) are coherent, whereas coarse ones are incoherent. To understand the role of the misfit strain in hydrogen trapping, a micromechanics analysis is performed. Elastic stress within a TiC particle and in the Fe matrix at the interface is computed, and its

geometric mean is defined as a trap stress for hydrogen. The results show that if the shape is plate-like, the trapping strength is greater for incoherent than for coherent particles. Within TiC particles, hydrogen atoms are proposed to replace some carbons due to the compressive stress. In the bcc Fe matrix, however, hydrogen atoms are to take on expanded interstitial sites for the coherent case and dislocation cores for the incoherent case.

2:55 PM Invited

Synchrotron X-Ray Microscopy Studies on Electromigration of a Two-Phase Material: *K. Subramanian*¹; *Andre Lee*¹; *Cheng-En Ho*¹; *Wenjun Liu*²; ¹Michigan State University; ²Argonne National Laboratory

Electromigration in multi-phase alloys has become important due to their utilization in microelectronic interconnects. Synchrotron X-ray microscopy has provided information regarding 2- and 3-dimensional crystallographic orientations and strain fields, providing documentation of microstructural evolution and surface features from current stressing of such alloys. Micro-beam X-ray fluorescence investigations indicated different conducting species move at different rates during electromigration. The continuous build-up of slow moving dominating species just behind the fast moving species causes significant compressive deformation in the anode region to push out the fast moving species towards the free surface forming the hillock. Micro-beam X-ray diffraction studies indicated the existence of significant compressive strain along the direction of electron flow near the anode, as well as tensile strains in directions perpendicular to the electron flow. Electron wind forces provide extra impetus for rapid morphological changes to produce larger grains of individual phases towards the anode.

3:25 PM

The Effect of Grain Boundary Character Distribution on Coble Creep: *Ying Chen*¹; *Christopher Schuh*¹; ¹Massachusetts Institute of Technology

As the properties of an individual interface largely depend on its atomic structure, the broad distribution of interfacial structures in polycrystalline materials presents a challenge to understanding the structure-property relationship. In this talk, we will discuss the effect of grain boundary network heterogeneity on grain boundary diffusional (Coble) creep. The grain boundaries are classified into slow-diffusing "special" boundaries and fast-diffusing "general" ones. The creep viscosity of the polycrystal is obtained from computer simulations, and is characterized as a function of the fraction of the different types of boundaries. This basically defines a new class of percolation problem where mass diffusion and force equilibrium are coupled. In addition to the percolation aspects, we also explore stress concentrations induced by the grain boundary character distribution, and an empirical effective medium equation that may be used with classical creep constitutive laws in order to predict the viscosity of a heterogeneous material.

3:50 PM Break

4:00 PM Invited

The Formation of Wear-Induced Microstructures during Sliding Contact: *Corbett Battaile*¹; *Somuri Prasad*¹; *Joseph Michael*¹; *Bhaskar Majumdar*²; ¹Sandia National Laboratories; ²New Mexico Tech

Friction can lead to complex mechanical and microstructural evolution near the worn surface, and these changes can impact the properties of the material. Recent results from tribological experiments on nickel single crystals reveal the formation of microstructural features ranging from nanometers (very near the surface) to microns in size. The formation and mechanical response of these zones is sensitive to crystallography, and can dramatically alter the frictional properties of the material itself. We have modeled these phenomena using combined treatments of crystal plasticity, microstructure formation, and grain boundary sliding. The loading conditions are adopted from an analysis of static frictional contact. A phenomenological treatment of wear debris and asperity-mediated contact is included to appropriately describe the mechanical mixing that occurs very near the contact interface. We will provide an overview of the experimental evidence, discuss the wear model in detail, and present results for kilocycle wear on nickel single crystals-in-different-crystallographic-orientations.

4:25 PM Invited

The Role of Interfaces on the Mechanics of Shape Memory Alloy (SMA) Fiber Reinforced Pb-Free Solder Composites: *Nikhilesh Chawla*¹; *J. Coughlin*¹; *J. Williams*¹; ¹Arizona State University

It is well known that solder joints must retain their mechanical integrity under conditions of isothermal aging, thermal fatigue, and creep. In recent years, shape memory alloys (SMA) have received significant attention due to their ability to be deformed and return to their original dimensions, upon unloading and/or the application of heat. Recently, SMA has been used as a reinforcement phase to form "smart" composite materials. The unique properties of SMA are being exploited to design damage tolerant materials that exhibit a beneficial response under applied loading. In this paper, we report on the interfacial reactions and mechanics of NiTi shape memory alloy fiber reinforced Sn matrix composites. It will be shown that the reaction products and kinetics are quite complex. The load transfer to the fiber is governed by the strength of the interface, aspect ratio of the fiber, and yield stress of the matrix. The evolution of the microstructural constituents and the influence on deformation behavior will be discussed.

4:55 PM

Formation and Growth of Ag Crystallites in Screen-Printed Ag Contacts for Crystalline Si Solar Cells: *Kyoung-Kook Hong*¹; *Sung-Bin Cho*¹; *Joo-Youl Huh*¹; *JaeSung You*²; *Ji-Weon Jong*²; ¹Korea University; ²LG Chem, Ltd. Research Park

The PbO-based glass frits contained in Ag paste are known to play an important role in the screen-printed Ag contact formation. Recently, there is an environmental demand for the development of a Pb-free glass frit to replace the conventional PbO-based frit. In search of the PbO replacement, it is crucial to understand first the role of PbO in the Ag contact formation. However, it still remains unclear how PbO in Ag pastes plays a role in the formation and growth of Ag crystallites at the paste/Si interface. In this study, we investigated the reactions between leaded Ag pastes and n-type [100] Si wafer coated with SiNx antireflection layer in an tube furnace at 800°C for 5 to 30 min, in order to understand the mechanism for the formation and growth of the inverse pyramidal Ag crystallites at the interface between the Ag paste and Si during the firing process.

5:20 PM

A Study of Interfacial Growth Kinetics and Mechanics for an Fe Fibre Reinforced Al Alloy: *Scott Kenningley*¹; *Simon Barnes*²; ¹Federal Mogul and Manchester University; ²Manchester University

The incorporation of long Fe based fibres into Al alloys has shown promise for significantly increased levels of high temperature fatigue resistance. This fatigue resistance, in combination with a relatively inexpensive manufacturing route, makes this composite a strong candidate material for highly loaded automotive engine products such as pistons. One of the problems with using this composite at highly elevated temperatures, is the reaction between the Fe based fibres and the Al matrix to produce brittle intermetallic phases. In the current study, fibre-matrix interfacial intermetallic growth has been characterised and modelled as a function of fibre volume fraction, heat soak temperature and time. The influence of changing interface intermetallic composition, morphology and size on the high temperature fatigue resistance of the composite has also been examined in an attempt to produce an FE model to predict behaviour of the composite as a function of its loading and thermal history.

Minerals, Metals and Materials under Pressure: High Pressure Phase Transitions and Mechanical Properties

Sponsored by: The Minerals, Metals and Materials Society, TMS Structural Materials Division, TMS: Chemistry and Physics of Materials Committee
Program Organizers: Richard Hennig, Cornell University; Dallas Trinkle, University of Illinois; Ellen Cerreta, Los Alamos National Laboratory

Tuesday PM Room: 385
 March 11, 2008 Location: Ernest Morial Convention Center

Session Chairs: Dallas Trinkle, University of Illinois; Richard Hennig, Cornell University

2:00 PM Invited

On Failure in Polycrystalline and Amorphous Brittle Materials: *Neil Bourne*¹; ¹Los Alamos National Laboratory

Materials found across natural environments experience mechanical extremes of pressure, temperature and strain rate or survive electromagnetic loads of great violence. Reaching an understanding of such states and the response of materials subject to them is key in fully describing operating deformation mechanisms. Armed with physically based models, it is possible to contemplate designing not only structures to operate within such environments, but also to adopt strategies to engineer materials with optimized properties to survive there. Key features of the dynamic response of brittle solids will be reviewed leading to understanding of natural materials under dynamic loads and to a new understanding of material design for use in extreme environments.

2:30 PM

Shear Strength and Texture Evolution in Tantalum Foils: *Juan Escobedo*¹; David Field¹; David Lassila²; ¹Washington State University; ²Lawrence Livermore National Laboratory

A new experimental apparatus has been developed for performing shear tests on specimens held under moderately high hydrostatic pressures. The experiments provide calibration data for models of materials subjected to extreme pressures such as the Steinberg-Guinan hardening model, among others. This paper reports the development of the experimental procedures and the results of experiments on thin foils of 111 textured polycrystalline Ta performed under hydrostatic pressures ranging from 1 to 5 GPa. Both yielding and hardening behavior of Ta are observed to be sensitive to the imposed pressure. EBSD was performed on the deformed specimens in order to determine what fraction of the specimen underwent a shear-type of deformation, these observations were correlated with the predicted texture that results by shearing a 111 texture material to a shear strain of 1 according to the visco-plastic self-consistent model. Finally burgers vector determination, dislocation cell structures were characterized by post-mortem TEM analysis.

2:50 PM Break

3:00 PM

Interpretation of Shock Damage Quantification Results through Polycrystalline Computer Simulations: *Davis Tonks*¹; Veronica Livescu¹; John Bingert¹; ¹Los Alamos National Laboratory

Quantification of ductile incipient damage in Tantalum samples from plate impact experiments has been performed using serial sectioning, EBSD, and optical microscopy. The influence of local crystal grain structure on void nucleation and growth and the role of plastic flow localization were investigated and will be reported on in another paper in this meeting (Livescu et al). This analysis is incomplete, however, without including the effects local stress and strain histories on damage creation. In this work, we compare the quantified damage results with computer simulations in which the experimental crystal grain structure has been explicitly represented in the mesh and the crystal grain plasticity is modeled phenomenologically. Void growth is treated in a simplified way. The calculated results reveal the stress and strain concentrations, which induce damage. The calculations and quantified damage will be analyzed for systematic trends that will then be modeled.

3:20 PM

First-Principles Studies of Structural and Mechanical Properties of XB₂ (X = W, Os, Re): *Xing-Qiu Chen*¹; C. L. Fu¹; ¹Oak Ridge National Laboratory, Materials Science and Technology Division

Transition-metal diborides, XB₂ (X = W, Os, Re), have attracted great interest due to their hard, ultra-incompressible behavior. Using ab initio density functional approach, we have studied the structural, electronic, and elastic properties of these compounds. The orthorhombic OsB₂ is found to undergo a phase transition into the ReB₂-type hexagonal phase above 2.5 GPa. For WB₂, we predict a ReB₂-type hexagonal structure at zero pressure; above 62 GPa, however, WB₂ transforms into the experimentally reported AlB₂-type structure. Among all of the studied structures, the ReB₂-type hexagonal structure exhibits the largest incompressibility along the c-axis, comparable to that of diamond. The origin of the ultra-incompressibility correlates not only with the strong covalence between B-B and X-B but also with the local buckled structure interconnected with covalent bonds. Research sponsored by the Division of Materials Sciences and Engineering, U.S. DOE, under contract DE-AC05-00OR22725 with UT-Battelle, LLC.

3:40 PM Break

4:00 PM Invited

High Pressure Materials Research Using Advanced Third Generation Synchrotron X-Ray: *Choong-Shik Yoo*¹; ¹Washington State University

Compression energy (PΔV) at 100 GPa (10⁶ atmospheres or 1 Mbar) often exceeds 1 eV or 100 KJ/mol, rivaling the energy of strong chemical bond. Therefore, the application of such a high pressure significantly alters chemical configuration, electronic and crystal structure, thermal, mechanical and chemical properties of solid and, in turn, provides a way to test condensed matter theory and to exploit novel properties and exotic materials. Furthermore, recent advances in diamond-anvil cell (DAC) high-pressure technologies coupled with advanced third-generation synchrotron x-ray offer unprecedented opportunities to discover exotic states of matter at high pressure-temperature conditions of Earth and other Giant planetary interiors. In this paper, I will discuss several recent results of high-pressure chemistry arising from pressure-induced electron delocalization in simple low-z molecular solids and in strongly correlated f- and d-transition metals at pressures of 100 GPa, following the brief descriptions of modern DAC technologies coupled with laser-heatings and synchrotron x-ray diffraction and spectroscopy. Also presented are the future directions of high-pressure synchrotron materials research in an emerging/complementary phase and time scales of shock and static high pressures.

4:20 PM

Delta to Alpha-Prime Phase Transformation in a Pu-Ga Alloy under Hydrostatic Compression: *Adam Schwartz*¹; Mark Wall¹; Daniel Farber¹; Kevin Moore¹; Kerri Blobaum¹; ¹Lawrence Livermore National Laboratory

Delta-phase Pu-Ga specimens, 2.3 mm diameter by 100 microns thick were compressed to approximately 1 GPa in a large volume moissanite anvil cell to induce the transformation to the alpha-prime phase. The recovered samples were characterized at ambient pressure with optical microscopy, x-ray diffraction, and transmission electron microscopy. Optical microscopy revealed a very fine microstructure that appears to be single phase. This preliminary conclusion was supported by x-ray diffraction, which showed only the monoclinic reflections from the alpha-prime phase. However, transmission electron microscopy revealed small regions of delta-phase with a very high dislocation density. From these results, we conclude that hydrostatic compression to 1 GPa is not fully sufficient to form and retain 100% alpha-prime. This work was performed under the auspices of the United States Department of Energy by the University of California, Lawrence Livermore National Laboratory, under Contract No. W-7405-Eng-48.

4:40 PM Break

4:50 PM

Pressure Induced Phase Transitions in PTFE: *Eric Brown*¹; Philip Rae¹; George Gray¹; Dana Dattelbaum¹; David Robbins¹; ¹Los Alamos National Laboratory

We present an experimental study of crystalline structure evolution of polytetrafluoroethylene (PTFE) due to pressure-induced phase transitions

in a semi-crystalline polymer using soft-recovery, shock-loading techniques coupled with mechanical and chemical post-shock analysis. Gas-launched, plate impact experiments have been performed on pedigreed PTFE 7C, mounted in momentum-trapped, shock assemblies, with impact pressures above and below the phase II to phase III crystalline transition. Below the phase transition only subtle changes were observed in the crystallinity, microstructure, and mechanical response of PTFE. Shock loading of PTFE 7C above the phase II–III transition was seen to cause both an increase in crystallinity from 38% to ~53% (by Differential Scanning Calorimetry, DSC) and a finer crystalline microstructure, and changed the yield and flow stress behavior. Results are discussed in the context of class shock hysteresis measurements and diamond anvil cell measurements on polymers.

5:10 PM

High-Pressure Amorphization of Boron Carbide: *Mingwei Chen*¹; ¹Tohoku University

Super-hard materials with strong covalent bonds can withstand very high stress prior to failure. However, the underlying mechanisms of high-pressure deformation and damage that lead to the failure of super-hard materials are poorly known. Boron carbide, B₄C, is one of the hardest materials and has been demonstrated to have outstanding ballistic armor properties. A variety of constitutive models have been developed to predict its performance at high shock pressures. However, the results have been mixed because the actual deformation/damage micromechanisms remain indefinite, which have been the subject of much intense work over the last 30 years. Here we report unusual depressurization amorphization in single-crystal B₄C subjected to diamond anvil cell experiments with nonhydrostatic pressures up to 50 GPa. Our findings provide a comprehensive portrayal on the high-pressure damage mechanisms of B₄C that will allow for more robust models and may be generically applicable to other super-hard materials in similar environments.

Neutron and X-Ray Studies for Probing Materials Behavior: Recrystallization

Sponsored by: National Science Foundation, The Minerals, Metals and Materials Society, TMS Structural Materials Division, TMS: Advanced Characterization, Testing, and Simulation Committee

Program Organizers: Rozaliya Barabash, Oak Ridge National Laboratory; Yandong Wang, Northeastern University; Peter K. Liaw, University of Tennessee

Tuesday PM
March 11, 2008

Room: 391
Location: Ernest Morial Convention Center

Session Chairs: Gabrielle Long, Argonne National Laboratory, Advanced Photon Source; Dorte Jensen, Riso National Laboratory

2:00 PM Keynote

Neutron and X-Ray Studies of Recrystallization: *Dorte Jensen*¹; ¹Riso National Laboratory

Neutron and x-ray methods offer complementary information to electron microscopy investigations of recrystallization. Of particular importance is the possibility of in-situ bulk studies. By following texture changes, overall kinetics information may be achieved and synchrotron x-rays allows studies of the local structural evolution in the bulk. These in-situ investigations have given results of importance for validation and for new developments of recrystallization models. Experimental methods, results and new modelling approaches are presented and discussed.

2:30 PM Invited

Spatially Resolved Elastic Strains in Dislocation Cell Structures Measured Using Sub-Micron X-Ray Beams: *Lyle Levine*¹; Jonathan Tischler²; Bennett Larson³; Michael Kassner³; Peter Geantli³; Wenjun Liu⁴; ¹National Institute of Standards and Technology; ²Oak Ridge National Laboratory; ³University of Southern California; ⁴Argonne National Laboratory

X-ray line profile measurements of deformed metals have long been used to study the elastic strains (and thus stresses) within dislocation cellular structures. These conventional X-ray studies use sample volumes that are much larger

than the dislocation structures being examined. Thus, only volume-averaged information can be obtained and attempts to interpret these results in terms of stress distributions within the underlying dislocation structures require ad hoc assumptions. We have used energy scanned, submicrometer X-ray beams to directly measure the axial elastic strains within individual dislocation cells in copper single crystals deformed in both tension and compression. Depth resolution was provided by translating a depth profiling wire through the diffracted beams and using triangulation to determine the depths of the diffracting volumes. More recent experiments have studied the distributions of elastic strains within individual dislocation cell walls and looked at elastic strains within extended contiguous sample volumes containing numerous dislocation cells.

2:55 PM

Study on the Texture and Micro-Structural Characters of IF Steel at Early Stage of Recrystallization by High-Energy X-Ray: *Yandong Liu*¹; Tong He¹; Qiwu Jiang²; Yang Ren³; Yandong Wang¹; Gang Wang¹; Liang Zuo¹; ¹Northeastern University; ²Anshan Iron and Steel Group Corporation; ³Argonne National Laboratory

High-energy synchrotron diffraction offers great potential for experimental study of recrystallization kinetics. A fine experimental design to study the recrystallization mechanism of Interstitial Free (IF) steel was implemented in this work. In-situ annealing process of cold-rolled IF steel with 80% reduction was observed using high-energy X-ray diffraction. The results shown that, at the early stage of recrystallization, new grains with {111}<110> orientation occurred at first and {111}<112> in sequence; the a-fiber texture component decreased with the annealing temperature increased, {111}<110> texture component does not change, while {111}<112> texture component increased.

3:15 PM

The Structure Dependence of Deformation Behaviour of TRIP Steel Monitoring by In-Situ Neutron Diffraction: *Jozef Zrník*¹; Ondrej Muransky²; Peter Sittner³; E.C. Oliver⁴; ¹COMTES FHT Sro; ²Nuclear Physics Institute; ³Institute of Physics; ⁴ISIS, CCLRC Rutherford Appleton Laboratory

Low alloyed TRIP steels are a class of multiphase steels offering an attractive combination of strength and ductility. By variation of thermomechanical processing parameters the transformation of conditioned austenite results in different structure characteristics. Qualitative microstructural characterization of the structure was carried out by SEM and TEM of thin foils. The volume fraction of retained austenite was measured by neutron diffraction and it varies in dependence of austenite conditioning. The tensile tests were performed at room temperature and different mechanical behaviour with different complex structure was found. The retained austenite mechanical stability during incremental loading was investigated by in-situ neutron diffraction. The results show that mechanical properties evaluated in-situ and by the standard tensile tests differ in total elongation and yield strength achieved. From evolution of phase strain was detected that the retained austenite bears a significantly larger load than the ferrite during the steel deformation.

3:35 PM

An In-Situ Investigation of Strain Partitioning and Variant-Selection Processes in Ti-6Al-4V at Elevated Temperatures Using Synchrotron Radiation: *Michael Glavicic*¹; S.L. Semiatin²; Gordon Sargent¹; ¹Air Force Research Laboratory (UES Inc.); ²Air Force Research Laboratory

The modeling of texture evolution during the hot working of two-phase, alpha/beta titanium alloys is complicated by several factors. First, the flow-stress behaviors of the hexagonal-close-packed (hcp) alpha phase and the body-centered-cubic (bcc) beta phase differ substantially and exhibit different dependences on temperature. Such differences result in an unequal partitioning of the imposed strain. Second, the beta phase decomposes to form alpha during cooling from the hot working temperature. At moderate cooling rates, this phase transformation follows a Burgers-type orientation relationship, in which there are twelve distinct possible variants that can form from a single orientation of a prior beta-phase grain. In this work, the partitioning of strain and the predisposition for one or several of the twelve variants to form preferentially over the others during the phase transformation from beta to alpha were investigated using novel in-situ high-temperature x-ray diffraction and x-ray line-broadening techniques.

3:55 PM Break

4:05 PM

Investigation of Fatigue Crack Growth in Superalloy Single Crystals by In Situ High Brilliance X-Ray Techniques: *Liu Liu¹; Naji Hussein²; Divine Kumah²; Chris Torbet¹; Roy Clarke²; Tresa Pollock¹; J. Wayne Jones¹*; ¹University of Michigan, Material Science and Engineering; ²University of Michigan, Physics

A portable ultrasonic fatigue instrument was designed and installed at the Advance Photo Source, Argonne National Laboratory to image, in situ, the initiation and propagation of fatigue cracks in the nickel-base superalloy CMSX-4 at 20 kHz with axial loading in the $\langle 001 \rangle$ direction. CMSX-4 specimens with 200 μm thickness have been examined. High brilliance x-ray undulator radiation was used to image (through-thickness) the initiation and growth of fatigue cracks from femtosecond laser machined notches and their interaction with the cast single crystal microstructure. Fatigue crack propagation occurred mainly on octahedral $\{111\}$ planes, and for some specimens, the transition from a mixed-loading-mode crystallographic crack on an octahedral plane to a mode I non-crystallographic crack was also observed. Images of crack morphology from x-radiation are compared with topographical information obtained by post-test fractography and optical microscopy. Extensions of this work to investigate fatigue damage accumulation in complex alloys and coatings is described.

4:25 PM

Effects of Asymmetric Rolling on Recrystallization Texture in Ultra-Thin Grain-Oriented Silicon Steel: *Yuhui Sha¹; Jing Chen¹; Fang Zhang¹; Liang Zuo¹*; ¹Northeastern University

Various modes of asymmetric rolling were applied to produce ultra-thin grain-oriented silicon steel strips, and the cold rolling and primary recrystallization textures were investigated by ODF (Orientation Distribution Function) method based on X-ray diffraction. Recrystallization texture development was found to depend strongly on asymmetric rolling modes and annealing temperature. Goss texture ($\{110\}\langle 001 \rangle$) and magnetic property can be significantly improved through appropriate processing parameters of asymmetric rolling and annealing. This indicates that asymmetric rolling has great potential to open up a new way for texture optimization in high-grade silicon steel thin strips. The effects of asymmetric rolling on recrystallization texture were explained in terms of the change in cold rolling texture and shear bands.

4:45 PM

Effect of Cold-Rolling on Texture Evolution and Mechanical Properties of a Ti-IF Steel Sheet: *Yongfeng Shen¹; Wenying Xue²; Yanhui Guo²; Yandong Wang¹*; ¹Northeastern University, Key Laboratory for Anisotropy and Texture of Materials (Ministry of Education); ²Northeastern University, The State Key Lab of Rolling and Automation

The dependence of crystallographic texture, deformation microstructure and flow stress on cold-rolling reductions in an interstitial-free (IF) steel sheet was investigated using X-ray diffraction (XRD), scanning electron microscope (SEM) and transmission electron microscope (TEM) techniques as well as tensile tests. The development of texture components was characterized for the specimens cold-rolled to various reductions from 13% to 75%. It was further observed that deformation microstructures consist of the geometrically necessary boundaries (GNBs) and incidental dislocation boundaries (IDBs). Dislocation and grain boundary hardening leads to an increase in flow stress with increasing rolling reduction. A fall in ductility found for the specimens with the rolling reductions between 13% and 46% is attributed to the onset of localized shearing. The increased ductility is closely related to the more uniform size distribution of cell blocks with increasing rolling reduction from 46% to 75%.

5:05 PM

In-Situ Tracing the Anomalous Recrystallization in the Ultrafine-Grained FeCo by High-Energy X-Ray Diffraction: *Jianning Deng¹; Chenchen Yuan¹; Yang Ren²; Ru Lin Peng³; Yanling Yang¹; Gang Wang¹; Dezhi Zhang⁴; Yandong Wang¹*; ¹Northeastern University; ²Argonne National Laboratory; ³Linköping University; ⁴Institute of Metal Research

Annealing texture in the traditional cold-rolled body-centered-cubic (BCC) metals or alloys consists mainly of $\{111\}/\text{ND}$. However, in a severely rolled FeCo alloy (with BCC structure) anomalous enhancement in the rotated-cube $(100)[011]$ texture component and a decrease in the $\{111\}/\text{ND}$ components were found after annealing, which is contrast to the recrystallization behaviors

reported in traditional BCC metals. So far the intrinsic physical nature of the anomalous recrystallization behavior in this material remains mysterious in the community of textures. In this investigation, the high-energy X-ray diffraction technique was used to trace the in-situ evolution of grain size, microstrain, and texture components during recrystallization. In combination with EBSP analysis in the SEM, the physical nature is revealed and will be presented in this talk.

5:25 PM

Influence of Hydrides on Fatigue Behavior of Zircaloy-4: *Elena Garlea¹; Hahn Choo¹; Gongyao Wang¹; Peter K. Liaw¹; Don Brown²; Jungwon Park¹; Phillip Rack¹*; ¹University of Tennessee; ²Los Alamos National Laboratory

The effect of zirconium hydrides, introduced by hydrogen-gas charging, on the mechanical behavior of Zircaloy-4 was investigated macroscopically using conventional mechanical testing and microscopically using neutron diffraction technique. Compact tension specimens were employed for which the specimen fatigue history plays a role on the distribution of hydrides and, thus, the crack propagation rate and fatigue life. It was observed that the hydrides were localized around a pre-existing crack, due to the stress gradient at the crack-tip, leading to faster crack propagation rates compared to the case when the hydrides were homogeneously spread if no flaws pre-existed in the sample. The synergetic effects of hydrides and crack tips on lattice strains of zirconium were observed by measuring the residual strain around the crack tip. The results from the hydrogenated specimens were compared with the as-received condition, allowing the evaluation of the stress produced at the crack-tip by the zirconium hydrides.

5:40 PM Invited

Novel Approaches for Non-Destructive 3D Grain Mapping: *Wolfgang Ludwig¹; Erik Lauridsen²; Søren Schmidt²; Henning Poulsen²*; ¹European Synchrotron Radiation Facility; ²Riso National Laboratory

Knowledge of the three-dimensional nature of material microstructures is of great importance for understanding, and optimization, of the microstructure – property relationship. This talk will provide an introduction to two novel approaches for 3D characterization of undeformed polycrystals. The two new approaches, termed topotomography and diffraction contrast tomography (DCT), respectively, are based on diffraction imaging using synchrotron radiation. Advantages and limitations of the two techniques are discussed as well as their relation to existing 3D x-ray based characterization techniques.

Particle Beam-Induced Radiation Effects in Materials: Ceramics and Nuclear Fuel Materials

Sponsored by: The Minerals, Metals and Materials Society, American Nuclear Society, TMS Structural Materials Division, TMS/ASM: Nuclear Materials Committee
Program Organizers: Gary Was, University of Michigan; Stuart Maloy, Los Alamos National Laboratory; Christina Trautmann, Gesellschaft für Schwerionenforschung; Maximo Victoria, Lawrence Livermore National Laboratory

Tuesday PM
March 11, 2008

Room: 389
Location: Ernest Morial Convention Center

Session Chairs: Kurt Sickafus, Los Alamos National Laboratory; Jian Gan, Idaho National Laboratory

2:00 PM

Accumulation of Radiation Damage in Ceramic Oxides: *Lionel Thomé¹; Jacek Jagielski²; Sandra Moll¹; Frederico Garrido¹*; ¹Nuclear Spectrometry and Mass Spectrometry Center-National Center for Scientific Research; ²Institute of Electronic Materials Technology

Ceramic oxides are employed in hostile media where efficient use of energy is a prime need. In most of applications ceramic oxides are submitted to intense irradiations which lead to strong modifications of their physico-chemical properties. The collect and analysis of data dealing with the production and recovery of radiation damage are thus tasks of prime interest. Ion beams provide very efficient tools for the simulation of the interactions involved during the slowing-down of energetic particles. A rather broad panoply of experimental techniques (RBS/C, TEM, XRD) can be implemented to monitor the damage

build-up and to characterize the nature of created defects. The aim of the present paper is to revisit the domain by the analysis of the damage accumulation in irradiated crystals in the framework of a new model (MSDA) based on the hypothesis that the damage results from multiple processes of atomic rearrangements occurring in successive steps.

2:40 PM

Comparison of the Damage in Sapphire Due to Implantation of Boron, Nitrogen, or Iron: *Carl McHargue*¹; Eduardo Alves²; Carlos Marques²;

¹University of Tennessee; ²Instituto Tecnológico e Nuclear

The damage microstructure and optical properties of sapphire implanted with boron, nitrogen, and iron were examined by RBS-C, TEM, and optical absorption. Implantations were conducted at RT and 1000 C at 150 keV and fluences from 3E16 to 1E17 ion/cm². Optical absorption measurements indicate that the boron-implanted samples contain the higher number of F-type centers and the nitrogen-implanted samples the fewest. The microstructure of the boron-implanted samples shows only "black-spot" defect clusters, as did the iron-implanted samples at low fluences. At higher fluences, the iron samples revealed the presence of nanometer sized single crystal bcc iron particles that contributed to additional optical scattering. Bubbles formed in the nitrogen-implanted samples at low fluences of nitrogen. A second damage region is apparent in the RBS-C spectra for higher fluences of nitrogen.

3:00 PM

Radiation Induced Effects in Magnesia and Dual Phase Magnesia-Zirconia Compounds: *Hannah Yount*¹; Todd Allen¹; Kurt Sickafus²; ¹University of Wisconsin-Madison; ²Los Alamos National Laboratory

Magnesia and magnesia zirconia dual phase ceramics are candidates for use as inert matrix materials in advanced reactor designs. Irradiations are being performed at Los Alamos National Laboratory (LANL) and the University of Wisconsin-Madison (UW) on magnesia and magnesia-zirconia dual phase ceramics to determine their radiation resiliency. The ceramics were irradiated with heavy ions to 1 dpa and 10 dpa and with protons to 1 dpa. Nanoindentation, microhardness analysis, XRD analysis, and TEM analysis was completed to investigate changes in lattice parameters, the presence of dislocations, and phase changes. Initial XRD results show broadening of the peaks and an increase in lattice parameter of less than 1.0% after irradiation. Initial Knoop microhardness analysis indicates a decrease after irradiation from 9.8 to 9.5 GPa at 10 dpa in the dual phase ceramic and 9.0 to 7.6 GPa at 10 dpa in the MgO.

3:20 PM

Particle Beam-Induced Radiation Effects in Strontium Titanate: *Yanwen Zhang*¹; William Weber¹; ¹Pacific Northwest National Laboratory

Strontium titanate (SrTiO₃) is of technological interest in microelectronics industries, where knowledge of particle beam-induced radiation effects, dynamic recovery and nanostructure evolution is critical. Irradiation-induced amorphization and recrystallization in SrTiO₃ under ion and electron irradiation have been studied in situ to characterize defects, dose rate effects, recrystallization rates and temperature dependence. The damage accumulation is consistent with a disorder accumulation model that describes interstitial and amorphous atom contributions. Significant dynamic recovery of the ion-induced damage occurs as irradiation temperature increases, and damage accumulation rate decreases dramatically at higher temperatures. The damage accumulation kinetics is consistent with irradiation-enhanced and thermal recovery processes with activation energies of 0.1 and 0.7 eV, respectively. Fast epitaxial recrystallization occurs through regrowth at a/c interface under electron-beam irradiation, with regrowth rates several orders magnitudes higher than thermal epitaxial growth, which may be attributed to localized electronic excitations that lower the energy barriers for rearrangement of interfacial atoms.

3:40 PM Break

4:00 PM

Bombardment of YSZ Thin Films with GeV U Ions: Alessio Lamperti¹; Anna Paola Caricato²; Paolo Maria Ossi³; Christina Trautmann⁴; Lia Vanzetti⁵; ¹University of Durham; ²Università di Lecce; ³Politecnico di Milano; ⁴Gesellschaft für Schwerionenforschung; ⁵Instituto Trentino di Cultura-Center for Scientific and Technological Research

The physico-chemical properties of Yttria Stabilised Zirconia (YSZ) make it a candidate for the containment of high activity nuclear wastes. To enhance the material stability under heavy irradiation, the evolution of its microscopic structure under extreme conditions has to be better understood. Amorphous and polycrystalline cubic YSZ thin films, about 400 nm thick, were deposited on (100) Si at RT and 673 K by UV pulsed laser ablation (248 nm; 20 ns; 4 Jcm⁻²), in oxygen atmosphere (1 Pa). The samples were exposed to 2.6 GeV U⁺ ions, at fluences between 2 and 8×10¹¹ cm⁻², completely penetrating the samples. The films were characterized, before and after irradiation, using SEM, GIXRD and XPS. In the crystalline films irradiation consistently broadens the diffraction reflections. A change is observed of Zr3d, Y3d and O1s core lines. The structural stability of polycrystalline and amorphous YSZ is discussed.

4:20 PM

Radiation Damage in Nanocrystalline UO₂: *Tapan Desai*¹; Dilpuneet Aidhy²; Paul Millett¹; Taku Watanabe²; James Tulenko²; Dieter Wolf¹; Simon Phillpot²; ¹Idaho National Laboratory; ²University of Florida

Displacement cascades in nanocrystalline UO₂ are studied using large-scale molecular dynamics (MD) simulation. A heavy cation (Uranium) is used as a primary knock-on atom (PKA) with energies ranging from 1 keV to 20 keV. Large number of point defect formation from radiation damage in single-crystal UO₂ have been studied previously¹. To understand the ion irradiation damage at the grain boundaries, a nanocrystalline material consisting of three dimensional grains of 10-40 nm diameter size is used. Due to the radiation, we expect large-scale defect formation in the grains followed by segregation of these defects to the grain boundaries. We compare the effects of different interatomic potentials for the description of the interactions in UO₂ on the defect evolution. The effect of the temperature on the defect formation/diffusion is also characterized. ¹L.V. Brutzel, M. Ravivamanantsoa and D. Ghaleb, Journal of Nuclear Materials, 354, (2006), 28.

4:40 PM

Gas Mobility in a Zirconium-Based Cermet Designed for Transuranic Isotope Burning: *Aaron Totemeier*¹; Lin Shao¹; Sean McDeavitt¹; ¹Texas A&M University

The development of UREX+ processes to recycle spent nuclear fuel has inspired the development of a zirconium matrix cermet storage/fuel form for transuranic (TRU) isotopes. Cermet fabrication is accomplished by hot extrusion at ~900°C. Accelerator-based ion beams are being used for irradiation simulation and sample characterization. The initial focus is on the degradation of mechanical properties and the mobility of fission products in zirconium. Samples prepared from zirconium crystal bar and extruded Zr-matrix cermets were prepared and ion irradiated using He and Kr ions with fluence levels between 1x10¹⁵ and 2x10¹⁷ atoms/cm² at temperatures up to 400°C. Microstructural and microchemistry changes are being quantified and mechanical property changes are measured using indentation methods. Further, He and Kr implanted samples are bombarded with Zr ions to increase damage without increasing gas concentrations in order to further isolate governing factors that are affecting mechanical properties.

5:00 PM

Charged Particle Beam Irradiation Creep Behavior of Pyrolytic Carbon: *Anne Davis*¹; Zhijie Jiao¹; Rongsheng Zhou¹; Gary Was¹; Lumin Wang¹; ¹University of Michigan

The creep behavior of pyrolytic carbon (PyC) in TRISO fuel particles under high temperature and neutron irradiation is critical to the fuel integrity of the Very High Temperature Reactor. To determine the irradiation creep behavior of PyC, experiments were conducted on thin (<70 μm) strip samples using a 3 MeV proton beam. The samples were loaded to stresses of 20.9 and 14.2 MPa at temperatures between 800 and 1200°C. The specially-designed irradiation stage in the Tandatron accelerator at the Michigan Ion Beam Laboratory includes a laser speckle extensometer for determining sample extension and a two-dimensional

thermal imager for temperature control. The temperature dependence of the creep rate under proton irradiation is compared to that under neutron irradiation at similar temperatures and loads. The relation between the creep behavior and the irradiated microstructure will also be discussed.

5:20 PM

Study of Silver Diffusion in Silicon Carbide: *Erich Friedland¹; Johan Malherbe¹; Nick van der Berg¹; ¹University of Pretoria*

Fuel elements of modern high-temperature nuclear reactors are encapsulated by CVD-layers of pyrolytic carbon and silicon carbide to reduce fission product release. Release of Ag-110m presents a major problem as the transport mechanism through polycrystalline silicon carbide is not well understood. The aim of this study is to obtain information on the importance of volume and grain boundary diffusion as well as their dependence on radiation damage. For this purpose silver diffusion in single crystal and in polycrystalline silicon carbide is compared at temperatures up to 2000 K. The contribution of grain boundary diffusion is extracted by correlating the diffusion results for single- and polycrystalline samples with the distributions of grain sizes and boundary thicknesses of the latter samples obtained by SEM analyses. Diffusion coefficients are obtained from the broadening of implantation profiles using RBS analysis. Different implantation temperatures are used to study the effect of radiation damage.

Phase Stability, Phase Transformations, and Reactive Phase Formation in Electronic Materials VII: Session II

Sponsored by: The Minerals, Metals and Materials Society, TMS Electronic, Magnetic, and Photonic Materials Division, TMS: Alloy Phases Committee

Program Organizers: Sinn-wen Chen, National Tsing Hua University; Srinivas Chada, Medtronic; Chih Ming Chen, National Chung-Hsing University; Hans Flandorfer, University of Vienna; A. Lindsay Greer, University of Cambridge; Jae-Ho Lee, Hong Ik University; Kejun Zeng, Texas Instruments Inc; Katsuaki Suganuma, Osaka University

Tuesday PM Room: 278
March 11, 2008 Location: Ernest Morial Convention Center

Session Chairs: Chih Ming Chen, National Chung-Hsing University; Daniel Lewis, Rensselaer Polytechnic Institute

2:00 PM Invited

Pronounced Electromigration of Cu in Molten Sn-Based Solders: *J. Huang¹; C. Robert Kao¹; ¹National Taiwan University*

The high local temperature in flip-chip solder joints of microprocessors has raised concerns that the solder, a low melting temperature alloy, might locally liquefy and consequently cause failure of the microprocessors. This presentation reports a highly interesting electromigration behavior when the solder is in the molten state. A 6.3×10^3 A/cm² electron current was applied to molten Sn_{3.5}Ag solder at 255°C through two Cu electrodes. The high current density caused the rapid dissolution of the Cu cathode. The dissolved Cu atoms were driven by electrons to the anode side and precipitated out as a thick and sometimes continuous layer of Cu₆Sn₅. The applied current caused the dissolution rate of the Cu cathode to increase by one order of magnitude. An equation for the minimum chemical potential gradient that is needed to balance the electromigration flux is derived.

2:20 PM

Measurement of Electromigration Activation Energy of the Eutectic SnPb Flip-Chip Solder Joints on Cu/Ni Thick-Film UBM Using Kelvin Probes: *Tsunghsien Chiang¹; Chih Chen¹; ¹National Chiao Tung University*

Activation energy of electromigration is investigated using Kelvin probes. The eutectic SnPb flip-chip solder joints with thick under bump metallization (UBM) of 5-μm Cu/3-μm Ni has been adopted for the electromigration test. We fabricate the Kelvin probes to monitor the bump resistance during the current stressing, and define the electromigration failure as the bump resistance increase reaches 20% of its initial value. Most of the previous studies defined the failure of the electromigration when the stressing circuit was open. Three-dimensional (3D) finite element modeling with void formation was established to compare

with the experiment results to confirm the increase of bump resistance. The stressing conditions were done on a hotplate with temperatures at 160°C, 150°C, and 140°C, and the current was 0.9 A. Also, the failure mode and the variation of the microstructure during various stages of electromigration will be discussed.

2:35 PM

Effect of Electromigration on the Mechanical Properties of Sn-3.5Ag Solder Joints with Ni and Ni-P Metallization: *Zhong Chen¹; Aditya Kumar²; Chee Cheong Wong¹; Subodh Mhaisalkar¹; Vaidhyanathan Kripesh³; ¹Nanyang Technological University; ²Nanyang Technological University/Institute of Microelectronics; ³Institute of Microelectronics*

The effect of moderate electric current density (1×10^3 to 3×10^3 A/cm²) on the mechanical properties of Ni-P/Sn-3.5Ag and Ni/Sn-3.5Ag solder joints were investigated after thermal aging at 160 degree for 100 hours. It was found that aged samples without current stressing failed mostly inside the bulk solder with significant plastic deformation in a tensile. The passage of current caused brittle failure to occur at the joint interface, and the tendency of such brittle failure increases with increasing current density. The fracture energy in the brittle failure decreased more rapidly with the Ni joint than the Ni-P joint. The IMC growth rate was also affected more in the Ni joint than the Ni-P joint.

2:50 PM

Recrystallization Induced Microstructure Change in Eutectic SnPb Flip Chip Solder Joints by Electromigration: *Fan-Yi Ouyang¹; K. Tu¹; ¹University of California, Los Angeles*

We observed frequently a refinement of the lamellar microstructure in eutectic SnPb solder joints in electromigration. We propose that the refinement is a consequence of recrystallization of the solder joint. Electromigration has both atomic flux and electron flow. The latter generates joule heating and the former causes strain. A strained solid at high temperature will undergo recrystallization. Since the eutectic solder is a two-phase alloy, a fine lamellar microstructure can be created, provided that the strain energy is much higher than the total interfacial energy. We calculated that the strain energy induced by electromigration can be three times of magnitude larger than the interfacial energy. Thus, recrystallization of a fine lamellar structure can occur in eutectic SnPb solder joints driven by electromigration.

3:05 PM

Study on the Electromigration Behavior in Sn-37Pb Flip Chip Solder Joint: *Sang-Su Ha¹; Jong-Woong Kim¹; Seung-Boo Jung¹; ¹Sungkyunkwan University*

Electromigration of solder joint under high current stressing has been an important concern of the reliabilities in the solder joint system, since the required device density and power of flip chip package increase. Thus, the size of the bumps shrinks continuously, causing rapid increase in the current density passing through the bumps. Recently, flip chip solder joint, when the current density reached the range of 104A/cm², drift of metal atoms occurred seriously, causing dissolution of under bump metallization at the cathode and the accumulation of the IMCs at the anode, meanwhile the current crowding accelerated at migration process. During the high current stressing in the solder joints, the effect of current crowding and Joule heating has been found to be responsible for the failure in the chip/anode side of the solder joints. In this study, electromigration behavior in Sn-37Pb solder bumps have been investigated for flip chip structure.

3:20 PM

Dual-Mode Failure Mechanisms of Electromigration in Pb-Free SnAg Solder Joints: *Hsiao-Yun Chen¹; Chih Chen¹; ¹National Chiao Tung University*

The effect of under bump metallization on electromigration failure mechanism has been investigated for eutectic SnAg composition under 9×10^3 A/cm² at 150°C. The thickness of the Cu UBM is 5 μm while the metallization on the substrate is 5 μm electroless Ni. Failure analysis revealed that Cu consumption in flip-chip solder joint structures plays important role in the failure mechanism. It is found that Cu would migrate to substrate end thus caused UBM depletion on the chip side regardless of the current direction, causing the intermetallic compounds spalled into solder. On the contrary, there would be no UBM depletion under current stressing for solder joints with a 5-μm Cu/3-μm Ni UBM. Typical pancake type void occurred when electron flow from chip side to substrate, while there is void formation near substrate with electron flow upward. More details on the failure mechanism will be discussed in the presentation.

3:35 PM Break

3:50 PM Invited

Undercooling of Pb-Free Solders on Various UBMs: Moon Gi Cho¹; Sung Kang²; Hyuck Mo Lee¹; ¹Korea Advanced Institute of Science and Technology; ²IBM Corp

The undercooling behavior of pure Sn, Sn-0.7Cu, Sn-3.5Ag and Sn-3.8Ag-0.7Cu solder alloys was observed in terms of various under bump metallurgies (UBMs). Four different UBMs (electroplated Cu, electroplated Ni, electroless Ni-P and electroless Ni-P/immersion Au) were employed. The amount of the undercooling of Pb-free solder alloys were reduced when reacted with Cu UBM and Ni-based UBMs, and the Ni-based UBMs was more effective than Cu UBM. When Ni₃Sn₄ was formed in the interfacial reactions with Ni-based UBMs, the reduction of undercooling was significant, especially for pure Sn and Sn-3.5Ag. The effects of UBMs on the undercooling of Pb-free solder alloys are discussed by comparing intermetallic compounds (IMCs) as well as the compositional change of each solder before and after interfacial reaction with UBMs. In addition, the microstructural changes of four solders on UBMs are discussed, which could be related to their undercooling behaviors.

4:10 PM Invited

Microstructural Evolution of Alloy Powder for Electronic Materials with Liquid Miscibility Gap: Ikuro Ohnuma¹; Takuro Saegusa¹; Yoshikazu Takaku¹; Ryosuke Kainuma¹; Kiyohito Ishida¹; ¹Tohoku University Graduate School of Engineering

Alloy powders manufactured from immiscible melts by a rapid quenching method exhibit characteristic morphologies, a so-called in situ composite, such as the egg-type, uniform second-phase dispersion microstructures reported by C.P. Wang et al., Science, 297 (2002), 990-993. In this paper, the microstructural evolution of rapidly quenched alloy powders, which are applicable for novel electronic materials, will be discussed based on a two-liquid miscibility gap predicted in the calculated phase diagrams using a thermodynamic database, ADAMIS (Alloy Database for Micro-Solders). Specifically, the microstructural evolution and properties of Bi-base Pb-free solders for high temperature use and Ag- or Au-base micro-powders with a high electric conductivity produced by a gas-atomizing method will be presented.

4:30 PM

Growth of SnPb Composite Whisker under Electrical Current Stressing: Cheng-Chang Wei¹; Pei Chiung Liu¹; Chih Chen¹; King Ning Tu²; ¹National Chiao Tung University; ²University of California, Los Angeles

The spontaneous growth of whiskers has become the most serious reliability problems in Pb-free electronic package industry. According to the previous literature, the optimum growth temperature for whisker is 60°C. And, it is hard to grow Sn whiskers in SnPb solder, since Pb can mitigate the growth of the Sn whiskers. In this study, composite SnPb whiskers were found to grow from the eutectic SnPb solder stripes. By employing FIB, solder stripes of various lengths, including 5µm, 10µm, 15µm and 270µm can be fabricated. Above the high current density of 5x10⁴ A/cm² at 100°C, the high compressive stress gradient exists in the SnPb solder and urges the composite whiskers formation. Pb-rich-phase whiskers grew first, followed by the growth of the Sn-rich-phase whiskers. According to the diffraction pattern of the Pb part in the composite whisker, the growth orientation was identified [110], [1-11] and [112].

4:45 PM

Improvement on Thermal Fatigue Properties of Sn-Ag-Cu Lead-Free Solder Interconnects on Casio's Wafer Level Packages Based on Morphology and Grain Boundary Character Distribution Changes: Shinichi Terashima¹; Taro Kohno²; Aiko Mizusawa³; Kazuyoshi Arai³; Osamu Okada³; Takeshi Wakabayashi³; Masamoto Tanaka¹; Kohei Tatsumi¹; ¹Nippon Steel Corporation; ²Ome Bumping Service Center, Nippon Steel Materials Corporation; ³Casio Computer Corporation

It has been well known that fatigue properties of lead-free Sn-Ag-Cu solder interconnects are affected by their silver contents; lower silver contents (ex. Sn-1Ag-0.5Cu) show better reliability at mechanically shock test than those with higher silver (ex. Sn-3Ag-0.5Cu) by absorbing shock energy, but have shorter thermal fatigue lives due to tin-grain coarsening caused by strain-induced dynamic recrystallization. In this presentation, thermal fatigue properties of commercial low-silver solder, LF35 (based on Sn-1.2Ag-0.5Cu), are evaluated

as compared with those of both low (Sn-1Ag-0.5Cu) and high silver (Sn-3Ag-0.5Cu) solders on Casio's wafer level packages. It is clarified that thermal fatigue properties of LF35 was remarkably improved from that of Sn-1Ag-0.5Cu, and moreover, LF35 showed longer fatigue life than Sn-3Ag-0.5Cu in spite of its lower silver content. This improvement can be explained from the viewpoints of both morphology and grain boundary character distribution changes.

5:00 PM

Mechanical and Electrical Properties of Cu-Sn Intermetallic Micro-Wire: Luhua Xu¹; King-Ning Tu¹; ¹University of California, Los Angeles

The size of solder joint in flip chip solder is becoming smaller, with a typical diameter of 50-100 micron. In through wafer vias, the diameter of copper interconnect and solder joint are as low as 20 micron. Solder and copper pad may rapidly react during both solder reflow and solid state aging. As a result, a high portion of intermetallic occupies in the small solder joint. It can even become a pure intermetallic joint. In this work, Cu-Sn intermetallic micro-wires were prepared by 100 micron copper wires reflowed with SnAgCu solder paste and followed by high temperature thermal annealing. Uni-axial tensile test on the intermetallic (Cu₆Sn₅+Cu₃Sn) showed the combined elastic modulus is 98 GPa, which is in agreement with previous result measured by nano-indentation. The resistivity of the intermetallic wire was determined by four probe method. Electromigration test on the Cu-IMC-Cu micro-wire showed a re-distribution of Cu₆Sn₅ and Cu₃Sn.

5:15 PM

Effect of Co Addition on Undercooling, Microstructures and Microhardness of Sn-3.5Ag Solder and Interfacial Reactions with Ni-P UBM: Dong Hoon Kim¹; Moon Gi Cho¹; Hyuck Mo Lee¹; ¹Korea Advanced Institute of Science and Technology

The effect of Co addition, from 0.01 to 0.7%, on undercooling, microstructure and microhardness of Sn-3.5Ag solder (number are all in wt.%) and interfacial reactions with Ni-P UBM are investigated. For addition of higher than 0.02%, the undercooling of Sn-3.5Ag solders was significantly reduced together with coarsened microstructures and increased eutectic regions. The hardness value also increased with increased alloying amount. The interfacial reaction with Ni-P UBM showed that spalling of intermetallic compounds (IMCs) during reflow was prevented in the Sn-3.5Ag-xCo (x=0.02%). And, the addition of higher than 0.05% Co changed the morphology of IMC from bulky (Ni₃Sn₄) to needle-shape (Ni-Sn-Co ternary compound). The optimum level of Co addition is also discussed.

5:30 PM

As-Solidified and Aged Microstructure Control through X Modification in SAC+X Alloys: Jason Wallester¹; Iver Anderson¹; Joel Harringa¹; David Rehbein¹; ¹Iowa State University

An ideal Pb-free electronic solder microstructure contains a fine phase distribution, while minimizing the size of any brittle phase. A coupled eutectic fits this description. Unfortunately, due to the difficulty of nucleating tin, a 100% eutectic microstructure for Sn-rich solders has remained elusive and pro-eutectic Ag₃Sn plates often plague Ag-bearing alloys. However, by careful study of Sn-Ag-Cu-X alloys using calorimetric solder joints (Cu substrates), pro-eutectic Ag₃Sn plates can be mitigated and eutectic volume maximized with specific near-eutectic SAC+X solders at low X concentrations (≤0.20 wt.%). One selection criteria for X was a demonstrated ability to suppress thermal aging effects, albeit at higher concentrations. Thermally aged samples (150C, up to 1000h), identical in composition and cooling rate to the DSC samples, also were examined and mechanically tested. Co, Zn, and Mn appeared most promising as substitutions for Cu in SAC(3595). Supported by Nihon-Superior, Inc., through Ames Lab contract no. DE-AC02-07CH11358.

Recycling: Micro-Organisms for Metal Recovery

Sponsored by: The Minerals, Metals and Materials Society, TMS Extraction and Processing Division, TMS Light Metals Division, TMS: Recycling and Environmental Technologies Committee

Program Organizers: Christina Meskers, Delft University of Technology; Greg Krumdiek, Argonne National Laboratory

Tuesday PM
March 11, 2008

Room: 280
Location: Ernest Morial Convention Center

Session Chairs: To Be Announced

2:00 PM

Chromate Reduction by a Novel Leucobacter Sp. Isolated from Chromite Ore Processing Residue Disposal Site of China: Zemin Ma¹; Wenjie Zhu¹; Liyuan Chai¹; ¹Central South University

A novel chromate [Cr(VI)] reducing bacterium was isolated from chromite ore processing residue disposal site of China and identified as a Leucobacter sp. by 16S rRNA gene sequence homology. The minimum inhibitory concentration of strain CRB1 was 820 mg l⁻¹ of Cr(VI). The reduction of Cr(VI) occurred only under aerobic conditions. With an initial concentration of 2.5×10⁸ cells ml⁻¹, 1800 mg l⁻¹ of Cr(VI) was reduced entirely within 38 h under the optimum conditions, at 30°C and pH 9.0. Increasing Cr(VI) concentrations prolonged reduction process and higher cell densities meant quicker reduction. A blue precipitate was produced during chromate reduction of strain CRB1, which was binding to the surface of bacterial cells and determined as trivalent chromium with electron paramagnetic resonance (EPR) spectrometry. The conspicuous chromate reduction ability of Leucobacter sp. CRB1 suggested a potential for bioremediation of Cr(VI) containing wastes.

2:20 PM

Detoxification of Chromite Ore Processing Residue with Novel Chromate Reducing Bacteria Leucobacter Sp. Ch1: Wenjie Zhu¹; Liyuan Chai¹; Zhihui Yang¹; ¹Central South University

Chromite ore processing residue (COPR) is a hazardous waste containing high concentration of chromium. We describe here a pioneer trial of detoxification of COPR in column reactor with an indigenous chromate reducing bacterium Leucobacter sp. Ch1, which showed high chromate reducing ability at high pH. Under the optimum conditions, at 30 °C and pH 10.0, pH of leachate decreased from 10.3 to 8.3, and Cr(VI) concentration in solution decreased to zero mg L⁻¹, and 76.4% of Cr(VI) was removed from COPR samples. The leaching toxicity of detoxified residue was 1.1 mg L⁻¹ that was lower than national standard of China.

2:40 PM

Effects of Chromium on the Population and Community Structure Diversity of Microorganism in Soils Contaminated by Chromium Slag in Alloy Steel Factory: ShunHong Huang¹; Zhihui Yang¹; Bing Peng¹; Liyuan Chai¹; ¹Central South University

The population of microorganisms and their diversity can reflect soil quality and contamination severity in soils. The objective of this study is to investigate the effects of hexavalent chromium (Cr(VI)) on the population of microorganism and their diversity in soils contaminated by chromium slag. The results showed that the population of microorganisms was significantly influenced by Cr(VI) contamination. The population of bacteria, fungi and actinomycetes in soils of chromium slag site were less than that in arable soils nearby and uncontaminated soils. Similar trend was also found in microbial diversity. In the incubation experiment, the population of microorganisms decreased with increasing Cr(VI) concentration. Furthermore, various microorganisms showed different sensitivity to Cr(VI) contamination. The sensitivity of microbial population to Cr(VI) contamination was in the order: bacteria>actinomycetes>fungi; while microbial diversity in the order: fungi>actinomycetes>bacteria.

3:00 PM

Influence of Cr(VI) on the Activity of Soil Enzymes: ShunHong Huang¹; Zhihui Yang¹; Bing Peng¹; Liyuan Chai¹; ¹Central South University

Soil microorganisms are sensitive to ambient environment and the changes of enzyme activities can indicate the pollution severity in soils. Field samples and incubation experiments were used for investigating the effects of Cr(VI) on enzyme activities in soils. Soil samples were taken from chromium slag site and nearby region in Xiangxiang Iron-Alloy factory in Hunan province. The results showed that the effect of Cr(VI) on activities of catalase, polyphenol oxidase and alkaline phosphatase was not significantly distinct. However, Cr(VI) showed a significantly inhibitory effect on dehydrogenase activity. Its value decreased with the increasing Cr(VI) concentration. The result imply that of dehydrogenase activity could be used as an indicator for the chromium pollution level in the area of Iron-Alloy factory and for the stability level of the soil ecosystem.

3:20 PM

Research on Bioleaching for Flotation Tailing of Cu-Ni Sulphide Ore in Karatungk: Linlin Tong¹; Hongying Yang¹; Maofa Jiang¹; Juan Yu¹; Yao Zhang¹; Youjing Fan¹; ¹Northeastern University

Today bacteria leaching of Cu-Ni sulfide ore becomes more and more popular. The study focus on the bioleaching for flotation tailing of Cu-Ni sulphide ore in Karatungk in Xinjiang of China. This tailing contains Cu of 0.11% and Ni of 0.19%. The bioleaching of the ore was conducted by bacteria HQ0211, an excellent bioleaching thermophilic strain, through the shake flask culture in different experimental conditions. The results showed that the highest leaching rate of Ni and Cu can reach 90.51% and 62.24% respectively, which is high-performance in oxidizing leach.

Structural Aluminides for Elevated Temperature Applications: Processing and Microstructure Control

Sponsored by: The Minerals, Metals and Materials Society, TMS Structural Materials Division, TMS: High Temperature Alloys Committee, TMS/ASM: Mechanical Behavior of Materials Committee

Program Organizers: Young-Won Kim, UES Inc; David Morris, Centro Nacional de Investigaciones Metalurgicas, CSIC; Rui Yang, Chinese Academy of Sciences; Christoph Leyens, Technical University of Brandenburg at Cottbus

Tuesday PM
March 11, 2008

Room: 394
Location: Ernest Morial Convention Center

Session Chairs: Kouichi Maruyama, Tohoku University; Birgit Skrotzki, BAM

2:00 PM Invited

Phase Transformations Studies of TiAl Based Alloys Solidifying through the β Phase: Marc Thomas¹; ¹ONERA

Following alloy development programs undertaken by ONERA with the aim to reduce the L→ α columnar as-cast structure, a new β -solidification TiAl (G4) alloy has been developed as a casting material with equiaxed microstructure for high temperature gas turbine applications. Since then, such a multi-phase material was found to induce a limited influence of aluminium content on mechanical properties. Further microscopic insights were however needed for a better understanding in the phase transformations mechanisms for such β solidification alloys. This paper highlights what are the structural factors, either related to the β solidification or to the subsequent cooling, that can be used to identify the precise step reactions from the liquid for this category of TiAl-based alloys. Then, emphasis is given to the various solid-state transformations involving the β phase such as $\beta \rightarrow \gamma$, $\beta \rightarrow \alpha_2$ and $\beta \rightarrow \omega$, those depending on the alloy chemistry and the heat treatment conditions.

2:30 PM

Recent Development in Gamma Titanium Aluminides Forging: Jacques Tschofen¹; Nicolas Rizzi¹; ¹Manoir Aerospace -Forges de Bologne

The gamma TiAl alloys present interesting properties to replace Ni base alloys for either rotational or hot components. They exhibit high temperature properties up to approx. 750°C combined with a low density. This study presents

recent work in forging of several grades. It shows difficulty to get good forgings and gives trends to have a more reliable forging route.

2:50 PM

Near Net Shape Manufacturing with Gamma Titanium Aluminide: *Edward Shelton¹; A. Wisbey¹; J.W. Brooks¹; ¹QinetiQ*

Alloys based on the intermetallic phase gamma titanium aluminide, TiAl, could replace other metallic materials in a range of applications. The principal benefits associated with TiAl are its low density and excellent properties at elevated temperatures. Commercial exploitation of the alloys has been restricted by technical difficulties and high costs associated with manufacturing components using conventional processing routes. The potential to produce components from TiAl alloys by thixoforming has been investigated. This process produces near net shape components by forcing the alloy into a mould while partially molten and is a well-developed technology applied to lower melting point alloys. There are significant technological difficulties to be overcome in developing it for TiAl alloys with melting points in excess of 1400°C. Process development studies are reported. Experimental trials have produced thixoformed specimen components from a TiAl-based alloy. Fundamental microstructural and mechanical properties of this thixoformed TiAl are reported.

3:10 PM

Towards the Thermodynamic Equilibrium of Titanium Aluminides after Consolidation by Back Pressure Equal Channel Angular Pressing: *Ross Whitfield¹; Klaus-Dieter Liss¹; Wei Xu²; Thomas Buslaps³; LaReine Yeoh¹; Xiaolin Wu²; Kenong Xia²; ¹Australian Nuclear Science and Technology Organisation; ²University of Melbourne; ³European Synchrotron Radiation Facility*

Mixtures of 50-Al and 50-Ti powders (atomic %) have been consolidated using the Back Pressure Equal Channel Angular Pressing (BP-ECAP) method starting with both raw and ball milled powders. We present in-situ high-energy X-ray diffraction studies with continuous Rietveld analysis obtained upon a heating ramp from 300 K to 1075 K performed after the consolidation process. Initial phase distributions contain all intermetallic compounds of this system but Al, with distribution maxima in the outer regions of the concentrations (α -Ti, TiAl₃). Upon annealing, we follow in detail the phase evolution and lattice parameter changes due to chemical segregation which is in favor for the more equilibrated phases such as γ -TiAl, α_2 -Ti₃Al and TiAl₂. An unexpected phase transition at about 625 K upon heating creates an intermediate β -Ti phase which gradually transforms into the final products.

3:30 PM Break

3:40 PM Invited

Processing and Properties of Gamma TiAl Sheet from Atomised Powder: *Rui Yang¹; Lei Xu¹; Yuyou Cui¹; Wei Sun¹; Chunguang Bai¹; Dong Liu¹; ¹Shenyang National Laboratory for Materials Science, Institute of Metal Research CAS*

Sheets made of light high-temperature materials such as gamma TiAl alloys have a variety of applications in aerospace structures. The compositional homogeneity of preforms inherent in the powder metallurgy approach helps to ensure uniform microstructure and mechanical properties of the sheet, especially at large dimension. This paper summarises our successful effort of sheet rolling using atomised powder of gamma alloys. Emphasis will be placed upon impurity pick-up and control of the atomised powder, the influence of degassing/HIPing parameters on the soundness of the preform, as well as identification of optimal combinations of rolling parameters. Temperature distribution in the preform at different stage of the rolling operation was accurately simulated using a finite element method. Thermomechanical deformation map of the gamma alloys obtained on a Gleeble simulator proves to be an excellent guide to identifying the "processing window" in which sheets with satisfactory mechanical properties can be produced.

4:10 PM

Solidification of Nb-Rich TiAl-Based Alloys: Grain Refinement by Boron Additions and the Role of Peritectic Growth: *Ulrike Hecht¹; Victor Witusiewicz¹; Anne Drevermann¹; ¹Access Materials and Processes*

Boron is an effective grain refiner for TiAl-based alloys, however its beneficial effect is sensitively depending on alloy composition and solidification conditions. In this paper we present a comprehensive analysis of the grain

refinement mechanism and its limits, based on thermodynamic and kinetic aspects of solidification and subsequent phase transformations: The analysis is based on unidirectional solidification experiments performed on samples with different composition, selected from within the range 43 to 46 at.% Al and 5 to 8 at.% Nb, both with and without boron additions. An adequate quenching technique allowed us to conserve high temperature phases, specifically the alpha-(Ti) phase, in all solidified samples. A clear distinction between peritectic alpha-(Ti) and alpha-(Ti) grown from solid state beta-(Ti) was possible. EBSD analysis of the grain orientation of alpha-(Ti) was directly feasible and proved to be the key for understanding grain refinement.

4:30 PM

Grain Refinement in TiAl-Based Materials Investigated by Directional Growth Experiments and Phase-Field Simulations: *Ingo Steinbach¹; Ulrike Hecht¹; Anne Drevermann¹; Janin Eiken¹; Christian Hartig²; Daniel Gosslar²; Robert Guenther²; Ruediger Bormann²; ¹Rheinisch-Westfälische Technische Hochschule-Aachen; ²Technische Universität Hamburg-Harburg*

Grain refinement of TiAl-based alloys can be achieved by thermal treatment or during solidification, the latter being commonly attributed to the effect of boron additions. The detailed mechanism of grain refinement by boron is however a subject of controversial discussion in literature, especially with regard to the role of boride phases on the nucleation of beta(Ti) and on nucleation of peritectic alpha(Ti). In this talk we present phase field simulations and well controlled directional growth experiments that focus on nucleation and subsequent growth of primary beta(Ti) and peritectic alpha(Ti) in the presence of third phases that may act as heterogeneous nucleation sites for either beta(Ti) or alpha(Ti). The microstructure evolution is compared to that of a reference TiAl-based alloy that does not contain, or form, third phases.

4:50 PM

Texture Formation in High Niobium Containing γ -TiAl Alloys during Hot Rolling: *Andreas Stark¹; Arno Bartels¹; Daniel Gosslar¹; Frank-Peter Schimansky²; Rainer Gerling²; Helmut Clemens³; ¹Hamburg University of Technology; ²GKSS Research Centre; ³Montanuniversität Leoben*

The texture formation during hot rolling was studied in Nb-rich γ -TiAl based alloys with compositions of Ti-45Al-(5-10)Nb-(0-0.5)C (at.%). Hot rolling is performed with texture-free powder compacts at temperatures in the upper range of the (α + γ) phase field. Additionally a third phase, β -Ti(Al), is present at that temperatures in Ti-45Al-10Nb. Samples for texture analysis were taken after various pass sequences of the rolling process as well as after additionally annealing. In the as-rolled samples the textures of γ -TiAl and α -Ti(Al) show components which are crystallographically correlated by the Blackburn orientation relationship. However this correlation is not caused by phase transformation but indicates co-deformation during hot rolling. For the first time we could measure the texture of β -phase in Ti-45Al-10Nb which exhibits components, typically observed in bcc-metals after rolling. In addition, the high number of slip systems which can be active in bcc β -Ti(Al) results in improved formability during the rolling process.

5:10 PM

Development of TiAl-Based Alloys for High Temperature Applications: *Fereshteh Ebrahimi¹; Sonalika Goyal¹; Michael Kesler¹; Orlando Rios¹; Hans Seifert²; ¹University of Florida; ²Technische Universität Bergakademie*

Polycrystalline gamma-TiAl has shown promising properties for high temperature applications below 1000°C. Precipitation of a second intermetallic phase can be exploited to extend its applicability to higher temperatures. Furthermore, since TiAl has limited workability, it is desirable to have a high temperature cubic phase, which upon cooling transforms to the aluminide phase. We have investigated additions of Nb and Cr to identify a compositional region that satisfies the above goals. Arc melted buttons using pure elements were prepared. Phase evolution in the alloys was evaluated by examination of samples heat treated in purified argon atmosphere and then quenched from critical temperatures identified by DSC experiments. Selected alloys were aged to study the phase stability at elevated temperatures. In this presentation the extension of the cubic beta phase field and the evolution of the two-phase gamma-TiAl and sigma-Nb2Al will be discussed. Financial support through NSF-DMR 0605702 grant is greatly appreciated.

Ultrafine-Grained Materials: Fifth International Symposium: Properties

Sponsored by: The Minerals, Metals and Materials Society, TMS Structural Materials Division, TMS Materials Processing and Manufacturing Division, TMS: Shaping and Forming Committee, TMS: Nanomechanical Materials Behavior Committee
Program Organizers: Yuri Estrin, Monash University and CSIRO Melbourne; Terence Langdon, University of Southern California; Terry Lowe, Los Alamos National Laboratory; Xiaozhou Liao, University of Sydney; Zhiwei Shan, Hysitron Inc; Ruslan Valiev, UFA State Aviation Technical University; Yuntian Zhu, North Carolina State University

Tuesday PM Room: 273
 March 11, 2008 Location: Ernest Morial Convention Center

Session Chairs: Terence Langdon, University of Southern California; Sergey Dobatkin, Russian Academy of Sciences, A.A.Baikov Institute of Metallurgy and Materials Science; Terry Lowe, Los Alamos National Laboratory; Karl Theodore Hartwig, Texas A&M University

2:00 PM Invited

Functional Properties Produced by Severe Plastic Deformation: *Zenji Horita*¹; ¹Kyushu University

Severe plastic deformation (SPD) through Equal-Channel Angular Pressing (ECAP) is applied to a Cu-6.5mass%Co alloy containing a fine dispersion of ferromagnetic Co precipitates in the Cu matrix. Changes in microstructures and crystal structures are examined using X-ray diffraction (XRD) analysis and transmission electron microscopy (TEM). Measurements of coercive force are carried out after ECAP with different numbers of passes and different processing routes. It is shown that the application of ECAP leads to an increase in the coercive force and introduces magnetic anisotropy. SPD through High-Pressure Torsion (HPT) is further applied to intermetallic MgNi₂ powders and the hydrogen storage capability of the intermetallic is examined. Quantitative analysis of hydrogen content including microstructural analyses using XRD and TEM show that HPT is effective to modify a non-hydrogen absorber, MgNi₂, to a hydrogen absorber without addition of ternary elements.

2:20 PM

Significant Size Effect in the Mechanical Behavior of Nanostructured Copper: Yonghao Zhao¹; Cheng Xu²; Terence Langdon³; *Yuntian Zhu*³; ¹University of California, Davis; ²University of Southern California; ³North Carolina State University, Department of Materials Science and Engineering

Nanostructured materials are usually characterized with small samples. Here we report that small sample sizes have unexpected size effects on the mechanical behavior, including on the ductility and work-hardening rate. Specifically, in addition to the size effect normally expected from the cross-section and gauge length, we demonstrate also that the gauge length significantly affects the strain hardening rate and the uniform elongation. The implications of these observations suggest that some of the literature data on mechanical behavior of nanostructured materials, especially the strain hardening rate and uniform ductility, may be partially incorrect. Also, the strain rate sensitivity may be affected by the sample size, casting some doubts on fundamental properties derived from this parameter such as the activation volume. In summary, the mechanical properties of nanostructured materials are not easily compared unless the sample sizes are the same.

2:35 PM Invited

Common Trends in Flow Anisotropy and Fatigue Response of Ultra-Fine Grained HCP and BCC Materials: *Ibrahim Karaman*¹; M. Haouaoui¹; G.G. Yipici¹; H.J. Maier²; I. Beyerlein³; C.N. Tome³; ¹Texas A&M University; ²University of Paderborn; ³Los Alamos National Laboratory

Recent findings show that large strains and abrupt strain path changes alter the microstructure and crystallographic texture of HCP and BCC materials, leading to considerable flow stress anisotropy. We have recently conducted an extensive investigation on the effect of strain path changes of a few HCP and BCC materials during and after severe plastic deformation on the resulting uniaxial (tensile and compressive) flow anisotropy and low cycle fatigue (LCF) response. In

particular, we have used Equal Channel Angular Extrusion (ECAE) to severely process: 1) commercial purity (CP) HCP Ti; 2) pure HCP Zr billets with strong basal texture; 3) Nb-1%Zr BCC alloy; and 4) interstitial free (IF) BCC steel, most of them processed at room temperature. A Visco-Plastic Self Consistent (VPSC) polycrystal plasticity model was used to predict the flow behavior and texture evolution after post-processing uniaxial experiments. In this talk, we will summarize the common trends and subtle differences on the texture evolution, flow anisotropy, and LCF response in these materials while also elaborating on the microstructural mechanisms responsible for these phenomena.

2:55 PM

Superplastic Deformation of Ultrafine-Grained Mg-Alloys Produced by Micro-Alloying and Equal Channel Angular Extrusion: *Florian Dalla Torre*¹; Anja Hänzi¹; Maciej Krystian²; Jörg Löffler¹; Peter Uggowitzer¹; ¹Swiss Federal Institute of Technology; ²ARC Seibersdorf Research GmbH

The 'grain growth restriction'-concept via the addition of elements such as Zn, Y, Ca, and Zr was used to cast and extrude Mg-alloys with mean grain sizes of < 10 micrometer. In combination with equal-channel-angular-extrusion (ECAE) processing, the mean grain size was further reduced to 200-300 nm. Tensile testing at room temperature of samples prior to ECAE showed a substantial increase in ductility and strength. After ECAE the yield strength increased further to values of 300 to 400 MPa, while maintaining a high strain to failure of 15-28%. Texture and mechanical anisotropy decreases with decreasing grain size. Above 250°C superplastic deformation with strains larger than 100% and with strain-rate-sensitivities of up to 0.6 were measured. These properties, combined with the stabilization of the grain size in the micrometer range, are very beneficial for superplastic net-shape-forming. In addition, their good biocompatibility makes these alloys potential candidates for biomedical applications.

3:10 PM Invited

Low-Temperature Superplastic Flow of Ultrafine Ti-6Al-4V: *S. Semiatin*¹; Gordon Sargent²; ¹Air Force Research Laboratory; ²UES, Inc

The superplastic-flow behavior at low temperatures (650 – 800°C) and a range of strain rates (10⁻⁴ to 10⁻² s⁻¹) of Ti-6Al-4V with an ultrafine microstructure has been established. Program materials comprised both billet product manufactured by warm isothermal ('abc') forging and sheet fabricated by warm rolling. Extensive metallography on undeformed and deformed samples water quenched from the various test temperatures was conducted to characterize microstructure stability. Despite the low deformation temperatures, both lots of material showed similar (measurable) dynamic coarsening, whose kinetics mirrored the flow-hardening observed during compression and tension tests. The plastic-flow phenomenology was interpreted in the context of the classical Bird-Mukherjee-Dorn relation. The stress and grain-size exponents of the strain rate were ~1.4-2 and ~2, respectively, for strain rates of 10⁻⁴ and 10⁻³ s⁻¹. The constitutive analysis suggested that multiple mechanisms (dislocation glide-climb, diffusion) control deformation, thus complicating the interpretation of the apparent activation energy.

3:30 PM Invited

Quasistatic and High-Strain Rate Response of Ultra-Fine Grained Copper: *Marc Meyers*¹; A. Mishra¹; B. Kad¹; M. Martin¹; N. Thadhani¹; ¹University of California

The quasistatic and high-strain rate mechanical response of UFG copper processed by ECAP was characterized by compressive, tensile, reverse Taylor impact and Hopkinson-bar experiments. Upon impact, the samples were found to undergo heat-induced static recrystallization at a calculated temperature of 360K, indicating that the UFG copper is thermally unstable. Reverse Taylor tests were conducted on as-received OFHC Cu rod and ECAP specimens with sequential ECAP passes (2 and 8). The dynamic deformation of the samples is modeled using AUTODYN-2D and a modified Johnson-Cook constitutive equation was found to well capture the dynamic response. Both the dynamic experiments and analysis from the Reverse Taylor tests indicate an enhanced strain-rate sensitivity in comparison with conventional polycrystalline copper, in agreement with predictions of reduced activation volume. Similar to the compression test results, the impacted front of the samples are found to recrystallize extensively and preferentially.

3:50 PM Break

4:05 PM Invited

Towards Enhancement of Fatigue of Ultra-Fine Grain Metals - Past and Future: Alexei Vinogradov¹; Satoshi Hashimoto¹; ¹Osaka City University

Common aspects and features of fatigue of UFG materials produced by ECAP are discussed. Special attention is paid to the influence of strain path, amount of strain and post-processing annealing on the structure, strength and ductility, fatigue life and cyclic hardening/softening. Available results on the grain size effect on high-cyclic and low-cyclic properties are reviewed aiming at understanding of the reasons for materials degradation. Mechanisms of plastic flow and degradation during fatigue are discussed from the standpoint of initial UFG structure and its evolution upon cycling. The role of dislocation accumulation and grain reduction is highlighted. It is shown that high fatigue limit can be achieved after first ECA-pressings if a uniform fine grain structure is formed during ECAP and post-processing annealing. Results of phenomenological modeling of the monotonic and cyclic response of UFG metals are presented in terms of dislocation kinetics and a satisfactory agreement with experiments is demonstrated.

4:25 PM

Mechanical and Service Properties of Nano- and Submicrocrystalline Low Carbon Steels at Temperatures between (-40) and (+700)°C: Sergey Dobatkin¹; Pavel Odessky¹; Evgeny Naidenkin¹; Svetlana Shagalina¹; ¹Russian Academy of Sciences, A.A.Baikov Institute of Metallurgy and Materials Science

The thermal stability, mechanical and service properties of low-carbon ferritic-pearlitic and martensitic 0.09%C-Mn-Si, 0.1%C-Mn-V-Ti and 0.06%C-Mo-Nb-V steels have been studied after severe plastic deformation (SPD) by high-pressure torsion (HPT) and equal-channel angular pressing (ECAP). HPT and ECAP of low carbon steels produce nanocrystalline (50-100nm) and submicrocrystalline (SMC) (200-300nm) structures, respectively. The initial martensitic state compared to the initial ferritic-pearlitic state of low carbon steels promotes the formation of finer structure, less intense grain growth upon heating after SPD up to 700°C and more significant strengthening. The high-strength state of the 0.1%C-Mn-V-Ti and 0.06%C-Mo-Nb-V steels after ECAP is retained up to a temperature of 500°C. The strength properties at 600°C (fire resistance) of these SMC steels are higher by 20-25% than those of the undeformed steels. A significant increase in impact toughness especially at subzero temperatures is shown. The work was supported by RFBR (project no. 07-03-00342).

4:40 PM Invited

The Effect of ECAP with Back-Pressure on Enhanced Superplasticity of Magnesium Alloy AZ31: Rimma Lapovok¹; Michael Popov²; Stuart Rundell¹; Yuri Estrin¹; ¹Monash University; ²Technical University of Clausthal

Enhanced superplastic behaviour of magnesium alloy AZ31 was studied as a function of the number of ECAP passes and the level of back-pressure. After homogenisation at 420°C for 4 hours the processing by ECAP with a back-pressure leads to microstructures more favorable for enhanced superplasticity, notably bi-modal grain structures. The role of back-pressure and temperature for obtaining bi-modality of microstructure has been studied. It was shown that a decrease in the temperature of ECAP processing and concurrent increase of the back-pressure result in a bi-modal structure which consequently leads to an increase in elongation-to-failure to a record level as compared to the reported results for this material. Samples processed by six passes of ECAP at 150°C and the applied back-pressure of 218 MPa demonstrated enhanced superplastic behaviour with maximum strain-to-failure above 1200%, which is by more than 300% higher than the best results published on AZ31 superplasticity to date.

5:00 PM

The Flow Behavior of Superplastic Materials Processed Using Severe Plastic Deformation: Megumi Kawasaki¹; Terence Langdon¹; ¹University of Southern California

When metallic alloys are processed using severe plastic deformation, the grain sizes are reduced to the submicrometer range and the materials exhibit exceptional properties including superplastic flow at elevated temperatures. There are many examples to date documenting the occurrence of superplastic behavior in materials processed by procedures such as equal-channel angular pressing. This presentation examines the characteristics of this behavior with special reference to a two-phase Zn-22% Al eutectoid alloy. Emphasis is placed

on the variation of the flow stress with strain rate, measurements of the strain rate sensitivity and the role and significance of internal cavitation.

5:15 PM

Ductility Enhancement of Ultrafine Grained Aluminium Processed by Constrained Groove Pressing: Jozef Zrník¹; Tomas Kovarik²; Miroslav Cieslar³; Libor Kraus⁴; ¹COMTES FHT Sro; ²West Bohemian University; ³Charles University; ⁴Comtes FHT, Ltd.

The constrained groove pressing was used to refine pure aluminium coarse structure. The cumulative effective strain ϵ_{eff} becomes ~ 9.3 . The impact of the groove pressing is investigated upon microstructure changes with transmission electron microscopy. The coarse grain structure is successfully refined to the mixture of subgrain and polygonized grains of submicron size. However, the structure nonhomogeneity is apparent regardless the number of passes performed. The changes in mechanical properties were evaluated by performing tensile tests and by hardness measurement. The substantial impact of straining upon the tensile strength increase was already observed after the first pressings. With increasing straining only small enhancement in strength and concomitant loss of ductility was apparent. To improve plastic properties of ultrafine grained Al a further annealing and deformation experiment was carried out. The results from tensile tests indicate the small decrease in YS and UTS but increase in the elongation.

5:30 PM

Mechanical Properties of Ultrafine Grained Ferritic Steel Sheets Fabricated by a New Process without Severe Plastic Deformation: Yoshitaka Okitsu¹; Naoki Takata²; Nobuhiro Tsuji²; ¹Honda R&D Company, Ltd.; ²Osaka University

It's been difficult to apply UFG metals to automobile body parts, because dimensions of the samples fabricated by SPD methods are limited. Recently the authors have developed a new process to produce UFG steel sheets through conventional rolling and annealing procedures. The purpose of this presentation is to show the process and the mechanical properties of the prototyped steels. A low-carbon hot-rolled steels composed of ferrite and martensite were cold-rolled by 90% reduction, and annealed in a salt bath set at 600°C to 700°C. The final microstructure consisted of sub-micrometer ferrite and fine cementite, and the ferrite grain size changed from 0.5 μ m to 1 μ m by changing the annealing temperature. The difference in flow stress between dynamic and quasi-static deformation of the obtained UFG steel was much larger than that of conventional high strength steels. It was concluded that the UFG steel has high potential of crash energy absorption.

5:45 PM

Enhancement of Fatigue Properties in Ultrafine-Grained Titanium Rods Produced by Means of Severe Plastic Deformation: Irina Semenova¹; Gulnaz Salimgareeva¹; Vladimir Latysh¹; Terry Lowe²; Ruslan Valiev¹; ¹Ufa State Aviation Technical University; ²Los Alamos National Laboratory

Our investigations are focused on the development of pilot technology to fabricate long-length ultrafine-grained (UFG) titanium rods. The technology combines equal channel angular pressing (ECAP) for the formation of UFG structure with additional thermomechanical treatments to further increase strength and produce rods of sufficient length for subsequent automated machining and forging of UFG titanium products. Among the set of properties fundamentally important for these products is fatigue resistance. This work summarizes experimental measurements of the fatigue properties of long-length rods of Grade 4 titanium. Fatigue tests were performed on smooth and notched samples. The formation of homogeneous UFG structures in commercial purity Grade 4 titanium rods is shown to enhance high cycle fatigue strength by 50%, exceeding the fatigue strength of Ti-6Al-4V. Additional experiments were conducted to evaluate how low-temperature annealing can further increase fatigue and other properties of UFG titanium.

6:00 PM

Influence of Iron Oxide Particles on the Strength of Ball-Milled Iron: Donald Lesuer¹; Chol Syn¹; Oleg Sherby²; ¹Lawrence Livermore National Laboratory; ²Stanford University

Detailed microstructural and mechanical property studies of ball-milled iron, in the powder and consolidated states, are reviewed and assessed. The analyses cover three and one-half orders of magnitude in grain size (from 6 nm to 20 μ m)

and focus on the influence of oxide particles on the strength. The study includes the early work of Jang and Koch, Kimura and Takaki and continues with the more recent work of Umemoto et al. and Belyakov, Sakai et al. It is shown that the major contributors to strength are the nano-oxide particles. These particles are created by adiabatic shear banding during ball-milling leading to a bimodal distribution of particles. The predicted strength from particles, σ_p , is given by $\sigma_p = B \cdot (D)^{-1/2}$ where D is the surface-to-surface interparticle spacing, and $B = 395 \text{ MPa} \cdot \mu\text{m}^{1/2}$. A model is proposed that accounts for the influence of the bimodal particle size distribution on strength.

PRELIMINARY

TUESDAY
P M

2008 Nanomaterials: Fabrication, Properties, and Applications: Random Topics

Sponsored by: The Minerals, Metals and Materials Society, TMS Electronic, Magnetic, and Photonic Materials Division, TMS: Nanomaterials Committee

Program Organizers: Seong Jin Koh, University of Texas; Wonbong Choi, Florida International University; Donna Senft, US Air Force; Ganapathiraman Ramanath, Rensselaer Polytechnic Institute; Seung Kang, Qualcomm Inc

Wednesday AM

Room: 274

March 12, 2008

Location: Ernest Morial Convention Center

Session Chair: To Be Announced

8:30 AM Invited

Optical Assembly of Nanomaterials: *Paul Braun*¹; ¹University of Illinois at Urbana-Champaign

The assembly of nanomaterials into higher order functional structures has remained a challenge, even as routes for the synthesis and chemical functionalization of nanomaterials has exploded. As a potential solution, we believe optically directed assembly may prove to be a powerful route for the assembly of nanomaterials into higher order complex and functional structures. Through optical holography, we have assembled semiconductor quantum dots and various ceramic nanoparticles into predefined 2 and 3 dimensional patterns within polymeric and multifunctional hosts. Also through optical holography, we have formed three-dimensionally patterned polymers and oxides. In both these systems, the resolution and 3-D control of structure obtained far surpassed that obtainable through conventional lithographic routes. In a related project, we have utilized laser tweezers to manipulate and assemble ZnS and Au nanoparticles inside of a self-assembled photonic crystal, giving us the ability to controllably place individual defect states within an ordered photonic lattice.

9:00 AM

Alkaline-Earth Metal Hexaboride One-Dimensional (1D) Nanostructures: Synthesis and Characterization: *Syed Amin*¹; *Shu-you Li*²; *John Roth*³; *Terry Xu*¹; ¹University of North Carolina, Charlotte; ²Northwestern University; ³University of Illinois, Chicago

In this presentation, we report our recent progress on synthesis and characterization of alkaline-earth metal hexaboride (MB₆, M=Sr, Ba) 1D nanostructures. The MB₆ 1D nanostructures are appealing candidates for applications such as thermoelectric energy conversion, nanocomposites and nanoelectronics. Catalyst-assisted growth of MB₆ 1D nanostructures was achieved by pyrolysis of diborane (B₂H₆) over alkaline-earth metal oxide (MO) or alkaline-earth metal carbonate (MCO₃) powders at elevated temperature (~890-960°C) and low pressure (~165 mTorr). Nickel, gold and palladium are effective catalytic materials. The as-synthesized MB₆ 1D nanostructures were characterized by scanning electron microscopy, transmission electron microscopy, and Raman spectroscopy. Results show that the MB₆ nanostructures are single crystalline with preferred growth direction along [001]. The MB₆ nanostructures are several tens of nanometer in diameter and up to ten micrometer in length. The growth of these nanostructures involved the vapor-solid growth mechanism. Thermal stability of MB₆ 1D nanostructures has also been studied.

9:15 AM

Synthesis of 1-D Nanostructures of Trititanate Thin Films on a Titanium Metal Flake: *Sun-Jae Kim*¹; *Yupeng Guo*¹; *Nam-Hee Lee*¹; *Hyo-Jin Oh*¹; *Chor-Rong Yoon*¹; ¹Sejong University

One-dimensional (1-D) layered trititanate nanotubes, nanoribbons films and self-assembled spherical aggregates were prepared by hydrothermal reacting Ti metal flake with concentrated NaOH solution. A combined TEM, SEM and XRD investigation of the reaction products as the functions of reaction temperature, duration, concentration of NaOH solution and post treatment conditions revealed that the 20-50 nm wide and ca. 1µm long nanoribbons with a 5 mol dm⁻³ NaOH aqueous solution at 140°C for 12 h. The 6-8 nm wide and several hundreds nanometer long nanotubes are prepared by using 10 mol dm⁻³ NaOH. Titanate sheets growth, split and roll-up model for the formation of 1-D titanate thin films was proposed.

9:30 AM

Wet Chemical Synthesis of Highly Aligned ZnO Nanowires with Optical Properties: *Jean-Claude Tedenac*¹; *Mezy Aude*¹; *Ravot Didier*¹; *Tichit Didier*¹; *Gerardin Corinne*¹; ¹Institut Gerhardt Universite de Montpellier 2

ZnO nanowires have a great commercial stake, due to their physical and chemical properties. Many methods have been employed for the growth of ZnO nanomaterials (sputtering, chemical vapour deposition, molecular beam epitaxy, metal-organic chemical vapour deposition) which greatly improve the crystalline quality. However, low cost and simplicity of the synthesis processes are required for commercial applications. The wet chemical synthesis route seems to meet these requirements, enabling the preparation of high crystal quality and proper growth orientation of ZnO nanowires. Nevertheless, control of the ZnO size, morphology, dimensionality, and self-assembly remains a very important stake, due to their tight influence on ZnO properties. Efficient control of both nanostructure dimensionality and assembly is obtained by using appropriate synthesis parameters during the seeded growth process. The synthesis of well aligned nanowires with a perpendicularly growth to the substrate and a high crystal quality is useful for the study of their physical properties.

9:45 AM

Characterization of Electrodeposited Nanocrystalline Al-Mg Powders: *Fereshteh Ebrahimi*¹; *Mahesh Tanniru*¹; *Sankara Sarma Tatiparti*¹; ¹University of Florida

Nanocrystalline aluminum-magnesium alloys were fabricated in the powder form using electrodeposition technique. The electrolyte was organometallic based and the synthesis was conducted in low oxygen argon atmosphere. XRD profiles showed that these powders consist of supersaturated fcc-Al(+Mg) and hcp-Mg(+Al) phases. Compositional analysis using EPMA revealed that the fcc phase can accommodate up to 20at%Mg, however the hcp phase may dissolve as high as 40at% of Al. SEM observations indicated that the hcp-Mg phase develops over the supersaturated fcc-Al phase. TEM studies showed that both phases consist of nanocrystalline grains. These powders were developed for hydrogen storage applications. Selected powders were hydrogenated at various temperatures and high pressures. In this presentation the results of characterization before and after hydrogenation will be presented. The financial support by NSF through grant DMR-0605406 is gratefully appreciated.

10:00 AM

Influence of Processing Mode on the Nanostructure Development of Flux Melted Ag-40at%Cu Alloy: *D Aujala*¹; *C. Davyl*¹; *P. Kalu*¹; *K. Han*²; *T. Shen*³; *D. Alexander*³; *R. Schwarz*³; ¹Florida Agricultural and Mechanical University-Florida State University-College of Engineering; ²National High Magnetic Field Laboratory; ³Los Alamos National Laboratory

The need to generate higher magnetic field has led to renewed research into the development of high strength conductor materials. This paper presents a comparison of the microstructure, texture and strength in Ag-40at%Cu alloy fabricated by two methods: drawing and cold rolling. The AgCu alloy was initially produced by flux melting technique and cast into 25.4 mm rods, and then severely deformed by either method to a true strain of 4.6. Several techniques including scanning electron microscopy, X-ray diffractometry and Nanoindentation were utilized in analyzing the material. It was found that both processing method produced nano-composites with alternating Ag and Cu laminates on the order of 60 to 200nm in thickness. A correlation was made between the microstructure and strength of the material. The general effect of processing mode on the mechanical properties of the material is discussed.

10:15 AM

Sonochemical Synthesis of Nanostructured Anatase and Study of the Kinetics among Phase Transformation and Coarsening as a Function of Heat Treatment Conditions: *Leonardo Gonzalez-Reyes*¹; *Isaias Hernández-Pérez*²; *Francisco Robles Hernandez*²; *Hector Dorantes Rosales*¹; *Elsa Arce Estrada*¹; ¹Instituto Politécnico Nacional; ²Universidad Autónoma Metropolitana; ³Transportation Technology Center, Inc.

The present paper shows that nanostructured anatase can be produced by sonochemical synthesis with an average particle size of 6.4nm and a specific surface area of 300m²g⁻¹. The results of microstructure coarsening evolution as well as phase transformation of nanometric anatase to rutile subjected to different heat treatment conditions are presented. The rates of transformation

from anatase to rutile, critical particle size of transformation anatase to rutile and coarsening are directly related to heat treatment temperature, which in turns allows developing a mathematical model to predict particle size evolution. The developed model can be used to precisely predict particle size for anatase and/or rutile using exponential like equations similar to those described in the LSW theory. The exponent of the LSW-like equations went from $\sim 1/8$ to $\sim 1/4$ as heat treatment times increase from 8 and 72 h respectively. This research was supported by means of BET, TGA, XRD and TEM.

10:30 AM

Initial Grain Growth Behavior during Sintering of Nanosized Powders:

Hongtao Wang¹; Zhigang Fang¹; ¹University of Utah

It is well known that rapid grain growth occurs in the final stage of the sintering of coarse powders. However, in the case of nanosized powder, notable grain growth has taken place during initial and intermediate stage of sintering, leading to loss of nano-structure. So it is critical for nanosintering to control initial grain growth in order to get full densification with final grain size on nanoscale. This paper is trying to understand enhanced grain growth behaviour during initial stage of sintering of nanosized powders from experiments observation to theoretical analysis by considering the unique issues of nanostructure such as high ratio of surface/interface area, non-equilibrium defects (vacancies, dislocations). The results show that the enhanced grain growth is related to recovery process during relaxation of excess energy in nanostructured materials.

10:45 AM Break

11:00 AM Invited

Magnetic Nanomaterials for Energy Efficient Systems: Raju Ramanujan¹:

¹Nanyang Technological University

Nanostructured magnetic materials are being intensively studied for novel energy efficient systems. Giant energy product magnets, high temperature magnetocaloric nanomaterials and high permeability soft magnetic nanomaterials for innovative permanent magnet MRI systems, solid state cooling and low loss transformer systems, respectively, are focus areas of our work. Exchange coupling at the nanoscale can be used as a common guiding principle to improve the magnetic properties; efficient coupling requires optimum microstructural control. Hence, mechanisms of nanocrystallization were studied for melt spun ribbons and powders using DSC, XRD, CTEM, EDX, VSM and in situ TEM techniques. Synergistic compositional changes at the crystal:matrix interface were found to play a key role in determining the crystal morphology, crystal size and nucleation density. Microstructural control, and associated change of magnetic properties, of specific magnetocaloric materials, nanocomposites with high energy product and high permeability magnets based on FeCo-B, Fe-Ni-Mo-B and Fe-Si-B-Nb-Cu alloy systems will be described.

11:30 AM

Co-Rich Nanocrystalline Soft Magnetic Ribbons with Improved Mechanical Strength: Maria Daniil¹; Todd Heil¹; Matthew Willard¹; ¹Naval Research Laboratory

Co-rich nanocrystalline have great technological interest due to their excellent response at high frequency magnetic fields and high temperature magnetic behavior. In this work we examine the crystallization behavior, crystal structure and mechanical properties of $(\text{Co,Fe,Ni})_{88}\text{Zr}_7\text{B}_4\text{Cu}_1$ and $(\text{Co}_{0.95}\text{Fe}_{0.05})_{88}\text{Zr}_6\text{M}_1\text{B}_4\text{Cu}_1$ ($M = \text{Zr, Nb, Hf and Ta}$) nanocrystalline ribbons. According to the X-ray diffraction measurements, the amorphous as-spun ribbons crystallize partially into a very fine mixture of FCC and BCC phases (7-8 nm) at low temperature, whereas at higher temperature it transforms into coarser FCC (20-28 nm) and $\text{Co}_{23}\text{Zr}_6$ grains. The lattice size of the BCC phase is $\sim 2.828 \text{ \AA}$, which is larger than the bulk (Fe,Co)-BCC phase. Bend test experiments showed a significant improvement of the fracture strength in samples with the highest Co content (83.6 at.%), whereas M substitutions for Zr add an extra small improvement. These results will be discussed in correlation with the fracture surface microstructure.

11:45 AM

Magnetic Properties of FePt: A Comparison between Nanodots and Continuous Thin Film: Gopinath Trichy¹; Jagdish Narayan¹; ¹North Carolina State University

We report on the synthesis and magnetic properties of L10 ordered FePt nanodots using pulsed laser deposition (PLD). Size reduction to nanoregime in

magnetic systems can lead to favorable changes in coercivity, remanence and domain reversal mechanisms. For an off-stoichiometric Fe₄₁Pt₅₉ system, we have shown that individual nanodots have higher coercivity (3200 Oe) when compared to a continuous thin film (2250 Oe). Improved coercivity for the nanodot system was attributed to the transition to single domain state. Another unique feature of this study is the integration of the FePt nanodots with Si (100). Remarkably, we achieved FePt growth along the magnetically hard c-axis using epitaxial TiN as a template buffer. Cross section and plan view TEM analysis showed that the FePt nanodots have an average size = 20 nm and thickness = 5nm. The magnetic storage density of such a system can potentially exceed 1 Tbit/inch².

12:00 PM

Atomic-Scale Segregation and Fluctuations in FePt Thin Films: Karen

Torres¹; Sundar Naga²; Jennifer Thompson²; Richard Martens¹; Gregory Thompson¹; ¹University of Alabama; ²West Virginia State University

A series of atom probe and transmission electron microscopy studies have been performed to investigate how compositional fluctuations in FePt contribute in the A1 to L1₀ phase transformation and grain coarsening. Fe₅₀Pt₅₀ and (Fe,Cu)₅₀Pt₅₀ thin films have been sputter-deposited onto Si substrates. The addition of Cu lowers the ordering temperature but also accelerates the grain growth in films during the phase transformation. Atom probe specimens were analyzed in an Imago Local Electrode Atom Probe (LEAP). The atom probe reconstruction showed small levels of Pt segregation and clustering at grain boundaries in the as-deposited films. These results provide experimental verification of modeling predictions that Pt will segregate to free surfaces in FePt to lower the total free energy of the system. The effect of different times and temperatures on segregation, ordering and grain morphology will be addressed.

12:15 PM

Millisecond Regime Flash Annealing of FePt Thin Films: Amanda Cole¹;

Ron Ott²; Timothy Klemmer³; Chandan Srivastava¹; James Harrell¹; Gregory Thompson¹; ¹University of Alabama; ²Oak Ridge National Laboratory; ³Seagate Technology

A pulsed-thermal-processing technique using a high density infrared plasma arc lamp with a radiant spectrum of 0.2 to 1.4 μm was used to facilitate the A1 to L1₀ phase transformation in FePt. The 20 nm and 100 nm films were annealed using single and multiple 100 or 250 ms pulse widths. XRD, TEM and AGM characterization confirmed that the time-temperature exposures studied were able to achieve L1₀ ordering. TEM micrographs confirmed that the mean grain size grew slightly with increasing time or temperature but was within the standard deviation of the as-deposited grain size. At lower annealing temperatures, a shoulder to the A1 {111} XRD peak was observed and indexed as L1₀, consistent with the nucleation of the L1₀ phase as a first-order phase transformation. At elevated temperatures, the L1₀ shoulder was not prevalent but the {111} peak qualitatively narrowed, consistent with the growth of the L1₀ phase.

12:30 PM

Hydrogen Uptake Properties of Nickel Doped Titanate Nanotubes: Nam-

Hee Lee¹; Hyo-Jin Oh¹; Yeong-Ung Yun¹; Yupeng Guo¹; Kyung-Sub Lee²; Sang-Chul Jung³; Sun-Jae Kim¹; ¹Sejong University; ²Hanyang University; ³Sunchon National University

Ni doped titanate nanotubes were hydrothermally synthesized using titania (TiO₂) nanoparticles with rutile phase as a starting material in 10M NaOH aqueous solution with NiCl₂. It was fully characterized by various techniques, including SEM, TEM, ICP, FT-IR, BET, and P-C-T test that conversions from nanoparticles to nanotubes were achieved at various temperatures and times for hydrothermal reaction. The Ni doped TNTs were found to be a multi-walled layered structure with an average outer diameter of $\sim 10 \text{ nm}$, an inner diameter $2 \sim 4 \text{ nm}$ and $\sim 0.75 \text{ nm}$ interlayer distance under optimized conditions. The hydrogen uptake amount of the Ni doped TNTs was shown more than 2.0 wt% into many mesoporous adsorption sites of interlayers and interiors of nanotube at room temperature under 20 atm.

WEDNESDAY AM

12:45 PM

Preparation of Hexagonal Barium Ferrite Nanoparticles by Carbon Combustion Synthesis: Karen Martirosyan¹; Long Chang²; Dan Luss¹; Dmitri Litvinov³; ¹University of Houston, Department of Chemical and Biomolecular Engineering; ²University of Houston, Department of Electrical and Computer Engineering; ³University of Houston, Department of Electrical and Computer Engineering, Department of Chemical and Biomolecular Engineering

We used high efficient carbon combustion synthesis method to produce well crystalline hexagonal barium ferrite nanoparticles (50-100nm). In this method exothermic oxidation of carbon nanoparticles ~5nm with surface area 80m²/g generates a thermal reaction wave with temperature of up to 1000C that propagates through the solid reactants (oxides and/or carbonates) mixture converting it to the desired complex oxide product. The carbon is not incorporated in the product and is emitted as a gas CO₂ from the sample. A stable self-propagating reaction front can be obtained only at carbon concentrations exceeding 6.5wt.%. A complete conversion to hexagonal structure was obtained only for carbon concentration exceeding 11wt.%. Solid-state interactions between the components and the nucleation of the nanoparticles started in the early period of combustion and continued in the post combustion zone. The magnetic properties H_c~2800Oe and M_s~80emu/g of the compact sintered ferrites compared well with those produced by other synthesis methods.

3-Dimensional Materials Science: Modeling and Characterization across Length Scales II

Sponsored by: The Minerals, Metals and Materials Society, TMS Structural Materials Division, TMS: Advanced Characterization, Testing, and Simulation Committee
Program Organizers: Michael Uchic, US Air Force; Eric Taleff, University of Texas; Alexis Lewis, Naval Research Laboratory; Jeff Simmons, US Air Force; Marc DeGraef, Carnegie Mellon University

Wednesday AM
March 12, 2008

Room: 286
Location: Ernest Morial Convention Center

Session Chairs: Mike Groeber, Ohio State University; Martin Glicksman, University of Florida

8:30 AM

Finite Element Modeling of the Deformation of 3D Polycrystals Including the Effect of Grain Size Distribution: Wei Li¹; Nicholas Zabaras¹; ¹Cornell University

A finite element analysis of the large deformation of 3D polycrystals is presented using pixel-based elements as well as elements conforming with grain boundaries. The macroscopic response is obtained through volume-averaging laws using a recently developed homogenization model. A constitutive framework for thermo-elastic-viscoplastic response of single crystals is utilized along with a fully-implicit Lagrangian finite element algorithm for modeling microstructure evolution. The effect of grain size distribution is included by considering a physically motivated measure of lattice incompatibility which provides an updated shearing resistance within grains. A domain decomposition approach is adopted for parallel computation to allow efficient large scale simulations. The computed mechanical properties of polycrystals are shown to be consistent with experimental results for different grain size distributions.

8:50 AM

Measuring the Evolution of the Crystal Scale Stress State in Polycrystalline Copper during Cyclic Loading: Jun-Sang Park¹; Matthew Miller¹; Alexander Kazimirov¹; ¹Cornell University

The micromechanical response of polycrystalline materials under cyclic loading is not well understood. Due to complicated microstructure and anisotropic single crystal mechanical properties the stress state of the crystals in the polycrystalline material can be significantly different from that imposed on the polycrystalline aggregate. In our study, cyclic loading was applied on recrystallized copper specimens. The loading was paused to perform high energy x-ray diffraction (XRD). Using XRD, the lattice strains and their evolution with respect to specimen life for many crystallographic planes of the crystals in the

aggregate were measured. The lattice strain measurements were then used to compute the lattice strain distribution function (LSDF) which is the elastic strain tensor field over crystallographic orientation space. Using the LSDF and anisotropic elasticity, the crystal stress distribution over orientation space was computed and its evolution was monitored at different points in specimen life.

9:10 AM

Realistic Microstructure Based 3D Indentation Modeling of Heterogeneous Materials: Arun Sreeranganathan¹; Arun Gokhale¹; ¹Georgia Institute of Technology

Instrumented indentation, which provides a continuous record of the indentation load P as a function of the depth of penetration h of the indenter into the material, is a widely used technique to study the mechanical behavior of small microstructural volumes. Indentation modeling of heterogeneous materials such as particulate reinforced composites is of interest so as to study the effect of the second phase particles on the indentation response of the material. In this contribution, we incorporate realistic 3D microstructures of particulate reinforced metal matrix composites, reconstructed from serial sectioning data, in finite element based simulations of microindentation. Effect of microstructural parameters such as the reinforcement volume fraction, spatial distribution etc. on the indentation response will be reported.

9:30 AM

3D Evolution of Precipitates in Binary Aluminum-Lithium: Martin Glicksman¹; Ben Pletcher¹; James Lebeau²; ¹University of Florida; ²University of California, at Santa Barbara

Phase coarsening in overaged Al-Li alloys is a diffusion-controlled process. Large particles grow by dissolution and mass transfer from smaller particles. Eight binary Al-Li alloys were aged for times between 3-240 h, to yield various distributions of δ' (Al₃Li) precipitates. Transmission electron microscopy was used to image 10-100 nm diameter, spherical δ' precipitates via centered dark-field techniques. TEM images were then autonomously analyzed using a novel Matlab[®] function to process and provide good statistical 3D results. Computer analysis provides objective characterization and fast image processing, allowing practical access to larger sample sizes. Results, including the particle size distribution and maximum particle size, agree with predictions from diffusion screening theory.

9:50 AM Break

10:10 AM

3D Microstructural Theories and 3D Experimental Techniques: Martin Glicksman¹; Paulo Rios²; ¹University of Florida; ²Universidade Federal Fluminense

Traditionally, materials scientists developed microstructure theories that relied on experimental quantities measured from planar sections. With the advent of 3D simulation of microstructures, and some recent advances in 3D characterization, this situation changed dramatically. Specifically, it is now possible, and desirable, to test microstructure theories with 3D data. Two theories will be examined along with the measurements required to test them. First, a proposed extension is presented of Johnson-Mehl, Avrami, Kolmogorov theory to situations where phase nuclei are not randomly located. This theory requires measurement of the Gaussian curvature of the interfaces, which may be extracted from the 3D microstructure. Second, a recent treatment of grain growth kinetics is presented in terms of its metrical and topological properties. In this case, measured quantities include the distribution of grain volumes and/or the distribution of the number of faces per grain. Again, these require microstructural measurements are only available via 3D characterization.

10:30 AM

Flow in Mushy Zones Using 3D Measurements of Microstructure: Dongchoul Kim¹; Roberto Mendoza²; Peter Voorhees³; Katsuyo Thornton²; ¹Sogang University; ²University of Michigan; ³Northwestern University

Dendritic microstructures that form during solidification modify fluid flow in a complex manner. While there have been investigations relating the solid volume fraction and other microstructural characteristics to permeability, a fundamental understanding of fluid flow in complex microstructures has not been fully developed. Using experimentally obtained three-dimensional reconstructions of microstructures, we determine the steady-state flow field

using the Navier-Stokes equation and the permeability using Darcy's law. The calculated values of permeability are compared to those predicted by previous investigations. This approach provides a method for assessing the empirically and theoretically obtained permeabilities and the limits of their applicability in realistic solidification microstructures.

10:50 AM

Porosity Distribution and Effective Elastic Modulus in ZrN as a Surrogate for PuN: Comparisons between 2-D and 3-D Measurements and Models: Manuel Parra Garcia¹; Sung-Ho Park²; Kirk Wheeler¹; Pedro Peralta¹; Ken McClellan³; ¹Arizona State University; ²Gyeongsang National University; ³Los Alamos National Laboratory

A serial sectioning process was used to develop a three-dimensional (3D) representation of the microstructure of a ZrN dense pellet sintered in Argon at 1600°C. Twenty five two-dimensional (2D) images of the microstructure obtained by imaging with an optical microscope at 200X (slides spaced 2µm apart from each other) were used as a basis for reconstructing the 3D microstructure of the ceramic for modeling using Finite Elements (FE). This representation allows the quantification of the spatial distribution of porosity in the samples as well as the creation of a three-dimensional finite-element model (FEM) that accounts for the presence of pores. The porosity distribution, Young's modulus and stress-strain behavior of the reconstructed volume were predicted from the 3D model of the microstructure and correlations with existing two-dimensional (2D) models and experimental results obtained at Los Alamos National Laboratory (LANL) are discussed. Work supported under DOE/NE Agreement # DE-FC07-05ID14654.

11:10 AM

Self-Assembly of Three-Dimensional Composite Materials with Multifunctionality: Hsun-Yi Chen¹; Yongwoo Kwon²; Peter Voorhees²; Katsuyo Thornton¹; ¹University of Michigan; ²Northwestern University

Multifunctional materials are of increasing interest because they facilitate the design of compact systems able to perform a variety of tasks. Composite materials are inherently suited for multifunctionality since desired properties can be achieved by hybridizing different materials. In recent research, microstructures having minimal-surface morphologies have been found to optimize simultaneous transport under certain symmetrical constraints. However, fabrication of microstructures with minimal-surface morphologies is challenging, often requiring special materials processing techniques. We find that bicontinuous structures resulting from coarsening after phase separation possess transport properties similar to those with minimal-surface morphologies. Our finding demonstrates that spinodal decomposition and other phase-separation processes may provide a plausible route to inexpensive self-assembly of three-dimensional two-phase composites with highly optimized multifunctionality.

11:30 AM

Three-Dimensional (3D) Visualization of Porosity in High Performance Sintered Steels: Jason Williams¹; Casey McClimon¹; Nikhilesh Chawla¹; ¹Arizona State University

Sintered steels are becoming attractive in replacing wrought alloys in many applications, particularly in the automotive industry, due to their low cost, high performance, and near-net shape manufacturing. Porosity in these materials controls mechanical behavior. In this talk we report on 3D visualization of porosity using a serial sectioning technique. The model revealed extensive interconnectivity among the pores, which was not readily apparent in two dimensions. Finite element modeling was conducted to elucidate the effect of 3D porosity on the local stress state in the material. The influence of the 3D porous structure on the micro- and macroscopic behavior of the steel will be discussed.

Alumina and Bauxite: Additives

Sponsored by: The Minerals, Metals and Materials Society, TMS Light Metals Division, TMS: Aluminum Committee

Program Organizers: Sringeri Chandrashekar, Rio Tinto Aluminium Limited; Peter McIntosh, Australus Management Services

Wednesday AM

Room: 296

March 12, 2008

Location: Ernest Morial Convention Center

Session Chair: Songqing Gu, Chalco

8:30 AM Introductory Comments

8:35 AM

New Crystal Growth Modifiers for Bayer Process: Dimitri Kouznetsov¹; Jianjun Liu¹; Kevin O'Brien¹; James Counter²; John Kildea²; ¹Nalco Company; ²Nalco Australia

In Bayer process, Crystal Growth Modifiers (CGM) help to increase alumina trihydrate yield and improve quality. Recent work aimed at mechanistic issues has led to the development of a second generation of CGM. Traditional, first generation products were well known to impact three critical process areas, trihydrate particle sizing, oxalate stability, and oxalate morphology. While some plants utilize all three properties to enhance and control trihydrate precipitation, it has long been recognized that all three properties are not always desirable and that products with a more selective impact could provide even greater benefits. The development of the second-generation CGM product range has focused not only on developing products that are more effective, but also products that are more selective in their properties. Results on a range of new formulations are presented.

9:00 AM

The Effect of DSP Structure on Impurities Removal from Refinery Liquors and Efficiency of Alkali Recovery: Andrey Panov¹; Alexander Suss¹; Anatoliy Lapin¹; Natalia Kuznetsova¹; Alyona Kuvyrkina¹; ¹Russian National Aluminium-Magnesium Institute

The influence of temperature and sulpho-, carbo-, chlorid ions containing in alumina refinery liquors on formation of different modifications of sodium hydroaluminosilicate (desilication products - DSP) obtained as a result of bauxite digestion was investigated. To solve the problem of impurity anions removal from recycled liquors the relation between adsorptive properties of DSP and conditions of its formation was examined. The effect of DSP structure and composition was studied in terms of alkali recoverability in the course of red mud treatment with lime. The possibility was shown of recovery up to 96% of alkali.

9:25 AM

Performance Appraisal of Evaporation System with Scale Inhibitor Application in Alunorte Plant: Ayana Oliveira¹; Juarez Moraes¹; Jefferson Batista¹; Jorge Lima¹; Ricardo Diniz²; Emiliano Repetto²; ¹Alunorte; ²Cytec Do Brasil Ltd.

Any alumina refinery plant has problems with sodalite scaling in heater exchange and pipes that promote a reducing in the life time of the evaporation train and other losses. Alunorte in conjunction with Cytec Industries Inc., has performed a plant trial with a bayer process scale inhibitor like a alternative action to reduce these losses in the process. This paper reports the plant trial results where the scale inhibitor achieved significant results like: increase the life time of the evaporation train, stability of the heater transfer coefficient, increase the availability of the evaporation and the condensate rate, improving on the operational maintenance safety. Additional benefits of this new polymer are currently under investigation.

9:50 AM

Cost Savings by Improved Filtration and Washing of Al-Hydrate Product: Juergen Hahn¹; Reinhard Bott¹; Thomas Langeloh¹; ¹Bokela GmbH

A new generation of pan filters enables filtering and washing of Al-Hydrate product with improved capacity, reduced maintenance and operation cost. Modern pan filters have many innovative features like the Forced Feeding

System, fast flow cells or the effective heel re-slurry system. The even filter cake and the excellent hydraulic improve cake washing and reduce wash water consumption by 25% which leads to significant evaporation cost saving. Steam can be used to improve cake washing and reduce cake moisture. The effective heel re-slurry system increases cycle times between filter cleaning and improves cloth lifetime. Thus, energy and operation cost reduce 10-15% compared to conventional pan filters. Another promising option enabled by the new filter technology is to replace the first washing step on pan filters by more compact and more efficient disc filters and re-slurrying the filter cake with wash filtrate from the pan filter.

10:15 AM Break

10:30 AM

Autoprecipitation Control with HXPAM Technology: *Qi Dai*¹; Scott Moffatt¹; Morris Lewellyn¹; ¹Cytec Industries Inc

Autoprecipitation poses serious problems to alumina refineries, such as more raw material consumption, alumina loss, scaling of equipment, unstable process, lower liquor productivity, etc. Cytec's SUPERFLOC HX® has been used as a main settler flocculant for over 1½ decades. It is known that the HX flocculant reduces autoprecipitation and settler scale in the presence of red mud solids. In fact, all hydroxamic acid-containing polymers of varying molecular weights can reduce gibbsite autoprecipitation. One particular product, SUPERFLOC HX-800, shows enhanced performance in reducing auto-precipitation in both settlers and washers. This paper presents laboratory results of HXPAM as an autoprecipitation inhibitor.

10:55 AM

Descalent and Corrosion Prevention Chemical for Korba Alumina Refinery: *P.K.N. Raghavan*¹; ¹Bharat Aluminium Company Ltd., (A Unit of Vedanta Resources Plc.)

During Alumina production by the Bayer Process, the bohemite bauxite ores are dissolved with Caustic Soda at elevated temperatures to extract the Alumina Hydrate. Most of the liquor Silica content recrystallizes out as part of the Red Mud while the remainder is retained in the supersaturated Sodium-aluminate solution used for hydrate precipitation. Subsequent to hydrate precipitation, the Spent Liquor is recycled via a series of Heat Exchangers for reheating and use in further bauxite digestion. Consequently, Spent Liquor heating in Heat Exchangers readily promotes scaling. Sodiumaluminosilicate scale formation in Heat Exchangers leads to serious tube-side fouling with a significant reduction in heat transfer efficiency and liquor throughput, resulting in increased energy and Caustic Soda consumption, higher labour demand, costly cleaning programme and loss of productivity. The Scales formed in the metal surface of Alumina Refinery, are generally removed by acid cleaning which is time consuming and causes acid corrosion.

11:20 AM

Application and Performance Characteristics of Superfloc® TF-8000 a New HX Based Hydrate Flocculant: Franklyn Ballentine¹; Scott Moffatt¹; Pat Clement²; ¹Cytec Industries Inc.; ²Ormet Alumina Company

HXPAM's emulsions have been shown to be very effective in improving overflow clarity and underflow flowability in tertiary trays, however the need for specialized equipment to invert the emulsions coupled with the need for high dilution in most applications has previously made them less convenient to use. Superfloc® TF-8000 is a HX based polymer designed for application in tertiary trays. It can be applied neat or pre-diluted with spent liquor. Application of Superfloc® TF-8000 in secondary trays has also been very successful because of its ability to significantly improve the flowability of the hydrate. This has expanded the possibility for application in other hydrate handling areas where flowability is a concern. This paper provides laboratory data comparing the performance of Superfloc® TF-8000 to dextran as well as other HX polymers. The paper also summarizes the results obtained when applied to the secondary trays for several months at Ormet.

Aluminum Alloys: Fabrication, Characterization and Applications: Corrosion and Protection

Sponsored by: The Minerals, Metals and Materials Society, TMS Light Metals Division, TMS: Aluminum Committee

Program Organizers: Subodh Das, Secat Inc; Weimin Yin, Secat Inc

Wednesday AM

March 12, 2008

Room: 293

Location: Ernest Morial Convention Center

Session Chairs: Subodh Das, Secat Inc; Weimin Yin, Secat Inc; Yansheng Liu, Secat Inc

8:30 AM

Naval Structural Aluminum Alloy Research: *Catherine Wong*¹; ¹Naval Surface Warfare Center

Recent focus on light-weight, high-speed naval ships has caused the Navy to re-evaluate aluminum as a structural material. Aluminum alloys generally offer good strength-to-weight ratio and corrosion resistance, which are both important properties in Navy ships. Light weight ships offer both higher speed and increased payload capacity, expanding mission capabilities. Although aluminum has been widely used in Navy patrol craft, small ship hulls, deckhouses, hydrofoils, and many other applications it has not been without problems. These problems resulted in the initiation of several programs which focus on understanding and coping with the four key aluminum material issues: reduced as-welded strength, low corrosion-fatigue strength in unpainted structures, in-service sensitization, and strength reduction during fires. This paper will present an overview of these programs.

8:50 AM

Effect of Grain Size and Substructure on Sensitization in 5083 Al Alloys: *Kinga Unocic*¹; Michael Mills¹; Glenn Daehn¹; Paul Kobe²; ¹Ohio State University; ²Alcan Rolled Products

This study focuses on the effects of microstructure on the intergranular corrosion (IGC) resistance of modified 5083 aluminum alloys. Previous research has shown that small additions of Cu and Zn to AA5083 can improve the resistance to IGC. Our present research shows that the same Cu and Zn modified composition can become susceptible to IGC following sensitization if the microstructure is altered. To demonstrate this effect, the material was heavily rolled then subjected to various sensitization heat treatments. For example, following a sensitization treatment at 150°C for 20hrs the heavily worked microstructure was virtually resistant to IGC. When compared to a sample that was given a short heat treatment in order to alter the heavily deformed microstructure, followed by the same sensitization heat treatment, resulted in IGC. Mg-rich grain boundary phases were identified through TEM characterization methods and were linked to the decreasing resistance to IGC.

9:10 AM

The Effect of Grain Boundary Character on the Intergranular Corrosion Susceptibility of 2124 Aluminum Alloy: *Lisa Chan*¹; Anthony Rollett¹; Gregory Rohrer¹; Hasso Weiland²; Soonwuk Cheong²; ¹Carnegie Mellon University; ²Alcoa Inc.

The objective of the research is to find a correlation between grain boundary character and intergranular corrosion in a 2124 aluminum alloy. In the present study, the alloy was subjected to different solutionizing temperatures and corrosion tested with full immersion in a sodium chloride and hydrogen peroxide solution according to ASTM G110 standards. The samples that were heat treated at 40°C above the standard solutionizing temperature of 500°C have shown susceptibility to intergranular corrosion. The grain orientations of the corroded samples were then obtained from automated Electron Back-Scatter Diffraction (EBSD). Preliminary results on the relationship of grain boundary character and intergranular corrosion will be presented.

9:25 AM

Solution and Aging Heat Treatment of a Cast Al-Si Alloy: Sergio Haro Rodriguez¹; Julian Ramirez²; Enrique Martinez²; ¹Universidad Autonoma de Zacatecas; ²Instituto Tecnológico de Zacatecas

In the present paper the influence of solutionizing (504-545°C) and aging (154-200°C) temperatures on microstructure and mechanical properties of the A319 (Al-6.5Si-0.86Fe-2.3Cu) cast aluminum alloy has been reported. The effect of these heat treatment parameters has been investigated with reference to microstructure and mechanical properties. Scanning electron microscopy (SEM) of tensile fractured surfaces was carried out to investigate the influence of solutionizing and aging temperatures on the mode of fracture. Finally, the heat treatment parameters to obtain the better mechanical properties are presented.

9:45 AM

The Corrosion Behaviour of Al-Zn Alloys in Abakaliki and Port Harcourt Rainwater: Ndubuisi Idenyi¹; Israel Owate²; Cajethan Okeke³; ¹Ebonyi State University; ²University of Port Harcourt; ³University of Nigeria

A study has been carried out on the corrosion behaviour of Al-Zn alloys exposed to rainwater sourced from Abakaliki, Ebonyi State, a highly residential urban town and Port Harcourt, Rivers State, a highly industrialized urban town, both in Nigeria. Corrosion test coupons of four (4) differing alloy grades of varying Zn concentrations produced at First Aluminium Plc., Port Harcourt under carefully controlled atmosphere were immersed in beakers containing each of the rainwater separately. The setup was allowed to stand for 30 days with a set withdrawn 5-daily for corrosion rate evaluation using the normal procedures. Results showed that all the alloy grades followed the usual corrosion trends associated with passivating metals, but that samples exposed to Abakaliki rainwater were more severely attacked possibly due to the heavy presence of clouds of carbonate particles in the atmosphere generated from predominant quarrying works in the town which must have made the rainwater somewhat acidic as compared to the possible presence of flared glasses in Port Harcourt resulting from petrochemical refining operations that predominate the town.

10:05 AM

The Corrosion Susceptibility and Electrochemical Impedance Spectroscopy of Al-Cu-Mg-Zr New Aerospace Aluminum Alloy: Sheng Yang¹; Sujuan Yao¹; Danqing Yi¹; Huiqun Liu¹; ¹Central South University, School of Materials Science and Engineering

In order to evaluate the degree and severity of Al-Cu-Mg-Zr alloy in 3.5%NaCl corrosion solution, the pit corrosion susceptibility and electrochemical impedance spectroscopy(EIS)of Al-Cu-mg-Zr alloy with different corrosive grades was studied to analyze the dynamic process of corrosion behavior by TEM and electrochemical. Compared with 2524-T4 aluminum alloy, Al-Cu-Mg-Zr alloy is good in corrosion property, Cu-rich particles are the main influence factor of pitting corrosion behavior. The impedance of EIS is characterized by a high frequency capacitive arc which gives information on the performance of the unattacked surface. At lower frequencies, a diffusion control is apparent suggesting the specific contribution of the surface in which the localized attack takes place. the micro-process and the influent mechanics of interface reaction and the electrode surface condition are studied by EIS and equivalent circuit.

10:20 AM Break

10:30 AM

The Effect of Fe-Rich Intermetallics on Sliding Wear and Mechanical Properties of Piston Alloy: Dheerendra Dwivedi¹; Mohit Dhiman¹; ¹Indian Institute of Technology, Roorkee

During the processing of cast piston alloys, iron frequently enters into the melt as an impurity and causes porosity and needle shaped Al-Fe-Si intermetallics. Literature however didn't reveal many reports on the effect of Fe and its intermetallics on wear behavior piston alloys. Therefore to increase the understanding in this area, an investigation has been undertaken to explore the effect of Fe (0.2 to 2.0) and consequently Fe-rich intermetallics and "Fe correctors" such as Mn in different Fe/Mn ratios. Sliding wear behavior was evaluated on pin-on-disk tribometer in the range of normal loads (1-4kg) at 2.0m/s speed. Metallurgical characterization of alloys were done by using image analyzer, scanning electron microscope (SEM), EDAX and EPMA. Sliding wear behaviour have been discussed in light of microstructure, particularly Fe-rich intermetallics and mechanical properties with and without the presence of "Fe corrector".

10:50 AM

Comparative Analysis of the Corrosion Susceptibility of Al-Zn Alloys in De-Ionized Water, Rainwater and Seawater: Ndubuisi Idenyi¹; C. Okeke²; Israel Owate³; S. Neife⁴; ¹Ebonyi State University; ²University of Nigeria, Nsukka; ³University of Port Harcourt, Choba; ⁴Enugu State University of Science and Technology

A study of the corrosion behaviour of aluminium – zinc alloy systems exposed to de-ionized water, rainwater and seawater has been carried out. Test coupons of four (4) grades of Al alloys with differing weight percentages of Zn were prepared and immersed in baths containing each of the environments separately. They were allowed to stand for a 30-day period with a set withdrawn every 5 days for weight loss measurements and subsequent corrosion rate profile evaluation using standard equations in mm/yr. The results obtained showed that samples exposed to seawater were more susceptible to corrosion and that the degree of severity increased with increased zinc content. This is attributed to the presence of dissolved salts and other complexes in seawater and increased grain boundaries in the alloys as more zinc was added; both conditions that favour corrosion attacks.

11:10 AM

The Effect of Zinc Additions to the Corrosion Rates and Tensile Strengths of Aluminium System: Israel Owate¹; Ephariam Chukwuocha¹; ¹University of Port Harcourt

Zinc oxide concentrations of 0.2778, 0.3012, 0.3821, 0.4942 and 0.5915 wt % were added to a mixture of the composition of an aluminium system. The designed component systems were produced into rectangular flat sheets of aluminium products measuring about 5mm thickness. Standard corrosion tests by weight loss method was applied to the samples under acid and base-media environment for 740 hours. Thereafter, the rates of corrosion, damages caused and tensile strengths were determined. The results obtained indicated progressive increase of corrosion rates from deionized water, base to acid medium. Whereas the tensile strengths decreased in the reverse. In addition, the corrosion rates increased relative to zinc concentrations except sample C which deviated from the trend. Sample C showed high values of tensile strengths and lower corrosion rates when compared to other specimens. This initial result presupposes that controlled zinc additions could be applied to achieving lower corrosiveness.

11:30 AM

The Role of Segregation in the Eutectic Modification of Hypoeutectic Al-Si Alloys: Kazuhiro Nogita¹; Masato Yoshiya²; Hideyuki Yasuda²; Arne Dahle¹; ¹University of Queensland; ²Osaka University

Modification of the eutectic silicon in hypoeutectic Al-Si alloys, which causes a structural transformation of the silicon phase from a needle-like to a fine fibrous morphology, is carried out extensively in industry to improve mechanical properties. It is known that the fibrous silicon phase in chemically modified alloys is heavily twinned. This impurity induced twinning has been explained by a twin plane re-entrant edge (TPRE) model. However, there are still some questions and contradictions that remain. In this paper, we discuss the mechanism of impurity induced twinning and modification in light of experimental data obtained by electron microscopy and synchrotron radiation, as well as predictions by first-principles calculations.

11:50 AM

The Effect of Chromium on Aluminum Base Alloy: Hua Shen¹; Guangchun Yao¹; Weidong Yang²; ¹Northeastern University; ²Shengyang Institute of Chemical Technology

Aluminum was noticed for its good characteristics of low density, high stress, easy machining and rich resource etc. But its application was limited by poor corrosion-resisting, hardness and mechanical strength. In this work, Cr was added to Al-Mg-Mn-RE complex alloy. Then it was compared with aluminum and Al-Mg-Mn-RE alloy in hardness and mechanical strength, finally the better property was found. This was because Cr had particular character in aluminum base alloy by observing the microstructures of alloys. Hardness and mechanical tests were carried out at room temperature. The results showed that the property of aluminum base alloy was improved.

WEDNESDAY AM

12:10 PM

Influence of Aging Time of Fracture Toughness Mechanisms of Al-Li Alloys:

Yongxin Wang¹; Zheng Chen¹; Ri Ma¹; Yanli Lu¹; ¹Northwestern Polytechnical University, State Key Laboratory of Solidification

The fracture toughness mechanisms in aluminum-lithium alloys aged for different time was studied. Based on semi-quantity statistical and analytical results, we specially discuss the effects of aging time and the condition of stress on delamination. The results show that the percentage of delamination increase, the percentage of dimples decrease and little of quasi-cleavage can be found at the beginning zone with aging time prolonged. The main fracture features is delamination at crack stable growth zone and is quasi-cleavage in near unstable crack growth zone. The percentage of delamination is increase at crack stable growth zone and decrease in near unstable crack growth zone with aging time prolonging. The aging time and the crack growth stage can take apparently effect on delamination percent, the longer aging time, the earlier delaminating, and those influence the effect of extrinsic toughness mechanism further.

Aluminum Reduction Technology: Aluminum Industry in Mid-East

Sponsored by: The Minerals, Metals and Materials Society, TMS Light Metals Division, TMS: Aluminum Committee

Program Organizers: Martin Iffert, Trimet Aluminium AG; Geoffrey Bearne, Rio Tinto Aluminium Tech

Wednesday AM

March 12, 2008

Room: 298/299

Location: Ernest Morial Convention Center

Session Chair: Abdulmunim Binbrek, DUBAL

8:30 AM Keynote

ALBA's Vision on Sustainable Development: Mahmood Daylami¹:

¹Aluminium Bahrain

Abstract not available.

9:00 AM Invited

Aluminium Smelting Greenhouse Footprint and Sustainability: Jeffrey Keniry¹; ¹Alumination Consulting Ltd

The continuing growth of smelting capacity in the Middle East and Russia, and the concurrent decline in Europe and the USA, demonstrate the vital importance of low-cost power in underpinning the industry's competitiveness. More recently, the greenhouse footprint of the smelter adds another dimension to competitive advantage, which will have increasing economic significance as concerns for global warming intensify. In this context, the power source itself may confer a competitive advantage well beyond the supply cost to the smelter. Direct greenhouse gas emissions from best-practice smelters are in the range 1.6-2.0 tonnes CO₂-e per tonne of aluminium, while the indirect emission attributable to power generation imposes an additional zero (hydro and nuclear sources) to as high as 16 tonnes CO₂-e for power sourced from low-grade coal. The implication of this indirect greenhouse footprint on the future competitive advantage of alternative smelting locations is discussed.

9:30 AM Invited

Development of Aluminum Production Capacity in the Middle East and Siberia: Halvor Kvande¹; ¹Hydro Aluminium AS

Aluminum production is expected to grow outside the US and Europe. New capacity is being developed in areas with available and affordable energy and small domestic markets. The Middle East is an area of particular interest for both Brownfield and Greenfield smelters. Both Alba and Dubal have expanded their production in Bahrain and Dubai to above 800 000 tpy. Construction of Greenfield smelters has started in Qatar and Oman, and there are plans to build new smelters in Abu Dhabi and Saudi Arabia. The Qatalum project in Qatar will be one of the largest primary aluminum plants ever built, with 585 000 tpy in the first step. The site and infrastructure are planned for expansions up to 1.2 million tonnes. Qatalum will then be a mega plant, with a very competitive cost position. Another area with available energy is Siberia, and the world's largest aluminum producer, UC Rusal, has announced the construction of the Taishet

aluminum smelter near Irkutsk, equipped with Rusal's new 400 kA cells. Also other Greenfield and Brownfield projects are under way in Siberia.

10:00 AM Break

10:20 AM Invited

Rusals Expansion Based on Hydropower: Horst Peters¹; ¹ATC

Since March 2007 United Rusal is ranked by Primary Production the largest Aluminum Producer in the world. The majority of this Primary Production is located in Siberia with the smelters Bratsk and Krasnojarsk each 1 Mio.t/a production as well as Sayansk with 850.000 t/a and Irkutsk with 300.000 t/a production. Energy basis for all of these smelters is Hydropower from the huge Jennisei and Angara river system. The installed capacity is 25.000 MW. More can be developed.

10:50 AM Invited

DX Technology: The Development and the Way Forward: Abdulla Kalban¹; Yousuf Alfarsi¹; Abdelhamid Meghlaoui¹; ¹Dubai Aluminium Company Limited

Dubai Aluminium Company Limited (DUBAL) developed and implemented Reduction Cell technologies, D18 (185kA), CD20 (200kA), D20 (240kA) between 1990 and 2007 for six Brownfield expansions which increased production from 135,000 t/y (1979) to 940,000 t/y (2008). DUBAL continued in the path of high amperage Reduction Cell development, and introduced the DX technology as its latest in-house technological development. 5 DX prototype cells were commissioned from September to December 2005 at an operating amperage of 325 kA. In 2007, through a series of improvements to the cell design and components, anode configuration, shell, process control, busbars, superstructure and operational practices, and based on a learning curve associated with the 5 Prototype Cells, an improved version of DX cell targeting 340-350 kA was designed and a section of 40 cells is currently under construction to be commissioned during the first quarter of 2008. This paper summarizes the design features of the DUBAL DX Reduction cell technology, and operation performance of the five prototype cells for two years.

11:20 AM

Alba Line 5 Expansion - Solios Solution for a Better Environment: Thierry Malard¹; Maxime Depinoy¹; Fabienne Virieux¹; ¹Solios

In spring 2003, Aluminium Bahrain B.S.C.(c) (ALBA) undertook to expand the capacity of its Manama Plant (Line 5). Solios has been awarded contracts for the supply of green anode plant, foundry, fume and gas treatment plants. Supported by its experience in the aluminium field and with the help of ALBA Engineer's professionalism, Solios Environnement has been in charge to supply economical solutions to minimize smelters emissions. This paper, focused on environmental challenges, recalls the project parameters including capacity and leading requirements, highlighting some specific solutions used for Gas Treatment Centre (pot gas). Pot room atmosphere study has been carried out in the frame of a cooperation agreement between ALBA and SOLIOS ENVIRONNEMENT. Benefits from the installed over suction system "YPRIOS" are described, and key factors to optimise such system efficiency are discussed.

Biological Materials Science: Functional Biomaterials

Sponsored by: The Minerals, Metals and Materials Society, TMS Structural Materials Division, TMS: Biomaterials Committee, TMS/ASM: Mechanical Behavior of Materials Committee

Program Organizers: Ryan Roeder, University of Notre Dame; Robert Ritchie, University of California; Mehmet Sarikaya, University of Washington; Lim Chwee Teck, National University of Singapore; Eduard Arzt, Max Planck Institute; Marc Meyers, University of California, San Diego

Wednesday AM Room: 390
March 12, 2008 Location: Ernest Morial Convention Center

Session Chairs: Ming-Yong Han, National University of Singapore, Institute of Materials Research and Engineering; Raju Ramanujan, Nanyang Technological University

8:30 AM Keynote

Size/Composition-Tunable Quantum Dots and Their Bioapplications: *Ming-Yong Han*¹; ¹National University of Singapore, Institute of Materials Research and Engineering

Colloidal semiconductor nanocrystals (quantum dots) have attracted great attention for their distinguished roles in fundamental studies and technical applications such as biological labeling and optoelectronic devices. In the last two decades, the main efforts have been focused on the preparation of size-tunable binary or core-shell nanocrystals with different emission colors. In our research, we also focus on the development of highly luminescent composition-tunable quantum dots across the whole visible spectrum. The successful preparation of high-quality composition-tunable quantum dots makes the new class of nanomaterials very promising as multicolor biological nanoprobe for imaging, sensing, and drug delivery applications. There is an emphasis on the development of ultrasensitive imaging/spectroscopic detection for multiplexed analysis at cellular or tissue levels. Quantitative multi-parameter analysis of multianalytes is being carried out, which could provide a direct way to identify sets of genes and proteins correlating with certain diseases.

9:10 AM

Biomimetic Assembly of Functional Nanomaterials onto Polymers: *Song Jin*¹; ¹University of Wisconsin-Madison

We employ a bottom-up, biomimetic strategy to assemble functional nanoscale inorganic materials into microarrays under low temperature, benign chemical conditions following principles derived from biomineralization. Our approach involves the selective functionalization of polymer surfaces to create regions of differing surface energy. By carefully controlling the surface functional groups heterogeneous nucleation can be promoted in designated regions but suppressed in others. We have demonstrated the arrays of CdS thin films and ZnO nanorods using a variety of engineering polymers. CdS materials assembled this way can be used as arrays of high performance photodetectors yet retains the low cost roll-to-roll solution processing on flexible polymer substrates. We will also report our success in using nanoscale self-assembled block copolymers and sequenced biopolymers to assemble nanoscale functional materials.

9:30 AM

Encapsulated Contrast Agent Marker (ECAM) for MRI Prostate Brachytherapy: *Karen Martirosyan*¹; R. Jason Stafford²; James Bankson²; Steven Frank³; ¹University of Houston, Department of Chemical and Biomolecular Engineering; ²University of Texas MD Anderson Cancer Center, Department of Imaging Physics; ³University of Texas MD Anderson Cancer Center, Department of Radiation Oncology

We report a novel Co²⁺-based contrast agent marker that provides high signal intensity in Magnetic Resonance Imaging (MRI) by shortening the spin lattice relaxation time (T1) of water protons. This contrast agent can be used to identify the radioactive titanium seeds used in prostate brachytherapy. Magnetic characterization of the contrast agent shows superparamagnetic properties with a large magnetic moment. Plastic (acrylic) and glass seeds with Co²⁺-based aqueous solution (1-10%) with amount ~2 microliters were well visualized by MRI with a relative signal intensity ranging from 10751 to 32767 in a phantom

under 1.5 T MRI (T1). Various combinations of plastic/(glass)-titanium-plastic/(glass) and titanium-plastic/(glass)-titanium row of seeds were identified in a dog prostate and the calculations verified the distance to the center of the titanium seeds. The developed marker is referred to as an Encapsulated Contrast Agent Marker (ECAM) and can provide a novel targeted magnetic resonance imaging for brachytherapy application.

9:50 AM

Targeted Dual Therapy for Disease Treatment by Multifunctional Coated Magnetic Nanoparticles: *Raju Ramanujan*¹; Sibnath Kayal¹; S. Purushotham¹; ¹Nanyang Technological University

Coated magnetic nanoparticles have a wide variety of important, novel and unique bioengineering applications. Multifunctional materials for combined drug targeting, triggered drug release and MRI imaging in the context of human cancer treatment will be presented. Chemical synthesis was used to prepare core-shell structures of magnetic nanoparticles coated with a shell of thermosensitive polymers and anti-cancer drug doxorubicin. Heating these particles in an external AC magnetic field results in combined dual therapy of hyperthermia and triggered drug release. Iron oxide nanoparticles were coated with thermosensitive polymers based on PNIPAA and doxorubicin. The temperature rise and drug release during AC field heating was examined for various magnetic particle sizes, concentration and external magnetic field strength. Our results show that temperature control is feasible and controlled drug release can be accomplished by this novel technique. MRI imaging, in vitro and in vivo studies in a buffalo rat model will be discussed.

10:10 AM Break

10:20 AM

Magnetic Nanocarrier for Tumor-Targeted Drug Delivery: *Qiang Yuan*¹; Rajesh Venkatasubramanian¹; Devesh Misra¹; ¹University of Louisiana

The primary challenge in the delivery of a drug to a tumor site is to target the anticancer drug specifically in and around tumors and at concentrations that would decrease the growth rate and/or viability of the tumors. An excellent vehicle to achieve targeted delivery of anticancer drug in and around tumors is magnetic nanocarrier. We describe here that the magnetic nanocrystals hooked with anticancer agents and encapsulated with novel stimuli-responsive polymer (temperature and/or pH-responsive) are viable drug carriers. The specialized synthesis of the nanocarrier and in-vitro experiments are described for its unique drug delivery properties of effective and controlled release of drug at the targeted site.

10:40 AM

Antibactericidal Function of Composite Nanoparticles Consisting of Doped-Titania Photocatalytic Shell and Nickel Ferrite Magnetic Core: *Rajesh Venkatasubramanian*¹; Devesh Misra¹; ¹University of Louisiana

Titania is a potential photocatalytic material in applications involving killing of bacteria and cancer cells. While it can be directly used for bio-applications, it cannot be extracted because it is an electrical insulator. However, the removal of titania can be facilitated with the help of a small magnetic field, if we can synthesize composite particles consisting of magnetic core and photocatalytic shell. The paper describes enhanced antibactericidal function of doped-titania composite nanoparticles. The modification of the band gap of titania by dopants minimizes the probability of electron-hole recombination process and enhances the effectiveness of destroying bacteria.

11:00 AM Invited

Inkjet Printing of Biopolymers and Cells: *Paul Calvert*¹; ¹University of Massachusetts

We are using inkjet printing to deposit patterns of silk, collagen and ionic complexes of polypeptides. These guide the growth of cells deposited on the patterns. Yeast has been printed onto agar and the effect of overprinted biopolymer layers on the growth of yeast is being studied. Human fibroblasts and mesenchymal stem cells can also be printed and subsequently grown. This allows organized structures of differing cells and biopolymers to be printed in order to study cell-cell interactions.

11:30 AM

Synthesis, Patterning and Characterization of Biocompatible Parylene Coatings: Varshni Singh¹; V. Gunda¹; Jost Goettert¹; ¹Louisiana State University

Microfabrication techniques and scale-up by replication have fueled advances in micro analysis chips and sensor systems for BioMEMS, medical, health, chemical and life science applications. The present and future technology in such areas is driven by the need for "miniaturization" without losing absolutely in terms of biocompatibility. In fabricating device(s) and their parts for these applications, it is extremely difficult to employ only such materials that are biocompatible and inert. Therefore, it is crucial to have a biocompatible coating (such as Parylene), conformably deposited on/in these devices, which is inert and has an excellent biocompatibility. Parylene coatings are known to possess the essential characteristics that includes excellent adhesion, conformal, pinhole free, smooth, lubricious or low friction coefficient, inert, autoclavable, thin, penetrate and coat complex surfaces and able to deposit at room temperature. Present study will discuss the synthesis, patterning and characterization of Parylene Coatings in perspective of BioMEMS devices.

11:50 AM

Novel Nanocomposite Biomaterials Based on Hydroxyapatite and Polyvinylidene Fluoride Ferroelectric Polymers: Vladimir Bystrov¹; Yuri Dekhtayr²; Natalia Bystrova³; Ekaterina Paramonova⁴; Andrei Kholkin¹; ¹University of Aveiro; ²Riga Technical University; ³Institute of Theoretical and Experimental Biophysics; ⁴Institute of Mathematical Problems of Biology

The development of novel multifunctional composite materials is very urgent for biomedicine and nanobiotechnology. Ferroelectric Polyvinylidene Fluoride (PVDF) and its copolymers are the most suitable for these aims owing their physical properties and compatibility with many organic and biological molecules. The creation of nanoscale polarization patterning of thin PVDF films was shown. Novel nanomaterial PERCERAMICS (<http://www.perceramics.vip.lv/>) consisting from hydroxyapatite (HAP) was developed. This material is one of the most wide used in medicine (implants) and biotechnology. The interface between HAP biomaterials and living cells is improved, if the HAP surface was charged (polarized) and nanostructured. Further development of PVDF composites consists of the polarization-driven assembly on a patterned ferroelectric surface HAP clusters and lipids. The formation of created PVDF-composites are explored experimentally and by computational modeling. Obtained data are used for development of novel nanocomposite biomaterials for biomedical applications. Work is supported by INTAS-05-1000008-8091 and Portugal FCT projects PTDC/CTM/73030/2006, SFRH/BPD/22230/2005.

12:10 PM

Antibacterial Effects of Copper Vermiculite against E. Coli, K. Pneumoniae and S. Aureus: Bowen Li¹; Jiann-Yang Hwang¹; Susan Bagley¹; ¹Michigan Technological University

Copper vermiculite is a new material with excellent antimicrobial ability. In this study, the antibacterial effects of copper vermiculite against E. coli, K. pneumoniae and S. aureus were investigated by diffusion method, respectively. The results show that copper vermiculite is efficient to inhibit the reproduction of these common bacteria indicators. The antibacterial mechanism of copper vermiculite is discussed.

Bulk Metallic Glasses V: Glass Forming Ability and Alloy Development

Sponsored by: The Minerals, Metals and Materials Society, TMS Structural Materials Division, TMS/ASM: Mechanical Behavior of Materials Committee
Program Organizers: Peter K. Liaw, University of Tennessee; Wenhui Jiang, University of Tennessee; Guojiang Fan, University of Tennessee; Hahn Choo, University of Tennessee; Yanfei Gao, University of Tennessee

Wednesday AM

March 12, 2008

Room: 393

Location: Ernest Morial Convention Center

Session Chairs: Wenhui Jiang, University of Tennessee; Hahn Choo, University of Tennessee

8:30 AM Invited

Glass-Forming Ability as a Function of Various Factors: Intrinsic vs. Extrinsic: Dmitri Louzguine¹; Akihisa Inoue¹; ¹Institute for Materials Research

Several parameters and factors have been applied so far to predict the glass-forming ability of bulk metallic glassy alloys, and none of them can be treated yet as a comprehensive one to predict the glass-forming ability upon solidification of a liquid phase. In the present work various factors influencing the glass-forming ability are discussed and separated as intrinsic (belonging to a glass itself) and extrinsic (depending upon external conditions) factors. Actual glass-forming ability can be significantly limited by the extrinsic factors. These factors should be also taken into consideration to predict a real glass-forming ability of the alloy.

8:50 AM Invited

Improving Glass Forming Ability of Zr50.5Cu38.5Al11 Alloy by Suppressing the Precipitation of CuZr Phase: S.T. Deng¹; Z.Q. Hu¹; H. F. Zhang¹; ¹Chinese Academy of Sciences

Based on Zr50.5Cu38.5Al11 alloy, substituting Cu with Ni and Ag can improve glass forming ability greatly. The content of various elements in CuZr phase is analyzed with energy dispersive spectrometer of scanning electron microscope. The XRD patterns verify that adding Ag is very helpful to restrain CuZr phase from precipitating. Especially, with the increment of Ag content in Zr53.5Cu29.5-xNi5Al12Agx alloy, the proceeding of suppressing CuZr phase precipitation is shown in the XRD patterns of arc melted ingots. Chemical interaction among various atoms plays an important role in affecting glass forming ability. From ternary alloy to quinary alloy, considering that Ni and Ag have similar chemical and physical properties with Cu, the additions of Ni and Ag cause competitions of Ni and Ag with Cu for Zr and this kind of competition weakens the interaction between Cu and Zr atoms.

9:10 AM

Enhanced Thermal Stability Amorphous Aluminum Alloys: Timothy Wilson¹; Jianming Bai¹; Hahn Choo¹; ¹University of Tennessee

Amorphous aluminum alloy powders with compositions of Al₈₅Y₇Fe₈, Al₈₃Y₇Fe₈Ti₂, and Al₇₉Y₇Fe₈Ni₃Ti₂Nd₁ were developed with crystallization temperatures of 342°C, 400°C, and 457°C, respectively. In-situ high-temperature synchrotron diffraction results were correlated with differential scanning calorimetry studies to investigate the structural evolution of the alloy during the crystallization. The results show that, through microalloying with Ti and Nd, the onset-of-crystallization temperature was increased by 115°C without increasing the melting temperature, and the resulting crystalline products changed from a mixture of fcc-Al and an intermetallic phase in the case of Al₈₅Y₇Fe₈ to only intermetallic phases. Pair distribution function studies have revealed insight into changes in the local atomic order.

9:25 AM

An Investigation of Viable Pathways to Achieve Highly Tunable Fe-Based BMG Composites: Hesham Khalifa¹; Kenneth Vecchio¹; ¹University of California-San Diego

Fe-based BMGs are an intriguing member of the metallic glass family on account of their impressive mechanical properties and reasonably low price. A new Fe-based glass forming system is introduced of the form Fe-Mo-Cr-W-C-

B. Alloys of varying compositions within this system were subjected to several heating and cooling treatments resulting in a broad spectrum of microstructures. Comprehensive mechanical, thermal, and XRD analyses indicate that extremely fine control over phase nucleation and crystal size is achievable upon heat treatment from the amorphous state or alternate cooling pathways from the molten state. The presence of Molybdenum is unique to these Fe-based alloys and plays a critical role in the phase nucleation cascade of re-heated amorphous alloys. Furthermore, Molybdenum rich second phase particles that form upon cooling slowly from the molten state offer tremendous reinforcement to the surrounding matrix and exhibit Vickers hardness in excess of 2500.

9:40 AM Invited

Microstructure, Mechanical Properties of Mg-Ni-Zn-Y Bulk Metallic Glass Matrix Composites: *Keqiang Qiu*¹; Qingfeng Li¹; Wenhui Jiang²; Yinglei Ren¹; Xiaoguang Yuan¹; ¹Shenyang University of Technology; ²University of Tennessee

Mg-Ni-Zn-Y bulk metallic glass (BMG) matrix composites were prepared by copper mold casting method. The microstructure, the mechanical properties were investigated by SEM, mechanical tester with different diameters. Compared with Mg-Cu-Zn-Y BMG matrix composites, Mg-Ni-Zn-Y BMG composites exhibit high fracture strength and lower mass density. The reinforcement was characterized as Mg solid solution flake of less than 5µm in thickness. The microstructure and mechanical properties vary according to diameters of the samples. The high fracture strength and plastic strain are discussed in term of amorphous phase effect and ductility of Mg flakes.

10:00 AM

Stabilization of Clusters in Metallic Glass Forming Melts: *Xiufang Bian*¹; ¹Shandong University

We propose a new concept, the stabilization of cluster in metallic liquids described by the parameter $B = dr/dT$, for the prediction of the glass-forming ability (GFA) before their quenching, from the viewpoint of classical homogeneous nucleation theory. Metallic liquids with low B value possess high GFA, i.e., strong stabilization of clusters benefits to glass formation. When the value of B is lower than 1, the metallic liquid can be prepared into a metallic glass. The results of sixteen kinds of metallic liquids investigated by a high temperature X-ray diffractometer demonstrates that the stabilization ability of clusters determines the GFA.

10:15 AM

Nanocrystallization of a Bulk Metallic Glass in the Zr-Al-CuNiCo System – Structure and Mechanical Properties: Rohit Satapathy¹; Rainer Wunderlich¹; Arnaud Caron¹; Indranil Manna¹; Hans-Jörg Fecht¹; ¹Ulm University

A controlled two-phase mixture in terms of volume fraction and morphology of nanocrystalline and amorphous components offers the possibility of tailoring the ductility and mechanical strength of BMG forming complex alloys. This has been investigated in the Zr-Al-CuNiCo alloy system as a function of the Al-concentration varied between 7 and 20 at%. At the composition limit of glass formation different amorphous to crystalline phase ratios and geometries have been obtained by casting. Minor compositional variations result in a BMG exhibiting excellent glass forming ability and two widely separated crystallization peaks which allows a wide variation of the nanocrystalline/glassy microstructure. Specimen were investigated by XRD, SEM, atomic resolution TEM, AFAM and nanoindentation. First results indicate that the microhardness and Young's modulus measured by nanoindentation considerably increase as a function of the nanocrystalline volume fraction while the Poisson ratio of the glass shows an unexpected maximum at some intermediate composition.

10:30 AM

Interfacial Reactions and Growth Kinetics for Intermetallic Compound Layer between Molten In-Sn Solder and CuZr-Based BMG: Guofeng Ma¹; Zhuang-qi Hu¹; ¹Chinese Academy of Sciences, Institute of Metal Research

The growth kinetics of intermetallic compound layers formed between In-Sn alloy and Cu₄₀Zr₄₄Al₈Ag₈ BMG substrates by solid state isothermal aging were examined at temperatures between 343 and 473 K for 1-10 hours. In the solder joints between the In-Sn solder and Cu₄₀Zr₄₄Al₈Ag₈ BMG, the intermetallic compound layer was composed of Zr, Cu, Sn as a whole, because the values of the time exponent (n) are approximately 0.5, the layer growth of the intermetallic compound was mainly controlled by a diffusion-controlled mechanism over the

temperature range studied. The intermetallic compound layer thickness reached 4µm after 10 hours of aging at 393 K. The apparent activation energy for growth of total intermetallic compound layers was 98.35 kJ/mol.

10:45 AM Break

10:50 AM Invited

Transition Metal Microadditions and Glass Formation in Rapidly-Quenched Al₈₈Y₇Fe₅ Alloys: *Kenneth Kelton*¹; Lydia Longstreth-Spoor¹; Nicholas Mauro¹; Karyn Spence¹; ¹Washington University

Studies of the influence of 3d transition metal microadditions on glass formation in Al₈₈Y₇Fe₅ are reviewed. Rapidly-quenched ribbons of Al₈₈Y₇Fe₅ show glass-like x-ray and transmission-electron-microscopy (TEM) diffraction patterns, but do not show the expected nucleation and growth peak in isothermal differential scanning calorimetry (DSC) measurements of primary crystallization to α-Al. The transformation kinetics, measured by DSC, TEM and electrical resistivity, are analyzed assuming both diffusion-limited nucleation and growth, and particle coarsening. Microalloying with any of the 3d transition metal elements improves glass formation and stability in this alloy, but to different degrees; the most effective element is Cr. High-q x-ray diffraction studies and EXAFS measurements made on Al₈₈Y₇Fe₅ and Al_{87.5}Y₅Ti_{0.5} show that the microaddition induces structural changes in the liquid/glass structure, raising the nucleation barrier for α-Al. Schematic TTT diagrams that reflect DSC measurements of the change in devitrification pathway with microalloying are presented.

11:10 AM Invited

Synthesis and Properties of New Cu-Zr-Based Glassy Alloys with Unusual Glass-Forming Ability: *Wei Zhang*¹; Akihisa Inoue¹; ¹Tohoku University

Addition of Al to Cu-Zr-Ag alloys increased the stabilization of supercooled liquid and the reduced glass transition temperature, leading to remarkable enhancement in the glass-forming ability (GFA). The quaternary glassy alloy samples of over 15.0 mm in diameter are formed in the composition range of 35 to 45 at% Cu, 40 to 50 at% Zr, 5 to 10 at% Ag, and 5 to 8 at% Al. The best GFA is recognized for Cu₃₆Zr₄₈Ag₈Al₈ alloy which is close a eutectic composition in the quaternary alloy system. The glassy alloy samples were successfully fabricated in the diameter range up to 25 mm by an injection copper mold casting method. The addition of a small amount of Pd to the quaternary alloy is effective for the further increase in GFA. The glassy sample diameter of over 30 mm was fabricated. The bulk glassy alloys exhibited excellent mechanical properties and high corrosion resistances.

11:30 AM

Structural Changes in Bulk Metallic Glasses Induced by Compression: *Wojciech Dmowski*¹; Takeshi Egami¹; Yoshihiko Yokoyama²; Akihisa Inoue²; Bogdan Palosz³; Yang Ren⁴; ¹University Tennessee/MSE; ²Tohoku University; ³Polish Academy of Science; ⁴Argonne National Laboratory

Mechanical properties of metallic glasses have been extensively studied, however much less is known about the underlying changes in the atomic structure. There is a general consensus that deformation must be accompanied by a local rearrangement of atoms to accommodate shear strain. However, disordered nature of a glass or small deformation volumes makes it difficult to observe experimentally. We have investigated changes in the atomic structure in a bulk metallic glass of Zr₅₀Cu_{40-x}Pd₁₀ (x=0,6,10) that have been compressed in an isostatic and inhomogeneous way with pressures up to 8 GPa and at temperatures up to 800 K. We used high energy X-ray scattering and area detector to obtain atomic pair density function. The results indicate that inhomogeneous deformation in a glass involves rearrangement in a cluster of atoms (like bond exchange) that leads to structural anisotropy. However, isostatic compression results in isotropic changes in the local atomic structure.

11:45 AM

Microstructure and Mechanical Properties of Stainless-Steel-Continuous-Fiber-Reinforced Zr-Based Amorphous Alloy Composites Fabricated by Liquid Pressing Process: *Kyuhong Lee*¹; Sang-bok Lee²; Sang-kwan Lee²; Sunghak Lee¹; Nack J. Kim¹; ¹Pohang University of Science and Technology; ²Korea Institute of Machinery and Materials

Stainless-steel-continuous-fiber-reinforced Zr-based amorphous alloy composites were fabricated without pores and misinfiltration by liquid pressing process, and their microstructures and mechanical properties were investigated in

this study. About 60 vol.% of continuous fibers were homogeneously distributed in the matrix, in which considerable amounts of polygonal crystalline particles and dendritic crystalline phases were formed by the diffusion of metallic elements from fibers to the matrix. In compressive test, strength of 700–830 MPa was maintained until reaching strain of 40% since fibers interrupted the propagation of shear bands initiated at the matrix and took over a considerable amount of loads. Under tensile loading, deformation and fracture occurred by consequent processes of crack formation at matrices, necking of fibers, fiber/matrix interfacial separation, and cup-and-cone-type fracture of fibers, thereby resulting in high tensile elongation over 6%. These findings suggested that new possibilities might be open to be applied to structural materials requiring excellent properties.

12:00 PM

Effect of Mo Addition to $\text{Fe}_{65}\text{Cr}_{15}\text{C}_{14}\text{B}_6$ Alloy during Mechanical: *Uma Maheswara Seelam*¹; C. Suryanarayana¹; ¹University of Central Florida

In this investigation, the effect of addition of Molybdenum to $\text{Fe}_{65-x}\text{Cr}_{15}\text{Mo}_x\text{C}_{14}\text{B}_6$ ($x = \text{Mo} = 0$ to 20 at.%) was studied on the ease of formation of an amorphous phase by MA. The milled powders were characterized using XRD, DSC and TEM methods. The alloy with 15 at.% Mo produced an amorphous phase after 30 h of milling. High temperature heat treatment (600–900°C) led to crystallization of the amorphous alloy. The type of crystallization products depended up on Mo content in the alloys. A carbide phase formed if the Mo content was less than 15 at.%. On the other hand, Fe solid solution and Fe/Mo borides formed if the Mo content was above 15 at.%. Thus, the type of phases present seems to be important in deciding whether amorphous alloys can be synthesized by MA.

12:15 PM

Thermodynamic Evaluations of Intermetallic Metallic Glass Systems Utilizing Interatomic Bond Energies: *James Dahlman*¹; ¹Air Force Research Laboratory/MLLMD^{*}

Experimental evidence has demonstrated the tendency for metallic glass systems to form structures with a high degree of short range order. Ordering amongst nearest neighbors indicates the presence of underlying thermodynamic criteria as interatomic bond strength largely governs localized interactions. Previous work has corroborated the assumption thermodynamic parameters influence glass stability by relating critical thickness to glass transition temperature, heat of formation and critical cooling rates. Additionally, it is understood that strong A-B bond energies in binary systems result in a high degree of short range order. However, previous work has failed to show a correlation between nearest neighbor bond energies and glass forming ability. This work seeks to establish whether a connection between nearest neighbor bond energy and structural stability is possible through evaluation of bond energies and the heat of formation for multiple intermetallic glass forming systems.

12:30 PM Invited

Rare-Earth Based Bulk Metallic Glasses with High Thermal Stability and Excellent Magnetocaloric Properties: *Xudong Hui*¹; Liang Liang¹; G. L. Chen¹; ¹University of Science and Technology Beijing

Several heavy rare-earth Gd-, Dy- and Er-based bulk metallic glasses (BMG) with high thermal stability and excellent magnetocaloric properties has been prepared by a copper mold casting. Compared with the other known rare-earth based BMGs, this BMG alloy possess higher glass transition temperature and crystallization temperature, larger effective activation energy for glass transition and crystallization. Under a modest magnetic field, this BMG alloy exhibits a comparable or even larger magnetocaloric effect than that the previously reported Re-based BMGs and crystalline compounds. The high thermal stability and the excellent magnetocaloric effect together with other merits of the BMGs make this BMG alloy suitable candidate for use as magnetic refrigerant in a temperature range below 100 K.

Carbon Dioxide Reduction Metallurgy: Electrolytic Methods

Sponsored by: National Materials Advisory Board, Metallurgical Society of the Canadian Institute of Mining Metallurgy and Petroleum, The Minerals, Metals and Materials Society, American Iron and Steel Institute, TMS Light Metals Division, TMS Extraction and Processing Division, TMS: Reactive Metals Committee, TMS: Recycling and Environmental Technologies Committee

Program Organizers: Neale Neelameggham, US Magnesium LLC; Masao Suzuki, Al Tech Associates; Ramana Reddy, University of Alabama

Wednesday AM

March 12, 2008

Room: 294

Location: Ernest Morial Convention Center

Session Chairs: Donald Sadoway, Massachusetts Institute of Technology; John Hryn, Praxair Inc

8:30 AM

Carbon-Free Metals Extraction by Molten Oxide Electrolysis: *Donald Sadoway*¹; ¹Massachusetts Institute of Technology

Molten oxide electrolysis (MOE), which is the electrolytic decomposition of molten metal-oxide into liquid metal and oxygen gas, represents an improvement over today's carbon-intensive thermochemical reduction processes for metal production. For MOE the feedstock can be concentrate derived from ore or from hazardous waste such as chromate sludge. The process avoids the use of consumable carbon anodes and thus eliminates greenhouse-gas emissions as the by-product of the metal-recovery step. The concept applies to a variety of chemistries including titanium, iron, and ferroalloys. The electrochemistry of multicomponent oxide melts from the family $\text{FeO} - \text{SiO}_2 - \text{TiO}_2 - \text{Al}_2\text{O}_3 - \text{MgO} - \text{CaO}$ has been studied by voltammetry at temperatures up to 1750°C. Galvanostatic electrolysis in laboratory-scale cells operating with a variety of feedstocks has demonstrated the extraction of liquid iron, ferrosilicon, and titanium with the simultaneous co-generation of oxygen.

8:50 AM

Electrochemical Reduction of Carbon Dioxide: *Melvin Miles*¹; ¹University of La Verne

Considerable research has been conducted on the anodic oxidation of methanol in fuel cells. The electrochemical reduction of carbon dioxide in aqueous solutions to form methanol is the same reaction in reverse, i.e. $\text{CO}_2 + 6\text{H}^+ + 6\text{e}^- \rightarrow \text{CH}_3\text{OH} + \text{H}_2\text{O}$. The same catalysts and conditions may operate for both reaction directions. This carbon dioxide reduction reaction, however, must be able to compete with the electrochemical reduction of water to form hydrogen gas. Thermodynamically, the reduction of CO_2 to form CH_3OH is slightly more favorable than the reduction of water. Kinetically, carbon dioxide reduction can be favored by electrodes that are poor catalysts for water reduction such as Mo, Cu, In, Sn, and Sb. The use of nearly neutral electrolytes rather than acidic electrolytes makes the reduction of CO_2 kinetically more favorable. The thermodynamics of various reaction steps will be presented.

9:10 AM

Soda Fuel Cycle Metallurgy – Choices for CO_2 Reduction: *Neale Neelameggham*¹; ¹US Magnesium LLC

Ferrous and non-ferrous metal industries are used to handling several billion tonnes a year of ore, fuel and fluxing agents by mineral processing techniques and varieties of extractive metallurgy "Reduction" processes. Metal industry know-how can be applied to meet the challenge of Reducing CO_2 to below 550 ppm in the atmosphere by the year 2050. Processes for generating alloys of carbon and hydrogen by Reducing the CO_2 and water mixture Soda, as in Carbonated water, to easily stored fuels are normally endothermic and are similar to generation of difficult to store hydrogen. This recycling of CO_2 and water are possible by using other forms of energy by innovative carbon capture methods. Thermodynamic diagrams for metal-soda [double oxide] reactions provide hints for using low cost unused stored energy in un-recycled metallic waste for thermal conversion. Choices for electrodes for electrometallurgical approaches [using solar - wind - hydro power] are also discussed.

9:30 AM

Electrocatalytic Reduction of CO₂ to C₂H₄ at a Gas/Solution/Metal Interface:

Kotaro Ogura¹; ¹Yamaguchi University

The problem of greenhouse effect should be largely mitigated if CO₂ can be recycled for use as fuels or chemicals. Although various processes for converting CO₂ to valuable compounds have been proposed, a matter of infinite importance is that the conversion process is feasible under mild conditions. This is because the secondary generation of CO₂ is feared if high energy is required and supplied with a fossil fuel. We have developed the electrochemical reduction process of CO₂ to C₂H₄ which occurs at a three-phase(gas/solution/metal)interface in concentrated potassium halide solutions. The input energy required for this process was supplied by a solar cell or a commercial power source. In the closed circulation system, the conversion efficiency of CO₂ increased with an increase of input electric charge to reach 100%, and the maximum selectivity for the formation of C₂H₄ was more than 80%.

9:50 AM Break

10:05 AM

Green Production of Light Metals in Ionic Liquid Electrolytes: *Mingming Zhang¹; Ramana Reddy²; ¹Univ of Alabama; ²University of Alabama*

Carbon dioxide (CO₂) is one of the most common by-products produced during light metals production. It is considered to be the cause of greenhouse effects. Efficient reduction of CO₂ can help to minimize the rate of global warming and improving energy sufficiency. In this paper, a novel light metals production process was proposed using ionic liquid electrolytes. This process has significant advantages compared with traditional high temperature processes such as zero CO₂ and CF₄ emission, low energy consumption due to the low temperature operation and non-consumable electrodes. Two types of anode materials (graphite, extruded carbon) were assessed in electrolysis experiment. The results showed that both anode materials were stable (negligible weight loss). However, the extruded carbon was found to be superior to graphite in terms of current density and current efficiency. The calculated energy consumption for aluminum production was less than 5kWh/kg at current densities up to 350 A/m².

10:25 AM

Carbon Dioxide Recycling by High Temperature Co-Electrolysis and Hydrocarbon Synthesis: *Joseph Hartvigsen¹; S. Elangovan¹; Lyman Frost¹; Anthony Nickens¹; Carl Stoots²; James O'Brien²; J. Herring²; ¹Ceramtec, Inc.; ²Idaho National Laboratory*

Carbon dioxide recovered from concentrated sources, such as metallurgical reduction furnaces, cement kilns and fossil power plants can provide a valuable feedstock for a synthetic fuels industry based on energy from nuclear, solar, wind and hydropower sources. High temperature co-electrolysis of CO₂ and steam to produce synthesis gas has been demonstrated using reversible solid oxide fuel cell technology. Where a source of high temperature process heat is available, such as from an advanced high temperature nuclear reactor or solar dish concentrator, the endothermic electrolysis reactions can utilize both thermal and electrical inputs in such a way that the conversion efficiency within the cell is 100%. Synthesis gas produced in a co-electrolysis cell has been further reacted over a catalyst to produce conventional hydrocarbon fuels. Widespread implementation of synfuel production from CO₂ will enable a much larger reliance on intermittent renewable energy than can be accommodated by conventional electric demand profiles.

10:45 AM

CO₂ Reduction by Nanoscale Galvanic Couples: *Kanchan Mondal¹; ¹Southern Illinois University*

Methanol, lower hydrocarbons, CO, and HCOOH formation have been by the reduction of CO₂ with H₂. Uncatalyzed electroreduction requires a significant overvoltage. An alternate route has been conceptualized. Production of hydrogen from water can be achieved by chemical oxidation of a metal in water followed by oxidation of the hydronium ion by the released electrons to form hydrogen radical. It is hypothesized that circumventing the problem of the formation of hydrogen molecule is essential while having the hydrogen radical to react with CO₂ forming methanol, etc. This may be possible by a bimetallic catalyst acting as a galvanic couple, wherein one metal acts as the electron donor for the production of hydrogen radical while the other acts as a catalyst for the reduction

of CO₂. This may enhance the reaction rates. The current concept circumvents the need for an external electric field unlike the electrochemical process.

11:05 AM

Reduction of Carbon Dioxide to Formate in an Electrochemical Membrane Reactor in KHCO₃ Buffer Solutions: *Kandasamy Subramanian¹; Krishnasamy Asokan¹; Govindarajan Gomathi¹; ¹Central Electrochemical Research Institute*

An electrochemical reactor with anode and cathode chambers separated by a composite perfluoro polymer cation exchange membrane was designed, fabricated and used for the reduction of dissolved carbon dioxide to formate under ambient conditions. The flow reactor enhanced the mass transfer of carbon dioxide compared to the batch reactor. Experiments were conducted using two different membranes - Nafion 961 and Nafion 430. Optimum values of flow rate and current density were evaluated for the formation of formate in aqueous KHCO₃ buffer solutions. The efficacy of various cathode materials (Cd, Pb, Sn and Zn plated stainless steel woven mesh) for the electro reduction of carbon dioxide is also reported.

11:25 AM Panel Discussion

11:40 AM Concluding Comments

Cast Shop Technology: Foundry Ingots and Alloys

Sponsored by: The Minerals, Metals and Materials Society, TMS Light Metals Division, TMS: Aluminum Committee

Program Organizers: Hussain AlAli, GM Casthouse and Engineering Services, Aluminium Bahrain Company (ALBA); David DeYoung, Alcoa Inc

Wednesday AM

Room: 295

March 12, 2008

Location: Ernest Morial Convention Center

Session Chair: Graham Banister, Bahrain Alloys Manufacturing Company

8:30 AM Keynote

Development of New Open Mould Conveyor Ingot Casting Technology:

John Grandfield¹; Vu Nguyen¹; Pat Rohan¹; ¹CSIRO

Operators of open mould chain conveyor remelt ingot casting machines are interested in reducing the oxide levels in the ingots and reducing production costs by improving the productivity of the machines. CAST has developed two patented technologies for ingot casting; a low dross filling system (CASTfill) and a mould design (CASTmould) with reduced ingot solidification time to achieve 20% higher production rates. This paper describes the development including application of Smooth Particle Hydrodynamic (SPH) modeling, prototype design testing on a full scale pilot system, fully coupled heat and stress modelling and a purpose built rig for measuring mould temperatures, air gaps and displacement. New mould designs were proposed and tested on the rig. Following successful plant testing both CASTfill and CAST mould have been adopted at a number of smelters.

8:50 AM

Quality and Productivity Improvements in the Manufacture of Foundry

(A356.2) Alloy Ingots at Aluminium Bahrain: *Michael Jacobs¹; Anand Sandhanam¹; Ebrahim Fathi¹; Aref Noor¹; ¹Aluminium Bahrain*

Aluminium Bahrain (Alba) produces 80,000 MT/annum of high quality remelt ingots for the aluminium foundry industry. This paper discusses the various technologies and practices implemented at Alba's new production facility to improve the productivity and quality of the alloys produced in order to meet the increasing quality demands of the customers. These improvements are related to pot room metal treatment, closed door furnace operation, an electromagnetic stirring system, in line degassing, filtration and rod feeder systems, ingot chain casting wheel and commissioning of a new Properzi bar casting machine in order to achieve consistently high quality product at the maximum productivity are discussed.

WEDNESDAY AM

9:10 AM

The Achievement of a Robust Al-Si Alloy Casting Process: Paul Cooper¹; Arne Dahle²; ¹London and Scandinavian Metallurgical Company Ltd.; ²University of Queensland

The Al-Si alloy casting process has suffered a long-standing reputation for lack of robustness when compared to wrought alloy casting. Both industries are able to benefit from the addition of effective master alloys for the purposes of grain refinement and structural modification. However the Al-Si alloy casting process has inherent disadvantages in terms of the achievement of a sound low porosity, high mechanical property casting. Recent advances in the technology of master alloy additives for Al-Si alloys are allowing this disadvantage to be effectively addressed. These advances are described and the potential for improved Al-Si alloy castings are explored.

9:30 AM

Microstructural Improvement of Semi Solid Al-Si Foundry Alloys through Boron Addition: Shahrooz Nafisi¹; Reza Ghomashchi²; ¹ISPCO Inc.; ²Advanced Materials and Processing Research Institute (AMPRI)

Comprehensive study was performed on the impact of grain refiners addition to the microstructural evolution of semi-solid Al-Si slurries. The most widely used industrial refiners for such alloys are AlTiB master alloys in spite of their well proven drawbacks including fading and settling of the so-called nucleant particles. Al-B master alloy is re-introduced as a potent substitute of traditional AlTiB master alloys. In semi solid casting of 356 alloy, it is shown that by boron addition, the number of primary Al-globules is increased. Improved globularity coupled with smaller primary particle size leads to superior rheological characteristics of the SSM billets.

9:50 AM

Effect of Transition Metals on the Grain Structure of a Model Al-4% Cu Alloy Solidified in the Presence of Cavitation: Tetyana Atamanenko¹; Dmitry Eskin²; Laurens Katgerman¹; ¹Delft Technical University; ²Netherlands Institute for Metals Research

In the casting of aluminium, ultrasonics can be used to promote the formation of a fine, uniform, non-dendritic grain structure. From previous investigations it is known that main condition for obtaining non-dendritic grain structure is a combined action of grain refiners and an intense ultrasound inducing developed cavitation on a solidifying melt. A small amount of transition metals (Zr, Ti etc.) can significantly increase the number of nucleation sites in the melt without using an Al-Ti-B master alloy. Many commercial wrought aluminium alloys contain these elements because they also prevent recrystallization. The paper describes the results on the influence of different transition metals on structure formation during ultrasonic melt treatment. In separate experiments, model Al-4%wt Cu alloys with small additions of transition metals, typical of commercial aluminium alloys, are solidified with and without UST. The final microstructure is analyzed.

10:10 AM Break

10:20 AM

Characterization of Zn-Al Alloys with Different Structures Using Solidification and Electrochemical Parameters: Alicia Ares¹; Liliana Gassa²; Carlos Schvezov¹; ¹CONICET/University De Misiones; ²CONICET/INIFTA

The objective of the present research consist on studying the type of structure (columnar, equiaxial or with the columnar to equiaxed transition, CET) using solidification and electrochemical parameters in Zn-Al alloys with different concentrations (Zn-2%Al, Zn-4wt%Al, Zn-16wt%Al, Zn-27wt%Al and Zn-50%Al, weight percent). In order to obtain columnar, equiaxial and the CET structures, the alloys were directionally solidified upwards in an experimental set up with a set of thermocouples in the samples which permit to determine the time dependent profiles during growth. From these profiles and the location of thermocouples it was possible to calculate the cooling rates, growth velocities and the temperature gradients along the samples. The electrochemical studies in the samples were realized by electrochemical impedance spectroscopy and polarization curves.

10:40 AM

Air Entrapment Due to Vertical Steps in the Mould Filling of A356 Sand Casting: Giovanni Sangiorgi Cellini¹; Luca Tomesani¹; ¹University of Bologna

The aim of research is to understand the formation of defects by air entrapment in the sand casting of A356 aluminum alloy in the mould filling phase, when the metal flow is subject to suddenly fall at vertical mould steps. For this purpose, a physical casting experiment was created to impose, during filling, a growing amount of turbulence in the different parts of the casting. The mould consists of one gate filling five different branches, each one being composed by two horizontal parts and an intermediate vertical one of growing height. Moreover, three different moulds were used, with different geometry of the terminal part: straight branches, goose beaked ends and blind risers. All the experiments were numerically simulated with PROcast2006. In order to discriminate the air entrapment effect from other defects origins, a correlation was sought between the porosity percentage and the simulation results for many defects-formation criteria.

11:00 AM

Study of AlTiBC Master Alloy: Liu Weimin¹; ¹Aida Aluminium Alloys Company, Ltd

The AlTiBC grain refining master alloy has been discussed and researched for years by some researchers, but now it's still in argument. So, by cooperating with Shandong University, Aida make a study of this master alloy. Experimental results showed that the AlTi5C0.4 master alloy which was after melting again exhibited better grain refining performance for commercially pure Al than the ones that had not been remelted. As a result, it was discussed a new preparation craft of AlTiBC master alloy in this paper in detail. And the grain refining potentiality of the AlTiBC master alloy was investigated in this article by optical microscopy and electron probe micro-analyzer (EPMA).

11:20 AM Panel Discussion

Characterization of Minerals, Metals, and Materials: Characterization of Microstructure and Properties of Materials III

Sponsored by: The Minerals, Metals and Materials Society, TMS Extraction and Processing Division, TMS: Materials Characterization Committee
Program Organizers: Jian Li, Natural Resources Canada; Toru Okabe, University of Tokyo; Ann Hagni, Intellection Corporation

Wednesday AM

March 12, 2008

Room: 284

Location: Ernest Morial Convention Center

Session Chairs: Arun Gokhale, Georgia Institute of Technology; Mingdong Cai, University of Houston

8:30 AM

Cathodic Polarization Behavior of Ionic Liquid (TMHA-Tf₂N) Containing Titanium Ions: Kazuaki Tsuchimoto¹; Tetsuya Uda¹; Kuniaki Murase¹; Yoshitaro Nose¹; Yasuhiro Awakura¹; ¹Kyoto University, Department of Materials Science and Engineering

To develop novel technology for the electroplating of titanium layers from ionic liquid (room temperature molten salt) baths at low temperatures, cathodic polarization behavior of trimethyl-*n*-hexylammonium bis[(trifluoromethyl)sulfonyl]amide (TMHA-Tf₂N) ionic liquid containing titanium ions was investigated at 50°C. Titanium electrode was dissolved anodically to feed titanium ions into the ionic liquid, and cyclic voltammograms were taken for the resulting baths. When a single-compartment electrolytic cell was used, two reduction waves were found at -1.0 V and -2.5 V. In contrast, an additional reduction wave appeared at 0 V with a two-compartment cell where anolyte and catholyte were separated by a sintered glass. It is considered that, in the single-compartment bath, Ti⁴⁺ ions generated through the anodic dissolution can migrate to cathode and reduced to a stable Ti³⁺ state, hence we can conclude here that the reduction at 0 V should be attributed to reduction of Ti⁴⁺ to Ti³⁺.

8:50 AM

Corrosion of Nickel-Based Superalloy in Molten Fluoride: Bowen Li¹; Xiaodi Huang¹; Jiann-Yang Hwang¹; ¹Michigan Technological University

Nickel-based alloys have been used in a wide variety of severe operating conditions, including corrosive environment, high temperature, high stress, and their combinations. To determine the feasibility of using nickel-based superalloy as an electrode material in primary aluminum production, the corrosion rate of a nickel-based superalloy from INCO was investigated in an industrial fluoride melt using the metallographic method. The results show that fluoride melt has high wettability to the alloy. When corrosion time was less than 0.5 hours at 1000°C, the microstructure of the specimen surface had no obvious change. The maximum corrosion rate of the fluoride solution to the superalloy is approximately 27 microns per hour.

9:10 AM

Comparison between Aluminium 6063 Hardened Thermochemical and Mecanochemically: Isaías Hilerio¹; Miguel Barrón¹; ¹Universidad Autonoma Metropolitana Azcapotzalco

The objective of this work is to compare the properties of a material treated thermochemically in relation to mecano-chemical treatment. The advantage of this last treatment is not to add a material to the substratum, because the hardened material with the mecanochemical treatment has not the adherence problem by hardened layer using thermochemical treatment. The process was carried out in 5 samples with the following dimensions: 35 x 100 x 8 mm. It has been utilized a vibrator machine with a different abrasive charge in each stage of the process. To study the kinetics of the process was withdrawn a sample for each stage of the process. It has been done the micro hardness study, MEB and Ray X diffraction. It has been founded higher hardness values in the material treated thermochemically, but the difference is in the cases which it is not possible to use that method.

9:30 AM

Thermally Activated Sintering of Kaolinitic Clay: Sergio Monteiro¹; Carlos Maurício Vieira¹; ¹State University of the Northern Rio de Janeiro - UENF

The sintering of kaolinitic clay ceramics can be achieved by solid state diffusion at temperatures below 900°C. Owing to the plate-shaped morphology of the kaolinitic clay particles, surface diffusion can consolidate the porosity by thermally activated mechanisms at temperatures as low as 500°C. In the present work, the thermally activated parameters for the sintering of a kaolinitic clay were characterized in the interval from 500 to 900°C. The mechanical strength obtained in cylindrical specimens, that were fired in this interval of temperatures for different times and then tested by diametral compression, serve to evaluate the thermally activated parameters. The results showed a relatively smaller value for the activation energy implying a more efficient mechanism of porosity consolidation, which justifies, in practice, the low temperature sintering of kaolinitic clay ceramic.

9:50 AM Break

10:10 AM

Investigations of Retained Deformation Energy after Hot Forming and Its Influence on the Abnormal Grain Growth for the Nickel Based Alloy 80a: Mirza Candic¹; Stefan Mitsche²; Baohui Tian³; Christof Sommitsch¹; ¹University of Leoben; ²University of Graz; ³Bohler Edelstahl GmbH

For a hot forming process, residual (i.e. retained) strains exist due to different degrees of recovery and recrystallization, which can be related to inhomogeneous deformation, strain rate and temperature gradients with deformation. During the subsequent annealing the retained strain may lead to non-uniformed grain structures, or even worse, coarse grains due to secondary recrystallization and abnormal grain growth, respectively. In the present work, for the nickel based alloy 80a, single and multi hit hot deformation tests followed by annealing were performed for variable deformation and annealing parameters. In order to evaluate the retained strain evolution, the strain distribution of related grain structures was investigated by using the finite element method as well as corresponding microhardness values and EBSD data. For the quantitative analysis of the local grain misorientation some new evaluation methods were developed.

10:30 AM

Fundamental Study on Titanium Production Process by Disproportionation Reactions of TiCl₂ in MgCl₂ Molten Salt: Taiji Oi¹; Toru Okabe¹; ¹University of Tokyo

In order to establish a novel titanium production process, the synthesis and disproportionation reactions of TiCl₂ in molten salt were investigated. This process comprised (1) the synthesis of TiCl₂ by reacting TiCl₄ with titanium metal in MgCl₂ molten salt at 1073-1273 K and (2) the formation of titanium by the disproportionation reactions of TiCl₂ in molten MgCl₂ at 1300-1373 K. The results revealed that TiCl₂ was successfully obtained in the synthesis step and the efficiency of TiCl₂ formation was drastically improved by using molten MgCl₂ as the reaction medium. Some preliminary experiments demonstrated that titanium powder of approximately 99% purity was produced by the disproportionation reactions of TiCl₂ in MgCl₂ molten salt. The titanium production methods investigated in this study can be applied to a new titanium production process and/or titanium plating technology.

10:50 AM

Influence of the Precursors Setup on the Yield and Properties of HPHT Synthesized Diamonds: Ana Lucia Skury¹; ¹Universidade Estadual do Norte Fluminense

The production yield of diamonds synthesized at HPHT conditions from graphite and catalyst metallic alloy precursors depends on parametric variables, which include the initial setup of the precursor materials. This setup is associated with the arrangement of both, the graphite and the catalyst alloy, in either homogeneous mixture or alternated layers. The present work studied the influence of the type of setup on the yield and properties of HPHT synthesized diamond crystals. Precursor reactive system composed of graphite and Ni-Mn alloy, in homogeneous mixture or layer, was processed at 4.7GPa and 1300°C for 10 minutes. It was found that the yield is sensibly affected by the type of setup. A 10% decrease in productivity occurs for the alternated layers setup, while the brittleness of the diamond, measured by friar tests, increases for the homogeneous mixture setup. Moreover, significant differences were observed in the shape and size distribution of the crystal.

11:10 AM

A New Pantograph Slider of High Speed Electric Locomotive: Lian Yang¹; ¹Tsinghua University

With devolvement of high-speed electric locomotive, current pantograph sliders are not satisfied electric locomotive demands because their shortcoming, such as higher resistance rate, lowers impact toughness, and bigger abrasion ratio. A new pantograph slider is developed to resolve the problems. The new pantograph slider is consisted of copper, carbon fiber, graphite etc. The influence of pressure and sintering temperature to the performance of pantograph slider is studied firstly. Then its performance of friction, abrasion and impact toughness is tested. Performance of the new pantograph slider is contrasted to current pantograph sliders at last. The results show that its performance of resistance ratio, friction coefficient, abrasion rate and impact toughness etc. is improved greatly compared with foreign immersed carbon slider MC with friction coefficient reduced 1.62 times, abrasion ratio decreased 1.27 times, impact toughness increased 3.09 times and conductance increased 45 times.

WEDNESDAY AM

Complex Oxide Materials - Synthesis, Properties and Applications: Scaling, Dynamics, and Switching

Sponsored by: The Minerals, Metals and Materials Society, TMS Electronic, Magnetic, and Photonic Materials Division

Program Organizers: Zhiming Wang, University of Arkansas; Ho Nyung Lee, Oak Ridge National Laboratory

Wednesday AM
March 12, 2008

Room: 277
Location: Ernest Morial Convention Center

Session Chair: To Be Announced

8:30 AM Invited

Atomic-Scale Characterization of Interfaces in Oxide Heterostructures:

Matthew Chisholm¹; Ho Nyung Lee¹; Maria Varela del Arco²; Stephen Pennycook¹; ¹Oak Ridge National Laboratory

Recent advances in materials synthesis, theoretical simulation and atomic scale imaging/spectroscopy is being used to design, create and characterize three-dimensional materials with functional physical properties resulting from electronic effects of two-dimensional interfaces. It is expected that correlating macroscopic properties of these new "interfacial solids" with atomic structures will lay the foundation for the ultimate miniaturization of devices. We will discuss some of our results on interface-induced, two-dimensional electrical conduction in thin film oxide superlattices. Macroscopic physical properties of these artificial solids will be correlated with results from ORNL's aberration-corrected scanning transmission electron microscopes, which provide the smallest electron probes. These instruments allow simultaneous sub-Å resolution imaging and electron energy-loss spectroscopy, which is currently the only means for obtaining a highly local measure of the chemical, crystallographic and electronic properties of materials. Research sponsored by the Office of Basic Energy Sciences, Division of Materials Sciences and Engineering.

9:00 AM Invited

Influence of Defects on the Dielectric and Transport Properties of SrTiO₃ Thin Films:

Susanne Stemmer¹; Junwoo Son¹; Nicholas Finstrom¹; ¹University of California Santa Barbara

In this presentation we report on the key properties of complex oxide thin films relevant for their application in metal/insulator/metal structures such as voltage tunable capacitors, and the relation of these properties to defects in the films. We study the dielectric and electrical properties of Pt/SrTiO₃/Pt thin film structures with controlled microstructures at frequencies up to 1 GHz. We discuss the origins of dielectric losses in these films and the role of point defects, such as oxygen vacancies. We report on dielectric deadlayers, which cause a significant reduction in the dielectric tunabilities. We discuss the influence of dielectric relaxation on the thermal leakage characteristics of Pt/SrTiO₃/Pt thin film structures. We show the influence of temperature and time-dependent leakage currents on phenomena such as anomalous positive temperature coefficient of resistivity and resistive switching.

9:30 AM Invited

Towards Defect Engineering in Resistive Switching Perovskite Thin Films:

Regina Dittmann¹; Kristov Szot¹; Ruth Münstermann¹; Paul Meuffels¹; Shaobo Mi¹; Chunlin Jia¹; Rainer Waser¹; ¹Forschungszentrum Juelich

A variety of perovskite materials exhibit electrically induced resistive switching effects and has been proposed for future non-volatile memories. For SrTiO₃ single crystals it was shown that switching occurs along crystalline defects which form a network of filamentary conduction paths (Szot et al., Nature Mater. 5, 312 (2006)). Since the distribution of defects in SrTiO₃ is generally very irregular, the application of this material class in future resistive RAM crucially depends on the success in developing thin film fabrication routes which guarantee a more registered arrangement of these filaments. We will present the impact of growth mode conditions and the corresponding defect distribution as well as the influence of doping atoms on the nanoscale resistive switching properties of titanate thin films analyzed by conductive-tip AFM (LC-AFM). For Nb-doped SrTiO₃ thin films epitaxially grown under appropriate deposition conditions, we succeeded to obtain well ordered arrays of nanoscale resistive switching blocks.

10:00 AM Break

10:20 AM Invited

Opportunities in Ferroelectrics and Multiferroics at Short Times and High Fields:

Paul Evans¹; ¹University of Wisconsin, Madison

Thin film structures with high-bandwidth electrical contacts make it possible to understand complex oxide materials at short timescales – in the range of hundreds of picoseconds at present and perhaps a few to tens of picoseconds in the near future. The magnitudes of electric fields applied under these conditions can reach several MV/cm, far higher than the fields associated with dielectric breakdown at low frequencies. Our time-resolved synchrotron microdiffraction structural studies of ferroelectric Pb(Zr,Ti)O₃ thin provide insight into polarization domain dynamics under electric fields close to the coercive field and into piezoelectricity at higher fields. Thin films of multiferroic BiFeO₃ has a more complicated symmetry than the tetragonal Pb(Zr,Ti)O₃ and structurally non-uniform at several length scales. We will describe structural studies of BiFeO₃ under high fields and switching between different polarization domain configurations.

10:50 AM Invited

The Mechanism of Pulsed Laser Deposition of Epitaxial Oxide Films

Studied by Time-Resolved Surface X-Ray Diffraction: Gyula Eres¹; ¹Oak Ridge National Laboratory

The laser plume ejected from a solid target consists of a complex mixture of neutral and ionized atoms, molecular fragments, and even small clusters with kinetic energies up to a few hundred eV. The extra kinetic energy provides a transient enhancement of surface mobility that affects the nucleation and growth of thin films. We use time-resolved surface x-ray diffraction to study the formation and evolution of surface structure during PLD of SrTiO₃. The use of x-ray diffraction greatly simplifies growth kinetics studies because in the kinematic limit the x-ray intensity changes correspond directly to coverage evolution. We analyze the intensity transients using a model independent approach that allows direct determination of the time-dependent surface coverages from the transient intensities. This analysis reveals that energy-enhanced interlayer transport occurs on a time scale of microseconds or less and it dominates crystallization and growth with the thermal component playing a negligible role.

11:20 AM Invited

Dynamics of Strained Film Growth on Vicinal Substrates:

Mina Yoon¹; ¹University of Tennessee

We theoretically study the morphological evolution in heteroepitaxial growth. We establish the existence of a deposition flux window within which stable and persistent step-flow growth can be achieved. We express the phase boundaries in terms of intrinsic physical parameters and experimentally controllable growth conditions.¹ Also, investigating the growth dynamics in the step-bunching regime, we found that there is a critical film thickness above which step-bunching occurs. The critical thickness shows a scaling behavior depending on the terrace width and the deposition flux.² We compare above predictions with experimental results from PLD growth studies of metal oxide thin films.^{1,2} Our results may open a way to grow films in a desired way. We will also discuss the role of step meandering in the above findings. ¹W. Hong et al., Phys. Rev. Lett. 95, 095501 (2005). ²M. Yoon et al., Phys. Rev. Lett. (2007).

11:50 AM

Domains Evolution under a Spatially Non-Uniform Applied Electric Potential: Phase-Field Simulation and Experiment:

Samrat Choudhury¹; Jingxian Zhang¹; Sergei Kalinin²; Long Chen¹; ¹Pennsylvania State University; ²Oak Ridge National Laboratory

A three-dimensional (3-D) phase-field model is developed for predicting the evolution of domain structures in ferroelectric thin films under a non-uniform externally applied electric potential. In this work, we considered lead zirconate titanate (PbZr(1-x)TiO₃) ferroelectric thin films as model systems. The temporal evolution of domain structures during switching will be presented. It was observed that the electric potential required to nucleate new domains during polarization switching in ferroelectric thin films varies spatially within a domain structure. The lowest electric field for nucleation is observed near the twin domain boundaries. Comparison of the spatial distribution of nucleation voltage obtained from phase-field approach shows an excellent agreement with our experimental measurements using Piezo-force microscopy technique.

Preliminary simulation and experimental results on the effect of grain boundary on switching behavior of ferroelectric thin films under a non-uniform applied electric potential will be discussed.

12:10 PM

Phase-Field Prediction of Enhanced Piezoelectric Response in Ferroelectric Islands: *Jingxian Zhang*¹; Ryan Wu¹; Samrat Choudhury¹; Shenyang Hu²; Yulan Li¹; Long-Qing Chen¹; ¹Pennsylvania State University; ²Los Alamos National Laboratory

In continuous ferroelectric thin films, the extrinsic contribution to piezoelectric response from the non-180° polarization switching is highly limited by the substrate constraint. Therefore, enhanced piezoelectric responses are expected by cutting the film into discrete islands to relieve the substrate clamp. In this work, a phase-field model has been developed for studying the domain structures and their evolutions in epitaxial ferroelectric islands. The piezoelectric properties of PbZr_{0.2}Ti_{0.8}O₃ ferroelectric islands are investigated by using the phase-field model. Much larger piezoelectric coefficients are obtained for the islands due to the 90° polarization switching, and the magnitude of the piezoelectric coefficients depends on the substrate strains and the lateral sizes of the islands. These results clearly demonstrate that the relaxation of substrate constraint plays a critical role on the piezoelectric response in the ferroelectric islands.

Computational Thermodynamics and Kinetics: Phase Transformations

Sponsored by: The Minerals, Metals and Materials Society, TMS Electronic, Magnetic, and Photonic Materials Division, TMS Materials Processing and Manufacturing Division, ASM Materials Science Critical Technology Sector, TMS: Chemistry and Physics of Materials Committee, TMS/ASM: Computational Materials Science and Engineering Committee, TMS/ASM: Phase Transformations Committee

Program Organizers: Yunzhi Wang, Ohio State University; Long-Qing Chen, Pennsylvania State University; Jeffrey Hoyt, McMaster University; Yu Wang, Virginia Tech

Wednesday AM
March 12, 2008

Room: 288
Location: Ernest Morial Convention Center

Session Chairs: Chen Shen, GE Global Research; Hamish Fraser, Ohio State University

8:30 AM Invited

On the Nucleation of Alpha-Ti in Alpha/Beta-Ti and Beta-Ti Alloys: Soumya Nag¹; Arda Genc¹; Rajarshi Banerjee²; Gopal Viswanathan¹; *Hamish Fraser*¹; ¹Ohio State University; ²University of North Texas

This paper presents experimental observations that lead to mechanistic details of the nucleation processes in alpha/beta and beta Ti alloys. For alpha/beta Ti alloys, the formation of Widmansaetten plates of the alpha phase from prior beta grain boundaries producing colony microstructures and the nucleation of the alpha plates that make up basketweave microstructures have been considered. Here, 3D characterization of the effects of grain boundary misorientation and grain boundary plane orientation on sideplate growth in has been studied, and observations have been made of the very early stages of nucleation in both types of microstructures. The nucleation of secondary alpha in beta ribs has been the subject of study, and the possible role of martensitic transformations in nucleation considered. Finally, the refined precipitation of alpha-Ti in beta stabilized alloys has been studied and the effects of beta phase separation and the omega phase on nucleation have been identified.

8:55 AM Invited

Physical Models for Heterogeneous Nucleation in Aluminium-Based Solid Solutions: *Barry Muddle*¹; Yury Kryvasheyev²; ¹Monash University, Centre for Design in Light Metals; ²Monash University, School of Physics

Effective computational analysis of phase transformations requires that not only are the algorithms employed sound in thermodynamic and kinetic principles, but that the physical models of the processes involved be reliably based. In the case of precipitation from supersaturated solid solution, this includes both the mechanisms of nucleation and growth, and the nature of any interactions

that influence, in particular, nucleation. In the specific case of precipitation-strengthened aluminium alloys, nucleation of key strengthening phases is invariably heterogeneous and preferred locations for nucleation may range from pre-existing static defects to sites defined dynamically during early stage decomposition. In most cases, the mechanisms by which such sites reduce the barrier to nucleation remain ill-defined and an inadequate physical basis limits the effectiveness of process models. The limitations of available physical models will be examined for a selection of the more common modes of heterogeneous nucleation in aluminium-based solid solutions as model systems.

9:20 AM

Phase Field Simulation of Autocatalytic Precipitation in the Al-Cu System: *Yury Kryvasheyev*¹; Barry Muddle¹; Chen Shen²; Yunzhi Wang²; ¹Monash University; ²Ohio State University

Phase transformations in coherent systems are strongly influenced by the matrix-product coherency strains, in some cases responsible for the formation of self-organized structures. In the case of θ' precipitation in Al-Cu, patterns of precipitates, formed in inclined parallel stacks or dual-variant cross-like arrays, are presumed to be the product of autocatalytic nucleation. It is suggested that elastic interaction promotes nucleation in specific locations within the strain field of a precursor crystal, leading to strong spatial correlation in the precipitate distribution. The model proposed is based on phase field evolution kinetics coupled with an explicit nucleation algorithm. Microstructural patterns formed during autocatalysis are compared for two forms of transformation strain – a pure uniaxial distortion and an invariant plane strain. The latter implies a diffusional-displacive mechanism of transformation and, aside from simulation of observed precipitate arrays, the model has the potential for verifying indirectly the nature of transformation strain during nucleation.

9:35 AM

A Comparison of Simulated Crystal Nucleation Times with Nucleation Theory for the Lennard-Jones Liquid: *Lujian Peng*¹; Rachel Aga²; James Morris²; ¹University of Tennessee; ²Oak Ridge National Laboratory

In previous work, we showed that when simulation size effects and transient nucleation theory were considered, crystal nucleation times from simulations could be predicted using classical theory. We have now extended this to the Lennard-Jones system. Homogeneous crystal nucleation is simulated by molecular dynamics. We study nucleation time as a function of system size and temperature. We present quantitative comparisons between our results and classical nucleation theory, including transient effects. This is done without parameter fitting, using interfacial free energies and other properties calculated from separate equilibrium simulations. The role of temperature-dependent interfacial free energies is explored. We compare with previous results that showed good agreement with the classical theory. This research has been sponsored by the Division of Materials Sciences and Engineering, Office of Basic Energy Sciences, U.S. Department of Energy under contract with DE-AC05-00OR-22725 with UT-Battelle.

9:50 AM Invited

Phase Field Modelling of Rafting in Ni Base Superalloys: Alphonse Finel¹; *Yann Le Bouar*²; Anaïs Gaubert¹; ¹ONERA; ²CNRS

Mechanical behaviour of Ni base superalloys depends largely on the microstructure at meso scale. Initially, the alloy consists in cuboidal precipitates of the γ' phase separated by channels of γ matrix. When such a material is submitted to a creep loading at high temperature, we observe a directional coalescence of the γ' precipitates. This morphological evolution, usually called rafting, is a result of the elastic stresses generated by the misfit between the precipitate and matrix phases. In addition, during rafting, plastic strain is generated in the matrix and enables a partial relaxation of the misfit stresses. The aim of this study is to propose a phase field model to represent in a quantitative way the microstructural changes in superalloys during a creep loading. In the model, the plastic activity in the γ phase is introduced by the means of a viscoplastic law coupled with the phase field model.

10:15 AM

The Pre-Wetting Transition at Anti-Phase Boundaries: An Atomistic Modeling Study of Ni₃Al: Chandler Becker¹; Yuri Mishin²; William Boettinger¹;¹National Institute of Standards and Technology; ²George Mason University

Using an embedded-atom potential for Ni-Al alloys, we have examined interfacial properties of antiphase boundaries (APBs) in the Ni₃Al-based γ phase. These interfaces between different ordering domains of the γ phase can undergo a pre-wetting transition, in which the APB region becomes disordered and then transforms into a thin layer of metastable γ phase. To understand this transition, we have performed detailed thermodynamic, compositional, and structural analyses of the APBs using semi-grand canonical Monte-Carlo simulations, with particular interest in composition profiles of Ni segregation and local atomic disorder. We discuss our findings in the context of previous studies of these interfaces and the possible impact of the APB pre-wetting on properties of γ - γ' alloys.

10:30 AM Break

10:50 AM Invited

Deterministic Sidebranching Mechanism in 3-D Dendritic Growth: Martin*Glicksman*¹; John Lowengrub²; Shuwang Li²; ¹University of Florida; ²University of California, at Irvine

We demonstrate the existence of a new mechanism for the generation of 3D side-branches in dendritic solidification. The proposed deterministic branching mechanism is induced directly via the interfacial boundary conditions, without benefit of noise or other stochastic phenomena. To support the new finding we developed accurate boundary integrals for simulating 3D solidification. Numerical results reveal that both anisotropic capillarity and kinetics induce non-monotone temperature distributions along the dendritic interface. The consequent dynamical process operates as a "limit cycle" generating a sequence of time-periodic protuberances near the dendrite tip. These protuberances grow and develop into secondary side-branches, setting the all-important scale of chemical microsegregation. Unlike conventional explanations of side branching, based on extrinsic influences, such as selective noise-amplification and loss of stability, we demonstrate that the generation of side-branches during dendritic growth is intrinsic to the solidification process, occurring via deterministic interactions at the solid-liquid interface.

11:15 AM

Orientation Selection in Dendritic Solidification of Materials with Hexagonal Symmetry: Tomorr Haxhimali¹; Alain Karma¹; Mark Asta²; Jeffrey Hoyt³;¹Northeastern University; ²University of California, Davis; ³McMaster University

The prediction of dendrite growth rate and orientation during dendritic solidification is crucial to control the morphology of solidification microstructures and thus the associated mechanical properties of cast and welded materials. In this talk we present recent results from a theoretical and phase-field study of dendrite growth rate and orientation selected during the dendritic solidification of materials with hexagonal symmetry with magnesium as a special case. The phase-field and theoretical study were performed by varying parameters that characterize the anisotropy of the crystal-melt interfacial free-energy. For anisotropy parameters that were estimated from recent atomistic simulation for pure magnesium, we show that dendrite grow along the basal plane as expected. Moreover we predict the existence of anomalous directions off basal plane by varying the anisotropic parameter, which is equivalent to changes in composition. These directions have been often observed by experimental studies in different magnesium and hcp alloys.

11:30 AM

Microstructure Formation in Ni-Base Superalloys during Solidification and Its Relation to the Eutectic-Peritectic Nature of the Gamma/Gamma-Prime Reaction: Nils Warnken¹; Roger Reed¹; ¹University of Birmingham

The microstructure formation in directionally solidified Ni-base superalloys is simulated using the phase-field method (MICRESS) with a special emphasize on the last stages of solidification and the interdendritic gamma-prime formation. The latter is commonly referred to as eutectic islands, although recent research indicates that it should be renamed to peritectic islands. Thermodynamic databases model it either way. The calculated microstructures yielded from both types of databases are compared in order to identify whether the type of the

reaction has a significant influence on the as-cast microstructure formed during directional solidification.

11:45 AM

Stress-Induced Instability and Break up in Multilayers: B. Chirranjeevi¹; Mogadalai Gururajan²; Thennathur Abinandanan³; ¹Indian Institute of Technology-Madras; ²Northwest University; ³Indian Institute of Science

Evolution of multilayers of elastically stiff and soft phases has been studied using a phase field model. When the interfaces are coherent and the phases have a lattice parameter mismatch, the hard phase is known to be unstable. Our phase field simulations capture — quantitatively — the key features of this instability for a single, isolated stiff film sandwiched between two semi-infinite soft matrix substrates. In a multi-layer setting (i.e., with an increasing volume fraction of the stiff phase), several new features emerge: (a) the onset of instability changes from a predominantly anti-symmetric mode to a symmetric one; (b) the dominant wavelength increases, thereby delaying the eventual break-up; (c) inter-layer correlations develop right from early stages of evolution, leading to a highly correlated microstructure after the complete break-up. These features will be presented and rationalized.

12:00 PM

A New Approach for Modeling Strongly Anisotropic Crystal Systems: Solmaz*Torabi*¹; John Lowengrub¹; Steven Wise²; ¹University of California-Irvine; ²University of Tennessee

We present a new approach for modeling strongly anisotropic crystal and epitaxial growth using regularized, anisotropic Cahn-Hilliard-type equations. Such problems arise during the growth and coarsening of thin films. When the surface anisotropy is sufficiently strong, sharp corners form and unregularized anisotropic Cahn-Hilliard equations become ill-posed. Our models contain a high order Willmore regularization to remove the ill-posedness. A key feature of our approach is the development of a new formulation in which the interface thickness is independent of crystallographic orientation. We also have added strain energy to this model to study the effect of elasticity. We present 3D numerical results using an adaptive, nonlinear multigrid finite-difference method. In particular, we find excellent agreement between the computed equilibrium shapes using the Cahn-Hilliard approach, with a finite but small Willmore regularization, and an analytical sharp-interface theory recently developed by B. J. Spencer [2004].

12:15 PM

Monte Carlo Simulation of Binary bcc Structured Layers Growth: Ruiqiang*Zhang*¹; Xiaohong Xu¹; Shunyan Zhang¹; Gillian Gehring²; ¹Shanxi Normal University; ²University of Sheffield

A very promising method for thin (of nanoscale thickness) layer fabrication is the pulsed laser deposition (PLD) method. In this paper, the growth of perovskite structured film grow on a perovskite substrate is simulated using the Monte Carlo procedure, and LaMnO₃ is taken as an example. In the model, we consider the La and Mn atoms and assume the oxygen atoms follow the metal atoms. The quality of the film is controlled by three parameters, namely, the temperature of the substrate, the kinetic energy of the atoms and the average coverage of each pulse. The simulated results show that the quality of the films is strongly dependent on the three parameters. We analyzed the mismatch of the films and find an interesting phenomenon; the displacement parameter presents odd-even staggering (OES) when the deposition condition near the best situation.

Emerging Interconnect and Packaging Technologies: Pb-Free Solders: Reliability and Microstructure Development

Sponsored by: The Minerals, Metals and Materials Society, TMS Electronic, Magnetic, and Photonic Materials Division, TMS: Electronic Packaging and Interconnection Materials Committee

Program Organizers: Carol Handwerker, Purdue University; Srinivas Chada, Medtronic; Fay Hua, Intel Corporation; Kejun Zeng, Texas Instruments, Inc.

Wednesday AM
March 12, 2008

Room: 275
Location: Ernest Morial Convention Center

Session Chairs: Laura Turbini, Research In Motion; Eric Cotts, Binghamton University

8:30 AM Invited

Microstructure, Defects, and Reliability of Mixed Pb Free/SnPb Assemblies: Polina Snugovsky¹; H. McCormick¹; S. Bagheri¹; Z. Bagheri¹; C. Hamilton¹; M. Romansky¹; ¹Selestica

The paper describes the results of an intensive study on Pb free BGA / SnPb solder assemblies as well as some lessons learnt dealing with mixed assembly production at Celestica. In the reliability study, four types of Pb free ball grid array components were assembled on test vehicles using the SnPb eutectic solder and typical SnPb reflow profiles with 205-220°C peak temperatures. Accelerated thermal cycling was conducted at 0 to 100°C. The microstructure after reflow and ATC was analyzed. The influence of the microstructure on Weibull plot parameters and failure mode will be shown. Interconnect defects such as non-uniform phase distribution, low melting structure accumulation, and void formation will be discussed. Recommendations on mixed assembly and rework parameters will be given.

9:00 AM Invited

Thermomechanical Behavior and Reliability of Pb-Free Solders: Nikhilesh Chawla¹; ¹Arizona State University

The thermal fatigue resistance of Sn-rich solder joints is dependent on the initial microstructure and the damage evolution during thermal cycling. In this talk we have report on the thermal fatigue behavior of single lap shear Sn-rich solder/Cu joints under cyclic thermal loading. Microstructure characterization of the initial and damaged solder joint microstructures was carried out by scanning electron microscopy (SEM). Persistent slip bands, was followed by crack nucleation and propagation at the tip of the lap shear geometry. The influence of Sn grain orientation on thermal fatigue damage was modeled using the finite element method (FEM). The grain orientation was determined by orientation image mapping (OIM) and a Schmid factor analysis was performed to determine the active slip systems in the Sn grains. It was found that the geometry of the lap shear joint, rather than Sn grain orientation, was more significant in determining the location of crack initiation.

9:30 AM Invited

Numerical and Experimental Analysis of Ball Grid Array Packages during Random Vibration: Fengjiang Wang¹; Matthew J. O'Keefe¹; Brandon Brinkmeyer¹; ¹University of Missouri-Rolla

With the transition from Sn-Pb to Pb-free solder, board level vibration testing for high reliability applications, i.e. the aerospace industry, is needed. In particular, ball grid array (BGA) packages are susceptible to mechanical failure due to the stress/strain in the solder balls from the relative motion between the BGA and substrate. The location of components on the printed circuit board (PCB) impacts reliability as a function of component type and solder alloy composition. Currently, there is limited information on the dynamic response of PCBs and Pb-free solder joints that relates stress/strain to solder joint reliability under random vibration. In this work, finite element modeling was used to determine how size and location impacts Pb-free and Sn-Pb BGA packages on a PCB. Random vibration in the frequency range of 20-2000 Hz was simulated using different root mean square accelerations. Correlation of the modeling to experimental results will also be discussed.

10:00 AM Break

10:15 AM

Bending Reliability of Combination Solder Joint in Mounted on Several Types of Pad Finish of Halogen Free PCB: Si-Suk Kim¹; Hun Han¹; Hyun-Jeong Ham¹; Yong-Hyun Kim¹; Dong-Chun Lee¹; Si-Don Choi¹; ¹Samsung Electronics

According to the transition of pb-free and demand for halogen free based on environmentally friendly product, we are considering applying low temperature soldering which is a combination solder joint between Sn3.0Ag0.5Cu solder ball and Sn57Bi.1.0Ag solder paste into halogen free pcb. It has lower soldering temperature compared to Sn3.0Ag0.5Cu solder system. So we have studied on bending reliability about this system. We used several types of halogen free pcb finish and pad designs in 512MB memory module. We carried out 3 point bending test. After bending test, we analyzed fracture mode using EDX, SEM and D&P(Dye & Pry). Consequently, we figured out good reliability in order ENIG+NSMD>OSP+SMD=Immersion Ag+SMD>OSP+NSMD=Immersion Ag+NSMD > ENIG+SMD. Solder joint strength for OSP or Immersion-Ag pad finish is stronger than that of ENIG pad. In addition, Cu adhesion strength of halogen free pcb is lower than normal FR4 pcb, which led to low reliability life.

10:30 AM Invited

Effect of Crystal Orientations of Copper and Tin on Recrystallization during Thermomechanical Cycling of Pb-Free Solder Joints: Amir Zamiri¹; Thomas Bieler¹; Adwait Telang¹; Farhang Pourboghra¹; ¹Michigan State University

It is known that many, and possibly most lead free solder joints consist of only a few crystal orientations. In many cases, sections of joints show only one orientation, suggesting that one crystal orientation may have a highly favorable orientation that minimizes elastic and/or plastic strain energy during thermal cycling. If so, then it is important to identify what orientations are energetically favored by the alternating stress states in a joint, and to determine how these orientations may grow to consume other existing orientations. Experimental measurements of a particular example of this phenomenon are presented along with computational modeling using elastic and plastic FEM analysis of particular orientations to quantify energy changes. Minimum elastic energy orientations are identified, and the texture of the copper appears to be influential, as copper has a strong elastic anisotropy.

11:00 AM

Interfacial Reaction between the Electroless Nickel Immersion Gold Substrate and Sn-3.0Ag-0.5Cu Solder: Ruihong Zhang¹; Zhidong Xia¹; Fu Guo¹; ¹Beijing University of Technology

Electroless nickel immersion gold (ENIG) is one of the most widely used surface finishes on the Cu substrate in electronic packages. The formation and growth of intermetallics compounds (IMCs) at the solder/substrate interface are key factors affecting the solderability and reliability of electronic solder joints. This study will be focused on the morphology and growth of the interfacial IMCs at the interface of Sn-3.0Ag-0.5Cu solder and ENIG substrate. Three kinds of ENIG finishes with different Au thickness will be chosen to study the effects of Ni and Au layer on the IMCs and reliability of solder joints through isothermal aging studies, shear testing, and thermomechanical fatigue testing. The effects of Au layer on the morphology of the IMCs both at the solder/substrate interface and in the bulk solder will be looked into in details. The relationship between interfacial IMCs and reliability in various solder/ENIG/ Cu substrate systems will be established.

11:15 AM

The Effect of Microstructure on the Fatigue Life of Lead Free Solders: Babak Arfaei¹; Peter Borgesen²; Pushkraj Tumne¹; James Woods¹; Jeremy Wolcott¹; Eric Cotts¹; ¹State University of New York; ²Unovis-Solutions

To understand the mechanical behavior of Sn-Ag-Cu solder joints, the evolution of Sn grains morphologies, Sn grain orientations, and precipitate (Ag₃Sn and Cu₆Sn₅) microstructures must be characterized. This study examined the mechanical response of Sn-Ag-Cu solder (SnAg₂Cu_{0.5} (weight percent) on Cu pads on a high-Tg FR-4 substrate) in a load controlled shear fatigue test on individual solder balls. After failure, balls were individually mounted, cross sectioned, polished and examined by means of optical microscopy (with cross polarizers and in bright field conditions), and by electron backscattered

diffraction in an scanning electron microscope. Differences in the plastic deformation fields in different Sn grains in selected solder joints were examined. Correlations of variations in fatigue life of solder balls with the Sn grain size, number and orientation, and with precipitate size and number are reported.

Emerging Methods to Understand Mechanical Behavior: Electron and Neutron Diffraction

Sponsored by: The Minerals, Metals and Materials Society, TMS Structural Materials Division, TMS Materials Processing and Manufacturing Division, TMS: Advanced Characterization, Testing, and Simulation Committee, TMS/ASM: Mechanical Behavior of Materials Committee, TMS: Nanomechanical Materials Behavior Committee
Program Organizers: Brad Boyce, Sandia National Laboratories; Mark Bourke, Los Alamos National Laboratory; Xiaodong Li, University of South Carolina; Erica Lilleodden, Forschungszentrum

Wednesday AM Room: 285
March 12, 2008 Location: Ernest Morial Convention Center

Session Chair: To Be Announced

8:30 AM Invited

New Insides in Deformed Microstructures by 3D EBSD-Based Orientation Microscopy: Stefan Zaefferer¹; ¹Max Planck Institute for Iron Research

We have developed a system for fully automated 3D orientation microscopy. It is based on precise serial sectioning by a focused ion beam (FIB) and EBSD-based orientation microscopy for characterisation of the sections. The technique delivers 3D crystal orientation maps with a resolution of 50 x 50 x 50 nm³. We have applied this new technique to the characterisation of various deformed microstructures: in order to get a better inside into the deformation process occurring during nano-indentation we observed the rotation fields and dislocation density distribution created by nano-indents into a copper single crystal. It was found that the deformation field expands in a self-similar manner with increasing indentation depth. Second, we applied the technique to study the microstructure of a heavily cold rolled FeNi alloy. Aim was to investigate the internal structure and local surrounding of cube-oriented areas. These areas are known to recrystallise first during an annealing treatment.

9:00 AM

The Importance of Grain Boundary Network Structures in Intergranular Failure: Bryan Reed¹; Robert Rudd¹; Eira Seppala²; Roger Minich¹; Mukul Kumar¹; ¹Lawrence Livermore National Laboratory; ²Noki Research Center

With the rising availability of electron backscatter diffraction (EBSD), it is now possible to generate reliable statistical information about the networks of grain boundaries in polycrystalline materials. This analysis reveals strongly correlated clusters containing tens (sometimes hundreds) of grains with unusually high concentrations of coincident site lattice (CSL) grain boundaries. These clusters are particularly well developed in grain boundary engineered materials. When engineered and normal versions of nickel alloy are subjected to intergranular stress-corrosion cracking (in which the engineered material failed up to five times more slowly), we find that the fracture surfaces look completely different on the length scale governed by these clusters. We show how the combination of EBSD, mathematical models, and fracture analysis yields insights into the workings of intergranular fracture in general and grain boundary engineered materials in particular.

9:20 AM

Combining Experimental and Simulation Methods for Investigation of Microstructural Cyclic Plasticity: Luke Brewer¹; Corbett Battaile¹; Brad Boyce¹; ¹Sandia National Laboratory

To develop truly predictive models that connect specific microstructures with changes in cyclical mechanical behavior, it is vital to combine experiment and simulation at the same, microstructural length scale. This talk will discuss the use of microstructurally-sensitive experimental techniques, such as electron back-scattered diffraction (EBSD), to provide starting microstructural information to simulation methods and to validate the predictions from these simulations. This study involves high-purity, polycrystalline nickel microstructures of

varying grain size. Individual microstructures were tracked throughout their deformation using both ex situ and in situ mechanical testing followed by EBSD after a certain number of cycles. This data is compared to crystal plasticity-based finite element method simulations (both local and non-local models) of the same, starting microstructure. We will discuss the technical aspects of comparing experimental and simulation data at these length scales: including choice of boundary conditions, merging of coordinate systems, and algorithms for quantification of the comparison.

9:40 AM

Effect of the Environment on Crack Initiation and Propagation within 7XXX Series Aluminum Alloys: Vipul Gupta¹; Sean Agnew¹; Richard Gangloff¹; ¹University of Virginia

Electron backscattered diffraction (EBSD) and SEM-based stereology have been applied along with focused ion beam surface preparation to investigate the crack path crystallography within 2-3 μ m of the fatigue crack initiation site of precipitation hardened aluminum alloys, 7075 and 7050. Fatigue cracking within humid air and vacuum never led to fracture surface facets parallel to {111} planes, calling into question the slip band initiation mechanism. Backscattered electron imaging and energy dispersive spectroscopy of fracture surface indicate that crack initiation always occurs at constituent clusters in alloy 7075, which are also the most common initiation site within comparatively purer alloy 7050. EBSD is used to map the grain orientations and local plastic damage near the crack initiation sites. Combining EBSD results with crack growth rates measured on the fracture surface within the microstructurally small crack (MSC) regime using a marker banding technique allows validation of microstructure-based models to explain MSC behavior.

10:00 AM

Nanoindentation-Correlated EBSD Study of Delamination Fracture in Al-Li Alloys: Wesley Tayon¹; Roy Crooks²; Marcia Domack³; John Wagner³; Abdelmageed Elmoustafa¹; ¹Old Dominion University and the Applied Research Center; ²National Institute of Aerospace; ³NASA Langley Research Center

Al-Li alloys offer attractive combinations of high strength and low density. However, a tendency for delamination fracture has limited their use. A better understanding of the delamination mechanisms may suggest a solution to this problem through processing modifications. We have brought a combination of new techniques to bear on this issue. Both high quality electron backscattered diffraction (EBSD) information and valid nanoindentation measurements were obtained from the same sampled regions. Samples were taken from as-received material and from fractured test specimens. Correlations were drawn between delamination, nanoscale property variations and local texture; and compared to associated processing parameters.

10:20 AM

Grain Boundary Engineering Alloy 800HT: Daniel Drabble¹; Milo Kral¹; ¹University of Canterbury

Grain boundary engineering has recently shown promise in its ability to improve mechanical properties of metals. The aim of the present work was to investigate the feasibility of using grain boundary engineering to improve the high-temperature properties of a common superalloy, alloy 800H/HT. A variety of sequential thermo-mechanically processing conditions were first applied to the alloy. Samples were then analysed using Electron Backscatter Diffraction (EBSD) to characterize the grain boundary character and Σ 3 grain boundary connectivity. The effects of the sequential thermo-mechanically processing on steady-state creep rate were then obtained in uniaxial tension creep tests with real-time strain measurement under common service conditions, in contrast to accelerated creep rupture tests for example.

10:40 AM Break

10:55 AM

Analysis of Orientation Gradients and Discontinuous Microstructure in Phase-Transformed Tantalum Thin Films: Ray Fertig¹; Robert Knepper¹; Max Aubain¹; Shefford Baker¹; ¹Cornell University

The equilibrium (alpha) phase of bulk Ta at room temperature and pressure is bcc, but it is possible to deposit thin films of Ta in the metastable tetragonal (beta) phase under certain conditions. We have recently discovered a unique microstructure in thin alpha-Ta films created by phase transformation from

the beta phase. This microstructure is characterized by continuous changes in orientation with position and a discontinuous boundary structure. In the present work, we use electron backscattered diffraction (EBSD) to study the orientation gradients in this microstructure. A detailed analysis of the crystal rotations was used to determine the minimum density of geometrically-necessary dislocations needed to generate the observed microstructure. Variations in dislocation density with film thickness and oxygen content suggest that the unusual microstructure arises from kinetic limitations during the phase transformation.

11:15 AM

Using Orientation Imaging Microscopy Data for Direct Input and Validation of Subgrain Texture and Microstructure Evolution of Polycrystalline Copper: *Ricardo Lebensohn*¹; Renald Brenner²; Olivier Castelnau²; ¹Los Alamos National Laboratory; ²Université Paris XIII

We present results of a numerical formulation based on Fast Fourier Transforms (FFT) to obtain the micromechanical fields in plastically deformed 3-D polycrystals using direct input from a digital image of their microstructures. The FFT-based formulation provides an exact solution of the governing equations in a periodic unit cell, has better performance than a Finite Element calculation for the same purpose and resolution, and can use voxelized microstructure data as input and for validation. To illustrate the capabilities of this model, we first discuss the construction of a 3-D unit cell using 2-D orientation maps obtained by means of Orientation Imaging Microscopy (OIM), and we then show FFT-based predictions, together with the corresponding OIM measurements, on subgrain texture evolution in a recrystallized Cu polycrystal deformed in uniaxial tension. The measured rotations of the average orientations and the orientation-dependent magnitudes of the average misorientations are well reproduced by the FFT-based model.

11:35 AM Invited

In-Situ Neutron Scattering Studies of Magnetic Shape Alloys under Stress, Temperature and Magnetic Fields: *Donald Brown*¹; Yandong Wang²; Saurabh Kabra¹; Thomas Sisneros¹; ¹Los Alamos National Laboratory; ²Northeastern University

We have utilized the SMARTS engineering diffractometer to study the crystallographic orientation and phase transformations in the ferromagnetic shape memory alloy NiMnGa under conditions of temperature and stress. Neutrons are uniquely suited to probe the crystallographic response of materials to external stimuli because of their high penetration, which allows them to sample the bulk of the material as well as pass through environmental chambers. We observed that the addition of relatively small stresses greatly effects the selection of variants during transformation from the austenitic to martensitic phase. Since the initial experiments, the capability to apply a magnetic field of 2T transverse to the loading direction has been integrated to SMARTS. The details of this new and unique capability to control all three stimuli simultaneously on a diffractometer will be presented in this talk. If all goes well in the upcoming run-cycle, preliminary results from initial experiments will also be presented.

12:05 PM

Detwinning of Pure Zirconium: In-Situ Neutron Diffraction Experiments: *Gwenaelle Proust*¹; George Kaschner¹; Donald Brown¹; Carlos Tome¹; Irene Beyerlein¹; ¹Los Alamos National Laboratory

Twinning is an important deformation mode in hexagonal polycrystalline metals to accommodate deformation along the c-axis. Twinning differs from slip in many ways, but we focus here on the behavior of twins during reversal loading. Previous in-situ neutron diffraction experiments performed on magnesium at the Lujan Neutron Scattering Center (LANSCE) show that during load reversal, the material detwins once the loading direction is changed. We have performed similar experiments on pure zirconium to see if it behaves as magnesium and to determine what role temperature plays in the detwinning mechanism. The experiments were motivated by previous studies of clock-rolled zirconium, deformed in the quasi-static regime for temperatures ranging from 76K to 450K, where it was observed that two tensile and one compressive twinning modes can be activated. We limit our study here to the behavior of the {10-12}{10-1-1} tensile twins during reversal loading at room temperature and 76K.

12:25 PM

Dynamical Diffraction Studies of Deformation Mechanisms in Ductile Intermetallic YCu: *Scott Williams*¹; Donald Brown²; Bjorn Clausen²; Alan Russell³; Karl Gschneidner³; ¹Iowa State University; ²Los Alamos National Laboratory; ³Ames Laboratory

A recent discovery has shown a family of rare earth intermetallic compounds having the B2 crystal structure which show intrinsic ductility. In-situ neutron diffraction tests while loading, conducted on YCu using SMARTS at LANSCE, have revealed the sample to be operating within the dynamical diffraction regime. The observed extinction effect is relatively uncommon within diffraction of engineering polycrystals, either because of the over-shadowing effect of true absorption (as with XRD) or because samples lack the necessary crystalline perfection. By analyzing diffraction data for changes in dynamical behavior, a new method arises for studying deformation and dislocation structure development. Examining these changes in YCu data indicate the development of large regions of perfect crystallinity as a result of annealing. With deformation, dislocation structures disrupt the perfect lattice, destroying the dynamical diffraction condition. These changes in the dislocation structure may be related to the deformation mechanisms within ductile rare earth intermetallic YCu.

Energy Conservation in Metals Extraction and Materials Processing: Session I

Sponsored by: The Minerals, Metals and Materials Society, TMS Extraction and Processing Division, TMS Light Metals Division, TMS: Aqueous Processing Committee, TMS: Pyrometallurgy Committee, TMS: Recycling and Environmental Technologies Committee

Program Organizers: Edgar Vidal, Colorado School of Mines; Cynthia Belt, Aleris International Inc

Wednesday AM
March 12, 2008

Room: 287
Location: Ernest Morial Convention Center

Session Chairs: Christopher Keller, Aleris International Inc; Cynthia Belt, Aleris International Inc

8:30 AM

Enhanced Energy Efficiency and Emission Reduction through Oxy-Fuel Technology: *Brian Patrick*¹; ¹Jupiter Aluminum Inc.

This paper describes an advanced oxy-fuel combustion technology for re-melting aluminum as well as alumina calcinations processing that significantly reduces energy consumption and emissions. This oxy-fuel combustion technology developed by Jupiter Oxygen is a patented process for combustion of fossil fuels with pure oxygen while excluding air, thereby creating an undiluted high flame temperature and increased efficiency for process heating in industrial furnaces. This unique process has led to improved heat transfer and longer residence time while maintaining the same process temperatures as with air combustion. This energy efficient combustion process allows aluminum companies to operate at a substantially lower cost due to dramatic fuel savings of approximately 70% for natural gas and waste oil. The results from more than 10 years of day-to-day experience with oxy-fuel combustion in the aluminum re-melting business are discussed.

8:50 AM

Computational Modeling of Gas Fired Immersion Heaters for Recycled Aluminum Melting: *Mohammed Hassan Ali*¹; Marwan Khraisheh¹; Shridas Ningilieri²; Subodh Das¹; ¹University of Kentucky; ²Secat Inc

Recent results have shown that the use of immersion heaters in aluminum melting is more efficient and clean compared to melting using the regular reverberatory furnaces. Immersion heater parameters including size, number, distribution, material, and heat flux characteristics affect the efficiency of the melting process. A detailed parametric study is needed to optimize the design of immersion heaters. In the present study a 3-D computational model is developed to simulate the melting process of pure aluminum using different immersion heater parameters and configurations. The results clearly show the effect of immersion heaters on the temperature distribution, molten metal natural circulation and solid fraction during melting.

WEDNESDAY AM

9:10 AM

Improving Combustion with a Low Velocity Vortex Generator Premix Industrial Gas Burner: *Tibbs Golladay*¹; ¹Burner Dynamics, Inc

Until recently, the resilience of our environment and unlimited availability of natural resources have been taken for granted and have not been seriously considered in the design of the machines that drive our industrialized world. The fact that the basic design of an industrial gas burner has not changed in over 100 years clearly demonstrates this. Unfortunately, many methods used to reduce emissions generated by the combustion of natural gas come with a trade off in efficiency and operating costs. This paper will present the advantages of utilizing a low velocity vortex generator as a method of thoroughly premixing the fuel and air immediately prior to combustion which results in closer to stoichiometric combustion than the typical design of industrial gas burners. The obvious benefits of stoichiometric combustion are more complete combustion, less undesirable by-products of combustion and more efficient heat generation.

9:30 AM

Oxyfuel - Solutions for Energy and Environmental Conservation: *Thomas Niehoff*¹; ¹Linde Gas

Many industrial processes require energy. The energy is often used for melting or heating purposes. The heat can be generated by electrical heating or combustion/oxidation of hydrocarbons. Oxygen supports the combustion process. Oxygen is naturally contained in air with about 20.9 vol.-%. The use of technical oxygen will allow an increase to the natural oxygen concentration of combustion air. Altering the combustion process by increasing the oxygen content has various effects. These effects are described and analyzed with regard to heat transfer, emissions and energy consumption. Industrial processes requiring oxyfuel are described and discussed regarding energy aspects.

9:50 AM

Global Warming Expands the Scope of Heat Pipe Applications: *Dumitru Fetcu*¹; ¹Econotherm (UK)

The paper examines several heat pipe heat exchanger approaches to heat recovery. In each approach waste energy is recovered and used to preheat air or water, to provide electricity, to provide free heat or simply to improve the efficiency of a system. The presented heat pipe concepts provide the waste heat recovery system designer with viable alternatives to classical heat transfer techniques and heat exchangers.

10:10 AM Break

10:30 AM

Waste Heat Recovery: Opportunities and Challenges: *Ilona Johnson*¹; William Choate¹; ¹BCS, Inc.

U.S. metal industries consume over 3×10^{15} Btu/year and emit > 200 million tonnes CO₂/year. Various studies estimate that as much as 30-50% of industrial energy is lost as excess or waste heat. Recovery of excess heat can conserve energy, reduce costs and lower environmental impacts. It would be useful to identify how much of this excess energy is feasibly recoverable. This can give opportunity insights to technology developers as well as organizations such as the Department of Energy Industrial Technologies Program, which funds high-risk R&D in energy efficient melting and furnace technologies. This paper discusses efforts to quantify and characterize waste heat sources and discusses opportunities for energy recovery. It examines both traditional technology applications and novel applications (e.g., advanced thermoelectric devices for recovering waste heat from exhaust gases as well as from sidewall radiation for thermal control of primary aluminum cells).

10:50 AM

Analysis of Energy Efficiency for Industrial Processes: *Cynthia Belt*¹; Ray Peterson¹; ¹Aleris International Inc

Improved energy efficiency has grown in importance within industry as energy costs have escalated. The analysis of trends and changes to a process is critical in making the best business decision in energy management. Frequently, energy use per day (Kilowatt-hour or British Thermal Units) is used to track energy efficiency. Sometimes, the somewhat more complex method of energy per processed weight (Kilowatt-hour per Metric Ton or BTU per Pound) is used to make this evaluation. Yet both methods ignore the effect due to throughput and weather. In this paper, different thermal processes and systems will be

evaluated using statistical methods to highlight alternate methods to evaluate energy efficiency. Examples and potential problems will be discussed for both a single process and a collection of processes within a plant or corporation.

11:10 AM

An Investigation of the Flame-Burden Interaction During Remelting in an Experimental Aluminum Reverberatory Furnace: *Ashwini Kumar*¹; Raj Venuturumilli¹; Paul King²; ¹ANSYS, Inc.; ²National Energy Technology Laboratory

Flame impingement on the burden is routinely encountered during the initial phase of melting in aluminum reverberatory furnaces. This impingement causes an obstructed pathway for the hot gases, and hence the circulation and residence time of the hot gases are greatly impacted. Moreover, as the load melts, the flames gradually achieve an unobstructed path leading to reduced gas residence times. This flame impingement and constantly changing combustion space volume will lead to vastly different fuel and oxidizer mixing patterns and thus affect the overall furnace performance. Fine tuning the burner operating conditions such as flow rates and injection angles with the changing combustion space could result in significant improvements to the furnace efficiency. However, one has to gain a better understanding of the furnace dynamics to know what parameters to adjust and by how much. Physical modeling can be elaborate and expensive to conduct on a regular basis while Computational Fluid Dynamics (CFD) can cost effectively address this challenge. In this study, a series of burden configurations within the furnace are modeled in a steady state manner. Each configuration can be thought of as a computational model of the furnace with the burden at a particular stage of the melting process. For each case, the thermal efficiency and behavior of the furnace are quantified. Model validation is performed by comparison with operational data from an experimental reverberatory furnace.

11:30 AM

Low Temperature Conversion of Organic Waste into Energy and Energetic Gases: *Edgar Vidal*¹; Scott Shuey²; Patrick Taylor¹; Paul Kruesi³; ¹Colorado School of Mines; ²Phelps Dodge Corporation; ³Cato Research Corporation

Abstract not available.

General Abstracts: Electronic, Magnetic, and Photonic Materials Division: Session I

Sponsored by: The Minerals, Metals and Materials Society, TMS Electronic, Magnetic, and Photonic Materials Division, TMS: Alloy Phases Committee, TMS: Biomaterials Committee, TMS: Chemistry and Physics of Materials Committee, TMS: Electronic Materials Committee, TMS: Electronic Packaging and Interconnection Materials Committee, TMS: Nanomaterials Committee, TMS: Superconducting and Magnetic Materials Committee, TMS: Thin Films and Interfaces Committee
Program Organizers: Long Qing Chen, Pennsylvania State University; Sung Kang, IBM Corporation

Wednesday AM
March 12, 2008

Room: 276
Location: Ernest Morial Convention Center

Session Chairs: Long Qing Chen, Pennsylvania State University; Sung Kang, IBM Corporation

8:30 AM

Studies on ZnO Based Diluted Magnetic Semiconductors: *Sasanka Deka*¹; ¹National Nanotechnology Laboratory of INFM

The carrier induced ferromagnetism in the transition metal (TM) doped wide band gap II-VI and III-V nonmagnetic semiconductors opened up a new area of research and potential applications in spintronics devices. Such systems, called diluted magnetic semiconductors (DMS), exhibit inherent properties from the 'charge' and 'spin' of an electron in a single material. DMSs combine their transport and optical properties with magnetism. The widely discussed DMS system, (Ga,Mn)As in the III-V series, shows the highest Curie temperature as 110 K. In the II-VI series, the widely discussed DMS system is Zn_{1-x}TM_xO (TM = Mn, Co, Ni, Fe, Cu, Cr, etc). However, the origin of ferromagnetism in this oxide based DMS is still under controversy. In most of the reports, the Curie temperature and the order of magnetism is not identical even for an identical

system. As most of the studies on DMSs were on thin films, we have carried out synthesis and studies on magnetic and optical properties on TM doped ZnO nano crystalline powder. We observed the evidence of the origin of ferromagnetism in the Co and Ni doped ZnO system as the metal nano-clusters, though optical and electronic structure studies indicate the incorporation of divalent metal ions inside the ZnO crystal lattice. ¹Pearton S. J., Abernathy C. R., Overberg M. E., Thaler G. T., Norton D. P., Theodoropoulou N., Hebard A. F., Park Y. D., Ren F., Kim J. and Boatner L. A. *J. Appl. Phys.* (2003) **93**, 1. ²Ohno H. *Science* (1998) **281**, 951. ³Deka S. and Joy P. A. *Chem. Mater.* (2005) **17**, 6507. ⁴Deka S. and Joy P. A. *Phys. Rev. B* (2006) **74**, 033201. ⁵Deka S. and Joy P. A. *Appl. Phys. Lett.* (2006) **89**, 032508.

8:50 AM

Characterization of 3-Phase (Ternary-Like) N-Type and P-Type Thermoelectric Materials Fabricated by Explosive (Shock) Consolidation: V. Muñoz¹; L. Murr²; D. Nemir³; R. Lovrenich³; E. Martinez²; S. Gaytan²; M. Lopez²; ¹OSRAM Sylvania, Inc.; ²University of Texas at El Paso; ³TXL Group

We prepared 3-phase powder mixtures of Bi-Te-Se and Bi-Te-Sb by cylindrical explosive consolidation to emulate traditional, melt-grown n-type and p-type doped Bi₂Te₃ thermoelectric materials. The powder diameters ranged from 40 μm to 3 μm, with starting Bi and Te particle Vickers microindentation hardnesses of 0.18 and 0.56 GPa, respectively in contrast to average shocked n-type and p-type monolith microindentation hardnesses of 1.15 and 1.31 GPa, respectively; compared to 0.72 and 0.68 GPa for the melt-grown n-type and p-type materials respectively. Shock consolidated monolith microstructures were characterized by optical metallography, SEM and TEM along with EDS analysis and XRD of all materials, including the melt-grown materials which had measured thermoelectric parameters considerably in excess of the shock (explosively) consolidated monoliths. Notable shock microstructures were characterized as deformation twins, while the melt-grown materials contained considerable, fine eutectic microstructures.

9:10 AM

Effect of Nb Addition on Magnetic Properties and the Microstructure of Fe₃B/Nd₂Fe₁₄B Nanocomposite Permanent Magnets: You Jun Hua¹; ¹Northeastern University

The microalloying effect of Niobium on the microstructure and magnetic properties of Nd₂Fe₁₄B/Fe₃B nanocomposite permanent magnet has been investigated. As a result, Niobium addition stabilizes the amorphous phase and hinders the kinetics of the crystallization of the Fe₃B particles. Niobium added in combination with Cu reduces grain size of Fe₃B particles more remarkably than that without Niobium; with Niobium addition enhances magnetic properties of the alloy, but the amount must be suitable. Optimum magnetic properties with B_r=1.15T, J_{Hc}=467kA/m and (BH)_{max}=132.7kJ/m³ were obtained by annealing a melt-spun Nd_{5.5}Fe_{70.0}Co₅Cu_{0.5}Nb_{0.5}B_{18.5} amorphous ribbon at 670°C for 40min.

9:30 AM

Electrical and Thermal Stress Effect on Switching Process of VDMOSFETs: Chafic Salame¹; Pierre Mialhe²; ¹Lebanese University; ²Perpignan University

Evolutions of the switching parameters of commercial VDMOSFET after a hot carrier injection are inspected. Experiment was done by hot carrier injection, where a large drain-source voltage is applied to reverse bias the Body drain junction then inducing a 30 mA reverse current. Switching time parameters were measured at different temperature and up to 300°C. The experimental results show that the device rise time decreases significantly for the first period of stress at room temperature, making the device faster during his turn-on switch. This event was associated to the high electric field in the junction that pulls electrons from the oxide gate into the channel, thus leaving trapped holes in the oxide bulk due to their low mobility. This study has an important value in terms of engineering application where speed of electronic devices is one of the most valuable parameters in communication and information technology fields.

9:50 AM Break

10:20 AM

Electrical Characterisation of Tantalum Anodes for Use in Semiconductors: Rizwan Rahman Rashid¹; Siva Jyothi¹; Rajkiran¹; Prasad Goud¹; ¹Mahatma Gandhi of Technology

This paper reveals the studies on the processing and electrical properties of tantalum anodes using tantalum powder. Processing methods of tantalum anodes using high purity sodium reduced tantalum powder, compaction, sintering and dielectric layer formation were studied. Different loads were applied while compacting the tantalum powder for making green anodes prior to high vacuum sintering to study its effect on the electrical properties of the Ta pellet. Different formation voltages were applied during the dielectric layer formation and then the capacitance measurements were carried out. This paper discusses these studies carried out as a project work in C-MET (Centre for Materials for Electronics Technology).

10:40 AM

Experimental Study of Co-Deposition of SiO₂ and GeO₂ in a Modified Chemical Vapor Deposition (MCVD) Reactor: Mainul Hasan¹; Shiliang Zhan¹; ¹McGill University

MCVD reactors are used to commercially manufacture high quality optical fibers. A MCVD reactor consists of a slowly rotating, fire polished silica tube wherein a mixture of gaseous silicon tetrachloride (SiCl₄), germanium tetrachloride (GeCl₄) and carrier oxygen gas is introduced at one or both ends of the tube. The tube is heated by slowly traversing an oxy-hydrogen torch to allow for the high temperature chemical reactions to produce fine particles of SiO₂ and GeO₂. These particles move with the un-reacted gas mixture and deposit onto the inner surface of the tube. Co-deposition experiments were carried out on a laboratory scale MCVD reactor. The thickness of the deposited layer and the concentrations of germanium, silicon and oxygen were measured by EDS. Experimental results were obtained by varying the torch heat fluxes (temperatures), torch moving speed, tube rotational speed, carry-on gas amount and in-take ratio of GeCl₄/SiCl₄.

11:00 AM

Extraction of MOSFET Devices Electrical Parameters Evolution at High Temperatures: Chafic Salame¹; Roland Habchi¹; ¹Lebanese University

Junction parameters of a MOSFET (Metal Oxide Semiconductor Field Effect Transistor) device are calculated based on a numerical double exponential model. The temperature dependence of these parameters is investigated; their evolution allows the evaluation of device's operation reliability in high temperature environments. The values of the shunt and series resistance, the ideality factor, the diffusion and recombination currents are determined. The accuracy of the model is investigated at high temperature.

General Abstracts: Materials Processing and Manufacturing Division: Forging, Forming, and Powder Processing

Sponsored by: The Minerals, Metals and Materials Society, TMS Materials Processing and Manufacturing Division, TMS/ASM: Computational Materials Science and Engineering Committee, TMS: Global Innovations Committee, TMS: Nanomechanical Materials Behavior Committee, TMS/ASM: Phase Transformations Committee, TMS: Powder Materials Committee, TMS: Process Technology and Modeling Committee, TMS: Shaping and Forming Committee, TMS: Solidification Committee, TMS: Surface Engineering Committee

Program Organizers: Ralph Napolitano, Iowa State University; Neville Moody, Sandia National Laboratories

Wednesday AM
March 12, 2008

Room: 282
Location: Ernest Morial Convention Center

Session Chairs: John Carsley, General Motors Corporation; Amine Benzerga, Texas A&M University

8:30 AM

Further Development on a Flashless Precision Forged Two-Cylinder-Crankshaft: *Sven Mueller*¹; ¹IPH - Institut für Integrierte Produktion Hannover gGmbH

Precision forging is defined as a flashless near-net-shape forging. A quality in the tolerance class from IT 8 to IT 10 can be achieved. The flashless precision forging offers an integrated heat treatment with the forging heat, because a clipping process is not necessary. After the forging and heat treatment often only a final fine machining of the functional surface with small chip volume is required. In the collaborative research project SFB 489 a two-cylinder-crankshaft is selected as an example for complex flat long pieces with a characteristic mass distribution along the longitudinal axis. The continuative development considers the thermal and mechanical tool stresses, which are also as complex as the crankshaft itself. Further on a parameter study on a bi-directional forging tool is made. It is planned to test the forging sequence, tools, cooling systems and measuring technology of the developed process in the end of 2007.

8:50 AM

The Effect of the Residual Stress on the Inner Surface Cracking during Small-Radius Bending of AA6111 Sheets: *Zhuoqun Li*¹; *Xin Wu*¹; ¹Wayne State University

Small-radius bending is one of the widely used methods in sheet metal hemming for manufacturing autobody closure panels, and by bending over a straight-edge the bendability of sheet metals can be assessed. During unloading from bending residual stress develops that not only causes geometrical change due to springback, but also leads to a residual tensile stress on the inner surface which, depending on the bending geometry and material's fracture behavior, can be sufficiently high to cause material fracture. To date, majority of the bending studies have emphasized mainly on outer surface fracture and springback, but limited study exists on inner surface fracture. In this paper, fracture of inner surface in bending AA6111 sheets was observed and characterized by SEM and OM, and the stress development during small-radius bending and springback were analyzed that can describe the inner surface cracking process.

9:10 AM

Controlled Sheet Metal Straightening: *Richard Krimm*¹; *Bernd-Arno Behrens*¹; ¹Institute for Metal Forming and Metal-Forming Machines

Straightening the sheet-metal in advance of forming operations needs to be improved. Today the straightening rolls are positioned manually or by means of an adjustment unit by the machines operator using his expert knowledge. A controlled adaptation of the rollers positions to the depending on the coil-radius variable curvature and properties of the sheet-metal is not realised yet. For this reason the flatness of the straightened sheet metal is limited and modifies while unreeling the coil. The paper shows a way to control the roller positions depending on the residual bending of the straightened sheet metal. The controlling system of a testing straightener was amended to vary the roller positions in dependence of the sheet metals residual bending. Using adequate controller settings it was

possible to stabilise the straightening process to a certain extend and to obtain good straightening results from coiled sheet metal.

9:30 AM

Metal Hardening Models at Large Strains - FEM Validation with Digital Image Correlation: *Wayne Cai*¹; *John Carsley*¹; *Dan Hayden*¹; *Louis Hector*¹; *Tom Stoughton*¹; ¹General Motors Corporation

Simulation accuracy of large strain deformation of sheet metals, as occurs during hemming and in vehicle crash situations, is limited because existing hardening laws (true stress - strain relationships) are calibrated from data only in the uniform deformation regime and require extrapolation in the diffuse and localized necking stages. A reverse engineering method was developed to predict hardening laws for large strains beyond uniform elongation. The method was implemented as a code requiring uniaxial tensile test data and finite element analysis. The true stress - true strain data pairs were determined when the load - displacement history of a tensile test matched the FEA results. Test cases showed that true stress - true strain relationships were generated for very large strains (75% for AA6111, and 85% for DP600). The method was validated using digital image correlation techniques for strain measurement on the surface of a tensile sample.

9:50 AM

An Improved Plasticity Model of Anisotropic Ductile Porous Solids: *Shyam Keralavarma*¹; *Ahmed Benzerga*¹; ¹Texas A&M University

Forming limits and fracture modes in structural materials are significantly influenced by microstructural details such as material texture, porosity, shape and distribution of microvoids. Accurate prediction of plastic flow localization and fracture during processing and product manufacturing requires the development of constitutive models that incorporate the effects of evolving microstructural parameters. In this work, we present a contribution toward this goal by developing, on rigorous micromechanistic bases, a constitutive model of porous solids incorporating the effects of plastic anisotropy and cavitation-induced damage. In particular, the model accounts for void shape effects and void closure. Plastic anisotropy data for a range of practically important materials is tabulated and the model predictions for the yield loci and microstructure evolution are compared with numerical limit analysis results and finite element simulations of porous unit cells for representative materials. Greater accuracy is obtained vis-a-vis previous models in predicting the plastic response of anisotropic solids.

10:10 AM

Drilling and Milling of Intermetallic Gamma-TiAl: *Stefan Bergmann*¹; *Dirk Biermann*¹; ¹Department of Machining Technology

Gamma-Titaniumaluminide is an intermetallic compound. It offers a very good hot strength, a high Young's Modulus and tensile strength as well as a low density (3.9 g/cm³). The fields of application are e. g. conrods, turbochargers for combustion engines and turbine blades. The advantage of deploying Gamma-TiAl results from a reduction of moving masses together with a minimization of engine vibrations. Contrasting with the outstanding lightweight material properties, problems occur when machining operations are carried out. These problems result from the very high hardness and brittleness, which leads to high cutting forces and rapid tool wear. The presentation features investigations on the machining of a Gamma-TiAl-alloy. For this reason, studies on drilling and milling were conducted, focusing on appropriate conditions for a high-quality machining process. The presentation shows results from selected machining tests, e. g. tool wear, cutting forces, surface integrity as well as tool and process optimizations.

10:30 AM Break

10:40 AM

Hot Isostatic Pressing of Titanium Powder Compacts Using a Ceramic Secondary Pressing Medium (HIP-SPM): *Fatos Derguti*¹; *Richard Dashwood*¹; ¹Imperial College London

We present a new low cost Near Net Shape (NNS) technique for titanium powder. Commercially pure Hydride DeHydride (HDH) Ti powder was compacted to rod samples of 70% of theoretical density using "wet-bag" Cold Isostatic Pressing (CIP) followed by HIPing using ceramic beads as a secondary pressing medium (SPM). The effect of SPM media and powder size of the mechanical properties will be presented, and compared to an FE model for

HIPing. Some observations are also presented on porosity, the reaction layers that form and oxygen uptake in the samples.

11:00 AM

The Adiabatic High Velocity Compaction of Titanium Powder: *Gordon Goranson*¹; ¹LMC Inc.

LMC compacts titanium powders to net shape components with reduced sintering time and temperature, or no sintering. One Tool – One Impact – One Part. The patented impact unit achieves ram velocities up to 100 meters per second creating adiabatic phenomena in powder, dislocating molecules and rejoining them in a solid state. Material yield is maximized. Surface finish is determined by tooling. High cycle rates are achieved. No lubricants. Part densities have been achieved to over 99%. The LMC process will produce: pellets that can be controlled for processing by smelters for extrusions, rolled or machined; near net shape billets to be finished machined; net shape parts. Presses capable of components to 20 kilos. The High Velocity Adiabatic Impact Process is fully commercialized for cutting, blanking, and forming. Environmentally friendly. No recyclables, minimum material waste and up to an 85% reduction in energy consumption compared to conventional presses.

11:20 AM

World Record Thermal Conductivity of Nano-Tungsten-Copper Powder: Seong Lee¹; Joon-Woong Noh¹; Young-Sam Kwon²; John Johnson³; *Seong Jin Park*⁴; Randall German⁴; ¹ADD; ²CetaTech; ³ATI Alldyne; ⁴Mississippi State University

Tungsten-copper is a leading candidate material for thermal management. However one of the huddles for this material is the difficulty to improve interfacial properties between tungsten and copper. In this study, nano tungsten coated copper powder has been developed with a range of compositions from 90W-10Cu to 10W-90Cu in weight percentage through a mechano-reduction process starting from oxides. Powder injection molding and die compaction were used to make samples to evaluate microstructure, thermal conductivity (TC) and coefficient of thermal expansion (CTE) with density and heat capacity for several compositions of tungsten coated copper powder. The measured TC lies among theoretical values predicted by the model with consideration of microstructure. Furthermore, the presentation will present mechanical properties such as hardness and compressive strength with shear rate dependency and electrical property of conductivity (or resistivity).

11:40 AM

Introduction of an Emerging Compaction Technology – Spark Plasma Sintering (SPS): *Robert Aalund*¹; Masao Tokita²; ¹Metal Processing Systems, Inc.; ²SPS Syntex Inc.

SPS is a compaction/sintering technology, utilizing uniaxial (Z axis) pressure, vacuum atmosphere (various gasses can be used), and a high amperage DC pulse power supply. Electrical current is drawn directly through the powder during compaction, netting numerous benefits. The process, basic machine configuration, and benefits will be explained at length. There are volumes of research in applying the SPS process to conventional powder metals, ceramics, hybrids and composites, and high purity materials (including many nanophase). Portions of various research papers will be shared. This technology is currently well established in Japan and numerous example parts will be discussed, including examples of near-net and net shapes.

12:00 PM

Preparation of High-Purity Strontium Carbonate from Celestite Concentrate by Double Decomposition-Roasting Process: *Mudan Liu*¹; Li Guanghui¹; Jiang Tao¹; ¹Central South University

The technology of using celestite concentrate to prepare high-purity strontium carbonate by double decomposition-roasting process was studied. The results showed that a maximal SrSO₄ conversion of 97.77% was obtained when Na₂CO₃ was used under the conditions of liquid/solid ratio of 5/1, Na₂CO₃ concentration of 1.1mol/L, Na₂CO₃/SrSO₄ molar ratio of 1.2, temperature of 75°C, and time of 75min. The maximal conversion was only 78.66% when (NH₄)₂CO₃ was used under the conditions of liquid/solid ratio of 5/1, (NH₄)₂CO₃ concentration of 1.7mol/L, (NH₄)₂CO₃/SrSO₄ molar ratio of 1.2, temperature of 60°C and time of 150min. The crude strontium carbonate were roasted at 1200°C for 45min with anthracite, and the ratio of strontium carbonate and anthracite was 10/1, then the conversion was 72.30%. The high-purity strontium carbonate were obtained

after the roasted products were leached, got rid of impurity and carbonated, in which the content of SrCO₃ exceeded 98%, and CaCO₃ was less than 0.5%.

General Abstracts: Structural Materials Division: Microstructure/Property Relations in Steel I

Sponsored by: The Minerals, Metals and Materials Society, TMS Structural Materials Division, TMS: Advanced Characterization, Testing, and Simulation Committee, TMS: Alloy Phases Committee, TMS: Biomaterials Committee, TMS: Chemistry and Physics of Materials Committee, TMS/ASM: Composite Materials Committee, TMS/ASM: Corrosion and Environmental Effects Committee, TMS: High Temperature Alloys Committee, TMS/ASM: Mechanical Behavior of Materials Committee, TMS/ASM: Nuclear Materials Committee, TMS: Product Metallurgy and Applications Committee, TMS: Refractory Metals Committee, TMS: Superconducting and Magnetic Materials Committee, TMS: Titanium Committee

Program Organizer: Ellen Cerreta, Los Alamos National Laboratory

Wednesday AM

March 12, 2008

Room: 387

Location: Ernest Morial Convention Center

Session Chair: Michele Manuel, University of Florida

8:30 AM

Austenite Grain Stability of Low-Manganese, High-Chromium Carburizing Steel: *Takeshi Fujimatsu*¹; Kazuya Hashimoto¹; Shinji Fukumoto²; Atsushi Yamamoto²; ¹Sanyo Special Steel Company Ltd.; ²University of Hyogo

Since automotive drive train parts require cost reduction as well as reduction in size and weight for improving fuel consumption, carburizing steel for those parts is expected to have lower cost, better cold formability and machinability, and higher strength. We found that the steel with reduced manganese and increased chromium contents meets these needs. It was also confirmed that this developed steel showed higher austenite grain coarsening temperature during carburizing than conventional steel. The microstructures of the low-manganese, high-chromium carburizing steel were investigated at various stages from hot forging through carburizing processes, and the improvement mechanisms of austenite grain coarsening temperature were discussed in this study.

8:50 AM

Deterioration of Fracture Toughness of Stainless Steel Due to the Phenomenon of Sensitization: *Swati Ghosh*¹; Kalyan Ray¹; Vivekananda Kain²; ¹Indian Institute of Technology; ²Bhaba Atomic Research Center

This investigation aims to illustrate how degree of sensitization of a stainless steel affects its fracture toughness, estimated by a simplified technique. Solutionized nuclear grade 304LN stainless steel were subjected to sensitization treatment at 1023 K for different time periods in the range 1-100 hr. Corrosion resistance of the differently heat-treated samples were assessed by oxalic acid-etch and electrochemical potentiokinetic reactivation tests. The fracture toughness of the heat treated specimens was determined by a recently developed procedure based on Ball Indentation principle and validated by standard J-integral tests. The results reveal that the fracture toughness of stainless steels gets significantly deteriorated by sensitization. The supplementary examination of microstructure, grain size and hardness and tensile tests explains the cause of such a degradation in toughness as to be due to martensite formation and stress build up due to the grain boundary carbide precipitation.

9:10 AM

Development of High Strength Non-Oriented 3% Silicon Steel: *Hee Yong Park*¹; Sam Kyu Chang¹; Bruno De Cooman¹; ¹GIFT

Current electrical steels usually are not fatigue resistant and so fatigue failure occurs during the operation, in motors for example, due to the overload from high frequencies. To use the electrical steels in large motors used in power plants, ship, aircraft and etc, we need to overcome this problem by increasing the yield strength and toughness of the electrical steel without losing its magnetic properties. Ability to withstand high frequencies and temperature is also required. To obtain the increase in mechanical properties without losing its magnetic properties, new elements such as B, Sb, Mo, Ni and Nb are added and higher amount of Al and Mn are added to the current electrical steel.

9:30 AM

Magnetic Properties and Textural Development of High Strength 3%Si Electrical Steels: *Sam Chang*¹; ¹Pohang University of Science and Technology

For the development of high strength electrical steels having yield strength of 450 N/mm² to meet the recent requirement for high fatigue resistance for large motors, it is also of important to investigate the magnetic properties and structural characteristics in such a high mechanical property electrical steel because in a high strength steel contains several alloying elements which are known detrimental to magnetic properties. Current electrical steels usually are not fatigue resistant and so fatigue failure occurs during the operation, in motors for example, due to the overload from high frequencies. To use the electrical steels in large motors used in power plants, ship, aircraft and etc, we need to overcome this problem by increasing the yield strength and toughness of the electrical steel without losing its magnetic properties. Ability to withstand high frequencies and temperature is also required. To obtain the increase in mechanical properties without losing its magnetic properties, new elements such as Sn, Sb, Ni and Nb are added and higher amount of Al and Mn are added to the current electrical steel.

9:50 AM

Characteristics of Hybrid Solid Solution Layer Formed on the Surface of 316 L Austenitic Stainless Steels: *Ozgur Celik*¹; Eyup Sabri Kayali¹; Huseyin Cimenoglu¹; ¹Istanbul Technical University

Among metallic materials, AISI 316L quality austenitic stainless steel is extensively used in manufacturing of orthopedic implants. Although it exhibits very good corrosion resistance in many acidic environments, synergetic attack of corrosion and wear in the body causes severe surface damage and loosening of the implant. It has been reported that surface hardening by low temperature plasma nitriding provides a considerable improvement in wear resistance as well as the corrosion properties of austenitic stainless steels. In the present study, low temperature nitriding was applied to an AISI 316L quality austenitic stainless steel in a fluidized bed to form a hybrid solid solution layer composed of nitrogen and carbon rich expanded austenite zones. The surface characteristics of nitrided alloy was examined through structural examinations, mechanical tests as well as biocompatibility tests and compared with those of Rex 734, which was recently produced austenitic stainless steel for manufacturing of implants.

10:10 AM

Deformation-Induced Martensitic Transformation in High-Nitrogen Metastable Austenitic Stainless Steels: *Chang-Seok Oh*¹; Tae-Ho Lee¹; Sung-Joon Kim¹; ¹Korea Institute of Materials Science

Deformation-induced martensitic transformation (DIMIT) in high-nitrogen metastable austenitic stainless steels was investigated in terms of the effects of nitrogen content and the microstructural change. During tensile deformation, the stress-strain response was changed at the transient point (at around 0.1–0.3) depending on nitrogen contents, induced by DIMIT. The critical strain for DIMIT was shifted to higher strain with increasing nitrogen contents, and DIMIT did not occur in the nitrogen contents above 0.5wt.%. At the beginning of deformation, the austenite to epsilon martensitic transformation occurred, whereas the formation of alpha prime martensite prevailed after the transient point, which caused the shape change of stress-strain curve. Based on analyses of SAD patterns, the orientation relationships between austenite and deformation-induced martensites were determined. The changes of martensite volume fraction and crystallographic features (lattice parameters and orientation change) during deformation were also analyzed using EBSD and neutron diffraction.

10:30 AM Break

10:50 AM

Effect of Cooling Rate on the Hot Ductility of Boron Bearing Steel: *Kyung Chul Cho*¹; Yang Mo Koo¹; Joong kil Park²; ¹Pohang University of Science and Technology; ²Pohang Iron and Steel Company

In boron bearing low carbon steels, corner cracking can occurs if the hot ductility of these steels at the unbending stage is poor during continuous casting. 25ppm boron bearing steel was examined in order to study the effect of cooling rate on the hot ductility. Since the rapid cooling in the corner of this slab during the continuous casting lead to as corner cracking, hot tensile test applied to the different cooling rate was taken into account. The results revealed that increasing cooling rate deteriorate hot ductility of B bearing steel. Low hot ductility of

B bearing steel is associated with intergranular fracture along the austenite grain boundaries. Rod-like BN precipitates co-precipitated with MnS were formed along austenite grain boundaries when the cooling rate was increased. Intergranular fracture of B bearing steel is caused by the formation and growth of grain boundary cavities which nucleate at grain boundary precipitates of BN+MnS.

11:10 AM

Microstructure and Properties of the HAZ in ASTM A709 HPS-100W Steel: *Avidipto Biswas*¹; ¹Illinois Institute of Technology, Thermal Processing Technology Center

HPS 100W is a new grade of bridge steel. In the present work an attempt has been made to characterize the weld heat affected zone (HAZ) microstructure of this steel. The material has been subjected to thermal profiles that simulate the HAZ and the resultant microstructures have been observed and mechanical properties determined. HAZ simulation was carried out in a GLEEBLE 3500 at different peak temperatures and fixed heat input followed by different stress relieving operations. Subsequently, impact toughness data have been obtained at different temperatures by means of a Charpy test. The microstructure was observed in order to correlate the structure-property relationship of the HAZ for HPS 100W steel.

11:30 AM

Fracture Toughness of Cast Stainless Steels for Shield Module Applications: *Mikhail Sokolov*¹; Randy Nanstad¹; Jeremy Busby¹; ¹Oak Ridge National Laboratory

Cast austenitic stainless steels are under consideration for structural components of the International Tokamak Experimental Reactor (ITER). An improved cast stainless steel has been developed as a substitute for wrought stainless steel for shield module applications. The improved castings were developed based on the commercially available CF3M specification. The modifications utilize combinations of Mn and N, which result in significant increases in strength. Additionally, two other alloys have been developed with enhanced solid solution strengthening by virtue of Cu and W additions to increase strength. The developmental process leading to these improved cast stainless steel alloys will be briefly reviewed, but the major focus of this paper will be the fracture toughness and other mechanical properties of at least two of the developmental alloys. Comparisons of these properties will be made with standard cast stainless steel. Metallography and scanning electron fractography of the tested steels will also be discussed.

11:50 AM

Impact of Sensitization on the Fracture Toughness of Austenitic Stainless Steel: *Swati Ghosh*¹; Kalyan Ray¹; Vivekananda Kain²; ¹Indian Institute of Technology; ²Bhaba Atomic Research Center

This investigation aims to illustrate how degree of sensitization of a stainless steel affects its fracture toughness, estimated by a simplified technique. Solutionized nuclear grade 304LN stainless steel were subjected to sensitization treatment at 1023 K for different time periods in the range 1–100 hr. Corrosion resistance of the differently heat-treated samples were assessed by oxalic acid-etch and electrochemical potentiokinetic reactivation tests. The fracture toughness of the heat treated specimens was determined by a recently developed procedure based on Ball Indentation principle and validated by standard J-integral tests. The results reveal that the fracture toughness of stainless steels gets significantly deteriorated by sensitization. The supplementary examination of microstructure, grain size and hardness and tensile tests explains the cause of such a degradation in toughness as to be due to martensite formation and stress build up due to the grain boundary carbide precipitation.

Hael Mughrabi Honorary Symposium: Plasticity, Failure and Fatigue in Structural Materials - from Macro to Nano: Mechanical Properties of Ultrafine-Grained (UFG) Metals I

Sponsored by: The Minerals, Metals and Materials Society, TMS Structural Materials Division, TMS Materials Processing and Manufacturing Division, TMS: High Temperature Alloys Committee, TMS/ASM: Mechanical Behavior of Materials Committee, TMS: Nanomechanical Materials Behavior Committee
Program Organizers: K. Jimmy Hsia, University of Illinois, Urbana-Champaign; Mathias Göken, Universitaet Erlangen-Nuernberg; Tresa Pollock, University of Michigan - Ann Arbor; Pedro Dolabella Portella, Federal Institute for Materials Research and Testing; Neville Moody, Sandia National Laboratories

Wednesday AM Room: 386
 March 12, 2008 Location: Ernest Morial Convention Center

Session Chairs: Neville Moody, Sandia National Laboratories; Cynthia Volkert, Forschungszentrum Karlsruhe

8:30 AM Keynote

Processing and Characterization of Nanocrystalline Materials with Interesting Physical Properties: Dongtao Jiang¹; Amiya Mukherjee¹; ¹University of California, Davis

Spark Plasma Sintering (SPS) method that allows the sintering to be completed in much shorter times has been used to produce ceramic nanocomposites. A three-phase alumina based nanoceramic composite demonstrated superplasticity at a lower temperature and at a higher strain rate. An alumina-carbon nanotube-niobium nanocomposite has a fracture toughness that is five times higher than that of pure alumina and an electrical conductivity that is thirteen orders of magnitude greater than that of pure nanocrystalline alumina. It also has excellent potential for use as a thermoelectric material. An alumina-spinel nanocomposite demonstrated optical transparency in the mid infrared range. A silicon carbide/silicon nitride nanocomposite produced by pyrolysis of liquid polymer precursor has produced one of the lowest creep rates in ceramics at a referred temperature of 1400°C. These structural and functional properties will be discussed in the context of microstructural investigations. This research is supported by ARO and ONR.

9:00 AM Invited

Effect of Nano-Scale Twins on Work Hardening Behaviors in Pure Copper: L. Lu¹; X.H. Chen¹; K. Lu¹; ¹Chinese Academy of Sciences, Institute of Metal Research

Work hardening is one of the most important mechanical behaviors for engineering materials. As a general trend, work hardening always decreases accompanied with strengthening of metals. In this work, we will present a novel finding that introduction of a high density of ultrathin nano-scale twins in pure Cu, its work hardening exponent can be significantly elevated relative to that of the coarse-grained polycrystalline Cu. The highest work hardening exponent achieved is about 0.66, almost twice that of conventional Cu (0.35), when the twin/matrix lamellar spacing is as small as 4 nm. The effect of nano-scale twins on work hardening exponent and rate will be demonstrated. The extra-ordinary high work hardening originates from the ultrathin twins patterns that effectively suppress the dynamic recovery of dislocations and enhance the dislocation storage ability. The results indicate that work hardening of metals can be elevated by means of proper nanostructure design.

9:20 AM

Thermal Stability and Stabilization of Ultrafine-Grained Copper: Yujiao Li¹; Wolfgang Blum¹; ¹University of Erlangen-Nürnberg

Ultrafine-grained (UFG) pure Cu produced by ECAP was subjected to thermal and thermomechanical treatment. Transmission electron microscopy and mechanical testing were combined to test the stability of the UFG structure. During deformation at temperature up to 373 K the material keeps the properties of UFG material. Annealing at 403 K for 2.5 h destroys them, indicating (partial) recrystallization of the UFG structure. This process can be retarded by a thermomechanical treatment (TMT) consisting of a series of small deformation

steps at increasing temperature. The TMT leads to growth of the cell size and decrease of flow stress. The cell size-stress relation equals the well-known stress dependence of the subgrain size in steady-state deformation. Tests of mechanical properties and structure observations indicate that the homogeneous coarsening of the cell structure during the TMT affects low- as well as high-angle boundary spacings and that the TMT significantly increases the resistance against recrystallization.

9:35 AM

Fracture Toughness and Fatigue Crack Propagation Measurements in Ultrafine Grained Iron and Nickel: Anton Hohenwarter¹; Reinhard Pippan¹; ¹Erich Schmid Institute Leoben

Nanocrystalline and Ultrafine-grained (UFG) materials are commonly known as materials with extraordinary mechanical properties. Due to the limited dimensions of HPT-deformed materials little is known about their fatigue properties whereas particularly this process delivers highly refined materials with little effort. In the framework of this study pure nickel and Armco-iron were subjected to High Pressure Torsion (HPT) and in combination with different heat treatments the grain-size was varied between approximately 100 nm and 10 µm. Afterwards crack-propagation measurements with reference to different grain-sizes were conducted and monitored. It could be shown that there is a distinctive difference in the crack path with respect to the grain size, which may has an influence on the threshold of fatigue crack propagation as well. With respect to fracture toughness measurements in the UFG regime a quite good combination of toughness and hardness was observed.

9:50 AM Invited

Lifetime and Damage Behavior of Engineering Ceramics under Fretting Fatigue Conditions: Thomas Schalk¹; Karl-Heinz Lang¹; Detlef Loehe¹; ¹Universitaet Karlsruhe (TH)

Fretting fatigue may appear in the contact zone between two components when they are exposed to cyclic loading and relative motion appears between the contact surfaces. This loading condition arises often in technical applications e.g. if forces are transmitted by form-fitting connections or at forming processes. To investigate the fretting fatigue behavior of engineering ceramics a new test rig was built up. The fretting fatigue loading is realized by the superposition of cyclic four point bending with local friction loading. The friction loading is achieved by the relative motion of a fretting pad which is well defined pressed on the tensile loaded surface of the four point bending specimen and moved by an electrodynamic actuator. With this testing system fretting fatigue experiments have been carried out at temperatures up to 900°C. The lifetime behavior of alumina and silicon nitride specimens will be presented and the arising damage characterized.

10:10 AM Invited

Fatigue Behavior of Railway Wheel Steels in the Very High Cycle Regime: Vadim Wagner¹; Frank Walther¹; Dietmar Eifler¹; ¹University of Kaiserslautern

The fatigue behavior of railway wheel steels has been investigated in the very high cycle regime under stress control at a frequency of 200 Hz on servohydraulic and resonance testing systems. Specimens machined from the rim of original wheels for high-speed passenger traffic exhibit a distinct change in the slope of the S-N curve at about 2×10^6 cycles. High-precision temperature and electrical resistance measurements influenced by deformation-induced changes of the microstructure are used to characterize the actual fatigue state under VHCF conditions. SEM investigations show crack initiation at the specimen surface as well as inside the specimen cross-section. The physically based fatigue life calculation "PHYBAL" on the basis of generalized Morrow, Coffin-Manson and Basquin equations leads to enormous scientific and economic advantages. The S-N curve calculated with temperature and resistance data measured after 10^4 cycles, i.e. 50 seconds, matches very well with the experimentally determined one until 2×10^8 cycles.

10:30 AM Break

10:40 AM Invited

Deformation Physics and Ductility of Nanostructured Materials: *Yuntian Zhu*¹; ¹North Carolina State University, Department of Materials Science and Engineering

Nanostructured materials usually have high strength but low ductility. To improve their ductility, we need to first understand their deformation physics. Past attempts to increase the ductility usually led to a decrease in strength. In this presentation, I'll first present the deformation physics in nanostructured materials and how they affect the ductility. I'll then present several strategies to tailor the structures and deformation physics of nanostructured materials with the aim of improving the ductility without sacrificing the strength. We have been able to simultaneously increase the ductility and strength using these strategies.

11:00 AM Invited

Length-Scale Effects on Fatigue of Thin Cu Films: *Cynthia Volkert*¹; Dong Wang²; Oliver Kraft²; ¹University of Goettingen, Institute of Materials Physics and Forschungszentrum Karlsruhe, Institute of Materials Research II; ²Forschungszentrum Karlsruhe, Institute of Materials Research II

Fatigue lives and fatigue damage morphology of Cu films (50 nm to 3 μ m in thickness) on polyimide substrates has been investigated under high cycle loading. As film thickness and grain size are decreased, characteristic fatigue damage such as extended dislocation structures and extrusions disappear and are replaced by cracks along boundaries. The transition in damage morphology with length scale is accompanied by a marked improvement in fatigue resistance. It is proposed that the transition is due to the inhibition of dislocation nucleation and motion at small length scales, and that the cracking observed in the thinnest films is evidence of a new fatigue mechanism promoted by high stresses and high boundary density. In addition, the eventual saturation of the extrusion and crack densities under total strain control allows schemes for the use of thin films in damage tolerant applications.

11:20 AM Invited

Thermal and Mechanical Stability of Nano- and Ultra-Fine-Grained Materials: *Zhirui Wang*¹; ¹University of Toronto

The involvement and the role of inter-crystalline constituents (such as high- and low-angle grain boundaries, twin boundaries and triple points) in submicron- and nano-meter grained materials could not be ignored when the materials' mechanical and physical properties are concerned. These constituents would also increase the internal energy of the material. In this report, effects of the energy associated to these constituents in electroformed Cu and CVD-deposited Ni materials will be discussed. The main thrust of the discussion will be two folds: First, experimental results will be presented to demonstrate the evolution of the ultra-fine-twin and nano-twin structures upon thermal activation, mechanical deformation; Bauschinger effect tests and DSE tests. The discussion will then be switched to correlate specifically the internal energy of such materials with their plastic deformation - strain hardening behaviour. Based on such analysis, a model has been established and would be presented which could be employed to predict the feature of work hardening in these materials.

11:40 AM

Inhomogeneity and Size of Microstructure - A New Paradigm in Understanding Deformation Mechanism of Nano Crystalline Metals: *Taher Saif*¹; Jagannathan Rajagopalan¹; Jong Han¹; ¹University of Illinois at Urbana-Champaign

We will present experimental evidence showing that plastically deformed polycrystalline free standing thin metal films with average grain size of 50-100nm recover all of the plastic strain under macroscopic stress-free condition. This recovery shows three distinct activation energies. When the grain size is increased to 100-200nm, the films do not recover plastic strain, but they show strong Bauschinger effect during unloading, while still under tension. We hypothesize, inhomogeneities in the microstructure (grain size and orientation variations) create non uniform local stress fields during loading as relatively larger or favorably oriented grain deform plastically while smaller or unfavorably oriented grains accommodate the strain elastically. Upon unloading, the elastically deformed grains, in order to reduce their strain energy, induce reverse plasticity in the larger grains leading to time dependent strain recovery in films with 50-100 nm grain size, and Bauschinger effect in films with 100-200 nm grain size.

11:55 AM

Emergence of Glass-Like Plasticity in the Finest Nanocrystalline Metals: *Jason Trelewicz*¹; Christopher Schuh¹; ¹Massachusetts Institute of Technology

Nanocrystalline metals exhibit a variety of unusual mechanical properties as grain size is refined towards the amorphous limit, a widely discussed peculiarity being the breakdown of the Hall-Petch relation. In this work, we study the mechanical properties of nanocrystalline Ni-W alloys, which can be produced with grain sizes spanning both the Hall-Petch and Hall-Petch breakdown regimes. We show that not only the hardness, but also its scaling with strain rate and superimposed pressure undergoes an inflection at a finite grain size coinciding with the Hall-Petch breakdown. We also illustrate how these mutually consistent inflections are a consequence of the shift to amorphous-like deformation mechanisms, with inhomogeneous shear banding taking place in samples with the finest nanocrystalline grain sizes. We finally explore how the grain boundary relaxation state affects the deformation mechanisms across the entire Hall-Petch breakdown regime.

12:10 PM

Damage Evolution and Lifetime Prediction of Thermal Barrier Coatings during Cyclic Oxidation: *Tilman Beck*¹; Olena Trunova¹; Roland Herzog²; Rolf Willi Steinbrech¹; Lorenz Singheiser¹; ¹Research Center Juelich; ²MAN Turbo AG

Thermal barrier coatings (TBCs) are applied to combustion chambers and turbine blades of gas turbines to raise efficiency by increasing maximum service temperature. For power generation units, TBC-lifetimes up to 40000hrs must be reached with high reliability. To fulfill this condition, in-depth understanding of microstructural damage as well as reliable tools for lifetime prediction are essential. Detailed damage analyses during cyclic oxidation of a plasma sprayed ZrO₂/8 wt-% Y₂O₃ - MCrAlY - CMSX-4 TBC system showed that formation and growth of an Al₂O₃ scale on the MCrAlY bondcoat plays a major role in the initiation of delamination cracks. The onset of stable crack propagation is strongly influenced by the TBC/bondcoat interface topography. Crack propagation itself can be described by fracture mechanics approaches. Based on the quantitative evaluation of damage evolution during cyclic oxidation with several dwell times at 1050°C, a phenomenological model for life prediction was developed and validated.

12:25 PM

The Effect of Environmental Exposure on the Dislocation Structure at the Fatigue Crack Wake: *YunJo Ro*¹; Sean Agnew¹; Richard Gangloff¹; ¹University of Virginia

Focused ion beam (FIB) milling was used to produce samples for transmission electron microscopy which successfully revealed the dislocation structure within 1 μ m of the fracture surface of an under-aged Al-Cu-Mg alloy tested in ultrahigh vacuum and high humidity air. Both different conditions exhibited a similar layer of dislocation cells just below the fracture surface, and the cell structure abruptly changed to localized slip bands away from the fracture surface. This abrupt change confirms the presence of the high strain gradient at the crack tip. In addition, the thickness of dislocation cell layer and the intensity of the slip bands observed in ultrahigh vacuum was much larger than those observed in high humidity air. Thus, the present results suggest that less plastic strain accumulation is required to propagate fatigue cracks at high humidity air relative to ultrahigh vacuum. Speculatively, the current study supports hydrogen enhanced decohesion.

Hot and Cold Rolling Technology: Session I

Sponsored by: The Minerals, Metals and Materials Society, TMS Light Metals Division, TMS: Aluminum Committee

Program Organizers: Ming Li, Alcoa Inc; Jürgen Hirsch, Hydro Aluminium Deutschland GmbH

Wednesday AM

Room: 297

March 12, 2008

Location: Ernest Morial Convention Center

Session Chair: To Be Announced

8:30 AM

Effects of Texture Evolution on Localized Deformation of AA2024: Soondo Kweon¹; Armand Beaudoin¹; Ming Li²; ¹University of Illinois at Urbana-Champaign; ²Alcoa Technical Center

An experimental and computational study is presented to examine the effects of texture evolution on localized deformation behavior in the alloy AA 2024-O. Routine monotonic mechanical testing is complemented by a novel cyclic test procedure to develop flow properties at temperatures from -100°C to 495°C and strain rates from 10⁻²/sec to 10⁻⁵/sec. A coupon test, where the stress state is similar to the slab edge, is then pursued to understand localized deformation that is taking place in the rolling process. Details of the deformation in the coupon test are developed through use of a 3D finite element model, with material response derived from the material characterization noted above. The evolution of crystallographic texture is also used as a means of drawing interpretation of the deformation history in the region of localization. The relevance of this coupon test to hot rolling is discussed.

10:35 AM

Process Chain Modelling of Al Sheet Production: Kai Karhausen¹; ¹Hydro Aluminium

Through Process Modelling (TPM) is a keyword in research activities with a view to optimising a process chain according to desired product properties. State variables need to be traced through a process chain. The linking of micro scale to macro scale models is required to feed realistic process information into the microstructural modules as well as to feed the process models with correct material behaviour. While the TPM can be validated directly on measured final or intermediate properties, it is often unclear to which extent the material behaviour affects the process performance. This presentation covers an exemplary TPM calculation of hot- and cold rolling passes as well as intermediate and final annealing. Variations are tested by computing extreme material conditions for single processing operations. This provides directives on which physical mechanisms and corresponding model combinations are required in specific process situations both with respect to accuracy and computational effort.

10:10 AM

Optimising the Winding of Aluminium Strip: Kai Karhausen¹; Cremer Albert¹; Michael Wimmer¹; Stefan Neumann¹; ¹Hydro Aluminium

The production process of Al-strip consists of a number of continuous processing steps like rolling, annealing or various strip treatments, which are interlinked semi-continuously by transport and storage operations. For these operations the strip is usually wound into a coil. Thus, the entire production may contain numerous winding and unwinding operations. Although winding is not a processing step of its own, it can change the strip properties and the performance of subsequent processing steps. Mastering the winding process is therefore mandatory to achieve a high quality level. Typical associated problems are e.g. telescoping of strip layers, coil collapse under its weight, buckling of strip layers or sticking of strip layers after annealing. Furthermore, the stress state can result in shape deviations and flatness errors of the strip upon unwinding. In this paper modeling and optimisation of the winding processes will be treated on case studies from aluminium foil production.

11:00 AM

Texture Evolution during Rolling of Aluminium Alloys: Jürgen Hirsch¹;

¹Hydro Aluminium Deutschland GmbH

For many applications of Aluminium alloy sheet crystallographic textures have a strong influence on specific (anisotropic) properties like strength, formability and etching behaviour, e.t.c.. For these cases textures are intentionally induced – or at least controlled – by the specific rolling conditions. Examples are given for industrial Aluminium alloy sheet processing and applications where strongly textures give superior properties to fulfill specific requirements in special applications, like deep drawing of cans, strength effects in can ends and capacity in deep etched high purity Aluminium foil for high quality electrolytic capacitors. The required control of specific processing steps during hot and cold rolling is described. The principles of microstructure evolution during processing are presented that are needed to ensure optimum material quality and product performance.

11:25 AM

The Role of Crystallographic Texture on the Performance of Flat Rolled Aluminium Products for Aerospace Applications: Roberto Rioja¹; Cindie Giummarra¹; Soonwuk Cheong¹; ¹Alcoa

In this paper, the evolution of crystallographic texture during hot and cold rolling of aluminum alloys is reviewed and the major texture components present in recrystallized and unrecrystallized products are discussed. In particular, the effect of the “brass” texture component on the anisotropy of mechanical properties in Al-Li alloys and the methods used to control it are presented. The influence of texture on strength, toughness and thermal stability of plate products for lower wing applications is discussed. Finally, the role of recrystallized and unrecrystallized microstructures on strength, toughness and fatigue performance of aerospace sheet is presented in light of different crystallographic textures. It is concluded that the role of crystallographic texture is necessary to optimize damage tolerant properties of Al-Li alloys for use in aerospace applications.

9:45 AM

Macro- and Micro-Surface Engineering to Improve Hot Roll Bonding of Aluminium Plate and Sheet: Jiantao Liu¹; Ming Li¹; Simon Sheu¹; Michael Karabin¹; Robert Schultz¹; ¹Alcoa Technical Center

Hot roll bonding of aluminum plate and sheet currently is the primary manufacturing method of fuselage skin sheet for aircraft and brazing sheet for automotive applications. This work explores the effects of macro- and micro-surface engineering on hot roll bonding process. It is concluded that micro-surface engineering yields better bonding quality than macro-surface engineering. The critical surface roughness of the core is about 0.58 micron below which bonding quality in terms of area contact and bonding energy can be significantly improved. However, no marked improvement was observed when the surface roughness was reduced further to 0.03 micron. Also, oxide layer on the surface of the core and local deformation on the surface of liner play a very important role. Ultrasonic test and roller peel test were employed to assess the bonding strength and quality. The quantitative ultrasonic test results are in good agreement with the roller peel test results.

8:55 AM

Innovations in Surface Quality Inspection as a Cornerstone for Production Optimization: Uwe Knaak¹; Elisa Jannasch¹; ¹Parsytec Computer GmbH

Surface defects impair the quality of the manufactured aluminium strip greatly; moreover, they may lead to strip breaks or even to equipment damage: less ability to deliver usable quality to customers, less throughput, and higher costs are the consequences. The solution of this problem is Surface Quality Inspection. Parsytec offers leading-edge solutions for an outstanding surface quality inspection: Parsytec Surface Inspection Systems deliver defect information, which can be turned into quality data for a most efficient production optimization. Parsytec's latest generation surface inspection solution - *espresso SI* - entails innovations for nearly all aspects of surface inspection: accessing inspection results via the web, employment of GBit Ethernet camera technology, and standard compact PCs. The benefits for customers comprise of highest detection sensitivity and accelerated access to relevant quality data, combined with highest availability and easiest handling and maintainability of the systems. Furthermore, based on Parsytec's unrivalled experience, *espresso SI* also adds so-called “production decision intelligence” solutions, which transform inspection

data to production benefit in selected applications. Production optimization can be achieved by combining surface quality data with all other available production and process data, as well as with customer and order information. One example, which will be presented here, is a productivity solution at coil slitting lines: The inspection system not only delivers information on surface defects, it supports the grading of complete coils, but also for individual stripes or coil segments on-line. This solution helps the aluminium producers to significantly improve yield and quality of their production. All in all, Surface Inspection by Parsytec serves two aims: increasing product quality, and turning surface quality information into production excellence.

9:20 AM

Investigation of Longitudinal Surface Cracks and Effective Metallurgical Parameters in Hot Rolling of Steels: *Anis Ghaderi Namin*¹; Seyyed Ahmad Jenabali Jahromi¹; ¹Shiraz University

Longitudinal surface cracks are often found on continuously cast billets. Compared to transversal cracks, longitudinal cracks are usually deeper. Often they are located in regions close to the centre line of billet surface. They found discontinuously in all of the billet surface, too. Many parameters can effect its generation such as FeS, Pinholes, Blowholes, trace elements (Cu, Sn), Inclusions and pre-heating condition of Hot Rolling. In this paper, we mentioned all of these parameters and the ways we can prevent longitudinal surface cracks. For example the optimum ratio between Fe and S is greater than 23.

Magnesium Technology 2008: Advanced Magnesium Materials

Sponsored by: The Minerals, Metals and Materials Society, TMS Light Metals Division, TMS: Magnesium Committee

Program Organizers: Mihriban Pekguleriyuz, McGill University; Neale Neelameggham, US Magnesium LLC; Randy Beals, Chrysler LLC; Eric Nyberg, Pacific Northwest National Laboratory

Wednesday AM
March 12, 2008

Room: 291
Location: Ernest Morial Convention Center

Session Chair: To Be Announced

8:30 AM

Mechanical Properties and Microstructure of Cast AS21 and AS31 Nanocomposites: *Guoping Cao*¹; Hongseok Choi¹; Juan Oportus¹; Hiromi Konishi¹; Xiaochun Li¹; ¹University of Wisconsin

SiC enhanced magnesium matrix nanocomposites, AS21/SiC and AS31/SiC were successfully cast after dispersion of SiC nanoparticles in magnesium alloy melts with ultrasonic cavitation. As compared to magnesium alloy matrix AS21 and AS31, the mechanical properties including room temperature tensile strength and yield strength of the nanocomposites were improved significantly, while the good ductility of magnesium alloy was retained. The high temperature (200°C) yield strength was also improved considerably in AS21/SiC and AS31/SiC nanocomposites. TEM study of the interface between SiC nanoparticles and AS21 magnesium alloy matrix indicates a good bonding.

8:50 AM

Mg-6Zn/SiC Nanocomposites Fabricated by Ultrasonic Cavitation Based Solidification Processing: *Guoping Cao*¹; Hongseok Choi¹; Juan Oportus¹; Hiromi Konishi¹; Xiaochun Li¹; ¹University of Wisconsin

Mg-6Zn/SiC nanocomposites were successfully fabricated by ultrasonic cavitation based dispersion of SiC nanoparticles in Mg-6Zn alloy melt. As compared to Mg-6Zn magnesium alloy matrix, the mechanical properties including tensile strength, yield strength and ductility of the Mg-6Zn/1.5% SiC nanocomposites were improved significantly. In the microstructure of Mg-6Zn/1.5% SiC nanocomposites, there are still some SiC micro-clusters, but in the areas free of micro-clusters, the SiC nanoparticles were dispersed very well. The grain size of Mg-6Zn was also refined considerably by adding 1.5% SiC nanoparticles. TEM study of the interface between SiC nanoparticles and magnesium matrix indicates a good bonding and no chemical reaction between SiC nanoparticles and Mg-6Zn matrix.

9:10 AM

Microstructure and Mechanical Properties of Cryomilled Magnesium Alloys: *Jeanette Blaine*¹; Sara Longanbach²; Carl Boehlert²; David Schwam³; ¹Advanced Ceramics Research Inc; ²Michigan State University; ³Case Western Reserve University

The microstructure and mechanical properties of cryomilled magnesium and magnesium alloys have been studied. The effect of milling duration and speed has been evaluated using sieve analysis, microstructural characterization, and mechanical testing. The relative percentage of fine grained magnesium powder produced increases with increased milling time, as does the ultimate tensile strength value of the hot pressed material. Cryomilled Mg-Y-Zn and Mg-ZrB₂ alloys have been evaluated, with the highest strength (150 MPa) and stiffness (82 GPa) values observed with the Mg-ZrB₂ system. Microstructure and mechanical properties of hot pressed cryomilled Mg and Mg alloys, in addition to properties of the forged Mg-ZrB₂ alloy, will be discussed.

9:30 AM

Microstructure and Mechanical Properties of Magnesium Alloys Consolidated in the Solid State from Granules: Rick Lee¹; Xiang Li¹; Sibashish Mukherjee¹; *Amit Ghosh*¹; ¹University of Michigan

Consolidation from granular stock can offer a low cost approach for preparing bulk Mg alloys in the solid state, if many steps in the rolling of plates and sheets can be avoided as practiced by wrought Mg industry. Processing of solid state consolidated Mg alloys has been studied by employing a variety of processing methods. Severe deformation techniques have been applied to the alloys to produce fine grain microstructure and superplastic properties. This paper will discuss potential for achieving high mechanical properties in Mg Alloys and its composites. (Work supported by National Science Foundation under Grants 0314218 and 0544920).

9:50 AM

Microstructure Evolution and Nucleation Kinetics of Rapidly Solidified Mg₇Zn_xY(0.55Zr) Alloys: Shijie Zhu¹; *Shaokang Guan*²; Qing Yang²; Mei Zhang²; ¹Department of Materials Science and Engineering, Zhengzhou University

The effects of solidifying condition and Y content on the microstructural evolution, phase selection and nucleation kinetics of Mg₇Zn_xY(0.55Zr) alloys were investigated with OM, SEM, XRD, DSC and TEM. The microstructures of as-cast alloys are dendritic morphology including preliminary α -Mg, interdendritic α -Mg/I-phase(Mg₃Y₂Zn₆) eutectic and W-phase(Mg₃Y₂Zn₃). Microstructures of the cross section of rapidly solidified alloys ribbons are composed of fine equiaxed, columnar grain and equiaxed region. The phase composition changes as the variation of alloying component and solidified condition. Rapidly solidified Mg₇Zn₃Y, Mg₇Zn₃Y0.55Zr alloys ribbons restrain the precipitation of (Mg₃Y₂Zn₆) phase. On the basis of heterogeneous nucleation theory, the connection between incubation period(τ) and temperature was induced and the curve of τ -T was obtained. The results show the second-phase of rapidly solidified Mg₇Zn_xY(0.55Zr) alloy nucleate firstly, which are concord with results of experiments.

10:10 AM Break

10:30 AM

Microstructures and Mechanical Properties of Magnesium Composite Alloys Dispersed with Carbon Nano-Tube via Powder Metallurgy Process: *Katsuyoshi Kondoh*¹; Hiroyuki Fukuda¹; Hisashi Imai¹; Bunshi Fugetsu²; ¹Osaka University; ²Hokkaido University

AZ31B powder coated by carbon nano-tubes (CNT) has been prepared by using surfactant (surface active agent), having both hydrophobic and hydrophilic groups, when employing CNT with 15nm and 75nm diameter. It was compacted at room temperature by applying 600MPa pressure, and consolidated by hot extrusion. Pre-heating temperature of the green compact before extrusion was higher than a sublimation point of the binder used in the surfactant which is determined by differential thermal analysis (DTA). Optical microscope and FE-SEM observation and EDS analysis were carried out on the above composite alloys. The dependence of their mechanical properties on CNT content was also discussed.

10:50 AM

Study on Cast Nano-Structured AZ91D/AlN: *Guoping Cao*¹; Hongseok Choi¹; Juan Oportus¹; Hiromi Konishi¹; Xiaochun Li¹; ¹University of Wisconsin

AZ91D is a widely used magnesium alloy, but its application is generally limited to below 175°C because of its inferior creep resistance and tensile properties at elevated temperatures. In this study, AlN nanoparticles were successfully added and dispersed into AZ91D melts by ultrasonic cavitation effect. The AZ91D melts dispersed with AlN nanoparticles were then cast into a permanent mold. The AlN nanoparticles were dispersed uniformly in the AZ91D matrix. The nanoparticles also markedly refined the grain sizes of as cast AZ91D and induced some new nanocrystalline structures. At both room temperature and 200°C, the yield and ultimate tensile strengths of AZ91D were improved significantly with an addition of 1.0wt% AlN nanoparticles. The good ductility of AZ91D was also retained in AZ91D/1%AlN nanocomposites. The nano-structured AZ91D/AlN is promising to serve as a structural material at much higher temperatures than expected before.

11:10 AM

Synthesis Structure Relationship in Cast Magnesium Periodic Cellular Materials: *Samson Ho*¹; Lukas Bichler²; Glenn Hibbard³; C. Ravi Ravindran²; ¹University of Toronto; ²Ryerson University; ³University of Toronto

Periodic cellular metals (PCMs) are weight efficient hybrids of space and metal. PCMs can deliver higher specific strengths and stiffnesses compared to conventional open cell structures like metallic foams. This study investigates the fabrication of cast magnesium PCMs using the lost foam casting (LFC) method. LFC is a near-net-shape process in which molten metal displaces a polystyrene pre-form embedded in refractory sand. The effect of mould geometry on fillability was studied with different process parameters such as foam characteristic, pouring temperature, casting section thickness and vacuum level. Micro-hardness measurements and optical microscopy were used to characterize the as-cast structure.

11:30 AM

Symmetry Control during Thixoextrusion for AZ31 Mg Alloy: *Young Ok Yoon*¹; Shae K. Kim¹; ¹Korea Institute of Industrial Technology

AZ31 Mg alloy was widely used in transportation industries in the field of extrusion process. However, mechanical properties of extruded AZ31 Mg alloy with symmetry were dependent on the microstructure of the material and could be characterized by their inhomogeneity, grain size distribution and crystallographic texture. Therefore, this correlation between microstructure and mechanical behavior offered the possibility to improve the mechanical properties, e.g. through optimization of the material production process. Thixoextrusion could allow symmetry with extrusion direction and reduced extrusion pressure. The present study was to characterize thixoextruded AZ31 Mg alloy in terms of its symmetric behavior through the optical microscope, electron back scattering diffraction and mechanical test. The results of thixoextrusion experiments about symmetric properties and mechanical properties were compared with conventional extrusion results. The symmetric properties of thixoextruded AZ31 Mg alloy could be obtained through the control of thixoextrusion parameters.

Magnesium Technology 2008: Alloy Microstructure and Properties

Sponsored by: The Minerals, Metals and Materials Society, TMS Light Metals Division, TMS: Magnesium Committee

Program Organizers: Mihriban Pekguleryuz, McGill University; Neale Neelameggham, US Magnesium LLC; Randy Beals, Chrysler LLC; Eric Nyberg, Pacific Northwest National Laboratory

Wednesday AM

March 12, 2008

Room: 292

Location: Ernest Morial Convention Center

Session Chair: To Be Announced

8:30 AM

An Assessment of High Pressure Die Cast Mg-Zn-Al Alloys: *Mark Easton*¹; Trevor Abbott²; Jian-Feng Nie¹; Gary Savage³; ¹Monash University; ²Advanced Magnesium Technologies; ³CSIRO

Most of the current commercial Mg high pressure die casting alloys are found in the Mg-Al-Zn system, mainly based on Mg-Al alloys with small additions of Zn. More recently some alloys containing higher Zn contents have been proposed mainly for alloys with higher creep resistance with some success. This paper investigates the mechanical properties (both creep and quasi-static tensile properties) and the castability of a range of Mg-Zn-Al alloys and indicates regions where each of the properties can be optimised. The yield strength of the alloys can be related by a simple regression relationship with the aluminium and zinc contents. Above approximately 8wt% alloying elements the ductility began to decrease, with alloys with very high alloy contents having little if any ductility. The findings confirmed the castability diagram presented by Foerster in the 1970's although the data shown here presents a continuous variation of properties with alloy content rather than the discrete categories for castable and non-castable alloys as was previously described

8:50 AM

Effect of Composition and Cooling Rate on the β Phase Formation in Mg-Al Alloys: *Suresh Sundarraj*¹; Mridula Bharadwaj¹; Shashank Tiwari¹; ¹General Motors Corporation

It is well known that the corrosion properties of Mg-Al alloys like the AM and AZ series are significantly affected by the formation of the microstructural beta phase ($Mg_{17}Al_{12}$) which forms during casting of these alloys as a result of microsegregation. In this paper we have studied the effect of the alloy composition and processing conditions which affect the amount and morphology of the beta phase formation. Binary Mg-Al alloys with varying amounts of Al content along with varying cooling conditions to mimic the sand, permanent mold, and die casting cooling rates were evaluated using this microsegregation model. The model results of the amount of beta have been verified with the in-house experimental data. Finally, a correlation was established between the corrosion behavior in these alloys with the model predictions.

9:10 AM

Effects of Composition on the Microstructure and Mechanical Properties of Mg-Al-Zn Alloys: *Songmao Liang*¹; Yuequn Ma¹; Rongshi Chen¹; *Enhui Han*¹; ¹Institute of Metal Research

For exploiting mechanical properties potential of low-cost Mg-Al-Zn casting magnesium alloys, the as-cast microstructure and mechanical properties of permanent-mould cast Mg-Al-Zn alloys with typical compositions within castable domain of the intermediate aluminum and zinc contents were investigated. This study disclosed the evolution rules of secondary phase type with variation in Zn/Al mass ratio. Within this domain, secondary phase changed from γ phase to ϕ phase, τ phase and quasi-crystalline phase (I phase) with the Zn/Al mass ratio increasing. By studying cooling curves acquired by thermal analysis technique, the forming temperatures of secondary phases were also determined. Mechanical property tests indicated that increasing the aluminum and/or zinc content, the Y.T.S (Yield Tensile Strength) increased and ductility decreased, while the U.T.S. (Ultimate Tensile Strength) firstly increased and then decreased. Both the U.T.S. and elongation of the alloy with optimum composition are superior to those of AZ91 alloy prepared at the same conditions.

WEDNESDAY AM

9:30 AM

Microstructure Development and Mechanical Behavior in High Pressure Die Cast Mg-Al Alloys: A. Nagasekhar¹; Carlos Caceres¹; Mark Easton²; ¹University of Queensland; ²Monash University

Binary Mg-Al alloys with varying content of aluminium from 0.5 to 12 mass% have been studied. The proof stress increase in two steps whereas the ductility exhibits two correlated stepwise drops, as the aluminum content increases. The first increase in strength, and attendant drop in ductility, is observed between 4 and 5 mass% Al. The second stepwise change is observed between 10 and 12 mass% Al. These effects are connected with well defined changes in the microstructure: at 4 mass% a dispersion of beta-phase intermetallic particles appears in the core region and a closed cell structure develops near the surface; at 12 mass% Al, the increased volume fraction of the beta-phase intermetallics extends the interconnected network of intermetallics to include the core region as well. The micromechanics of the strengthening and decreased ductility are discussed.

9:50 AM

Stabilization of Mg-Ca-Zn Alloys by Zr Additions: Dmitry Shepelev¹; Anton Gorny¹; Menahem Bamberger¹; Alexander Katsman¹; ¹Technion - Israel Institute of Technology

The microstructure and mechanical properties of Mg-Ca-Zn alloys with Zr additions were investigated in as-cast and heat treated conditions. Different concentrations of Zr (0.5 wt% and 1.0 wt%) were used to refine the grain structure. The alloys were exposed to solution treatment at 410°C for 96 hours followed by aging at 175°C for up to 96 hours. The microstructure obtained after heat treatment had equiaxed grains with evenly distributed binary phases, Mg₂Ca and Zn₂Zr. The ternary Mg₂Ca₆Zn₃ phase was identified at grain boundaries surrounded by precipitate depleted zones. Thermal stability of the Zr-modified alloys was examined by microhardness measurements conducted after prolonged exposures of the alloys to elevated temperatures. It was found that Zr is a structure stabilizing factor. Its influence was associated with formation of Zr-containing phases that do not undergo coarsening at elevated temperatures used (due to low diffusivity of Zr).

10:10 AM

The Effects of Alloying Elements on Microstructure and Mechanical Properties of Mg-MM-(Sn) Alloys: Hyun Kyu Lim¹; Do Hyung Kim¹; Ju Youn Lee¹; Won Tae Kim²; Do Hyang Kim¹; ¹Yonsei University; ²Cheongju University

In the present study, the effects of Sn addition on the microstructure and mechanical properties of Mg-MM (MM: misch metal) have been investigated. To optimize the mechanical properties of Mg-MM-Sn alloys, the effects of addition of Al or Zn have been further investigated. The secondary solidification phase in Mg-MM alloy changes dramatically with addition of Sn forming small rod-shaped phase. Although the strength of alloy is decreased with addition of Sn, the ductility is improved in Mg-rich Mg-MM-Sn alloys. To enhance the mechanical properties, a small amount of Al or Zn has been added in Mg-2MM-2Sn alloy. The rollability and mechanical properties are improved with addition of Al or Zn. From the result of conical cup test at 200°C, it has been found that the addition of alloying elements improved the formability of Mg-MM-Sn alloys.

10:30 AM

Phase Relations, Formation and Morphologies in Mg-Zn-RE (RE=Y, Rare Earth) Alloys: Alok Singh¹; ¹National Institute for Materials Science

Lattices of ternary and Mg-Zn binary phases are related to the matrix Mg phase through its basal plane. This characterizes the structural relationships among the phases and determines the orientation relationships formed by nucleation and growth of these phases over each other and the morphologies evolved, which finally affect strengthening. Orientation relationships and morphologies of icosahedral phase with ternary phases cubic W and pre-eutectic hexagonal H are described. A most important phase in this system is the binary monoclinic Mg₂Zn, which often nucleates over the icosahedral phase. In Mg-matrix this phase occurs in form of rods parallel to hexagonal axis, commonly known as β₁ phase, until now believed to be of structure of hexagonal MgZn₂ phase and the primary hardening phase in Mg-Zn alloys. Constraints to form low energy interfaces with the matrix produces a domain structure inside the rods, with four different orientations.

10:50 AM

A Study on the Microstructure of As-Cast and Homogenized Mg-Gd-Nd-Zr Alloys: Kaiyun Zheng¹; Jie Dong¹; Xiaolin Zeng¹; Wenjiang Ding¹; ¹Shanghai Jiao Tong University

Microstructure of Mg-xGd-2Nd-0.5Zr (x=6, 8, 11, Wt.%) alloys in as-cast and homogenized condition were investigated in this paper, using optical microscopy, scanning electron microscopy, transmission electron microscopy, energy dispersive X-ray spectrometry and X-ray diffraction. It was observed that all the as-cast alloys contained primary α-Mg solid solution, eutectic structures, cuboid-shaped phases, rod-like precipitates and Zr-rich clusters. The eutectic phase in Mg-11Gd-2Nd-0.5Zr was characterized to be of Mg₅Gd prototype with stoichiometry near Mg₅(Nd_xGd_{1-x}, x~0.43). Microstructural evolution of the alloys during homogenization can be divided into three coinstantaneous processes as follows: dissolving of eutectic phases, growth of cuboid-shaped phases and coarsening of grains. After appropriate homogenization, the alloys exhibit microstructure with little eutectic phases, small amount of cuboid-shaped phases and relatively fine grains, corresponding to excellent mechanical properties. The cuboid-shaped phase with a FCC crystal structure (a~0.56nm) was identified as a Gd-based ternary Gd-Nd-Mg phase.

11:10 AM

Heat Treatment and Tensile Properties of Cast Mg-5Gd-3Y-0.3Zr Alloy: Wangxing Li¹; Sujuan Yao¹; Sheng Yang²; Danqing Yi²; ¹Zheng Zhou Research Institute of Chalco; ²School of Materials Science and Engineering, Central South University

Microstructures, aging hardnesses and mechanical properties of as-cast Mg-5Gd-3Y-0.3Zr alloys were investigated. The microstructure is a typical dendritic structure of as-cast sample, after solution treated, the sample was aged at a temperature range of 200°C-250°C and at a different aging time, the hardness increases with the aging time prolonging, the aging peak hardness is high than 100HV at 200°C. Tensile strength was tested at temperature 25°C, 200°C, 250°C and 300°C, tensile strengths are 219 Mpa, 218 Mpa, 206 Mpa and 200 Mpa respectively. With the strengths decrease slightly, the elongations increase quickly. The results show that this alloy is a new type magnesium-rare earth alloy with high temperature excellent properties.

11:30 AM

A Comparative Study on the Solution Treatment of Mg-Al and Mg-Al-Ca Alloys: Lihong Han¹; Henry Hu¹; Derek Northwood¹; ¹University of Windsor

The solution treatment of permanent mold (PM) cast Mg- 5wt.% Al (AM50) and Mg- 5 wt.% Al- 2wt.% Ca (AC52) alloys was studied by Differential Scanning Calorimetry (DSC), microhardness and quantitative metallography. DSC showed that the temperature of the solution treatment was dependent on the type of the eutectic phases present in the alloys. The measurement of changes in microhardness with solution treatment time showed that it took about 10 hours for the AC52 alloy to reach a minimum value of microhardness while only 3 hours was required for the AM50 alloy. Quantitative metallography showed that the Mg₁₇Al₁₂ phase in the AM50 alloy dissolved quickly into the matrix at an early stage of solution treatment compared with the Ca-containing eutectics in the AC52 alloy. These observations on microstructural evolution and microhardness change suggest that these are different dissolution kinetics for the eutectic phases during solution treatment of the two alloys.

11:50 PM

Further Improvements in HPDC Mg Alloys for Powertrain Applications: Mark Gibson¹; Mark Easton²; Vinay Tyagi¹; Morris Murray³; Gordon Dunlop³; ¹CSIRO; ²Monash University; ³Advanced Magnesium Technologies

Rare earth containing magnesium alloys are the most promising alloys for powertrain applications. AM-HP2 has the best creep properties of currently proposed high pressure die casting alloys for elevated temperature applications. One of the most important issues for all creep resistant Mg alloys has been to obtain excellent creep properties and good castability simultaneously. A new die for assessing multiple aspects of castability has been designed. This die allows assessment of the many aspects of castability that are required for good casting quality including die filling, susceptibility to hot tearing and defects at flow fronts. Using this die, alloys with improved die castability and which retain the already excellent creep properties of AM-HP2, have been identified.

12:10 PM

Fracture Toughness in Magnesium Alloys by Dispersion of Quasicrystalline Phase: *Somekawa Hidetoshi*¹; Alok Singh¹; Toshiji Mukai¹; ¹National Institute for Materials Science

One of the most important criteria of safety and reliability of materials is the fracture toughness. However, the fracture toughness in magnesium alloys are lower than that in aluminum alloys. The dispersion of precipitates is generally the effective method to improving the mechanical properties in metallic material, but these particles easily become the origin of fracture. On the other hand, the characteristics of icosahedral phase are different from conventional crystalline phases, because this phase has quasi-periodic structure and very strong interface with matrix. This phase has been studied as the strengthening phase in magnesium alloys, but the effect of dispersion of quasi-crystalline phase on fracture toughness has not been investigated yet. In this study, the fracture toughness in Mg-Zn-RE alloys containing quasi-crystalline phase were examined, and the fracture mechanisms were observed in detail. The fracture toughness indicated higher values, and this phase pinned many dislocation movements and prevented void nucleation.

Materials for Infrastructure: Building Bridges in the Global Community: Session II

Sponsored by: The Minerals, Metals and Materials Society, Indian Institute of Metals, Chinese Society for Metals

Program Organizer: Brajendra Mishra, Colorado School of Mines

Wednesday AM
March 12, 2008

Room: 272
Location: Ernest Morial Convention Center

Session Chair: Subodh Das, Secat Inc

8:30 AM Invited

Steel for Bridges: *Virendra Kumar Mehta*¹; ¹Central Marketing Organisation, SAIL

Abstract not available.

9:00 AM Invited

The Development of High Performance Bridge Steel in China: *Chengjia Shang*¹; Huaxin Hou²; Aimin Guo³; Xinlai He¹; ¹School of Materials Science and Engineering, University of Science and Technology Beijing; ²Anshan Iron and Steel (Group) Corporation; ³Wuhan Iron and Steel (Group) Corporation

In the past decade, twenty six bridges have been constructed across Chinese longest river, Yangtze River. In the next decade, more than twenty bridges will be built across it. The first bridge on this river is Wuhan Bridge which established in 1950's, the steel, which was imported from USSR is Q235 grade; the second Yangtze river bridge is Nanjing Bridge which was constructed by domestic produced steel, Q345(16Mn, made by An-Steel). From then on, Q420 grade 15Mn-V-N produced by An-Steel was used to construct Jiujing Bridge in Jiangxi province with main span of 216m in 1990's, despite the disadvantage of welding ability; 14Mn-Nb (370MPa grade) was developed by WISCO to construct Wuhu Bridge with main span of 312m in early 2000's. These years, high performance bridge steel is urgently demanded by super bridge projects in China. A serial of 420,460,500 and 690MPa grade low carbon microalloying steel have been developed for steel bridge constructing. From the microalloying approach, low carbon or ultra-low carbon are accepted; Nb,V,Ti microalloys are used to fine the grain size, affect the TMCP and strengthen the matrix. On the other hand, the modern metallurgical technologies are applied and the steel achieves economy grade cleanness. The new developed bridge steels can achieve high strength, high toughness, good weldability and weathering resistance. The thickness can reach 80mm by TMCP. Last year, 12000 tons of high performance 420MPa grade plate steel had been used to construct Chongqing Yangtze River Bridge. The 460MPa grade steel has been accepted to design and construct the express railway bridge across Yangtze River in Nanjing. With the demanding and developing of high strength bridge steel, the employ performance, reliability should be paid more attention and the structural design theory and specification should also be improved.

9:30 AM Invited

Materials for Infrastructural Applications: *Jonathan Martin*¹; ¹National Institute of Standards and Technology

Recent natural (e.g., hurricanes Katrina and Rita) and anthropomorphic (e.g., the World Trade Centers and Boston's Big Dig) disasters have highlighted the important roles that construction materials play in catastrophic events. Construction materials also are playing an important role in the nation's aging and overburdened infrastructure. For example, the American Society of Civil Engineers (ASCE), in their 2005 Infrastructure Report Card, projects that the cost of repairing the nation's infrastructure back to good condition has escalated to over \$1.6 trillion dollars. To meet these challenges, advanced construction materials are needed. These construction materials will not only be expected to have improved initial and long-term performance properties (i.e., have longer service lives and longer mean times between repairs), but also, in many applications, will be expected to perform simultaneously multiple functions, e.g., enhancing the appearance of a structure while acting as a biocidal surface. In this presentation, field-observed construction material failures will be shown, and recent advances in the performance of construction materials will be documented.

10:00 AM Break

10:20 AM Invited

Steel for Buildings: *Supriya Das Gupta*¹; ¹MN Dastur and Company Pvt Ltd
Abstract not available.

10:50 AM Invited

Materials for Oil and Gas Transport: *David Olson*¹; ¹Colorado School of Mines

The demand on materials for transporting oil, natural gas, and other fluids, including hydrogen, ethanol, etc. is severe in terms of material strength, corrosion resistance, durability and maintainability. Lower temperatures and higher pressures are key factors in enhancing this demand on materials. The status and potential for performance ability of current materials available for transporting the fluids over long distances shall be reviewed. The research and development efforts for new ferrous and non-ferrous materials, including coating options, will be discussed. The strength and corrosion performance challenges will be highlighted.

11:20 AM Invited

High Strength Corrosion Resistant Fe/9Cr/0.1C Lath Martensitic Steels for Concrete Reinforcement: *Greg Kusinski*¹; Salem Faza²; ¹Clemson University; ²MMFX Technologies Corporation

One of the major problems facing the concrete construction industry today is the corrosion of steel reinforcement in concrete structures. In addition, congestion of reinforcement in heavily reinforced elements (such as mat foundations of high-rise buildings or confinement steel in columns of high-rises in seismic zones) is a critical constructability problem. In this paper, high-strength (YS > 100 ksi and 120 ksi) corrosion resistant steel, namely Microcomposite 9Cr steel, is presented from the aspect of alloy development, property characterization, and code implementation. We present principles of steel alloy design to produce nanophase multilayered structure composed of dislocated lath martensite separated by sheets of retained austenite. Such microstructure, which is free from interlath carbides, has an optimal combination of strength and corrosion resistance. A summary of a wide range of corrosion testing in saline environments carried out by many organizations including the Federal Highway Administration and many state Departments of Transportation (DOT's), will be presented to show that the MMFX-9Cr are a cost effective solution to offer 100 year design life of concrete structures. The steels conform to the new ASTM A1035 specification and their implementation into ACI 318-08 building code will be discussed. Structural engineering calculations will be presented to show that in certain cases it is possible to achieve up 50% steel reduction as compared with conventional grade 60 ksi steel. Furthermore, these principles of high strength design could also be applied for transportation and other applications to achieve significant cost savings.

WEDNESDAY AM

Materials in Clean Power Systems III: Fuel Cells, Hydrogen-, and Clean Coal-Based Technologies: Metallic Interconnects and Sealing in SOFCs

Sponsored by: The Minerals, Metals and Materials Society, TMS Structural Materials Division, TMS/ASM: Corrosion and Environmental Effects Committee

Program Organizers: Zhenguo "Gary" Yang, Pacific Northwest National Laboratory; Michael Brady, Oak Ridge National Laboratory; K. Scott Weil, Pacific Northwest National Laboratory; Xingbo Liu, West Virginia University; Ayyakkannu Manivannan, National Energy Technology Laboratory

Wednesday AM
March 12, 2008

Room: 392
Location: Ernest Morial Convention Center

Session Chairs: Paul Jablonski, NETL; Douglas Ivey, University of Alberta

8:30 AM Invited

Effects of Cell Operating Conditions on Degradation by Chromium: Terry Cruse¹; Michael Krumpelt¹; Brian Ingram¹; Gang Chen¹; Shanling Wang²; Paul Salvador²; ¹Argonne National Laboratory; ²Carnegie Mellon University

This research examines how the performance of solid oxides fuel cells (SOFC) degrades in the presence stainless steel bipolar plates as a result of chromium migration. The cells examined were commercially supplied anode supported cells with Ni/8YSZ cermet anodes, 8YSZ electrolytes, and LSM/8YSZ active cathodes. They were operated under varying temperatures and current densities, which influenced operating cell potential, degradation rate and chromium deposition for the cells. Several techniques were used to examine the cells after operation (e.g., 500 hours): transmission electron microscopy (TEM), scanning electron microscopy (SEM), energy dispersive spectroscopy (with both TEM and SEM), and high energy x-ray analysis at Argonne National Laboratory's Advance Photon Source. This research will provide information and a better understanding of how degradation of SOFC's by chromium occurs which will lead to a minimization of deleterious interactions between the SOFC cathode and chromium.

9:00 AM

Development of Multi-Component Air Braze Filler Metals for High-Temperature Electrochemical Application: K. Scott Weil¹; Jin Kim¹; Jens Darsell¹; Jung Pyung Choi¹; John Hardy¹; ¹Pacific Northwest National Laboratory

A silver-based joining technique referred to as reactive air brazing (RAB) has been recently developed for joining high temperature structural ceramic components of the type used in high-temperature electrochemical devices. In prior work, it was found that additions of CuO to silver have a significant effect on the wettability and joint strength characteristics of the resulting braze on polycrystalline alumina substrates. More recently it has been found that various ternary additions can further improve the wetting characteristics of these filler metals and/or increase their potential operating temperatures. This presentation will describe the use of several different types of additions, including: (1) a titania dopant added to increase wetting, (2) a palladium alloying agent added to increase use temperature, and (3) inert particulate such as alumina and yttria-stabilized zirconia powder/fiber added to increase joint strength.

9:25 AM

Effects of Y, Co, and Y/Co Coatings on the Oxidation Kinetics of Ferritic Stainless Steels for SOFC Interconnect Applications: Seong-Hwan Kim¹; Joo-Youl Huh¹; Jae-Ho Jun²; Do-Hyeong Kim²; Joong-Hwan Jun²; ¹Korea University; ²RIST

Ferritic stainless steels are considered as promising interconnect materials for SOFCs, owing to their low cost and good thermo-mechanical compatibility with other components in SOFCs. However, the continuous growth of poorly conducting oxide scales in the SOFC operating environment, which degrades the stack performance, is the major challenges to be overcome for the used of ferritic stainless steels as interconnect materials. In this study, we have investigated the effects of Y, Co and Y/Co coatings on the oxidation behavior of STS444 and Crofer 22 APU. After oxidation for times up to 1000 h in air at 800°C, uncoated and coated samples were characterized using thermogravimetry (TG), X-ray

diffraction (XRD), scanning electron microscopy (SEM), glow discharge spectrometry (GDS), and area specific resistance (ASR) measurements. In the presentation, the correlation between the oxidation behavior and electrical properties of oxide scales will be discussed in terms of the redistribution of the coating elements.

9:45 AM

Niobium-Clad Stainless Steel for Bipolar Plate Material of PEMFC: Sung-tae Hong¹; K. Scott Weil¹; ¹Pacific Northwest National Laboratory

Niobium (Nb)-clad 304L stainless steel (SS) is currently under consideration for use as a bipolar plate material in polymer electrolyte membrane fuel cell (PEMFC) stacks. The Nb-clad SS was fabricated via roll bonding. Results from mechanical testing suggest that annealing treatment after roll bonding may be necessary to improve the ductility and reduce the springback of the material. Microstructural analysis of the specimens indicates that two failure conditions can potentially arise, dependent on the thermomechanical condition of the material. In the as-rolled condition, failure initiates via fracture through the Nb cladding. In the annealed specimens, failure can occur by brittle fracture of an interfacial intermetallic layer that forms during the annealing treatment. This generates a series of crack-induced pores along the interface between the Nb cladding and the SS core, which eventually leads to ductile failure of the Nb cladding via localized necking.

10:10 AM Break

10:25 AM Invited

Observation of Metal Nanoparticles in Oxide Scale by Synchrotron X-Ray Nano-Beam: Zuotao Zeng¹; Ken Natesan¹; Zhonghou Cai¹; ¹Argonne National Laboratory

Oxide scale is generally considered to consist of oxides. However, our recent nano-X-ray beam analysis indicated the scale to be a mixture of oxides and metal particles. This result can have broad influence on several research areas. For example, how carbon diffuses through oxide scale and leads to carburization and metal dusting have not been well understood. If metal particles are present in the oxide scale, carbon can diffuse through the channels that established by metal particles in the scales. Currently, solid oxide fuel cell requires low resistivity for oxide scales that develop on alloys for metallic interconnects. If metal particles are present in oxide scale, it may lead to electrical short and greatly reduce the area resistance of metallic interconnects. On the other hand, if we can prevent the formation of metal particles in oxide scale, carburization can be retarded by elimination of the carbon transfer channels.

10:55 AM

Selecting the Appropriate Air Brazing Conditions for Joining Reactive Substrates: K. Scott Weil¹; Jens Darsell¹; John Hardy¹; ¹Pacific Northwest National Laboratory

Air brazing technology is being developed at Pacific Northwest National Laboratory as means of joining and/or hermetically sealing metal and ceramic components used in high-temperature electrochemical devices such as solid oxide fuel cells, oxygen and hydrogen gas concentrators, and sensors. On several occasions, it has found that when molten, the conventional air braze filler metal (Ag-CuO) will react excessively with a given substrate; cobalt-containing oxide or metal alloys tend to be particularly reactive. We have developed several processing strategies that mitigate the extent of interfacial reaction and thereby avoid the associated loss in joint strength typically observed. Select examples and applications will be discussed in this presentation.

11:20 AM Invited

The Operating Characteristics of Diesel-Driven SOFC: Inyong Kang¹; Yunhyeok Kang¹; Sangho Yoon¹; Gyujeong Bae¹; Joongmyeon Bae¹; ¹Korea Advanced Institute of Science and Technology

The flowrates and composition of the reformat produced by the diesel autothermal reformer were changed according to the reforming conditions, such as GHSV, H₂O/C and O₂/C. Therefore, the reforming conditions directly affect the SOFC performance. And, although the reforming performance at a certain point is known, the performance of the autothermal reformer and SOFC often degrades steadily due to carbon deposition from lighter hydrocarbons. Fortunately, CH₄ did not cause any problems when an appropriate H₂O/C was determined for direct internal reforming (DIR) with a Ni-based anode. But other

light hydrocarbons, such as normal butane($n\text{-C}_4\text{H}_{10}$), caused severe carbon deposition, even at experimentally-proven carbon free conditions for $\text{CH}_4\text{-DIR}$. Therefore, the maintenance of high diesel conversions is very important for the longer-term performance of the diesel-driven SOFC system. In this study, the SOFC single stacks and the 5-cell stack were provided by the Korea Electric Power Research Institute(KEPRI).

11:45 AM

Comparison of High Velocity and Quasi-Static Forming of Sheet Metals: *Kristin Banik*¹; Scott Golowin¹; John Bradley²; Keith Newman²; Steve Hatkevich³; Glenn Daehn¹; ¹Ohio State University; ²General Motors Corporation; ³American Trim Corporation

The ability to manufacture sheet metal components of complex shape by stamping is limited by the ductility limits. In this study, the formability of a variety of sheet metals were evaluated both quasi-statically and with high-velocity forming. A single-sided die with narrow serpentine channels was used with a high pressure urethane pad to establish baseline quasi-static conditions. The austenitic stainless steel and Ni-based alloy exhibited adequate formability, whereas the other materials failed by splitting. Using the same die, the materials were subjected to high-velocity electromagnetic forming. This resulted in enhanced ductility. Ti and ferritic stainless steel sheets could now be formed without splitting. All samples were evaluated for hardness, microstructure, deformation depth and other properties. The improvement in formability may be due to the high strain rates ($\sim 10^5 \text{ s}^{-1}$) or the largely compressive stress state on impact. Efforts to make high velocity processes suitable for commercial use will be discussed.

Materials Informatics: Enabling Integration of Modeling and Experiments in Materials Science: Informatics and Materials Theory and Modeling

Sponsored by: The Minerals, Metals and Materials Society, TMS Materials Processing and Manufacturing Division, TMS/ASM: Computational Materials Science and Engineering Committee

Program Organizer: Krishna Rajan, Iowa State University

Wednesday AM
March 12, 2008

Room: 271
Location: Ernest Morial Convention Center

Session Chair: To Be Announced

8:30 AM

Applying Informatics to Semi-Empirical First Principles Calculations: *S. Broderick*¹; H. Aourag²; Krishna Rajan¹; ¹Iowa State University; ²Tlemcen University

In this presentation we discuss how statistical learning techniques can be used to augment more classical approaches to computational based design of materials. The role of data mining to identify dominant parameters influencing phase stability calculations is demonstrated. The use of such informatics based techniques to accelerate the computational approaches for first principle calculations is discussed. NSF International Materials Institute: Combinatorial Sciences and Materials Informatics Collaboratory (CoSMIC-IMI).

8:55 AM

Applying Information Theory to Crystal Structure Design: *Chang Kong*¹; Changwon Suh¹; S. Arapan²; R. Ahuja²; Krishna Rajan¹; ¹Iowa State University; ²Uppsala University

Data mining and informatics are becoming one of the main areas in the computational methodologies for the materials design. The classification and visualization of data structure by applying appropriate criteria enable us to readily extract useful knowledge through the discovery of the trends within the database. The concepts of information theory, which originally started from the telecommunication systems, have been widely used in various fields including materials science especially at the single atom or molecule level. However, there has rarely been a scientific search of their application for the analysis of crystal-level, yet atomically defined, materials. In this presentation, we provide the

examples of the analysis using information theory for the multivariate data of inorganic crystal structures. The application of the information theory is mainly focused on the classification of structure data and the evaluation of the used criteria, as the part of the prediction procedure of inorganic crystal-structure. NSF-International-Materials-Institute:-Combinatorial-Sciences-and-Materials-Informatics-Collaboratory-(CoSMIC-IMI).

9:20 AM

Data Mining, First-Principles Calculations and Thermodynamic Modeling for Ir-W Alloys: *Tao Wang*¹; Krishna Rajan¹; ¹Iowa State University

Ir-base alloy has been found to be a promising material for high-temperature applications. Most studies on Ir-base systems have suffered from limited and inaccurate thermodynamic information. Our work here has focused on the construction of thermodynamic database for the Ir-W system using first-principles approach, thermodynamic modeling and data mining techniques. We have found that a combination of data mining, first-principles calculations and thermodynamic modeling can not only provide a reliable thermodynamic database but also help us to understand the role of key electronic factors.

9:40 AM

Informatics Aided Structure Maps: *C. Suh*¹; S. Iwata²; Krishna Rajan¹; ¹Iowa State University; ²University of Tokyo, Research into Artifacts, Center for Engineering

It is shown how conventional structure maps of spinel nitrides are created from data mining techniques. It is shown how data driven analysis of structural data coupled to property calculations can also help establish structure-property relationships unlike traditional structure maps. Examples are shown for nitrides and how these results compare with classical bi-variate mapping of structure classification. The value of informatics as a powerful tool for developing new structure maps and their role in materials design is discussed. NSF International Materials Institute: Combinatorial Sciences and Materials Informatics Collaboratory (CoSMIC-IMI).

10:05 AM

Predicting Multi-Component Crystal Structures Using Data Mining and Quantum Mechanics: *Geoffroy Hautier*¹; Chris Fischer¹; Gerbrand Ceder¹; ¹Massachusetts Institute of Technology

Crystal structure prediction is a fundamental problem in computational materials science. Although material property predictions can now be reliably addressed ab initio, for predictions to be relevant, they must be performed on the stable crystal structure of the compound. Predicting crystal structure is therefore an essential step in any computational materials design scheme. We have developed a method to predict the structure of multi-component systems using data mining and quantum mechanics. We demonstrate an algorithm that detects similarities between crystal structure in order to find the structure prototypes in any database. Correlations between prototypes can then be extracted from the prototyped database to assess the probability for a compound to form in a given crystal structure. The results of our prototyping and data mining algorithm on the Inorganic Crystal Structure Database (ICSD) are discussed.

10:30 AM

Representation of Complex Microstructures: A Data Perspective: *Richard LeSar*¹; ¹Iowa State University

One of the challenges facing those seeking to apply materials informatics methods is that properties of materials often depend critically on the three-dimensional distribution of interfaces, defects, impurities, etc., i.e., properties depend on the microstructures of the materials. The key challenge is to represent those microstructures in a way that captures the essential structural features yet is simple enough for inclusion in a searchable materials database. In this talk we will discuss ways to represent the microstructures of systems of dislocations. We will base the discussion on results from discrete dislocation simulations and will discuss various scaling relations, cluster expansions, correlation functions, etc. that have been used to capture aspects of the dislocation microstructures.

11:05 AM

Superalloy Grain Growth Model Development through Simulation-Experimentation Integration: *Eric Payton*¹; Gang Wang¹; Ning Ma¹; Yunzhi Wang¹; Michael Mills¹; ¹Ohio State University

Grain size is an important input for prediction of mechanical behavior of structural materials. Accurate physics-based modeling of grain growth is expected to accelerate the insertion of advanced alloys. During thermomechanical processing, the variation of distributions and volume fractions of pinning particles with thermal exposure control grain growth behavior and hence determine the grain size and distribution. Various electron microscopy techniques and digital image processing methods are being used to characterize the grain size distribution and populations of pinning phases in Ni-base superalloys during thermal exposure. Characterization results are being fed into phase-field and mean-field simulations. Simulation results are being compared to experimental observations, then used to elucidate the microstructural parameters for which additional characterization is needed to increase accuracy and generality of a model for predicting grain size during heat treatment. The established feedback loop between experimentation and simulation has enabled focused experimentation and development of fast-acting predictive models.

11:30 AM

Pandat Software for Materials Property Simulation of Multi-Component Systems Linking Calphad with Materials Informatics: *Weisheng Cao*¹; Shuanglin Chen¹; Fan Zhang¹; Kaisheng Wu¹; Ying Yang¹; Y. Chang²; ¹CompuTherm LLC; ²University of Wisconsin

The Pandat, integrating PanEngine, PanOptimizer and PanStar, bridges all the functionalities for thermodynamic calculation, property optimization, and precipitation simulation of multi-component systems based on Calphad approach. This software package, in combination with thermodynamic/kinetic/thermophysical databases, provides an integrated workspace for simulating materials properties of multi-component systems. The simulation results, which include phase equilibria, thermophysical properties, and microstructure related information, are critically needed in alloy design, selection of parameters for fabrication steps such as heat treatment, prediction of performance, and failure analysis. In addition to the functionalities provided in Pandat, its calculation/optimization engines (PanEngine, PanStar and PanOptimizer) are built as shared libraries and enable their integrations with other models for wider applications in materials science and engineering. This provides a linkage of Calphad approach with materials informatics.

11:55 AM

Virtual Candidate Spaces: Developing Design Rules for Data-Driven Exploration: *Kim Ferris*¹; Bobbie-Jo Webb-Robertson¹; Dumont Jones²; ¹Pacific Northwest National Laboratory; ²Proximate Technologies, LLC

Traditional approaches to materials development rely upon a data point by data point approach, becoming highly dependent upon prior art and variations of current topical materials. This presentation will discuss strategies for identification of candidate materials for gamma radiation detection as prototypical examples for more efficient virtual candidate exploration. An information-based approach has been applied to ranking the alkali/alkali earth halide series on their energy conversion efficiency and luminosity response. Relevant data are sparse (25% coverage), but sufficient to complete the forward mapping of materials properties through materials signatures. These mappings are used to explore the limits of the conversion efficiency as a function of chemical composition, and examine its relationship with weight density. For scintillator luminosities, we illustrate that forward mappings are only the starting point for development of design rules, which provide both synthetic guidance for materials chemists as well as a measure of bounding materials performance.

Mechanical Behavior, Microstructure, and Modeling of Ti and Its Alloys: Microstructure/Property Correlation II

Sponsored by: The Minerals, Metals and Materials Society, TMS Structural Materials Division, TMS: Titanium Committee

Program Organizers: Ellen Cerreta, Los Alamos National Laboratory; Vasisht Venkatesh, TIMET; Daniel Evans, US Air Force

Wednesday AM

March 12, 2008

Room: 384

Location: Ernest Morial Convention Center

Session Chairs: Thomas Bayha, ATI Allvac/Research and Development; M. Ashraf Imam, Naval Research Laboratory

8:30 AM

Ageing Behavior of Deep-Hardenable Ti-10V-6Cu Alloy: *Hoi Pang Ng*¹; Colleen Bettles¹; Barry Muddle¹; ¹Monash University

The phase stability map proposed by Morinaga for titanium alloys indicates a potential locus for deep-hardenable alloys in the Bo vs Md space. A novel heat-treatable beta alloy Ti-10V-6Cu in the vicinity of the locus has been developed and the dependence of its isothermal ageing behaviour on initial quench rates has been studied. Transmission electron microscopy reveals distinct sizes and morphologies of omega phase in water-quenched and air-quenched samples. However, their effect on the ageing behaviours at 350°C and 500°C, respectively, is confined only to the first few minutes of ageing; after which the hardness profiles are indistinguishable, implying a deep-hardenable character of the alloy. In this work, emphasis is put on the effect of omega phase on the transformation of alpha phase occurred at 500°C ageing. A transitional rhombohedral omega phase has been characterised and its potential role as the nucleation site for alpha phase is discussed.

8:50 AM

Elevated Temperature Oxidation Resistance of Boron Modified Titanium Alloys: *Deborah Sweeney*¹; *Raghavan Srinivasan*¹; ¹Wright State University

It has been established that the addition of trace amounts (~0.1 wt%) of boron to titanium alloys refines the as-cast grain size by an order of magnitude. Reports also indicate that the room temperature corrosion resistance of the boron containing alloys may be substantially greater than conventional titanium alloys. In this study, the effects of boron addition on oxidation resistance are investigated, since conventional titanium alloys have limited corrosion resistance in air above 650°C. The mass gain per unit surface area is measured at an elevated temperature to compare the oxidation of alpha-beta and beta titanium alloys with boron and without boron additions, by exposure to air. These findings are presented in conjunction with the overall characterization of boron modified titanium alloys. Results include microstructural characterization of the oxide layer and the formation of the alpha case and also the hardness of each layer.

9:10 AM

Effect of Oxygen on Fracture Toughness and Stress-Corrosion Cracking of Ti-6211: *Peter Pao*¹; M. Imam¹; Harry Jones¹; Robert Bayles¹; Jerry Feng¹; ¹Naval Research Laboratory

Oxygen is a potent solid solution strengthener in titanium alloys and, in relatively small concentrations, can significantly increase the tensile strength and affect the cracking resistance of these alloys. The effect of oxygen concentrations ranging from 0.075 to 0.29 wt% on the fracture toughness, stress-corrosion cracking (SCC) resistance, and fatigue crack growth of Ti-6Al-2Nb-1Ta-0.8Mo (Ti-6211) is investigated. While oxygen has little effect on the fracture toughness below 0.236 wt%, it can significantly reduce the fracture toughness at higher concentrations. Oxygen strongly affects the SCC resistance of Ti-6211. The SCC threshold decreases from more than 120 MPavm for an alloy that contains 0.075 wt% O to 40 MPavm for an alloy that contains 0.29 wt% O. The fatigue crack growth kinetics for Ti-6211 is not affected by the oxygen concentration. The interplay of SCC susceptibility, fracture paths, and fracture mechanisms in Ti-6211 with various amounts of oxygen will be discussed.

9:30 AM

The Effect of Thermal Oxidation on the Fatigue Behavior of Ti6Al4V and Ti6Al7Nb Alloys: *Onur Meydanoglu¹; Mehmet Cingi¹; Murat Baydogan¹; Huseyin Cimenoglu¹; Eyup Kayali¹*; ¹Istanbul Technical University

Ti6Al4V alloy is the most favorable titanium alloy because of good combination of improved strength-to-weight ratio, high fatigue resistance with an excellent corrosion resistance. It covers more than 50% of total titanium usage. Recently Ti6Al7Nb alloy has been developed as an alternative to Ti6Al4V by substitution of vanadium by niobium. In this study, the effect of thermal oxidation on fatigue behavior of Ti6Al4V and Ti6Al7Nb has been examined. Based on our previous study which gives the optimum oxidation conditions, thermal oxidation of alloys was performed by holding the samples at 600°C for 60h in atmospheric conditions. The fatigue tests were performed on as-received and thermally oxidized samples utilizing a rotating bending fatigue tester. Characterization of the oxide layer was made by means of optical microscopy, X-ray diffractometer and hardness measurement. The fractured surfaces of the samples were investigated by scanning electron and stereo microscopes.

9:50 AM

Effect of Heat Treatment on Microstructures and Properties of Y-Bearing TiAl Alloy: *Yuyong Chen¹*; ¹Harbin Institute of Technology

In this article, the microstructure control and properties for various microstructures of Ti-45Al-5Nb-0.3Y have been studied using relatively large forged pancake. The canned forging pancake was successfully gained. The effect of processing and heat treatment on microstructure and properties was studied using X-ray diffraction, optical microscopy, scanning electron microscopy (SEM) and transmission electron microscopy (TEM). Results showed that the microstructure of forged pancake consisted of major curved lamellar, broken lamellar and minor dynamic recrystallized grains (DRX) with the size of about 1-2µm and the YAl₃ phase at grain boundaries. Three different microstructures, duplex, nearly lamellar and fully lamellar, have been obtained through heat treatment, respectively. And the microstructure evolution was also analyzed. The alloy with duplex microstructure owed the best ductility, the elongation reached 1.9%, and which with fully lamellar microstructure took on better strength, yield strength and fracture strength were 557.1MPa and 715MPa, at room temperature, respectively.

10:10 AM

Effect of Hot Isostatic Pressing(HIP) and Heat Treatment(HT) on Microstructure and Properties of As Cast Ti-15-3 Alloy: *Hai Nan¹*; ¹Beijing Institute of Aeronautical Materials

Because as cast Ti-15-3 alloy has very high strength compared with as cast Ti-6-4 alloy, some critical aero-components are needed cast by Ti-15-3 alloy to substitute other alloy in aviation industry. Before and after HIP and HT, as cast Ti-15-3 alloy microstructure and mechanical properties were investigated. After HIP, the cast defects such as shrinkage voids, microvoids and gas holes almost disappeared. After HIP and HT, as cast Ti-15-3 alloy mechanical properties increased greatly. Especially its ultimate tensile strength was over 1100MPa. The elongation of as cast Ti-15-3 alloy still need more research to increase it over 4% in order to be widely used.

10:30 AM Break

10:50 AM

Microstructural and Mechanical Behavior Characterization of Ultrasonically Consolidated Titanium – Aluminum Laminates: *Tomoko Sano¹*; James Catalano¹; Daniel Casem¹; Dattatraya Dandekar¹; ¹US Army Research Laboratory

Multilayered hybrid metal laminates have been studied for structural applications due to their potential for higher strength, toughness, and stiffness. The goal of this study is to modify and engineer the microstructure and mechanical properties of commercial purity titanium (CP-Ti) and 1100 aluminum (Al) laminates for potential applications in mine blast mitigation. Alternating layers of 50 µm thick CP-Ti and Al layers were ultrasonically consolidated. To provide high hardness and stiffness, the consolidated material was heat treated in a variety of conditions to form intermetallic TiAl₃ layers. The CP-Ti/TiAl₃/Al layers processed by the various heat treatments were characterized by scanning electron microscopy to choose the best laminate microstructure for plate impact testing, an instrumented laboratory scale test to characterize the dynamic spall

behavior of the material. From those tests, it was determined that the sample with the TiAl₃ layers had greater spall strength than the sample without the TiAl₃ layers.

11:10 AM

Microstructure and Mechanical Properties of Sponge Ti and Its Alloy Powders with Various Powder Metallurgical Processes: *Haitham El Kadiri¹; William Peter²; Robert Whitehorn¹; Seong Jin Park¹; Youssef Hammi¹; Randall German¹; Craig Blue²; Jim Kiggans²*; ¹Mississippi State University; ²Oak Ridge National Laboratory

Newly developed sponge Ti powder and its alloys have price competitiveness in automotive application. In this study, sponge Ti and several alloys with Al, V, Fe, Zn, Mo, Mn, Sn, Nb, and Cr₃C₂ were investigated in various powder metallurgical processes such as vacuum hot press and rolling process, conventional press and sinter, and powder injection molding. All samples were analyzed in term of density, microstructure, and mechanical properties. The microstructures generated by different compositions and processes were characterized and modeled to rationalize the conflicting effects of substitutional elements on the density, yield strength, ductility, and cost.

11:30 AM

The Effect of Processing Parameters on Biocompatibility of Micro-Arc Oxidized Titanium Alloys: *Mert Gunyuz¹*; Murat Baydogan¹; Huseyin Cimenoglu¹; Eyup Kayali¹; ¹Istanbul Technical University

In this study, the effect of micro arc oxidation process on surface morphology of Ti₆Al₄V alloy. Micro arc oxidation was performed by using an AC power supply operating in constant voltage mode between 450-600V using two different electrolyte. Mechanical and physical properties were evaluated on the surface including hardness, wettability, surface roughness and scratch resistance of the oxide film. Rockwell C testing was used to compare the relative adhesion characteristics of the oxide film. The surface oxidized samples were hold in simulated body fluid (SBF) to compare the biocompatibility. The surface oxide layer was examined by an X-ray diffractometer and a scanning electron microscope before and after SBF testing. Mechanical and physical properties as well as surface morphology relative biocompatibility of the samples were discussed on the basis of micro arc oxidation parameters such as applied voltage and electrolyte composition.

11:50 AM

An Investigation on Biocompatibility of Titanium Alloys: *Nuray Balaban¹; Murat Baydogan¹*; Huseyin Cimenoglu¹; Eyup Kayali¹; ¹Istanbul Technical University

Titanium alloys can successfully be used in manufacturing dental and orthopedic implants because of high biocompatibility of oxide layer formed at the surface. Thermal oxidation is the simplest way in forming an oxide layer at the surface and bioactivity of this layer can be further improved with optimizing processing parameters such as time and temperature. In this study, biocompatibility of Ti₆Al₄V and Ti₆Al₇Nb alloys was evaluated by means of holding the samples in a simulated body fluid (SBF) for seven days. The samples were subjected to acidic etching and then thermal oxidation at 400°C and 600°C for different times. Characterization of surface layers before and after SBF tests were carried out by means of surface roughness, wettability measurements, XRD and SEM equipped with EDS. Ti6Al7Nb alloy exhibited best bioactivity after acidic etching prior to thermal oxidation at 400°C for 4 hours.

12:10 PM

Thermo-Mechanical Processing of Boron Modified Beta Titanium Alloys: *Balakrishna Cherukuri¹*; Raghavan Srinivasan¹; Sesh Tamirisakandala²; Shibayan Roy³; Satyam Suwas³; ¹Wright State University; ²FMW Composite Systems; ³Indian Institute of Sciences

Trace Boron additions to titanium alloys have shown to reduce the grain size in as-cast condition. Two beta titanium alloys: Beta-21S and Ti-5553 with 0.1 wt% B and without boron additions were used in this investigation. The effect of Boron on the thermo-mechanical processing is investigated. Isothermal compression tests were carried out at temperatures ranging from 775 to 950 °C at different strain rates ranging from 0.001/s to 1/s. The effect of boron on the processing of beta alloys will be presented in the light of micro-structural effects and the deformation behavior.

WEDNESDAY AM

Mechanics and Kinetics of Interfaces in Multi-Component Materials Systems: Joint Session with Advances in Semiconductors, Electro Optic and Radio Frequency Materials

Sponsored by: The Minerals, Metals and Materials Society, TMS Electronic, Magnetic, and Photonic Materials Division, TMS Structural Materials Division, TMS/ASM: Composite Materials Committee, TMS: Thin Films and Interfaces Committee

Program Organizers: Bhaskar Majumdar, New Mexico Tech; Rishi Raj, University of Colorado, Boulder; Indranath Dutta, US Naval Postgraduate School; Ravindra Nuggahalli, New Jersey Institute of Technology; Darrel Frear, Freescale Semiconductor

Wednesday AM
March 12, 2008

Room: 279
Location: Ernest Morial Convention Center

Session Chairs: Anthony Fiory, New Jersey Institute of Technology; Bhaskar Majumdar, New Mexico Tech

8:30 AM Introductory Comments

8:40 AM Invited

Morphological Evolution in Polycrystalline Films: *Ramanathan Krishnamurthy*¹; Mikko Haataja²; ¹Caterpillar Inc., Technical Center; ²Princeton University

Growth models for polycrystalline films commonly used in optoelectronic/materials applications do not consider grain size effects. We address this issue via a thermodynamics-based method that effectively handles grain grooving, lateral growth and surface fluctuations. Groove profiles formed upon annealing (zero flux) deviate considerably from the Mullins' result. Depending upon whether the annealing transport mechanism conserves mass or not, grooving stops completely at late times/small grain sizes L , or a steady state wherein the entire film is translated along its thickness is attained. The surface roughness, for all annealing transport mechanisms, varies as $1/\sqrt{L}$ and L for large/small L , in agreement with recent STEM observations. Using electrodeposition as an example, we demonstrate that height profiles for growing films (non-zero flux) depend critically upon the ratio of the maximally unstable wavelength for growth and the grain size. We also present results for the effect of lateral grain motion on growth morphologies.

9:05 AM Invited

Engineered Interfaces for Silicon Solar Cell Applications: *Bhushan Sopori*¹; ¹National Renewable Energy Laboratory

Fabricating high-efficiency Si solar cells requires precise control of bulk material quality and of the electrical and optical properties of interfaces. To control the optical properties, interfaces are designed to provide minimum reflection and maximum light trapping within the desired, broad, spectral range. This is accomplished by providing shaped, rough interfaces and by antireflection/reflection coatings. These features result in optical scattering, leading to very high absorption of the light within a useable spectrum (i.e., in the 0.4–1.1 μm wavelength range) and a concomitant high photo-carrier generation. Electronically, interfaces must provide a very low carrier recombination to prevent loss of photogenerated carriers. One additional consideration for interfaces relates to process design. Solar cell fabrication requires processes such as plasma depositions that can produce surface damage, which can introduce undesirable losses. Hence, such damage must be "healed" during subsequent processing. This paper reviews methods used in fabricating solar cells to achieve interface control. In particular, we discuss interface design features such as texturing, passivation using insulating films with control charge, and minority-carrier reflecting mirrors by dopant grading.

9:30 AM

Simulations of Absorption Efficiency for Three Dimensional Carbon Nanotube Based Photovoltaics: *Jack Flicker*¹; Jud Ready¹; ¹Georgia Tech Research Institute

The production of cheap energy from the sun will be a major research objective in the coming years. Major strides must be made in solar cell efficiency, including increasing the absorbance efficiency of a cell by etching or texturing.

In order to increase the absorbance efficiency of solar cells, we have developed a three dimensional solar cell structure by depositing a cadmium telluride thin film overtop carbon nanotube towers. These towers act as both a scaffolding and electrical interconnect. Multiple photon interactions as they reflect between these towers increase the absorption efficiency. We have developed a theoretical model and computer simulation to maximize the number of photon interactions due to the geometrical characteristics of the system (aspect ratio, spacing, size, shape, etc). Simulated modeling has shown that by optimization of parameters a three dimensional cell can obtain up to a 300% increase in power production over traditional cells.

9:50 AM Invited

Electromigration Related Effects at Hetero-Interfaces in Multi-Component Systems: *Indranath Dutta*¹; S. Menon¹; C. Park¹; P. Kumar¹; ¹US Naval Postgraduate School

In many applications with interfaces between dissimilar materials, at least one of the components adjoining the interface is subjected to a large current density and concurrent Joule heating to high homologous temperatures. Under these conditions, electromigration (EM) becomes prominent, and superposed on other thermo-mechanical effects, can cause unusual, scale-sensitive phenomena. In this paper, two instances of EM-related effects next to hetero-interfaces are discussed. First, the influence of EM-induced interfacial diffusion on diffusionaly accommodated interfacial sliding in thin film structures in microelectronic devices will be discussed. Model and experiments capturing the interaction between EM and interfacial creep will be presented. Secondly, experimental observations of EM-driven liquid transport along thin film surfaces will be presented, along with potential implications for railgun technology. Based on this, a new method for conformally coating thin film structures with low melting metals, results from which will also be presented. Supported by NSF-DMR-0513874 and ONR-MURI-N00014-04-1-0599RQ-M.

10:15 AM Break

10:25 AM Invited

Interface Reliability in Microelectronic Packages: *Vijay Sarihan*¹; ¹Freescale Semiconductor, Inc.

Microelectronics and MEMs use a very large variety of packages determined by specific application requirements. This can be from the traditional SOICs all the way to recent advanced packages like the Redistributed Chip Package (RCP). These packages are multilayered structures, use a variety of different materials in the same package and as a result have a large number of distinct interfaces. These packages during assembly, reliability testing and field applications are subjected to a wide variety of processing and environmental exposures like high humidity exposure, high temperature reflow, thermal cycling, shock and drop testing. One of the key package reliability concerns is the interfacial reliability, and interfacial integrity is crucial to the success of all packages. In this paper a number of different package types will be addressed where interfacial integrity was the primary failure mode. These include exposed pad SOIC packages, molded multi chip packages on insulated metal substrates, anisotropic conductive film packages and molded flip chip modules. The emphasis will be on the use of finite element approach with the incorporation of interfacial fracture mechanics.

10:50 AM

Magnetic Field Assisted Assembly-Theory and Experiments: *Rene Rivero*¹; V. Kasisomayajula¹; Shanmugamurthy Fnu¹; Tzesar Seman¹; Sudhakar Shet¹; Michael Booty¹; Anthony Fiory¹; Nuggahalli Ravindra¹; ¹New Jersey Institute of Technology

Principles of magnetic field assisted assembly are summarized. Experimental techniques for the assembly process with an optimal control system with feedback is described. The results of the study are analyzed in relation to applications in manufacturing of heterogeneous systems.

11:10 AM

Recyclable Clean Copper: A New Generation EMI Shielding Material: *Colin Tong*¹; Doug Tilghman¹; ¹Laird Technologies

Recyclable clean copper (RCC) is new generation high strength conductive material for a wide range of slotted EMI shielding applications. CuBe has long set the benchmark for EMI shielding and elastic performance. Other alloys come with compromises in terms of both shielding effectiveness and elastic

performance. Offering attenuation performance nearly comparable to CuBe and stress relaxation similar to that of CuBe, this novel RCC alloy offers an appealing alternative to traditional CuBe gaskets. Meeting the attenuation and installation requirements of many products, this new alloy fulfills the needs of manufacturers who face an increasingly competitive global marketplace, in which consumers are both environmentally concerned and price conscious. RCC meets their needs by providing excellent attenuation and mechanical properties while softening the cost impact of rising copper prices. This paper gives a broad overview of how RCC performs and highlights the key advantages of the novel RCC products.

11:30 AM

A Fabry-Perot Interferometric Pressure Sensor with Alignment Tolerance and High Temperature Performance: *Ivan Padron*¹; *Anthony Fiory*¹; *Nuggehalli Ravindra*¹; ¹New Jersey Institute of Technology

The Fabry-Perot interferometry is one of the most popular of the several optical techniques available for the fabrication of an optical sensor that can provide high degree of sensitivity, versatility and immunity to environmental noise. The Fabry-Perot Interferometric Sensor (FPIS), to be discussed in this presentation, consists of a Fabry-Perot cavity formed between two bonded surfaces: a corrugated diaphragm with a center rigid body (or boss) which deflects under external pressure and keeps a high alignment tolerance and a glass surface with an optical fiber insert. The Fabry-Perot cavity and optical fiber have been used as the sensing element and interconnect, respectively. The Fabry-Perot cavity has been fabricated using the MEMS technology. Micromachining techniques make Fabry-Perot sensors very attractive by reducing the size and the cost of the sensing element.

11:50 AM

Studies of PMD Intrinsic Dynamics of Spooled Fibers under Highly Stable Conditions: *Julio Martinez*¹; ¹New Jersey Institute of Technology

State of polarization (SOP) and polarization mode dispersion (PMD) of optical communications fibers in an environmentally controlled atmosphere were measured at 1550 nm with a 100 nm bandwidth over extended time periods. The test fibers, which comprised various dispersion compensation module (DCM) spools, were sealed within a vibration-isolated isothermal chamber (three-sigma temperature variation less than 0.02°C). Autocorrelation function analysis, which is used to establish the average drift time associated with intrinsic fiber decorrelation, reveals slowly varying intrinsic dynamics and suggests non-constant dielectric properties of the fibers in a stabilized environment. However, the dynamical magnitudes are much smaller than in fiber-optic communications links, particularly in buried sections, which are subject to seasonal temperature changes and other environmental disturbances. The results are particularly relevant to the hinge model of PMD, which attributes most of the PMD variability in a fiber-optic link to environmental exposure of the DCMs.

Neutron and X-Ray Studies for Probing Materials Behavior: Stresses/Strains and Structure

Sponsored by: National Science Foundation, The Minerals, Metals and Materials Society, TMS Structural Materials Division, TMS: Advanced Characterization, Testing, and Simulation Committee

Program Organizers: Rozaliya Barabash, Oak Ridge National Laboratory; Yandong Wang, Northeastern University; Peter K. Liaw, University of Tennessee

Wednesday AM
March 12, 2008

Room: 391
Location: Ernest Morial Convention Center

Session Chairs: Yandong Wang, Northeastern University; Peter Liaw, University of Tennessee

8:30 AM Keynote

In-Situ Monitoring of Weld Transformations and Their Effect of Weld Residual Stresses: *Philip Withers*¹; *Harry Bhadeshia*²; *John Francis*¹; *Laura Pocock*¹; *Howard Stone*²; ¹University of Manchester; ²University of Cambridge

The volume and shear changes that occur during martensitic transformation can have a marked effect on the final weld residual stress field. Until recently

it has not been possible to follow the transformation in real time for realistic weld cooling cycles. In this paper time resolved synchrotron X-ray diffraction measurements are used to follow the transformation, texture and residual stress changes taking place during weld cooling for three weld metals having different transformation characteristics and transformation temperatures. These results are used to interpret the state of residual stress, as measured by neutron diffraction, and texture, as measured by electron back scattered diffraction, found in single-pass groove welds deposited by manual-metal-arc welding using each of the three weld filler metals on 12 mm thick ferritic steel plates.

9:00 AM Invited

The Development of Internal Strains and Texture during Cyclic Deformation of Extruded Mg Az31B: *Donald Brown*¹; *Sean Agnew*²; *Ashutosh Jain*²; *Bjorn Clausen*²; ¹Los Alamos National Laboratory; ²University of Virginia

It has been shown that Mg can twin reversibly during cyclic deformation to relatively small strains. We have recently completed in-situ neutron diffraction measurements during strain controlled C-T cycling of extruded Mg to monitor the development of the twin volume fraction and microstructure. Twins appear with compressive deformation along the extrusion axis and withdraw with subsequent tensile deformation. The recovery (de-twinning) of the twins at the maximum tensile strain is observed to decrease with increased cycles, that is the overall twin volume fraction increases. In particular, parent grains which initially have their plane normals parallel to the straining direction cease to de-twin completely at higher cycles. Despite this, no significant repartition of the internal stresses amongst the different grain orientations was observed. However, a significant increase in peak breadth was observed with increased cycle, indicative of increased defect or dislocation density which may inhibit the motion of the twin boundaries.

9:25 AM

Elastic and Plastic Behaviors in Duplex Steel Characterized by In-Situ Neutron Diffraction and Self-Consistent Model: *Nan Jia*¹; *Yandong Wang*¹; *Ru Lin Peng*²; *D. W. Brown*³; ¹Northeastern University, Key Laboratory for Anisotropy and Texture of Materials (MOE); ²Linköping University; ³Los Alamos National Laboratory

For duplex alloy being subjected to thermo-mechanical treatments, the respective thermal expansion and different mechanical behaviours of each constituent phase may lead to a non-uniform partition of stresses between the phases. In addition, the grain-orientation-dependent elastic/plastic anisotropy in each phase may cause micro-mechanical interactions which modify further the microscopic load partitioning. In current work, neutron diffraction experiments on the spectrometer for materials research at temperature and stress (SMARTS) was employed on an austenite-ferrite stainless steel for tracing the evolution of micro-stresses that underlies the load sharing among different grain orientations in phases under stress and temperatures fields. Based on the diffraction measured lattice strain distributions on multiple lattice reflections, the anisotropic elastoplastic properties of the duplex steel were simulated using a Visco-Plastic Self Consistent (VPSC) model. Some modelling parameters describing the mechanical behaviours of constituent phases were derived from nanoindentation experiments in combination with EBSD technique.

9:45 AM

Cyclic Twinning-Detwinning Behavior during the Cyclic Deformation of a Wrought Magnesium Alloy, ZK60A: *Liang Wu*¹; *Ashutosh Jain*²; *Donald Brown*³; *Grigoreta Stoica*¹; *Sean Agnew*²; *Bjorn Clausen*³; *Douglas Fielden*¹; *Peter Liaw*¹; ¹University of Tennessee; ²University of Virginia; ³Los Alamos National Laboratory

The twinning and detwinning behavior in a strongly textured magnesium alloy was investigated using in-situ neutron diffraction during the cyclic deformation along the prior extrusion direction. The initial preferred orientation places the c-axis in most grains perpendicular to the loading axis, and this favors extensive {10-12}<10-11> tensile twinning under compressive loading. In contrast, the grains are not favorably oriented to undergo such twinning during monotonic tensile loading along the prior extrusion axis. This is the reason for the well-known tension-compression strength asymmetry of wrought magnesium alloys. The unique orientation relationship between the parent grains and the twin grains also favors detwinning during the subsequent loading reversal. The neutron diffraction indicates that such twinning and detwinning alternates with

the cyclic loading. However, a small volume fraction of residual twins gradually increases with increasing cycles, which may be an important factor in dictating the low-cycle fatigue behavior of the magnesium alloy.

10:05 AM Break

10:15 AM Invited

Microstructure, Texture, and Residual Stresses in a Friction Stir Processed AZ31B Magnesium Alloy: *Hahn Choo*¹; Wanchuck Woo¹; Michael Prime²; Zhili Feng³; Bjorn Cluasen²; ¹University of Tennessee; ²Los Alamos National Laboratory; ³Oak Ridge National Laboratory

Spatial variations of microstructure, hardness, chemical composition, tensile behavior, and texture were investigated in a friction-stir processed (FSP) AZ31B magnesium alloy. Residual stresses were also measured using two different methods: neutron diffraction and contour method. No significant variations in the hardness and chemical composition were found in the FSP zones including the severely deformed stir zone (SZ), which had a finer grain size compared to the heat-affected zone and base material. On the other hand, significant changes in the yield strength, texture, and residual stresses were observed in the FSP zones. The relationship between the texture variations and yield-strength reduction; and its influence on the decrease in the residual stress near the SZ is discussed. Finally, the residual stresses measured by neutron diffraction and contour method are compared, and the effect of the texture on the neutron diffraction residual stress measurements will be discussed.

10:40 AM

Residual Stresses in LENS®-Deposited AISI 410 Stainless Steel Plates: *Liang Wang*¹; Haitham Kadi¹; Sergio Felicelli²; Phillip Pratt²; John Berry²; Camden Hubbard³; ¹Mississippi State University, Center for Advanced Vehicular Systems; ²Mississippi State University; ³Oak Ridge National Laboratory

The residual stress in thin plate components deposited by the Laser Engineered Net Shaping (LENS®) process was investigated experimentally and numerically. Neutron and X-ray diffraction residual stress mapping was used to characterize the through-thickness stresses and surface stresses in LENS®-deposited AISI 410 stainless steel thin wall plates. Using the commercial welding software SYSWELD, a thermo-mechanical three-dimensional finite element model was developed, which considers also the effect of metallurgical phase transformations. The model was employed to predict the temperature history and the residual stress field during the LENS® process. Several simulations were performed with the geometry and process parameters that were used to build the experimental samples. The origin of the residual stress distribution is discussed based on the thermal histories of the samples, and the modeling results are compared with measurements obtained by diffraction mapping.

11:00 AM Invited

Application of In-Situ Characterization Methods in Developing the Advanced Numerical Models to Predict the Constitutive Behaviors of TRIP Steels: *Xin Sun*¹; W.N. Liu¹; M.A. Khaleel¹; Z.H. Cong²; N. Jia²; Yandong Wang²; P.K. Liaw³; ¹Pacific Northwest National Laboratory; ²Northeastern University; ³University of Tennessee

Compared to other advanced high-strength steels, TRIP steels exhibit better ductility at a given strength level and can be used to produce complicated automotive parts. This enhanced formability comes from the transformation of retained austenite to martensite during plastic deformation. Development of an advanced quantitative microstructure-based constitutive model for capturing the deformation behavior of the TRIP steels is the first step in predicting optimum processing parameters in steel productions. To develop the micro-mechanical model accounting for the complex deformation behaviors of TRIP steels, in-situ high-energy X-ray and neutron diffraction experiments have been used in this study to quantify the lattice stress-strain relations to validate various numerical results. Some new progresses of experimental and theoretical work will be presented in this talk. The applications of those advanced models in the development of newer steel products as well as the associated manufacturing processes will be elucidated.

11:25 AM

Variation of Residual Stresses in Drawn Copper Tube: *Adele Carradó*¹; Sebastian Brueck²; Laurant Barrallier³; A. Fabre³; Uwe Struhr⁴; Thomas Pirling⁵; Heinz Palkowski²; ¹Institut de Physique et Chimie des Matériaux de Strasbourg (IPCMS); ²Technical University of Clausthal; ³ENSAM Aix en Provence; ⁴Paul-Scherrer-Institut; ⁵Institut Laue-Langevin

Seamless tubes are used for many applications, e.g. in heating, transport gases and fluids, evaporators as well as medical use and as intermediate products for hydroforming and various mechanical applications. They are produced by cold drawing in one or several steps to reach the final dimension. The production of rough tubes is normally done by extrusion or rolling on 3-roll-mills, typically resulting in ovality and eccentricity in the tubes. Ovality and eccentricity lead to non-symmetric material flow during the cold drawing process and therewith to inhomogeneous deformation. Because of this non-axisymmetric behavior and deviations over the length of the tube caused by moving tools, inhomogeneous residual stresses are generated. To understand the interconnections between the geometrical changes in the tubes and the residual stresses, the residual strains in a copper tube were measured by neutron diffraction and compared with its changing geometry over length and circumference.

11:45 AM Invited

Neutron and X-Ray Diffraction Study of Internal Stress in Thermomechanically Fatigued Single Crystal Superalloy: *Erdong Wu*¹; Jun Zhang¹; Sucheng Wang¹; Bo Chen²; Guangai Sun²; Vincent Ji³; Darren Hughes⁴; Thilo Pirling⁴; ¹Chinese Academy of Sciences, Institute of Metal Research; ²Chinese Academy of Engineering Physics, Institute of Nuclear Physics and Chemistry; ³Laboratoire d'Ingénierie des Matériaux, École Nationale Supérieure d'Arts et Métiers; ⁴Institut Laue-Langevin

The relationship between internal stress and thermomechanical fatigue (TMF) in a Ni-based single crystal superalloy grown along [001] axis is studied by neutron and X-ray diffraction. The macroscopic internal stresses in the alloy generally increase with the TMF cycles until the sample is necked. However, the internal stress in the precipitate γ' phase increases more significantly than that in the matrix γ phase during TMF. The stress developed during TMF cycles in the vertical channel of the γ phase along the loading axis is compressive, whereas that in the horizontal channel is tensile. The microstrains and mosaicity in the γ/γ' phases also increase during TMF, but the trends of their developments are not consistent with that of the internal stresses. These trends and the associated TEM examination indicate that the failure by TMF is mostly caused by the development of defect related stresses in the γ' phase.

12:10 PM

Investigation of Residual Stresses in Austenitic Stainless Steel with X-Ray Area Detector: *Leng Chen*¹; ¹University of Science and Technology Beijing

An approach to residual stresses measurement was proposed based on X-ray area detector diffraction system, which gives a direct relationship between the diffraction cone distortion and strain tensor. The benefit of the new method is that all the data points on diffraction rings are used to calculate stresses so as to get better measurement result with less data collection time, and have many advantages over the conventional X-ray diffraction in dealing with highly textured materials, coarse-grained materials, or weak diffraction intensity which attributed to "virtual oscillation" function of X-ray area detector. Results of the residual stresses measurements in austenitic stainless steel with X-ray area detector were described.

Particle Beam-Induced Radiation Effects in Materials: Carbides, Semiconductors and Other Non-Metals

Sponsored by: The Minerals, Metals and Materials Society, American Nuclear Society, TMS Structural Materials Division, TMS/ASM: Nuclear Materials Committee
Program Organizers: Gary Was, University of Michigan; Stuart Maloy, Los Alamos National Laboratory; Christina Trautmann, Gesellschaft für Schwerionenforschung; Maximo Victoria, Lawrence Livermore National Laboratory

Wednesday AM
 March 12, 2008
 Room: 389
 Location: Ernest Morial Convention Center

Session Chairs: Christina Trautmann, Gesellschaft für Schwerionenforschung (GSI); William Weber, Pacific Northwest National Laboratory

8:30 AM

The Evolution of Charged-Particle Irradiation Damage in Silicon Carbide: William Weber¹; Fei Gao¹; Ram Devanathan¹; Yanwen Zhang¹; Weilin Jiang¹; In-Tae Bae¹; ¹Pacific Northwest National Laboratory

Experimental charged-particle irradiations and multi-scale computer simulations have been used to investigate the primary damage state and evolution of radiation damage in silicon carbide as functions of temperature and charged-particle mass and energy. Atomistic simulations of energetic collision cascades indicate that single interstitials, vacancies, antisite defects, and small defect clusters are produced. Atomistic simulations have determined the activation energies for close-pair recombination and long-range diffusion, which are used in a kinetic Monte Carlo (MC) simulation model to describe isochronal annealing of defects in SiC between cascade events. At the charged-particle fluxes normally used in the laboratory to simulate neutron irradiation damage, the ratio of ionization rate to displacement rate in SiC has a significant impact on observed temperature-dependent processes. A fundamental understanding of these ionization effects is needed if charged-particle irradiation results are to be used to develop predictive models of damage evolution in SiC.

9:10 AM

Proton Irradiation Study of GFR Candidate Ceramics: Jian Gan¹; Yong Yang²; Clayton Dickerson²; Todd Allen²; ¹Idaho National Laboratory; ²University of Wisconsin-Madison

This work investigated the microstructural response of ZrC, ZrN, TiC, TiN and SiC irradiated with 2.6 MeV protons at 800°C to a single dose in the range of 1.5 to 3.0 dpa depending on the material. The change of lattice constant evaluated using HOLZ patterns is not observed and is small when measured using XRD for the irradiated samples up to 1.5 dpa for 6H-SiC and up to 3.0 dpa for ZrC and ZrN. In comparison to Kr ion irradiation at 800°C to 10 dpa from the previous studies, the proton-irradiated ceramics at 3.0 dpa show less irradiation damage to the lattice structure. The irradiated ZrC exhibits faulted loops which are not observed in the Kr ion irradiated sample. The irradiated ZrN shows the least microstructural change from proton irradiation. The microstructure of 6H-SiC irradiated to 3.0 dpa consists of black dot type of defects at high density.

9:30 AM

Light and Heavy Ions Effects on the Electrical and Mechanical Properties of GPC/SiC Composites: B. Chhay¹; Claudiu Muntele¹; D. Ila¹; ¹Alabama A&M University

Glassy Polymeric Carbon (GPC) is a unique biocompatible material that can withstand high temperature and present excellent mechanical and electrical properties. When nanoparticles of Silicon Carbide (SiC) is added in the GPC matrix, the electrical conductivity of the composite increases as well as the mechanical performance. In this work, we used a molding method to prepare samples of SiC/GPC composite with 3 different concentrations of SiC and we bombarded them with light and heavy ions to study the induced changes in the electrical resistivity and in the Young's modulus of the composites. Results will be presented during the meeting. This research was sponsored by the Center for Irradiation of Materials, Alabama A&M University and by the AAMURI Center for Advanced Propulsion Materials under the contract number NNM06AA12A from NASA, and by National Science Foundation under Grant No. EPS-0447675.

9:50 AM

Magnetic Order in Proton Irradiated Graphite: Curie Temperatures and Magnetoresistance Effects: Jose Barzola-Quiquia¹; Pablo Esquinazi¹; D. Spemann¹; M. Rothermel¹; T. Butz¹; N. García²; ¹University of Leipzig; ²Consejo Superior de Investigaciones Científicas

Defect induced magnetic order is a new phenomenon in material science that refers to the triggering and manipulation of magnetic order and magnetic moments in nominally non-magnetic materials by lattice defects and/or non-magnetic add atoms. A noticeable example of this effect is the magnetic order at room temperature produced by proton irradiation of graphite. In this work we have managed to increase the ferromagnetic signal by cooling the graphite samples at 110K during proton irradiation, diminishing in this way annealing effects. SQUID measurements of the magnetization show a fluence dependent Curie temperature. The longitudinal magnetoresistance and the Hall effect show an irreversible behavior similar to that found in ferromagnetic films indicating spin/domain reorientation effects. The observed magnetoresistance effects and Curie temperatures above room temperature are promising facts that may lead to useful carbon-based devices in the near future.

10:10 AM Break

10:30 AM

Search for Radiation Cation Defects in Binary Ionic Crystals: Aleksandr Lushchik¹; ¹University of Tartu

The creation processes of anion and cation structural defects under irradiation of wide-gap (7-15 eV) binary dielectrics by fast electrons, alpha-particles, heavy ions and VUV radiation of 7-35 eV have been investigated in a wide temperature range (5-750 K) using the methods of optical and thermoactivation spectroscopy. Besides universal impact mechanism, Frenkel defects are formed at the decay of various intrinsic and impurity-related electronic excitations. Using pure and doped LiF and NaCl crystals as an example, it is shown that the nonimpact creation of cation Frenkel defects via the decay of electronic excitations is responsible for several radiation effects at 400-800 K. At low temperatures, the creation efficiency of cation defects by X-rays in these crystals is low. Thus, a search for cation defects is especially promising under crystal irradiation by heavy ions providing extremely high density of excitations and suitable conditions for high-temperature defect stabilization.

10:50 AM

Behavior of 6H-SiC Irradiated to Extremely Low Doses: Weilin Jiang¹; Ponnusamy Nachimuthu¹; William Weber¹; Lev Ginzburg²; ¹Pacific Northwest National Laboratory; ²L.G. Tech-Link

Irradiation of 6H-SiC single crystals was performed using energetic H⁺ ions. The changes in lattice parameters were measured as a function of dose using high-resolution x-ray diffraction. In general, the lattice parameter changes are small and anisotropic at extremely low doses. The c-axis lattice parameter c increases monotonically with the increasing dose, which could be attributed to aligned interstitials along the c-axis. In contrast, the a-axis lattice parameter a decreases at the extremely low doses, which may originate from the irradiation-induced vacancies and the possible formation of antisite defects. As a result, an initial volumetric contraction of the unit cell occurred. To our best knowledge, this behavior of 6H-SiC has not been reported previously. As the dose increases, both parameters a and c increase with respect to the initial disordering stage. Eventually, the interstitial concentration reaches to such a level that lattice expansion becomes dominant along all directions.

11:10 AM

Vacancy Cluster Dynamic in Silicon: Nélida Smetniansky-De Grande¹; Martín Alurralde¹; Julian Fernández¹; ¹National Commission of Atomic Energy

Most of electronic devices in satellites are made of silicon. In space environment they are in extreme conditions including radiation due to charged particles (mainly electron and protons). At microscope scale the impinging particle can transfer enough energy to lattice atoms to displace from its position producing defects (self-interstitials, vacancies and clusters). In order to predict the degradation of the device it is necessary to know the evolution and distribution of defects. Most of studies on defect evolution were done on defects produced during fabrication process or implanted for doping, both cases at substantially high temperature. In space the temperature changes from -100 to 100°C. At this temperatures the mobility of vacancies is several order higher

than of interstitials, the proposed model consider that only vacancies are moving to study the evolution of the distribution of vacancies, interstitials and clusters using computational techniques.

11:30 AM

Trim as a Tool to Study Radiation Effects on Solar Cells: *Martín Alurralde*¹; Alberto Filevich¹; ¹National Commission of Atomic Energy

The Trim code is a very used tool to study ions in matter, but has its limitations specially when several layers with very different thickness are together. This paper shows how to applied this code to predict the degradation of a multijunction solar cell, the so call CAC method.

Phase Stability, Phase Transformations, and Reactive Phase Formation in Electronic Materials VII: Session III

Sponsored by: The Minerals, Metals and Materials Society, TMS Electronic, Magnetic, and Photonic Materials Division, TMS: Alloy Phases Committee

Program Organizers: Sinn-wen Chen, National Tsing Hua University; Srinivas Chada, Medtronic; Chih Ming Chen, National Chung-Hsing University; Hans Flandorfer, University of Vienna; A. Lindsay Greer, University of Cambridge; Jae-Ho Lee, Hong Ik University; Kejun Zeng, Texas Instruments Inc; Katsuaki Suganuma, Osaka University

Wednesday AM

Room: 278

March 12, 2008

Location: Ernest Morial Convention Center

Session Chairs: Yee-wen Yen, National Taiwan University of Science and Technology; Alexandre Kodentsov, Eindhoven University of Technology

8:30 AM Invited

Interactions in the Sn-Cu-Ni System: *Alexandre Kodentsov*¹; ¹Eindhoven University of Technology

It was found that small additions (a few percents) of Ni in Cu significantly alter the course of the interfacial reactions. No Cu₃Sn is formed at the substrate/solder interface, and the Cu₆Sn₅-based reaction product was found to grow almost an order of magnitude faster compared to that in the Cu/Sn binary diffusion couple. Though this demonstration is a really remarkable one, given the fact that the Sn-Cu-Ni system is, perhaps, the most important material system for Pb-free solder technology, little is yet known in a detail way on the mechanism governing this peculiar reaction phenomenon. Since the additions of the alloying element to the Cu₆Sn₅-superlattice results in changes of electron concentration in the system, it may be conjectured that the presence of Ni-atoms stabilizes a long-period superlattice of the low-temperature modification of the Cu₆Sn₅-phase.

8:50 AM

Interfacial Behavior between Bi-Ag Solders and the Ni Substrate: *Hsin-Yi Chuang*¹; Jenn-Ming Song¹; ¹National Dong Hwa University

This present study investigated the interfacial reaction between molten Bi-Ag alloys and Ni substrate. The kinetics of substrate dissolution and the growth of the intermetallic compounds (IMCs) were explored. The results show that the dissolution could be divided in two stages, namely, the linear stage and the steady stage. Ni dissolution obeyed the parabolic relationship in the former stage about 20 minutes, afterward the dissolution remained almost constant. Two IMCs, NiBi₃ and NiBi, were observed at the interface. Based on the differences in the composition and morphology, it could be demonstrated that NiBi₃ formed via interfacial reaction as well as crystallization in isothermal period and also during solidification. The NiBi layer formed between NiBi₃ and Ni substrate was believed growing through a solid-state transformation. It was also found that the Ag addition accelerated the dissolution of Ni and thus the growth of Ni-Bi IMCs.

9:05 AM

Interfacial Reaction and Thermal Fatigue of Zn-4wt.%Al-1wt.%Cu/Ni Solder Joint: *Yoshikazu Takaku*¹; Ikuo Ohnuma¹; Yasushi Yamada²; Yuji Yagi²; Ikuo Nakagawa³; Takashi Atsumi³; Kiyohito Ishida¹; ¹Tohoku University Graduate School of Engineering; ²Toyota Central Research and Development Laboratory Inc.; ³Toyota Motor Corporation

The Zn-Al-Cu eutectic alloy (T_m=381°C) is a candidate for use as a Pb-free high temperature solder as a substitute for Pb-base high solders. It is suitable for severe working environments such as the engine room of hybrid vehicles equipped with an inverter system as well as a heat engine. In this study, the interfacial reaction between Zn-Al-Cu alloys and the Ni substrate during soldering and thermal cycling was investigated. Semiconductor chips and Ni-plated Cu substrates were soldered with Zn-Al-Cu alloys at various temperatures under a nitrogen atmosphere. The soldered assemblies were then heat-treated at 200°C and 300°C to examine the microstructural evolution at the soldered interface. The effect of severe thermal cycles between -40°C and 250°C in the air on the microstructure and fracture behavior at the solder joint was investigated. Even after a 1000-cycle test, the thickness of Al₃Ni₂ layer formed at the interface was quite small.

9:20 AM

Dissolution and Interfacial Reaction between Cu and Sn-Ag-Cu Solders: *Chih-Chiang Chang*¹; C. Robert Kao¹; ¹National Taiwan University

In electronic packaging, the dissolution of the Cu layer of the under-bump metallizations or surface finishes during reflow is one of the most important processing concerns. Therefore, the objective of this study is to investigate in depth the dissolution of Cu into SnAgCu solders with various Cu concentrations. The effect of solder volume on dissolution rate will also be studied. In this study, solder balls of different concentrations Sn₃Ag_xCu_{1-x} (x=0/0.3/0.5/0.7wt.%) and different diameters, 500 or 760µm, are employed to study the influence of Cu concentration as well as the solder volume. It is found that the Cu concentration and solder ball volume have very strong effect on the Cu consumption rate. The different initial Cu concentration in the SnAgCu ternary solder changed the dissolution driving force (the Cu concentration gradient). The results of this study suggest that a high Cu-content SnAgCu solder can be used to reduce the dissolution of Cu pad.

9:35 AM

Interfacial Reaction between Sn-Ag-Bi-In Lead-Free Solder and Copper Substrate: *Ming-Hsiun Chen*¹; Che-Hsiun Huang¹; Wei-Tang Chen¹; *Albert Wu*²; ¹National Taipei University of Technology; ²National Central University

It is still important to find a new solder alloy system for the replacement of eutectic SnPb solder. Though Sn-Ag-Bi alloy is one of the choices for lead-free solder, bismuth usually deteriorates the mechanical properties of the joints. The addition of indium can lower the melting point of the alloy but will not reduce the mechanical strength of the joints. In this study, we investigated the interfacial reaction between Sn-Ag-Bi-In solder and Cu substrate. By using different reflow conditions, the growth of intermetallic compound was conducted by measuring the thickness versus reflow time and temperature. The interfacial reaction for different contents of indium added in the Sn-Ag-Bi system was also studied. The compounds formed in the reaction are mainly Cu₃Sn₅ and Cu₃Sn at the interface. The kinetics of compound growth was also investigated in this study.

9:50 AM

Thermal Stability Improvements in Cu Metallization on Barrierless GaAs: *Wean-Kuan Leaw*¹; Jinn. P. Chu¹; V.S. John¹; ¹National Taiwan Ocean University

Barrierless copper metallization of GaAs device was performed using Cu/GaAs and Cu(TaNx)/GaAs structures by co-sputtering system. The pure Cu and Cu(TaNx) films were characterized by X-ray diffractometry, focussed ion beam, X-ray photoelectron spectroscopy and low angle X-ray diffractometry, which authenticates the results. The Cu films on GaAs were very stable up to 350°C for 1 hour. The Cu(TaNx) films on GaAs show better thermal stability up to 450°C for 1 hour. The thermal stability improvement by doping a minor amount of TaNx into Cu has been confirmed. The thermal property and microstructure results will be presented and discussed.

10:05 AM Break

10:20 AM Invited

Suppressing the Growth of Cu₅Zn₈ Intermetallic Layer in Sn-Zn-Ag-Al-Ga/Cu Solder Joints: Kwang-Lung Lin¹; R. Lai¹; Budiman Salam¹; ¹National Cheng Kung University

The presence of the intermetallic compound (IMC) layer at the interface between solder and substrate indicated a bond actually formed between the solder and the substrate. Besides its advantage for bonding the solder and the substrate, its disadvantage is that it is generally the most brittle part of the solder joint. In this study, the growth of IMC layers was seen slower as the silver content increased in the Sn-8.5Zn-Ag-Al-Ga/Cu alloy systems. The experimental results show that the total thickness of the IMC layers in the studied solder alloy with 1.5wt.% silver content is about half that in the studied solder alloy without silver added. The reduction might be due to the formation of the (Ag, Cu)-Zn intermetallic at the interface of the silver added solder which in the no silver solder, Cu₅Zn₈ was normally found.

10:40 AM

Interfacial Reaction between Eutectic SnZn Solder and Thin-Film Cu Substrate: Chih Ming Chen¹; Chih Hao Chen¹; ¹National Chung-Hsing University

SnZn eutectic alloy is a promising lead-free solder. Copper is a common metallic substrate in electronic devices. Thus, interfacial reactions at the SnZn/Cu solder joints are studied extensively. However, the Cu is usually the bulk type; interfacial reaction regarding the thin-film Cu substrate is not studied yet. In this talk, we will present that the interfacial reaction of thin-film Cu is different from that of bulk Cu. Reaction product and interfacial morphology will be discussed and compared between the bulk and thin-film Cu types.

10:55 AM

Interfacial Reactions between Pb-Free Solders and In/Ni/Cu Substrates: Yee-wen Yen¹; Wei-kai Liou¹; Hong-yao Wei¹; Chiapng Lee¹; ¹National Taiwan University of Science and Technology

This study investigated the interfacial reactions between Pb-free solders-Sn-3.0 wt% Ag-0.5 wt% Cu (SAC) and Sn-0.7 wt% Cu (SC), and In/Ni/Cu multilayer substrates by the diffusion bonding method. The reflow temperatures were at 160, 180 and 200°C for various lengths of time, and then samples were annealed at 100°C for 100 to 500 hours. The experimental results show that the scalloped Cu₆Sn₅ phase was formed and spread over the SAC/In/Ni/Cu and SC/In/Ni/Cu interface. The ternary Ni-In-Sn intermetallic compound (IMC) was formed when the samples were aged at 100°C. At the reflow temperature was increased to 200°C, only one Cu₆Sn₅ phase was formed on the solder/substrate interface even the reaction couple was aged at 100°C for 500 hours. According to mechanical test, the formation of the Ni-In-Sn ternary IMC cause the mechanical strength of the solder joint decrease.

11:10 AM

Local Resistance Measurements via Four Points Probe (4pp) Method in Eutectic Solder Assembly after Temperature Cycling Test by SEM Internal Probing Technique: T.I. Shih¹; Yung-Chi Lin¹; Jeng-Gong Duh¹; Tom Hsu²; ¹National Tsing Hua University; ²United Microelectronics Corporation

Interfacial reaction for the flip chip solder bump of Sn63-Pb37 structure and electrical characterization for lead-free materials in the bump technology under TCT of environmental tests were investigated. In the industry, there is very limited success in understanding the precision of electrical resistance via four points probe method, as well as in reducing resistance errors due to inaccuracy in the positions of the probes. The present study was aimed to provide an innovative attempt to cast additional light on this critical subject through local nano-probing in a high-resolution scanning analytical electron microscope (FEI XL-30). The microstructure, elemental distribution and electrical characterization of IMCs were thoroughly examined using an integrated combination set-up of FE-EPMA, SEM nano-probing system and SELA-EM2. This allows us to obtain a well-documented correlation between the electrical properties of the specific IMCs and their morphology as well as microstructure.

11:25 AM

Modelling Sn-Cu Interfacial Reactions with the Phase Field Method: An Serbruyns¹; Nele Moelans¹; Bart Blanpain¹; Patrick Wollants¹; ¹Katholieke Universiteit Leuven

During soldering and subsequent thermal cycling, an intermetallic compound (IMC) layer is formed between the molten solder and the solid substrate, which is required for a strong bond. However, thick IMC layers are detrimental for mechanical properties of the joint. Therefore, their growth has to be controlled. The behaviour of the IMC layers in Sn-Cu systems is studied using a phase-field model. In the phase field method, microstructures are represented by a set of phase field variables that are continuous functions of the spatial coordinates and time. The model uses a diffuse interface approach, which allows the consideration of several concurrent microstructural processes for complex morphologies, without a considerable increase of the mathematical complexity. Influence of diffusion coefficient ratios, start concentrations, elastic properties and other parameters are investigated.

11:40 AM

Prediction of the IMC Formation at the Interface between Two Metals: Huashan Liu¹; ZhanPeng Jin¹; ¹Central South University

Formation of intermetallic compounds (IMCs) at the interface between 2 metals during soldering processing may inevitably affect the electrical and mechanical performance of integrate circuits (ICs). Hence prediction of the formation sequence of IMCs benefits the design of electronic packaging process and packaging structure as well. By involving the effect of both thermodynamic and kinetic factors (including nucleation and growth) on phase formation, 2 empirical models were respectively proposed to predict the phase formation at the interface between 2 metals with different structures and with the same structure. Applications of these models on the interfacial reactions between pure elemental pairs of metals such as Ni/Sn, Cu/In, Cu/Sn, Ni/Bi and Co/Sn, and Al/Cu and Al/Ni at different temperatures show good agreement with experiments and the examination of their credibility for multi-component systems is underway.

Pyrometallurgy - General Sessions: Pyrometallurgy

Sponsored by: The Minerals, Metals and Materials Society, TMS Extraction and Processing Division, TMS: Pyrometallurgy Committee
Program Organizer: Boyd Davis, Queens University

Wednesday AM
March 12, 2008

Room: 283
Location: Ernest Morial Convention Center

Session Chair: Michael Potesser, University of Leoben

8:30 AM

Enhanced Reduction of Self-Reducing Pellet of Chromites with Fe-Si Addition in the Reductant: Cyro Takano¹; Adolfo Zambrano¹; Marcelo Mourao¹; ¹University of Sao Paulo

Fe-Cr-C production is a very high electrical energy consuming process. When self-reducing agglomerates are used it is expected to decrease up to 10% of this electrical energy. This research aims to understand how the synergetic effects are when stronger reductant, like Fe-Si, is substituted for coke. Brazilian chromites containing 41.2%Cr₂O₃ were mixed with petroleum coke, small amount, 1%, 2% and 4% of Fe-75%Si and agglomerated with cement as the binder. The mixture was pelletized, dried and submitted at temperatures 1773K up to complete the reactions. The results showed that the reduction reactions were 1.4 and 2 times faster with 1% and 2%Fe-Si addition, respectively, than with no addition. The microscopic analysis showed that a liquid phase formed but the pellet did not collapse and indicated that the coalescence of the metallic phase depends on the dissolution of the pre-reduced particles of the chromites into slag.

8:55 AM

Improvements Carried out at Huelva Smelter in the 2007 General Shutdown: A Review: *Rafael Fernandez-Gil Bando¹; Carlos Ortiz¹; Juan Moreno¹; ¹Atlantic Copper SA*

The Huelva Flash Smelting Furnace was commissioned in September 1975. The Smelter and the Acid Plant was expanded in 1995 to its present capacity of 300,000 tpa new copper equivalent and one million tonnes of concentrate per year. During these years of operational experience, most of the initial practices have been reviewed, process control has drastically improved and main process equipment has been modernised. The fourth Flash Furnace campaign lasted 9 years (1995-2004) during which 8 million tonnes concentrate were smelted. Increasing in sulphur content in concentrates and new environmental requirements imply new challenges for smelters to keep production and operation costs. This paper is an overview of the modifications and improvements carried out in the 2007 general shutdown in Smelter and Acid Plants. Also environmental improvements carried out on Smelter gasses treatment systems are described.

9:20 AM

Impurities Behavior under Oxidization and Reduction Conditions of Non-Ferrous Pyrometallurgical Process: *German Wastavino¹; ¹IM2 Codelco*

In recent years the amount of the impurities such as As and Sb in the smelting process has increased because of the quality of the copper concentrate, producing a high variation of the concentration of impurities in the anode. This behavior create an additional problem in the electrolytic refining because it affects the ratio As/(Sb+Bi), increasing the concentration of As and Sb in the cathode. The objective of this study is to clarify the effects of oxidization and reduction conditions in different processes. Teniente Converter, Pierce Smith Converter and Slag Cleaning Electric Furnace were evaluated under different industrial sceneries to achieve a high impurities volatilization. The present work describes the main results and conclusions of this study. It was found that the behavior of impurities in electric furnace might limit the process, because the recovered metal contains high concentration of As and Sb which is usually recirculated to conventional converting process.

9:45 AM Break

10:05 AM

New Pyrometallurgical Bullion Lead Refining Process: *Michael Potesser¹; Burkhardt Holleis¹; Helmut Antrekowitsch¹; ¹University of Leoben; ²Messer Austria GmbH*

After the primary or secondary lead production the bullion lead is remelted and charged into a vessel with following refining process. The removing of arsenic, antimony and tin takes place by salt slags or oxidizing gases like air or pure oxygen. Due to the increasing lead price Messer Austria GmbH and in cooperation with the institute of Nonferrous Metallurgy at the University of Leoben developed a new process named OXIPOT for the refining of Sn, As and Sb. The OXIPOT process bases on the bottom purging technology with a ceramic or steel purging device. This leads to an increased retention time of the refining products due to the deeper bath level and an optimized specific reaction volume concerning the bubble size. This paper describes the process, pilot plant, thermodynamic calculations for the optimisation concerning the selectivity of element removal and an economic calculation.

10:30 AM

The Investigation of Domestic Iron Ores for Sponge Iron Production: *Ercin Ersundu¹; Nuri Solak¹; Süheyla Aydin¹; ¹Istanbul Technical University*

In the present work, three different domestic iron ores; Sivas Divrigi B Head high grade hematite, Malatya-Hekimhan-Hasançelebi medium and low grade magnetite lump ores reduced with Soma-Kisrakdere lignite coal to investigate their suitability for sponge iron production. In the experimental studies different operation parameters were selected being Cfix/Fetot ratio, temperature in the range of 1100-1250°C and time, to determine their effects on metallization. Metallization degree of 88% was calculated in the reduction experiments realized by using Sivas Divrigi B Head lump ore, whereas for Malatya-Hekimhan-Hasançelebi magnetite lump ores 65-70% metallization degrees were obtained. Additionally, kinetic calculations have been performed and it was found that the reduction reactions obey the Ginstling – Brounshtein type diffusion controlled model. Activation energy values were determined in the range of 55–150 kJ/mol for different types of iron ores, which is in agreement with the literature data.

10:55 AM

Production of Separating Precious Metals from Base Metals in Gold-Antimony Alloys by Selective Chlorination Leaching under Controlling Potential: *Liu Weifeng¹; Yang Tianzu¹; Dou Aichun¹; Chen Fangbin¹; Liu Yong¹; ¹Central South University*

Owing to the existing problems in the electrolysis of gold-antimony alloys process, the new hydro-technology of separating precious metals from base metals have been studied in china. In this paper, the new hydro-technology of separating precious metals from base metals has been introduced in detail. The technology of selective chlorination leaching under controlling potential has been applied to treat the gold-antimony alloys. The impurity metals were removed effectively since the leaching efficiencies of copper, nickel and antimony are over 99%, with direct recovery of gold being 99.83%. Silver, antimony, copper and nickel were recovered effectively. The crude gold powder containing 94% gold can be obtained from the residue. The direct recovery of gold can be improved from 70% to 99.83%. This technology has been applied successfully in the treatment of gold-antimony alloys since September 2005. Many former procedures have been cancelled, such as electrolysis, Anode slime leaching by nitric acid, smelting in crucible and blowing in muffle.

Recycling: Light Metals

Sponsored by: The Minerals, Metals and Materials Society, TMS Extraction and Processing Division, TMS Light Metals Division, TMS: Recycling and Environmental Technologies Committee

Program Organizers: Christina Meskers, Delft University of Technology; Greg Krundick, Argonne National Laboratory

Wednesday AM

March 12, 2008

Room: 280

Location: Ernest Morial Convention Center

Session Chair: Christina Meskers, Delft University of Technology

8:30 AM

Dynamic Processes for the Recycling of Low-Quality Aluminum Charge Materials: *Simon Lekakh¹; David Robertson¹; Sergey Rimoshevsky²; Leonid Tribyshevsky²; Vladimir Tribyshevsky²; ¹University of Missouri-Rolla; ²Belarusian National Technical University*

Melting processes may be classified into two groups – stationary and dynamic. In stationary processes the melt and solid charge are immovable or listlessly moving by natural convection. In dynamic processes there is active motion of the solid charge and melt inside the furnace by external mechanical or electromagnetic forces. Features of these processes were analyzed from the point of view of metal recovery and energy efficiency when charge materials with different metallurgical quality were used. The dynamic melting processes have the possibility of increased aluminum recovery from low-quality scrap with oxidized surface, such as turnings and dross, by effective separation of melt from slag with using special fluxes. The melting parameters in a dynamic rotary furnace were experimentally studied and computationally modeled. Technical results will be presented of using a small size (0.5 t) rotary furnace for recycling locally-sourced low-quality aluminum charge materials over a period of several years.

8:50 AM

Fundamental Study of the Decoating of Aluminium Beverage Can: *Xiangjun Zuo¹; Lifeng Zhang¹; ¹Norwegian University of Science and Technology*

The first step of the recycling of aluminium beverage can is decoating, removing surface layer of plastic (polyester coat on the inwall of can) and paint (on the ectotheca). In the current study, Small pieces of Carlsberg beer can were heated in TG/DTA and MS machines at different heating rates and different carrying gas flow rates. SEM is used to observe the structure of the samples before and after decoating. The activation energy of reactions at different temperature is deduced according to the experimental data. A model has been developed to describe the decoating process.

9:10 AM

The Recycling of Aluminum from Building and Construction (B and C) Applications: *Subodh Das*¹; John Green²; John Kaufman¹; ¹Secat Inc; ²JASG Consulting

The aluminum industry is a leading proponent of global sustainability and has for many decades strongly advocated recycling of the metal. Recycled aluminum is a key and growing component of the U.S. metal supply and in recent years has actually exceeded the aluminum supplied from primary production. The use of recycled aluminum saves ~95% of both the energy and emissions associated with the smelting of aluminum and reduces reliance on foreign imports. This paper explores the recycling of aluminum from the building and construction (B and C) markets, taking advantage of a European study by Delft Technical University. Significant potential savings from recycling during building demolition with aluminum recoveries averaging ~95% are demonstrated. A rudimentary on-site alloy sorting scheme is proposed and a pathway forward is suggested to validate the sorting approach and confirm the recycling potential. Further, the potential for reuse of the resultant alloy content is considered.

9:30 AM

Microstructures Evolution and Mechanical Properties of Rare Earth Magnesium Alloy Machined Chips Recycled by Severe Plastic Deformation: *Tao Peng*¹; Qudong Wang²; ¹Shanghai Jiaotong University, School of Materials Science and Engineering; ²Shanghai Jiaotong University, State Key Laboratory of Metal Matrix Composite

GW103K Rare earth magnesium alloy machined chips were recycled by CEC (cyclic extrusion compression) technology. In this work, the total recycling course mainly included sintering technology of Machined chips and CEC of the sintered billets. Machined chips were sintered at the temperature of 673K, 723K and 773K with a pressure of 250 Mpa in air. Those sintered billet were then extruded at 773K. CEC not only made machined chips excellent metallurgical bonding, reduced the porosity, but made uniform dispersion of oxide contaminants and grains refinement with the increasing of extrusion passes. The extrusions processed from machined chips showed a good combination of high ultimate tensile strength of 400~460Mpa, high 0.2% proof stress of 300~350 Mpa and elongation to failure of 5~10% at the room temperature which had higher strength and equivalent elongation compared with those of extrusions processed from the cast ingot.

Refractory Metals 2008: Processing

Sponsored by: The Minerals, Metals and Materials Society, TMS Structural Materials Division, TMS: Refractory Metals Committee

Program Organizers: Todd Leonhardt, Rhenium Alloys Inc; Jim Ciulik, University of Texas at Austin

Wednesday AM
March 12, 2008

Room: 388
Location: Ernest Morial Convention Center

Session Chairs: Todd Leonhardt, Rhenium Alloys, Inc; James Ciulik, University of Texas at Austin

8:30 AM Introductory Comments

8:35 AM

Transitions from Tool Steels (H-13) to Refractory Metals (Mo, Ta, W) through Laser Powder Deposition: *James Sears*¹; ¹South Dakota School of Mines and Technology

Laser powder deposition of refractory metals, such as tantalum, molybdenum, rhenium and tungsten, is being evaluated for manufacturing of permanent molds for titanium casting, as internal cladding for gun barrels and shot liners for Mg and Al die casting. This work is focused on transitions from tool steel (H-13) to these refractory metals via an intermediary material by successive layering by Laser Powder Deposition. Issues related to transition materials used, powder type and morphology, clad quality and dilution control that were encountered during this project are discussed. This work was performed under a grant from the U.S. Department of Energy (DOE), Office of Industrial Technology under contract DE-PS07-03ID14425: Industrial Materials for the Future Program.

9:00 AM

Molybdenum and Molybdenum Alloy Seamless Tubing: *Donald Mitchell*¹; Todd Leonhardt¹; ¹Rhenium Alloys Inc

An increase in demand for longer length and thinner wall tubing, along with technological advancements in design and applications have resulted in requirements of higher quality and greater precision of molybdenum and molybdenum alloy seamless tubing. Several methods of production will be discussed; including plug drawing and mandrel drawing. Mechanical properties and microstructures will also be illustrated and discussed. Several of the industries benefiting from these materials are temperature measurement, medical, nuclear, and aerospace.

9:25 AM

The Response of an NbSi Alloy to Net Shape HIPping: *Qiang Li*¹; Roger Morrell²; *Xinhua Wu*¹; ¹University of Birmingham; ²National Physical Laboratory

Hot Isostatic pressing (HIPping) has been used to consolidate atomised Nb-16Si-25Ti-8Hf-2Cr-2Al using a three stage HIPping process to produce a near net shape component. The creep and oxidation behaviour of the as-HIPped powder have been assessed. The consolidation during HIPping has been monitored using analytical scanning and transmission electron microscopy and X-Ray diffraction. The powder is HIPped in mild steel tooling to define the shape after which it is de-canned and HIPped at higher temperatures in order to remove the remaining porosity. Young's modulus and the shear moduli of the powder-HIPped samples have been measured and are similar to those found in cast samples. The oxidation properties are similar to those of cast samples but the creep properties are worse, presumably because of the fine scale of the microstructure. These observations are discussed in terms of using HIPping of powder to produce Net Shape components of NbSi-based alloys.

9:50 AM

Development of Irradiation Hardening of Unalloyed and ODS Molybdenum during Neutron Irradiation to Low Doses at 300C and 600C: *Brian Cockeram*¹; Lance Snead²; Richard Smith¹; ¹Bechtel Bettis Inc.; ²Oak Ridge National Laboratory

Unalloyed molybdenum and Oxide Dispersion Strengthened (ODS) molybdenum were neutron irradiation at nominally 300C and 600C in the high fluence isotope reactor (HFIR) at relatively low fluences that correspond to nominal displacement doses of 0.01, 0.1 and 1.3 dpa. Following Irradiation hardening occurred at neutron fluences of 1.3 dpa with an increase in yield stress, a significant decrease in uniform elongation, and elevation of the Ductile to Brittle Transition Temperature (DBTT). The hardening behavior was evaluated by comparing the observed defect and defect cluster formation and accumulation with indirect measures of defect density obtained from electrical resistivity measurements, hardness measurements, and tensile properties. The influence of temperature on the mobility of defects and resulting properties also was evaluated. Additionally, the role of microstructure and grain size on irradiation hardening was evaluated by comparing the results for unalloyed molybdenum and ODS molybdenum.

10:15 AM Break

10:25 AM

Consequences of Crystal Orientation on Fabricating Single or Multi-Crystal Nb SRF Cavities: *Derek Baars*¹; Thomas Bieler¹; Chris Compton¹; Terry Grimm¹; ¹Michigan State University

Manufacturing superconducting radio frequency (SRF) cavities from single crystal niobium is being investigated as an alternative to polycrystalline niobium for several reasons: 1) single crystal sheets may be cut directly from the purified ingot, eliminating the cost of rolling into polycrystalline sheet, 2) polycrystalline sheet texture varies among manufactures and even between batches, leading to variability in forming and surface finish, 3) a single crystal cavity has already been tested and matches the capability of polycrystalline cavities. The effect of various crystal orientations on dislocation density, surface quality, and recrystallization after plastic deformation similar to that anticipated for normal cavity assembly steps such as forming operations, chemical etches, and welding will be presented.

WEDNESDAY AM

10:50 AM

Small-Scale Resistance Spot Welding of 50Mo-50Re Thin Sheet: *Jianhui Xu¹; Williams Umstead²; John Farrell²; Michael Effen²; Tongguang Zhai¹*
¹University of Kentucky; ²Semicon Associates

A 50Mo-50Re alloy, in a form of thin sheet (0.127 mm thick), was joined by small-scale resistance spot welding (SSRSW). The effects of six important welding parameters, such as hold time, electrode, ramp time, weld current, electrode force and weld time, were studied systematically, in an attempt to optimize the welding quality. It was found that the commonly used criterion that the suitable nugget penetration was 80% of the thickness of the welded sheet in large-scale resistance welding was not applicable to SSRSW of the 50Mo-50Re sheet, since a penetration larger than 80% found in this study did not deteriorate the strength of the weld. The diameter of a nugget was only 30-40% of the electrode diameter in SSRSW due to the relatively low electrode force, compared with the high electrode force employed in large-scale resistance welding where the diameter of nugget was almost 100% of the electrode diameter.

11:15 AM

High Temperature Mo-Si-B Alloy Designs and Microstructures: *J. Perepezko¹; R. Sakidja¹*; ¹University of Wisconsin-Madison

The multiphase microstructures that can be developed in the Mo-Si-B system offer useful options for high temperature applications. Alloys based upon the coexistence of the high melting temperature (>2100C) ternary intermetallic Mo₅SiB₂ (T₂) phase with Mo(ss) and Mo₃Si phases allow for in-situ toughening and offer favorable oxidation resistance. A focal point of the microstructural designs is the T₂ phase which exhibits a range of solubility. Selected refractory metal substitutional alloying has been examined to alter the solubility of the T₂ phase and the relative phase stability as a method to develop multiphase microstructure design options. The observed alloying trends also highlight the fundamental geometric and electronic factors that influence the relative stability of the T₂ phase. Similarly, the systematic investigation of reaction kinetics involving the T₂ phase has a direct application to the analysis of oxidation behavior and to the design of effective coating systems with self-healing and gradient characteristics.

11:40 AM

Influence of Texture and Velocity on the Dynamic Tensile Extrusion Response of Tantalum: *Fang Cao¹; Ellen Cerreta¹; George Gray¹*; ¹Los Alamos National Laboratory

The mechanical behavior and damage evolution of tantalum are influenced by texture, strain rate, and grain size. The effects of original rolling texture and grain size on the large-strain dynamic tensile extrusion process in a high purity Ta have been investigated and quantified in this research. The post-extrusion macroscopic evolution of the samples was captured using high-speed photography in a modified Taylor Gun Facility. Post-mortem characterization of the microstructure, surface topography, texture, and substructure evolution was conducted using optical metallography, scanning electron microscopy (SEM), electron backscatter diffraction (EBSD), and transmission electron microscopy (TEM), respectively. The dynamic tensile extrusion behavior and microstructure evolution in Ta have been compared to its responses under quasi-static and controlled high strain rate shear conditions to evaluate "path dependency" effects on defect storage processes.

Structural Aluminides for Elevated Temperature Applications: Phase and Microstructure Evolution

Sponsored by: The Minerals, Metals and Materials Society, TMS Structural Materials Division, TMS: High Temperature Alloys Committee, TMS/ASM: Mechanical Behavior of Materials Committee

Program Organizers: Young-Won Kim, UES Inc; David Morris, Centro Nacional de Investigaciones Metalurgicas, CSIC; Rui Yang, Chinese Academy of Sciences; Christoph Leyens, Technical University of Brandenburg at Cottbus

Wednesday AM

March 12, 2008

Room: 394

Location: Ernest Morial Convention Center

Session Chairs: Rui Yang, Chinese Academy of Sciences; Michael Loretto, University of Birmingham

8:30 AM Invited

Modulated Microstructures: A Novel Approach for the Design of TiAl Alloys: *Fritz Appel¹*; ¹GKSS Research Centre

Phase decomposition and ordering reactions in beta/B2-phase containing TiAl alloys were utilized to establish a novel, previously unreported, type of in-situ composite. The characteristic constituents of this composite are laths with a modulated substructure that are comprised of several stable and metastable phases involving gamma, alpha-2, beta/B2, and orthorhombic B19. The modulation occurs at the nanometre-scale and thus leads to a significant structural refinement. Interfacial dislocations and ledges accommodate the lattice mismatch between the different phases and provide a fine dispersion of nucleation sites for mechanical twins. The phase transformations involved in the formation of the microstructure were characterized by high-resolution electron microscopy. Microstructural control of the alloys can be achieved by conventional thermo-mechanical processing, which however has to be tightly tailored to the alloy composition. Potential applications will be discussed by addressing the strength, creep resistance and fracture toughness of the material.

9:00 AM

Strengthening of Lamellar TiAl Alloys by Dynamic Precipitation of Beta Phase during Creep: *Hanliang Zhu¹; Kouichi Maruyama²*; ¹University of Queensland; ²Tohoku University

Further improvement of their strength at elevated temperatures is necessary for widespread applications TiAl alloys. In TiAl alloys, alpha2 Ti3Al phase transforms to gamma TiAl phase during high temperature exposure. This transformation results in disappearance of gamma/alpha2 boundaries, and the consequent weakening of the alloys. Recent TiAl alloys often contain beta stabilizing elements to have their better formability. In such alloys, precipitation of beta particles takes place during the alpha2 to gamma transformation, and precipitation zones of dense beta particles are formed in place of prior alpha2 plates. The precipitation zones can act as barriers to dislocation motion, and can bring about strengthening. Microstructural changes during creep exposure were studied up to 9000 h at 760C with Ti-47Al-2W-0.2Si alloy. Dynamic precipitation and dissolution of beta particles were observed during the creep tests. It will be discussed how to design the beta precipitation to improve its creep strength.

9:20 AM

In-Situ Characterization of Phase Transformations and Microstructure Evolution in a γ -TiAl Based Alloy: *Klaus-Dieter Liss¹; Andreas Stark²; Arno Bartels²; Helmut Clemens³; Thomas Buslaps⁴; Dominic Phelan⁵; LaReine Yeoh¹*; ¹Australian Nuclear Science and Technology Organisation; ²Hamburg University of Technology; ³Montanuniversität Leoben; ⁴European Synchrotron Radiation Facility; ⁵University of Wollongong

Phase diagrams and microstructures of titanium aluminides are rather complex and, so far, little data were observed in-situ at elevated temperatures. We report on two-dimensional high energy X-ray diffraction and complementary laser scanning confocal microscopy to characterize the appearing phases and to follow the phase evolution in-situ in real time. As an example, the microstructure evolution of a quenched γ -TiAl alloy, consisting of α 2-Ti3Al grains at RT, has been followed in both reciprocal and direct space as a function of temperature up

to 1400°C. At 600-800°C extremely fine γ -laths are formed in α -2-grains occurring through an oriented rearrangement of atoms. Streaks linking reflections of both phases testify from coherent lattice and orientation gradients in the transforming crystallite. At temperatures above the eutectoid temperature recrystallization effects and the $\gamma \rightarrow \alpha$ phase transition take place leading to grain refinement.

9:40 AM

Evaluation of Experimental Beta Gamma Alloys Produced via Powder Metallurgy: Charles Yoltan¹; Jean Stewart¹; Young-Won Kim²; Alojz Kajinic¹; ¹Crucible Materials Corporation; ²UES

Beta gamma alloys are a new class of gamma titanium aluminide alloys that are under continued exploration to offer refined cast structures and improved hot-workability and machine-ability over conventional gamma alloys. The improved process-ability is associated with beta solidification and solid-state phase transformation pathways that yield significant amounts of finely dispersed stable beta at processing temperatures. While beta gamma alloys offer improved cast-ability, melting and casting of large ingots may still present challenges. Powder processing of beta gamma alloys can offer certain advantages over ingot metallurgy processing and the only size limitation is the volume of the vessel used for consolidation by hot isostatic pressing (HIP). Two experimental beta-gamma alloys, Ti-44Al-7(Nb, Mn) at% and Ti-44Al-4(Nb, Mo) (at%), were selected for the present work and their powders were produced by gas atomization. This paper will present the initial findings on production of beta gamma alloys via a pre-alloyed powder route.

10:00 AM

Microstructure Evolution in Directionally Solidified Ti-(44,50)Al Alloy: Zhong Li¹; ¹Harbin Institute of Technology

The microstructure evolutions in directionally solidified Ti-(44, 50) at%Al alloys have been investigated at different growth rates. The detailed phase and microstructure formation from initial transient to steady growth and the lamellar structure in the subsequent solid phase transition were observed. For Ti-44at%Al, the primary phase was beta. Only beta growth was observed at a low growth rate, having a lamellar orientation of 0 or 45° to the growth direction. But at a high growth rate, the primary beta(β) of dendrites surrounded by peritectic alpha(α) and solidification gamma(γ) phase in interdendritic region were observed. The lamellar orientation was 45° to the growth direction. For Ti-50at%Al, the primary phase was alpha. In present growth rate range, dendrite of alpha(α) surrounded by the peritectic gamma(γ) was observed. The gamma(γ) by peritectic reaction shows a typically facet growth parallel to growth direction. The lamellar orientation was 90° to the growth direction.

10:20 AM Break

10:30 AM Invited

Alloy Design Concept for Development of Wrought Gamma Titanium Aluminides - Role of Interstitial and Substitutional Elements in Microstructural Control: Masao Takeyama¹; ¹Tokyo Institute of Technology

Cast TiAl based alloys are in practical use for automobile and jet engine components. In contrast, the wrought alloys are currently under progress. This talk gives the alloy design concept and thermo-mechanical controlled processing (TMCP) methods for the development of wrought gamma alloys, based on the phase equilibria, phase transformations and kinetics of precipitation in Ti-Al-M ternary systems. Emphasis will be placed on the role of substitutional and interstitial elements in microstructure control. The appropriate addition of substitutional β stabilizer M (V, Nb, Cr, Mo) creates the novel transformation pathway of $\beta \rightarrow \alpha \rightarrow \beta + \gamma$. This transformation makes it possible to impart both hot deformability in process and toughness in service by dispersing the β particles within lamellae. The combined addition of an interstitial element, carbon, stabilizes γ phase at lower temperatures, allowing us to control a fine-grained fully lamellar microstructure with fine dispersion of p-type carbide (Ti_3AlC) within lamellae.

11:00 AM

Thermal and Stress Induced Formation of Ordered ω -Phase in Nb-Rich γ -TiAl Based Alloys: Andreas Stark¹; Arno Bartels¹; Frank-Peter Schimansky²; Rainer Gerling²; Helmut Clemens³; ¹Hamburg University of Technology; ²GKSS Research Centre; ³Montanuniversitaet Leoben

The occurrence of ordered ω -phase B8₂ in γ -Ti-45at%Al with 5-10at% Nb and with or without small carbon additions was investigated. For the preparation of the alloys a powder metallurgical approach was used. The formation of ω -phase was observed and analyzed by X-ray diffraction and SEM/EBSD. In Ti-45at%Al-10at%Nb the B2-phase transforms into ω -phase during cooling after HIP at 1280°C. With ≤ 7.5 at% Nb the ω -phase occurs during isothermal compressive deformation at temperatures around 800°C. Here the supersaturated α_2 -phase after HIP transforms into ω -phase. Under compression stress at 800°C the transformation is fast and needs only some minutes to take place. Without applied stress also a transformation of α_2 to ω -phase is observed at 800°C, but it takes several 100 hours. The amount of ω -phase increases with content of Nb. Otherwise, carbon additions stabilize the α_2 -phase and thus hamper its transformation into ω -phase.

11:20 AM

A Numerical Model for the Effect of Nb on the Lamellar and Massive Transformation in Ti-Al-Nb Alloys: Amin Rostamian¹; Alain Jacot¹; ¹Computational Materials Laboratory, Ecole Polytechnique Fédérale de Lausanne, Switzerland

A phenomenological modelling approach has been developed for the description of the massive and lamellar microstructures which form during cooling of TiAl-based alloys from the α phase region at high and moderate cooling rates, respectively. The nucleation of both massive and lamellar γ is described by classical heterogeneous nucleation theory which takes into account that nuclei are formed predominantly at α grain boundaries. The growth rate of the massive phase is calculated with an expression for interface-controlled reactions, while the thickening rate of the lamellae is described with a modified multi-component Zener model of precipitation. The model permits to investigate the influence of nominal composition and cooling rate on the proportion of massive and lamellar γ in the microstructure. The effect of Nb additions on the transformation kinetics is discussed and calculated CCT diagrams for different Nb contents are compared with experimental data published in the literature.

11:40 AM

Understanding the Massive Transformation in TiAl Alloys Using End Quenching: H. Saage¹; D. Hu¹; H. Jiang¹; Michael Loretto¹; X. Wu¹; ¹University of Birmingham, IRC in Materials

The influence of composition and of other variables such as cooling rate and grain size on the massive transformation in a wide range of TiAl alloys has been studied with the aim of developing alloys that can transform massively on air cooling rather than on quenching. The main experimental tool which has been used is end quenching using the Jominy technique. Examination of longitudinal samples taken from different alloys reveals in a particularly simple way the factors which influence the transformation. Optical and analytical scanning and transmission electron microscopy have been used to characterise the microstructures of TiAl alloys with limited additions of alloying elements and alloys with significant additions of Ta and Nb with a range of oxygen contents and different grain sizes. The observations made on the Jominy samples allow an understanding of the sensitivity of the transformation behaviour to all of these experimental variables and it has been shown that 25mm diameter samples of Ta-containing TiAl which have low oxygen contents (below 500wtpm) can transform through thickness when air-cooled. These observations will be discussed in terms of the possibility of using the massive transformation to refine the microstructure of cast components of TiAl.

12:00 PM

Microstructure and Compressive Property in Aluminum-Titanium-Vanadium Ternary Alloys with Phase Constitutions Containing γ Intermetallics and β Phase: *Tohru Takahashi*¹; Koshiro Otsuka²; Yohji Kojima²; Yukiko Toyoda²; Daisuke Ashida²; ¹Department of Mechanical Systems Engineering, Tokyo University of Agriculture and Technology; ²Graduate Student, Tokyo University of Agriculture and Technology

Microstructure and compressive behavior have been investigated on several aluminum-titanium-vanadium ternary alloys whose chemical compositions are varied along a conceivable conjugate line spanning between γ single phase and β single phase. The $Al_{50}Ti_{40}V_{10}$ alloy (V10) with the subscript numbers showing the atomic fraction of each component, contained a small amount of β besides the γ phase. The $Al_{40}Ti_{30}V_{30}$ alloy (V30) showed a fine-grained dual phase microstructure of about a half-and-half mixture, and the $Al_{35}Ti_{25}V_{40}$ alloy (V40) was a coarse-grained β material. At an ambient temperature the V30 and V40 alloys were much stronger than the V10 alloy. But the harder phase interchanged from β to γ at around 1000K as the temperature increased. Accordingly, the compressive creep rate at elevated temperatures became much lower in V10 alloy.

Ultrafine-Grained Materials: Fifth International Symposium: Deformation Mechanisms

Sponsored by: The Minerals, Metals and Materials Society, TMS Structural Materials Division, TMS Materials Processing and Manufacturing Division, TMS: Shaping and Forming Committee, TMS: Nanomechanical Materials Behavior Committee
Program Organizers: Yuri Estrin, Monash University and CSIRO Melbourne; Terence Langdon, University of Southern California; Terry Lowe, Los Alamos National Laboratory; Xiaozhou Liao, University of Sydney; Zhiwei Shan, Hysitron Inc; Ruslan Valiev, UFA State Aviation Technical University; Yuntian Zhu, North Carolina State University

Wednesday AM
March 12, 2008
Room: 273
Location: Ernest Morial Convention Center

Session Chairs: Zhiwei Shan, Hysitron Inc; Hans Fecht, Ulm University; Tongde Shen, Los Alamos National Laboratory; Igor Alexandrov, UFA State Aviation Technical University

8:30 AM Invited

Mechanisms of Deformation Behavior of Ultrafine-Grained Ti: *Igor Alexandrov*¹; Roza Chembarisova¹; Vil Sitdikov¹; ¹Ufa State Aviation Technical University

A grain size is known to be one of the factors which define mechanical properties of metallic materials. At the same time the mechanisms which regulate the deformation behavior of bulk ultrafine-grained (UFG) metals produced by the severe plastic deformation method are still a subject for intensive study and fixed ambiguously. The report presents the developed model and the results of its application for kinetic modeling of the deformation behavior of UFG CP Ti. Conservative slip and non-conservative climb of dislocations, deformation twinning, dynamic strain ageing are considered as potential deformation mechanisms. A wide temperature-rate range of deformation modes is considered. Conclusions about the role of the investigated mechanisms in the appearance of the peculiarities of the deformation behavior of UFG CP Ti are made.

8:50 AM

Dislocation-Twin Interactions in a Nanostructured Cu-30%Zn Alloy: Zhiwei Wang¹; Xiaozhou Liao¹; Yonghao Zhao²; Enrique Lavernia²; Yuntian Zhu³; Zenji Horita⁴; Terence Langdon⁵; ¹University of Sydney; ²University of California, Davis; ³Los Alamos National Laboratory; ⁴Kyushu University; ⁵University of Southern California

Nanostructured metals and alloys usually demonstrate very high strength but suffer from poor ductility because of the lack of work hardening. This lack of work hardening in nanostructured materials has been explained as a lack of mechanisms in accumulating dislocations within the grains of nanostructured materials during deformation. Recently, it was reported that twin boundaries may be good barriers to block and accumulate dislocations and thereby contribute

to work hardening. In this presentation, we discuss detailed high-resolution transmission electron microscopy observations of dislocation-twin interactions in a nanostructured Cu-30%Zn alloy processed by high-pressure torsion. We also discuss the impact of these interactions on the ductility of the material.

9:05 AM Invited

Deformation and Toughening Mechanisms of Nanograins – Lessons from Nature: *Xiaodong Li*¹; ¹University of South Carolina

Seashells are natural nanocomposites with superior mechanical strength and toughness. What is the secret recipe that Mother Nature uses to fabricate seashells? What roles do the nanoscale structures play in the inelasticity and toughening of seashells? Can we learn from this to produce seashell-like nanocomposites? Here we will limit our focus to nacre (mother-of-pearl). The presentation summarizes the recent discovery of nanoparticles “nanograins” in nacre and elucidates the roles that these nanograins play in nacre’s toughness. It was found that rotation and deformation of aragonite nanograins are the two prominent mechanisms contributing to energy dissipation in nacre. The biopolymer spacing between nanograins facilitates the grain rotation process. The digital image correlation technique was used to map local, nanoscale strains to elucidate deformation and fracture mechanisms. This presentation also presents future challenges in the study of nacre’s nanoscale structure and mechanical properties.

9:25 AM

Multiple Deformation Mechanisms in Bulk Nanocrystalline Silver: *Tongde Shen*¹; Can Aydinler¹; Donald Brown¹; ¹Los Alamos National Laboratory

We monitored the stress-strain relations of nanocrystalline silver in tension and simultaneously recorded the synchrotron x-ray diffraction patterns. From the diffraction data, we deduced the grain sizes (GS), dislocation densities (DD), and deformation texture. Our results suggest that the deformation of nanocrystalline silver can be divided into three stages. In stage 1 (before yielding), strain increases GS but decreases the density of glissile dislocations. In stage 2 (after yielding but before stage 3), strain largely increases the stress, but only slightly decreases GS and increases DD. The change in both GS and DD is completely reversible during unloading, suggesting that resistance for the plastic deformation mainly comes from the rotation of grains, as evidenced by the fact that no deformation texture is observed. In stage 3, strain increases both the dislocation density and the deformation texture, indicative of the pile-up of dislocations, similar to the plastic deformation of coarse-grained metals.

9:40 AM

Orientation Splitting and Its Contribution to Grain Refinement during Equal Channel Angular Extrusion: *Yan Huang*¹; Philip Prangnell¹; ¹University of Manchester

Mechanisms of grain refinement during ECAE of a single-phase aluminium alloy have been studied using the high resolution EBSD technique. It was found that, in addition to the formation of shear-plane cell bands (CBs) and shear bands (SBs) by “simple shear”, the development of deformation bands due to orientation splitting contributed significantly to the refinement of microstructure during the early stages of ECAE processing. “Regular” slab-like deformation bands and “irregular” transitional bands were observed after 1st pass; both developed boundaries of high misorientations. During 2nd pass deformation, moderate orientation splitting took place within the deformation bands, although new deformation bands were not detected. With increased strains, orientation splitting tended to occur within small volumes of material, assisting the evolution of the shear plane CBs and SBs into a fibre structure dominated by boundaries of high misorientations. The crystallographic features of the orientation splitting were examined.

9:55 AM

Plastic Deformation of Fully Dense Nanocrystalline Material: *Hans Fecht*¹; Youlia Ivanisenko²; ¹Ulm University; ²Research Centre Karlsruhe

We present results on the fundamentals of plastic deformation in fully dense bulk nanocrystalline metals with a mean grain size between 10 and 30 nm prepared by an innovative and new combination of Inert Gas Condensation (IGC) and subsequent Severe Plastic Deformation (SPD) technique. The model system investigated is Pd (fcc) at the first stage and several single-phase Pd alloys. The experiments focus on mechanical tests using new testing equipment for miniaturized specimens. The aim is to obtain a significantly improved database of materials behaviour for these alloys at this very small grain size, since this

has previously only been explored sporadically, and to elucidate and describe the microscopic mechanisms that mediate the deformation. The obtained results are important not only for fundamental material science, but also allows to elaborate the principles of development of technically feasible nanostructured materials providing the highest level of strength and ductility of these materials.

10:10 AM Break

10:25 AM Invited

Mechanical Properties and Deformation Mechanisms in Ultrafine-Grained Metals: Heinz Werner Höppel¹; Johannes May²; Doris Amberger²; Mathias Göken²; ¹Institute of General Materials Properties WW I; ²University of Erlangen-Nuernberg

Ultrafine-grained (UFG) metals exhibit very promising mechanical properties under monotonic loads: High specific strength is paired with a relatively high ductility. Although, some authors reported a strongly increased ductility (elongation to failure), others observed a reduced ductility compared to the CG counterparts. The enhanced ductility has been found so far for UFG Cu and Al and Al-alloys. In all these cases, the ductility increases as the strain rate decreases. Unfortunately, the deformation mechanisms behind are currently unclear and are in the centre of the scientific discussion. Grain boundary sliding, Coble creep as well as thermally activated annihilation processes are the proposed mechanisms. By reviewing relevant results published in literature on SPD-processed and PED-materials and also analysing new results obtained on UFG Aluminium alloys the objective has been to clarify that point. The proposed mechanisms are also discussed with respect to the cyclic deformation behaviour of UFG materials.

10:45 AM

In Situ TEM Compression Tests on FIB Fabricated Single Crystal Ni Pillars: Zhiwei Shan¹; Raj Mishra²; S.A. Syed Asif¹; Oden Warren¹; Andy Minor³; ¹Hysitron Inc; ²General Motors; ³Lawrence Berkeley National Laboratory

Single-crystal Ni pillars of nominal diameters between 150 and 400 nm were micromachined using focused ion beam (FIB). TEM observations showed that the pillars had a high density of defects after FIB processing and a side wall taper angle of about 4.5 degree. In-situ TEM compression tests using a diamond flat punch were performed on pillars of several different sizes. Our observations showed that: i) dislocation density always decreased dramatically during the deformation test and in some cases a dislocation-free pillar was the end result; ii) the high resolution load vs. displacement curves exhibit extremely irregular profile and were very sensitive to the loading conditions and the sample size; iii) Unlike those bulk materials, the strain hardening observed in our work resulted from the dislocation starvation. The underlying physical mechanisms controlling the nanoscale pillars during deformation will be discussed in light of the above findings.

11:00 AM Invited

Dislocation Dynamics in Nanocrystalline Nickel: Scott Mao¹; Zhiwei Shan¹; Eric Stach²; Jorg Wietzorek¹; David Follstaedt³; James Knapp³; ¹University of Pittsburgh; ²Purdue University; ³Sandia National Laboratories

It is believed that the dynamics of dislocation processes during the deformation of nanocrystalline materials can only be visualized by computational simulations. Here we demonstrate that observations of dislocation processes during the deformation of nanocrystalline Ni with grain sizes as small as 10nm can be achieved by using a combination of in situ tensile straining and high-resolution transmission electron microscopy. Trapped unit lattice dislocations are observed in strained grains as small as 5 nm, but subsequent relaxation leads to dislocation recombination.

11:20 AM

The Role of Twinning in UFG Fcc and Hexagonal Metals Determined by X-Ray Line Profile Analysis: Levente Balogh¹; Tamas Ungar¹; ¹Eotvos University

The appearance of stacking faults or twin boundaries in coarse grain materials is determined by the stacking faults energy (SFE). In most of the pure fcc or bcc metals the SFE is so large that plastic deformation is carried almost solely by dislocation activity. In submicron or nanometer grain size materials the creation and/or mobility of dislocations can be so difficult that faulting or twinning can become an alternative channel for carrying of plastic deformation. Faulting and

twinning has recently been incorporated into the line profile analysis procedure: CMWP. The extended procedure, eCMWP is applied to HPT processed Al alloys, pure Ni, Cu and Cu-Zn alloys and ECAP processed Ti. The frequency of twin boundaries is determined and discussed in correlation with dislocation density, crystallite or subgrain size, size-distribution and mechanical properties.

11:35 AM

Dynamic Deformation Behavior of Ultrafine Grained Materials Produced by ARB and Subsequent Annealing: Naoki Takata¹; Yoshitaka Okitsu²; Nobuhiro Tsuji¹; ¹Osaka University; ²Honda R&D Company, Ltd.

For automobile applications, dynamic deformation behaviors of materials are important to guarantee the safety in collision. In the present study, we fabricated the ultra-low carbon steel and pure aluminum sheets with various grain sizes ranging from 0.2 to 10 micrometer through accumulative roll bonding (ARB) and subsequent annealing at various temperatures. Mechanical properties of these materials were examined at various strain rates ranging from 10⁻² s⁻¹ to 10³ s⁻¹ for clarifying the dynamic deformation behaviors of the ultra-fine grained materials. The flow stress in the dynamic deformation was much higher than that in the quasi-static deformation. It was found that yield-drop phenomenon of the ultra-fine grained materials significantly depended on the strain rate. It could be concluded that the dynamic deformation behavior of the ultra-fine grained materials was attractive compared with that of the same materials with conventional grain size.

11:50 AM

Strain Rate Sensitivity of Ultrafine-Grained Copper with Nano-Scale Twins: Lei Lu¹; Ming Dao²; Suresh Subra²; ¹Chinese Academy of Science, Institute of Metal Research; ²Massachusetts Institute of Technology

We have conducted systematic experimental studies of the effects of nano-scale twin concentration, at a fixed ultra-fine grain size, on the deformation and ductility of ultrafine-grained copper prepared by pulsed electrodeposition technique. It is demonstrated that increasing the nano-scale twin density, while keeping the grain size fixed, results in significant increases in strength and strain-rate sensitivity. It is also found that the activation volume associated with this deformation process significantly decreases with increasing twin volume fraction. These results point to the trend that refining structural dimensions through the introduction of nano-scale twins has the same effect on strength and hardness as grain refinement. In addition, nano-scale twins are also found to provide enhanced ductility. Results of uniaxial tension, strain-rate jump, and instrumented nanoindentation tests will be reported in this presentation and some related modeling results will be briefly referred to with respect to the possible deformation mechanisms.

12:05 PM

Effect of Initial Morphology on Low-Temperature Superplasticity of Submicrocrystalline Ti-6Al-4V: Young Gun Ko¹; Dong Hyuk Shin²; Chong Soo Lee³; ¹Massachusetts Institute of Technology; ²Hanyang University; ³Pohang University of Science and Technology

A present study was made to investigate the superplastic deformation behavior of ultra-fine grained (UFG) Ti-6Al-4V in relation to its initial morphology of alpha/beta phase. Ultra-fine grained microstructures were produced via equal-channel angular (ECA) pressing at 873 K using two different initial microstructures, i.e., equiaxed and lamellar microstructures. After imposing an effective strain up to 4, alpha and beta grains in both microstructures were significantly refined to ~ 300 nm in diameter, and however, beta-phase grains were more uniformly distributed in the initial lamellar microstructure resulting in higher area fraction of alpha/beta interface than the initial equiaxed structure. The flow behavior of UFG Ti-6Al-4V alloy was well described by the constitutive equations which consisted of grain matrix deformation and grain/phase boundary sliding. It was found that higher superplasticity can be obtained in the UFG microstructure when using the fine lamellar microstructure as an initial material.

12:20 PM Award Ceremony for Posters

2008 Nanomaterials: Fabrication, Properties, and Applications: Theory

Sponsored by: The Minerals, Metals and Materials Society, TMS Electronic, Magnetic, and Photonic Materials Division, TMS: Nanomaterials Committee

Program Organizers: Seong Jin Koh, University of Texas; Wonbong Choi, Florida International University; Donna Senft, US Air Force; Ganapathiraman Ramanath, Rensselaer Polytechnic Institute; Seung Kang, Qualcomm Inc

Wednesday PM

Room: 274

March 12, 2008

Location: Ernest Morial Convention Center

Session Chair: To Be Announced

2:00 PM Invited

Understanding Mechanisms of Growth of Nanostructures during Wet Chemical Synthesis: *N. Ravishanker*¹; ¹Indian Institute of Science

In spite of their simplicity, most wet chemical synthetic methods are too reagent-specific and there is very limited fundamental understanding of nanostructure growth. While control of shape during synthesis is reasonably well understood, understanding the general mechanisms of shape control are still elusive. In this talk, I shall illustrate two examples of anisotropic shapes (1-D nanowires and 2-D platelets) and discuss the mechanisms of their formation. In particular, I will illustrate that the mechanism of shape control for the formation of 2-D crystals is directly related to the driving force available for interface motion and is far more general than imagined earlier. The proposed mechanism is applicable for a variety of situations ranging from wet chemical synthesis, vapor phase methods and the formation of inorganic phases by biomineralisation. Such an analysis provides predictive capabilities and enables rational synthesis of 2-D nanostructures.

2:30 PM

Chemical Synthesis and Magnetic Properties of Cubic Morphology Fe₃-Pt Nanoparticles: *Mohammad Shamsuzzoha*¹; *Madhuri Mandal*¹; *David Nikles*¹; ¹University of Alabama

Fe₃-Pt nanoparticles of cubic crystal morphology with sizes in the order of 40 nm were prepared by the use of TX-100 micelles template during the reduction and decomposition of platinum acetylacetonate and iron pentacarbonyl respectively. The nanoparticles thus prepared have an ordered simple cubic structure and are supermagnetic. However, upon annealing with progressively increasing temperature, the nanoparticles showed a drastic drop in the value of magnetic moment at 47°C. This anomalous magnetic behavior is attributed to the occurrences of the Curie temperature for the particles. These cubic morphology particles owing to their faceted morphology as well as of magnetic properties appear a suitable candidate for the hyperthermia therapy in cancer treatment.

2:45 PM

Structural and Thermodynamical Study of CoPt Nanoparticles: *Yann Le Bouar*¹; *Christian Ricolleau*²; *Damien Alloyeau*³; *Cyril Langlois*²; *Annick Loiseau*³; *T. Oikawa*⁴; ¹Laboratoire d'Etudes des Microstructures, Centre Nationaux de la Recherche Scientifique; ²LMPQ, Université Paris 7; ³Laboratoire d'Etudes des Microstructures, Office National d'Etudes et Recherches Aérospatiales; ⁴Jeol Ltd.

The present work is focused on the study of the size effect on the thermodynamical behavior of CoPt nanoparticles. Pulsed laser deposition technique (PLD) is used to synthesize nanoparticles of controlled composition and size, on amorphous carbon or alumina. To characterize the particles, we use conventional TEM, nanoprobe electron diffraction, High Resolution Transmission Electron Microscopy (HRTEM) and Energy Dispersive X-ray Analysis (EDX). The crystal parameters of the particle, determined by electron diffraction, is found proportional to the composition of the particle. The 3D morphology of the nanoparticles has been determined using focal series and electron tomography experiments. The particles (from 2 nm to 12 nm) are slightly faceted and exhibit ellipsoidal shapes elongated in the plane of the substrate. Finally, we study the order-disorder transition in the nanoparticles as a function of their size by annealing either ex situ or in situ in the microscope.

3:00 PM

Grain Growth Behavior and Consolidation of Ball Milled: *Rajeev Gupta*¹; *Raman Singh*¹; *Carl Koch*²; ¹Monash University; ²North Carolina State University

Nanocrystalline iron-chromium alloys may provide considerable corrosion resistance, even at low chromium contents. However, processing of such alloys could be a challenge. This paper describes successful synthesis of nanocrystalline Fe-10%Cr alloy by ball-milling route. In the absence of suitable hot compaction facility, the alloy powder could be successfully compacted close to the desired density, by employing a step of prior annealing of the powder. Grain growth behaviour of Fe-10%Cr nanocrystalline alloy was investigated at 500, 600 and 700°C. At 500°C, no appreciable grain growth was observed, after the initial grain growth. However, sudden and rapid grain growth was observed after 90 at 600°C, and 30min at 700°C. The paper will present the grain growth kinetics and successful processing of nanocrystalline iron-chromium alloys, and preliminary results of their corrosion tests.

3:15 PM

Theory of the Large Melting Point Hysteresis of Ge Nanocrystals Confined within Silica: *Daryl Chrzan*¹; *I. Sharp*¹; *Q. Xu*¹; *C. Yuan*¹; *C. Liao*¹; *J. Ager*²; *E. Haller*¹; ¹University of California, Berkeley and Lawrence Berkeley National Laboratory; ²Lawrence Berkeley National Laboratory

Recent experiments demonstrate that Ge nanocrystals confined within a silica matrix display an extremely large (470 K) melting-point hysteresis centered (approximately) on the bulk melting point of Ge. This behavior stands in marked contrast to bulk solids that, in general, cannot be superheated. Further, since the silica is amorphous, one cannot invoke lattice registry effects to explain the observations. We show that a classical nucleation theory is able to explain quantitatively experimental observations. The theory properly reflects the geometry of the confined nanocrystals, and the impact of this geometry on the nucleation kinetics. Further, the theory relies on generally accepted values for interface energies and latent heats. Thus, there is no need to assume that interface energies depend on nanocrystal radii, nor to invoke atomic scale effects to explain the observations. This work is supported by the U. S. Department of Energy under contract No. DE-AC02-05CH11231.

3:30 PM

Cold Rolling of Nano-Crystalline Nickel: *Andreas Kulovits*¹; *Scott Mao*¹; *Jorg Wozorek*¹; ¹University of Pittsburgh

Good quality bulk nanocrystalline (NC) metals offer potential property enhancements compared to their coarse-grained (CG) counterparts. However, effects of the reduction of the grain size to the nanoscale involve changes in plasticity mechanisms. Dislocation processes responsible for work hardening and deformation texture development in CG metals may not be directly applicable to otherwise equivalent NC metals. Thus, it is important to study the microstructural changes occurring during manufacture of engineered components from NC metals. We use fully dense electrodeposited NC Ni (grain size ~30nm) to study the microstructural evolution during cold-rolling at room temperature to reduction in thickness up to 85% (true strain equivalent ~ 1.9). We determined the changes in texture, grain boundary character and grain sizes as a function of rolling strain using X-ray diffraction and transmission electron microscopy, and measured the hardness. Results for NC and CG Ni are compared.

3:45 PM Break

4:00 PM Invited

Understanding of Ultra-Low Thermal Conductivity Layered Crystals and Nanolaminates: *Pawel Koblinski*¹; ¹Rensselaer Polytechnic Institute

Using molecular dynamics simulations and vibration mode analysis we investigate the mechanism underlying ultra-low thermal conductivity of layered crystals thin films observed in recent experiments (Chiritescu et al, Science 315, 351-353, 2007). In particular, we compare film size dependence of thermal conductivity of ordered and out-of-plane disordered layered crystals. The disorder, indeed, significantly reduces thermal conductivity. It also makes the film thickness dependence weak by comparison with that characterizing ordered layered crystals, however, the film thickness dependence it is not completely eliminated. We will also discuss the potential of designing low thermal conductivity nanolaminates involving alternating layers of soft and hard materials.

4:30 PM

Specific Heat and Thermal Conductivity Measurements Parallel and Perpendicular to the Long-Axis of Cobalt Nanowires: *Nihar Pradhan*¹; Huanan Duan¹; Jianyu Liang¹; Germano Iannacchione¹; ¹Worcester Polytechnic Institute

We present specific heat (C_p) and thermal conductivity (κ) measurements on cobalt nanowires (CoNWs) parallel and perpendicular to the nanowire long-axis from 300 to 400 K. Parallel measurements were done by growing the nanowires within the highly ordered, dense packed, array of parallel pores in aluminum-oxide. Measurements perpendicular to the long-axis of CoNW were done by depositing a thin film of CoNWs within the calorimetric cell. The specific heat both parallel C_p and perpendicular C_p deviates at higher temperatures strongly from bulk, amorphous, powder cobalt. The perpendicular thermal conductivity follows a similar bulk-like behavior, exhibiting a maximum value near 365 K indicating the onset of boundary-phonon scattering. The parallel thermal conductivity does not display any maximum but rather is a smooth increasing function of temperature over the range studied and appears dominated by phonon-phonon scattering.

4:45 PM

Nanoscale Properties Resulting from d States in Complex Metallic Alloys: Esther Belin-Ferré¹; Jean-Marie Dubois²; ¹National Center of Scientific Research; ²Institut Jean Lamour

Many complex compounds exist in alloys like Al-Mg, Al-Mg-Zn or Al-Metal and Mg-Metal. The electronic structure of their valence band was investigated using X-ray emission spectroscopy, which provides separately the electron energy distribution around each chemical species in the solid, averaging the data over all sites. We discuss the nanoscale properties originating from Al 3s,d and Mg 3s,d states in several complex alloys comparatively to the pure metals as well as to other simpler structures, thus evidencing the importance of Al and (or) Mg d-like states at the Fermi level. By comparison to simple alloys containing a transition metal, it is suggested that Al or Mg d-like states play a significant role in the formation of a pseudo-gap at the Fermi level and therefore contribute to select and stabilize complex structures based on icosahedral clusters of nanometer size.

5:00 PM

Structure and Hardness Evolution in Nanocrystalline LIGA Fabricated Ni-6.7at%W Alloy at 873 K: *A.S.M.A. Haseeb*¹; Klaus Bade²; ¹University of Malaya; ²Forschungszentrum Karlsruhe

Nanocrystalline Ni-W alloys have good potential in LIGA fabricated MEMS. Thermal stability of Ni-6.7at%W alloy prepared on silicon wafer using PMMA resist irradiated by synchrotron x-ray, as well as on copper is investigated. The grain size of Ni-6.7at%W alloy increases from 21 nm to 31 nm upon heating at 873 K for 48 hours. Grain growth exponent is found to be 2.25, which indicates an insignificant role of grain boundary diffusion. The microhardness of the alloy decreases from 705 to 420 HV following the Hall-Petch relationship with grain size. Under the same heating condition, the hardness of sulphamate Ni decreases from 324 to 92 HV. The initial cross sectional banded microstructure of LIGA test microcomponent persists during heating at 873 K for 48 hours. A comparison with literature data on nanocrystalline Ni and Ni-P alloys reveals that Ni-6.7at%W alloy possesses a much more stable structure at 873 K.

5:15 PM

Phase Formation in (Co_{0.95}Fe_{0.05})₈₉Zr₇B₄ Nanocrystalline Alloys during In-Situ Heating: *Ramasis Goswami*¹; Matthew Willard²; ¹SAIC/Naval Research Laboratory; ²Naval Research Laboratory

Nanocrystalline soft magnetic alloys are interesting for inductor applications due to their balanced magnetic properties resulting, in part, from their unique microstructure. Understanding the microstructure formation is an important for optimization of the magnetic properties. In this study, phase transformations in a (Fe_{0.05}Co_{0.95})₈₉Zr₇B₄ melt spun alloy have been investigated by in-situ heating in the transmission electron microscope. The sample in the as spun condition consists of fine BCC crystallites dispersed in amorphous matrix. At higher temperatures, above secondary crystallization, the amorphous matrix dissociates into Zr-intermetallics and the grains coarsen significantly. HRTEM on samples annealed at 550°C showed 8-10 nm grains, both BCC and FCC, are surrounded by with the residual amorphous matrix, forming a barrier for diffusion

between grains that prevents the grain growth at intermediate temperatures. Z-contrast imaging showed the nanocrystalline pockets containing higher Zr, which stabilizes the amorphous region.

5:30 PM

Mechanical Properties of Nanocrystalline Cu-Sn Alloys Produced by Hot Rolling of Ball-Milled Powders: *Hee-Tae Jeong*¹; Jae-Hyuk Shin¹; Hyun-Joo Choi¹; Donghyun Bae¹; ¹Yonsei University

During the past decade, lots of interests have been given to the fabrication of bulk nanostructured metallic materials for structural applications. In the present study, the mechanical properties of hot-rolled Cu_{100-x}Sn_x, $x=5, 10, 15$, and 22 wt.%, alloys were investigated. The powders for the consolidation process were produced by mechanical alloying. With a proper milling condition, the produced powders, in the range of Sn content up to 22 wt.%, were found to have single phase of α -(Cu,Sn) solid solution and the grain size of the powder was below 50 nm. Hot-rolling process was employed to fabricate the plates. The microstructures, mechanical properties, such as tensile strength and ductility, and strain rate effects, of the as-rolled and heat-treated plates and their deformation mechanism will be presented.

3-Dimensional Materials Science: Modeling and Characterization across Length Scales III

Sponsored by: The Minerals, Metals and Materials Society, TMS Structural Materials Division, TMS: Advanced Characterization, Testing, and Simulation Committee
Program Organizers: Michael Uchic, US Air Force; Eric Taleff, University of Texas; Alexis Lewis, Naval Research Laboratory; Jeff Simmons, US Air Force; Marc DeGraef, Carnegie Mellon University

Wednesday PM

March 12, 2008

Room: 286

Location: Ernest Morial Convention Center

Session Chairs: Eric Taleff, University of Texas; Jaimie Tilely, US Air Force

2:00 PM Invited

3D X-Ray Microscopy Investigation of Materials Microstructure: *Bennett Larson*¹; ¹Oak Ridge National Laboratory

X-ray structural microscopy using polychromatic x-ray microbeams now provides the capability to measure local crystal microstructure and strain in deformed materials with submicron spatial resolution in three-dimensions. 3D x-ray microscopy measurements performed on 3D grids lead to dislocation density tensors for characterizing deformation in terms of geometrically necessary dislocation (GND) densities. 3D x-ray microscopy measurements made on single crystal copper indented with a 100 micron radius spherical indenter will be presented in terms of 3D spatially resolved rotation maps and dislocation density tensors. These measurements will be compared with (collaborative) computer simulations for spherically indented copper to illustrate the connection between experiment and computations. Exploiting the confined deformation volumes associated with indentation provides a direct and absolute linkage between 3D x-ray microscopy measurements and computer simulations on mesoscopic length scales. Research sponsored by the DOE BES-DMS&E and performed at the DOE supported APS at ANL and SHARE at ORNL.

2:30 PM

Non-Destructive 3-D X-Ray Diffraction Imaging at the Nanoscale: *Barry Muddle*¹; Rouben Dilanian²; Nadia Zatsepin²; Andrei Nikulin²; ¹Monash University, Centre for Design in Light Metals; ²Monash University, School of Physics

Approaches to non-destructive, 3-D x-ray imaging with nanoscale (10-30nm) spatial resolution typically fall into two categories: (i) those employing refractive x-ray lenses to deliver 3-D microscopy in scanning or full-field transmission modes, and (ii) those using an iterative oversampling algorithm to retrieve phase from multiple 2-D maps of diffracted intensity to deliver lens-free, coherent diffractive imaging. Both approaches require highly coherent x-rays and tomography is necessary for full 3-D imaging. The present alternative employs a crystal analyser to collect diffracted intensity as a function of spherical coordinates in reciprocal space and an iterative algorithm is used to reconstruct

WEDNESDAY PM

the 3-D form of the average diffracting object with a spatial resolution of a few nanometres. The technique is insensitive to the coherence of the x-ray beam, and 3-D reconstruction is possible without tomographic synthesis. Application to characterisation of nanoparticulate in a range of dispersed-phase nanocomposite structures will illustrate the approach.

2:50 PM

Reconstructing 3D Microstructure from X-Ray Diffraction Microscopy

Data: Robert Suter¹; Chris Hefferan¹; Frankie Li¹; Robert Moore¹; Brian Tieman²; Ulrich Lienert²; ¹Carnegie Mellon University; ²Argonne National Laboratory

X-ray diffraction microscopy makes it possible to non-destructively measure volumes of microstructure. As such, it is possible to perform dynamic measurements of the response of ensembles of grains to stimuli such as heat or stress. Forward modeling methods for analyzing the data use computer simulation to adjust simulated local crystallographic parameters to match observed diffraction. This method is flexible since multiple phases and complex scattering can be incorporated but it is also computationally intensive. We describe successful reconstruction of an aluminum polycrystal. We interpolate layer-by-layer reconstructions onto a cubic array of voxels, mesh boundaries with triangles, and use smoothing algorithms to remove steps and optimize grain boundary locations. The resulting map includes grain geometries, boundary types, and internal structure such as orientation gradients. The feasibility of extending this type of analysis to large volume data sets and the necessity of parallel computing architectures will be discussed.

3:10 PM

NanoCT: Analysis of Internal Microstructures with High Resolution Computed Tomography: Kathleen Brockdorf¹; David Lehmann¹; ¹Phoenix X-ray

High-resolution X-ray tomography allows the visualisation and spatial analysis of internal microstructures of small samples. The nanotom of phoenix|x-ray is the first 180 kV nanofocus computed tomography system tailored specifically to the highest-resolution applications in the fields of material science, micro electronics, geology etc. with exceptional voxel-resolutions down to <0.5 microns. By granting the user the ability to navigate the internal structure of an object slice-by-slice in a non-destructive manner, the system creates new analysis capabilities thus far have been unreachable: Any internal detail showing a contrast in material, density or porosity can be visualized and distances can be measured. By this way different metal phases of alloys or the texture of fibres in composite materials with only a few microns diameter may be analysed. This opens a new dimension of the 3D-microanalysis and will partially substitute destructive methods like traditional slicing – saving costs and time per sample inspected.

3:30 PM Break

3:50 PM

Atom Probe Tomography: Reconstructing and Quantifying Microstructural Features from Atoms: Michael Miller¹; ¹Oak Ridge National Laboratory

Major advances have occurred in atom probe instrumentation of over the last few years. Datasets containing the atomic coordinates and the mass-to-charge state ratios of almost a billion atoms have been generated. Although standard visualizations methods such as atom maps and isoconcentration surfaces provide valuable information on the phase distribution and morphology, it is difficult to extract quantitative information on the distribution of solutes and sizes of the microstructural features present directly from these methods. Therefore, statistical based methods have been developed to perform these types of analysis. The concepts underlying these methods and the issues of implementing them at the atomic level will be discussed. Research at the Oak Ridge National Laboratory SHaRE User Facility was sponsored by Basic Energy Sciences, U.S. Department of Energy.

4:10 PM

Subnanoscale Characterization of a Multicomponent Steel by 3-Dimensional Atom-Probe Tomography: R. Prakash Kolli¹; David Seidman¹; ¹Northwestern University

We describe briefly the atom-probe tomography (APT) methodology, which possesses a resolution of ca. 0.2 to 0.5 nm, and the compositional and morphological results that can be obtained using it. We then present results from

a precipitation hardened, multicomponent, high-strength low-carbon (HSLC) ferritic steel being developed for naval applications. We illustrate that the mean radius, $R(t)$, and number density, $N_v(t)$, of the precipitates can be measured directly thereby characterizing their morphology. Furthermore, we demonstrate that the elemental concentration profiles, solute partitioning, phase compositions, and supersaturations can be obtained; yielding detailed compositional information about the precipitates, matrix, and interfacial region. The acquired results are correlated to bulk mechanical properties (yield stress, ultimate tensile stress, plasticity at failure, Charpy V-Notch values) and strengthening mechanisms, precipitate growth and coarsening models, or can be used as input or to refine computational models such as the commercially available *Thermo-Calc* or *Precipi-Calc* programs.

4:30 PM

Microanalysis and Modeling of TiNi-Based Shape Memory Alloys with 3-D Local Electrode Atom Probe Tomography: Matthew Bender¹; Gregory Olson¹; ¹Northwestern University

3-D local electrode atom probe (LEAP) tomography is utilized to support the computational design of nanoscale precipitation-strengthened TiNi-based shape-memory alloys. Using LEAP tomography, the otherwise unattainable B2-L21 phase relations for Ni-Ti-Al-Zr alloys at 600°C are mapped. Results indicate that Zr addition has the unintended effect of stabilizing unwanted metastable Ni_3Ti_3 phase; therefore, phase relations of Ni-rich precipitates are also studied and optimized alloy compositions are designed to avoid them. Precipitate growth and coarsening of aluminide precipitates is investigated with LEAP tomography, revealing that optimal microstructures occur in the early stages of precipitation rather than at equilibrium. Using experimentally calibrated models, a superelastic biomedical Ni-Ti-Al-Zr alloy for the application of stenting a superficial femoral artery is designed to have low-misfit coherent precipitation strengthening, desired transformation temperatures, and enhanced radiopacity absorption, within the constraint of practical processing temperatures. Mechanical testing validates the expected high-performance properties of designed alloys.

4:50 PM

Pulsed-Laser (3D) Atom Probe Tomography of Spinodal Decomposition and Transition Carbide Formation during Tempering of Low C-High Si-Low Ni Martensitic Steel: Padmanava Sadhukhan¹; Don Sherman²; Gregory Olson³; ¹Northwestern University; ²Caterpillar Inc; ³Northwestern University, Questek Innovations LLC

Pulsed-Laser Atom-Probe(AP) tomography has been used to study kinetics of spinodal decomposition/transition ϵ' -carbide formation in 0.29C-1.52Si-0.19Ni low-alloy tough-steel. The as-quenched martensite specimens were (1)aged at room-temperature for prolonged period, and (2)tempered at 215C for various times. Carbon segregation was analyzed using (3D) Local-electrode AP(LEAPTM) carbon distribution maps, with an average of 35-40 Million ions collected. Composition of carbon-enriched regions,modulations and transition-carbides have been analyzed using both cylindrical 1D-composition profile method along different axes and proximity-histogram concentration profile method. The latter separates the interfacial regions from the precipitate/concentrated cores, with the precipitates binned in 1nm3 volume increments. Analysis of concentration-profiles of these carbides have been compared to earlier observed modulations/transition carbides using APFIM/TEM in high-Carbon Fe-Ni-C martensites. Steel specimens were provided by AMT, Caterpillar. Financial support from ONR(N00014-01-1-0953) is acknowledged. Atom-probe analyses were performed at Northwestern-University Center for Atom-Probe Tomography(NUCAPT). LEAPTM tomograph was purchased with funding from NSF-MRI(DMR-0420532) and ONR-DURIP(N00014-0400798) programs.

5:10 PM

Microstructure Evolution of the High Carbon Pearlitic Steel Wires by Using LA-3DAP: Yang Yo Sep¹; Park Chan Gyung¹; Bae Jong Gu²; ¹POSTECH MSE; ²KISWIRE Research and Development Center

A three dimensional knowledge of the atom-scale structure is necessary for improving the design and understanding of the modern materials. Laser assisted atom probe is used to obtain atom by atom 3D reconstruction to characterize three versions of several alloys in high carbon steel wires. Since steel wires experience the heavy drawing process, the carbon atoms in cementite moved into

ferrite matrix. It is worthy to find the reasons why carbon dissolution is occurred, since the cementite dissolution is strongly related with mechanical properties, especially fatigue resistance. To identify the carbon movement in the cementite and ferrite, the steel wires were fabricated depending on the carbon content and drawing condition. The carbon atoms moved into ferrite with increase of drawing strain, regardless carbon contents. It revealed that the fatigue resistance of all steel wires decreased with increase of carbon content and drawing strain resulted from the increase of cementite dissolution.

Alumina and Bauxite: Operations

Sponsored by: The Minerals, Metals and Materials Society, TMS Light Metals Division, TMS: Aluminum Committee

Program Organizers: Sringeri Chandrashekar, Rio Tinto Aluminium Limited; Peter McIntosh, Australus Management Services

Wednesday PM
March 12, 2008

Room: 296
Location: Ernest Morial Convention Center

Session Chair: Milind Chaubal, Sherwin Plant

2:00 PM Introductory Comments

2:05 PM

The Kinetics of Quartz Dissolution in Caustic Solutions and Synthetic Bayer Liquors: Bingan Xu¹; Christine Wingate¹; Peter Smith¹; ¹CSIRO

The Oku-Yamada (O-Y) equation (1971) has successfully estimated quartz attack for many bauxites. However it is often used outside its development conditions (particularly temperature). This paper examines the kinetics of quartz attack for quartz in pure caustic and synthetic Bayer liquor, and for an Australian bauxite in synthetic liquor. Under typical conditions, the attack of quartz in pure caustic was well modeled by the O-Y equation but it tended to over-estimate attack in synthetic liquor. The equation also over-estimated attack on coarse particles and under-estimated attack on fine particles, suggesting quartz surface area (not a factor in the O-Y equation) is important. Quartz attack on bauxite was modeled well suggesting that the quartz size distribution was comparable to that in Oku and Yamada's bauxite. Measured quartz attack at higher temperatures (240-280°C) showed the same trends as lower temperatures, suggesting the equation can be used for bauxite in this temperature range.

2:30 PM

Improvement in Vanadium Salt Separation: P.K.N. Raghavan¹; ¹Bharat Aluminium Company Ltd., (A Unit of Vedanta Resources Plc.)

In the work presented here an attempt has been made for improving the extraction of Vanadium Sludge from the Bayer's Liquor and improving the quality of the Sludge. This paper also deals with our experiments on the processing of Vanadium Sludge for the recovery of Caustic Soda and the other value added products. Laboratory Scale experiments were carried out with the Vanadium Sludge produced from our Alumina Plant by treating it with Wash Water to improve the Vanadium Salt quality. Our experiments on improving the Vanadium Salt yield by chilling the strong liquor, has shown an improved salt yield. This paper also deals with the optimum temperature to which the liquor is to be cooled to get higher yields at Plant Condition.

2:55 PM

Potential of Improvement of Atmospheric Pressure Bauxite Digestion Circuit: Alexander Suss¹; Nikolay Ivanushkin²; Irina Paromova¹; Andrey Panov¹; Anatoly Lapin¹; Tatiana Gabrielyan¹; ¹Russian National Aluminium-Magnesium Institute; ²Russian Aluminum Company

The paper describes the work on elaboration of two - stages counter current digestion circuit for pure gibbsite bauxites from Fria deposit in Guinea. With the alumina recovery at the same level as for single stage digestion the transition to the 2 stages allows to obtain higher RP in the liquid phase for non-autoclave digestion in agitations. The expected production growth after implementation of 2 stages counter current digestion circuit at Friguia Alumina Refinery will be ~ 50 ktpy. The higher RP ratio increases the agglomeration capacity of green

liquor with stronger hydrate crystals. It will allow to reduce the attrition index from ~ 33-35 to ~ 20%.

3:20 PM

Using a Statistical Model in the Red Mud Filtration by Means of DOE: Jorge Lima¹; Américo Borges¹; ¹Alunorte

ALUNORTE was conceived to dispose the red mud using dry-stacking technology, making use of deep-thickeners in the last stage of the washing circuit and vacuum drum filters in the red mud filtration area, reducing the caustic concentration from 65 g/L in the last washers down to 7 g/L at filters discharge. This paper aims to present a DOE program with two levels and five factors at red mud filtration. Dilution, rotation, condensate, level in the basin and vacuum had been considered as variables of control. The output variable considered was the caustic concentration in the filtered red mud. The DOE measured the magnitude of the control variables and the influences on the output variable, making possible to model the filtration process, aiming to control the caustic concentration in the red mud below the target of 7 g/L.

3:45 PM Break

4:00 PM

Process Diagnosis Based on Neural Network Expert System for Gas Suspension Calcination of Aluminum Hydroxide: Dai fei Liu¹; Jie Li¹; Feng qi Ding¹; Zhong Zou¹; Xiang tao Chen¹; ¹Central South University

Stable and effective operations in the gas suspension calcination of aluminum hydroxide can save energy, increase yield and reduce exhaust emission. But this goal hasn't been reached because the roasting process is too complex. Until now there is few process diagnosis models discussed or built in the published literatures. This paper presents a process diagnosis system, which uses neural network and expert system, and comprises four parts, namely state analysis module, energy evaluation module, parameter optimization module and control guidance module. In the system the state analysis module is used to analyze process state, the energy evaluation module is to compute energy costs and the parameter optimization and control guidance module are to deduce other useful results and optimization parameters. The application of this system indicates that the identifying accuracy for abnormal process achieved 90% and temperature error was within $\pm 5^\circ\text{C}$, real-time evaluation and optimization provided good guidance for practice.

4:25 PM

Review on the Quality of Alumina: Wangxing Li¹; Dalin Fan¹; Zhonglin Yin¹; Zhanwei Liu¹; ¹Zhengzhou Research Institute of Aluminum Corporation of China Limited

After China entered WTO, the important tasks facing our alumina industry are actively participating in international cooperation and competition in a global economy. With the development of aluminium smelting technology and greater attention given to the environmental protection, the quality requirements of alumina are more strictly. The effects of alumina quality on the aluminium smelting are discussed in this paper. The differences between domestic and foreign alumina products in chemical components and physical properties are also presented in this paper. The measures of improving the quality of alumina are explored, so the alumina products can meet the requirements of aluminium smelting.

4:50 PM

Bauxite Digestion Studies for Optimiztion of Operating Parameters: P.K.N. Raghavan¹; ¹Bharat Aluminium Company Ltd., (A Unit of Vedanta Resources Plc.)

Alumina extraction from bauxite by the Bayer's process requires an efficient digestion process. Bauxite digestion depends much on the temperature-pressure conditions, the recycled liquor concentration bauxite mineralogy and charge quantity. The productivity of the entire Bayer process depends to a large extent on the digestion process. High-pressure digestion (235 to 245 Oc) is used for boehmitic and diasporic bauxite. A need has been felt to optimize the digestion conditions in order to achieve low caustic soda loss coupled with minimum bauxite consumption. In an effort to achieve the above-mentioned goals a series of experiments were conducted to find out the best parameter for conducting digestion at laboratory scale. The effect of deslucation and digestion temperature, bauxite charge, lime quantity and digestion liquor MR is discussed in these paper.

Aluminum Alloys: Fabrication, Characterization and Applications: Composites and Foams

Sponsored by: The Minerals, Metals and Materials Society, TMS Light Metals Division, TMS: Aluminum Committee

Program Organizers: Subodh Das, Secat Inc; Weimin Yin, Secat Inc

Wednesday PM

Room: 293

March 12, 2008

Location: Ernest Morial Convention Center

Session Chairs: Subodh Das, Secat Inc; Weimin Yin, Secat Inc; Shridas Ningilieri, Secat Inc

2:00 PM

Development of High-Strength Hypereutectic Al-Si Alloys by Nano-Refining the Constituent Si Phases: *Mohammad Shamsuzzoha¹; Frank Juretzko¹; Anwarul Haque¹; ¹University of Alabama*

Among the structural light weight materials, Al-Si alloys have established itself as the most widely used Al-alloys for aerospace and automotive applications. Our recent efforts have demonstrated that it is possible to develop primary Si-phase free hypereutectic Al-Si alloys by a casting method. In the continuation of this effort, an Al-17wt%Si alloy that has a microstructure in which silicon phase assumes nano sized fibrous morphology has been developed by directional casting. The fabrication and characterization of this unique Al-Si alloys are presented. The mechanical properties of this alloy based on first principle, are also discussed.

2:20 PM

Fabrication of Aluminum Composites with Gradient Cladding Interface by Continuous Casting: *Weiwen Zhang¹; Datong Zhang¹; Yuanyuan Li¹; ¹South China University of Technology*

A method named double-stream-pouring continuous casting (DSPCC) was proposed to produce bimetallic composites with gradient cladding interface. The characteristics of DSPCC and the differences between DSPCC and conventional continuous casting were highlighted. According to the trials in Al-Zn-Mg, Al-Cu-Mg, Al-Mn and Al-Mg-Si alloy systems, it is found that the interfacial zone dimensions can be controlled by adjusting the alloy composition and solidification processing parameters, such as the temperature of the melts, the casting speed and the depth of the submerged nozzle in the mold. A 2024/3003 composite having the equivalent corrosion resistance to 3003 alloy was prepared by DSPCC. After plastic deformation and T6 heat treatment, the tensile strength and yield strength of the composite are 2.56 and 4.05 times of that of 3003 alloy, respectively and the elongation of the composite is still as high as 21.6%.

2:40 PM

Study of Different Magnesium or Silicon Content on Microstructures in In-Situ Mg₂Si/Al Alloy Composites: *Jing Qingxiu¹; Zhu Yinglu¹; ¹Institute of Material and Chemistry Engineering, Jiangxi University of Science and Technology*

In-situ Mg₂Si reinforced Al alloy composites were fabricated by common weight casting technique. Effects of different Mg and Si content and heat treatments on microstructures of materials were studied. The results indicate that effect of combined modification of rare earths and Strontium salt on primary α -Al is very good, while not obvious on eutectic α -Al. Eutectic Mg₂Si nucleates at crystal boundaries, with shaping undeveloped Chinese characters-like in a hypoeutectic Al-Mg₂Si system which contains more Si element, while eutectic Mg₂Si is surrounded by α -Al and grows to integrated Chinese characters-like shape in a nearly eutectic Al-Mg₂Si system in which little Si contained. Eutectic Mg₂Si is fined to particle or short cosh in a heat treatment process, and the size of primary Mg₂Si is also reduced at some extent, from about 15 μ m to 8 μ m.

3:00 PM

Influences of Pressing Modes to the Density of Precursor: *Zhiqiang Guo¹; Guangchun Yao¹; Yihan Liu¹; ¹Northeastern University, School of Materials and Metallurgy*

There are many factors influence the preparation of foam aluminum, but the density of precursors is the first important thing to get high quality foam aluminum

materials. In this paper influences of pressing modes to powder compact method are studied. Mix Al powders with foaming agent (TiH₂), and then press them into precursors with two different pressing modes: 300MPa cold pressing mode and 300MPa cold pressing + 300MPa hot pressing mode. The precursors are analyzed by SEM. It can be shown that there are many tiny holes existed in the precursor using cold pressing mode, and it's adverse to the preparation of foam aluminum. However, using cold pressing +hot pressing mode, it can be shown that tiny holes are eliminated after hot pressing, high density precursors are obtained, and it's useful to the preparation of foam aluminum.

3:15 PM

Influencing Factors on Preparation of Aluminum Foam Core Sandwich Panels by the Elemental Powder Metallurgy Method: *Hong Li¹; Guangchun Yao¹; Guoyin Zu¹; Yihan Liu¹; ¹Northeastern University*

Pure Al powder was applied as raw material. Foaming agent TiH₂ and pure Al powder were blended with different amounts of element powders Si and Mg. Pure aluminum panels Al-foam sandwich were fabricated through cold rolling of mixed powder with two panels and then foaming in a furnace. The effects of cold rolling reduction rate, foaming temperature and time on foaming results were studied. The results show that when the cold rolling reduction rate is in the range of (60~70%), the binding between panels and core is perfect after foaming, which is metallurgical binding. Moreover, foaming effect of the core shows good. The optimal foaming temperature and foaming time for good foaming results are 630~640°C and 7~9 min, respectively.

3:30 PM

Foam Structure and Mechanical Properties of AlCu₃Mn Foam Stabilized by Short Carbon Fibers: *Zhuokun Cao¹; Bing Li¹; Guangchun Yao¹; Yihan Liu¹; ¹Northeastern University of China*

Categories of commercial aluminum alloy foams are quite limited. As for Al-Cu alloy, which possess good mechanical property and machinability, manufacture of such alloy foams encounters technical difficulties involving foam stability and chemical component change. In the present paper, AlCu₃Mn alloy foam was fabricated using short carbon fibers with copper coating as stabilizer. The volume fraction of fibers used is as low as 0.7vol.%, so its influence on mechanical property is quite little. Relative density, average cell wall thickness and mean cell size is measured, and the mechanical property of this new foam is also characterized. It is evidence that this foam show uniform structure, high weight efficiency and good energy absorption.

3:45 PM

Effects of Si and Mg on Preparation of Aluminum Foam Core Sandwich Panels: *Hong Li¹; Guangchun Yao¹; GuoYin Zu¹; Yihan Liu¹; Bing Li¹; Zhiqiang Guo¹; ¹Northeastern University*

Pure Al powder was applied as raw material. Foaming agent TiH₂ and pure Al powder were blended with different amounts of element powders Si and Mg. Pure aluminum panels Al-foam sandwich were fabricated through cold rolling of mixed powder with two panels and then foaming in a furnace. The effects of particle size of Si and addition of Mg on foam structure were discussed. The results show that, the melting temperature of the core decreases and pure aluminum panels are protected from softening when Si is added to produce AlSi alloy through powder metallurgy. The cell structure could be improved by decreasing the particle size of Si. When a little amount of Mg is added, complex compound Al₃Si₂O₇ and Mg₃Al₂(SiO₄)₃ are produced and stable cell walls are obtained.

4:00 PM Break

4:10 PM

Study on the Bubble Stable Mechanism of Foam Aluminum: *Li Wei¹; ¹Shenyang Ligong University, Materials Science and Engineering College*

This is a study on preparing foam aluminum by powder metallurgy. In this research raw materials are pure aluminum powder, aluminum powder added carborundum and aluminum powder added aluminum oxide. The microstructure of cell wall of foam aluminum, the viscosity and surface tension of melt are investigated. The bubble stabilities which are controlled through adding carborundum and aluminum oxide are discussed, and the mechanism of bubble's stability is analyzed. The results showed that the homogeneity of bubble holes of foam aluminum is better which is obtained by adding carborundum and

aluminum oxide practical into the raw materials. Observing SEM can indicate that carborundum and aluminum oxide practical distribute evenly on cell wall of foam aluminum. It means that during foaming a lot of carborundum and aluminum oxide practical distribute diffusively in liquid aluminum melted or mid-melted. It increases the viscosity of melt so that stability of bubble is increased.

4:30 PM

Study on the Control of Foam Gradient by Foam Melting: Wang Yong¹; Guangchun Yao¹; Li Bing¹; Cao Zuo-kun¹; ¹Northeastern University

The solidification modes of foamed Al and its influence on the cell structure are studied, and the changes of volume and porosity of foamed melt during solidification process are discussed. It is demonstrated that the evolution of the cellular structure is influenced by different solidification mode in the process. The relation of the foam growth height with time is researched. The foam evolvement of the melt in the solidification phase is discussed. Some conclusions are obtained: the evolution of cellular structure is influenced by many processing factors such as viscosity, foaming time and solidification mode. Al foam melt is prone to solidify with planar front, using special solidification mode can control the gradient of the cellular structure effectively, and the bubble size has a certain relation with the cooling time.

4:50 PM

The Effect of Complex Modification and Melt Mixing Treatment on Microstructure in In-Situ Mg₂Si/Al-Si Composite: Jing Qingxiu¹; Huang Xiaodong²; ¹Jiangxi University of Science and Technology, Institute of Material and Chemistry Engineering; ²Jiangxi University of Science and Technology

The effect of SrCl₂ and RE complex modification and melt mixing treatment on microstructure in in-situ Mg₂Si/Al-Si composite was investigated in this paper. It is found that primary Mg₂Si particles have been greatly refined from 25μm to below 8μm with morphology changing from polygonal to quadrangle in the optimum melt mixing condition and with the optimum content of SrCl₂ and RE addition. The result also indicates that, with the increase of SrCl₂ and RE content, the pseudo-eutectic Mg₂Si is changed gradually from agglomerated coarse tablet to dispersed spots or slim bars. The growth of Mg₂Si follows not only the twin plane re-entrant edge (TPRE) mechanism, but also layer mechanism as well.

5:10 PM

Study on Sound Insulation Performance of Al Foam Sandwich Board: Guoyin Zu¹; Guangchun Yao¹; Hong Li¹; ¹Northeastern University, School of Materials and Metallurgy

Sound reduction index of Al foam bare board and sandwich board was tested using standing wave method, the effect of density and thickness on acoustical behavior of Al foam sandwich board was studied. The results showed that, sound reduction index of Al foam sandwich board increased with the increase of sound wave frequency, sound reduction index during difference frequency was controlled by difference mechanism, it could be divided into three regions: rigidity and damp control region, quality control region and mixing influence region. With the increase of density and thickness of Al foam sandwich board, the sound insulation performance enhanced gradually, sound reduction index increased with the increase of sound wave frequency.

5:30 PM

Effect of Cold-Rolling Bonding Process on Microstructure and Properties of the Sandwich Aluminum Foil for Automobile Heat Exchanger: Guoyin Zu¹; Ning Wang¹; Jiuming Yu¹; ¹Northeastern University, School of Materials and Metallurgy

The cold-rolling bonding process of sandwich aluminum foil for automobile heat exchanger was investigated, and the effect of deformation rate in the first pass, the clad thickness and the final annealing schedule on microstructure and properties of the sandwich foil was analyzed. The results showed that under deformation rate of 30%-50% in the first pass, the initial bonding can be gained between the clad A4045 and the core A3003, the upper clad thickness of the product was probably the same as the lower one. The final clad radio was influenced by deformation rate and initial thickness of the rolled piece; it increases with the increasing of deformation rate and initial thickness. The cladding foil had the best sagging resistance when the cold-rolling deformation rate was 25%-35%.

5:50 PM

The Effects of Mg Addition and TiH₂ Pre-treated on the Stability of Aluminum Foams Made by Powder Compact Method: Zhiqiang Guo¹; Guangchun Yao¹; Yihan Liu¹; ¹Northeastern University, School of Materials and Metallurgy

Aluminum foams produced by melting powder compacts containing a blowing agent are usually non-uniform which might lead to inferior mechanical properties. The reasons for this can be thermal gradients during foaming and a blowing agent which is not adapted to the melting range of the alloy to be foamed. In this paper TiH₂ is pre-treated in air at 520°C, and Mg with different contents are also added to improve the stability of foams. It can be found that precursors foamed in an early time and with the oxidation treatment of TiH₂ powders at 520°C. An increase in expansion was affected by the addition of Mg particles to Al foams and the stability is also improved. Enhanced wetting, due to reaction with Mg, enables the particles to be embedded in the cell walls, making them more effective at foam stabilization.

6:05 PM

Study on Powder Metallurgy Foaming Process of Rolled Precursor: Guoyin Zu¹; Guangchun Yao¹; Hong Li¹; Liang Hao¹; ¹Northeastern University, School of Materials and Metallurgy

The powder metallurgy foaming process of rolled precursor was investigated in this paper, evolvement process of high tightness core to foam structure was analyzed, efficiency approach to increase stability of foam structure was studied, and the optimal foaming process was obtained. The results showed that cracks and drainage during foaming were inhibited by heat treatment of foaming agent TiH₂ and proper quantities addition of Mg to body system. The optimum heat treatment way of TiH₂ was that heat preserving at 450°C for 1 hour, and Mg addition was 1wt.%. The optimum foaming temperature of rolled precursor was 620-630°C, ideal core foam structure was obtained when at 620°C for 4-6min.

Aluminum Reduction Technology: Fundamentals, Low Melting Electrolytes, New Technologies

Sponsored by: The Minerals, Metals and Materials Society, TMS Light Metals Division, TMS: Aluminum Committee

Program Organizers: Martin Iffert, Trimet Aluminium AG; Geoffrey Bearne, Rio Tinto Aluminium Tech

Wednesday PM
March 12, 2008

Room: 298
Location: Ernest Morial Convention Center

Session Chair: Victor Buzunov, United Company «Russian Aluminum»

2:00 PM

Technical Contributions of the Late Warren Haupin – A Review: Jay Bruggeman¹; Alcoa Inc.

From his pioneering work in pot heat balance measurements and modeling to his fundamental studies on anode effects and electrode processes, the late Warren Haupin often laid a foundation of understanding for others to build on. This paper reviews Haupin's major technical contributions as a tribute to the man who impacted the aluminum industry so much.

2:25 PM

Top Heat Loss in Hall-Heroult Cells: Xian Chun Shen¹; Margaret Hyland²; Barry Welch³; ¹CITIC International Cooperation Co., Ltd.; ²University of Auckland; ³Centre for Electrochemical and Mineral Processing, University of New South Wales

The top heat losses were measured in industrial Hall-Heroult cells, including heat losses from different cover materials, anode assemblies and off-gas. The effect of the top heat loss on cell energy balance was discussed.

2:45 PM

Electrolysis of Aluminum in the Low Melting Electrolytes Based on Potassium Cryolite: Yuriy Zaikov¹; Andrey Khramov¹; Vadim Kovrov¹; Vasily Kryukovsky¹; Alexey Apisarov¹; *Olga Tkacheva*¹; Nikolay Shurov¹; ¹Institute of High Temperature Electrochemistry

The aluminum electrolysis in electrolytes with composition (mas.%): KF(47,37)-AlF₃(52,63) with CR=1,3 and KF(49,0)-AlF₃(49,0)-LiF(2,0) with CR=1,58 at temperature 750°C was carried out in the lab scale cell with liquid aluminum cathode. As anodes, metallic Al-Cu and Ni-Cu-Al-Fe or cermet Cu-Cu₂O or ceramic SnO₂ materials were used. The alumina concentration was kept on the 4,5 mas.% level. The region of anode current density was 0,4-0,6 A/cm². Duration of experiments reached 96 hours. Temperature, voltage and current on the cell during electrolysis, voltage at the moment of current interruption were recorded. The most steady anode materials have proved to be Cu-Al(3 or 5 mas.%) and Cu₂O-Cu(15 mas.%).

3:05 PM

Influence of CaF₂ on the Properties of the Low-Temperature Electrolyte Based on the KF-AlF₃ (CR=1,3) System: Alexander Dedyukhin¹; Alexey Apisarov¹; Alexander Redkin¹; *Olga Tkacheva*¹; Yuriy Zaikov¹; ¹Institute of High Temperature Electrochemistry

The low melting electrolyte based on the KF-AlF₃ (CR=1,3) system is very prospective for development of the new energy saving aluminum production technology. The low electrical conductivity of the KF-AlF₃ (CR=1,3) system can be increased by the LiF addition. Calcium fluoride is always brought into the electrolyte as an impurity of the alumina. The influence of CaF₂ on the properties of the low melting electrolytes at temperature below 800°C is not studied properly. Therefore electrical conductivity, melting point and calcium fluoride solubility in the KF-AlF₃ (CR=1,3) and KF-LiF-AlF₃ (CR=1,3) systems within temperature range 700-800°C have been studied. The CaF₂ solubility increases with LiF additions. The electrical conductivity dependence varies not linearly with the content of dissolved CaF₂. The melting point of the electrolytes under study rises with the calcium fluoride concentration increase.

3:25 PM

Temperature of Primary Crystallization in Part of System Na₃AlF₆-K₃AlF₆-AlF₃: Wang Jiawei¹; *Lai Yanqing*¹; Tian Zhongliang¹; Li Jie¹; Liu Yexiang¹; ¹Central South University

Methods for testing temperature of primary crystallization in aluminum electrolyte melts were summarized, a classical thermo-analysis method was chosen, an experimental setup was built and its reliability was proved detailly. To get base datum of electrolytes and provide theoretical guidance for low temperature aluminum electrolysis, temperature of primary crystallization in part of system Na₃AlF₆-K₃AlF₆-AlF₃ were tested, the ratio of K₃AlF₆ to K₃AlF₆+Na₃AlF₆ was 0-20wt.%, and AlF₃ would occupy 0-30wt.% of total electrolytes weight. Results showed that, when AlF₃ was below 20wt.%, adding of K₃AlF₆ decreased temperature of primary crystallization, but when above 20wt.%, the effect of K₃AlF₆ on it was not obvious. To the samples with ratio of K₃AlF₆ to K₃AlF₆+Na₃AlF₆ 0, 10, 20, when AlF₃ was below 18wt.%, every adding 1wt.% AlF₃ would decrease approximate 3.49, 2.33 and 1.59 respectively, but when above 18wt.%, the effect of AlF₃ on it became notable, every adding 1wt.% AlF₃ would all decrease about 10.

3:45 PM Break

3:55 PM

Electrical Conductivity of the Na₃AlF₆-K₃AlF₆-AlF₃ Melts: Huang Youguo¹; *Lai Yanqing*¹; Tian Zhongliang¹; *Li Jie*¹; Liu Yexiang¹; ¹Central South University

The electrical conductivity of Na₃AlF₆-K₃AlF₆-AlF₃ melts was studied with a Continuously Varying Cell Constant technique (CVCC). The reliability of experiment device was validated by testing the electrical conductivity of KCl solution, molten KCl, and molten cryolite. To be used as a low temperature electrolyte for inert anodes, the melts contained 0, 20, 24, and 30 wt % AlF₃ with 40 wt%K₃AlF₆ in Na₃AlF₆ + K₃AlF₆ mixture. The superheat was 20, 40, 60, and 80°C. The electrical conductivity data in the molten mixtures can be described by a simple equation of the Arrhenius type: $\ln \kappa = A + B/T$ where κ represents electrical conductivity (S·cm⁻¹), T is temperature (K), A and B are constants for the measured system.

4:15 PM

Chemical and Electrochemical Reactions in the Al-Al₂O₃-Na₂SO₄ System at 927°C: *Xiao Yan*¹; Marshall Lanyon¹; ¹CSIRO

Solubilities of a-Al₂O₃, ZrO₂, and Y₂O₃ in Na₂SO₄-based melts and aluminum interaction with molten Na₂SO₄ were studied using an equilibration technique. The Al₂O₃ solubility was determined to be 0.012 wt% in a pure Na₂SO₄ melt in air, increased with increasing Na₂O content over 0.2-4 mol% Na₂O. The ZrO₂ and Y₂O₃ solubilities in the melts were below the detection limits. An Al₂O₃ layer formed on the solidified aluminum surface after immersion in fused Na₂SO₄ in argon for 24 hours, whereas Al-Na-S mattes were not detected due to their dissolutions into molten Na₂SO₄. Cathodic reactions at platinum, gold, and aluminum cathodes in the melts were also investigated using electrolytic cells with a graphite rod or SOFC-type anode. The results indicated that both aluminum and sodium were electrochemically deposited from the α -Al₂O₃ saturated electrolytes. The possibility of using molten Na₂SO₄ as an alternative solvent for Al₂O₃ in aluminum electrowinning is discussed.

4:35 PM

Experimental Studies on Carbothermal Reduction of Andalusite Ore for Al-Si Alloy Production: *Jilai Xue*¹; Jianghua Ma¹; Zhu Jun¹; Lei Wang¹; ¹School of Metallurgical and Ecological Engineering, University of Science and Technology Beijing

There are large reserves of andalusite ore in the northwest China, which have great potential to use as raw materials for metal production. Experimental studies on carbothermal reduction of andalusite ore for Al-Si alloy production were carried out in laboratory. Selected andalusite ore containing about 50%-60% Al₂O₃ and 30%-40% SiO₂ was mixed with petroleum coke and bitumenite and briquetted under pressure. Gas emission during the carbothermal reduction process was online monitored on the smelting furnace, and the products was analysed for metal purity and solid inclusions. The effects of briquette porosity, reaction temperature and the amount of reducing agents on metal quality, recovery rate and Al/Si ratio will be described in details. The reaction mechanism involved will also be discussed.

4:55 PM

Effect of LiF on Physicochemical Properties of Molten Cryolite-Based Aluminum Electrolyte: *Hongmin Kan*¹; Zhongning Shi¹; Zhaowen Wang¹; Yungang Ban¹; Shaohua Yang¹; Xiaozhou Cao¹; Xianwei Hu¹; ¹Northeastern University

Effect of LiF on physicochemical properties of molten Cryolite-based aluminum electrolyte system was investigated. Liquidus temperature, density and electrical conductivity of melts in the Na₃AlF₆-AlF₃-Al₂O₃-CaF₂-LiF system were measured. The activation energy of conductance was obtained on the basis of the electrical conductivity data. The results showed that the liquidus temperature and the activation energy of conductance were reduced and the electrical conductivity was increased greatly by adding LiF. However, the density was increased with increasing LiF content in the acidic electrolytes. It is disadvantageous for the operation of industry cell. The effects of LiF content on physicochemical properties of molten Cryolite-based aluminum electrolyte were analyzed in theory.

5:15 PM

The Development of 85kA Three-Layer Electrolysis Cell for Refining of Aluminum: Hengchao Zhao¹; *Huimin Lu*¹; ¹Beijing University of Aeronautics and Astronautics

After studying the thermal-electric distribution, magnetic field of the 85kA three-layer electrolysis cell deeply and systematically, some influence regulations of the operating parameters to the cells have been disclosed. Based on these works, a series of 85kA three-layer electrolysis cells with the Gadeau process electrolyte system for capacity of 20,000t/y refined aluminum have been designed optimally; the operating parameters of the cells have been optimized; some improvements have been applied on the 85kA three-layer electrolysis cells in order to operate the aluminum refining course automatically. The aim of high current efficiency 98.5% and low DC power consumption 14000kWh/t has come true.

Aluminum Reduction Technology: Reduction Cell Modelling

Sponsored by: The Minerals, Metals and Materials Society, TMS Light Metals Division, TMS: Aluminum Committee

Program Organizers: Martin Iffert, Trimet Aluminium AG; Geoffrey Bearne, Rio Tinto Aluminium Tech

Wednesday PM
March 12, 2008

Room: 297
Location: Ernest Morial Convention Center

Session Chair: Dagoberto Severo, PCE Ltd.

2:00 PM

Optimization in Magnetic Modeling: *Stéphane Wan Tang Kuan*¹; Denis Jacquet²; Thierry Tomasino¹; Carlos Canutas De Wit²; ¹Alcan; ²GIPSA-Laboratory, CNRS

The stability of the electrolysis cells represents a major challenge in terms of safety and current efficiency. In order to control stability, models are used to determine the magnetic field in the cells but also in the potrooms with final outcome being an optimal cell busbar circuit. They also can be used to determine the current intensity and the position of a compensation loop if required. The method we used allows a rapid optimization of the induced magnetic field distribution at the various parts of a production line. It is based on a static and nonlinear optimization technique. The paper presents a practical case of magnetic optimization on a plant of AP30 technology integrating cost aspects. The constraints and limits of such an approach are also mentioned.

2:20 PM

Shallow Water Model for Aluminium Electrolysis Cells with Variable Top and Bottom: *Valdis Bojarevics*¹; Koulis Pericleous¹; ¹University of Greenwich

The MHD wave instability in commercial cells for electrolytic aluminium production is often described using 'shallow water' models. The model is extended for a variable height cathode bottom and anode top to account for realistic cell features. The variable depth of the two fluid layers affects the horizontal current density, turbulent horizontal velocity circulation and the resulting wave development. Instructive examples for the 500 kA demonstration cell are presented.

2:40 PM

Impact of the Vertical Potshell Deformation on the MHD Cell Stability Behavior of a 500kA Aluminum Electrolysis Cell: *Marc Dupuis*¹; Valdis Bojarevics²; Daniel Richard³; ¹GeniSim Inc; ²University of Greenwich, School of Computing and Mathematics; ³Hatch

In previous publications, it was rationalized that a large vertical potshell deformation may have a negative impact on the operations of very high amperage cells. The MHD-Valdis non-linear Magneto-Hydro-Dynamic model was therefore extended to take into account the displacement of the potshell. The MHD cell stability behavior of a 500 kA cell with a 17.3 meters long potshell was then studied.

3:00 PM

Comparison of Various Methods of Modeling the Metal-Bath Interface: *Dagoberto Severo*¹; Andre Schneider¹; Elton Pinto¹; Vanderlei Gusberti¹; Vinko Potocnik²; ¹PCE Ltd.; ²Vinko Potocnik Consultant

Correct evaluation of the stationary metal-bath interface in aluminum reduction cells is still a source of discussion and controversy. The objective of this paper is to present some calculations of the interface performed by different methods, used in software packages and to compare them with measured metal-bath interface profile in a real cell. Our comparison includes shallow layer approach and 3D multiphase methods, such as homogeneous and inhomogeneous volume of fluid (VOF). Different boundary conditions on the top of bath channels and different turbulence models are tested. Finally, a simple generic magnetic field is proposed which could be used for future software benchmarking of this problem.

3:20 PM

Modelling and Measurement of Metal Pad Velocity in a 208 Ka End-to-End Prebake Cell: *Mohamed Mahmoud*¹; Mohamed Doheim²; Abdel Fatah El-Kersh³; Nabil Kotb⁴; Mohamed Ali¹; ¹Egyptalum; ²Assiut University; ³El Taif University; ⁴El Minia University

Measurements and modeling of flow characteristics are presented for turbulent flow subjected to current-magnetic field interaction in 208 kA end to end prebaked cells. The numerical calculations of incompressible turbulent flow have been carried out by solving full time-averaged Navier-Stokes equation using finite difference method. The k-epsilon turbulence model is modified to account for near wall function. In this part, the electromagnetic force is introduced in the governing equations as source term. Velocity measurements in the metal pad were established using iron rod method. The calculated and measured velocities showed a good agreement and the model can be used to predict the velocity profiles inside the molten melt regions at different operating conditions.

3:40 PM Break

3:50 PM

Dynamics of the Gas Emission from Aluminum Electrolysis Cells: *Laszlo Kiss*; *Klára Vékony*¹; ¹Université du Québec a Chicoutimi

The evolution of gas has a strong impact on the operation of the aluminum reduction cell. The dynamics of the bubble related phenomena involves the nucleation travel and coalescence of the bubbles under the anode, and finally their escape from the bath. Generally, it is assumed that the bubbles escape freely and easily as they arrive to the upper horizontal surface of the bath. In the present paper, we analyze the case when the escape of the gas is hindered above the bath, for example by the presence of a crust layer. If the gas accumulates and forms a cushion under certain zones of the crust, its escape can provoke oscillations. This frequency is independent of the nucleation and even of the formation of big coalesced bubbles under the anode. The dynamic character of this phenomenon, which depends strongly on the geometry, will be illustrated by a simple mathematical model.

4:10 PM

Freeze Thickness in the Aluminum Electrolysis Cells: *Laszlo Kiss*¹; Véronique Dassylva-Raymond¹; ¹Université du Québec a Chicoutimi

The presence of a frozen electrolyte layer (ledge) on the sidewall is vital for the aluminum reduction cell. The thickness of the ledge is the result of the complex interaction between heat balance, amperage, bath chemistry, cell resistance, bath movement etc. In the present paper, the general tendencies like the effects of increasing the amperage, the correlation between bath-ledge heat transfer and freeze thickness are analyzed. The analysis is based on the mathematical modeling of the heat balance of an aluminum reduction pot. The tendencies extracted from the results of the numerical simulations can be cast into simple functional or graphical forms that characterize the given cell design.

4:30 PM

Application of Mathematical Methods to Optimize Aluminium Production in Pre-baked Anode Cells: *Vaycheslav Veselkov*¹; *Alex Knizhnik*²; Yuriy Bogdanov¹; Alexandr Kusakov¹; Boris Zelberg¹; ¹JSC; ²RUSAL

The OA-300 cell as well as the aluminium production technology in 300 kA cells were developed by "SibVAMI". At present studies aimed at increasing current load in the cell are performed. 330 kA amperage has been reached and a possibility of further amperage increase is studied. Mathematical modeling methods were used in order to study possibilities of current load increase and forecast results. The paper is dedicated to two of them: numerical modeling in the ANSYS system and proper estimation coefficient to make up the anode change sequence. Numerical modeling of temperature fields in the cell was performed using parametrical construction of the model. Such an approach allowed estimation of the cell efficiency at increased amperage. Estimation coefficient of current distribution irregularity in anodes is suggested as well as software allowing making up anode change sequences is described in the paper. The principle for the anode change sequence is suggested to provide the most uniform current distribution in the anodes.

4:50 PM

Two-Dimensional Model of Melt Flows and Interface Instability in Aluminum Reduction Cells: *Mehdi Kadkhodabeigi*¹; ¹Sharif University of Technology

We derive a new non-linear two dimensional model for melt flows and interface instability in aluminum reduction cells. This model is based on non-linear de St. Venant shallow water equations and contains the main features of an aluminum reduction cell. In this model we consider linear friction terms but in a new way that has not been considered in previous works. Our results are in good agreement with the results of simulation of viscous flow. This model is applicable both in determination of melt flows in molten aluminum and cryolite layers and also in finding the extreme limit for stability of interfacial waves in an aluminum reduction cell.

5:10 PM

Busbar Designing and Its Impacts on Steady Magneto-Hydrodynamic Characters of Aluminum Reduction Cells: *Wei Liu*¹; Jie Li¹; Yanqing Lai¹; Yujie Xu¹; ¹Central South University

A simulation model was built to directly couple resulted currents in inside conductive parts and the busbars into the magnetic analysis, and electromagnetic forces into the flow motion analysis. The model aided the design of the whole busbar system of a 320 kA based aluminum reduction cell involving the use of the L/S value of the resistance definition and the coefficient between the flex's resistance and that of the connecting cathodic busbar between every two flexes. The results from optimized Scheme G2 showed that this model effectively adjusted the distribution of currents in local flexes, global busbars and the distribution of voltage potential in the metal. The vertical magnetic component was found to have max/min values 33 Gauss. The flow field was investigated with the k-ε model. The max velocity of the metal was 20.1 cm/s and the averaged was 8.9 cm/s with the interface heaved about 3.0 cm.

Biological Materials Science: Mechanical Behavior of Biological Materials II

Sponsored by: The Minerals, Metals and Materials Society, TMS Structural Materials Division, TMS: Biomaterials Committee, TMS/ASM: Mechanical Behavior of Materials Committee

Program Organizers: Ryan Roeder, University of Notre Dame; Robert Ritchie, University of California; Mehmet Sarikaya, University of Washington; Lim Chwee Teck, National University of Singapore; Eduard Arzt, Max Planck Institute; Marc Meyers, University of California, San Diego

Wednesday PM
March 12, 2008

Room: 390
Location: Ernest Morial Convention Center

Session Chair: John Nychka, University of Kentucky

2:00 PM **Invited**

Effects of Cytoskeletal Dynamics on Cell Deformation and Function: *Subra Suresh*¹; Ju Li²; George Lykotraftis¹; ¹Massachusetts Institute of Technology; ²Ohio State University

All living matter such as tissues and cells differ fundamentally from traditional engineering materials in that they require the input of energy (ATP) to function. Such metabolism introduces interesting non-equilibrium effects, which fundamentally alter their mechanical behavior. A general framework for simulating cellular cytoskeletal dynamics (CD) (PNAS 104 (2007) 4937; Biophys. J. 88 (2005) 3707) has been developed so as to model the self-assembly of cytoskeleton of human red blood cells (RBC). The questions addressed include: (a) how do applied mechanical forces and ATP input influence cytoskeletal reorganization? (b) how does such cytoskeletal reorganization facilitate cell shape changes and motility through small blood vessels? and (c) how does the cytoskeleton recover its original shape upon release of the mechanical or chemical energy? The CD simulation results resolve some long-standing questions regarding RBC equilibrium shape and deformation response.

2:30 PM

Surface Phase Separation and Flow in Vesicle Bio-Membranes: *Shuwang Li*¹; *John Lowengrub*¹; ¹University of California, Irvine

Recent experiments of giant unilamellar vesicles (GUV) reveal that lipid bilayer membranes exhibit rich shape transition behaviors, such as bud formation. Physical processes like phase separation and bending are usually coupled with morphology changes in membranes. Because of the presence of high-order nonlinear terms in these physical processes, it is highly challenging to simulate phase decomposition and motion of phase boundaries on a moving surface. In this talk, we present a mathematical model describing the nonlinear coupling among the flow, vesicle morphology and the evolution of the surface phases. Our numerical method combines the immersed interface method to solve the flow equations and the Laplace-Young jump conditions, the level-set method to represent and evolve the surface, and a non-stiff Eulerian algorithm to update the mass concentration on the surface. Numerical results show detailed dynamics of phase separation and shape transformation (e.g. bud formation).

2:50 PM

Coupled Composition-Deformation Phase-Field Simulation of Multicomponent Lipid Membranes: *Chloe Funkhouser*¹; William Jaquind¹; Francisco Solis²; Katsuyo Thornton¹; ¹University of Michigan; ²Arizona State University

We investigate the morphological evolution of binary lipid membranes via a phase-field simulation. We consider membranes in which the local composition and shape are coupled through composition-dependent spontaneous curvature. The evolution of the composition field is described by a Cahn-Hilliard-type equation, while shape changes are described by relaxation dynamics. Our method explicitly treats the nonlinear form of the geometrical scalars, tensors, and differential operators associated with the shape of the membrane. We study morphological evolution and stability of lipid membranes initialized in a variety of compositional and geometric configurations. Nearly planar membranes and spherical vesicles are considered. We discuss the effects of spontaneous curvature, bending rigidity, and line tension on the dynamics and final configurations. For the nearly planar case, microstructures are characterized quantitatively using average domain size, shape anisotropy, and other statistical measurements.

3:10 PM

On Affinity in the Deformation of Biopolymer Networks: *Erik Van der Giessen*¹; Patrick Onck¹; ¹University of Groningen

Networks of (usually cross-linked) biopolymers play a key role in various biological functions, in particular in mechanotransduction. Well-known examples are the cytoskeleton and collagen. The peculiar strain stiffening exhibited by many of these materials has been the topic of intense investigations. The current explanations can be classified in two groups. The first attributes strain stiffening to the stiffening of individual filaments caused by entropic effects. The second explanation charges the non-affine distortion of the network, allowing for a transition from a soft, bending-dominated response to one dominated by stretching of the filaments. By contrast, the entropic stiffening theory available to date presumes affinity of the network distortion. Affinity or not has thus become a critical issue. Theoretical and simulation considerations, first in two and more recently in three dimensions, are slowly getting supplemented with experimental observations. This paper aims at presenting a comprehensive, state-of-the-art view on affinity.

3:30 PM **Break**

3:40 PM

Evaluation of the Elastic Properties of Human Corneas via Nanoindentation: *Rut Rivera*¹; *David Bahr*²; Julie Last³; Christopher Murphy³; ¹University of Puerto Rico at Humacao; ²Washington State University; ³University of Wisconsin

The assessment of the mechanical properties of the cornea requires the ability to probe spatially unique regions of the tissue, both laterally and through the thickness. Nanoindentation allows for these properties to be measured, but brings specific challenges due to the material's compliance and environmental requirements. Utilizing a nanoscale dynamic mechanical analysis method we have carried out indentations in human corneas and hydrogel based contact lenses in a phosphate buffer solution. For the cornea the target layers of interest were the basement membrane and stroma. The elastic response of these surfaces for depths between 50 and 5000 nm is on the order of 10-1 MPa as a function of depth, with a viscoelastic response that appears to be relatively constant

with depth. Challenges related to quantification of properties are discussed, particularly issues of sensitivity to surface detection in solution with a material that exhibits significant adhesion to mechanical probes.

4:00 PM

Evidence of Van Der Waals Adhesion Found in Abalone Foot: *Albert Lin*¹; Ralf Brunner¹; Po-Yu Chen¹; Frank Talke¹; Marc Meyers¹; ¹University of California, San Diego

The attachment of abalone to surfaces was investigated and the stress for separation was measured and determined to be 0.15 MPa. The surface of the abalone foot in contact with surfaces was characterized and is found to be composed of fibers (setae) terminated by spatulae with a diameter of 200 nm in a similar fashion to gekko feet. The areal density of the spatulae is $1.9 \times 106/\text{mm}^2$. Atomic force microscopy measurements show that the spatulae show bonding to surfaces and that the bonding force per spatula is 3 μN . This is characteristic of van der Waals forces in a similar way to gekko feet. This corresponds to a theoretical attachment stress of 0.18 MPa, in accordance with the experimental measurements. Other effects, such as capillarity and suction are also being investigated. Research funded by the National Science Foundation Grant DMR 0510138.

4:20 PM

Mechanics of Permanent Biological Attachment Systems: *Tina Steinbrecher*¹; Deane Harder²; Thomas Speck²; Oliver Kraft¹; Ruth Schwaiger¹; ¹Forschungszentrum Karlsruhe; ²University of Freiburg

Climbing plants have developed a variety of mechanical strategies to permanently attach to supporting structures thereby achieving vertical growth. Boston ivy (*Parthenocissus tricuspidata*) has specialized attachment pads that exhibit excellent mechanical performance. However, they have not yet been investigated systematically with respect to interface, microstructure or mechanical behavior. In this study, the mechanical properties of attachment pads on various substrates as well as the interface were investigated. Boston ivy was found to attach to many different substrates, e.g. to very smooth inorganic as well as to rough organic substrates. In contact, the attachment structures lignify and stay attached even under extreme environmental conditions. Our tensile tests show that a pad withstands stresses up to 4 MPa; failure never occurred at the interface. Based on microscopical investigations, which indicate an almost perfect plant/substrate form closure, the strategy of the plant to achieve this strong attachment is discussed.

4:40 PM

Growth and Mechanical Behavior of Hydroxyl-Carbonate Apatite Layer on 45S5 Bioactive Glass: *Ding Li*¹; Fuqian Yang¹; John Nychka²; ¹University of Kentucky; ²University of Alberta

Bioactive glasses have been known for applications in bone replacement implants. The formation of hydroxyl-carbonate apatite (HCA) layer and the mechanical behavior of the HCA layer potentially determine the bioactive response of bioglasses in bone implants. In this work, the growth behavior of the HCA layer over 45S5 bioglass is evaluated in a simulated body fluid at a temperature of 37°C. After 24 hours immersion, the HCA layer fully covers the surface of the 45S5 bioglass. The thickness of the HCA layer increases with the immersion time, following a parabolic relation. The localized mechanical behavior of the HCA layers is studied by using the indentation technique. The effect of the HCA layer thickness on the mechanical response is probed.

5:00 PM

Microstructure and Mechanical Behavior of Biocompatible TiO₂/Ti: *Grant Crawford*¹; Nikhilesh Chawla¹; Jack Houston²; Jan Ringnalda³; Tony Carpenter³; ¹Arizona State University; ²Sandia National Laboratory; ³FEI Company

Titanium oxide coatings have been shown to exhibit desirable properties as biocompatible coatings. In this talk we report on mechanical properties and deformation behavior of TiO₂ nanotubes grown on pure titanium substrates through anodic oxidation. By adjusting the processing conditions, the coating thickness, tube diameter and tube wall thickness were varied. Characterization of the as-processed coatings was conducted using scanning electron microscopy, Focused Ion Beam milling, and transmission electron microscopy. Nanoindentation, using an Interfacial Force Microscope, was employed to accurately probe the Young's modulus of the nanotubes. This technique was also used to study the inelastic deformation behavior of the nanotubes. The relationship between the

nanostructure of the tubes and the mechanical response will be discussed.

5:20 PM

The Design of Material and Mechanical Property of Stabilization Systems and Special Medical Tools for Alloplastic of Hip Joint: *Szota Michal*¹; Malgorzata Lubas¹; Jozef Jasinski¹; Bogdan Stodolnik²; ¹Czestochowa Technical University; ²ZWM of Bialysto University of Technology in Suwalki

There are different reasons for which the results of hip alloplasty become worse with time. Aseptic slackening of endoprosthesis is the main reason affecting a growth in dysfunction of the limb. In such cases the most effective method of repair the bone defects occurring in the vicinity of endoprosthesis is an application both tightly stuffed allogenic bone grafts and metallic stabilizers. Secondary hip arthroplasty needs the massive and frozen bone grafts and metal stabilizers in the form of nets and baskets, which strengthen and fasten the bone defects. Stabilizers protect the graft against excessive overload occurring in its surrounding, especially during heal process. In order to complete the bone defects a prototype batch of: -the bridging baskets in 12 type dimensions, -strengthening baskets in 2 diameters, -strengthening meshes shaping by bending and stamping.

5:40 PM

Microstructure and Property of Titanium Using for Implants: *Szota Michal*¹; Jozef Jasinski¹; Bogdan Stodolnik²; ¹Czestochowa Technical University; ²ZWM Bialystok University of Technology in Suwalki

Oxidation is one of the most employed methods to improve titanium and its alloys properties especially due to medical application. This process like most of the thermo-chemical treatment processes substantially influences on the characteristic of surface layers and the same on its mechanical and useful properties. Oxide coatings produced during titanium oxidation were examined due to their composition identification. Titanium was oxidized in fluidized bed in temperature range between 500-700°C. Microstructures of titanium with a visible oxide coating on its surface after thermo-chemical treatment and changes of grain size in core of titanium samples are described. Moreover X-ray phase analysis of obtained oxides coatings was made as well as microhardness measurements of titanium surface layers after oxidation process. Finally, the surfaces of titanium after oxidation in fluidized bed were measured by Auger electron spectroscopy.

Bulk Metallic Glasses V: Structures and Modeling II

Sponsored by: The Minerals, Metals and Materials Society, TMS Structural Materials Division, TMS/ASM: Mechanical Behavior of Materials Committee

Program Organizers: Peter K. Liaw, University of Tennessee; Wenhui Jiang, University of Tennessee; Guojiang Fan, University of Tennessee; Hahn Choo, University of Tennessee; Yanfei Gao, University of Tennessee

Wednesday PM

March 12, 2008

Room: 393

Location: Ernest Morial Convention Center

Session Chairs: Katharine Flores, Ohio State University; Daniel Miracle, US Air Force

2:00 PM Invited

Effect of Liquid Fragility on Glass Forming Ability of Metallic Alloys: *Oleg Senkov*¹; ¹UES Inc

Analysis of the fragile behavior of glass-forming liquid in the temperature range between the liquidus T_l and glass transition T_g temperatures allowed us to identify unique correlation between the critical cooling rate for glass formation R_c , liquid fragility index m and reduced glass transition temperature $T_{rg} = T_g/T_l$. Correspondingly, a new GFA parameter F_1 , which is proportional to $-\log(R_c)$ and is a function of T_{rg} and m was proposed. F_1 increases with an increase in T_{rg} and a decrease in m and varies from ~ 0 in the case of the extremely fragile liquid (e.g. pure metals) to ~ 0.8 in the case of the extremely strong liquid (e.g. SiO₂). Validity and universality of this GFA parameter F_1 was experimentally verified for a number of bulk metallic and non-metallic glasses. On the other hand, when used separately, T_{rg} and m were shown to be able to predict GFA only in special cases.

2:20 PM Invited

New Generation of Structural Materials: Solid Solution Alloys with High Entropy of Mixing and Bulk Metallic Glasses: *Zhang Yong*¹; ¹University of Science and Technology Beijing

According to Gibbs phase rule, a great number of intermediate phases will form for the multi-principal components materials (also high-entropy alloys, HEAs), which are located at the center of the phase diagram, and solid solution phase generally forms at the terminal side of the phase diagram. However, it is recently reported that some HEAs form simple solid solution rather than many intermediate phases. In this paper, phase-formation rule of HEAs was obtained in terms of the atomic-size factor (δ) and enthalpy of mixing (ΔH_{mix}) by summarizing the literature data reported, and its validity was also verified by our experimental results. The mechanical properties of the HEAs were compared with those of the bulk metallic glasses.

2:40 PM Invited

The Influence of Shear on the Viscosity and Crystallization of Bulk Metallic Glass Forming Liquids: *Ralf Busch*¹; ¹Saarland University

The shear rate and temperature dependence of the viscosity and the onset of crystallization in several bulk metallic glass (BMG) forming liquid has been measured in the liquid and undercooled liquid state. The alloys show pronounced shear thinning especially close to the liquidus temperature. With increasing temperature this behavior gets less pronounced and in certain alloys a transition to a Newtonian liquid is observed, which is associated with the change from strong to fragile liquid behavior. In general, we find that the shear rate effects are more pronounced in strong liquids than in fragile liquids. Shearing the liquid accelerates the crystallization process and shifts the time-temperature transformation diagrams to shorter times. We discuss the influence of shearing not only on the kinetics but also on the thermodynamic driving force that leads to faster crystallization.

3:00 PM Invited

Structure and Phase Transformation in Metallic Glasses: *Xun-li Wang*¹; Alexandru Stoica²; Dong Ma¹; Matthew Kramer²; James Richardson³; Chain Liu¹; Michael Miller¹; ¹Oak Ridge National Laboratory; ²Iowa State University; ³Argonne National Laboratory

Bulk metallic glasses were discovered more than 20 years ago. Despite extensive research efforts since then, mostly experimental, the structure of metallic glasses is still not well understood. In this talk, we describe some recent neutron and synchrotron diffraction experiments and the insights thus gained on the local and medium-range ordering in these glassy alloys. The structural evolutions at local and nano scales are studied by in-situ scattering experiments during devitrification. The experimental results are correlated with analysis by atomic probe tomography. This research was supported by Office of Basic Energy Sciences, U.S. Department of Energy under Contract DE-AC05-00OR22725 with UT-Battelle, LLC. The work at Ames Laboratory was supported by the U.S. Department of Energy through Iowa State University under contract No. W-7405-ENG-82. Work at Argonne National Laboratory was supported by U.S. Department of Energy under Contract No. W-31-109-Eng-38.

3:20 PM

Characterization of Glass and Nanocrystalline Composite Structure in Highly Driven Marginal Glass Forming Alloys: *Eren Kalay*¹; Scott Chumbley¹; Iver Anderson¹; ¹Ames Laboratory/Iowa State University

Al-Rare Earth (RE) based alloys are important marginal glass forming alloys, where glass formation is often accompanied by the presence of nanocrystals during solidification. Among these alloys, the Al-Sm system has attracted interest due to its wide glass formation range. Thus, Al(100-x)Smx (x=8,10,12, and 14) binary alloys were produced using Cu-block single-roller melt spinning. The as-quenched phase was studied by high resolution electron microscopy (HRTEM) in combination with energy loss (EELS) and energy dispersive spectroscopy (EDS) and by x-ray diffractometry (XRD). The structure of the as-quenched nanocrystalline phase is sensitive to initial composition of liquid and has a typical length scale of 5 nm. The appearance of pre-peaks on XRD diffraction patterns and low calculated activation energies for the decomposition of amorphous product phases at different compositions indicate some local ordering on quenching.

3:35 PM Invited

Amorphous Structure with Inhomogeneity for Enhancement of Plasticity: *Do Hyang Kim*¹; Hye Jung Chang¹; Eun Soo Park²; Won Tae Kim³; ¹Yonsei University, Department of Metallurgical Engineering; ²Harvard University, School of Engineering and Applied Sciences; ³Chongju University, Division of Applied Science

Design of amorphous structure with inhomogeneity, which includes inhomogeneous distribution of chemical bonding, clustering and free volume is suggested as one of the possible ways for enhancement of plasticity in monolithic metallic glasses. In the present study, the possible routes and mechanisms for the enhancement of plasticity in monolithic glass alloys will be presented. Ti-Zr-Ci-Ni-Be and Zr-Ti-Cu-Ni-Nb-Al metallic glass alloys exhibit enhanced compressive plasticity due to the presence of quenched-in icosahedral nuclei in as-cast state. While Ni-Nb and Cu-Zr based alloys exhibit enhanced plasticity with the addition of elements having positive heat of mixing with constituent elements. The detailed structural analysis implies that the degree of preferential bonding increases with increasing the difference in the heat of mixing between the elements and with increasing the amount of additional element. The inhomogeneous amorphous structure might induce more sites for initiation of shear bands and finally can distribute the localized stress.

3:55 PM Break

4:00 PM Invited

Characterizations of Mechanically Alloyed Ti-Based Bulk Metallic Glass Composites Containing Carbon Nanotube: *Chih-Feng Hsu*¹; Pee-Yew Lee¹; ¹National Taiwan Ocean University

This study explored the feasibility of preparing Ti50Cu28Ni15Sn7 bulk metallic glass composite by powder metallurgy route. The CNT / Ti50Cu28Ni15Sn7 metallic glass composite powders can be formed by mechanical alloying process. The DSC result shows that the thermal stability of the Ti50Cu28Ni15Sn7 amorphous matrix is affected by the presence of the CNT particles. The bulk metallic glass composite was successfully prepared by vacuum hot pressing the as-milled CNT / Ti50Cu28Ni15Sn7 metallic glass composite powders. A significant hardness and fracture strength increase with the CNT additions was observed for the consolidated composite compacts. The compressive fracture strength and elastic strain of the composites reaches 1937 MPa and 13 %, respectively, for the 12 vol. % CNT specimen. The effects of the CNT addition on the thermal stability and mechanical property of CNT/Ti50Cu28Ni15Sn7 bulk metallic glass composites were discussed.

4:20 PM

Neutron Diffraction Studies of Zr-Cu Metallic Glasses: *Dong Ma*¹; Alexandru Stoica¹; Xun-li Wang¹; ¹Oak Ridge National Laboratory

Recently we reported an observation of negligibly small volume of mixing in the formation of bulk metallic glasses (BMGs).¹ In particular, as the basis of most technologically usefully BMGs, binary Zr-Cu glasses exhibit an ideal-mixing characteristic by following Vegard's law in terms of atomic volume. Here we present a neutron diffraction study to show a close correlation between local structural configuration and atomic volume in Zr-Cu glasses. Our study offers a new perspective on the disordered structure in metallic glasses. This research was supported by Division of Materials Science and Engineering, U.S. Department of Energy under Contract No. DE-AC05-00OR22725 with UT-Battelle. ¹D. Ma, A.D. Stoica, and X.-L. Wang, "Volume conservation in bulk metallic glasses", Applied Physics Letter, 91(2007)021905.

4:35 PM

A Simple Model to Predict the Temperature Dependence of Elastic Moduli of Bulk Metallic Glasses: *Zhiying Zhang*¹; Veerle Keppens¹; Takeshi Egami¹; ¹University of Tennessee

In the past few years, significant research efforts have been devoted to the study of the elastic moduli of bulk metallic glasses. These studies are partially triggered by the reported correlation between the energy of fracture and the Poisson ratio for bulk metallic glasses, with brittle glasses displaying a low Poisson ratio. However, reliable measurements as a function of temperature on high-quality materials are often time-consuming. We report a simple model to predict the temperature dependence of elastic moduli of bulk metallic glasses from room temperature measurements, using the Varshni Equation and the basic assumption that between absolute zero and the melting point, the shear and

bulk moduli change resp. by 45% and 22%. This model has been tested using experimental data obtained on a large variety of bulk metallic glasses, and the predicted values are found to be in very good agreement with the experimental results.

4:50 PM

Ni and Cu Free Vitreloy: Aaron Wiest¹; Gang Duan¹; Annellen Kahl¹; Joseph Schramm¹; Landon Wiest²; Andrew Peck³; Georg Kaltenboeck¹; Marios Demetriou¹; William Johnson¹; ¹Caltech; ²Brigham Young University; ³Pasadena City College

Investigation of the ZrTiBe system revealed three regions of interest. One region contains bulk glass forming alloys having critical casting thicknesses as high as 6mm and densities as low as titanium. Another region forms in-situ beta phase composites that exhibit moderate ductility. The third region contains alloys exhibiting large supercooled liquid regions and eutectic crystallization. We will show that partial substitution of Be in a base ternary glass with various late transition metals (excluding Ni and Cu) yields a glass with properties drastically improved over the ternary base alloy. This suggests that Vitreloy alloys derive their properties from their ternary counterparts. Using our ternary map as an alloy development tool, Ni and Cu free compositions with casting thicknesses in excess of 1cm, yield strengths > 1.7GPa, $\Delta T=150C$, and compressive ductility in excess of 2% were found.

5:05 PM

Structural Evolution and Phase Analysis of Bulk Amorphous $Zr_{56.6}Cu_{17.3}Ni_{12.5}Al_{9.6}Ti_4$ Alloy: Dawei Xing¹; Jun Shen¹; Jianfei Sun¹; Gang Wang¹; Yulai Gao¹; Demin Chen¹; Peter K. Liaw²; ¹Harbin Institute of Technology, School of Materials Science and Engineering; ²University of Tennessee

The structural evolution of bulk amorphous $Zr_{56.6}Cu_{17.3}Ni_{12.5}Al_{9.6}Ti_4$ alloy in a as-cast wedge ingot was studied by OM, SEM, and TEM to clarify the competing relationship between the crystalline phases and amorphous phase during cooling. It was found that there were three clear zones; amorphous, partially-crystallized, and crystallized areas, from the thin to thick ends of the wedge ingot. These three zones were dominated by the amorphous, the intermetallic phase $CuZr_2+NiZr_2$, $Cu_{10}Zr_7+Zr_3Al$, and Zr_2Ni , respectively. The precipitation of these phases was dependent on the cooling rate. The observations were discussed in terms of a schematic Time Temperature Transition (TTT) curve of $Zr_{56.6}Cu_{17.3}Ni_{12.5}Al_{9.6}Ti_4$. This finding may give a direct evidence to that Zr-Cu has a larger glass-forming tendency than that of Zr-Ni, and GFA may be improved by restraining Zr_2Ni phases through removing all the Ni elements in a Zr-based multi-component alloy.

5:20 PM

A New Criterion for Predicting the Onset of Glass-Like Temperature Dependent Behavior in Simple Liquids: Rachel Aga¹; James Morris¹; Valentin Levashov²; Takeshi Egami²; ¹Oak Ridge National Laboratory; ²University of Tennessee

We present simulations on the temperature-dependence of the shear viscosity and diffusion coefficient of a monatomic glass-forming liquid. Changes in temperature-dependent properties include deviation from Arrhenius behavior, and temperature-dependence of the effective diameter from the Stokes-Einstein relation. We introduce a definition for the term "liquid-like" based on experimental viscosities from various atomic liquids at their melting temperatures. The above changes in dynamical behavior occur when the system has departed the liquid-like dynamical regime, and is now exhibiting glass-like temperature-dependent behavior. In the glass-like regime, there is an increasing spread in the values of time correlations for shear stress components. In contrast, the spread is constant when the system is liquid-like. The development of a double-peaked $g(r)$ is strongly correlated with the transition from liquid-like to glass-like temperature-dependent dynamics. This research has been sponsored by the Division of Materials Sciences and Engineering, Office of Basic Energy Sciences, US Department of Energy under Contract DE-AC05-00OR-22725 with UT-Battelle.

5:35 PM

A Thermodynamic Description of the Metallic Glass State Using the Central Atoms Model: Eric Lass¹; Gary Shiflet¹; Aiwu Zhu¹; Joseph Poon¹; ¹University of Virginia

The thermodynamic properties of the metastable amorphous phase in metallic glass systems have been studied using the central atoms model. By consideration of the shell or "cage" of nearest neighbors (NN) surrounding a given atom, an understanding of short range order, its temperature dependence, and the effects on the thermodynamics of the system are obtained. Certain NN combinations are more stable relative to others, depending on bulk composition, atomic size, chemical heats of mixing between elements, etc. The resulting expressions for the thermodynamic functions are dependent on the probability distribution of the possible NN cages. This model allows for a more accurate description of the supercooled liquid state by the introduction of such irregularities as a variable number of NN between atoms of like and unlike species. It is shown the even in a simple binary system the local structure around the different species varies dramatically.

5:50 PM

Diffusion Mechanism in Metallic Glasses from Bond Defects Perspective: Aiwu Zhu¹; Gary Shiflet¹; S. Poon¹; ¹University of Virginia

Diffusion in metallic glasses and deeply undercooled liquids is analyzed from the perspective of structural defects induced by the bond deficiencies (BD). The elementary process is considered to be thermally activated hopping of diffusing atoms between the first-neighbor and the second neighbor positions at the BD defects that requires cooperative movement of multiple adjacent atoms. The activation energy Q will then depend on the bond strengths, size of diffusing atoms, the elastic constant of the matrix and the effective number of matrix atoms that are involved. Application to the Zr-Ni and Ti-Ni systems shows the atomic size effect of diffusing atoms agrees with experimental measurements. Most of the other observations including the effects of isotopes, of pressure and the shape slope of the Q versus pre-exponential factor can also be explained accordingly.

Cast Shop Technology: Casting Processes and Quality Analysis

Sponsored by: The Minerals, Metals and Materials Society, TMS Light Metals Division, TMS: Aluminum Committee

Program Organizers: Hussain AlAli, GM Casthouse and Engineering Services, Aluminium Bahrain Company (ALBA); David DeYoung, Alcoa Inc

Wednesday PM

March 12, 2008

Room: 295

Location: Ernest Morial Convention Center

Session Chair: Neil Hall, BHPBilliton - Bayside Aluminium

2:00 PM

A Comparison of Various Technologies in Mold Metal Level Sensing Applications: Mike Anderson¹; ¹Wagstaff, Inc.

This paper offers a comparison of various technologies utilized in open top direct chill aluminum casting molten metal level sensor applications. The strengths and weaknesses of each technology along with their effects on the mold metal level control process are discussed.

2:20 PM

Characterization of the Microstructure of the 8006 Alloy Sheets and Foils: Carmen Stanica¹; Petru Moldovan²; Gheorghe Dobra¹; Cristian Stanescu¹; ¹ALRO S A; ²Polytechnic University of Bucharest

The paper presents the evolution of the 8006 alloy microstructure in the plastic deformation process; the paper's purpose is to set the causes for the defective conditions of the different size sheets and foils. The experiments put in evidence the defective conditions caused by the presence of iron, manganese and silicon compounds in the 8006 alloy structure, as well as the conditions occurred in the rolling process. The slab microstructures before and after homogenization were compared to the microstructures of foils and sheets obtained by plastic deformation. The techniques of optical quantitative microscopy, electronic

microscopy SEM/EDS and electronic microscopy at the JXA micro analyzer to highlighting the process and material factors responsible for the presented defective conditions.

2:40 PM

Determination of TiB₂ Inclusions in Al-Billets by Single Spark Emission Spectrometry: *Marcel Rosefort¹; Frank Urbanek¹; Joerg Niederstrasser²; Hubert Koch¹; ¹Trimet Aluminum AG; ²OBLF Gesellschaft fuer Elektronik- und Feinwerktechnik mbH*

Aluminum safety parts and aluminum bright shining components, especially for automotive applications, have to be nearly free from inclusions due to their influences on mechanical properties and surface quality, respectively. On the other hand grain refinement is essential. For this purpose Titanium/Boron based master alloys are used, which can lead to TiB₂ agglomerations in the billet. The usual method for quality control is microscopic examination of the specimen. The growing demand for high quality billets has created a need for faster and cost-efficient methods of quality control. Single spark spectrometry promises fast determination of inclusions, especially of TiB₂-particals or agglomerations. Statistical evaluation of single spark spectrometry data allows the determination of distribution and size of TiB₂-agglomerations. This paper covers the application of single spark emission spectrometry to Al-billets, the graphical and statistical analysis and an outlook on the quality control using this new technique.

3:00 PM

Mastering the Strip Geometrical Tolerances with the Twin-Roll Continuous Strip-Casting Technology: *Frederic Basson¹; Marc Bosch¹; Philippe Charlier¹; ¹Novelis PAE*

From Pechiney to Novelis, and today with Hindalco in the Aditya Birla Group, Novelis PAE has been a major actor in developing twin-roll continuous strip-casting technology for more than five decades. In the recent years, driven by the higher speed capabilities of the latest generation rolling mills, customer requirements and technological developments have both been focused on tightening the strip geometrical tolerances, in order to improve the consistency of the strip cross profile and longitudinal gauge variations. To meet these demanding requirements, the highly proven Jumbo 3CM® continuous casting technology includes advanced technological features addressing each casting process parameter impacting the solidification and thus the strip geometry: metal feeding system with accurate metal level regulation and temperature control, homogeneous roll water cooling system, highly reactive hydraulic gap control, improved shell coating control, together with an in-line cross and longitudinal strip profile monitoring.

3:20 PM

On the Formation of Interdendritic Cracking Phenomena in Direct Chill Casting of Aluminum Alloy Slabs: *Mostafa El-Bealy¹; ¹Ain Shams University*

The formation mechanism of interdendritic cracking phenomena of continuously cast aluminum alloy slabs has been studied by metallographically examining slab sample and by performing a set of mathematical analyses of heat flow, solidification and interdendritic strain phenomena. The model also combines an interdendritic cracking model with concept of the effect of different dendritic solidification behaviors on Bealy's interdendritic cracking susceptibility function "BICSF" and elementary interdendritic area "EIA". The study has revealed that the interdendritic cracking phenomena can be classified principally into macro and micro cracks. The type of interdendritic crack depends mainly on the degree and pattern of macrosegregation. The analysis of interdendritic cracking by mathematical modeling indicates that Bealy's interdendritic cracking susceptibility function (BICSF) measures qualitatively the susceptibility of interdendritic micro or macrocracking during the interdendritic coherent region in the mushy zone. However, the elementary interdendritic area EIA is to simulate qualitatively crack initiation and propagation.

3:40 PM Break

3:50 PM

Wagstaff Bleedout Detection System: *Mike Anderson¹; ¹Wagstaff, Inc.*

Bleedouts during continuous casting of extrusion billets are undesirable. Typically damage to equipment and large amounts of metal in the casting pit can result. In extreme cases an explosion can occur. To prevent this, a plug is inserted

into the mold as soon as the detection of the bleedout occurs to stop the flow of molten metal. Due to the number of strands on a typical table it can be difficult to detect the location of the bleedout until a considerable amount of molten metal has entered the pit. A bleedout detection system has been developed that quickly detects the bleedout and alerts the operator to its location. Testing of the system has been completed and will be presented.

4:10 PM

Wrinkling Phenomena to Explain Vertical Fold Defects in DC-Cast Al-Mg4.5 Sheet Ingots: *J. Lee Davis¹; Patricio Mendez²; ¹Novelis; ²Colorado School of Mines*

Some Al-Mg4.5 aluminum ingots cast by the direct chill method are subject to surface defects which appear to originate on the molten surface while others are not. Defects – commonly called “vertical folds” – are frozen into the solid ingot and must be removed prior to rolling. Vertical folds are found on top of the molten ingot surface where areas of thin oxide skin are (1) bounded by physical constraints and (2) stretched. The mechanism of wrinkling is suggested for the formation of vertical folds. Wrinkling behavior is described by physical and mathematical expressions for an elastic sheet in tension. The frequency and amplitude of vertical folds in DC-cast aluminum is found to obey wrinkling laws based on the thickness, length, Young's modulus, and Poisson's ratio of the thin, elastic oxide sheet.

4:30 PM

Hydrogen Measurement Practices in Liquid Aluminium at Low Hydrogen Levels: *Mark Badowski¹; Werner Droste¹; ¹Hydro Aluminium Deutschland GmbH*

Today, the most common measurement systems for hydrogen content in aluminium melt use the principal of a carrier gas and heat flux sensitivity (thermal conductivity cell). Current publications indicate, that the ambient humidity might influence hydrogen readings due to diffusion of water into the measurement loop. New systems – using the principal of electro-motoric-force-measurements between different hydrogen levels – enter the market. A comparison of these newer and older ways to determine hydrogen levels in liquid aluminium in a low hydrogen regime will be presented.

4:50 PM

Investigation of Hydrogen Measurement Technique for Molten Aluminum: *Juan Moreno Exebio¹; Daniel Larouche¹; Dany Paquin²; Jasmin Proulx²; Claude Dupuis³; ¹Laval University; ²ABB; ³Alcan International Limited*

On-line measurement of hydrogen content in molten aluminum alloys based on the Sievert's law is the most widely used method in the aluminium industry. For more than 15 years, the AISCAN analyzer has been recognized as the industry reference for hydrogen measurement because of its good reproducibility and its high robustness. It is well known that ambient conditions surrounding the molten aluminium are the main factors affecting the concentration of dissolved hydrogen. This paper presents the results of a detailed investigation of the key components and operating parameters of the AISCAN technique on the measurement of dissolved hydrogen in molten aluminium alloys. Impact of ambient humidity in the vicinity of the measurement circuit is highlighted. Improvement to the current technology is proposed.

5:10 PM

Ab-Initio Predictions of Interfacial Heat Flows during the High Speed Thin Strip Casting of Metals and Alloys: *Jinsoo Kim¹; Donghui Li¹; Mihaiela Isac¹; Roderick Guthrie¹; ¹McGill University, McGill Metals Processing Centre*

The purpose of this study was to develop ab-initio mathematical and computational models aimed at predicting instantaneous heat fluxes when a liquid metal or alloy contacts a colder substrate. Semi-analytical and fully computational models have been developed to determine whether measured instantaneous heat fluxes associated with the strip casting of aluminum and magnesium alloys on copper, steel, and variously plasma-coated steel substrates, can be inferred from first principles. It is shown that the thermal properties of the melt and substrate are critical in determining the peak heat fluxes achieved during metal/mould contact, a cold copper substrate being more effective than steel. However, the net amount of heat extracted tends to favor a steel substrate. The surface texture of a belt and presence of gas, and or liquid/solid films among the “valleys” between the peaks where perfect thermal contact is assumed, is also shown to be of great significance. The way in which the liquid metal first contacts

the substrate (i.e. the liquid metal delivery system), is similarly important in determining the shapes of the instantaneous heat flux curves, as are the rates at which the metal strip decouples from the substrate. The computational models developed, allows various scenarios to be effectively studied, and experimental curves matched with “predicted” curves based on reasonable assumptions. The use of such models can help guide operators of near-net shape casting machines in their quest to effectively control interfacial heat fluxes during the formation of sheet products.

5:30 PM Panel Discussion

Characterization of Minerals, Metals, and Materials: Characterization of Microstructure and Properties of Materials IV

Sponsored by: The Minerals, Metals and Materials Society, TMS Extraction and Processing Division, TMS: Materials Characterization Committee

Program Organizers: Jian Li, Natural Resources Canada; Toru Okabe, University of Tokyo; Ann Hagni, Intellection Corporation

Wednesday PM
March 12, 2008

Room: 284
Location: Ernest Morial Convention Center

Session Chairs: Toru Okabe, University of Tokyo; Yoshitaro Nose, Kyoto University

2:00 PM

Formation of Silicon Carbide Crystals on Porous Silicon Substrate by Reaction Diffusion at Low Temperatures: Yoshitaro Nose¹; Kohei Hosokawa¹; Tetsuya Uda¹; Yasuhiro Awakura¹; ¹Kyoto University

We tried the formation of silicon carbide crystals by reaction diffusion of silicon and carbon at low temperatures. In general, silicon carbide crystals form on a silicon substrate by chemical vapor deposition at temperatures above 1200°C since atomic diffusion is very slow in this system; however, the formation at low temperatures is desirable. We thus considered utilizing porous silicon substrate, which has many pores of the nano-micron size on the surface, to promote carbon diffusion. Porous silicon substrates were fabricated by electrochemical method and its porosity and pore size were controlled by the kind of bath, current density and time. When the substrate was annealed at 1000°C for 10h after carbon deposited, the formation of silicon carbide crystals was observed on the porous silicon by Raman spectroscopy, while it was not observed on the single crystal substrate.

2:20 PM

Effects of Microalloying on an Innovative Quenched and Tempered Plastic Mold Steel: Donato Firrao¹; Paolo Matteis¹; Pasquale Russo Spena¹; Giovanni Mortarino¹; Maurizio Chiarbonello¹; Maria Pina²; Maria Ienco²; Matteo Fabbreschi²; Giuseppe Silva³; Barbara Rivolta³; Riccardo Gerosa³; Maria Tata⁴; Severino Missori⁴; Roberto Montanari⁴; Andrea Ghidini⁵; ¹Politecnico di Torino; ²Università di Genova; ³Politecnico di Milano; ⁴Università di Roma Tor Vergata; ⁵Lucchini Sidermeccanica

Molds for large plastic automotive components are machined from pre-hardened steel blooms. Due to the size, the heat treatment of the commonly employed ISO 1.2738 steel yields mixed microstructures (varying from surface to core) and low toughness. An alternative steel is examined, which is microalloyed (noticeably with Nb, Zr and B) with the aim of limiting the austenitic grain growth, increasing the hardenability, and ultimately improving the strength and toughness combination. Although the hardenability calculated without the microalloying elements would be similar to the 1.2738 steel, perlite was avoided at core of a large quenched and tempered bloom (1x1.2 m section), whereas it occurred at core of similar 1.2738 blooms. Previous investigations of the microalloyed bloom pointwise microstructural and mechanical properties are extended. Moreover, microalloying effects are examined by comparing the properties of samples with and without the microalloying elements, that were laboratory heat-treated simulating a bloom core thermal history.

2:40 PM

Titanium Smelting Process Using Selective Chlorination and Preform Reduction Process: Haiyan Zheng¹; Toru Okabe¹; ¹University of Tokyo

For efficiently producing metallic titanium with high productivity and low cost, a new high-speed, semi-continuous, and environmentally sound titanium production process is investigated. In practice, iron (Fe) removal directly from titanium ore (ilmenite) by selective chlorination using calcium chloride (CaCl₂) and water vapor at 1023~1293 K was carried out. The obtained deironized titanium ore was directly reduced to metal by calcium (Ca) vapor at 1273 K using the preform reduction process (PRP), which is based on the metallothermic reduction of titanium oxide in the preform. After the PRP, titanium powder with 98% purity was obtained from the upgraded ilmenite ore. It is demonstrated that Fe in the ilmenite was successfully removed and PRP is a feasible process for producing metallic titanium powder with certain purity (>98%). Recovery of chlorine from iron chloride waste—generated by the chlorination process—is also investigated in order to develop an environmentally sound process.

3:00 PM

Thermal Resistant Polymers Modified with Ionic Groups for Ion Selective Membranes: Ana Lucia Skury¹; Márcia Azevedo¹; ¹Universidade Estadual do Norte Fluminense

The development of polymer materials capable of standing elevated temperatures and still exhibiting high permeability and selectivity for protons, is of interest in fuel cell technology. Many engineering thermoplastic polymers have been considered as possible substitutes for perfluorinated ionomers, provide that a charge group (sulfonic) is introduced into the structural unit. However, the final properties of such polymers do not allow their application in an industrial scale. In this work, polyetherimide (PEI) and poly(4,4'-diphenylether-1,3,4-oxadiazole) (POD-DPE) were investigated. The polymer characterization was accomplished by TGA, intrinsic viscosity, IEC and ion permeability. The IEC and an increase in the water sorption showed that both polymers were effectively sulfonated. The results indicated that the sulfonation lead to a significant reduction in the degradation temperature of the polymer. In comparison with commercial polymers, the degradation temperature of the PEI(S) is higher, which makes this polymer useful for applications involving ion transport.

3:20 PM Break

3:40 PM

Influence of Centrifugal Casting Processing Parameters on the Distribution of Reinforcing Particles in Aluminum Matrix Composites: Tunde Adelakin¹; Gustavo Gutierrez¹; Oscar Suarez¹; ¹University of Puerto Rico

In the whole range of functionally-graded materials (FGM), aluminum metal matrix composites (AMC) have attracted much interest partly due to their high wear resistance and high mechanical strength and toughness. Additional features, such as low density and low production costs, can be obtained when the aforementioned FGM AMCs are reinforced with AlB₂ and AlB₁₂ particles. Centrifugal casting process then allows gradually redistributing those denser reinforcements. With increasing rotational speed the reinforcing particle distribution changes along the centrifugal force (longitudinal) direction of the cast, the highest being at the periphery decreasing towards the inner zone close to the pouring end. The effect of the functional compositional gradient on superficial hardness and micro hardness measured along the casting longitudinal direction is discussed. The relationship between casting time and pouring temperature with the attained particle distribution is also investigated.

4:00 PM

High Pressure Assisted Sintering of Nanostructured B-Si-Cu-Diamond Composites: Ana Lucia Skury¹; Sergio Monteiro¹; Guerold Bobrovitchii¹; Márcia Azevedo¹; ¹Universidade Estadual do Norte Fluminense

The synthesis of advanced materials with superior performance and properties is of growing scientific and technological interest. In particular, significant achievements have been attained in the synthesis of nanocomposites associated with superhard materials. This work investigates nanostructured composites obtained by high pressure and high temperature sintering of synthetic diamonds combined with boron, silicon and copper. Diamond powder was mixed with B, Si and Cu, also in the form of powder. The mixture was then submitted to high energy wet milling until a nanopowder was formed. Sintering of this resulting nanopowder was carried out at 5.6GPa of pressure and 1300°C. X-ray diffraction

and scanning electron microscopy analysis revealed the formation of new phases in a well consolidated nanostructure with relatively high density.

4:20 PM

Studied Carbon Paste Electrode Modified by Nickel(II) Complex of Taurine-5-Bromosalicylaldehyde Schiff Base: *Wen Yuqing*¹; Liu Zheng¹; ¹Guilin University of Technology, Department of Material and Chemical Engineering

Synthesized 5-bromosalicylaldehyde Schiff base and its nickel complex by the solution method, carried on the attribute and the confirmation to the product structure by the ultra-violet spectrograph, IR Spectrum, TG. With oxidation peak current of the cyclic voltammograms changing, studied the characteristic of the carbon paste electrode modified by the bromide salicylaldehyde Schiff base nickel (II) complexes as active substances, the effect of electric activity of the type and loadings. Graphite loadings, paraffin loadings to the cyclic voltammetry of electrode. Studying the chemical modified carbon paste electrode for the electrocatalytic oxidation activeness of the formaldehyde by oxidation peak current and redox peak of the cyclic voltammograms as the target. When the formaldehyde range of the concentration from 0.001 mol/L to 0.01 mol/L, the linear relations is the peak electric current changing and the concentration of formaldehyde, the result show can the quantitative analysis of formaldehyde by the modified carbon paste electrode.

4:40 PM

The Surface Interaction of Pyrite in No Water Conditions: *Dan Li*¹; Qiyuan Chen¹; Zhoulan Yin¹; ¹Central South University

Ultrafine grinding pyrite was used ball grinder with particle size analysis. Results show that grinding pyrite powder in anhydrous ethanol is better than grinding in dry-mill powder particle size changes, anhydrous ethanol grinding was more efficient; Add several common aids, Sodium hexameta phosphate was found in pyrite ultrafine grinding process played better grinding effects; Powder saturated with vertical velocity measurement pyrite powder at different liquid medium of wettability, It was found pyrite powder in the body of anhydrous ethanol wettability was the best, followed by anhydrous acid, other organic solvents pyrite wettability was bad; turbidimetric method using the principle, spectrophotometer using different solvents pyrite dispersion effect, drawn in the aids solution, Pyrite Powder in the sodium hexameta phosphate solution to the dispersion stability was the best, but in non-aqueous environment, pyrite powder in anhydrous ethanol in the dispersion stability was the best, pyrite powder in water dispersion stability was bad.

Complex Oxide Materials - Synthesis, Properties and Applications: Ferroelectric/Dielectric Oxides

Sponsored by: The Minerals, Metals and Materials Society, TMS Electronic, Magnetic, and Photonic Materials Division

Program Organizers: Zhiming Wang, University of Arkansas; Ho Nyung Lee, Oak Ridge National Laboratory

Wednesday PM
March 12, 2008

Room: 277
Location: Ernest Morial Convention Center

Session Chair: To Be Announced

2:00 PM

Effect of Delithiation Rate on the Microstructure in Li_xCoO_2 - A Transmission Electron Microscopy Study: *Heike Gabrisch*¹; Tanghong Yi¹; Qingfeng Xing¹;

¹University of New Orleans

LiCoO_2 in the rhombohedral R-3m form is used as intercalation compound in rechargeable Li-ion batteries. During electrochemical charge/discharge cycling lithium is extracted and re-inserted into the crystal lattice accompanied by reversible changes in the stacking order of the lattice. With lithium extraction the electrostatic repulsion between neighboring CoO_2 slabs increases, leading to an expansion of the crystal lattice along the c-axis accompanied by a smaller contraction of the a-lattice parameter. Only little is known on the homogeneity of the lithium distribution within a population of powder particles of average composition Li_xCoO_2 or on concentration gradients within one particle, ($0 \leq x \leq 1$). We compare the microstructure of Li_xCoO_2 using transmission electron

microscopy. The powders are produced by chemical delithiation using a solution of NO_2BF_4 in acetonitrile (CH_3CN) at different ratios of LiCoO_2 : NO_2BF_4 . Our results show at high removal rates an inhomogeneous and highly strained microstructure is formed.

2:20 PM

Application of High- ϵ Ceramics for Enhanced Sensitivity of Electron Paramagnetic Resonance Spectrometer: *Ilia Geifman*¹; Iryna Golovina¹; Anatoliy Belous²; ¹Institute of Semiconductor Physics of NASU; ²Institute of General and Inorganic Chemistry of NASU

Earlier the application of single-crystal ferroelectric resonators improved the sensitivity of electron paramagnetic resonance (EPR) method up to 44 times.¹ In the present work new EPR resonators were developed and tested by using ceramic materials having high dielectric constant, $\epsilon=80-160$. Designed resonators have high quality, $Q=10^3-10^4$, and enhance the sensitivity of EPR spectrometer up to 60 times. The advantages of new ceramic resonators are: 1) cheaper synthesis and simplified fabricating technology; 2) wider temperature interval of usage; 3) higher precision in registering EPR spectra. Due to high ϵ and low $\tan\delta$ of applied ceramic material, the resonator increases microwave magnetic field on a sample, thereby improving EPR signal strength. The ceramics is made on the basis of titanates of complex oxides of rare-earth and alkali metals, and have perovskite or potassium-tungsten bronze type structure. I.N.Geifman, I.S.Golovina, J. Magn. Reson. 174, no.2, 292-300 (2005).

2:40 PM

Characterization of Anatase Synthesized by Sonochemical Means and Effects of Heat Treatments: *Leonardo Gonzalez-Reyes*¹; Isaias Hernández-Pérez²; Francisco C. Robles Hernández³; Jose de Jesus Cruz Rivera⁴; Elsa Miriam Arce-Estrada¹; ¹Instituto Politécnico Nacional; ²Universidad Autónoma Metropolitana-A, Departamento de Ciencias Básicas; ³Transportation Technology Center Incorporated; ⁴University of San Luis Potosí, Facultad de Ingeniería-Instituto de Metalurgia

In the present research were characterized anatase particles produced by sonochemical means. The TEM, XRD and SEM confirmed that sonochemical synthesis is an effective method to produced nanometric anatase. Relatively low temperature, 500°C, heat treatments show that anatase can be coarsened from 6.4 nm to 28.3 nm after 72 hours of heat treatment and in the absence of phase transformations. Anatase coarseness following a behavior similar to the one described by the LSW theory. The heat treated anatase particles show significant morphological changes as a function of heat treatment time and this directly affects the surface area of the anatase particles. In addition, the results of the effects of heat treatment on Photocatalytic activity are presented. The characterization of the anatase particles were carried out by means of BET, TGA, XRD, Raman, FTIR, UV-Vis and TEM.

3:00 PM

Current Density Influences on Morphology and Adhesion of $\text{RuO}_2 \cdot n\text{H}_2\text{O}$ Films Electrodeposited on Tantalum Substrate: *Hui Qin*¹; ¹Central South University

Effects of the different current density on morphology and adhesion of $\text{RuO}_2 \cdot n\text{H}_2\text{O}$ films were investigated by galvanostatic deposition. The mechanism of electrodeposition of hydrous ruthenium oxide was discussed. We can observe some morphological changes as the samples under SEM (Scanning Electron Microscope). When different current density are applied but the capacitance appears to be sensitive to this variable. Elements of films were analyzed by Energy Dispersive Spectroscopy (EDS); Phases of films were analyzed by X-ray Diffraction meter (XRD); Zeta potential of colloid solution was analyzed by DELSA 440SX Analyzer. It can be concluded that the thickness of $\text{RuO}_2 \cdot n\text{H}_2\text{O}$ films on tantalum substrate would increased with the cathodic current density, but the trend of the crack of $\text{RuO}_2 \cdot n\text{H}_2\text{O}$ films proportional to the cathodic current density after they were dried in atmosphere. when cathodic current density up to 10 mA/cm², $\text{RuO}_2 \cdot n\text{H}_2\text{O}$ film flaked away from the tantalum substrate, adhesion of $\text{RuO}_2 \cdot n\text{H}_2\text{O}$ film was very poor and hydrous ruthenium oxide easily drop from tantalum substrate.

3:20 PM

The Rule of NanoBoehmite on Spinel Formation in Magnesia Spinel Micro Composites: *Hamid Zargar*¹; Farhad Golestanifard¹; Hamidreza Rezaie¹; ¹Iran University of Science and Technology

The amounts of formed spinel were investigated systematically at temperatures of 700-1500°C for four different groups of micro composites starting material containing 0,3,5 and 7 percents nano boehmite as an additive. In this regard, nanobohmite added dead burnt magnesia and reactive alumina were mixed, pressed and fired orderly. FTIR was utilized in order to prove spinel formation as well as XRD patterns for both low and elevated temperatures. Results are shown that nano spinel was homogeneously formed on MgO surface at temperature as low as 700°C which these may act as seeds for spinel formation. It was cleared that the more nano boehmite results in lower permanent linear change (PLC). It was also found that spinel formation prohibited at temperatures above 1100°C with nanobohmite addition. This project is aimed to applying nanotechnology in Iranian refractory industry where is the largest producer in the Middle East.

3:40 PM Break

3:55 PM

Study of the Superficial Behavior of Inorganic Pigments (Iron Oxides): *Oscar Restrepo*¹; Federico Vásquez¹; Oswaldo Bustamante¹; ¹Universite Nacional De Colombia

Present work present the variation of the surface conditions of a pigment (iron oxide Fe₂O₃). We determine how the surface effects of particles, governed to a great extent by pH of the suspension, affect the behaviour of the fluid like colloid as far as viscosity and fluidity, and as well, those changes generated in the surface of particles modify the behaviour like pigment. The best conditions to work a pigment suspension and the best conditions settle down to which the pigment offers excellent benefits, directed to reductions of costs in manufacture and application of the pigment because of smaller costs of operation, low power consumptions in agitation and handling of higher concentrations in suspensions (obtaining of the low viscosities), and as pigment their characteristics of dispersability and colorimetric improved.

4:15 PM

Study on Structure and Properties of Glass Ceramics from Converter Slag: *Jiang Maofa*¹; Zhang Dayong¹; Shi Peiyang¹; ¹Northeastern University

Glass ceramics with converter slag as a raw material were prepared with the melting method. The effects of the mass fraction of converter slag on crystallization behavior and properties were studied by SEM, XRD and EDS. The results showed: With the mass fraction of converter slag increasing, the transition temperature and melting temperature of glass gradually decreased; the intensity of diffraction peak gradually increased, and the crystal phase of glass ceramics were Ca_{1.018}(Mg_{0.733}Fe_{0.293})(Si_{1.67}Fe_{0.304}O₆) with Ca(Fe, Mg)Si₂O₆, and the results of EDS showed there were Fe, Ca, Si, Mg and Al in glass, which the same as the results of XRD; the crystals rate increased, and the dimension of the crystals firstly increased and then decreased; the microhardness and the bulk density firstly decreased and then increased, which were the maximum when the mass fraction of converter slag was equal to 70%.

4:35 PM

Synthesis of Superconductor Oxide Ceramics by Combustion of Carbon Nanoparticles: *Karen Martirosyan*¹; Eduard Galstyan²; Y. Xue²; Dan Luss³; ¹University of Houston, Department of Chemical and Biomolecular Engineering; ²University of Houston, Texas Center for Superconductivity; ³Department of Chemical and Biomolecular Engineering, University of Houston

We report a novel cost-effective and simple method to produce a superconductor YBa₂Cu₃O_{7-x} powder (1-2µm) by self-sustaining one step process, named Carbon Combustion Synthesis of Oxides (CCSO). It produces YBCO much faster (order of seconds) than the common calcination process (order of hours) without any external power consumption and using rather inexpensive raw materials. In CCSO the exothermic oxidation of carbon (-393.5 kJ/mol) nanoparticles generates a thermal reaction wave with temperature up to 850°C that propagates at a velocity of 1 mm/s through the solid reactant Y₂O₃, BaO₂, CuO mixture converting it to the YBCO. The carbon is not incorporated in the product and is emitted as CO₂ from the sample generating high porous (~70%) and friable product. The variations of the magnetization of as-synthesized samples have been determined by SQUID magnetometer and show the onset

of superconducting transition at ~91K with shielding fraction of 44% of the -1/(4p) value.

4:55 PM

Oxidation Resistance and Characterization of Nb-Cr-W Superalloys at Elevated Temperatures: *Daniel Castro*¹; ¹University of Texas - El Paso

The importance of turbine engines in aerospace and energy sectors of industry has lead to the research of high temperature, low oxidation, super alloys for turbine engine component fabrication. An interest in niobium based superalloys has developed due to it's high service temperature capability and oxidation resistance when alloyed with chromium and tungsten. Samples from two different Nb-Cr-W alloy compositions were oxidized at temperatures 700-1400°C and analyzed under a SEM. Previous research on similar alloys with significantly less Chromium illustrated Nb₂O₄ as the primary oxide constituent. However, alloys studied in this research have affirmed new oxides and oxidation mechanisms in the Nb-Cr-W alloy system. A change in oxidation mechanism is apparent in the samples exposed to temperatures in excess of 900°C. In the resolve of this research, identifying a new oxide formation and mechanism has affirmed the need for more oxidation research in Nb-Cr-W alloys.

Computational Thermodynamics and Kinetics: Integrated Computational Materials Engineering

Sponsored by: The Minerals, Metals and Materials Society, TMS Electronic, Magnetic, and Photonic Materials Division, TMS Materials Processing and Manufacturing Division, ASM Materials Science Critical Technology Sector, TMS: Chemistry and Physics of Materials Committee, TMS/ASM: Computational Materials Science and Engineering Committee, TMS/ASM: Phase Transformations Committee
Program Organizers: Yunzhi Wang, Ohio State University; Long-Qing Chen, Pennsylvania State University; Jeffrey Hoyt, McMaster University; Yu Wang, Virginia Tech

Wednesday PM
March 12, 2008

Room: 288
Location: Ernest Morial Convention Center

Session Chairs: Jeff Simmons, Air Force Research Laboratory; Zi-Kui Liu, Pennsylvania State University

2:00 PM Invited

MatCASE and CCMD: Integrating Materials Simulation and Design: *Zi-Kui Liu*¹; ¹Pennsylvania State University

Individual phases are the building blocks of microstructures which dictate the performance of materials. Developing efficient approaches in accurately obtaining properties of individual phases is critically important in creating knowledge base for materials design and simulation, and promoting the paradigm shift towards integrated computational-prediction and experimental-validation approaches. In this presentation, our approach integrating first-principles calculations and CALPHAD modeling is presented through calculations of thermodynamic properties, thermal expansion coefficient, lattice parameters, elastic coefficients, and diffusion coefficients. Those properties are further used as guidance in processing design and input data in phase-field simulations of microstructure evolutions in the framework of our Materials Computation and Simulation Environment (MatCASE) [J. Comput-Aided Mater. Des., Vol.11, 2004, 183-199] and the NSF Center for Computational Materials Design [Proceedings Education and Professional Development, Materials Science & Technology 2006, Cincinnati, Ohio, 2006, pp. 111-118].

2:25 PM Invited

Discovery of Novel Hydrogen Storage Materials: An Atomic Scale Computational Approach: *Christopher Wolverton*¹; ¹Northwestern University

Practical hydrogen storage for mobile applications requires materials that contain large amounts of hydrogen, have low decomposition temperatures, and fast kinetics for absorption and desorption. Unfortunately, no reversible materials are currently known that possess all of these attributes. We present here results from an effort we have been developing over the past few years directed a predicting novel hydrogen storage materials from a computational first-principles approach. Such an approach requires several key capabilities: (i)

W
E
D
N
E
S
D
A
Y

P
M

Accurate prediction of decomposition thermodynamics, (ii) Prediction of crystal structures for unknown hydrides, and (iii) Prediction of preferred decomposition pathways. We show examples of progress we've made in these three areas: (i) prediction of hydriding enthalpies and free energies across a wide range of hydride materials, (ii) prediction of crystal structures for multivalent alanates and borohydrides, [such as $\text{Ca}(\text{AlH}_4)_2$ and $\text{Mg}(\text{BH}_4)_2$], and (iii) predicted decomposition pathways for $\text{Li}_4\text{BN}_3\text{H}_{10}$ and destabilized systems based on combinations of LiBH_4 , $\text{Ca}(\text{BH}_4)_2$ and metal hydrides. These capabilities have led to the prediction of several novel high-density hydrogen storage materials and reactions.

2:50 PM

Multiscale Simulation of Processing of Ni-Base Superalloys: Nils Warnken¹; Henrik Larsson²; Roger Reed¹; ¹University of Birmingham; ²KTH

The solidification and subsequent homogenisation treatment of a Ni-base superalloy have been simulated using phase-field (MICRESS), a front-tracking method and a method based on homogenisation (part of the DICTRA software). Obtained results are compared with experimental data. Directional solidification and further cooling are modelled using macro-scopic heat transfer Finite Element Analysis (ProCAST), yielding temperature history data for use in the micro models. We discuss the relative advantages of the different methods and demonstrate how these tools can be used to optimise the homogenization heat treatment of complex Ni-base superalloys.

3:05 PM

Modelling of the Discontinuous Precipitation Reaction with the Phase-Field Method: Lynda Amirouchel¹; Mathis Plapp²; ¹Université des Sciences et de la Technologie Houari Boumediene; ²Ecole Polytechnique

The discontinuous precipitation reaction appears in many industrial alloys and often results in a degradation of the alloy microstructure, accompanied by a drastic deterioration of its mechanical properties. It transforms a supersaturated mother phase into a two-phase structure consisting of lamellar precipitates and the depleted mother phase. The rate-limiting process is the surface diffusion of solute along grain boundaries and interfaces. We formulate a phase-field model for the description of the discontinuous precipitation reaction and study the structure and growth speed of regular (spatially periodic) precipitation fronts. We find that the shape and the steady-state growth speed of the precipitates are strongly influenced by the relative magnitude of surface diffusivity, volume diffusivity, and grain boundary mobility. We also find that steady states do not exist for certain ranges of these parameters. These findings will be discussed and compared to several theories for discontinuous precipitation.

3:20 PM

Diffusion Databases for Mg-ICME: Nagraj Kulkarni¹; Peter Todd¹; Yong-ho Sohn²; ¹Oak Ridge National Laboratory; ²University of Central Florida

The development of high fidelity diffusion databases is an integral component of a global Integrated Computational Materials Engineering (ICME) initiative in Mg-based alloys. In the current approach, an experimental approach for the development of robust tracer diffusion databases in light metal alloys systems is proposed that does not invoke any of the previous assumptions in the phenomenological theory of diffusion. Such an approach is based on modern SIMS measurements of diffusion depth profiles of stable isotopes (tracers) on samples prepared using conventional or combinatorial techniques. In comparison with previous diffusion measurements made using radioactive isotopes, it is expected that the time required for measurements and the subsequent analysis to develop a tracer diffusion database using stable isotopes will be significantly reduced. The current effort will include 4 ternaries from the Mg-Al-Mn-Zn system. Preliminary results will be presented.

3:35 PM Break

4:05 PM Invited

Developments in Phase Field Modeling for Ni-Base Alloys in Industrial Applications: Jeff Simmons¹; Y.H. Wen²; B. Wang³; Yunzhi Wang³; James Lill⁴; S.L. Chen⁵; Fan Zhang⁵; ¹Air Force Research Laboratory; ²UES, Inc; ³Ohio State University; ⁴HPTi; ⁵CompuTherm, LLC

Phase Field modeling has become popular because of its ability to simulate realistic microstructures that compare directly with microscopy and give information about local heterogeneities. Industrial applications generally require

non-isothermal processing of complex alloy systems of 10 or more elements, so modifications of the method were required to simulate concurrent nucleation and growth of reduced constitutional complexity systems. The concurrent nucleation and growth model allows for simulations of non-isothermal transformations and for validation of proposed transformation mechanisms. A pseudobinary model was developed that reduces the constitutional complexity, but involves approximating a complex system with a fictitious binary system, so an exact fit is not possible. We are, thus, developing an algorithmic calibration method that minimizes deviations from target values. Finally, a ternary model is being developed that accounts for transient diffusional effects. This model directly integrates commercial CALPHAD-type databases into the simulation. Selected results will be given.

4:30 PM Invited

Phase-Field Model for Grain Growth in Nanocrystalline Metals: Ingo Steinbach¹; Xiaoyan Song²; ¹RWTH-Aachen; ²Beijing University of Technology

We investigate the correlation between size dependent thermodynamics and grain growth kinetics of nano crystalline metals both theoretically and experimentally. The theoretical approach is based on the multi-phase-field method considering volume expansion of the grain boundaries with respect to the bulk crystal. Also temperature dependence of the elastic constants is taken into account to investigate the destabilizing effect of increased temperatures on nanograin structures. Experimental results in pure nano crystalline Co showing a discontinuous nanograin growth at a certain temperature are used to verify the model.

4:55 PM

Model for Ion Beam Synthesis of Nanocrystals: C. Yuan¹; I. Sharp¹; S. Shin¹; C. Liao¹; J. Guzman¹; J. Ager III¹; E. Haller¹; D. Chrzan¹; ¹Lawrence Berkeley National Laboratory; Department of Materials Science, University of California at Berkeley; ²Lawrence Berkeley National Laboratory

A model for the ion beam synthesis of nanocrystals within an amorphous matrix is developed. The model includes implantation of high-energy ions, motion of these ions in the matrix, and ion beam damage to the growing clusters. The model is studied using both a rate-equation based theory and kinetic Monte Carlo simulations, and the predictions of both methods are in substantial agreement. The model demonstrates that during implantation the island size distribution evolves through a nucleation phase to a growth phase and, ultimately, to a distribution that represents the balance between growth and ion beam damage. The model is compared with experimental results for Ge implanted into silica and results in a scaled nanocrystal size distribution that is in excellent agreement with experimental observations. This work was supported by the U. S. Department of Energy under contract No. DE-AC02-05CH11231.

5:10 PM

Examination and Simulation of the Transformation Path in Ti-Al-Nb Alloys: Orlando Rios¹; Damian Cupid¹; Hans Seifert²; Fereshteh Ebrahimi¹; ¹University of Florida; ²Technical University Bergakademie Freiberg

Ti-Al-Nb alloys with at least 40% Al have shown promising properties for high temperature applications. The phase diagram for this system has been well researched however several controversies including the extension of the beta phase field into the aluminum rich corner exist. We have combined computational and experimental efforts to evaluate the transformation paths in Al rich corner of this system. We have limited our studies to the two-phase region where gamma, TiAl(+Nb) and sigma, Nb₂Al(+Ti) phase are stable in the 1200 to 800°C temperature range. DTA and high temperature XRD techniques with capabilities up to 1600°C were employed in order to determine the transformation temperatures and stable majority constituent phases, respectively. Experimental observations revealed an extended beta phase field beyond the previously reported phase boundary. The CALPHAD methodology was used to calculate the liquidus surface and isothermal phase diagrams which were subsequently optimized implementing the experimental results. NSF-DMR0605702.

5:25 PM

A Ternary Phase-Field Model and Its Application to Precipitation Behavior in Ni-Al-Cr Alloys: *You-Hai Wen*¹; James Lill²; Shuang-Lin Chen³; Jeff Simmons⁴; ¹UES Inc.; ²High Performance Technologies, Inc.; ³CompuTherm LLC; ⁴Air Force Research Laboratory/MLLM

We developed a ternary phase-field model linking to Pandat software directly [CompuTherm, LLC] for thermodynamic evaluations. Using this model, we examined the effect of diffusivity and initial compositional/ordering profiles on the growth process of precipitate. We focused on the composition evolution with time in both the precipitates (gamma prime) and the matrix (gamma) and compared them with experimental observations by Sudbrack et al. [Acta mater., 54:3199,2006]. Our results indicate that random distribution of Cr in the nuclei is important to achieve comparable results with experimental observations. Some analysis of these results will be presented.

5:40 PM

Phase Field Simulations of Substrate-Coating Interactions for Nb-Si Based Alloys: *Sujoy Kar*¹; Bernard Bewlay¹; Ying Yang²; Bernd Boettger³; ¹GE Global Research; ²CompuTherm LLC; ³ACCESS Materials and Processes

Nb-Si based composite alloys are promising materials for application as high-temperature structural materials. Typically Nb based alloys are used in conjunction with a silicide based coating. The phase stability issues at the substrate-coating interface are critical during exposure at elevated temperatures. Phase field modeling techniques can be used effectively to simulate the behavior of the matrix-coating interface during exposure. In this work, a binary Nb-Si based matrix with a Si based coating has been simulated using the Phase-field methods to study the phase stability and motion of the interface at high temperature. The nucleation and growth mechanisms of the different phases that form at the interface have been studied.

Electrode Technology Symposium (formerly Carbon Technology): Cathodes Manufacturing and Developments

Sponsored by: The Minerals, Metals and Materials Society, TMS Light Metals Division, TMS: Aluminum Committee

Program Organizers: Carlos Zangiacomi, Alcoa Aluminum Inc; John Johnson, RUSAL Engineering and Technological Center LLC

Wednesday PM
March 12, 2008

Room: 299
Location: Ernest Morial Convention Center

Session Chairs: Morten Sorlie, Elkem Aluminium ANS; Ketil Rye, Elkem Aluminum

2:00 PM

Constitutive Laws of Carboneous Materials of Aluminium Electrolysis Cell: Current Knowledge and Future Development: *Donald Picard*¹; Guillaume D'Amours²; Mario Fafard¹; ¹Laval University, Aluminium Research Centre - REGAL; ²NRC Aluminium Technology Centre

The Hall-Héroult cell behaviour at different stages of the electrolysis process is an important point to take into consideration in the design and the optimization of the cell. Nowadays, numerical simulation has become a powerful and essential tool since in situ measurements are difficult to perform and cost expensive. For those numerical simulations, constitutive laws and their parameters' identification in laboratory are required for all the relevant physics of the cell materials. For the mechanical behaviour of the cell, many efforts have been done to characterize, to understand and to develop constitutive laws for the carboneous materials. Plasticity, viscosity, visco-elasticity, baking, etc., are examples of phenomena which have been addressed up to date, on both transient and steady state situations. This paper presents an overview on various level of modeling of the mechanical behaviour of the carbon cell lining material, from elastic to more complex like a thermo-(chemo)-visco-elasto-plastic one.

2:20 PM

Cathode Hot Patching to Prolong Cathode Life at DUBAL: *Maryam Al-Jallaft*¹; Ali Mohamed¹; Joseph Antony¹; ¹Dubai Aluminium Company Limited

The deterioration of cathode blocks may occur by general erosion, characterised by 'W' wear in more graphitised materials and by localised erosion, also known as potholing. Pothole failure is predominant in some cell technologies due to high amperage or certain cathode grades. The three main factors to contribute in the theory of pothole formation are cathode weakness area, high current density and an increase in metal pad velocity. Until 2003, Dubal focussed on using fused alumina, corundum, to hot patch the potholes in order to cease iron attack, thereby prolong cathode life. The cost-benefit analysis was derived in terms of key performance indicators, labour and corundum cost to determine the break even point of extended cathode life in a patched cell. This paper summarises Dubal's experience with fused alumina hot patching in D18 cell technology with respect to stall location and perform overall cost-benefit analysis.

2:40 PM

Lining Materials and Their Arrangement for Longer Life of Aluminum Reduction Cells: *Qi Quan*¹; ¹Northeastern University Engineering and Research Institute, Company, Ltd

With ever increasing size and current, lining materials and structure are playing more and more important role for longer life of aluminum reduction cells. Traditionally, bottom lining is required to possess better heat insulation and better heat dissipation for side lining. Meanwhile, these lining materials are also required to have better resistivity against erosion and penetration from molten bath and have better thermal stability. They must also be able to absorb cathode dilation to alleviate tension in it and ensure even and better thermal distribution inside cathode and lining. For these purpose, a rational lining structure and material option are presented for reduction cells of long life and high performance based on author's understanding over reduction cell lining and experience.

3:00 PM

High-Performance Preparation Plant for Cathode Paste: *Berthold Hohl*¹; Valery Burjak²; ¹Maschinenfabrik Gustav Eirich GmbH and Company KG; ²AOA Ukrgrafit

In the course of a modernization program, the Ukrainian company Ukrgrafit has converted part of their paste preparation line for cathodes and carbon blocks from conventional mixing technology to Eirich intensive mixers. The new plant was put into operation in the middle of 2006. Apart from the mixer, it comprises coke heating, intermediate storage of the finished mix, transport to the presses as well as the entire automation. The substantially improved homogeneity of the mix as well as the complete documentation of the preparation process clearly refined the quality of the final products. The paper describes the criteria leading to the decision on the system as well as the realization of the task definition. Moreover, first operating results are presented.

3:20 PM

Twelve Years of Experience with a Fully Automated Gas Preheating System for Söderberg and Prebake Cells: *Odd-Arne Lorentsen*¹; Ketil Rye²; ¹Hydro Aluminium; ²Elkem Aluminium

A preheating system with propane burners suitable for both Prebake and Söderberg cells was successfully developed more than 10 years ago at Elkem Aluminium. Two burners are controlled by a fully automated computer program with a predetermined heating rate, and they are pulsing according to the temperature on top of the cathode blocks. The new preheating concept makes it possible to increase the temperature in the cathode lining in a smooth and uniform manner up to 970°C. By improving the start-up procedure, we now start the cells without an initial anode effect. The paper presents our experience with the preheating system and how to obtain a smooth start-up and early operation.

3:40 PM

Cell Preheat/Start-up and Early Operation: *Ketil Rye*¹; ¹Elkem Aluminium

The most common methods for preheating industrial aluminum pots are reviewed and advantages and disadvantages of each method are presented. Also, the present industrial trend of reducing pot turnaround times is commented and measurements of deep-lining temperatures at start-up are related to the pot behavior in early operation. In general it is seen that shorter preheating times is unfavorable for pot stability in early operation and this effect may limit

WEDNESDAY PM

the potential for further pot turnaround time reductions or lead to operational problems and/or reduced potlife.

4:00 PM Break

4:10 PM

Properties of Pitch and Furan-Based TiB₂-C Cathodes: Mohamed Mahmoud¹; Trygve Foosnæs²; Harald Øye²; ¹Aluminium Company of Egypt (Egyptalum); ²Norwegian University of Science and Technology

Some characteristic properties of pitch and furan-based TiB₂-C bulk samples were studied. The open porosity of pitch and furan-based TiB₂-C bulk materials is 13.3% and 34.6%, respectively. The compressive strength of pitch-based samples is twice the value of furan samples (39 and 16.5 MPa, respectively). The X-ray diffraction patterns of baked pitch and furan-based TiB₂-C samples showed the presence of TiC and TiBO₃ due to the oxidation of TiB₂ and/or the reaction between TiB₂ and carbon in the presence of diffusing oxygen. The TGA study in nitrogen atmosphere showed weight losses of 6.2% and 2% for green and baked pitch-based TiB₂-C samples, and 11.2% and 7% for green and baked furan-based TiB₂-C samples, respectively. There was a significantly different behaviour between pitch and furan-based TiB₂-C samples in thermal dilatometer experiments. Pitch-based TiB₂-C samples showed higher shrinkage than furan-based TiB₂-C samples after soaking.

4:30 PM

Numerical Simulations and Experimental Studies on the Strain and Expansion of Carbon/TiB₂ Function Gradient Materials: Jilai Xue¹; Qingsheng Liu¹; Baisong Li¹; ¹University of Science and Technology, Beijing

Thermal strain and sodium expansion of carbon/TiB₂ function gradient materials (FGM) for aluminium reduction cathodes was investigated by numerical simulations and experimental tests. Carbon/TiB₂ FGM was made of TiB₂-rich layer as a wettable surface, TiB₂-containing layers as transition interfaces and carbons as matrix. Simulation studies using ANSYS indicate that the 3 or 4-layers of carbon/TiB₂ function gradient materials can offer lower thermal strain and sodium expansion in the cathode body and cell bottom structure. Then FGM samples were prepared with the number of function layers $n = 4$, and the gradient coefficient = 0.6. Experimental tests show a satisfactory thermal stability and good resistance to sodium expansion.

4:50 PM

Electrodeposition of TiB₂ from Cryolite-Alumina Melts: Dmitry Simakov¹; Sergei Vassiliev²; Parviz Tursunov²; N. Khasanova²; Viktor Ivanov¹; Artem Abakumov²; N. Alekseeva²; Evgenii Antipov²; Galina Tsirlina²; ¹Russian Engineering Company Ltd.; ²Moscow State University

Formation of TiB₂ and various by-products under cathodic polarization is studied in relation to in situ deposition of coatings on graphite directly from cryolite-alumina bath. This procedure can provide a cheap cathode coating having very good wettability. In order to evaluate the nature of products, voltammetry and multistep potentiostatic technique are applied in combination with XRD, SEM and local analysis. For CR between 2 and 3 and alumina content of 2-8 wt.%, current efficiency of TiB₂ formation is found to pass a maximum at current densities of ca. 0.4-0.5 A/cm². Parallel deposition of Ti₂O₃ and silicides is confirmed in certain potential regions. Wetting test demonstrated the formation of homogeneous Al film on as-deposited coatings even under open circuit conditions. Wettability was much better as compared to samples with brushed TiB₂-based coating. A disadvantage of the deposited coatings is its dendrite microstructure which may be improved upon in future.

5:10 PM

Diffusional Creep Deformation in Carbon/TiB₂ Cathode Materials during Aluminum Electrolysis: Jilai Xue¹; Qing-Sheng Liu¹; ¹University of Science and Technology

Diffusional creep deformation in carbon/TiB₂ cathode materials mainly due to sodium penetration during aluminum electrolysis was investigated in a modified Rapoport apparatus. Experimental data for the cathode materials with varying amount of TiB₂ addition were obtained against varying temperature and compressive pressure. Sodium penetration and expansion were measured at the same time along with the diffusional creep process under compressive pressure. In general the creep deformation process shows a trend of increasing with prolonged time of aluminum electrolysis and increased temperatures

of cell operation. The addition of TiB₂ into the carbons can, however, reduce the diffusional creep deformation. Numerical simulations were also applied to compare and analyze the effects of various material properties and processing parameters. The technical information obtained is useful for cell design and relining by using the carbon/TiB₂ cathode materials.

5:30 PM

Penetration of Sodium and Electrolyte to Vibratory Compaction TiB₂ Cathode: Zhaowen Wang¹; Yungang Ban¹; Zhongning Shi¹; Shaohua Yang¹; Hongmin Kan¹; Xiaozhou Cao¹; ¹Northeastern University, College of Materials and Metallurgy

Vibratory compaction TiB₂ and 30 mass% graphite contained block were used as cathodes in aluminum electrolysis. In the same condition, after 5 h electrolysis, the depth of electrolyte penetrated into the 30 mass% graphite cathode was about 13 mm. It was deeper than that into TiB₂ cathode which was less than 1 mm. SEM and EDS analysis showed that Na, F, Al penetrated slightly into the vibratory compaction TiB₂ cathode much less than that into the 30 mass% graphite cathode. Vibratory compaction TiB₂ cathode can decrease sodium penetration effectively, but it can not hinder sodium penetration thoroughly. The penetration resistance mechanism of vibratory compaction TiB₂ cathode to sodium and electrolyte was also discussed in this paper.

5:50 PM

Effect of Grain Gradation on Vibratory Packing Efficiency in Preparing TiB₂-C Composite Cathode for Aluminum Electrolysis: Xiaojun Lü¹; Jie Li¹; Yan-qing Lai¹; Qing-yu Li¹; Zhang-Liang Tian¹; Zhao Fang¹; ¹Central South University

The effect of the size distribution of coarse-fine binary particles and the volume fraction of fine particles on the vibratory packing efficiency and porosity of TiB₂ powder were investigated. The results showed that the vibratory packing efficiency increased and the porosity decreased when the size ratio (R) of coarse particles to fine particles increased. In addition, the vibratory packing efficiency was also governed by the volume fraction of coarse or fine particles, and reached its maximum when the volume fraction of fine particles is 30%-40%. Comparing the experimental results to the values calculated by the Furnas model, it is found that the Furnas model suits TiB₂ ceramic powder system, and the value of the parameter C2 in Furnas model is determined according to experimental results.

Emerging Interconnect and Packaging Technologies: Pb-Free Solders and Other Interconnects: Microstructure, Modeling, and Test Methods

Sponsored by: The Minerals, Metals and Materials Society, TMS Electronic, Magnetic, and Photonic Materials Division, TMS: Electronic Packaging and Interconnection Materials Committee

Program Organizers: Carol Handwerker, Purdue University; Srinivas Chada, Medtronic; Fay Hua, Intel Corporation; Kejun Zeng, Texas Instruments, Inc.

Wednesday PM
March 12, 2008

Room: 275
Location: Ernest Morial Convention Center

Session Chairs: C. Robert Kao, National Taiwan University; Carol Handwerker, Purdue University

2:00 PM

In-Situ Observations of Unidirectional Solidification in Sn-0.7Cu and Sn-0.7Cu-0.06Ni by X-Ray Imaging: Yosuke Yamamoto¹; Kazuhiro Nogita²; Christopher Gourlay²; Arne Dahle²; Kentaro Uesugi³; Hideyuki Yasuda¹; ¹Osaka University; ²University of Queensland; ³Japan Synchrotron Radiation Research Institute, SPring-8

It has previously been shown that Ni additions in the range of 400-1000ppm alter the microstructure and improve the wave soldering performance of Sn-0.7Cu-xNi alloys. However, the influence of Ni additions on the microstructure formation during solidification is not fully understood. In recent years, in-situ observations of solidification of metallic alloys have been developed using time-resolved X-ray radiation in the synchrotron. This paper reports on the results from in-situ observations of unidirectional solidification of Sn-Cu and Sn-Cu-

Ni solders at the SPring-8 synchrotron radiation facility. The solidification characteristics of Sn-0.7Cu and Sn-0.7Cu-0.06Ni at growth rates in the range of 1-10 μ m.s⁻¹ are compared and discussed.

2:15 PM

As Solidified and Aged Microstructure Control Through X Modification in SAC+X Alloys: *Jason Wallester¹; Iver Anderson²; Fran Laabs²; Joel Harringa²; ¹Iowa State University; ²Ames Laboratory*

The ideal solder microstructure contains a fine phase distribution while minimizing the size of any brittle phase. A coupled eutectic fits this description. Unfortunately, due to the difficulty in nucleating tin, a 100% eutectic microstructure for Sn rich solder alloys has remained elusive and pro-eutectic Ag₃Sn plates often plague Ag bearing alloys. However, by careful study of Sn-Ag-Cu-X alloys using simulated DSC solder joints, pro-eutectic Ag₃Sn plates can be mitigated and eutectic volume maximized by controlling X and its concentration. Additionally, previous research shows that certain X additions also slow diffusion and resulting IMC growth. Aged samples, identical in composition to the DSC samples, will also be prepared, examined, and mechanically tested. The primary difference is that at this time, the lower concentrations of X will be used. Zn and Mn appear most promising.

2:30 PM

An Investigation of Microstructure and Mechanical Properties of Pb-Free Solders as a Function of Alloy Composition and Cooling Rate: *Sun-Kyoung Seo¹; Sung Kang²; Hyuck Mo Lee¹; Da-Yuan Shih²; ¹Korea Advanced Institute of Science and Technology; ²IBM Corporation*

The microstructure and microhardness are investigated for various Pb-free solders; Sn-Cu, Sn-Ag, and Sn-Ag-Cu. The Cu content examined varies from 0.5 to 2 wt % in Sn-Cu, while the Ag content varies from 0.5 to 3.5 wt % in Sn-Ag or Sn-Ag-Cu. The effects of minor alloying elements such as Cu, Ni and Zn are also examined with various Sn-rich solders. The cooling rates employed during solidification range from 0.02°C/s, to 1-5°C/s and to 100°C/s. Sn grain size and orientation are observed by cross-polarization light microscopy and electron backscatter diffraction (EBSD). The microhardness is measured to find the variation of mechanical properties in terms of alloying contents and cooling rates. It is found that the alloy composition, minor alloying elements, and cooling rate significantly affect the Sn grain size and hardness in various solder alloys. Sn grains become smaller with increasing minor alloying contents, and also with the fast cooling rate.

2:45 PM

Effect of Reflow Profile on Sn Undercooling and Microstructure Evolution of Sn-3.5Ag and Sn-3.9Ag-0.6Cu Lead Free Alloys: *Yan Xing¹; James Woods¹; Eric Cotts¹; ¹Binghamton University, Department of Physics and Materials Science*

This study focuses on the effects of high temperature annealing on the Sn solidification temperature in Sn-Ag-Cu solder, and on the final microstructure of Sn-Ag-Cu samples. Reflow temperature, reflow time and number of reflows were varied in eutectic Sn-3.5Ag and Sn-3.9Ag-0.6Cu alloys. It was found that the solidification temperature of the Sn phase decreases with higher reflow temperature, and with longer annealing times at elevated temperatures. Cross sectioned samples were examined by means of optical microscopy and scanning electron microscopy. The size and number of Ag₃Sn and Cu₆Sn₅ precipitates was found to vary dramatically with reflow conditions. For instance, in samples which had been reflowed at high temperatures (~400C-500C), no primary Ag₃Sn precipitates (plates) were observed in the cross sections of both Sn-3.5Ag and Sn-3.9Ag-0.6Cu solder balls. The rate of nucleation and growth of Ag₃Sn in undercooled melts was examined and found to vary with reflow conditions.

3:00 PM

Role of Au in the Massive Spalling at the SnAgCu/Ni Interface: *Su-Chun Yang¹; C. Rober Kao¹; ¹National Taiwan University*

Massive spalling of intermetallic compound in the SnAgCu/Ni system has been reported in the literature. In this study, we pointed out that the presence of a Au layer between solder and Ni has the effect of triggering the massive spalling at even earlier stage. Experimentally, Sn-Ag-Cu lead-free solders of various compositions were reflowed on Au/Ni metallization. The thickness of Au layer was varied from 0 to 3 μ m. The thicker the Au layer is, the easier massive spalling can occur. The reason for the Au effect will be presented in this talk.

3:15 PM Break

3:30 PM

Effects of Phosphorus on Fluidity and Microstructure of Sn-xCu-yNi Lead-Free Solder: *Kazuhiro Nogita¹; Jonathan Read¹; Christopher Gourlay¹; Tetsuro Nishimura²; Shoichi Suenaga²; Arne Dahle¹; ¹University of Queensland; ²Nihon Superior Company, Ltd*

Phosphorus is sometimes added to lead-free solders as an anti-oxidation agent during wave soldering. This paper reports on the effect of phosphorus on the maximum fluidity length, and microstructure of Sn-xCu-yNi alloys. Fluidity tests were conducted by the vacuum fluidity test (the Ragone method) using Pyrex elbow tubes (800mm x 150mm and ID:3mm) at a constant superheat of TLiq+40K. The results clearly demonstrate that phosphorus additions decrease the maximum fluidity length. The most significant decrease in fluidity length occurs in the range 20 to 90 ppm P in Sn-0.7Cu-0.05Ni-zP alloys. The mechanisms responsible for these effects are discussed in terms of the nucleation and growth dynamics and microstructure in this system.

3:45 PM

Cross-Interaction between in Ni/Sn5Ag/Cu and Ni/Sn/Cu Solder Joints: *Hua-wei Tseng¹; Liu Chengyi¹; ¹National Central University*

Recently, peoples start realizing the importance of the mutual interaction between two different interfacial reactions in solder joints. It has been reported by many researchers that the dissolved elements from metal pads, such as Cu and Au, would diffuse across the molten solder and influence the opposite solder/metal pad interfacial reactions. Cross-interaction between two interfacial reactions in Ni/Sn5Ag/Cu and Ni/Sn/Cu solder joints were investigated. In this talk, we will report: (1) In Ni/Sn/Cu sandwich structure, the asymmetrical microstructure across Ni/Sn and Sn/Cu interfaces was found, which greatly affects the interfacial strength in Ni/Sn/Cu solder joint. (2) In Ni/Sn5Ag/Cu sandwich structure, we found that Ag tend to migrate and form Ag₃Sn compound on the Ni side with longer reflow time. The Ag migration mechanism will be discussed based on the isothermal Sn-Ag-Cu diagram.

4:00 PM

First Principles Modeling of Copper Interconnect Resistance: *Donald Nicholson¹; X.-G. Zhang¹; Bala Radhakrishnan¹; Nagraj Kulkarni¹; Sirish Namilae¹; Li An-Ping¹; ¹Oak Ridge National Laboratory*

First principles quantum mechanical methods are needed to accurately model electron transport in interconnects once they are so narrow that the width and grain size approach the electron mean free path. We have used a local density based approach to calculate the resistance of individual grain boundaries. The Layer KKR multiple scattering code is used to calculate the transmission of Bloch waves through tilt and twist boundaries. Various levels of atomic and electronic relaxation of the grain boundary are investigated. A procedure for incorporating local electronic transport results into a lattice Boltzmann model corresponding to particular interconnect grain structures will be described. Research sponsored by the Laboratory Directed Research and Development Program of Oak Ridge National Laboratory (ORNL), managed by UT-Battelle, LLC for the U. S. Department of Energy under Contract No. DE-AC05-00OR22725.

4:15 PM

Characterization of Tungsten Carbide Electrical Contacts for High-Temperature Electronics: *Claudiu Muntele¹; Kennesha Nettles²; Daniel Walker²; Satilmis Budak¹; Abdalla Elsamadicy²; Daryush Ila¹; ¹Alabama A&M University; ²University of Alabama in Huntsville*

Silicon carbide based electronics components are sought after for applications in harsh environments (high temperature, corrosive atmosphere etc.). For such applications, electric connects made of tungsten carbide seems to be the best choice, for chemical and mechanical stability. In this work we are investigating the stoichiometry, microstructure, and electrical behavior of tungsten carbide thin films on silicon carbide substrates. We used Rutherford Backscattering spectrometry and X-ray photoelectron spectroscopy for measuring the stoichiometry and depth profile, scanning electron microscopy to monitor the surface morphology change, and Van der Pauw electrical measurements for determining the sheet resistivity as a function of operating temperature, ranging from room temperature to 800°C.

Emerging Methods to Understand Mechanical Behavior: X-Ray Diffraction

Sponsored by: The Minerals, Metals and Materials Society, TMS Structural Materials Division, TMS Materials Processing and Manufacturing Division, TMS: Advanced Characterization, Testing, and Simulation Committee, TMS/ASM: Mechanical Behavior of Materials Committee, TMS: Nanomechanical Materials Behavior Committee
Program Organizers: Brad Boyce, Sandia National Laboratories; Mark Bourke, Los Alamos National Laboratory; Xiaodong Li, University of South Carolina; Erica Lilleodden, Forschungszentrum

Wednesday PM

Room: 285

March 12, 2008

Location: Ernest Morial Convention Center

Session Chair: To Be Announced

2:00 PM Invited

Using Quantitative Texture Methods and Finite Element Analysis to Understand Internal Stresses in Deforming Polycrystals: *Matthew Miller¹; Jun Park¹; Tong Han²; Paul Dawson¹; ¹Cornell University; ²Yonsei University*

Stress state is a key factor for many important phenomena related to processing and performance of engineering alloys. Microplasticity, recrystallization, phase transformation and crack initiation are driven by stress state on the size scale of the individual crystal. In this talk, a synchrotron x-ray based experimental method – motivated by quantitative texture analysis – designed to measure the orientation-dependent distributions of crystal stresses over a deforming aggregate is described. The experimental data from tests conducted on sintered copper are compared to finite element results from a crystal-based simulation methodology. Stress distributions are compared component by component at each load level. To better understand trends over orientation space, we also expand both sets of data in a series of spherical harmonic functions and compare the modes and coefficients between experiment and simulation.

2:30 PM

A Method to Determine the Full Second Order Strain Tensor from a Single 2D Diffraction Pattern: *Apurva Mehta¹; David Bronfenbrenner²; James Belasco¹; Matthew Bibee³; Monica Barney⁴; M.R. Mitchell⁴; Alan Pelton⁴; ¹Stanford Synchrotron Radiation Laboratory; ²University of California, Berkeley; ³Stanford University; ⁴Nitinol Devices Corporation*

When a structural element is subjected to external load, the resultant mechanical deformation is a complex response function best captured by a second order strain tensor. This tensor can be thought of as a description of a 3D ellipsoidal surface, where the deviation (eccentricity) from a spherical surface is the measure of local strain along that direction. Conventional x-ray diffraction strain measurement analyzes one point on this ellipsoid. The sample is rotated along two non-colinear axes to sample many different locations on the ellipsoid and thus determine the full strain tensor. This forms the basis of the sin-squared-psi (ssp) technique. We will present an adaptation of the ssp technique using a large area detector, which will yield the full second order strain tensor from a single diffraction pattern. We will show a comparison of the strain tensors obtained from “stationery”, single-shot method to the ones obtained from standard ssp method.

2:50 PM

Determination of Local Strain for a More Fundamental Understanding of Mechanical Response in Materials: *Monica Barney¹; David Bronfenbrenner²; Sam Daly³; Apurva Mehta⁴; M.R. Mitchell¹; Alan Pelton¹; ¹Nitinol Devices Corporation; ²University of California, Berkeley; ³California Institute of Technology; ⁴Stanford Synchrotron Radiation Laboratory*

In order to move toward a more fundamental understanding of the strain response to load on a local level in materials, development of a non-destructive, spatially resolved strain measurement technique using highly coherent, monochromatic synchrotron X-rays is underway. By studying conventional elastic-plastic strain behavior of the common metallic crystal structures (FCC, BCC, HCP), the validity of this newly developed approach can be verified and these X-ray measurements compared to global strain quantities to shed light on a more detailed understanding of mechanical behavior. In addition, the precise

onset of plastic deformation should be readily determined from the changes in the X-ray diffraction peaks and compared to the transition between deformation modes observed in global strain measurements.

3:10 PM

Micromechanical Study of Superelastic and Shape Memory NiTi by Novel Synchrotron X-Ray Diffraction Techniques: *David Bronfenbrenner¹; Monica Barney²; M. Mitchell²; Apurva Mehta³; Alan Pelton²; Ronlad Gronsky¹; ¹University of California-Berkeley; ²Nitinol Devices Corporation; ³Stanford Synchrotron Radiation Laboratory*

Conventional strain measurements treat the specimen as a homogeneous continuum and provide a macroscopic assessment of the elastic and plastic strain in response to applied force. In the current study, strain is assessed at the microscopic level for superelastic and shape memory NiTi. In response to an applied global displacement, NiTi experiences four modes of micromechanical deformation. Reversible deformation consists of both bond stretching (Hookian elastic) as well as thermodynamically driven phase transformations. Irreversible deformation consists of dislocation driven deformation (conventional plasticity) as well as low-symmetry crystallite reorientation. The ellipsoidal X-ray diffraction technique used in this study is ideally suited to distinguish between these four deformation modes at the microscopic level. Our group has used in-situ synchrotron x-ray diffraction to distinguish and quantify the micromechanical response of deforming superelastic and shape memory NiTi and has compared these with conventional global strain measurements.

3:30 PM

Strain and Texture Evolution during Mechanical Loading of a Crack Tip in Martensitic Shape-Memory Nit: *Mark Daymond¹; Marcus Young²; Jon Almer³; David Dunand²; ¹Queens University; ²Northwestern University; ³Argonne National Laboratory*

In situ synchrotron X-ray diffraction measurements are used to create maps of elastic strain and texture, averaged over a compact-tension specimen thickness, near a crack tip in martensitic NiTi. After fatigue crack propagation, the material ahead of the crack and in its wake exhibits strong texture, which is eliminated by subsequent shape-memory heat treatment, indicating that this texture is due to detwinning, the main deformation mechanism of NiTi. Upon subsequent application of tensile stresses, the textured zone reappears and grows around the crack tip as applied stress is increased. At the highest applied stress intensity of 35MPa-root-m, large tensile strains are measured ahead of the crack tip and considerable elastic anisotropy is observed. The detwinning zone is similar to the plastic zone produced by dislocation slip present around cracks in other metals. The texture in the zone is not significantly altered after mechanical unloading, despite substantial triaxial compressive residual strains.

3:50 PM Break

4:05 PM Invited

Diffraction Stress/Strain Analysis in Integrated Circuits: *Conal Murray¹; Ismail Noyan²; ¹IBM T.J. Watson Research Center; ²Columbia University*

Modern microelectronic circuits are heterogeneous devices which contain very significant locked-in manufacturing strains. These strains form the basis of “strained-silicon” devices with enhanced performance characteristics. Because of the current device dimensions, independent measurement of these strains is a non-trivial exercise. In this paper we will discuss the technology, physics and mechanics relevant to strained-Si devices and summarize our attempts at measuring these strain fields using microbeam x-ray diffraction.

4:35 PM Invited

Single Grain Characterization Techniques at the APS 1-ID Beamline: *Ulrich Lienert¹; Jonathan Almer¹; Bo Jakobsen²; Wolfgang Pantleon²; Henning Poulsen²; Christopher Hefferan³; Robert Suter³; ¹Argonne National Laboratory; ²Risø National Laboratory; ³Carnegie Mellon University*

The use of high-energy synchrotron x-rays provides a unique combination of bulk penetration power (mm to cm) with high spatial (about 1 micrometer) and temporal resolution. The APS 1-ID beamline is dedicated to high-energy diffraction and the status of the single grain diffraction program will be presented. Recently, a dedicated setup for diffraction imaging has been installed. A forward modeling algorithm has been developed to reconstruct the grain boundary outlines. Grain maps of polycrystalline aluminum have been reconstructed.

Strain sensitivity is achieved in the far-field regime. The technique has been extended to high reciprocal space resolution by novel x-ray optics providing a narrow bandwidth beam and by positioning an area detector at very long distance behind the sample. The use of area detectors provides fast data acquisition, and therefore three-dimensional reciprocal space maps can be recorded. The reciprocal space resolution of about 0.001 1/\AA is almost isotropic.

5:05 PM

Using X-Ray Microbeams to Assess Long Range Internal Stresses in Materials: *Michael Kassner*¹; Lyle Levine²; Bennett Larson³; Jon Tischler³; Peter Geantil¹; ¹University of Southern California; ²National Institute of Standards and Technology; ³Oak Ridge National Laboratory

The presence of counterbalanced stresses within microscopic volumes (or cells) in deformed materials was predicted more than two decades ago and has been inferred from numerous indirect experiments. Yet, direct proof of their existence had been elusive, as spatially-resolved measurements of the stress magnitudes and distributions critical for testing theories and computer modeling were not possible until recently. Researchers using the intense, submicron, x-ray beams at the Advanced Photon Source made the first quantitative, spatially resolved measurements of elastic strains within dislocation cells. The measurements indicated that the structural materials were under significant, variable internal stresses of opposite direction on submicron length scales corresponding to the dislocation substructure. The results provide critical data for validating and guiding the development of detailed dislocation-based simulations and models for every major facet of dislocation structure evolution and dislocation transport.

5:25 PM

In-Situ Investigation of Twinning in Individual Mg Grains with Synchrotron X-Rays: *Cahit Aydinler*¹; Bjorn Clausen¹; Joel Bernier²; Ulrich Lienert³; Don Brown¹; Carlos Tome¹; ¹Los Alamos National Laboratory; ²Lawrence Livermore National Laboratory; ³Argonne National Laboratory

Formation of tensile twins and their stress evolution in individual Mg grains is investigated with a state-of-the-art, high-energy synchrotron X-ray diffraction method. In-situ measurements are performed under compressive load where sample rotations in each step allow recording of diffraction spots from most atomistic planes of targeted grains. Analysis of these spots allows identification of individual grains through their orientation and yields their strain tensor. It is crucial to note that these grains are investigated in the bulk, in their native environment. Here, the known crystallographic relation between the parent grain and twin variant means that the location of the diffraction spots of the prospective twin can be predicted. We have observed the realization of these spots (formation of the twin) and the increase in their intensity with further loading (growth of the twin). Ultimately, we detail the stress interaction between the twin and the parent at a single grain level.

5:45 PM

Microstructure as Seen by X-Ray Line Broadening, Its Relevance to Mechanical Behavior: *Tamas Ungar*¹; ¹Eotvos University

Mechanical behavior, in a broader sense, is determined by the microstructure. The major constituents of microstructure are composition, second phases, dislocations, grain boundaries and planar defects, especially stacking faults and twin boundaries. X-ray line profile analysis proves to be a powerful method for characterizing these microstructure elements both, qualitatively and quantitatively. The dislocation model of strain anisotropy enables the precise determination of dislocation densities and characters together with subgrain size and size-distribution. The Taylor and Hall-Petch models of strength can be evaluated by using these data. Twinning can be determined quantitatively by X-ray diffraction and, together with scanning electron microscopy, provides a comprehensive microstructure characterization, especially in hexagonal metals.

Energy Conservation in Metals Extraction and Materials Processing: Session II

Sponsored by: The Minerals, Metals and Materials Society, TMS Extraction and Processing Division, TMS Light Metals Division, TMS: Aqueous Processing Committee, TMS: Pyrometallurgy Committee, TMS: Recycling and Environmental Technologies Committee

Program Organizers: Edgar Vidal, Colorado School of Mines; Cynthia Belt, Aleris International Inc

Wednesday PM

Room: 287

March 12, 2008

Location: Ernest Morial Convention Center

Session Chair: Edgar Vidal, Colorado School of Mines

2:00 PM

Develop a Synergic Thermal-Mechanical Process for Al-Mg-Si Alloys: *Mingdong Cai*¹; ¹University of Houston

AlMgSi extrusion alloys are usually processed sequentially as casting, homogenization, extrusion and artificial ageing treatment (T5/T6). Due to low ageing temperature, it usually takes over 1000 minutes for peak-ageing treatment. This largely limits the manufacturing efficiency and requires large energy consumption. We propose to overcome this issue through combining conventional processing techniques (such as rolling, extrusion and forging) and ageing, a synergic thermal-mechanical process named dynamic ageing. Preliminarily, dynamic ageing of two AlMgSi alloys at 170°C was conducted by equal channel angular extrusion (ECAE). It is shown that the ageing time-scale is reduced to around 10 minutes, and the dynamically aged samples have higher ultimate tensile strength than statically peak-aged samples with comparable ductility. It is therefore concluded that ECAE-aided dynamic ageing is efficient in executing ageing treatment that results in superior mechanical properties. We expect that this new technique have great potential in automobile and aerospace industries.

2:20 PM

Direct Electrochemical Production of Titanium Alloys from Oxide Precursors: *Kevin Dring*¹; ¹Norsk Titanium

Current production of titanium alloys is accomplished via the Kroll process; a discontinuous, greenhouse gas emitting process that is labor intensive. A more efficient process based on electrolysis was forecasted by Kroll himself over fifty years ago, however, this prophecy has remained unfulfilled. The present work demonstrates the production of low-oxygen beta titanium alloys - of both conventional and novel compositions - via the direct electrochemical reduction of blended oxide precursors in molten salt electrolytes at elevated temperatures. Electroanalytical and materials characterisation techniques were applied to partially and fully deoxidized material in order to ascertain the reduction mechanisms and pathways. A beneficial effect on the reduction pathway of titanium dioxide was obtained from the presence of secondary oxides during the reduction process. The earlier onset of beta titanium formation greatly facilitated the extraction of the final remnants of oxygen from the metallic titanium.

2:40 PM

Sulfide Ore Looping Oxidation Process: Maximizing Energy Recovery and Minimizing Environmental Impact: *Larry McHugh*¹; *Jean Mozolic*²; ¹Orchard Material Technology LLC; ²The Mozolic Consulting Group LLC

This paper is the subject of a recent patent application demonstrating major improvements in sulfide ore processing. This two-step "looping oxidation" process effectively removes sulfur while producing materials of adequate purity in an energy proficient and environmentally friendly manner. The first step results in a metal sub-oxide and a highly concentrated sulfur oxide off-gas stream. This gas stream can be processed for recovery in a more effective manner regarding both energy and capital equipment costs. In the second step, this metal sub-oxide is further oxidized to efficiently generate energy that can be recovered and utilized without the typical complications of an "acid gas" stream process. Additionally, a portion of the final fully oxidized product can be looped back to the first step as the oxidizing agent. The process will be described in detail and compared to existing technologies in the following areas: production efficiency, energy utilization, sulfur recovery and cost.

WEDNESDAY PM

3:00 PM

On Promoting Energy Conservation in Hydrometallurgical Processing of Complex Materials: *Katragadda Rao*¹; ¹Institute of Minerals and Materials Technology (Formerly Regional Research Laboratory (CSIR), Bhubaneswar)

Current potential technologies of aqueous processing of minerals, metals and materials include the treatment of nickel, zinc and gold ores; processing of complex multimetal sulphides, chromite overburden/nickel laterites and ocean-floor manganese nodules; and biomaterial technology. Hydrometallurgical processes involving single units that combine reaction and separation operations have received considerable attention as they offer major advantages over conventional processes due to the interaction of reaction, mass and energy transfer. A better understanding of the whole materials supply chain has become essential in today's world that is defined by materials and not by metallurgy. With the above background, the present paper describes the importance of interdisciplinary nature of hydrometallurgy, some recent energy saving measures practiced in leaching processes, solution separation and purification, and environmental aspects.

3:20 PM

Control and Optimization of Teniente and PS Converters Operations for Energy Efficiency and Process Intensification: *Florian Kongoli*¹; F. Condore²; R. Riveros²; I. McBow¹; E. Z. O'Brien¹; J. Bobadilla²; G. Achurra²; ¹Flogen Technologies, Inc.; ²Codelco-Chile

Energy efficiency is one of the most important issues for various existing and new extraction processes. An efficient process uses the minimum possible energy in various forms and ways in order to extract or process several materials. This is closely related to several factors from decreasing the number of operational problems and accidental shutdowns to the control, optimization and automation of these processes. In this paper, the authors discuss their recent work in effectively controlling and optimizing the day-to-day operational parameters in Teniente and PS Converters as well as the intensification, optimization and automation of these processes through a unique non-equilibrium physical process modeling that correctly simulate the industrial furnace processes and avoid guessing and uncertainties. The advantages of this new approach have been discussed.

3:40 PM Break

4:00 PM

Electrochemical Synthesis of Non-Oxide Ceramic Powders in a Eutectic CaCl₂-NaCl Melt: *Xiao Yan*¹; Mark Pownceby¹; Mark Cooksey¹; Marshall Lanyon¹; ¹CSIRO

A fused salt electrochemical process was investigated for synthesis of non-oxide ceramic powders directly from metal oxide, boric oxide, and carbon powders by electro-deoxidation. Sintered pellets of the mixed powders were designed to act as a composite cathode in the electrolytic cell. Electrolysis was carried out in molten CaCl₂-NaCl eutectic at 3.1 V and at 600-900°C under argon. The favoured cathodic reaction was the removal of the oxygen from the oxides to produce metal atoms that reacted with either the reduced boron atoms, forming a metal boride, or the carbon initially present in the sintered pellets to produce a metal carbide. The technical viability of the process was demonstrated by the electro-deoxidation of the sintered pellets of TiO₂/B₂O₃ and TiO₂/C to produce TiB₂ and TiC, respectively. Compared to the existing carbothermic reduction process, this new electrochemical process is much less energy intensive and may lead to lower production costs.

4:20 PM

Simulation of the Thermopower of Zn₄Sb₃: *Zhongliang Xiao*¹; Dan Liu¹; Qiyuan Chen¹; ¹Changsha University of Science and Technology

A new method was proposed to calculate the absolute thermopower of semiconductors from their density of states. In metals the electrochemical potential of the electrons is a unique function of the temperature. In semiconductors, the potential is also a unique function of temperature T, if valence electron concentration n_v in turn is a well-defined function of T. The temperature dependence of the potential can then be represented by two parts, one at constant electron concentration plus one due to the known change of the electron concentration. The second term is small in semiconductors. The thermopower of a semiconductor is related to the ratio either of two transport coefficients or of the gradients of the electrochemical potential of the electrons

and the temperature. A function obtainable from the density of states of the metal as illustrated on a thermopower isotherm of Zn₄Sb₃.

4:40 PM

Preparation of Metal Lithium by Molten Salt Electrolysis with Li₂CO₃ as Raw Material: *Jidong Li*¹; Mingjie Zhang¹; Tingan Zhang¹; Dan Li¹; Zhuo Zhang¹; ¹Northeastern University

Metal lithium was prepared by using graphite anode, wire cathode and a mixture of LiF-LiCl as the molten salt electrolysis with Li₂CO₃ as raw material in a laboratory cell. The back electromotive force was measured by continuous pulse-computer. The result is as follows: with the current density and temperature increasing, the back electromotive force increases in terms of logarithm and decreases respectively. When 2g Li₂CO₃ is added into the fused mass of LiF-LiCl, the back electromotive force decreases significantly by 0.8V. Then the back electromotive force comes back gradually with Li₂CO₃ consumed by electrolyzing continuously, so it is determined that the period of feeding Li₂CO₃ is 20mins. At 550°C, the 3.8g metal lithium was obtained finally by electrolyzing in 5A for 4h, which the current efficiency can reach 72%.

5:00 PM

The Influence of Different Calcination Atmosphere on the Photocatalytic Reactivity of Water Splitting to O₂ over Rutile TiO₂: *Daixin Wu*¹; Qiyuan Chen¹; Zhoulun Yin¹; Jie Li¹; ¹Central South University

The Rutile TiO₂ were prepared under air, Ar and H₂ calcination atmosphere by low temperature hydrolysis using Tetrabutyl titanate. Powers were characterized by by power X-ray diffraction, UV-vis diffuse reflectance and X-ray photoelectron spectroscopy. The influence of the calcination atmosphere on the photocatalytic reactivity of Rutile TiO₂ for oxygen production was investigated. The photocatalytic reactivity of Rutile TiO₂ prepared under air, Ar and H₂ atmosphere was compared under ultraviolet and visible light radiation with Fe³⁺ as electron acceptor. The results showed that Rutile TiO₂ prepared under Ar and H₂ atmosphere had higher photocatalytic activity for oxygen production than that prepared under air atmosphere. The oxygen production rates under ultraviolet irradiation were 427.5, 378.2 and 357 μmol · L⁻¹ · h⁻¹ respectively when Rutile TiO₂ was prepared under Ar, H₂ and air atmosphere. The oxygen production rates under visible light irradiation were 78.2, 52.2 and 13.5 μmol.

5:20 PM

Electrochemical Behavior of Pb-Ag-Bi Alloys as Anodes in Zinc Electrowinning: *Zhong Shui-ping*¹; Lai Yan-qing¹; Jiang Liang-xing¹; Li Jie¹; Liu Yexiang¹; ¹Central South University

A new type Pb-Ag(0.8wt%)-Bi(0~5wt%) alloy for used as anode in electrowinning of zinc from sulphuric acid electrolytes was prepared. The electrochemical and corrosion properties of this ternary lead alloys have been tested and compared with those of the Pb-Ag(1wt%) anodes used in industry. Results showed that the corrosion resistance and anodic overpotential of the new anodes was not affected when the content of Bi was less than 3 wt%, but when the content of Bi was 3 wt%, the anodic overpotential was about 40-80 mV lower than that of Pb-Ag(1wt%) alloy. The formation of oxide layers on the surface of these alloys was traced by cyclic voltammetric methods and the composition of the anodic oxide layers was characterized by X-ray and SEM analyses. The surface layer on the two type anodes examined was composed mainly of PbSO₄, α-PbO₂ and β-PbO₂. But different structure of the surface layer was observed.

General Abstracts: Electronic, Magnetic, and Photonic Materials Division: Session II

Sponsored by: The Minerals, Metals and Materials Society, TMS Electronic, Magnetic, and Photonic Materials Division, TMS: Alloy Phases Committee, TMS: Biomaterials Committee, TMS: Chemistry and Physics of Materials Committee, TMS: Electronic Materials Committee, TMS: Electronic Packaging and Interconnection Materials Committee, TMS: Nanomaterials Committee, TMS: Superconducting and Magnetic Materials Committee, TMS: Thin Films and Interfaces Committee

Program Organizers: Long Qing Chen, Pennsylvania State University; Sung Kang, IBM Corporation

Wednesday PM Room: 276
March 12, 2008 Location: Ernest Morial Convention Center

Session Chairs: Long Qing Chen, Pennsylvania State University; Sung Kang, IBM Corporation

2:00 PM

Lightning Causes and Effects – A Systematic Protection Approach for the Aluminum Industry: *Franco D'Alessandro*¹; ¹ERICO Products Australia Pty Ltd

The continuous production of primary aluminum relies on a reliable electricity supply and the use of data acquisition, automation and control technologies to maximise profits. The losses incurred as a result of a lightning incident in the aluminum industry cannot be underestimated, e.g., Alcoa Tennessee shutdown in April 2007 and the subsequent downtime of about 7 weeks. A key first step in today's highly technological environment is the implementation of a risk management plan, so the paper discusses how to carry out a lightning risk assessment. Secondly, the paper presents the theme that, whilst no single technology can guarantee 100% prevention of damage, a "six point protection approach" provides a comprehensive yet practical checklist covering the major damage mechanisms related to direct-strike, surge and transient effects. Finally, the paper discusses the importance of a low impedance ground plane and good connections throughout the site.

2:20 PM

Magnetic Domain Evolution and Strain Mechanism in Terfenol-D Crystals: *Yongxin Huang*¹; *Yongmei Jin*¹; ¹Texas A&M University

Phase field model is used to simulate the magnetic domain evolution and the corresponding deformation process in magnetostrictive Terfenol-D crystals. The model considers the two competing magnetization mechanisms, i.e., magnetization rotation and domain wall movement, addresses the magnetic field-induced deformation by magnetoelastic coupling through magnetostriction phenomenon, and takes into account the domain microstructure-dependent long-range magnetostatic and elastostatic interactions. The simulations quantitatively describe the magnetization and deformation processes. The results reveal the interplays of the two magnetization mechanisms, the interactions of magnetic domains with underlying crystallographic microstructures (growth twins, polycrystals), and the effects of compressive stresses on magnetostrictive behaviors.

2:40 PM

Magneto-Optical Study of Cobalt Ferrite Nanoparticles: *Byron Scott*¹; *Kevin Stokes*¹; ¹University of New Orleans

We present a magneto-optical study of $\text{Co}_x\text{Fe}_{1-x}\text{Fe}_2\text{O}_4$ nanoparticles, where $0 \leq x \leq 1$. The ferrite nanoparticles were produced using a generic wet-chemical synthesis procedure. Stoichiometric amounts of Fe^{2+} , Fe^{3+} and Co^{2+} salts are dissolved in a non-aqueous polar medium (diethylene glycol). A coprecipitation reaction with sodium hydroxide produces ferrite nanoparticles with average diameter of 6 nm. The nanoparticles can be stabilized in water, or, alternatively, the nanoparticles can be treated with a hydrophobic capping ligand with a carboxylic acid or amine head group and suspended in a non-polar organic solvent. Faraday rotation was measured on nanoparticle samples dried on an amorphous silica substrate. The magneto-optical spectra show the characteristic features of both Fe_3O_4 and CoFe_2O_4 as x increases as well as evidence of

electronic transitions involving both Co^{2+} and Fe^{2+} . The results are discussed in terms of the distribution of cations in the crystal lattice.

3:00 PM

Microwave Response of Patterned Nanosize Stripes of Exchange Biased Bilayers: *Leszek Malkinski*¹; *Minghui Yu*¹; *Donald Scherer*¹; ¹University of New Orleans

The exchange bias is the interface phenomenon originating from the spin coupling of two different magnetic materials and it manifests as asymmetry or a shift of the hysteresis loop. The understanding of this phenomenon is still incomplete and there exist a few competitive theories of the effect. Majority of research on exchange bias systems was carried out on thin film systems. We present experimental study of static and dynamic magnetic properties of exchange biased nanostructures of Co and IrMn. The samples have a form of arrays of nanosized stripes. They were fabricated by electron beam nanolithography, magnetron sputtering and lift off process. The results of the hysteresis loop measurements using SQUID magnetometer and microwave response by the means of ferromagnetic resonance technique of the arrays will be compared to those of the continuous reference bilayers. The results will be discussed in the light of existing models of exchange bias.

3:20 PM Break

3:50 PM

Monte Carlo Simulation Model for Charge Transport in Polymers: *Nenian Charles*¹; *Brandon Howard*¹; *Pedro Derosa*²; ¹Grambling State University; ²Louisiana Tech University/Grambling State University

Since the discovery that conjugated polymers can conduct electricity, provided adequate doping is added to them, there has been vast research to better understand the physical, electrical and chemical properties of these molecules. Furthermore, tools to simulate the conductive behavior are of great interest nowadays. A number of models have been proposed so far. A Monte Carlo-based method early proposed by Bäessler and coworkers have proved successful in reproducing a number of experimental findings. We propose a model based on the Bäessler model to study conduction in polymers which adds a realistic description of the polymer network. Configurational disorder is reproduced by disordered arrangements of hopping sites rather than by a parameter. In addition, the model proposed here allows for the association between hopping sites and polymers, thus intramolecular conduction can be distinguish from intermolecular conduction. The initial testing of this model vs. the Bäessler model has produced encouraging results.

4:10 PM

Structures and Properties of La and Sm-Doped BaTiO_3 Sputtered Films: Post-Annealing and Dopant Effects: *Cheng-Hui Wu*¹; *Jinn Chu*¹; *Sea-Fue Wang*²; *C. H. Lin*²; *Wen-Zhi Chang*¹; *V. S. John*¹; ¹National Taiwan Ocean University; ²National Taipei University of Technology

200-nm-thick La- and Sm-doped BaTiO_3 thin films with A/B ratio of unity fabricated by r.f. magnetron sputtering on the $\text{Pt/Ti/SiO}_2/\text{Si}$ substrate have been characterized. The effects of post-annealing and the amount of dopant on structure and electrical properties were studied. X-ray diffraction studies reveals that all the films show tetragonal BaTiO_3 crystal structure without any detectable second phase or reaction phase formation after annealed at 750°C. X-ray photoelectron spectroscopy results confirm that the dopant substitutes the A or B site and La_2O_3 and Sm_2O_3 are present in the BaTiO_3 structure, when the dopant content is more than 1.4La and 1.0Sm in atom%. The permittivity increases with increasing annealing temperature up to 750°C and may be due to the grain growth and better crystallinity. The leakage current property is found to vary with the type of dopant.

4:30 PM

Transparent Al-Doped ZnO Thin Films Synthesized by RF Magnetron Sputtering: *Soo Young Seo*¹; *Changha Kwak*¹; *Yongbyung Lee*¹; *Sunhong Park*²; *Seonhyo Kim*¹; *Sangwook Han*³; ¹POSTECH; ²Research Institute of Industrial Science and Technology; ³Chonbuk National University

Transparent and conductive Al-doped zinc oxide thin films were fabricated on Al_2O_3 substrates by a RF-magnetron sputtering procedure from a ZnO target mixed with a various wt% Al_2O_3 . The quantity of aluminum at the target was varied from 2 to 5 weight %. The structural and optical characteristics of Al-doped

ZnO thin-films were studied using field emission scanning electron microscopy (FE-SEM), X-ray diffraction (XRD), UV-VIS-IR and photoluminescence (PL) measurements. The XRD measurements revealed that all of Al-doped ZnO thin-films had a wurtzite crystal structure and had the (002) preferred orientation. We did not observe any extra peak from the XRD patterns. The best visual light transparency of the films was 90%. The band gap of the films was about 3.35 eV and the visual light absorption edge was about 350 nm. We will discuss the chemical and optical properties, comparing with the structural properties and Al-doping ratio.

General Abstracts: Structural Materials Division: Microstructure/Property Relations of Steels II

Sponsored by: The Minerals, Metals and Materials Society, TMS Structural Materials Division, TMS: Advanced Characterization, Testing, and Simulation Committee, TMS: Alloy Phases Committee, TMS: Biomaterials Committee, TMS: Chemistry and Physics of Materials Committee, TMS/ASM: Composite Materials Committee, TMS/ASM: Corrosion and Environmental Effects Committee, TMS: High Temperature Alloys Committee, TMS/ASM: Mechanical Behavior of Materials Committee, TMS/ASM: Nuclear Materials Committee, TMS: Product Metallurgy and Applications Committee, TMS: Refractory Metals Committee, TMS: Superconducting and Magnetic Materials Committee, TMS: Titanium Committee
Program Organizer: Ellen Cerreta, Los Alamos National Laboratory

Wednesday PM Room: 387
March 12, 2008 Location: Ernest Morial Convention Center

Session Chair: To Be Announced

2:00 PM

Substructural Analysis of Adiabatic Shear Bands in Standard and Enhanced Rebar Steel Using Transmission Electron Microscopy: *Lisa Dougherty*¹; Ellen Cerreta¹; George Gray¹; Carl Trujillo¹; Mike Lopez¹; ¹Los Alamos National Laboratory

Rebar steel that has been enhanced in composition and microstructure for optimal corrosion and strength characteristics exhibits greater microstructural instability at high strain rates than standard rebar. Adiabatic shear bands have been observed to form in enhanced rebar steel at strain rates below that required for shear band formation in standard rebar, indicating an increased propensity for shear localization in the enhanced rebar steel. Optical microscopy and scanning electron microscopy, as well as electron backscattered diffraction, indicate complete annihilation of the original microstructure within the shear bands of enhanced rebar, whereas residual, highly deformed grains can be found within the shear bands of standard rebar. This current study utilizes transmission electron microscopy to examine the microstructure inside the shear bands and at the boundaries of the sheared regions in both the standard and the enhanced rebar steels to understand the differing mechanisms operating during shear localization in these materials.

2:20 PM

Microstructure Evolution in Nano/Submicron AISI 301 Austenitic Stainless Steel: Shreyas Rajasekhara¹; Paulo Ferreira¹; Pentti Karjalainen²; Antero Kyrolainen³; ¹University of Texas at Austin; ²University of Oulu; ³Outokumpu Stainless Oy

Nano/submicron grained AISI 301 austenitic stainless steel has been achieved by heavy cold rolling to 52% reduction, to induce the formation of martensite, and subsequent annealing at 600°C, 800°C and 1000°C from 1 to 100 seconds. The microstructural evolution was analyzed using transmission electron microscopy (TEM) and X-ray diffraction (XRD), which reveal that the as-cold rolled samples are textured and primarily consist of heavily deformed lath-type martensite. Subsequent annealing at 600°C results in negligible martensite to austenite reversion, while the texture is retained from the cold-rolled samples. However, upon annealing at a higher temperature of 800°C and 1000°C, significant austenite reversion and M23C6 carbide precipitation is observed. As carbide precipitation typically occurs in stainless steels that are annealed for long durations (>0.1 hours/360 seconds), this work shows for the first time carbide

precipitation in short annealed (1, 10 and 100 seconds) commercial austenitic stainless steels.

2:40 PM

Oxide-Dispersion Strengthened Ferritic Alloys by Internal Oxidation: *Joachim Schneibel*¹; Sang Shim¹; ¹Oak Ridge National Laboratory

Oxide-dispersion strengthened (ODS) ferritic alloys such as MA956, MA957, and PM2000 contain high number densities of fine oxide particles with diameters as small as a few nm. Their processing involves mechanical alloying of metallic powders with Y2O3, which is an expensive and energy-intensive process. An alternative process, which is used commercially in ODS copper alloys, is internal oxidation. This process was applied to the intermetallic compounds Fe7Y2 and Fe11TiY at temperatures ranging from 600 to 1000°C. Oxide particles or lamellae as small as ~10 nm were obtained, and the room temperature nano-hardness increased significantly with decreasing particle size. Preliminary results on the internal oxidation of Fe-Ti-Y solid solution alloys will also be presented.

3:00 PM

Structure and Strength of Quenched Martensite in Fe-C Steels: *Oleg Sherby*¹; Jeffrey Wadsworth²; Donald Lesuer³; Chol Syn³; ¹Stanford University; ²Battelle Memorial Institute; ³Lawrence Livermore National Laboratory

The lattice parameters of quenched martensite change discontinuously as a function of carbon content. The discontinuity occurs at 0.6 wt%C, designated as the H point. Martensite in quenched Fe-C steels is described based on the formation of two different, but sequential, martensitic transformations. The first transformation, designated as primary martensite, is the only transformation process for steels from nearly zero to the H point. Primary martensite (known as lath martensite) is interpreted as evidence for the formation of martensite with a BCC structure containing meta-stable carbide particles. Above the H point, the structural changes during quenching occur by the formation of primary martensite followed by secondary martensite where the BCT structure is obtained. Secondary martensite is the acicular structure of martensite. The hardness of quenched martensite is reviewed and explained on the basis of the two different martensites. Nano-carbides and fine cell/subgrain structures are the principal contributors to strength.

3:20 PM

Textural Characteristics and Magnetic Properties of High Strength Electrical Steels: *Sam Chang*¹; Hee Park¹; ¹Pohang University of Science and Technology

For the recent development of new high strength electrical steel to meet the requirement for high fatigue resistance of core materials using for large electric motors, it is of important to investigate the textural characteristics and its relation with magnetic properties and fatigue strength. The steels are designed to obtain yield strength of 450 N/mm² and core loss less than 3 Watt/Kg and some special elements like Nb, Sn, and Ni are added to 3%Si steel to increase strength as well as to improve magnetic properties. Textural features depending on alloying elements are quantitatively analyzed and relationship of texture with tensile strength and fatigue strength is clarified.

3:40 PM Break

4:10 PM

The Effect of Boronizing and Austempering on the Wear Behavior of a Ductile Iron: Seckin Akay¹; Murat Baydogan¹; Huseyin Cimenoglu¹; Eyup Kayali¹; ¹Istanbul Technical University

Boronizing is a surface hardening method to improve hardness and wear resistance creating a hard layer at the surface. Austempering is an isothermal annealing to improve strength and toughness giving an acicular ferrite morphology in the microstructure. In this study, combining effect of these two processes on surface hardness and wear resistance were investigated. A ferritic ductile iron was boronized at 900°C for 90 min. and then transferred to an isothermal salt bath at 300°C and held at that temperature for several durations, and then air cooled. Borided layer was characterized by XRD and SEM. Microhardness measurements were performed from the surface to the center of the specimen, indicating that a high hardness of 1200 HV was obtained at the surface. Reciprocating wear tests performed revealed that wear resistance

increased 6.5 times after boronizing and austempering when compared to the as cast state.

4:30 PM

Effect of Strain Rate on High Temperature Mechanical Properties of PM2000 Alloy for Advanced Nuclear Reactor Applications: Md Rahman¹; K. Raja¹; Carl Nesbitt¹; Manoranjan Misra¹; ¹University of Nevada Reno

Next generation nuclear reactors will operate at relatively higher temperatures and severe environmental conditions. It is critical to understand the behavior of structural materials under these severe conditions. Ferritic ODS alloy (PM 2000) which has excellent creep and oxidation resistance at temperature up to 1200°C is a candidate for these purposes. In this study high temperature mechanical properties of PM2000 has been evaluated as a function of strain rate. Failed specimens were characterized by using an ex-situ Scanning Kelvin Probe Force Microscope which measures the variation of work function of specimen surface due to microstructural variations and can be used for estimating the remnant lifetime of the component. Preliminary Results showed a decrease in stress and strain as the strain rate decreased from 1.0×10^{-3} s to 1.0×10^{-5} s. Results from mechanical tests as well as characterization of failed specimen using SKPFM, SEM, EDX and optical microscopy will be presented in the paper.

4:50 PM

Passive Film Characteristics and Corrosion Performance of 9Cr/0.1C Microcomposite Steel in Simulated Concrete Pore Solutions: Greg Kusinski¹; Mauricio Mancio²; Tom Devine²; ¹Clemson University; ²University of California, Berkeley

The passive film formed on the Microcomposite steels, (wt%: C 0.1, Cr 9.0, Mn 0.6, bal. Fe; microstructure consisting of multilayers of lath martensite with thin films of retained austenite at lath boundaries), in highly alkaline environments was investigated. A series of in-situ Surface-Enhanced Raman Spectroscopy (SERS) experiments were conducted in conjunction with cyclic potentiodynamic polarization curves over a wide range of potentials, in order to characterize the formation and breakdown mechanisms of the passive films. A solution of 0.55M KOH + 0.16M NaOH, with and without chlorides (0% and 3.5% NaCl), was used for the SERS experiments. In addition, the corrosion performance of Microcomposite steels as a function of pH (9–14) and ionic strength of the solution (from 10⁻⁵ to 1M) was evaluated via polarization resistance (Rp) experiments, and compared to the performance of regular carbon steel rebar.

5:10 PM

Structural Strength Variation of Freight Car Carbody during Static Loadings: Jeongguk Kim¹; Jung-Won Seo¹; Sung-Cheol Yoon¹; Sung-Tae Kwon¹; ¹Korea Railroad Research Institute

The structural strength assessment for carbody of freight car in railway applications was performed using engineering analysis techniques to verify the structural strength of newly manufactured carbody. The freight car was designed with A441 steel and stainless steel for the railway transportation. Prior to the assessment of structural strength, finite element method (FEM) characterization was used for the stress and structural analyses on stress distribution in a carbody of freight car. The strain gages were attached on the carbody based on the FEM results. The actual vertical loading test and horizontal compression loading test were conducted, and the results were compared with the previous FEM results. In this investigation, the evaluation method for the structural strength in a structural component has been introduced using several engineering techniques, and experimental and theoretical results were compared.

Hael Mughrabi Honorary Symposium: Plasticity, Failure and Fatigue in Structural Materials - from Macro to Nano: Mechanical Properties of Ultrafine-Grained (UFG) Metals II

Sponsored by: The Minerals, Metals and Materials Society, TMS Structural Materials Division, TMS Materials Processing and Manufacturing Division, TMS: High Temperature Alloys Committee, TMS/ASM: Mechanical Behavior of Materials Committee, TMS: Nanomechanical Materials Behavior Committee
Program Organizers: K. Jimmy Hsia, University of Illinois, Urbana-Champaign; Mathias Göken, Universitaet Erlangen-Nuernberg; Tresa Pollock, University of Michigan - Ann Arbor; Pedro Dolabella Portella, Federal Institute for Materials Research and Testing; Neville Moody, Sandia National Laboratories

Wednesday PM
March 12, 2008

Room: 386
Location: Ernest Morial Convention Center

Session Chairs: Marc Meyers, University of California, San Diego; Oliver Kraft, Forschungszentrum Karlsruhe

2:00 PM Keynote

Mechanical Properties of Nanocrystalline Ni as Studied by Nanoindentations and Creep Tests: Mathias Göken¹; Johannes Mueller¹; ¹University Erlangen-Nürnberg

Nanocrystalline Ni with average grain sizes between 25 nm and some hundred nm was produced by pulsed electrodeposition (PED) to study the mechanical properties in the temperature range from 298 K to 473 K by nanoindentation tests and compression creep tests. Nanoindentation is a suitable method to characterise the mechanical properties of these materials including strain rate sensitivity. The maximum flow stress, the strain rate sensitivity of flow stress and the rate of work hardening increase with decreasing grain size. The results are compared with data available for coarse grained and ultrafine-grained materials and an interpretation of the data is given in terms of the responsible deformation mechanism. It is shown by Auger analysis of in-situ fractured specimens that impurities which are deposited during the electrodeposition process at the grain boundaries play an important role on the deformation behavior.

2:30 PM Invited

Stress Generation Mechanisms in Thin Films Impacted by Energetic Ions: Sulin Zhang¹; Sachin Terdalkar²; Joseph Rencis²; K. Jimmy Hsia¹; ¹National Science Foundation; ²University of Arkansas

Molecular dynamics simulations are performed to study the stress generation mechanisms in carbon thin films in the forms of graphene sheet (2D) and diamond (3D) impacted by energetic carbon neutrals. The simplicity of the 2D cantilever graphene sheet model enables direct observation of free-end deflection during the impact, while the 3D model captures more realistic physics. Both simulations demonstrate that the stress due to the impact of energetic C neutrals is strongly dependent on the incident energy. At low-energy impact, the film undergoes tensile stress; a transition from tensile to compressive stresses occurs at an intermediate impacting energy; the compressive stress peaks at around 50eV; further increasing the incident energy lowers the compressive stress. Examinations of the atomic stress and film microstructures reveal that the formation of the film stress is attributed to competing mechanisms between production and annihilation of point defects. A simple analytical model satisfactorily explains the results.

2:50 PM Invited

Deformation of Nanocrystalline Metals and Alloys Investigated by Microcompression and Nanoindentation: Ravi Kottada¹; Ruth Schwaiger¹; Jörg Weismüller¹; Jürgen Markmann¹; Yulia Ivanisenko¹; Oliver Kraft¹; ¹Forschungszentrum Karlsruhe

Pure nanocrystalline metals have been studied with an overwhelming interest in the last two decades due to their attractive and unusual mechanical properties. However, only little information is available on the mechanical behavior of nanocrystalline metallic alloys. Here, we show comparative micro-compression and nanoindentation test results for nanocrystalline metals and alloys, namely electrodeposited nanocrystalline Ni and Ni-20%Fe, and Pd and

Pd-Au prepared by inert gas condensation and subsequent densification via high pressure torsion. Micro-columns with diameters ranging from 1 – 3 μm were prepared by Focused Ion Beam (FIB) machining. Subsequently, the micro columns were uniaxially compressed to strains of 10-50% using a nanoindenter equipped with a flat diamond punch. Nanoindentation experiments at various indentation strain rates complement the mechanical testing. The results, which were analyzed with respect to strain hardening and strain rate sensitivity indicate that the alloyed metals show a weaker strain rate sensitivity compared to their pure counterparts.

3:10 PM

Influence of Grain Boundary Character on Nanocrystalline Plasticity: *Mark Tschopp*¹; Shreevant Tiwari²; Sudipto Ghosh²; David McDowell¹; ¹Georgia Institute of Technology; ²Indian Institute of Technology Kharagpur

The objective of this research is to use atomistic simulations to investigate the influence of the grain boundary character distribution on the plasticity of nanocrystalline materials. In this work, we generate a 3D periodic columnar grain structure about the $\langle 110 \rangle$ tilt axis using an algorithm that enables the preferential assignment of low order CSL boundaries. Three nanocrystalline configurations are generated: one with increased $\Sigma 3$ content, a random distribution, and one with increased $\Sigma 9$ content (lower nucleation stresses). Deformation simulations under uniaxial tension show that the strength of nanocrystalline materials is enhanced with higher populations of $\Sigma 3$ boundaries. However, the grain boundary plane inclination also plays a role in plastic deformation. Last, the influence of the grain size in plastic response is investigated to determine if increasing the low order CSL boundary content has a diminished influence in regimes where grain rotation and grain boundary sliding are the dominant deformation mechanisms.

3:25 PM

Mechanical Properties of Nanostructured Al-Cu Alloy Produced by High Energy Ball Milling and Hot Isostatic Pressing: T. Shanmugasundaram¹; V. Subramanya Sarma¹; B. Murty¹; Holger Saage²; *Martin Heilmaier*²; ¹Indian Institute of Technology Madras; ²Otto von Guericke University

Nanostructured materials exhibit usually improved strength but at the expense of ductility. The development of bi-modal grain size distribution with micron-sized grains embedded in a matrix of nanostructured grains has been shown to restore ductility without significant loss in strength. In the present work, we present the mechanical properties of nanostructured precipitation hardening Al-Cu alloy prepared by high energy ball milling of the inert gas atomized Al-Cu alloy powder. After milling, X-ray diffraction (XRD) analysis was used to evaluate the grain size. After 15 h of milling, 30 nm crystallite size was obtained. Subsequently, these nano powders were blended with 15 and 30 wt.pct. coarse alloy powder (1 to 10 μm). Blended powders were degassed and consolidated by hot isostatic pressing. The microstructures and mechanical properties of the samples will be characterized with the aim of establishing optimized microstructures and processing conditions for simultaneously achieving high strength and ductility.

3:40 PM Break

3:50 PM Invited

Micro and Nano Defects Formation During Grain Refinement by ECAP: *Rimma Lapovok*¹; Peter McKenzie¹; Dacian Tomus¹; Yuri Estrin¹; Terry Lowe²; ¹Monash University; ²Los Alamos National Laboratory

Severe plastic deformation via ECAP is a method to refine the grain size of metals. Generally, UFG metals have a superior strength and high cycle fatigue life compared to their coarse grained counterparts. However, the fatigue performance of various UFG metals is not always consistent with trends in tensile properties due to defects introduced during ECAP. A study of micro defects, such as decohesion of particles within the matrix, brittle fracture of particles, formation of voids at the grain boundaries have been performed using SEM and TEM. To investigate the formation of nano-defects, namely the voids of 1 to 200 nm size, Small-Angle Neutron Scattering technique has been employed. The SANS measurements on CP-Ti processed by ECAP revealed that defects in the range of 5-20 nm were not influenced by the level of back-pressure, whereas defects of the 20-200 nm size could be manipulated by application of hydrostatic pressure.

4:10 PM Invited

Analytical and Molecular Dynamics Modeling of Void Growth: Sirirat Traiviratana¹; Eduardo Bringas¹; David Benson¹; *Marc Meyers*¹; ¹University of California

Void growth is the principal failure mechanism in ductile metals. Yet, it is only recently that a dislocation mechanism was postulated by Lubarda et al (Acta Mat, 1397, 2004), who showed that both prismatic and shear loops nucleating at the void surface can provide the material transport required for growth. Atomistic simulations on monocrystalline and polycrystalline copper (using the Mishin-Farkas potential) reveal the detailed nature of the dislocation activity surrounding a growing void. The emission of dislocations is the first stage, followed by their reactions and interactions. Calculations are carried out for voids having different sizes and predict different critical stresses for plasticity, in disagreement with the Gurson model, which is size independent. The calculations are applied to grain-boundary voids, important in polycrystals.

4:30 PM

Single Crystals Deformed by High Pressure Torsion: *Martin Hafok*¹; Reinhard Pippan¹; ¹Erich Schmid Institute of Materials Science

The fragmentation process of high pressure torsion deformed samples is commonly studied by the use of polycrystalline specimens. Usually it is widely accepted that the interaction between adjacent crystallites facilitates the fragmentation process, but how is the fragmentation process influenced in a single crystalline material? On account of this, single crystalline nickel samples were manufactured in the form of small discs with $\langle 111 \rangle$ and $\langle 001 \rangle$ orientation parallel to the cylinder axis to characterize the evolution of microstructure and microtexture. Due to the shear deformation a characteristic microtexture has developed that exhibits preferred orientations, depending on the alignment of the crystal system with respect to the deformation state. In addition to the characterisation of the microstructure and microtexture by BSE and EBSD measurements, the torque during the deformation can be readily measured and analysed with respect to the two different crystallographic orientations.

4:45 PM

Mechanical Anisotropy in Ultrafine Grained Copper and IF Steel Processed via Equal Channel Angular Extrusion (ECAE): Effects of Grain Morphology and Texture: *Mohammed Haouaoui*¹; Majid Al-Maharbi¹; Ibrahim Karaman¹; Hans Maier²; ¹Texas A&M University; ²University of Paderborn

The effect of strain path and level on the flow stress anisotropy and Bauschinger effect (BE) in UFG OFHC copper and IF steel was investigated considering grain morphology, dislocation mean free path and texture evolution. The materials were deformed via multipass ECAE using a 90° square die. The room temperature experiments were conducted under tension and compression along three perpendicular directions in each billet. Bauschinger experiments were conducted in both forward tension/reverse compression and forward compression/reverse tension modes. The strong anisotropy in flow stress, softening and BE were correlated to grain morphology and texture. The observed stronger tension strength and tension/compression asymmetry was attributed, in addition to the effect of hydrostatic pressure on dislocations, to the dislocation mean free path via grain morphology. The comparison between copper (fcc) and IF steel (bcc) elucidated further the contribution of texture on the flow anisotropy in UFG materials.

5:00 PM

High-Strain-Rate Shearing of Nanocrystalline Aluminum Film: *Buyang Cao*¹; Zhizhou Zhang¹; Kaliai Ramesh¹; ¹Johns Hopkins University

Nanocrystalline aluminum film is made through vapor deposition with a mean grain size of 30nm. It is then subjected to high-rate shearing deformations with strain rates of 10^3 – 10^6 s^{-1} . The experimental configuration is that of a compression-torsion kolsky bar, where the specimen is a thin film mounted on a stainless steel ring. Superimposed pressures of 400 MPa are also developed. The experimental technique provides high-rate stress-strain curves as well as deformed films for microstructure analysis. The results of microscopic characterization using TEM and HRTEM are described.

5:15 PM

Effect of Annealing Twins on Microstructure Evolution in Electrodeposited Nanostructured Ni: *Indranil Roy*¹; Farghalli Mohamed¹; ¹University of California, Irvine

This paper presents evidence for the effect of annealing twin boundaries on microstructure evolution in electrodeposited nanostructured Ni based. This evidence is illustrated by means of transmission electron micrographs (TEM) and orientation maps generated by electron backscatter diffraction (EBSD). Statistics of annealing twin boundaries and corresponding lamellar spacing as a function of several variables, including grain size, temperature, and annealing time, to engineer a microstructure having a maximum twin density are also investigated. The results are discussed with reference to the role of annealing twinning not only in improving intergranular corrosion resistance but also in simultaneously increasing strength and ductility in nanocrystalline materials.

5:30 PM

Application of the Normalization JIC Fracture Methodology to Ductile Polymers: *Eric Brown*¹; ¹Los Alamos National Laboratory

The single specimen normalization technique is extensively investigated for ductile polymers. This employs an analytical solution with power law behavior for tip blunting and crack initiation and transitions smoothly to a linear relationship for steady-state crack growth to accurately estimate the position of the crack tip throughout the test. The evolution and validation of the normalization technique and its application to ductile polymers is discussed. Results are presented for PTFE7C, PCTFE, Kel-F800, THV500, and PEEK450G with a focus on the effects of transitioning through the glass transition temperature and temperature induced phase transitions. Results are compared to the literature and presented in the context of extensive fractography to elucidate fracture mechanisms on length scales from the nano- to macro-scale.

Magnesium Technology 2008: Corrosion, Surface Finishing and Joining

Sponsored by: The Minerals, Metals and Materials Society, TMS Light Metals Division, TMS: Magnesium Committee

Program Organizers: Mihriban Pekguleryuz, McGill University; Neale Neelameggham, US Magnesium LLC; Randy Beals, Chrysler LLC; Eric Nyberg, Pacific Northwest National Laboratory

Wednesday PM Room: 291
March 12, 2008 Location: Ernest Morial Convention Center

Session Chair: Neale Neelameggham, US Magnesium LLC

2:00 PM

3D Observation of Corroding AZ91D by Synchrotron-Radiation Based Microtomography: Frank Witte¹; Norbert Horst²; Hajo Dieringa²; Michael Störmer²; Felix Beckmann²; Karl Kainer²; ¹Hannover Medical School; ²GKSS Research Center

The beta phase Mg₁₇Al₁₂ develops during casting and is assumed to influence strength as well as corrosion properties of Mg Al alloys. The distribution of beta-phases and Al-Mn phases after corrosion tests can be determined using the 2D technique of standard metallography. This destructive method has some limitations especially with the brittle and dissolvable magnesium corrosion products. Synchrotron-radiation based microtomography (SRμCT) was used to obtain a non-destructive 3D image the local distribution of beta phases and Al-Mn phases in un-corroded AZ91D alloy as well as in its corrosion layer after 8 hours immersion in 3.5% NaCl. SRμCT results have been supplemented by XRD and standard methods of metallography.

2:20 PM

Characteristics of the Phosphate Conversion Coating on AZ91D Magnesium Alloy and Its Corrosion Resistance: *Suqiu Jia*¹; S.S Jia²; Yao Jun²; S.M. Yu¹; ¹School of Materials Science and Engineering, Changchun University of Technology; ²Key Laboratory of Automobile Materials, Jilin University

Phosphate treatment is one of effective ways to prevent magnesium alloy from attack. In the paper characteristics of phosphate conversion coatings and

corrosion resistance of the coatings on AZ91D magnesium alloy were studied. Three phosphatation solutions containing phosphoric acid, phosphate ions, nitrates and nitrites added with or without zinc ions and fluorides were used. The morphology and composition of the coatings were analyzed by SEM, EDX, XRD and TEM. The phosphate coating for bath 1, which composed of amorphous Mg₃(PO₄)₂ and Mg₁₇Al₁₂, is different from those for other two solutions. The phosphate coatings of bath 2 and bath 3 are mainly composed of tetra-hydrated zinc phosphate by XRD and TEM. The corrosion potential of the coatings in 3.5% NaCl solution is ranked in the following decreasing order: Ebath2>E bath3>E bath1 >EAZ91D.

2:40 PM

Electrochemical Fabrication and Biocompatibility of the Hydroxyapatite Coating on Magnesium Alloy for Implanted Applications: *Shaokang Guan*¹; Li Peng¹; Qun Luo¹; Cuilian Wen¹; ¹Department of Materials Science and Engineering, Zhengzhou University

The hydroxyapatite coating composed by needle-like hydroxyapatite(HAP) fiber was fabricated on magnesium alloy substrate by electro-deposition method to improve the corrosion resistance and biocompatibility. There were vibrations of HPO₄²⁻, PO₄³⁻, CO₃²⁻ and OH⁻ in the coating, which was the composition of bone. The biocompatibility of the coating was deeply investigated. It reveals that there was obviously specific mass gain in the first week and the HAP coating could protect the Mg substrate from quickly degradation during the first period of immersion. The degradation in psychological environment could not cause the rise of magnesium in the serum. The HAP coating could reduce the corrosion of magnesium alloy at the first period of implanting and the HAP/Mg could stimulate the growth of the bone tissue. The histopathology result further testified that HAP/Mg could improve the circulation of the blood of bone defects and stimulate the growth of new bone tissue.

3:00 PM

Electroless Ni-P Plating on Mg-10Li-1Zn Alloy: *Hua Zhang*¹; Guangchun Yao¹; Shulan Wang²; Chunlin Liang¹; ¹School of Materials and Metallurgy, Northeastern University; ²School of Science, Northeastern University

A uniform Ni-P coating was successfully obtained on Mg-10Li-1Zn alloy by the electroless plating technology. The pretreatment process, the micro-morphology and the corrosion resistance of the coating were studied. Experimental results indicated that the treated surface was coarser with prolonging the acid pickle time, and the fluoride film on surface of the alloy became thicker with increasing activation treatment time. Moreover, the pretreatment process obviously influenced the micro-morphology of the electroless Ni-P plating. Under the optimal pretreatment process of acid pickle for 20s and activation for 10min, the Ni-P coating deposited was compact and even, which was connected tightly to the substrate. The result of potentiodynamic polarization showed that the Ni-P coating had good corrosion resistance, which could provide an effective protection for Mg-10Li-1Zn alloy.

3:20 PM

Gas Dynamic Spray (GDS) Coatings for Improving Galvanic Corrosion and Sliding Wear Resistance of Magnesium Alloys: *Jiaren Jiang*¹; Lijue Xue¹; ¹National Research Council of Canada (NRC)

Magnesium alloys are very attractive for many industrial applications, particularly, for reducing vehicle weight in the automobile and aerospace industry to reduce greenhouse gas emission. However, the poor wear and galvanic corrosion resistance seriously limits the wider industrial applications of magnesium alloys. In this paper, the improvement of galvanic corrosion and dry sliding wear resistance of magnesium alloys has been investigated by applying aluminum-based coatings on cast AZ91D and AM60B magnesium alloy substrates using gas dynamic spray (GDS) process. It is shown that GDS coatings can be directly applied on dry-machined or cast magnesium alloy substrate with very good bonding without requiring special surface preparations. Salt spray testing showed excellent galvanic corrosion protection results for die-cast AM60B magnesium alloy by applying the developed innovative GDS coatings. The dry sliding wear resistance of the cast magnesium alloys is also significantly improved by the aluminium-based GDS coatings.

3:40 PM Break

WEDNESDAY PM

4:00 PM

The Microstructure and Performance of AZ31 Joint Welded by Gas Tungsten Arc: *Yefeng Bao*¹; Yongfeng Jiang¹; ¹Hohai University

Welds of AZ31 magnesium alloy was carried out using gas tungsten arc (GTA) welding. The microstructures of AZ31 magnesium alloy base metal, heat affected zone(HAZ) and weld metal were investigated by optical and scanning electron microscopy (OM and SEM) and EDS. The fusion line between weld metal and HAZ was distinct. The HAZ was overheated and the grain size was coarser. However, the grain size of weld, which was quenched like casting and fine equiaxed grains were formed, was smaller than that of base metal and HAZ. The discontinuous network phase, Mg₁₇Al₁₂ and Mg₁₇(AlZn)₁₂ and divorced eutectic distributed around grain boundary in weld metal was detected. The hardness of weld metal was higher than base metal, where, was lower than HAZ. The corrosion resistances in weld and base metal were similar, in contrast, that of HAZ was lower.

4:20 PM

Influence of Cutting and Non-Cutting Processes on the Corrosion Behavior and the Mechanical Properties of Magnesium Alloys: *Martin Bosse*¹; ¹Leibniz Universität Hannover

An important aim for the automotive industry is to reduce vehicle weight in order to decrease fuel consumption and emission of CO₂. The use of light metals as construction materials is generally considered of key importance for the future. Magnesium alloys fulfill the demands of a low specific weight with excellent machining properties and high recycling potential. The low corrosion resistance in comparison with other light materials is one of the reasons for the rare application as construction material. The aim of the presented joint research project within the priority program 1168 of the German Research Foundation is to influence the mechanical properties and corrosion resistance by cutting processes and mechanical surface treating through deep rolling. The corrosion and mechanical properties are significantly affected by the surface and subsurface properties of the workpiece. Therefore the influence of surface treatment and different alloy compositions on the corrosion rate has been studied.

4:40 PM

Mechanical Properties of Self-Pierce Riveted Joints of Magnesium: *William Song*¹; Y. Durandet¹; M. Easton²; S. Blacket³; M. Brandt¹; ¹IRIS, Swinburne University of Technology; ²Monash University; ³Henrob (UK) Party Ltd.

Magnesium-to-magnesium and aluminium-to-magnesium joints of various ply thicknesses and alloys were produced using a thermally assisted self-pierce riveting (SPR) technique to prevent cracking of the magnesium ply placed on the bottom in the design of the joint. Materials included; 2 to 3mm thick high pressure die cast AM50 and AM60 alloys, 3.3mm thick strip cast AZ31-O, 2mm thick Al 5005-H34 sheet, and 1.5 or 3mm thick Al6060-T5 extruded plate. The mechanical properties of single-point joint specimens were assessed by static lap shear tensile testing. Maximum loads of 2500N to 7200N were obtained, and specific absorbed energy values were determined from measurements of area under the curve up to the maximum load displacement. The effects of ply thickness and alloy, rivet type, size of test piece or joint overlap on the properties of the joints are presented and discussed.

5:00 PM

Micro Galvanic Corrosion Behavior of Mg Alloys as a Function of Aluminum Content: *Mridula Bharadwaj*¹; Shashank Tiwari¹; Yar-Ming Wang¹; Vijayalakshmi Mani¹; ¹General Motors

The corrosion behavior of the cast Mg-Al alloys was studied as a function of varying Al concentration. The beta phase is cathodic to the more reactive (anodic) primary phase called the alpha phase and hence it is critical to control the amount and distribution of this beta phase around the alpha phase. We present the polarization and direct galvanic current measurement results of the above alloys along with electrochemical impedance spectroscopy response of the surface oxide layer. These results are presented in correlation with the microstructural mapping of component phases to interpret the beta phase functionality. It was observed that a continuous network of the beta phase around the alpha phase imparts anodic-barrier role to the beta phase. The objective of these studies is to better design the Mg alloy microstructure so as to minimize the micro galvanic corrosion between component microstructural phases.

5:20 PM

New Bio-Absorbable Magnesium Alloys for Medical Applications: *Anja Hänzli*¹; Mischa Weder¹; Bodo Gerold²; Jörg Löffler¹; Peter Uggowitzer¹; ¹ETH Zurich; ²Biotronik GmbH and Company

Today, stenting is a well-established technique in the treatment of vascular diseases. Stents provide mechanical support to blood vessels and are generally permanent implants. Recent studies, however, have demonstrated the potential of bio-absorbable devices in the field of vascular intervention. The two new bio-absorbable magnesium-based alloys described in this study approach the mechanical and electro-chemical properties required in stents. After extrusion both reveal fine and even microstructures with grains smaller than 10 µm generating exceptional plasticity at ambient temperature. One alloy features high uniform elongation of 17% at a tensile strength level of 270 MPa, while the other reaches a superior 20% at 250 MPa. The alloys' outstanding mechanical properties are accompanied by good electro-chemical performance in a simulated physiological medium, manifested in slow and homogeneous degradation. The application potential of these new alloys in the field of vascular intervention seems very promising.

5:40 PM Invited

Thread Forming In Magnesium Alloys: *Klaus Pantke*¹; ¹University of Dortmund

With cold forming tapping tools, it is possible to produce internal threads by cold forming. Due to this, thread strength could be significantly enhanced. The core requirement for cold forming is the adequate plasticity of the workpiece material. Insufficient plasticity of magnesium alloys limits cold tap forming. A new process of pre-forming tap offers a good opportunity to handle the described problem. To implement this, threads are produced in a two-stage operation. In the first step, an incomplete thread will be generated (machined) by a modified thread tool. The diameter of this tap is slightly less than the normal tap. In the second step, a cold forming tap is finishes the thread to final diameter. Through this procedure it is possible to increase thread strength up to 40 percent. This article will address the microstructure influence of thread forming in magnesium alloys and the resulting thread strength.

Magnesium Technology 2008: Creep Resistant Magnesium Alloys

Sponsored by: The Minerals, Metals and Materials Society, TMS Light Metals Division, TMS: Magnesium Committee

Program Organizers: Mihriban Pekguleriyuz, McGill University; Neale Neelameggham, US Magnesium LLC; Randy Beals, Chrysler LLC; Eric Nyberg, Pacific Northwest National Laboratory

Wednesday PM

March 12, 2008

Room: 292

Location: Ernest Morial Convention Center

Session Chair: To Be Announced

2:00 PM

Creep and Hot Working Behaviour of a New Magnesium Alloy Mg-3Sn-2Ca: Norbert Hort¹; Kamineni Rao²; Tarek Abu Leil¹; Hajo Dieringa¹; V.Y.R.K. Prasad³; Karl Kainer¹; ¹GKSS Research Center; ²City University Hong Kong

With regard to the limited number of magnesium alloys in use, an approach has been undertaken to develop a new class of magnesium alloys based on the system Mg-Sn-Ca. From recent investigations the alloy Mg₃Sn₂Ca has been identified as one of the most promising magnesium alloys. It will be shown that this alloy offers superior creep properties even compared to the creep resistant alloy AE42. Mechanical properties will be presented as well as results from compressive creep experiments at 80 MPa and temperatures of 135-175°C. Additionally, the Mg₃Sn₂Ca alloy also offers good hot deformation behaviour in the temperature range of 300-550°C and deformation rates of 10⁻³-10⁻¹ s⁻¹, as revealed by the processing maps generated for the alloy. Compared with the most widely used alloy AZ31 the Mg₃Sn₂Ca can be easily hot worked over the entire temperature range investigated at fairly high strain rates, and the alloy recrystallized completely.

2:20 PM

Creep Properties and Texture Evolution in Hot Processing of Creep Resistant Magnesium Alloys: *Dimitry Sediako*¹; Michael Gharghoury¹; ¹National Research Council of Canada

Recent efforts to develop high-temperature creep-resistant alloys for automotive applications have resulted in a number of experimental alloys. Chemical composition and the casting/rolling production routes frequently determine the cost and properties of the wrought material. The scope of this study was limited to evaluation of creep properties and texture evolution for the following alloying systems: Mg-Al-Ca, Mg-Al-Sr, Mg-Al-RE, and Mg-Zn-RE. Crystallographic texture strongly influences the deformation behaviour of magnesium alloys during hot forming operation. Neutron diffraction was used to characterize the texture of several creep resistant alloys produced using exactly the same sequence of permanent-mold casting and one-stage extrusion processes. Alloys with large variations in chemical composition were used in order to clearly show the effects of the major alloying elements on the resulting microstructure, crystallographic texture, and high-temperature creep properties.

2:40 PM

DSM's High Performance HPDC Alloys as a Replacement to A380 Aluminum Alloy: *Boris Bronfin*¹; Nir Moscovitch¹; ¹Dead Sea Magnesium

One of the most direct methods of improving fuel economy and reducing CO₂ emissions is automotive light weighting. Currently the automotive industry is searching for lightweight materials for powertrain parts, which are subjected to both high temperature and dynamic loads. However, until recently, the utilization of magnesium alloys in powertrain parts was very limited due to some reasons mainly associated with increased magnesium cost compared to aluminum and, to great extent, with lack of suitable HPDC magnesium alloys with properties that match closely those of HPDC aluminum alloys like A380. The present paper addresses high-pressure die cast magnesium alloys MRI153M and MRI230D that combine numerous advantages of standard magnesium alloys over aluminum alloys with enhanced general corrosion resistance and creep performance at competitive cost. Specific benefits and weight reduction associated with the use of MRI alloys in different applications are discussed and disclosed.

3:00 PM

Microstructural Evolution and Creep Resistance in Mg-Sn-Ca Alloy: *Do Hyung Kim*¹; Hyun Kyu Lim¹; Ju Youn Lee¹; Won Tae Kim¹; Do Hyang Kim¹; ¹Center for Noncrystalline Materials

Among the trace elements to improve creep resistance in magnesium alloys, Sn and Ca have attracted many researcher's attention due to the formation of thermally stable phases such as Mg₂Sn and Mg₂Ca. In the present study, creep properties of Mg-Sn-Ca alloys depending on the microstructural evolution have been investigated. As-cast microstructures of the Mg-5Sn-0-4Ca (wt%) alloys exhibit typical dendritic structure consisted of primary α -Mg and secondary solidification phases. The secondary solidification phases have been identified as Mg₂Sn, CaMgSn or Mg₂Ca depending on the Ca/Sn ratio. Although the CaMgSn phase shows high thermal stability, its coarse morphology deteriorates the creep resistance, acting as crack initiation sites. On the other hand, the alloy containing the Mg₂Ca phase (higher Ca/Sn ratio) shows remarkably enhanced creep resistance. The detailed analysis indicates that improved creep resistance is originated from the precipitation of the Mg₂Ca phase preserving coherency with α -Mg matrix.

3:20 PM

Influence of Applied Pressure on Tensile Properties of Mg-Al-Sr Alloy: *Shuping Wang*¹; Henry Hu¹; ¹University of Windsor

The focus of this study is on development of alternative manufacturing processes for potential high temperature magnesium-aluminium-strontium alloys. The effect of external pressure on tensile properties of squeeze cast Mg-Al-Sr alloy was investigated. Four different applied levels, 0, 30, 60 and 90 MPa, were employed to exert on a Mg-6 wt.% Al - 0.5 wt.% Sr alloy during squeeze casting. The results of tensile testing indicate that the ultimate tensile strength (UTS), yield strength (YS) and elongation (Ef) of the squeeze cast Mg-Al-Sr alloy increase with increasing applied pressure level. The microstructural analysis and porosity measurements suggest that the tensile property enhancement resulting from applied pressure should be attributed to microstructure refinement and porosity reduction of the squeeze cast alloy.

3:40 PM

The Mg-Al-Zn-Mn-Ca-Sr Alloy System: Backbone of Understanding Phase Formation in AXJ Alloys and Modifications of AZ and AM Alloys with Ca or Sr: *Andreas Janz*¹; Joachim Groebner¹; *Rainer Schmid-Fetzer*¹; ¹Clausthal University of Technology

Progress is reported on experimental study and thermodynamic modeling of phase formation in key subsystems pertinent to the Mg-Al-Zn-Mn-Ca-Sr alloy system, or abbreviated as (Mg)-AZMXJ. This ongoing work enables thermochemical calculations, which are an important tool for the focused alloy development and process optimization. As an example, additions of Ca and Sr to alloys of the AZ series may provide improved mechanical and corrosion properties. Understanding the contribution of phase formation to these effects and, based on that, tackling a purposeful optimization is hardly possible without that information. This applies also in the case of Sr-addition to AM, essentially forming AJ alloys or, including the Ca-addition, to the potential offered by the AXJ system. This work is supported by the German Research Foundation (DFG) in the Priority Programme "DFG-SPP 1168: InnoMagTec."

4:00 PM

Development of Creep Resistant Magnesium Die Casting Alloy RSM-9#: *Weijian Tao*¹; *Shu Wang*¹; *Fang Yu*¹; ¹Nanjing Welbow Metals Company, Ltd.

This paper presents a creep resistant magnesium alloy (RSM-9#) with high performance and low cost. The effects of alloying elements Al, Ca, Sr and Ce on the mechanical properties at both room and high temperature have been studied by using die cast specimens. It was found that this alloy (RSM-9#) has a steady state creep rate of 3.43×10^{-10} /s at 175°C and 70MPa. Microstructure Examination, SEM and EDAX show that the integration of reduced β -Mg17Al12 phase and appearance of high melting point inter-metallic phases with Ca and Ce improved the high temperature mechanical properties of RSM-9# alloy.

4:20 PM

A Comparative Study of Microstructures and Creep Behaviour of AE42 and AE44 Die-Casting Alloys: *Suming Zhu*¹; Mark Gibson²; *Jian-Feng Nie*¹; Mark Easton¹; Trevor Abbott³; Per Bakke⁴; ¹CAST, Monash University; ²CAST, CSIRO Manufacturing and Materials Technology; ³Advanced Magnesium Technologies; ⁴Hydro Magnesium Competence Centre

It has been reported that the creep performance of AE42 tends to deteriorate at temperatures above 150°C while AE44 exhibits much better creep performance at elevated temperatures. However, the relationship between microstructures and creep resistance in these Mg-Al-RE die-casting alloys has not been well understood. In the present work, the microstructures and creep behaviour of AE42 and AE44 die-casting alloys were investigated and compared. The creep tests were conducted at 175°C in a stress range of 75 - 90 MPa. The microstructures in the as-cast and the aged conditions were characterised in detail by transmission electron microscopy. The correlation between creep resistance and microstructure suggests that it is the level of Al solute retained in the α -Mg matrix after die-casting that is the key factor in influencing creep resistance, with high levels leading to the precipitation of Mg₁₇Al₁₂ during creep and thus reducing the creep resistance.

4:40 PM

Effects of RE Additions on the Creep Behavior of AZ91 Alloy: *Reza Mahmudi*¹; Farhoud Kabirian¹; ¹University of Tehran

Creep behavior of AZ91 with 1-3 wt.% RE element additions was studied by impression testing. The tests were carried out under constant stress in the range 100-700 MPa and at temperatures in the range 425-525 K. Assuming a power law relationship between the impression velocity and stress, stress exponents of 5-8 were obtained. Analysis of the data showed that for all loads and temperatures, the activation energy for all materials was almost stress-independent with an average value of 100 kJ mol⁻¹. Based on the obtained stress exponents and activation energy data, which is very close to the 80-100 kJ mol⁻¹ for grain boundary diffusion of Mg, it is proposed that the operative creep mechanism is dislocation climb. It is found that the introduction of 2% rare earth elements has the maximum improvement in the creep resistance due mainly to the formation of thermally stable Al-La compounds with branched-shape morphology.

WEDNESDAY PM

Materials in Clean Power Systems III: Fuel Cells, Hydrogen-, and Clean Coal-Based Technologies: PEM Fuel Cells and Solar Technologies

Sponsored by: The Minerals, Metals and Materials Society, TMS Structural Materials Division, TMS/ASM: Corrosion and Environmental Effects Committee
Program Organizers: Zhenguo "Gary" Yang, Pacific Northwest National Laboratory; Michael Brady, Oak Ridge National Laboratory; K. Scott Weil, Pacific Northwest National Laboratory; Xingbo Liu, West Virginia University; Ayyakkannu Manivannan, National Energy Technology Laboratory

Wednesday PM Room: 392
 March 12, 2008 Location: Ernest Morial Convention Center

Session Chairs: Jin Yong Kim, Pacific Northwest National Laboratory; Xingbo Liu, West Virginia University

2:00 PM Invited

High Temperature Polymer Electrolyte Membrane Fuel Cells: *Dominic Gervasio*¹; ¹Arizona State University

A High Temperature Proton Electrolyte Membrane Fuel Cell (HT PEM FC) has an ion conducting membrane that operates with little or no need for hydration at temperatures above 100°C. Plastic PEMs are shock and vibration tolerant and operating above the water boiling temperature gives simplified one-phase fluids, heat rejection and tolerance to impurities for a more robust, compact and efficient system. Unfortunately, the state-of-the-art HT PEM FC, which uses a phosphoric acid loaded polybenzimidazole membrane, operates at 0.6 volt and 200 milliamp per square centimeter at ambient pressure and 170°C, so the cell is only 50% efficient and has low areal power density. New membranes based on protic salt electrolytes and thin lightweight corrosion-resistant metal-foil cell housings are under study at Arizona State University and recent results in these two efforts for making improved fuel cells will be discussed.

2:30 PM

Alloy Effects and Processing of Nitrided Metallic Bipolar Plates for Proton Exchange Membrane Fuel Cells: Michael Brady¹; Peter Tortorelli²; Harry Meyer¹; Heli Wang²; John Vitek¹; John Turner²; Dan Connors³; Mahlon Wilson⁴; Fernando Garzon⁴; Josh Pihl¹; Don Gervasio⁵; James Rakowski⁶; ¹Oak Ridge National Laboratory; ²National Renewable Energy Laboratory; ³GenCell Corporation; ⁴Los Alamos National Laboratory; ⁵Arizona State; ⁶Allegheny Ludlum

Formation of protective Cr-nitride surface layers on stainless steel proton exchange membrane fuel cell (PEMFC) bipolar plates by gas nitridation necessitates decreasing the high nitrogen permeability in these materials. This is accomplished by preoxidation of the material to form a Cr-rich oxide surface followed by thermal conversion of this surface oxide to Cr-nitride by nitridation. Small additions of vanadium to the alloy improve the behavior by modifying the Cr-oxide to make it more amenable to nitridation. A multi-organization effort to scale up and evaluate this approach with thin stamped and nitrided V-modified Fe-Cr base stainless steel bipolar plates was recently initiated. Initial results related to alloy design and processing efforts to lower the levels of Cr and V needed to yield the protective Cr-nitride surface, in order to reduce alloy cost and improve amenability to stamping, will be presented.

2:55 PM

Corrosion Behavior of Construction Materials for the Sulfur Iodine Thermochemical Hydrogen Cycle: *Bunsen Wong*¹; Gottfried Bsenbruch¹; Lloyd Brown¹; Ajit Roy²; ¹General Atomics; ²University of Nevada, Las Vegas

The sulfur-iodine thermochemical cycle is one of the most efficient water splitting means to produce hydrogen but the reaction environments are extremely corrosive. An extensive screening program has been undertaken to identify materials that can be used for heat exchanger construction for the HI decomposition section. Immersion corrosion tests results show that only Ta based alloys and SiC based ceramics are suitable for use with HIX (HI + I₂ + H₂O) and 95wt% conc. phosphoric acid. The stress corrosion behavior of Ta based alloys has been studied using c-ring and u-bend specimens. Furthermore, stainless components coated with Ta by various deposition means have also been

tested in environments with flowing chemicals. The results indicate that they can be suitable replacements for monolithic Ta parts for this application.

3:20 PM

Metallurgical and Corrosion Evaluation of 316L Stainless Steel for PEM Fuel Cell Bipolar Plate Application: *Daniel Wilkosz*¹; Mark Ricketts¹; Tsung-Yu Pan¹; Michael Santella²; Alan Frederick²; ¹Ford Motor Company; ²Oak Ridge National Laboratory

The austenitic stainless steel 316L is a candidate material for PEM fuel cell bipolar plates. The process to make a bipolar plate involves stamping, trimming, and laser welding. The effect of laser welding on the microstructure and corrosion of 316L was investigated in this study. Full-penetration linear weld beads were produced in 0.1-mm-thick samples using a 400W pulsed YAG laser. Weld translation speeds were 8.5-12.7 mm/s. Corrosion and metallurgical evaluations were conducted between weld-bead and original samples. The welded materials were corrosion tested using electrochemical polarization measured between -0.5Vnhe and 1.5Vnhe at a scan rate of 5mV/s. Static polarization at 1Vnhe for 6hour duration were also undertaken. The current response was measured and the test solution was analyzed to determine the quantity of metal ion leached. All electrochemical tests were carried out in pH 3 sulfuric acid solution. Metallurgical specimens were prepared by cross-sectioning and examined by light microscope.

3:45 PM Break

3:55 PM Invited

Tantalum Oxide for PEM Electrode Applications: *Jin Kim*¹; Jeff Bonnett¹; K. Scott Weil¹; ¹Pacific Northwest National Laboratory

Over the past decades, a significant amount of research effort has been made to reduce the cost of PEM fuel cell stacks by minimizing or eliminating the use of platinum in the electrodes. Even though several alternative materials have been attempted to replace expensive Pt-based catalysts, none of them show satisfactory properties in term catalytic activity and stability. Our preliminary research exhibits that tantalum oxide has high oxygen reduction potential comparable to Pt even though the reduction current is by and large limited by its poor electrical conductivity. One of the approaches to improve the reduction current of tantalum oxide is to increase its triple-phase boundaries where the oxygen reduction occurs. In this study, the feasibility of sputtered tantalum oxide for PEM catalysts has been investigated. The detailed results to date will be discussed.

4:25 PM

Characterization and Stability of Carbon Supported Pt and PtCo Alloy Fuel Cell Catalysts: *Obiefune Ezekoye*¹; Karen Adams²; Chi Paik²; George Graham¹; Xiaoqing Pan¹; ¹University of Michigan; ²Ford Motor Company

Carbon supported PtCo is a promising catalyst material that has the potential to mitigate some of the performance and durability issues associated with pure Pt proton-exchange membrane (PEM) fuel cells catalysts. In this work, the electrocatalytic activity and durability of fuel cell electrodes containing carbon supported Pt and PtCo catalysts were investigated using voltage cycling methods for 450 minutes in 1M H₂SO₄. After voltage cycling, powders removed from these electrodes were investigated with high resolution transmission electron microscopy (HRTEM) and compared with untreated commercial catalyst powder. HRTEM results support conclusions, reported elsewhere, that cobalt alloying significantly reduces platinum particle size growth after voltage cycling. In this study, however, HRTEM was used to quantify the effects of alloying on both the mean particle size and the particle size distribution in carbon supported Pt and PtCo fuel cell catalyst.

4:50 PM

Photoelectrochemical Investigation of InN Thin Film Electrodes: *Sushil Sitaula*¹; *Aurangzeb Khan*¹; Mohammad Alam¹; ¹University of South Alabama

The photoelectrochemical (PEC) method of renewable hydrogen production is a promising alternative to generate environment friendly energy to alleviate the current energy crisis. It produces clean energy with only sunlight as an energy source and only water as a by-product. Finding a suitable material for the harvesting of sunlight to break water has been a major challenge. This work reports photoresponse of indium nitride thin film electrodes prepared by pulsed laser deposition. X-ray diffraction and scanning electron microscopy were used

for the structural characterization of the films. Indium nitride electrodes showed n-type behavior. Maximum photocurrent of several μA was observed. The effect of growth parameters on the photoresponse of the films was studied with the intent of optimization. No clear trend between the photoresponse of the films and the growth parameters was observed. At 175 mJ of pulse energy and 5000 laser pulses, optimum photocurrent was observed.

5:15 PM

Growth of InN on Silicon and Sapphire Substrates Using Direct Pulsed Laser Deposition: Sushil Sitaula¹; Aurangzeb Khan¹; Mohammad Alam¹; Albert Gapud²; ¹University of South Alabama, Department of Electrical and Computer Engineering; ²University of South Alabama, Department of Physics

InN is a novel material, and many of its physical and optical properties are yet to be established. Recently, it has received a significant attention in optoelectronic applications as well as in photoelectrochemical hydrogen production. Due to lower dissociation temperature of around 550°C, high quality growth of InN is very difficult. This paper reports successful deposition of InN films on silicon and sapphire substrates using direct pulsed laser deposition. Laser pulse energy and the growth temperature were found to be important growth parameters. Higher pulse energy led to splashing of the molten target, forming a rough surface morphology. As observed from scanning electron microscope, optimum surface morphology was obtained with 175 mJ of pulse energy. At 525°C, the best surface morphology was obtained. The X-ray diffraction pattern of the films reveals the growth of polycrystalline InN, with (002) and (111) as major peaks.

5:40 PM

Study on the Preparation of Dendritic Zinc Powder for Zinc-Air Battery by Electrodeposition: Qing-hua Tian¹; Xueyi Guo¹; ¹Central South University

Dendritic zinc powder is applied in preparation of cathode of zinc-air battery. Based on a series of experiments, the electrodeposition was determined for the preparation of dendritic zinc powder in the solution system of Zn^{2+} - NH_4^+ - SO_4^{2-} - H_2O . The thermodynamic equilibrium analysis was conducted for this system, and the thermodynamics curves were drawn. Then the effects of current density temperature pH of solution concentration of reactants were explored by experiments, the pure and well crystalized zinc was obtained. Based on the test results the optimal conditions were as follows: $[\text{Zn}^{2+}]$ is 15g/L, $[(\text{NH}_4)_2\text{SO}_4]$ is 30~40g/L, pH of electrolyte is 4.5~5.45, and temperature of it is 25°C. SEM Photos of the obtained powder shows that the particles are dendritic in narrow size distribution.

Materials Informatics: Enabling Integration of Modeling and Experiments in Materials Science: Informatics and Cyberinfrastructure

Sponsored by: The Minerals, Metals and Materials Society, TMS Materials Processing and Manufacturing Division, TMS/ASM: Computational Materials Science and Engineering Committee

Program Organizer: Krishna Rajan, Iowa State University

Wednesday PM
March 12, 2008

Room: 271
Location: Ernest Morial Convention Center

Session Chair: To Be Announced

2:00 PM

CyberDesign: Mark Horstemeyer¹; Tomasz Haupt¹; ¹Mississippi State University

This presentation discusses the concept of the CyberDesign, that is, the application of emerging IT technologies to exploit the recent transformative research in material science involving multiscale physics based predictive modeling, multiscale experiments and bio-inspired design, in conjunction with robust design and manufacturing process optimizations with uncertainty. The cyberinfrastructure will enable the integration of otherwise independent research areas to accelerate agglomeration of structure-properties relations into material models. The results of such agglomeration will lead to higher fidelity, validated

designs of structural components and predictive material models that can capture structure-properties relations and include material history, thus closing the significant knowledge gaps in a unifying physics based modeling theme that captures a broad range of materials, admits structure-property relations, can be used in simulation-based design, can be implementable into finite elements codes, can be experimentally validated, can capture history effects, and can morph into a metamodel for rapid use prognostics.

2:20 PM

Cyberinfrastructure for Design Optimizations: Tomasz Haupt¹; Mark Horstemeyer¹; ¹Mississippi State University

Simulation-based design optimization is playing an increasingly important role in engineering product development, reducing or eliminating the need for physical prototyping, and increasing the quality of manufactured products. The complexity of the new generation of simulation codes demands the employment of high-performance computing platforms. Currently, it is a very tedious and error-prone manual effort by the designer to submit, monitor and coordinate hundreds of jobs in heterogeneous distributed environments which requires the designer to learn the arcana of ever-changing IT technologies such as operating systems, batch systems, storage systems, networking, and security. This presentation demonstrates the use of the modern information infrastructure based on Service Oriented Architecture (SOA), Web Services and Grid computing streamlining of the process of gathering experimental results, and deriving the material properties for a particular material model and employing the material model in finite element analysis in the process of building validated metamodels and design optimizations.

2:40 PM

Data/Modeling-Driven toward Innovation of Materials Design: Ying Chen¹; Hao Wang²; Yasunori Kaneta¹; Shuichi Iwata²; ¹University of Tokyo, School of Engineering; ²University of Tokyo, Graduate School of Frontier Sciences

One of the most challenging tasks in material science is designing materials with certain atomic constitutions, which achieves the pre-defined properties. As a typical inverse problem, it is very hard to find the best solution from a large amount of possibilities. There are two typical approaches in materials design. One is the inductive approach based on the empirical regularities from analyzing a materials data collected, another is the deductive approach based on theoretical calculations on specific systems following general physical laws. These two approaches so far have been developed almost independently. In recent years, we proposed an integrating approach by combining two types of approach, the data mining and the first principles calculations, as an efficient way to accelerate the speed of finding target atomic configuration from huge number of candidates and predicting properties of new materials. Several examples will be presented.

3:00 PM

Incorporating Collaborative Tools in MatDL Pathway: Laura Bartolo¹; Cathy Lowe¹; ¹Kent State University

The NSF supported National Science Digital Library Materials Digital Library Pathway (MatDL) is implementing an information infrastructure to disseminate government funded materials research results and to provide content as well as services to support the integration of research and education in materials. This paper describes how we are incorporating open-source collaborative tools, such as wikis and collaborative source code development systems, into the MatDL Pathway to support users in materials research and education as well as interactions between the two. These tools also have the potential to facilitate interactions between theorists and experimentalists.

Mechanical Behavior, Microstructure, and Modeling of Ti and Its Alloys: Physical/Mechanical Property Prediction

Sponsored by: The Minerals, Metals and Materials Society, TMS Structural Materials Division, TMS: Titanium Committee

Program Organizers: Ellen Cerreta, Los Alamos National Laboratory; Vasisht Venkatesh, TIMET; Daniel Evans, US Air Force

Wednesday PM
March 12, 2008

Room: 384
Location: Ernest Morial Convention Center

Session Chair: Kuang-Tsan Chiang, Southwest Research Institute

2:00 PM Invited

Modeling of Phase Transformation in Titanium Alloys: Amit Chatterjee¹; David Furrer¹; Michael Glavicic²; Jonathan Miller²; S. Semiatin²; ¹Rolls-Royce Corporation; ²Air Force Research Laboratory

The evolution of microstructure in commercial titanium alloys is critical to the optimal development of final component mechanical properties. The growth of primary alpha upon cooling from solution heat treatment and subsequent decomposition of remaining beta grains in alpha-beta alloys, such as Ti64 and Ti6242 has been studied and applied to production process development and optimization. Similarly, the prediction of the decomposition microstructure within beta processed alloys, such as Ti6246, is critical to understanding the resultant mechanical properties. The decomposition of beta phase follows the Burger's relationship between the BCC and HCP phases making 12 total possible alpha orientation variants possible. Current studies have shown the potential of preferentially selecting specific variant orientations resulting in the potential of a precipitation texture. Results from initial efforts to identify the mechanisms and a modeling approach to predict anisotropic variant selection will be presented. Deformation texture is also prevalent within the processing of alpha-beta titanium alloys. Beta phase deformation texture can occur during high strain processing and alpha phase texture can also rapidly occur during deformation processing as a result of rigid-body rotation and crystallographic slip. A modeling tool to predict the texture evolution during deformation processing has developed and demonstrated. An overall assessment of how these types of microstructure modeling tools can be linked with and can support component and process design processes will also be discussed.

2:30 PM

The Application of Bayesian Neural Network Modeling for the Prediction of Fracture Toughness in α/β Ti Alloys: Santhosh Koduri¹; Vikas Dixit¹; Peter Collins¹; Hamish Fraser¹; ¹Ohio State University

The development of computational tools that permit microstructurally-based predictions of tensile and fracture toughness properties of Ti-based alloys is an essential step towards the accelerated maturation of materials. This paper will discuss the development of Bayesian Neural Network Models to predict the fracture toughness of Ti-6Al-4V at room temperature. The development of these rules-based models has required the population of extensive databases, including both compositional and microstructural information. Once trained and tested, these models have been successfully used to identify the influence of individual microstructural features on the mechanical properties through the use of virtual experiments. For example, they have been used to identify the importance of the equiaxed α size/fraction and the thickness of grain boundary α on fracture toughness for $\alpha+\beta$ and β -processed Ti-6-4, respectively. Such critical features have been further investigated using state-of-the-art characterization techniques (including 3D techniques) to determine their role in fracture toughness.

2:50 PM

Microstructural Evolution and Mechanical Property Prediction in Beta Ti Alloys: Soumya Nag¹; Arda Genc¹; Peter Collins¹; Gopal Viswanathan¹; Srin Rajagopalan¹; Rajarshi Banerjee²; Hamish Fraser¹; ¹Ohio State University; ²University of North Texas

This paper describes research aimed at understanding the evolution of microstructure in beta-Ti alloys as a function of heat-treatment. Of particular

interest are the nucleation mechanisms that influence the distribution of alpha Ti from the beta phase. Here, attention is paid to the influence of beta phase separation and the omega phase on process of nucleation. The differences between the precipitation processes in alpha/beta Ti alloys and those observed in beta Ti alloys will be discussed. The understanding gained is used to predict ways to optimize microstructure for given combinations of properties. The prediction of mechanical properties, through microstructure/property relationships, is effected through data mining techniques. Specifically, neural networks have been developed to relate microstructure to mechanical properties, and these will be demonstrated and discussed. Additionally, these models are used to develop an understanding of functional dependencies of properties on specific microstructural features. These will be presented and discussed.

3:10 PM

A Constitutive Model of Cavitation-Induced Damage in Ti Alloys: Shyam Keralavarma¹; Ahmed Benzerga¹; ¹Texas A&M University

One major challenge in the hot working of Ti-based alloys is minimizing cavitation induced damage such as flow localization in shear bands that limit the formability of such metals. There is a need for accurate modeling of microstructure evolution under various loading conditions to ensure that such defects are minimized in the final product. We present a rigorous micromechanics based constitutive model of porous solids incorporating the effects of void shape and plastic anisotropy of the matrix. An important feature of the model is that it predicts the influence of plastic anisotropy and cavity shape on the evolution of porosity, which can potentially yield more accurate modeling of cavitation induced damage during material processing and cavity sealing upon strain-path changes. The model predictions for the yield surface and microstructure evolution for representative materials are compared with numerical limit analysis and finite element simulation results on porous unit cells for validation.

3:30 PM Break

3:50 PM

Dislocation Characterization and Modeling of Creep Mechanisms in Zirconium Alloys: Benjamin Morrow¹; Robert Kozar²; Ken Anderson²; Michael Mills¹; ¹Ohio State University; ²Bechtel Bettis, Inc.

Zirconium alloys are important as a material in nuclear reactors. Accurately predicting creep deformation of zirconium alloys throughout the lifecycle of a reactor depends on reliable deformation models. The Modified Jogged-Screw Model asserts that the motion of tall jogs in screw dislocations act as the rate controlling mechanism during creep in certain regimes. Previous studies at The Ohio State University have shown that the Modified Jogged-Screw Model accurately describes creep behavior in titanium alloys, which have a similar (HCP) crystal structure to zirconium alloys. Scanning transmission electron microscopy (STEM) was used to directly observe and characterize the dislocation structure of creep tested Zircaloy-4 over a broad range of test conditions. The applicability of the Modified Jogged-Screw Model was demonstrated and physically-based values for model parameters were determined. Thorough characterization will provide a better understanding of thermal creep in zirconium alloys, which will ultimately result in more robust creep deformation predictions.

4:10 PM

Micromechanical Modeling of Deformation Behavior of Duplex Type TNB Alloy with a Multi-Scale Modeling Approach: Mohammad Rizviul Kabir¹; Liudmila Chernova¹; Marion Bartsch¹; ¹German Aerospace Center

Room temperature deformation behavior of niobium-containing two-phase TiAl alloy has been investigated numerically using a two-scale micromechanical FE model. A polycrystal with duplex microstructure consisting of globular and lamellar grains is modeled with 3D unit cells that take into account specific volume fractions and orientations of the grains. The constitutive behavior of the α_2 and γ -phases is described by continuum mechanics based crystal plasticity model. Quantitative representations of microstructural details are obtained from the SEM analysis of a particular TNB alloy. The material parameters of the α_2 and γ -phases are initially taken from literatures and modified to fit the tensile behavior of the TNB alloy. The model provides an insight into the local variation of stresses and strains of the duplex microstructure consisting of globular and lamellar colonies. The role of dislocations and slip systems on the evolution of local plastic deformation is discussed.

4:30 PM

High Strain-Rate Modeling of Titanium-Aluminum Laminates: *Charles Radow*¹; George Gazonas²; ¹Bucknell University; ²U.S. Army Research Laboratory

Laminate composites created by alternating layers of titanium and aluminum have shown an improved resistance to fracture with a reduction in density. In these studies, hot pressing has been used to bond the layers together, resulting in the creation of the intermetallic TiAl₃. In the present work, commercially pure titanium (CP-Ti) and 1100-Al are bonded using an ultrasonic consolidation process before hot pressing to form a CP-Ti/TiAl₃/Al laminate, with the goal of developing a system capable of withstanding the high strain-rate loads encountered in ballistic impact and blast applications. One of the difficulties in modeling such systems is the lack of information available on the high strain-rate properties of TiAl₃. Through the use of dynamic finite element modeling and plate impact experiments, the effect of TiAl₃ on the laminate strength is investigated. These results are used in predictive models of the laminate subjected to impact loading.

4:50 PM

Modeling High Temperature Strength and Flow Stress Curves of Titanium Alloys: Zhanli Guo¹; Nigel Saunders¹; Peter Miodownik¹; Jean-Philippe Schille¹; ¹Sente Software, Ltd.

Process design and simulation for any metals requires an understanding of their high temperature mechanical behavior, particularly with respect to flow stress as a function of temperature and strain rate. This paper describes the recent developments of JMatPro, a computer software for material property simulation, on calculating the high temperature mechanical properties of titanium alloys. Extensive validation has been carried out and shown in the present work. Good agreement between calculated and experimental results has been achieved for a variety of titanium alloys, including alpha, near-alpha, alpha+beta, and beta types, over a wide range of temperature and strain rates. The material properties calculated from JMatPro can now be passed directly into computer-aided engineering packages for process simulation.

Neutron and X-Ray Studies for Probing Materials Behavior: Scattering and Understanding of Materials Properties

Sponsored by: National Science Foundation, The Minerals, Metals and Materials Society, TMS Structural Materials Division, TMS: Advanced Characterization, Testing, and Simulation Committee

Program Organizers: Rozaliya Barabash, Oak Ridge National Laboratory; Yandong Wang, Northeastern University; Peter K. Liaw, University of Tennessee

Wednesday PM Room: 391
March 12, 2008 Location: Ernest Morial Convention Center

Session Chairs: Emil Zolotoyabko, Technion-Israel Institute of Technology; Gene Ice, Oak Ridge National Laboratory

2:00 PM Invited

Small-Angle Scattering of Neutrons and X-Rays in Materials Science - A Comparison: *Gernot Kosterz*¹; ¹ETH Zurich

After a short comparison of the basic features of small-angle scattering of X-rays and neutrons, examples of recent applications will be given. Experimental results will be discussed, in particular those concerning phase separation of alloys, emphasizing the possibilities of spatial and temporal resolution of the decomposition process, high temperature-in-situ studies, and combinations with diffuse scattering and transmission electron microscopy. In some Al-, Cu- and Ni-base alloys, shape, volume fraction, spatial arrangement and other details of precipitates can be analyzed with great precision.

2:25 PM

Understanding Particle Morphology during High Energy Milling of Complex Metal Hydrides: *Tabbatha Dobbins*¹; Ejiroghene Oteri¹; Jan Ilavsky²; ¹Louisiana Tech University; ²Advanced Photon Source, Argonne National Laboratory

A program comprised of ultrasmall-angle x-ray scattering (USAXS) experiments was performed at sector 33-ID at the UNI-CAT for the study of particle morphology changes in the aluminates (e.g. NaAlH₄—both before and after transition metal salt catalytic dopant additions by high energy ball milling). The variation in surface fractal dimension and particle size with milling time and dopant content was tracked. These studies have shown that dopant content level (e.g. 2 mol % and 4 mol %) and dopant type (i.e. TiCl₂, TiCl₃, VCl₃, and ZrCl₄) markedly affects NaAlH₄ powder particle surface area (determined using surface fractal dimension). This study was able to link powder particle surface area to catalytic doping. We will report links among codopants (i.e. two dopants) and powder particle surface area studied using USAXS.

2:45 PM Invited

Diffuse Scattering and Monte Carlo Studies of Relaxor Ferroelectrics: *Thomas Welberry*¹; ¹Australian National University

A renewed interest in the field of ferroelectricity has taken place in recent years since the finding of exceptional piezoelectric properties in the lead-oxide class of relaxor ferroelectric (RF) materials typified by the disordered perovskite PbZn_{1/3}Nb_{2/3}O₃ (PZN). Although PZN and numerous related materials have been extensively studied over a long period a detailed understanding of the exact nature of their polar nanostructure has still not emerged. In this paper we describe experiments in which full three-dimensional diffuse neutron scattering data have been recorded from a single crystal of PZN using the time-of-flight (tof) Laue technique. Monte Carlo simulation has been used to demonstrate that the observed diffuse patterns are due to planar nano-domains oriented normal to the six <110> directions. A simple model has been developed which explains the observed scattering.

3:10 PM Invited

Concomitant Determination of Planar Faults, Dislocations and Subgrain Size by X-Ray Line Profile Analysis: *Tamas Ungar*¹; Levente Balogh¹; ¹Eotvos University

X-ray line profile analysis is based on (i) the different profile shapes and (ii) the different hkl dependence of line broadening or shifts corresponding to the different types of lattice defects: (a) grain or subgrain boundaries, (b) dislocations and (c) planar defects, i.e. stacking faults and twin boundaries. It is shown that physically well established, theoretically calculated profile functions can be attributed to the three fundamental defect types, (a) to (c). These *defect-related profile-functions* have the same mathematical form for each Bragg reflection throughout the entire diffraction pattern. However, their breadths and positions are scaled by defect specific, hkl dependent scaling rules. Since the scaling rules are only weakly correlated the diffraction effects of the three different defect types can be separated and the defect properties well characterized.

3:35 PM Break

3:45 PM Invited

Probing Phonons and Phase Transitions in Solids with X-Ray Thermal Diffuse Scattering: *Tai Chiang*¹; ¹University of Illinois

X-ray scattering by thermally populated phonons in crystals give rise to diffuse scattering. Measurements of such thermal diffuse scattering (TDS) intensities as functions of momentum transfer and sample temperature yield information about the lattice dynamics including the phonon dispersion relations. This method has a long history, and after being largely ignored for decades, it has revived and become a powerful tool with the advent of intense synchrotron x-ray sources. In this talk, we review the basics of TDS together with recent experiments of phonon studies in various systems. Issues of high order scattering and background contributions will be discussed in connection with details of data analysis. Examples will be presented to illustrate the power of TDS as a probe of phase transitions that involve phonons. The method is well suited for detailed studies of soft mode behavior and critical exponents.

4:10 PM Invited

Local Structure of Decagonal Quasicrystals by DAFS: *Hiroshi Abe*¹; Hiroyuki Saitoh²; Hironori Nakao³; ¹National Defense Academy; ²Japan Atomic Energy Research Institute; ³Tohoku University

Al-Ni-Co (ANC) and Al-Ni-Fe (ANF) system is well known to be decagonal quasicrystals, which have two-dimensional quasiperiodic planes. The structures depend both on concentrations and on temperature extensively. Recently, short-range order (SRO) in quasicrystals was detected on a quasiperiodic plane by anomalous-X-ray scattering method.¹ In this study, local structure of quasicrystals was examined along the periodic direction compared with a quasiperiodic plane by X-ray diffraction anomalous fine structure (DAFS) technique. In principle, DAFS possesses site and spatial selectivity. DAFS experiment was performed on the beamline BL-4C of the Photon Factory at the High Energy Accelerator Research Organization in Japan. Apparent differences of DAFS between periodic and quasiperiodic directions were shown in ANC and ANF. ¹H. Abe, H. Saitoh, T. Ueno, H. Nakao, Y. Matsuo, K. Ohshima and H. Matsumoto, J. Phys.: Condens. Matter 15 (2003) 1665.

4:35 PM Invited

Diffuse Scattering in Quasicrystals of Icosahedral Symmetry: *Sonia Francoual*¹; Marc de Boissieu²; Roland Currat³; Shiro Kashimoto⁴; Tsutomu Ishimasa⁴; ¹National High Magnetic Field Laboratory; ²Sciences et Ingenierie des Matériaux et Procédés; ³Institut Laue-Langevin; ⁴Hokkaido University

According to the hydrodynamic theory of quasicrystalline materials, the long-range quasiperiodic order yields in quasicrystals new long-wavelength modes, the phason modes, in addition to the acoustic phonons. Phason excitations are diffusive and associated with internal atomic rearrangements the dynamics of which is expected to lead to a distinctive diffuse scattering signal around Bragg peaks in reciprocal space. Up to now, experimental demonstration for the existence of phason diffuse scattering was given in the enlightening single case of the Al-Pd-Mn Mackay-type icosahedral (i-) phase from which the phason elastic constants were extracted and the thermal activation revealed. In the present communication, we report on X-ray Synchrotron investigations of the diffuse scattering in the i-Zn-X-Sc (X = Mg, Ag, Co) phases and the Zn-Sc 1/1 periodic approximant bringing evidence for the presence of long-wavelength phasons also in this new class of icosahedral quasicrystals and ruling it out in the 1/1 approximant structure.

5:00 PM Invited

Towards Systematic Procedures for Interpreting Diffuse Scattering from Disordered Molecular Materials: *Hans-Beat Bürgi*¹; Christina Hoffmann²; ¹University of Zuerich; ²Oak Ridge National Laboratory

Real crystals show many kinds of disorder giving rise to diffuse scattering which may cover the whole reciprocal space and is generally much weaker than Bragg scattering. However, with the advent of new, more intense radiation sources like synchrotrons and neutron Spallation sources it has become possible to measure diffuse features accurately. New X-ray and neutron single crystal diffractometers have been designed for fast data collection and repeatability of experiments at controlled conditions. X-ray and neutron experiments will be measured on the same sample by both methods, allowing to analyze the collected data simultaneously. Although state of the art computing resources allow to process the large amounts of data produced in such experiments, the methods to produce reliable models of disorder are less developed in comparison to single crystal structure analysis. Here we will sketch steps towards systematic procedures for interpreting diffuse scattering from molecular materials.

5:25 PM Invited

X-Ray Imaging for Materials and Biomedical Sciences: *Jung Ho Je*¹; Y. Hwu²; G. Margaritondo³; ¹Pohang University of Science and Technology; ²Academia Sinica, Institute of Physics; ³Ecole Polytechnique Fédérale de Lausanne

Radiology is the oldest and by far the largest field of application of x-rays. In recent years, this domain has been literally revolutionized by the exploitation of the unique characteristics of synchrotron sources. The results are particularly spectacular when the high spatial coherence of the radiation is used for novel and powerful approaches to radiology. The results are very high quality microradiology and microtomography images and movies - taken with a limited x-ray dose - that find a variety of applications in materials science, biology and medical research. In this talk we review basic theory and selected applications

of phase contrast x-ray microscopy to materials and biomedical sciences. Furthermore we introduce a new strategy of combining phase contrast radiology and diffraction x-ray microscopy to visualize atomic level defects such as misfit dislocations and micropipes in semiconductor single crystals. Finally phase contrast x-ray imaging in nanometer-resolution (<30 nm) will be demonstrated.

5:50 PM Panel Discussion:

Donald Nicholson, Oak Ridge National Laboratory

Wolfgang Pantleon, Risø National Laboratory

Gernot Kostorz, ETH Zurich

Emil Zolotoyabko, Technion-Israel Institute of Technology

Vaclav Holy, Charles University

Thomas Welberry, Australian National University

Henning Poulsen, Risø National Laboratory

Philip Withers, Manchester University

Donald Brown, Los Alamos National Laboratory

Sunil Sinha, University of California, San Diego

Ulrich Lienert, Argonne National Laboratory

Hiroshi Abe, National Defense Academy

Branton Campbell, Brigham Young University

6:20 PM Concluding Comments

Particle Beam-Induced Radiation Effects in Materials: Nanostructures

Sponsored by: The Minerals, Metals and Materials Society, American Nuclear Society, TMS Structural Materials Division, TMS/ASM: Nuclear Materials Committee
Program Organizers: Gary Was, University of Michigan; Stuart Maloy, Los Alamos National Laboratory; Christina Trautmann, Gesellschaft für Schwerionenforschung; Maximo Victoria, Lawrence Livermore National Laboratory

Wednesday PM

March 12, 2008

Room: 389

Location: Ernest Morial Convention Center

Session Chairs: Daryush Ila, Alabama A&M University; Tongde Shen, Los Alamos National Laboratory

2:00 PM

Studies of the Ion Irradiation Effects in Bulk Nanocrystalline TiNi:

*Askar Kilmametov*¹; Adam Balogh²; Horst Hahn³; Ruslan Valiev¹; ¹Ufa State Aviation Technological University; ²Darmstadt University of Technology; ³Forschungszentrum Karlsruhe GmbH

Nanocrystalline intermetallic alloys, which possess a long-range chemical ordering, considered being a good object to examine irradiation effects on the stability or degradation of crystal superlattice in the ordered state. TiNi alloy as one of the most important engineering materials due to its superior shape memory and mechanical properties was studied at present work. Bulk ordered nanocrystalline samples of altered grain size values (25 and 40 nm) were processed using the method of severe plastic deformation, namely high pressure torsion technique. Ordered nanocrystalline and coarse-grained samples were subjected to 1.5 MeV Ar ion irradiation at room temperature with damage dose up to 5.6 displacements per atom. Comparative analysis of long-range disordering and amorphisation kinetics revealed the enhanced irradiation resistance of nanocrystalline TiNi alloy. It was shown that at the equal damage dose nanostructured state is able to retain a long-range ordering meanwhile the coarse-grained counterpart was just essentially amorphised.

2:40 PM

Nanoscale Nano-Systems by MeV Ion Beam: *Daryush Ila¹; Robert Zimmerman¹; ¹Alabama A&M University*

MeV ion beam used to form Nanolayers of Nanocrystals of various materials within selected host materials by sequentially co-depositing host, selected species and depositing the host. The Nanocrystals are formed along the direction of MeV Ion beam passage due to the electronic ionization of the substrate. Example: a system consists of Nanolayers of Nanocrystals generating highly efficient thermoelectric generators (TEG). TEG produced by enhancing the electrical conductivity, enhancing the thermal insulation and increasing the Seebeck Coefficient. Some material systems, we had to dope the nanolayers by keV implantation of selected species before MeV bombardment. We measured thermal conductivity, electrical conductivity, and the Seebeck coefficient as a function of ion bombardment fluence. The induced nanoscale effects enhanced the thermoelectric properties of selected materials, which is increased figure of merits. We will discuss the mechanism behind such ion beam bombardment effects and the reason why thermoelectric properties may be changed.

3:00 PM

Modeling of Point Defect Cluster Evolution in the Framework of Mean Field Approximation: *Stanislav Golubov¹; Alexey Ovcharenko²; Roger Stoller¹; Steven Zinkle¹; ¹Oak Ridge National Laboratory; ²All Russia Institute for Agricultural Microbiology*

Nucleation, growth and coarsening of point defect clusters or secondary phase precipitates are generic processes in the study of defect accumulation in crystalline solids. These processes are responsible for numerous changes one observes in the physical and mechanical properties of materials during thermal treatment or under irradiation. If random spatial distribution of defect clusters is assumed, the evolution is described in terms of their size distribution, which obeys the kinetic equation describing growth and dissolution of the clusters due to different reactions with mobile defects. The kinetic equation in the form of a Master Equation or Fokker-Plank Equation has been treated by means of both analytical and numerical methods. In this work the numerical methods, which permit approximate solutions to be obtained for practically interesting cases are critically reviewed and analyzed. Application of different methods to the evolution of different types of clusters is presented.

3:20 PM Break

3:40 PM

Nanostructuring by Energetic Ions: *Devesh Avasthi¹; ¹Inter University Accelerator Centre*

The ions in different energy regims can (i) produce nano particles (ii) change the shape of particle or nano structure and (iii) alter the size and the size distribution of nano particles. In low energy regime, 1 keV Ar atom source producing a wide beam is used to synthesize metal particles in insulating matrix with definite advantages over other conventional methods. C nanowires are created in fullerene matrix by irradiation of fullerene film by 100 MeV Au ions. The nucleation and growth of Ag nano particles in insulating matrix by ion irradiation is investigated. The growth of Au nanoparticles in silica matrix is studied in the in-situ XRD experiment during ion irradiation. There have been major activities in nanostructuring by ions at IUAC Delhi, in recent past, which show the unique features of ion beam in different energy regime in creating or modifying the nanostructures in a controlled way.

4:00 PM

Nanostructure under Irradiation: Is Smaller Better?: *Tongde Shen¹; Shihai Feng¹; Ming Tang¹; James Valdez¹; Yongqiang Wang¹; Kurt Sickafus¹; ¹Los Alamos National Laboratory*

Previous experimental observations indicate that nanosized zirconia or silicon, when embedded in an amorphous silica matrix (thus forming two-phase nanocomposites), are more susceptible to radiation-induced amorphization when compared to their corresponding large-grained counterparts. We compare and contrast ion-induced radiation damage in a single-phase oxide MgGa_2O_4 , with microstructures consisting of either large (10 μm) or nanosized (10 nm) grains. We demonstrate a substantial enhancement in amorphization resistance for nanocrystalline versus large-grained MgGa_2O_4 . In particular, we observed an amorphization transformation in large-grained MgGa_2O_4 at a relatively low ion dose of about 10 displacements per atom (dpa), while we found nanocrystalline

MgGa_2O_4 to be unaffected by ion irradiation to a dose nearly an order of magnitude higher (100 dpa). Our experimental results and thermodynamic analysis suggest that smaller can be better under certain conditions.

4:20 PM

Nanoscale Surface Modifications of Conductors and Insulators Induced by Slow, Highly Charged Ion Impact: *Rene Heller¹; Stefan Facsko¹; ¹Forschungszentrum Dresden*

In the interaction of highly charged ions (HCI) with solids a large amount of potential energy is released. Each ion carries thereby up to several tens of keV potential energy which is mainly deposited into a strongly localized area ($\sim\text{nm}^2$) on the surface within a very short time ($\sim\text{fs}$). Due to the highly excited electronic system and the subsequent relaxation various structural as well as morphological changes are induced. We present scanning probe investigations (AFM/STM) of surface modification in conductors and insulators induced by slow, highly charged ions with different potential energies. In addition, a theoretical model for the interaction process of HCIs with alkali halides is proposed.

Phase Stability, Phase Transformations, and Reactive Phase Formation in Electronic Materials VII: Session IV

Sponsored by: The Minerals, Metals and Materials Society, TMS Electronic, Magnetic, and Photonic Materials Division, TMS: Alloy Phases Committee

Program Organizers: Sinn-wen Chen, National Tsing Hua University; Srinivas Chada, Medtronic; Chih Ming Chen, National Chung-Hsing University; Hans Flandorfer, University of Vienna; A. Lindsay Greer, University of Cambridge; Jae-Ho Lee, Hong Ik University; Kejun Zeng, Texas Instruments Inc; Katsuaki Suganuma, Osaka University

Wednesday PM

March 12, 2008

Room: 278

Location: Ernest Morial Convention Center

Session Chairs: Jae-Ho Lee, Hong Ik University; Hans Flandorfer, University of Vienna

2:00 PM Invited

The Intermetallic System Cu-Ni-Sn: *Hans Flandorfer¹; Clemens Schmetterer¹; Usman Saeed¹; Herbert Ipser²; ¹University of Vienna; ²University of Wien*

The intermetallic system Cu-Ni-Sn is highly important for lead-free soldering as it concerns the majority of solder/substrate interactions of hitherto used solders. Although first phase diagram data for this system have been published approx. 30 years ago literature information turned out to be still confusing. Contradictions concern mainly the ternary solubilities and the possible existence of ternary compounds. Experimental work is hampered by several phase transformations in the Cu-Sn and Ni-Sn binaries and difficulties to quench the corresponding high-temperature phases. We prepared approx. 100 samples and annealed them at 400, 500 and 600°C; a temperature of 200°C was only applied on samples with high Sn-contents. We investigated the samples performing XRD, metallography including EPMA and thermal analysis. Based on our recent results for the Ni-Sn binary system, we could provide more detailed information on the phase relations of Cu-Ni-Sn and clarify some of the contradictions.

2:20 PM

Thermodynamic Assessment in the Cu-In-Sn System: *Jan Vrestal¹; Ales Kroupa²; Jaromir Drapala³; ¹Masarykova University, Brno; ²Institute of Physics of Materials, Academy of Sciences of the Czech Republic; ³Technical University, Ostrava*

Knowledge of phase stability in the Cu-In-Sn system is important for revealing interaction of Sn-based lead-free solders with Cu substrate. Phase equilibrium data on this system from literature are complemented by new data published recently. The isothermal long-term annealing, followed by fast quenching, was employed to freeze thermodynamic equilibrium, followed by metallography, SEM (Scanning Electron Microscope) and EDX (Energy Dispersive X-ray) analysis. Phase transformation temperatures were determined by DTA (Differential Thermal Analysis). New thermodynamic data based on vapor pressure measurements, calorimetry and electromotive force measurements were also published very recently. Thermodynamic modeling by the CALPHAD

WEDNESDAY PM

(Calculation of Phase Diagrams) method reconcile corresponding thermodynamic and phase equilibrium data yielding the best set of thermodynamic parameters describing phase equilibria in this system. Resulting assessment of thermodynamic parameters will be presented. Financial support of Ministry of Education of Czech Republic Nos. OC531.001, OC531.002, OC531.003, MSM0021622410 and AV0Z20410507 is gratefully acknowledged.

2:35 PM

Thermodynamic Modeling of the Sn-Sb-Ag and Sn-Sb-Cu Systems: *Wojciech Gierlotka*¹; Sinn-wen Chen¹; An-ren Zi¹; Po-yin Chen¹; ¹National Tsing Hua University

Sn-Sb-Cu and Sn-Sb-Ag ternary systems are of interests for lead-free solder applications. Thermodynamic models of these two ternary systems are developed based on the CALPHAD method using the experimental information found in the literature as well as our own experimental data. There are 2 binary phases, 2 continuous solid solutions and three terminal phases in the Sn-Sb-Ag system, and there are 15 binary phases 1 ternary phase and three terminal phases in the Sn-Sb-Cu system. Sublattice models were adopted as a new description of intermetallic compounds and compositional homogeneities of promising solder materials were reproduced. Results of the calculation, such as thermodynamic properties of liquid and solid phases, isothermal and isopleths sections, and liquidus projections are compared with the experimental data. The calculated results are in good agreement with the experimental determinations.

2:50 PM

Liquidus Projection of the Sn-Zn-Cu Ternary System: *Yu-Chih Huang*¹; Sinn-wen Chen¹; Chin-yi Chou¹; Wojciech Gierlotka¹; ¹National Tsing Hua University

Liquidus projection of the Sn-Zn-Cu ternary system has been experimentally determined and thermodynamically calculated. Sn-Zn-Cu alloys of various compositions were prepared. These alloys were melted at high temperatures, removed from the furnace and solidified in air. The solidified samples were metallographically examined to determine the primary solidification phases. There is no ternary compound and all the primary solidification phases are the terminal solid solutions and binary intermetallics. They are Sn, η -Cu₆Sn₅, ϵ -Cu₃Sn, γ -(Cu-Sn), β -Cu₁₇Sn₃, α -Cu, β -CuZn, γ -Cu₅Zn₈, δ -CuZn₃, ϵ -CuZn₅ and Zn. Thermodynamic modeling was developed based on the thermodynamic models of the constituent binary systems and the experimental results from this study and those in the literatures. The calculated liquidus projection is in agreement with the experimental determinations. Solidification curves of the Sn-Zn-Cu alloys were determined using DTA, and the solidification paths of these Sn-Zn-Cu alloys were illustrated based on the solidification curves and the determined liquidus projection.

3:05 PM

Characterization of Ni-Si Phase Transformation: *Shiang Yu Tan*¹; ¹Chinese Culture University

The interest in the low resistivity NiSi increased significantly because of the foreseeable use as contact to the source, drain, and gate of sub-65 nm and 45 nm CMOS devices. However, the thermal stability of NiSi is worse as the high resistivity phase NiSi₂ nucleates at about 750°C and film agglomeration occurs even at a temperature as low as 600°C. The phase transformation from NiSi to NiSi₂ is of crucial importance for understanding the properties of nickel silicide and improving the process of IC industry. In order to obtaining a thermally stable Ni-FUSI gate electrode, we introduced properly tuned thickness of the initial Ni film and two-step RTP process during the poly-gate formation to push the transformation of NiSi₂ to higher temperatures and retard agglomeration. Several measurement techniques such as XRD, TEM, Resistivity, AFM and XPS were carried out to characterize its physical and electrical properties.

3:20 PM

Phase Equilibria and Diffusion Paths to Fabricate Single-Phase Half-Heusler MNiSn (M=Ti, Zr, Hf) Thermoelectric Alloys: *Yoshisato Kimura*¹; Chihiro Asami¹; Hazuki Ueno¹; ¹Tokyo Institute of Technology

Half-Heusler compounds MNiSn (M=Ti, Zr, Hf) are well-known to show excellent n-type thermoelectric properties at elevated temperatures around 1000 K. They are attractive because not only of high thermoelectric performance, but also of eco-friendly compositions containing no toxic element. However, it is very hard to prepare monolithic MNiSn alloys. Heterogeneous multi-phase

microstructures are inevitable to form via non-equilibrium solidification in cast metallurgy, and even in powder metallurgy, since the melting point of Sn (505 K) is too much lower than other constituent elements. In the present work, phase equilibria in the M-Ni-Sn ternary systems were examined to establish the phase diagram information by means of electron probe microanalysis. Moreover, diffusion paths to form MNiSn phase were investigated using various types of diffusion couples. Based on these results, we have succeeded to fabricate single-phase MNiSn alloys, for instance, by directional solidification using the floating zone method.

3:35 PM Break

3:50 PM Invited

Effect of Water-Base Flux Containing Oxalic Acid on Interfacial Reaction between Cu Substrate and Pb-Free Solders: *Xing Jun Liu*¹; Shun Mao Lin¹; Cui Ping Wang¹; ¹Xiamen University

In recent years, great attention has been given to the development of Pb-free solders for electronic interconnection materials because of the health and environmental safety problems caused by conventional Sn-Pb solders. However, for the Pb-free solders, it is required to further improve their wettability, and to restrain the growth of the intermetallic compounds (IMC) between solders and Cu substrate, which is associated with the reliability problem. In this work, a new type water-base flux containing oxalic acid was developed and good wettability between solders and Cu substrate was obtained by using this water-base flux. The effects of the water-base flux containing oxalic acid on growth of the intermetallic compounds were investigated. Results indicate that the water-base flux with oxalic acid can hinder the growth of IMC, and improve the wettability and reliability in electronic packaging.

4:10 PM Invited

The Effect of Additives on Small Copper via Filling by Electroplating Method: *Sukei Lee*¹; *Jae-Ho Lee*¹; ¹Hong Ik University

Copper via filling by electroplating method became a common technology for interlayer metallization in 3D SiP(System In Package) and then it has been actively studied. The void free copper via can be obtained with varying the additives of the electrolytes and, the current density and types, pulse and pulse reverse. The effects of additives on the copper via filling were investigated. The acid copper electrolytes containing additives such as PEG, SPS, JGB and PEI were examined to fill 10~20 micron via hole without void. The 10~20 micron small vias were successfully filled by copper electroplating.

4:30 PM

Study of Cu Surface Oxidation: *Zi-ming Huang*¹; Chengyi¹; ¹National Central University

Wettability of Pb-free solders on Cu metal bond pad highly depends on the oxidation condition of Cu bond pad surface. In this study, the oxidation behavior on Cu surface was studied. In this talk, two main parts will be presented: (1) Kinetic and phase formation of oxidation on Cu surface. The kinetic of Cu oxidation will be measured by ESCA and XPS. XRD will be used to analyze the Cu oxidation phase and structure. (2) We found that water contact angle is highly sensitive to the degree and condition of Cu surface oxidation. A correlation between the water contact angle and the Cu surface oxidation was established and will be reported.

4:45 PM

The System Ni-P-Sn and Its Binary Constituents: *Clemens Schmetterer*¹; Jiri Vizdal¹; Alexandre Kodentsov²; Herbert Ipser¹; ¹University of Vienna; ²Eindhoven University of Technology

Due to the use of phosphorus containing nickel substrates in microelectronics, understanding their reaction with Sn-based solders and the knowledge of the corresponding reaction products is highly important. Therefore, the ternary Ni-P-Sn system and relevant subsystems (Ni-P, P-Sn) have been studied experimentally (SEM + EDS, DTA/DSC, XRD) and theoretically (CALPHAD approach). On the basis of these investigations new versions of the binary phase diagrams were established. In the ternary Ni-P-Sn system the phase equilibria at various temperatures between 200 and 1050°C were determined. These results were enhanced with information obtained from a diffusion couple technique. New ternary phases were characterized with respect to their stability range and crystal structure.

5:00 PM

Evaluation of Peel Strength on Flexible Copper Clad Laminate with Ni-Cr Layer: *Bo-In Noh*¹; Seung-Boo Jung¹; ¹Sungkyunkwan University

In the rapid development of ultra large scale integrated (ULSI), Cu/polyimide system has been one of crucial technical concerns in multi interconnection scheme. In particular, as the number of output channel of IC driver increases and inner lead bonding (ILB) pitch in chip on flex (COF) demands the size below 30 μ m, the direct Cu deposition in two-layer flexible copper clad laminate (FCCL) fabrication will replace the present tie-coating process. Therefore, Cu metallization on polyimide will have steadily receive a great deal of attention because of continuous growing of IT market. The good adhesion between the metallic layer and the substrate in combination with the small foil thickness make flexible printed circuit boards (FPCBs) mechanically flexible. In addition, if polyimide is used for substrate material, the circuit board can operate at high temperatures. Therefore, we estimated that the reliability of FCCLs was affected by Ni-Cr layer using peel test method.

5:15 PM

The Effects of Pulse Plating Parameters on Ni-W Alloy Electroplating for UBM Application: Yeong Kwon Ko¹; *Jae-Ho Lee*¹; ¹Hong Ik University

Nickel has been used as a diffusion barrier material in UBM. Electro and electroless nickel plating have been extensively investigated. Even though nickel did not form IMC with tin at low temperature, nickel formed IMC with tin at high temperature. Nickel consumed the solder materials and then it affects on reliability of UBM. Tungsten is very good diffusion barrier material, however tungsten cannot be electroplated and has poor adhesion with tin. To utilize the advantage of nickel and tungsten, Ni-W alloy electroplating was investigated. Ni-W alloy film with crack free and low residual stress were obtained when pulse electroplating were employed. The interface of Ni-Sn and Ni(W)-Sn were analyzed by AES and EDS.

Recycling: General Sessions

Sponsored by: The Minerals, Metals and Materials Society, TMS Extraction and Processing Division, TMS Light Metals Division, TMS: Recycling and Environmental Technologies Committee

Program Organizers: Christina Meskers, Delft University of Technology; Greg Krumbick, Argonne National Laboratory

Wednesday PM

Room: 280

March 12, 2008

Location: Ernest Morial Convention Center

Session Chair: Joseph Pomykala, Argonne National Laboratory

2:00 PM Introductory Comments

2:05 PM

On the Separation of Zinc from Dust in Ironmaking and Steelmaking Off-Gas Cleaning Systems: *Naiyang Ma*¹; ¹Mittal Steel USA

Ironmaking and steelmaking off-gas cleaning system solid wastes often contain too high zinc to recycle for iron recovery through blast furnaces, but contain too low zinc to economically recover zinc from the wastes. The status of zinc in the ironmaking and steelmaking off-gas cleaning systems has been analyzed from three aspects: thermodynamics and kinetics of zinc deposition, correlation of zinc concentration with size and density of particles, and aerodynamics of dust particles in the off-gas cleaning systems. Theory and supporting data show that spontaneous separation of zinc from iron-bearing dust occurs in the ironmaking and steelmaking off-gas cleaning systems. Dry off-gas cleaning systems provide the most favorable conditions and environments for zinc to separate from dust. The coarser and heavier fraction of iron-rich solid wastes would be zinc-free or have low-zinc content if high-efficiency separators were to be used and appropriately arranged in the off-gas cleaning systems.

2:25 PM

Evaporation Behavior of ZnO with Ar-O₂-HCl-H₂O Atmosphere: *Kohei Yajima*¹; Hiroyuki Mastuura¹; Fumitaka Tsukihashi¹; ¹University of Tokyo

The dusts and fly ash in the steelmaking industry and municipal solid waste incineration process contain metallic elements such as Fe, Zn, Pb and Cd with considerable amount of halogens. In Japan, zinc in dusts is recovered by Waelz kiln or MF process, etc. However, the presence of halogen in the dust affects the evaporation and condensation behavior of zinc and other metals, and disturbs the direct recycling of dust to steelmaking processes, because alkali or heavy metals reacted with halogen vaporize easily as halides and/or oxyhalide compounds in pyrometallurgical process. Recently, the formation mechanism of zinc oxychloride vapor was investigated and the formation of zinc oxychloride such as ZnOCl was proposed. However, considering the practical operation, the effect of water vapor on the evaporation behavior of oxychloride is not fully clarified yet. This study is focused on the investigation of evaporation behavior of ZnO with Ar-O₂-HCl-H₂O atmosphere.

2:45 PM

The New Resourcing Method of Converter Slag: *Liu Chengjun*¹; ¹Northeastern University

According to the status of lower comprehensive utilization level for the converter slag in the word, and base on the chemical compositions and phase features of converter slag, the new resourcing method of converter slag were developed that some value-added products could be prepared such as calcium sulfate whisker and nano-Fe₂O₃. After converter slag was leached in H₂SO₄, calcium sulfate whisker and nano-Fe₂O₃ could be prepared from leaching liquid and solid products by the hydrothermal method. Effects of the temperature and solid-to-liquid ratio on the slenderness ratio of calcium sulfate whisker were investigated, and effects of the pH and reaction temperature on the style, size and color of nano-Fe₂O₃ crystal were investigated also by XRD, TEM and chemical analysis. The growth mechanism, transformation condition and control method for calcium sulfate whisker and nano-Fe₂O₃ were set up by thermodynamic analysis and kinetic model.

3:05 PM

Study of Phosphorus Recovery from Rare Earth Solution with Phosphorus by Citric Acid Coordination: *Bian Xue*¹; Wu Wenyuan¹; ¹Northeastern University

Citric acid coordinated with rare earth elements, and the coordination products dissolved in water. So in this paper, the citric acid was used to separate rare earth with phosphorus. The relationship among the ratio of phosphorus recovery, citric acid addition, pH, temperature, and time was studied by the quadratic regression orthogonal analysis, and then the regression equation was obtained. The optimum process conditions of phosphorus recovery were obtained as follows: citric acid addition: 0.05mol·L⁻¹, pH: 10, temperature: 30°C, and time: 20min, the ratio phosphorus recovery: 99.8%, rare earth loss: 0.98%. In addition, XRD analysis was used to investigate the sediment, and the reaction of alkalinity process was determined.

3:25 PM Break

3:35 PM

Study on the Adsorption Behavior of Modified Orange Peel Biosorbent on Cu²⁺: *Ningchuan Feng*¹; Xueyi Guo¹; ¹Central South University

A biosorbent, the chemically modified orange peel, was prepared from hydrolysis of the grafted copolymer, which was prepared by reacting methyl acrylate with cross-linking orange peel and the infrared spectroscopy (IR) was used for ensuring the structure of the biosorbent. Adsorption characteristics and effects of various factors of the biosorbent on Cu²⁺ were discussed including pH, adsorption time and initial concentration of Cu²⁺. Experiment results show that when pH was 6.0 and the initial concentration of Cu²⁺ was 50mg/L, the removal rate was 91.73% and adsorption capability was 80.53 mg/g after 6 h adsorption. After five times being reused, 85% removal rate could be obtained by the biosorbent.

WEDNESDAY PM

3:55 PM

Removal of Pb²⁺ from Aqueous Solutions Using Modified Spent Grains: Qingzhu Li¹; Liyuan Chai¹; Qingwei Wang¹; ¹Central South University

The adsorption process of Pb²⁺ from aqueous solutions by spent grains modified with 1mol/L NaCl solution was investigated. The effects of solution pH, contact time, adsorbent concentration, initial Pb²⁺ concentration, particle size on Pb²⁺ removal were also studied. The initial adsorption process was rapid and 90.35% of Pb²⁺ adsorption occurred within 30 min. The absorption equilibrium was obtained at 4h. When pH was 5.5, Pb²⁺ concentration in aqueous solutions decreased from the initial content of 20 mg/L to 0.01 mg/L after 5 hours by application of 10g/L adsorbent at 25°C, Pb²⁺ removal efficiency reached up to 99.95% and the Pb²⁺ remaining in aqueous solutions was under China Sanitary Standard for Drinking Water (GB5749-85). Adsorption data fitted well with Langmuir and Freundlich models. However, Langmuir isotherm model was better to describe Pb²⁺ adsorption than Freundlich model, indicating that the applicability of monolayer coverage of Pb²⁺ on the surface of adsorbent.

4:15 PM

Recycling of Wastes from Water Treatment Plant into Clayey Ceramic: Carlos Maurício Vieira¹; Jhonatas Vitorino¹; Sergio Monteiro¹; ¹State University of the Northern Fluminense

In this work the properties and the microstructure of a clayey ceramic incorporated, up to 10 wt.%, with three type of wastes from a water treatment plant was evaluated. To determine the physical and mechanical properties such as linear shrinkage, water absorption and flexural strength, specimens were prepared by 18 MPa uniaxial pressure and then fired in laboratory furnace at 700°C. The microstructure of the ceramics was analyzed by SEM and XRD. The results indicated that the wastes changed the fired phases and increased the porosity of the ceramic. The results showed that these wastes modified the plasticity/workability of the clayey body as well as the evaluated properties of the fired ceramic. From the results it was found possible to recycle these wastes into clayey ceramic in low amounts to avoid deleterious effect on the quality of the fired product.

4:35 PM

The Shrinkage Behaviour of Recycled Glass Compacts: Adele Garkida¹; Jiann-Yang Hwang²; Xiaodi Huang²; Charles Okuofu¹; Bowen Li²; Abashiya Ahuwan¹; ¹Ahmadu Bello University; ²Michigan Technological University

Compacts of crushed waste window glass, fluorescent tubes, drinking glasses and laboratory glass wares were made at various proportions from 106 microns and minus 75 microns powders in combination with 5% bentonite as binder for each glass type, after several trials to determine compactibility of particle sizes. They were made using the uniaxial press at 10,000 psi and sintered at a temperature range of 700-750°C. The results showed anisotropic shrinkage behavior for all the samples, exhibiting an axial shrinkage lower than the radial shrinkage. Sintered compact from waste drinking glass which comprised of 60% 106 microns and 40% minus 75 microns powders showed the least sintering shrinkage factor of 1.125, fused at 700°C and the highest shrinkage factor of 1.286 at 750°C. This shrinkage behavior connotes that sintering can be employed to utilize these waste glasses up to the maximum of 95% recycled glass content in ceramic tile production.

Refractory Metals 2008: Characterization

Sponsored by: The Minerals, Metals and Materials Society, TMS Structural Materials Division, TMS: Refractory Metals Committee

Program Organizers: Todd Leonhardt, Rhenium Alloys Inc.; Jim Ciulik, University of Texas at Austin

Wednesday PM

March 12, 2008

Room: 388

Location: Ernest Morial Convention Center

Session Chairs: James Ciulik, University of Texas at Austin; Omar Dogan, Albany Research Center, National Energy Technology Laboratory

2:00 PM

Analysis of the Purification of Iridium by Electron Beam Melting: Evan Ohriner¹; ¹Oak Ridge National Laboratory

The purification of iridium metal by electron beam melting has been characterized for 48 impurity elements using glow discharge mass spectrographic (GDMS) analysis. No significant removal of six refractory metal elements occurred. The elements B, C, Al, Si, Cr, Fe, Ru, Rh, and Pt were partially removed by vaporization during electron beam melting. The remaining elements were undetectable following melting. Purification was analyzed using Langmuir's equation for vaporization with equilibrium vapor pressures calculated using Henry's law. Activity coefficients were obtained from published data for the elements Fe, Ti, and Pt. Activity coefficients were estimated from enthalpy data for several elements known to bond strongly to iridium. An ideal solution model was used for the remaining elements. The results are consistent with ideal mixing and some localized heating of the melt pool. Sponsor: Office of Radioisotope Power Systems, U. S. Department of Energy, under Contract DE-AC05-00OR22725 with UT-Battelle, LLC.

2:25 PM

New Method for Measuring Potassium Impurities in Molybdenum: Dick Beercheck¹; Leanna Ergin²; David Kluk²; John Shields³; ¹Goldstein Group Communications; ²NSL Analytical Services; ³Mill Creek Materials Consulting

Potassium impurities in molybdenum can cause defects in sputtered coatings on LCD displays, leading to expensive coated glass having to be scrapped. To reduce defects, screen manufacturers are demanding higher purity molybdenum (in the 3 ppm potassium range), and the testing community is scrambling to develop more accurate techniques to verify these purity levels. Flame Atomic Absorption Spectroscopy (Flame AA) has been the preferred method for measuring potassium content of molybdenum. However, at the low levels being demanded by industry, Flame AA does not provide the required measurement accuracy. A method based on Gas Chromatography Mass Spectroscopy (GC/MS) shows promise as an alternative to Flame AA in measuring potassium at the 3 ppm level. At its present stage of development, GC/MS can provide repeatable measurements at the 10 ppm level, and 5 ppm is in sight. Future work is aimed at providing accurate, repeatable measurements at the 3 ppm level.

2:50 PM

In-Situ Fracture Studies and Modeling of the Toughening Mechanism Present in Wrought LCAC, TZM, and ODS Molybdenum Flat Products: Brian Cockeram¹; Kwai Chan²; ¹Bechtel Bettis Inc.; ²Southwest Research Institute

Fractographic examinations of tensile and fracture toughness specimens from unalloyed LCAC, TZM, and Oxide Dispersion Strengthened molybdenum have indicated that these alloys exhibit a ductile laminate toughening mechanism that is characterized as thin sheet toughening. In-situ examinations of fracture toughness specimens using a DISMAP method provide information on the stress-intensity values needed for crack propagation, path of crack propagation, and localized measurements of strain at the crack tip. C-scan measurements confirm that delaminations occur at the crack tip, and the development of the delamination zone with increasing stress-intensity is determined for each molybdenum alloy. A micromechanical model is developed to relate the toughness values to the features of the microstructure. Molybdenum alloys with a finer grain size, such as ODS molybdenum, are shown to exhibit higher toughness values at lower

temperatures. The improvement in DBTT with respect to microstructural features is understood in terms of the thin sheet toughening mechanism.

3:15 PM

Measurement of High Temperature Properties of Refractory Metals: *Samuel Causey*¹; Randall Jenkins¹; Jack Spain¹; Jason Wood¹; ¹Southern Research Institute

Southern Research Institute has been characterizing materials for use in extreme environments for well over 50 years. The applications have included re-entry bodies, rocket motors, antenna windows, and nuclear reactor materials among many others. The range of temperatures has been from cryogenic up to about 3030°C (5500°F). These materials have included ceramics, composites, graphites, metals, and cermets. The specimens developed have been recently modified for testing rhenium, tungsten, and molybdenum, and their alloys across a wide temperature range. These modifications as well as important aspects of the techniques and hardware designs used in the testing of refractory metals are discussed. Two companion papers will discuss data generated on rhenium and molybdenum-rhenium using these specimen geometries and test techniques.

3:40 PM Break

3:50 PM

Anomalous Strain Rate Dependence of Ductility in a 50Mo-50Re Alloy at Room Temperature: *Jianhui Xu*¹; Todd Leonhard²; John Farrell³; Michael Effgen³; Tongguang Zhai¹; ¹University of Kentucky; ²Rhenium Alloys Inc.; ³Semicon Associates

Tensile tests were conducted on a fully recrystallized 50Mo-50Re alloy, in the form of sheet of 0.216 mm thick, at different strain rates ranging from 10⁻⁶ s⁻¹ to 1 s⁻¹ at room temperature. It was found that the total elongation of the alloy increased significantly with increasing the strain rate. The fracture surface changed from brittle to ductile with increase in strain rate. Plastic deformation was found to occur by both slip and twinning in this alloy. The electron back scatter diffraction measurement revealed non-uniform plastic strain within individual grains, especially in the vicinity of grain boundary triple junctions. The decrease in ductility at low strain rates in this alloy was possibly related to the interaction between dislocations and trace interstitial elements.

4:15 PM

Tensile Ductility Reduction in Pure Rhenium at High Temperature: *Mark Opeka*¹; Jie Zhang¹; Samuel Causey²; Randall Jenkins²; Jennifer Gaies¹; Keisha Sylvestre¹; ¹Naval Surface Warfare Center; ²Southern Research Institute

Mechanical and thermal properties were obtained from pure rhenium samples produced by sintering and hot isostatic pressing, sintering and cold rolling, electroforming, and by chemical vapor deposition. Mechanical and thermal properties for these materials were obtained from room temperature up to 3500°F. The tensile testing results will be summarized. For all manufacturing processes, the highest tensile strains of 10 to 40% were observed at room temperature, with strain varying strongly with sample texture. The tensile strains decreased significantly with increasing temperature and values of 3 to 5% were observed at 3500°F and independent of texture. Reductions-in-area were very low or not measurable and grain boundary cleavage type failure was typically observed.

4:40 PM

Anisotropic Yield Function for Modeling Formability of Conventionally Rolled RRR Niobium: *Amir Zamiri*¹; Hairong Jiang¹; *Thomas Bieler*¹; Farhang Pourboghra¹; Chris Compton¹; Terry Grimm¹; ¹Michigan State University

The overall mechanical properties of the high purity niobium (RRR) sheets, which are used in fabrication of the superconducting accelerator cavities, were investigated. High purity niobium has microstructure and texture gradients that lead to a rough surface and anisotropic deformation. High purity niobium is a rate sensitive material and its strength and ductility increases with increasing strain rate. Due to the presence of an unstable texture, the *r* values in high purity niobium sheets decrease with plastic deformation. From tensile tests in different in-plane directions and bi-axial bulge tests, a new mathematical model was developed to describe the evolving yield function that predicts the variation of the *r* values with respect to the effective strain and angle to the rolling direction. From this analysis, suggestions for optimal microstructure and texture for fabricating cavities from high purity niobium are proposed.

5:05 PM

First Principles Design of Ductile Refractory Alloys Validated by Experiments: *Michael Gao*¹; Michael Widom¹; Omer Dogan²; Paul King²; ¹Carnegie Mellon University; ²National Energy Technology Laboratory

The purpose of this work is to demonstrate that the synergy that integrates first-principles calculations, computational thermodynamics and kinetics, and experimental design can be appropriately used to develop new materials for high-temperature applications in energy systems. Specifically, the Rice-Thomson parameter will be used as a computational screening tool for identifying ductilizing additives to the refractory alloys in addition to Poisson ratio. The advantage of using the Rice-Thomson parameter and Poisson ratio derives from the fact that they can be evaluated completely from first principles with virtually no empirical information. The calculations will be applied first to model simple prototype binary alloys based on Cr. Further, experimental measurements concerning selected Cr-binaries such as Cr-W will be conducted and used as benchmarks to examine theoretical calculations. Applications of current first principles calculations for phase diagrams and thermodynamics of refractory alloys will also be presented.

Structural Aluminides for Elevated Temperature Applications: New Class of Gamma Alloys

Sponsored by: The Minerals, Metals and Materials Society, TMS Structural Materials Division, TMS: High Temperature Alloys Committee, TMS/ASM: Mechanical Behavior of Materials Committee

Program Organizers: Young-Won Kim, UES Inc; David Morris, Centro Nacional de Investigaciones Metalurgicas, CSIC; Rui Yang, Chinese Academy of Sciences; Christoph Leyens, Technical University of Brandenburg at Cottbus

Wednesday PM
March 12, 2008

Room: 394
Location: Ernest Morial Convention Center

Session Chairs: Young-Won Kim, UES Inc; Vijay Vasudevan, University of Cincinnati

2:00 PM Invited

A β -Stabilized γ -TiAl Based Alloy for Improved Processing Performance: *Helmut Clemens*¹; Harald Chladil¹; Wilfried Wallgram¹; Sascha Kremmer²; Andreas Otto³; Volker Guether³; Arno Bartels⁴; ¹University of Leoben; ²Bohler Schmiedetechnik GmbH&CoKG; ³GfE Metalle und Materialien GmbH; ⁴Hamburg University of Technology

The development of high-temperature materials is the key to technological advancements in aero-engines, where materials have to withstand extremely demanding conditions. TiAl alloys offer many attractive properties, such as low density, good oxidation and burn resistance as well as good creep properties and high strength at elevated temperatures. Conventional high Nb bearing γ -TiAl based alloys exhibit a relatively strong tendency to segregations because of their peritectic solidification path. This leads to local microstructural inhomogeneities causing severe problems regarding hot-working behaviour and a scatter in mechanical properties. The investigated β -solidifying Ti-43Al-4Nb-1Mo-0.1B alloy (at.%) shows a homogeneous and fine grained microstructure in the cast state. Due to a high volume fraction of β -phase the alloy can be, e.g., forged under near conventional conditions. With subsequent heat-treatments a significant reduction of the β -phase is achieved, as predicted by thermodynamic calculations. Alloy characterization was conducted by SEM, EBSD, TEM, texture measurements, and mechanical testing.

2:30 PM

Microstructure and Properties of Beta-Solidifying Gamma-Titanium Aluminide Alloys: *Michael Oehring*¹; Fritz Appel¹; Jonathan Paul¹; Renat Imayev²; Valery Imayev²; Viola Küstner³; ¹GKSS Research Centre; ²Institute of Metals Superplasticity Problems; ³Max-Planck-Institut für Metallforschung

Gamma titanium aluminide alloys solidifying solely via the beta-phase exhibit characteristic solidification microstructures, which often involve equiaxed instead of columnar structures, weak textures, and modest segregation. These features result from single-phase solidification and the subsequent solid-state

transformations. In view of the development of improved cast alloys, the potential of the beta/alpha transformation with respect to microstructural refinement and its dependence on the addition of several alloying elements has been investigated. It was found, that particularly fine and very homogeneous microstructures can be obtained for certain alloy compositions. The microstructural refinement can be attributed to the alloying effect on the kinetics of the beta/alpha transformation and even can be achieved after slow cooling from high-temperature heat treatments. The paper discusses alloy concepts aiming at refined cast alloys that also appear to be useful with respect to ingot material for wrought processing routes.

2:50 PM Invited

Microstructure and Corresponding Tensile Properties of as Cast β -Solidifying γ -TiAl Based TNM Alloys: *Volker Guether*¹; *Andreas Otto*¹; *Joachim Klose*²; *Christiane Rothe*²; *Helmut Clemens*³; *Werner Kachler*⁴; *Susanne Winter*⁴; *Sascha Kremmer*⁵; ¹GfE Metalle und Materialien GmbH; ²FNE Forschungsinstitut fuer Nichteisen-Metalle Freiberg GmbH; ³University of Leoben; ⁴Zentrum fuer Werkstoffanalytik Lauf GmbH; ⁵Bohler Schmiedetechnik GmbH&CoKG

VAR ingots of γ -TiAl based TNM alloys which solidify completely via the β -phase exhibit fine grained microstructure consisting of lamellar γ / α_2 - colonies and globular γ - and β /B2-grains. The volumetric ratio between the three phases depends mainly on the aluminum content and the content of the major β -stabilizing alloying elements molybdenum, niobium and boron. The thermodynamic stability of the microstructure at operation temperature is characterized by the investigation of the equilibrium phase formation at elevated temperatures using high temperature XRD measurements. The excellent tensile properties at room temperature and 700°C of thermally stress relieved as cast VAR materials are related to the microstructure and, thus, to the chemical composition of the TiAl alloy. It is expected that γ -TiAl based alloy compositions can be adjusted to the specific needs of both final application and further processing steps.

3:20 PM

“Near Conventional” Forging of a β -Stabilized γ -TiAl Based Alloy: *Sascha Kremmer*¹; *Harald Chladil*²; *Wilfried Wallgram*²; *Helmut Clemens*²; *Andreas Otto*³; *Volker Güther*³; *Arno Bartels*⁴; *Wilfried Smarsly*⁵; ¹Bohler Schmiedetechnik GmbH&CoKG; ²Montanuniversität Leoben; ³GfE Metalle und Materialien GmbH; ⁴Hamburg University of Technology; ⁵MTU Aero Engines GmbH

Due to the strong demand for higher efficiencies, reduced CO₂ emissions and weight reduction in aircraft engines, the substitution of presently used materials by novel light-weight, high-temperature alloys like γ -TiAl based alloys is at the edge of realization. This paper summarizes detailed investigations on a “near conventional” forging route for the fabrication of TiAl components. γ -TiAl based alloys with high Nb contents exhibit a narrow forging window, which show severe shifts if only slight changes in alloy composition occur. However, when using an alloy with an optimized content of β -stabilizing elements the forging window can be widened with respect to billet temperature, die temperature and die speed. Forging experiments conducted on this specially developed Nb and Mo containing γ -TiAl based alloy (TNM), demonstrate the feasibility of a robust and economic manufacturing route. Additionally, the results of texture measurements are shown and the mechanical properties of forged TNM material are presented.

3:40 PM Break

3:50 PM Keynote

Development of Beta Gamma TiAl Alloys: Opening Robust Processing and Greater Application Potential: *Young-Won Kim*¹; *Sang-Lan Kim*¹; *Dennis Dimiduk*²; *Christopher Woodward*²; ¹UES Inc.; ²Air Force Research Laboratory

The primary material and manufacturing limitations of gamma TiAl alloys include large cast lamellar grains, an inhomogeneous distribution of microstructure and composition, and processing difficulties. Efforts have been made in developing a new class of TiAl-based alloys, called beta gamma, which would overcome or reduce such barriers. The design concept was to identify gamma alloy systems, which are solidified through the beta-solidification process, thereby producing phase fields where the β phase amount is adequate at elevated temperatures but low or negligible at the anticipated use temperatures. Such alloy compositions were determined to exist within Ti-(40-45)Al-(2-8)Nb-

(1-9)(Cr, Mn, V, Mo)-(0-0.3)B in and around the ternary phase field (γ + β /B2 + α / α_2). Three groups of beta gamma alloys, rich with gamma phase and having distinct transformation pathways, were explored, featuring remarkably refined microstructures and compositional homogeneity. The ongoing development process will be discussed, along with the initial properties and associated engineering implications.

4:30 PM

Effect of Small Boron and Carbon Additions on the Mechanical Properties of a Novel High Niobium-Containing Gamma Titanium Aluminide Alloy: *Janny Lindemann*¹; *Maria Glavatskikh*¹; *Stefan Schmidt*¹; *Christoph Leyens*¹; *Dan Roth-Fagaraseanu*²; ¹BTU Cottbus; ²Rolls-Royce Deutschland

Recently, the alloy design of high niobium-containing gamma titanium aluminide alloys is focused on increased beta-stabilized alloys (TNM alloys). Increased beta-stabilizing of TNM alloys compared to conventional high niobium-containing alloys (TNB alloys) leads to an increased beta-volume content in these alloys which can be beneficial with regard to ductility and formability of the alloys. However, the fatigue performance and the creep resistance of the TNM alloys can be reduced due to the beta-volume content. In the present work the mechanical properties of an extruded TNM alloy were compared with those of a conventional TNB alloy. Furthermore, the effect of a small amount of boron and carbon on the mechanical properties was investigated. While the presence of borides could significantly improve microstructure refinement and homogenization during extrusion, a small amount of carbon can lead to higher strength and creep resistance due to precipitation hardening.

4:50 PM

Development of Multiphase Gamma-TiAl Alloys with Enhanced Mechanical Properties: *Renat Imayev*¹; *Valery Imayev*¹; *Timur Khismatullin*¹; *Tatiana Oleneva*¹; ¹Institute for Metals Superplasticity Problems

The effect of heat and thermomechanical treatment on the microstructure and mechanical properties of two groups of beta-solidifying gamma-TiAl alloys with the metastable or stable beta (B2) phase in the composition range of Ti-(43-46)Al-(4.5-7)(Nb,Mo)-0.2B-(0-0.3)C has been considered. In the first group of the alloys the molybdenum content was within the limits of solubility in the gamma and alpha-2 phases, in the second group the content exceeded this limit. The metastable beta (B2) phase promotes refinement of the structure upon freezing and cooling and can be dissolved by heat treatment that allows a good balance of mechanical properties to be obtained. The stable beta phase gives rise to some a reduction in high temperature mechanical properties, but improves significantly ductility and workability. Both the alloy groups possess improved processing characteristics in comparison with currently known gamma-TiAl alloys.

5:10 PM

Forging of β -Phase Containing γ -TiAl Alloys: *Jiulai Zhang*¹; *Stefan Schmidt*¹; *Fritz Appel*²; *Christoph Leyens*¹; *Bernd Viehweger*¹; ¹Brandenburg University of Technology Cottbus; ²GKSS Research Centre

Forging of conventional γ -TiAl alloys is difficult due to their ordered structure. Up to now the only feasible closed-die forging process is the isothermal forging. The introduction of β -phase in γ -TiAl alloys may make the conventional closed-die forging possible. Upsetting tests were carried out on some newly developed β -phase containing γ -TiAl alloys with warm dies made from a Ni-base superalloy with varied strain rates and die temperatures. Both bare and canned specimens were used. The canning consists of three layers of steel foil (foil thickness 0.1 mm) and a layer of glass. 75% upsetting was reached at optimal forging parameter. The forged specimens were examined with light microscopy and SEM. The results show that the newly developed β -phase containing γ -TiAl alloys can be forged at much higher strain rates than those conventional γ -TiAl alloys. Canning reduces drastically the die temperatures needed for a defect free forging.

Structural Aluminides for Elevated Temperature Applications: Poster Session

Sponsored by: The Minerals, Metals and Materials Society, TMS Structural Materials Division, TMS: High Temperature Alloys Committee, TMS/ASM: Mechanical Behavior of Materials Committee

Program Organizers: Young-Won Kim, UES Inc; David Morris, Centro Nacional de Investigaciones Metalurgicas, CSIC; Rui Yang, Chinese Academy of Sciences; Christoph Leyens, Technical University of Brandenburg at Cottbus

Wednesday PM

Room: 394

March 12, 2008

Location: Ernest Morial Convention Center

Session Chairs: Maria Perez-Bravo, ITP; Chao Jiang, Los Alamos National Laboratory; Christoph Leyens, Technical University of Brandenburg at Cottbus; Rui Yang, Chinese Academy of Sciences; David Morris, Centro Nacional de Investigaciones Metalurgicas, CSIC

An Electron Microscope Study of Low-Cycle Fatigue of a High Niobium Containing and Precipitation Hardened TiAl Alloy: Fritz Appel¹; Thomas Haeckel²; Hans-Jürgen Christ²; ¹GKSS Research Centre; ²Universität Siegen

The fatigue behaviour of an extruded TiAl alloy with the composition Ti-45Al-8Nb-0.2C (at. %) will be described. Fully reversed isothermal tests were performed under strain control at a strain amplitude of 0.7% and the temperatures 25, 550 and 850°C. TEM examination of the samples fatigued at 25 and 550°C revealed dense structures of ordinary dislocations and debris that were accumulated in tangles. The dipole defects apparently serve as additional glide obstacles but may also contribute to dislocation multiplication if the local stress rises. Another important low temperature deformation mechanism is the stress-induced transformation of the orthorhombic B19 phase, which is a significant constituent of the microstructure. The B19 phase is apparently unstable under tetragonal distortion and transforms into gamma phase via distinct shuffle operations. Under high-temperature fatigue the lamellar microstructure degrades by dynamic recrystallization. Details of these processes were investigated by high-resolution electron microscopy.

Fracture Toughness of an Intermetallic TiAl: Nicolas Barbi¹; Russell Goodall¹; Frédéric Diolent¹; Andreas Mortensen¹; ¹Ecole Polytechnique Fédérale de Lausanne

Cast TiAl-based alloys have potential in several applications such as valves or turbocharger wheels; however, the suitability of these materials in critical applications such as gas-turbine blades may be limited by their generally brittle behaviour. We present results from a study of the toughness of gamma/alpha2 titanium aluminides conducted within the framework of a wider collaborative project on these materials. Three-point bend fracture toughness tests conducted under controlled atmosphere on precracked specimens, varying the alloy composition, heat treatment and test temperature are used to assess the suitability of these cast alloys for applications, as well as relations between basic microstructural parameters, such as the alpha2 phase contents and distribution, and their resistance to crack propagation.

Environment Protection of γ -TiAl Alloys Coated with CrAlYN/CrN Nanoscale Multilayer Coatings and EB-PVD Thermal Barrier Coatings: Reinhold Braun¹; David Müßner¹; Christoph Leyens²; Papken Hovsepian³; Christina Reinhard³; Arutun Eghiasarian³; ¹DLR - German Aerospace Center; ²Technical University of Brandenburg at Cottbus; ³Sheffield Hallam University

The oxidation protection capability of nanostructured CrAlYN/CrN multilayer coatings for gamma titanium aluminides was studied at 750 and 850°C under cyclic oxidation conditions. Nitride coatings of about 5 μ m thickness with an oxy-nitride top coat were deposited on γ -TiAl samples with Cr-, CrAl- and Y-etched interfaces. EB-PVD thermal barrier coatings of yttria stabilized zirconia were deposited on some of the samples using CrAlYN/CrN + CrAlYON as bond coat. CrAlYN/CrN coatings exhibited excellent oxidation resistance at 750°C. A significantly reduced mass gain was observed for coated samples in comparison to the bare γ -TiAl alloy. With regard to the different surface pre-treatments, the Y-etched interface exhibited the most beneficial effect on oxidation resistance. The multilayer nitride coatings provided also good oxidation protection at

850°C. No spallation of the thermal barrier coating systems was observed during 2000 cycles at 850°C. The TBCs exhibited excellent adhesion to the oxy-nitride top coat.

Fabrication of TiAl Foils by Heat Treatment Only: Jiulai Zhang¹; Christoph Leyens¹; Bernd Viehweger¹; ¹Brandenburg University of Technology Cottbus

TiAl foils were prepared by heat treatment of Ti/Al foil packs. After heat treatment at high temperatures for 0.5h TiAl foils with a thickness of 85 μ m were attained. Different from the results in literature, where Ti and TiAl₃ instead of γ phase were achieved, the foils are free from Ti, TiAl₃ and contain only γ phase and α_2 phase. The as-heat-treated foils show good surface quality too. The foils show a coarse lamellar microstructure through the whole thickness of the foils. A row of pores were found in the middle plane of the foils. The reason of the pore formation was discussed and methods were tried to remove the pores.

Microstructure Characterization and Mechanical Property of Ti/TiAl Sheets Prepared by EBPVD: Liping Shi¹; Xiaodong He¹; Li Ma¹; Yesheng Zhong¹; ¹Harbin Institute of Technology

By the double resource method of electron beam physical vapor deposition, Ti and TiAl ingot were evaporated in their given order onto the substrate. And Ti/TiAl sheets with total thickness of 1 mm were fabricated, in which Ti is served as tough phase to improve the fracture toughness property of base phase TiAl. This basic concept of the toughness procedure is defined that tough particles were bridged to connect the main crack surface of the brittle matrix. Based on the results of DSC, XRD and SEM analyses, the microstructure of Ti/TiAl sheets were characterized. Additionally, the mechanical property including tensile, creep and fatigue testing were performed. According to the experimental results, the property of the Ti/TiAl sheets is up to the structure and property of each composition and its main influencing factor includes body content, interlayer spacing and mutual solubility.

Multiple F-Implantation for Improved Oxidation Protection of Gamma-TiAl Alloys: Hans-Eberhard Zschau¹; Michael Schuetz¹; ¹DECHEMA e. V.

To overcome the insufficient oxidation resistance of Gamma-TiAl above 750°C the fluorine effect is well established. After fluorine doping on the TiAl surface an alumina scale is formed. Several methods of fluorine treatment were considered. The fluorine content at the metal/oxide interface was found to be an important stability parameter. Its time behaviour follows an exponential decay function with a constant term of about 1 at.-% after oxidation for 1000 h at 900°C. To improve the long-time stability of the protective effect a fluorine reservoir was established by using multiple implantation techniques. Implantation energies between 20 keV and 120 keV and ion fluences between 5E16 and 6E17 F cm⁻² were considered. The implantation profiles varied between two step and multiple implantation. The fluorine depth profiles were obtained by using the non-destructive PIGE technique showing an optimized shape suitable for long oxidation times.

On the Influence of Nb and C on the Phase Transition Temperatures in γ -TiAl Based Alloys: Harald Chladi¹; Helmut Clemens¹; Ernst Kozeschnik²; Arno Bartels³; Rainer Gerling⁴; Sascha Kremmer⁵; ¹Montanuniversität Leoben; ²Graz University of Technology; ³Hamburg University of Technology; ⁴GKSS Research Centre; ⁵Böhler Schmiedetechnik GmbH&Co KG

Intermetallic titanium aluminides are of increasing technical importance for high-temperature applications in automotive and aerospace industries due to their low density, combined with high yield strength, good creep properties and good oxidation behaviour. Current γ -TiAl based alloys are an example of complex multi-phase materials. Therefore, the knowledge of the constituting phases and their solid-state transition temperatures as well as the influence of alloying elements is the basis for thermo-mechanical processing and for smart heat treatments, e.g. for the optimization of mechanical properties. In the present study phase transition temperatures and constituting phases of alloys showing a baseline composition of Ti-45Al-(5-10)Nb-(0-0.5)C (at.%) were investigated by means of DSC, scanning electron microscopy, electron back-scattered diffraction and X-ray diffraction. For the prediction of phases and phase transition temperatures, thermodynamic calculations based on the CALPHAD method were performed using a commercially available database, which also was adapted with some corrections.

Phase and Microstructure Evolution and Tensile Properties in a Beta Gamma Alloy Ti-44Al-4Nb-3.5(Mn, Cr)-0.2B: Young-Won Kim¹; Christopher Woodward²; Dennis Dimiduk³; ¹UES Inc; ²Air Force Research Laboratory

Beta gamma alloys are under exploration as possibly "more robust" gamma-base alloys. Their compositions exist within a range of Ti-(40-45)Al-(2-8)Nb-(1-9)(Mn, Cr, V, Mo, Cu)-(0-0.3)B-(0-0.4)C. Three groups of beta gamma alloys, rich with gamma phase (>85%) at use temperatures, were determined to exist in and around the ternary phase field (γ -TiAl + β -Ti + α_2 -Ti₃Al). A three-phase alloy, Ti-44Al-4Nb-3.5(Mn, Cr)-0.2B, was investigated to evaluate its phase transformation pathways and microstructure evolution taking place upon heat treatments for both ISM ingot material and an extruded material. These processes were analyzed using phase and grain size distribution measured as a function of temperature and heat treatment condition. The resulting information and data was used to determine extrusion conditions and also define new useful microstructure types with a desirable phase and microstructure distribution. Property testing is underway, and the results will be correlated to measured microstructures to define their relationships.

Surface Strengthening for Enhanced Fatigue Performance of Gamma Titanium Aluminides: Maria Glavatskikh¹; Janny Lindemann¹; Christoph Leyens²; Michael Oehring²; Fritz Appel¹; ¹Brandenburg University of Technology Cottbus; ²GKSS Research Centre

The fatigue performance of modern high niobium-containing gamma titanium aluminides can be significantly improved by mechanical surface treatments such as shot peening and roller burnishing. Fatigue strength improvements depend on the process-induced work hardening, the residual compressive stresses in the surface layer and on the surface roughness. While at ambient temperature the improvement of the fatigue strength is mainly caused by the process-induced residual compressive stresses, the residual stresses hardly affect the fatigue performance at elevated temperatures since they are quickly relaxed at service temperatures above 650°C. Nevertheless, surface strengthening can be beneficial for fatigue performance even at elevated temperatures. In the present work the potential of surface strengthening to enhance the fatigue performance of high niobium-containing gamma titanium aluminides at elevated temperatures was assessed. Furthermore, methods for improving the thermal stability of defect structures produced by surface strengthening were investigated.

Thermodynamic and Diffusion Modelling for Nanostructured Coatings Design on Gamma-TiAl Aluminides for High Temperature Applications: Francisco Perez-Trujillo¹; Juan Nieto¹; Maria Hierro de Bengoa¹; Sophia Tsipas¹; Juan Leal¹; Sonia Mato¹; ¹Universidad Complutense

Thermodynamic and diffusion modelling on gamma-TiAl have been applied in order to model the oxidation behaviour in different aggressive environments at high temperatures. From these data, solid phases can be model and use it to optimize the coating composition and design. Moreover diffusional approaches have been done to know the interdiffusion processes and metallic elements depletion in the process to form protective oxidized layer on the nanostructured coated gamma-aluminide. Some validation of this modelling approach will be given for micro/nano structured coatings.

Diffusion Bonding between TiAl and Ti₂AlNb: Jianying Zou¹; Yuyou Cui¹; Rui Yang¹; ¹Institute of Metal Research CAS

Direct diffusion bonding of orthorhombic Ti₂AlNb-base alloy to TiAl-base alloy was carried out and the interface microstructure, formation of new phase at the interface and joint strength were characterised. At low temperature, a new phase with AlNb₂-structure, Al(Nb,Ti)₂, was formed at interface adjacent to the O-based alloy. The α_2 was found to be the major reaction product and developed at interface adjacent to the TiAl alloy as well as at interface adjacent to the O-base alloy accompanying Al(Nb,Ti)₂. The formation of Al(Nb,Ti)₂ has been attributed to the different diffusion velocity of Nb and Al leading to a eutectoid-like reaction. At relatively high temperature, Al(Nb,Ti)₂ did not form due to enhanced diffusivity of Nb but a B2-enriched zone formed instead after long holding time. Only when an appropriate phase composition was achieved through diffusion could the shear strength of the joint reach 80% of that of the TiAl base metal.

Deformation in TiAl by the Formation of L11 Pseudotwin: Dongsheng Xu¹; Hao Wang¹; Rui Yang¹; ¹Institute of Metal Research, Chinese Academy of Sciences

The shear deformation of twinned and perfect TiAl with L10 structure at various temperature and hydrostatic pressure was investigated using atomistic simulations. By shearing in [211] direction on the (111) plane under hydrostatic compression, an L11 structured pseudo-twin was found to form at low temperature. The critical conditions for activating different twinning system were identified with the help of molecular dynamic and static simulation. The activation of the pseudo-twinning is expected to benefit the strain transfer and the reduction of the stress concentration at the grain or lamella boundary. The L11 pseudo-twin in TiAl was observed only in limited experiments, consistent with the difficulty of its formation. Our results showed that the L11 phase has a higher energy than normal twins, and can only form by shearing under hydrostatic compression. Further first principles calculation showed that some alloying elements may have the potential to promote this transformation.

Anisotropic Properties of Interfaces in Fe-Al: Vaclav Paidar¹; Jaromir Kopecek¹; Pavel Lejcek¹; ¹Institute of Physics

The properties of interfaces such as grain and antiphase boundaries are primarily derived from the atomic structure in their core regions. Structural and chemical inhomogeneity of these planar interfaces can play a decisive role for material behaviour including mechanical properties. Dislocation motion is affected by their core structure that depends on the stacking-fault-like defects and by the interaction with barriers as grain boundaries. Fracture is essentially governed by processes on atomic scale when the interatomic bonds are interrupted. In polycrystalline materials where the grain boundaries represent regions of different atomic arrangements, the cracks can nucleate and propagate under specific conditions along the boundary planes. The processes identified on interfaces will be discussed from the point of view of different grain boundary types and their behaviour will be deduced from experimentally studied grain boundaries in bicrystals and from theoretical considerations.

Effects of Ru Addition on Phase Equilibria, Microstructures and Mechanical Properties of E₂ Co₃AlC_{1-x} Based Alloys: Yosuke Uotani¹; Yoshisato Kimura¹; Yoshinao Mishima¹; ¹Tokyo Institute of Technology

E₂ Co₃AlC_{1-x} is one of the most possible candidates for a new strengthening phase in Co based heat resistant alloys. E₂ Co₃AlC_{1-x} transforms to E₂' Co₃AlC_{0.5} at 1325K due to the extra-ordering of C atoms associated with the APD formation. E₂' consists of alternate stacking of E₂ and L1₂ type close-packed {111} planes. Single crystal of Co₃AlC_{1-x} exhibits excellent ductility and high strength in a temperature range from 300 to 1373K. The influence of APD size on room temperature ductility was investigated using single crystals. Co₃AlC_{1-x} with fine APDs shows no plastic deformability. From the viewpoint of the improvement in elevated temperature strength, small amount of Ru addition was conducted and phase equilibria were investigated to establish the pathway to design new Co based heat resistant alloys. We have found that Ru is a B2 former and a solubility of Ru in Co₃AlC_{1-x} is limited to a few at.%.

Effects of Ternary Additions on Mechanical Behaviour of B2-Ordered Fe-40 at.% Al Alloys: Anna Fraczkiewicz¹; Sanaa Najjar¹; David Colas¹; Adrien Chapuis¹; ¹Ecole Nationale Supérieure des Mines

Forty years after beginning of development of B2-ordered FeAl for structural applications, their poor room temperature ductility still remains the main locking point. Nowadays, all existing solutions of avoiding this problem involve an extreme grain size refining by P/M-type technologies that make the fabrication cost of FeAl prohibitive. A new way of progress could come with development of optimised, ternary or quaternary, alloy compositions. Fe-40Al alloys, B-doped and containing some ternary elements (Ni, Co, Mo, Ti, Nb, Mn) have been studied. Their behaviour was appreciated from RT tensile tests and high temperature (20 – 900°C) compression tests. Among studied additions, Ni, Co and Mn seem the most interesting. Nickel and cobalt provoke a significant hardening associated with an important RT brittleness. In Mn-alloyed FeAl, an increase of RT ductility is associated with an unchanged YS value. These results will be analysed on the basis of alloys fine microstructure.

Fabrication and Strengthening of Ni-Based Thermostructural Panels: *Sara Johnson*¹; Tresa Pollock¹; ¹University of Michigan

Thermostructural panels for use in emerging hypersonic flight systems require the use of advanced materials able to support substantial loads at elevated temperatures. The major challenge in this advancing technology is identifying formable structural materials that are both strong and oxidation resistant. A new processing path beginning with sheets of Ni-based alloys has been developed where the solid-solution alloy is formed and subsequently strengthened by vapor phase aluminization. Fabrication, microstructure, mechanical properties, and oxidation behavior of these panels will be discussed.

Flow Behavior Characteristics and Constitutive Equation for IC10 Alloy: Hongjian Zhang¹; Weidong Wen¹; Haitao Cui¹; ¹Nanjing University of Aeronautics and Astronautics

IC10 is a newly developed Ni₃Al-based superalloy, with its nominal composition (wt%): 0.07-0.12% C, 11.5-12.5% Co, 6.5-7.5% Cr, 5.6-6.2% Al, 4.8-5.2% W, 1.0-2.0% Mo, 6.5-7.5% Ta, 1.3-1.7% Hf, 0.01-0.02% B, and Bal. Ni. In order to investigate flow behaviors of IC10, tensile experiments were conducted over a wide range of temperatures (25–800°C) and strain rates (0.0001–0.01/s) on a material-testing-system. Experimental results reveal that: 1) flow behaviors are not sensitive to strain rates at ambient temperature; 2) flow behaviors various with the temperature at the same strain rate; 3) the yield stress various little with temperature. In order to capture the major flow features of IC10, we apply and modify the Johnson-Cook equation in this paper. In Johnson-Cook equation, strain-rate effects and temperature effects are multiplied simply with hardening effects which cause some deviations in real prediction. So, we modify Johnson-Cook equation and use it to predict flow behaviors of IC10 at different experimental conditions. The comparisons between predicted and experimental data reveal that the modified equation works well in real prediction something.

Ternary Interdiffusion in Ni₃Al with Ir or Ta Additions: *Narayana Garimella*¹; M. Ikeda²; Machiko Ode³; Hideyuki Murakami³; Yong-ho Sohn¹; ¹University of Central Florida; ²Kobe Steel Company; ³National Institute for Materials Science

Average ternary interdiffusion coefficients in Ni₃Al with Ir or Ta additions have been determined using solid-to-solid diffusion couples annealed at 1200°C for 5 and 25 hours. Disc shaped alloy specimens were prepared by vacuum arc melting at various compositions within the Ni₃Al with minor alloying up to 3 at.% Ir or 1.5 at.% Ta. Concentration profiles of individual components were measured by electron probe microanalysis and interdiffusion fluxes were determined and examined to calculate the average ternary interdiffusion coefficients. Average main interdiffusion coefficients of Ir or Ta were observed to be two orders of magnitude lower than those of Al and Ni. A significant diffusional interaction between Ir and Ni, and between Ta and Al was observed, highlighted by large magnitudes in average cross interdiffusion coefficients. Variation of average ternary interdiffusion coefficients is presented with respect to sublattice sites of Ni₃Al and applications in high temperature alloys and coatings.

The Development of High Specific Strength Wrought Fe₃Al-Based Alloys: *Satoru Kobayashi*¹; Stefan Zaefferer²; Takayuki Takasugi¹; ¹Tohoku University; ²Max-Planck-Institut Fuer Eisenforschung GmbH

Our recent research on grain refinement of Fe₃Al-based alloys through thermomechanical process revealed that coarse κ -Fe₃AlC precipitate particles are effective in introducing nucleation sites for recrystallization, and thereby refining grain size.^{1,2} Between room temperature and 600°C, fine-grained materials showed specific strengths as high as Ti-based alloys, indicating that Fe₃Al-based alloys might be useful for structural components such as low-pressure turbine blades and compressors. Fatigue properties and tensile properties in water vapor atmosphere will be presented. ¹Kobayashi S, Zaefferer S: Microstructure Control Using Recrystallization in Particle-containing Fe₃Al-based Alloys, Materials Science Forum Vol. 558-559, pp. 235-240 (2007). ²Kobayashi S, Takasugi T: Grain Refinement of a Fe₃Al-based Alloy Using κ -Fe₃AlC Precipitate Particle Stimulating Nucleation of Recrystallization, Intermetallics, accepted.

Microstructure and Mechanical Properties of a Eutectoid FeNiMnAl Alloy: *Yifeng Liao*¹; Ian Baker¹; ¹Dartmouth

The microstructure and mechanical properties of a novel eutectoid alloy with the composition (in at.%) of Fe-20Ni-35Mn-15Al have been studied. The alloy was arc melted from elemental powders, and SEM/EDS and TEM/EDS

were used to determine the microstructures and compositions of the phases present. The results revealed that the compound was composed of FCC and B2 lamellae, whose widths were ~300 nm and ~200 nm, respectively. Straining under compression produced yield strengths ranging from 750 MPa at 300 K to 160 MPa at 1000 K, with a rapid drop in yield strength at ~600 K. Elongations of 25%-30% were observed in tensile tests at room temperature, with fracture surface analysis indicating a ductile fracture mode. The dislocation behavior was also investigated. Research supported by NSF grant DMR-0505774.

The Role of Engineers in Meeting 21st Century Societal Challenges — AIME Keynote Session

Sponsored by: The Minerals, Metals and Materials Society, TMS; Public and Governmental Affairs Committee

Program Organizers: Diran Apelian, Worcester Polytechnic Institute; Iver Anderson, Iowa State University

Wednesday PM

Room: 272

March 12, 2008

Location: Ernest Morial Convention Center

Session Chair: Dan Thoma, Los Alamos National Laboratory

2:00 PM Introductory Comments by Dan Thoma, Los Alamos National Laboratory

2:10 PM Invited

The Role of Engineers and the Profession in the 21st Century: *Diran Apelian*¹; ¹Worcester Polytechnic Institute

Globalization of the economy has amplified the impact of technology on modern societies in ways that could not have been predicted. The connectivity provided by the Internet has generated new markets for products and services, but has also made available labor that is often both educated and cheap. This is likely to have a profound impact on the distribution of wealth in both the developed and the developing part of the world and may, in particular, alter the socio-economic structure of countries where the general well-being of the population has been taken for granted. The role of engineers and the profession is critical for the sustainable development of our planet. The 21st Century presents us with challenges (as well as opportunities) that will require a “new” breed of engineers. These issues and the impending actions that we need to take will be discussed in this presentation.

2:30 PM Invited

People First: Global Mission: *Jaleel Al-Khalifa*¹; ¹Saudi Aramco

In the past, share holders’ emphasis on maximizing short-term commercial interest (The bottom line) has steered corporate management. The notion of management by values was introduced to better engage the workforce. Introducing the corporate social responsibility (CSR) to help local communities has also gained significant momentum. The notion of the three bottom-line (share holders, customers, workforce) was also introduced. The next essential reform is to apply “People First” paradigm, i.e. the four bottom-line (share holders, customers, workforce, and humanity at-large). “People First” ensures the commercial success of the organization, while meeting the global mission of advancing growth and prosperity of mankind. It represents a very systematic approach to running business while serving humanity. It aims at ensuring the commercial success while availing adequate food, water, shelter, health and education for the neighbor community. The role of professional societies to promote “People First” paradigm cannot be further emphasized. We, professionals, need to continually sharpen our technical competency and at the same time nurture the human side of our character. It is both technical competency and personal character that ensure excellence in our future careers.

2:50 PM Invited

Energy Sources for the 21st Century - Implications and Challenges: *Tomas Diaz De La Rubia*¹; ¹Lawrence Livermore National Laboratory

Economic development and population growth trends indicate that global energy demand will double by the year 2050 to 25 TW-yr and will reach 50-60 TW-yr by 2100. At the same time, climate models indicate that continued

emissions of greenhouse gases into the atmosphere will likely lead to global surface temperature increase by the year 2100 ranging from 1.1 C to 2.9 C in the low impact scenario. Fossil fuels, the main culprits behind current increases in CO₂ concentration in the atmosphere, currently provide 85% of the world's energy demand, but are likely to deplete over the next decades for oil and gas, or the next two centuries for coal. Meeting the growth in energy demand while mitigating climate change will demand new energy sources beyond fossil fuels such as solar, nuclear and ultimately fusion. The development and massive worldwide deployment of these clean, alternative sources to produce energy at economically competitive rates will require new, advanced materials capable of performing with high efficiency, safety and reliability, often in very extreme environments. In this talk, I will describe some of the world wide efforts to develop new materials for energy applications with an emphasis on fission and fusion energy.

3:10 PM Break

3:20 PM Invited

Sustainable Mobility: The Grand Challenges: *John Moavenzadeh*¹; ¹World Economic Forum

Transportation of both people and goods will face a number of interconnected challenges over the next decades, including: Urbanization: The world's urban population will grow from roughly 3.2 billion today to roughly 4.9 billion by 2030, an increase of over 50%.¹ United Nations World Urban Population Prospects: 2005 Revision. How will this fundamental transformation in where we live affect the automotive industry? How will people get around in the city of the future? Global Climate Change: Public awareness of global climate change continues to grow, and governments are increasingly ready to act. Does the automotive industry have the best strategy to engage governments and other stakeholders on the climate change issue? Developing World Motorization: Tata Motors of India is launching a \$2500 car for the Indian market. China is now the second largest automotive market in the world. What are the implications of a rapidly motorizing developing world? Other noteworthy challenges include the global volume of vehicle-related fatalities, the overwhelming dependence of the transport sector on fossil fuels, an ageing air transport infrastructure that cannot keep up with increasing demand, and others. Engineers have a critical role to play in developing technology that will enhance the sustainability of the transport network for future generations; however, engineers will need to work closely with other stakeholders. ¹United Nations World Urban Population Prospects: 2005 Revision.

3:40 PM Invited

Housing for the 21st Century – Design, Technology and Construction: *Stephen Lee*¹; ¹Carnegie Mellon

Traditional American methods of homebuilding are not adequately responding to the need for flexible, affordable, energy effective and resource efficient homes. This session will take a fresh look at the housing delivery process in response to global and regional change. From climate change, to power deregulation, to suburban sprawl to the rapid proliferation of information technology, change is occurring at a more rapid pace than at any other time in our history. Yet, the housing industry is a fragmented, multi-headed beast in which change is slow to occur, if at all. Our houses of today are not meeting the needs of the users, nor are they performing as good "global" citizens. Applying industrial engineering principles to the housing delivery process could potentially offer solutions to directly solve these problems. History however, shows us that the houses constructed in this fashion, from the panelized houses of Konrad Wachsmann and Walter Gropius to Operation Breakthrough and HUD-code homes, have not been the solution to our housing needs. While these historic efforts introduced new technologies and processes, they were not fully integrated into the structure of the domestic homebuilding industry. Japan and the European Community, faced with higher energy costs and high density housing conditions, have been leading the way globally with innovative ideas and financial incentives to produce better housing. The concepts of "low-", "zero-" and "plus-" house are well known and describe the annual energy balance for homes with respect to the grid. This session will speak directly to our future housing needs and will illustrate potential design, technology and construction process solutions using the 2007 Carnegie Mellon Solar Decathlon house as a case study.

4:00 PM Invited

Biomaterials: Evolving Technologies and Applications: *Arthur Coury*¹; ¹Genzyme Corporation

Biomaterials, the components of medical devices that interact directly with tissue, have enabled the development of a worldwide industry of over \$200 billion. From its infancy a half-century ago, the device industry has evolved from the use of commercially available commodity materials for mainly structural applications to custom-designed materials with specific properties and biological interactions. Accompanying this transition, the complexity and functionality of device designs have increased to include products such as device-drug, device-biologic and device-cell combinations. Therapeutic goals have increasingly evolved from replacement of structure and function of body tissues to their restoration and regeneration using principles of tissue engineering, i.e., systematic control of cells, matrices and fluids of the body. By my estimate, some 25% of device and combination products involve tissue engineering. Regenerative and restorative therapies currently involve expensive development and production protocols, but economic efficiencies to come will improve the availability of advanced medical therapies worldwide.

4:20 PM Invited

Recycling Technologies and Environmental Stewardship: *David Spencer*¹; ¹wTe Corporation

The ever burgeoning quantities of waste that our society produces are a positive sign of economic growth and human wealth. This new world-wide industrial revolution, however, also spawns new challenges to effective environmental stewardship. Historically, these end-of-life products have been wasted — either disposed in landfills or incinerated — often with adverse environmental consequences. Early methods of recycling were incapable of dismantling and recycling manufactured products whereby the inherent value of the processed materials going into the end-product was preserved. Recently, with support from NSF and NIST/ATP, new optoelectronic recycling processes are under development or being piloted to recycle end-of-life goods in a fully automated way. These advanced technologies can run at high capacity and sort a wide array of materials with extreme accuracy yielding high-value recycled raw materials. As a result, a paradigm shift in recycling, with significant consequent benefits to the environment is both possible and probable, along with the generation of still more opportunities for manufacturing new products with much higher quantities of recycled content.

Ultrafine-Grained Materials: Fifth International Symposium: Structure and Evolution

Sponsored by: The Minerals, Metals and Materials Society, TMS Structural Materials Division, TMS Materials Processing and Manufacturing Division, TMS: Shaping and Forming Committee, TMS: Nanomechanical Materials Behavior Committee
Program Organizers: Yuri Estrin, Monash University and CSIRO Melbourne; Terence Langdon, University of Southern California; Terry Lowe, Los Alamos National Laboratory; Xiaozhou Liao, University of Sydney; Zhiwei Shan, Hysitron Inc; Ruslan Valiev, UFA State Aviation Technical University; Yuntian Zhu, North Carolina State University

Wednesday PM

March 12, 2008

Room: 273

Location: Ernest Morial Convention Center

Session Chairs: Xiaozhou Liao, University of Sydney; Terry McNeley, Naval Postgraduate School; David Morris, Centro Nacional de Investigaciones Metalurgicas, CSIC; Pei-Ling Sun, Feng Chia University

2:00 PM Invited

Deformation-Induced Grain Growth and Texture Evolution in Nanocrystalline Materials: Li Li¹; Yandong Wang²; Guojian Fan¹; Y. L. Yang²; N. Jia²; Yang Ren³; Hahn Choo¹; *Peter K. Liaw*¹; ¹University of Tennessee; ²Northeastern University, School of Materials and Metallurgy; ³Argonne National Laboratory, X-Ray Science Division

Grain growth was observed recently in nanocrystalline materials (grain size < 100 nm) during the plastic deformation. However, the underlying mechanisms of this deformation-induced grain growth were not well understood. In our

studies, nanocrystalline Ni-Fe alloys with grain size $\sim 23\text{nm}$ were investigated after rolling under both room and liquid-nitrogen temperatures. The high-energy x-ray diffraction technique was used to investigate their mechanical deformation behaviors. Compared with as-deposited one, the nanocrystalline Ni-Fe alloy shows great grain growth (up to $\sim 50\text{ nm}$) after rolling at room temperature. Moreover, a strong texture is found to develop in the deformed nanocrystalline materials during rolling. Based on the above experiments and the associated simulations, deformation mechanisms in nanocrystalline material will be discussed in this presentation. This research is supported by NSF-IMI program (DMR-0231320) and NSF-MRI program (DMR-0421219).

2:20 PM

Towards the Basic Rules for Grain Refinement by SPD Processing: *Ruslan Valiev*¹; ¹Ufa State Aviation Technical University

Intensive investigations of the past 10-15 years oriented at fabrication of bulk nanostructured materials using severe plastic deformation (SPD) processing have made it possible to conclude that grain refinement is determined by three main factors: the SPD technique in use, SPD processing regimes and routes, as well as the nature of the material processed. In the present report, critical processing parameters (accumulative strains, processing temperature and applied pressure) that determine efficiency of grain refinement are investigated, taking the two most popular SPD techniques (namely, equal-channel angular pressing and high-pressure torsion) as an example. The problem of ultimate microstructure refinement by SPD processing is considered as well.

2:35 PM Invited

High Pressure Torsion in Mg: Effect of Strain and Hydrostatic Pressure on Texture Evolution: Bartłomiej Bonarski¹; Erhard Schafner¹; Borys Mikulowski²; Michael Zehetbauer¹; ¹University of Vienna; ²AGH-University of Science and Technology

Single crystals, and polycrystalline samples of 99.8% Mg with different initial grain size, have been subjected to High Pressure Torsion at RT. The evolution of texture has been investigated as a function of shear strain (up to 120) and of hydrostatic pressure (up to 4 GPa). Apart from a compression component which arises from the early stages of HPT deformation, a clear shear texture evolves. However, at the largest strains investigated, a new texture is observed which exhibits clear evidence for recrystallization. As concerns the texture evolution at higher pressures, the same sequence of textures appears but the onset of recrystallization occurs at lower strains. The results are compared with previous investigations of HPT induced texture evolution in hexagonal and cubic face centered metals, and discussed in terms of c/a ratio and of lattice symmetry, respectively.

2:55 PM

The Limiting Grain Size during Severe Deformation of Dilute Aluminium at Cryogenic Temperatures: *Philip Prangnell*¹; Yan Huang¹; ¹University of Manchester

The deformation structures formed in a dilute aluminium alloy have been studied down to liquid nitrogen temperatures, with the aim of investigating the factors that limit the formation of a true nano-scale grain structure. It was found that a steady state was approached, where a minimum grain size was reached irrespective of the temperature. Even at -198°C a nanoscale high angle boundary spacing was only approached in the normal direction. It is shown that the minimum grain size achievable in severe deformation is controlled by a balance between the rate of compression of the HABs and dynamic recovery, with a minor effect of texture and changing the deformation mode. The required boundary migration rate to maintain a constant boundary spacing was found to be far higher than can be justified from conventional diffusion controlled grain growth and at low temperatures, can only be explained by invoking an athermal mechanism.

3:10 PM

Microstructure Refinement in Iron Aluminide by Severe Plastic Deformation: *David Morris*¹; Ivan Gutierrez-Urrutia¹; María Muñoz-Morris¹; ¹Centro Nacional de Investigaciones Metalúrgicas, CSIC

Microstructural refinement of ductile alloys can be achieved by severe plastic deformation carried out to different strain levels using various processing methods. Changes of microstructure of iron aluminides have been examined after severe plastic deformation, with the extremes of low and high strain levels

achieved by heavy rolling and by mechanical milling. Processes such as ECAP provide intermediate strain levels. The deformation substructure obtained during the initial stages of straining is inhomogeneous, showing changes that appear to correspond to different textures or grain orientations. At extremely high strain levels, as the structural scale refines towards the nanoscale, the microstructure becomes homogeneous once again. The relationship between grain orientation, local texture, and the microstructure generated by severe plastic deformation will be examined. These factors play also an important role in determined the way the microstructure coarsens or recrystallizes during annealing after deformation.

3:25 PM Invited

Microstructure and Microhardness of FCC Metals Subjected to Ultra-High Strain Deformation: *Alexander Zhilyaev*¹; Azat Gimazov²; Ádam Révész³; Terence Langdon⁴; ¹Centro Nacional de Investigaciones Metalúrgicas, Consejo Superior de Investigaciones Científicas; ²Russian Academy of Sciences, Institute for Metals Superplasticity Problems; ³Eötvös University; ⁴University of Southern California, Los Angeles

Microhardness measurements, TEM and X-ray were used to study the microstructure and tensile properties of highly strained nickel and copper processed from bulk master metal strained to different levels and from electrodeposited, ball milled (BM), rapidly quenched (RQ) ribbons and machined chips. High resolution X-ray showed BM+HPT specimens have the smallest coherent domain size of 9 nm and RQ+HPT possesses the highest dislocation density of $6.7 \times 10^{15}\text{ m}^{-2}$. A gradual increasing strain in bulk nickel gave increasing dislocation density and decreasing coherent domain size. Microstructure and microhardness of pure copper was compared after ECAP (4 passes, route BC), HPT ($P=6\text{ GPa}$, $N=5$), machining and their combinations, including machining of ECAP specimens, HPT of ECAP copper and HPT of machining chips. Microstructure, dislocation density and microhardness were evaluated by X-ray, transmission and scanning electron microscopy. The influence of different processing routes is discussed in terms of accumulated strain and microstructure refinement.

3:45 PM Break

4:00 PM Invited

Vacancies by Severe Plastic Deformation and Their Effects in Ultrafine-Grained Al: X.L. Wu¹; B. Li²; *Evan Ma*³; ¹Institute of Mechanics; ²Materials Science; ³Johns Hopkins University

Severe plastic deformation (SPD) introduces into a metal an extraordinarily high population of vacancies, in addition to dislocations that evolve into grain boundaries. These vacancies also cluster to form nanoscale entities that should have major impact on the microstructure-mechanical property relationship; but this aspect has not received adequate attention so far and remains to be systematically studied. Here we report the size, density, distribution, and stability of vacancy clusters in aluminum after SPD-processing at liquid nitrogen temperature. Vacancy-type dislocation loops as large as 16 nm, at a density as high as $1\text{E}15/\text{m}^2$, have been observed under transmission electron microscope. Molecular dynamics simulations indicate that such large faulted loops (stacking faults), when at these high densities, contribute in a major way to impeding moving dislocations. These stacking faults should hence be taken into account when interpreting the high strength of ultrafine-grained or nanostructured metals processed by SPD.

4:20 PM

Strain Path and Microstructure Evolution during ECAP of Al-Si Alloys: Juan Maria Garcia de la Infanta Belio¹; Srinivasan Swaminathan²; Alexander Zhilyaev¹; Fernando Carreño¹; Oscar Ruano¹; *Terry McNelley*²; ¹Centro Nacional de Investigaciones Metalúrgicas (CENIM), CSIC; ²Naval Postgraduate School

As-cast Al-Si alloys were subjected to repetitive ECAP at ambient temperature by route A, which involves monotonically increasing strain through a sequence of passes, or by route BC, wherein the strains are redundant after every four passes. The shape change of the primary and eutectic constituents mirror the idealized straining expected for repetitive processing by either of these routes. This leads to strain path dependence of grain refinement in the primary constituent: grain subdivision combined with geometric effects are operative in material processed by route A, while grain subdivision alone predominates in material processed by route BC. Also, the morphology and distribution of the eutectic constituent in processed materials reflect mainly geometrical effects.

4:35 PM Invited

Phase Separation in Ultrafine Grained Materials Produced by Severe Plastic Deformation: *Xavier Sauvage*¹; *Xavier Quelennec*¹; *Abdelahad Chbihi*¹; *Dmitry Gunderov*²; *François Vurpillot*¹; ¹University of Rouen, GPM; ²Ufa State Aviation Technical

Ultrafine Grained (UFG) structures produced by Severe Plastic Deformation (SPD) usually exhibit a much higher yield stress than their coarse grained counterparts; however in most cases applications are limited due to the relatively low ductility. It has recently been suggested that a combination of UFG structure with precipitation of a second phase may give rise to some significant strain hardening and ductility. In this context, we have investigated phase separation and precipitation in FeCu, CuCr and FePdAu alloys processed by SPD. Microstructures were characterized thanks to transmission electron microscopy and three-dimensional atom probe. A special emphasis was given on the competition between phase separation and recrystallisation. In such non equilibrium structures, we show that even if the driving force for recrystallisation is extremely high, phase separation usually occurs first. This feature is attributed to an accelerated precipitation kinetics resulting from enhanced atomic mobility of solute elements.

4:55 PM

Grain Refinement Mechanisms and Mechanical Properties in Copper Subjected to Severe Plastic Deformation: *Nairong Tao*¹; *K. Lu*¹; ¹Chinese Academy of Sciences, Institute of Metal Research

The grain refinement in copper subjected to plastic deformation was investigated by means of TEM. Strain-induced three different grain refinement approaches were identified. At low strain rate, plastic deformation is dominated by dislocation activities. Submicro-sized grains were obtained via formation and development of dislocation cells. The final size of the refined grain is usually 100-300 nm. At high strain rate, mechanical twins were induced and deformation twinning plays an important role in grain refinement process. The structure refinement was achieved by the break-up of twin/matrix lamellae. The average transverse size of refined grains is about 47 nm. Nano-sized grains were also formed inside the shear bands. The nanostructured Cu sample prepared at cryogenic temperatures and high strain rate exhibits tensile yield strength of over 600 MPa, evidently higher than that of the Cu prepared at room temperature and low strain rate (~ 400 MPa).

5:10 PM Invited

Gradient Multiscale Structure and Tensile Property of Cobalt by Surface Mechanical Attrition Treatment: *Xiao-Lei Wu*¹; ¹Chinese Academy of Sciences, Institute of Mechanics

The formation of the gradient multiscale structure (GMS) in hcp-cobalt during surface mechanical attrition treatment was investigated. The GMS showed grain size distribution ranging from 25 nm to 500 nm in the deformed surface. The mechanism of grain refinement was interpreted in terms of the structural subdivision of grains subjected to plastic deformation. Moreover, plastic deformation induced the phase transformation from hcp into fcc structure. The nanocrystalline fcc phase exhibited also gradient distribution in grain size and volume fraction as well. The tensile properties of GMS cobalt were discussed.

5:30 PM

Irradiation Behavior of Nanostructured Austenitic Steels: *Philippe Pareige*¹; *Auriane Etienne*¹; *Bertrand Radiguet*¹; *Xavier Sauvage*¹; *Ruslan Valiev*¹; ¹Rouen University

The evolution of mechanical properties of austenitic stainless steels in internal structures of pressure water reactor is due to complex intragranular and intergranular induced segregation. An atomic description of the phenomena is needed to increase the level of understanding of the mechanisms at the origin. This means for example that careful examination of grain boundaries is needed and elimination of intragranular segregation would be interesting. In order to bring information, austenitic materials have been nanostructured, annealed and ion irradiated. This allows to investigate a large density of grain boundaries and also to understand the effect of nanograins on the elimination of irradiation point defects. Atomic description of the nanostructure and grain boundaries with Tomographic Atom Probe and TEM will be given. Point defects evolution will be followed with rate theory.

5:45 PM

Deformation Behavior during Tensile Straining of Nano/Ultrafine-Grained Structures Formed by Reversion in Metastable Austenitic Steels: *Devesh Misra*¹; *B. Ravi Kumar*¹; *Sashank Naik*¹; *Mahesh Somani*²; *Pentti Karjalainen*²; ¹University of Louisiana at Lafayette; ²University of Oulu

The deformation behavior of nano/ultrafine-grained structures during tensile deformation has been examined by transmission electron microscopy in metastable austenitic steels. Special fine-grained structures were obtained by controlled reversion annealing of strain-induced martensite. Proper gradual strain hardening by the formation of ultra-fine martensite results in excellent tensile strength-ductility property combination.

3-Dimensional Materials Science: Modeling and Characterization across Length Scales IV

Sponsored by: The Minerals, Metals and Materials Society, TMS Structural Materials Division, TMS: Advanced Characterization, Testing, and Simulation Committee
Program Organizers: Michael Uchic, US Air Force; Eric Taleff, University of Texas; Alexis Lewis, Naval Research Laboratory; Jeff Simmons, US Air Force; Marc DeGraef, Carnegie Mellon University

Thursday AM Room: 286
 March 13, 2008 Location: Ernest Morial Convention Center

Session Chair: Michael Uchic, US Air Force

8:30 AM

HAADF-STEM Tomography of Intrinsically Low Contrast Materials: *David Morgan*¹; *Miriam Herrera*¹; *Shareghe Maheraeen*¹; *Volkan Ortalan*¹; *Nigel Browning*¹; ¹University of California, Davis

Materials science tomography has traditionally involved materials exhibiting large contrast variation. Examples of such materials are catalytic nanoparticles and quantum dots sitting on or embedded within a matrix of lighter elements. The large contrast difference between such particles and their matrix is highlighted using high angle annular darkfield (HAADF) scanning transmission electron microscopy (STEM) and tomography based on HAADF-STEM images can clearly reveal particle shape and arrangement in three-dimensions. Indeed, data processing for tomography makes use of the high contrast nature of such images. However, materials where the structure is dominated by features such as grain boundaries or dislocations do not exhibit such contrast and have proven difficult to analyze using conventional tomographic methods. We are developing methods to deal with such low contrast materials and will present results based on a variety of image processing filters utilized at various steps during the tomographic data processing procedure.

8:50 AM

Dark-Field Electron Tomography for Three-Dimensional Domain Morphology in Ni-Based Ordered Alloys: *Syo Matsumura*¹; *Kosuke Kimura*¹; *Kanae Matsuyama*¹; *Satoshi Hata*¹; ¹Kyushu University

Electron tomography is rapidly getting popular these days for three-dimensional material characterization in nanometer scale with development of computer-assisted operation of transmission electron microscopes. So far, this technique has been mostly applied to fine structures and morphologies due to element aggregation with spatial variation of mass density, in which transmittance of incident electrons decays monotonically with mass-thickness. In contrast, dark-field transmission electron microscopy with diffracted electrons can image morphologies of crystal grains and ordered domains, which are due to spatial change in crystal orientation. In this study, we made a trial to reconstruct three-dimensional morphologies of ordered domains in Ni-based alloys from tilt series of dark-field images by the computed-tomography procedure. In the present talk, we will demonstrate three-dimensional characterization of domain shapes and dispersion of $D1_a$ ordered variants in a Ni_4Mo alloy as well as of precipitates of gamma and gamma-prime phases in Ni-Al-Ti alloys.

9:10 AM

A Femtosecond Laser-Aided Serial Sectioning Process and 3D Dendrite Reconstruction of a Nickel Based Superalloy: *McLean Echlin*¹; *Jonathan Madison*¹; *Tresa Pollock*¹; ¹University of Michigan

A laser-aided technique for acquisition of three-dimensional microstructural datasets has been developed. This technique has been utilized to image dendritic structure at the solidification front in a nickel-base single crystal superalloy. The solid-liquid interface is obtained by draining molten metal from an investment mold in a partially solidified casting. The 3D reconstruction was produced using a fully automated serial sectioning process that employs a femtosecond laser to ablate material from the sample surface. Between material removal steps 2D images are captured using an optical lens and a fiber light illumination system. The collection of images are stacked and reconstructed using IDL™ into a 3D dataset. Sectioning slice thicknesses range from the ablation fluence threshold for René N4 (~30-50 μm), and have no apparent slice thickness upper bound.

The efficiencies of this serial sectioning process relative to FIB-based and mechanical serial sectioning techniques will be discussed.

9:30 AM

Micromechanics-Based Modeling of Ductile Fracture with Experimental Integration of 3-D Microstructural Data: *Amine Benzerga*¹; ¹Texas A&M University

In ductile fracture of structural materials, damage initiates at second-phase particles. Therefore, the spacing between these sets the relevant scale of analysis. A unifying framework for analyzing ductile damage by void nucleation, growth and coalescence will be presented. It relies on constitutive descriptions that incorporate shape, relative spacing and orientation of particles in addition to their volume fraction. One peculiar feature of this framework is that crack initiation and growth are natural outcomes to competing plastic mechanisms. The counterpart to the enriched microstructural description is the need to collect more experimental information, both in the undeformed and deformed states. Use of two-dimensional imaging, aided by suitable stereological transformations, has traditionally been the method of choice in providing critical input and model assessment data. In strongly anisotropic materials, however, there is a need for full three-dimensional input and avenues in exploring such input in our modeling strategies will be discussed.

9:50 AM Break

10:10 AM

Three-Dimensional Characterization of Dendritic Structure in Nickel-Base Single Crystals: *Jonathan Madison*¹; *Jonathan Spowart*²; *David Rowenhorst*³; *Tresa Pollock*¹; ¹University of Michigan; ²US Air Force; ³Naval Research Laboratory

During solidification, solute-induced convective instabilities at the solid - liquid interface can result in the formation of defects such as freckles and misoriented grains. These defects can be particularly detrimental in the directional solidification of single crystal nickel-base superalloys. Unfortunately, detailed understanding of fluid flow at the scale of the dendritic structure has yet to be fully understood, particularly under conditions in which heat extraction is non-axial. The objective of this research is to develop a technique for quantifying the dendritic substructure at the solid - liquid interface for the purposes of providing direct input into computational fluid flow modeling. Using the RoboMET.3D serial sectioning system, three-dimensional datasets of dendritic structures within decanted René N4 have been obtained and will be shown. Distributions and arrangements of solid and liquid in the vicinity of dendrite tips will also be presented along with discussion of implications for defect formation.

10:30 AM

Advanced Characterization to Determine Chemical Segregation in Nickel Super Alloys: *Jaimie Tiley*¹; ¹US Air Force

Advanced neutron diffraction, high resolution transmission electron microscopy, and atomic probe tomography techniques were employed to determine the three dimension microstructure characteristics of several commercial nickel superalloys. This includes the volume fraction and morphology of ordered gamma prime phases, the chemical segregation between phases as a function of processing conditions and temperature, and the lattice misfit, site occupancies, and thermal expansion parameters for the studied materials.

10:50 AM

Three Dimensional Characterization of Microstructure in Hot-Deformed AA5083 for Understanding Cavitation Damage: *Jung-Kuei Chang*¹; *Eric Taleff*¹; *Paul Krajewski*²; ¹University of Texas; ²General Motors Corporation

Fine-grained aluminum alloy AA5083 sheet is hot formed into complex body panels by the Quick Plastic Forming process for the mass production of automobiles. Cavity formation and interlinkage during hot tensile straining can limit the formability of this material in production. Cavitation is strongly influenced by a number of microstructural features, particularly intermetallic particles. The relationship between intermetallic particles and cavities is complex. Standard microstructural observations of two-dimensional material cross sections have not produced data sufficient to understand this relationship. Serial sectioning was used to produce three-dimensional, 3-D, microstructure data sets. These 3-D data sets reveal relationships between intermetallic particles and cavities not previously observable. In particular, cavity percolation and

cavity-particle adjacency are available and quantifiable from the 3-D data. These data provide definitive evidence for the association of cavities with particular intermetallic particle types and particle spatial distributions.

Alumina and Bauxite: Precipitation/Conclusion

Sponsored by: The Minerals, Metals and Materials Society, TMS Light Metals Division, TMS: Aluminum Committee

Program Organizers: Sringeri Chandrashekar, Rio Tinto Aluminium Limited; Peter McIntosh, Australus Management Services

Thursday AM
March 13, 2008

Room: 296
Location: Ernest Morial Convention Center

Session Chair: Luiz Correa, Companhia Vale do Rio Doce

8:30 AM Introductory Comments

8:35 AM

The Effects of Wet Oxidation on Hydrate Yield Inhibitors in Alkaline Aluminate Solutions: *Joanne Loh*¹; *Greta Brodie*¹; *Greg Power*¹; *Chris Vernon*¹; ¹CSIRO Minerals

Wet oxidation can be an effective means of removing organics from Bayer liquor. Total removal of organics by wet oxidation requires extreme conditions, so partial organics removal is generally considered to be a more economically viable approach. However the mechanisms of degradation by wet oxidation are complex and the products of partial wet oxidation are not well understood. This allows the possibility that there may be conditions under which harmful products, in particular hydrate yield inhibitors, could be produced. This fundamental study was conducted to determine the susceptibility of known yield inhibitors to destruction by wet oxidation. It is shown that of the yield inhibitors investigated, compounds with more than 5 carbons in a chain and aromatic compounds are readily destroyed by wet oxidation at 165°C in the presence of oxygen. Members of the C4 family of inhibitors are more stable and require higher temperatures for full destruction.

9:00 AM

Using Mass Balance for Solids Concentration Control at Precipitation Agglomerator Tanks: *Anderson Amaral*¹; *Cleto Junior*¹; *Luiz Gustavo Correa*¹; *Jorge Lima*¹; *Joaquim Filho*¹; *Luiz Santos*¹; ¹Alunorte

The solids concentration control at agglomerator tanks is used as a tool to control the hydrate PSD at precipitation, as well as, to guarantee the alumina attrition index in suitable levels. The range of solids concentration used at Alunorte agglomerator tanks to achieve these objectives is allowed to vary around 180-220 gpl. This paper aims to present the application of one transient mass balance to control the solids concentration at agglomerator tanks. JAVA programming language was used to implement routine for calculations and the PI - Plant Information software, connected with DCS was used for control loop implementation. The relative mean error between the results of calculated solids concentration, by mass balance, and the analyzed samples is around 10%, indicating an excellent applicability of the transient mass balance to control the solids concentration at agglomerator tanks.

9:25 AM

Influence of Ultrasonic Processing on Sodium Aluminate Solution and Alumina Hydrate Precipitation Process: *Jibo Liu*¹; *Qiyuan Chen*¹; *Zhoulan Yin*¹; ¹Aluminum Corporation of China Limited

The influence of ultrasonic processing on sodium aluminate solution and alumina trihydrate precipitation process were studied. The cavitation phenomenon caused by ultrasound were detected by hydrophone and sonofluorescence, the structure alterations of sodium aluminate solution were investigated by ESR, 27Al-NMR spectra, and RAMAN spectra, the alumina trihydrate precipitation processes from sodium aluminate solution with ultrasonic processing were also studied, it was found that the ultrasonic processing can cause cavitation and molecular structure change in sodium aluminate solution, the precipitation rate can also be enhanced by ultrasonic processing, and the appearance and granularity of the crystalline produced by the precipitation process were also affected.

9:50 AM

The Impact of Conversion from Batch to Continuous Agglomeration at the Ewerton Alumina Refinery: *Patrick Harris*¹; ¹West Indies Alumina Company

The agglomeration circuit at the Ewerton Alumina Refinery was converted from batch to continuous mode. The change was achieved by a reconfiguration of existing tanks and pipework. Open launders were installed between the continuous tanks. The final arrangement is a continuous agglomeration circuit followed by a short continuous growth circuit and batch growth precipitators. The impact of the reconfigured precipitation circuit on yield, particle size control and residual soda were assessed and are presented in this paper. There was significant increase in precipitation yield and reduction in residual soda in the final alumina tri-hydrate, while maintaining alumina particle size within customer specification.

10:15 AM Break

10:30 AM

Characterization Profile in Scales from CVG-Bauxilum: *Ricardo Galarraaga*¹; *Royman Cañas*¹; *Nelson Piñero*¹; ¹CVG Bauxilum

One of the most current and challenging issues affecting Bauxite processing Plants is the constant scale formation in equipment and main process piping. From the Red to the White Side, no one area is exempted from this situation. Based on this, the present work focuses on a detailed investigation of the chemical composition of the scale according to its origin site. Samples were collected, analyzed and dissolution tests made for each of the scales. The purpose of the investigation converges in the study and optimization of the ideal process parameters for the elimination, control or reduction of the formation. The final recommendation is centered around the determination of each type of cleaning system to be used, mechanical, high pressure water, or chemical. For the later case emphasis has been put on temperature conditions, caustic concentration, RMC, contact time and frequency of cleaning that do not impact considerably on plant capacity.

10:55 AM

Ibbsite Precipitated from Caustic Aluminate Solutions Irradiated by Ultrasound: *Guohui Chen*¹; *Chen Yuan*¹; *Yin Lan*¹; *Yin Min*¹; ¹Central South University

Stereoscopic microscope, SEM and Laser diffraction sizer measurements are used to study gibbsite precipitation from caustic aluminate solutions irradiated by low frequency ultrasound waves. The observed phenomena showed that low frequency ultrasonic wave could enhance not primary nucleation but secondary nucleation, the new secondary nuclei on mother seeds were pseudo hexagonal slices with diameter less than 1µm and thickness at nanometer grade, these new nuclei on seeds could break away from seeds and aggregate, change the size distribution of precipitates, form a new peak below 10µm, but the size of the main peak was not affected.

11:20 AM

Simulation on Seeded Precipitation Process of Alumina Production from Diasporic Bauxite: *Jibo Liu*¹; *Xinping Tang*¹; ¹Aluminum Corporation of China Limited

The diasporic bauxite has to be digested by high concentration sodium hydroxide, and the pure liquor for seeded precipitation process has relatively higher caustic concentration and low supersaturation, in this condition, the seeded precipitation process is not easy to produce sandy alumina trihydrate. And the mechanisms of alumina trihydrate precipitation process from high concentrated sodium aluminate solution is different from that from high supersaturation pure liquor and have to be studied. In this article, a model considering nucleation, crystal growth and agglomeration during the seeded precipitation process was established. The relationship between reaction conditions and parameters of the nucleation rate (B_0), growth rate (G), and agglomeration kernel (β) were studied. The values predicted by model is compared to the data obtained in experiments, the model prediction are fit well with experimental detection.

11:45 AM Panel Discussion

Challenges Facing Alumina and Bauxite Industry

12:40 PM Concluding Comments

Aluminum Reduction Technology: Cell Development Part II

Sponsored by: The Minerals, Metals and Materials Society, TMS Light Metals Division, TMS: Aluminum Committee

Program Organizers: Martin Iffert, Trimet Aluminium AG; Geoffrey Bearne, Rio Tinto Aluminium Tech

Thursday AM
March 13, 2008

Room: 298
Location: Ernest Morial Convention Center

Session Chair: Gary Tarcy, Alcoa Inc

8:30 AM

Last Development in AP50 Cell: Jean-Luc Basquin¹; Ben Benkahla¹; Yves Caratini¹; Hervé Mezin¹; Steve Renaudier¹; ¹Alcan

Alcan has achieved a new step in AP50 technology development: by 2009 44 AP50 cell will be in operation at Jonquiere complex in Quebec, demonstrating on industrial phase the cutting edge of this technology. In the last 3 years an intensive program has been launched to optimize the AP50 design and performances. Using new development of thermo-electrical and MHD models, cell design has been improved. A new anodic assembly, an optimised cathode, has allowed to reduce specific energy consumption and to improve cell stability. Full measurement campaign and performance test has validated this high level of performance. The AP50 process control has integrated the last development of ALPSYS pot control system insuring a benchmark result for thermal control and Anode Effect frequency. The AP50 technology with a single potline having an annual output of 500 kt will increase dramatically productivity per employee and reduce investment cost compared to previous technologies.

8:50 AM

Fjardaal Smelter Project, Iceland-Modular Construction: Bernard Cloutier¹; Joe Wahba²; Warren McKenzie³; Sam Maliha¹; ¹Solios Environnement Inc; ²Bechtel; ³Alcoa, Inc

The Construction of the Fjardaal Smelter Project in Iceland represented a challenge in terms of logistics and construction. This challenge is primarily due to the unavailability of a local workforce and the Icelandic climatic conditions. Faced with such constraints, the project Owner ALCOA and the nominated EPC contractor BECHTEL Corp. encouraged the engineering and construction off-site of large pre-assembled modules that would be shipped using specialized maritime transportation vessels. The modules were moved from the plant harbor to the final destination using SPMT's (Self Propelled Mobile Transporters). This paper describes SOLIOS experience in applying this concept to the potlines Gas Treatment Centers and the Bath Treatment Plant. Large pre-assembled modules weighing from 80T to 340T were delivered in a record time and the construction team managed by Bechtel/Alcoa has received several awards for Health, Safety and Environmental protection. The application of this concept is of high interest for new smelters that are built in remote areas coastal locations and driven by tight schedules.

9:10 AM

Successful Dry Re-Start of the Hamburg Aluminum Smelter: Till Reek¹; Joerg Prepenit¹; ¹Trimet Aluminium AG

In December 2005, the 133,000 tons smelter in Hamburg, Germany was shut-down. The phase-out process was very controlled and efficient, which was essential for the restart. The assets were acquired by TRIMET ALUMINIUM AG late in 2006. Beginning of March 2007, only 3 months after the transaction took place, the first pot was started successfully. The first two pots were specially prepared with a full-shadow resistor-coke bed for electrical preheating. Temperatures of above 1100°C were reached and pure synthetic cryolite was molten. Seven newly relined pots were started before the first shut down cell was restarted with its original lining. Depending on the condition of the old cathodes either gas or electrical pre-heating was used. This paper highlights the experiences of the dry start-up and the challenges involved in restarting an idle smelter in record time without any pot failures.

9:30 AM

20 Years of Continues Improvements in TALUM Smelter: Cus Zlatko¹; Avgust Sibila¹; ¹Talum

TALUM is the only primary aluminium producer in Slovenia. In February 1954, the first alumina production plant was introduced, and first aluminium was produced in November of the same year. Various lines and technologies were in operation the last 54 years. Currently the only AP18 technology is used for TALUM primary aluminium production. AP18 pots were started in 1988. During last 20 years the TALUM continues improvements program bring us to be one of the most efficient producer of aluminium in AP18 technology. The average CE of 95,28%, 13.166 kWh/t DC energy consumption and average pot life of more then 3000 days is result of technical improvements using best practice with minimum cost approach which mainly covers optimization of operational parameters, improvement of cathode design, optimization of process control system and application of slotted anodes as well as improvement of anode quality.

9:50 AM Break

10:10 AM

Faster Normalization of Cells after Bath up: B. Kakkar¹; Ali Al Zarouni¹; Arvind Kumar¹; ¹Dubai Aluminum Company

It is always the endeavour to normalise cells as early as possible after bath up. A newly started cell has several notable features. current efficiency being one of them. All efforts are directed at improving this aspect right from the time a cell is bathed up. The closely monitored parameters during early operation are bath temperature and excess AIF₃. Their control is better in graphitized cathodes due to lower adsorption of sodium. When Dubal switched over to graphitized cathodes, early cell operation strategy was comprehensively revamped in terms of voltage reduction, alumina feed rate, metal level and bath chemistry control. The change in bath up strategy has positively responded and current efficiency of 96.5% could be achieved from second week onwards. Current efficiency improvement in new cells is in line with the strategy of maximising metal output from a cell during its service life.

10:30 AM

Development of New Generation SY300 Technology: Kangjian Sun¹; ¹ShenYang Aluminium and Magnesium Institute

SAMI have developed SY300 technology in 2002. There are more than two thousand SY300 pots in operation. SAMI have made further improvement in SY300 technology and develop the new generation SY 300 technology and applied the technology in Hennan Wanji smelter. When the first new generation SY300 potline (Wanji) starts up in Jan 2006, the current has increased from 300kA to 335kA. The potline have get the high current efficiency and lower energy consumption than the first generation SY300 pot. SAMI is doing further work to improve the new generation SY300 technology to the world benchmark.

10:50 AM

Thyristor Rectifiers for Aluminium Plants with Advanced Freewheeling Control: Krystal Futter¹; Eric Lambert¹; ¹ABB Inc.

Potline current demand for aluminium plants is constantly increasing. Many potlines with 350 kA are in operation and the trend is to push towards 500 kA in the near future, requiring the installation of many units in parallel. Due to the physical limitations of the size of each unit and the redundancy requirements, it could pose a problem to handle current when all the units are tripped simultaneously. As a result of uneven switching off of the rectifiers, there is a good chance that the last unit will carry full potline current. In a diode plant, this phenomenon can be handled easily as all diodes go into a natural freewheeling mode. Whereas in thyristor plants, special techniques need to be implemented to prevent overloading of the last switched unit. ABB High Power Rectifiers have developed a sophisticated technique which can handle such an occurrence without over sizing any units.

Biological Materials Science: Implant Biomaterials II

Sponsored by: The Minerals, Metals and Materials Society, TMS Structural Materials Division, TMS: Biomaterials Committee, TMS/ASM: Mechanical Behavior of Materials Committee

Program Organizers: Ryan Roeder, University of Notre Dame; Robert Ritchie, University of California; Mehmet Sarikaya, University of Washington; Lim Chwee Teck, National University of Singapore; Eduard Arzt, Max Planck Institute; Marc Meyers, University of California, San Diego

Thursday AM
March 13, 2008

Room: 390
Location: Ernest Morial Convention Center

Session Chairs: Carlos Elias, Instituto Militar de Engenharia; Ryan Roeder, University of Notre Dame

8:30 AM

Fatigue of Zirconia Bioceramics: *Carlos Elias¹; Claudinei dos Santos²; Renato Souza²; Luiz Bicalho²; Miguel Barboza²; ¹Instituto Militar de Engenharia; ²Escola de Engenharia de Lorena*

When ceramic is used for implant material such as artificial joints or dental implant abutment, it demands for generation of design-relevant fatigue data. In this paper, the fatigue behavior of tetragonal zirconia polycrystals (TZP) with 3mol.% of Y_2O_3 stabilized (3Y-TZP) under four-point bending in load cyclic conditions was investigated. Mechanical properties of hardness, fracture toughness and modulus of rupture were also evaluated. The results showed that dense 3Y-TZP was obtained after sintering, and present HV, K_{IC} and modulus of rupture of 13.5 GPa, 8.15 MPa.m^{1/2} and 880 MPa, respectively. In this ceramic submitted to the 4 point bending cyclic load, the propensity for cyclic fatigue is very strong and presents a considerable range of loading conditions, where cyclic fatigue can be detected. The results obtained indicates that the fatigue strength limit over 5×10^6 cycles stress is about 550 MPa or around 63% static bending strength.

8:50 AM

Nanocrystalline Hydroxyapatite for Biomedical Applications: *Tien Tran¹; Cosan Unuvar¹; Joanna Groza¹; James Shackelford¹; ¹University of California*

Hydroxyapatite, a bioactive and resorbable material, has been limited to non-load bearing applications due to its poor mechanical properties. Although nanocrystalline bioceramics exhibit enhanced strength, hardness, and wear resistance as well as protein adsorption and cell adhesion, the fracture toughness of non-cubic ceramics in relation to grain size remains a concern. Conventional processing methods lead to rapid grain coarsening and decomposition making it difficult to achieve fully dense nanocrystalline hydroxyapatite. Consequently, published fracture toughness values at the submicron to nanocrystalline levels often reflect the effects of porosity rather than grain size. Near-theoretical densities can be achieved in minutes by the field-assisted sintering technique (FAST), thereby restraining grain growth to the nanoscale regime and reducing decomposition. Eliminating the effects of porosity allows optimization of the mechanical properties of hydroxyapatite. The application of this approach to producing nanoscale hydroxyapatite is reported, including both biological and mechanical characterization of the resulting material.

9:10 AM

Synthesis and Characterization of Sodium Calcium Phosphate for Biological Applications: *Hande Demirkiran¹; Pranesh Aswath¹; ¹University of Texas at Arlington*

New ceramic products were developed by sintering mixtures of Hydroxyapatite (HA) and Bioglass®(BG) at 1200°C. The phase composition and microstructure of the blends were examined by x-ray diffraction (XRD) and scanning electron microscope (SEM), respectively. Bioactivity of the ceramics by soaking in simulated body fluid (SBF) solution maintained at 37°C and pH of 7.4 for 10 weeks. Surface compositions and microstructures of the disks were analyzed after immersion in SBF solution by FTIR and SEM, respectively. Sodium, calcium, and phosphorus ion concentrations were examined by inductive coupled plasma. The results demonstrated that the bioactivity of the 25wt% BG-HA blends were found to be the most promising blend among all the blends with

crystalline sodium calcium phosphate [$Na_3Ca_6(PO_4)_5$] and amorphous silicon phases. A thick layer of carbonate-apatite covered the surface of sodium calcium phosphate disks after 1 week of immersion.

9:30 AM

In-Vitro Response of Sodium Calcium Phosphate Surfaces to Growth and Proliferation of Bone Marrow Stromal Cells: *Hande Demirkiran¹; Arunesh Mohandas¹; Motokazi Dohi¹; Kytai Nguyen¹; Pranesh Aswath¹; ¹University of Texas at Arlington*

Mixtures of $3NaH_2(PO_4) + 2CaH(PO_4) + 4CaO$ were sintered at temperatures ranging from 600–1500°C for 1 hour. The phases formed were characterized using X-ray diffraction and the microstructure of the ceramic product was examined with scanning electron microscopy and optical microscopy. Compositions sintered at temperatures greater than 1200°C or for times longer than 1 hour at 1200°C yielded $Ca_{10}Na(PO_4)_7$. In addition blends of Bioglass® and Hydroxyapatite were sintered together to yield new ceramic products with compositions with 25 wt.% Bioglass® yielding $Ca_{10}Na(PO_4)_7$. In this study, compositions that yielded $Ca_{10}Na(PO_4)_7$ were examined further by culturing bone marrow stromal cells on the surfaces over a period of six days. The proliferation and differentiation of BMSC was determined by picogreen DNA assay's and alkaline phosphatase activity.

9:50 AM

Biocompatibility Evaluation of Potassium Mica-Fluorapatite Based Glass Ceramics as a Function of CeO₂ Addition: *Ipek Akin¹; Hilal Yazici¹; Candan Tamerler Behar¹; Gultekin Goller¹; ¹Istanbul Technical University*

For a material to be machinable and bioactive, it should contain both mica and apatite crystals. Apatite containing glass ceramics are greatly important for surgical implantation due to the high bioactivity, close crystallographic and chemical similarity to human bone tissue. The crystalline phases occurring in these glass ceramics include essentially apatite which provides the biocompatibility and bioactivity of the glass ceramics, and mica phase, crystallized at higher temperature and provides the interesting mechanical properties such as machinability and strength. Osteoblasts are the cells that support the formation, secretion and mineralization of extracellular bone matrix. The purpose of this study is to investigate the behavior of these cells of a glass ceramic having 70wt% potassium mica and 30wt% fluorapatite as a function of 1 and 2wt% CeO₂ addition.

10:10 AM

Influence of ZrO₂ Addition on In-Vitro Bioactivity Properties of Potassium Mica-Fluorapatite Based Glass Ceramics: *Gultekin Goller¹; Ugur Ceylan¹; ¹Istanbul Technical University*

Glass ceramics containing microcrystalline phases of mica and fluorapatite can be considered as new materials for bone implants and substitutes in human body. Such a glass-ceramic has a better machinability due to the large amount of layered mica phase which is oriented randomly and distributed uniformly in glass matrix. For a material to be machinable and bioactive, it should contain both mica and apatite crystals. Apatite containing glass ceramics are important due to the high bioactivity, close crystallographic and chemical similarity to human bone tissue. In the production of glass ceramics, nucleating agents (ZrO₂) can be used in order to induce bulk crystallization of the phases. The purpose of this study is to investigate the in-vitro bioactivity character of glass ceramics having 3:7 weight ratio of fluorapatite ($Ca_5(PO_4)_3F$) to potassium mica ($K_2Mg_3AlSi_3O_{10}F_2$) as a function of ZrO₂ addition, and compare the morphology of HCA layer formation depending on ZrO₂ addition.

10:30 AM Break**10:40 AM**

Nanostructured Silica Enforced Hydroxyapatite: *Tzy-Jiun Luo¹; Ching-Chang Ko²; ¹North Carolina State University; ²University of North Carolina*

Silica materials synthesized via sol-gel solution have shown excellent biocompatibility towards biomolecules, cell culture, and tissue engineering. A unique bioceramic based on nanostructured silica, when integrated with gelatin-induced hydroxyapatite (HAP-GEL) nanocrystals (Ko et al., 2006), exhibits enhanced mechanical properties. This new process allowed modification of forming and porosity of the material for potential tissue engineering applications. The nanostructure of silica produced from polycondensation of aminosilane was

found to be affected by HAP-GEL phases allowing chemical additives (e.g. glycerol) for enhanced stability of encapsulated enzyme. Efforts have been made to optimize the synthesis procedure to show short curing time, improved optical properties for bioassay characterization, and tailor-made surfaces for better cell adhesion.

11:00 AM

Microstructure and Bioactivity of Laser Induced Geometrically Textured and Porous Ca-Pon Ti-6Al-4V: Sameer Paital¹; Narendra Dahotre¹; ¹University of Tennessee

In the present work the feasibility of synthesizing porous and geometrically textured calcium phosphate (Ca-P) coating on Ti-6Al-4V by a Continuous wave (CW) Nd:YAG system has been demonstrated. Phases developed due to various laser processing parameters are studied using XRD. TiO₂, Ti and α -TCP phases are obtained as the most predominant phases. Crystallite size for all the above three phases increased with increasing laser fluence. The bioactivity of the coatings was further demonstrated by the formation of an apatite like phase by immersing the sample for varying time periods in a simulated biofluid (SBF). Microstructure and morphological evolutions before and after immersion in a SBF were studied using scanning electron microscopy.

11:20 AM

Control of Microbial and Cell Adhesion to Biomaterials by Ion Beam Implantation: Robert Zimmerman¹; Claudiu Muntele¹; Daryush Ila¹; ¹Alabama A&M University

Medical implants usually require seamless adaptation with adjacent living tissue. For example, temporary carbon trans cutaneous electrodes or drainage tubes interface with skin, or permanent replacements of artificial teeth and the femur head interface with bone of the jaw and femur, respectively. We have shown that ion beam induced roughening of specific surfaces of these implanted materials enhance the adhesion with adjacent living tissue, and that implantation of silver ions below the surface of otherwise biocompatible materials completely inhibits cell attachment, while leaving neighboring areas hospitable to cell attachment and adherence. This patterning permits precise control of the formation of tissue on implanted biomaterials. Similarly, we have shown that silver implantation at the surface of Ultra High Molecular Weight Polyethylene (UHMWPE) gives the material anti microbial properties, as well as increasing the wear resistance. Both are improvements to the UHMWPE liner for the acetabular cup replacement for the hip joint.

11:40 AM

The Effect of Mechanical Processing on the Bio-Corrosion and Fatigue Resistance of Mg Alloy AZ31: Yuri Estrin¹; Hao Wang²; H. Fu³; Guangling Song³; Zuzana Zuberova⁴; ¹Monash University; ²University of Southern Queensland; ³University of Queensland; ⁴Technical University of Clausthal

The effect of mechanical working by hot rolling and equal channel angular pressing (ECAP) on the fatigue resistance and corrosion kinetics in Hank's solution of Mg alloy AZ31 was studied. This alloy is considered as a possible candidate material for biodegradable implant surgery (possibly for resorbable stents and bone implants), and its suitability depends critically on both the fatigue behaviour and the bio-corrosion resistance. It was shown that grain refinement of the as cast structure by hot rolling leads to a very significant improvement of fatigue properties and a sizeable decrease of the corrosion rate in Hank's solution. However, additional grain refinement by a further processing step (ECAP) did not enhance the fatigue endurance limit and caused a slight increase of the corrosion rate. The study has demonstrated the possibility of improving (and possibly controlling) corrosion and fatigue behaviour of alloy AZ31 using relatively simple mechanical processing routes.

12:00 PM

Corrosion Resistance of Ti₆Al₄V in Fluoride Solutions: Carlos Elias¹; Fabio Souza²; Tânia Nogueira²; ¹Instituto Militar de Engenharia; ²Universidade Federal Fluminense

The purpose of this work is to evaluate the electrochemical behavior of Ti₆Al₄V alloy in fluoride solutions after surface treatments with acid and mechanical polishing. The study was carried out by anodic voltammetry in 1% NaCl solutions with 0.1% to 1.6% NaF contents at a pH of 2.0 and 6.50. The samples were observed by SEM before and after the voltammetric assays. The samples submitted to acid etching tested in pH 2.0 solution showed the

appearance of pit corrosion at high potentials. The samples submitted to polishing remained passivated. In the case of pH 6.50 solution, a passivation process with the appearance of crystals on the surface of both samples was observed. These results showed that the acid etching treatment, despite leading to better titanium osseointegration, needs careful attention in relation to corrosion. It was observed that the corrosion was more pronounced with increasing fluoride concentration.

Bulk Metallic Glasses V: Processing and Properties

Sponsored by: The Minerals, Metals and Materials Society, TMS Structural Materials Division, TMS/ASM: Mechanical Behavior of Materials Committee

Program Organizers: Peter K. Liaw, University of Tennessee; Wenhui Jiang, University of Tennessee; Guojing Fan, University of Tennessee; Hahn Choo, University of Tennessee; Yanfei Gao, University of Tennessee

Thursday AM
March 13, 2008

Room: 393
Location: Ernest Morial Convention Center

Session Chairs: Yanfei Gao, University of Tennessee; Marios Demetriou, California Institute of Technology

8:30 AM Invited

Processing of Bulk Metallic Glass: Jan Schroers¹; ¹Yale University

The sluggish crystallization kinetic of bulk metallic glass results in two fundamentally different processing opportunities. BMG can be directly cast. But even for the low critical cooling rates measured for BMGs geometries with high aspect ratio are particularly challenging since during casting cooling and filling of the entire mold cavity are coupled and thereby occur simultaneously. This limits the complexity of the geometries that can be cast even when processing parameters are carefully balanced. Alternatively, BMG can be thermoplastically formed in the supercooled liquid region. In this case the required fast cooling and forming are decoupled. The BMG is formed in a high viscous state where it behaves very similar to plastics when compared by processing temperature and forming pressure. A measure for the formability of BMGs will be introduced. Processing potentials and challenges will be discussed and various examples will be given including blow-molding, microfabrication, and nano-patterning.

8:50 AM Invited

Oxidation Behavior of a Pd₄₃Cu₂₇Ni₁₀Pb₂₀ Bulk Metallic Glass in Dry Air: Wu Kai¹; I. Ren¹; Bryan Barnard²; Peter Liaw²; Marios Demetriou³; William Johnson³; ¹National Taiwan Ocean University; ²University of Tennessee; ³California Institute of Technology

The oxidation behavior of a Pd₄₃Cu₂₇Ni₁₀Pb₂₀ bulk metallic glass (Pd4-BMG) was investigated over the temperature range of 70 to 325°C in dry air. The results showed that virtually no oxidation occurred in Pd4-BMG at T < 250°C, revealing the alloy's favorable oxidation resistance in this temperature range. A very thin film formed on Pd4-BMG at higher temperatures. This film consisted of copper, and its compositions depended strongly on temperature. In addition, the amorphous structure remained unchanged below the glass-transition temperature (T_g), while a duplex structure developed after oxidation at higher temperatures. The duplex structure consisted of Pd-Cu-Ni and Pd-P phases.

9:10 AM

Microstructural and Mechanical Characterization of a Laser Processed Zr-Based Bulk Metallic Glass: Hongqing Sun¹; Katharine Flores¹; ¹Ohio State University

Laser processing is a novel manufacturing technology which offers the possibility of creating or repairing metallic coatings and components with highly non-equilibrium microstructures. Due to the localized heat input and high cooling rate inherent to the process, this technology has great potential to be applied in the production of metallic glasses. In the present work, we use the Laser Engineered Net Shaping (LENSTM) process to deposit Zr-based glass forming powder on amorphous and crystalline substrates of the same nominal composition. Amorphous melt zones surrounded by distinct crystalline heat-affected zones (HAZs) are observed in single- and multi-layer deposits. The microstructural evolution of the deposits and underlying substrate depend strongly on the total heat input per pass. SEM, TEM, XRD, and DSC analyses are

performed to identify and characterize the observed amorphous and crystalline phases. In light of their unique composite microstructures, the mechanical behavior of laser deposited coatings is also investigated.

9:25 AM Invited

Thermodynamic, Structural and Mechanical Properties of Zr 63-x Alx Cu24 Ni10 Co3 Bulk Metallic Glass Forming Alloys: Rainer Wunderlich¹; Arnaud Caron¹; Hans-Jörg Fecht¹; ¹Ulm University

The correlation between thermodynamic, structural and mechanical properties is of strong current interest in bulk metallic glass research in the quest of improving the ductility of metallic glasses. As a model system, the Zr-Al-(CuNiCo) equivalent three component phase diagram has been investigated along the (CuNiCo)=37at% isoconcentration line with the Al-concentration varied from 7 to 20 at%. As a function of Al-concentration, a decrease in the average atomic distance was found which correlates with an increase of the glass transition temperature. An increase in the bulk modulus was observed while the Poisson ratio exhibited a pronounced and unexpected maximum at some intermediate composition. This trend is also reflected in an increase of the cavitation-erosion resistance as a function of Al-concentration. These findings are in contrast to the generally accepted linear rule of mixing, showing that chemical and topological short range order considerably influence the macroscopic mechanical properties of BMGs.

9:45 AM Invited

Thermoplastic Forming Properties and Microreplication Ability of an Mg-Base Bulk Metallic Glass: Shian-Ching Jang¹; C. C. Tseng¹; Y. C. Yeh²; J. L. Jou²; Jacob Huang³; ¹I-Shou University; ²Metal Industries Research and Development Centre; ³National Sun Yat Sen University

The thermoplastic forming properties of Mg58Cu531Nd5Y6 bulk metallic glass (BMG) was evaluated via compressive test at different temperature with various strain rates. Then the process window of thermoplastically forming of the Mg-base BMG is developed according to this data obtained from those compressive tests. The result reveals that the Mg-base BMG possess an excellent superplastic formability with the m-value being nearly 1.0 in the supercooled liquid region under a strain rate around 0.001 ~ 0.01 s⁻¹. In parallel, a relatively low flow stress (less than 10 MPa) within the supercooled liquid region can be obtained with a strain rate of 0.001 s⁻¹. Additionally, the result of replication of a hologram pattern with 10 micro meter depth also shows extremely good microforming ability of this Mg-base BMG in the supercooled liquid region with suitable working condition.

10:05 AM Invited

Superplastic Micro/Nano Formation of Pd₄₀Ni₂₀P₄₀ Bulk Metallic Glass: Jinn Chul¹; Y. C. Chen²; T. Y. Lin²; C. W. Wu²; V. S. John²; ¹National Taiwan University of Science and Technology; ²National Taiwan Ocean University

In recent decades, bulk metallic glasses (BMGs) are an interesting class of new materials with unique properties that offer exciting applications to a broad range of technologies. The micro/nano system fabrication is performed in the supercooled liquid region (SCLR), where the BMGs exist as a viscous liquid under an applied pressure into a mold. BMGs are thus malleable forming devices with complicated shapes. In the present investigation, the compressive deformation behavior of Pd₄₀Ni₂₀P₄₀ bulk metallic glasses were examined in the SCLR (589-670K) at strain rates ranging from 10⁻² to 10⁻⁴ s⁻¹. We demonstrate that various high aspect-ratio structures and optical gratings of BMGs can be fabricated from dies in air. The surface morphology and the roughness were measured by scanning electron microscopy and atomic force microscopy, respectively. Significantly the material exhibited excellent deformability in the supercooled liquid region and indicates that BMG is enable to promote microdevices in the future.

10:25 AM Invited

Effects of Processing Conditions on Plastic Deformation of Bulk Metallic Glasses: Z. P. Lu¹; H. Bei²; ¹University of Science and Technology Beijing; ²Oak Ridge National Laboratory

It was recently reported that the misalignment has a great influence on the plastic displacement of bulk metallic glasses under compression. Based on our experimental data, however, the compressive displacement data are quite scattered even for the same bulk metallic glass with reasonable alignment and the same testing conditions including the strain rate and sample diameter. In this

talk, we will focus on effects of processing conditions such as purities on the plastic deformation of bulk metallic glasses. Using the recently reported super plastic Zr-based bulk metallic glass and other relatively brittle Zr-based glassy alloys as model systems, we attempt to explore the underlying mechanisms that dictate the localized plastic deformation for the samples with various preparation circumstances and thus understand the fundamental variables that control the mechanical behavior of the bulk metallic glasses investigated.

10:45 AM Break

10:50 AM

Crystallization and Mechanical Behaviors of Electroless Ni-P Amorphous Coatings: Yongfeng Shen¹; Wenying Xue²; Wenming Wang¹; Yandong Wang¹; ¹Northeastern University, Key Laboratory for Anisotropy and Texture of Materials (Ministry of Education); ²Northeastern University, State Key Laboratory of Rolling and Automation

The crystallization behavior of electroless Ni-P was investigated by using differential scanning calorimetry method and X-ray diffraction technique. The crystallization temperature of amorphous Ni-P deposits is 337.1°C, which is lower than that of Ni-10.2P (343.7°C). The crystallization behavior of the Ni-P coating was evaluated for the specimens treated at different temperature ranges from 300 to 500°C. It was shown that the amorphous Ni-P was transformed into a stable Ni₃P phase and some metastable phases, such as, NiP₂, Ni₅P₃ and Ni₁₂P₅. The volume fraction of Ni₃P was raised with increasing treatment temperature. The hardness of the Ni-P coating is remarkably improved at higher heat-treatment temperature due to the dispersion of Ni₃P phase in the matrix.

11:05 AM

Sliding Wear Resistance of the Ni-Based Metallic Glass: Nozomu Togashi¹; Yasunori Saotome²; Mamoru Ishida³; Hideki Takeda³; Yukiharu Shimizu⁴; Nobuyuki Nishiyama¹; Akihisa Inoue²; ¹RIMCOF Tohoku University Laboratory; ²Tohoku University, Institute for Materials Research; ³YKK Corporation; ⁴Namiki Precision Jewel Corporation

We have reported that wear resistance of the metallic glass (MG) bearing is more excellent than that of the sintered Fe-Cu alloy bearing under lubrication. But then, the worn loss of the MGs is larger than that of the conventional steel in the sliding wear tests under no lubrication.¹ So wear resistance of the MGs changes greatly depending on a lubrication condition. In order to clarify the relation between wear behavior and lubrication, we conducted the pin-on-disk wear tests under lubrication for Ni-based MG. It was found that the wear rate of the MGs under lubrication decreased as the load increases. It was therefore assumed that the friction of MGs made slippery with the oil slick, leading to reduction of the adhesion wear. ¹M. Ishida, H. Takeda, N. Nishiyama, K. Kita, Y. Shimizu, Y. Saotome and A. Inoue, Mater. Sci. and Eng. A, 449 (2007) 149.

11:20 AM

Solid State Joining of a Zr-Based Bulk Metallic Glass: Nicholas Hutchinson¹; Yuan Zhang¹; Justin Bennet¹; Glenn Daehn¹; Katharine Flores¹; ¹Ohio State University

Bulk metallic glasses have excellent mechanical properties, including exceptionally high strength, high toughness, and low damping, which make them well suited for structural applications. A significant barrier to expanding the use of metallic glasses is a lack of well characterized manufacturing processes, particularly joining techniques to create large scale or complex shaped components. The present work focuses on the characterization and optimization of three solid state welding techniques which rely on mechanical work and plastic deformation at mating interfaces to create joints. Specimens were joined by the friction stir process, a high velocity electromagnetic welding process, and an electro-thermo-mechanical process. The effectiveness of each joining technique and changes in microstructure at the joint are characterized as functions of appropriate operating parameters, applied stress and strain rates and material surface preparation. The results of these experiments will be discussed.

11:35 AM

Solid State Synthesis of Bulk Composites of Amorphous and Nano-Crystalline Structures in Ni-Ti Alloys: *Niven Mosengue*¹; Kai Zhang¹; Alex Aning¹; ¹Virginia Polytechnic Institute and State University

Equimolar powder mixtures of nickel and titanium are cryomilled in a modified attritor mill filled with liquid nitrogen to create lamella structures with 20 to 100 nm spacing in the powder particles. The milled powders are consolidated in a hot isostatic press at temperatures between 300 and 350°C. During the HIPing process, the synthesis of the amorphous structure and the consolidation of the powders take place at the same time. The resulting compacts are composites of amorphous and crystalline nano-structures of the Ni-Ti alloy. Results from TEM, and the dependence of hardness on the microstructure of the composites will be presented and discussed.

11:50 AM

A Continuous Casting Process by Using Electromagnetic Vibrations for Fe-Based Bulk Metallic Glasses: *Takuya Tamura*¹; Daisuke Kamikihara¹; Naoki Omura¹; Mingjun Li¹; Kenji Miwa¹; ¹National Institute of Advanced Industrial Science and Technology

It is known that cooling rate from the liquid state is an important factor for producing the bulk metallic glasses. However, almost no other factors such as electric and/or magnetic fields were investigated. The present authors reported that a new method for producing Mg-Cu-Y bulk metallic glasses by using electromagnetic vibrations is effective in forming the metallic glass phase. Moreover, the present authors have reported that the glass-forming ability of Fe-Co-B-Si-Nb alloys also enhances with increasing the electromagnetic vibration force. Thus, we try to develop a continuous casting process by using the electromagnetic vibrations for Fe-based bulk metallic glasses.

12:05 PM

Effects of Vibration on Micro Forming of an Al Superplastic Alloy and a Zr-Based Bulk Metallic Glass: *Young-Sang Na*¹; Seon-Cheon Son²; Kyu-Yeol Park²; Jong-Hoon Lee¹; ¹Korea Institute of Materials Science, Korea Institute of Machinery and Materials; ²University of Ulsan

Vibrational micro forming of pyramidal shape patterns was conducted for an Al superplastic alloy, Al5083 and a Zr-based bulk metallic glass, Zr₆₂Cu₁₇Ni₁₃Al₈. A PZT actuator combined with a signal generator was adopted for generating vibrational load in a specially-designed vibrational micro forming system. Si micro dies with wet-etched pyramidal patterns were used as master dies for vibrational micro forming. The height of the micro formed pyramids for Al 5083 alloy was increased as the vibrational frequency increased from 1 Hz up to 100 Hz. This was the similar case for Zr₆₂Cu₁₇Ni₁₃Al₈ bulk metallic glass. In addition, the micro-formed pattern quality was improved by applying vibrational load and by increasing the vibration frequency in terms of surface defects and in terms of pattern asymmetry, as well.

12:20 PM

Laser Pulse Induced Shock Processing of Zr-Based Bulk Metallic Glass: *Sameer Paital*¹; Gong Wang¹; Peter Liaw¹; Narendra Dahotre¹; ¹University of Tennessee

In the present work attempts are made to introduce residual stresses at the surface of Zirconia-based bulk metallic glass (BMG) using a pulsed Nd:YAG laser. Shock processing was carried out in the direct laser impact mode. It is observed that there is an improvement in plasticity due to the residual stresses generated from the shock waves and rise in temperature. This combined effect has resulted in a composite phase microstructure at the near surface region of the bulk metallic glass and resulted in improved plasticity at this region. This improvement in plasticity may be attributed to the retardation in initiation and propagation of the shear bands. The detailed microstructural, stress and strength analyses of laser surface modified Zr-based samples under various laser processing conditions are ongoing and will be discussed during presentation.

12:35 PM

Air-Oxidation of a Cu₄₅Zr₄₅Al₅Ag₅ Bulk Metallic Glass: *Wu Kai*¹; I.-F. Ren¹; C.-P. Chuang²; M. Freels²; Peter Liaw²; ¹National Taiwan Ocean University; ²University of Tennessee

The oxidation behavior of a Cu₄₅Zr₄₅Al₅Ag₅ bulk metallic glass (CZA4-BMG) was studied over the temperature range of 375-500°C in dry air. The role of Ag addition on the oxidation kinetics was investigated, and the results were

compared to those of the ternary Cu_{47.5}Zr_{47.5}Al₅ BMG (CZA3-BMG). In general, the oxidation kinetics of CZA4-BMG followed a multi-stage parabolic rate law, and the oxidation-rate constants at the steady-state stage were slightly lower than those of CZA3-BMG, indicating that the addition of Ag provided a better oxidation resistance for CZA4-BMG. The scales formed on CZA4-BMG consisted mostly of ZrO₂, copper oxides, dissolved with Ag, and a minor amount of Al₂O₃. The exact composition and constitution of the scales strongly depended on the temperature. In addition, the amorphous structure retained unchanged at the temperature below the glass-transition temperature (T_g), while a triple-phase structure was developed after oxidation at higher temperatures, being also temperature-dependent.

Cast Shop Technology: Modelling

Sponsored by: The Minerals, Metals and Materials Society, TMS Light Metals Division, TMS: Aluminum Committee

Program Organizers: Hussain AlAli, GM Casthouse and Engineering Services, Aluminium Bahrain Company (ALBA); David DeYoung, Alcoa Inc

Thursday AM
March 13, 2008

Room: 295
Location: Ernest Morial Convention Center

Session Chair: Bjorn Henriksen, Elkem Aluminium ASA Research

8:30 AM Keynote

Mushy Zone Mechanics and the Modeling Solidification Defects in DC Cast Aluminum: *Mohammed M'Hamdi*¹; ¹SINTEF

Many casting defects occur while the material is in the mushy state. An accurate description of mushy zone phenomena is, therefore, essential for the development of mathematical models and simulation tools for defect prediction, and an important step towards the virtual casthouse. In particular the mechanical behavior of the mushy zone can have a significant impact on several of these defects. The paper focus on the aluminum direct chill casting process, and discusses recent development on the modeling of the mushy zone mechanical behavior and its impact on the modeling of solidification defects such microporosity, hot tearing, surface exudation and bulk macrosegregation.

8:50 AM

Coupled Modeling of Air-Gap Formation and Surface Exudation during DC-Casting of Aluminium Extrusion Ingots: *Dag Mortensen*¹; Bjorn Henriksen²; Mohammed M'Hamdi³; Hallvard Fjær¹; ¹Institute for Energy Technology; ²Elkem Aluminium ANS; ³SINTEF

During casting of aluminium extrusion ingots the surface against the mould experiences a pull-in force that magnifies the air-gap during solidification close to the mould surface. This is a global phenomenon that results in early and large air-gap formations compared to the shape-casting situation. Due to the semi-solid surface created under such conditions, exudation through the surface may appear. In this study a coupled heat and fluid flow, stresses and deformation modelling tool are applied on the process. Results from the mechanical calculation are back-coupled to the thermal boundary conditions. The metallostatic head is the driving force for exudation through the dendritic network and the resulting fluid flow through this network is used to calculate a dynamic thickness of the exuded layer. Measurements from two different alloys, with rather small changes in composition, but with large variations on surface quality, are compared with the modelling results.

9:10 AM

DC Cast Thermal and Fluid Flow Simulation Using a Semi-Permeable Model of TF Combo Bag: *Sylvain Tremblay*¹; *Daniel Larouche*²; Andre Arseneault²; Jean-Philippe Dube³; ¹Pyrotek Inc.; ²Laval University; ³A.B.I. Aluminerie de Bécancour Incorporated

In the process of aluminum ingot casting, the heat transfer is a key issue in the final quality of the ingot. Hot liquid metal reaches the ingot through the liquid metal distribution system. The distribution action in the pool is mainly achieved by the combo bag as a part of the distribution system. In the present article, we propose a model allowing the coupling between combo bag thermal fluid flow circulations with those into the pool without over-constraints on the physical

conservation equations (mass, momentum and energy). The need of such a model is essential to define the complete heat transfer analysis of ingot casting process if pre-imposed solutions are not fed into the mathematical equations. More specifically, it will allow evaluating the impact of combo bag parameter on the thermal flow circulation in metal pool.

9:30 AM

Cyclone Application for Molten Aluminium: Numerical Approach: *Andrey Turchin*¹; Dmitry Eskin¹; John Courtenay²; Laurens Katgerman³; ¹Netherlands Institute for Metals Research; ²Melt Quality Partnership Ltd.; ³Technical University Delft

In this paper a numerical simulation technique has been used to evaluate the possibilities of cyclone application in molten aluminium processing by determining the fluid flow for flow velocities of 0.01 m/s, 0.1 m/s and 1 m/s; particle behavior for discrete particle sizes in the range of 20–100 µm; and the collection efficiency of the cyclone. The geometrical aspects have been discussed. The results show that the cyclone concept can be effectively used as an alternative method to remove the impurities from a stream of molten aluminium in a wide range of flow regimes. A pilot installation is being built for validation of the used model in terms of collection efficiency; and for casting trials (see a separate presentation by J. H. Courtenay et al.).

9:50 AM

Computational Heat-Transfer Model of Melt-Spinning of Al-7% Si Alloy on a Cu-Be Wheel: *Aravind Sundararajan*¹; Brian Thomas¹; ¹University of Illinois

A one-dimensional transient finite-difference heat-transfer model (STRIP1D) has been developed to simulate the Planar Flow Melt-Spinning (strip casting) of Al-7% Si on a Cu-Be wheel. The model includes the effects of two-dimensional fluid flow in the liquid pool on heat transfer and solidification in the strip, coupled with transient conduction in the rotating wheel. The strip-wheel interface is characterized with a time-dependent heat transfer coefficient. The complete model has been validated with experimental data from a pilot caster at Cornell University, and reasonably matches the measured strip thickness, wheel thermocouple temperature, strip surface temperature and secondary dendrite arm spacings. The model provides fundamental insights into the effect of process conditions like wheel speed, gap height, puddle length, and superheat on solidification. Interfacial imperfections observed in the strip are predicted to occur owing to gas bubbles formed at the wheel-strip interface, and have been validated using two-dimensional computations with ABAQUS.

10:10 AM Break

10:20 AM

Inclusion Transport Phenomena in Casting Furnaces: *Stephen Instone*¹; Andreas Buchholz¹; Gerd-Ulrich Gruen¹; ¹Hydro Aluminium Deutschland GmbH

The presence of non-metallic inclusions in Aluminium is one of the most important factors determining its processability and the quality of finished products. The concentration of such inclusions in the liquid metal has been observed to vary greatly. To better understand the contribution of furnace processes to melt quality, a mathematical model of casting furnace processes has been developed at Hydro Aluminium's Research and Development Centre in Bonn, Germany. The model is capable of simulating the most important fluid flow and particle (inclusion) transport phenomena occurring in the furnace during both settling and casting operations. Output from the model is compared with results from industry standard inclusion measurement techniques (LiMCA and PodFA) for different furnace geometries. The results show that the model is a powerful tool and can be used to improve understanding of these processes and help in explaining observations in the cast house.

10:40 AM

Gas Fluxing of Aluminium: Modeling Fluid Dynamics and Magnesium Removal: *Autumn Fjeld*¹; James Evans²; D. Chesonis³; ¹University of Leoben; ²University of California, Berkeley; ³Alcoa Technical Center

A demagging reaction model was developed which combines the efforts of a multi-part investigation on the gas fluxing of aluminum. Bubble size distribution and residence times taken from a computational fluid dynamics model are incorporated into an external demagging reaction model, which predicts chlorine

utilization efficiency. This model includes assumptions regarding the kinetics and reaction path, however the model shows reasonable agreement to prior experimental magnesium removal data and provides insight into the interplay of reaction progress in a fluxing unit and the fluid dynamics in terms of bubble size, trajectory, and resulting bubble residence time. Better understanding of these factors can lead to more sophisticated process control systems and more efficient gas delivery in a gas fluxing unit.

11:00 AM

Analysis of the Interaction of Particles with Non-Planar Solidifying Interfaces: *Eliana Agalotis*¹; Mario Rosenberger¹; Alicia Ares¹; *Carlos Schvezov*¹; ¹CONICET/University De Misiones

The results of model calculations for the interaction of particles with non-planar interfaces during solidification are presented. The model is based on finite element methods for the calculation of the shape of the solidifying interface which is modified by the presence of a solid particle, and for the drag forces resulting on the particle for the geometrical configuration of the system particle-melt-solid. The drag force on the particle is calculated for different conditions of steady pushing by the solid. The results are compared with the corresponding drag force for a planar interface and a particle at the same separation. Thermal conditions resulting in concave and convex interface shapes are considered. The results show that a concave interface generate higher drag forces than a planar interface and the opposite for a concave shape. The magnitude of the force could differ in as much as one order of magnitude.

11:20 AM Panel Discussion

Characterization of Minerals, Metals, and Materials: Characterization of Microstructure and Properties of Materials V

Sponsored by: The Minerals, Metals and Materials Society, TMS Extraction and Processing Division, TMS: Materials Characterization Committee
Program Organizers: Jian Li, Natural Resources Canada; Toru Okabe, University of Tokyo; Ann Hagni, Intellection Corporation

Thursday AM
March 13, 2008

Room: 284
Location: Ernest Morial Convention Center

Session Chairs: Ann Hagni, Intellection Corporation; Mingdong Cai, University of Houston

8:30 AM

Mechanisms of Texture Evolution in Annealed Wire-Drawn OFHC Copper: *Daudi Waryoba*¹; Peter Kalu²; ¹Florida State University, National High Magnetic Field Laboratory; ²Florida A&M University

Despite the large volume of research work on texture transformation from strong<111>+weak<100> wire texture into strong<100>+weak<111> on recrystallization or to <111> on secondary recrystallization, there has been limited report on the mechanisms governing this transformation. This study was therefore carried out to present a comprehensive analysis of the mechanisms governing texture transition in wire drawn materials. The investigation was performed on OFHC copper wire drawn to a true strain of 3.56, and annealed at 750°C for durations ranging from 20s to 1 hr. The results show that at the early stage of recrystallization, strain induced grain boundary migration (SIGBM) occurs. This enhances the density of <100> grains which dominate the recrystallization texture due to their higher stored strain energy difference. For prolonged annealing time, continuous recrystallization of the <111> grains coupled with their high grain boundary mobility provide growth advantage of this orientation, leading to a <111> growth texture.

8:50 AM

Rupture Mechanisms in Composites Reinforced with Curaua Fiber: *Sergio Monteiro*¹; Ailton Ferreira¹; Felipe Perisse Lopes¹; ¹State University of the Northern Rio de Janeiro - UENF

A high strength lignocellulosic fiber can be extracted from leaves of the curaua plant to reinforce polymeric composites. Each curaua fiber is composed

of naturally bonded aligned filaments that may be separated under applied load and contribute to the composite fracture. This work investigates the rupture mechanism associated with the flexural fracture of polyester composites reinforced with curaua fibers. Plates with up to 50 vol.% of continuous curaua fibers embedded in orthophthalic polyester resin were press-molded at room temperature and cured for 24 hours. Composite specimens cut from the plate were bend tested and had their fracture analyzed by SEM. It was found that the composite rupture is associated with a complex mechanism of individual interaction of the filaments, which compose each fiber, with the matrix during crack initiation and further propagation. A model of stress concentration due to the specific fiber/matrix interface geometry explains the experimental fracture strength results.

9:10 AM

Local Electrode Atom Probe (LEAP) Analysis of Rhenium Segregation and Secondary Precipitates in Single Crystal, Nickel Base Superalloy PWA 1484:

Brandon Wilson¹; Anantha Puthicod²; Gerhard Fuchs¹; Michael Kaufman²; ¹University of Florida; ²University of North Texas

A second generation single crystal nickel base superalloy, PWA 1484, was studied with a Local Electrode Atom Probe (LEAP) to observe Re segregation near gamma/gamma' interfaces as a function of heat treatment. Additionally, the secondary gamma' precipitates that form in the gamma matrix channels were observed as they also strongly influence creep behavior, most notably in the primary creep regime. Two different aging heat treatments were used in order to produce varied amounts of secondary gamma' particles in the alloy. Following aging, samples were also given a brief (30 min) solution heat treatment and rapid quench in an attempt to resolution the gamma' precipitates. This was done to observe any shell or cluster formation along the prior gamma/gamma' interface. Three dimensional composition data as produced by the LEAP allowed for examination of these features as a function of aging heat treatment and subsequent resolution heat treatment.

9:30 AM

Thermal Shock Behaviour and Mechanical Properties of Refractory Materials: Bouressace Zina¹; Meddour Athman¹; ¹Université de Guelma

Our refractory material was elaborated from grog. It was used as aggregates. Kaolin was also introduced as a binder. An X-ray diffraction (XRD) analysis showed that the prepared basic refractory samples (without addition) are composed obviously, of Mullite and silica in its various forms. In addition, the presence of the Indialite phase was detected for the reinforced talc samples. This phase is characterized by some advantageous properties affecting the thermomechanical properties final material. The porosity of the samples takes diversified values. It differs from one batch to another. Therefore, the mechanical tests and thermal carried out revealed different behaviours of the refractory material according to prepared compositions. The amorphous phase governs considerably the sample thermomechanical properties variation with temperature increasing. This study shows that the thermal shock tests realized proved that our refractory elaborated, by addition of talc particles, takes the good thermal shock resistance.

9:50 AM Break

10:10 AM

Characterization of the Impact Resistance of Coir Fiber Reinforced Polyester Composites: Sergio Monteiro¹; Lucas da Costa¹; Felipe Lopes¹; Luiz Augusto Terrones¹; ¹State University of the Northern Rio de Janeiro - UENF

Polymeric composites reinforced with natural lignocellulosic fibers are being considered for applications in which low cost and malleability are desirable conditions. In particular, the fibers extracted from the coconut fruit, known as coir fiber, are nowadays used as composite reinforcement in automobile components such as panels and cushions. This investigation focused on the characterization of the impact resistance of coir fiber reinforced composites with polyester matrix. Both Charpy and Izod impact specimens made of polyester composites with up to 40wt.% of coir fibers were tested in an instrumented hammer pendulum. The results showed that the introduction of coir fibers significantly improves the impact resistance due to the energy transferred to a large number of cracks developed at the fiber/matrix interface.

10:30 AM

Characterisation of Silicon Nitride Thin Films Used as Stressor Liners on CMOS FETS: Measurement of Young's Modulus and Hardness: Gaetan Raymond¹; Pierre Morin²; Muriel Braccini¹; Fabien Volpi¹; ¹Simap; ²ST Microelectronics

This paper presents a study of the physical, chemical, and in particular mechanical properties of nitride films used for this application. Its aim is to determine the most important material characteristics and establish the best correlations between these properties. CESL nitride films are deposited by Plasma Enhanced Chemical Vapour Deposition. Thanks to process tuning, film stress ranging from -3 to 1.6 GPa can be achieved. Typical thicknesses used in CMOS technologies are ranging from 30 to 80 nm. For the purpose of the material characterisation, layers up to 300 nm have been deposited on 300 mm silicon substrates. These characterisations and results will help the optimisation of the nitride film used for stressor applications in current and future CMOS technological nodes.

10:50 AM

Characterizing Crystalline Ceramics in the Presence of a Glass Phase: Jessica Riesterer¹; Jeffrey Farrer²; N. Ravishankar³; C. Barry Carter¹; ¹University of Connecticut; ²Brigham Young University; ³Indian Institute of Science

EBS and XEDS in the SEM allow the orientation and phase of grains as small as 100nm to be determined simultaneously for samples ~1mm or greater. AFM provides quantitative high-resolution information on the topology. These techniques have been combined with TEM of FIBed samples to monitor solid-liquid interfaces in ceramic materials prepared for liquid-phase sintering (LPS) studies. Grain boundary migration in bicrystals of rutile TiO₂ and Al₂O₃ have been prepared as model samples. Hot pressed single crystals of known orientation with an intentional controlled interlayer of glass (SiO₂ or CaAl₂Si₂O₈, respectively) were prepared. The same process was repeated with one of the single crystal slabs replaced with polycrystalline material to give a single/poly 'bicrystal'. The effect of the orientation on grain boundary migration was examined by combining the above microscopy techniques to assess the driving force for migration. Exudation of glass from the boundaries may also be analyzed.

11:10 AM

Challenges in Materials Processing: Role of Heterogeneity in Chemistry and Structure: Sudha Cheruvathur¹; Vijayalakshmi Muraleedharan¹; ¹Indira Gandhi Centre for Atomic Research

Challenges in the processing of materials arising due to restructuring of microchemistry and microstructure during service life, are illustrated with the following examples: (1) Prediction and experimental confirmation of formation and prevention of hard brittle zone in dissimilar joints of ferritic steels. (2) Optimizing the formation of dilution layer in Colmonoy weld overlay on AISI 304 (L) stainless steel. (3) Prediction and confirmation of alternate structural material for electrodes of elementary neutral particle detectors. (4) "Self wastage" of 9Cr-1Mo steel in Sodium water reaction testing facility. In all the above examples, it is demonstrated that detailed computations along with selected confirmatory experiments are essential to recommend appropriate process parameters and also to ensure satisfactory performance of materials.

Computational Thermodynamics and Kinetics: Diffusion and Phase Stability

Sponsored by: The Minerals, Metals and Materials Society, TMS Electronic, Magnetic, and Photonic Materials Division, TMS Materials Processing and Manufacturing Division, ASM Materials Science Critical Technology Sector, TMS: Chemistry and Physics of Materials Committee, TMS/ASM: Computational Materials Science and Engineering Committee, TMS/ASM: Phase Transformations Committee
Program Organizers: Yunzhi Wang, Ohio State University; Long-Qing Chen, Pennsylvania State University; Jeffrey Hoyt, McMaster University; Yu Wang, Virginia Tech

Thursday AM
 March 13, 2008

Room: 288
 Location: Ernest Morial Convention Center

Session Chairs: John Morral, Ohio State University; Sujoy Kar, GE Global Research

8:30 AM Invited

The Formation of Single Phase Layers at the Interface of Diffusion Bonded Multiphase Alloys: John Morral¹; Ximiao Pan¹; Yunzhi Wang¹; ¹Ohio State University

When multiphase alloys are diffusion bonded there are a number of mechanisms by which a single phase layer can form at the initial interface. Often the formation is predictable by consulting a phase diagram. However in two cases, the phase diagram alone may suggest that the interface will be free of a single phase layer. One is when bonding two phase alloys that only differ in their average composition. Another is when bonding two phase alloys that differ in both their phases and their average composition. In the former case the layer may form if the diffusion path contains a singularity, while in the latter case they will form if the diffusion path passes through a special point on the phase diagram. Both experimental and computer simulation examples of the two cases will be given using diffusion couples made from model systems and Ni-Cr-Al alloys.

8:55 AM

Diffusion Kinetics at Ultra-High Stresses: Amit Samanta¹; Ju Li¹; Ting Zhu²; ¹Ohio State University; ²Georgia Institute of Technology

We assess point-defect diffusion kinetics in the ultra-strength regime, when materials sustain stresses at significant fractions of their ideal strengths. Since atomic bonds are already weakened, one expects reduced diffusion barrier that could lead to earlier onset of massive processes such as creep. As an example, the formation energy and migration energy barrier of vacancy in Cu are systematically evaluated in bulk, along grain boundaries and inside dislocation cores, and compared to zero-stress values. Surface diffusion is also modeled at the limit of large surface stresses.

9:10 AM

Multicomponent Diffusion in Single-Phase Multilayered Assemblies: Kaustubh Kulkarni¹; Mysore Dayananda¹; L. Ram-Mohan²; ¹Purdue University; ²Worcester Polytechnic Institute

A transfer matrix method is employed to examine concentration profiles developed in multicomponent 'multilayer diffusion assemblies' (MDAs) consisting of a number of finite layers sandwiched between two infinite terminal alloys. Analytical expressions for the temporal and spatial evolution of the concentration profiles are developed for single-phase multilayered assemblies characterized by a set of constant interdiffusion coefficients. The evolution of concentration profiles is explored for test MDAs assembled with ternary, single phase layers characterized by an arbitrary set of interdiffusion coefficients. The results indicate that the diffusion path of an MDA varies with time appreciably and approaches at long times asymptotically that for a solid-solid infinite diffusion couple between the two terminal alloys. Experimental MDAs were also assembled with $\alpha(\text{fcc})$ Cu-Ni-Zn alloys with a thin alloy layer sandwiched between two thick terminal alloys and annealed at 775°C for various times. The results of these studies are also presented and discussed.

9:25 AM

Calculation of Impurity Diffusivities in Ferrite from First-Principles: Daniel Worthington¹; Shenyang Huang²; Chris Retford¹; Gautam Ghosh³; Morris Fine³; Peter K. Liaw²; Mark Asta¹; ¹University of California, Davis; ²University of Tennessee; ³Northwestern University

First-principles calculations of impurity diffusion constants in body-centered-cubic (bcc) Fe have been undertaken in support of an effort aimed at the computationally-assisted design of a creep-resistant precipitate-strengthened ferritic "superalloy." To augment existing kinetic databases, which lack experimental measurements for a number of 4d and 5d solutes, diffusivities have been derived by incorporating first-principles calculated jump-rate probabilities into a generalized five-frequency model of vacancy-mediated diffusion in the dilute limit. We carried out both kinetic Monte Carlo and transition-matrix methods to compute correlation factors incorporating calculated vacancy-solute binding energies, which were found to extend beyond second neighbor. First-principles calculations were also conducted to determine the induced magnetization of the host atoms in the first and second coordination shells of the impurity, to compute the magnetization dependence of the diffusion activation energy, employing a previously published empirical relation between these quantities.

9:40 AM

Multibody Expansions: An Ab Initio Based Transferable Potential for Computational Thermodynamics: Baskar Ganapathysubramanian¹; Nicholas Zabarav¹; ¹Cornell University

Ab initio based techniques provide by far the most comprehensive and accurate details for computational thermodynamic and structure evolution studies. The computational complexity of these methods precludes the application of such first-principal analysis to configurations beyond a few hundred atoms. But in many cases, long-ranged and many-body interactions are necessary to model the energy accurately. We utilize a multibody based representation of the potential energy landscape to accurately represent these interactions in a computationally efficient manner. The many-body expansion is constructed via accurate sparse grid interpolation over a large database of ab-initio cluster energies. This framework results in the construction of transferable potentials that can be seamlessly integrated into various MD and MC platforms. We will illustrate the accuracy, efficiency and transferability of the proposed potential expansion using several computational thermodynamics based applications including the computation of stable structures of binary alloys.

9:55 AM

Extension of Miedema's Semi-Empirical Model for Estimation of Formation Enthalpies of Multicomponent Intermetallics: Pratik Ray¹; Mufit Akinci¹; Matthew Kramer²; Haoran Gong²; ¹Iowa State University; ²Ames Laboratory

We propose a simple extension of Miedema's semi-empirical model for estimation of formation enthalpies of multicomponent intermetallics and compare the model predictions with first principles calculations and experimental data on ternary intermetallics. The Miedema model has been extended by using a simple averaging scheme of the Wigner-Seitz cell boundary electron density of different elements. Thereafter, the enthalpy calculations are carried out within the framework of a sub-regular solution model. The results show fairly good agreement with the first principles calculations for Mo-Nb-Si alloys, as well as with the experimental data available in the literature.

10:10 AM Break

10:40 AM

Two-Phase Coexistence in Nanoscale Systems: Peter Bunzel¹; Gerhard Wilde²; Jörg Weissmüller³; ¹Forschungszentrum Karlsruhe; ²Westfälische Wilhelms-Universität Münster; ³Forschungszentrum Karlsruhe and Universität des Saarlandes

We inspect the equilibrium conditions governing the coexistence of two alloy phases within a system of finite size, for instance, a matrix-embedded alloy nanoparticle. The magnitude of the excess energy associated with the internal interface may here be comparable to that of the relevant bulk energy terms, and it depends on the phase fraction in a nonlinear way. Consequently, the common tangent rule does not apply, and the topology of the alloy phase diagram is found to differ from that of macroscopic alloy systems. As an example, we discuss a eutectic alloy system. We find, that the eutectic point splits up into an interval

of discontinuous phase change, and that the solidus temperature as well as the compositions of phases coexisting at equilibrium become functions of the overall composition. Calorimetric experiments on Cd-Bi alloy nanoparticles embedded in Al are well compatible with the predictions.

10:55 AM

A Statistical-Thermodynamic Modeling of Behavior and Properties in Thin-Film Intermetallic $L1_2$ -Structures: Olga Semenova¹; Regina Krachler¹; ¹University of Vienna

A statistical-thermodynamic modeling based on an Ising approach and the Bethe-Bragg-Williams random-mixing approximations is proposed for description of thermodynamic behavior and ordering phenomena in many layers nano-crystalline thin-film materials with $L1_2$ -structure. New modeling approach takes into account the presence of all possible defects in the structure, both vacancies and anti-structure atoms and includes a description of Long-Range Ordering and Short-Range Ordering in the crystal lattice. The derived equations define the fluctuations of the internal variables, such as interaction energies between atoms and defects and their contributions to macroscopic properties. As a validation of the suitability and high reliability of the chosen methodology, the obtained theoretical results are tested using experimental data on thermodynamic and structural properties of bulk intermetallic phases such as Ni_3Ga , and point defect concentrations, the degree of long-range order in the structure, as well as critical transition temperatures were predicted and compared to the experimental data.

11:10 AM

Ordering and Clustering Instabilities in FCC-Based Alloys: Importance of Second Nearest Neighbors: Nitin Singh¹; David Laughlin²; William Soffa¹; ¹University of Virginia; ²Carnegie Mellon University

Various investigators have employed the generalized Bragg-Williams model including second-, third-, etc nearest neighbor interactions to describe the energetics and kinetics of the precipitation of ordered phases in FCC-based alloys such as Al-Li, Ni-Ti and Ni-Al. In these systems where the order-disorder transformation is thermodynamically first-order, a synergism between ordering, clustering and spinodal decomposition has been revealed giving rise to a so-called conditional spinodal, for example. In this analysis specific attention is called explicitly to the importance of second nearest neighbour interactions in the occurrence of ordering and phase separation in FCC alloys involving the precipitation of an ordered $L1_2$ phase within a supersaturated FCC solid solution. The salient features of the generalized Bragg-Williams model applied to FCC alloys ($A1-L1_2$) will be elucidated and compared to the BCC case ($A2-B2$).

11:25 AM

Influence of Interaction Energy on the Mechanism of Ordered Precipitates of Al-Li Alloy: Yongxin Wang¹; Haichuan Miao¹; Zheng Chen¹; Yanli Lu¹; ¹State Key Laboratory of Solidification, Northwestern Polytechnical University

Influence of interaction energy on the precipitation kinetics mechanism of δ' (Al_3Li) was investigated by simulating the atomic pictures and calculating the order parameters, etc. The variation in precipitation mechanism with the nearest interchange interaction energy ($W1$). It is found that the ordering reaction take place before the atom cluster processing. With the $W1$ increased, the precipitation incubation period of δ' shortened, the range of ordered phase decreased, and the number of ordered phase increased. The ordering process and atom clustering promoted and the formation of the disordered phase blocked while the nearest interchange interaction energy increased. The maximum value that the long-range-order parameter advanced by increasing the $W1$.

11:40 AM

Thermodynamic Modeling of Phase Equilibrium in the Mo-Ti-Zr-C System: Sujoy Kar¹; Don Lipkin¹; Thomas Tiearney²; ¹GE Global Research; ²GE Healthcare

Alloys in the Mo-rich corner of the Mo-Ti-Zr-C system have found broad application in non-oxidizing environments requiring structural integrity at temperatures well beyond 1000C. Alloys such as TZM (Mo-0.5Ti-0.08Zr-0.03C) and TZC (Mo-1.2Ti-0.3Zr-0.1C) owe much of their high-temperature strength and microstructural stability to MC and M₂C carbide phases. The stability of the respective carbides, and the subsequent mechanical behavior of the alloy, is strongly dependent on the alloying additions. A CALPHAD-based thermodynamic modeling approach was employed to elucidate the effect of

alloying on the phase equilibrium in the Mo-Ti-Zr-C system. Key aspects of the thermodynamic descriptions of the constituent binary and ternary systems are described, the supporting experimental validation data is reviewed, and implications for developing improved molybdenum-based alloys are discussed.

11:55 AM

Phase Equilibria and Thermodynamic Assessment of the Ti-Al-Nb System: Hans Seifert¹; Damian Cupid²; Olga Fabrichnaya¹; Orlando Rios²; Fereshteh Ebrahimi²; ¹Technische University Bergakademie; ²University of Florida

Alloys in the Ti-Al-Nb system are promising for many high-temperature applications such as turbines for aero-engines. To refine the currently available thermodynamic description of the Ti-Al-Nb system, the extension of the bcc primary solidification field of the liquidus surface was investigated by observing the as-cast microstructures of selected alloys using optical microscopy, X-ray diffraction, scanning electron microscopy, and electron probe microanalysis. Also, differential thermal analysis was performed to determine the temperature of the invariant reaction between the liquid, σ -Nb₂Al, bcc, and γ -TiAl phases. The results of the experiments were used to re-optimize the Gibbs energy descriptions of the phases in the Ti-Al-Nb system for better agreement between calculated and experimentally observed liquidus surfaces. For further refinement during optimization, the calculated temperatures of predicted solid state reactions in the Ti-Al-Nb system were checked using differential thermal analysis and also additionally included as experimental data in the optimization.

12:10 PM

Phase Stability between the $(Al_{1-x}Mg_x)_2B_{12}$ Phase and the Al-Mg Intermediate Phases: Sungtae Kim¹; Donald Stone¹; Jae-Ik Cho²; Chang Yeol Jeong²; Chang-Seog Kang²; Jung-Chan Bae²; ¹University of Wisconsin - Madison; ²Korea Institute of Industrial Technology

In-situ composites based on Al-Mg matrices and $(Al_{1-x}Mg_x)_2B_{12}$ reinforcement phases are being investigated as candidate alloys for transportation applications where such alloys offer the potential to reduce weight and improve fuel efficiency. A key to the synthesis of these alloys is the ability to tailor their microstructures, an issue that is intimately related to phase stability in the Al-Mg-B system. Therefore, we investigate that stability; but in order to avoid attempting alloy system design with an arbitrary selection of composition and temperature, we utilize additive entropy formulation and ab initio calculations to estimate thermodynamic properties of phases in the Al-Mg-B system. Based on experimentally updated and theoretically evaluated thermodynamic properties of intermediate phases, the CALPHAD method has constructed the Al-Mg-B phase diagram over a wide range of temperature and composition to guide in alloy design. The financial support of the Korea Institute of Industrial Technology is gratefully acknowledged.

Electrode Technology Symposium (formerly Carbon Technology): Inert Anode

Sponsored by: The Minerals, Metals and Materials Society, TMS Light Metals Division, TMS: Aluminum Committee

Program Organizers: Carlos Zangiacomi, Alcoa Aluminum Inc; John Johnson, RUSAL Engineering and Technological Center LLC

Thursday AM
March 13, 2008

Room: 299
Location: Ernest Morial Convention Center

Session Chairs: Odd-Arne Lorentsen, Hydro Aluminium; Jomar Thonstad, Norwegian University of Science and Technology

8:30 AM

Inert Anodes: An Update: Rudolf Pawlek¹; ¹Technical Information Services and Consulting

This overview covers the development of inert anodes for the primary aluminium industry in the period 2003-2007. It reviews further on cermet, including their mechanical and physical properties and their behaviour and their manufacture; especially Cu (NiO-NiFe₂O₄) cermets in cryolite melts. However, the overview focuses particularly on the manufacture and behaviour metal anodes, including steels and Ni-Fe alloys. These alloys must be passivated

before use in electrolysis, otherwise they will dissolve in the cryolite electrolyte. Low temperature electrolytes are used to avoid aggravated corrosion; KF-based electrolytes for low temperature electrolysis have proved suitable. Multi-polar electrolysis in a mushy electrolyte using metal electrodes could be a solution in the future. Inert anodes were tested on laboratory and batch scales, but no information about industrial scale tests is yet available.

8:50 AM

X-Ray Visualization of Gas Bubble Ohmic Contribution: Comparison between Carbon and Inert Anodes: Veronique Laurent¹; Patrice Palau¹; Patrick Buttard¹; ¹Alcan CRV

Cermet anodes are today considered as one of the most promising candidate for replacing carbon anode in the aluminium industry. Nevertheless, the standard Gibbs energy of the oxygen evolution reaction is higher than the carbon dioxide one and leads to an increase of the electromotive force of around 1V at 960°C. Consequently, energy saving must be found in the different ohmic contribution of the cell voltage with inert anodes. An X-Ray set up has thus been developed in order to visualize a lab cell under electrolysis conditions. Observations during polarisation allowed us to compare the gas bubble effect on the cell voltage between a cermet and a carbone electrode.

9:10 AM

Effects of the NaF to AlF₃ Ratio on Fe-Ni-Al₂O₃ Anode Properties for Aluminum Electrolysis: Junli Xu¹; Zhongning Shi¹; Zhaowen Wang¹; ¹Northeastern University

Fe-Ni-Al₂O₃ anodes for aluminum electrolysis were prepared by powder metallurgy method and were tested in different ratio of NaF to AlF₃. It was discovered that the anode corrosion rate increased with the decrease of the ratio of NaF to AlF₃. The appropriate ratio was between 1.6~1.8, and the produced aluminum purity reached 98% while the corrosion rate of anode was about 22mm/a. The effects of the ratio of NaF to AlF₃ to the corrosion rate of Fe-Ni-Al₂O₃ anode were explained using electrochemical impedance analysis and cyclic voltammetry.

9:30 AM

Al₃Ti Alloy as an Inert Anode for Aluminium Electrolysis: Jianyun Wang¹; Zhaowen Wang¹; Zhongning Shi¹; Yaxin Yu¹; ¹Northeastern University

The Al₃Ti alloy, which is produced by the powder metallurgy technique, has been studied as inert anode for aluminium electrolysis. The goal for Al₃Ti is to produce an oxide layer at the electrolyte/anode interface, which can protect the anode from molten cryolite. Tests were carried out with conventional bath chemistry (CR=2.1) at around 940°C. A short-term electrolysis approach was taken to understand the anodic reaction and oxidation behaviour. The scales of anode, both before and after electrolysis, have been characterized through XRD and SEM. In general, inert anode was confirmed by the oxygen producing from anode. After electrolysis, there was no evidence that the size of sample changed. The SEM of sample after electrolysis showed that there was no Al except grainy Al₃Ti alloy inside the anode.

9:50 AM Break

10:00 AM

Anti-Oxidation Properties of Iron-Nickel Alloy at 800-900°C: Xingliang Zhao¹; Xiaozhou Cao¹; Zhongning Shi¹; Zhaowen Wang¹; Ying Nie¹; ¹Northeastern University

Fe-Ni base alloy as a kind of candidate materials for metal inert anode in aluminum electrolysis, three Fe-Ni (with different wt %) alloys with mass ratio of 50:50, 60:40 and 70:30 respectively were prepared by powder metallurgy process. Oxidation behavior of the three alloys were studied at 900°C. The results indicated that the oxidation kinetic curves follow the parabolic law and anti-oxidation properties enhanced with increasing ratio of Fe to Ni in the alloy. X-Ray Diffraction showed that the oxide film formed on the anodic surface consisted of Fe₂O₃ and Fe₃O₄. 5wt% Al and 30wt% Co were added in different Fe-Ni alloy respectively. The results showed that anti-oxidation properties of Fe-Ni-Co is better than Fe-Ni-Al at 900°C

10:20 AM

Effects of Rare Earth Element on Oxidation Behavior of Fe-Ni Metal Anode for Aluminium Electrolysis: Xiaozhou Cao¹; Zhongning Shi¹; Zhaowen Wang¹; Ting'an Zhang¹; Xianwei Hu¹; Xingliang Zhao¹; ¹Northeastern University

The addition of rare earth elements have significant effect on the oxidation behavior of Fe-Ni metal anode for aluminium electrolysis in air at 900°C by thermogravimetry method. The microstructure and composition of oxide film have been analyzed by XRD and SEM. The results show that rare earth element can change the content of oxide film on the surface of metal anode. Rare earth element is inclined to distribute on grain interfaces and refined casting grains. The oxide film is compact and can prevent the matrix from oxidizing further. The oxidation mechanism was suggested by the component of oxide film of metal anode.

10:40 AM

Effect of Additive CaO on Corrosion Resistance of 10NiO-NiFe₂O₄ Ceramic Inert Anodes in Aluminium Electrolysis: Zhongliang Tian¹; Lifeng Huang¹; Yanqing Lai¹; Jie Li¹; Yexiang Liu¹; ¹Central South University, School of Metallurgical Science and Engineering

10NiO-NiFe₂O₄ composite ceramic inert anodes with additive CaO content of 0, 1, 2 and 4%(mass fraction) were prepared and their corrosion resistance to Na₃AlF₆-K₃AlF₆-Al₂O₃ melts was studied in laboratory electrolysis tests. The results show that the content of additive CaO in anodes had little effects on the steady-state concentrations of impurities in electrolyte. Considering the corrosion resistance and thermal shock resistance, among 10NiO-NiFe₂O₄ ceramic anodes with different content of additive, 2% CaO/(10NiO-NiFe₂O₄) ceramic inert anode behaves best and should be further studied.

11:00 AM

The Effect of Additives on the Performance of the Nickel Ferrite Cermet Inert Anode for Aluminum Electrolysis: Yihan Liu¹; ¹Northeastern University

The inert anode cermet based on the nickel ferrite spinel was prepared by the powder metallurgy method using NiO, Fe₂O₃, Ag, and small amount additives as primary ingredients. The effect of additives on the microstructure and performance of the inert anode was researched. The results indicate that the additives can significantly improve the characteristics of the inert anode such as the conductivity and the corrosion resistance. The tests show the corrosion rate and the electricity conductivity of the sample containing additives are much better than that of the sample without additives. The fact has been observed that the additives could make the grains of the ceramic with the shape of octahedron grow completely and apparently. The fact has also been picked up that the additives could ameliorate the distribution of silver in the inert anode. The performance of the inert anode can visibly be improved by means of adding foreign super additions.

Hael Mughrabi Honorary Symposium: Plasticity, Failure and Fatigue in Structural Materials - from Macro to Nano: Cyclic Deformation and Fatigue of Metals II

Sponsored by: The Minerals, Metals and Materials Society, TMS Structural Materials Division, TMS Materials Processing and Manufacturing Division, TMS: High Temperature Alloys Committee, TMS/ASM: Mechanical Behavior of Materials Committee, TMS: Nanomechanical Materials Behavior Committee
Program Organizers: K. Jimmy Hsia, University of Illinois, Urbana-Champaign; Mathias Göken, Universitaet Erlangen-Nuernberg; Tresa Pollock, University of Michigan - Ann Arbor; Pedro Dolabella Portella, Federal Institute for Materials Research and Testing; Neville Moody, Sandia National Laboratories

Thursday AM Room: 386
 March 13, 2008 Location: Ernest Morial Convention Center

Session Chairs: J. Wayne Jones, University of Michigan; Tatsuo Sakai, Ritsumeikan University

8:30 AM Keynote

Mechanisms of Fatigue Failure of Polycrystalline Copper in the VHCF-Regime: Stefanie Stanzl-Tschegg¹; ¹BOKU University

In order to understand the mechanisms of fatigue damage of metallic materials, ductile single-phase metals have been studied by distinct authors like Mughrabi extensively in the past. More recently, since the non-existence of a fatigue limit in inhomogeneous high-strength steels became evident in tests in the VHCF regime, the question on the microstructural mechanisms of cyclic deformation in ductile metals was actualized by Mughrabi, and investigations with new testing techniques were started. Some results are reported in this paper, like on the formation of persistent slip bands (PSBs) in the VHCF regime and their role for the initiation of fatigue cracks in polycrystalline copper. The experiments were performed with the ultrasound fatigue technique up to 10^{11} cycles, and AFM as well as SEM and TEM studies were performed. The existence and correlation of PSB threshold and a questionable fatigue limit are treated.

9:00 AM Invited

Microstructure Variability and Fatigue Behavior at Very Long Life Fatigue:

J. Wayne Jones¹; John Allison²; Tresa Pollock¹; Christopher Szczepanski¹; Xiaoxia Zhu¹; Jiashi Miao¹; Liu Liu¹; ¹University of Michigan; ²Ford Motor Company

The is a growing body of research on the interesting and sometime unique interactions between microstructure, cyclic deformation mechanisms and damage accumulation that affect very high cycle fatigue behavior (VHCF) at lifetimes at or beyond 10^9 cycles. Models have emerged, such as proposed by Mughrabi, that extend our current understanding of cyclic deformation processes and microstructure variability to explain VHCF behavior. At such long lifetimes, critical microstructure features (e.g. large grains, inclusion, pores, surface condition) exert a strong influence on fatigue damage accumulation and, hence on the variability of fatigue life. This presentation describes recent research that uses ultrasonic fatigue to investigate VHCF behavior in a wide range of structural alloys, including cast aluminum alloys, wrought titanium alloys, particulate reinforced aluminum alloys and nickel-base single crystal and polycrystalline superalloys at ambient and elevated temperature. Current understanding from these studies of the role of microstructure in VHCF behavior will be summarized.

9:20 AM Invited

Long Life Fatigue-Critical Crack Length Concept: Alan Plumtree¹;

¹University of Waterloo

Long life fatigue is expressed by examining the critical lengths and threshold stress ranges for small surface and internal cracks. Competition between the two occurs after a very large number of cycles. The crack (surface or internal) that attains the critical length first becomes dominant, causing eventual failure. The critical length of surface cracks is related to crack closure and surface strain distribution. Failure occurs at the corresponding maximum threshold stress range ie. endurance limit. For much longer lives, the maximum threshold stress range

for the initiation and growth of internal cracks exceeds that of surface cracks. The more highly stressed internal regions such as flaws are preferred sites for the critical cracks. This critical length concept is applied to describe the long life fatigue of aluminum alloys and steels.

9:40 AM Invited

Development of Multi-Type High Efficiency Fatigue Testing Machines in Rotating Bending and Axial Loading: Tatsuo Sakai¹; Tatsuya Furusawa²; Ryohei Takizawa³; Noriyasu Oguma⁴; Hiroshi Hojo⁵; Hajime Ikuno⁶; ¹Ritsumeikan

University; ²Tokyokoki Seizosho Ltd.; ³Toyota Motor Corporation; ⁴University of Toyama; ⁵Toyota Central Research and Development Laboratories, Inc.

In usual fatigue tests, cyclic load are applied to the specimens toward ten million cycles to obtain S-N characteristics of the structural materials. But, the fatigue property in gigacycle regime is also focused as an important subject in recent years. In such a long life region, a tremendous long period is required to perform fatigue tests. In order to overcome this difficulty, the authors have developed special types of fatigue testing machines under rotating bending and axial loading in which some multiple specimens can be tested simultaneously. In rotating bending, two different type of testing machines for 4 or 10 specimens were developed. On the other hand, two different types of testing machines in axial loading were also developed by using special hydraulic technology. Their fundamental performance was confirmed through actual fatigue tests in gigacycle regime.

10:00 AM

Focused Ion Beam Tomography for the 3D-Investigation of Fatigue Cracks and Their Interaction with Micro-Structural Barriers: Horst Vehoff¹; Michael Marx¹; Wolfgang Schaefer¹; ¹Saarland University

The influence of the microstructure on fatigue is often discussed on the basis of mean values. For developing materials with a better fatigue resistance, local information about the interaction of cracks with microstructural obstacles is needed. The problem is how to image three dimensional cracks with the available techniques? Imaging by SEM or AFM is two dimensional, the resolution of high resolving x-ray tomography is not sufficient to image crack opening displacements in the order of less than one micron and in TEM only thin films can be investigated. Therefore three dimensional FIB tomography is used to visualize the crack path inside the specimens. It will be shown, by which mechanisms cracks interact with grain boundaries and how precipitates are bypassed by activating additional slip systems. Microstructural data like the inclination angel of the active slip systems can be coupled with the crack propagation rate which decreases significantly during interaction.

10:15 AM

High Cycle Fatigue Behavior of Copper Deformed by High Pressure Torsion: Golta Khatibi¹; Jelena Horky¹; Brigitte Weiss¹; Michael Zehetbauer¹;

¹University of Vienna

So far, investigations of fatigue behaviour of bulk nanomaterials achieved by Severe Plastic Deformation (SPD) have been restricted to those from Equal Channel Angular Pressing (ECAP). This contribution presents first results of fatigue tests of Cu processed by High Pressure Torsion (HPT). A special resonance ultrasonic fatigue testing system has been used which allows for symmetrical loading ($R = -1$) of freestanding small samples with thicknesses down to $10\mu\text{m}$. From disk-shaped HPT samples, miniaturized dumbbell-shaped specimens were cut and subjected to 10^6 to 10^9 loading cycles. The influence of purity and of grain/subgrain size on high cycle fatigue of HPT copper was investigated. Comparing the fatigue life curves of HPT Cu with those of coarse grained Cu, a significant increase of fatigue life was found. During cycling, high purity copper specimens showed softening and related grain coarsening while specimens of commercially pure copper did not reveal this effect.

10:30 AM

A Comparative Study on Fatigue Behavior of Shot Peened and Surface Severe Plastically Deformed Nickel Alloys: J. W. Tian¹; J. C. Villegas²; K. Dai³; A. L. Ortiz⁴; R. Ren⁵; M. Manjarres⁶; Leon Shaw⁶; Peter K. Liaw¹; D. L. Klarstrom⁷;

¹University of Tennessee; ²Intel Corporation; ³Quality Engineering and Software Technology; ⁴Universidad de Extremadura; ⁵Dalian Jiaotong University; ⁶University of Connecticut; ⁷Haynes International

A surface severe plastic deformation (S2PD) method has been applied to bulk specimens of a nickel-base C-2000 alloy. The fatigue behavior of the

S2PD-processed samples has been characterized and compared with that of the shot-peened samples. The microstructure of the near-surface layer, macroscopic residual stresses, and cross-sectional hardness profiles have been quantified using a variety of instruments. Both shot peening (SP) and S2PD improve the fatigue resistance of the C-2000 alloy with S2PD showing better enhancement. The different improvements in the fatigue resistance resulting from SP and S2PD are related to differences in the nano-grains at the surface region, the residual compressive stresses, and the work-hardened surface layer. Finite element modeling is performed to provide quantitative description of these differences and insights into the mechanism responsible for the observed improvements. This study demonstrates that S2PD can provide better fatigue resistance than SP.

10:45 AM

Development of Damage in Cast Iron During Superimposed Low Frequency Thermal-Mechanical and Higher Frequency Mechanical Loading: Thilo Hammers¹; Andreas Uihlein¹; Karl-Heinz Lang¹; Detlef Loehe¹; ¹Universitaet Karlsruhe (TH)

More and more thermally and mechanically highly stressed components fail due to the superposition of low and higher frequency loadings. A typical example are cylinder heads of combustion engines. Permanently rising temperatures and pressures of the combustion increase both the thermal-mechanical loading as well as the superimposed higher frequency mechanical induced loadings. The superposition of a higher frequency loading may reduce the number of low frequency basic cycles to failure drastically. It has to be assumed that the superimposed loading changes both the conditions for the initiation as well as the growth behaviour of fatigue cracks. To clarify the mechanisms of the damage development thermal-mechanical fatigue tests without and with a superimposed higher frequency loading were carried out on a cast iron material. Broken specimens as well as specimens from disrupted experiments were examined using light and scanning electron microscopy to identify the fatigue damages on hand.

11:00 AM

Investigation of Microstructure for AA7050 to Assist in Identifying the Fatigue Crack Initiation Sites: Jonathan LeDonne¹; Steve Sintay¹; Anthony Rollett¹; ¹Carnegie Mellon University

The fatigue life of aerospace aluminum alloys is governed primarily by crack initiation, which is accelerated by the presence of particles in the microstructure. Although much is known qualitatively about the relationships between fatigue life and the size of microstructural features, quantitative models suffer because of the lack of detailed microstructural data. Characteristics of coarse constituent particles are investigated for AA7050. Size distributions of second phase particles are characterized. The sizes and positions of particles are analyzed for 2-dimensional orthogonal sections, which are then used for reconstruction of a 3-dimensional microstructure of particles. The conversion assumes that the particles can be approximated as ellipsoids. Fracture surfaces are also investigated to establish a defined fatigue crack-initiating feature. The results are compared to previous results on AA7075.

11:15 AM Concluding Comments

Materials in Clean Power Systems III: Fuel Cells, Hydrogen-, and Clean Coal-Based Technologies: Hydrogen Technologies

Sponsored by: The Minerals, Metals and Materials Society, TMS Structural Materials Division, TMS/ASM: Corrosion and Environmental Effects Committee
Program Organizers: Zhenguo "Gary" Yang, Pacific Northwest National Laboratory; Michael Brady, Oak Ridge National Laboratory; K. Scott Weil, Pacific Northwest National Laboratory; Xingbo Liu, West Virginia University; Ayyakkannu Manivannan, National Energy Technology Laboratory

Thursday AM

March 13, 2008

Room: 392

Location: Ernest Morial Convention Center

Session Chairs: Leon Shaw, University of Connecticut; Guozhong Cao, University of Washington

8:30 AM Invited

Coherent Carbon-Cryogel-Ammonia-Borane Nanocomposites for H₂ Storage: Guozhong Cao¹; ¹University of Washington

Coherent carbon cryogel - ammonia borane (C-AB) nanocomposites are synthesized and the improved H₂ storage properties are reported. Porous carbon cryogels were impregnated with AB in tetrahydrofuran solution at 25°C under Argon. 30% of the carbon cryogel pore volume was filled to produce a 24 wt% C-AB nanocomposite. Nitrogen sorption isotherms, X-ray diffraction, differential scanning calorimetry, differential thermal / thermal gravimetric analyses, mass spectrometry, Fourier Transform Infrared Spectroscopy and 11B NMR were used to characterize the coherent C-AB nanocomposites. Findings include a merged two-step hydrogen release reaction with an appreciable reduction in the dehydrogenation temperature to <90°C, as well as the suppression of borazine release. Our results indicate that incorporation of AB in CC will lead to its destabilization, which is responsible for the improvement of hydrogen release kinetics as well as formation of different nonvolatile products for thermally reacted CC-AB compared to solid state AB.

9:00 AM

Hydrogen Uptake and Release Behavior of Lithium Amide and Hydride Systems for Hydrogen Storage Applications: W. Osborn¹; T. Markmaitree¹; X. Wan¹; Leon Shaw¹; Z. Gary Yang²; ¹University of Connecticut; ²Pacific Northwest National Laboratory

The DOE FreedomCAR requires that the on-board hydrogen storage system for PEM fuel cells can provide stable hydrogen fuel in about 1,500 uptake and release cycles. This study investigates the reaction pathway and rate-limiting step of dehydrogenation of the nanostructured LiNH₂ + LiH mixture in order to identify the strategy for enhancing its hydrogen uptake and release rates. The study reveals that dehydrogenation of the LiNH₂ + LiH mixture is diffusion controlled and the rate-limiting step is NH₃ diffusion through the Li₂NH product layer outside the LiNH₂ shrinking core. Furthermore, long-term hydrogen uptake/release stability is observed. These phenomena are explained based on a model describing the major steps of the dehydriding reaction of the mixture, and related to the evidence obtained from X-ray diffraction and specific surface area measurements of the mixture before and after isothermal hydrogen uptake/release cycles at high homologous temperatures.

9:25 AM

Structural Behavior Studies of Li-Based Hydrogen Storage Materials during Pressure Hydriding/De-Hydriding Cycling: Wen-Ming Chien¹; Joshua Lamb¹; Dhanesh Chandra¹; ¹University of Nevada

Li-based complex hydrides (imide/amide and LiNH₂/Li₂AlH₆) have been performed X-ray diffraction studies during pressure hydriding/de-hydriding cycling. The degradation of hydrogen storage capacities after pressure cycling was also determined. Equilibrium isotherms were obtained by Sievert's apparatus after 1, 56, 163, 501 and 1100 pressure cycles on imide/amide system, and observe hydrogen capacity changes as a function of cycles at 255°C. Structural studies of the products after pressure cycling showed mainly Li₂NH and LiH phases, and the impurity Li₂O phase. X-ray diffraction results showed the Li₂NH reduced from 77% to 13%, and LiH phase increases from 18% to 57% after 1100

cycles. Pressure cycling results showed 2.55 (~10.25 bar) and 2.95 wt% (~0.86 bar) hydrogen storage loss after 1100 cycles. X-ray diffraction study results of $\text{LiNH}_2/\text{Li}_3\text{AlH}_6$ system show that there is a phase transformation between 165°C to 200°C. Detail results of structural behaviors and pressure isothermals of different cycles will be presented.

9:50 AM

Development of Catalysts for Hydrogen Generation from Hydride Compounds: Valentina Simagina¹; Pavel Storozhenko²; Olga Netskina¹; Oksana Komova¹; ¹Boriskov Institute of Catalysis; ²State Research Institute of Chemistry and Technology of Organoelement Compounds

Investigation of hydrogen generation from NaBH_4 and NH_3BH_3 over catalysts has been carried out. It was shown, that the nature of a support and an active component of the catalyst affects the rate of H_2 generation. Development of active and stable catalysts, optimization of the catalytic bed and application of new engineering solutions have permitted to develop of hydrogen generator providing uniform hydrogen generation both in uninterrupted and in periodic modes of operation.

10:15 AM Break

10:30 AM

Elastic Constants and Internal Friction of Beta-Phase and Alpha+Beta-Phase Pd-Hydride between 1.4 and 300 K: Douglas Safarik¹; Ricardo Schwarz¹; ¹Los Alamos National Laboratory

Recently we measured¹ the room-temperature elastic constants of single-crystal PdH_x , where $0.01 < x < 0.62$. In this composition range, the crystals are two-phase mixtures of coherent beta-hydride precipitates in an alpha-hydride matrix, or coherent alpha-hydride precipitates in a beta-hydride matrix, depending on the value of x . We found that C_{44} and B decrease linearly with increasing x , whereas $C' = (C_{11} + C_{12})/2$ shows a parabolic dependence on x . The unusual composition dependence of C' was attributed¹ to anelastic relaxations involving changes in the shape of the coherent lenticular-shaped precipitates when subjected to an acoustic stress. To further investigate this anomalous behavior, we have measured the elastic constants and internal friction of single crystal PdH_x in the temperature range $1.4 < T < 300$ K and the composition range $0.58 < x < 0.72$. We discuss our results in terms of thermally activated relaxations of the coherent precipitates and ordering of the H-atoms in the beta phase. ¹R.B. Schwarz, H.T. Bach, U. Harms, D. Tugge, *Acta Mat.* 53, 569 (2005).

10:55 AM

Effects of Partial Substitution of Al for Mg on the Electrode Properties of Mg_2Ni Thin Film: Junli Xu¹; Ying Li²; Fuhui Wang²; ¹Northeastern University; ²Institute of Metal Research of Chinese Academy of Sciences

Mg_2Ni films with Mg partially substituted by Al were prepared by magnetron sputtering. Their charge-discharge property was tested, and the effect of the partial substitution of Al for Mg on thermal parameter of the films was studied. The charge-discharge experiments showed that the discharge property of Mg_2Ni film was improved by the substitution of Al for Mg. The gradation of discharge capacity of $\text{Mg}_{2-x}\text{Al}_x\text{Ni}$ film was: $\text{Mg}_{1.8}\text{Al}_{0.2}\text{Ni} > \text{Mg}_{1.7}\text{Al}_{0.3}\text{Ni} > \text{Mg}_{1.6}\text{Al}_{0.4}\text{Ni} > \text{Mg}_2\text{Ni}$. P-C-T curves revealed that the equilibrium hydrogen pressure increased and the formation enthalpy of hydrides in $\text{Mg}_{2-x}\text{Al}_x\text{Ni}$ film decreased with the increment of Al content, which indicated that the stability of the hydrides in $\text{Mg}_{2-x}\text{Al}_x\text{Ni}$ film decreased with the increment of Al content.

11:20 AM

Cytotoxicity and Reactive Oxygen Species Generation for Aggregated Carbon and Carbonaceous Nanoparticulate Materials: K. Garza¹; K. Soto²; L. Murr¹; ¹University of Texas; ²Lockheed Martin Aeronautics Company

We have investigated the cytotoxicity and reactive oxygen species (ROS) generation for indoor and outdoor soots: candle, wood, diesel, tire, and natural gas burner soots – along with surrogate black carbon, various multiwall carbon nanotube aggregate materials, TiO_2 (anatase) and chrysotile asbestos as reference materials. All soots were observed by TEM and FESEM to be composed of aggregated, primary spherules (20–80 nm diameter) forming complex, branched fractal structures. These spherules were composed of intercalated, turbostratic arrangements of curved graphene fragments with varying concentrations of polycyclic aromatic hydrocarbon (PAH) isomers. In vitro cultures with an immortalized human lung epithelial cell line (A549) treated with these materials

showed decreased cell viability and variations in ROS production, with no correlations to PAH content. The data demonstrates that soots are cytotoxic and that cytotoxicity is not related to PAH content but is a function of ROS generation, suggesting that soot induces cellular oxidative stress.

Refractory Metals 2008: Properties of Refractory Metals

Sponsored by: The Minerals, Metals and Materials Society, TMS Structural Materials Division, TMS: Refractory Metals Committee

Program Organizers: Todd Leonhardt, Rhenium Alloys Inc; Jim Ciulik, University of Texas at Austin

Thursday AM
March 13, 2008

Room: 388
Location: Ernest Morial Convention Center

Session Chairs: Todd Leonhardt, Rhenium Alloys Inc; Brian Cockeram, Bechtel Bettis Inc.

8:30 AM

Influence of Microstructure on the Fracture Toughness of Tungsten Alloys:

Bernd Gludovatz¹; Mario Faleschini²; Andreas Hoffmann³; Reinhard Pippan²;

¹Christian Doppler Laboratory for Local Analysis of Deformation and Fracture;

²Austrian Academy of Sciences, Erich Schmid Institute of Materials Science;

³Plansee Metall GmbH

Tungsten and tungsten alloys show the typical change in fracture behaviour from brittle (low temperatures) to ductile (high temperatures). In order to improve the understanding of the effect of microstructure the fracture toughness of pure tungsten, potassium doped tungsten and tungsten with 1wt% La_2O_3 has been investigated by means of 3-point bending -, double cantilever beam - and compact tension specimens. Though all these materials show the expected increase in fracture toughness with increasing temperature, influences like texture, chemical composition, grain boundary segregation and dislocation density have an extreme influence on the obtained results. These influences can especially be seen in the fracture behaviour and morphology, where two kinds of fracture can occur: on one hand the transcrystalline and on the other hand the intercrystalline fracture. Therefore techniques like electron backscatter diffraction, auger electron spectroscopy and x-ray line profile analysis were used to determine the parameter influencing fracture toughness.

8:55 AM

Physical Properties of Tungsten Wire for Halogen Lamp Manufacture:

James Downs¹; ¹Rhenium Alloys Inc.

Tungsten is the choice for halogen lamp filaments because of its good conductivity, high melting point, and low vapor pressure. Controlling the mechanical properties of the tungsten wire is critical to meet the demand for high intensity infrared lamps, for industrial and semiconductor industry that last longer and perform better. This presentation examines physical properties of tungsten, metallurgical structure and halogen cycle and how these affect fabrication and manufacture of the lamps and lamp performance.

9:20 AM

Microstructural Characterization of Dynamic Abnormal Grain Growth in Molybdenum: James Ciulik¹; Eric Taleff¹; ¹University of Texas at Austin

Large single crystals of commercial-purity molybdenum were grown by dynamic abnormal grain growth (DAGG). The microstructures were characterized using several methods: serial sectioning to show the three dimensional microstructure at the polycrystalline/single crystal interface; electron backscatter diffraction (EBSD) to characterize the crystallographic orientations of the grown single crystals and the crystallographic texture of the parent polycrystalline molybdenum; and Laue backscatter X-ray diffraction to identify the orientation of the single crystals grown. Results are presented to show that DAGG is a viable method of growing large single crystals of refractory metals at temperatures well below the melting temperature.

9:45 AM

High Temperature Properties of Molybdenum-Rhenium Alloys: Jason Wood¹; Samuel Causey¹; Randall Jenkins¹; Jennifer Gaies²; Mark Opeka²; Keisha Sylvester²; Xian Zhang²; ¹Southern Research Institute; ²Naval Surface Warfare Center – Carderock Division

Mechanical and thermal properties were obtained from different alloy compositions of molybdenum-rhenium (Mo-Re). The Mo-Re compositions characterized were Mo-41%Re, Mo-44.5%Re and Mo-47.5%Re and the manufacturing processes for these compositions were sinter and hot isostatic press (HIP) or swaged. Mechanical and thermal properties for these materials were obtained from room temperature to 3500°F. Manufacturing process differences and material property comparisons will be presented.

10:10 AM Break

10:20 AM

Oxidation Behavior of Alloys from the Nb-W-Cr System Containing C Modifiers: Maria Gonzalez De Moricca¹; Shailendra Varma¹; ¹University of Texas at El Paso, Department of Metallurgical and Materials Engineering

A comparison of the oxidation behavior between alloys of the Nb-W-Cr System containing C as a modifier has been performed. Selection of alloy compositions was based on the ternary isothermal sections of Nb-W-Cr at 1000 and 1500°C. Oxidation experiments were conducted in air at different time intervals in a range of temperatures from 700 to 1400°C. Mass gain per unit area as function of the temperature was used to determine the alloy's oxidation resistance. The oxidation products were characterized by XRD, EDS, SEM, and XPS. An intermediate temperature range indicates the formation of complete powder after 24 hours. The oxidation resistance at 1200°C and above has been found to be superior to their monolithic form as well as the alloys with boron (B) addition. The characterization results will be presented to delineate the effect of the carbon as a modifier to the ternary alloys on the oxidation kinetics.

10:45 AM

Effect of Al on High Temperature Oxidation of Cr-W Alloys: Omer Dogan¹; ¹Albany Research Center, National Energy Technology Laboratory

There is an increasing demand for new materials with good high temperature properties for new energy technologies developed to increase generating efficiency and reduce environmental pollution. Along with other refractory metals, chromium-tungsten alloys possess good strength well above the application temperatures of Ni-based superalloys. However, they have limitations with room temperature ductility and elevated temperature oxidation. The Cr-W alloys develop Cr₂O₃ scale under oxidizing conditions at elevated temperatures. Under cyclical temperature conditions, the oxide scale spalls resulting in a mass loss. In this study, effect of Al on the high temperature oxidation behavior of Cr-10wt%W alloy was investigated using a pseudo-cyclical oxidation test. Forming an Al-Cr layer on the Cr-W alloy reduced oxidation rate significantly and eliminated spalling completely.

11:10 AM

Mechanical Properties of High Purity Niobium Processed via Severe Plastic Deformation: Shreyas Balachandran¹; Richard Griffin¹; Robert Barber²; Karl Hartwig¹; ¹Texas A&M University; ²Shear Form Inc

High purity Niobium (Nb) is used for superconducting radio frequency accelerator cavities. This application requires the Nb sheet to have good formability and uniform mechanical and physical properties. The motivation of the study is to develop a fabrication process for Nb sheet with a more uniform microstructure and improved ductility. In order to obtain such sheet, the authors have worked bulk Nb by multipass equal channel angular extrusion (ECAE) and then rolled the bars to sheet. Preliminary results of tensile test and hardness measurements along with microstructural analysis shows improved ductility and mechanical property uniformity when compared to commercially available Nb sheet.

Structural Aluminides for Elevated Temperature Applications: Environmental Effects and Protection

Sponsored by: The Minerals, Metals and Materials Society, TMS Structural Materials Division, TMS: High Temperature Alloys Committee, TMS/ASM: Mechanical Behavior of Materials Committee

Program Organizers: Young-Won Kim, UES Inc; David Morris, Centro Nacional de Investigaciones Metalurgicas, CSIC; Rui Yang, Chinese Academy of Sciences; Christoph Leyens, Technical University of Brandenburg at Cottbus

Thursday AM

Room: 394

March 13, 2008

Location: Ernest Morial Convention Center

Session Chairs: Christoph Leyens, Technical University of Brandenburg at Cottbus; Guo Liang Chen, University of Science and Technology Beijing

8:30 AM Invited

Recent Progress on Oxidation Resistance of High Nb Containing TiAl Alloys: Guo Liang Chen¹; N. Zhang¹; L. L. Zhao¹; W. J. Wang¹; J. P. Lin¹; ¹University of Science and Technology Beijing

The presentation deal with the oxidation behavior of high Nb containing TiAl alloys. It has been confirmed that the outside thin layer of scale is Al₂O₃ at initial stage of the oxidation of high Nb containing TiAl alloys. The depletion in Al from surface is consistent with the selective oxidation of the alloy to form the alumina oxide layer. But the growth of the alumina layer is limited by the diffusion of Al in the underneath oxide layer. The depletion of Al leads to the onset of (Ti,Nb)O₂ layer. The (Ti,Nb)O₂ layer consists of two sublayers, (Ti,Nb)O₂ and (Ti,Nb)O₂+Al₂O₃. The morphology of (Ti,Nb)O₂ layer is finer and denser than TiO₂ layer of the TiAl alloys without Nb content. The alloying Nb significantly reduces the diffusion of oxygen in the scale, resulting in great improvement of oxidation resistant. The long time oxidation resistant can be significantly improved by Y additions. Suitable Y content can completely depress the abnormal increase of the oxidation of TiAl + 7/8 Nb alloys after about 500 hr long time exposure at 900. The optimum content is related to the Nb content in the alloy. Adding Y to high Nb containing TiAl alloys is a suitable way to keep excellent oxidation resistance after long time exposure at high temperature. The detailed effects of Y addition on the oxide scale are also discussed.

9:00 AM

Oxidation Behavior of TiAlYN and CrAlYN Nanocomposite Coatings Deposited on γ -TiAl Based Alloy Ti-45Al-8Nb: Reinhold Braum¹; David Müßener¹; Martin Moser²; Florian Rovere²; Paul Mayrhofer²; Christoph Leyens³; ¹DLR - German Aerospace Center; ²Montanuniversität Leoben; ³Technical University of Brandenburg at Cottbus

The oxidation behaviour of nanocomposite TiAlYN and CrAlYN coatings was investigated in the temperature range between 750 and 950°C conducting cyclic oxidation tests in air. The about 4 μ m thick layers were deposited on γ -TiAl samples using unbalanced magnetron sputtering. The yttrium content varied from 0 to 4 at%. Post-oxidation micro-structural examination was carried out using scanning electron microscopy and energy-dispersive X-ray spectroscopy. The TiAlYN coatings provided reasonable oxidation protection to γ -TiAl alloy at 750°C, but they decomposed after short time periods at 850°C. Samples with nanocomposite CrAlYN coatings exhibited significant lower mass gains in comparison to the bare substrate material when thermally cycled at 900°C. Although the coatings were entirely oxidised, oxidation of the substrate was considerably reduced compared to uncoated samples. When exposed at 950°C, the CrAlYN coatings with 1 and 4 at% Y provided initial protection which vanished after longer exposure times.

9:20 AM

High Temperature Oxidation of Beta-Gamma Ti Alloys: Michiko Yoshihara¹; Young-Won Kim²; ¹Yokohama National University; ²UES Inc

A new class of TiAl based multi-component alloys, called beta gamma alloys, have been explored at UES/AFRL in an effort to ease the processing and improve the machinability of gamma-TiAl alloys. Additional requirements were that the new alloys should have refined structures and also adequate resistance to creep and oxidation at high temperatures. It was found out that such alloys

may exist within the broad composition range of Ti-(40-45)Al-(1-7)Nb-(1-8)(Cr,Mn,V,Mo)-(0-0.5)(B,C). In the present study, the cyclic oxidation behavior of several beta-gamma alloys has been investigated in air in the temperature range between 600°C and 870°C. The results show that the oxidation resistance varies widely depending upon the phase distribution and alloying elements. Some of beta-gamma alloys show the oxidation resistance as good as that of best conventional gamma alloys. The results will also be compared with those of representative titanium alloys and explained in terms of beta distribution and alloying elements.

9:40 AM

Influence of Oxidation Protective Coatings on the Ductility of γ -TiAl Based Alloys: *Martin Moser*¹; *Florian Rovere*¹; *Reinhold Braun*²; *Helmut Clemens*¹; *Paul Mayrhofer*¹; ¹Montanuniversität Leoben; ²DLR-German Aerospace Centre

Using γ -TiAl alloys in high temperature applications requires coatings that effectively protect the material from oxidation. Here, three commercial coating systems, Al/Cr deposited by pack-cementation, NiAl prepared by Ni-electroplating, and a CoNiCrAlY coating deposited by atmospheric plasma spraying, as well as two novel physical vapour deposition (PVD) films, AlAu and CrAlYN are investigated. Ti-47Al-2Cr-0.2Si sheet material was selected as substrate as this alloy exhibits high ductility at room temperature but low oxidation resistance. Thermal exposure in air reveals that all selected coatings improve significantly the oxidation resistance of the base material. The interaction between the coatings and γ -TiAl was investigated by 4-point-bending tests at room temperature. After coating all samples show a decrease in bending strength. The PVD coatings as well as the CoNiCrAlY films show the smallest influence on ductility, whereas the pack cementated Al/Cr- and electroplated Ni-films resulted in strong degradation of mechanical properties.

10:00 AM

Oxidation Characteristics of γ -TiAl-8Nb Coated with a CrAlYN/CrN Nanoscale Multilayer Coating: *William Rainforth*¹; *Ian Ross*¹; *Christina Reinhard*²; *Papken Eh.Hovsepian*²; *Arutium Ehasarian*²; *Reinhold Braun*³; *Christoph Leyens*⁴; ¹Sheffield University; ²Sheffield Hallam University; ³German Aerospace Centre (DLR); ⁴Technical University of Brandenburg at Cottbus

There is a major desire to introduce gamma-TiAl into a range of high performance applications in order to reduce weight. However, this will require the development of coatings that protect against oxidation at high temperature, but do not adversely affect the mechanical properties. This work reports the high temperature degradation mechanisms of a nanoscale CrAlYN/CrN multilayer coating deposited on gamma-TiAl(8Nb) by a combined high power impulse magnetron sputtering/unbalanced magnetron sputtering. Detailed TEM/STEM analysis of FIB prepared specimens from isothermal static oxidation tests at 850°C for up to 1030 hours is presented. The evolution of the complex oxide and significant structural modification of the gamma-TiAl(8Nb) substrate is reported. The implication of these observations for future coating development is discussed.

10:20 AM Keynote

Recent Progress in the Science and Technology of Gamma Titanium Aluminides: *Christoph Leyens*¹; *Janny Lindemann*¹; *Maria Glavatskikh*¹; *Susanne Gebhard*²; *Maik Fröhlich*²; *Dan Roth-Fagaraseanu*³; ¹Technical University of Brandenburg at Cottbus; ²German Aerospace Center; ³Rolls-Royce Deutschland

Titanium aluminides have attracted significant attention since materials properties have been strongly improved over the last years, and engineers have become more familiar to design with a material that shows limited ductility and damage tolerance. Part of the reason of slow introduction into service is the complexity of materials processing which is attributed to a strong dependency of component properties on alloy chemistry and microstructure. Among others, the paper will provide an overview of recent progress in the understanding of processing-related fluctuations in chemical composition and their effects on the mechanical properties of Ti-Al-Nb- and Ti-Al-Nb-Mo-based gamma TiAl alloys which are designed for moderately elevated temperature applications. Moreover, recent results on the retained strength of these classes of modern alloys and materials behavior after impact will be highlighted. Also, latest findings regarding mechanical and chemical surface treatments including coatings will be discussed.

11:00 AM

Hot Corrosion Behavior of Nanostructured Coatings on Gamma-TiAl for High Temperature Applications: *Francisco Perez-Trujillo*¹; *Juan Nieto Hierro*¹; *Maria Hierro de Bengoa*¹; *Sonia Mato Díaz*¹; ¹Universidad Complutense

Gamma-TiAl aluminides have a temperature limit for high temperature applications. In order to increase the operation temperature, different micro and nano structured coatings have been applied in order to increase this temperature. Among the different corrosive environments at high temperature, molten salts are the most aggressive environment to test. To know the hot corrosion resistance of this novel coatings, experiments in sulfate-chloride molten mixtures have been performed at 750°C for more than 300 h. Since this test has not been performed before, equivalent circuits have been established, as well as the corresponding modelling. The advantages to establish coatings performance of the electrochemical impedance spectroscopy (EIS) applied will be established. Mechanistic approach and coatings performance will be given.

11:20 AM

Oxidation Behavior of Nb Additional TiAl Alloys: *Wei Lu*¹; *Lianlong He*¹; ¹Institute of Metal Research

The oxidation behavior of different stages of three kinds of Nb additional TiAl based alloy, Ti-46.5Al-5Nb, Ti-45Al-8Nb-0.2W-0.2B-0.02Y and Ti-45Al-15Nb (at%) have been investigated at 900°C in static air. The adherence between nitride layer and base alloy is good. However, an obvious interface between the mixed layer and the under layer existed at the initial oxidation stage. Meanwhile, oxygen absorption and refining of the base alloy lead to the increase of the volume fraction of grain boundary at the initial stage. The first reason why Nb addition improves the oxidation resistance of TiAl alloys is that the doping of Nb⁵⁺ in the TiO₂ enriched layer can not only reduce the diffusion path of Ti cation and O anion but also promote the formation of Al₂O₃ enriched layer. The second reason is that Nb based compound was formed at the subsurface layer, which can prevent a continuous formation of X phase.

11:40 AM

The Fluorine Effect for High Temperature Oxidation Protection of TiAl-Alloys for Automotive and Aero-Engine Applications: *Alexander Donchev*¹; *Michael Schütze*¹; *Rossen Yankov*²; *Andreas Kolitsch*²; ¹Society for Chemical Engineering and Biotechnology; ²Forschungszentrum Dresden Rossendorf

The insufficient oxidation resistance of TiAl above roughly 800°C is a major disadvantage for its use but it can be improved significantly by small amounts of halogens in the surface zone of the TiAl-material. Especially fluorine has proven to be a beneficial doping element. The fluorine effect is stable at least for one year at temperatures up to 900°C under thermocyclic conditions. In this paper results of fluorine treated and untreated TiAl-coupons, turbocharger rotors for automotive use and turbine blades for aero-engines are shown. The specimens were exposed isothermally and thermocyclically in the temperature range from 700–1050°C in laboratory air or synthetic air. The specimens can be treated with fluorine in several ways e.g. spraying. Without any treatment some components were totally destroyed during high temperature oxidation but after fluorine treatment the components were still intact. Post oxidation investigations showed the formation of a thin and protective Al₂O₃-scale.

12:00 PM

Ti-Al-Cr-X Coatings for High Temperature Oxidation Protection of Gamma Titanium Aluminides: *Maik Fröhlich*¹; *Reinhold Braun*¹; *Christoph Leyens*²; ¹DLR-German Aerospace Center; ²Technical University of Brandenburg at Cottbus

To extend the oxidation resistance of gamma titanium aluminides for applications above 750°C the formation of non-protective titania has to be prevented. The primary objective to improve the resistance of titanium aluminides against oxidation is the use of alumina forming coatings. The paper is focussed on the development of oxidation resistant metallic coatings on the basis of Ti-Al-Cr. Ti-Al-Cr and Ti-Al-Cr-X coatings with X=Ag,Hf,Y,Si were produced by magnetron-sputtering-techniques. The coated specimens were examined under cyclic conditions at 900°C and 950°C up to 1000 cycles, respectively. All coatings formed a thin alumina layer on top providing a diffusion barrier for oxygen at the beginning. But internal diffusion between substrate and coating led to a depletion of Laves phase which promotes the formation of alumina. The effect of cross diffusion between coating and substrate for the various coating chemistries will be discussed on the basis of post-oxidation SEM/EDX and oxidation kinetics analysis.

A

Aalund, R.....	283
Abakumov, A.....	326
Abbott, T.....	289, 337
Abdel Maksoud, I.....	134
Abdelmalek, F.....	219
Abe, H.....	342
Abedrabbo, S.....	63
Abeykoon, A.....	197
Abidzina, V.....	143
Abinandanan, T.....	43, 276
Abot, J.....	59
Abromeit, C.....	71, 94
Abu Leil, T.....	336
Accorsi, I.....	122
Achurra, G.....	330
Adams, J.....	88
Adams, K.....	338
Addemir, O.....	123, 233
Adedokun, S.....	65
Adelakin, T.....	321
Adharapurapu, R.....	182
Afanasjev, V.....	168
Aga, R.....	275, 319
Agaliotis, E.....	362
Agarwal, A.....	60
Agarwal, R.....	74
Ager, J.....	66, 308, 324
Agnew, S.....	95, 118, 189, 241, 278, 286, 297
Aguiar, M.....	213
Aguiar, J.....	125
Ahart, M.....	92
Ahluwalia, R.....	224
Ahmed, H.....	65, 134
Ahn, B.....	51, 52, 122
Ahn, K.....	105
Ahn, S.....	48
Ahuja, R.....	293
Ahuwan, A.....	346
Aichun, D.....	78, 302
Aidhy, D.....	252
Ajayan, P.....	59
Akbari Mousavi, S.....	53, 54
Akin, I.....	358
Akinc, M.....	364
Akray, S.....	332
Akuzawa, N.....	227
Al-Fadhalah, K.....	82
Al-Jallaf, M.....	325
Al-Jassim, M.....	105
Al-Khalifa, J.....	351
Al-Maharbi, M.....	52, 334
Al-Sharab, J.....	41
AlAli, H.....	112, 164, 220, 271, 319, 361
Alam, M.....	338, 339
Albe, K.....	99
Albert, C.....	287
Alekseeva, N.....	326
Alexander, D.....	149, 151, 170, 230, 260
Alexandrov, I.....	51, 306
Alfarsi, Y.....	266
Alge, D.....	216
Ali, M.....	315
Alisch, G.....	57
Alkorta, J.....	225
Allain, S.....	118

Allen, A.....	64, 147
Allen, T.....	198, 199, 252, 299
Allison, J.....	49, 80, 85, 86, 126, 367
Alloyeau, D.....	308
Allred, L.....	194
Alman, D.....	189
Al Marzouqi, A.....	226
Almer, J.....	142, 143, 328
Alterach, M.....	181
Alurralde, M.....	299, 300
Alves, E.....	252
Al Zarouni, A.....	357
Amaral, A.....	107, 356
Amberger, D.....	307
Amin, S.....	260
Amini, S.....	40
Amirouche, L.....	324
Amjad, J.....	134
An, H.....	80
An-Ping, L.....	327
Anand, K.....	234
Andermann, L.....	211
Anderoglu, O.....	174
Andersen, P.....	229
Anderson, I.....	90, 108, 140, 145, 200, 254, 318, 327, 351
Anderson, K.....	340
Anderson, M.....	319, 320
Anderson, P.....	39, 131
Andersson, J.....	87
Ando, D.....	241
Ando, T.....	177
Andrievskaya, N.....	57
Angulo, R.....	192
Aning, A.....	361
Ankem, S.....	73, 246
Anopuo, O.....	186
Antipov, E.....	326
Antônio Reis, M.....	119
Antony, J.....	325
Antrekowitsch, H.....	113, 125, 165, 202, 220, 302
Anumalasetty, V.....	100
Anyalebechi, P.....	86, 87, 136, 192, 245
Aoki, K.....	45, 47, 48, 135
Aourag, H.....	293
Aoyagi, T.....	245
Apel, M.....	146
Apelian, D.....	147, 202, 351
Apisarov, A.....	314
Appel, F.....	74, 149, 304, 347, 348, 349, 350
Appel, J.....	64
Aquino, R.....	221
Arabaci, A.....	79
Arai, K.....	254
Arai, M.....	193
Arapan, S.....	293
Arce-Estrada, E.....	260, 322
Ares, A.....	87, 181, 272, 362
Arfaei, B.....	277
Argon, A.....	139, 182
Arjunan, S.....	51
Armstrong, P.....	135
Arockiasamy, A.....	107
Arora, V.....	213
Arruda, A.....	119
Arseneault, A.....	361
Arsenlis, T.....	72

Arzt, E.....	66, 110, 160, 215, 267, 316, 358
Asa, Y.....	193
Asadi, M.....	87
Asami, C.....	344
Asgari, S.....	118
Ashcroft, N.....	196
Ashida, D.....	306
Asif, S.....	76
Askin, J.....	39
Asokamani, R.....	51
Asokan, K.....	271
Aspen, E.....	164
Asta, M.....	72, 78, 139, 191, 224, 276, 364
Aswath, P.....	215, 358
Atamanenko, T.....	272
Athman, M.....	363
Athreya, B.....	169
Atmeh, M.....	40
Atsumi, T.....	300
Atzmon, M.....	67
Aubain, M.....	278
Aude, M.....	260
Aujla, D.....	260
Auld, J.....	187
Avasthi, D.....	343
Averback, R.....	71
Avraham, S.....	187
Awakura, Y.....	272, 321
Aydin, S.....	79, 302
Aydiner, C.....	143, 306, 329
Azevedo, M.....	321
Azhazha, V.....	57

B

Baars, D.....	303
Bache, M.....	235
Bacon, D.....	73, 169
Bade, K.....	309
Badillo, A.....	71
Badowski, M.....	320
Bae, C.....	152
Bae, D.....	39, 47, 309
Bae, G.....	292
Bae, I.....	299
Bae, J.....	292, 365
Bagheri, S.....	277
Bagheri, Z.....	277
Bagley, S.....	268
Bahadur, H.....	71
Bahr, D.....	174, 195, 316
Bai, C.....	219, 256
Bai, H.....	86
Bai, J.....	268
Bajenaru, O.....	180
Baker, I.....	204, 351
Baker, K.....	216
Baker, S.....	278
Bakke, P.....	337
Balaban, N.....	295
Balachandran, S.....	370
Balani, K.....	60
Balasubramanian, J.....	39
Ballard, D.....	70
Ballato, J.....	105
Ballentine, F.....	264
Ballou, T.....	106

- Balogh, A.....342
 Balogh, L.....307, 341
 Bamberger, M.....187, 188, 290
 Ban, Y.....191, 314, 326
 Bandaru, P.....59, 60
 Banerjee, R.....166, 181, 193, 194, 275, 340
 Bang, W.....48
 Banhart, J.....178
 Banik, K.....293
 Banister, G.....271
 Banks, J.....267
 Banovic, S.....211
 Bao, Y.....239, 336
 Baoyan, Z.....178
 Barabash, O.....221
 Barabash, R.....92, 93, 141, 197, 221, 250, 297, 341
 Barbee, T.....218, 236
 Barber, R.....370
 Barbi, N.....349
 Barbosa, E.....210
 Barboza, M.....358
 Barker, E.....170
 Barnard, B.....359
 Barnes, S.....248
 Barnett, M.....100
 Barney, M.....328
 Baron, J.....172
 Barrallier, L.....298
 Barron, M.....137, 166, 273
 Barsoum, M.....40
 Bartels, A.....256, 304, 305, 347, 348, 349
 Barthélemy, A.....115
 Bartolo, L.....339
 Bartsch, M.....340
 Barzola-Quiquia, J.....299
 Basletic, M.....115
 Basquin, J.....357
 Bass, M.....105
 Bassler, K.....197
 Basson, F.....320
 Basu, J.....76
 Batane, N.....236
 Bates, B.....122
 Batey, J.....190
 Batista, E.....213
 Batista, J.....263
 Battaile, C.....104, 155, 247, 248, 278
 Battiste, R.....233
 Bauer, G.....142
 Bauer, R.....125
 Bauer, V.....129
 Baxi, J.....181
 Baydogan, M.....295, 332
 Bayha, T.....294
 Bayles, B.....234
 Bayles, R.....294
 Bazan, G.....91
 Beall, G.....114
 Beals, R.....85, 86, 132, 133, 186, 188, 238, 240, 288, 289, 335, 336
 Beardsley, M.....123
 Beame, G.....108, 159, 213, 266, 313, 315, 357
 Beaudoine, A.....287
 Beck, T.....50, 286
 Becker, A.....95
 Becker, C.....276
 Becker, R.....72
 Beckmann, F.....335
 Beercheck, D.....346
 Behrens, B.....282
 Bei, H.....360
 Belak, J.....169, 175
 Belasco, J.....328
 Bele, E.....107, 234
 Belin-Ferré, E.....184, 309
 Bellon, P.....49, 71
 Belous, A.....322
 Belova, I.....44
 Belt, C.....279, 280, 329
 Bender, M.....310
 Bengus, V.....57
 Benhaddad, S.....243
 Benkahla, B.....357
 Bennet, J.....360
 Benoit, G.....204
 Benson, D.....334
 Benson, M.....197
 Bentancur, M.....229
 Bentley, J.....90
 Benzerga, A.....45, 179, 184, 282, 340, 355
 Berghmans, A.....104
 Bergmann, S.....282
 Berkley, M.....164
 Bernabai, U.....231
 Bernier, J.....329
 Berramane, N.....204
 Berry, C.....105
 Berry, J.....140, 298
 Berteaux, O.....129
 Berzansky, J.....164
 Bessa, E.....213
 Bessada, C.....227
 Besser, M.....90
 Bestor, M.....128, 175
 Bettles, C.....294
 Bewlay, B.....325
 Beyerlein, I.....100, 117, 229, 257, 279
 Bhadesia, H.....297
 Bhadrachalam, P.....153
 Bharadwaj, M.....289, 336
 Bharathula, A.....163
 Bhattacharjee, A.....247
 Bhattacharya, P.....176
 Bhattacharya, R.....134
 Bhattacharyya, D.....102, 171, 230
 Bian, X.....269
 Bibee, M.....328
 Bibes, M.....115
 Bicalho, L.....358
 Bichler, L.....289
 Bie, H.....145
 Bieler, T.....90, 148, 170, 228, 229, 277, 303, 347
 Biermann, D.....282
 Biermann, H.....236
 Bilani, O.....168
 Binbrek, A.....171, 266
 Bindl, D.....212
 Biner, S.....95
 Bing, L.....313
 Bingert, J.....141, 209, 249
 Birat, J.....219
 Biswas, A.....284
 Biswas, P.....154, 158
 Bjelkengren, C.....65
 Bjørneklett, B.....158
 Blacket, S.....336
 Blaine, J.....288
 Blanpain, B.....117, 301
 Blau, P.....89, 233
 Blicharski, M.....80
 Blobaum, K.....249
 Blochwitz, C.....183
 Blue, C.....295
 Blum, W.....285
 Boakye, E.....118
 Bobadilla, J.....330
 Bobrovitchii, G.....222, 321
 Bock, U.....79
 Bodde, S.....67
 Bodepalli, S.....42
 Boehlert, C.....90, 194, 195, 246, 288
 Boettger, B.....325
 Boettinger, W.....72, 169, 276
 Bogdanov, Y.....315
 Bohn, T.....206
 Bohner, H.....213
 Bojarevics, V.....315
 Bolcavage, A.....78
 Bonarski, B.....52, 353
 Bonfrisco, L.....176
 Bonnett, J.....338
 Booty, M.....296
 Borbely, A.....84
 Border, K.....64
 Borges, A.....311
 Borgeisen, P.....277
 Boris, A.....115
 Borisenko, K.....184
 Bormann, R.....133, 186, 241, 256
 Bosch, M.....320
 Bosse, M.....336
 Botelho, J.....171
 Bott, R.....156, 157, 263
 Böttcher, H.....165, 220
 Bouaziz, O.....118
 Bourgeois, L.....146
 Bourke, M.....75, 121, 173, 229, 278, 328
 Bourne, G.....69
 Bourne, N.....249
 Bouville, M.....224
 Bouwhuis, B.....107
 Bouzehouane, K.....115
 Bower, A.....46, 157, 228
 Bowers, R.....157, 171, 172
 Boyce, B.....75, 121, 122, 173, 229, 278, 328
 Boyce, D.....153
 Boyle, K.....85
 Boysen, K.....244
 Braccini, M.....363
 Bradley, J.....157, 293
 Brady, M.....86, 135, 189, 190, 243, 292, 338, 368
 Bramhoff, D.....165
 Brandimarte, G.....140
 Brandt, M.....336
 Brant, D.....161
 Braun, P.....260
 Braun, R.....349, 370, 371
 Brederholm, A.....87
 Brenner, R.....279
 Brewer, L.....278
 Brewster, A.....165

Bridi, R	220	Calderón, H	47	Cha, D	102
Brigmon, R	105	Calin, M	56	Cha, S	39, 59
Bringa, E	169, 334	Calonne, O	203	Chada, S	74, 119, 172, 199, 228, 253, 277, 300, 326, 343
Bringas, Jr., P	160	Calvert, P	267	Chai, L	255, 346
Brinkmeyer, B	277	Camara, J	213	Chakhalian, J	115
Brittes, G	210	Camili, R	213	Chakkingal, U	51
Brockdorf, K	310	Campbell, A	177, 232	Chakraborti, D	105
Brockenbrough, J	49	Campbell, B	342	Chakraborty, P	61
Brockman, R	78	Campbell, C	97	Chamberlain, O	156
Broderick, S	293	Campbell, J	107	Champion, Y	100
Brodie, G	356	Campillo, B	45	Chan, K	346
Bronfenbrenner, D	328	Cañas, R	356	Chan, L	264
Bronfin, B	337	Candic, M	273	Chan, P	169
Brookes, S	149	Cannova, F	171, 172	Chancellor, T	101
Brooks, J	193, 256	Canutas De Wit, C	315	Chandra, D	368
Brooks, R	247	Cao, B	334	Chandra, S	71
Brown, A	128, 175	Cao, F	81, 304	Chandrasekar, S	55, 57, 151
Brown, D	93, 118, 142, 143, 166, 170, 197, 198, 230, 251, 279, 297, 306, 329, 342	Cao, G	239, 288, 289, 368	Chandrashekar, S	106, 156, 210, 263, 311, 356
Brown, E	91, 140, 198, 249, 335	Cao, H	187	Chang, C	75, 300
Brown, L	183, 338	Cao, W	138, 294	Chang, H	318
Brown, S	145	Cao, X	78, 177, 314, 326, 366	Chang, J	200, 355
Browning, N	355	Cao, Y	174	Chang, L	262
Bruder, E	206	Cao, Z	312	Chang, R	185
Brueck, S	298	Capdevila, C	146	Chang, S	283, 284, 332
Bruggeman, J	313	Capdevila-Montes, C	54	Chang, W	331
Brunner, R	317	Cappiello, M	144	Chang, Y	96, 102, 112, 138, 158, 184, 187, 294
Bsesnbruch, G	338	Caputo, A	120	Chan Gyung, P	310
Buchanan, D	78	Caratini, Y	357	Chanturiya, V	114
Buchholz, A	362	Carden, Z	165	Chao, J	54
Buchholz, D	185	Caricato, A	252	Chapuis, A	350
Buchovecky, E	228	Carlton, C	76	Charles, N	331
Budai, J	93	Carolan, M	135	Charlier, P	320
Budak, S	41, 208, 327	Caron, A	269, 360	Chasiotis, I	122
Buenavista, S	125	Caron, P	82	Chason, E	228
Buergi, H	342	Carpenter, J	69	Chatterjee, A	185, 340
Bugge, M	159	Carpenter, T	317	Chatterjee, U	65
Bulanova, M	181	Carradó, A	298	Chau, R	141
Bulatov, V	72	Carreño, F	353	Chaubal, M	311
Bunin, I	114	Carrétero, C	115	Chawla, N	74, 210, 248, 263, 277, 317
Bunzel, P	364	Carroll, L	130	Chbihi, A	354
Burjak, V	325	Carroll, M	94	Chembarisova, R	306
Burkatsky, O	160	Carsley, J	282	Chen, B	98, 231, 298
Burkins, M	133	Carter, C	76, 363	Chen, C	75, 91, 102, 120, 153, 173, 199, 253, 254, 300, 301, 343
Burleigh, T	233	Carter, J	133, 134, 199	Chen, D	319
Busby, J	199, 284	Carter, M	208	Chen, G	42, 60, 270, 292, 356, 370
Busch, R	318	Carvalho Costa, L	119	Chen, H	130, 132, 188, 243, 244, 253, 263
Buslaps, T	256, 304	Casem, D	295	Chen, J	41, 80, 101, 213, 230, 251
Bustamante, O	323	Casolco, S	127	Chen, L	42, 71, 72, 84, 92, 116, 140, 168, 200, 222, 223, 224, 274, 275, 280, 298, 323, 331, 364
Buttard, P	366	Castellero, A	68	Chen, M	139, 218, 250, 300
Butz, T	299	Castelnau, O	279	Chen, P	66, 317, 344
Buzunov, V	160, 313	Castillo, D	245	Chen, Q	95, 105, 322, 330, 356
Byler, D	92	Castro, D	323	Chen, R	121, 289
Bystrov, V	268	Castro-Colin, M	197	Chen, S	75, 84, 131, 138, 174, 184, 199, 237, 238, 240, 253, 294, 300, 324, 325, 343, 344
Bystrova, N	268	Catalano, J	295	Chen, T	113
C		Caton, M	50	Chen, W	243, 245, 246, 300
Caballero, F	146	Catoor, D	81, 82	Chen, X	62, 64, 119, 249, 285, 311
Cabrera, J	56	Causey, S	347, 370	Chen, Y	72, 148, 169, 184, 200, 248, 295, 339, 360
Caceres, C	290	Cavins, M	87	Chen, Z	116, 253, 266, 365
Caceres-Valencia, P	244	Cawkwell, M	141, 174	Cheng, L	107
Cady, C	121, 170	Caya, C	157	Cheng, S	142, 198
Cai, J	55	Cazacu, O	81, 118, 180	Cheng, Y	218
Cai, M	69, 272, 329, 362	Ceder, G	293		
Cai, W	49, 282	Celik, O	284		
Cai, Z	292	Cerreta, E	73, 74, 81, 88, 91, 117, 128, 138, 140, 169, 171, 180, 193, 196, 225, 234, 246, 249, 283, 294, 304, 332, 340		
		Ceylan, U	358		

- Cheng-Yi, L..... 120
 Chengyi..... 344
 Chengjun, L..... 44, 345
 Chengyi, L..... 327
 Cheong, S..... 93, 264, 287
 Cheong, Y..... 117
 Chernova, L..... 340
 Cherukuri, B..... 295
 Cheruvathur, S..... 363
 Chesonis, C..... 113, 164
 Chesonis, D..... 362
 Chhay, B..... 70, 299
 Chhowalla, M..... 41, 60
 Chiang, H..... 201
 Chiang, K..... 246, 340
 Chiang, T..... 341
 Chiarbonello, M..... 237, 321
 Chichkov, B..... 110
 Chien, W..... 368
 Chirranjeevi, B..... 276
 Chisholm, M..... 274
 Chiu, W..... 135, 189
 Chladil, H..... 347, 348, 349
 Cho, H..... 59
 Cho, J..... 47, 88, 188, 195, 365
 Cho, K..... 284
 Cho, M..... 254
 Cho, S..... 248
 Choate, W..... 280
 Choi, B..... 174, 218
 Choi, H..... 39, 288, 289, 309
 Choi, I..... 174
 Choi, J..... 117, 190, 240, 292
 Choi, S..... 237, 277
 Choi, W..... 39, 42, 59, 101, 152, 207, 260, 308
 Choo, H..... 67, 69, 93, 110, 111, 161, 197,
 198, 216, 251, 268, 298, 317, 352, 359
 Chou, C..... 344
 Chou, K..... 42
 Chou, L..... 131
 Chou, Y..... 85
 Choudhury, S..... 224, 274, 275
 Chrissey, D..... 208
 Christ, H..... 129, 130, 349
 Christen, H..... 222
 Christie, G..... 135
 Christodoulou, J..... 60
 Chrzan, D..... 66, 76, 116, 308, 324
 Chu, J..... 200, 217, 300, 331, 360
 Chu, K..... 116
 Chu, M..... 120
 Chu, P..... 42, 238
 Chu, T..... 216
 Chuang, C..... 218, 361
 Chuang, H..... 300
 Chuang, P..... 103
 Chukwuocha, E..... 265
 Chumbley, L..... 95
 Chumbley, S..... 108, 318
 Chung, J..... 93
 Chwee Teck, L..... 66, 110, 160, 215, 267, 316, 358
 Cieslar, M..... 258
 Cimenoglu, H..... 284, 295, 332
 Cingi, M..... 295
 Cipoletti, D..... 46
 Ciulik, J..... 303, 346, 369
 Clarke, A..... 166, 170, 230
 Clarke, J..... 84
 Clarke, R..... 251
 Clarry, D..... 164
 Clausen, B..... 93, 118, 198, 279, 297, 329
 Clemens, H..... 256, 304, 305, 347, 348, 349, 371
 Clement, P..... 264
 Clifton, R..... 91
 Cloutier, B..... 357
 Cluasen, B..... 298
 Cochran, J..... 128
 Cockayne, D..... 84, 131, 184, 237
 Cocke, D..... 114, 214
 Cockeram, B..... 303, 346, 369
 Coimbra, A..... 213
 Colas, D..... 203, 350
 Cole, A..... 261
 Collins, P..... 61, 88, 166, 209, 230, 246, 340
 Collins, S..... 146
 Colombo, G..... 89
 Comer, M..... 103
 Compton, B..... 68
 Compton, C..... 303, 347
 Compton, W..... 55, 57, 151
 Condore, F..... 330
 Cong, Z..... 298
 Conner, B..... 161
 Conner, R..... 68
 Connors, D..... 338
 Converse, G..... 215
 Cooksey, M..... 330
 Cooley, J..... 206
 Cooper, P..... 272
 Copie, O..... 115
 Coratolo, A..... 243
 Cordill, M..... 173
 Corinne, G..... 260
 Corlu, B..... 125, 126
 Corr, D..... 208
 Correa, L..... 356
 Cortés S., V..... 125
 Costa, J..... 159
 Costanza, G..... 140
 Cotts, E..... 277, 327
 Coughlin, J..... 248
 Coulter, K..... 136
 Counter, J..... 263
 Couper, M..... 220
 Courtenay, J..... 220, 362
 Coury, A..... 352
 Cowen, C..... 189
 Cox, C..... 145
 Cox, W..... 169
 Crawford, G..... 317
 Crawford, P..... 155
 Crimp, M..... 148, 170
 Cristol, B..... 106
 Crooks, R..... 278
 Cross, C..... 243
 Cruise, T..... 292
 Cruz Rivera, J..... 322
 Cui, H..... 351
 Cui, J..... 78
 Cui, Y..... 98, 256, 350
 Cuong, N..... 240
 Cupid, D..... 44, 324, 365
 Cupidon, S..... 105
 Currat, R..... 342
 Currie, K..... 239
 Curtin, W..... 43, 116
 Cutler, E..... 46
- ## D
- D'Abreu, J..... 79
 D'Alessandro, F..... 331
 D'Amours, G..... 325
 D'Armas, H..... 92
 da Costa, L..... 167, 363
 Daehn, G..... 67, 175, 264, 293, 360
 Dahle, A..... 75, 265, 272, 326, 327
 Dahlman, J..... 162, 270
 Dahotre, N..... 47, 60, 80, 359, 361
 Dai, K..... 367
 Dai, Q..... 156, 264
 Dai, Y..... 94, 143
 Daigle, E..... 123
 Dailey, N..... 46
 Dalla Torre, F..... 68, 99, 217, 257
 Daly, S..... 328
 Dandekar, D..... 295
 Dando, N..... 109, 119
 Dangelewicz, A..... 150
 Daniil, M..... 261
 Dantzig, J..... 169
 Dao, M..... 82, 307
 Darell, O..... 227
 Darling, K..... 205
 Darsell, J..... 292
 Das, J..... 112
 Das, K..... 65
 Das, M..... 235
 Das, S..... 64, 107, 112, 147, 157, 202,
 211, 242, 264, 279, 291, 303, 312
 Dash, P..... 180
 Dashwood, R..... 139, 247, 282
 Dassylva-Raymond, V..... 315
 Dattelbaum, D..... 92, 198, 249
 Dauskardt, R..... 89
 David, S..... 221, 233
 Davidson, D..... 83
 Davies, P..... 138
 Davis, A..... 252
 Davis, B..... 78, 124, 134, 301
 Davis, J..... 320
 Davy, C..... 260
 Dawson, P..... 153, 328
 Dayananda, M..... 364
 Daylami, M..... 266
 Daymond, M..... 197, 328
 Dayong, Z..... 323
 de Boissieu, M..... 342
 Decamps, B..... 203
 de Carvalho, E..... 70
 Deck, C..... 60
 Decker, R..... 188
 De Cooman, B..... 283
 Dedyukhin, A..... 314
 DeGraef, M..... 60, 102, 103, 153,
 154, 209, 262, 309, 355
 Dehm, G..... 139
 Deibert, M..... 243, 244
 Deisenroth, J..... 79
 Deiters, C..... 165
 Deka, S..... 280

Dekhtayr, Y	268	Docekalova, K	97	Durandet, Y	336
De Klerk, R	214	Dogan, O	346, 347, 370	Durst, K	174
Delaire, O	43	Doheim, M	315	Dursun, A	125, 126
Delimova, L	168	Dohi, M	358	Duszczuk, J	65
Delplanque, J	179	Dojc, D	119	Dutrizac, J	113
De Lucas, R	133, 177	Domack, M	278	Dutta, I	89, 139, 194, 228, 229, 247, 296
Delucas, R	124	Domínguez, M	125	Dutta, T	45
Demetriou, M	67, 68, 319, 359	Domínguez M., S	125	Duz, V	88
Demirkiran, H	358	Donchev, A	371	Dwivedi, D	265
Demkowicz, M	199	Dong, J	290	Dye, D	139, 247
De Moares, J	210	Dong, L	53	Dymek, S	80
Demopoulos, G	214	Dong, Z	60, 101		
den Bakker, A	189	Donner, W	197	E	
Deng, J	251	Doraiswamy, A	110	Easton, M	289, 290, 336, 337
Deng, S	268	Dorantes Rosales, H	260	Ebeling, T	133, 241
Dennis, K	145	Dörnenburg, F	123, 124	Eberl, C	121
Depinoy, M	266	Dorr, K	168	Ebrahimi, F	256, 260, 324, 365
Deppisch, C	74	Dorr, M	169	Echlin, M	355
Depres, C	83	dos Santos, C	358	Eckert, J	39, 56, 59, 110, 112
Derahkshan, S	144	dos Santos, L	221	Eden, T	64
Deranlot, C	115	Dotson, K	233	Edwards, L	171
Derguti, F	282	Dotson, T	233	Efe, M	57
Derin, B	192	Dougherty, L	180, 209, 332	Effgen, M	304, 347
Derosa, P	331	Downey, J	62	Egami, T	111, 161, 167, 197, 269, 318, 319
deRosset, A	151	Downs, J	369	Eggeler, G	149, 222, 223, 224, 236
Deryugin, Y	158	Doyle, C	123	Egorov, I	191
Desai, T	99, 252	Drabble, D	278	Eh.Hovsepien, P	371
Despinasse, S	159	Drache, M	200	Ehiasarian, A	349, 371
Desrosiers, P	159	Drapala, J	343	Eifler, D	285
Deutsch, T	105	Draper, S	148	Eiken, J	239, 256
Devanathan, R	299	Dressler, J	165	Eisenlohr, P	118, 148, 170
Devincere, B	72, 83	Drevertmann, A	98, 256	Eivani, A	65
Devine, T	333	Dreyer, C	189	Ekuma, C	125
DeWald, A	77	Dring, K	329	El-Awady, J	131
DeYoung, D	112, 113, 164, 220, 271, 319, 361	Driver, J	84	El-Bealy, M	320
Dhiman, M	265	Droste, W	320	El-Desouky, A	192
Dias, D	119	Druschitz, E	87	El-Kersh, A	315
Diaz De La Rubia, T	351	Dryepondt, S	123	Elangovan, S	271
Dickerson, C	299	Du, D	217	El Bekkali, A	227
Dickerson, P	102, 209, 230	Du, L	240	Elder, K	168, 169
Dickerson, R	92	Du, N	157	Elias, C	358, 359
Dickinson, J	69	Du, P	81	El Kadir, H	140, 155, 295
Didier, R	260	Du, Q	72	Elkholy, A	49
Didier, T	260	Du, X	68	Elkin, I	143
Dieringa, H	335, 336	Du, Z	55	Ellis, D	168, 222, 223
DiGiacomo, S	92	Duan, G	319	El Mehtedi, M	188
Dilanian, R	309	Duan, H	309	Elmustafa, A	128, 278
Dillard, S	141, 209	Dubach, A	217	Elsamadicy, A	327
Dimiduk, D	72, 97, 101, 102, 104, 114, 131, 154, 183, 209, 348, 350	Dube, G	164	Elsayed, F	134
Ding, F	311	Dube, J	361	Emamian, A	39
Ding, W	134, 188, 239, 240, 290	Dubey, M	122	Emerson, S	136
Dinh, L	205	Dubois, J	184, 309	Engberding, N	98
Diniz, R	263	Duchesne, C	159, 213	Enomoto, M	247
Dinkel, M	56	Dudek, M	74	Enright, P	165
Dinu, C	208	Dudnik, E	181	Eom, C	222
Diologent, F	82, 349	Dufour, G	159, 213, 225	Erb, A	53, 221
Dion, M	79	Duh, J	131, 301	Erdogan, R	125
Dittmann, R	274	Dulikravich, G	191	Eremets, M	196
Dixit, V	340	Dunand, D	247, 328	Eres, G	274
Djambazov, G	98, 177	Dundar, M	125	Ergin, L	346
Dlouhy, A	97, 148	Dündar, M	126	Ernst, F	233, 234
Dlouhy, I	97	Dunlop, G	290	Ersundu, E	79, 302
Dmowski, W	197, 218, 269	Dunne, R	229	Es-Said, O	65
Dobatkina, S	257, 258	Dupas, N	226	Escobedo, J	249
Dobbins, T	46, 47, 48, 341	Dupon, E	79	Escuadro, A	236
Dobra, G	319	Dupuis, C	113, 320	Esit, F	107
		Dupuis, M	315		

Eskin, D.....209, 220, 272, 362
 Esquinazi, P.....299
 Esquivel, E.....110
 Essadiqi, E.....134
 Estrin, Y.....50, 99, 100, 149, 205,
257, 258, 306, 334, 352, 359
 Etienne, A.....198, 354
 Etzion, R.....227
 Evangelista, E.....188
 Evans, A.....121, 175, 176
 Evans, D.....88, 99, 138, 193, 246, 294, 340
 Evans, J.....109, 213, 219, 362
 Evans, N.....146
 Evans, P.....274
 Ewing, R.....59, 101
 Ezekoye, O.....338

F

Fabbreschi, M.....321
 Fabre, A.....298
 Fabrichnaya, O.....44, 365
 Facsko, S.....343
 Fafard, M.....325
 Falah, A.....49
 Faleschini, M.....369
 Falk, M.....162
 Fan, D.....311
 Fan, G.....67, 110, 161, 216, 268, 317, 352, 359
 Fan, X.....62
 Fan, Y.....255
 Fanchini, G.....41
 Fang, J.....200
 Fang, Z.....193, 261, 326
 Fangbin, C.....78, 302
 Farber, D.....249
 Farias, S.....67
 Farrell, J.....304, 347
 Farrer, J.....363
 Fashanu, A.....65
 Fathi, E.....271
 Fattebert, J.....169
 Faulhaber, S.....176
 Faulkner, R.....144
 Favilla, P.....181
 Faza, S.....291
 Fecht, H.....51, 247, 269, 306, 360
 Feldman, J.....219
 Felicelli, S.....137, 155, 298
 Fell, B.....179
 Felli, F.....47, 231
 Feng, C.....178
 Feng, J.....196, 294
 Feng, N.....345
 Feng, S.....343
 Feng, W.....72
 Feng, Y.....177
 Feng, Z.....198, 221, 233, 298
 Fengchun, J.....66
 Fennie, C.....167
 Fenton, G.....175
 Feret, F.....214
 Fergus, J.....243
 Fernandez, J.....46, 299
 Fernandez-Gil Bando, R.....302
 Ferreira, A.....362
 Ferreira, H.....213
 Ferreira, P.....76, 332
 Ferrell, S.....233
 Ferrer, D.....184
 Ferris, K.....294
 Ferron, C.....214
 Ferron, J.....124
 Fert, A.....115
 Fertig, R.....278
 Fetcu, D.....280
 Fevre, M.....42
 Field, D.....158, 249
 Field, F.....64, 147
 Field, R.....166, 170, 230
 Fielden, D.....297
 Figueiredo, F.....119
 Figueiredo, R.....52
 Filevich, A.....300
 Filho, J.....107, 356
 Filius, J.....62
 Fillit, R.....84
 Findley, K.....94
 Fine, M.....96, 191, 364
 Finel, A.....42, 224, 275
 Finsterbusch, M.....243
 Finstrom, N.....274
 Fiory, A.....63, 296, 297
 Firrao, D.....69, 140, 237, 321
 Fischer, C.....293
 Fischer, J.....236
 Fisher, W.....46
 Fivel, M.....83
 Fjær, H.....158, 361
 Fjeld, A.....137, 362
 Flanagan, T.....136
 Flandorfer, H.....199, 253, 300, 343
 Flicker, J.....296
 Florando, J.....91, 111
 Flores, K.....67, 131, 163, 317, 359, 360
 Flores, M.....127
 Flowers, J.....60
 Fnu, S.....296
 Foecke, T.....211
 Foiles, S.....116, 170
 Foley, D.....143
 Follstaedt, D.....307
 Fonda, R.....146
 Fong, H.....66
 Foosnæs, T.....226, 227, 326
 Foosnas, T.....119
 Fortenberry, N.....185
 Fracziewicz, A.....203, 350
 Francis, J.....297
 Francoual, S.....342
 Frank, S.....267
 Franz, C.....156
 Frary, M.....46, 176, 182, 229
 Fraser, H.....61, 88, 166, 181, 194,
209, 230, 246, 275, 340
 Frear, D.....74, 89, 139, 172, 194, 228, 247, 296
 Frederick, A.....338
 Frederick, D.....233
 Fredrickson, G.....62
 Free, M.....78, 124, 214
 Freeland, J.....115
 Freels, M.....217, 361
 Freeman, A.....128, 234
 Freibert, F.....155

Freitas, M.....80
 Frerichs, A.....95
 Fridy, J.....49
 Friedland, E.....253
 Friedman, L.....207
 Friedrich, B.....98
 Fries, S.....181
 Froehlich, M.....371
 Fröhlich, M.....371
 Frost, L.....271
 Frosta, O.....226
 Fu, C.....249
 Fu, E.....143, 199
 Fu, H.....359
 Fu, R.....238
 Fu, Y.....108
 Fuchs, G.....46, 363
 Fugetsu, B.....288
 Fujii, T.....184
 Fujimatsu, T.....283
 Fujino, S.....223
 Fujiwara, E.....142
 Fujiyoshi, M.....194
 Fukuda, H.....288
 Fukumoto, S.....283
 Fullwood, D.....103
 Fultz, B.....43
 Funakubo, H.....223
 Funkhouser, C.....316
 Furrer, D.....340
 Furu, T.....212
 Furuhashi, T.....193
 Furusawa, T.....367
 Furuya, K.....208, 245
 Futter, K.....357

G

Gaal, S.....201
 Gabay, S.....233
 Gabb, T.....176
 Gabrielyan, T.....311
 Gabrisch, H.....322
 Gagne, J.....225
 Gagnidze, T.....202
 Gaies, J.....347, 370
 Galarraga, R.....356
 Gallagher, M.....127
 Galli, G.....78
 Galstyan, E.....323
 Gama, S.....197
 Gamweger, K.....113
 Gan, J.....251, 299
 Ganapathysubramanian, B.....154, 155, 364
 Gandhi, R.....210
 Ganesan, Y.....76
 Ganesan, S.....186
 Gang, S.....88
 Gangloff, R.....278, 286
 Gangopadhyay, A.....162
 Gannon, P.....232, 243, 244
 Ganuza, A.....67
 Gao, B.....140
 Gao, F.....299
 Gao, M.....43, 44, 98, 347
 Gao, X.....146

Gao, Y	67, 110, 111, 130, 161, 180,	Gimazov, A.....	52, 353	Greenberg, B	81
.....	216, 217, 268, 317, 319, 359	Ginzburgsky, L.....	299	Greene, R	196
Gapud, A	339	Girard, Y.....	204	Greer, A	110, 199, 253, 300, 343
Garay, J	192	Giribaskar, S.....	53	Greer, L	162
Garcia, E	190	Gittard, S	105	Gregory, J	64, 147
García, N.....	299	Giummarra, C	287	Grekhov, I	168
Garcia, R	224	Glaessgen, E.....	99	Griffin, R	370
García-Hinojosa, A.....	211	Glavatskikh, M.....	348, 350, 371	Grimm, T.....	303, 347
Garcia-Mateo, C.....	146	Glavicic, M	88, 250, 340	Groeber, M.....	102, 154, 209, 262
Garcia-Moreno, F.....	178	Gleeson, B	77, 122, 175, 231	Groebner, J.....	337
Garcia de Andrés, C	146	Glicksman, M.....	262, 276	Groeschel, F.....	94
Garcia de la Infanta Belio, J.....	353	Gludovatz, B	369	Gronbech-Jensen, N.....	224
García H., A.....	45	Glushchenko, V.....	143	Gronsky, R	328
Gardner, T	164	Godet, S.....	97	Groza, J	179, 223, 358
Garimella, N.....	190, 351	Godlewski, L.....	126	Gruber, J.....	117, 154
Garkida, A	346	Goebel, W	216	Gruber, P	172
Garlea, E	251	Goel, M	219	Gruen, G.....	362
Garrido, F.....	251	Goesele, U.....	131	Grunschel, S.....	91
Garza, K	369	Goettert, J.....	268	Grunspan, J	178, 179
Garzon, F.....	338	Göken, M	49, 56, 82, 129, 130, 174,	Gschneider, K.....	95, 279
Gascoin, F	145	182, 236, 285, 307, 333, 367	Gu, S	210, 263
Gassa, L.....	272	Gokhale, A.....	262, 272	Guan, S	288, 335
Gaubert, A	275	Goldenfeld, N.....	169	Guangchun, Y.....	60
Gaudreault, B	159	Golestanifard, F.....	323	Guanghui, L	283
Gaustad, G.....	155	Golladay, T.....	280	Gudbrandsen, H	227
Gauthier, C	159, 213, 225, 226	Goller, G.....	358	Guebels, C.....	179
Gavrielatos, I.....	190	Golovina, I.....	322	Gueijman, S.....	87
Gaytan, S.....	110, 281	Golowin, S	293	Guenther, R.....	256
Gazonas, G.....	341	Golubov, S.....	343	Guether, V.....	347, 348
Ge, Y	233	Gomathi, G.....	271	Guimarães, M.....	159, 214
Geantil, P.....	83, 183, 250, 329	Gomes, J.....	114, 214	Guimarães, O	210
Gebhard, S.....	148, 371	Gong, H.....	364	Gulsoy, E.....	209
Gehring, G.....	276	González, B.....	50	Gunda, V.....	268
Geifman, I	322	Gonzalez, J.....	137	Gunderov, D.....	354
Geltmacher, A.....	209, 210	Gonzalez-Carrasco, J.....	54	Guner, S	41, 208
Gemmen, R	243	Gonzalez-Reyes, L.....	260, 322	Gungor, M.....	194
Gemming, T	39, 59	Gonzalez De Moricca, M.....	370	Günther, R.....	186
Genc, A	166, 194, 275, 340	Gooch, W	133	Gunyuz, M	295
Gendron, M.....	171, 225	Goodall, R.....	349	Guo, A	291
Geng, H.....	72	Goranson, G.....	283	Guo, F	121, 277
George, E.....	198	Gordon, J.....	164	Guo, X	42, 246, 339, 345
George, P.....	123	Gordon, P	116	Guo, Y	59, 101, 251, 260, 261
Gerberich, W.....	76, 173	Gornostyrev, Y.....	234	Guo, Z	232, 312, 313, 341
Gerling, R.....	256, 305, 349	Gorny, A.....	290	Guofeng, C.....	48
German, R.....	107, 155, 283, 295	Gorokhovskiy, V	243	Gupta, A	240
Gerold, B.....	336	Gossler, D.....	256	Gupta, N.....	129
Gerosa, R.....	237, 321	Goswami, R.....	309	Gupta, R.....	308
Gershenson, M.....	109	Gottstein, G.....	130, 205, 206, 207	Gupta, S.....	291
Gervasio, D	338	Goud, P	80, 281	Gupta, V.....	41, 132, 278
Ghaderi Namin, A	288	Goundla, P.....	46	Guruprasad, P.....	45, 184
Gharghouri, M.....	337	Gourlay, C.....	326, 327	Gururajan, M.....	43, 61, 117, 276
Ghiban, B.....	180	Gout, D	144	Gusberti, V.....	315
Ghidini, A.....	237, 321	Gouthama.....	53	Güther, V.....	348
Ghomashchi, R.....	272	Goutière, V.....	113	Guthrie, R.....	320
Ghoniem, N.....	94, 131, 182	Gower, L.....	160	Gutierrez, G.....	321
Ghosh, A.....	138, 188, 288	Goyel, S.....	256	Gutiérrez, I.....	183
Ghosh, G	191, 364	Gräb, H	165	Gutierrez, M.....	137
Ghosh, K	65	Graham, G.....	338	Gutierrez-Urrutia, I	203, 353
Ghosh, S.....	61, 102, 154, 247, 283, 284, 334	Grandfield, J.....	271	Guyer, J	72
Gianola, D.....	121, 229	Grassi, J.....	107	Guzman, J	324
Gibala, R	104	Grater, J.....	204		
Gibson, M	290, 337	Gray, G.....	73, 74, 117, 169, 170,		
Gierlotka, W.....	344	174, 225, 249, 304, 332		
Gil-Sevillano, J	183, 225	Grazier, J	122		
Gila, B	101	Greco, R	95, 144		
Gill, A	221	Greedan, J	144		
Gilman, J.....	73, 183	Green, J.....	147, 303		

H

Ha, D	136
Ha, S	253
Haase, R.....	231
Haataja, M.....	116, 169, 296

- Habchi, R 281
 Hackenberg, R. 166, 230
 Hackett, M. 199
 Haddad, A. 63
 Hadorn, J. 111
 Haeckel, T. 349
 Hafok, M. 57, 334
 Hagelstein, K. 46
 Hagiwara, M. 227
 Hagni, A. 69, 113, 166, 221, 272, 321, 362
 Hahn, H. 342
 Hahn, J. 156, 157, 263
 Haines-Butterick, L. 161
 Haley, B. 224
 Hall, N. 319
 Halle, T. 57
 Haller, E. 308, 324
 Ham, H. 277
 Hamann, B. 209
 Hamburg, B. 141
 Hamdan, A. 195
 Hamdi, F. 118
 Hamer, S. 165
 Hamilton, B. 79, 80
 Hamilton, C. 277
 Hamilton, J. 238
 Hammers, T. 368
 Hammi, Y. 295
 Hamza, A. 218
 Hamzic, A. 115
 Han, B. 98
 Han, E. 289
 Han, H. 277
 Han, J. 123, 286
 Han, K. 260
 Han, L. 290
 Han, M. 267
 Han, Q. 187, 239
 Han, S. 53, 153, 331
 Han, T. 328
 Han, W. 192
 Han, X. 75
 Han, Z. 40
 Handa, T. 201
 Handwerker, C. 74, 119, 172, 228, 277, 326
 Hanlummyuang, Y. 116
 Hanna, M. 126
 Hänninen, H. 87
 Hansen, N. 52, 150, 206
 Hantcherli, L. 118
 Hänzi, A. 257, 336
 Hao, L. 313
 Haouaoui, M. 52, 151, 257, 334
 Haque, A. 312
 Harder, D. 317
 Harding, R. 98
 Hardy, J. 292
 Harel, G. 188
 Harimkar, S. 60
 Hark, R. 64
 Harlow, D. 217
 Harmon, B. 96
 Haro Rodriguez, S. 265
 Harrell, J. 207, 261
 Harringa, J. 200, 254, 327
 Harris, P. 356
 Hartig, C. 133, 186, 241, 256
 Hartvigsen, J. 271
 Hartwig, K. 58, 143, 206, 257, 370
 Hartwig, T. 151
 Harvey, É. 157
 Harwood, N. 106
 Hasan, M. 80, 281
 Haseeb, A. 309
 Hashemian, S. 92
 Hashiguchi, M. 136
 Hashimoto, K. 283
 Hashimoto, S. 258
 Hass, D. 176
 Hassan, H. 90
 Hassan Ali, M. 279
 Hata, S. 71, 355
 Hatano, M. 150
 Hatcher, N. 128
 Hatkevich, S. 293
 Hattiangadi, A. 123
 Haugh, M. 215
 Haupt, T. 339
 Hautier, G. 293
 Haxhimali, T. 276
 Hay, R. 118
 Hayashi, T. 56
 Hayden, D. 282
 Haynes, A. 231
 Hazel, B. 176, 231
 He, H. 121
 He, L. 371
 He, M. 121
 He, T. 250
 He, X. 291, 349
 He, Y. 74, 97, 147, 149
 Heard, R. 176
 Hebert, R. 68, 235
 Hecht, U. 256
 Hector, Jr., L. 85, 121, 145, 157
 Hector, L. 282
 Hefferan, C. 310, 328
 Heggset, B. 164
 Heifets, E. 222
 Heil, T. 261
 Heilmair, M. 55, 98, 334
 Heinze, J. 46
 Heller, R. 343
 Hemburrow, P. 159
 Hemker, K. 121, 122, 195, 229
 Hemley, R. 92
 Henaff, G. 129, 204
 Hengelmolen, A. 113
 Henkel, S. 236
 Hennig, R. 91, 140, 196, 249
 Henriksen, B. 361
 Henry, P. 214
 Her, E. 46
 Herbst, J. 145
 Herklotz, A. 168
 Hernandez, D. 110
 Hernandez-Garcia, A. 211
 Hernandez-Majoral, M. 143
 Hernández-Pérez, I. 260, 322
 Herranz, G. 115
 Herrera, M. 355
 Herring, J. 271
 Herzog, R. 50, 286
 Hess, W. 69
 Heuer, A. 233, 234
 Heying, M. 244
 Hibbard, G. 107, 234, 289
 Hibbins, S. 239
 Hidetoshi, S. 291
 Hierro de Bengoa, M. 350, 371
 Higashi, K. 239
 Hilck, A. 156
 Hilerio, I. 137, 166, 273
 Hilgraf, P. 156
 Hill, M. 77
 Hill, T. 87
 Hiltunen, P. 156
 Hines, J. 86, 104, 155
 Hirata, T. 239
 Hirsch, J. 287
 Hisatsune, K. 142
 Hixson, R. 74, 141
 Ho, C. 120, 142, 248
 Ho, S. 289
 Ho, W. 86
 Hoag, E. 147
 Hoagland, R. 39, 102, 174, 199, 230
 Hoc, T. 83
 Hockauf, M. 57
 Hockridge, R. 106
 Hodge, A. 236
 Hodgson, P. 69, 100, 112, 216
 Hoelzer, D. 90, 128
 Hoffelner, W. 230
 Hoffmann, A. 369
 Hoffmann, C. 342
 Hoffmann, R. 196
 Hofmeister, W. 207
 Hohenwarter, A. 285
 Hohl, B. 325
 Hojo, H. 367
 Holby, E. 72
 Holden, I. 226
 Hollang, L. 225
 Holleis, B. 113, 302
 Holm, E. 116
 Holt, N. 108
 Holy, V. 141, 142, 342
 Hommes, G. 72
 Hong, K. 248
 Hong, S. 39, 59, 190, 292
 Honghui, T. 40
 Hongqiang, R. 43
 Honma, T. 241
 Hono, K. 55, 146, 187, 241
 Hooks, D. 141, 174
 Hoppe, R. 149
 Hoppe, T. 110
 Höppel, H. 56, 236, 307
 Horita, Z. 257, 306
 Horky, J. 367
 Horstemeyer, M. 77, 155, 158, 339
 Hort, N. 186, 239, 335, 336
 Hoseman, P. 143
 Hosemann, P. 95, 144
 Hosokawa, K. 321
 Hosoya, Y. 146
 Hostetter, G. 194
 Hou, C. 127
 Hou, H. 291
 Houda, H. 100

Houghton, B	112
Hourlier, D	199
Houston, J	317
Houston, K	53
Hovsepian, P	349
Howard, B	331
Howe, J	89
Hoyos, L	137
Hoyt, J	42, 71, 116, 168, 223, 275, 276, 323, 364
Hryn, J	270
Hsia, K	49, 82, 129, 182, 236, 285, 333, 367
Hsiao, H	173
Hsieh, K	68, 217
Hsiung, L	141
Hsu, C	45, 318
Hsu, E	241
Hsu, T	301
Hsu, Y	120
Hu, D	178, 194, 305
Hu, H	290, 337
Hu, J	42
Hu, S	72, 275
Hu, W	130, 244
Hu, X	78, 140, 314, 366
Hu, Z	208, 268, 269
Hua, F	74, 119, 172, 173, 228, 277, 326
Hua, Y	281
Huang, C	300
Huang, E	93
Huang, H	208
Huang, J	59, 68, 217, 218, 253, 360
Huang, L	366
Huang, P	150
Huang, S	191, 255, 364
Huang, W	136
Huang, X	52, 150, 206, 273, 346
Huang, Y	223, 238, 306, 331, 344, 353
Huang, Z	169, 344
Hubbard, C	298
Hubbard, J	103
Huber, D	230
Huda, M	105
Hudson, J	194
Hufnagel, T	111
Hughes, D	298
Huh, J	248, 292
Hui, X	270
Hulbert, D	48
Hull, L	74
Hundley, M	174
Husseini, N	251
Hutchins, C	151
Hutchins, J	114
Hutchinson, N	360
Hvidsten, R	213
Hwang, C	74
Hwang, H	114
Hwang, J	64, 114, 193, 221, 240, 268, 273, 346
Hwang, K	193
Hwang, S	126
Hwang, T	202
Hwu, Y	342
Hyers, R	70, 162, 244
Hyland, M	106, 233, 313

I

Iadicola, M	211
Iannacchione, G	309
Ibarra, L	246
Ice, G	92, 93, 142, 341
Idenyi, N	125, 126, 265
Ienco, M	140, 321
Iffert, M	108, 159, 213, 266, 313, 315, 357
Iijima, T	223
Ikeda, M	351
Ikeda, T	145
Ikuno, H	367
Ila, D	41, 70, 208, 299, 327, 342, 343, 359
Ilavsky, J	175, 341
Iliev, M	197
Im, J	58
Imagawa, H	227
Imai, H	288
Imam, M	294
Imanaka, N	96
Imayev, R	205, 347, 348
Imayev, V	347, 348
Inaba, Y	207
Inami, T	245
Inel, C	126
Ingram, B	292
Inoue, A	163, 217, 268, 269, 360
Instone, S	362
Inui, H	203, 204
Inzunza, E	171
Ionescu, I	129
Ipsier, H	229, 343, 344
Iqbal, F	130
Irons, G	137
Irsen, S	98
Isac, M	320
Isanaka, S	87
Ishida, K	254, 300
Ishida, M	360
Ishikawa, K	45, 47, 48, 135
Ishimasa, T	342
Islam, Z	141
Islamgaliev, R	54
Isoda, S	84, 131, 184, 237, 238, 240
Itsumi, Y	193
Ivanisenko, Y	51, 306, 333
Ivanov, M	81
Ivanov, V	326
Ivanushkin, N	311
Ivey, D	243, 292
Iwasawa, M	72
Iwata, S	293, 339
Izmailova, N	205

J

Jablonski, P	189, 292
Jackson, M	139, 235, 247
Jacob, T	222
Jacobs, M	271
Jacobson, A	197
Jacot, A	305
Jacques, P	97
Jacquet, D	315
Jacquet, E	115
Jadhav, N	228

Jagielski, J	251
Jahed, H	77
Jain, A	297
Jain, J	189
Jain, P	81
Jain, V	174
Jakobsen, B	93, 328
James, B	123, 179, 233
Jang, D	67
Jang, H	178
Jang, J	68, 111, 174, 217, 218
Jang, S	360
Jang, Y	47, 212
Jannasch, E	287
Janz, A	337
Jaquinde, W	316
Jarmakani, H	169
Jasinski, J	191, 245, 317
Jayaraman, N	77
Je, J	342
Jean, Y	67
Jean-Charles, R	105
Jeandin, M	123, 233
Jee, S	160
Jenabali Jahromi, S	288
Jenkins, D	94
Jenkins, M	143, 144
Jenkins, R	347, 370
Jensen, D	250
Jensen, M	109
Jeon, H	39, 102
Jeon, M	39
Jeong, C	365
Jeong, H	45, 309
Jeong, I	171
Jeong, J	202
Jeong, Y	59, 212
Jha, A	235
Jha, G	107
Jha, M	163, 202
Jha, S	50, 78, 237
Jhon, M	66
Ji, H	142
Ji, V	298
Jia, C	274
Jia, N	297, 298, 352
Jia, Q	98
Jia, S	335
Jia Ming, Z	160
Jiang, C	204, 349
Jiang, D	48, 285
Jiang, F	69
Jiang, H	194, 215, 305, 347
Jiang, J	335
Jiang, L	240
Jiang, M	124, 255
Jiang, Q	250
Jiang, R	246
Jiang, T	62
Jiang, W	67, 68, 110, 111, 161, 216, 217, 268, 269, 299, 317, 359
Jiang, X	215, 245
Jiang, Y	239, 244, 336
Jiao, J	195
Jiao, L	89, 139
Jiao, T	91
Jiao, Z	143, 252

- Jiawei, W 314
 Jie, L 314, 330
 Jimbo, I 193
 Jin, L 134, 188, 240
 Jin, M 76
 Jin, S 85, 96, 101, 152, 267
 Jin, X 42, 60
 Jin, Y 223, 331
 Jin, Z 301
 Jinhong, L 214
 Johansson, B 96
 John, R 78
 John, V 200, 300, 331, 360
 Johnson, C 243, 244
 Johnson, I 280
 Johnson, J... 119, 171, 175, 225, 226, 283, 325, 365
 Johnson, R 195
 Johnson, S 351
 Johnson, W 67, 68, 319, 359
 Jolly, B 233
 Jolly, M 79
 Jonas, J 97, 147, 240
 Jones, D 294
 Jones, H 294
 Jones, J 49, 130, 172, 182, 187, 237, 251, 367
 Jones, N 139, 247
 Jones, R 122
 Jones, T 133
 Jong, J 248
 Jong Gu, B 310
 Jonnalagadda, K 122
 Joseph, D 61
 Joshi, S 100
 Jou, J 360
 Jouiad, M 129
 Joung, J 171
 Ju, J 240
 Juhas, M 246
 Jun, H 112
 Jun, J 292
 Jun, Y 335
 Jun, Z 314
 Jung, J 174
 Jung, S 201, 253, 261, 345
 Jung, Y 45
 Jungwirth, T 142
 Junior, C 356
 Juretzko, F 312
 Jyoth, S 281
- K**
- K., A 176
 Kabir, M 340
 Kabirian, F 337
 Kabra, S 198, 279
 Kachler, W 348
 Kad, B 257
 Kadiri, H 298
 Kadkhodabeigi, M 316
 Kaftelen, H 40
 Kahl, A 319
 Kahler, D 104
 Kahn, H 233, 234
 Kai, H 42
 Kai, W 359, 361
 Kain, V 283, 284
 Kainer, K 335, 336
 Kainuma, R 254
 Kaiyu, Z 191
 Kajinic, A 305
 Kajiwara, Y 185
 Kakkar, B 357
 Kalay, E 108, 318
 Kalban, A 266
 Kale, P 200
 Kalembo, I 80
 Kalgraf, K 109
 Kalidindi, S 103
 Kalinin, S 274
 Kalkan, K 207
 Kaltenboeck, G 319
 Kalu, P 53, 221, 241, 260, 362
 Kamado, S 241
 Kamal, M 194, 246
 Kamegawa, A 237
 Kamikawa, N 52, 150
 Kamikihara, D 361
 Kan, H 314, 326
 Kaneta, Y 72, 339
 Kang, B 101, 153, 163
 Kang, C 365
 Kang, F 51
 Kang, H 122
 Kang, I 292
 Kang, J 127
 Kang, S 39, 59, 101, 152, 172, 188, 207, 254, 260, 280, 308, 327, 331
 Kang, Y 292
 Kannan, R 216
 Kanthala, T 105
 Kao, C 75, 238, 253, 300, 326, 327
 Kao, P 91
 Kappes, B 43, 116
 Kar, A 233
 Kar, S 325, 364, 365
 Kar, Y 181
 Karabelchtchikova, O 234
 Karabin, M 287
 Karaman, I 52, 151, 236, 257, 334
 Karhausen, K 287
 Karjalainen, P 332, 354
 Karma, A 116, 168, 276
 Karnesky, R 247
 Karumuri, S 207
 Kaschner, G 117, 229, 279
 Kashimoto, S 342
 Kasisomayajula, V 296
 Kasouf, C 203
 Kassner, M 83, 182, 183, 206, 250, 329
 Katgerman, L 209, 220, 272, 362
 Kato, A 189
 Kato, M 184
 Kato, S 124
 Kato, T 45
 Katoda, T 223
 Katsman, A 187, 290
 Katz, J 124
 Kaufman, J 147, 242, 303
 Kaufman, M 64, 193, 363
 Kauzlarich, S 145
 Kavanagh, L 219
 Kavich, J 115
 Kawalla, R 240
 Kawamura, Y 241
 Kawasaki, M 71, 258
 Kayal, S 267
 Kayali, E 284, 295, 332
 Kazimirov, A 93, 262
 Kazyhanov, V 54
 Keblinski, P 308
 Keck, A 210, 237, 247
 Kecses, L 149, 151, 204, 206
 Keimer, B 115
 Keles, Ö 107
 Keller, C 279
 Kelly, T 97
 Kelm, K 98
 Kelton, K 162, 269
 Kempkes, M 226
 Keniry, J 160, 266
 Kennedy, M 81, 195
 Kenningley, S 124, 248
 Kent, M 195
 Keppens, V 318
 Keralavarma, S 282, 340
 Kern, K 60
 Kesavan, M 178
 Kesler, M 256
 Ketabchi, M 52
 Key, C 243
 Khaleel, M 298
 Khalifa, H 268
 Khan, A 338, 339
 Khan, S 239
 Khasanova, N 326
 Khater, H 73
 Khatibi, G 367
 Khismatullin, T 348
 Kholkin, A 268
 Khoroshilov, D 181
 Khraisheh, M 279
 Khramov, A 314
 Kiessling, W 123
 Kiggans, J 295
 Kildea, J 263
 Kilmametov, A 54, 342
 Kim, B 55, 202
 Kim, C 47, 63, 104, 105
 Kim, D 39, 44, 45, 47, 173, 240, 254, 262, 290, 292, 318, 337
 Kim, H 57, 118, 188
 Kim, J 102, 117, 166, 201, 253, 292, 320, 333, 338
 Kim, K 39, 59, 173, 200, 228
 Kim, M 98, 102, 158, 202
 Kim, N 269
 Kim, S 39, 45, 74, 102, 107, 152, 154, 155, 173, 200, 212, 228, 260, 261, 277, 284, 289, 292, 331, 348, 365
 Kim, T 44, 45
 Kim, W 44, 45, 47, 240, 290, 318, 337
 Kim, Y 48, 55, 97, 98, 117, 148, 149, 203, 238, 255, 277, 304, 305, 347, 348, 349, 350, 370
 Kimura, H 70, 192, 202
 Kimura, K 355
 Kimura, M 201
 Kimura, T 245
 Kimura, Y 344, 350
 King, A 151

L

- Laughlin, D 365
 Launois, S 204
 Laurent, V 227, 366
 Lauridsen, E 61, 251
 Lavernia, E 51, 52, 53, 150, 151, 306
 Lawson, D 211
 Leal, J 350
 Leau, W 300
 Lebeau, J 262
 LeBeau, S 188
 Lebensohn, R 81, 118, 170, 210, 279
 LeBlanc, M 111
 Le Bouar, Y 42, 275, 308
 Le Brun, P 220
 Lechner, R 142
 Leckie, R 175
 LeDonne, J 49, 368
 Lee, A 120, 142, 248
 Lee, B 48, 102
 Lee, C 48, 55, 301, 307
 Lee, D 277
 Lee, E 65
 Lee, G 212
 Lee, H 70, 114, 115, 167, 222, 254, 274, 322, 327
 Lee, I 91
 Lee, J 71, 102, 112, 136, 188, 199, 201, 202, 212, 240, 247, 253, 290, 300, 337, 343, 344, 345, 361
 Lee, K 45, 78, 102, 112, 117, 152, 173, 212, 261, 269
 Lee, M 112
 Lee, N 260, 261
 Lee, P 45, 46, 318
 Lee, R 138, 288
 Lee, S 46, 53, 55, 71, 91, 93, 136, 154, 209, 212, 269, 283, 344, 352
 Lee, T 65, 74, 84, 120, 284
 Lee, Y 136, 188, 201, 223, 331
 Lefebvre-Legry, P 199
 Lefrançois, L 159
 Lehmann, D 310
 Lei, Y 160
 Lei, Z 122
 Leisenberg, W 119
 Leite, P 213
 Leitner, H 221
 Lejava, T 202
 Lejcek, P 350
 Lekakh, S 219, 302
 Lele, T 101
 Lemieux, T 234
 Lena, C 177
 Lenosky, T 169
 Léonard, F 170
 Leonhardt, T 303, 346, 347, 369
 Lepselter, M 63
 Lerch, B 148
 LeSar, R 293
 Lesuer, D 258, 332
 Letzig, D 241
 Leu, M 87
 Levashov, V 319
 Levesque, R 113
 Levi, C 175
 Leviatan, T 187
 Levine, L 83, 103, 175, 183, 250, 329
 Lewandowska, M 57
 Lewandowski, J 89, 90
 Lewellyn, M 156, 264
 Lewinsohn, C 135
 Lewis, A 60, 61, 102, 103, 153, 209, 210, 262, 309, 355
 Lewis, D 253
 Lewis, G 110
 Leyens, C 97, 148, 203, 255, 304, 347, 348, 349, 350, 370, 371
 Li, B 100, 114, 127, 132, 133, 148, 170, 268, 273, 312, 326, 346, 353
 Li, C 64, 89
 Li, D 108, 317, 320, 322, 330
 Li, F 310
 Li, G 62, 124, 184
 Li, H 87, 312, 313
 Li, J 62, 69, 91, 108, 111, 113, 118, 130, 132, 133, 138, 166, 169, 180, 185, 187, 218, 221, 225, 272, 311, 316, 321, 326, 330, 362, 364, 366
 Li, K 182
 Li, L 352
 Li, M 80, 126, 134, 287, 361
 Li, N 121, 143, 199
 Li, Q 50, 82, 214, 269, 303, 326, 346
 Li, R 111, 218
 Li, S 190, 208, 260, 276, 316
 Li, W 106, 109, 119, 214, 262, 290, 311
 Li, X 41, 75, 91, 121, 138, 173, 207, 229, 243, 278, 288, 289, 306, 328
 Li, Y 69, 98, 101, 111, 212, 216, 224, 231, 275, 285, 312, 369
 Li, Z 64, 157, 242, 282, 305
 Lian, J 59, 101
 Liang, C 335
 Liang, H 181
 Liang, J 81, 309
 Liang, L 270
 Liang, S 120, 289
 Liang, Y 43
 Liang, Z 43
 Liang-xing, J 330
 Liao, C 127, 308, 324
 Liao, X 50, 99, 149, 150, 205, 257, 306, 352
 Liao, Y 204, 351
 Liaw, P 67, 68, 69, 92, 93, 110, 111, 141, 161, 163, 191, 197, 198, 216, 217, 218, 250, 251, 268, 297, 298, 317, 319, 341, 352, 359, 361, 364, 367
 Lie, J 62
 Lienert, U 93, 310, 328, 329, 342
 Lill, J 43, 324, 325
 Lilleodden, E 75, 121, 173, 229, 278, 328
 Lim, C 53, 222
 Lim, G 233
 Lim, H 47, 240, 290, 337
 Lim, K 44, 45
 Lim, S 223
 Lima, A 166
 Lima, J 106, 107, 210, 263, 311, 356
 Lin, A 110, 317
 Lin, C 200, 331
 Lin, D 134
 Lin, J 69, 101, 112, 153, 216, 370
 Lin, K 301
 Lin, M 230
 Lin, P 176
 Lin, S 344
 Lin, T 51, 58, 125, 360
 Lin, Y 301
 Lindemann, J 348, 350, 371
 Lindhe, U 110
 Lindley, T 235
 Lindsay, S 109
 Linga, H 108
 Lin Peng, R 251
 Linyong, F 114
 Liou, W 301
 Liping, N 234
 Lipkin, D 365
 Lipko, S 39
 Liss, K 256, 304
 Litvinov, D 262
 Liu, B 51, 58, 85, 125, 127
 Liu, C 118, 121, 124, 153, 191, 230, 318
 Liu, D 62, 238, 256, 311, 330
 Liu, F 111, 172, 217
 Liu, G 101
 Liu, H 265, 301
 Liu, J 50, 106, 132, 133, 150, 175, 263, 287, 356
 Liu, K 98
 Liu, L 81, 182, 238, 251, 367
 Liu, M 62, 283
 Liu, P 254
 Liu, Q 326
 Liu, R 226
 Liu, T 177, 201
 Liu, W 61, 83, 92, 93, 135, 142, 193, 248, 250, 298, 316
 Liu, X 86, 135, 189, 193, 216, 232, 243, 244, 292, 338, 344, 368
 Liu, Y 64, 138, 157, 172, 197, 198, 220, 231, 250, 264, 312, 313, 366
 Liu, Z 72, 92, 140, 148, 186, 187, 311, 323
 Livescu, V 128, 141, 209, 249
 Llorca, N 56
 Lochbichler, C 98
 Lockhart, G 134
 Lodzik, J 159
 Loehe, D 285, 368
 Löffler, J 68
 Löffler, J 217, 257, 336
 Loh, J 356
 Loiseau, A 308
 Lomatayo, C 101
 Lombard, D 227
 Long, B 143
 Long, G 250
 Long, H 62
 Long, Z 157
 Longanbach, S 90, 288
 Longo, F 124
 Longstreth-Spoor, L 269
 Loomis, E 92
 Lopes, F 362, 363
 Lopez, C 137
 Lopez, M 110, 281, 332
 Lopez P, N 125
 Lorentsen, O 325, 365
 Loretto, M 88, 178, 194, 304, 305
 Lossius, L 171
 Lou, J 76

Louchet, F.....	203	Madhavan, V.....	180	Martinez, J.....	110, 297
Lourie, O.....	76	Madison, J.....	355	Martínez, L.....	45
Louzuine, D.....	268	Maeda, M.....	70, 192, 202	Martins, J.....	159, 214
Lovato, M.....	118, 229	Mahajan, S.....	73, 117, 169, 225	Martirosyan, K.....	262, 267, 323
Lovrenich, R.....	281	Mahammed, Q.....	63	Marton, Z.....	167
Lovvik, O.....	136	Mahapatra, R.....	53, 204	Maruyama, K.....	255, 304
Lowe, C.....	339	Maheraeen, S.....	355	Marx, M.....	367
Lowe, T.....	50, 54, 99, 149, 205,	Mahmoud, M.....	315, 326	Mason, J.....	110
	257, 258, 306, 334, 352	Mahmudi, R.....	337	Massalski, T.....	95
Lowengrub, J.....	208, 276, 316	Maier, H.....	151, 236, 257, 334	Mastuura, H.....	345
Lozano, A.....	144	Maijer, D.....	134	Masuda, C.....	88, 178
Lu, C.....	85	Maiti, S.....	69	Mataya, M.....	93
Lu, G.....	78	Maiwald, D.....	119	Matej, Z.....	142
Lu, H.....	41, 63, 245, 247, 314	Majaniemi, S.....	168	Mathaudhu, S.....	99, 151, 206
Lu, K.....	85, 150, 200, 285, 354	Majumdar, B.....	89, 139, 194, 195, 247, 248, 296	Mathur, A.....	171
Lu, L.....	285, 307	Makaraci, M.....	181	Mato, S.....	350
Lu, N.....	40	Makitka, A.....	135	Mato Díaz, S.....	371
Lu, W.....	371	Malard, T.....	266	Matos, J.....	50
Lu, X.....	190	Malherbe, J.....	253	Matsukawa, Y.....	102
Lü, X.....	326	Maliha, S.....	357	Matsumoto, K.....	193
Lu, Y.....	43, 76, 174, 266, 365	Malkinski, L.....	331	Matsumura, S.....	71, 355
Lu, Z.....	144, 360	Mallik, U.....	127	Matsushita, T.....	247
Luan, B.....	216	Maloy, S.....	94, 95, 143, 144,	Matsuyama, K.....	355
Lubas, M.....	317		198, 199, 251, 299, 342	Matteis, P.....	140, 237, 321
Lucadamo, G.....	238	Maltais, B.....	112	Maurice, C.....	84
Lucas, J.....	243	Malysheva, S.....	205	Mauro, N.....	269
Lucas, M.....	43	Mamforia, M.....	202	Maveety, J.....	74
Ludwig, A.....	137, 244	Man, J.....	183	May, G.....	192
Ludwig, W.....	251	Mancio, M.....	333	May, J.....	307
Lugo, M.....	77	Mandal, M.....	308	Mayrhofer, P.....	370, 371
Lugo, N.....	56	Mani, V.....	336	Maziasz, P.....	146
Lui, L.....	231	Maniruzzaman, M.....	108, 126, 127, 234	McBow, I.....	330
Lukas, P.....	236	Manivannan, A.....	86, 135, 189, 243, 292, 338, 368	McCabe, R.....	117, 170, 171, 230
Luo, A.....	85, 188, 240	Manivasagam, G.....	51	McCallum, R.....	145
Luo, H.....	220	Manjarres, M.....	367	McClain, D.....	195
Luo, J.....	132	Manley, M.....	224	McClellan, K.....	92, 179, 195, 263
Luo, Q.....	335	Mann, J.....	55	McClimon, C.....	263
Luo, S.....	92	Mann, V.....	160	McClintock, D.....	128
Luo, T.....	207, 358	Manna, I.....	269	McCormick, H.....	277
Luo, W.....	160, 163	Mannava, S.....	77, 221	McCune, R.....	86
Luo, X.....	140	Manohar, P.....	232	McDeavitt, S.....	252
Lushchik, A.....	299	Mansoor, B.....	188	McDonald, A.....	51, 58, 125
Luss, D.....	262, 323	Mansour, B.....	188	McDowell, D.....	49, 83, 170, 334
Lv, M.....	40, 235	Manuel, M.....	283	McDowell, D.....	104
Lykotrafitis, G.....	316	Mao, S.....	307, 308	McEvily, A.....	237
		Mao, X.....	89	McFadden, G.....	72
M		Maofa, J.....	44, 323	McHargue, C.....	252
M'Hamdi, M.....	361	Maoz, Y.....	187	McHugh, L.....	329
Ma, D.....	318	Maple, M.....	95	McIntosh, P.....	106, 156, 210, 263, 311, 356
Ma, E.....	76, 100, 170, 216, 218, 353	Mar, A.....	145	McKenna, I.....	61, 117
Ma, F.....	42	Mara, N.....	102, 143, 230	McKenzie, P.....	334
Ma, G.....	269	Marathe, G.....	235	McKenzie, W.....	357
Ma, J.....	180, 314	Mardare, C.....	244	McKinney, S.....	172
Ma, K.....	78	Margarella, A.....	104	McKittrick, J.....	66
Ma, L.....	132, 349	Margaritondo, G.....	342	McLaughlin, S.....	104
Ma, N.....	96, 138, 163, 169, 294, 345	Margem, F.....	166	McNabb, P.....	195
Ma, R.....	266	Markmaitree, T.....	368	McNelly, T.....	52, 53, 352, 353
Ma, S.....	42, 130	Markmann, J.....	51, 99, 333	McNutt, J.....	203
Ma, X.....	181	Marques, C.....	252	Mechler, S.....	94
Ma, Y.....	98, 289	Marquis, E.....	170	Meco, H.....	244
Ma, Z.....	255	Martens, R.....	175, 261	Medina, F.....	110
Macdonald, W.....	239	Martin, F.....	234	Medlin, D.....	170, 238
Macht, M.....	94	Martin, J.....	291	Medvedev, S.....	196
MacSleyne, J.....	103	Martin, M.....	199, 257	Meghlaoui, A.....	266
Madariaga, I.....	148	Martin, O.....	159	Mehta, A.....	328
Madhavan, R.....	202	Martin, P.....	70, 100, 246	Mehta, V.....	63
		Martinez, E.....	110, 265, 281	Mei, J.....	194, 235

Meier, M.....	225	Mishima, Y.....	350	Morin, P.....	363
Meier, W.....	226	Mishin, Y.....	276	Morisaku, K.....	48
Mejia, S.....	184	Mishra, A.....	257	Morishige, T.....	239
Mellenthin, J.....	168	Mishra, B.....	242, 291	Morral, J.....	364
Mencer, D.....	114	Mishra, C.....	211	Morrell, R.....	303
Mendelev, M.....	162	Mishra, R.....	154, 157, 158, 188, 240, 307	Morris, C.....	141
Mendes, F.....	119	Mishra, S.....	203	Morris, D.....	97, 148, 203, 255, 304, 347, 349, 352, 353, 370
Mendez, J.....	84	Misra, A.....	102, 104, 143, 155, 171, 174, 199, 230	Morris, J.....	69, 76, 84, 95, 120, 144, 162, 173, 275, 319
Mendez, P.....	191, 320	Misra, D.....	216, 267, 354	Morris, R.....	207
Mendis, C.....	187, 241	Misra, M.....	333	Morrison, D.....	236
Mendoza, R.....	262	Missalla, M.....	156	Morrissey, R.....	182
Menéndez, O.....	47	Missori, S.....	321	Morrow, B.....	340
Meng, F.....	245	Mitchell, D.....	303	Morsi, K.....	90, 140, 192
Menon, S.....	296	Mitchell, M.....	328	Mortarino, G.....	237, 321
Mercer, G.....	147	Mitsche, S.....	221, 273	Mortensen, A.....	349
Merrill, F.....	141	Mitsuishi, K.....	208	Mortensen, D.....	361
Merrill, J.....	152	Mitsuoka, N.....	245	Moscoco, W.....	57
Meskers, C.....	201, 255, 302, 345	Miwa, K.....	134, 361	Moscovitch, N.....	337
Mesquita, A.....	119	Miyake, M.....	70, 192, 202	Mosengue, N.....	361
Messner, T.....	202	Miyamoto, G.....	193	Moser, M.....	370, 371
Metson, J.....	106, 227	Miyamoto, H.....	150	Moss, S.....	197
Meuffels, P.....	274	Mizusawa, A.....	254	Mottern, M.....	135
Meydanoglu, O.....	295	Moats, M.....	163	Mourao, M.....	301
Meyer, H.....	338	Moavenzadeh, J.....	352	Mourer, D.....	77, 122, 175, 176, 231
Meyer, L.....	57	Modinaro, D.....	190	Moxson, V.....	88
Meyer, M.....	79	Moeck, P.....	40	Mozolic, J.....	329
Meyers, M.....	66, 67, 110, 160, 169, 215, 257, 267, 316, 317, 333, 334, 358	Moelans, N.....	43, 117, 301	Mrozinski, T.....	245
Meyers, W.....	110	Moenig, R.....	229	Mubarok, A.....	68
Mezin, H.....	357	Moffatt, S.....	264	Muddle, B.....	196, 275, 294, 309
Mhaisalkar, S.....	253	Mogilevsky, P.....	118	Mueller, J.....	333
Mi, S.....	274	Mohamed, A.....	325	Mueller, S.....	282
Mialhe, P.....	281	Mohamed, F.....	205, 335	Mukai, T.....	100, 189, 291
Miao, H.....	365	Mohamed, W.....	153	Mukherjee, A.....	48, 285
Miao, J.....	130, 367	Mohandas, A.....	358	Mukherjee, M.....	178
Michael, J.....	248	Mohri, T.....	169	Mukherjee, R.....	43
Michael, N.....	105	Moitra, A.....	155	Mukherjee, S.....	288
Michal, G.....	233, 234	Moldovan, D.....	50, 100	Mulder, A.....	213
Michal, S.....	191, 245, 317	Moldovan, P.....	180, 319	Müller, C.....	206
Michler, J.....	230	Molina, J.....	225	Mulyadi, M.....	193
Middlemas, M.....	128	Moll, A.....	46	Mulyukov, R.....	205
Middleton, C.....	106	Moll, S.....	251	Munoz, J.....	43
Migchielsen, J.....	165	Molodova, X.....	206	Muñoz, V.....	281
Mihalkovic, M.....	44	Moloney, M.....	232	Muñoz-Morris, M.....	203, 353
Mikulowski, B.....	52, 353	Mondal, K.....	219, 271	Münstermann, R.....	274
Miles, M.....	126, 127, 270	Montanari, R.....	140, 321	Muntele, C.....	41, 94, 152, 208, 235, 299, 327, 359
Miller, B.....	225	Monteiro, A.....	222	Murakami, H.....	351
Miller, G.....	145	Monteiro, S.....	70, 114, 166, 167, 221, 222, 273, 321, 346, 362, 363	Murakami, M.....	223
Miller, H.....	117, 176	Moody, N.....	49, 79, 82, 126, 129, 173, 179, 182, 233, 236, 282, 285, 287, 288, 289, 333, 367	Muraleedharan, V.....	363
Miller, J.....	163, 340	Mook, W.....	76	Muransky, O.....	250
Miller, M.....	54, 93, 146, 162, 166, 262, 310, 318, 328	Moon, H.....	47	Murase, K.....	272
Miller, S.....	41	Moon, J.....	88	Murayama, N.....	208
Miller, W.....	86	Moon, K.....	192	Murch, G.....	44
Millett, P.....	99, 252	Mooney, A.....	211	Murdoch, D.....	159
Mills, M.....	56, 73, 131, 146, 183, 193, 225, 247, 264, 294, 340	Moore, K.....	47, 249	Murphy, C.....	316
Mimaki, T.....	150	Moore, R.....	310	Murphy, K.....	175
Min, S.....	47	Moosbrugger, J.....	236	Murr, L.....	110, 281, 369
Min, Y.....	356	Moraes, J.....	263	Murray, C.....	328
Minh, N.....	86	Moran, B.....	61	Murray, M.....	290
Minich, R.....	278	Moreno, H.....	214	Murty, B.....	334
Minor, A.....	76, 307	Moreno, J.....	302	Murty, K.....	153
Miodownik, P.....	232, 341	Moreno Exebio, J.....	320	Murzinova, M.....	54
Miracle, D.....	162, 246, 317	Morgan, D.....	72, 199, 223, 355	Musil, J.....	142
Mironov, S.....	54	Morgenstern, R.....	123	Müßener, D.....	349, 370
Miryala, M.....	214	Moriarty, J.....	91	Muthubandara, N.....	44

N

Na, M.....	61
Na, Y.....	112, 361
Nachimuthu, P.....	243, 299
Nadano, T.....	48
Nafisi, S.....	272
Nag, S.....	166, 181, 194, 275, 340
Naga, S.....	261
Nagai, T.....	70
Nagaraj, B.....	231
Nagasawa, K.....	94
Nagasekhar, A.....	290
Nagem, N.....	213
Nahar, M.....	221
Naidenkin, E.....	258
Naik, S.....	354
Nair, A.....	215
Nair, M.....	211
Najjar, S.....	350
Nakagawa, I.....	300
Nakai, Y.....	217
Nakajima, K.....	146
Nakamura, T.....	186
Nakao, H.....	342
Nalagatla, D.....	75
Namilae, S.....	327
Nan, H.....	295
Nanninga, N.....	212
Nanstad, R.....	128, 284
Napolitano, R.....	79, 86, 126, 179, 233, 282
Narayan, J.....	45, 105, 145, 261
Narayan, R.....	105, 110, 215
Narayana, C.....	196
Narayanan, B.....	146
Narendra Kumar, G.....	159
Narita, H.....	48
Narvekar, R.....	171
Nascimento, D.....	221
Nasipuri, T.....	213
Nastac, L.....	138
Nastasi, M.....	71
Natesan, K.....	292
Natishan, P.....	234
Navarra, P.....	234
Navarro, F.....	119
Nawaz, A.....	182
Nayak, S.....	180
Nazarov, A.....	205
Needleman, A.....	230
Needs, R.....	196
Neelakantan, S.....	88
Neelameggham, N.....	85, 125, 132, 133, 163, 178, 186, 188, 219, 238, 240, 270, 288, 289, 335, 336
Neife, S.....	125, 126, 265
Neil, C.....	189
Neira, A.....	193
Nelson, S.....	242
Nelson, T.....	127
Nemanich, R.....	84, 131, 132, 184, 237
Nemir, D.....	281
Neophytides, S.....	190
Nesbitt, C.....	333
Netskina, O.....	369
Nettles, K.....	327
Neumann, P.....	83

Neumann, S.....	287
Newbauer, T.....	234
Newbery, A.....	51
Newman, J.....	77
Newman, K.....	293
Ng, H.....	294
Nghiem, N.....	202
Nguyen, K.....	358
Nguyen, T.....	122
Nguyen, V.....	271
Ni, C.....	60
Nicholson, D.....	162, 327, 342
Nichtova, L.....	142
Nickel, D.....	57
Nickens, A.....	271
Nicola, L.....	230
Nicolaou, P.....	88
Nie, J.....	146, 289, 337
Nie, Y.....	132, 366
Nie, Z.....	190, 198
Niederstrasser, J.....	320
Nieh, T.....	111, 216
Niehoff, T.....	280
Niendorf, T.....	236
Nieto, J.....	350
Nieto Hierro, J.....	371
Niezgoda, S.....	103
Nikles, D.....	308
Nikulin, A.....	309
Ningileri, S.....	64, 157, 171, 172, 279, 312
Nishida, K.....	223
Nishimiya, Y.....	178
Nishimura, T.....	75, 327
Nishiyama, N.....	163, 360
Niu, X.....	67
Nixon, M.....	81, 118
Niyomwas, S.....	192
Nobuhiro, I.....	245
Noda, T.....	98
Nogita, K.....	75, 265, 326, 327
Nogueira, T.....	359
Noh, B.....	345
Noh, J.....	283
Noh, S.....	98
Noh, T.....	115
Noldin, J.....	79
Noll, H.....	153
Noor, A.....	271
Norfleet, D.....	131, 183
Noro, J.....	204
Northwood, D.....	290
Norton, D.....	101, 153
Nose, Y.....	272, 321
Novak, V.....	142
Nowak, J.....	76
Nowell, M.....	69
Nowill, C.....	108
Noyan, I.....	328
Nuggehalli, R.....	89, 139, 194, 247, 296
Nurislamova, G.....	54
Nürnberg, M.....	241
Nutt, S.....	52, 122
Nyberg, E.....	85, 132, 133, 186, 188, 238, 240, 288, 289, 335, 336
Nychka, J.....	68, 316, 317
Nye, R.....	114

O

O'Brien, E.....	330
O'Brien, F.....	215
O'Brien, J.....	271
O'Brien, K.....	263
O'Dell, L.....	106
O'Dovero, P.....	114
O'Keefe, M.....	277
Oberson, P.....	73, 246
Ode, M.....	351
Odessky, P.....	258
Oechsner, A.....	44
Oehring, M.....	149, 347, 350
Oguma, N.....	367
Ogunmola, B.....	65
Ogura, K.....	271
Oh, C.....	74, 284
Oh, H.....	260, 261
Oh, K.....	46, 88
Oh, T.....	117
Oh-ishi, K.....	55, 187, 241
Ohashi, T.....	92, 204
Ohba, Y.....	79
Ohm, V.....	125
Ohno, M.....	169
Ohnuma, I.....	254, 300
Ohnuma, T.....	72
Ohriner, E.....	346
Ohtomo, A.....	71
Oi, T.....	273
Oikawa, T.....	308
Oishi, K.....	146
Okabe, S.....	186
Okabe, T.....	69, 113, 166, 221, 272, 273, 321, 362
Okada, M.....	237
Okada, N.....	193
Okada, O.....	254
Okamoto, S.....	115, 223
Okeke, C.....	126, 265
Oki, S.....	239
Okino, H.....	223
Okitsu, Y.....	258, 307
Okuofu, C.....	346
Okura, T.....	186
Olaya-Luengas, L.....	48
Oleneva, T.....	348
Oliana, R.....	79
Oliveira, A.....	210, 263
Oliveira, H.....	119
Oliver, E.....	250
Olmsted, D.....	116
Olsen, A.....	109
Olsen, E.....	127
Olson, D.....	291
Olson, G.....	61, 145, 188, 234, 310
Omran, A.....	39
Omura, N.....	361
Onaka, S.....	184
Onck, P.....	316
Ontman, A.....	103
Opalka, S.....	136
Opeka, M.....	347, 370
Oportus, J.....	288, 289
Orlikowski, D.....	72
Orlov, D.....	150
Orlovskaya, N.....	243

- Orsborn, J 88
 Ortalan, V 355
 Ortiz, A 367
 Ortiz, C 302
 Ortiz, U 184
 Osborn, W 368
 Osenbach, J 119, 121, 173, 228
 Osetskiy, Y 73
 Osetsky, Y 102
 Ossi, P 252
 Oster, N 145
 Ostolaza, K 148
 Oswald, M 240
 Ota, N 47
 Oteri, E 48, 341
 Otsuka, K 306
 Ott, R 162, 261
 Otto, A 347, 348
 Ou, S 229
 Ouimet, L 86
 Ouyang, F 228, 253
 Ovcharenko, A 343
 Öveçoglu, M 40, 91
 Ovsianikov, A 110
 Owate, I 126, 265
 Oye, H 226
 Øye, H 226, 326
 Ozaki, C 227
 Özgün, E 91
 Ozolins, V 245
- P**
- Packard, C 68
 Padilla, R 245
 Padron, I 297
 Paglieri, S 135
 Paidar, V 350
 Paik, C 338
 Paine, M 160
 Paisley, D 92
 Paital, S 47, 359, 361
 Pal, U 124, 133, 177
 Palanisamy, B 234
 Palau, P 366
 Palkowski, H 87, 298
 Palm, M 98, 204
 Palmlund, D 172
 Palmstrom, C 131
 Palomar, M 137
 Palosz, B 269
 Pan, T 338
 Pan, X 338, 364
 Pan, Z 71, 206
 Pandey, R 200
 Pang, J 92, 228
 Pang, L 63
 Paninski, M 98
 Panov, A 211, 263, 311
 Pantke, K 336
 Pantleon, W 83, 93, 328, 342
 Pao, P 294
 Paquin, D 320
 Paramonova, E 268
 Pareige, P 198, 354
 Park, C 296
 Park, E 318
 Park, H 97, 283, 332
 Park, J 44, 45, 93, 136, 251, 262, 284, 328
 Park, K 361
 Park, S 48, 107, 155, 195, 238, 263, 283, 295, 331
 Paromova, I 211, 311
 Parra, M 247
 Parra Garcia, M 195, 263
 Parry, S 156
 Parthasarathy, T 72, 183
 Parvin, N 52
 Paster, F 178
 Patel, K 233
 Patel, V 192
 Pati, S 124, 133
 Patrick, B 279
 Paturaud, F 56
 Paul, J 149, 347
 Pawlek, R 365
 Payton, E 294
 Pearton, S 101, 153
 Peaslee, K 219
 Pecharsky, V 95, 144
 Peck, A 319
 Pedersen, T 109
 Peiyang, S 323
 Pekgulyuz, M 85, 132, 133, 186, 188, 238, 240, 288, 289, 335, 336
 Pellati, G 140
 Pelton, A 328
 Peng, B 255
 Peng, K 205
 Peng, L 239, 240, 275, 335
 Peng, R 297
 Peng, T 303
 Peng, Y 51
 Pennycook, S 274
 Peralta, P 92, 179, 195, 237, 247, 263
 Perander, L 106
 Pereira, C 213
 Perepezko, J 304
 Perez, R 45
 Perez-Bravo, M 148, 349
 Perez-Tijerina, E 184
 Perez-Trujillo, F 350, 371
 Periaswamy, P 200
 Pericleous, K 98, 177, 315
 Perrot, P 199
 Pesyna, G 147
 Péteín, A 97
 Peter, W 295
 Peters, H 266
 Peters, P 148
 Peterson, B 230, 246
 Peterson, E 106, 114, 214
 Peterson, R 155, 163, 280
 Petralia, S 140
 Petrov, A 168
 Pettersen, T 212
 Pfitzing, J 149
 Phanikumar, G 137
 Phelan, D 304
 Phillips, D 99
 Phillips, E 210
 Phillpot, S 252
 Picard, D 325
 Piccardo, P 140
 Pickard, C 196
 Pickens, J 194
 Pihl, J 338
 Pilchak, A 246
 Pillai, S 177
 Pilone, D 47, 231
 Pimentel, N 79
 Pinasco, M 140, 321
 Piñero, N 356
 Pint, B 77, 122, 123, 175, 231
 Pinto, E 315
 Pippa, R 56, 57, 285, 334, 369
 Pirhoseinloo, H 158
 Pirling, T 298
 Pirouz, P 73
 Piskunov, S 222, 223
 Pisutha-Armond, N 72
 Plapp, M 168, 324
 Pletcher, B 262
 Plumtree, A 367
 Pochan, D 161
 Pocock, L 297
 Podolskiy, A 57
 Poirier, J 227
 Polat, A 181
 Polcawich, R 122
 Polesak III, J 189
 Pollard, M 146
 Pollock, T 49, 82, 129, 130, 182, 187, 236, 251, 285, 333, 351, 355, 367
 Pomykala, J 345
 Ponnusamy, M 160
 Poole, W 53, 189
 Poon, J 319
 Poon, S 68, 319
 Poorganji, B 193
 Popa-Simil, L 94, 152, 235
 Popescu, C 180
 Popescu, G 180
 Popko, D 114
 Popov, M 258
 Popova, L 181
 Porfiri, M 129
 Portella, P 49, 82, 129, 182, 236, 285, 333, 367
 Porter, W 182
 Potesser, M 113, 301, 302
 Potirniche, G 155
 Potocnik, V 315
 Pouchon, M 230
 Poudel, B 59
 Poulain, X 179
 Poulsen, H 76, 93, 251, 328, 342
 Pourboghra, F 277, 347
 Pourmostadam, S 128
 Powell, A 177, 186, 232
 Powell, B 86
 Powell, J 174
 Power, G 356
 Powers, M 125
 Pownceby, M 330
 Pozzi, C 140
 Pradeilles, N 181
 Pradhan, D 178
 Pradhan, N 309
 Prangnell, P 306, 353
 Prasad, S 89, 90, 173, 248
 Prasad, V 336

Prasanna Kumar, T.....	137
Prater, J.....	105
Pratt, P.....	298
Prebble, J.....	220
Prepenit, J.....	357
Preuss, M.....	178
Prevey, P.....	77
Prillhofer, B.....	125, 165, 202, 220
Prime, M.....	298
Pritantha, W.....	244
Privé, D.....	112
Priyantha, W.....	243
Proffen, T.....	144
Proshkin, A.....	226
Proulx, J.....	320
Proust, G.....	117, 118, 229, 279
Provatas, N.....	168
Provenzano, V.....	176
Przybyla, C.....	49
Pshenichuk, A.....	54
Pucci, A.....	157
Pugazhenth, L.....	242
Pulskamp, J.....	122
Purcek, G.....	52
Purushotham, S.....	267
Puthicode, A.....	363
Puthucode, A.....	193, 194
Puxley, D.....	157
Pyczak, F.....	56, 130
Pyshkin, S.....	105

Q

Qazi, J.....	194
Qi, Y.....	46
Qian, H.....	132
Qian, K.....	205, 226
Qidwai, M.....	209, 210
Qin, H.....	322
Qin, W.....	244
Qingxiu, J.....	312, 313
Qiu, D.....	124
Qiu, K.....	269
Qiu, S.....	109, 214
Qiu, X.....	204
Qu, J.....	89, 233
Quach, D.....	223
Quan, Q.....	325
Quast, J.....	195
Quelennec, X.....	354
Querín, J.....	212
Quinones, S.....	110
Quintana, M.....	146
Quintino, L.....	80

R

Raab, G.....	54
Raabe, D.....	118, 148, 170
Rabba, S.....	226
Rack, H.....	138, 194
Rack, P.....	217, 251
Radhakrishnan, B.....	327
Radiguet, B.....	198, 354
Rae, A.....	172
Rae, P.....	174, 198, 249
Raeisinia, B.....	53

Rafea, M.....	165
Raffaella, R.....	152
Raghavan, P.....	264, 311
Raghavan, R.....	158
Raghunathan, S.....	247
Rahbar, N.....	67
Rahman, M.....	333
Rahman Rashid, R.....	46, 80, 281
Rainforth, M.....	134, 138
Rainforth, W.....	371
Raj, R.....	89, 139, 194, 247, 296
Raja, K.....	333
Rajagopalan, J.....	286
Rajagopalan, S.....	181, 340
Rajamoorthy, S.....	178
Rajan, K.....	191, 244, 293, 339
Rajasekhara, S.....	332
Rajgarhia, R.....	140
Rajkiran.....	281
Rajkiran, G.....	46, 80
Rajulapati, K.....	67
Rakowski, J.....	189, 190, 338
Ram-Mohan, L.....	364
Ramanath, G.....	39, 59, 101, 152, 207, 260, 308
Ramanujan, R.....	261, 267
Ramaswamy, J.....	159
Ramesh, K.....	100, 170, 334
Ramesh, R.....	167
Ramirez, J.....	265
Ramos, A.....	204
Ramos, K.....	141, 174
Randall, N.....	174
Randow, C.....	341
Ranganathan, S.....	186
Rangasamy, V.....	106, 160
Rao, A.....	59
Rao, B.....	55
Rao, K.....	330, 336
Rao, P.....	240
Rao, S.....	72, 183
Rao, W.....	224
Rashmi.....	71
Rata, D.....	168
Ratvik, A.....	227
Ravelo, R.....	140
Ravi, V.....	134
Ravindra, N.....	105
Ravindra, N.....	63, 64, 104, 105, 247, 296, 297
Ravindran, C.....	289
Ravindranath, R.....	77
Ravishankar, N.....	308, 363
Rawlins, C.....	219
Ray, K.....	283, 284
Ray, P.....	364
Ray, V.....	153, 208
Raymond, G.....	363
Read, C.....	171
Read, J.....	327
Ready, J.....	296
Real, C.....	137
Reddy, R.....	163, 178, 219, 270, 271
Reddy, S.....	46, 80
Redfern, A.....	109
Redkin, A.....	179, 314
Reed, B.....	169, 278
Reed, M.....	114
Reed, R.....	276, 324

Reedy, E.....	195
Reek, T.....	357
Rehbein, D.....	162, 200, 254
Reichstein, S.....	123, 124
Reilly, C.....	79
Reinbold, L.....	228
Reinhard, C.....	349, 371
Reis, J.....	214
Reis, L.....	80
Reis, R.....	119
Reitan, B.....	99
Reiten, E.....	99
Reiter, G.....	197
Reitz, J.....	98
Ren, F.....	101, 153
Ren, I.....	359, 361
Ren, J.....	133
Ren, R.....	367
Ren, Y.....	69, 93, 142, 197, 250, 251, 269, 352
Ren, Z.....	59
Renaudier, S.....	357
Renavikar, M.....	228
Rencis, J.....	333
Repetto, E.....	263
Restrepo, O.....	323
Retford, C.....	224, 364
Rettenmayr, M.....	40
Reusch, F.....	220
Reuther, K.....	225
Révész, Á.....	353
Reyes-Villanueva, G.....	122
Reynante, B.....	60
Rezaie, H.....	41
Rezvanian, O.....	184
Rhee, M.....	72
Richard, C.....	51, 159
Richard, D.....	315
Richards, C.....	195
Richards, D.....	169
Richards, R.....	195
Richards, V.....	87, 219
Richardson, J.....	198, 318
Ricketts, M.....	338
Rickman, J.....	116
Ricolleau, C.....	308
Ried, P.....	86
Rieken, J.....	90
Riesterer, J.....	363
Rigg, P.....	141
Rijkeboer, A.....	211
Rijnders, G.....	115
Rimoshevsky, S.....	302
Rinderer, B.....	164
Ringnald, J.....	317
Rioja, R.....	287
Rios, O.....	256, 324, 365
Rios, P.....	262
Risanti, D.....	108
Rist, M.....	193
Ritchie, R.....	66, 110, 130, 160, 215, 267, 316, 358
Ritter, C.....	159
Ritter, Y.....	99
Rivas, C.....	245
Rivera, R.....	316
Rivera Diaz del Castillo, P.....	108
Rivero, R.....	64, 296
Riveros, R.....	330

- Rivolta, B 237, 321
 Rizzi, N 255
 Ro, Y 286
 Robbins, D 249
 Roberts, C 179, 180
 Robertson, C 83
 Robertson, D 302
 Robertson, I 117, 225
 Robinson, A 64
 Robles Hernandez, F 260, 322
 Rödel, J 134
 Rodrigo, R 213
 Rodriguez, M 189
 Rodriguez G., X 125
 Roeder, R 66, 110, 160, 161, 215, 267, 316, 358
 Rogers, J 70, 162, 244
 Roh, J 212
 Rohan, P 271
 Rohrer, G 117, 209, 264
 Rokhlin, S 247
 Rollett, A 43, 45, 49, 100, 117, 153, 154,
 180, 209, 210, 212, 222, 264, 368
 Romansky, M 277
 Rong, Y 155, 156
 Ronning, F 174
 Roos, A 72
 Rosefort, M 320
 Rosen, G 188
 Rosenberger, A 77, 122, 175, 231, 246
 Rosenberger, M 181, 362
 Ross, F 84
 Ross, I 371
 Rostamian, A 305
 Roters, F 118, 148, 170
 Roth, J 260
 Roth, R 65
 Roth-Fagaraseanu, D 148, 348, 371
 Rothe, C 348
 Rothermel, M 299
 Roussel, P 200
 Rovere, F 370, 371
 Rowenhorst, D 61, 103, 153, 210, 355
 Rowson, J 113
 Roy, A 338
 Roy, I 205, 335
 Roy, S 295
 Royva, T 202
 Rozenak, P 107
 Ruano, O 353
 Rudd, R 278
 Rui, G 41
 Ruiz, G 165
 Ruiz, M 245
 Rumpf, K 56
 Rundell, S 258
 Ruoff, A 196
 Rupert, T 229
 Rusche, S 109
 Russ, S 149
 Russell, A 95, 279
 Russell, K 94, 166
 Russo Spena, P 237, 321
 Rutledge, S 213
 Rutman, D 114, 214
 Ruvalcaba-Jimenez, D 209
 Ryabkov, D 123
 Rye, K 213, 325
 Ryu, T 193
S
 Saage, H 98, 194, 305, 334
 Sabirov, I 100
 Sachdev, A 107, 154, 188, 240
 Sadayappan, K 85
 Sadhukhan, P 310
 Sadoway, D 270
 Sadrabadi, P 174
 Saeed, U 229, 343
 Saegusa, T 254
 Saether, E 99
 Safarik, D 135, 369
 Sahin, F 192
 Sahu, T 226
 Saif, T 286
 Saito, K 223
 Saitoh, H 342
 Sakai, J 223
 Sakai, T 202, 367
 Sakamoto, D 48
 Saket Kashani, M 180
 Sakidja, R 304
 Salam, B 301
 Salamanca-Riba, L 223
 Salame, C 281
 Salazar-Villalpando, M 164
 Saldana, C 55
 Saleh, T 155
 Salehpour, B 158
 Salem, A 88
 Sales, B 144
 Salick, D 161
 Salimgareeva, G 258
 Salishchev, G 54, 205
 Salman, U 224
 Salvador, P 292
 Samant, A 80
 Samanta, A 118, 130, 364
 Samaras, M 230
 Sanchez, R 167
 Sánchez, R 114
 Sandhanam, A 271
 Sandhu, P 232
 Sands, T 102
 Sangiorgi Cellini, G 272
 Sano, T 295
 Santafé, H 167
 Santella, M 338
 Santerre, R 159
 Santos, E 119
 Santos, H 210
 Santos, L 166, 356
 Santos, T 80
 Saotome, Y 163, 360
 Saphin, E 205
 Sargent, G 250, 257
 Sarihan, V 228, 296
 Sarikaya, M 66, 110, 160, 161,
 215, 267, 316, 358
 Sarma, D 93
 Sarma, V 55, 334
 Sarosi, P 56, 73, 146
 Sarvinis, J 164
 Sasaki, H 202
 Sastry, S 53, 89
 Satapathy, R 269
 Sato, H 181
 Sato, N 124
 Sato, Y 201, 227
 Saunders, A 141
 Saunders, N 232, 341
 Sauvage, X 354
 Savage, G 289
 Savan, A 244
 Saw, C 141
 Saxena, A 140
 Saylor, D 72
 Scattergood, R 205
 Scavino, G 140
 Schaedler, T 175
 Schaef, W 367
 Schafier, E 52, 353
 Schalk, T 285
 Scharf, T 90
 Scherer, D 331
 Scheriau, S 56
 Schille, J 232, 341
 Schilling, J 196
 Schillo, M 135
 Schimansky, F 256, 305
 Schlegel, S 182
 Schmauder, S 158, 237, 239
 Schmetterer, C 343, 344
 Schmid-Fetzer, R 186, 337
 Schmidt, C 240
 Schmidt, H 156
 Schmidt, S 251, 348
 Schmidt, T 165
 Schmitz, G 98
 Schneibel, J 56, 332
 Schneider, A 315
 Schneider, J 53, 141, 161, 212
 Schoning, C 227
 Schramm, J 319
 Schroers, J 359
 Schroth, J 126
 Schuetze, M 349
 Schuh, C 68, 248, 286
 Schultz, R 287
 Schumacher, G 94
 Schütze, M 371
 Schvezov, C 87, 181, 272, 362
 Schwaiger, R 174, 317, 333
 Schwam, D 288
 Schwardt, J 110
 Schwartz, A 249
 Schwarz, M 177
 Schwarz, R 135, 260, 369
 Scott, B 331
 Scott, C 118
 Scott, M 70
 Schwartz, C 141
 Sears, J 104, 155, 208, 303
 Sebright, J 123
 Sediako, D 232, 239, 337
 Sediako, O 232
 Sedlacek, D 109
 Seelaboyina, R 42
 Seelam, U 270
 Seetharaman, S 247

Seidman, D.....	61, 247, 310	Sherby, O.....	258, 332	Singheiser, L.....	50, 286
Seifert, H.....	44, 256, 324, 365	Sherman, D.....	310	Sinha, S.....	141, 342
Seki, Y.....	48, 67	Shet, S.....	105, 296	Sinha, V.....	70
Sekulic, D.....	75	Sheu, S.....	287	Sinita, N.....	181
Seman, T.....	296	Shi, D.....	59, 101	Sintay, S.....	49, 154, 368
Semenova, I.....	258	Shi, J.....	184	Sisneros, T.....	279
Semenova, O.....	365	Shi, L.....	349	Sisson, R.....	108, 127, 234
Semiatin, L.....	54	Shi, W.....	85	Sitaula, S.....	338, 339
Semiatin, S.....	88, 180, 250, 257, 340	Shi, X.....	132	Sitdikov, V.....	306
Semones, J.....	205	Shi, Z.....	78, 140, 314, 326, 366	Sittner, P.....	250
Senft, D.....	39, 59, 101, 152, 207, 260, 308	Shibata, J.....	113, 208	Sjöberg, G.....	87
Seniw, M.....	236	Shields, J.....	346	Skladan, K.....	159
Senkov, O.....	65, 317	Shifflet, D.....	228	Skrotzki, B.....	149, 255
Senkova, S.....	65	Shifflet, G.....	44, 68, 103, 111, 319	Skrotzki, W.....	183, 225
Senn, J.....	189	Shih, D.....	172, 327	Skury, A.....	222, 273, 321
Seo, D.....	174	Shih, T.....	301	Skybakmoen, E.....	227
Seo, J.....	333	Shim, S.....	332	Slater, T.....	110
Seo, S.....	327, 331	Shimizu, Y.....	360	Sloan, T.....	233
Seppala, E.....	278	Shin, B.....	47	Smarsly, W.....	97, 101, 104, 114, 348
Serbruyns, A.....	301	Shin, C.....	83	Smelser, N.....	140
Sereni, S.....	188	Shin, D.....	48, 55, 126, 307	Smetniansky-De Grande, N.....	299
Serra, A.....	73	Shin, H.....	102, 152	Smirnov, S.....	57
Setty, K.....	139	Shin, J.....	47, 309	Smith, C.....	47, 225
Severo, D.....	315	Shin, K.....	127, 187, 240	Smith, M.....	106
Sewell, T.....	141, 174	Shin, S.....	324	Smith, P.....	311
Sha, Y.....	251	Shingledecker, J.....	146, 221	Smith, R.....	189, 243, 244, 303
Shaarbaf, M.....	57	Shinozaki, D.....	174	Smyslov, A.....	205
Shackelford, J.....	358	Shipova, O.....	211	Snead, L.....	303
Shagalina, S.....	258	Shiu, K.....	230	Snead, M.....	160
Shaghiev, M.....	65	Shivkumar, S.....	108	Snugovsky, P.....	277
Shahab, A.....	53, 54	Shiwen, B.....	178	Snyder, G.....	145
Shahbazian Yassar, R.....	158, 241	Shoji, T.....	177, 189	Soare, M.....	43, 116
Shaidulin, E.....	160	Shqau, K.....	135	Soboyejo, W.....	67
Shaigan, N.....	243	Shuey, S.....	201, 280	Soffa, W.....	365
Shalini, T.....	176	Shui-ping, Z.....	330	Sohn, H.....	193
Shamsuzzoha, M.....	200, 308, 312	Shuiping, Z.....	214	Sohn, S.....	44, 45
Shan, Z.....	50, 76, 99, 149, 205, 257, 306, 307, 352	Shull, R.....	185	Sohn, Y.....	175, 190, 324, 351
Shang, C.....	291	Shunwen, W.....	91	Sokolov, M.....	128, 284
Shang, L.....	134	Shurov, N.....	314	Sokolowski, P.....	145
Shang, S.....	186	Shurygin, A.....	179	Solak, N.....	302
Shankar, M.....	55, 151	Shutthanandan, V.....	94, 243	Solheim, A.....	227
Shanmugasundaram, T.....	334	Sibila, A.....	357	Solis, F.....	316
Shao, L.....	199, 252	Sicha, J.....	142	Solli, L.....	108
Shao, R.....	136	Sickafus, K.....	251, 252, 343	Somani, M.....	354
Shao-Horn, Y.....	72	Siddiq, A.....	237	Somekawa, H.....	189
Sharafat, S.....	94	Sievert, R.....	149	Someran, M.....	66
Sharafutdinov, A.....	54	Sigworth, G.....	164	Sommer, K.....	57
Sharma, A.....	70	Sikha, S.....	105	Sommitsch, C.....	221, 273
Sharon, J.....	229	Sillekens, W.....	189	Son, C.....	136
Sharp, I.....	308, 324	Silva, G.....	237, 321	Son, J.....	274
Sharp, J.....	58	Silva, H.....	210	Son, S.....	361
Sharpe, W.....	64	Silva, M.....	119	Song, C.....	81
Shaw, L.....	205, 218, 367, 368	Simagina, V.....	369	Song, G.....	359
She, Y.....	136	Simakov, D.....	326	Song, H.....	221
Shechtman, D.....	90	Simmons, J.....	43, 60, 102, 103, 153, 154, 209, 262, 309, 323, 324, 325, 355	Song, J.....	300
Shelton, E.....	256	Simões, T.....	159, 214	Song, M.....	208
Shen, C.....	73, 138, 224, 225, 275	Simpkins, R.....	149	Song, S.....	111, 216
Shen, H.....	265	Sinclair, C.....	53, 118, 189	Song, W.....	336
Shen, J.....	111, 319	Sinclair, R.....	84	Song, X.....	40, 193, 324
Shen, T.....	260, 306, 342, 343	Singh, A.....	87, 189, 199, 290, 291	Song, Y.....	59
Shen, X.....	313	Singh, G.....	156	Sopori, B.....	63, 64, 104, 296
Shen, Y.....	251, 360	Singh, J.....	49	Sordelet, D.....	162
Sheng, H.....	218	Singh, N.....	63, 104, 365	Sorlie, M.....	325
Sheng, W.....	72	Singh, P.....	86, 190	Soto, K.....	369
Shenoy, G.....	93	Singh, R.....	308	Souza, F.....	359
Shepard, M.....	77, 122, 175, 231	Singh, V.....	268	Souza, R.....	358
Shepelev, D.....	290			Spaepen, F.....	43, 117

Spain, J.....	347	Strachan, A.....	91	Tack, W.....	194
Spaldin, N.....	167	Streitz, F.....	169	Tada, S.....	127
Spanos, G.....	61, 103, 210	Struhr, U.....	298	Tafra, E.....	115
Spearot, D.....	140	Stuart, P.....	203	Tagliavia, G.....	129
Specht, E.....	142	Stukowski, A.....	99	Taheri Hashjin, M.....	158
Speck, T.....	317	Stukowski, M.....	244	Tajik, A.....	77
Spemann, D.....	299	Su, J.....	53	Takahashi, A.....	94, 131
Spence, K.....	269	Su-Chi, I.....	138	Takahashi, T.....	71, 306
Spencer, D.....	352	Suarez, M.....	48	Takai, K.....	182
Spiegel, M.....	244	Suarez, O.....	321	Takai, O.....	161
Spitzer, D.....	156	Suárez, O.....	47	Takaku, Y.....	254, 300
Spohr, E.....	222	Subbaian, B.....	106	Takano, C.....	301
Spoljaric, D.....	113	Subbarayan, G.....	139	Takasu, I.....	79
Spowart, J.....	355	Subhash, G.....	69	Takasugi, T.....	351
Spranklin, J.....	220	Subra, S.....	307	Takata, N.....	258, 307
Sreenivas Rao, K.....	137	Subramanian, K.....	119, 120, 121, 142, 248, 271	Takechi, H.....	97
Sreeranganathan, A.....	262	Subramanian, R.....	153	Takeda, H.....	360
Srinivasan, R.....	294, 295	Sudhakar, N.....	145	Takeda, O.....	201
Srivastava, A.....	71	Suenaga, S.....	75, 327	Takeguchi, M.....	208
Srivastava, C.....	39, 200, 261	Suganuma, K.....	173, 199, 200, 228, 253, 300, 343	Takeuchi, I.....	223
Srolovitz, D.....	116	Sugimoto, J.....	74	Takeyama, M.....	305
Stach, E.....	307	Suh, C.....	293	Takizawa, R.....	367
Stacy, J.....	231	Suh, D.....	74	Talavera, M.....	210
Stafford, R.....	267	Sukumaran, C.....	159	Taleff, E.....	60, 102, 153, 157, 209, 262, 309, 355, 369
Stafford, S.....	110	Sun, F.....	81	Talke, F.....	317
Stam, M.....	213	Sun, G.....	298	Talling, R.....	247
Stanescu, C.....	319	Sun, H.....	42, 359	Tamerler, C.....	161
Stanica, C.....	319	Sun, J.....	319	Tamerler Behar, C.....	358
Stanzl-Tschegg, S.....	367	Sun, K.....	357	Tamimi, S.....	52
Stark, A.....	256, 304, 305	Sun, N.....	133	Tamiris, S.....	246
Starostenkov, M.....	181	Sun, P.....	150, 206, 352	Tamirisakandala, S.....	295
Stas, M.....	159	Sun, W.....	256	Tamura, K.....	48
Stein, F.....	98	Sun, X.....	198, 298	Tamura, T.....	134, 361
Stein, V.....	135	Sun, Y.....	56, 93	Tan, C.....	51, 58, 125
Steinbach, I.....	146, 239, 256, 324	Sun, Z.....	132	Tan, P.....	246
Steinberg, M.....	163	Sunda-Meya, A.....	132	Tan, S.....	63, 344
Steinbrech, R.....	50, 286	Sundararajan, A.....	362	Tanaka, H.....	184
Steinbrecher, T.....	317	Sundarraj, S.....	232, 289	Tanaka, K.....	204
Steingart, D.....	109, 213	Sung, S.....	98	Tanaka, M.....	48, 208, 254
Stelzer, N.....	153	Suñol, J.....	56	Tanaka, T.....	193
Stemmer, S.....	274	Suput, M.....	124	Tanaka, Y.....	146
Stephenson, K.....	94	Suresh, S.....	82, 118, 316	Tang, H.....	135
Stevens, A.....	203	Suryanarayana, C.....	270	Tang, L.....	215, 226
Stevens, R.....	43	Suss, A.....	211, 263, 311	Tang, M.....	71, 72, 343
Stevenson, J.....	190	Suter, R.....	310, 328	Tang, W.....	145
Stewart, I.....	234	Sutton, M.....	121	Tang, X.....	41, 356
Stewart, J.....	180, 305	Suwas, S.....	51, 295	Tanner, C.....	200
Stockinger, M.....	221	Suzuki, M.....	48, 163, 219, 270	Tanniru, M.....	260
Stodolnik, B.....	317	Svoboda, M.....	236	Tao, D.....	42
Stoecker, C.....	130	Swadener, J.....	144, 230	Tao, J.....	50, 62, 150, 283
Stoica, A.....	142, 318	Swaminathan, S.....	52, 53, 151, 353	Tao, N.....	150, 354
Stoica, G.....	297	Swamy, V.....	196	Tao, W.....	337
Stokes, A.....	66	Swamydhas, V.....	154	Taptik, I.....	107
Stokes, K.....	101, 192, 331	Swart, D.....	192	Tarcy, G.....	213, 357
Stolken, J.....	130	Sweatman, K.....	75	Tata, M.....	140, 321
Stoller, R.....	102, 343	Sweeney, D.....	294	Tatenuma, K.....	164
Stone, D.....	365	Syed, B.....	82	Tateyama, M.....	208
Stone, H.....	297	Syed Asif, S.....	307	Tatiparti, S.....	260
Stonis, M.....	107	Sylvester, K.....	347, 370	Tatsumi, K.....	254
Stoos, C.....	271	Syn, C.....	258, 332	Tauson, V.....	39
Støre, A.....	227	Szczepanski, C.....	237, 367	Tavsanoglu, T.....	123, 233
Störmer, M.....	335	Szot, K.....	274	Taylor, B.....	121
Storozhenko, P.....	369	Szpunar, J.....	241	Taylor, M.....	112, 213
Stotter, C.....	221			Taylor, P.....	201, 280
Stoudt, M.....	103			Tayon, W.....	278
Stoughton, T.....	282			Tchakhalian, J.....	167
Stout, M.....	229				
		T			
		Tabachnikova, E.....	57		

Teale, R	237, 247
Tedenac, J	181, 260
Telang, A	277
Telesman, J	176
Templeton, J	190
Teng, Z	191
Tenhundfeld, G	123
Terada, D	100
Terashima, S	254
TerBush, J	187
Terdalkar, S	333
Tereshko, A	143
Tereshko, I	143
Terrones, L	166, 363
Tessier, J	159, 213
Teter, D	166
Tewari, A	154
Thadhani, N	257
Thein-Han, W	216
Thibault, M	112, 225
Thirumalai, N	116
Thoma, D	166, 209, 230, 351
Thomas, B	110, 362
Thomas, M	129, 255
Thomé, L	251
Thompson, G	39, 207, 261
Thompson, J	261
Thompson, R	42, 122
Thonstad, J	365
Thornton, K	72, 169, 235, 262, 263, 316
Threadgill, P	178
Tian, B	273
Tian, J	218, 367
Tian, Q	42, 246, 339
Tian, Z	326, 366
Tianzu, Y	78, 302
Tiearney, T	365
Tieman, B	310
Tien, L	101, 153
Tierney, C	215
Tikhonovsky, M	57
Tilak, R	165
Tiley, J	191, 198, 309, 355
Tilghman, D	296
Timokhina, I	100
Ting-an, Z	234
Tirschler, W	183
Tischler, J	83, 92, 93, 183, 250, 329
Tiwari, A	95, 144
Tiwari, S	289, 334, 336
Tkacheva, O	179, 314
Tkachuk, A	145
Tobler, E	145
Tochiyama, O	124
Todaka, Y	56, 150
Todd, P	324
Togashi, N	163, 360
Tokita, M	283
Tomasino, T	159, 315
Tome, C	117, 118, 170, 171, 225, 229, 257, 279, 329
Tomesani, L	272
Tomsett, A	225
Tomsia, A	215
Tomus, D	334
Tong, C	44, 230, 296
Tong, L	157, 255

Tong, Z	143
Tonks, D	141, 209, 249
Topic, I	56
Topping, T	51
Torabi, S	276
Torbet, C	182, 251
Toribio, J	50
Toroghinejad, M	57
Torres, K	261
Tortorelli, P	338
Tosta, R	171
Totemeier, A	252
Toyoda, Y	306
Traiviratana, S	334
Tran, T	179, 358
Trau, M	101
Trautmann, C	94, 143, 198, 251, 252, 299, 342
Trautt, Z	116
Trelewicz, J	286
Tremblay, S	361
Trenkler, J	197
Triantafylopoulos, N	190
Tribyshevsky, L	302
Tribyshevsky, V	302
Trichy, G	45, 145, 261
Trinkle, D	91, 140, 196, 224, 249
Trojan, I	196
Truci, H	119
Trujillo, C	174, 332
Trumble, K	55, 57, 136, 151
Trunova, O	50, 286
Tsai, A	87, 199
Tsai, C	244
Tschofen, J	255
Tschopp, M	49, 83, 170, 334
Tseng, C	360
Tseng, H	327
Tseng, Y	101
Tsipas, S	350
Tsirlina, G	326
Tsuchimoto, K	272
Tsuji, N	56, 100, 149, 150, 258, 307
Tsujikawa, M	239
Tsujimoto, M	228
Tsukazaki, A	71
Tsukihashi, F	345
Tsurkan, V	223
Tu, G	140
Tu, K	84, 85, 119, 131, 184, 194, 200, 228, 229, 237, 245, 253, 254
Tubman, N	168
Tucker, G	49
Tucker, J	199
Tulenko, J	252
Tumne, P	277
Turbini, L	120, 277
Turchi, P	169
Turchin, A	220, 362
Turco, T	79
Turner, C	39
Turner, J	105, 338
Turri, G	105
Tursunov, P	326
Tyagi, V	290

U

Ubertalli, G	140
Uche, O	238
Uchic, M	60, 72, 102, 131, 153, 154, 183, 209, 262, 309, 355
Ucisik, A	181
Ucok, I	194
Uda, T	221, 272, 321
Uddin, S	80
Ueno, H	344
Ueshima, M	74
Uesugi, K	326
Uggowitz, P	257, 336
Uhlenhaut, D	68
Uihlein, A	368
Uju, S	184
Ulfig, R	162
Ullmann, M	240
Umemoto, M	56, 150
Umstead, W	304
Underwood, R	135
Ungar, T	83, 236, 307, 329, 341
Ungár, T	83
Unocic, K	264
Unocic, R	73
Unuvar, C	358
Uotani, Y	350
Upadhyaya, A	180, 234
Upmanyu, M	40, 43, 100, 116
Urbanek, F	320
Usta, M	181
Uttarwar, M	215
Utyashev, F	54
Uyar, F	154

V

Vaagland, J	164
Vaidyanathan, R	128
Vainik, R	220
Valanoor, N	223
Valdez, J	343
Valdez, S	45, 127
Valiev, R	50, 51, 54, 99, 149, 205, 257, 258, 306, 342, 352, 353, 354
van Dalen, M	247
van der Berg, N	253
Van der Giessen, E	230, 316
van der Linden, D	189
Vandermeer, R	206
Van der Meyden, H	109
Vanderspurt, T	136
van der Winden, M	158
van der Zwaag, S	88, 108
Van De Walle, A	139
vanHassel, B	135
Van Hauwermeiren, M	159
Van Quyet, N	129
Van Tyne, C	186
Vanzetti, L	252
Varatharajan, A	223
Varela del Arco, M	274
Varma, S	370
Vasconcelos, P	119
Vásquez, F	323
Vassiliev, S	326

- Vasudevan, V 77, 221, 347
 Vattre, A 72
 Vaughan, G 54
 Vazquez B., L 125
 Vecchio, K 60, 66, 268
 Vedamanickam, S 127
 Vehoff, H 367
 Vékony, K 315
 Velasco, E 165
 Velikodniy, A 57
 Venkatasubramanian, R 267
 Venkatesh, V 88, 138, 193, 194, 246, 294, 340
 Venuturumilli, R 234, 280
 Veprek, S 139
 Verbrugge, M 85
 Vergazova, G 227
 Verlinden, B 57
 Verma, R 64, 134, 157, 241
 Verma, V 39
 Vernon, C 356
 Verweij, H 135
 Veselkov, V 315
 Veyssiere, P 93, 183
 Veyssière, P 73
 Vichikganina, L 51
 Victoria, M 94, 143, 198, 251, 299, 342
 Vidal, E 279, 280, 329
 Vidal, V 57
 Vieh, C 144
 Viehweger, B 348, 349
 Vieira, C 114, 273, 346
 Vieira, T 204
 Vilaça, P 80
 Villechaise, P 84
 Villegas, J 367
 Vinogradov, A 258
 Virieux, F 266
 Viswanathan, A 51
 Viswanathan, G 181, 275, 340
 Vitchus, B 171, 172
 Vite, M 125
 Vitek, J 338
 Vitorino, J 114, 346
 Vizdal, J 344
 Vogel, S 198
 Voggenteiter, H 148
 Vogt, H 240
 Voice, W 235
 Volkert, C 229, 285, 286, 287, 288, 289
 Voller, V 232
 Volpi, F 363
 Volz, H 166
 Voorhees, P 61, 117, 169, 262, 263
 Vratsanos, L 135
 Vrestal, J 343
 Vurpillot, F 354
- W**
- Wadsworth, J 332
 Wagner, B 104
 Wagner, J 221, 278
 Wagner, M 224
 Wagner, V 285
 Wagner, W 94
 Wahba, J 357
 Wain, N 194
- Wakabayashi, T 254
 Walczak, G 191
 Walker, D 327
 Walker, L 89, 90
 Wall, J 198
 Wall, M 249
 Walleser, J 254, 327
 Wallgram, W 347, 348
 Wallick, M 110
 Walter, G 234
 Walther, F 285
 Wan, X 368
 Wanderka, N 94
 Wang, A 194
 Wang, B 43, 44, 96, 221, 324
 Wang, C 75, 344
 Wang, D 42, 136, 215, 286
 Wang, F 112, 277, 369
 Wang, G 68, 156, 163, 187, 191, 197,
 198, 217, 250, 251, 294, 319, 361
 Wang, H 73, 98, 101, 124, 153, 174, 199,
 215, 245, 247, 261, 338, 339, 350, 359
 Wang, J 50, 51, 52, 55, 56,
 150, 204, 216, 241, 366
 Wang, K 101, 193
 Wang, L 81, 87, 89, 101, 137, 155, 252, 298, 314
 Wang, M 41, 193
 Wang, N 313
 Wang, P 155
 Wang, Q 55, 156, 303, 346
 Wang, S 56, 59, 212, 214,
 292, 298, 331, 335, 337
 Wang, T 293
 Wang, W 41, 98, 101, 360, 370
 Wang, X 66, 142, 162, 198, 318
 Wang, Y 42, 43, 61, 69, 71, 73, 75, 92,
 93, 96, 116, 122, 138, 140, 141, 142,
 144, 149, 168, 169, 186, 188, 197, 198,
 205, 207, 217, 218, 223, 224, 225, 250,
 251, 266, 275, 279, 294, 297, 298, 323,
 324, 336, 341, 343, 352, 360, 364, 365
 Wang, Z 70, 75, 78, 114, 132, 140,
 152, 167, 185, 191, 215, 222, 245,
 274, 286, 306, 314, 322, 326, 366
 Wan Tang Kuan, S 315
 Ward, C 104, 246
 Warner, J 113
 Warnken, N 276, 324
 Warren, J 72, 169
 Warren, O 76, 307
 Waryoba, D 53, 221, 362
 Was, G 82, 94, 143, 182, 198,
 199, 251, 252, 299, 342
 Waser, R 274
 Wasson, A 46
 Wastavino, G 302
 Watanabe, C 184
 Watanabe, T 252
 Watling, K 75
 Weaver, M 128, 175
 Webb-Robertson, B 294
 Weber, W 252, 299
 Weder, M 336
 Weertman, J 236
 Wei, C 254
 Wei, H 301
 Wei, L 231, 312
- Wei, Q 151, 205, 206, 207
 Wei, W 243
 Weidner, A 183
 Weifeng, L 78, 302
 Weil, K 86, 135, 189, 190, 243, 292, 338, 368
 Weiland, H 49, 264
 Weimer, M 97
 Weimin, L 272
 Weismüller, J 51, 333
 Weiss, B 229, 367
 Weiss, I 160
 Weissmüller, J 99, 364
 Wejdemann, C 93
 Wejrzanowski, T 57
 Welberry, T 341, 342
 Welch, B 313
 Wells, D 168
 Wells, M 134
 Wen, C 69, 112, 216, 335
 Wen, L 219
 Wen, W 351
 Wen, X 157, 211
 Wen, Y 43, 324, 325
 Wenyan, W 345
 Werner, E 50
 West, J 208
 Westerlund, K 79
 Weston, M 210
 Wheeler, D 169
 Wheeler, K 179, 195, 263
 Whelan, S 171
 Whetten, J 64
 White, C 212
 White, D 113
 White, P 243
 White, S 160
 Whitehorn, R 295
 Whitfield, R 256
 Whitley, V 141, 174
 Wicker, R 110
 Wickett, M 169
 Wickins, M 98
 Widom, M 44, 347
 Wielage, B 57
 Wierzbicka, A 173
 Wiest, A 68, 319
 Wiest, J 39
 Wiest, L 319
 Wiezorek, J 55, 307, 308
 Wignacourt, J 200
 Wilde, G 364
 Wildey, B 219
 Wilkosz, D 338
 Willard, M 261, 309
 Williams, C 178
 Williams, E 113, 164
 Williams, J 131, 246, 247, 248, 263
 Williams, P 146
 Williams, R 61, 209, 246
 Williams, S 95, 279
 Wilson, B 363
 Wilson, J 135
 Wilson, M 338
 Wilson, S 45, 117, 154
 Wilson, T 268
 Wimmer, M 287
 Windl, W 163

Wingate, C	311
Winter, S	348
Wiredu, L	220
Wisbey, A	256
Wise, S	208, 276
Withers, P	178, 297, 342
Withey, E	76
Witte, F	335
Witusiewicz, V	256
Wögerer, C	153
Wojewoda, J	173
Wolcott, J	277
Wolf, A	156
Wolf, D	99, 252
Wolfson, N	68
Wollants, P	117, 301
Wollmershauser, J	95
Wolverton, C	140, 323
Wombles, R	172
Wong, B	338
Wong, C	158, 253, 264
Wong, H	81
Woo, C	71
Woo, K	39
Woo, W	298
Wood, A	243
Wood, J	187, 347, 370
Woodrow, B	119
Woods, J	277, 327
Woodward, C	72, 139, 149, 224, 348, 350
Worthington, D	141, 191, 209, 364
Wright, P	109, 213
Wright, S	69
Wright, W	111
Wu, A	300
Wu, C	331, 360
Wu, D	105, 330
Wu, E	298
Wu, H	41, 200
Wu, J	243, 244
Wu, K	96, 138, 169, 238, 294
Wu, L	297
Wu, Q	221
Wu, R	275
Wu, W	111, 200
Wu, X	178, 235, 256, 282, 303, 305, 353, 354
Wu, Y	145
Wunderlich, R	247, 269, 360
Wuttig, M	223
Wynne, B	134, 138, 178

X

Xia, F	219
Xia, G	190
Xia, K	256
Xia, S	51
Xia, Y	149
Xia, Z	277
Xiangfa, L	65
Xiangxin, X	43
Xiao, B	156
Xiao, S	148
Xiao, Z	70, 330
Xiaodong, H	313
Xiao Dong, Y	160
Xie, H	69, 112

Xie, S	95
Xie, X	41
Xing, C	139
Xing, D	319
Xing, Q	322
Xing, Y	327
Xiquan, Q	214
Xu, B	311
Xu, C	149, 150, 257
Xu, D	73, 245, 350
Xu, G	121
Xu, H	233
Xu, J	304, 347, 366, 369
Xu, K	42
Xu, L	41, 228, 245, 254, 256
Xu, Q	308
Xu, S	144
Xu, T	260
Xu, W	109, 256
Xu, X	194, 276
Xu, Y	194, 229, 316
Xu, Z	121, 124
Xue, B	345
Xue, J	215, 245, 314, 326
Xue, L	80, 335
Xue, P	246
Xue, W	251, 360
Xue, Y	77, 323

Y

Yablinsky, C	131
Yacaman, M	184
Ya Feng, L	160
Yagi, Y	300
Yajima, K	345
Yakimicki, D	110
Yamada, H	115
Yamada, Y	300
Yamaguchi, M	193
Yamaguchi, S	186, 202
Yamakov, V	99
Yamamoto, A	283
Yamamoto, K	190
Yamamoto, T	223
Yamamoto, Y	326
Yamasaki, T	163
Yamashita, D	208
Yan, H	109
Yan, Q	51, 58, 125
Yan, S	41
Yan, X	314, 330
Yan, Y	41, 63, 104, 105
Yan-qing, L	330
Yanada, I	228
Yang, B	72
Yang, F	44, 68, 121, 148, 217, 317
Yang, H	42, 128, 205, 215, 255
Yang, L	72, 273
Yang, M	40, 235
Yang, Q	288
Yang, R	73, 97, 98, 148, 203, 218, 255, 256, 304, 347, 349, 350, 370
Yang, S	132, 265, 290, 314, 326, 327
Yang, W	265
Yang, X	235
Yang, Y	138, 239, 251, 294, 299, 325, 352

Yang, Z	86, 135, 189, 190, 242, 243, 255, 292, 338, 368
Yankov, R	371
Yanli, J	43
Yanqing, L	314
Yao, G	231, 265, 312, 313, 335
Yao, J	89, 139
Yao, S	265, 290
Yao, Z	143, 144
Yapici, G	257
Yashin, A	181
Yasuda, H	265, 326
Yavari, A	54
Yavari, R	162
Yazgan Kokuzoz, B	138
Yazici, H	358
Ye, B	89
Ye, F	197
Ye, J	76
Yeager, J	195
Yeh, Y	360
Yen, Y	300, 301
Yeoh, L	256, 304
Yeon, D	169
Yexiang, L	314, 330
Yi, D	265, 290
Yi, G	70
Yi, T	322
Yim, C	238
Yin, D	50, 150
Yin, H	137
Yin, W	64, 107, 157, 211, 264, 312
Yin, Z	311, 322, 330, 356
Yinglu, Z	312
Yip, T	100
Yokka, Y	201
Yokoyama, S	223
Yokoyama, Y	163, 216, 217, 218, 269
Yolton, C	149, 305
Yong, L	78, 302
Yong, W	313
Yong, Z	318
Yoo, B	174, 218
Yoo, C	249
Yoo, H	152
Yoo, J	202
Yoo, K	202
Yoon, C	260
Yoon, M	274
Yoon, S	292, 333
Yoon, Y	289
Yordanov, P	115
Yo Sep, Y	310
Yoshihara, M	370
Yoshiya, M	265
You, B	238
You, J	248
Youguo, H	314
Young, D	231
Young, G	104
Young, M	328
Yount, H	252
Yu, F	337
Yu, G	218
Yu, H	48, 231
Yu, J	132, 133, 255, 313
Yu, L	42

- Yu, M..... 331
 Yu, P..... 72
 Yu, S..... 126, 127, 335
 Yu, W..... 228
 Yu, Y..... 366
 Yu-Ting, Y..... 120
 Yuan, C..... 251, 308, 324, 356
 Yuan, Q..... 216, 267
 Yuan, X..... 269
 Yücel, O..... 192
 Yue, L..... 178
 Yue, S..... 134, 241
 Yuferev, V..... 168
 Yün, Y..... 261
 Yunusova, N..... 54
 Yuqing, W..... 322
 Yuri, G..... 144
- Z**
- Zabar, N..... 154, 155, 156, 225, 262, 364
 Zaefferer, S..... 278, 351
 Zaikov, Y..... 314
 Zaluzec, M..... 104
 Zambrano, A..... 301
 Zamiri, A..... 277, 347
 Zan, X..... 149
 Zangiaccomi, C..... 119, 171, 225, 226, 325, 365
 Zarandi, F..... 241
 Zargar, H..... 41, 323
 Zatsepin, N..... 309
 Zbib, A..... 195
 Zehetbauer, M..... 52, 353, 367
 Zelberg, B..... 39, 315
 Zelinska, O..... 145
 Zeman, M..... 132
 Zemcik, L..... 97
 Zeng, K..... 74, 119, 172, 199, 228, 229, 253, 277, 300, 326, 343
 Zeng, Q..... 211
 Zeng, X..... 134, 188, 290
 Zeng, Z..... 101, 292
 Zenobia, S..... 94
 Zestrea, V..... 223
 Zhai, Q..... 81, 87, 180
 Zhai, T..... 157, 211, 304, 347
 Zhai, X..... 108, 138
 Zhan, S..... 281
 Zhang, C..... 187
 Zhang, D..... 251, 312
 Zhang, F..... 96, 116, 138, 157, 251, 294, 324
 Zhang, H..... 62, 69, 186, 268, 335, 351
 Zhang, J..... 40, 44, 127, 193, 221, 231, 274, 275, 298, 347, 348, 349
 Zhang, K..... 140, 361
 Zhang, L..... 56, 155, 156, 201, 220, 302
 Zhang, M..... 108, 138, 185, 271, 288, 330
 Zhang, N..... 370
 Zhang, R..... 80, 139, 276, 277
 Zhang, S..... 60, 187, 188, 276, 333
 Zhang, T..... 69, 89, 108, 111, 139, 177, 218, 238, 330, 366
 Zhang, W..... 50, 217, 269, 312
 Zhang, X..... 41, 143, 174, 185, 199, 205, 231, 241, 327, 370
 Zhang, Y..... 52, 56, 122, 123, 162, 205, 231, 252, 255, 299, 360
 Zhang, Z..... 53, 57, 75, 108, 138, 180, 240, 318, 330, 334
 Zhao, H..... 75, 314
 Zhao, J..... 122
 Zhao, L..... 370
 Zhao, Q..... 109, 177, 214
 Zhao, S..... 193
 Zhao, X..... 78, 132, 366
 Zhao, Y..... 77, 150, 206, 257, 306
 Zheng, B..... 70
 Zheng, G..... 59
 Zheng, H..... 321
 Zheng, K..... 290
 Zheng, L..... 322
 Zheng, S..... 87
 Zheng, Y..... 124
 Zherebtsov, S..... 54, 205
 Zhihe, D..... 234
 Zhihui, X..... 178
 Zhilyaev, A..... 52, 353
 Zhong, Y..... 130, 349
 Zhongliang, T..... 314
 Zhou, F..... 51, 58, 125
 Zhou, J..... 65, 141
 Zhou, N..... 224
 Zhou, R..... 252
 Zhou, W..... 41, 60, 101
 Zhou, X..... 44, 142
 Zhou, Y..... 53, 150
 Zhu, A..... 319
 Zhu, C..... 215
 Zhu, H..... 40, 133, 235, 304
 Zhu, J..... 187, 190
 Zhu, M..... 89
 Zhu, S..... 288, 337
 Zhu, T..... 118, 130, 364
 Zhu, W..... 255
 Zhu, X..... 49, 367
 Zhu, Y..... 50, 54, 99, 149, 150, 205, 206, 207, 257, 286, 306, 352
 Zhuang, L..... 158
 Zhukovskii, Y..... 223
 Zi, A..... 344
 Zieba, P..... 173
 Ziegler, D..... 213
 Zigoneanu, L..... 100
 Zikry, M..... 184
 Zimmerman, R..... 343, 359
 Zimmermann, M..... 130
 Zimprich, P..... 229
 Zina, B..... 363
 Zindel, J..... 126
 Zinkle, S..... 104, 343
 Zlatko, C..... 357
 Zmierczak, W..... 163
 Zolotoyabko, E..... 93, 341, 342
 Zou, J..... 350
 Zou, Z..... 311
 Zrnik, J..... 250, 258
 Zschack, P..... 92
 Zschau, H..... 349
 Zu, G..... 312, 313
 Zuberova, Z..... 359
 Zujovic, Z..... 106
 Zuo, L..... 197, 198, 250, 251
 Zuo, X..... 201, 302
 Zuo-kun, C..... 313